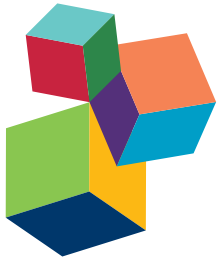


MOLECULAR AND METABOLIC MECHANISMS ASSOCIATED WITH FLESHY FRUIT QUALITY

EDITED BY: Ana M. Fortes, Antonio Granell, Mario Pezzotti and
Mondher Bouzayen

PUBLISHED IN: Frontiers in Plant Science and Frontiers in Physiology



Frontiers Copyright Statement

© Copyright 2007-2017 Frontiers Media SA. All rights reserved.

All content included on this site, such as text, graphics, logos, button icons, images, video/audio clips, downloads, data compilations and software, is the property of or is licensed to Frontiers Media SA ("Frontiers") or its licensees and/or subcontractors. The copyright in the text of individual articles is the property of their respective authors, subject to a license granted to Frontiers.

The compilation of articles constituting this e-book, wherever published, as well as the compilation of all other content on this site, is the exclusive property of Frontiers. For the conditions for downloading and copying of e-books from Frontiers' website, please see the Terms for Website Use. If purchasing Frontiers e-books from other websites or sources, the conditions of the website concerned apply.

Images and graphics not forming part of user-contributed materials may not be downloaded or copied without permission.

Individual articles may be downloaded and reproduced in accordance with the principles of the CC-BY licence subject to any copyright or other notices. They may not be re-sold as an e-book.

As author or other contributor you grant a CC-BY licence to others to reproduce your articles, including any graphics and third-party materials supplied by you, in accordance with the Conditions for Website Use and subject to any copyright notices which you include in connection with your articles and materials.

All copyright, and all rights therein, are protected by national and international copyright laws.

The above represents a summary only. For the full conditions see the Conditions for Authors and the Conditions for Website Use.

ISSN 1664-8714

ISBN 978-2-88945-272-9

DOI 10.3389/978-2-88945-272-9

About Frontiers

Frontiers is more than just an open-access publisher of scholarly articles: it is a pioneering approach to the world of academia, radically improving the way scholarly research is managed. The grand vision of Frontiers is a world where all people have an equal opportunity to seek, share and generate knowledge. Frontiers provides immediate and permanent online open access to all its publications, but this alone is not enough to realize our grand goals.

Frontiers Journal Series

The Frontiers Journal Series is a multi-tier and interdisciplinary set of open-access, online journals, promising a paradigm shift from the current review, selection and dissemination processes in academic publishing. All Frontiers journals are driven by researchers for researchers; therefore, they constitute a service to the scholarly community. At the same time, the Frontiers Journal Series operates on a revolutionary invention, the tiered publishing system, initially addressing specific communities of scholars, and gradually climbing up to broader public understanding, thus serving the interests of the lay society, too.

Dedication to Quality

Each Frontiers article is a landmark of the highest quality, thanks to genuinely collaborative interactions between authors and review editors, who include some of the world's best academicians. Research must be certified by peers before entering a stream of knowledge that may eventually reach the public - and shape society; therefore, Frontiers only applies the most rigorous and unbiased reviews.

Frontiers revolutionizes research publishing by freely delivering the most outstanding research, evaluated with no bias from both the academic and social point of view.

By applying the most advanced information technologies, Frontiers is catapulting scholarly publishing into a new generation.

What are Frontiers Research Topics?

Frontiers Research Topics are very popular trademarks of the Frontiers Journals Series: they are collections of at least ten articles, all centered on a particular subject. With their unique mix of varied contributions from Original Research to Review Articles, Frontiers Research Topics unify the most influential researchers, the latest key findings and historical advances in a hot research area! Find out more on how to host your own Frontiers Research Topic or contribute to one as an author by contacting the Frontiers Editorial Office: researchtopics@frontiersin.org

MOLECULAR AND METABOLIC MECHANISMS ASSOCIATED WITH FLESHY FRUIT QUALITY

Topic Editors:

Ana M. Fortes, Universidade de Lisboa, Portugal

Antonio Granell, Instituto de Biología Molecular y Celular de Plantas (CSIC-UPV), Spain

Mario Pezzotti, University of Verona, Italy

Mondher Bouzayen, INRA, University of Toulouse, France

Fleshy Fruits are a late acquisition of plant evolution. In addition of protecting the seeds, these specialized organs unique to plants were developed to promote seed dispersal via the contribution of frugivorous animals. Fruit development and ripening is a complex process and understanding the underlying genetic and molecular program is a very active field of research. Part of the ripening process is directed to build up quality traits such as color, texture and aroma that make the fruit attractive and palatable. As fruit consumers, humans have developed a time long interaction with fruits which contributed to make the fruit ripening attributes conform our needs and preferences. This issue of *Frontiers in Plant Science* is intended to cover the most recent advances in our understanding of different aspects of fleshy fruit biology, including the genetic, molecular and metabolic mechanisms associated to each of the fruit quality traits. It is also of prime importance to consider the effects of environmental cues, cultural practices and postharvest methods, and to decipher the mechanism by which they impact fruit quality traits.

Most of our knowledge of fleshy fruit development, ripening and quality traits comes from work done in a reduced number of species that are not only of economic importance but can also benefit from a number of genetic and genomic tools available to their specific research communities. For instance, working with tomato and grape offers several advantages since the genome sequences of these two fleshy fruit species have been deciphered and a wide range of biological and genetic resources have been developed. Ripening mutants are available for tomato which constitutes the main model system for fruit functional genomics. In addition, tomato is used as a reference species for climacteric fruit which ripening is controlled by the phytohormone ethylene. Likewise, grape is a reference species for non-climacteric fruit even though no single master switches controlling ripening initiation have been uncovered yet. In the last period, the genome sequence of an increased number of fruit crop species became available which creates a suitable situation for research communities around crops to get organized and information to be shared through public repositories. On the other hand, the availability of genome-wide expression profiling technologies has enabled an easier study of global transcriptional changes in fruit species where the sequenced genome is not yet available.

In this issue authors will present recent progress including original data as well as authoritative reviews on our understanding of fleshy fruit biology focusing on tomato and grape as model species.

Citation: Fortes, A. M., Granell, A., Pezzotti, M., Bouzayen, M., eds. (2017). Molecular and Metabolic Mechanisms Associated with Fleshy Fruit Quality. Lausanne: Frontiers Media.
doi: 10.3389/978-2-88945-272-9

Table of Contents

- 06 Editorial: Molecular and Metabolic Mechanisms Associated with Fleshy Fruit Quality**
Ana M. Fortes, Antonio Granell, Mario Pezzotti and Mondher Bouzayen
- 11 Use of Natural Diversity and Biotechnology to Increase the Quality and Nutritional Content of Tomato and Grape**
Quentin Gascuel, Gianfranco Diretto, Antonio J. Monforte, Ana M. Fortes and Antonio Granell
- REGULATION OF FRUIT DEVELOPMENT AND RIPENING**
- 35 DNA Methylation and Chromatin Regulation during Fleshy Fruit Development and Ripening**
Philippe Gallusci, Charlie Hodgman, Emeline Teyssier and Graham B. Seymour
- 49 Fruit Calcium: Transport and Physiology**
Bradleigh Hocking, Stephen D. Tyerman, Rachel A. Burton and Matthew Gillham
- 66 Identification of Peach NAP Transcription Factor Genes and Characterization of their Expression in Vegetative and Reproductive Organs during Development and Senescence**
Fang Li, Jinjin Li, Ming Qian, Mingyu Han, Lijun Cao, Hangkong Liu, Dong Zhang and Caiping Zhao
- 79 Implication of Abscisic Acid on Ripening and Quality in Sweet Cherries: Differential Effects during Pre- and Post-harvest**
Verónica Tijero, Natalia Teribia, Paula Muñoz and Sergi Munné-Bosch
- 94 Structural and Functional Analysis of the GRAS Gene Family in Grapevine Indicates a Role of GRAS Proteins in the Control of Development and Stress Responses**
Jérôme Grimpel, Patricia Agudelo-Romero, Rita T. Teixeira, Jose M. Martinez-Zapater and Ana M. Fortes
- 116 Evolutionary Recycling of Light Signaling Components in Fleshy Fruits: New Insights on the Role of Pigments to Monitor Ripening**
Briardo Llorente, Lucio D'Andrea and Manuel Rodríguez-Concepción
- 123 In silico Transcriptional Regulatory Networks Involved in Tomato Fruit Ripening**
Stilianos Arhondakis, Craita E. Bita, Andreas Perrakis, Maria E. Manioudaki, Afroditi Krokida, Dimitrios Kaloudas and Panagiotis Kalaitzis
- 133 Nitric Oxide Overproduction in Tomato shr Mutant Shifts Metabolic Profiles and Suppresses Fruit Growth and Ripening**
Reddaiah Bodanapu, Suresh K. Gupta, Pinjari O. Basha, Kannabiran Sakthivel, Sadhana, Yellamaraju Seelakshmi and Rameshwar Sharma

RIPENING ASSOCIATED PROCESSES AND FRUIT QUALITY

- 151 *On the Developmental and Environmental Regulation of Secondary Metabolism in Vaccinium spp. Berries***
Katja Karppinen, Laura Zoratti, Nga Nguyenquynh, Hely Häggman and Laura Jaakola
- 160 *Phenylpropanoids Accumulation in Eggplant Fruit: Characterization of Biosynthetic Genes and Regulation by a MYB Transcription Factor***
Teresa Docimo, Gianluca Francese, Alessandra Ruggiero, Giorgia Batelli, Monica De Palma, Laura Bassolino, Laura Toppino, Giuseppe L. Rotino, Giuseppe Mennella and Marina Tucci
- 178 *Metabolic and Molecular Changes of the Phenylpropanoid Pathway in Tomato (Solanum lycopersicum) Lines Carrying Different Solanum pennellii Wild Chromosomal Regions***
Maria Manuela Rigano, Assunta Raiola, Teresa Docimo, Valentino Ruggieri, Roberta Calafiore, Paola Vitaglione, Rosalia Ferracane, Luigi Frusciante and Amalia Barone
- 193 *Exploiting Genomics Resources to Identify Candidate Genes Underlying Antioxidants Content in Tomato Fruit***
Roberta Calafiore, Valentino Ruggieri, Assunta Raiola, Maria M. Rigano, Adriana Sacco, Mohamed I. Hassan, Luigi Frusciante and Amalia Barone
- 207 *Exploring New Alleles Involved in Tomato Fruit Quality in an Introgression Line Library of Solanum pimpinellifolium***
Walter Barrantes, Gloria López-Casado, Santiago García-Martínez, Aranzazu Alonso, Fernando Rubio, Juan J. Ruiz, Rafael Fernández-Muñoz, Antonio Granell and Antonio J. Monforte
- 219 *Identification of Loci Affecting Accumulation of Secondary Metabolites in Tomato Fruit of a Solanum lycopersicum × Solanum chmielewskii Introgression Line Population***
Ana-Rosa Ballester, Yury Tikunov, Jos Molthoff, Silvana Grandillo, Marcela Viquez-Zamora, Ric de Vos, Ruud A. de Maagd, Sjaak van Heusden and Arnaud G. Bovy
- 233 *Metabolite Profiling of Italian Tomato Landraces with Different Fruit Types***
Svetlana Baldina, Maurizio E. Picarella, Antonio D. Troise, Anna Pucci, Valentino Ruggieri, Rosalia Ferracane, Amalia Barone, Vincenzo Fogliano and Andrea Mazzucato
- 246 *The Relationship between CmADHs and the Diversity of Volatile Organic Compounds of Three Aroma Types of Melon (Cucumis melo)***
Hao Chen, Songxiao Cao, Yazhong Jin, Yufan Tang and Hongyan Qi
- 258 *Gene-Metabolite Networks of Volatile Metabolism in Airen and Tempranillo Grape Cultivars Revealed a Distinct Mechanism of Aroma Bouquet Production***
José L. Rambla, Almudena Trapero-Mozos, Gianfranco Diretto, Angela Rubio-Moraga, Antonio Granell, Lourdes Gómez-Gómez and Oussama Ahrazem
- 281 *How Does Host Carbon Concentration Modulate the Lifestyle of Postharvest Pathogens during Colonization?***
Dov B. Prusky, Fangcheng Bi, Juan Moral and Shiri Barad
- 287 *Inter-Species Comparative Analysis of Components of Soluble Sugar Concentration in Fleshy Fruits***
Zhanwu Dai, Huan Wu, Valentina Baldazzi, Cornelis van Leeuwen, Nadia Bertin, Hélène Gautier, Benhong Wu, Eric Duchêne, Eric Gomès, Serge Delrot, Françoise Lescourret and Michel Génard
- 299 *Insights into molecular and metabolic events associated with fruit response to post-harvest fungal pathogens***
Noam Alkan and Ana M. Fortes

IMPACT OF ENVIRONMENTAL CUES, CULTURAL PRACTICES, AND POSTHARVEST STRATEGIES ON FRUIT QUALITY

- 313 *Field-Grown Grapevine Berries Use Carotenoids and the Associated Xanthophyll Cycles to Acclimate to UV Exposure Differentially in High and Low Light (Shade) Conditions***
Chandré Joubert, Philip R. Young, Hans A. Eyéghé-Bickong and Melané A. Vivier
- 330 *Grapevine Rootstocks Differentially Affect the Rate of Ripening and Modulate Auxin-Related Genes in Cabernet Sauvignon Berries***
Massimiliano Corso, Alessandro Vannozzi, Fiorenza Ziliotto, Mohamed Zouine, Elie Maza, Tommaso Nicolato, Nicola Vitulo, Franco Meggio, Giorgio Valle, Mondher Bouzayen, Maren Müller, Sergi Munné-Bosch, Margherita Lucchin and Claudio Bonghi
- 344 *Kaolin Foliar Application Has a Stimulatory Effect on Phenylpropanoid and Flavonoid Pathways in Grape Berries***
Artur Conde, Diana Pimentel, Andreia Neves, Lia-Tânia Dinis, Sara Bernardo, Carlos M. Correia, Hernâni Gerós and José Moutinho-Pereira
- 358 *Plasticity of the Berry Ripening Program in a White Grape Variety***
Silvia Dal Santo, Marianna Fasoli, Stefano Negri, Erica D'Incà, Nazareno Vicenzi, Flavia Guzzo, Giovanni Battista Tornielli, Mario Pezzotti and Sara Zenoni
- 375 *Rootstocks/Scion/Nitrogen Interactions Affect Secondary Metabolism in the Grape Berry***
Aude Habran, Mauro Commissio, Pierre Helwi, Ghislaine Hilbert, Stefano Negri, Nathalie Ollat, Eric Gomès, Cornelis van Leeuwen, Flavia Guzzo and Serge Delrot
- 386 *The Influence of Genotype and Environment on Small RNA Profiles in Grapevine Berry***
Daniela Lopes Paim Pinto, Lucio Brancadoro, Silvia Dal Santo, Gabriella De Lorenzis, Mario Pezzotti, Blake C. Meyers, Mario E. Pè and Erica Mica
- 409 *The Potential of the MAGIC TOM Parental Accessions to Explore the Genetic Variability in Tomato Acclimation to Repeated Cycles of Water Deficit and Recovery***
Julie Ripoll, Laurent Urban and Nadia Bertin
- 424 *Identification, Expression and IAA-Amide Synthetase Activity Analysis of Gretchen Hagen 3 in Papaya Fruit (*Carica papaya L.*) during Postharvest Process***
Kaidong Liu, Jinxiang Wang, Haili Li, Jundi Zhong, Shaoxian Feng, Yaoliang Pan and Changchun Yuan



Editorial: Molecular and Metabolic Mechanisms Associated with Fleshy Fruit Quality

Ana M. Fortes^{1*}, Antonio Granell², Mario Pezzotti³ and Mondher Bouzayen⁴

¹ Faculdade de Ciências de Lisboa, BioSI, Universidade de Lisboa, Lisboa, Portugal, ² Instituto de Biología Molecular y Celular de Plantas (CSIC-UPV), Valencia, Spain, ³ Department of Biotechnology, University of Verona, Verona, Italy,

⁴ Laboratory of Genomics and Biotechnology of Fruit, INRA, University of Toulouse, Toulouse, France

Keywords: breeding, fruit ripening, fruit quality, grapevine, molecular mechanisms, metabolic profiling, tomato

Editorial on the Research Topic

Molecular and Metabolic Mechanisms Associated with Fleshy Fruit Quality

INTRODUCTION

OPEN ACCESS

Edited by:

Vasileios Fotopoulos,
Cyprus University of Technology,
Cyprus

Reviewed by:

Angelos K. Kanellis,
Aristotle University of Thessaloniki,
Greece

George A. Manganaris,
Cyprus University of Technology,
Cyprus

*Correspondence:

Ana M. Fortes
amfortes@fc.ul.pt

Specialty section:

This article was submitted to
Plant Physiology,
a section of the journal
Frontiers in Plant Science

Received: 28 April 2017

Accepted: 29 June 2017

Published: 13 July 2017

Citation:

Fortes AM, Granell A, Pezzotti M and
Bouzayen M (2017) Editorial:
Molecular and Metabolic Mechanisms
Associated with Fleshy Fruit Quality.
Front. Plant Sci. 8:1236.
doi: 10.3389/fpls.2017.01236

Fleshy fruits constitute a commercially important and nutritionally indispensable food commodity. In 2014, the total production of tomatoes and grapes worldwide was 170,750,767 and 74,499,859 tones, respectively (FAOSTAT).

This issue covers the most recent advances in our understanding of different aspects of fleshy fruit biology. In fact, fruit development and ripening involves several processes that were addressed in this issue namely accumulation of bioactive compounds (Calafiore et al.; Docimo et al.; Karppinen et al.; Rigano et al.) and modification of components that affect nutritional quality (Baldina et al.; Barrantes et al.; Dai et al.; Karppinen et al.; Rambla et al.) as well as modifications in texture triggered by cell wall changes and increased susceptibility to pathogens (Alkan and Fortes; Hocking et al.; Prusky et al.). The reprogramming of fruit development and ripening involves several transcription factors (Arhondakis et al.; Docimo et al.; Grimplet et al.; Li et al.), hormones (Tijero et al.; Alkan and Fortes; Karppinen et al.), nitric oxide (Bodanapu et al.), light signaling (Llorente et al.), calcium (Hocking et al.), small ncRNAs (Paim Pinto et al.), and epigenetic regulation (Gallusci et al.). Furthermore, environmental cues (Joubert et al.; Karppinen et al.; Paim Pinto et al.; Ripoll et al.; Dal Santo et al.), cultivation practices (Conde et al.; Corso et al.; Habran et al.), and postharvest strategies (Tijero et al.; Li et al.; Liu et al.) were shown to have an impact in ripening properties and fruit quality traits. Finally, in the review by Gascuel et al. were addressed the available genetic resources for breeding purposes of commercially important commodities such as tomato and grape. Furthermore, the technologies that facilitate the identification of genes/alleles of interest within the natural or generated variability gene pool were explored.

REGULATION OF FRUIT DEVELOPMENT AND RIPENING

Fruit development and ripening involves hormonal regulation in which auxins, cytokinins, ethylene, and ABA play an important role among other hormones (Fortes et al., 2015). The involvement of ABA in promoting ripening and quality of climacteric and non-climacteric fleshy fruits was reported by several authors in this issue (Alkan and Fortes; Hocking et al.; Karppinen et al.; Li et al.; Tijero et al.).

Endogenous ABA was mentioned to be involved in the regulating of ripening of climacteric tomato fruit (Bodanapu et al.). Fruit ripening in the short root (*shr*) mutant of tomato

that hyperaccumulates nitric oxide was delayed compared with the wild type. Central carbon metabolism and endogenous phytohormones levels were affected in the *shr* fruits. The authors highlighted that a crosstalk among nitric oxide and auxin, ABA and ethylene may regulate ripening and that selective manipulation of nitric oxide levels during ripening may increase shelf life of tomato.

In sweet cherries, a non-climacteric fruit, Tijero et al. studied the role played by ABA during pre-harvest and post-harvest room temperature/cold treatments. Endogenous ABA concentrations positively influenced quality parameters (accumulation of anthocyanins and vitamin E) during pre-harvest but not during post-harvest. Cold treatment increased ABA levels and led to an inhibition of senescence. The authors concluded that endogenous ABA promotes fruit ripening on the tree, but delays over-ripening in detached fruits.

Transcription factors play an important role in the regulation of fruit ripening (Docimo et al.; Grimplet et al.; Li et al.). The GRAS and the NAP gene families were characterized in grape and peach, respectively (Grimplet et al.; Li et al.). Both families play an important role in plant growth and development. By comparing the information available for tomato and grapevine GRAS genes, Grimplet et al. identified candidate genes that might constitute conserved transcriptional regulators of both climacteric and non-climacteric fruit ripening and that deserve further functional analysis. Co-expression analysis of GRAS genes provided insights into the molecular networks related with development and stress responses involving these transcription factors. On the other hand, Li et al. identified peach NAP genes that are responsive to ABA post-harvest treatment and that may regulate peach ripening. ABA-treated fruits softened faster and released more ethylene resulting in a shorter maximum storage period. In accordance, the promoters of four fruit-specific NAP genes presented ABA-responsive elements. Moreover, Arhondakis et al. identified two transcription factors, a SLWRKY22-like and a SIER24 transcriptional activator which were shown to regulate modules by using the LeMoNe algorithm for the analysis of microarray datasets representing four stages of tomato ripening. The WRKY22-like module comprised a subgroup of six various calcium sensing transcripts. In agreement, the promoter of these genes contained a *cis*-acting element, the W-box, recognized by WRKY transcription factors that might be involved in their coordinated regulation of expression. This approach can be applied for the construction of general fruit ripening regulatory module networks in particular those involving transcription factors.

Manipulation of individual components of light perception and signaling networks in tomato (*Solanum lycopersicum*) affects the metabolism of ripening fruit (Llorente et al.). In this mini-review, the authors explored how molecular mechanisms originally devoted to respond to environmental light cues have been re-adapted during evolution to inform plants on fruit ripening progression. The spectral composition of the light filtered through the fruit pericarp can be transduced by phytochromes and phytochromes-interacting factors, respectively, to regulate gene expression and in turn modulate the production of carotenoids. This process

involves recycling of light-signaling components to finely adjust pigmentation. This trait may have evolved as an advantageous trait. In fact, the ability to display a change in color when the fruit is ripe would attract more seed dispersers among early fleshy-fruited plants.

The effect of calcium on fruit ripening was documented in the review by Hocking et al. The authors reported on the major components that determine calcium supply and distribution in grape. Moreover, calcium-pectin cross-links are a key factor in determining pectin properties and therefore influence remodeling of fruit cell walls. In turn, this affects fruit mechanical properties (softening), water relations and pathogen susceptibility. Calcium is a secondary messenger during hormone signaling and therefore can influence ripening through interaction with hormones. The authors concluded that improved understanding of the calcium nutritional requirements of plants may aid in optimizing fruit quality as both calcium deficiency and toxicity can affect the productivity, characteristics and pathogen susceptibility of the fruit.

Recent strong evidence suggests that fruit ripening is under not only genetic but also epigenetic regulation (Gallusci et al.). In this review, it was described how post-translational modifications of histones influence chromatin organization and contribute to the epigenetic regulation of gene expression during fruit ripening. They further explored the impact of variation in DNA methylation levels on the expression of ripening-related genes. In tomato and probably in other species such as grape (Fortes and Gallusci, 2017) the process of fruit ripening requires active DNA demethylation (Liu et al., 2015). Changes in DNA methylation due to spontaneous mutations or genome duplications can lead to the generation of natural epialleles affecting fruit phenotypes. The authors concluded that epi-marks on gene promoter regions could be used for “fine tuning” of gene expression in breeding strategies and for crop improvement.

RIPENING ASSOCIATED PROCESSES AND FRUIT QUALITY

Karpinnen et al. focused on the mechanisms associated with the regulation of key secondary metabolites in *Vaccinium* berries. Bilberry is a very rich source of anthocyanins that start to accumulate with the onset of ripening. The variation in flavonoid profile during berry development is related to seed dispersal and defense responses, subjected to hormonal control and involves transcription factors namely from the R2R3 MYB family. Many berries also accumulate carotenoid derived volatile flavor compounds at ripening (Agudelo-Romero et al., 2013; Karppinen et al.). Furthermore, light conditions, temperature, altitude, and genotype X environment interactions affect the composition of secondary metabolites in fruits.

Docimo et al. reported on metabolite abundance, regulation of chlorogenic acid, and anthocyanin biosynthesis, and characterization of candidate chlorogenic acid biosynthetic genes in eggplant, a fruit known to accumulate health-promoting phenylpropanoids. Analysis of the promoters of the biosynthetic genes (*SmPAL1*, *SmHQT1*, *SmANS*, and *SmMyb1*) revealed the

presence of several MYB regulatory elements. Furthermore, the authors also determined that deletion of the C-terminal region of SmMYB1 does not limit its capability to regulate chlorogenic acid accumulation, but impairs anthocyanin biosynthesis, proposing therefore a functional role of the C-terminal domain of this transcription factor.

Genomics resources were exploited in order to identify candidate genes underlying antioxidants content in tomato (Calafiore et al.). The authors used *Solanum pennellii* introgression lines harboring quantitative trait loci (QTL) that increase the content of these bioactive compounds in the fruit. The differential expression of six candidate genes associated to ascorbic acid and one with carotenoids' metabolism together with polymorphisms in the sequences of the wild and the cultivated alleles of these genes may account for increased content in these metabolites. In another work from the same group, two genotypes carrying loci from the same wild species were crossed and two genotypes carrying introgressions at the homozygous condition (DHOs) were shown to present increased antioxidants content, revealing a positive interaction between the two wild regions pyramided in DHO genotypes (Rigano et al.). In these genotypes, occurs a putative redirection of the phenylpropanoid flux toward the biosynthesis of phenolic acid glycosides. Gene mapping, transcriptional profiling and biochemical analyses suggested a central role of the 4-coumarate:CoA ligase in redirecting the phenylpropanoid pathways whereas Myb4 and bHLH transcription factors may regulate these pathways. This work highlighted that interaction effects between QTLs must be studied in order to design an efficient pyramiding strategy for increasing fruit nutritional quality.

On the other hand, Barrantes et al. evaluated the breeding potential of introgression lines from the *Solanum pimpinellifolium* accession TO-937 into the genetic background of the "Moneymaker." The authors identified using a genomic library chromosomal regions associated with both vegetative and fruit-related traits. QTLs were detected for fruit weight and organoleptic traits whose stability across generations depended on the trait. Ballester et al. characterized fruits grown in two locations of a population of introgression lines derived from a cross between *Solanum lycopersicum* and the wild species *Solanum chmielewskii*. Robust metabolite QTLs were identified for content in flavonoids, phenylpropanoids and alkaloids. Furthermore, *chalcone isomerase 1* was identified as the key gene underlying the variation in quercentin- and kaempferol glycosides. Altogether, the results demonstrated that by combining genetic and genomic resources in tomato with bioinformatics tools and metabolomics, dissection of QTLs and mQTLs can be achieved in order to improve the nutritional value and attributes of tomato.

The need to improve organoleptic characteristics in fruits is driving attention toward wild relatives but also traditional fruit varieties. Baldina et al. studied the content of several metabolites in tomato landraces categorized into three broad fruit type classes. The round/elongate types showed a higher content in glycoalkaloids, whereas flattened types had higher levels of phenolic compounds and were rich in aminoacids in particular

glutamate, a compound directly related to organoleptic quality. The positions of several SNPs markers showed correspondence with already described genomic regions and QTLs. This work indicated that the future detection of mQTLs for important metabolites will give valuable tools to improve traditional tomato varieties by assisted breeding.

Aroma compounds are key elements in fruit quality. Chen et al. explored the involvement of *Cucumis melo* alcohol dehydrogenases (ADHs) and alcohol acyl-transferase (AAT) in the formation of volatile organic compounds. Ethyl acetate and hexyl acetate (E,Z)-3,6-nonadien-1-ol were found to be the principle aroma compounds of two cultivars whereas (E, Z)-3,6-nonadien-1-ol was the most abundant volatile in the non-aromatic cultivar. Several *CmADH* genes were specifically expressed in ripe fruits and differences were noticed between aromatic and non-aromatic varieties; these genes may code for isoenzymes with different substrates preference. Total AAT activity but not ADH seems to regulate esters abundance. Finally, *CmADH3* and *CmADH12* were selected as putative candidates involved in the synthesis of aroma compounds of oriental melon.

In two grape varieties (one white and one red) the emission of volatile and non-volatile compounds during berry maturation was investigated (Rambla et al.). Early stages were characterized in both cultivars by higher levels of some apocarotenoids, terpenoids and several furans, while the final stages were characterized by the highest amounts of benzenoid phenylacetaldehyde, 2-phenylethanol, 3-methylbutanol, among others. The study also highlighted that different varieties may have different content in certain volatile precursors. By also monitoring the expression of genes putatively involved in the synthesis of these compounds, the authors explored gene-metabolite networks of volatile metabolism and establish candidate genes involved in aroma formation. Furthermore, correlation analysis showed a higher degree of overall correlation in precursor/volatile metabolite-metabolite levels in the white variety, highlighting the different mechanism occurring in white varieties to develop an enriched aroma bouquet.

One of the characteristics that makes the fruits attractive to human consumption is the soluble sugar concentration that depends on sugar import, sugar metabolism, and water dilution (Dai et al.). These authors performed an inter-species comparison in order to identify common and/or species specific modes of regulation in sugar accumulation. By using a mathematical framework for the analysis of 104 combinations of species (grape, peach, and tomato), genotypes, and growing conditions, the authors concluded that different regulation modes of soluble sugar concentration operate being either import-based, dilution-based, or shared. The distinct modes appear to be species-specific, but the intensity of the effect may depend on the genotype and management practices. These results provided novel insights into the drivers causing the inter-species variability in soluble sugar concentration in fleshy fruits.

Increased sugar concentration in ripe fruits leads to increased susceptibility toward pathogens as reviewed by Prusky et al. and Alkan and Fortes. During fruit ripening physiological shifts occur: cell wall remodeling, decrease in the amount of phytoanticipins and phytoalexins, decline of inducible host

defense responses, cuticle biosynthesis and changes in the ambient host pH. These changes are regulated by a complex interplay of hormonal signals that involve ethylene, ABA, jasmonic acid, and salicylic acid, among others and they release the fungus from its quiescent state and promote a necrotrophic life style (Alkan and Fortes). Recent data suggests that carbon availability in the environment (sugar levels) is a key factor triggering the production and secretion of small pH-modulating molecules (ammonia, gluconic acid) that contribute to colonization by postharvest pathogens (Prusky et al.). These pathogens modulate the expression of genes contributing to pathogenicity according to environmental pH-inducing conditions. The authors emphasized that knowledge on the processes responsible for the onset of necrotrophic stage may lead to strategies aiming at enhancing fruit defense and decreasing fungal virulence that will result in increased quality of fruits.

IMPACT OF ENVIRONMENTAL CUES, CULTURAL PRACTICES, AND POSTHARVEST STRATEGIES ON FRUIT QUALITY

Environmental factors such as water deficit may negatively impact fruit yield and quality. The effect of three successive cycles of moderate water deficit and recovery was analyzed during the plant reproductive period in parental accessions of Multi-Parent Advanced Generation Inter-Cross population which presents the largest allelic variability observed in tomato (Ripoll et al.). Independent responses were observed in the leaf and fruit whereas negative effects on fruit fresh weight were dependent on stress intensity. Fruit quality was improved under water deficit mainly through concentration effects. The authors concluded that responses to drought are strongly genotype-dependent as well as highly variable depending on the stage of development at the time water deficit was applied. However, repeated cycles of water deficit and recovery may be used to improve fruit taste if the full variability of genotypic responses and crop performance is explored considering developmental stages.

Joubert et al. concluded that grape berries employed carotenoids and the associated xanthophyll cycles to acclimate to UV exposure. The berry responses differed between high light and low light conditions, in particular when the berries are still photosynthetically active (green developmental stage). Furthermore, in the highlight environment, certain monoterpenes and norisoprenoids were decreased by UVB attenuation confirming that UVB exposure stimulates volatile organic compounds in exposed ripe berries. These volatile terpenes may play a role in stress sensing and signaling related with UVB radiation. This work extended the current understanding of light/UV impacts in grapes and their metabolic plasticity in response to this environmental cue providing valuable data for stress management and improvement of grape quality.

Phenotypic and metabolic plasticity were also addressed in a white berry variety grown at four sites presenting different

pedoclimatic conditions (Dal Santo et al.). Several genes that control transcription, translation, transport, and carbohydrate metabolism showed different expression depending on the environmental conditions. An important conclusion from this work was that genes representing the phenylpropanoid/flavonoid pathway showed highly plastic responses to the environment mirroring the accumulation of the corresponding metabolites. Furthermore, phenotypic plasticity varies among cultivars and may depend on whether the berries are white or red, highlighting the importance of conducting these studies in order to understand how grape and wine characters are developed in different environments from the same genotype.

Not only the epigenome and the RNA transcriptome but also the small RNA transcriptome participates in the dynamic regulatory network occurring in genotype-environment interactions (Paim Pinto et al.). These authors studied grapevine berries at four developmental stages from two varieties growing in three different environments. The results indicated that the distribution of small RNA-producing loci is variable between the cultivars, with the two cultivars showing a completely different small RNA profile across environments. On the other hand, the profile of miRNA accumulation mainly depends on the developmental stage. Several known vvimiRNAs and novel vvimiRNA candidates presented an accumulation in the berries modulated by at least one of the variables studied. The *in silico* prediction of miRNA targets suggests their involvement in berry development and in secondary metabolism.

Grafting commercial grapevine varieties on interspecific rootstocks is a common cultural practice for improving stress resistance and vigor. Corso et al. reported on the acceleration of grape ripening under the influence of a new rootstock comparing to a commercial one. Molecular and biochemical analyses revealed that auxin signaling is strongly affected by the rootstock genotype and the existence of a link between the rate of berry development and the modulation of auxin metabolism which is more pronounced in skin tissue. On the other hand, Habran et al. addressed the combined effects of nitrogen supply and rootstock on berry composition. The authors used four rootstock/scion combinations fertilized with three different levels of nitrogen. The results showed complex responses of the metabolites' content (sugars, organic acids, aminoacids, anthocyanins, flavonols, flavan-3-ols/procyanidins, stilbenes, hydroxycinnamicB, and hydroxybenzoicacids) that depend on soil composition/rootstock/scion/climate interactions. These studies are fundamental in modern viticulture in order to clarify the impact of rootstock on berry scion development and ripening, and how this can be affected by adjustments in nitrogen fertilization.

The foliar exogenous application of kaolin, a radiation-reflecting inert mineral, has been proven effective in mitigating the negative impacts of abiotic stresses in grapevine. By performing a combined molecular and biochemical analysis, Conde et al. showed that kaolin treatment stimulated the expression of genes, and the activity of enzymes involved in the phenylpropanoid, flavonoid, and stilbenoid pathways at latter ripening stages. Metabolomic analysis corroborated this data and indicates that application of kaolin in grapevine leaves may be

used as a summer stress mitigating strategy with positive impacts on berry quality.

Postharvest decay impacts significantly fruit quality and market value especially in climacteric fruits such as papayas that present a short-term shelf life. Liu et al. studied the role of *GH3* genes (encoding IAA-amido synthetases) in the regulation of postharvest physiology in papaya. The observed induced IAA-amido synthetase activities during the postharvest period may lead to the maintenance of low levels of endogenous IAA which is an inhibitor of ripening. Additionally, ascorbic acid treatment seems to regulate postharvest fruit ripening and softening by inducing a decrease in *GH3* genes expression, and IAA-amido synthetase activities, and therefore promoting endogenous IAA levels. Fruits treated with ascorbic acid showed a relatively lower production rate of ethylene than non-treated. These findings may provide a way to develop novel strategies for improving fruit quality during postharvest storage.

REFERENCES

- Agudelo-Romero, P., Erban, A., Sousa, L., Pais, M. S., Kopka, J., and Fortes, A. M. (2013). Search for transcriptional and metabolic markers of grape pre-ripening and ripening and insights into specific aroma development in three portuguese cultivars. *PLoS ONE* 8:e60422. doi: 10.1371/journal.pone.0060422
- Fortes, A. M., and Gallusci, P. (2017). Plant stress responses and phenotypic plasticity in the epigenomics era: perspectives on the grapevine scenario, a model for perennial crop plants. *Front. Plant Sci.* 8:82. doi: 10.3389/fpls.2017.00082
- Fortes, A. M., Teixeira, R. T., and Agudelo-Romero, P. (2015). Complex interplay of hormonal signals during grape berry ripening. *Molecules* 20, 9326–9343. doi: 10.3390/molecules20059326
- Liu, R., How-Kit, A., Stammitti, L., Teyssier, E., Rolin, D., Mortain-Bertrand, A., et al. (2015). A DEMETER-like DNA demethylase governs

AUTHOR CONTRIBUTIONS

AF wrote the editorial with input from AG, MP, and MB.

FUNDING

Funding to AF was provided by the Portuguese Foundation for Science and Technology (FCT Investigator IF/00169/2015, PEst-OE/BIA/UI4046/2014). Research in the AG lab was supported by the EC H2020 Program: TRADITOM-634561 and TOMGEM679796 and networking activities by COST FA1106.

ACKNOWLEDGMENTS

The authors would like to thank the COST (European Cooperation in Science and Technology) Action FA1106 “Quality fruit.”

tomato fruit ripening. *Proc. Natl. Acad. Sci. U.S.A.* 112, 10804–10809. doi: 10.1073/pnas.1503362112

Conflict of Interest Statement: The authors declare that the research was conducted in the absence of any commercial or financial relationships that could be construed as a potential conflict of interest.

The reviewer GM and handling Editor declared their shared affiliation, and the handling Editor states that the process met the standards of a fair and objective review.

Copyright © 2017 Fortes, Granell, Pezzotti and Bouzayen. This is an open-access article distributed under the terms of the Creative Commons Attribution License (CC BY). The use, distribution or reproduction in other forums is permitted, provided the original author(s) or licensor are credited and that the original publication in this journal is cited, in accordance with accepted academic practice. No use, distribution or reproduction is permitted which does not comply with these terms.



Use of Natural Diversity and Biotechnology to Increase the Quality and Nutritional Content of Tomato and Grape

Quentin Gascuel^{1*}, Gianfranco Diretto², Antonio J. Monforte³, Ana M. Fortes⁴ and Antonio Granell^{3*}

¹ Laboratory of Plant-Microbe Interactions, Centre National de la Recherche Scientifique, Institut National de la Recherche Agronomique, Toulouse University, Castanet Tolosan, France, ² Italian National Agency for New Technologies, Energy, and Sustainable Development, Casaccia Research Centre, Rome, Italy, ³ Instituto de Biología Molecular y Celular de Plantas, Agencia Estatal Consejo Superior de Investigaciones Científicas, Universidad Politécnica de Valencia, Valencia, Spain, ⁴ Faculdade de Ciências de Lisboa, Instituto de Biossistemas e Ciências Integrativas (BiolISI), Universidade de Lisboa, Lisboa, Portugal

OPEN ACCESS

Edited by:

Irene Murgia,
Università degli Studi di Milano, Italy

Reviewed by:

Golam Jalal Ahammed,
Zhejiang University, China
Marco Zancani,
University of Udine, Italy

*Correspondence:

Quentin Gascuel
qgascuel@quentingascuel.web4me.fr
Antonio Granell
agranell@ibmcp.upv.es

Specialty section:

This article was submitted to
Plant Physiology,
a section of the journal
Frontiers in Plant Science

Received: 21 December 2016

Accepted: 10 April 2017

Published: 12 May 2017

Citation:

Gascuel Q, Diretto G, Monforte AJ, Fortes AM and Granell A (2017) Use of Natural Diversity and Biotechnology to Increase the Quality and Nutritional Content of Tomato and Grape. *Front. Plant Sci.* 8:652.
doi: 10.3389/fpls.2017.00652

Improving fruit quality has become a major goal in plant breeding. Direct approaches to tackling fruit quality traits specifically linked to consumer preferences and environmental friendliness, such as improved flavor, nutraceutical compounds, and sustainability, have slowly been added to a breeder priority list that already includes traits like productivity, efficiency, and, especially, pest and disease control. Breeders already use molecular genetic tools to improve fruit quality although most advances have been made in producer and industrial quality standards. Furthermore, progress has largely been limited to simple agronomic traits easy-to-observe, whereas the vast majority of quality attributes, specifically those relating to flavor and nutrition, are complex and have mostly been neglected. Fortunately, wild germplasm, which is used for resistance against/tolerance of environmental stresses (including pathogens), is still available and harbors significant genetic variation for taste and health-promoting traits. Similarly, heirloom/traditional varieties could be used to identify which genes contribute to flavor and health quality and, at the same time, serve as a good source of the best alleles for organoleptic quality improvement. Grape (*Vitis vinifera* L.) and tomato (*Solanum lycopersicum* L.) produce fleshy, berry-type fruits, among the most consumed in the world. Both have undergone important domestication and selection processes, that have dramatically reduced their genetic variability, and strongly standardized fruit traits. Moreover, more and more consumers are asking for sustainable production, incompatible with the wide range of chemical inputs. In the present paper, we review the genetic resources available to tomato/grape breeders, and the recent technological progresses that facilitate the identification of genes/alleles of interest within the natural or generated variability gene pool. These technologies include omics, high-throughput phenotyping/phenomics, and biotech approaches. Our review also covers a range of technologies used to transfer to tomato and grape those alleles considered of interest for fruit quality. These include traditional breeding, TILLING (Targeting Induced

Local Lesions in Genomes), genetic engineering, or NPBT (New Plant Breeding Technologies). Altogether, the combined exploitation of genetic variability and innovative biotechnological tools may facilitate breeders to improve fruit quality taking more into account the consumer standards and the needs to move forward into more sustainable farming practices.

Keywords: fruit quality, germplasm, grape, omics, new plant breeding techniques, tomato, QTLs

INTRODUCTION

Since the dawn of agriculture in Neolithic communities some 12,000–10,000 years ago, the selection of plants exhibiting the most desirable traits has never ceased. This, so-called, domestication process appears to have been instrumental in our ancestors' transition from a hunter-gatherer to an agricultural lifestyle (Gepts, 2014), and was characterized by the low number of plant species to succeed as widely-grown crops in modern societies. Initially an intuitive process, selection was made on a few easy-to-observe desirable traits (e.g., fruit size, shape and color, or seed quality; Chalhoub et al., 2014; Vogel, 2014). As in species reduction, only a few genes exercising large phenotypic effects within this limited number of species were selected (Tang et al., 2010).

In fruit crops, initial selection was probably based on nutritious, non-toxic, and palatable features. Hedonic and culinary qualities, including flavor, succulence, juiciness, and other consumer-desirable characteristics were added later (Table 1). However, since the 1930s breeders, including tomato breeders, have centered their efforts on productivity and have basically neglected fruit quality, including traits of interest to consumers (e.g., flavor or nutritious). This can be explained in many ways: one is the fact that it is difficult to breed for complex multigene traits such as flavor; another is our lack of understanding of the molecular genetic basis of fruit quality

(Klee, 2010; Lim et al., 2014). Together with changes in consumer habits, this has led to lower fruit quality and loss of flavor, which indirectly have a negative impact on fruit consumption (Klee, 2010; Orzaez et al., 2010). Hence, scientists and breeders are faced with a real challenge to improve grapes and tomatoes so that they meet the needs both of producers, i.e., productivity, and consumers, i.e., taste and healthiness (Handa et al., 2014). The relevance of this goal lies in the importance of nutrition (i.e., vitamins, antioxidants, and minerals) to remedy physiological disorders and reduce the incidence of human diseases (Klee, 2010). Today, regarding what quality parameters are crucial to improve, yield, and sustainability are the first, because of their role to ensure food security and healthiness. So, we need to maintain the yield per hectare, reducing fertilizers, and pesticides and increasing resilience to biotic and abiotic stresses in a global climate change scenario. The next objective should be increasing nutritional content, especially for crops that will be cultivated in poor areas. Enable crop diversification in poor areas could be a solution. Moreover, depending on the crop, different nutritional contents will be easier to increase. In the case of tomato, carotenoid related compounds are a clear target. For grapes, polyphenols are the main topic of studies. Finally, consumer preferences and taste should be taking into account.

Grape (*Vitis vinifera* L.) and tomato (*Solanum lycopersicum* L.) are the focus of the present review. Both produce fleshy, berry-type fruit, and have undergone important domestication and selection processes that have dramatically reduced their genetic variability. Tomato and grapevine have been selected to satisfy the quality standards required by humans. This has entailed a preference for varieties that were more productive, gave larger fruits or displayed defined organoleptic characteristics. In grapevine, despite the thousands of cultivars available, the market is dominated by a few and these are classified as a function of the final product: table grapes or raisins, or their use in winemaking (This et al., 2006). In tomato, there has also been a progressive/dramatic reduction in variability during the domestication process in the original centers of diversification and, later, when introduced into Europe, and then reintroduced into North America (Blanca et al., 2015). Initially, selection was performed by farmers; later, breeders and researchers became involved. Ultimately, this has led to the development of tomato cultivars yielding fruits of the shape, color, and size of choice. For a long time, tomatoes have been used both as a fresh product and as a processed commodity in soups, juices, sauce, pastes, powders, or concentrates, all of which require different characteristics (Bai and Lindhout, 2007; Bergougnoux, 2014). While grape and tomato share a past history of reduced variability, important differences exist: loss of flavor has more dramatically affected

TABLE 1 | Quality standards according to the different stakeholders in the Agri-Food chain.

Standards	Quality traits
Producer	Resistant against biotic and abiotic stresses. High yield (size...). Easy to harvest and handle. Synchronization of flowering or fruiting time.
Market	Shelf-life. Less prone to handling and shipping damages. Biochemical products (soluble solid concentration for processing tomatoes, resveratrol for grapes).
Consumer	Flavor/succulent/juicy. Crispness/chewiness/oiliness. Appearance/color. Healthy/sustainably produced. Nutritious.
Environmental	Reduction of synthetic fertilizers and pesticides.

tomato, in part, due to more active breeding for productivity than in grapevine. Knowledge of the molecular genetic basis of fruit quality traits and of environmental impact on these traits will facilitate the maintenance of and/or an increase in production while enabling us to improve or change flavor at will.

Despite the biotechnological advances of recent decades, breeding programs often fail when dealing with complex quality traits (Handa et al., 2014). Progress in biotechnology and omics technologies applied to the variability available are likely to help us decode the underlying genetic basis of complex traits. Best alleles could subsequently be transferred into cultivars by crossing, genetic engineering, or NPBT (New Plant Breeding Technologies), to improve the quality of tomato or grape fruit. The present review is based on four fundamental approaches to increase fruit quality: (i) to enhance/maintain germplasm diversity as the source for best alleles; (ii) to understand the biochemical and genetic basis of fruit quality traits using this genomic and phenotypic diversity; (iii) to develop and use tools to dissect fruit quality traits, including improved computational technologies and network analysis; and (iv) to conduct functional studies of cultivar improvement. In conclusion, we will present an up-to-date view of the genetic resources and technologies that can improve fruit quality.

THE CONTRIBUTIONS OF BIOTECHNOLOGICAL TOOLS TO LINK GENOMIC VARIABILITY PRESENT IN *IN-SITU* AND *EX-SITU* GERMPLASM COLLECTIONS WITH THE DERIVED PHENOTYPIC DIVERSITY

Germplasm Diversity

Sources of germplasm, here defined as the collection of genes and their alleles available for plant improvement, include cultivated species and sexually-compatible wild species but could also include sexually-incompatible species harboring genes that can impact on fruit quality and be transferred through genetic engineering. Only a minimal part of the wide variability present in wild germplasm was domesticated and resulted in selective gain of phenotypical or physiological traits of interest for humans. Similarly, the domestication process also resulted in a loss of genes that were left behind in non-selected wild relatives, but were needed to improve crop adaptation to environmental changes. Modern plant breeding programs are based on a process of human selection which differs dramatically from that of natural evolution: selective pressure is no longer defined primarily by a multifactorial changing environment but by narrow human standards that focus on a few traits. Hence, even if the number and nature of genes under selection may vary across the different domesticated species, phenotypic, and genetic diversity are more heavily reduced in “domesticated” germplasm than in their wild relatives. These so-called bottlenecks occurred during domestication and cultivar development, and have recently been confirmed by sequencing (Tang et al., 2010; Abbo et al., 2014; Amini et al., 2014; Andersen et al., 2015). This reduction in genetic variability is particularly evident in

cultivated grapevine, in part, as a consequence of its vegetative propagation (Roby et al., 2014), but it also occurs in tomato. On the whole, as the (agronomical) traits selected by humans differed from those oriented toward optimal adaptation to the natural environment, a clear dichotomy arose between crops and their wild progenitors (Gepts, 2014). This particular genetic bottleneck, known as genetic erosion, could compromise modern cultivars as they may be unable to cope with global warming or newly emerging diseases (Prada, 2009; Chen et al., 2013; Bai et al., 2016). For instance, the wild North American grapevine species *Muscadinia rotundifolia* is known to be resistant to both powdery and downy mildew (Feechan et al., 2013). This resistance was mapped to a single locus that contains a family of seven *TIR-NB-LRR* genes known to be involved in effector-triggered immunity. Therefore, these wild species could constitute a source of resistance-related genes to be introgressed into susceptible cultivars.

In light of the consequences of genetic erosion and the importance of preserving sources of genetic and phenotypic diversity in crops, the scientific community has developed germplasm banks (Prada, 2009). Nowadays, there are more than a thousand seed banks distributed all over the world. Tomato genetic resources in gene banks have been reviewed by (Bai and Lindhout, 2007; Di Matteo et al., 2011) (**Table 2**) and altogether may account for over 20,000 accessions. Grapevine germplasm also exhibits great diversity with up to 10,000 cultivars predicted (Laucou et al., 2011). In this context, many seed centers have been dedicated specifically to grapevine species—especially in countries with a tradition of viticulture (**Table 2**). Furthermore, the Svalbard Global Seed Vault conserves in permafrost the seeds of over four thousand plant species (>774,601 accessions, of which 7,382 correspond to tomato or wild relatives of tomato clade) (www.seedvault.no) (Fowler, 2008; Westengen et al., 2013).

Genetic resources include wild, landraces (heirlooms and old cultivars of local importance), modern cultivars, and synthetic populations, and constitute the ground material for breeders. Populations of wild relatives offer breeders untapped genetic and phenotypic diversity that has evolved over millions of years to adapt to a wide range of environmental niches (Honnay et al., 2012). It is very much in our interest to study this in depth (Khan et al., 2012). Landraces/heirlooms or traditional varieties represent old cultivars that may be of more or less local importance and were developed/selected by traditional farmers over hundreds or a few thousand years to best fit their needs. Landraces (local varieties) generally display greater diversity than modern cultivars as they have been selected to adapt to local, sometimes hostile environments, at a time when agronomic technology (i.e., irrigation, fertilizers, pesticides) was not yet widely available. Cultivar uniformity was not desirable when varieties had to successfully adapt to a range of environmental conditions (Fernie et al., 2006; Cebolla-Cornejo et al., 2013). Modern agronomic practices often result in more homogeneous environmental conditions: tomato cultivation in greenhouses entails controlled watering, facilitating the selection/development of genetically uniform cultivars to enhance yield performance. Hence, landraces constitute a source

TABLE 2 | Main seed bank collections worldwide where tomato and grapevine germplasm can be found.

Name	Plants	Resources	Website	References
The Solanaceae database	Non-tuberous Solanaceae germplasm collection	<i>Ex situ</i> plant collections	http://www.bgard.science.ru.nl/	Bai and Lindhout, 2007
The isogenic tomato 'mutation library'	Solanaceae	About 3,500 tomato monogenic mutants from the genetic background of the inbred variety M82 by treatment with EMS (ethyl methane sulfonate) and fast-neutron mutagenesis	http://zamir.sgn.cornell.edu/mutants/	Menda et al., 2004
French Network of Vine Conservatories	Grapevine (<i>Vitis vinifera</i> L.)	7,000 accessions from 40 countries	http://www1.montpellier.inra.fr/vassal/	French Network of Vine Conservatories
The EuropeanVitisdatabase	Grapevine (<i>Vitis vinifera</i> L.)	27,000 <i>Vitis</i> accessions from 13 european wine-growing countries	http://www.eu-vitis.de/index.php	
FAO/IAEA Mutant Variety Database (MVD)	Wide range of plant mutant including tomato and grapevine		http://mvd.iaea.org/#!Home	FAO/IAEA

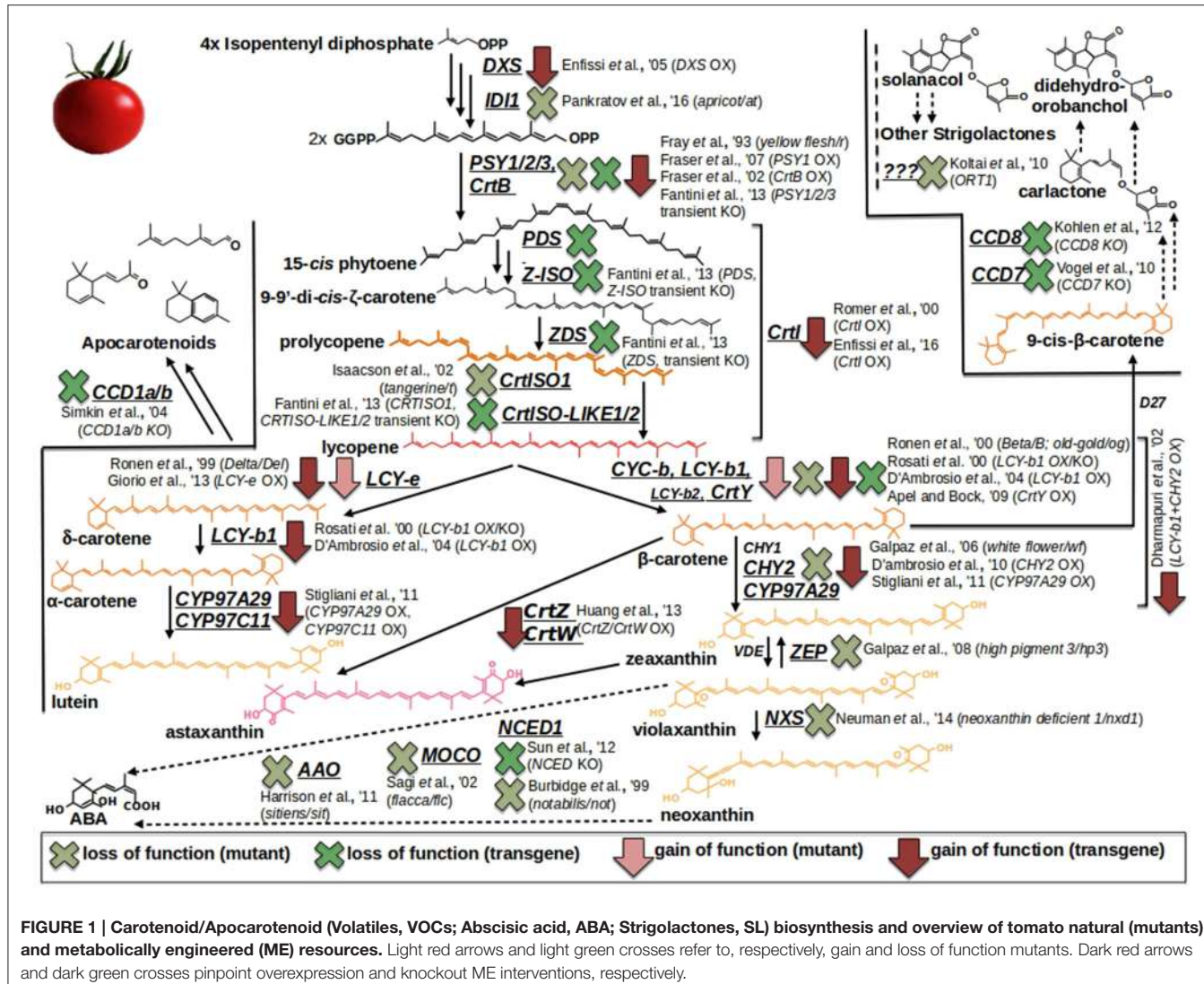
of allelic variants lost to modern breeding (i.e., over the last 80 years) but potentially available for variety improvement (Mazzucato et al., 2008; Prada, 2009; Leida et al., 2015). Because of their greater proximity to modern cultivars than their wild relatives, landrace cultivars with the desired phenotypes hold great potential for cultivar improvement (Zhu et al., 2008; Prada, 2009; Biasi and Brunori, 2015). For example, Corrado et al. (2013), studied variability in a set of 214 tomato accessions which included wild relatives, cultivated landraces, and commercial varieties. They identified a number of loci which were under strong positive selection among landrace and commercial cultivars. Although the diversity present in wild and landrace populations makes them useful for the identification of genotypes carrying genes of agronomic importance, they are of less use when we attempt to accurately dissect the underlying genetic basis. To overcome these difficulties, researchers and breeders have developed a wide range of cross populations such as Recombinant Inbred Lines (RILs), Near Isogenic Lines (NILs) or Introgression Lines (ILs), Double Haploid Lines (DHLs), Induced Mutant Lines (IMLs), TILLING (Targeting Induced Local Lesions in Genomes) Lines (TLs) (Varshney et al., 2014; Henikoff et al., 2004), Multiparent Advanced Generation Intercross (MAGIC, Cavanagh et al., 2008) and Nested Association Mapping (NAM, McMullen et al., 2009; Table 3). In grape, as in other perennial/long generation time and/or self-incompatible species, for which it is difficult or impossible to generate inbred lines, F₁ segregating populations (also termed Cross-Pollinators, CP) have been developed for genetic mapping (Grattapaglia and Sederoff, 1994) and propagated by grafting. Finally, germplasm collection can also be used directly as a mapping population in Genome-Wide Association Studies (GWAS; Rosenberg et al., 2010).

One way to unravel the genetic basis of fruit quality traits is by analyzing spontaneous/natural or induced mutant lines (Di Matteo et al., 2011; Bauchet and Causse, 2012). For tomato, several natural mutants have been identified but these resources are limited in comparison with induced mutant collections (Bauchet and Causse, 2012; and Table 1). The carotenoid

pathway, for example, is one of the best elucidated metabolism in tomato fruit due to the availability of a series of well-characterized mutations (Figure 1). These mutants provide distinct berry color phenotypes: *apricot*, *at*, loss of function in the isopentenyl diphosphate 1 (*ID11*) gene (Pankratov et al., 2016); *yellow flesh*, *r*, knockout of the *phytoene synthase 1* (*PSY1*) gene (Fray and Grierson, 1993); *tangerine*, *t*, loss of function in the carotenoid isomerase 1 (*CrtISO1*) enzymatic activity (Isaacson et al., 2002); *Beta*, *B*, and *Delta*, *Del*, gain of function in the *lycopene β*- and *ε*-cyclase (*CYC-b*; *LCY-e*) genes (Gil et al., 1999; Ronen et al., 2000); *high-pigment 3*, *hp3*, loss of function in the transcript coding for the *zeaxanthin epoxidase* (*ZEP*) (Galpaz et al., 2008); neoxanthin deficient 1, *nxd1*, defected in the neoxanthin synthase (*NXS*) enzymatic activity (Neuman et al., 2014). In this context, the only known exception of a carotenoid structural gene which, if mutated, does not affect the berry color is represented by the *β-carotene hydroxylase 2* (*CHY2*), whose knock out produce the, so called, *white flower* (*wf*) mutant, displaying, respectively, regular and not pigmented fruits and flowers (Galpaz et al., 2006). Additionally, a series of well-known mutants in ABA biosynthesis are also available thanks to the studies carried out by the german scientist Hans Stubbe: *notabilis*, *not*, loss of function in the *9-cis-epoxycarotenoid dioxygenase* (*NCED*) gene (Burbidge et al., 1999); *flacca*, *flc*, knockout of the gene coding for a *molybdenum cofactor* (*MoCo*) (Sagi et al., 2002); *sitiens*, *sit*, deficient in the aldehyde oxidase (*AAO*) enzymatic activity (Harrison et al., 2011). More recently, the first mutant in the strigolactone pathway (*ORT1*) has been identified, although the source of the mutation has not yet been elucidated (Kohlen et al., 2012) (Figure 1). In addition, The *Solanaceae* genome network (SGN) and the Tomato Genetic Resource Center (TGRC) host large collections of tomato genotypes and mutants, which are available to researchers (Di Matteo et al., 2011; Saito et al., 2011; Bauchet and Causse, 2012; Sacco et al., 2013). More recently, a collection of ethyl methanesulfonate (EMS) and γ-ray-derived tomato mutants in the Micro-Tom dwarf background has been generated (Saito et al., 2011; Shikata et al., 2016). To date, it comprises over a thousand genotypes which have been used to

TABLE 3 | Breeding populations developed in tomato and grape.

Name	Definition	Advantages/Disadvantages	Tomato and wine populations publicly available	References
Recombinant inbred lines (RILs)	A Recombinant inbred line is developed by crossing inbred lines followed by repeated selfing up to create an inbred line whose genome is a mosaic of the parental genomes and total or nearly homozygous.	Due to the different events of recombination that happen in parental gametes, two RILs resulting from the same cross present different mosaics of the parental genomes. Hence, RILs populations allow to estimate the recombination rate between two genomic loci, constituting powerful tools for preliminary genetic mapping even for recessive traits. A relatively large number of generations are needed (>8), making difficult to be implemented in species with long generation time.	Several tomato RILs population were hosted by the Tomato Genetics Resource Center (TGRC), whereas grapevine population are quite rare, probably due very long generation time.	Broman, 2005; Carrera et al., 2012; Khan et al., 2012; Viquez-Zamora et al., 2014; Thapa et al., 2015
Near isogenic lines (NILs)/Introgenous Lines (ILs)	NILs are a set of lines that are genetically identical, except for few loci, which result from several backcrosses between a donor line and an acceptor line, selecting at each generation the descendants with the trait of interest.	A population of Introgression Lines (ILs) is made of NILs in which introgression fragments cover the whole genome of the donor line. Introgression effects are evaluated in an elite genetic background, being ideal to introgress wild variability. The breeding scheme requires intensive marker assisted selection.	<i>S. pennelli</i> and <i>S. habrochaites</i> IL collections are available at TGRC. <i>S. pimpinellifolium</i> ILs at CSIC. Barrantes et al., 2014	Eshed and Zamir, 1995; Monforte and Tanksley, 2000;
Multiparent Advanced Generation Intercross (MAGIC)	Recombinant Inbred Lines derived from the intercross of several genotypes (typically 8).	Multiple alleles are tested in a sib population, together with multiple recombinant events, thus providing a very high mapping resolution. The development of this populations is very time consuming, extensive genotyping is also needed and genetic analysis is complex.	Eight-way MAGIC population from four <i>S. lycopersicum</i> and four <i>S. lycopersicum</i> var. <i>cerasiforme</i> cultivars.	Pascual et al., 2015
Cross-Pollinator (CP) or F ₁ segregating population	Population consisted of full sibling plants after crossing two highly heterozygous genotypes.	The generation of this population is fast and inexpensive. Up to four alleles can be segregated. Only one meiosis has been carried out in each chromosome, so the mapping resolution is low.	Picovine × Ugni Blanc, Syrah × Pinot Noir.	Houel et al., 2015; Malacarne et al., 2015
Genome-wide Association studies	Collection of germplasm/cultivars that retain some extent of linkage disequilibrium.	Collections of germplasm are already available. The selection of the proper collection and the analysis is complex.	Major germplasm banks are listed in Table 2 .	Fodor et al., 2014; Ruggieri et al., 2014



create the TOMATOMA database, representing an interesting resource to research scored traits/phenotypes easily. Other EMS tomato mutant collections include the M82 processing tomato collection (<http://zamir.sgn.cornell.edu/mutants/>) and the Red Setter collection (<http://www.agrobios.it/tilling/>). These monogenic mutant populations could be directly screened to identify the genes responsible for a specific function (Menda et al., 2004; Long et al., 2006), or individual mutant lines could be analyzed to confirm the function of a gene previously identified by other means, such as QTL analysis (Goldsborough et al., 1994).

Unlike tomato, collections of grapevine-induced mutants are quite rare (Forte et al., 2015). Consequently, almost all studies in grape aimed at deciphering the molecular basis of traits use natural mutants (This et al., 2006). The FAO/IAEA Mutant Variety Database (MVD) maintains a wide range of plant mutant cultivars including tomato and grapevine. In grape, the counterpart of the conspicuous tomato/carotenoid system is represented by the phenylpropanoid pathway and,

more specifically, by the synthesis of high-value sub-classes of phenylpropanoid compounds (anthocyanins, stilbenes etc.). An overview of grape genes and genetic resources for important phenylpropanoids affecting fruit quality is shown in **Figure 2**. While, contrary to the situation in tomato, it is not possible to clearly define grapevine monogenic mutants, several studies have unraveled the genetic basis of the difference between red and white cultivars, which is mainly due to a group of *MYB* transcription factors (*MYBA1-1/2*, *MYBA2*, *MYB5a/b*), mutated in the latter and, thus, preventing anthocyanin synthesis (Kobayashi et al., 2002; Deluc et al., 2006, 2008; Walker et al., 2007; Rinaldo et al., 2015; **Figure 2**). Similarly, Rinaldo et al. (2015) have reported that the acylated-anthocyanin phenotype is associated to the expression of the *3AT* gene, coding for an *ANTHOCYANIN 3-O-GLUCOSIDE-6''-O-ACYLTRANSFERASE*, which is lacking in white cultivars, as well in some red varieties as Pinot-Noir, that do not accumulate acylated anthocyanins. TILLING was also used to screen the

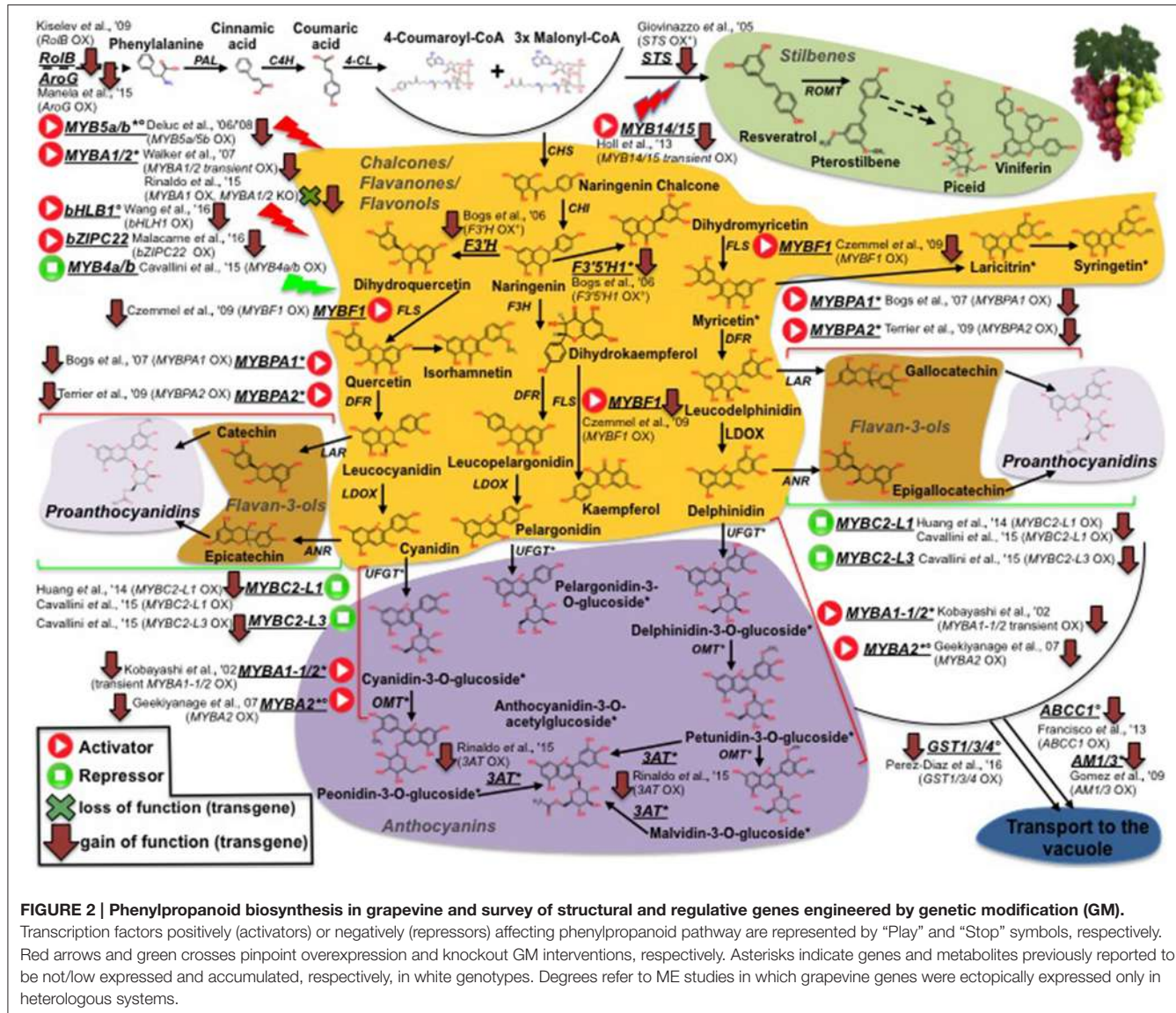


FIGURE 2 | Phenylpropanoid biosynthesis in grapevine and survey of structural and regulative genes engineered by genetic modification (GM).

Transcription factors positively (activators) or negatively (repressors) affecting phenylpropanoid pathway are represented by "Play" and "Stop" symbols, respectively. Red arrows and green crosses pinpoint overexpression and knockout GM interventions, respectively. Asterisks indicate genes and metabolites previously reported to be not/low expressed and accumulated, respectively, in white genotypes. Degrees refer to ME studies in which grapevine genes were ectopically expressed only in heterologous systems.

tomato mutant database (Kurowska et al., 2011) for validation of gene function and as a source/tool for crop improvement (Minoia et al., 2010). Furthermore, it can also be applied to the identification of SNPs in spontaneous mutants (EcotILLING) making it, thus, extremely useful in characterizing the variability present in germplasm banks (Mba, 2013).

Genome and Epigenome Sequencing and Genotyping Methods

Genomic variations can be the result of SNPs, insertions/deletions (Indels), copy number variations (CNV), and presence absence variations (PAV); they are responsible for crop evolution and domestication (Xu and Bai, 2015). Historically, to decipher genomic diversity, two types of molecular markers were developed (reviewed by Yang et al., 2015). The first were generated before the genomic era and were able to identify genetic diversity in a wide range of

genotypes (and different conditions) without the need for DNA or genome sequences. For example, the first markers developed in the 1980s were the restriction fragment length polymorphism (RFLP). Anonymous PCR-based markers such as Random Amplified Polymorphic DNA (RAPD) markers and Amplified fragment length polymorphism (AFLP) were developed later. Single Sequence Repeat (SSR) or microsatellite markers were more popular during the 1990s and the early 2000s, when a large source of reliable medium-throughput markers was generated. However, even with these markers, molecular mapping remained time-consuming, expensive, and yielded relatively low mapping resolution (Xu and Bai, 2015). While several QTLs were identified on large genomic regions, few have been used in breeding programs (Bernardo, 2008).

Three generations of sequencing technologies resulting in three "waves" of genome sequencing facilitated the study of

germplasm diversity and, thus, the production of new markers and high-throughput genotyping technologies that impact on breeding methods (Bolger et al., 2014; Varshney et al., 2014; Xu and Bai, 2015; Yang et al., 2015). In 2007, the genomes of an inbred line (PN40024) derived from Pinot Noir (Jaillon et al., 2007) and a heterozygous genotype nowadays used by winemakers (Velasco et al., 2007), were published by two groups independently. Both studies used whole genome shotgun (WGS) methods and predicted around 30 k protein-coding genes (Jaillon et al., 2007; Velasco et al., 2007) distributed around 38 chromosomes ($n = 19$). On the other side, a high quality, well-annotated reference genome is available for tomato (Sato et al., 2012). From this genome (around 900 Mb divided up to 12 chromosomes), 34,727 protein-coding genes were identified and 30,855 of these were confirmed by RNA sequencing. Moreover, using comparative genomics with grape and *A. thaliana* genomes, this study highlighted that two consecutive genome triplication events might have occurred during its evolution (Sato et al., 2012). The use of NGS methods is not limited to sequencing and *de novo* assembly but, thanks to an increase in high-throughput read lengths, single-base accuracy, reduced costs, and assembling methods, NGS enables whole-genome resequencing to identify genetic variations on a genome-wide basis (Xu and Bai, 2015). A number of resequencing projects have already identified genomic variations by resequencing and identifying a huge number of DNA markers (cited above). Divergence between the wild (*S. pimpinellifolium*) and domesticated tomato genomes was estimated at around 0.6%, representing 5.4 million SNPs, distributed along the chromosomes mostly in the gene-poor regions (Sato et al., 2012). Despite this, more than 12,500 genes carry non-synonymous changes. Another study has revealed that the Micro-Tom genome presents about 1,230,000 SNPs and 190,000 indels, by comparison with the “Heinz 1706” genome (Aoki et al., 2013). Using a high-density polymorphism array (7,720 SNPs, also known as the SolCAP array), Sim et al. (2012) genotyped a collection of 426 tomato accessions, which revealed that over 97% of the markers in the collection were polymorphic. Currently, several hundred resequenced genomes of tomato varieties, *S. lycopersicum* vr cerasiformes, and *S. pimpinellifolium* are available for marker and variability studies at https://solgenomics.net/jbrowse_solgenomics/. They are being used to gain an understanding of genetic base domestication and improvement, and for GWAS (Lin et al., 2014). WGS of induced tomato mutants reveals many DNA markers, such as SNPs (Menda et al., 2004; Saito et al., 2011; Xu and Bai, 2015). In some cases, NGS can be applied to a limited number of sites in the genome and the throughput can be increased using Genotyping By Sequencing (GBS) (Kumar and Khurana, 2014; Xu and Bai, 2015). For example, Víquez-Zamora et al. (2014) used GBS on a RIL population of a cross between *S. lycopersicum* cv. Moneymaker and *S. pimpinellifolium* G1.1554 to develop a linkage map of 715 unique genetic loci from 1,974 SNPs. These results were subsequently used to map QTL responsible for TYLCV (Tomato yellow leaf curl virus) resistance. A similar strategy based on the SolCAP was used by Rambla et al. (2017a) to define a volatile QTL map in an RIL population derived from the

cross between *S. lycopersicum* (Money maker) and the TO-937 accession of *S. pimpinellifolium*.

Recent studies have shown the differential regulation of genes encoding epigenetic regulators as well as local chromatin and DNA methylation changes in response to a variety of abiotic stresses including cold, salinity, drought, osmolality, or mineral nutrition (reviewed by Fortes and Gallusci, 2017). Epigenetics constitutes another process that greatly influences gene expression and, therefore, contributes to genetic plasticity. DNA methylation represents a layer of regulatory complexity beyond that encoded in the basic structure of the plant genome (Harrigan et al., 2007). Using techniques such as bisulfite Sanger sequencing, whole-genome bisulfite sequencing, and chromatin immunoprecipitation sequencing (ChIP-seq), Zhong et al. (2013) have shown that tomato ripening involves specific epigenetic remodeling. They found that binding sites for *RIN*, one of the key ripening transcription factors, were frequently localized in the demethylated regions of the promoters of numerous ripening genes. This binding process occurred in concert with demethylation. The binding of *RIN* to regulate fruit ripening genes is attenuated in the *cnr* ripening mutant. In addition, they found that DNA regions near the 5' ends of genes were hypermethylated in the *cnr* mutant (Zhong et al., 2013). In a more recent study (Liu et al., 2015), a direct relationship between DNA demethylase (*SDML2*) activity and tomato fruit ripening was reported. Briefly, silencing *SDML2* caused ripening inhibition via hypermethylation. Simultaneously, a drastic reduction in the expression of both transcription factors controlling fruit ripening and of down-stream pathways (e.g., carotenoids) occurred. Consequently, crop-improvement strategies should take account of both DNA sequence variation between plant lines and information encoded in the epigenome. In this context, the grape was recently proposed as an essential model for epigenetic and epigenomic studies in agriculturally-important, woody perennials to enable so-called epigenetic breeding (Fortes and Gallusci, 2017). Currently, a Tomato Epigenome database (<http://ted.bti.cornell.edu/epigenome/1196099620>) is available to investigate the presence of DNA methylation phenomena for each tomato gene. Epigenetic mechanisms have also been reported as being involved in defining the levels of Vitamin E accumulation in tomato fruits (Quadrana et al., 2014). Epigenetic marks may participate in the priming mechanisms to better withstand biotic and abiotic stresses, a topic that deserves attention in order to moderate stress susceptibility and increase climate change resilience in grapevine and tomato (reviewed by Fortes and Gallusci, 2017).

Phenomics

While sequencing and genotyping technologies have leaped forward significantly, limited progress in the throughput and price affordability of phenotyping technologies has slowed the identification of genetic-phenotypic associations (Fiorani and Schurr, 2013; Bolger et al., 2014).

Phenotype-based selection came long before DNA discovery and the use of genotyping technologies. However, sequencing and molecular biotechnologies made rapid progress while phenotyping biotechnologies still need to be improved. Indeed,

while the sequence of genomic DNA gives a comprehensive view of genetic capacity, the information it contains is cryptic and does not directly explain the differences between cells and all plant phenotypes (Angel et al., 2012). When it comes to fruit such as tomato or grape, it is the phenotype that is directly linked to our interest. Until now, plant phenotyping mainly focused on a single scale (molecule, cell, organ, plant, field, or canopy) depending on the organ of interest (shoots or roots) and the technology used. However, Rousseau et al. (2015) insist on the importance of multi-scale analysis. Indeed, genome expression can be observed at multiple microscopic and macroscopic levels including proteomics, metabolomics, physiological traits, and others that are visible/invisible to the naked eye. Hence, phenotypic traits provide more direct information about plant production and health than genomic data do. Nevertheless, because few technologies are available, phenotyping methods have traditionally been restricted to macroscopic traits.

Fortunately, the recent improvement in phenotyping methods (reviewed by Fiorani and Schurr, 2013) enable us to broaden the concept of phenotyping and include both molecular mechanisms (proteomic and metabolomic) and all intermediate layers that result in macroscopic physiological and phenological traits (architecture, yield, taste). Progress is mainly related to the development of a wide range of sensors, their automatization and adaptation to both indoor and outdoor conditions. Hence, advances in phenotyping technologies, including cost reductions and time gains, facilitate an increase in throughput phenotyping for multi-level traits under control or field conditions (reviewed by Fiorani and Schurr, 2013; Araus and Cairns, 2014). In fact, the global phenotype can be considered the result of all the measurable traits, influenced in a complex and dynamic manner (time and space) by both genome expression and environmental effects.

Macroscopic shoot phenotyping improvements have mainly been due to the development of new sensors (**Table 4**) (Araus and Cairns, 2014; Fahlgren et al., 2015). For root phenotyping, new technologies were recently established (Wasson et al., 2012; Fiorani and Schurr, 2013; Kuijken et al., 2015) by easily accessing the roots (artificial growth medium and dynamic 2D or 3D imaging), and by indirect methods which phenotype roots in the soil (**Table 5**). For example, using a time-lapse scanning system, Dresbøll et al. (2013) demonstrated that the growth rate of tomato roots decreased under waterlogging. More recently, a series of platforms that integrate morphological parameters and, in some cases, gene expression have been developed. Among these, for example, MorphoGraphX is able to quantify several morphogenetic processes in 4D (Barbier de Reuille et al., 2015). New sensors were also developed to improve post harvested practices such as shelf life (Abano and Buah, 2014). For example, NIR spectroscopy was used to optimize the storage time of apple lots (Giovanelli et al., 2014).

On the other hand, automated facilities have evolved into high-throughput phenotyping platforms providing a powerful tool to fundamental research that can be conducted at growth chamber, greenhouse or field levels. In order to reduce error variance under field conditions, most of the sensors described above could be adapted to allow high-throughput

measures, thus increasing the number of samples under analysis (reviewed by Araus and Cairns, 2014). Ground vehicles equipped with sensors were used in several studies (Andrade-Sanchez et al., 2014), while aerial vehicles with dedicated instruments facilitate rapid plant characterization in many plots, notably for phenotyping canopy traits (Araus and Cairns, 2014; Sankaran et al., 2015). Among them, due to their reduced cost, user-friendly flying control, and high autonomy, polycopters also called Unmanned Aerial Platforms (UAPs) could constitute the future of field phenotyping. The laboratory of plant-microbe interactions (INRA, Toulouse, France) set up a low cost phenotyping platform so called “Heliaphen,” which allows the growth and the high throughput phenotyping of 1,300 plants in outdoor semi-natural conditions (<https://www.youtube.com/watch?v=vZSVgeWuhlw>). The development of plants in high capacity pots (15 L) makes possible the study of crops during their entire life cycle. In this way, the effect of soil heterogeneity is reduced compared to field conditions. The use of a mobile robot, which phenotypes and monitors hydric conditions for each plant, is one of the original aspects of this platform (personal communication from N. Langlade).

In microscopic imaging technologies, improvements in time acquisition, automatization, and user-friendly interface make high-throughput phenotyping possible on a microscopic scale (Sozzani et al., 2014; Rousseau et al., 2015). In a recent study, Legland et al. (2012) coupled microscopic and macroscopic approaches to create a synthetic representation of cell morphology variations at the whole fruit level. The complexity and the high volume of data produced by high-throughput phenotyping platforms require computing power and robust bioinformatic tools (Araus and Cairns, 2014). Furthermore, to date, phenotyping data are still dispersed in different file types, programs, and databases and, therefore, efforts to comply with defined standards, which enable comparison and information exchange between phenotyping experiments and conditions, are needed (Krajewski et al., 2015).

Proteomics

The proteome integrates environmental and genetic information and is, therefore, fundamental. Knowledge of the proteome permits a more direct connection between proteins and the corresponding phenotypes (Boggess et al., 2013). Nowadays, significant improvements have been achieved in this field (reviewed by Angel et al., 2012). For example, coupling liquid chromatography (LC) separations with mass spectrometry (MS)-based technologies that enable the characterization of a protein at the proteome and sub-proteome levels, such as post-translational modifications (PTMs) of proteins like, for instance, lysine succinylation (Jin and Wu, 2016). Hence, many studies have used proteomic analyses to highlight the link between proteomic and phenotypic variations (Tanou et al., 2009; Zhao et al., 2013; Kumar and Khurana, 2014). Several studies of tomato proteome have provided both qualitative and quantitative data (reviewed by Kumar and Khurana, 2014). For example, using shotgun proteomic analysis of fruit tissues, Shah et al. (2012) presented data about the interaction between tomato fruit and *Botrytis cinerea* showing that the proteins produced by the

TABLE 4 | New sensors and their application to plant macroscopic phenotyping.

Sensor technology	Measure	Applications	References
Sensitive cameras in the visible spectral range of the electromagnetic spectrum.	Produce raw data in the RGB or in the HSV (hue, saturation, value) spaces.	Shoot phenology and color.	Fiorani and Schurr, 2013; Araus and Cairns, 2014
Fluorescence cameras.	Analysis of fluorescence parameters.	Photosynthesis status. Identification of biotic and abiotic stresses before visible phenotypes could be detected.	Maxwell and Johnson, 2000; Berger et al., 2004; Bélanger et al., 2008; Chaerle et al., 2009; Fiorani et al., 2012; Fiorani and Schurr, 2013; Araus and Cairns, 2014
Thermal cameras.	Measure the leaf temperature.	Identification of abiotic (Fuentes et al., 2012; Mishra et al., 2012), and biotic (Calderón et al., 2014; Raza et al., 2015) stresses. Evaluation of fruit maturity and bruise (Vadivambal and Jayas, 2011; Ishimwe et al., 2014).	Review by (Fiorani and Schurr, 2013; Meron et al., 2013; Araus and Cairns, 2014; Calderón et al., 2014; Prashar and Jones, 2014)
Imaging spectroscopy.	Scanning specific wavebands of interest through high resolution cameras.	Water status by the analysis of the Near-Infrared (NIR) to the mid-infrared wavebands. Photosynthesis status by the analysis of the peak of green reflectance at 550 nm. Determination of nitrogen content and pigment composition (Fiorani and Schurr, 2013). Estimation of storage time for apple using NIR.	Fiorani and Schurr, 2013; Giovanelli et al., 2014
I-sensor.	Measurement of electrical impedance.	Estimation of cuticle and wax characteristics on vine berries and the link with disease resistance.	Herzog et al., 2015

TABLE 5 | 3D imaging technology for plant phenotyping.

3D sensor	Measures	Application
Stereo camera.	3D imaging.	Biomass and shoot structure.
High resolution volumetric imaging (X-ray tomographs, Magnetic resonance imaging, and positron emission detectors).	3D imaging of physiological status.	Water content, morphometric parameters.
Laser scanning technologies such as Light Detection And Range (LiDAR) (Menzel et al., 2009; Eitel et al., 2011; Hosoi and Omasa, 2012; Araus and Cairns, 2014; Deery et al., 2014; Raza et al., 2015; Rousseau et al., 2015).	Measures the distance between a target and the sensor by analyzing the reflected light of a laser.	Canopy characterization such as phenology, and leaf area index (Llorens et al., 2011; Rinaldi et al., 2013; Sanz et al., 2013; Hosoi et al., 2011).

fungus include those that facilitate the pathogen's penetration and growth on the plant tissue, those that inhibit resistance responses by the plant, and those that enable the pathogen to use the nutrient resources within the plant. On the other hand, the proteins produced by the plant include those that limit pathogenic infection and protect the plant tissue from additional damage.

A similar study by (Parker et al., 2013) analyzed the interaction between tomato and the *Pseudomonas syringae* bacteria through an iTRAQ (isobaric tags for relative and absolute quantification) quantitative proteomic approach. Proteomic data could also be used as biomarkers to facilitate the rapid identification of biotic or abiotic stress before it becomes visible through diagnostic tools (Angel et al., 2012). An interesting, novel approach involves the use of combined genomic-proteomic data to predict DNA-binding proteins (like transcription factors), integrated through computational models which can greatly promote functional

annotation of tomato or other plant genomes (Motion et al., 2015). However, in contrast to the genomic data common to all cells of the same organism, proteomic data could be highly tissue-, cell-, or compartment-specific, making it more difficult to access the overview offered by plant proteome. In this context, another important issue is represented by the characterization of the protein fraction at sub-cellular level, like those specifically synthesized in plastids (Barsan et al., 2012), which can significantly influence a series of physiological processes such as fruit ripening. In another example, the characterization of proteomic changes induced during ripening processes into grape fruit skin provided important information to determine the skin parameters which could impact on wine quality (Deytieux et al., 2007). Furthermore, alterations in sugar and phenylpropanoid metabolism due to thermal stress were revealed by a quantitative proteomic study of Cabernet Sauvignon grape cells (George et al., 2015).

Metabolomics

Metabolomics has played a remarkable role in assessing genotypic and phenotypic diversity in plants, in defining biochemical changes associated with developmental changes during plant growth and, increasingly, in compositional comparisons. Furthermore, metabolic information is often viewed as a more accurate reflection of biological endpoints than transcript or protein analysis (Harrigan et al., 2007). Therefore, metabolomic data may strongly support breeding and selection of novel yield-enhanced and nutritionally improved crops (Harrigan et al., 2007). It also seems that metabolite composition, although genetically based, is heavily influenced by environmental factors, much more, even, than enzyme activity (Biais et al., 2014). Reassuring results have proved that the hereditability of the tomato fruit metabolome, including that part of the metabolome affecting flavor, in terms of mQTL, was relatively high, in both primary metabolites (sugars and acids) (Schauer et al., 2008) and volatiles (Rambla et al., 2016). Obviously, flavor-related traits have attracted much attention. The combination of a taste panel and other omics technologies have facilitated the definition of sugars, organic acids, and volatile compounds underlying flavor and consumer preferences (Mathieu et al., 2009). Furthermore, the robustness of the mQTL and the release of flavor compounds often depend on enzymatic activities that cleave the chemical bond between the flavor compound and a glycosyl moiety. One example is represented by the *non-smoky glycosyltransferase1* (*NSGT1*) gene, that takes part in the phenylpropanoid pathway, which was shown to prevent the “smoky” aroma attribute (Tikunov et al., 2013). Similar glycosylation/glycosidation mechanisms operate in grape varieties that usually accumulate large amounts of volatile precursors as conjugated compounds that are released following tissue maceration (Rambla et al., 2016, 2017b). Using target approaches based on knowledge of metabolic pathways has led to the characterization of several genes involved in the biosynthesis of phenylpropanoids (Tieman et al., 2010; Mageroy et al., 2012), fatty acid-derived volatiles (Speirs et al., 1998; Chen et al., 2004; Matsui et al., 2007; Shen et al., 2014), apocarotenoids (Simkin et al., 2004), esters (Goulet et al., 2015), and other phenylalanine-derived volatile compounds (Tieman et al., 2010), and in the conjugation and/or deconjugation and emission of volatiles (Tikunov et al., 2013). Moreover, Schauer et al. (2005) performed one of the first GC-MS-based surveys of the relative metabolic levels of leaves and fruits of *S. lycopersicum* and five sexually-compatible wild tomato species (*S. pimpinellifolium*, *S. neorickii*, *S. chmielewskii*, *S. habrochaites*, and *S. pennelli*). Interestingly, several biochemical markers associated with the desired traits (stress resilience, nutritional quality) were identified in the wild species. A series of robust LC-MS-based protocols for tomato metabolome have been developed at WUR (De Vos et al., 2007) and KAZUSA (Iijima et al., 2008), and exploited in several studies of fruit development and physiology (Yin et al., 2010; Mounet et al., 2012), and stress response (Etalo et al., 2013; Lucatti et al., 2013). In a recent study (D'Esposito et al., 2017), genotype × environment interaction, particularly related to sensorial attributes, was investigated in three tomato varieties using a combination of genomic, transcriptomic and

metabolomic technologies. The varieties in question included the “cosmopolitan” Heinz 1706—which showed high resilience in the different environments tested—and two Italian Protected Designation of Origin (DOP) ecotypes—San Marzano and Vesuviano—which displayed high plasticity to environmental variations.

In grape, studies focusing on ripening and using complementary platforms such as NMR and GC-MS to identify metabolic markers of pre-ripening and ripening stages, are available (Forte et al., 2011; Agudelo-Romero et al., 2013). Using an integrated transcriptomic/metabolomic approach, Agudelo-Romero et al. (2013) provided hints about how the development of a grape cultivar-specific aroma is controlled at transcriptional level. In the same context, the distinctive processes regulating the accumulation of polyphenols in berry skins of Cabernet Sauvignon and Shiraz cultivars were investigated at gene expression and metabolite levels (Degu et al., 2014).

One important phenological aspect, the terroir (i.e., the complex of all environmental factors responsible for the qualities of a grapevine cultivar grown in a specific habitat), was studied for the Corvina variety using volatile/non-volatile metabolomics, and transcriptomics. On the whole, a strong terroir-specific effect was revealed in clones grown in different vineyards—an effect that persists over several vintages (Anesi et al., 2015). The primary aromatic profile of a wine is mainly due to the genotype × environment-derived relationship between volatile metabolites and their precursors. Volatiles have been extensively studied in grape (reviewed in: González-Barreiro et al., 2015), whereas volatile precursors have scarcely been investigated (Martin et al., 2012). Recently, Rambla et al. (2016) performed an in-depth analysis of volatile and precursor metabolites in white (Airén) and red (Tempranillo) grape variety berries at different developmental stages. The use of a series of bioinformatic approaches—such as correlation networks—proved the existence of complex metabolite-metabolite patterns that were more complex in Airén, as would be expected given the enriched aroma bouquet typical of white varieties. Metabolomics has contributed much to our increased understanding of the molecular basis of biotic stress resistance. A series of metabolites, including quercetin-3-O-glucoside and a *trans*-feruloyl derivative, have been shown to underlie cultivar resistance to downy mildew infection (Kashif et al., 2009). More recently, Agudelo-Romero et al. (2015) concluded that berries infected with *B. cinerea*, reprogram carbohydrate and lipid metabolisms toward increased synthesis of secondary metabolites like *trans*-resveratrol and gallic acid, which are involved in plant defense.

Furthermore, metabolomic approaches have been used to assess the impact on the metabolome and fruit quality traits of mutations or genetically engineered approaches in structural/regulatory genes. Of special significance are the metabolic boost identified in tomato fruit by the light-hyperresponsive *high-pigment* (*hp*) gene (Bino et al., 2005). The authors concluded that fruits from *hp* plants overproduced many metabolites with antioxidant or photoprotective activities. A number of additional tomato fruit color mutants that affect the metabolite profile have been identified (list available at

<http://kdcomm.net/~tomato/Tomato/color.html>). However, not all of these them resulted in the accumulation of quality molecules (with positive health or organoleptic effects) in the fruit. Among these mutants are the *B* (*Beta*) and *B^c/B^g* mutants, yielding high amounts in β-carotene and lycopene, respectively, due to a gain or loss of function in chromoplast-specific lycopene β-cyclase (*Cyc-B*) activity (Ronen et al., 2000, and **Figure 1**). Similarly, the *Abg* (*Aubergine*), *Aft* (*Anthocyanin fruit*) and *Atv* (*Atrovioletaceum*) loci result in anthocyanin-accumulating fruits (Mes et al., 2008; Schreiber et al., 2012), phenotypes associated with a perturbation in the expression of the transcription factors controlling anthocyanin synthesis, such as *ANTHOCYANIN 1* (*ANT1*) and *ANTHOCYANIN 2* (*AN2*). In contrast to classical mutants, metabolic engineering overcomes a number of classic breeding constraints, including a limited gene-pool, time consuming processes, etc. Against this broader scenario, tomato fruits have been engineered to accumulate large amounts of many high-value nutrients (in an approach known as metabolic engineering, ME): vitamins such as folate (Díaz de la Garza et al., 2007) and ascorbate (Nunes-Nesi et al., 2005); secondary metabolites such as carotenoids, for which tomato represents a model system. An overview of ME studies of carotenoids in tomato is shown in **Figure 1**: so far, transgenic fruits enriched in lycopene [(Fraser et al., 2002, 2007); (ectopic expression of the bacterial (*CrtB*) or the tomato (*PSY1*) *phytoene synthase* genes); (Rosati et al., 2000) (down-regulation by antisense technology, of the *lycopene-b-cyclase 1* (*LCY-b1*) gene)], β-carotene [(Apel and Bock, 2009); transplastomic expression of the bacterial lycopene-β-cyclase (*CrtY*) activity]; (D'Ambrosio et al., 2004, 2011) (stable transgenics for the tomato *LCY-b1* gene); (Römer et al., 2000) [ectopic expression of the bacterial *carotenoid isomerase* (*CrtI*)]; (Rosati et al., 2000) (stable transformants expressing the arabidopsis *LCY-b1* gene), lutein (Giorio et al., 2013; over-expression of the endogenous lycopene ε-cyclase (*LCY-ε*-) activity)], and β-xanthophylls [Dharmapuri et al., 2002; simultaneous expression of the arabidopsis *LCY-b1* and of a pepper β-carotene hydroxylase 1 (*CHY1*)]; (D'Ambrosio et al., 2011) [overexpression of the tomato β-carotene hydroxylase 2 (*CHY2*)] have been achieved. Furthermore, ME tomatoes accumulating high-value ketocarotenoids (e.g., astaxanthin) have been obtained by the simultaneous expression of the β-carotene hydroxylase (*CrtZ*) from *Haematococcus pluvialis* and the algal β-carotene ketolase (*CrtW*) from *Chlamydomonas reinhardtii* (Huang et al., 2013) (**Figure 1**). In some cases, it is not possible to achieve stable silenced transgenic plants for a specific activity, likely due to the occurrence of a lethal phenotype in the transformant cells; in this context, an useful alternative is represented by virus induced gene silencing (VIGS), which allows to study a specific enzymatic step by transient transformation assays. In tomato fruits, this tool has been exploited to investigate the functions of all the genes involved in lycopene biosynthesis (*PSY1, 2, 3*; phytoene desaturase, *PDS*; 15-cis-ζ-carotene isomerase, *Z-ISO*; ζ-carotene desaturase, *ZDS*; carotenoid isomerase 1, like-1, like-2, *CrtISO1*, *CrtISO-LIKE1*, *CrtISO-LIKE2*), and the presence of three functional units, comprising *PSY1*, *PDS/ZISO*, and *ZDS/CrtISO* has been found (Fantini et al., 2013). ME has also been used to elucidate

enzymatic activities taking place in carotenoid catabolism: with this purpose, apocarotenoid emission has been strongly reduced by the down-regulation, via RNAi technology, of the *carotenoid cleavage dioxygenase 1b* (*CCD1b*) gene (Simkin et al., 2004). Similarly, ABA biosynthesis has been investigated by through the production of RNAi plants for the *9-cis-epoxycarotenoid dioxygenase* (*NCED1*) gene (Sun et al., 2012); and two CCD (*CCD7* and *CCD8*) transcripts, involved in strigolactone pathway, have been characterized by tomato stable transformants, in which the two enzymatic functions had been knocked out (Vogel et al., 2010; Kohlen et al., 2012). Engineering tomatoes for high flavonoids in the fruit is a biotechnology goal as these types of healthy metabolites are deficient in the fruit. To this end, successful efforts for flavonoid increase (Schijlen et al., 2006) and *de novo* anthocyanin accumulation (Zhang et al., 2013) have been reported; in a recent study, Zhang et al. (2015) used the *AtMYB12* transcription factor to engineer high levels of novel phenylpropanoids in tomato. This up-regulation of specific branches of phenylpropanoid metabolism was disclosed by a combination of RNA sequencing and LC-MS analyses. Phenylpropanoids have also been the target molecules of the few ME attempts reported in grape (illustrated in **Figure 2**): interestingly, while only limited studies have modified the expression of structural genes, most efforts have focused on the identification of biosynthetic transcriptional regulators. Within the formers, *flavonoid 3'-hydroxylase* (*F3'H*) and *flavonoid 3',5'-hydroxylase* (*F3'5'H*), key genes for flavonoid hydroxylation (and, thus, for their stability, color and antioxidant capacity) have been cloned in red grapevine, cv Shiraz, and their functionality has been proved by ectopic expression in *Petunia hybrida* (Bogs et al., 2006); in another study, Giovinazzo et al. (2005) have achieved stilbene accumulation in tomato fruits by expressing a grape *stilbene synthase* (*STS*). In the latter, a vast range of MYB transcription factors acting as activators or repressors of the pathway have been described: interestingly, some of them have been found to perturb the whole biosynthesis [positively: *MYBA1-1/2*, *MYBA2*, *MYB5a/b* (Kobayashi et al., 2002; Deluc et al., 2006, 2008; Walker et al., 2007; Rinaldo et al., 2015); negatively: *MYB4a/b* (Cavallini et al., 2015)], while another group looks to affect distinct phenylpropanoid subclasses [*MYB14/15*, directly activating *STS* genes (*STSs*)] (Höll et al., 2013); *MYBF1*, positively regulating *flavanol synthase* (*FLS*) expression (Czembel et al., 2009); *MYBPA1/2* and *MYBC2-L1/3*, respectively boosting or repressing flavan-3-ols/proanthocyanidin synthesis (Bogs et al., 2007; Cavallini et al., 2015; **Figure 2**). Besides MYBs, additional transcription factors affecting phenylpropanoid metabolite pool have been isolated and characterized in grape: Wang et al. (2016), for instance, have identified a *VvbHLH1* factor, whose ectopic expression in Arabidopsis resulted in increased flavonoid content, although this factor looks to be also associated to ABA-related processes, like drought and salt stresses; similarly, Malacarne et al. (2016) have recently described a new bZIP factor, named *VvbZIPC22*, whose ectopic expression in tobacco has proved its role in triggering flavonoid synthesis and accumulation (**Figure 2**). Once synthesized, flavonoids and anthocyanins are rapidly transported to the vacuole: basically, three mechanisms including

vesicle trafficking, membrane transporters and glutathione S-transferase (GST)-mediated transport have been described. In grape, in particular, two kinds of anthocyanin active transporters, and localized to the tonoplast, have been discovered: two belonging to the Multidrug And Toxic Extrusion (MATE) family and called *anthoMATE1-3* (*AM1* and *AM3*), which can bind acylated anthocyanins and translocate them to the vacuole in the presence of MgATP (Gomez et al., 2009); and an ABC-type transporter, *ABCC1*, shown to perform the transport of glucosylated anthocyanidins (Francisco et al., 2013). More recently, three GSTs (*VviGST1*, *VviGST3*, *VviGST4*) have been tested for their ability to bind glutathione and monomers of different phenylpropanoids (anthocyanin, PAs, and flavonols): interestingly, all the three genes displayed the binding activity, although with distinct specificity according the phenylpropanoid class (Pérez-Díaz et al., 2016).

HOW KNOWLEDGE OF THE GENETIC BASIS OF THE OBSERVED VARIABILITY COULD CONTRIBUTE TO IMPROVE FRUIT QUALITY

Over the last 25 years, a number of papers have started to dissect the genetic basis of fruit quality traits by means of QTL analysis (Duchêne et al., 2012; Klee and Tieman, 2013). In tomato, fruit morphology, yield, fruit color, and soluble solid concentration were the major focus of attention during the early QTL mapping years but recently, more complex traits such as primary metabolites, nutritional, antioxidant, and volatile compounds have received more attention (reviewed by Grandillo et al., 2013; see **Table 6**). The translation of those early studies into gene discovery and/or application to breeding programs remains slow. This low impact can be explained in several ways, including the limited accuracy of QTL mapping experiments due to the lack of sufficient markers; the accuracy of phenotypic evaluations; or the limitations or poor suitability of mapping population designs (Collard et al., 2005), among others.

In spite of these shortcomings, genes involved in tomato fruit morphology and sugar content QTLs have been isolated (Fridman et al., 2000; Monforte et al., 2014). Recent advances in sequencing, genotyping, and phenotyping technologies, combined with the development of a wide range of plant germplasm collections and populations, facilitate more accurate QTL detection (Chen et al., 2015; Li and Sillanpää, 2015). Today, these technologies permit the fine mapping of QTLs and candidate genes for a wide range of complex traits such as seed characteristics (Doligez et al., 2013), developmental stages (Duchêne et al., 2012), or tolerance to root chilling (Arms et al., 2015). In this last study, Arms et al. (2015) took advantage of a sub-NILs population in order to identify and functionally test candidate genes. Recently, Houel et al. (2015) worked on QTLs related to leaf area and berry quality using high-throughput genotyping technology from the Illumina® 18 K SNP chip and a mapping population of 129 microvines derived from Picovine × Ugni Blanc flb. The compact size, early flowering, and continuous production of reproductive organs make the Microvine or Dwarf

and Rapid Cycling and Flowering (DRCF) mutant a valuable tool for QTL mapping (Houel et al., 2015). Combined with the 6,000 SNP markers given by the 18 K SNP chip, this microvine population has facilitated the identification of 10 QTLs of the 43 traits analyzed simultaneously (Houel et al., 2015). In tomato, the development of the Illumina® 8 K SNP chip (Sim et al., 2012) gave the research community access to affordable high-throughput genotyping. The combination of bulk segregant analysis with whole genome sequencing (i.e., QTL-seq) is another approach that has proved a cost-effective method of identifying QTLs involved in tomato fruit morphology (Illa-Berenguer et al., 2015).

Hence, several studies insist on the importance of the populations used to permit QTL fine mapping (Nicolas et al., 2016). Indeed, the choice of an appropriate genotype panel from the vast germplasm available is particularly relevant for QTL identification either in the case of using a segregating mapping population (**Table 2**) or in GWASenome Wide Association Studies (GWAS). Take, for example, one of the biggest collection of grapevine cultivars: that of the Institut National de la Recherche Agronomique (France). The 2,486 unique grapevine cultivars in this collection can be used to identify new QTLs (Nicolas et al., 2016). From this huge population, Nicolas et al. (2016) designed a diversity core panel of 247 grapevine cultivars with limited relatedness to use in identifying new QTLs with the GWAS approach as it captures most of the genetic and phenotypic diversity present in the original collection. Even though GWAS is a very promising strategy, the development of bi-/multi-parent populations is still highly relevant (Pascual et al., 2016) when comparing QTL detection in tomato RIL, MAGIC populations and GWAS, to find significant differences between the populations. RILs and MAGICs are especially powerful tools for rare allele mappings, whereas GWAS provides a more general view of common variants. An integration of different populations and mega QTL analysis (Monforte et al., 2014), would help detect an increasing number of small effect loci. High-throughput genotyping methods also help speed up the construction of time-consuming populations as IL collections (Barrantes et al., 2014). We would encourage the development of a larger number of these populations (especially ILs and MAGICs/NAMs) in the near future, to allow easy access to a wide range of germplasm resources.

One critical issue following QTL identification is to determine the stability and robustness of their genetic basis in different backgrounds and environments. Several studies have addressed the stability of QTLs over time and generation, as well as across environments (Monforte et al., 2001; Gur and Zamir, 2004; Chaïb et al., 2006; Doligez et al., 2013; Arms et al., 2015; Houel et al., 2015). These authors have shown that selecting stable QTLs to introgress into agronomic cultivars is feasible, a finding that must especially be taken into account considering issues relating to global warming. Introgression lines have been proved to be a highly suitable population design to address these questions (Monforte et al., 2001; Gur and Zamir, 2004).

Quantitative trait loci maps have been published for most descriptors of tomato fruit quality (color, texture, flavor) and also for specific metabolites associated with these quality descriptors.

TABLE 6 | QTL analysis in tomato and grape.

Species	QTL or Candidate Genes (CG)	Characters	References
Tomato	QTL and CG	Tolerance to chilling	Oyanedel et al., 2001; Elizondo and Oyanedel, 2011; Arms et al., 2015
Tomato	QTL	Shot turgor maintenance	Truco et al., 2000
Tomato	QTL	Flavor and gustative quality of berries	Saliba-Colombani et al., 2001; Causse et al., 2004; Schauer et al., 2006; Tieman et al., 2006; Mathieu et al., 2009; Zanor et al., 2009; Zhang et al., 2015; Calafiore et al., 2016
Tomato	QTL	Flowering characteristics	Tanksley et al., 1996; Doganlar et al., 2002; Jiménez-Gómez et al., 2007; Nakano et al., 2016
Tomato	QTL	Fruit Morphology, color, soluble solid concentration, yield	Eshed and Zamir, 1995; Fulton et al., 1997; Bernacchi et al., 1998; Saliba-Colombani et al., 2001; Monforte et al., 2001; Van der Knaap et al., 2002; Gur and Zamir, 2004; Huang and van der Knaap, 2011
Tomato	QTL	Carotene/nutritional/vitamins	Saliba-Colombani et al., 2001; Liu et al., 2003; Rousseaux et al., 2005; Schauer et al., 2006; Capel et al., 2015
Grape	QTL	Disease resistance	Fischer et al., 2004; Marguerit et al., 2009; Riaz et al., 2006, 2011
Grape	CG	Disease resistance	Barker et al., 2005; Coleman et al., 2009; Barba et al., 2014; Feechan et al., 2013
Grape	QTL	Pest resistance	Doucet et al., 2004; Fischer et al., 2004; Zyprian et al., 2016; Krivanek et al., 2006; Xu et al., 2008
Grape	QTL		

For these tomato fruit volatiles, QTLs have been identified in experimental populations obtained from crosses between tomato cultivars and different germplasm sources used as donor parents—e.g., cherry tomato (Saliba-Colombani et al., 2001; Zanor et al., 2009) or the distantly related, green-fruited, wild tomato species *Solanum pennellii* (Tadmor et al., 2002; Tieman et al., 2006) and *Solanum habrochaites* (Mathieu et al., 2009). In some cases, QTL validity (Zanor et al., 2009; Rambla et al., 2016, 2017a) has been confirmed in other populations which are, therefore, useful for breeding. Genomics has been successfully used in a limited number of cases to narrow down the regions of several hundreds of genes to a plausible candidate gene, as in the aforementioned case of the “smoky” aroma (Tikunov et al., 2013), and the gene for Brix (Zanor et al., 2009). In most cases, however, the gene underlying the QLT has yet to be identified.

NEW PLANT BREEDING TECHNIQUES (NPBT) FOR FRUIT QUALITY STUDIES

Over the past 10 years, the introduction of so-called, new plant breeding techniques (NPBT) has constituted a breakthrough in the field of crop improvement. A number of technologies have been developed to produce new plants with desired traits, in which the main bottlenecks to standard genetic modification (i.e., the presence of foreign DNA in the modified food plant) are no longer an issue. In this context, several different strategies, based on the exploitation of chimeric nucleases have been applied. Overall, they rely on a system composed of sequence-specific DNA-binding domains coupled to a non-specific DNA cleavage module (reviewed in: Gaj, 2014; Sprink et al., 2015; Schaart et al., 2016) that expedite efficient genomic modifications through the introduction of sequenced specific/targeted DNA double-strand breaks (DSBs), which boost all the DNA repair components, like error-prone non-homologous end joining (NHEJ), and homology-directed repair (HDR). To date, the most widely utilized NPBTs are:

zinc finger nucleases, ZFNs; transcription activator-like effector nucleases, TALENs; and Clustered Regulatory Interspaced Short Palindromic Repeats (CRISPR)/CRISPR-associated (Cas) system, CRISPR/Cas. Each strategy has its own advantages and disadvantages, as illustrated in Table 7. To date, no TALEN and ZNF studies of grape are available, whereas two proof-of-concept trials have been described in tomato: Lor et al. (2014) knocked out the *PROCERA (PRO)* gene involved in the negative regulation of gibberellin signaling; in contrast, Hilioti et al. (2016) have shown the effectiveness of the ZFN approach by targeting the expression of the *LEAFY-COTYLEDON1-LIKE4 (LIL4)* transcription factor, coding for the β subunit of nuclear factor Y and severely affecting plant development.

Currently, the most promising NPBT is based on the exploitation of the CRISPR/Cas9 system. Involved in the immune response processes of the prokaryotes (Barrangou et al., 2007), CRISPRs have been identified in 90% of sequenced archaea (Grissa et al., 2007). A simplified CRISPR system, relying on a single protein (Cas9), has been shown capable of modulating expression of specific one-by-one targets in human cells, insects and plants (Shalem et al., 2014; Konermann et al., 2015). More recently, a powerful tool for multi-modular expression of several plant genes in a single construct (with so-called “Goldenbraid” technology; Sarrion-Perdigones et al., 2011, 2013) has been adapted to CRISPR/Cas9 technology to build constructs able to modify the expression of a series of targets of interest (Vazquez-Vilar et al., 2016). Examples of efficient modifications of specific target genes have been reported both for tomato and grape: by using the CRISPR/Cas9 system. In fact, the *ripening inhibitor (RIN)* gene, encoding a MADS-box transcription factor regulating ethylene synthesis and, thus, fruit ripening, has been successfully mutagenized (Ito et al., 2015); simultaneously, the efficient knockout of the *Lidonate dehydrogenase* gene (*IdnDH*), involved in the tartaric acid pathway, has been achieved in both grape cell suspension and plants (Ren et al., 2016). Additionally, still in grape, a

TABLE 7 | Overview of the three main strategies for plant gene editing: ZFN, TALEN, and CRISPR/Cas9.

Technology	Acronym	Type	System components	Mechanism of action	Sensitivity to methylation	Off-target effects	Design difficulty	Scaling up for library production	Studies in tomato and grape
Zinc finger nuclease	ZFN	Protein-DNA	Zinc finger DNA binding domain fused with an endonuclease (usually FokI); specific recognition of 3 bp sequences	A DNA-cutting/DNA-grabbing-based system, able to recognize target genes	Yes	High	Difficult	No (custom protein selection for each gene)	Hilliot et al., 2016
Transcription activator-like effector nuclease	TALEN	Protein-DNA	Endonuclease (usually FokI) catalytic domain fused to Xanthomonas spp. DNA binding domain of transcription activator-like effectors. Composed by 33–35 amino acid (aa) multiple repeats containing a repeat variable diresidue (RDV; usually, the aa 12 and 13)	Same as ZFN	Yes	Low	Medium	Possible but complicate	Lor et al., 2014
Clustered regularly-interspaced short palindromic repeat/CRISPR-associated	CRISPR/Cas9	RNA-DNA	20 nt crRNA fused to tracrRNA and Cas9 endonuclease	A DNA-cutting protein associated to a guided RNA which can specifically recognize target genes	No	Low	Easy	Easy (generation of 20 nt adapter/s for each gene)	Brooks et al., 2014; Ron et al., 2014; Černík et al., 2015; de Toledo Thomazella et al., 2016; Jacobs and Martin, 2016; Ito et al., 2015; Klap et al., 2016; Pan et al., 2016; Xu et al., 2016; Ren et al., 2016; Wang et al., 2016

Technical characteristics and a survey of all the studies described, to date, in tomato and grape are also provided.

computational survey of all the CRISPR/Cas9 sites available in the genome has been performed. This has revealed the presence of 35,767,960 potential CRISPR/Cas9 target sites, distributed across all chromosomes with a preferential localization at the coding region level (Wang et al., 2016). A Grape-CRISPR website of all possible protospacers and target sites has been created and made available to the public (<http://biodb.sdau.edu.cn/gc/index.html>).

New plant breeding techniques have already proved successful in the potential improvement of apple and citrus fruit quality (Jia and Nian, 2014; Nishitani et al., 2016), although the feasibility of the technology has been exploited as proof-of-concept by the knockout of the *PDS* gene, acting on carotenoid biosynthesis at vegetative and reproductive levels. In contrast, to date, only two advanced studies in tomato have been described: precise targeting of the *pectate lyase* (*PL*) gene, which resulted in delayed fruit softening without perturbing other ripening-related parameters (Uluisik et al., 2016); and editing the *SIAGAMOUS-LIKE6* (*SIAGL6*), a MADS-box transcription factor which provides tolerance to heat stress conditions and results in parthenocarpic fruits (Klap et al., 2016).

Taking into consideration the potential of these technologies, a more precise metabolic refinery is expected to come by selecting specific targets for nutritional and anti-nutritional molecules. This would imply the loss (knock out) and/or gain of function (activation) of selected enzymatic activities, respectively. Overall, these technologies potentially represent a powerful, innovative opportunity to introduce fine modifications in specific target genes. However, although the effect of knocking out genes has already proved successful, more work is needed for other kinds of gene remodeling (e.g., activation, production of allelic variants, etc.). To this end, significant contributions are likely to be provided by combining the CRISPR systems with additional enzymatic activities acting on DNA, such as recombinases, transposases, and DNA histone methyltransferases/acetyltransferases. These additional editing capabilities could potentially enable a vaster array of gene changes that, in the case of the fruit quality trait, may lead to a revolution in efficiency and respond better to consumer interests.

CONCLUSION AND PERSPECTIVES

Three elements required to identify the genetic basis responsible for suitable phenotypes, and to use them to improve fruit quality produced in fields, have experienced huge technological progresses in the recent years. The first one is the constitution of germplasm banks in order to conserve the existing genetic diversity, including both natural and artificially-induced variability. The second one is the ability to identify suitable phenotypes, notably innovations from wild genotypes, and to decipher their genetic basis. Finally, the third element is represented by the capacity to introduce the genetic elements into agronomic germplasm, remarkably through NPBT or selection assisted by markers. Altogether, the important advances in plant biotechnologies described in this review could last for long time, further facilitating plant breeding.

Indeed, biotechnologies are often praised for assuring food security to a growing Human population, through their impact on crop yield, and *de facto*, hunger has diminished drastically. Nevertheless, malnutrition still remains a global health problem, which also concerns developed countries (e.g., obesity) (FAO, 2015 hunger report; Steiber et al., 2004), suggesting that access to balanced and quality food is a combination of multiple factors besides agronomic yield as food allocation, waste and nutritional quality (Foley et al., 2011; Tilman and Clark, 2015). Hence, the responsibility of plant scientist is to develop solution in order to try to solve the society concerns. This could be achieved by a wide range of biotechnologies, dedicated to setting up the best suited genotypes, and producing knowledge that enables the optimization of agronomic practices (Chappell and LaValle, 2011; Amini et al., 2014).

However, in the context of recent societal mistrust about biotechnologies, sustainability of fruit production is becoming a quality trait more and more demanded by consumers, and awareness by research institutes. If one wants biotechnologies to be synonym of sustainability, improving yields and fruit quality in a long run on diverse field conditions, the notion of cost-benefits should be weighted ensuring that (i) Human and environmental health are not threatened, (ii) scientist and farmer self-reliance is not jeopardized by monopolies hold by international conglomerates including seed, chemical, and processing companies (Francis et al., 2003; Altieri and Nicholls, 2005; Chappell and LaValle, 2011; Guillemaud et al., 2016), and (iii) biotechnologies bring real benefits compared to existing processes (Temple et al., 2011; Abbo et al., 2014; Amini et al., 2014; Andersen et al., 2015; Reganold and Wachter, 2016). This debate around biotechnology use is well-illustrated by the debate around GMOs whose use could be more problematic than genetic manipulation itself (Altieri and Rosset, 1999; Chappell and LaValle, 2011; Amini et al., 2014; Guillemaud et al., 2016).

Therein, biotechnologies have their place within agroecology which bases the design of agricultural systems on the valorization of ecosystemic services to set up agri-food system economically viable, socially fair, and sustainable for the environment (Francis et al., 2003; Altieri and Nicholls, 2005; Wezel et al., 2009, 2014; García et al., 2013; Kershen, 2013). In this frame, evaluation of of biotechnologies relevance taking into account their global impact on all components of our societies, could be considered as a sustainable way to integrate biotechnologies to agriculture.

AUTHOR CONTRIBUTIONS

QG, AF, and AG designed the perspective and all the authors wrote the manuscript.

FUNDING

AF was provided by the Portuguese Foundation for Science and Technology (SFRH/BPD/100928/2014, FCT

Investigator IF/00169/2015, PEst-OE/BIA/UI4046/2014), and to AG by the EC H2020 program (TRADITOM project 634561). QG benefited of the support of the Sunrise project ANR-11-BTBR-0005 funded by the ANR.

REFERENCES

- Abano, E. E., and Buah, J. N. (2014). Biotechnological approaches to improve nutritional quality and shelf life of fruits and vegetables. *Int. J. Eng. Technol.* 4.
- Abbo, S., Pinhasi van-Oss, R., Gopher, A., Saranga, Y., Ofner, I., and Peleg, Z. (2014). Plant domestication versus crop evolution: a conceptual framework for cereals and grain legumes. *Trends Plant Sci.* 19, 351–360. doi: 10.1016/j.tplants.2013.12.002
- Agudelo-Romero, P., Erban, A., Rego, C., Carbonell-Bejerano, P., Nascimento, T., Sousa, L., et al. (2015). Transcriptome and metabolome reprogramming in *Vitis vinifera* cv. Trincadeira berries upon infection with *Botrytis cinerea*. *J. Exp. Bot.* 66, 1769–1785. doi: 10.1093/jxb/eru517
- Agudelo-Romero, P., Erban, A., Sousa, L., Pais, M. S., Kopka, J., and Fortes, A. M. (2013). Search for transcriptional and metabolic markers of grape pre-ripening and ripening and insights into specific aroma development in three portuguese cultivars. *PLoS ONE* 8:e60422. doi: 10.1371/journal.pone.0060422
- Altieri, M. A., and Nicholls, C. I. (2005). *Agroecology and the Search for Truly Sustainable Agriculture*. United Nations Environmental Programme, Environmental Training Network for Latin America and the Caribbean.
- Altieri, M. A., and Rosset, P. (1999). Ten reasons why biotechnology will not ensure food security, protect the environment and reduce poverty in the developing world. *AgBioForum* 2, 155–162.
- Amini, S., Sharaf, S., Komeili, H. R., and Tabaei, N. A. (2014). Effect of biotechnology on biodiversity. *Int. J. Farm. Allied Sci.* 3, 910–915.
- Andersen, M. M., Landes, X., Xiang, W., Anyshchenko, A., Falhof, J., Østerberg, J. T., et al. (2015). Feasibility of new breeding techniques for organic farming. *Trends Plant Sci.* 20, 426–434. doi: 10.1016/j.tplants.2015.04.011
- Andrade-Sánchez, P., Gore, M. A., Heun, J. T., Thorp, K. R., Carmo-Silva, A. E., French, A., et al. (2014). Development and evaluation of a field-based, high-throughput phenotyping platform. *Funct. Plant Biol.* 41, 68–79. doi: 10.1071/FP13126
- Anesi, A., Stocchero, M., Dal Santo, S., Commissio, M., Zenoni, S., Ceolino, S., et al. (2015). Towards a scientific interpretation of the terroir concept: plasticity of the grape berry metabolome. *BMC Plant Biol.* 15:191. doi: 10.1186/s12870-015-0544
- Angel, T. E., Aryal, U. K., Hengel, S. M., Baker, E. S., Kelly, R. T., Robinson, W., et al. (2012). Mass spectrometry-based proteomics: Existing capabilities and future directions. *Chem. Soc. Rev.* 41, 3912–3928. doi: 10.1039/c2cs15331a
- Aoki, K., Ogata, Y., Igarashi, K., Yano, K., Nagasaki, H., Kaminuma, E., et al. (2013). Functional genomics of tomato in a post-genome-sequencing phase. *Breed. Sci.* 63, 14–20. doi: 10.1270/jbsbbs.63.14
- Apel, W., and Bock, R. (2009). Enhancement of carotenoid biosynthesis in transplastomic tomatoes by induced lycopene-to-provitamin A conversion. *Plant Physiol.* 151, 59–66. doi: 10.1104/pp.109.140533
- Araus, J. L., and Cairns, J. E. (2014). Field high-throughput phenotyping: the new crop breeding frontier. *Trends Plant Sci.* 19, 52–61. doi: 10.1016/j.tplants.2013.09.008
- Arms, E. M., Bloom, A. J., and St. Clair, D. A. (2015). High-resolution mapping of a major effect QTL from wild tomato *Solanum habrochaites* that influences water relations under root chilling. *Theor. Appl. Genet.* 128, 1713–1724. doi: 10.1007/s00122-015-2540-y
- Bai, H., Tao, F., Xiao, D., Liu, F., and Zhang, H. (2016). Attribution of yield change for rice-wheat rotation system in China to climate change, cultivars and agronomic management in the past three decades. *Clim. Change* 135, 539–553. doi: 10.1007/s10584-015-1579-8
- Bai, Y., and Lindhout, P. (2007). Domestication and breeding of tomatoes: what have we gained and what can we gain in the future? *Ann. Bot.* 100, 1085–1094. doi: 10.1093/aob/mcm150
- Barba, P., Cadle-Davidson, L., Harriman, J., Glaubitz, J. C., Brooks, S., Hyma, K., et al. (2014). Grapevine powdery mildew resistance and susceptibility loci identified on a high-resolution SNP map. *Theor. Appl. Genet.* 127, 73–84. doi: 10.1007/s00122-013-2202-x
- Barbier de Reuille, P., Routier-Kierzkowska, A.-L., Kierzkowski, D., Bassel, G. W., Schüpbach, T., Tauriello, G., et al. (2015). MorphoGraphX: a platform for quantifying morphogenesis in 4D. *eLife* 4:5864. doi: 10.7554/eLife.05864
- Barker, C. L., Donald, T., Pauquet, J., Ratnaparkhe, M. B., Bouquet, A., Adam-Blondon, A. F., et al. (2005). Genetic and physical mapping of the grapevine powdery mildew resistance gene, Run1, using a bacterial artificial chromosome library. *Theor. Appl. Genet.* 111, 370–377. doi: 10.1007/s00122-005-2030-8
- Barrangou, R., Fremaux, C., Deveau, H., Richards, M., Boyaval, P., Moineau, S., et al. (2007). CRISPR provides acquired resistance against viruses in prokaryotes. *Science* 315, 1709–1712. doi: 10.1126/science.1138140
- Barrantes, W., Fernández-del-Carmen, A., López-Casado, G., González-Sánchez, M. Á., Fernández-Muñoz, R., Granell, A., et al. (2014). Highly efficient genomics-assisted development of a library of introgression lines of *Solanum pimpinellifolium*. *Mol. Breed.* 34, 1817–1831. doi: 10.1007/s11032-014-0141-0
- Barsan, C., Zouine, M., Maza, E., Bian, W., Egea, I., Rossignol, M., et al. (2012). Proteomic analysis of chloroplast-to-chromoplast transition in tomato reveals metabolic shifts coupled with disrupted thylakoid biogenesis machinery and elevated energy-production components. *Plant Physiol.* 160, 708–725. doi: 10.1104/pp.112.203679
- Bauchet, G., and Causse, M. (2012). “Genetic diversity in tomato (*Solanum lycopersicum*) and its wild relatives,” in *Genetic Diversity in Tomato (*Solanum lycopersicum*) and Its Wild Relatives, Genetic Diversity in Plants*, ed. M. Caliskan (InTech), 133–162. Available online at: <http://www.intechopen.com/books/genetic-diversity-in-plants/genetic-diversity-in-tomato-solanum-lycopersicum-and-its-wild-relatives>
- Bélanger, M. C., Roger, J. M., Cartolaro, P., Viau, A. A., and Bellon-Maurel, V. (2008). Detection of powdery mildew in grapevine using remotely sensed UV-induced fluorescence. *Int. J. Remote Sens.* 29, 1707–1724. doi: 10.1080/01431160701395245
- Berger, S., Papadopoulos, M., Schreiber, U., Kaiser, W., and Roitsch, T. (2004). Complex regulation of gene expression, photosynthesis and sugar levels by pathogen infection in tomato. *Physiol. Plant.* 122, 419–428. doi: 10.1111/j.1399-3054.2004.00443.x
- Bergougoux, V. (2014). The history of tomato: from domestication to biopharming. *Biotechnol. Adv.* 32, 170–189. doi: 10.1016/j.biotechadv.2013.11.003
- Bernacchi, D., Beck-Bunn, T., Eshed, Y., Lopez, J., Petiard, V., Uhlig, J., et al. (1998). Advanced backcross QTL analysis in tomato. I. Identification of QTLs for traits of agronomic importance from *Lycopersicon hirsutum*. *Theor. Appl. Genet.* 97, 381–397. doi: 10.1007/s001220050908
- Bernardo, R. (2008). Molecular markers and selection for complex traits in plants: learning from the last 20 years. *Crop Sci.* 48, 1649–1664. doi: 10.2135/cropsci2008.03.0131
- Biais, B., Bénard, C., Beauvoit, B., Colombié, S., Prodhomme, D., Ménard, G., et al. (2014). Remarkable reproducibility of enzyme activity profiles in tomato fruits grown under contrasting environments provides a roadmap for studies of fruit metabolism. *Plant Physiol.* 164, 1204–1221. doi: 10.1104/pp.113.231241
- Biasi, R., and Brunori, E. (2015). The on-farm conservation of grapevine (*Vitis vinifera* L.) landraces assures the habitat diversity in the viticultural agro-ecosystem. *Vitis J. Grapevine Res.* 54, 265–269.
- Bino, R. J., De Vos, C. H. R., Lieberman, M., Hall, R. D., Bovy, A., Jonker, H. H., et al. (2005). The light-hyperresponsive high pigment-2dg mutation of tomato: alterations in the fruit metabolome. *New Phytol.* 166, 427–438. doi: 10.1111/j.1469-8137.2005.01362.x

ACKNOWLEDGMENTS

The authors would like to thank the COST (European Cooperation in Science and Technology) Action FA1106 “Quality fruit” and Action CA15136 “EUROCAROTEN.”

- Blanca, J., Montero-Pau, J., Sauvage, C., Bauchet, G., Illa, E., Díez, M. J., et al. (2015). Genomic variation in tomato, from wild ancestors to contemporary breeding accessions. *BMC Genomics* 16:257. doi: 10.1186/s12864-015-1444-1
- Boggess, M. V., Lippolis, J. D., Hurkman, W. J., Fagerquist, C. K., Briggs, S. P., Gomes, A. V., et al. (2013). The need for agriculture phenotyping: moving from genotype to phenotype. *J. Proteomics* 93, 20–39. doi: 10.1016/j.jprot.2013.03.021
- Bogs, J., Ebadi, A., McDavid, D., and Robinson, S. P. (2006). Identification of the flavonoid hydroxylases from grapevine and their regulation during fruit development. *Plant Physiol.* 140, 279–291. doi: 10.1104/pp.105.073262
- Bogs, J., Jaffe, F. W., Takos, A. M., Walker, A. R., and Robinson, S. P. (2007). The grapevine transcription factor VvMYBPA1 regulates proanthocyanidin synthesis during fruit development. *Plant Physiol.* 143, 1347–1361. doi: 10.1104/pp.106.093203
- Bolger, M. E., Weisshaar, B., Scholz, U., Stein, N., Usadel, B., and Mayer, K. F. X. (2014). Plant genome sequencing - applications for crop improvement. *Curr. Opin. Biotechnol.* 26, 31–37. doi: 10.1016/j.copbio.2013.08.019
- Broman, K. W. (2005). The genomes of recombinant inbred lines. *Genetics* 169, 1133–1146. doi: 10.1534/genetics.104.035212
- Brooks, C., Nekrasov, V., Lippman, Z. B., and Van Eck, J. (2014). Efficient gene editing in tomato in the first generation using the clustered regularly interspaced short palindromic repeats/CRISPR-associated9 system. *Plant Physiol.* 166, 1292–1297. doi: 10.1104/pp.114.247577
- Burbridge, A., Grieve, T. M., Jackson, A., Thompson, A., McCarty, D. R., and Taylor, I. B. (1999). Characterization of the ABA-deficient tomato mutant *notabilis* and its relationship with maize *Vp14*. *Plant J.* 17, 427–431. doi: 10.1046/j.1365-313X.1999.00386.x
- Calafiore, R., Ruggieri, V., Raiola, A., Rigano, M. M., Sacco, A., Hassan, M. I., et al. (2016). Exploiting genomics resources to identify candidate genes underlying antioxidants content in tomato fruit. *Front. Plant Sci.* 7:397. doi: 10.3389/fpls.2016.00397
- Calderón, R., Castro, O., Arauz, F., and Bonatti, J. (2014). “Use of infrared sensors for early detection of bacterial wilt caused by *Ralstonia solanacearum* in tomato plants,” in *CIGR Proceedings, Vol. 1* (San Jose, CL: Costa Rica).
- Capel, C., Del Carmen, A. F., Alba, J. M., Lima-Silva, V., Hernández-Gras, F., Salinas, M., et al. (2015). Wide-genome QTL mapping of fruit quality traits in a tomato RIL population derived from the wild-relative species *Solanum pimpinellifolium* L. *Theor. Appl. Genet.* 128, 2019–2035. doi: 10.1007/s00122-015-2563-4
- Carrera, J., Fernández del Carmen, A., Fernández-Muñoz, R., Rambla, J. L., Pons, C., Jaramillo, A., et al. (2012). Fine-tuning tomato agronomic properties by computational genome redesign. *PLoS Comput. Biol.* 8:e1002528. doi: 10.1371/journal.pcbi.1002528
- Causse, M., Duffe, P., Gomez, M. C., Buret, M., Damidaux, R., Zamir, D., et al. (2004). A genetic map of candidate genes and QTLs involved in tomato fruit size and composition. *J. Exp. Bot.* 55, 1671–1685. doi: 10.1093/jxb/erh207
- Cavallini, E., Matus, J. T., Finezzo, L., Zenoni, S., Loyola, R., Guzzo, F., et al. (2015). The phenylpropanoid pathway is controlled at different branches by a set of R2R3-MYB C2 repressors in grapevine. *Plant Physiol.* 167, 1448–1470. doi: 10.1104/pp.114.256172
- Cavanagh, C., Morell, M., Mackay, I., and Powell, W. (2008). From mutations to MAGIC: resources for gene discovery, validation and delivery in crop plants. *Curr. Opin. Plant Biol.* 11, 215–221 doi: 10.1016/j.pbi.2008.01.002
- Cebolla-Cornejo, J., Roselló, S., and Nuez, F. (2013). Phenotypic and genetic diversity of Spanish tomato landraces. *Sci. Hortic.* 162, 150–164. doi: 10.1016/j.scienta.2013.07.044
- Čermák, T., Baltes, N. J., Čegan, R., Zhang, Y., and Voytas, D. F. (2015). High-frequency, precise modification of the tomato genome. *BMC Genomics* 16:232. doi: 10.1186/s13059-015-0796-9
- Chærle, L., Lenk, S., Leinonen, I., Jones, H. G., Van Der Straeten, D., and Buschmann, C. (2009). Multi-sensor plant imaging: towards the development of a stress-catalogue. *Biotechnol. J.* 4, 1152–1167. doi: 10.1002/biot.200800242
- Chaib, J., Lecomte, L., Buret, M., and Causse, M. (2006). Stability over genetic backgrounds, generations and years of quantitative trait locus (QTLs) for organoleptic quality in tomato. *Theor. Appl. Genet.* 112, 934–944. doi: 10.1007/s00122-005-0197-7
- Chalhoub, B., Denoeud, F., Liu, S., Parkin, I. A., Tang, H., Wang, X., et al. (2014). Early allopolyploid evolution in the post-Neolithic *Brassica napus* oilseed genome. *Science* 345, 950–953.
- Chappell, M. J., and LaValle, L. A. (2011). Food security and biodiversity: can we have both? An agroecological analysis. *Agric. Hum. Values* 28, 3–26. doi: 10.1007/s10460-009-9251-4
- Chen, G., Hackett, R., Walker, D., Taylor, A., Lin, Z., and Grierson, D. (2004). Identification of a specific isoform of tomato lipoxygenase (TomloxC) involved in the generation of fatty acid-derived flavor compounds. *Plant Physiol.* 136, 2641–2651. doi: 10.1104/pp.104.041608
- Chen, J., Wang, N., Fang, L.-C., Liang, Z.-C., Li, S.-H., and Wu, B.-H. (2015). Construction of a high-density genetic map and QTLs mapping for sugars and acids in grape berries. *BMC Plant Biol.* 15:28. doi: 10.1186/s12870-015-0428-2
- Chen, X., Chen, F., Chen, Y., Gao, Q., Yang, X., Yuan, L., et al. (2013). Modern maize hybrids in Northeast China exhibit increased yield potential and resource use efficiency despite adverse climate change. *Glob. Chang. Biol.* 19, 923–936. doi: 10.1111/gcb.12093
- Coleman, C., Copetti, D., Cipriani, G., Hoffmann, S., Kozma, P., Kovács, L., et al. (2009). The powdery mildew resistance gene REN1 co-segregates with an NBS-LRR gene cluster in two Central Asian grapevines. *BMC Genet.* 10:89. doi: 10.1186/1471-2156-10-89
- Collard, B. C. Y., Jahufer, M. Z. Z., Brouwer, J. B., and Pang, E. C. K. (2005). An introduction to markers, quantitative trait loci (QTL) mapping and marker-assisted selection for crop improvement: the basic concepts. *Euphytica* 142, 169–196. doi: 10.1007/s10681-005-1681-5
- Corrado, G., Piffanelli, P., Caramante, M., Coppola, M., and Rao, R. (2013). SNP genotyping reveals genetic diversity between cultivated landraces and contemporary varieties of tomato. *BMC Genomics* 14:835. doi: 10.1186/1471-2164-14-835
- Czemmel, S., Stracke, R., Weisshaar, B., Cordon, N., Harris, N. N., Walker, A. R., et al. (2009). The Grapevine R2R3-MYB transcription factor VvMYBF1 regulates flavonol synthesis in developing grape berries. *Plant Physiol.* 151, 1513–1530. doi: 10.1104/pp.109.142059
- D'Ambrosio, C., Giorio, G., Marino, I., Merendino, A., Petrozza, A., Salfi, L., et al. (2004). Virtually complete conversion of lycopene into β-carotene in fruits of tomato plants transformed with the tomato lycopene β-cyclase (tlcy-b) cDNA. *Plant Sci.* 166, 207–214. doi: 10.1016/j.plantsci.2003.09.015
- D'Ambrosio, C., Stigliani, A. L., and Giorio, G. (2011). Overexpression of CrtR-b2 (carotene beta hydroxylase 2) from *S. lycopersicum* L. differentially affects xanthophyll synthesis and accumulation in transgenic tomato plants. *Transgenic Res.* 20, 47–60. doi: 10.1007/s11248-010-9387-4
- D'Esposito, D., Ferriello, F., Dal Molin, A., Diretto, G., Sacco, A., Minio, A., et al. (2017). Unraveling the complexity of transcriptomic, metabolomic and quality environmental response of tomato fruit. *BMC Plant Biol.* 17:66. doi: 10.1186/s12870-017-1008-4
- de Toledo Thomazella, D. P., Brail, Q., Dahlbeck, D., and Staskawicz, B. J. (2016). CRISPR-Cas9 mediated mutagenesis of a DMR6 ortholog in tomato confers broad-spectrum disease resistance. *bioRxiv*, 064824. doi: 10.1101/064824
- De Vos, R. C., Moco, S., Lommen, A., Keurentjes, J. J., Bino, R. J., and Hall, R. D. (2007). Untargeted large-scale plant metabolomics using liquid chromatography coupled to mass spectrometry. *Nat. Protoc.* 2, 778–791. doi: 10.1038/nprot.2007.95
- Deery, D., Jimenez-Berni, J., Jones, H., Sirault, X., and Furbank, R. (2014). Proximal remote sensing buggies and potential applications for field-based phenotyping. *Agronomy* 4, 349–379. doi: 10.3390/agronomy4030349
- Degu, A., Hochberg, U., Sikron, N., Venturini, L., Buson, G., Ghan, R., et al. (2014). Metabolite and transcript profiling of berry skin during fruit development elucidates differential regulation between Cabernet Sauvignon and Shiraz cultivars at branching points in the polyphenol pathway. *BMC Plant Biol.* 14:188. doi: 10.1186/s12870-014-0188-4
- Deluc, L., Barrieu, F. C., Marchive, C., Lauvergeat, V., Decendit, A., Richard, T., et al. (2006). Characterization of a grapevine R2R3-MYB transcription factor that regulates the phenylpropanoid pathway. *Plant Physiol.* 140:499. doi: 10.1104/pp.105.067231
- Deluc, L., Bogs, J., Walker, A. R., Ferrier, T., Decendit, A., Merillon, J.-M., et al. (2008). The transcription factor VvMYB5b contributes to the regulation of anthocyanin and proanthocyanidin biosynthesis in developing grape berries. *Plant Physiol.* 147, 2041–2053. doi: 10.1104/pp.108.118919

- Deytieux, C., Geny, L., Lapaillerie, D., Claverol, S., Bonneau, M., and Donèche, B. (2007). Proteome analysis of grape skins during ripening. *J. Exp. Bot.* 58, 1851–1862. doi: 10.1093/jxb/erm049
- Dharmapuri, S., Rosati, C., Pallara, P., Aquilani, R., Bouvier, F., Camara, B., et al. (2002). Metabolic engineering of xanthophyll content in tomato fruits. *FEBS Lett.* 519, 30–34. doi: 10.1016/S0014-5793(02)02699-6
- Di Matteo, A., Rigano, M. M., and Sacco, A. (2011). Genetic transformation in tomato: novel tools to improve fruit quality and pharmaceutical production,” in *Genetic Transformation*. Available online at: http://www.intechopen.com/source/pdfs/18813/InTech-Genetic_transformation_in_tomato_novel_tools_to_improve_fruit_quality_and_pharmaceutical_production.pdf
- Díaz de la Garza, R. I., Gregory, J. F., and Hanson, A. D. (2007). Folate biofortification of tomato fruit. *Proc. Natl. Acad. Sci. U.S.A.* 104, 4218–4222. doi: 10.1073/pnas.0700409104
- Doganlar, S., Frary, A., Daunay, M. C., Lester, R. N., and Tanksley, S. D. (2002). Conservation of gene function in the Solanaceae as revealed by comparative mapping of domestication traits in eggplant. *Genetics* 161, 1713–1726.
- Doligez, A., Bertrand, Y., Farnas, M., Grolier, M., Romieu, C., Esnault, F., et al. (2013). New stable QTLs for berry weight do not colocalize with QTLs for seed traits in cultivated grapevine (*Vitis vinifera* L.). *BMC Plant Biol.* 13:217. doi: 10.1186/1471-2229-13-217
- Doucet, M., Jin, Y., Gao, F., Riaz, S., Krivanek, A. F., and Walker, M. A. (2004). A genetic linkage map of grape, utilizing *Vitis rupestris* and *Vitis arizonica*. *Theor. Appl. Genet.* 109, 1178–1187. doi: 10.1007/s00122-004-1728-3
- Dresboll, D. B., Thorup-Kristensen, K., McKenzie, B. M., Dupuy, L. X., and Bengough, A. G. (2013). Timelapse scanning reveals spatial variation in tomato (*Solanum lycopersicum* L.) root elongation rates during partial waterlogging. *Plant Soil* 369, 467–477. doi: 10.1007/s11104-013-1592-5
- Duchêne, E., Butterlin, G., Dumas, V., and Merdinoglu, D. (2012). Towards the adaptation of grapevine varieties to climate change: QTLs and candidate genes for developmental stages. *Theor. Appl. Genet.* 124, 623–635. doi: 10.1007/s00122-011-1734-1
- Eitel, J. U., Vierling, L. A., Long, D. S., and Hunt, E. R. (2011). Early season remote sensing of wheat nitrogen status using a green scanning laser. *Agric. For. Meteorol.* 151, 1338–1345. doi: 10.1016/j.agrformet.2011.05.015
- Elizondo, R., and Oyanedel, E. (2011). Field testing of tomato chilling tolerance under varying light and temperature conditions. *Chilean J. Agric. Res.* 70, 552–558. doi: 10.4067/S0718-58392010000400004
- Eshed, Y., and Zamir, D. (1995). An introgression line population of *Lycopersicon pennellii* in the cultivated tomato enables the identification and fine mapping of yield-associated QTL. *Genetics* 141, 1147–1162.
- Etalo, D. W., Stulemeijer, I. J. E., Esse, H. P., van Vos, R. C. H., de Bouwmeester, H. J., and Joosten, M. H. A. J. (2013). System-wide hypersensitive response-associated transcriptome and metabolome reprogramming in tomato. *Plant Physiol.* 162, 1599–1617. doi: 10.1104/pp.113.217471
- Fahlgren, N., Gehan, M. A., and Baxter, I. (2015). Lights, camera, action: high-throughput plant phenotyping is ready for a close-up. *Curr. Opin. Plant Biol.* 24, 93–99. doi: 10.1016/j.pbi.2015.02.006
- Fantini, E., Falcone, G., Frusciante, S., Giliberto, L., and Giuliano, G. (2013). Dissection of tomato lycopene biosynthesis through virus-induced gene silencing. *Plant Physiol.* 163, 986–998. doi: 10.1104/pp.113.224733
- FAO, IFAD, WFP (2015). “The State of Food Insecurity in the World 2015,” in *Meeting the 2015 International Hunger Targets: Taking Stock of Uneven Progress*. Rome: Food and Agriculture Organization Publications.
- Feechan, A., Anderson, C., Torregrosa, L., Jermakow, A., Mestre, P., Wiedemann-Merdinoglu, S., et al. (2013). Genetic dissection of a TIR-NB-LRR locus from the wild North American grapevine species *Muscadinia rotundifolia* identifies paralogous genes conferring resistance to major fungal and oomycete pathogens in cultivated grapevine. *Plant J.* 76, 661–674. doi: 10.1111/tpj.12327
- Fernie, A. R., Tadmor, Y., and Zamir, D. (2006). Natural genetic variation for improving crop quality. *Curr. Opin. Plant Biol.* 9, 196–202. doi: 10.1016/j.pbi.2006.01.010
- Fiorani, F., and Schurr, U. (2013). Future scenarios for plant phenotyping. *Annu. Rev. Plant Biol.* 64, 267–291. doi: 10.1146/annurev-arplant-050312-120137
- Fiorani, F., Rascher, U., Jahnke, S., and Schurr, U. (2012). Imaging plants dynamics in heterogenic environments. *Curr. Opin. Biotechnol.* 23, 227–235. doi: 10.1016/j.copbio.2011.12.010
- Fischer, B. M., Salakhutdinov, I., Akkurt, M., Eibach, R., Edwards, K. J., Töpfer, R., et al. (2004). Quantitative trait locus analysis of fungal disease resistance factors on a molecular map of grapevine. *Theor. Appl. Genet.* 108, 501–515. doi: 10.1007/s00122-003-1445-3
- Fodor, A., Segura, V., Denis, M., Neuenschwander, S., Fournier-Level, A., Chatelet, P., et al. (2014). Genome-wide prediction methods in highly diverse and heterozygous species: proof-of-concept through simulation in grapevine. *PLoS ONE* 9:e110436. doi: 10.1371/journal.pone.0110436
- Foley, J. A., Ramankutty, N., Brauman, K. A., Cassidy, E. S., Gerber, J. S., Johnston, M., et al. (2011). Solutions for a cultivated planet. *Nature* 478, 337–342. doi: 10.1038/nature10452
- Fortes, A. M., Agudelo-Romero, P., Silva, M. S., Ali, K., Sousa, L., Maltese, F., et al. (2011). Transcript and metabolite analysis in Trincadeira cultivar reveals novel information regarding the dynamics of grape ripening. *BMC Plant Biol.* 11:149. doi: 10.1186/1471-2229-11-149
- Fortes, A. M., and Gallusci, P. (2017). Plant stress responses and phenotypic plasticity in the epigenomics era: perspectives on the grapevine scenario, a model for perennial crop plants. *Front. Plant Sci.* 8:82. doi: 10.3389/fpls.2017.00082
- Fortes, A. M., Teixeira, R. T., and Agudelo-Romero, P. (2015). Complex interplay of hormonal signals during grape berry ripening. *Molecules* 20, 9326–9343. doi: 10.3390/molecules20059326
- Fowler, C. (2008). The Svalbard seed vault and crop security. *Bioscience* 58:190. doi: 10.1641/B580302
- Francis, C., Lieblein, G., Gliessman, S., Breland, T. A., Creamer, N., Harwood, R., et al. (2003). Agroecology: the ecology of food systems agroecology: the ecology of food systems. *J. Sustain. Agric.* 22, 99–118. doi: 10.1300/J064v22n03_10
- Francisco, R. M., Regalado, A., Ageorges, A., Burla, B. J., Bassin, B., Eisenach, C., et al. (2013). ABCC1, an ATP binding cassette protein from grape berry, transports anthocyanidin 3-O-glucosides. *Plant Cell* 25, 1840–1854. doi: 10.1105/tpc.112.102152
- Fraser, P. D., Enfissi, E. M. A., Halket, J. M., Truesdale, M. R., Yu, D., Gerrish, C., et al. (2007). Manipulation of phytoene levels in tomato fruit: effects on isoprenoids, plastids, and intermediary metabolism. *Plant Cell* 19, 3194–3211. doi: 10.1105/tpc.106.049817
- Fraser, P. D., Romer, S., Shipton, C. A., Mills, P. B., Kiano, J. W., Misawa, N., et al. (2002). Evaluation of transgenic tomato plants expressing an additional phytoene synthase in a fruit-specific manner. *Proc. Natl. Acad. Sci. U.S.A.* 99, 1092–1097. doi: 10.1073/pnas.241374599
- Fray, R. G., and Grierson, D. (1993). Identification and genetic analysis of normal and mutant phytoene synthase genes of tomato by sequencing, complementation and co-suppression. *Plant Mol. Biol.* 22, 589–602. doi: 10.1007/BF00047400
- Fridman, E., Pleban, T., and Zamir, D. (2000). A recombination hotspot delimits a wild-species quantitative trait locus for tomato sugar content to 484 bp within an invertase gene. *Proc. Natl. Acad. Sci. U.S.A.* 97, 4718–4723. doi: 10.1073/pnas.97.9.4718
- Fuentes, S., De Bei, R., Pech, J., and Tyerman, S. (2012). Computational water stress indices obtained from thermal image analysis of grapevine canopies. *Irrigat. Sci.* 30, 523–536. doi: 10.1007/s00271-012-0375-8
- Fulton, T. M., Beck-Bunn, T., Emmatty, D., Eshed, Y., Lopez, J., Petiard, V., et al. (1997). QTL analysis of an advanced backcross of *Lycopersicon peruvianum* to the cultivated tomato and comparisons with QTLs found in other wild species. *Theor. Appl. Genet.* 95, 881–894. doi: 10.1007/s001220050639
- Gaj, T. (2014). ZFN, TALEN and CRISPR/Cas based methods for genome engineering. 31, 397–405. doi: 10.1016/j.tibtech.2013.04.004.ZFN
- Galpaz, N., Ronen, G., Khalfa, Z., Zamir, D., and Hirschberg, J. (2006). A chromoplast-specific carotenoid biosynthesis pathway is revealed by cloning of the tomato white-flower locus. *Plant Cell* 18, 1947–1960. doi: 10.1105/tpc.105.039966
- Galpaz, N., Wang, Q., Menda, N., Zamir, D., and Hirschberg, J. (2008). Abscisic acid deficiency in the tomato mutant high-pigment 3 leading to increased plastid number and higher fruit lycopene content. *Plant J.* 53, 717–730. doi: 10.1111/j.1365-313X.2007.03362.x
- García, A. C., Izquierdo, F. G., Hernández, O. L., Margarita, M., Armas, D., De López, R. H., et al. (2013). Biotechnology of humified materials obtained from

- vermicomposts for sustainable agroecological purposes. *Afr. J. Biotechnol.* 12, 625–634. doi: 10.5897/AJBX12.014
- George, I. S., Pascoiu, D., Mirzaei, M., and Haynes, P. A. (2015). Quantitative proteomic analysis of cabernet sauvignon grape cells exposed to thermal stresses reveals alterations in sugar and phenylpropanoid metabolism. *Proteomics* 15, 3048–3060. doi: 10.1002/pmic.201400541
- Gepts, P. (2014). The contribution of genetic and genomic approaches to plant domestication studies. *Curr. Opin. Plant Biol.* 18, 51–59. doi: 10.1016/j.pbi.2014.02.001
- Gil, R., Merav, C., Dani, Z., and Joseph, H. (1999). Regulation of carotenoid biosynthesis during tomato fruit development: expression of the gene for lycopene epsilon-cyclase is down-regulated during ripening and is elevated in the mutant *Delta*. *Plant J.* 17, 341–351. doi: 10.1046/j.1365-313X.1999.00381.x
- Giorio, G., Yildirim, A., Stigliani, A. L., and D'Ambrosio, C. (2013). Elevation of lutein content in tomato: a biochemical tug-of-war between lycopene cyclases. *Metab. Eng.* 20, 167–176. doi: 10.1016/j.ymben.2013.10.007
- Giovannelli, G., Sinelli, N., Beghi, R., Guidetti, R., and Casiraghi, E. (2014). NIR spectroscopy for the optimization of postharvest apple management. *Postharvest Biol. Technol.* 87, 13–20. doi: 10.1016/j.postharvbio.2013.07.041
- Giovinazzo, G., D'Amico, L., Paradiso, A., Bollini, R., Sparvoli, F., and DeGara, L. (2005). Antioxidant metabolite profiles in tomato fruit constitutively expressing the grapevine stilbene synthase gene. *Plant Biotechnol. J.* 3, 57–69. doi: 10.1111/j.1467-7652.2004.00099.x
- Goldsborough, A., Belzile, F., and Yoder, J. (1994). Complementation of the Tomato anthocyanin without (aw) mutant using the Dihydroflavonol 4-Reductase Gene. *Plant Physiol.* 105, 491–496.
- Gomez, C., Terrier, N., Torregrosa, L., Viallet, S., Fournier-Level, A., Verries, C., et al. (2009). Grapevine MATE-type proteins act as vacuolar H⁺-dependent acylated anthocyanin transporters. *Plant Physiol.* 150, 402–415. doi: 10.1104/pp.109.135624
- González-Barreiro, C., Rial-Otero, R., Cancho-Grande, B., and Simal-Gándara, J. (2015). Wine aroma compounds in grapes: a critical review. *Crit. Rev. Food Sci. Nutr.* 55, 202–218. doi: 10.1080/10408398.2011.650336
- Goulet, C., Kamiyoshihara, Y., Lam, N. B., Richard, T., Taylor, M. G., Tieman, D. M., et al. (2015). Divergence in the enzymatic activities of a tomato and *Solanum pennellii* alcohol acyltransferase impacts fruit volatile ester composition. *Mol. Plant* 8, 153–162. doi: 10.1016/j.molp.2014.11.007
- Grandillo, S., Termolino, P., and van der Knaap, E. (2013). Molecular mapping of complex traits in tomato. *Genet. Genomics Breed. Tomato* 150–227. doi: 10.1201/b14578-7
- Grattapaglia, D., and Sederoff, R. (1994). Genetic linkage maps of *Eucalyptus grandis* and *Eucalyptus urophylla* using a pseudo-testcross: mapping strategy and RAPD markers. *Genetics* 137, 1121–1137. doi: 10.1007/s11033-010-0612-2
- Grissa, I., Vergnaud, G., and Pourcel, C. (2007). The CRISPRdb database and tools to display CRISPRs and to generate dictionaries of spacers and repeats. *BMC Bioinformatics* 8:172. doi: 10.1186/1471-2105-8-172
- Guillemaud, T., Lombaert, E., and Bourguet, D. (2016). Conflicts of interest in GM Bt crop efficacy and durability studies. *PLoS ONE* 11:e0167777. doi: 10.1371/journal.pone.0167777
- Gur, A., and Zamir, D. (2004). Unused natural variation can lift yield barriers in plant breeding. *PLoS Biol.* 2:245. doi: 10.1371/journal.pbio.0020245
- Handa, A. K., Anwar, R., and Mattoo, A. K. (2014). Biotechnology of fruit quality. *Fruit Ripening Physiol. Signal. Genomics* 259–290. doi: 10.1079/9781845939625.0259
- Harrigan, G. G., Martino-Catt, S., and Glenn, K. C. (2007). Metabolomics, metabolic diversity and genetic variation in crops. *Metabolomics* 3, 259–272. doi: 10.1007/s11306-007-0076-0
- Harrison, E., Burbidge, A., Okyere, J. P., Thompson, A. J., and Taylor, I. B. (2011). Identification of the tomato ABA-deficient mutant sitiens as a member of the ABA-aldehyde oxidase gene family using genetic and genomic analysis. *Plant Growth Regul.* 64, 301–309. doi: 10.1007/s10725-010-9550-1
- Henikoff, S., Till, B. J., Comai, L., Division, B. S., Hutchinson, F., and Washington, S. H. (2004). TILLING. Traditional mutagenesis meets functional genomics. *Plant Physiol.* 135, 630–636. doi: 10.1104/pp.104.041061.630
- Herzog, K., Wind, R., and Töpfer, R. (2015). Impedance of the grape berry cuticle as a novel phenotypic trait to estimate resistance to *Botrytis cinerea*. *Sensors* 15, 12498–12512. doi: 10.3390/s150612498
- Hilioti, Z., Ganopoulos, I., Ajith, S., Bossis, I., and Tsafaris, A. (2016). A novel arrangement of zinc finger nuclease system for *in vivo* targeted genome engineering: the tomato LEC1-LIKE4 gene case. *Plant Cell Rep.* 35, 1–15. doi: 10.1007/s00299-016-2031-x
- Höll, J., Vannozi, A., Czembel, S., D'Onofrio, C., Walker, A. R., Rausch, T., et al. (2013). The R2R3-MYB transcription factors MYB14 and MYB15 regulate stilbene biosynthesis in *Vitis vinifera*. *Plant Cell* 25, 4135–4149. doi: 10.1105/tpc.113.117127
- Honnay, O., Jacquemyn, H., and Aerts, R. (2012). Crop wild relatives: more common ground for breeders and ecologists. *Front. Ecol. Environ.* 10:121. doi: 10.1890/12.WB.007
- Hosoi, F., and Omasa, K. (2012). Estimation of vertical plant area density profiles in a rice canopy at different growth stages by high-resolution portable scanning lidar with a lightweight mirror. *ISPRS J. Photogramm. Remote Sens.* 74, 11–19. doi: 10.1016/j.isprsjprs.2012.08.001
- Hosoi, F., Nakabayashi, K., and Omasa, K. (2011). 3-D modeling of tomato canopies using a high-resolution portable scanning lidar for extracting structural information. *Sensors* 11, 2166–2174. doi: 10.3390/s110202166
- Houel, C., Chatbanyong, R., Doligez, A., Rienth, M., Foria, S., Luchaire, N., et al. (2015). Identification of stable QTLs for vegetative and reproductive traits in the microvine (*Vitis vinifera* L.) using the 18 K Infinium chip. *BMC Plant Biol.* 15, 205. doi: 10.1186/s12870-015-0588-0
- Huang, J. C., Zhong, Y. J., Liu, J., Sandmann, G., and Chen, F. (2013). Metabolic engineering of tomato for high-yield production of astaxanthin. *Metab. Eng.* 17, 59–67. doi: 10.1016/j.ymben.2013.02.005
- Huang, Z., and van der Knaap, E. (2011). Tomato fruit weight 11.3 maps close to fasciated on the bottom of chromosome 11. *Theor. Appl. Genetics* 123, 465–474. doi: 10.1007/s00122-011-1599-3
- Iijima, Y., Nakamura, Y., Ogata, Y., Tanaka, K., Sakurai, N., Suda, K., et al. (2008). Metabolite annotations based on the integration of mass spectral information. *Plant J.* 54, 949–962. doi: 10.1111/j.1365-313X.2008.03434.x
- Illa-Berenguer, E., Van Houten, J., Huang, Z., and van der Knaap, E. (2015). Rapid and reliable identification of tomato fruit weight and locule number loci by QTL-seq. *Theor. Appl. Genet.* 128, 1329–1342. doi: 10.1007/s00122-015-2509-x
- Isaacson, T., Ronen, G., Zamir, D., and Hirschberg, J. (2002). Cloning of tangerine from tomato reveals a carotenoid isomerase essential for the production of beta-carotene and xanthophylls in plants. *Plant Cell* 14, 333–342. doi: 10.1105/tpc.01303.2001
- Ishimwe, R., Abutaleb, K., and Ahmed, F. (2014). Applications of thermal imaging in agriculture—A review. *Adv. Remote Sens.* 3, 128. doi: 10.4236/ars.2014.33011
- Ito, Y., Nishizawa-Yokoi, A., Endo, M., Mikami, M., and Toki, S. (2015). CRISPR/Cas9-mediated mutagenesis of the RIN locus that regulates tomato fruit ripening. *Biochem. Biophys. Res. Commun.* 467, 76–82. doi: 10.1016/j.bbrc.2015.09.117
- Jacobs, T. B., and Martin, G. B. (2016). High-throughput CRISPR vector construction and characterization of DNA modifications by generation of tomato hairy roots. *J. Vis. Exp.* e53843–e53843. doi: 10.3791/53843
- Jaillon, O., Aury, J.-M., Noel, B., Policriti, A., Clepet, C., Casagrande, A., et al. (2007). The grapevine genome sequence suggests ancestral hexaploidization in major angiosperm phyla. *Nature* 449, 463–467. doi: 10.1038/nature06148
- Jia, H., and Nian, W. (2014). Targeted genome editing of sweet orange using Cas9/gRNA. *PLoS ONE* 9:93806. doi: 10.1371/journal.pone.0093806
- Jiménez-Gómez, J. M., Alonso-Blanco, C., Borja, A., Anastasio, G., Angosto, T., Lozano, R., et al. (2007). Quantitative genetic analysis of flowering time in tomato. *Genome* 50, 303–315. doi: 10.1139/G07-009
- Jin, W., and Wu, F. (2016). Proteome-wide identification of lysine succinylation in the proteins of tomato (*Solanum lycopersicum*). *PLoS ONE* 11:0147586. doi: 10.1371/journal.pone.0147586
- Kashif, A., Federica, M., Eva, Z., Martina, R., Young, H. C., and Robert, V. (2009). NMR metabolic fingerprinting based identification of grapevine metabolites associated with downy mildew resistance. *J. Agric. Food Chem.* 57, 9599–9606. doi: 10.1021/jf902069f
- Kershen, D. L. (2013). The contested vision for agriculture's future: sustainable intensive agriculture and agroecology. *Creighton Law Rev.* 46, 1–36.
- Khan, N., Kazmi, R. H., Willems, L. A. J., van Heusden, A. W., Ligerink, W., and Hilhorst, H. W. M. (2012). Exploring the natural variation for seedling traits and their link with seed dimensions in tomato. *PLoS ONE* 7:e43991. doi: 10.1371/journal.pone.0043991

- Klap, C., Yeshayahou, E., Bolger, A. M., Arazi, T., Gupta, S. K., Shabtai, S., et al. (2016). Tomato facultative parthenocarpy results from Sl AGAMOUS-LIKE 6 loss of function. *Plant Biotechnol. J.* 15, 634–647. doi: 10.1111/pbi.12662
- Klee, H. J. (2010). Improving the flavor of fresh fruits: genomics, biochemistry, and biotechnology. *New Phytol.* 187, 44–56. doi: 10.1111/j.1469-8137.2010.03281.x
- Klee, H. J., and Tieman, D. M. (2013). Genetic challenges of flavor improvement in tomato. *Trends Genet.* 29, 257–262. doi: 10.1016/j.tig.2012.12.003
- Kobayashi, S., Ishimaru, M., Hiraoka, K., and Honda, C. (2002). Myb-related genes of the Kyoho grape (*Vitis labruscana*) regulate anthocyanin biosynthesis. *Planta* 215, 924–933. doi: 10.1007/s00425-002-0830-5
- Kohlen, W., Charnikhova, T., Lammers, M., Pollina, T., Tóth, P., Haider, I., et al. (2012). The tomato carotenoid cleavage dioxygenase8 (SlCCD8) regulates rhizosphere signaling, plant architecture and affects reproductive development through strigolactone biosynthesis. *New Phytol.* 196, 535–547. doi: 10.1111/j.1469-8137.2012.04265.x
- Konermann, S., Brigham, M. D., Trevino, A. E., Abudayeh, O. O., Barcena, C., Hsu, P. D., et al. (2015). Genome-scale transcriptional activation by an engineered CRISPR-Cas9 complex. *Nature* 517, 61422–61427. doi: 10.1038/nature14136.Genome-scale
- Krajewski, P., Chen, D., Ćwiek, H., Van Dijk, A. D. J., Fiorani, F., Kersey, P., et al. (2015). Towards recommendations for metadata and data handling in plant phenotyping. *J. Exp. Bot.* 66, 5417–5427. doi: 10.1093/jxb/erv271
- Krivanek, A. F., Riaz, S., and Walker, M. A. (2006). Identification and molecular mapping of PdR1, a primary resistance gene to Pierce's disease in Vitis. *Theor. Appl. Genet.* 112, 1125–1131. doi: 10.1007/s00122-006-0214-5
- Kuijken, R. C. P., Van Eeuwijk, F. A., Marcelis, L. F. M., and Bouwmeester, H. J. (2015). Root phenotyping: from component trait in the lab to breeding. *J. Exp. Bot.* 66, 5389–5401. doi: 10.1093/jxb/erv239
- Kumar, R., and Khurana, A. (2014). Functional genomics of tomato: opportunities and challenges in post-genome NGS era. *J. Biosci.* 39, 917–929. doi: 10.1007/s12038-014-9480-6
- Kurowska, M., Daszkowska-Golec, A., Gruszka, D., Marzec, M., Szurman, M., Szarejko, I., et al. (2011). TILLING - a shortcut in functional genomics. *J. Appl. Genet.* 52, 371–390. doi: 10.1007/s13353-011-0061-1
- Laucou, V., Lacombe, T., Dechesne, F., Siret, R., Bruno, J. P., Dessup, M., et al. (2011). High throughput analysis of grape genetic diversity as a tool for germplasm collection management. *Theor. Appl. Genet.* 122, 1233–1245. doi: 10.1007/s00122-010-1527-y
- Legland, D., Devaux, M. F., Bouchet, B., Guillon, F., and Lahaye, M. (2012). Cartography of cell morphology in tomato pericarp at the fruit scale. *J. Microsc.* 247, 78–93. doi: 10.1111/j.1365-2818.2012.03623.x
- Leida, C., Moser, C., Esteras, C., Sulpice, R., Lunn, J. E., de Langen, F., et al. (2015). Variability of candidate genes, genetic structure and association with sugar accumulation and climacteric behavior in a broad germplasm collection of melon (*Cucumis melo* L.). *BMC Genet.* 16:28. doi: 10.1186/s12863-015-0183-2
- Li, Z., and Sillanpää, M. J. (2015). Dynamic quantitative trait locus analysis of plant phenomic data. *Trends Plant Sci.* 20, 822–833. doi: 10.1016/j.tplants.2015.08.012
- Lim, W., Miller, R., Park, J., and Park, S. (2014). Consumer sensory analysis of high flavonoid transgenic tomatoes. *J. Food Sci.* 79, S1212–S1217. doi: 10.1111/1750-3841.12478
- Lin, T., Zhu, G., Zhang, J., Xu, X., Yu, Q., Zheng, Z., et al. (2014). Genomic analyses provide insights into the history of tomato breeding. *Nat. Genet.* 46, 1220–1226.
- Liu, R., How-Kit, A., Stammitti, L., Teyssier, E., Rolin, D., Mortain-Bertrand, A., et al. (2015). A DEMETER-like DNA demethylase governs tomato fruit ripening. *Proc. Natl. Acad. Sci. U.S.A.* 112, 10804–10809. doi: 10.1073/pnas.1503362112
- Liu, Y. S., Gur, A., Ronen, G., Causse, M., Damidaux, R., Buret, M., et al. (2003). There is more to tomato fruit colour than candidate carotenoid genes. *Plant Biotechnol. J.* 1, 195–207. doi: 10.1046/j.1467-7652.2003.00018.x
- Llorens, J., Gil, E., and Llop, J. (2011). Ultrasonic and LIDAR sensors for electronic canopy characterization in vineyards: advances to improve pesticide application methods. *Sensors* 11, 2177–2194. doi: 10.3390/s110202177
- Long, M., Millar, D. J., Kimura, Y., Donovan, G., Rees, J., Fraser, P. D., et al. (2006). Metabolite profiling of carotenoid and phenolic pathways in mutant and transgenic lines of tomato: identification of a high antioxidant fruit line. *Phytochemistry* 67, 1750–1757. doi: 10.1016/j.phytochem.2006.02.022
- Lor, V. S., Starker, C. G., Voytas, D. F., Weiss, D., and Olszewski, N. E. (2014). Targeted mutagenesis of the tomato PROCERA gene using TALENs. *Plant Physiol.* 166, 1288–1291. doi: 10.1104/pp.114.247593
- Lucatti, A. F., van Heusden, A. W., de Vos, R. C., Visser, R. G., and Vosman, B. (2013). Differences in insect resistance between tomato species endemic to the Galapagos Islands. *BMC Evol. Biol.* 13:175. doi: 10.1186/1471-2148-13-175
- Mageroy, M. H., Tieman, D. M., Floystad, A., Taylor, M. G., and Klee, H. J. (2012). A *Solanum lycopersicum* catechol-O-methyltransferase involved in synthesis of the flavor molecule guaiacol. *Plant J.* 69, 1043–1051. doi: 10.1111/j.1365-313X.2011.04854.x
- Malacarne, G., Coller, E., Czembel, S., Vrhovsek, U., Engelen, K., Goremykin, V., et al. (2016). The grapevine VvibZIPC22 transcription factor is involved in the regulation of flavonoid biosynthesis. *J. Exp. Bot.* 67, 3509–3522. doi: 10.1093/jxb/erw181
- Malacarne, G., Costantini, L., Coller, E., Battilana, J., Velasco, R., Vrhovsek, U., et al. (2015). Regulation of flavonol content and composition in (Syrah × Pinot Noir) mature grapes: integration of transcriptional profiling and metabolic quantitative trait locus analyses. *J. Exp. Bot.* 66, 4441–4453. doi: 10.1093/jxb/erv243
- Marguerit, E., Boury, C., Manicki, A., Donnart, M., Butterlin, G., Némorin, A., et al. (2009). Genetic dissection of sex determinism, inflorescence morphology and downy mildew resistance in grapevine. *Theor. Appl. Genet.* 118, 1261–1278. doi: 10.1007/s00122-009-0979-4
- Martin, D. M., Chiang, A., Lund, S. T., and Bohlmann, J. (2012). Biosynthesis of wine aroma: transcript profiles of hydroxymethylbutenyl diphosphate reductase, geranyl diphosphate synthase, and linalool/nerolidol synthase parallel monoterpenol glycoside accumulation in Gewürztraminer grapes. *Planta* 236, 919–929. doi: 10.1007/s00425-012-1704-0
- Mathieu, S., Cin, V. D., Fei, Z., Li, H., Bliss, P., Taylor, M. G., et al. (2009). Flavour compounds in tomato fruits: identification of loci and potential pathways affecting volatile composition. *J. Exp. Bot.* 60, 325–337. doi: 10.1093/jxb/ern294
- Matsui, K., Ishii, M., Sasaki, M., Rabinowitch, H. D., and Ben-Oliel, G. (2007). Identification of an allele attributable to formation of cucumber-like flavor in wild tomato species (*Solanum pennellii*) that was inactivated during domestication. *J. Agric. Food Chem.* 55, 4080–4086. doi: 10.1021/jf063756b
- Maxwell, K., and Johnson, G. N. (2000). Chlorophyll fluorescence—a practical guide. *J. Exp. Bot.* 51, 659–668.
- Mazzucato, A., Papa, R., Bitocchi, E., Mosconi, P., Nanni, L., Negri, V., et al. (2008). Genetic diversity, structure and marker-trait associations in a collection of Italian tomato (*Solanum lycopersicum* L.) landraces. *Theor. Appl. Genet.* 116, 657–669. doi: 10.1007/s00122-007-0699-6
- Mba, C. (2013). Induced mutations unleash the potentials of plant genetic resources for food and agriculture. *Agronomy* 3, 200–231. doi: 10.3390/agronomy3010200
- McMullen, M. D., Kresovich, S., Villeda, H. S., Bradbury, P., Li, H., Sun, Q., et al. (2009). Supporting online material for: genetic properties of the maize nested association mapping population. *Science* 325, 737–741. doi: 10.1126/science.1174320
- Menda, N., Semel, Y., Peled, D., Eshed, Y., and Zamir, D. (2004). *In silico* screening of a saturated mutation library of tomato. *Plant J.* 38, 861–872. doi: 10.1111/j.1365-313X.2004.02088.x
- Menzel, M. I., Tittmann, S., Buehler, J., Preis, S., Wolters, N., Jahnke, S., et al. (2009). Non-invasive determination of plant biomass with microwave resonators. *Plant Cell Environ.* 32, 368–379. doi: 10.1111/j.1365-3040.2009.01931.x
- Meron, M., Sprintsin, M., Tsipris, J., Alchanatis, V., and Cohen, Y. (2013). Foliation temperature extraction from thermal imagery for crop water stress determination. *Precis. Agric.* 14, 467–477. doi: 10.1007/s11119-013-9310-0
- Mes, P. J., Boches, P., Myers, J. R., and Durst, R. (2008). Characterization of tomatoes expressing anthocyanin in the fruit. *J. Am. Soc. Hort. Sci.* 133, 262–269.
- Minoia, S., Petrozza, A., D'Onofrio, O., Piron, F., Mosca, G., Sozio, G., et al. (2010). A new mutant genetic resource for tomato crop improvement by TILLING technology. *BMC Res. Notes* 3:69. doi: 10.1186/1756-0500-3-69
- Mishra, K. B., Iannaccone, R., Petrozza, A., Mishra, A., Armentano, N., La Vecchia, G., et al. (2012). Engineered drought tolerance in tomato plants is reflected in chlorophyll fluorescence emission. *Plant Sci.* 182, 79–86. doi: 10.1016/j.plantsci.2011.03.022

- Monforte, A. J., and Tanksley, S. D. (2000). Development of a set of near isogenic and backcross recombinant inbred lines containing most of the *Lycopersicon hirsutum* genome in a *L. esculentum* genetic background: a tool for gene mapping and gene discovery. *Genome* 43, 803–813. doi: 10.1139/gen-43-5-803
- Monforte, A. J., Diaz, A., Caño-Delgado, A., and Van Der Knaap, E. (2014). The genetic basis of fruit morphology in horticultural crops: lessons from tomato and melon. *J. Exp. Bot.* 65, 4625–4637. doi: 10.1093/jxb/eru017
- Monforte, A. J., Friedman, E., Zamir, D., and Tanksley, S. D. (2001). Comparison of a set of allelic QTL-NILs for chromosome 4 of tomato: deductions about natural variation and implications for germplasm utilization. *Theor. Appl. Genet.* 102, 572–590. doi: 10.1007/s001220051684
- Motion, G. B., Howden, A. J. M., Huitema, E., and Jones, S. (2015). DNA-binding protein prediction using plant specific support vector machines: validation and application of a new genome annotation tool. *Nucleic Acids Res.* 43:e158. doi: 10.1093/nar/gkv805
- Mounet, F., Moing, A., Kowalczyk, M., Rohrmann, J., Petit, J., Garcia, V., et al. (2012). Down-regulation of a single auxin efflux transport protein in tomato induces precocious fruit development. *J. Exp. Bot.* 63, 4901–4917. doi: 10.1093/jxb/ers167
- Nakano, H., Kobayashi, N., Takahata, K., Mine, Y., and Sugiyama, N. (2016). Quantitative trait loci analysis of the time of floral initiation in tomato. *Sci. Hortic.* 201, 199–210. doi: 10.1016/j.scienta.2016.02.009
- Neuman, H., Galpaz, N., Cunningham, F. X., Zamir, D., and Hirschberg, J. (2014). The tomato mutation *nxd1* reveals a gene necessary for neoxanthin biosynthesis and demonstrates that violaxanthin is a sufficient precursor for abscisic acid biosynthesis. *Plant J.* 78, 80–93. doi: 10.1111/tpj.12451
- Nicolas, S. D., Péros, J.-P., Lacombe, T., Launay, A., Le Paslier, M.-C., Bérard, A., et al. (2016). Genetic diversity, linkage disequilibrium and power of a large grapevine (*Vitis vinifera* L.) diversity panel newly designed for association studies. *BMC Plant Biol.* 16:74. doi: 10.1186/s12870-016-0754-z
- Nishitani, C., Hirai, N., Komori, S., Wada, M., Okada, K., Osakabe, K., et al. (2016). Efficient genome editing in apple using a CRISPR/Cas9 system. *Sci. Rep.* 6:31481. doi: 10.1038/srep31481
- Nunes-Nesi, A., Carrari, F., Lytovchenko, A., Smith, A. M. O., Loureiro, M. E., Ratcliffe, R. G., et al. (2005). Enhanced photosynthetic performance and growth as a consequence of decreasing mitochondrial malate dehydrogenase activity in transgenic tomato plants. *Plant Physiol.* 137, 611–622. doi: 10.1104/pp.104.055566
- Orzaez, D., Monforte, A. J., and Granell, A. (2010). Using genetic variability available in the breeder's pool to engineer fruit quality. *GM Crops* 1, 120–127. doi: 10.4161/gmc.1.3.12327
- Oyanedel, E., Wolfe, D. W., Monforte, A. J., Tanksley, S. D., and Owens, T. G. (2001). Using *Lycopersicon hirsutum* as a source of cold tolerance in processing tomato breeding. *Acta Hortic.* doi: 10.17660/ActaHortic.2001.542.51
- Pan, C., Ye, L., Qin, L., Liu, X., He, Y., Wang, J., et al. (2016). CRISPR/Cas9-mediated efficient and heritable targeted mutagenesis in tomato plants in the first and later generations. *Sci. Rep.* 6:24765. doi: 10.1038/srep24765
- Pankratov, I., McQuinn, R., Schwartz, J., Bar, E., Fei, Z., Lewinsohn, E., et al. (2016). Fruit carotenoid-deficient mutants in tomato reveal a function of the plastidial isopentenyl diphosphate isomerase (IDI1) in carotenoid biosynthesis. *Plant J.* 88, 82–94. doi: 10.1111/tpj.13232
- Parker, J., Koh, J., Yoo, M.-J., Zhu, N., Feole, M., Yi, S., et al. (2013). Quantitative proteomics of tomato defense against *Pseudomonas syringae* infection. *Proteomics* 13, 1934–1946. doi: 10.1002/pmic.201200402
- Pascual, L., Albert, E., Sauvage, C., Duangjitt, J., Bouchet, J. P., Bitton, F., et al. (2016). Dissecting quantitative trait variation in the resequencing era: complementarity of bi-parental, multi-parental and association panels. *Plant Sci.* 242, 120–130. doi: 10.1016/j.plantsci.2015.06.017
- Pascual, L., Desplat, N., Huang, B. E., Desgroux, A., Bruguier, L., Bouchet, J.-P., et al. (2015). Potential of a tomato MAGIC population to decipher the genetic control of quantitative traits and detect causal variants in the resequencing era. *Plant Biotechnol. J.* 13, 565–577. doi: 10.1111/pbi.12282
- Pérez-Díaz, R., Madrid-Espinoza, J., Salinas-Cornejo, J., González-Villanueva, E., and Ruiz-Lara, S. (2016). Differential roles for VviGST1, VviGST3, and VviGST4 in proanthocyanidin and anthocyanin transport in *Vitis vinifera*. *Front. Plant Sci.* 7:1166. doi: 10.3389/fpls.2016.01166
- Prada, D. (2009). Molecular population genetics and agronomic alleles in seed banks: searching for a needle in a haystack? *J. Exp. Bot.* 60, 2541–2552. doi: 10.1093/jxb/erp130
- Prashar, A., and Jones, H. G. (2014). Infra-red thermography as a high-throughput tool for field phenotyping. *Agronomy* 4, 397–417. doi: 10.3390/agronomy4030397
- Quadrana, L., Almeida, J., Asís, R., Duffy, T., Domínguez, P. G., Bermúdez, L., et al. (2014). Natural occurring epialleles determine vitamin E accumulation in tomato fruits. *Nat. Commun.* 5, 3027. doi: 10.1038/ncomms5027
- Rambla, J. L., Gianfranco, D., Angela, R.-M., Giovanni, G., Antonio, G., Lourdes, G.-G., et al. (2017b). Evolution of volatile compounds and their relationship with their precursors and the expression profiles of some genes involved in their release during maturation of Airén and Tempranillo grape varieties. *Front. Plant Sci.* 7:1619. doi: 10.3389/fpls.2016.01619
- Rambla, J. L., Medina, A., Fernández-del-Carmen, A., Barrante, W., Garndillo, S., Cammareri, M., et al. (2017a). Identification, validation and introgression of fruit volatile QTLs from a red-fruited wild tomato species. *J. Exp. Bot.* 68, 4269–4442. doi: 10.1093/jxb/erw455
- Rambla, J. L., Trapero-Mozos, A., Diretto, G., Rubio-Moraga, A., Granell, A., Gómez-Gómez, L., et al. (2016). Gene-metabolite networks of volatile metabolism in airen and Tempranillo grape cultivars revealed a distinct mechanism of aroma bouquet production. *Front. Plant Sci.* 7:1691. doi: 10.3389/fpls.2016.01619
- Raza, S. E., Prince, G., Clarkson, J. P., and Rajpoot, N. M. (2015). Automatic detection of diseased tomato plants using thermal and stereo visible light images. *PLOS ONE* 10:e0123262. doi: 10.1371/journal.pone.0123262
- Reganold, J. P., and Wachter, J. M. (2016). Organic agriculture in the twenty-first century. *Nat. Plants* 2, 1–8. doi: 10.1038/nplants.2015.221
- Ren, C., Liu, X., Zhang, Z., Wang, Y., Duan, W., Li, S., et al. (2016). CRISPR/Cas9-mediated efficient targeted mutagenesis in Chardonnay (*Vitis vinifera* L.). *Sci. Rep.* 6:32289. doi: 10.1038/srep32289
- Riaz, S., Krivanek, A. F., Xu, K., and Walker, M. A. (2006). Refined mapping of the Pierce's disease resistance locus, PdR1, and Sex on an extended genetic map of *Vitis rupestris* × *V. arizonica*. *Theor. Appl. Genet.* 113, 1317–1329. doi: 10.1007/s00122-006-0385-0
- Riaz, S., Tenscher, A. C., Ramming, D. W., and Walker, M. A. (2011). Using a limited mapping strategy to identify major QTLs for resistance to grapevine powdery mildew (*Erysiphe necator*) and their use in marker-assisted breeding. *Theor. Appl. Genet.* 122, 1059–1073. doi: 10.1007/s00122-010-1511-6
- Rinaldi, M., Llorens, J., and Gil, E. (2013). “Electronic characterization of the phenological stages of grapevine using a LIDAR sensor,” in *Precision Agriculture*, Vol. 13. (Wageningen: Academic Publishers), 603–609.
- Rinaldo, A. R., Cavallini, E., Jia, Y., Moss, S. M. A., McDavid, D. A. J., Hooper, L. C., et al. (2015). A grapevine anthocyanin acyltransferase, transcriptionally regulated by VvMYBA, can produce most acylated anthocyanins present in grape skins. *Plant Physiol.* 169, 1897–1916. doi: 10.1104/pp.15.01255
- Roby, J. P., van Leeuwen, C., Gonçalves, E., Graça, A., and Martins, A. (2014). “The preservation of genetic resources of the vine requires cohabitation between institutional clonal selection, mass selection and private clonal selection,” in *BIO Web of Conferences*, Vol. 3. (EDP Sciences).
- Römer, S., Fraser, P. D., Kiano, J. W., Shipton, C. A., Misawa, N., Schuch, W., et al. (2000). Elevation of the provitamin A content of transgenic tomato plants. *Nat. Biotechnol.* 18, 666–669. doi: 10.1038/76523
- Ron, M., Kajala, K., Pauluzzi, G., Wang, D., Reynoso, M. A., Zumstein, K., et al. (2014). Hairy root transformation using *Agrobacterium rhizogenes* as a tool for exploring cell type-specific gene expression and function using tomato as a model. *Plant Physiol.* 166, 455–469. doi: 10.1104/pp.114.239392
- Ronen, G., Carmel-Goren, L., Zamir, D., and Hirschberg, J. (2000). An alternative pathway to β-carotene formation in plant chloroplasts discovered by map-based cloning of Beta and old-gold color mutations in tomato. *Proc. Natl. Acad. Sci. U.S.A.* 97, 11102–11107. doi: 10.1073/pnas.190177497
- Rosati, C., Aquilani, R., Dharmapuri, S., Pallara, P., Marusic, C., Tavazza, R., et al. (2000). Metabolic engineering of beta-carotene and lycopene content in tomato fruit. *Plant J.* 24, 413–419. doi: 10.1046/j.1365-313x.2000.00880.x
- Rosenberg, N. A., Huang, L., Jewett, E. M., Szpiech, Z. A., Jankovic, I., and Boehnke, M. (2010). Genome-wide association studies in diverse populations. *Nat. Rev. Genet.* 11, 356–366. doi: 10.1038/nrg2760

- Rousseau, D., Chéné, Y., Belin, E., Semaan, G., Trigui, G., Boudehri, K., et al. (2015). Multiscale imaging of plants: current approaches and challenges. *Plant Methods* 11, 6. doi: 10.1186/s13007-015-0050-1
- Rousseaux, M. C., Jones, C. M., Adams, D., Chetelat, R., Bennett, A., and Powell, A. (2005). QTL analysis of fruit antioxidants in tomato using *Lycopersicon pennellii* introgression lines. *Theor. Appl. Genet.* 111, 1396–1408. doi: 10.1007/s00122-005-0071-7
- Ruggieri, V., Francese, G., Sacco, A., D'Alessandro, A., Rigano, M. M., Parisi, M., et al. (2014). An association mapping approach to identify favourable alleles for tomato fruit quality breeding. *BMC Plant Biol.* 14:337. doi: 10.1186/s12870-014-0337-9
- Sacco, A., Ruggieri, V., Molisso, M., and Barone, A. (2013). "Omics" approaches in tomato aimed at identifying candidate genes for ascorbic acid accumulation in the fruit. *Afr. J. Biotechnol.* 12, 6791–6800. doi: 10.5897/AJBX12.007
- Sagi, M., Scazzocchio, C., and Fluhr, R. (2002). The absence of molybdenum cofactor sulfuration is the primary cause of the *flacca* phenotype in tomato plants. *Plant J.* 31, 305–317. doi: 10.1046/j.1365-313X.2002.01363.x
- Saito, T., Ariizumi, T., Okabe, Y., Asamizu, E., Hiwasa-Tanase, K., Fukuda, N., et al. (2011). TOMATOMA: a novel tomato mutant database distributing micro-tom mutant collections. *Plant Cell Physiol.* 52, 283–296. doi: 10.1093/pcp/pcr004
- Saliba-Colombani, V., Causse, M., Langlois, D., Philouze, J., and Buret, M. (2001). Genetic analysis of organoleptic quality in fresh market tomato. 1. Mapping QTLs for physical and chemical traits. *Theor. Appl. Genet.* 102, 259–272. doi: 10.1007/s001220051643
- Sankaran, S., Khot, L. R., Espinoza, C. Z., Jarolmasjed, S., Sathuvalli, V. R., Vandemark, G. J., et al. (2015). Low-altitude, high-resolution aerial imaging systems for row and field crop phenotyping: a review. *Eur. J. Agron.* 70, 112–123. doi: 10.1016/j.eja.2015.07.004
- Sanz, R., Rosell, J. R., Llorens, J., Gil, E., and Planas, S. (2013). Relationship between tree row LIDAR-volume and leaf area density for fruit orchards and vineyards obtained with a LIDAR 3D dynamic measurement system. *Agric. For. Meteorol.* 171, 153–162. doi: 10.1016/j.agrformet.2012.11.013
- Sarrion-Perdigones, A., Falconi, E. E., Zandalinas, S. I., Juárez, P., Fernández-del-Carmen, A., Granell, A., et al. (2011). GoldenBraid: An iterative cloning system for standardized assembly of reusable genetic modules. *PLoS ONE* 6:e21622. doi: 10.1371/journal.pone.0021622
- Sarrion-Perdigones, A., Vazquez-Vilar, M., Palaci, J., Castelijns, B., Forment, J., Ziarsolo, P., et al. (2013). GoldenBraid 2.0: a comprehensive DNA assembly framework for plant synthetic biology. *Plant Physiol.* 162, 1618–1631. doi: 10.1104/pp.113.217661
- Sato, S., Tabata, S., Hirakawa, H., Asamizu, E., Shirasawa, K., Isobe, S., et al. (2012). The tomato genome sequence provides insights into fleshy fruit evolution. *Nature* 485, 635–641. doi: 10.1038/nature11119
- Schaart, J. G., van de Wiel, C. C. M., Lotz, L. A. P., and Smulders, M. J. M. (2016). Opportunities for products of new plant breeding techniques. *Trends Plant Sci.* 21, 438–449. doi: 10.1016/j.tpls.2015.11.006
- Schauer, N., Semel, Y., Balbo, I., Steinfath, M., Repsilber, D., Selbig, J., et al. (2008). Mode of inheritance of primary metabolic traits in tomato. *Plant Cell* 20, 509–523. doi: 10.1105/tpc.107.056523
- Schauer, N., Semel, Y., Roessner, U., Gur, A., Balbo, I., Carrari, F., et al. (2006). Comprehensive metabolic profiling and phenotyping of interspecific introgression lines for tomato improvement. *Nat. Biotechnol.* 24, 447–454. doi: 10.1038/nbt1192
- Schauer, N., Zamir, D., and Fernie, A. R. (2005). Metabolic profiling of leaves and fruit of wild species tomato: a survey of the *Solanum lycopersicum* complex. *J. Exp. Bot.* 56, 297–307. doi: 10.1093/jxb/eri057
- Schijlen, E., Ric de Vos, C. H., Jonker, H., van den Broeck, H., Molthoff, J., van Tunen, A., et al. (2006). Pathway engineering for healthy phytochemicals leading to the production of novel flavonoids in tomato fruit. *Plant Biotechnol. J.* 4, 433–444. doi: 10.1111/j.1467-7652.2006.00192.x
- Schreiber, G., Reuveni, M., Evenor, D., Oren-Shamir, M., Ovadia, R., Sapir-Mir, M., et al. (2012). ANTHOCYANIN1 from *Solanum chilense* is more efficient in accumulating anthocyanin metabolites than its *Solanum lycopersicum* counterpart in association with the ANTHOCYANIN FRUIT phenotype of tomato. *Theor. Appl. Genet.* 124, 295–307. doi: 10.1007/s00122-011-1705-6
- Shah, P., Powell, A. L., Orlando, R., Bergmann, C., and Gutierrez Sanchez, G. (2012). Proteomic analysis of ripening tomato fruit infected by *Botrytis cinerea*. *J. Proteome Res.* 11, 2178–2192. doi: 10.1021/pr200965c
- Shalem, O., Sanjana, E. N., Hartenian, E., and Zhang, F. (2014). Genome-scale CRISPR-Cas9 knockout. *Science* 343, 84–88. doi: 10.1126/science.1247
- Shen, J., Tieman, D., Jones, J. B., Taylor, M. G., Schmelz, E., Huffaker, A., et al. (2014). A 13-lipoxygenase, TomloxC, is essential for synthesis of C5 flavour volatiles in tomato. *J. Exp. Bot.* 65, 419–428. doi: 10.1093/jxb/ert382
- Shikata, M., Hoshikawa, K., Ariizumi, T., Fukuda, N., Yamazaki, Y., and Ezura, H. (2016). TOMATOMA update: phenotypic and metabolite information in the micro-tom mutant resource. *Plant Cell Physiol.* 57, e11. doi: 10.1093/pcp/pcv194
- Sim, S. C., Durstewitz, G., Plieske, J., Wieseke, R., Ganal, M. W., van Deynze, A., et al. (2012). Development of a large SNP genotyping array and generation of high-density genetic maps in tomato. *PLoS ONE* 7:e40563. doi: 10.1371/journal.pone.0040563
- Simkin, A. J., Schwartz, S. H., Auldrige, M., Taylor, M. G., and Klee, H. J. (2004). The tomato carotenoid cleavage dioxygenase 1 genes contribute to the formation of the flavor volatiles β-ionone, pseudoionone, and geranylacetone. *Plant J.* 40, 882–892. doi: 10.1111/j.1365-313X.2004.02263.x
- Sozzani, R., Busch, W., Spalding, E., and Benfey, P. (2014). Advanced imaging technique for the study of plant growth and development. *Trends Plant Sci.* 19, 304–310. doi: 10.1016/j.biotechadv.2011.08.021.Secreted
- Speirs, J., Lee, E., Holt, K., Yong-Duk, K., Steelen Scott, N., Loveys, B., et al. (1998). Genetic manipulation of alcohol dehydrogenase levels in ripening tomato fruit affects the balance of some flavor aldehydes and alcohols. *Plant Physiol.* 117, 1047–1058. doi: 10.1104/pp.117.3.1047
- Sprink, T., Metje, J., and Hartung, F. (2015). Plant genome editing by novel tools: TALEN and other sequence specific nucleases. *Curr. Opin. Biotechnol.* 32, 47–53. doi: 10.1016/j.copbio.2014.11.010
- Steiber, A., Hegazi, R., Herrera, M., Landy Zamor, M., Chimanya, K., Pekcan, A. G., et al. (2004). Spotlight on global malnutrition: a continuing challenge in the 21st century. *J. Acad. Nutr. Diet.* 115, 1335–1341. doi: 10.1016/j.jand.2015.05.015
- Sun, Y. D., Liang, Y., Wu, J. M., Li, Y. Z., Cui, X., and Qin, L. (2012). Dynamic QTL analysis for fruit lycopene content and total soluble solid content in a *Solanum lycopersicum* x *S. pimpinellifolium* cross. *Genet. Mol. Res.* 11, 3696–3710. doi: 10.4238/2012.August.17.8
- Tadmor, Y., Fridman, E., Gur, A., Larkov, O., Lastochkin, E., Ravid, U., et al. (2002). Identification of malodorous, a wild species allele affecting tomato aroma that was selected against during domestication. *J. Agric. Food Chem.* 50, 2005–2009. doi: 10.1021/jf011237x
- Tang, H., Sezen, U., and Paterson, A. H. (2010). Domestication and plant genomes. *Curr. Opin. Plant Biol.* 13, 160–166. doi: 10.1016/j.pbi.2009.10.008
- Tanksley, S. D., Grandillo, S., Fulton, T. M., Zamir, D., Eshed, Y., Petiard, V., et al. (1996). Advanced backcross QTL analysis in a cross between an elite processing line of tomato and its wild relative *L. pimpinellifolium*. *Theor. Appl. Genet.* 92, 213–224. doi: 10.1007/BF00223378
- Tanou, G., Job, C., Rajjou, L., Arc, E., Belghazi, M., Diamantidis, G., et al. (2009). Proteomics reveals the overlapping roles of hydrogen peroxide and nitric oxide in the acclimation of citrus plants to salinity. *Plant J.* 60, 795–804. doi: 10.1111/j.1365-313X.2009.04000.x
- Temple, L., Kwa, M., Tetang, J., and Bikoi, A. (2011). Organizational determinant of technological innovation in food agriculture and impacts on sustainable development. *Agron. Sustain. Dev.* 31, 745–755. doi: 10.1007/s13593-011-0017-1
- Thapa, S. P., Miyao, E. M., Davis, R. M., and Coaker, G. (2015). Identification of QTLs controlling resistance to *Pseudomonas syringae* pv. tomato race 1 strains from the wild tomato, *Solanum habrochaites* LA1777. *Theor. Appl. Genet.* 128, 681–692.
- This, P., Lacombe, T., and Thomas, M. R. (2006). Historical origins and genetic diversity of wine grapes. *Trends Genet.* 22, 511–519. doi: 10.1016/j.tig.2006.07.008
- Tieman, D. M., Zeigler, M., Schmelz, E. A., Taylor, M. G., Bliss, P., Kirst, M., et al. (2006). Identification of loci affecting flavour volatile emissions in tomato fruits. *J. Exp. Bot.* 57, 887–896. doi: 10.1093/jxb/erj074
- Tieman, D., Zeigler, M., Schmelz, E., Taylor, M. G., Rushing, S., Jones, J. B., et al. (2010). Functional analysis of a tomato salicylic acid methyl transferase and its role in synthesis of the flavor volatile methyl salicylate. *Plant J.* 62, 113–123. doi: 10.1111/j.1365-313X.2010.04128.x
- Tikunov, Y. M., Molthoff, J., de Vos, R. C. H., Beekwilder, J., van Houwelingen, A., van der Hooft, J. J. J., et al. (2013). Non-smoky glycosyltransferase1 prevents

- the release of smoky aroma from tomato fruit. *Plant Cell* 25, 3067–3078. doi: 10.1105/tpc.113.114231
- Tilman, D., and Clark, M. (2015). Food, agriculture andamp; the environment: can we feed the world andamp; save the earth? *Daedalus* 144, 8–23. doi: 10.1162/DAED_a_00350
- Truco, M. J., Randall, L. B., Bloom, A. J., and St. Clair, D. A. (2000). Detection of QTLs associated with shoot wilting and root ammonium uptake under chilling temperatures in an interspecific backcross population from *Lycopersicon esculentum* × *L. hirsutum*. *Theor. Appl. Genet.* 101, 1082–1092. doi: 10.1007/s001220051583
- Uluisik, S., Chapman, N. H., Smith, R., Poole, M., Adams, G., Gillis, R. B., et al. (2016). Genetic improvement of tomato by targeted control of fruit softening. *Nat. Biotechnol.* 1, 1–11. doi: 10.1038/nbt.3602
- Vadivambal, R., and Jayas, D. S. (2011). Applications of thermal imaging in agriculture and food industry—a review. *Food Bioprocess. Technol.* 4, 186–199. doi: 10.1007/s11947-010-0333-5
- Van der Knaap, E., Lippman, Z. B., and Tanksley, S. D. (2002). Extremely elongated tomato fruit controlled by four quantitative trait loci with epistatic interactions. *Theor. Appl. Genet.* 104, 241–247. doi: 10.1007/s00122-001-0776-1
- Varshney, R. K., Terauchi, R., and McCouch, S. R. (2014). Harvesting the promising fruits of genomics: applying genome sequencing technologies to crop breeding. *PLoS Biol.* 12:e1001883. doi: 10.1371/journal.pbio.1001883
- Vazquez-Vilar, M., Bernabé-Orts, J. M., Fernandez-Del-Carmen, A., Ziarsolo, P., Blanca, J., Granell, A., et al. (2016). A modular toolbox for gRNA-Cas9 genome engineering in plants based on the GoldenBraid standard. *Plant Methods* 12, 10. doi: 10.1186/s13007-016-0101-2
- Velasco, R., Zharkikh, A., Troggio, M., Cartwright, D. A., Cestaro, A., Pruss, D., et al. (2007). A high quality draft consensus sequence of the genome of a heterozygous grapevine variety. *PLoS ONE* 2:e1326. doi: 10.1371/journal.pone.0001326
- Víquez-Zamora, M., Caro, M., Finkers, R., Tikunov, Y., Bovy, A., Visser, R. G., et al. (2014). Mapping in the era of sequencing: high density genotyping and its application for mapping TYLCV resistance in *Solanum pimpinellifolium*. *BMC Genomics* 15:1152. doi: 10.1186/1471-2164-15-1152
- Vogel, B. (2014). Marker assisted selection: a biotechnology for plant breeding without genetic. *Greenpeace Res. Lab.* 59.
- Vogel, J. T., Walter, M. H., Giavalisco, P., Lytovchenko, A., Kohlen, W., Charnikhova, T., et al. (2010). SICCD7 controls strigolactone biosynthesis, shoot branching and mycorrhiza-induced apocarotenoid formation in tomato. *Plant J.* 61, 300–311. doi: 10.1111/j.1365-313X.2009.04056.x
- Walker, A. R., Lee, E., Bogs, J., McDavid, D. A. J., Thomas, M. R., and Robinson, S. P. (2007). White grapes arose through the mutation of two similar and adjacent regulatory genes. *Plant J.* 49, 772–785. doi: 10.1111/j.1365-313X.2006.02997.x
- Wang, Y., Liu, X., Ren, C., Zhong, G.-Y., Yang, L., Li, S., et al. (2016). Identification of genomic sites for CRISPR/Cas9-based genome editing in the *Vitis vinifera* genome. *BMC Plant Biol.* 16:96. doi: 10.1186/s12870-016-0787-3
- Wasson, A. P., Richards, R. A., Chatrath, R., Misra, S. C., Prasad, S. V. S., Rebetzke, G. J., et al. (2012). Traits and selection strategies to improve root systems and water uptake in water-limited wheat crops. *J. Exp. Bot.* 63, 3485–3498. doi: 10.1093/jxb/ers111
- Westengen, O. T., Jeppson, S., and Guarino, L. (2013). Global Ex-Situ crop diversity conservation and the svalbard global seed vault: assessing the current status. *PLoS ONE* 8:e64146. doi: 10.1371/journal.pone.0064146
- Wezel, A., Bellon, S., Doré, T., Francis, C., Vallod, D., and David, C. (2009). Agroecology as a science, a movement and a practice. *Sustain. Agric.* 2, 27–43. doi: 10.1007/978-94-007-0394-0_3
- Wezel, A., Casagrande, M., Celette, F., Vian, J.-F., Ferrer, A., and Peigné, J. (2014). Agroecological practices for sustainable agriculture. A review. *Agron. Sustain. Dev.* 34, 1–20. doi: 10.1007/s13593-013-0180-7
- Xu, K., Riaz, S., Roncoroni, N. C., Jin, Y., Hu, R., Zhou, R., et al. (2008). Genetic and QTL analysis of resistance to Xiphinema index in a grapevine cross. *Theor. Appl. Genet.* 116, 305–311. doi: 10.1007/s00122-007-0670-6
- Xu, X., and Bai, G. (2015). Whole-genome resequencing: changing the paradigms of SNP detection, molecular mapping and gene discovery. *Mol. Breed.* 35, 33. doi: 10.1007/s11032-015-0240-6
- Xu, C., Park, S. J., Van Eck, J., and Lippman, Z. B. (2016). Control of inflorescence architecture in tomato by BTB/POZ transcriptional regulators. *Genes Dev.* 30, 2048–2061. doi: 10.1101/gad.288415.116
- Yang, H., Li, C., Lam, H. M., Clements, J., Yan, G., and Zhao, S. (2015). Sequencing consolidates molecular markers with plant breeding practice. *Theor. Appl. Genet.* 128, 779–795. doi: 10.1007/s00122-015-2499-8
- Yin, Y. G., Kobayashi, Y., Sanuki, A., Kondo, S., Fukuda, N., Ezura, H., et al. (2010). Salinity induces carbohydrate accumulation and sugar-regulated starch biosynthetic genes in tomato (*Solanum lycopersicum* L. cv. "Micro-Tom") fruits in an ABA-and osmotic stress-independent manner. *J. Exp. Bot.* 61, 563–574. doi: 10.1093/jxb/erp333
- Zanor, M. I., Rambla, J. L., Chaib, J., Steppa, A., Medina, A., Granell, A., et al. (2009). Metabolic characterization of loci affecting sensory attributes in tomato allows an assessment of the influence of the levels of primary metabolites and volatile organic contents. *J. Exp. Bot.* 60, 2139–2154. doi: 10.1093/jxb/erp086
- Zhang, J., Zhao, J., Xu, Y., Liang, J., Chang, P., Yan, F., et al. (2015). Genome-wide association mapping for tomato volatiles positively contributing to tomato flavor. *Front. Plant Sci.* 6:1042. doi: 10.3389/fpls.2015.01042
- Zhang, Y., Butelli, E., De Stefano, R., Schoonbeek, H. J., Magusin, A., Pagliarani, C., et al. (2013). Anthocyanins double the shelf life of tomatoes by delaying overripening and reducing susceptibility to gray mold. *Curr. Biol.* 23, 1094–1100. doi: 10.1016/j.cub.2013.04.072
- Zhao, Q., Zhang, H., Wang, T., Chen, S., and Dai, S. (2013). Proteomics-based investigation of salt-responsive mechanisms in plant roots. *J. Proteomics* 82, 230–253. doi: 10.1016/j.jprot.2013.01.024
- Zhong, S., Fei, Z., Chen, Y., Zheng, Y., Huang, M., Vrebalov, J., et al. (2013). Single-base resolution methylomes of tomato fruit development reveal epigenome modifications associated with ripening. *Nat. Biotechnol.* 31, 154–159. doi: 10.1038/nbt.2462
- Zhu, C., Gore, M., Buckler, E. S., and Yu, J. (2008). Status and prospects of association mapping in plants. *Plant Genome* 1, 5–20. doi: 10.3835/plantgenome2008.02.0089
- Zyprian, E., Ochßner, I., Schwander, F., Šimon, S., Hausmann, L., Bonow-Rex, M., et al. (2016). Quantitative trait loci affecting pathogen resistance and ripening of grapevines. *Mol. Genet. Genomics* 291, 1573–1594. doi: 10.1007/s00438-016-1200-5

Conflict of Interest Statement: The authors declare that the research was conducted in the absence of any commercial or financial relationships that could be construed as a potential conflict of interest.

Copyright © 2017 Gascuel, Diretto, Monforte, Fortes and Granell. This is an open-access article distributed under the terms of the Creative Commons Attribution License (CC BY). The use, distribution or reproduction in other forums is permitted, provided the original author(s) or licensor are credited and that the original publication in this journal is cited, in accordance with accepted academic practice. No use, distribution or reproduction is permitted which does not comply with these terms.



DNA Methylation and Chromatin Regulation during Fleshy Fruit Development and Ripening

Philippe Gallusci^{1*}, Charlie Hodgman², Emeline Teyssier¹ and Graham B. Seymour²

¹ EGFV, Bordeaux Sciences Agro, INRA, Université de Bordeaux, Villenave d'Ornon, France, ² School of Biosciences, University of Nottingham, Sutton Bonington, UK

OPEN ACCESS

Edited by:

Antonio Granell,
Consejo Superior de Investigaciones
Científicas, Spain

Reviewed by:

Miyako Kusano,
University of Tsukuba and RIKEN
Center for Sustainable Resource
Science, Japan
Akira Kanazawa,
Hokkaido University, Japan

*Correspondence:

Philippe Gallusci
philippe.gallusci@bordeaux.inra.fr

Specialty section:

This article was submitted to
Plant Physiology,
a section of the journal
Frontiers in Plant Science

Received: 11 February 2016

Accepted: 23 May 2016

Published: 14 June 2016

Citation:

Gallusci P, Hodgman C, Teyssier E
and Seymour GB (2016)
DNA Methylation and Chromatin
Regulation during Fleshy Fruit
Development and Ripening.
Front. Plant Sci. 7:807.
doi: 10.3389/fpls.2016.00807

Fruit ripening is a developmental process that results in the leaf-like carpel organ of the flower becoming a mature ovary primed for dispersal of the seeds. Ripening in fleshy fruits involves a profound metabolic phase change that is under strict hormonal and genetic control. This work reviews recent developments in our understanding of the epigenetic regulation of fruit ripening. We start by describing the current state of the art about processes involved in histone post-translational modifications and the remodeling of chromatin structure and their impact on fruit development and ripening. However, the focus of the review is the consequences of changes in DNA methylation levels on the expression of ripening-related genes. This includes those changes that result in heritable phenotypic variation in the absence of DNA sequence alterations, and the mechanisms for their initiation and maintenance. The majority of the studies described in the literature involve work on tomato, but evidence is emerging that ripening in other fruit species may also be under epigenetic control. We discuss how epigenetic differences may provide new targets for breeding and crop improvement.

Keywords: DNA methylation, epigenetics, ripening, tomato, crop improvement

INTRODUCTION

The fruit is an organ that is unique to the Angiosperms or flowering plants and a true fruit is defined as a mature ovary, although accessory tissues can form the bulk of the fleshy fruit tissue in some cases (Seymour et al., 2013). Ripening in fleshy fruits involves a profound phase change in the leaf-like tissues that encase or are associated with the mature seeds and it can completely alter the metabolic state of a carpel organ or associated tissues. Recent discoveries indicate that ripening is under both strict genetic and epigenetic control.

Epigenetics refers to heritable changes in gene expression that occur without modification of the underlying DNA sequence. It involves histone Post-Translational Modifications (PTMs) and DNA methylation which are transmitted through DNA replication and cell propagation, thereby determining and maintaining cell-type specific gene expression patterns (Vermaak et al., 2003; Chan et al., 2005; Reyes, 2006; Li et al., 2007; Eichten et al., 2014; Pikaard and Mittelsten Scheid, 2014). We do not discuss alterations in small RNA composition or abundance in any detail because the relationship between inherited small RNA levels and fruit development and ripening has been little studied and their general role in plant development has been the subject of recent reviews (for example Borges and Martienssen, 2015). Studies in *Arabidopsis* and other plants, including tomato have demonstrated the relevance of epigenetic mechanisms in the

control of plant developmental processes (Choi et al., 2002; Hsieh and Fischer, 2005; Lauria and Rossi, 2011) and their potential impact on traits of agronomical interest such as flowering time (for a review He G. et al., 2011), heterosis (Dapp et al., 2015), and fleshy fruit ripening (Manning et al., 2006; Zhong et al., 2013; Liu et al., 2015). So far, much of the work analyzing the impact of epigenetic regulation on fleshy fruit quality has been undertaken mainly in tomato (*Solanum lycopersicum*), because this is the model system for investigating the molecular basis of ripening in fleshy fruits. Even in this fruit the extent and role of the epigenetic regulation of ripening is still relatively poorly understood. Here, we review the available literature and identify areas for further investigation. The limited information on the potential role of histone PTMs in fruit development and ripening is discussed, but the review focuses on recent evidence demonstrating that DNA methylation plays a crucial role in ripening. Major questions that need to be addressed include the nature, extent and stability of epigenetic variation that may impact ripening and whether epigenetic control of this process is a common feature of all fruit bearing species. A better understanding of epigenetic control of ripening has the potential to provide novel strategies for generating sources of variation for crop improvement.

HISTONE POST-TRANSLATIONAL MODIFICATIONS MAY HAVE IMPORTANT FUNCTIONS IN FLESHY FRUITS

Post-translational modifications of histones influence chromatin organization and contribute to the epigenetic regulation of gene expression. Histone PTMs include phosphorylation, methylation, acetylation, or ubiquitination and depend on a wide range of enzymes that determine their genome wide distribution and abundance (reviewed in Berr et al., 2011). So far, four major chromatin states, corresponding to specific combinations of 11 different histone PTMs and of DNA methylation, have been determined in *Arabidopsis* that are preferentially associated with active or repressed genes, intergenic regions and transposons (Roudier et al., 2011). These chromatin states appear similar to the situation described in *Drosophila*, although five different chromatin states were defined in this case (Filion et al., 2010). In addition, some marks seem preferentially associated to specific chromatin states. For example, histone acetylation is preferentially linked to gene expression whereas dimethylation at lysine 9 of histone H3 seems to correlate with constitutive heterochromatin and trimethylation of lysine 27 with gene repression (Roudier et al., 2011). There are many enzymes that participate in PTMs and the functions of a few of them are starting to be deciphered, mainly in the model plant *Arabidopsis* (For a review, Berr et al., 2011). In this case, it is becoming clear that histone PTMs are critically important for several aspects of plant development and adaptation to stress (for reviews see Ahmad et al., 2010; Mirouze and Paszkowski, 2011; Eichten et al., 2014), but no direct effect on *Arabidopsis* fruit development has been documented so far.

Several recent studies have described the expression pattern of histone modifiers, including histone deacetylases (HDACs), histone acetyltransferase (HATs), or histone methyl transferases (HMT) in a range of fleshy fruits including apple (Janssen et al., 2008), citrus (Xu et al., 2015a), grape (Aquea et al., 2010, 2011; Almada et al., 2011), and tomato (Cigliano et al., 2013; Zhao et al., 2014). The results indicate that some of the genes involved in histone PTMs are preferentially or specifically expressed in fruits and may present stage preferential expression, suggesting their recruitment for the regulation of fruit development. For example, a few tomato HMT genes, among which those encoding the ENHANCER OF ZESTE [E(z)] proteins, were shown to be expressed during early phases of tomato fruit development (How Kit et al., 2010; Cigliano et al., 2013) suggesting an early programming of chromatin structure necessary for proper fruit development. This is consistent with the functional analysis of the two tomato *SIEZ1* and *SIEZ2* genes which encode the tomato E(z) proteins orthologous to the *Arabidopsis* SWINGER and CURLY LEAF, respectively (How Kit et al., 2010; Boureau et al., 2016). E(z) proteins, together with EXTRA SEX COMB protein, FERTILISATION INDEPENDENT ENDOSPERM DEVELOPMENT (FIE) and the SUPPRESOR OF ZESTE 12; FERTILISATION INDEPENDENT SEED DEVELOPMENT 2 (FIS2) are the core elements of the POLYCOMB REPRESSIVE COMPLEXES 2 (PRC2s, Table 1), that govern transition phases during the development of *Arabidopsis* plants and determine cell type specificity (for a recent review: Mozgova and Hennig, 2015). Knock down of *SIEZ1* had no impact on tomato plant and fruit development, and resulted in alteration of flower shape and development of fruits with a moderate increase in carpel number suggesting that *SIEZ1* is mainly involved in flower formation (How Kit et al., 2010). In contrast, *SIEZ2* repression led to fruits with modified shapes, texture and color, eventually presenting ectopic carpels (Figure 1; Boureau et al., 2016). Color alteration was due to reduced cutin content rather than to changes in carotenoid composition, and these cutin changes also resulted in a rapid shrinking of fruits when left overripe on plants. In addition, ripe *SIEZ2* RNAi fruits were characterized by a high trichome density as compared to WT fruits of the same age consistent with *SIEZ2* being involved in the control of tomato fruit epidermal cell identity. It is noteworthy that, fruit shape, aspects of texture and cutin

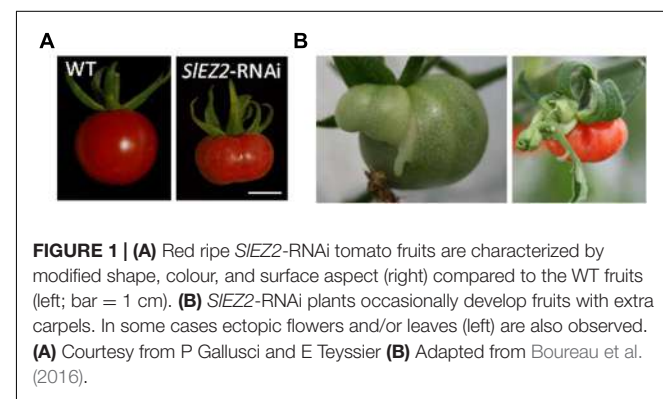


TABLE 1 | Tomato genes encoding the proteins of the Polycomb Repressive Complex 2.

Gene accession (Solgene)	Gene id (NCBI)	Proposed names: actual review	Proposed <i>Arabidopsis</i> ortholog (gene id)	Reference
Solyc01g079390	100134891	SIEZ1	AtSWN (828165)	How Kit et al., 2010
Solyc03g044380	100134892	SIEZ2	AtCLF (816870)	How Kit et al., 2010; Boureau et al., 2016
Solyc02g093190/ Solyc02g093200	101267964	SIEZ3	AtCLF (816870)	How Kit et al., 2010; Boureau et al., 2016
Solyc03g093640	100134887	SIEMF2	AtEMF2 (835198)	
Solyc07g064090	100136877	SIFIE	AtFIE (821622)	

content are dependent on events occurring early during fruit development (Chaib et al., 2007; Mintz-Oron et al., 2008; van der Knaap et al., 2014) and these events occur contemporaneously with the highest expression level of *SIEZ2* (How Kit et al., 2010; Boureau et al., 2016). These results indicate a more prominent role of the *SIEZ2* protein in the control of fruit development and are consistent with polycombs being primarily involved in early stages of fruit development (Boureau et al., 2016). Interestingly, repression of the gene encoding the tomato FIE protein had a stronger effect than either of the *SIEZ* RNAi lines described above and resulted in parthenocarpic fruit development, modified flower and fruit shapes. As FIE is encoded by a unique gene in the tomato genome (Liu et al., 2012; Boureau et al., 2016), this protein is likely to participate in all PRC2 complexes; which may result in effects stronger than those caused by knocking down single *EZ* genes.

Other evidence of chromatin regulation during fruit development and ripening comes from the study of the high pigment mutants in tomato, *hp1* and *hp2*. These are caused by lesions in the genes encoding the UV-damaged DNA binding protein 1 (DDB1) and de-etiolated-1 protein (DET1), respectively, and result in enhanced fruit color and levels of carotenoids in the pericarp (Mustilli et al., 1999; Liu et al., 2004). Both the *DDB1* and *DET1* gene products associate with Cullin 4 (CUL4) to form the CUL4-DDB1-DET1 complex (Chen et al., 2006), which plays a central role in controlling protein degradation. Evidence indicates that DET1 also binds to non-acetylated amino-terminal tails of the core histone H2B in the context of the nucleosome and is likely to be involved in transcriptional repression (Benvenuto et al., 2002; Fisher and Franklin, 2011). Interestingly, a methyl CpG binding domain protein (SIMBD5) was recently shown to physically interact with DDB1 in tomato. Overexpression of *SIMBD5* in tomato plants led to a fruit phenotype similar to the *hp1* loss of function mutant indicating that this protein and DDB1 have antagonistic effects in fruits. DDB1 together with DET1 and CUL4 inhibits gene expression whereas SIMBD5, following its binding to methylated CG, would act as a transcriptional activator (Li et al., 2015). Although the precise mechanisms and targets of the CUL4-DDB1-DET1 complex and SIMBD5 have not been identified yet, these results suggest a complex interplay between histone marks and DNA methylation in the regulation of fruit development and ripening (Li et al., 2015). Indeed, there is also strong evidence that DNA methylation *per se* plays an important role in the control of fruit development and ripening, as discussed below.

DNA METHYLATION IN PLANTS: AN OVERVIEW

Epigenetic modifications involving changes in DNA methylation are the main focus of this review, because these types of changes have been demonstrated to be major regulators of fruit ripening. In eukaryotes, DNA methylation refers to the addition of a methyl group to the carbon 5 of cytosine [5-Methylcytosine (5mC)]. Changes in DNA methylation are associated with a wide range of biological processes such as gene and transposon silencing (Law and Jacobsen, 2010; He G. et al., 2011; He X.-J. et al., 2011). These also include the control of maternal imprinting (FitzGerald et al., 2008; García-Aguilar and Gillmor, 2015) and homologous recombination during meiosis (Mirouze et al., 2012; Yelina et al., 2015). Indeed, plants with experimentally induced hypomethylated genomes present several developmental defects (Finnegan et al., 1996) consistent with DNA methylation being essential for proper plant growth. It is only recently, however, that an understanding of the central role for DNA methylation in controlling traits of agronomical relevance has begun to emerge, among which its role in responses to biotic and abiotic stresses (Baulcombe and Dean, 2014; Probst and Scheid, 2015), heterosis (Shen et al., 2012), and ripening in tomato and other fleshy fruits (Manning et al., 2006; Teyssier et al., 2008; Msogoya et al., 2011; Zhong et al., 2013; Liu et al., 2015; Xu et al., 2015b) are important examples.

Genomic DNA methylation in plants can occur at cytosines in a symmetrical context, CG or CHG, where H is any nucleotide except G or a non-symmetrical context CHH. Cytosine methylation is maintained by a variety of different methyltransferases during DNA replication. Pathways for maintenance of symmetric methylation involve DNA METHYLTRANSFERASE 1 (MET1) which, together with Variant in Methylation proteins 1 and 2 maintains CG methylation (Woo et al., 2008) and CHROMOMETHYLASE (CMT3) which is targeted to specific sequences through its interaction with KRYPTONITE (KYP), SUVH5 and SUVH6, maintains the CHG context (Jackson et al., 2002; Law and Jacobsen, 2010; Du et al., 2014). Asymmetric CHH methylation, which unlike symmetrical methylation, is not found in both daughter DNA molecules, needs an siRNA trigger and requires re-establishment following each cycle of DNA replication and is maintained through persistent *de novo* methylation by the DOMAINS REARRANGED METHYLTRANSFERASE 2

(DRM2) or following a different pathway by CMT2. This requires the nucleosome remodelers DRD1 and DDM1, respectively (**Figure 2**, Kanno et al., 2004; Zemach et al., 2013; Matzke and Mosher, 2014). In the model plant *Arabidopsis*, the mechanism underlying the initiation of methylation marks by DRM2 has been deciphered. This mechanism, known as the RNA-directed DNA methylation (RdDM), is specifically directed at transposons and notably at small and recently acquired transposons in euchromatin. This includes those transposons or repeats in the promoters, introns or coding regions of genes (Matzke and Mosher, 2014). The currently accepted mechanisms of RdDM are summarized in **Figure 3**, and their detailed description is covered in a number of recent publications (Matzke and Mosher, 2014; Bond and Baulcombe, 2015; Matzke et al., 2015).

DNA methylation can also be either lost when active maintenance of DNA methylation is not functional or actively reversed by DNA Glycosylase-Lyases (DNA-GL). DNA-GL, also called DNA demethylases, catalyze the removal of 5mCs which are subsequently replaced by a non-methylated cytosines (**Figure 2**; Gong et al., 2002; Zhu, 2009; Law and Jacobsen, 2010). In *Arabidopsis*, DEMETER, DEMETER-LIKE (DML), and REPRESSOR OF SILENCING 1 (ROS1) recognize and remove methylated cytosines from DNA at specific loci thereby impacting gene expression in developmental processes such as maternal imprinting (Choi et al., 2002; Zhu, 2009; Gehring et al., 2009), male gametophyte development (Schoft et al., 2011), epidermal cell differentiation (Yamamoto et al., 2014) or in response to pathogen attack (Yu et al., 2013). ROS1 activity appears to be regulated through the action of the histone H3 acetyltransferase, INCREASE in DNA METHYLATION 1 (IDM1), an alpha crystallin protein, IDM2, and a Methylcytosine Binding Protein, MBD7 (Qian et al., 2012, 2014; Wang et al., 2015). Recent work has also shown that the final level of DNA methylation is determined by the combined action of both methyltransferases and demethylases in a regulatory loop where *ROS1* gene expression is determined by its methylation level (Lei et al., 2015; Williams et al., 2015).

EPIALLELES CAN GENERATE FLESHY FRUIT PHENOTYPIC VARIATIONS

The potential importance of DNA methylation in sculpting phenotypic variation in tomato was recognized 25 years ago in a study by Messeguer et al. (1991). This study focused on the level, target sites and inheritance of cytosine methylation in nuclear DNA and revealed significant differences in 5mC content between tomato tissues, with highest levels in seeds. Methylation polymorphisms were found between the cultivated tomato (*S. lycopersicum* cv. VF36) and the wild tomato species, *S. pennellii* (LA716) and these polymorphisms were inherited in a normal Mendelian fashion (Messeguer et al., 1991). Hadfield et al. (1993) then reported that a decrease in DNA methylation (DDM) in genes highly expressed in tomato fruits was coincident with the onset of ripening, but the first demonstration that DNA methylation marks could impact ripening was reported in tomato

as a result of the cloning of the gene at the *Colourless non-ripening* (*Cnr*) locus (Manning et al., 2006).

The *Cnr* mutant has a non-ripening phenotype where the fruits turn white and then yellow and remain firm (Thompson et al., 1999). The *Cnr* fruits show none of the usual features associated with ripening such as accumulation of carotenoids in the pericarp, softening, or flavor changes (Thompson et al., 1999; Eriksson et al., 2004). The *CNR* gene was cloned using a genetic map-based approach (Manning et al., 2006). Positional cloning delineated a mapping interval of 13 kb containing the *Cnr* locus. This 13 kb region of tomato chromosome 2 harbored three open reading frames and the regulatory region of a fourth gene model. However, there were no sequence differences between mutant and wild-type genomic DNA within the mapping interval. Only one gene model in the 13 kb interval showed strong differential gene expression between mutant and wild type fruits. This gene encoded a SQUAMOSA Promoter Binding Protein (SBP-box/SPL) transcription factor, which are normally associated with control of the expression of SQUAMOSA class of MADS-box genes (Manning et al., 2006). Further investigation revealed that part of the regulatory region of this gene was hypermethylated in a 286-bp contiguous region 2.4 kb upstream from the first ATG and this epimark only occurred in lines harboring the *Cnr* mutation (Manning et al., 2006). *Cnr* was a spontaneous mutation and this demonstrates that natural methylation polymorphisms can, under certain circumstances, dramatically affect tomato fruit phenotypes, supporting the potential importance of epigenetic variation in this species as postulated earlier by Messeguer et al. (1991).

A range of natural epialleles affecting fruit phenotypes have now been reported in addition to *Cnr* in tomato and in other plants. A gene encoding a 2-methyl-6-phytylquinol methyltransferase underlying a quantitative trait locus (QTL) for vitamin E from the wild tomato species *S. pennellii* was shown to be associated with differential methylation (Quadrana et al., 2014). Both in apples and pears changes in skin color were associated with hypermethylation of the *MYB10* gene promoter region resulting in repression of this gene expression and the absence of anthocyanin accumulation (Telias et al., 2011; Wang et al., 2013; El-Sharkawy et al., 2015). Very recently, it has been reported that methylation of a CACTA transposon underlies the mantled somaclonal variant of oil palm (*Elaeis guineensis*) fruit (Ong-Abdullah et al., 2015) which is characterized by feminization of flower organs and reduced oil yield.

HOW ARE EPIALLELES GENERATED AND MAINTAINED?

Epialles as contributors of phenotypic diversity in plants have been produced in the model plant *Arabidopsis* through the generation of EpiRILs (Epigenetic Recombinant Inbred lines). Crossing of *ddm1* or *met1* mutants, characterized by hypomethylated genomes, with isogenic wild type parents were used to generate an *F₁* progeny which were genetically identical, but with contrasting sets of DNA methylation marks. The EpiRIL populations were obtained from the *F₁* after seven or

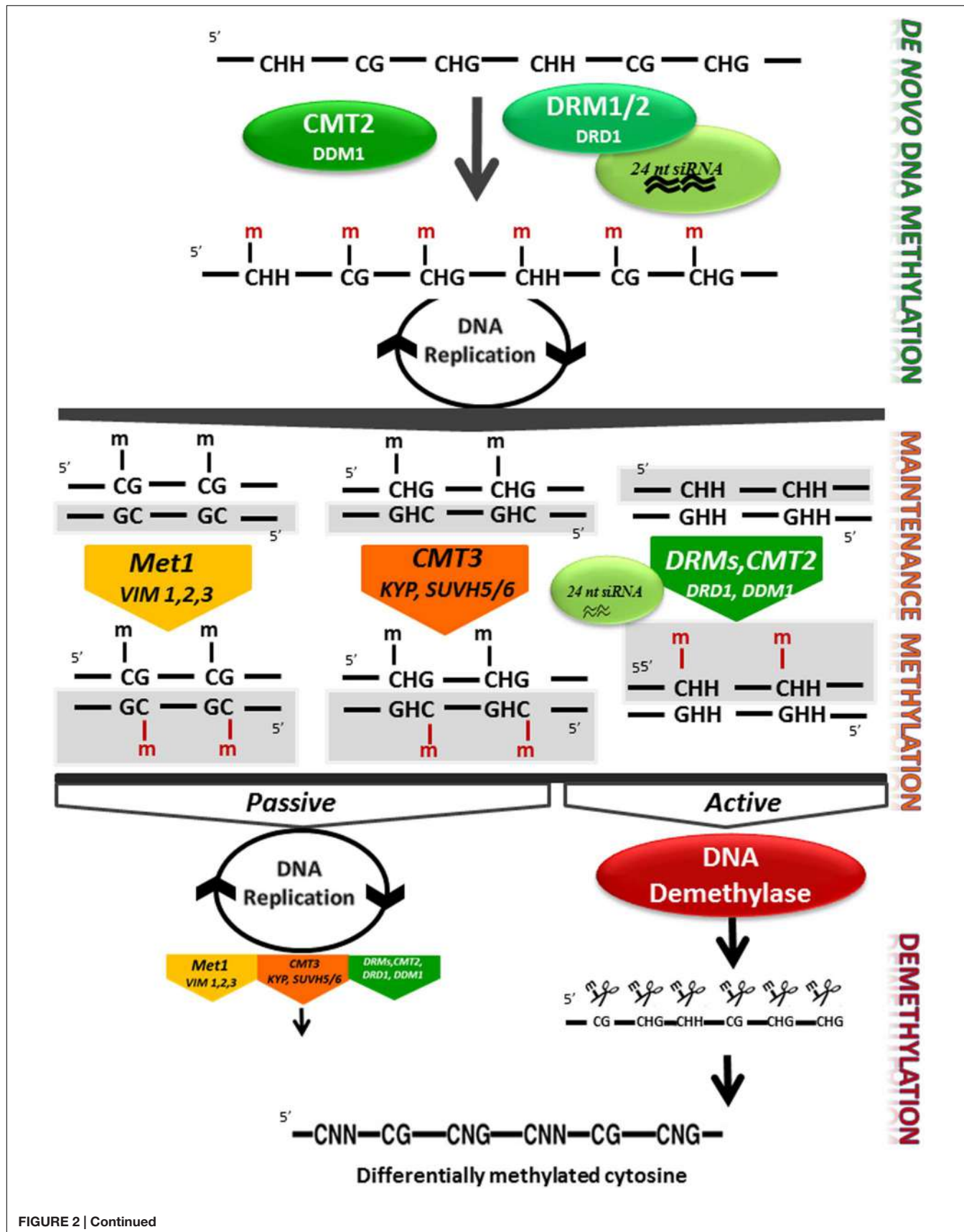


FIGURE 2 | Continued

FIGURE 2 | Continued

DNA methylation control in plants. Methyltransferases and DNA demethylases are involved in 5mC *de novo* methylation, maintenance methylation, and demethylation in higher plants. *De novo* DNA methylation is set up by the RNA directed DNA Methylation (RdDM) pathway involving the DRM1/2 methyltransferases, DRD1 and 24 nt long small RNAs, and by the chromomethylase CMT2 with DDM1 in the CHH sequence context at heterochromatic regions (Zemach et al., 2013). Details of the RdDM pathways are shown in **Figure 3**. After replication, newly produced DNA will be hemi-methylated at CG and CHG symmetrical sites, but at CHH sites one of the two newly synthesized DNA molecules will not be methylated. Maintenance methylation in the CG context depends on MET1 and VIM1, 2 and 3, and maintenance in the CHG context is catalyzed by CMT3. CHH methylation maintenance depends both on the RdDM pathway and on CMT2 activity. Both CMTs are dependent on histone methylation mediated by KYP and SUVH5 and 6. DNA demethylation can occur passively in a replication dependant way, when the methylation machinery is not or poorly active. 5mC cytosine can be actively removed by DNA glycosylase lyase independently from DNA replication. Newly synthesized DNA strands are highlighted in gray. Enzymes names are based on the *Arabidopsis* model. DRM1/2, CMT2/3 (CHROMOMETHYLASE 2/3), MET1 (cytosine-DNA-methyltransferase 1), VIM1-3 (VARIANT IN METHYLATION 1-3), KYP/SUVH4 [KYP/Su-(var)3-9 homolog 4], SUVH5/6 [Su-(var)3-9 homolog 5/6], DRD1 (DEFECTIVE IN RNA-DIRECTED DNA METHYLATION), DDM1 (DECREASE IN DNA METHYLATION), and 24 nt siRNA (24 nucleotide small interfering RNAs).

eight generations of inbreeding leading to the demonstration that experimentally induced epialleles could stably affect plant traits such as flowering time and plant height, although some reversion was observed (Johannes et al., 2009; Teixeira et al., 2009; Cortijo et al., 2014; Hu et al., 2015; Kooke et al., 2015). However, despite the description of several natural epialleles the mechanisms leading to their generation have remained poorly understood so far. Indeed, genome duplications, which are recognized as important engines of evolution in the Angiosperms (Paterson et al., 2010; Rensing, 2014; Vanneste et al., 2014), might, in addition to the generation of spontaneous mutations, result in transposon movement and in new DNA methylation patterns through the RdDM pathway stimulated by genome shock. It has been estimated that in unstressed *Arabidopsis* the rate of spontaneous gains and losses of DNA methylation is 1000 times higher than the genetic mutation. Whether such genome wide changes in DNA methylation patterns can generate new stable epialleles is an appealing possibility that requires further investigation (Matzke and Mosher, 2014; Matzke et al., 2015). Alternatively, epialleles could be generated following interspecific hybridization as suggested by the analysis of hybrids between *S. lycopersicum* and *S. pennellii*. Results show that there were significant changes in DNA methylation and siRNA populations in the progeny (Shivaprasad et al., 2012). These data provided evidence that phenotypic differences generated following interspecific hybridization in tomato could be due to both epigenetic and genetic variation, and may generate stable epialleles. In several cases epialleles occur in the close vicinity of transposable elements (TEs). For example, the event that initiated the *Cnr* mutation although not yet known, may have arisen because of the proximity of the CNR promoter to a Copia-like retrotransposon (Manning et al., 2006) which could direct RdDM to the region of the *Cnr* locus (see work on maize by Gent et al., 2013). Associations between transposon sequences and natural epialleles have also been observed for the *VTE3* gene in tomato (Quadrana et al., 2014), the *FWA* gene in *Arabidopsis* (Lippman et al., 2004), and the *CmWIP1* gene in melon (Martin et al., 2009). All these examples are consistent with the hypothesis that transposons may contribute to the generation of spontaneous epialleles. However, in some cases associations between transposon and natural epialleles were not identified, as for the *CYCLOIDEA* gene in *Linaria vulgaris* (Cubas et al., 1999) and the *MyB A10* gene in pear (Wang et al., 2013) suggesting a diversity of mechanisms being involved in epiallele formation.

The maintenance of many epialleles seems to rely essentially on the normal methylation machinery. Recently Chen et al. (2015) have shown that a CMT that is expressed in developing tomato fruits was up-regulated in the immature fruits of the *Cnr* mutant. Virus induced silencing (VIGS) of this gene in the mutant resulted in increased expression of the *CNR* gene and triggered ripening in the epimutant. VIGS of *SiDRM7*, *SiMET1*, and *SiCMT2* also all had some positive effect on the ripening process in the *Cnr* mutant background. These data indicate that genes involved in DNA maintenance methylation are necessary for the somatic maintenance of this epimutation. A similar observation was made more than a decade ago in *Arabidopsis* by demonstrating that the *clarkent* epiallele of *SUPERMAN* could be reversed by a mutation in the *CMT3* gene (Lindroth et al., 2001). This mutation resulted in a depletion of CHG methylation in *Arabidopsis*, although with no major effect on plant phenotype except for the reversion of the epiallele, demonstrating that the ability to maintain CHG methylation in the superman promoter region was strictly linked to the stability of the epiallele. Mutation of *KYP* a H3 Lys 9 methyltransferase gene had effects similar to mutants in *CMT3* with loss of cytosine methylation at CHG sites and reversion of the *clark kent* epiallele (Jackson et al., 2002). This demonstrated the requirement of *KYP* for CHG maintenance methylation and further illustrates the complex interactions between histone marks and DNA methylation processes (**Figure 3**).

FRUIT RIPENING IN TOMATO INVOLVES MAINTENANCE OF DNA METHYLATION AND REQUIRES ACTIVE DNA DEMETHYLATION

In the tomato genome eight 5mC methyltransferases (MTases) and four DMLs genes have been identified (Teyssier et al., 2008; Cao et al., 2014; Chen et al., 2015; Liu et al., 2015). Comparing the protein coding sequences with those of related genes from *Arabidopsis* allows identification of the likely tomato orthologs of genes such as *MET1* and *ROS1* (**Table 2**). For genes involved in maintenance methylation expression analysis based on microarray data (**Figure 4**)¹ and previous work by Teyssier et al. (2008) indicated that *MET1*, *CMTs*, and several *SiDRMs* are most active during early fruit development while

¹[ftp://ftp.solgenomics.net/microarray/](http://ftp.solgenomics.net/microarray/)

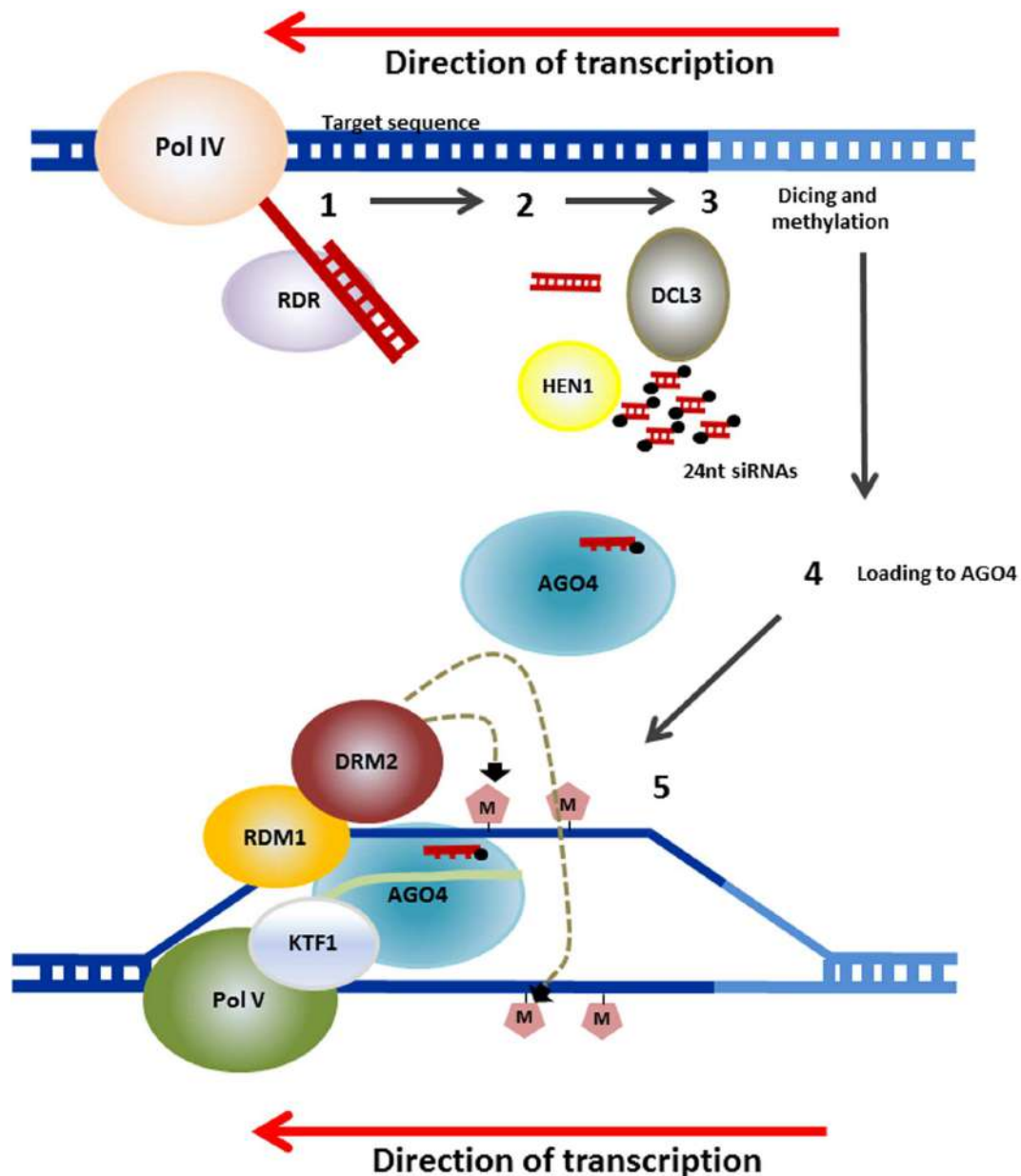


FIGURE 3 | Mechanism for RdDM. RNA transcripts are generated from repetitive sequences (transposons and others) by an RNA polymerase known as Pol IV. RNA-DEPENDENT RNA POLYMERASE (RDR) then converts the RNA to double stranded transcripts. These are processed into 24-nucleotide small RNAs (siRNAs) by DICER-LIKE3 (DCL3). These are methylated at their 3' ends by HUA ENHANCER 1 (HEN1) and the guide strand complementary to the genomic DNA, that will be the target of the RdDM, is incorporated into ARGONAUTE (AGO4). AGO4 is recruited through interactions with Pol V and with KOW DOMAIN-CONTAINING TRANSCRIPTION FACTOR 1 (KTF1). RNA-DIRECTED DNA METHYLATION 1 (RDM1) links AGO4 and DOMAINS REARRANGED METHYLTRANSFERASE 2 (DRM2), which catalyzes *de novo* methylation of DNA (after Matzke and Mosher (2014) and Matzke et al. (2015)). Several mechanisms for RdDM have been reported to deviate from this canonical pathway and these are also described in the latter reviews.

SIDRM7 expression peaks during early phases of fruit ripening. The importance of maintenance methylation in determining the onset of ripening was first suggested by the work of Zhong et al. (2013). They reported that treatment of immature tomato fruit with the methyltransferase inhibitor 5-azacytidine could induce premature ripening. During tomato fruit development several rounds of endoreduplication occurs with cells of mature fruits

reaching 216 to 512 C depending on the variety (Chencllet et al., 2005; Teyssier et al., 2008). Hence, in the absence of maintenance methylation the genomes of fruit pericarp cells would gradually become demethylated resulting in the premature induction of the ripening process. The maintenance of DNA methylation in immature fruits is therefore likely to be necessary to block ripening induction before seed maturation.

TABLE 2 | Tomato DNA methyltransferases and DNA Glycosylase-Lyase (Demethylase).

Gene accession (Solgene)	Gene id (NCBI)	Proposed name: actual review	Arabidopsis ortholog (Gene id)	References
DNA Methyltransferase				
Solyc11g030600	543721	SIMET1	AtMET1 (834975)	Teyssier et al., 2008; Cao et al., 2014; Chen et al., 2015
Solyc12g100330	101267211	SICMT2	AtCMT3 (843313)	Teyssier et al., 2008; Cao et al., 2014; Chen et al., 2015
Solyc01g006100	101265056	SICMT3	AtCMT3 (843313)	Teyssier et al., 2008; Cao et al., 2014; Chen et al., 2015
Solyc08g005400	101244018	SICMT4	AtCMT2 (827640)	Teyssier et al., 2008; Cao et al., 2014; Chen et al., 2015
Solyc02g062740	100135704	SIDRM5	AtDRM2 (831315)	Teyssier et al., 2008; Cao et al., 2014; Chen et al., 2015
Solyc10g078190	101266376	SIDRM6	AtDRM1 (831390)	Teyssier et al., 2008; Cao et al., 2014; Chen et al., 2015
Solyc04g005250	101255191	SIDRM7	AtDRM1 (831390)	Teyssier et al., 2008; Cao et al., 2014; Chen et al., 2015
Solyc05g053260	101267313	SIDRM8	AtDRM3 (820994)	Teyssier et al., 2008; Cao et al., 2014; Chen et al., 2015
Solyc08g067070*		SIDNMT2*	AtDNMT2* (832623)	Teyssier et al., 2008; Cao et al., 2014; Chen et al., 2015
DNA Glycosylase Lyases (DNA demethylase)				
Solyc09g009080	101244311	SIDML1	AtROS1 (818224)	Cao et al., 2014; Liu et al., 2015
Solyc10g083630	101263652	SIDML2	AtROS1 (818224)	Cao et al., 2014; Liu et al., 2015
Solyc11g007580	101252835	SIDML3	AtDEMETER (830335)	Cao et al., 2014; Liu et al., 2015
Solyc03g123440	101251080	SIDML4	ATDML2/AtDML3 (820162)/(829552)	Liu et al., 2015

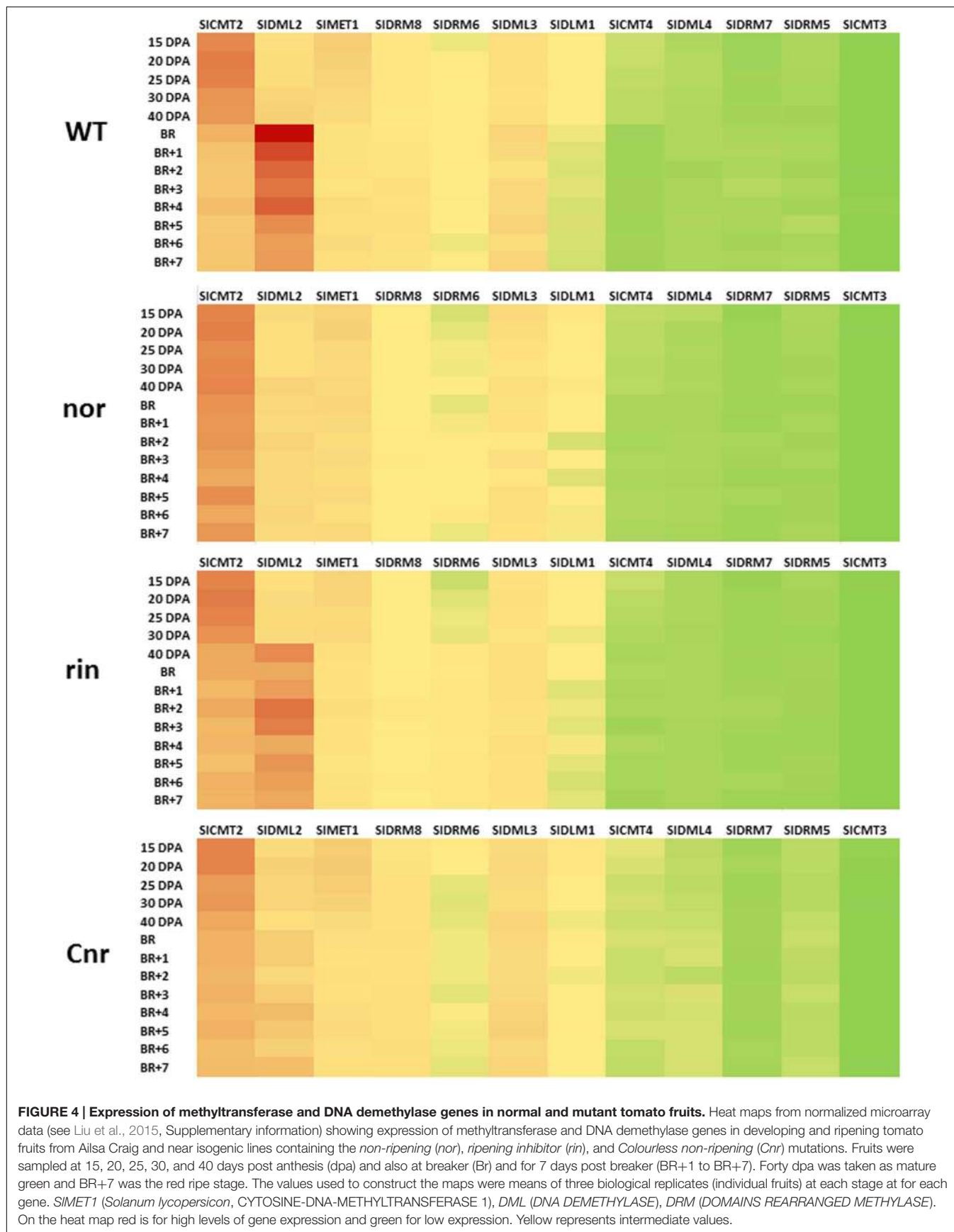
*It is unclear whether DNMT2 is an active DNA methyltransferase in plants.

The importance of DNA demethylation in regulating fruit ripening initially suggested by Hadfield et al. (1993) was highlighted in studies by Teyssier et al. (2008) who showed a 30% decrease of the global DNA methylation levels in tomato pericarp, but not in locular tissues, during tomato fruit maturation. This work suggested tissue specific control of DNA methylation in fruits which is consistent with the tissue dependent differential expression of DNA MTases genes during the development and ripening of fruit tissues (Teyssier et al., 2008). However, the DDM observed in fruit pericarp occurred when cell division and endoreduplication is limited, making unlikely a replication dependent passive loss of DNA methylation (Teyssier et al., 2008, **Figure 4**). This was consistent with locus-specific loss of DNA methylation in ripening-related genes reported by Hadfield et al. (1993) who showed a decrease in methylation at the *POLYGALACTURONASE* (PG) and *CELLULASE* gene promoters at the onset of tomato ripening and more recently similar changes in the CNR promoter in the cultivar Liberto (Manning et al., 2006).

A breakthrough study providing new insights into the importance of DNA demethylation in ripening was reported by Zhong et al. (2013). In a genome wide analysis of DNA methylation in tomato they found dynamic changes in 5mC distribution during fruit development and revealed a loss of 5mC in the promoters of more than 200 ripening-related genes, a list of which can be found in Zhong et al. (2013; Supplementary Tables S10 and S12). These included genes encoding proteins involved in carotenoid accumulation (PHYTOENE SYNTHASE: PSY1; 15-CIS-ZETA-CAROTENE ISOMERASE), in ethylene

synthesis (ACO1, ACS2) and reception (NR, ETR4), in fruit softening (PG; PECTIN METHYLESTERASE: PMEU1), and several transcription factors of various classes (MADS-box, WRKY, or NAC), among which those controlling ripening induction such as RIPENING INHIBITOR (RIN), NON-RIPENING (NOR), COLORLESS NON-RIPENING (CNR), and TAGL1. The differentially methylated regions in these genes were typically adjacent to binding sites for RIN (Zhong et al., 2013), a MADS-box transcription factor that acts as a master regulator of ripening in tomato (Vrebalov et al., 2002). In addition to providing compelling evidence that ripening is governed by epigenetic in addition to genetic and other components, these data indicated that demethylation does not occur in a random way, but is rather targeted at specific sites, again consistent with active DNA demethylation being intimately involved in the ripening process.

Liu et al. (2015) have now been able to demonstrate that active DNA demethylation is the mechanism responsible for the loss in 5mC at the onset of ripening. They showed that among the four potential DNA demethylases found in the tomato genome, there was one gene, SIDML2, which was strongly induced at the onset of ripening concomitantly with the DDM (Teyssier et al., 2008; Zhong et al., 2013). RNAi or VIGS mediated SIDML2 silencing resulted in extremely delayed ripening and ripening defects associated with repression of essential ripening induced transcription factors and of PSY1, which controls carotenoid accumulation during ripening. Silencing of these genes was correlated to the hypermethylation of their promoter regions in contrast to their demethylation in WT fruits. This causal



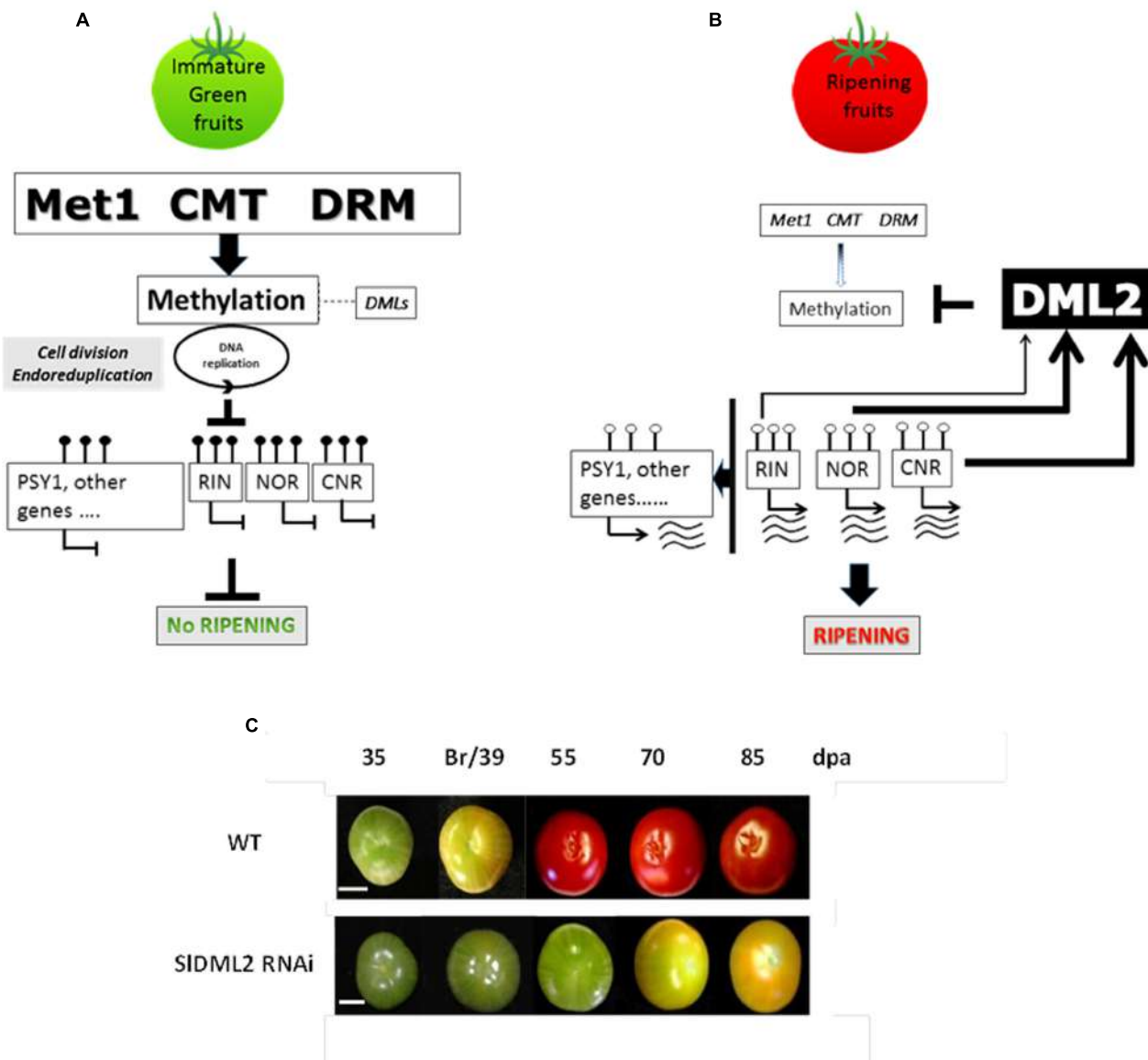


FIGURE 5 | Model of molecular framework linking the induction of ripening with the action of methyltransferases, DNA demethylases and DNA methylation. (A) The *RIN*, *NOR*, and *CNR* genes encode master regulators of ripening. Their expression in immature tomato fruit is inhibited along with that of other ripening genes including *PSY1* by 5mC marks in their regulatory regions. Potential additional targets are listed in the Supplementary Table S10 of Zhong et al. (2013) and include genes involved in ethylene biosynthesis and perception, fruit softening as well as many transcription factors of various classes. These are maintained in immature green fruit. **(B)** However, at the onset of ripening these epi-marks are removed by DNA demethylases. Expression of the *NOR*, *RIN*, and *CNR* genes then occurs and the ripening process is initiated. *SIMET1* (cytosine-DNA-methyltransferase 1), *CMT* (CHROMOMETHYLASE), *DRM*. **(C)** Example of fruits from transgenic RNAi plants affected for *SIDML2* gene expression (adapted from Liu et al., 2015).

relationship between active demethylation and induction of fruit ripening demonstrated that there is an epigenetic layer of control for fruit ripening, at least in tomato.

In addition, *SIDML2* was shown to be down regulated in the *Cnr* and *nor* backgrounds, and to a lower extent in a *rin* background, suggesting a regulatory loop between transcription factors controlling fruit ripening and DNA demethylation (Figure 5). Liu et al. (2015) also reported that the hypermethylation of the genomic DNA of *Cnr* and *rin* fruit

occurred to a level and intensity that was correlated with the repression level of *SIDML2* in the corresponding mutant fruits. The demonstration that *SIDML2* is also repressed in the *nor* mutant background indicates that genomic DNA in this mutant may be hypermethylated to a similar extent as in *Cnr*. It is possible that the ripening defects in *rin*, *nor*, and *Cnr* may, at least in part, be due to limited demethylation in addition to, and as a result of, the absence of these transcription factors. Whether *SICMT2* which is upregulated in *Cnr* during fruit ripening (Figure 4), also

contributes to the hypermethylated phenotype observed in these fruits is so far unclear, as the increase in 5mC levels are not limited to the CHG context normally mediated by CMT enzymes, but occurs in all sequence contexts (Zhong et al., 2013).

CONCLUSION

Recent work on various plants including *Arabidopsis* (Zhang et al., 2006; Zilberman et al., 2007; Cokus et al., 2008), rice (Li et al., 2012), maize (Gent et al., 2013), and tomato (Zhong et al., 2013) has demonstrated that remodeling of epigenomes occurs at various stages during plant development. Indeed, *Arabidopsis* plants with altered control of histones PTMs or hypomethylated genomes present numerous phenotypes consistent with epigenome homeostasis being critically important for proper plant development (Finnegan et al., 1996), but also adaptation to environmental changes (Baulcombe and Dean, 2014). Considering the plethora of enzymes involved in the control of histone PTMs (Kouzarides, 2007; Lauria and Rossi, 2011) and their complex expression patterns in fleshy fruits (Janssen et al., 2008; Aquea et al., 2010, 2011; Almada et al., 2011; Cigliano et al., 2013; Zhao et al., 2014; Xu et al., 2015a), it is very likely that they will be involved in several aspect of this development process. Among them, the H3K27me3mark, established by the Polycomb group proteins, appears to be important at early stages of tomato fruit development (How Kit et al., 2010; Liu et al., 2012; Boureau et al., 2016). Yet, there is still much to do to get a clear understanding of the precise function of histone modifications in fruits as most studies performed so far are correlative, and functional analysis of the histone modifiers is now necessary. It is also unclear to which extent variations in histone PTMs will be stably inherited and impact fruit phenotypes across generations. Alternatively, it is also plausible that genetic diversity of histone modifiers (diversification of gene families) as well as changes in their expression pattern could contribute to shape epigenetic driven phenotypic changes within or between species.

The understanding of the functions of DNA methylation in fleshy fruits is by far more advanced than that relating to histone PTMs, at least in the tomato plant. The results discussed in this review clearly show that fruit ripening is under strict epigenetic control mediated by changes in DNA methylation levels and distribution, in addition to genetic and hormonal controls (for review Gapper et al., 2013). The current model of ripening proposes that active demethylation is necessary to trigger fruit ripening (Figure 5, Liu et al., 2015), and this process should target several hundred of genes as shown by the methylome analysis in ripening fruits (Zhong et al., 2013). Changes in DNA methylation patterns might therefore play a more important role in the control of gene expression during plant developmental processes than anticipated from previous studies mainly based on the *Arabidopsis* model (Eichten et al., 2014). Indeed, when considering DNA methylation *Arabidopsis* may be an “epigenetic exception” with only 5% of methylated cytosine in the genome (Lister et al., 2008) and very few TEs, limiting the likelihood for DNA methylation control of gene

expression. This contrasts with TE and DNA methylation-rich crops that contain more than 20% of methylated cytosines in their genomes (Teyssier et al., 2008; Li et al., 2012; Gent et al., 2013) and high transposon contents (Tenailleon et al., 2010; Lee and Kim, 2014). In addition the distribution of DNA methylation also differs between *Arabidopsis* and other plants including tomato or maize where a substantial proportion of methylation is in the CHH context (Gent et al., 2013; Zhong et al., 2013). Thus DNA methylation may play more important role in plant species with more ‘complex’ genomes as illustrated by its central function in tomato fruit ripening.

In the context of tomato fruits, it is possible to speculate that the regulation of ripening mediated by the DNA methylation/demethylation balance has evolved as a ‘double-lock’ mechanism, along with changes in gene expression as a result of developmental cues, to prevent premature dispersal of seeds prior to their full maturation. It remains now to be determined whether the epigenetic control of ripening has emerged similarly in other types fleshy fruits or is limited to the tomato and related wild species.

In relation to crop improvement and breeding strategies, epi-marks on gene promoter regions could be used for ‘fine tuning’ of gene expression. Examples published for tomato include the biosynthesis of vitamin E and gene expression at the *Cnr* locus. VTE3 gene expression in Andean landraces of tomato (*S. lycopersicum*) and commercial cultivars is related to the extent of methylation in the VTE3 promoter region (Quadrana et al., 2014) and differences in the extent of methylation in the *CNR* promoter are apparent in normally ripening fruits of the cultivars Liberto and Ailsa Craig. Higher levels of expression of *CNR* in Ailsa Craig, in comparison to Liberto, are associated with reduced DNA methylation in a region of the gene upstream of the first ATG (Manning et al., 2006). A comprehensive analysis of the distribution of epi-marks and DNA methylation in tomato and other fruit crops in relation with gene expression profiles and fruit quality traits would likely identify epialleles that could be used as important new targets for plant breeding.

AUTHOR CONTRIBUTIONS

CH provided experimental data and helped write the manuscript. ET helped write the article. PG and GS conceived the review, provided data and wrote the manuscript.

ACKNOWLEDGMENTS

GS acknowledges financial support from the UK Biotechnology and Biological Sciences Research Council and specifically ESB-LINK and TomNet, grant numbers BB/F005458/1 and BB/J015598/1 and support from the European Cooperation in Science and Technology (COST) Action FA1106, ‘An integrated systems approach to determine the developmental mechanisms controlling fleshy fruit quality in tomato and grapevine.’

REFERENCES

- Ahmad, A., Zhang, Y., and Cao, X. F. (2010). Decoding the epigenetic language of plant development. *Mol. Plant* 3, 719–728. doi: 10.1093/mp/ssq026
- Almada, R., Cabrera, N., Casaretto, J. A., Peña-Cortés, H., Ruiz-Lara, S., and Villanueva, E. G. (2011). Epigenetic repressor-like genes are differentially regulated during grapevine (*Vitis vinifera* L.) development. *Plant Cell Rep.* 30, 1959–1968. doi: 10.1007/s00299-011-1104-0
- Aquea, F., Timmermann, T., and Arce-Johnson, P. (2010). Analysis of histone acetyltransferase and deacetylase families of *Vitis vinifera*. *Plant Physiol. Biochem.* 48, 194–199. doi: 10.1016/j.plaphy.2009.12.009
- Aquea, F., Vega, A., Timmermann, T., Poupin, M. J., and Arce-Johnson, P. (2011). Genome-wide analysis of the SET DOMAIN GROUP family in Grapevine. *Plant Cell Rep.* 30, 1087–1097. doi: 10.1007/s00299-011-1015-0
- Baulcombe, D. C., and Dean, C. (2014). Epigenetic regulation in plant responses to the environment. *Cold Spring Harb. Perspect. Biol.* 6:a019471. doi: 10.1101/cshperspect.a019471
- Benvenuto, G., Formiggini, F., Laflamme, P., Malakhov, M., and Bowler, C. (2002). The photomorphogenesis regulator DET1 binds the amino-terminal tail of histone H2B in a nucleosome Context. *Curr. Biol.* 12, 1529–1534. doi: 10.1016/S0960-9822(02)01105-3
- Berr, A., Shafiq, S., and Shen, W. H. (2011). Histone modifications in transcriptional activation during plant development. *Biochim. Biophys. Acta* 1809, 567–576. doi: 10.1016/j.bbagr.2011.07.001
- Bond, D. M., and Baulcombe, D. C. (2015). Epigenetic transitions leading to heritable, RNA-mediated de novo silencing in *Arabidopsis thaliana*. *Proc. Natl. Acad. Sci. U.S.A.* 112, 917–922. doi: 10.1073/pnas.1413053112
- Borges, F., and Martienssen, R. A. (2015). The expanding world of small RNAs in plants. *Nat. Rev. Mol. Cell Biol.* 16, 727–741. doi: 10.1038/nrm4085
- Boureau, L., How-Kit, A., Teyssier, E., Drevensek, S., Rainieri, M., Joubès, J., et al. (2016). A CURLY LEAF homologue controls both vegetative and reproductive development of tomato plants. *Plant Mol. Biol.* 90, 485–501. doi: 10.1007/s11103-016-0436-0
- Cao, D., Ju, Z., Gao, C., Mei, X., Fu, D., Zhu, H., et al. (2014). Genome-wide identification of cytosine-5 DNA methyltransferases and demethylases in *Solanum lycopersicum*. *Gene* 550, 230–237. doi: 10.1016/j.gene.2014.08.034
- Chaïb, J., Devaux, M.-F., Grotte, M.-G., Robini, K., Causse, M., Lahaye, M., et al. (2007). Physiological relationships among physical, sensory, and morphological attributes of texture in tomato fruits. *J. Exp. Bot.* 58, 1915–1925. doi: 10.1093/jxb/erm046
- Chan, S. W. L., Henderson, I. R., and Jacobsen, S. E. (2005). Gardening the genome: DNA methylation in *Arabidopsis thaliana*. *Nat. Rev. Genet.* 6, 351–360. doi: 10.1038/nrg1601
- Chen, H., Shen, Y., Tang, X., Yu, L., Wang, J., Guo, L., et al. (2006). Arabidopsis CULLIN4 forms an E3 ubiquitin ligase with RBX1 and the CDD complex in mediating light control of development. *The Plant Cell* 18, 1991–2004. doi: 10.1105/tpc.106.043224
- Chen, W., Kong, J., Qin, C., Yu, S., Tan, J., Chen, Y.-R., et al. (2015). Requirement of CHROMOMETHYLASE3 for somatic inheritance of the spontaneous tomato epimutation colourless non-ripening. *Sci. Rep.* 5:9192. doi: 10.1038/srep09192
- Cheniclet, C., Rong, W. Y., Causse, M., Frangne, N., Bolling, L., Carde, J. P., et al. (2005). Cell expansion and endoreduplication show a large genetic variability in pericarp and contribute strongly to tomato fruit growth. *Plant Physiol.* 139, 1984–1994. doi: 10.1104/pp.105.068767
- Choi, Y., Gehring, M., Johnson, L., Hannon, M., Harada, J. J., Goldberg, R. B., et al. (2002). DEMETER, a DNA glycosylase domain protein, is required for endosperm gene imprinting and seed viability in *Arabidopsis*. *Cell* 110, 33–42. doi: 10.1016/S0092-8674(02)00807-3
- Cigliano, R. A., Sanseverino, W., Cremona, G., Ercolano, M. R., Conicella, C., and Consiglio, F. M. (2013). Genome-wide analysis of histone modifiers in tomato: gaining an insight into their developmental roles. *BMC Genomics* 14:57. doi: 10.1186/1471-2164-14-57
- Cokus, S. J., Feng, S., Zhang, X., Chen, Z., Merriman, B., Haudenschild, C. D., et al. (2008). Shotgun bisulphite sequencing of the *Arabidopsis* genome reveals DNA methylation patterning. *Nature* 452, 215–219. doi: 10.1038/nature06745
- Cortijo, S., Wardenaar, R., Colomé-Tatché, M., Gilly, A., Etcheverry, M., Labadie, K., et al. (2014). Mapping the epigenetic basis of complex traits. *Science* 343, 1145–1148. doi: 10.1126/science.1248127
- Cubas, P., Vincent, C., and Coen, E. (1999). An epigenetic mutation responsible for natural variation in floral symmetry. *Nature* 401, 157–161. doi: 10.1038/43657
- Dapp, M., Reinders, J., Bédiée, A., Balsera, C., Bucher, E., Theiler, G., et al. (2015). Heterosis and inbreeding depression of epigenetic *Arabidopsis* hybrids. *Nat. Plants* 1:15092. doi: 10.1038/nplants.2015.92
- Du, J., Johnson, L. M., Groth, M., Feng, S., Hale, C. J., Li, S., et al. (2014). Mechanism of DNA methylation-directed histone methylation by KRYPTONITE. *Mol. Cell.* 55, 495–504. doi: 10.1016/j.molcel.2014.06.009
- Eichten, S. R., Schmitz, R. J., and Springer, N. M. (2014). Epigenetics: beyond chromatin modifications and complex genetic regulation. *Plant Physiol.* 165, 933–947. doi: 10.1104/pp.113.234211
- El-Sharkawy, I., Liang, D., and Xu, K. (2015). Transcriptome analysis of an apple (*Malus × domestica*) yellow fruit somatic mutation identifies a gene network module highly associated with anthocyanin and epigenetic regulation. *J. Exp. Bot.* 66, 7359–7376. doi: 10.1093/jxb/erv433
- Eriksson, E. M., Bovy, A., Manning, K., Harrison, L., Andrews, J., De Silva, J., et al. (2004). Effect of the Colorless non-ripening mutation on cell wall biochemistry and gene expression during tomato fruit development and ripening. *Plant Physiol.* 136, 4184–4197. doi: 10.1104/pp.104.045765
- Filion, G. J., van Bemmel, J. G., Braunschweig, U., Talhout, W., Kind, J., Ward, L. D., et al. (2010). Systematic protein location mapping reveals five principal chromatin types in drosophila cells. *Cell* 143, 212–224. doi: 10.1016/j.cell.2010.09.009
- Finnegan, E. J., Peacock, W. J., and Dennis, E. S. (1996). Reduced DNA methylation in *Arabidopsis thaliana* results in abnormal plant development. *Proc. Natl. Acad. Sci. U.S.A.* 93, 8449–8454. doi: 10.1073/pnas.93.16.8449
- Fisher, A. J., and Franklin, K. A. (2011). Chromatin remodelling in plant light signalling. *Physiol. Plant.* 142, 305–313. doi: 10.1111/j.1399-3054.2011.01476.x
- FitzGerald, J., Luo, M., Chaudhury, A., and Berger, F. (2008). DNA methylation causes predominant maternal controls of plant embryo growth. *PLoS ONE* 3:e2298. doi: 10.1371/journal.pone.00002298
- Gapper, N. E., McQuinn, R. P., and Giovannoni, J. J. (2013). Molecular and genetic regulation of fruit ripening. *Plant Mol. Biol.* 82, 575–591. doi: 10.1007/s11103-013-0050-3
- García-Aguilar, M., and Gillmor, C. S. (2015). Zygotic genome activation and imprinting: parent-of-origin gene regulation in plant embryogenesis. *Curr. Opin. Plant Biol.* 27, 29–35. doi: 10.1016/j.pbi.2015.05.020
- Gehring, M., Reik, W., and Henikoff, S. (2009). DNA demethylation by DNA repair. *Trends Genet.* 25, 82–90. doi: 10.1016/j.tig.2008.12.001
- Gent, J. I., Ellis, N. A., Guo, L., Harkess, A. E., Yao, Y., Zhang, X., et al. (2013). CHH islands: de novo DNA methylation in near-gene chromatin regulation in maize. *Genome Res.* 23, 628–637. doi: 10.1101/gr.146985.112
- Gong, Z., Morales-Ruiz, T., Ariza, R. R., Roldán-Arjona, T., David, L., and Zhu, J. K. (2002). ROS1, a repressor of transcriptional gene silencing in *Arabidopsis*, encodes a DNA glycosylase/lyase. *Cell* 111, 803–814. doi: 10.1016/S0092-8674(02)01133-9
- Hadfield, K. A., Dandekar, A. M., and Romani, R. J. (1993). Demethylation of ripening specific genes in tomato fruit. *Plant Sci.* 92, 13–18. doi: 10.1016/0168-9452(93)90061-4
- He, G., Elling, A. A., and Deng, X. W. (2011). The epigenome and plant development. *Annu. Rev. Plant Biol.* 62, 411–435. doi: 10.1146/annurev.applant-042110-103806
- He, X.-J., Chen, T., and Zhu, J.-K. (2011). Regulation and function of DNA methylation in plants and animals. *Cell Res.* 21, 442–465. doi: 10.1038/cr.2011.23
- How Kit, A. H., Boureau, L., Stammiotti-Bert, L., Rolin, D., Teyssier, E., and Gallusci, P. (2010). Functional analysis of SIEZ1 a tomato Enhancer of zeste (E (z)) gene demonstrates a role in flower development. *Plant Mol. Biol.* 74, 201–213. doi: 10.1007/s11103-010-9657-9
- Hsieh, T. F., and Fischer, R. L. (2005). Biology of chromatin dynamics. *Annu. Rev. Plant Biol.* 56, 327–351. doi: 10.1146/annurev.applant.56.032604.144118
- Hu, Y., Morota, G., Rosa, G. J., and Gianola, D. (2015). Prediction of plant height in *Arabidopsis thaliana* using DNA methylation data. *Genetics* 201, 779–793. doi: 10.1534/genetics.115.177204
- Jackson, J. P., Lindroth, A. M., Cao, X., and Jacobsen, S. E. (2002). Control of CpNpG DNA methylation by the KRYPTONITE histone H3 methyltransferase. *Nature* 416, 556–560. doi: 10.1038/nature731

- Janssen, B. J., Thodey, K., Schaffer, R. J., Alba, R., Balakrishnan, L., Bishop, R., et al. (2008). Global gene expression analysis of apple fruit development from the floral bud to ripe fruit. *BMC Plant Biol.* 8:16. doi: 10.1186/1471-2229-8-16
- Johannes, F., Porcher, E., Teixeira, F. K., Saliba-Colombani, V., Simon, M., Agier, N., et al. (2009). Assessing the impact of transgenerational epigenetic variation on complex traits. *PLoS Genet.* 5:e1000530. doi: 10.1371/journal.pgen.1000530
- Kanno, T., Mette, M. F., Kreil, D. P., Aufsatz, W., Matzke, M., and Matzke, A. J. (2004). Involvement of putative SNF2 chromatin remodeling protein DRD1 in RNA-directed DNA methylation. *Curr. Biol.* 14, 801–805. doi: 10.1016/j.cub.2004.04.037
- Kooke, R., Johannes, F., Wardenaar, R., Becker, F., Etcheverry, M., Colot, V., et al. (2015). Epigenetic basis of morphological variation and phenotypic plasticity in *Arabidopsis thaliana*. *Plant Cell* 27, 337–348. doi: 10.1105/tpc.114.114205
- Kouzarides, T. (2007). Chromatin modifications and their function. *Cell* 128, 693–705. doi: 10.1016/j.cell.2007.02.005
- Lauria, M., and Rossi, V. (2011). Epigenetic control of gene regulation in plants. *Biochim. Biophys. Acta* 1809, 369–378. doi: 10.1016/j.bbaprm.2011.03.002
- Law, J. A., and Jacobsen, S. E. (2010). Establishing, maintaining and modifying DNA methylation patterns in plants and animals. *Nat. Rev. Genet.* 11, 204–220. doi: 10.1038/nrg2719
- Lee, S. I., and Kim, N. S. (2014). Transposable elements and genome size variations in plants. *Genomics Inform.* 12, 87–97. doi: 10.5808/GI.2014.12.3.87
- Lei, M., Zhang, H., Julian, R., Tang, K., Xie, S., and Zhu, J. K. (2015). Regulatory link between DNA methylation and active demethylation in *Arabidopsis*. *Proc. Natl. Acad. Sci. U.S.A.* 112, 3553–3557. doi: 10.1073/pnas.1502279112
- Li, B., Carey, M., and Workman, J. L. (2007). The role of chromatin during transcription. *Cell* 128, 707–719. doi: 10.1016/j.cell.2007.01.015
- Li, X., Zhu, J., Hu, F., Ge, S., Ye, M., Xiang, H., et al. (2012). Single-base resolution maps of cultivated and wild rice methylomes and regulatory roles of DNA methylation in plant gene expression. *BMC Genomics* 13:300. doi: 10.1186/1471-2164-13-300
- Li, Y., Deng, H., Miao, M., Li, H., Huang, S., Wang, S., et al. (2015). Tomato MBD5, a methyl CpG binding domain protein, physically interacting with UV-damaged DNA binding protein-1, functions in multiple processes. *New Phytol.* 210, 208–226. doi: 10.1111/nph.13745
- Lindroth, A. M., Cao, X., Jackson, J. P., Zilberman, D., McCallum, C. M., Henikoff, S., et al. (2001). Requirement of CHROMOMETHYLASE3 for maintenance of CpXpG methylation. *Science* 292, 2077–2080. doi: 10.1126/science.1059745
- Lippman, Z., Gendrel, A. V., Black, M., Vaughn, M. W., Dedhia, N., McCombie, W. R., et al. (2004). Role of transposable elements in heterochromatin and epigenetic control. *Nature* 430, 471–476. doi: 10.1038/nature02651
- Lister, R., O’Malley, R. C., Toniati-Filippini, J., Gregory, B. D., Berry, C. C., Millar, A. H., et al. (2008). Highly integrated single-base resolution maps of the epigenome in *Arabidopsis*. *Cell* 133, 523–536. doi: 10.1016/j.cell.2008.03.029
- Liu, D.-D., Dong, Q.-L., Fang, M.-J., Chen, K.-Q., and Hao, Y.-J. (2012). Ectopic expression of an apple apomixis-related gene *Mhf1E* induces co-suppression and results in abnormal vegetative and reproductive development in tomato. *J. Plant physiol.* 169, 1866–1873. doi: 10.1016/j.jplph.2012.07.018
- Liu, R., How-Kit, A., Stammitti, L., Teyssier, E., Rolin, D., Mortain-Bertrand, A., et al. (2015). A DEMETER-like DNA demethylase governs tomato fruit ripening. *Proc. Natl. Acad. Sci. U.S.A.* 112, 10804–10809. doi: 10.1073/pnas.1503362112
- Liu, Y., Roof, S., Ye, Z., Barry, C., van Tuinen, A., Vrebalov, J., et al. (2004). Manipulation of light signal transduction as a means of modifying fruit nutritional quality in tomato. *Proc. Natl. Acad. Sci. U.S.A.* 101, 9897–9902. doi: 10.1073/pnas.0400935101
- Manning, K., Tör, M., Poole, M., Hong, Y., Thompson, A. J., King, G. J., et al. (2006). A naturally occurring epigenetic mutation in a gene encoding an SBP-box transcription factor inhibits tomato fruit ripening. *Nat. Genet.* 38, 948–952. doi: 10.1038/ng1841
- Martin, A., Troadec, C., Boualem, A., Rajab, M., Fernandez, R., Morin, H., et al. (2009). A transposon-induced epigenetic change leads to sex determination in melon. *Nature* 461, 1135–1138. doi: 10.1038/nature08498
- Matzke, M. A., Kanno, T., and Matzke, A. J. M. (2015). RNA-directed DNA methylation: the evolution of a complex epigenetic pathway in flowering plants. *Ann. Rev. Plant Biol.* 66, 243–267. doi: 10.1146/annurev-arplant-043014-114633
- Matzke, M. A., and Mosher, R. A. (2014). RNA-directed DNA methylation: an epigenetic pathway of increasing complexity. *Nat. Rev. Genet.* 15, 394–408. doi: 10.1038/nrg3683
- Messeguer, R., Ganal, M., Steffens, J., and Tanksley, S. D. (1991). Characterization of the level, target sites and inheritance of cytosine methylation in tomato nuclear DNA. *Plant Mol. Biol.* 16, 753–770. doi: 10.1007/BF00015069
- Mintz-Oron, S., Mandel, T., Rogachev, I., Feldberg, L., Lotan, O., Yativ, M., et al. (2008). Gene expression and metabolism in tomato fruit surface tissues. *Plant Physiol.* 147, 823–851. doi: 10.1104/pp.108.116004
- Mirouze, M., Lieberman-Lazarovich, M., Aversano, R., Bucher, E., Nicolet, J., Reinders, J., et al. (2012). Loss of DNA methylation affects the recombination landscape in *Arabidopsis*. *Proc. Natl. Acad. Sci. U.S.A.* 109, 5880–5885. doi: 10.1073/pnas.1120841109
- Mirouze, M., and Paszkowski, J. (2011). Epigenetic contribution to stress adaptation in plants. *Curr. Opin. Plant Biol.* 14, 267–274. doi: 10.1016/j.pbi.2011.03.004
- Mozgova, I., and Hennig, L. (2015). The polycomb group protein regulatory network. *Annu. Rev. Plant Biol.* 66, 269–296. doi: 10.1146/annurev-arplant-043014-115627
- Msogoya, T. J., Grout, B. W., and Roberts, A. (2011). Reduction in genome size and DNA methylation alters plant and fruit development in tissue culture induced off-type banana (*Musa* spp.). *J. Anim. Plant Sci.* 3, 1450–1456.
- Mustilli, A. C., Fenzi, F., Ciliento, R., Alfano, F., and Bowler, C. (1999). Phenotype of the tomato high pigment-2 mutant is caused by a mutation in the tomato homolog of DEETIOLATED1. *Plant Cell* 11, 145–157. doi: 10.1105/tpc.11.2.145
- Ong-Abdullah, M., Ordway, J. M., Jiang, N., Ooi, S., Kok, S.-Y., Sarpan, N., et al. (2015). Loss of Karma transposon methylation underlies the mantled somaclonal variant of oil palm. *Nature* 525, 533–537. doi: 10.1038/nature15365
- Paterson, A. H., Freeling, M., Tang, H., and Wang, X. (2010). Insights from the comparison of plant genome sequences. *Annu. Rev. Plant Biol.* 61, 349–372. doi: 10.1146/annurev-arplant-042809-112235
- Pikaard, C. S., and Mittelsten Scheid, O. (2014). Epigenetic regulation in plants. *Cold Spring Harb. Perspect. Biol.* 6:a019315. doi: 10.1101/cshperspect.a019315
- Probst, A. V., and Scheid, O. M. (2015). Stress-induced structural changes in plant chromatin. *Curr. Opin. Plant Biol.* 27, 8–16. doi: 10.1016/j.pbi.2015.05.011
- Qian, W., Miki, D., Lei, M., Zhu, X., Zhang, H., Liu, Y., et al. (2014). Regulation of active DNA demethylation by an alpha-crystallin domain protein in *Arabidopsis*. *Mol. Cell.* 55, 361–371. doi: 10.1016/j.molcel.2014.06.008
- Qian, W., Miki, D., Zhang, H., Liu, Y., Zhang, X., Tang, K., et al. (2012). A histone acetyltransferase regulates active DNA demethylation in *Arabidopsis*. *Science* 336, 1445–1448. doi: 10.1126/science.1219416
- Quadrana, L., Almeida, J., Asís, R., Duffy, T., Dominguez, P. G., Bermúdez, L., et al. (2014). Natural occurring epialleles determine vitamin E accumulation in tomato fruits. *Nat. Commun.* 5:4027. doi: 10.1038/ncomms5027
- Rensing, S. A. (2014). Gene duplication as a driver of plant morphogenetic evolution. *Curr. Opin. Plant Biol.* 17, 43–48. doi: 10.1016/j.pbi.2013.11.002
- Reyes, J. C. (2006). Chromatin modifiers that control plant development. *Curr. Opin. Plant Biol.* 9, 21–27. doi: 10.1016/j.pbi.2005.11.010
- Roudier, F., Ahmed, I., Berard, C., Sarazin, A., Mary-Huard, T., Cortijo, S., et al. (2011). Integrative epigenomic mapping defines four main chromatin states in *Arabidopsis*. *EMBO J.* 30, 1928–1938. doi: 10.1038/emboj.2011.103
- Schoft, V. K., Chumaka, N., Choi, Y., Hannom, M., García-Aguilar, M., Machlicovaa, A., et al. (2011). Function of the DEMETER DNA glycosylase in the *Arabidopsis thaliana* male gametophyte. *Proc. Natl. Acad. Sci. U.S.A.* 108, 8042–8047. doi: 10.1073/pnas.1105117108
- Seymour, G. B., Østergaard, L., Chapman, N. H., Knapp, S., and Martin, C. (2013). Fruit development and ripening. *Annu. Rev. Plant Biol.* 64, 219–241. doi: 10.1146/annurev-arplant-050312-120057
- Shen, H., He, H., Li, J., Chen, W., Wang, X., Guo, L., et al. (2012). Genome-wide analysis of DNA methylation and gene expression changes in two *Arabidopsis* ecotypes and their reciprocal hybrids. *Plant Cell* 24, 875–892. doi: 10.1105/tpc.111.094870
- Shivaprasad, P. V., Dunn, R. M., Santos, B. A., Bassett, A., and Baulcombe, D. C. (2012). Extraordinary transgressive phenotypes of hybrid tomato are

- influenced by epigenetics and small silencing RNAs. *EMBO J.* 31, 257–266. doi: 10.1038/emboj.2011.458
- Teixeira, F. K., Heredia, F., Sarazin, A., Roudier, F., Boccara, M., Ciaudo, C., et al. (2009). A role for RNAi in the selective correction of DNA methylation defects. *Science* 323, 1600–1604. doi: 10.1126/science.1165313
- Telias, A., Lin-Wang, K., Stevenson, D. E., Cooney, J. M., Hellens, R. P., Allan, A. C., et al. (2011). Apple skin patterning is associated with differential expression of MYB10. *BMC Plant Biol.* 11:93. doi: 10.1186/1471-2229-11-93
- Tenaillon, M. I., Hollister, J. D., and Gaut, B. S. (2010). A triptych of the evolution of plant transposable elements. *Trends Plant Sci.* 15, 471–478. doi: 10.1016/j.tplants.2010.05.003
- Teyssier, E., Bernacchia, G., Maury, S., How Kit, A., Stammitti-Bert, L., Rolin, D., et al. (2008). Tissue dependent variations of DNA methylation and endoreduplication levels during tomato fruit development and ripening. *Planta* 228, 391–399. doi: 10.1007/s00425-008-0743-z
- Thompson, A. J., Tor, M., Barry, C. S., Vrebalov, J., Orfila, C., Jarvis, M. C., et al. (1999). Molecular and genetic characterization of a novel pleiotropic tomato-ripening mutant. *Plant Physiol.* 120, 383–390. doi: 10.1104/pp.120.2.383
- van der Knaap, E., Chakrabarti, M., Chu, Y. H., Clevenger, J. P., Illa-Berenguer, E., Huang, Z., et al. (2014). What lies beyond the eye: the molecular mechanisms regulating tomato fruit weight and shape. *Front. Plant Sci.* 5:227. doi: 10.3389/fpls.2014.00227
- Vanneste, K., Baele, G., Maere, S., and Van de Peer, Y. (2014). Analysis of 41 plant genomes supports a wave of successful genome duplications in association with the Cretaceous-Paleogene boundary. *Genome Res.* 24, 1334–1347. doi: 10.1101/gr.168997.113
- Vermaak, D., Ahmad, K., and Henikoff, S. (2003). Maintenance of chromatin states: an open-and-shut case. *Curr. Opin. Cell Biol.* 15, 266–274. doi: 10.1016/S0955-0674(03)00043-7
- Vrebalov, J., Ruezinsky, D., Padmanabhan, V., White, R., Medrano, D., Drake, R., et al. (2002). A MADS-box gene necessary for fruit ripening at the tomato ripening-inhibitor (Rin) locus. *Science* 296, 343–346. doi: 10.1126/science.1068181
- Wang, C., Dong, X., Jin, D., Zhao, Y., Xie, S., Li, X., et al. (2015). Methyl-CpG-binding domain protein MBD7 is required for active DNA demethylation in *Arabidopsis*. *Plant Physiol.* 167, 905–914. doi: 10.1104/pp.114.252106
- Wang, Z., Meng, D., Wang, A., Li, T., Jiang, S., Cong, P., et al. (2013). The methylation of the PcMYB10 promoter is associated with green-skinned sport in Max Red Bartlett pear. *Plant Physiol.* 162, 885–896. doi: 10.1104/pp.113.214700
- Williams, B. P., Pignatta, D., Henikoff, S., and Gehring, M. (2015). Methylation-sensitive expression of a DNA demethylase gene serves as an epigenetic rheostat. *PLoS Genet.* 11:e1005142. doi: 10.1371/journal.pgen.1005142
- Woo, H. R., Dittmer, T. A., and Richards, E. J. (2008). Three SRA-domain methylcytosine-binding proteins cooperate to maintain global CpG methylation and epigenetic silencing in *Arabidopsis*. *PLoS Genet.* 4:e1000156. doi: 10.1371/journal.pgen.1000156
- Xu, J., Xu, H., Liu, Y., Wang, X., Xu, Q., and Deng, X. (2015a). Genome-wide identification of sweet orange (*Citrus sinensis*) histone modification gene families and their expression analysis during the fruit development and fruit-blue mold infection process. *Front. Plant Sci.* 6:607. doi: 10.3389/fpls.2015.00607
- Xu, J., Xu, H., Xu, Q., and Deng, X. (2015b). Characterization of DNA Methylation variations during fruit development and ripening of sweet orange. *Plant Mol. Biol. Reporter* 33, 1–11. doi: 10.1007/s11105-014-0732-2
- Yamamoto, C., Miki, D., Zheng, Z., Ma, J., Wang, J., Yang, Z., et al. (2014). Overproduction of stomatal lineage cells in *Arabidopsis* mutants defective in active DNA demethylation. *Nat. Commun.* 5:462. doi: 10.1038/ncomms5062
- Yelina, N. E., Lambing, C., Hardcastle, T. J., Zhao, X., Santos, B., and Henderson, I. R. (2015). DNA methylation epigenetically silences crossover hot spots and controls chromosomal domains of meiotic recombination in *Arabidopsis*. *Genes Dev.* 29, 2183–2202. doi: 10.1101/gad.270876.115
- Yu, A., Lepère, G., Jay, F., Wang, J., Bapaume, L., Wang, Y., et al. (2013). Dynamics and biological relevance of DNA demethylation in *Arabidopsis* antibacterial defense. *Proc. Natl. Acad. Sci. U.S.A.* 110, 2389–2394. doi: 10.1073/pnas.1211757110
- Zemach, A., Kim, M. Y., Hsieh, P. H., Coleman-Derr, D., Eshed-Williams, L., Thao, K., et al. (2013). The *Arabidopsis* nucleosome remodeler DDM1 allows DNA methyltransferases to access H1-containing heterochromatin. *Cell* 153, 193–205. doi: 10.1016/j.cell.2013.02.033
- Zhang, X., Yazaki, J., Sundaresan, A., Cokus, S., Chan, S. W. L., Chen, H., et al. (2006). Genome-wide high-resolution mapping and functional analysis of DNA methylation in *Arabidopsis*. *Cell* 126, 1189–1201. doi: 10.1016/j.cell.2006.08.003
- Zhao, L., Lu, J., Zhang, J., Wu, P. Y., Yang, S., and Wu, K. (2014). Identification and characterization of histone deacetylases in tomato (*Solanum lycopersicum*). *Front. Plant Sci.* 5:760. doi: 10.3389/fpls.2014.00760
- Zhong, S., Fei, Z., Chen, Y.-R., Zheng, Y., Huang, M., Vrebalov, J., et al. (2013). Single-base resolution methylomes of tomato fruit development reveal epigenome modifications associated with ripening. *Nat. Biotechnol.* 31, 154–159. doi: 10.1038/nbt.2462
- Zhu, J. K. (2009). Active DNA demethylation mediated by DNA glycosylases. *Annu. Rev. Genet.* 43, 143–166. doi: 10.1146/annurev-genet-102108-134205
- Zilberman, D., Gehring, M., Tran, R. K., Ballinger, T., and Henikoff, S. (2007). Genome-wide analysis of *Arabidopsis thaliana* DNA methylation uncovers an interdependence between methylation and transcription. *Nat. Genet.* 39, 61–69. doi: 10.1038/ng1929

Conflict of Interest Statement: The authors declare that the research was conducted in the absence of any commercial or financial relationships that could be construed as a potential conflict of interest.

Copyright © 2016 Gallusci, Hodgman, Teyssier and Seymour. This is an open-access article distributed under the terms of the Creative Commons Attribution License (CC BY). The use, distribution or reproduction in other forums is permitted, provided the original author(s) or licensor are credited and that the original publication in this journal is cited, in accordance with accepted academic practice. No use, distribution or reproduction is permitted which does not comply with these terms.



Fruit Calcium: Transport and Physiology

Bradleigh Hocking^{1,2}, Stephen D. Tyerman¹, Rachel A. Burton² and Matthew Gillham^{1*}

¹ Plant Transport and Signaling Laboratory, ARC Centre of Excellence in Plant Energy Biology, School of Agriculture, Food and Wine, Waite Research Institute, University of Adelaide, Glen Osmond, SA, Australia, ² ARC Centre of Excellence in Plant Cell Walls, School of Agriculture, Food and Wine, Waite Research Institute, University of Adelaide, Glen Osmond, SA, Australia

OPEN ACCESS

Edited by:

Mario Pezzotti,
University of Verona, Italy

Reviewed by:

Serge Delrot,
University of Bordeaux, France
Cristos Xiloyannis,
University of Basilicata, Italy

***Correspondence:**

Matthew Gillham
matthew.gillham@adelaide.edu.au

Specialty section:

This article was submitted to
Plant Physiology,
a section of the journal
Frontiers in Plant Science

Received: 19 December 2015

Accepted: 13 April 2016

Published: 29 April 2016

Citation:

Hocking B, Tyerman SD, Burton RA and Gillham M (2016) Fruit Calcium: Transport and Physiology. *Front. Plant Sci.* 7:569.
doi: 10.3389/fpls.2016.00569

Calcium has well-documented roles in plant signaling, water relations and cell wall interactions. Significant research into how calcium impacts these individual processes in various tissues has been carried out; however, the influence of calcium on fruit ripening has not been thoroughly explored. Here, we review the current state of knowledge on how calcium may impact the development, physical traits and disease susceptibility of fruit through facilitating developmental and stress response signaling, stabilizing membranes, influencing water relations and modifying cell wall properties through cross-linking of de-esterified pectins. We explore the involvement of calcium in hormone signaling integral to the physiological mechanisms behind common disorders that have been associated with fruit calcium deficiency (e.g., blossom end rot in tomatoes or bitter pit in apples). This review works toward an improved understanding of how the many roles of calcium interact to influence fruit ripening, and proposes future research directions to fill knowledge gaps. Specifically, we focus mostly on grapes and present a model that integrates existing knowledge around these various functions of calcium in fruit, which provides a basis for understanding the physiological impacts of sub-optimal calcium nutrition in grapes. Calcium accumulation and distribution in fruit is shown to be highly dependent on water delivery and cell wall interactions in the apoplasm. Localized calcium deficiencies observed in particular species or varieties can result from differences in xylem morphology, fruit water relations and pectin composition, and can cause leaky membranes, irregular cell wall softening, impaired hormonal signaling and aberrant fruit development. We propose that the role of apoplastic calcium-pectin crosslinking, particularly in the xylem, is an understudied area that may have a key influence on fruit water relations. Furthermore, we believe that improved knowledge of the calcium-regulated signaling pathways that control ripening would assist in addressing calcium deficiency disorders and improving fruit pathogen resistance.

Keywords: calcium, fruit ripening, xylem, pectin, water

Abbreviations: ABA, abscisic acid; Ca^{2+} , Calcium ion; CEC, Cation exchange capacity; GA, Gibberellic acid; IAA, Indole acetic acid; K^+ , Potassium ion; OGA, Oligogalacturonide; PME, Pectin methyl-esterase; R_h , hydraulic resistance; WAK, Wall associated kinase.

INTRODUCTION

Fruit are economically important plant organs that face unique challenges in terms of calcium nutrition and physiology. Fruit are architecturally isolated; their supply of water and nutrients changes during fruit development; they often have low rates of transpiration and have low xylem transport rates when compared with the rest of the plant, which limits fruit calcium delivery. We describe how these unique circumstances can create a situation in which calcium deficiencies can easily arise, leading to numerous disorders that impact fruit development and reduce crop quality. Although the strict botanical definition of fruit includes wheat grain and bean pods we mostly restrict ourselves in this review to discussing the multifaceted role of calcium in the flesh-rich seed-associated structures that are commonly referred to as fruit. In particular, this review often uses the role of calcium in grape, tomato, and kiwifruit as a model systems for understanding fruit calcium physiology. Much of our current knowledge on calcium signaling in plants is drawn from specific cell-types such as the guard cell or pollen tube. Different tissues and cell types possess their own protein network, developmental programming and physiology (Henderson and Gillham, 2015); fruit are not guard cells, mesophyll tissue or pollen tubes – they differ in how they develop and how they respond to stress. Therefore, despite deficiency and toxicity symptoms often being most noticeable in fruit, generally we have a poor understanding of the physiological roles of calcium in fruit development.

The irreplaceable nature of the calcium ion (Ca^{2+}) as a signal transduction agent, and in cell wall polysaccharide interactions is undisputed; it is through these processes that calcium is central to stress responses, cell wall growth and remodeling, and to plant tissue development (Dodd et al., 2010; Hepler and Winship, 2010; Kudla et al., 2010; Gillham et al., 2011b). As Ca^{2+} is such a biologically active ion its concentration and transport must be tightly controlled within plant tissue down to the level of cellular and extracellular compartments. If tissue calcium concentration is high, this can result in cellular toxicity, in overly rigid cell walls and in developmental abnormalities (Conn et al., 2011; Cybulská et al., 2011). When calcium supply is low or transport is disturbed, local calcium deficiencies result. This can lead to membrane breakdown and/or cell wall failure; in fruit this has been proposed to result in disorders such as blossom end rot (de Freitas and Mitcham, 2012). Whether this is the cause of such a disorder or whether calcium deficiency is a result of this condition has been recently debated (de Freitas et al., 2014; Saure, 2014); further insights into how cell wall calcium can influence tissue integrity are provided here.

The cell wall properties of fruit epidermal cell layers are important determinants of pathogen susceptibility. Fruit cell walls are pectin rich, and calcium-pectin cross-links are a major factor in determining the physical and structural properties of fruit. The cell wall is also the source of pectin derived OGAs that elicit pathogen defense responses (Decreux and Messiaen, 2005); cytosolic Ca^{2+} signaling also occurs during defense responses (Dodd et al., 2010), so the interactions between calcium in

the cell wall and its cytosolic signaling role warrants further investigation from a fruit-pathogen susceptibility perspective. Treatment of some fruit with calcium-containing sprays is a routine horticultural practice, which can improve cell integrity and disease resistance (Manganaris et al., 2005; Dayod et al., 2010), demonstrating the importance of calcium in determining fruit quality at harvest and improving post-harvest traits. Here, we review the field, and nominate what are the most pressing research questions in this area.

Hormonal controls on cell division and expansion are active in the development of fruit. Many of these phytohormonal pathways utilize changes in cytoplasmic calcium concentration ($[\text{Ca}^{2+}]_{\text{cyt}}$) as a secondary signal messenger (e.g., ABA, jasmonic acid, auxin, GA, ethylene, brassinosteroids, and cytokinins; Fortes et al., 2015). Therefore, the reliance upon Ca^{2+} as a signaling element in a tissue with low and variable calcium supply has been said to create physiological disorders during development, such as blossom end rot in tomatoes (de Freitas et al., 2012). The case for calcium nutrition being an important consideration in establishing normal fruit development and optimizing stress responses is made here. As it is a phloem immobile nutrient, calcium is mainly reliant on transpirational water flow for its accumulation within fruit; however, calcium can regulate water flow through modification of aquaporin activity and cell wall properties that affect cell wall permeability to water so calcium has the potential to affect its own delivery locally (Gillham et al., 2011b). The influence of calcium in pectin modification and micro-domain gel formation is also a potential source of influencing xylem water transport, water relations and calcium delivery (Zsivanovits et al., 2004). Therefore, the complex relationship between calcium, water, cell walls and signaling pathways make calcium a significant player in fruit physiology and development worthy of further attention.

FRUIT CALCIUM TRANSPORT

Fruit calcium nutrition is dependent upon the physical and molecular pathways of water and calcium delivery, and the impact that calcium signaling can have on cell wall interactions, transpiration, and water transport. The major factors that influence calcium delivery and distribution in aerial tissues include: the rate of xylem water mass flow (as Ca^{2+} is virtually phloem immobile), the competition between ions for binding sites in xylem vessel walls and pit membranes (including H^+ , making pH an important factor), formation of lowly soluble or insoluble complexes (e.g., calcium oxalate) and cellular water/ionic transport mechanisms (Franceschi and Nakata, 2005; Saure, 2005; Gillham et al., 2011b). Calcium concentration in different cellular compartments can impact water transport processes via membrane-delimited pathways. For instance, increases in $[\text{Ca}^{2+}]_{\text{cyt}}$ can decrease water transport through aquaporins (Alleva et al., 2006; Verdoucq et al., 2008). This has been proposed to affect the relative contribution of apoplastic and symplastic water flow and the magnitude of calcium delivery (Gillham et al., 2011b), with symplastic pathways having a lower capacity for long distance Ca^{2+} movement.

Long-Distance Calcium Transport

The link between water and calcium transport is particularly apparent when examining sink organs with relatively low transpiration rates, such as those that typically occur in fruit (**Figure 1**). At fruitset the transpiration rate of fruit is at its highest, for instance in kiwifruit this can be as high as $2.3 \text{ mmol m}^{-2} \text{ s}^{-1}$, but this quickly declines to almost a tenth of this value later in development, whereas leaf transpiration is maintained greater than $10 \text{ mmol m}^{-2} \text{ s}^{-1}$ (Montanaro et al., 2014). It is at these early stages of fruit development that most Ca^{2+} is delivered to fruit (Montanaro et al., 2012a,b). In most species the delivery of water, sugar, and basic nutritional inputs during the later stages of fruit ripening occurs largely via the phloem (Drazeta et al., 2004; Rogiers et al., 2006b; Choat et al., 2009). As Ca^{2+} has low phloem mobility, calcium accumulation in aerial sink organs such as fruit is dependent upon its delivery by the xylem (Rogiers et al., 2000; Drazeta et al., 2004). The low phloem mobility of Ca^{2+} can create a situation that leads to localized calcium deficiencies in fruit. The relationship between calcium accumulation, fruit transpiration, and environmental variables is exemplified by observations made in kiwifruit (Montanaro et al., 2014). In kiwifruit, both phloem and xylem appear to contribute to fruit hydration during late development, but their relative contributions are affected by environmental conditions (Clearwater et al., 2012). Under high vapor pressure deficit, kiwifruit calcium accumulation is coupled to transpiration; under low vapor pressure deficit, lower transpiration and fruit water uptake occurs, with calcium accumulation instead more closely coupled with fruit growth rates (Montanaro et al., 2015).

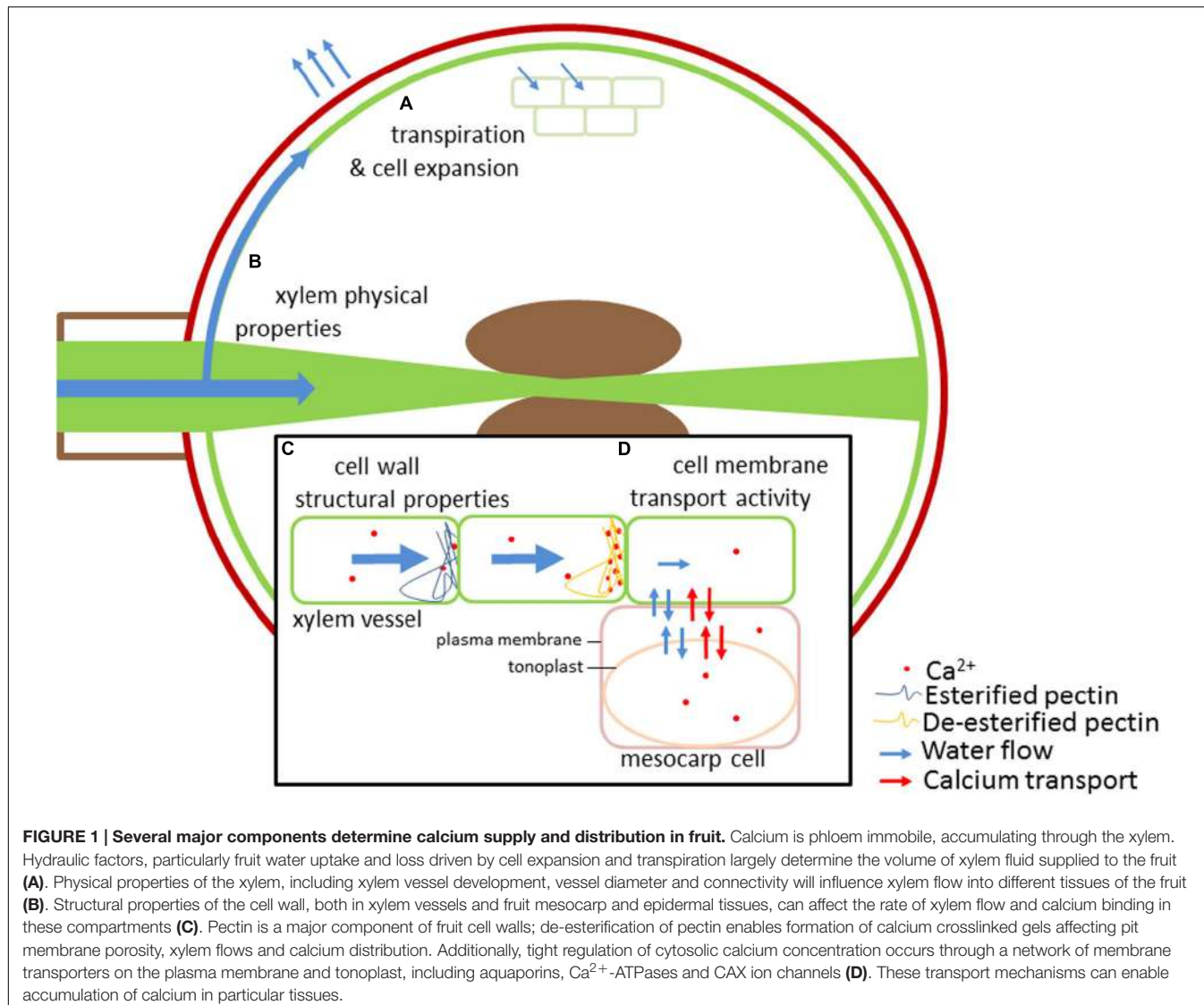
Calcium accumulation in tomato fruit has been shown to be dependent on rates of xylem sap flow, influenced by transpiration and growth rates (Ho et al., 1993; de Freitas et al., 2014). The strength of other calcium sinks in the plant can affect calcium accumulation in the tomato, and may lead to calcium related physiological disorders such as blossom end rot (Ho and White, 2005). ABA treatment of whole plants reduced leaf peduncle xylem sap flow rate and leaf calcium uptake whilst increasing fruit peduncle xylem sap flow rate and fruit calcium uptake; these fruit demonstrated lower susceptibility to development of blossom end rot (de Freitas et al., 2014). However, accumulation of ionic nutrients in fruit is determined not only by water import rates, but also by their relative prevalence and mobility in the phloem and xylem. Unlike, Ca^{2+} , which is only xylem mobile, K^+ is both xylem and phloem-mobile, with K^+ concentrations in the phloem being up to ten times that found in the xylem (Hocking, 1980). Grape berry potassium accumulation occurs throughout berry development, reaching a maximum uptake rate during early post-veraison with uptake continuing throughout ripening (Rogiers et al., 2006b). In contrast, calcium content (i.e., Ca per berry) generally does not increase after veraison (Rogiers et al., 2006a). The large drop in xylem hydraulic conductance into the berry, which occurs post-veraison, is correlated with a loss of cell vitality and berry shrivel, and also results in a reduction in calcium import (Tyerman et al., 2004; Rogiers et al., 2006b; Tilbrook and Tyerman, 2009). A varietal survey revealed genotype differences in the occurrence of cell vitality loss and berry shrivel in mature

grapes (Fuentes et al., 2010). It is not inconceivable that the reduction in Ca^{2+} import could contribute to cell vitality, with those grape varieties that maintain longer periods of water and Ca^{2+} potentially less susceptible to shrivel. The shift away from xylem water delivery during ripening also effectively buffers the fruit against fluctuations in plant water status and water stress events that may affect the plant during ripening (Thomas et al., 2006; Choat et al., 2009). Determining the hydraulic pathways of ionic delivery is vital for understanding patterns of distribution and accumulation and their effects upon fruit development and ripening.

Cation exchange within the xylem plays an important role in Ca^{2+} delivery; CEC is a measure of the abundance of fixed negative charges in the cell wall, a key determinant of the diffusion pattern of cations through the apoplasm. However, studies that have measured the CEC of the xylem are few. The CEC of cell walls for calcium from different root and shoot tissues of *Picea abies* has been measured using transmission electron microscopy energy-dispersive microanalysis. Whilst there was a wide variation between root and shoot tissue CEC was observed, the CEC of the secondary cell wall of xylem tracheids was consistently low ($\sim 24 \text{ meq/kg}$ wall material; Fritz, 2007). This suggests that the composition of other zones within the xylem (e.g., pit membranes) and cellular membrane transport mechanisms may also be important for determining Ca^{2+} transport and buffering fluctuations in xylem sap calcium concentration (**Figure 1**).

Calcium and Hydraulic Conductivity

Compartmentation resulting in high hydraulic resistance in the apoplasm occurs in many tissues. Examples of this include; separation of the extracellular space of the outer root from the root endodermis by the Caspary strip (Nawrath et al., 2013), separation of adjacent xylem conduits by pit membranes (Zwieniecki et al., 2001; Plavcova and Hacke, 2011; van Doorn et al., 2011), separation of the leaf xylem from the leaf apoplasm by bundle sheath cells, and separation of external surfaces of the plant and the underlying apoplasm by the cuticle (Nawrath et al., 2013). Changes in the hydraulic resistance (R_h) of components of the bunch and berry vascular architecture of grapes may account for some of the observed varietal differences in susceptibility to berry shrivel. By studying the R_h of each component the contributions of particular variables to observed changes in xylem flows may be identified (Tyerman et al., 2004; Choat et al., 2009; Mazzeo et al., 2013). These variables may include; physical barriers (i.e., pit membrane porosity and xylem vessel diameter), structural changes (i.e., formation of pectin gels within the xylem), and cellular water permeability (i.e., through changes in temporal and spatial expression of aquaporins; **Figure 1**). A recent study has demonstrated that hydraulic conductivity of xylem vessels in grape pedicels decreased at veraison and throughout ripening, potentially due to blockages formed by pectin deposition (Knipfer et al., 2015). This effective compartmentation of the apoplasmic space highlights the importance of understanding physical transport barriers as well



as cellular transport mechanisms for controlling Ca^{2+} movement and utilization.

A developmental switch to phloem water delivery from predominantly xylem driven delivery reduces the direct hydraulic link of fruit water status to that of the plant (Greenspan et al., 1994). During normal grape development a decrease in mesocarp turgor coincides with the onset of veraison, indicative of phloem solute unloading. Water stress can also cause a drop in fruit mesocarp turgor; however, after veraison, berry mesocarp turgor does not appear to respond to vine water deficit (Thomas et al., 2006). When pre-veraison berries were physically boxed to restrict veraison associated cell expansion, both sugar accumulation and the drop in mesocarp turgor pressure were delayed. When the box was ventilated to allow transpiration, delayed sugar accumulation was not observed and the mesocarp turgor drop was less delayed (Matthews et al., 2009). This suggests that fruit transpiration is required to assist in phloem sugar loading into fruit (by removing excess water;

Lang and Thorpe, 1989), and that ripening related changes in mesocarp cell turgor pressures are linked to both rapid cell expansion and sugar accumulation (Matthews et al., 2009). Calcium is involved in the regulation of cell expansion and elongation during pollen tube tip growth through dynamic pectin binding (Jiang et al., 2005; Rounds et al., 2011), binding signaling proteins and modifying ion channel activity (Konrad et al., 2011). Calcium may also be involved in the changes in cell turgor pressure and cell expansion observed during the progression of fruit ripening. The relative contributions of turgor and cell wall changes to fruit softening are still a major point of discussion. However, it is clear that both factors contribute to the onset and development of ripening processes in fruit through complex interactive pathways and feedback mechanisms.

Fruit water relations and ripening-linked shifts in fruit hydraulic conductance vary between species. Kiwifruit (*Actinidia chinensis*) maintains positive water fluxes from both the phloem

and xylem into the fruit throughout development, with each pathway contributing approximately equally to the water balance (Clearwater et al., 2012). However, when grown in high vapor pressure deficit conditions *A. chinensis* var. *chinensis* 'Hort16A' exhibits late ripening shrivel, similar to the phenomenon observed in Shiraz grapes. The high surface conductance and transpiration rate observed in Hort16A may cause an imbalance between water delivery to the fruit and transpiration losses (Clearwater et al., 2012). Additionally, kiwifruit does not accumulate sugars until late in the ripening phase; this difference may explain its ability to maintain xylem flow from the plant into the fruit throughout development. A study of kiwifruit xylem hydraulic resistance (R_h) throughout development using pressure chamber and flow meter techniques showed a general increase in R_h during the second half of fruit development, consistent with previous reports in grapevine and kiwifruit (Tyerman et al., 2004; Choat et al., 2009; Mazzeo et al., 2013). However, the increase in R_h began prior to ripening, indicating that decreasing xylem inflows in kiwifruit may be attributable to increasing xylem hydraulic resistance (Mazzeo et al., 2013). This contrasts to observations in grape; xylem flow rates into the berry drop around veraison whereas increases in R_h are observed after veraison (Tyerman et al., 2004; Choat et al., 2009). The parallel use of pressure chamber and flow meter techniques (Mazzeo et al., 2013), and an evaporative flux method (Clearwater et al., 2012), showed differences in the magnitude of resistance measured depending on the methodology employed. The flow meter technique may also underestimate xylem resistance, with the calculations used for estimation of berry hydraulic isolation and the potential for xylem backflow being questioned (Mazzeo et al., 2013). Despite difficulties in accurately and consistently measuring hydraulic resistance, it is highly likely that differences in xylem sap ionic composition and xylem physical properties will contribute to fruit water relations.

Interactions between Membrane Transport and Fruit Calcium Physiology

The influence of transport proteins on the long distance transport of Ca^{2+} has been reviewed previously (Gillham et al., 2011b), and varies at both the inter- and intra-species level (White, 2001; Cholewa and Peterson, 2004; Conn et al., 2012); in grapevine the choice of rootstock has also been shown to influence shoot accumulation of calcium (Kidman et al., 2014). The presence of a suberized endodermis limits root apoplasmic flow making symplastic transport a necessity, and the dominant pathway of root xylem loading at low transpiration. Regulation of Ca^{2+} transport across the plasma membrane and organelar membranes is tightly controlled by the expression pattern, interaction and post-transcriptional control of many Ca^{2+} transporters (Kudla et al., 2010; **Figure 1**). For example, the differentially regulated expression of a number of membrane ion transporters is responsible for cell-specific calcium accumulation patterns in plants (Conn and Gillham, 2010; Conn et al., 2011; Gillham et al., 2011a). The use of both cell-specific ion and transcript profiling and of genomic

and transcriptional natural variation amongst varieties of certain plant species has been useful in the identification of these transporters (Conn et al., 2012). In *Arabidopsis*, knockout of the vacuolar $\text{Ca}^{2+}/\text{H}^+$ antiporters AtCAX1 and AtCAX3 resulted in lower mesophyll Ca^{2+} sequestration and higher apoplasmic Ca^{2+} , with physiological impacts ranging from reduced stomatal aperture, stomatal conductance and CO_2 assimilation to reduced cell wall extensibility and leaf growth rate (Conn et al., 2011). Constitutive expression of sCAX1, the *Arabidopsis* vacuolar calcium transporter with its auto-inhibitory region removed, in transgenic tomatoes, increased fruit calcium concentration and vacuolar Ca^{2+} transport (Park et al., 2005). Interestingly, susceptibility to blossom end rot was also increased in these transgenic lines (Park et al., 2005; de Freitas et al., 2011). The constitutive expression of the sCAX1 increased vacuolar calcium accumulation, depleting pools of apoplasmic and cytosolic Ca^{2+} , causing increased membrane leakage and blossom end rot (de Freitas et al., 2011). Although some calcium transport mechanisms have been investigated in fruit, calcium signaling in fruit has not, so the broader impact of calcium nutrition, transport and signaling pathways on fruit development and ripening is still largely unknown.

Plants tightly control cellular Ca^{2+} transport in order to keep $[\text{Ca}^{2+}]_{\text{cyt}}$ within the range ($\sim 0.1\text{--}10 \mu\text{M}$) required for signal transduction (Evans et al., 1991; White, 2000; Dodd et al., 2010). Regulated fluctuations in $[\text{Ca}^{2+}]_{\text{cyt}}$ form the "calcium signature" which is a major determining factor in the specificity of downstream transcriptional and physiological responses (McAinsh and Pittman, 2009; Dodd et al., 2010; Kudla et al., 2010). Different environmental stimuli create specific calcium signatures in particular cell-types (Kiegle et al., 2000; Dodd et al., 2010; Marti et al., 2013). The channels responsible for regulating these calcium transients are still largely unknown, with progress having been reviewed by Swarbreck et al. (2013). Electrically induced calcium transients with different amplitudes and frequencies were shown to induce distinct patterns of gene expression (Whalley and Knight, 2013), indicating that environmental stimuli can translate into specific expression profile changes in calcium signaling components. There is considerable evidence indicating that Ca^{2+} signaling transients also occur in compartments other than the cytosol, e.g., the nucleus, chloroplasts and the apoplasm (Johnson et al., 1995, 2006; Tang et al., 2007; McAinsh and Pittman, 2009). However, these mechanisms are not nearly as well characterized as the cytosolic pathways. Furthermore, Ca^{2+} transient signaling in fruit specific cell types has not been studied. Generic models for how transients are developed in plant tissue and which transporters are involved in their generation are illustrated in reviews such as Kudla et al. (2010) and de Freitas and Mitcham (2012), these are also useful in the context of understanding the nutritional fluxes of Ca^{2+} and how these may affect compartmentation of Ca^{2+} apoplasmically, in the cytoplasm and intracellularly.

Increases in apoplasmic calcium can result in increases in $[\text{Ca}^{2+}]_{\text{cyt}}$; this has been used to control the duration and

amplitude of $[Ca^{2+}]_{cyt}$ oscillations in stomatal guard cells to affect guard cell closure (Allen et al., 2001; Webb et al., 2001). *In planta* manipulation of apoplastic calcium ($[Ca^{2+}]_{apo}$) can reduce CO₂ assimilation and transpiration rate, through reducing stomatal aperture (Conn et al., 2011). Some components of an extracellular calcium-sensing pathway have been described; where a plastid localized calcium sensor protein (CAS) mediates stomatal closure in response to changes in extracellular calcium (Han et al., 2003; Wang et al., 2012). Antisense *cas* lines showed reduced water use efficiency and photosynthetic electron transport rate, due to reduced control of stomatal aperture and transcription of electron transport components (Wang et al., 2014), demonstrating the importance of the extracellular calcium signaling pathways in optimizing photosynthesis and water use. The supply of Ca²⁺ to fruit is dependent upon transpirational water flow and storage rate (i.e., Ca²⁺ transport into the vacuole via CAX transporters; Conn et al., 2011), therefore $[Ca^{2+}]_{apo}$ in both leaves and fruit are likely to have an impact on Ca²⁺ supply; furthermore, high $[Ca^{2+}]_{apo}$ in fruit will directly regulate $[Ca^{2+}]_{cyt}$, cell wall properties, gene expression and water relations of the fruit, but the impact that this has on fruit quality outcomes at harvest and during storage is totally unexplored.

Characterization of changes in apoplasmic and vacuolar solute composition that supply grapes supports the notion of a switch from symplasmic to apoplasmic unloading of phloem solutes during late ripening. The table grape variety Concord maintains high apoplasmic pH (relative to vacuolar pH) late into ripening, whereas, in the shrivel susceptible variety Merlot the pH difference between these compartments is reduced to zero during late ripening, indicating a loss of membrane selectivity in this variety (Keller and Shrestha, 2014). This is supported by recent measurements of electrical impedance in Shiraz berries (Caravia et al., 2015). The switch to apoplasmic phloem unloading enables accumulation of high sugar levels in ripening fruit but also modifies the conditions of the apoplast with potential impacts on cell wall modification and calcium binding. Merlot demonstrates a dramatic jump in apoplasmic glucose and fructose concentrations during the transition from red to ripe berries (Keller and Shrestha, 2014). The accumulation of sugars in the apoplasm activates cell wall localized invertases and hexose/proton transport pathways in berries (Hayes et al., 2007). The loss of cell turgor, vitality, and membrane integrity in the locular tissues during ripening may be related to apoplasmic unloading and the ongoing accumulation of solutes from the adjacent central vasculature (Tyerman et al., 2004; Krasnow et al., 2008). However, the onset of berry death normally occurs after the transition to apoplasmic unloading. Additionally, cell membrane capacitance in the berry is maintained through the cell death phase, indicating intact membranes (Caravia et al., 2015). This suggests that rather than 'cell death,' the loss of cell vitality often observed may actually represent a loss of membrane selectivity allowing distribution of some solutes (e.g., sugars, ions, and perhaps the cell vitality stain fluorescein diacetate) into the apoplasm. The effect of solute accumulation in the apoplasm and associated changes in cell turgor on fruit water relations requires further investigation.

CALCIUM-CELL WALL INTERACTIONS DURING FRUIT DEVELOPMENT

The cell wall is composed of a diverse array of complex polysaccharides. In dicots, the primary cell wall consists of cellulose microfibrils bound in a matrix of pectins and hemicelluloses. The Cellulose is extruded through the plasma membrane by cellulose synthase complexes, whereas pectins and hemicelluloses are synthesized within the Golgi apparatus, and are transported to the cell surface where further synthesis and modification may take place (Gendre et al., 2013). The matrix polysaccharides are very diverse in their composition, with a variety of sugar residues, linkages and side chains present; their synthesis and modification is therefore accomplished by a large number of genes (Burton et al., 2010). The cell wall is a dynamic structure that responds to both developmental and environmental stimuli by structural remodeling; environmental perturbations include pathogen attack, light, and touch (Hoson, 1998; Seifert and Blaukopf, 2010). Cell wall modifying enzymes activated at different stages of development, and under certain conditions (e.g., heat, pH changes in the apoplasm), are responsible for modification and degradation of cell wall polysaccharides (Grignon and Sentenac, 1991; Brummell, 2006). The chemical changes that occur in fruit cell walls during development include; modification of pectin side chains, depolymerisation of pectins, and degradation of xyloglucan (a hemicellulose), and the activity of non-catalytic proteins such as expansins and AGPs. Together with other ripening related processes (such as the accumulation of solutes) this leads to a number of physical and textural changes in fruit that can help us to classify different types of fruit by their ripening mechanisms. Physical changes in fruit cell walls are associated with ongoing modification and solubilisation of pectins; calcium-pectin cross-links are a key factor in determining pectin physical properties.

General Calcium and Pectin Interactions

Pectins are a complex family of polysaccharides that are structurally related by the occurrence of (1,4)- α -linked galacturonan in the backbone, commonly as homogalacturonan, or as the rhamnose/galacturonan disaccharide repeat rhamnogalacturonan-I (Mohnen, 2008). The galacturonan residues of the backbone may be methyl-esterified or acetylated; homogalacturonan is secreted into the cell wall in an esterified form (Willats et al., 2001). A wide variety of linear and branched side chains are also observed, forming the pectin structural classes rhamnogalacturonan-II, xylogalacturonan, and apiogalacturonan. Rhamnogalacturonan-II is the most complex pectin, it can include up to 12 different sugar residues and more than 20 different linkage types. These have been reviewed previously (Vorwerk et al., 2004; Mohnen, 2008; Burton et al., 2010). The structural complexity of pectin, driven by the expression of a range of pectin synthesizing and modifying enzymes throughout development, implicates pectin in an array of potential interactions and functional roles.

The prevalence of ionic and ester bonds between adjacent pectins play an important role in the physical properties

of fruit cell walls. These bond interactions influence the solubility of pectins. Suitable ions for cross-linking adjacent pectins include calcium-forming junctions between de-esterified homogalacturonans and boron forming di-ester bonds between rhamnogalacturonan II units. Associations between adjacent homogalacturonans ionically linked by calcium ions have been characterized as forming an “egg-box” structure. Although this structure has been demonstrated in pectin extracts (Tibbits et al., 1998), the diversity of side chains and modifications within the pectic polysaccharides, as well as the complexity of other cell wall components makes such interactions difficult to characterize *in planta*. The importance of pectin structure for determining the hydraulic and elastic properties of pectin gels has been examined mostly *in vitro*; understanding the complexity of these cell wall interactions *in planta* requires further research.

The majority of pectins occur in the middle lamella (outermost part of the extracellular matrix; where cell junctions occur), with smaller amounts observed in the primary cell wall (Lee et al., 2011). Micro-domain localization of calcium in particular

extracellular domains is hypothesized to affect cell wall loosening and cell separation (Figure 2). This may be particularly relevant at three way cell junctions where turgor pressure is driving the separation of cells and the formation of large intra-cellular spaces (Willats et al., 2001). It has been suggested that the major physical effects of pectin modification will therefore be in cell-cell adhesion rather than strength of the primary cell wall (Ferguson, 1984). However, species and tissue differences in patterns of pectin deposition and modification (through controlled expression of an array of cell wall modifying enzymes) indicate that the situation may be much more complex.

Cell wall acidification promotes cell growth and expansion by displacing pectin-bound calcium through protonation of pectin carboxyl groups. The pH of the apoplasm may be affected by the pH of the xylem sap when water delivery is high, depending on the buffering capacity of the xylem solutes. Control of apoplasm pH occurs through the activity of the plasma-membrane localized H⁺-ATPase and is buffered by the CEC of the apoplasm. When exposed to high concentrations of NaCl

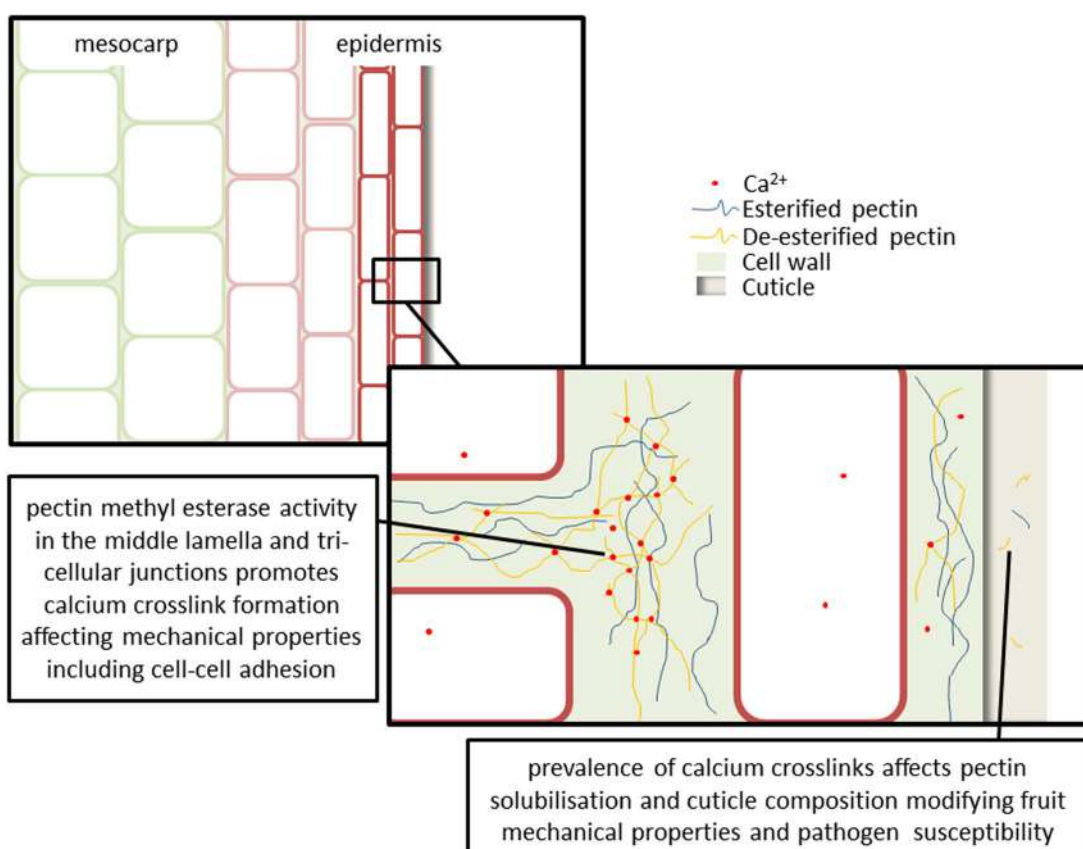


FIGURE 2 | Cell wall changes and calcium-pectin crosslink formation affects fruit mechanical properties, water relations and pathogen susceptibility.

Upregulation of cell wall modifying and hydraulic regulatory genes (e.g., pectin methyl esterases, polygalacturonases, and aquaporins) occurs in the mesocarp at veraison. The majority of pectins occur in the middle lamella, with smaller amounts observed in the primary cell wall. Localization of calcium in particular extracellular domains is hypothesized to affect cell wall loosening and cell separation. This may be particularly relevant at three way cell junctions where turgor pressure is driving the separation of cells and the formation of large intra-cellular spaces. Cuticle composition is an important variable in determining both fruit physical properties and transpiration water losses throughout berry development. Processes affecting polysaccharide solubilisation and movement into the cuticle, such as pectin de-esterification and calcium crosslinking, and production of oligogalacturonides will modify fruit mechanical properties and pathogen susceptibility.

in the growth media a decrease in leaf growth rate of a salt-sensitive maize cultivar is correlated with a reduction in H⁺-ATPase activity, resulting in increased apoplastic pH whilst a tolerant hybrid cultivar showed none of these effects (Pitann et al., 2009). This finding is contrasted by work measuring ion fluxes in bean leaf, which showed H⁺ efflux from the mesophyll upon addition of NaCl directly to the mesophyll (Shabala, 2000), although this may be in part related to the displacement of H⁺ from the cell wall by Na⁺. Amelioration of the effects of salinity on growth by high calcium has been observed; this may result from interactive effects with plasma membrane transport proteins (such as H⁺/cation exchangers), or through a reduction in the rate of Ca²⁺ displacement from pectin cross links by Na⁺ and H⁺ ions (Shabala, 2000). Additionally, cell wall localized expansions show optimal activity at low pH. They are believed to act by reducing hydrogen bonding between primary cell wall components, allowing slippage between adjacent polysaccharides and hence cell wall expansion (Sampedro and Cosgrove, 2005; Dal Santo et al., 2013). Thus, changes in apoplastic pH can have significant effects on the dynamics and composition of the cell wall.

Calcium, Pectin, and Fruit Softening

Fruit softening is often attributed to changes in the composition of the cell wall, and particularly to the impact of pectin de-esterification and calcium crosslink formation on cell wall physical properties including strength and elasticity, cell wall loosening and swelling (**Figure 2**). Changes in [Ca²⁺]_{apo} and the secretion and modification of pectins are important for the physical development of fruit. Some species (e.g., strawberry and plum) exhibit cell wall swelling during ripening which results in a soft textured fruit, whereas other species (e.g., watermelon and apple) do not exhibit swelling and maintain crisp textured fruit (Redgwell et al., 1997).

Throughout fruit ripening, pectin de-esterification occurs by the action of PMEs. This exposes the carboxyl residues that can be cross-linked by calcium. The level of PME activity and Ca²⁺ availability within the apoplasm has a direct impact on cell wall strength and expansion (Conn et al., 2011). Studies in grapes suggest that PME expression begins before veraison and continues throughout ripening (Barnavon et al., 2001; Schlosser et al., 2008; **Figure 2**). Mesocarp and skin tissues exhibit different patterns of PME expression in grapes (Nunan et al., 1998; Schlosser et al., 2008; Lacampagne et al., 2010). During the initiation of ripening a raft of cell wall modifying and hydraulic regulatory genes in grape (including expansions EXP3 and EXPL, pectate lyase, a pectin methyl esterase, and aquaporin PIP2;1) are upregulated (Schlosser et al., 2008). This occurs initially in mesocarp; the delayed activation of these genes in the skin suggests a role for the skin in moderating berry growth during ripening. The degree of pectin de-esterification also varies between varieties (Ortega-Regules et al., 2008).

The expression and activity patterns of cell wall modifying enzymes in grapes change throughout development, as well as varying between varieties. In both Cabernet Sauvignon and Semillon, polygalacturonase activity appears correlated with ABA levels, reaching a maximum at veraison (Deytieux et al.,

2005). Polygalacturonase activity in skin was not detected, however, transcripts of two isoforms showed different expression patterns, with a common feature being greater expression late in development (100 days after anthesis), indicating a variety of roles for the polygalacturonase family, and a concerted role in cell wall disassembly at maturity (Deytieux-Belleau et al., 2008). However, other research has also indicated that transcript expression of polygalacturonases does not necessarily translate to detectable enzyme activity (Nunan et al., 2001). *In vitro* calcium has an inhibitory effect on polygalacturonase activity; a reduction in calcium concentration and availability following veraison may be linked to a concurrent increase in polygalacturonase activity (Cabanne and Doneche, 2001). In grape skin tissue pectin methylesterase is present throughout ripening with enzyme activity reaching a peak at the beginning of veraison, then decreasing sharply in the subsequent 10 days and increasing steadily thereafter (Deytieux-Belleau et al., 2008). Low levels of polygalacturonase and pectate lyase activity are observed during some stages of ripening; however, hormonal cues may regulate the targeted expression of specific isoforms to drive the depolymerisation of pectin observed during ripening (Nunan et al., 2001).

In addition to the de-esterification of pectins observed in fruit cell walls during ripening, depolymerisation of pectins to shorter sub-units is also an important factor. By using a chelator (e.g., CDTA) followed by size exclusion chromatography to extract and characterize ionically bound pectins, the diversity in timing and degree of depolymerisation that occurs between species can be observed. Some species show almost no change in pectin composition or solubilisation throughout development (e.g., capsicum), whilst others (e.g., tomato) show high degrees of depolymerisation and high levels of chelator soluble pectins (i.e., high levels of calcium bound pectins; Brummell, 2006). This depolymerisation is achieved through the action of polygalacturonases and pectate lyases. Polygalacturonases are absent or detected at very low levels in the fruit of some species which may account for some of the differences in levels of pectin solubilisation. Additionally, it has been demonstrated that reduced expansion activity (normally responsible for loosening of xyloglucan and cellulose networks in the primary cell wall during cell expansion) decreases solubilisation of primary cell wall pectins, possibly through reduced access of polygalacturonases to their substrates in this space (Brummell et al., 1999). This finding suggests that it is important to consider more than just transcript levels or enzyme activity when assessing potential for degradation of particular components; calcium availability and activity of other cell wall enzymes may influence substrate accessibility.

The combinatorial effects of pectin modifying enzyme activity, apoplasm pH and calcium concentration determine various mechanical properties of pectin gels including compressive strength, water holding capacity, porosity, and elasticity (Tibbits et al., 1998; Willats et al., 2001; Ngouemazong et al., 2012). The strength of calcium crosslinks is pH dependent, with the strongest bonds forming at apoplasmic pH 6–7. Formation and dissolution of pectin gels by calcium crosslinks is highly dependent on the level of de-esterification (i.e., available carboxyl groups) and free calcium ion concentration (Tibbits et al., 1998). Gel swelling can

be observed during cell wall dissolution, due to both the osmotic pressure created by free carboxyl groups in the pectin matrix (occurring when ionic strength is low), and the disassociation of calcium cross-linked pectins. This can be expressed as the ratio of free calcium ions to carboxyl groups (i.e., if $[Ca^{2+}]_{free} : COO^- < 0.05$ significant swelling is likely to occur). As gel dissolution and swelling occurs, the breakdown of calcium crosslinks reduces the stiffness of the gel. Swelling of a gel is generally at maximum around pH 3, which is also the pH at which calcium crosslinking and gel shear strength are at a minimum (Tibbits et al., 1998). Reported work with pectin concentrations similar to those observed in plant cell walls (films with $\sim 30\%$ pectin), demonstrate that pectin hydration status (or degree of swelling) has a linear inverse relationship with tensile strength (Zsivanovits et al., 2004). Additionally, the hydraulic properties and susceptibility to swelling of the pectin matrix are determined by both the pectin composition and the ionic composition of the space (Zsivanovits et al., 2004). Through understanding the pectin ion interaction effects on gel properties *in vitro* it is likely we will advance our comprehension of fruit ripening processes.

Calcium, Pectin and Pathogens

Plant and fungal PMEs have different modes of function; plant PMEs generally operate in a blockwise manner, de-esterifying multiple homogalacturonan residues along a single chain, whereas fungal PMEs operate in a non-blockwise manner (Willats et al., 2001). Patterning of pectin modification and calcium binding may affect the attachment and rate of pectin cleavage by polygalacturonases (Figure 2). Three botrytis (*Botrytis cinerea*) isolates exhibited calcium inhibition of polygalacturonase activity. The calcium concentration required to inhibit enzyme activity varied between isolates (Chardonnet et al., 2000). The pathogenicity of these isolates also varied between four apple varieties, indicating that the interaction between the pathogen cell-wall degrading enzymes and the composition of the fruit cell wall is important for determining pathogenicity (Chardonnet et al., 2000). It has been demonstrated that the calcium content of grape skin cell walls is negatively correlated with susceptibility to botrytis enzymatic digestion (Chardonnet and Doneche, 1995). Calcium infiltration reduced the level of pectin degradation by botrytis in grapes (Chardonnet et al., 1997), and reduced the level of decay in apples (Chardonnet et al., 2000). Complex interactions between calcium nutrition and the diversity of pectin profiles seen in different species, varieties, tissues, organs, and developmental points influence susceptibility to fungal pathogens. These studies indicate that calcium treatments may be worthwhile exploring as a management option for some fruit pathogens (Dayod et al., 2010).

Degradation of pectic homogalacturonan backbones generates short chain molecules known as OGAs; these have been implicated in pathogen defense signaling activation. This role is carried out through OGA binding by the wall-associated kinase (WAK) family (Decreux and Messiaen, 2005). It is likely that functional OGAs may be prevalent in fruit, and often affect ripening, as ripening fruit has high pectin content and is attractive to a variety of pathogens. Many factors influence the defense response eliciting capacity and specificity of OGAs,

including; calcium availability, length of OGA, degree of methyl-esterification and degree of acetylation (Decreux and Messiaen, 2005; Vallarino and Osorio, 2012; Figure 2). The extracellular domain of *Arabidopsis* WAK1 binds OGAs only in the presence of calcium and calcium crosslink forming conditions (Decreux and Messiaen, 2005). Transgenic expression of a fruit-specific PME from cultivated strawberry in wild strawberry (*Fragaria vesca*) resulted in a modified pattern of OGA esterification in the transgenic fruit. This change was sufficient to constitutively activate defense responses in the transgenic plant, thereby increasing botrytis resistance (Osorio et al., 2008). A variety of evidence suggests that, in addition to WAKs binding specific OGAs during pathogen responses, they also bind cell wall pectins during normal development to regulate cell expansion (e.g., reduction in WAK expression via antisense has been shown to reduce cell size) reviewed in Kohorn and Kohorn (2012). It is apparent that the specificity of calcium-pectin-WAK interactions may facilitate multiple signaling pathways important in pathogen defense activation as well as during the normal developmental control of cell expansion.

The Influence of the Cuticle

Changes in cuticle composition (e.g., relative abundance of polysaccharides) can affect fruit mechanical properties and transpiration rate. Fruit cuticles are typically thicker (but also more water permeable) than leaf cuticles; the scarcity of stomata on fruit also suggests that cuticle composition is important for fruit water relations (Martin and Rose, 2014). A study modeling the impacts of environmental variables on kiwifruit transpiration revealed both seasonal and diurnal variation in transpiration rates, with skin conductance being the key fruit variable in determining fruit transpiration rates (Montanaro et al., 2012b). A tomato cultivar ('Delayed Fruit Deterioration') with altered cuticle architecture was shown to have low fruit transpiration and increased cell turgor pressure, leading to delayed softening despite undergoing normal ripening related cell wall modifications (Saladie et al., 2007), and application of gibberellins was shown to increase cuticle thickness in tomato (Knoche and Peschel, 2007). In grapes (cv. Riesling), a drop in the transpiration permeability of the cuticle occurs from pre-veraison to post-veraison (Becker and Knoche, 2011), and this drop is strongly correlated with increased cuticle deposition (Becker and Knoche, 2012). Indeed, recent work has identified both varietal differences and developmental changes in the cuticular conductance of grape berries, possibly attributable to cuticle composition (Keller et al., 2015). The composition of the cuticle changes throughout development in cherry tomato (cv. Cascada); cuticle mass per unit fruit surface area increased rapidly from 10 days after anthesis to reach a maximum 15 days after anthesis (subsequent increases in cuticle thickness were attributed to reduced cuticle density; Dominguez et al., 2008). Interestingly, another study in the same cultivar looking at the cuticle mechanical properties found a shift from elastic to predominantly viscoelastic behavior from 10 to 15 days after anthesis. These changes in the cuticle mechanical properties were correlated with the ratio of cutin:polysaccharide present; high ratios were associated with cell enlargement growth stages,

and lower ratios (approaching 1:1) were associated with stages where cell expansion is minimal (i.e., early cell division and later ripening phases; Espana et al., 2014). As such, it is hypothesized that polysaccharides in the cuticle contribute elastic properties, and cutin confers viscoelastic properties. It is clear that cuticle composition is an important variable in determining both fruit physical properties and transpiration water losses.

CALCIUM-HORMONE INTERACTIONS DURING FRUIT DEVELOPMENT

Calcium is a secondary messenger during hormone signaling. Calcium is known to participate in GA, auxin, and ABA signaling to regulate fruitset, initiation of ripening, cell division, cell expansion, and fruit softening (Ferguson, 1984; Saure, 2005; Yu et al., 2006). Additionally, hormonal regulation of cell expansion, cell wall modification, xylem development, and sugar unloading from the phloem can affect calcium distribution within the fruit (Saure, 2005; de Freitas et al., 2014). Although the physiological pathways and interactions of plant hormones and calcium are still being uncovered, many hormone and calcium treatments are already used for horticultural improvement. The role of plant hormones in fruit development and ripening processes has been extensively reviewed (Ruan et al., 2012; McAtee et al., 2013; Osorio et al., 2013; Wang and Ruan, 2013; Kumar et al., 2014; Leng et al., 2014). As both are components of an array of complex signaling pathways, the accumulation and activity of calcium and phytohormones is tightly controlled at the tissue level. Subsequently, perturbed calcium nutrition may create multiple plant hormonal responses that are difficult to characterize. This section will therefore articulate the current knowledge and gaps in our understanding of calcium and hormone interactions in fruit.

Auxin

Auxin has key roles in fruitset, cell division and cell expansion. These developmental pathways both utilize calcium as a secondary messenger and affect patterns of calcium distribution. Fruitset and early development are triggered by auxin synthesis in the ovules during fertilization, which induces GA synthesis, reviewed in Kumar et al. (2014). GA signaling in the pericarp of *Arabidopsis* fruit has been demonstrated to activate a pathway degrading the growth inhibiting DELLA proteins (Fuentes et al., 2012; Kumar et al., 2014). The relationship between GA and auxin is complex, with a GA independent pathway for fruitset being demonstrated in tomato (Serrani et al., 2008; McAtee et al., 2013). High levels of GA are commonly associated with rapid cell expansion and this has also been linked to low or reduced calcium concentrations by disrupting calcium transport (Saure, 2005); the mechanism through which this occurs requires further investigation.

Calcium acts as a secondary messenger downstream of auxin through the acid growth pathway. This pathway has been demonstrated in *Arabidopsis*; auxin efflux from cells is facilitated by PIN-FORMED (PIN) membrane proteins. PIN activity and targeted endocytotic transport of PIN are regulated

by PINOID (PID) protein kinase and PP2A phosphatase complex mediated phosphorylation (Fozard et al., 2013). Extracellular auxin (possibly through the binding of ABP1) activates plasma membrane calcium transport in wheat embryos, creating $[Ca^{2+}]_{cyt}$ transients that activate the plasma membrane localized H⁺-ATPase to reduce apoplastic pH. Lower apoplastic pH activates pH sensitive cell wall loosening enzymes (Rober-Kleber et al., 2003; Shishova and Lindberg, 2010; Wang and Ruan, 2013). This proton influx into the cell wall compartment also increases competition with calcium for binding sites on de-esterified pectin, resulting in looser cell walls; as such higher levels of calcium can inhibit auxin-activated acid growth (Ferguson, 1984). H⁺-ATPase transport also activates voltage dependent inward rectifying K⁺ channels, this results in an increase in K⁺ content, causing osmotically driven movement of water into the cell, increasing cell turgor pressure. This acid growth pathway is responsible for cell elongation and expansion; it has been observed during growth and hormone-stimulated cell expansion of many tissues. Examples of auxin-calcium interactions in fruit growth are given below.

Auxin is also involved in calcium uptake and distribution in fruit. Application of CME (an auxin transport inhibitor) reduced calcium uptake into developing fruit of some tomato cultivars differing in susceptibility to blossom end rot (Brown and Ho, 1993). This reduced calcium uptake may occur through modification of cellular transport activity or perturbed cell expansion (disrupting xylem development). Calcium is also involved in fruit basipetal auxin transport. CME induced reductions in basipetal IAA efflux were only observed in tomato fruit grown under high salinity conditions where calcium uptake was reduced (Brown and Ho, 1993). In kiwifruit, light induction of higher levels of auxin-protecting hydroxycinnamic acids decreased auxin degradation, resulting in increased calcium uptake (Montanaro et al., 2007). These results suggest that tomato susceptibility to blossom end rot may be determined not just by differences in capacity for calcium uptake and distribution, but also by related factors such as auxin transport and metabolism, and rate of cell enlargement (Bangerth, 1976).

Abscisic Acid

Fruit ripening processes typically involve ABA and ethylene signaling. Non-climacteric fruit show a greater reliance upon ABA for initiation of ripening processes and do not demonstrate the same extent of ethylene responsiveness as climacteric fruit. ABA signaling in *Arabidopsis* acts through a network of calcium binding signal receptors (PYR/PYL/RCAR) and phosphorylation status modifiers including PP2C protein phosphatases ABI1 and ABI2 (Leung et al., 1994; Allen et al., 1999), and an array of CBL (Pandey et al., 2004), CIPK (Kim et al., 2003), and CDPK (Zhu et al., 2007) protein kinases (Fortes et al., 2015). A systems biology approach has been applied to understand the complexity of interactions and crosstalk between these networks (Cramer et al., 2011).

The concentration of ABA in grapes increases dramatically at the beginning of veraison; it is possible that the drop in cell turgor that occurs at this time triggers increases in ABA content (Castellarin et al., 2011). There are varietal differences in the time

during veraison (measured as % color change) at which maximal berry ABA is reached; Merlot (10% color change), Cabernet Sauvignon (50% color change), and Semillon (100% color change; Deytieu-Belleau et al., 2008). The partitioning of ABA between mesocarp and skin shifts from 100% in mesocarp prior to veraison, to approximately 40% in skin by maturity (Deytieu-Belleau et al., 2008). In non-climacteric fruit (e.g., strawberries and grapes) several other factors have been identified as potential ripening signal elements; auxin treatment of unripe fruit delays ripening (Boettcher et al., 2011) whilst reactive oxygen species accumulate in grape berries at the onset of ripening (Pilati et al., 2014). The transduction of these ripening triggers through the calcium signaling network suggests that calcium also plays a role in sugar accumulation and fruit softening and evidence for these functions are examined below.

Higher ABA levels at ripening leads to hexose accumulation through up-regulation of hexose transporters and increased apoplastic invertase activity (Pan et al., 2005; Deluc et al., 2009; Hayes et al., 2010). ABA activates sugar cell wall bound invertases at the initiation of grape ripening, catalyzing sucrose cleavage, decreasing the apoplastic sucrose concentration, and thereby allowing for continued phloem unloading of sucrose into the berry apoplasm (Pan et al., 2005). Phloem unloading of sugars becomes crucial for driving expansion, as well as efficiently maintaining the accumulation of sugars in the fruit. ABA and sugar responsive elements involved in these pathways have been identified, including an ABA and sugar responsive protein (VvMSR1) that forms part of a complex regulating expression of monosaccharide transporter VvHT1 (Cakir et al., 2003). Microarray expression analysis of cells overexpressing an ABA response element binding transcription factor (VvABF2) demonstrate elevated transcript levels of a vacuolar invertase, a hexose transporter, and cell wall modifying genes linked to fruit softening (i.e., polygalacturonase, pectin methyl esterase and rhamnogalacturonase; Nicolas et al., 2014). It has been demonstrated that ABA activates the calcium dependent protein kinase (ACPK1) in grape mesocarp through a complex mechanism involving influx of apoplastic calcium to the cytosol (Yu et al., 2006). AC PK1 in turn activates plasma membrane H⁺-ATPase in the berry mesocarp, possibly energizing the cell for solute uptake (Yu et al., 2006). A transient decrease in calcium concentration is observed in the apoplasm of *Vicia faba* leaves following ABA treatment, providing further evidence for apoplastic calcium as a transducer of ABA signaling (Felle et al., 2000). The timing of ABA accumulation, metabolic responses and the drop in turgor varies between varieties with differing ripening profiles (Deluc et al., 2009; Castellarin et al., 2011).

Combined Effects of Hormones

Endogenous hormone levels influence fruit softening by altering expression levels of enzymes that modify cell turgor pressure, apoplasm solute accumulation, and cell wall modification. Application of GA has been shown to increase berry firmness and shelf life in the table grape variety Thompson Seedless (Marzouk and Kassem, 2011). Suppression of a key enzyme involved in tomato ABA biosynthesis (*9-cis*-epoxycarotenoid dioxygenase) resulted in the transcriptional down regulation of

polygalacturonase, pectin methylesterase, expansion, and many other cell wall modifying enzymes (Sun et al., 2012; Osorio et al., 2013). In Cabernet Sauvignon berries treated with sucrose or sucrose and ABA, a drop in berry firmness (as occurs at the onset of ripening in the field) was only observed in the sucrose and ABA treated berries (Gambetta et al., 2010). The combined effect of ABA-activation of sugar invertases and cell wall modifying enzymes in the apoplasm is to simultaneously reduce cell turgor pressure and loosen cell walls (Pan et al., 2005; Gambetta et al., 2010). Auxin and ABA pathways utilize calcium as both a protein binding secondary messenger and in membrane transport mechanisms that modify turgor and solute accumulation to drive cell expansion and ripening.

IMPLICATIONS OF CALCIUM NUTRITION FOR FRUIT DISEASE SUSCEPTIBILITY

Understanding the role of calcium in fruit development is important for addressing ripening disorders (e.g., berry shrivel in Shiraz grapes), tissue localized calcium deficiencies (e.g., blossom end rot in tomatoes, bitter pit in apples), and pathogen susceptibilities (e.g., botrytis). Improved understanding of the calcium nutritional requirements of plants may also aid in optimizing fruit quality outcomes as both calcium deficiency and toxicity can affect the productivity of horticultural systems, and the post-harvest characteristics of the crop. Calcium deficiency can occur due to an insufficient mobilization of calcium from internal stores or a reduced supply of calcium through the xylem (often a result of low transpiration rates; White and Broadley, 2003). Calcium toxicity can occur due to high concentrations of available calcium in the soil solution; this can result in reduced growth rates and the ectopic deposition of calcium oxalate crystals (White and Broadley, 2003).

An ABA deficient tomato mutant (*sitiens*; which exhibits botrytis resistance) exhibits a lower degree of epidermal cell wall pectin de-esterification, reduced cuticle thickness, and increased cuticle permeability, when compared to wild type (Asselbergh et al., 2007; Curvers et al., 2010). The consequent reduction in botrytis susceptibility of *sitiens* may be as a result of: (a) plant detection of defective cuticle, prompting constitutive expression of chitinases and β -glucosidases into the cell wall, enabling rapid release of fungal elicitors upon infection, and/or (b) a lower level of de-esterification in *sitiens* cell walls providing a source of more bio-active OGAs upon infection; thereby producing a more rapid and effective response to pathogen attack (Curvers et al., 2010). The level of esterification in OGAs is one of several factors that determine their activity and specificity in triggering plant responses; it has been shown that the level of de-esterification in strawberry OGAs contributes to their capacity to elicit defense responses (Osorio et al., 2008). Although the exact mechanism of botrytis resistance in *sitiens* is unknown, it is clear that the interaction between epidermal cell wall derived pectins and the cuticle, either as defense signaling OGAs or as structural components, is important. In addition to the processes controlling deposition of cutin into the cuticle, processes affecting polysaccharide solubilisation and

movement into the cuticle, such as pectin de-esterification and calcium crosslinking, will modify fruit mechanical properties and pathogen susceptibility.

Blossom end rot in tomatoes is often cited as being a result of calcium deficiency. Tomatoes grown in low calcium nutrient solution show an increase in the incidence of blossom end rot (Coolong et al., 2014). Pericarp elasticity increased with calcium levels in the growth solution (Coolong et al., 2014). GA treatment of tomatoes leads to increased occurrence of blossom end rot while treatment with GA biosynthesis inhibitor prohexadione-calcium eliminated blossom end rot (de Freitas et al., 2012). GA treated tomatoes showed increased expression of CAX and Ca-ATPase genes and reduced apoplastic $[Ca^{2+}]$, whereas GA inhibitor treated fruit showed higher pericarp total calcium levels and an increased number of functional fruit xylem vessels (de Freitas et al., 2012). GA-induced gene expression for CAX and putative endoplasmic reticulum localized Ca-ATPase results in depletion of the apoplastic calcium pool, possibly below the critical concentration required for pectin-calcium crosslinks in the cell wall to maintain membrane stability and moderate cell expansion. Similarly, constitutive expression of an *Arabidopsis* CAX gene with its autoinhibitory region removed (sCAX1) in tomatoes led to increased calcium accumulation in the fruit pericarp, but lower calcium levels in apoplasm and cytosol compartments (de Freitas et al., 2011). The sCAX1 line showed leakier plasma membranes, with 100% of fruit demonstrating blossom end rot by 15 days after pollination (de Freitas et al., 2011), highlighting the need for targeted approaches to address localized calcium deficiencies. In addition to the localized decrease in calcium concentration, rapidly expanding tissue (such as the blossom end of tomatoes) may further impede normal fruit calcium distribution due to cellular intrusions causing obstruction or breakage of xylem vessels (Drazeta et al., 2004; de Freitas et al., 2012). Apogee-treated fruit showed increased numbers of functional xylem vessels; the impact of GA on xylem differentiation and development modifies normal pathways for calcium distribution (Saure, 2005). Additionally, GA triggers increased cuticle deposition (Knoche and Peschel, 2007), potentially modifying fruit water relations and calcium uptake. All of these factors provide possible linkages between GA responses and changes in calcium localization leading to blossom end rot.

Other examples of complications arising from sub-optimal calcium nutrition occur in apples and melons. Calcium accumulation in apples is also reduced by progressive breakdown of xylem connectivity as the result of growth related damage, potentially increasing occurrence of bitter pit disorder (Drazeta et al., 2004). In contrast, dye studies in post-veraison grapes indicate that the xylem not only remains relatively intact, but also continues to develop and mature (Chatelet et al., 2008). Application of exogenous calcium has also been proposed as a way to increase apple sugar content and post-harvest shelf life. However, the relationship between calcium and sugar accumulation is complex and many factors appear to affect the effectiveness of this strategy including soil calcium availability, timing of spray/application, apple variety, tree calcium status

and *in planta* interactions with other ions (e.g., boron; Lu et al., 2013). Levels of apple tree shading also have a complex effect, with conflicting reports as to whether apple calcium uptake is increased or decreased with shading (Chen et al., 1997; de Freitas et al., 2013). Melons suffer from a water-soaking condition that has been linked to apoplastic calcium deficiency where it has been hypothesized that depletion of apoplastic calcium supply can lead to insufficient pectin crosslinks in the middle lamella of the mesocarp, resulting in water-soaked tissue (Madrid et al., 2004; Nishizawa et al., 2004).

FUTURE PERSPECTIVES

Whilst advances in the understanding of water relations in the fruit vasculature are being made, interactions between water and specific extracellular domains are still largely uncharacterised. This review has discussed much of the existing literature that explores the interplay between cell wall composition, calcium binding, and water movement through plants. The observed diversity of ripening patterns demonstrates that, even within a species, inferences from these studies should be made with caution when looking at different species, varieties, or conditions.

Target areas for further research

How do calcium-pectin interactions affect water movement through fruit xylem vasculature? Are there critical 'control points' in the apoplasm that contribute to fruit water or nutrient deficiencies?

How does the developmental switch from phloem to xylem unloading of solutes affect apoplastic calcium levels, cell wall properties and membrane integrity?

How can our knowledge of calcium delivery, calcium-pectin binding conditions, and calcium signaling pathways during ripening be utilized to address calcium deficiency disorders and improve pathogen resistance?

The relative contributions of xylem and phloem to fruit water influx (or loss) are still a subject of contention. Studies of phloem flows and sap composition are notoriously difficult due to the fine and fragile nature of the compartment. Structural changes, the influence of ionic interactions, and osmotic effects within the xylem also make it a complex and dynamic compartment. It is hoped that a more holistic approach which incorporates not only measures of bulk tissue water balance and molecular mechanisms, but also knowledge of osmotic effects, changes in calcium distribution, pectin gels, and diffusion barriers, will help understand some of the idiosyncrasies of fruit water relations during ripening.

Further studies of calcium distribution in the cell wall and xylem vessels would increase our comprehension of the interactions between calcium nutrition, cell wall processes, and berry water relations. Techniques utilizing fluorescent and luminescent chemical or genetic indicators (e.g., Fluor-4, aequorin, CaR-GECO1 and pHlourin) could be used for quantifying calcium and pH differences (and treatment responses) across different fruit cell types. These techniques have already been applied in other plant tissues (e.g., pollen

tubes) to characterize the role of transport and signaling pathway components (e.g., CDPKs; Michard et al., 2008). Application of microscopy techniques for mapping ion concentrations and histochemical localization of cell wall component modifications throughout fruit ripening would also be beneficial. Particularly, combining calcium localization at a sub-cellular level using X-ray microanalysis, or equivalent techniques, with localization of esterified and de-esterified pectins using antibody probes could describe patterns of calcium movement and accumulation in fruit as well as identifying the location of calcium-pectin binding and gel formation (Conn et al., 2011). These results could be correlated with physical properties of fruit (e.g., fruit firmness, elasticity, and skin strength) determined by standard and high throughput methodologies on materials testing devices. This type of approach would bridge the gap between understanding of molecular mechanisms of ion transport and cell wall modification, and observations of fruit physiology impacts on harvest and post-harvest traits.

As the molecular mechanisms of calcium and water transport across cellular membranes are elucidated, and more RNA expression studies in particular fruit and cell types become available (e.g., Fasoli et al., 2012; Sato et al., 2012; Karlova et al., 2014; Palumbo et al., 2014), understanding of the influence of molecular mechanisms on pathways of water and calcium distribution will be improved. Additionally, these studies would help to describe the expression of genes involved in the developmental and stress-induced changes to cell wall composition and modification. This includes elucidation of transcription factor controls, pathogen responses through OGA release from the cell wall and binding by WAKs. The transduction of hormonal signals through calcium dependent kinase networks is also gaining more attention; translation of the functions of these networks in fruit will be an important future development.

REFERENCES

- Allen, G. J., Chu, S. P., Harrington, C. L., Schumacher, K., Hoffman, T., Tang, Y. Y., et al. (2001). A defined range of guard cell calcium oscillation parameters encodes stomatal movements. *Nature* 411, 1053–1057. doi: 10.1038/35082575
- Allen, G. J., Kuchitsu, K., Chu, S. P., Murata, Y., and Schroeder, J. I. (1999). *Arabidopsis* abi1-1 and abi2-1 phosphatase mutations reduce abscisic acid-induced cytoplasmic calcium rises in guard cells. *Plant Cell* 11, 1785–1798. doi: 10.2307/3871054
- Alleva, K., Niemietz, C. M., Maurel, C., Parisi, M., Tyerman, S. D., and Amodeo, G. (2006). Plasma membrane of *Beta vulgaris* storage root shows high water channel activity regulated by cytoplasmic pH and a dual range of calcium concentrations. *J. Exp. Bot.* 57, 609–621. doi: 10.1093/jxb/erj046
- Asselbergh, B., Curvers, K., Franca, S. C., Audenaert, K., Vuylsteke, M., Van Breusegem, F., et al. (2007). Resistance to *Botrytis cinerea* in sitiens, an abscisic acid-deficient tomato mutant, involves timely production of hydrogen peroxide and cell wall modifications in the epidermis. *Plant Physiol.* 144, 1863–1877. doi: 10.1104/pp.107.099226
- Bangerth, F. (1976). A role for auxin and auxin transport inhibitors on the Ca content of artificially induced parthenocarpic fruits. *Physiol. Plant.* 37, 191–194. doi: 10.1111/j.1399-3054.1976.tb03956.x
- Barnavon, L., Doco, T., Terrier, N., Ageorges, A., Romieu, C., and Pellerin, P. (2001). Involvement of pectin methyl-esterase during the ripening of grape berries: partial cDNA isolation, transcript expression and changes in the degree of methyl-esterification of cell wall pectins. *Phytochemistry* 58, 693–701. doi: 10.1016/S0031-9422(01)00274-6
- Becker, T., and Knoche, M. (2011). Water movement through the surfaces of the grape berry and its stem. *Am. J. Enol. Vitic.* 62, 340–350. doi: 10.5344/ajev.2011.10056
- Becker, T., and Knoche, M. (2012). Deposition, strain, and microcracking of the cuticle in developing 'Riesling' grape berries. *Vitis* 51, 1–6.
- Boettcher, C., Harvey, K., Forde, C. G., Boss, P. K., and Davies, C. (2011). Auxin treatment of pre-veraison grape (*Vitis vinifera* L.) berries both delays ripening and increases the synchronicity of sugar accumulation. *Aust. J. Grape Wine Res.* 17, 1–8. doi: 10.1111/j.1755-0238.2010.00110.x
- Brown, M. M., and Ho, L. C. (1993). Factors affecting calcium-transport and basipetal IAA movement in tomato fruit in relation to blossom-end rot. *J. Exp. Bot.* 44, 1111–1117. doi: 10.1093/jxb/44.7.1111
- Brummell, D. A. (2006). Cell wall disassembly in ripening fruit. *Funct. Plant Biol.* 33, 103–119. doi: 10.1071/FP05234
- Brummell, D. A., Harpster, M. H., Civello, P. M., Palys, J. M., Bennett, A. B., and Dunsmuir, P. (1999). Modification of expansin protein abundance in tomato fruit alters softening and cell wall polymer metabolism during ripening. *Plant Cell* 11, 2203–2216. doi: 10.1105/tpc.11.11.2203
- Burton, R. A., Gidley, M. J., and Fincher, G. B. (2010). Heterogeneity in the chemistry, structure and function of plant cell walls. *Nat. Chem. Biol.* 6, 724–732. doi: 10.1038/nchembio.439
- Cabanne, C., and Doneche, B. (2001). Changes in polygalacturonase activity and calcium content during ripening of grape berries. *Am. J. Enol. Vitic.* 52, 331–335.

With this data in hand, a more informed comprehension of the relationships between different components of these pathways will be established.

Although many of the individual roles of calcium in fruit are now being demonstrated, the effect of changes in calcium nutrition on fruit development, susceptibility to pathogens and calcium-related disorders is still lacking. The importance of calcium nutrition in determining susceptibility to major horticultural disorders has been established. However, the amelioration of these disorders and improvement in pathogen resistance through calcium fertilization does not deliver reliable results. Further studies that modify calcium nutrition without affecting other ionic interactions may improve the understanding of optimum plant calcium nutrition and enable better strategies for avoiding fruit physiological disorders and improving fruit physical traits at harvest.

AUTHOR CONTRIBUTIONS

BH wrote the majority of the manuscript with input from MG. MG, ST, and RB supervised BH's Ph.D. from where this review originated. All authors edited and commented on the manuscript.

ACKNOWLEDGMENTS

We would like to thank the University of Adelaide for supporting the Ph.D. research by BH, which produced this review. This research was conducted in the Australian Research Council funded Centre of Excellence in Plant Energy Biology (CE140100008) and Centre of Excellence in Plant Cell Walls (CE110001007); MG is supported by an ARC Future Fellowship (FT130100709).

- Cakir, B., Agasse, A., Gaillard, C., Saumoneau, A., Delrot, S., and Atanassova, R. (2003). A grape ASR protein involved in sugar and abscisic acid signaling. *Plant Cell* 15, 2165–2180. doi: 10.1105/tpc.013854
- Caravia, L., Collins, C., and Tyerman, S. D. (2015). Electrical impedance of Shiraz berries correlates with decreasing cell vitality during ripening. *Aust. J. Grape Wine Res.* 21, 430–438. doi: 10.1111/ajgw.12157
- Castellarin, S. D., Gambetta, G. A., Wada, H., Shackel, K. A., and Matthews, M. A. (2011). Fruit ripening in *Vitis vinifera*: spatiotemporal relationships among turgor, sugar accumulation, and anthocyanin biosynthesis. *J. Exp. Bot.* 62, 4345–4354. doi: 10.1093/jxb/err150
- Chardonnnet, C., and Doneche, B. (1995). Relation between calcium content and resistance to enzymatic digestion of the skin during grape ripening. *Vitis* 34, 95–98.
- Chardonnnet, C., Lhyvernat, A., and Doneche, B. (1997). Effect of calcium treatment prior to *Botrytis cinerea* infection on the changes in pectic composition of grape berry. *Physiol. Mol. Plant Pathol.* 50, 213–218. doi: 10.1006/pmpp.1996.0075
- Chardonnnet, C. O., Sams, C. E., Trigiano, R. N., and Conway, W. S. (2000). Variability of three isolates of *Botrytis cinerea* affects the inhibitory effects of calcium on this fungus. *Phytopathology* 90, 769–774. doi: 10.1094/PHYTO.2000.90.7.769
- Chatelet, D. S., Rost, T. L., Shackel, K. A., and Matthews, M. A. (2008). The peripheral xylem of grapevine (*Vitis vinifera*). 1. Structural integrity in post-veraison berries. *J. Exp. Bot.* 59, 1987–1996. doi: 10.1093/jxb/ern060
- Chen, K., Hu, G. Q., and Lenz, F. (1997). Training and shading effects on vegetative and reproductive growth and fruit quality of apple. *Gartenbauwissenschaft* 62, 207–213.
- Choat, B., Gambetta, G. A., Shackel, K. A., and Matthews, M. A. (2009). Vascular function in grape berries across development and its relevance to apparent hydraulic isolation. *Plant Physiol.* 151, 1677–1687. doi: 10.1104/pp.109.143172
- Cholewa, E., and Peterson, C. A. (2004). Evidence for symplastic involvement in the radial movement of calcium in onion roots. *Plant Physiol.* 134, 1793–1802. doi: 10.1104/pp.103.035287
- Clearwater, M. J., Luo, Z. W., Ong, S. E. C., Blattmann, P., and Thorp, T. G. (2012). Vascular functioning and the water balance of ripening kiwifruit (*Actinidia chinensis*) berries. *J. Exp. Bot.* 63, 1835–1847. doi: 10.1093/jxb/err352
- Conn, S., and Gillham, M. (2010). Comparative physiology of elemental distributions in plants. *Ann. Bot.* 105, 1081–1102. doi: 10.1093/aob/mcq027
- Conn, S. J., Berninger, P., Broadley, M. R., and Gillham, M. (2012). Exploiting natural variation to uncover candidate genes that control element accumulation in *Arabidopsis thaliana*. *New Phytol.* 193, 859–866. doi: 10.1111/j.1469-8137.2011.03977.x
- Conn, S. J., Gillham, M., Athman, A., Schreiber, A. W., Baumann, U., Moller, I., et al. (2011). Cell-specific vacuolar calcium storage mediated by CAX1 regulates apoplastic calcium concentration, gas exchange, and plant productivity in *Arabidopsis*. *Plant Cell* 23, 240–257. doi: 10.1105/tpc.109.072769
- Coolong, T., Mishra, S., Barickman, C., and Sams, C. (2014). Impact of supplemental calcium chloride on yield, quality, nutrient status, and postharvest attributes of tomato. *J. Plant Nutr.* 37, 2316–2330. doi: 10.1080/01904167.2014.890222
- Cramer, G., Urano, K., Delrot, S., Pezzotti, M., and Shinozaki, K. (2011). Effects of abiotic stress on plants: a systems biology perspective. *BMC Plant Biol.* 11:163 doi: 10.1186/1471-2229-11-163
- Curvers, K., Seifi, H., Mouille, G., De Rycke, R., Asselbergh, B., Van Hecke, A., et al. (2010). Abscisic acid deficiency causes changes in cuticle permeability and pectin composition that influence tomato resistance to *Botrytis cinerea*. *Plant Physiol.* 154, 847–860. doi: 10.1104/pp.110.158972
- Cybulska, J., Zdunek, A., and Konstankiewicz, K. (2011). Calcium effect on mechanical properties of model cell walls and apple tissue. *J. Food Eng.* 102, 217–223. doi: 10.1016/j.foodeng.2010.08.019
- Dal Santo, S., Vannonzi, A., Tornielli, G. B., Fasoli, M., Venturini, L., Pezzotti, M., et al. (2013). Genome-wide analysis of the expansin gene superfamily reveals grapevine-specific structural and functional characteristics. *PLoS ONE* 8:e62206. doi: 10.1371/journal.pone.0062206
- Dayod, M., Tyerman, S. D., Leigh, R. A., and Gillham, M. (2010). Calcium storage in plants and the implications for calcium biofortification. *Protoplasma* 247, 215–231. doi: 10.1007/s00709-010-0182-0
- de Freitas, S. T., Do Amarante, C. V. T., Dandekar, A. M., and Mitcham, E. J. (2013). Shading affects flesh calcium uptake and concentration, bitter pit incidence and other fruit traits in “Greensleeves” apple. *Sci. Hortic.* 161, 266–272. doi: 10.1016/j.scientia.2013.07.019
- de Freitas, S. T., Jiang, C. Z., and Mitcham, E. J. (2012). Mechanisms involved in calcium deficiency development in tomato fruit in response to gibberellins. *J. Plant Growth Regul.* 31, 221–234. doi: 10.1007/s00344-011-9233-9
- de Freitas, S. T., McElrone, A. J., Shackel, K. A., and Mitcham, E. J. (2014). Calcium partitioning and allocation and blossom-end rot development in tomato plants in response to whole-plant and fruit-specific abscisic acid treatments. *J. Exp. Bot.* 65, 235–247. doi: 10.1093/jxb/ert364
- de Freitas, S. T., and Mitcham, E. J. (2012). “Factors involved in fruit calcium deficiency disorders,” in *Horticultural Reviews*. (New York, NY: John Wiley & Sons, Inc.), 107–146.
- de Freitas, S. T., Padda, M., Wu, Q. Y., Park, S., and Mitcham, E. J. (2011). Dynamic alternations in cellular and molecular components during blossom-end rot development in tomatoes expressing sCAX1, a constitutively active Ca²⁺/H⁺ antiporter from *Arabidopsis*. *Plant Physiol.* 156, 844–855. doi: 10.1104/pp.111.175208
- Decreux, A., and Messiaen, J. (2005). Wall-associated kinase WAK1 interacts with cell wall pectins in a calcium-induced conformation. *Plant Cell Physiol.* 46, 268–278. doi: 10.1093/pcp/pci026
- Deluc, L. G., Quilici, D. R., Decendit, A., Grimpel, J., Wheatley, M. D., Schlauch, K. A., et al. (2009). Water deficit alters differentially metabolic pathways affecting important flavor and quality traits in grape berries of Cabernet Sauvignon and Chardonnay. *BMC Genom.* 10:212. doi: 10.1186/1471-2164-10-212
- Deytieux, C., Geny, L., and Doneche, B. (2005). “Relation between hormonal balance and polygalacturonase activity in grape berry,” in *Proceedings of the 5th International Postharvest Symposium*, Vol. 1–3, eds F. Mencarelli and P. Tonutti (Leuven 1: International Society Horticultural Science), 163–170. doi: 10.17660/actahortic.2005.682.15
- Deytieux-Belleau, C., Vallet, A., Doneche, B., and Geny, L. (2008). Pectin methylesterase and polygalacturonase in the developing grape skin. *Plant Physiol. Biochem.* 46, 638–646. doi: 10.1016/j.plaphy.2008.04.008
- Dodd, A. N., Kudla, J., and Sanders, D. (2010). The language of calcium signalling. *Annu. Rev. Plant Biol.* 61, 593–620. doi: 10.1146/annurev-arplant-070109-104628
- Dominguez, E., Lopez-Casado, G., Cuartero, J., and Heredia, A. (2008). Development of fruit cuticle in cherry tomato (*Solanum lycopersicum*). *Funct. Plant Biol.* 35, 403–411. doi: 10.1071/FP08018
- Drazeta, L., Lang, A., Hall, A. J., Volz, R. K., and Jameson, P. E. (2004). Causes and effects of changes in xylem functionality in apple fruit. *Ann. Bot.* 93, 275–282. doi: 10.1093/aob/mch040
- Espana, L., Heredia-Guerrero, J. A., Segado, P., Benitez, J. J., Heredia, A., and Dominguez, E. (2014). Biomechanical properties of the tomato (*Solanum lycopersicum*) fruit cuticle during development are modulated by changes in the relative amounts of its components. *New Phytol.* 202, 790–802. doi: 10.1111/nph.12727
- Evans, D. E., Briars, S. A., and Williams, L. E. (1991). Active calcium-transport by plant-cell membranes. *J. Exp. Bot.* 42, 285–303. doi: 10.1093/jxb/42.3.285
- Fasoli, M., Dal Santo, S., Zenoni, S., Tornielli, G. B., Farina, L., Zamboni, A., et al. (2012). The grapevine expression atlas reveals a deep transcriptome shift driving the entire plant into a maturation program. *Plant Cell* 24, 3489–3505. doi: 10.1105/tpc.112.100230
- Felle, H. H., Hanstein, S., Steinmeyer, R., and Hedrich, R. (2000). Dynamics of ionic activities in the apoplast of the sub-stomatal cavity of intact *Vicia faba* leaves during stomatal closure evoked by ABA and darkness. *Plant J.* 24, 297–304. doi: 10.1046/j.1365-313x.2000.00878.x
- Ferguson, I. B. (1984). Calcium in plant senescence and fruit ripening. *Plant Cell Environ.* 7, 477–489. doi: 10.1111/j.1365-3040.1984.tb01438.x
- Fortes, A. M., Teixeira, R. T., and Agudelo-Romero, P. (2015). Complex interplay of hormonal signals during grape berry ripening. *Molecules* 20, 9326–9343. doi: 10.3390/molecules20059326
- Fozard, J. A., King, J. R., and Bennett, M. J. (2013). Modelling auxin efflux carrier phosphorylation and localization. *J. Theoret. Biol.* 319, 34–49. doi: 10.1016/j.jtbi.2012.11.011
- Franceschi, V. R., and Nakata, P. A. (2005). Calcium oxalate in plants: formation and function. *Annu. Rev. Plant Biol.* 56, 41–71. doi: 10.1146/annurev.arplant.56.032604.144106

- Fritz, E. (2007). Measurement of cation exchange capacity (CEC) of plant cell walls by X-ray microanalysis (EDX) in the transmission electron microscope. *Microsc. Microanal.* 13, 233–244. doi: 10.1017/S1431927607070420
- Fuentes, S., Ljung, K., Sorefan, K., Alvey, E., Harberd, N. P., and Ostergaard, L. (2012). Fruit growth in *Arabidopsis* occurs via DELLA-dependent and DELLA-independent gibberellin responses. *Plant Cell* 24, 3982–3996. doi: 10.1105/tpc.112.103192
- Fuentes, S., Sullivan, W., Tilbrook, J., and Tyerman, S. (2010). A novel analysis of grapevine berry tissue demonstrates a variety-dependent correlation between tissue vitality and berry shrivel. *Aust. J. Grape Wine Res.* 16, 327–336. doi: 10.1111/j.1755-0238.2010.00095.x
- Gambetta, G. A., Matthews, M. A., Shaghassi, T. H., McElrone, A. J., and Castellarin, S. D. (2010). Sugar and abscisic acid signaling orthologs are activated at the onset of ripening in grape. *Planta* 232, 219–234. doi: 10.1007/s00425-010-1165-2
- Gendre, D., McFarlane, H. E., Johnson, E., Mouille, G., Sjodin, A., Oh, J., et al. (2013). Trans-Golgi network localized ECHIDNA/Ypt interacting protein complex is required for the secretion of cell wall polysaccharides in *Arabidopsis*. *Plant Cell* 25, 2633–2646. doi: 10.1105/tpc.113.112482
- Gillham, M., Athman, A., Tyerman, S. D., and Conn, S. J. (2011a). Cell-specific compartmentation of mineral nutrients is an essential mechanism for optimal plant productivity—another role for TPC1? *Plant Signal. Behav.* 6, 1656–1661. doi: 10.4161/psb.6.11.17797
- Gillham, M., Dayod, M., Hocking, B. J., Xu, B., Conn, S. J., Kaiser, B. N., et al. (2011b). Calcium delivery and storage in plant leaves: exploring the link with water flow. *J. Exp. Bot.* 62, 2233–2250. doi: 10.1093/jxb/err111
- Greenspan, M. D., Shackel, K. A., and Matthews, M. A. (1994). Developmental changes in the diurnal water-budget of the grape berry exposed to water deficits. *Plant Cell Environ.* 17, 811–820. doi: 10.1111/j.1365-3040.1994.tb00175.x
- Grignon, C., and Sentenac, H. (1991). pH and ionic conditions in the apoplast. *Ann. Rev. Plant Physiol.* 42, 103–128. doi: 10.1146/annurev.pp.42.060191.000053
- Han, S. C., Tang, R. H., Anderson, L. K., Woerner, T. E., and Pei, Z. M. (2003). A cell surface receptor mediates extracellular Ca²⁺ sensing in guard cells. *Nature* 425, 196–200. doi: 10.1038/nature01932
- Hayes, M. A., Davies, C., and Dry, I. B. (2007). Isolation, functional characterization, and expression analysis of grapevine (*Vitis vinifera* L.) hexose transporters: differential roles in sink and source tissues. *J. Exp. Bot.* 58, 1985–1997. doi: 10.1093/jxb/erm061
- Hayes, M. A., Feechan, A., and Dry, I. B. (2010). Involvement of abscisic acid in the coordinated regulation of a stress-inducible hexose transporter (VvHT5) and a cell wall invertase in grapevine in response to biotrophic fungal infection. *Plant Physiol.* 153, 211–221. doi: 10.1104/pp.110.154765
- Henderson, S. H., and Gillham, M. (2015). “Cell-type specific molecular mechanisms of plant adaptation to abiotic stresses,” in *Mechanisms in Plant Adaptation*, ed. R. Laitinen (London: Wiley Blackwell).
- Hepler, P. K., and Winship, L. J. (2010). Calcium at the cell wall-cytoplasm interface. *J. Integr. Plant Biol.* 52, 147–160. doi: 10.1111/j.1744-7909.2010.00923.x
- Ho, L. C., Belda, R., Brown, M., Andrews, J., and Adams, P. (1993). Uptake and transport of calcium and the possible causes of blossom-end rot in tomato. *J. Exp. Bot.* 44, 509–518. doi: 10.1093/jxb/44.2.509
- Ho, L. C., and White, P. J. (2005). A cellular hypothesis for the induction of blossom-end rot in tomato fruit. *Ann. Bot.* 95, 571–581. doi: 10.1093/aob/mci065
- Hocking, P. J. (1980). The composition of phloem exudate and xylem sap from tree tobacco (*Nicotiana glauca* Grah.). *Ann. Bot.* 45, 633–643.
- Hoson, T. (1998). Apoplast as the site of response to environmental signals. *J. Plant Res.* 111, 167–177. doi: 10.1007/BF02507163
- Jiang, L. X., Yang, S. L., Xie, L. F., Puah, C. S., Zhang, X. Q., Yang, W. C., et al. (2005). VANGUARD1 encodes a pectin methylesterase that enhances pollen tube growth in the *Arabidopsis* style and transmitting tract. *Plant Cell* 17, 584–596. doi: 10.1105/tpc.104.027631
- Johnson, C. H., Knight, M. R., Kondo, T., Masson, P., Sedbrook, J., Haley, A., et al. (1995). Circadian oscillations of cytosolic and chloroplastic free calcium in plants. *Science* 269, 1863–1865. doi: 10.1126/science.7569925
- Johnson, C. H., Shingles, R., and Ettlinger, W. (2006). “Regulation and role of calcium fluxes in the chloroplast,” in *The Structure and Function of Plastids*, eds R. Wise and J. Hoober. (Dordrecht: Springer), 403–416.
- Karlova, R., Chapman, N., David, K., Angenent, G. C., Seymour, G. B., and De Maagd, R. A. (2014). Transcriptional control of fleshy fruit development and ripening. *J. Exp. Bot.* 65, 4527–4541. doi: 10.1093/jxb/eru316
- Keller, M., and Shrestha, P. M. (2014). Solute accumulation differs in the vacuoles and apoplast of ripening grape berries. *Planta* 239, 633–642. doi: 10.1007/s00425-013-2004-z
- Keller, M., Zhang, Y., Shrestha, P. M., Biondi, M., and Bondada, B. R. (2015). Sugar demand of ripening grape berries leads to recycling of surplus phloem water via the xylem. *Plant Cell Environ.* 38, 1048–1059. doi: 10.1111/pce.12465
- Kidman, C. M., Dry, P. R., McCarthy, M. G., and Collins, C. (2014). Effect of rootstock on nutrition, pollination and fertilisation in ‘Shiraz’ (*Vitis vinifera* L.). *Vitis* 53, 139–145.
- Kiegler, E., Moore, C. A., Haseloff, J., Tester, M. A., and Knight, M. R. (2000). Cell-type-specific calcium responses to drought, salt and cold in the *Arabidopsis* root. *Plant J.* 23, 267–278. doi: 10.1046/j.1365-313x.2000.00786.x
- Kim, K. N., Cheong, Y. H., Grant, J. J., Pandey, G. K., and Luan, S. (2003). CIPK3, a calcium sensor-associated protein kinase that regulates abscisic acid and cold signal transduction in *Arabidopsis*. *Plant Cell* 15, 411–423. doi: 10.1105/tpc.006858
- Knipfer, T., Fei, J., Gambetta, G. A., McElrone, A. J., Shackel, K. A., and Matthews, M. A. (2015). Water transport properties of the grape pedicel during fruit development: insights into xylem anatomy and function using microtomography. *Plant Physiol.* 168, 1590–1602. doi: 10.1104/pp.15.00031
- Knoche, M., and Peschel, S. (2007). Gibberellins increase cuticle deposition in developing tomato fruit. *Plant Growth Regul.* 51, 1–10. doi: 10.1007/s10725-006-9107-5
- Kohorn, B. D., and Kohorn, S. L. (2012). The cell wall-associated kinases, WAKs, as pectin receptors. *Front. Plant Sci.* 3:88. doi: 10.3389/fpls.2012.00088
- Konrad, K. R., Wudick, M. M., and Feijo, J. A. (2011). Calcium regulation of tip growth: new genes for old mechanisms. *Curr. Opin. Plant Biol.* 14, 721–730. doi: 10.1016/j.pbi.2011.09.005
- Krasnow, M., Matthews, M., and Shackel, K. (2008). Evidence for substantial maintenance of membrane integrity and cell viability in normally developing grape (*Vitis vinifera* L.) berries throughout development. *J. Exp. Bot.* 59, 849–859. doi: 10.1093/jxb/erm372
- Kudla, J., Batistic, O., and Hashimoto, K. (2010). Calcium signals: the lead currency of plant information processing. *Plant Cell* 22, 541–563. doi: 10.1105/tpc.109.072686
- Kumar, R., Khurana, A., and Sharma, A. K. (2014). Role of plant hormones and their interplay in development and ripening of fleshy fruits. *J. Exp. Bot.* 65, 4561–4575. doi: 10.1093/jxb/eru277
- Lacampagne, S., Lambert, C., Belleau-Deytieux, C., L'Hyvernat, A., Doneche, B., and Geny, L. (2010). “Expression, activity and cellular localization of pectin methylesterase in grape berry skin during ripening,” in *Proceedings of the VI International Postharvest Symposium*, eds M. Erkan and U. Aksoy (Leuven 1: Int Soc Horticultural Science), 1057–1062. doi: 10.17660/actahortic.2010.877.143
- Lang, A., and Thorpe, M. R. (1989). Xylem, phloem and transpiration flows in a grape – application of a technique for measuring the volume of attached fruits to high-resolution using Archimedes principle. *J. Exp. Bot.* 40, 1069–1078. doi: 10.1093/jxb/40.10.1069
- Lee, K. J. D., Marcus, S. E., and Knox, J. P. (2011). Cell wall biology: perspectives from cell wall imaging. *Mol. Plant* 4, 212–219. doi: 10.1093/mp/ssf075
- Leng, P., Yuan, B., and Guo, Y. (2014). The role of abscisic acid in fruit ripening and responses to abiotic stress. *J. Exp. Bot.* 65, 4577–4588. doi: 10.1093/jxb/eru204
- Leung, J., Bouvierduran, M., Morris, P. C., Guerrier, D., Chefdeville, F., and Giraudat, J. (1994). *Arabidopsis* ABA response gene AB11 - features of a calcium-modulated protein phosphatase. *Science* 264, 1448–1452. doi: 10.1126/science.7910981
- Lu, Y. Q., Liu, H. P., Wang, Y., Zhang, X. Z., and Han, Z. H. (2013). Synergistic roles of leaf boron and calcium during the growing season in affecting sugar and starch accumulation in ripening apple fruit. *Acta Physiol. Plant.* 35, 2483–2492. doi: 10.1007/s11738-013-1283-0
- Madrid, R., Valverde, M., Alcolea, V., and Romojaro, F. (2004). Influence of calcium nutrition on water soaking disorder during ripening of *Cantaloupe melon*. *Sci. Hortic.* 101, 69–79. doi: 10.1016/j.scientia.2003.10.005
- Manganaris, G. A., Vasilakakis, M., Mignani, I., Diamantidis, G., and Tzavella-Klonari, K. (2005). The effect of preharvest calcium sprays on quality attributes,

- physicochemical aspects of cell wall components and susceptibility to brown rot of peach fruits (*Prunus persica* L. cv. Andross). *Sci. Hortic.* 107, 43–50. doi: 10.1016/j.scientia.2005.06.005
- Marti, M. C., Stancombe, M. A., and Webb, A. A. R. (2013). Cell- and stimulus type-specific intracellular free Ca²⁺ signals in *Arabidopsis*. *Plant Physiol.* 163, 625–634. doi: 10.1104/pp.113.222901
- Martin, L. B. B., and Rose, J. K. C. (2014). There's more than one way to skin a fruit: formation and functions of fruit cuticles. *J. Exp. Bot.* 65, 4639–4651. doi: 10.1093/jxb/eru301
- Marzouk, H. A., and Kassem, H. A. (2011). Improving yield, quality, and shelf life of Thompson seedless grapevine by preharvest foliar applications. *Sci. Hortic.* 130, 425–430. doi: 10.1016/j.scientia.2011.07.013
- Matthews, M. A., Thomas, T. R., and Shackel, K. A. (2009). Fruit ripening in *Vitis vinifera* L.: possible relation of veraison to turgor and berry softening. *Aust. J. Grape Wine Res.* 15, 278–283. doi: 10.1111/j.1755-0238.2009.00060.x
- Mazzeo, M., Dichio, B., Clearwater, M. J., Montanaro, G., and Xiloyannis, C. (2013). Hydraulic resistance of developing *Actinidia* fruit. *Ann. Bot.* 112, 197–205. doi: 10.1093/aob/mct101
- McAinch, M. R., and Pittman, J. K. (2009). Shaping the calcium signature. *New Phytol.* 181, 275–294. doi: 10.1111/j.1469-8137.2008.02682.x
- McAtee, P., Karim, S., Schaffer, R., and David, K. (2013). A dynamic interplay between phytohormones is required for fruit development, maturation, and ripening. *Front. Plant Sci.* 4:79. doi: 10.3389/fpls.2013.00079.
- Michard, E., Dias, P., and Feijo, J. A. (2008). Tobacco pollen tubes as cellular models for ion dynamics: improved spatial and temporal resolution of extracellular flux and free cytosolic concentration of calcium and protons using pHluorin and YC3.1 CaMleon. *Sex. Plant Reprod.* 21, 169–181. doi: 10.1007/s00497-008-0076-x
- Mohnen, D. (2008). Pectin structure and biosynthesis. *Curr. Opin. Plant Biol.* 11, 266–277. doi: 10.1016/j.pbi.2008.03.006
- Montanaro, G., Dichio, B., Lang, A., Mininni, A. N., Nuzzo, V., Clearwater, M. J., et al. (2014). Internal versus external control of calcium nutrition in kiwifruit. *J. Plant Nutr. Soil Sci.* 177, 819–830. doi: 10.1002/jpln.201400396
- Montanaro, G., Dichio, B., Lang, A., Mininni, A. N., and Xiloyannis, C. (2015). Fruit calcium accumulation coupled and uncoupled from its transpiration in kiwifruit. *J. Plant Physiol.* 181, 67–74. doi: 10.1016/j.jplph.2015.04.004
- Montanaro, G., Dichio, B., Xiloyannis, C. (2012a). "Fruit transpiration: mechanisms and significance for fruit nutrition and growth," in *Advances in Selected Plant Physiology Aspects*, ed. G Montanaro (Rijeka: Intech),
- Montanaro, G., Dichio, B., Xiloyannis, C., and Lang, A. (2012b). Fruit transpiration in kiwifruit: environmental drivers and predictive model. *AoB Plants* 6, pls036. doi: 10.1093/aobpla/pls036
- Montanaro, G., Treutter, D., and Xiloyannis, C. (2007). Phenolic compounds in young developing kiwifruit in relation to light exposure: implications for fruit calcium accumulation. *J. Plant Interact.* 2, 63–69. doi: 10.1080/17429140701429228
- Nawrath, C., Schreiber, L., Franke, R. B., Geldner, N., Reina-Pinto, J. J., and Kunst, L. (2013). Apoplastic diffusion barriers in *Arabidopsis*. *Arabidopsis Book* 11, e0167. doi: 10.1199/tab.0167
- Ngouemazong, D. E., Jolei, R. P., Cardinaels, R., Fraeye, I., Van Loey, A., Moldenaers, P., et al. (2012). Stiffness of Ca²⁺-pectin gels: combined effects of degree and pattern of methylesterification for various Ca²⁺ concentrations. *Carbohydr. Res.* 348, 69–76. doi: 10.1016/j.carres.2011.11.011
- Nicolas, P., Lecourieux, D., Kappel, C., Cluzet, S., Cramer, G., Delrot, S., et al. (2014). The basic leucine zipper transcription factor ABCSICIC ACID RESPONSE ELEMENT-BINDING FACTOR2 is an important transcriptional regulator of abscisic acid-dependent grape berry ripening processes. *Plant Phys.* 164, 365–383. doi: 10.1104/pp.113.231977
- Nishizawa, T., Kobayashi, T., and Aikawa, T. (2004). Effect of calcium supply on the physiology of fruit tissue in 'Andesu' netted melon. *J. Hortic. Sci. Biotechnol.* 79, 500–508. doi: 10.1080/14620316.2004.11511796
- Nunan, K. J., Davies, C., Robinson, S. P., and Fincher, G. B. (2001). Expression patterns of cell wall-modifying enzymes during grape berry development. *Planta* 214, 257–264. doi: 10.1007/s004250100609
- Nunan, K. J., Sims, I. M., Bacic, A., Robinson, S. P., and Fincher, G. B. (1998). Changes in cell wall composition during ripening of grape berries. *Plant Physiol.* 118, 783–792. doi: 10.1104/pp.118.3.783
- Ortega-Regules, A., Ros-Garcia, J. M., Bautista-Ortin, A. B., Lopez-Roca, J. M., and Gomez-Plaza, E. (2008). Changes in skin cell wall composition during the maturation of four premium wine grape varieties. *J. Sci. Food Agric.* 88, 420–428. doi: 10.1002/jsfa.3102
- Osorio, S., Castillejo, C., Quesada, M. A., Medina-Escobar, N., Brownsey, G. J., Suau, R., et al. (2008). Partial demethylation of oligogalacturonides by pectin methyl esterase 1 is required for eliciting defence responses in wild strawberry (*Fragaria vesca*). *Plant J.* 54, 43–55. doi: 10.1111/j.1365-313X.2007.03398.x
- Osorio, S., Scossa, F., and Fernie, A. R. (2013). Molecular regulation of fruit ripening. *Front. Plant Sci.* 4:198. doi: 10.3389/fpls.2013.00198
- Palumbo, M. C., Zenoni, S., Fasoli, M., Massonnet, M., Farina, L., Castiglione, F., et al. (2014). Integrated network analysis identifies fight-club nodes as a class of hubs encompassing key putative switch genes that induce major transcriptome reprogramming during grapevine development. *Plant Cell* 26, 4617–4635. doi: 10.1105/tpc.114.133710
- Pan, Q. H., Li, M. J., Peng, C. C., Zhang, N., Zou, X., Zou, K. Q., et al. (2005). Abscisic acid activates acid invertases in developing grape berry. *Physiol. Plant.* 125, 157–170. doi: 10.1111/j.1399-3054.2005.00552.x
- Pandey, G. K., Cheong, Y. H., Kim, K. N., Grant, J. J., Li, L. G., Hung, W., et al. (2004). The calcium sensor calcineurin B-Like 9 modulates abscisic acid sensitivity and biosynthesis in *Arabidopsis*. *Plant Cell* 16, 1912–1924. doi: 10.1105/tpc.021311
- Park, S., Cheng, N. H., Pittman, J. K., Yoo, K. S., Park, J., Smith, R. H., et al. (2005). Increased calcium levels and prolonged shelf life in tomatoes expressing *Arabidopsis* H+/Ca²⁺ transporters. *Plant Physiol.* 139, 1194–1206. doi: 10.1104/pp.105.066266
- Pilati, S., Brazzale, D., Guella, G., Milli, A., Ruberti, C., Biasioli, F., et al. (2014). The onset of grapevine berry ripening is characterized by ROS accumulation and lipoxygenase-mediated membrane peroxidation in the skin. *BMC Plant Biol.* 14:87. doi: 10.1186/1471-2229-14-87
- Pitann, B., Schubert, S., and Muehling, K. H. (2009). Decline in leaf growth under salt stress is due to an inhibition of H⁺-pumping activity and increase in apoplastic pH of maize leaves. *J. Plant Nutr. Soil Sc.* 172, 535–543. doi: 10.1002/jpln.200800349
- Plavcova, L., and Hacke, U. G. (2011). Heterogeneous distribution of pectin epitopes and calcium in different pit types of four angiosperm species. *New Phytol.* 192, 885–897. doi: 10.1111/j.1469-8137.2011.03842.x
- Redgwell, R. J., Macrae, E., Hallett, I., Fischer, M., Perry, J., and Harker, R. (1997). In vivo and in vitro swelling of cell walls during fruit ripening. *Planta* 203, 162–173. doi: 10.1007/s004250050178
- Röber-Kleber, N., Albrechtova, J. T. P., Fleig, S., Huck, N., Michalke, W., Wagner, E., et al. (2003). Plasma membrane H⁺-ATPase is involved in auxin-mediated cell elongation during wheat embryo development. *Plant Physiol.* 131, 1302–1312. doi: 10.1104/pp.013466
- Rogiers, S. Y., Greer, D. H., Hatfield, J. M., Orchard, B. A., and Keller, M. (2006a). Mineral sinks within ripening grape berries (*Vitis vinifera* L.). *Vitis* 45, 115–123.
- Rogiers, S. Y., Greer, D. H., Hatfield, J. M., Orchard, B. A., and Keller, M. (2006b). Solute transport into Shiraz berries during development and late-ripening shrinkage. *Am. J. Enol. Vitic.* 57, 73–80.
- Rogiers, S. Y., Keller, M., Holzapfel, B. P., and Virgona, J. M. (2000). Accumulation of potassium and calcium by ripening berries on field vines of *Vitis vinifera* (L) cv. Shiraz. *Aust. J. Grape Wine Res.* 6, 240–243. doi: 10.1111/j.1755-0238.2000.tb00184.x
- Rounds, C. M., Lubeck, E., Hepler, P. K., and Winship, L. J. (2011). Propidium iodide competes with Ca²⁺ to label pectin in pollen tubes and *Arabidopsis* root hairs. *Plant Physiol.* 157, 175–187. doi: 10.1104/pp.111.182196
- Ruan, Y. L., Patrick, J. W., Bouzayen, M., Osorio, S., and Fernie, A. R. (2012). Molecular regulation of seed and fruit set. *Trends Plant Sci.* 17, 656–665. doi: 10.1016/j.tplants.2012.06.005
- Saladie, M., Matas, A. J., Isaacson, T., Jenks, M. A., Goodwin, S. M., Niklas, K. J., et al. (2007). A reevaluation of the key factors that influence tomato fruit softening and integrity. *Plant Physiol.* 144, 1012–1028. doi: 10.1104/pp.107.097477
- Sampedro, J., and Cosgrove, D. J. (2005). The expansin superfamily. *Genome Biol.* 6, 242. doi: 10.1186/gb-2005-6-12-242

- Sato, S., Tabata, S., Hirakawa, H., Asamizu, E., Shirasawa, K., Isobe, S., et al. (2012). The tomato genome sequence provides insights into fleshy fruit evolution. *Nature* 485, 635–641. doi: 10.1038/nature11119
- Saure, M. C. (2005). Calcium translocation to fleshy fruit: its mechanism and endogenous control. *Scientia Hortic.* 105, 65–89. doi: 10.1016/j.scienta.2004.10.003
- Saure, M. C. (2014). Why calcium deficiency is not the cause of blossom-end rot in tomato and pepper fruit – a reappraisal. *Sci. Hortic.* 174, 151–154. doi: 10.1016/j.scienta.2014.05.020
- Schlosser, J., Olsson, N., Weis, M., Reid, K., Peng, F., Lund, S., et al. (2008). Cellular expansion and gene expression in the developing grape (*Vitis vinifera* L.). *Protoplasma* 232, 255–265. doi: 10.1007/s00709-008-0280-9
- Seifert, G. J., and Blaukopf, C. (2010). Irritable walls: the plant extracellular matrix and signaling. *Plant Physiol.* 153, 467–478. doi: 10.1104/pp.110.153940
- Serrani, J. C., Ruiz-Rivero, O., Fos, M., and Garcia-Martinez, J. L. (2008). Auxin-induced fruit-set in tomato is mediated in part by gibberellins. *Plant J.* 56, 922–934. doi: 10.1111/j.1365-313X.2008.03654.x
- Shabala, S. (2000). Ionic and osmotic components of salt stress specifically modulate net ion fluxes from bean leaf mesophyll. *Plant Cell Environ.* 23, 825–837. doi: 10.1046/j.1365-3040.2000.00606.x
- Shishova, M., and Lindberg, S. (2010). A new perspective on auxin perception. *J. Plant Physiol.* 167, 417–422. doi: 10.1016/j.jplph.2009.12.014
- Sun, L., Sun, Y. F., Zhang, M., Wang, L., Ren, J., Cui, M. M., et al. (2012). Suppression of 9-cis-epoxycarotenoid dioxygenase, which encodes a key enzyme in abscisic acid biosynthesis, alters fruit texture in transgenic tomato. *Plant Physiol.* 158, 283–298. doi: 10.1104/pp.111.186866
- Swarbreck, S. M., Colaco, R., and Davies, J. M. (2013). Plant calcium-permeable channels. *Plant Physiol.* 163, 514–522. doi: 10.1104/pp.113.220855
- Tang, R. H., Han, S. C., Zheng, H. L., Cook, C. W., Choi, C. S., Woerner, T. E., et al. (2007). Coupling diurnal cytosolic Ca²⁺ oscillations to the CAS-IP3 pathway in *Arabidopsis*. *Science* 315, 1423–1426. doi: 10.1126/science.1134457
- Thomas, T. R., Matthews, M. A., and Shackel, K. A. (2006). Direct in situ measurement of cell turgor in grape (*Vitis vinifera* L.) berries during development and in response to plant water deficits. *Plant Cell Environ.* 29, 993–1001. doi: 10.1111/j.1365-3040.2006.01496.x
- Tibbitts, C. W., Macdougall, A. J., and Ring, S. G. (1998). Calcium binding and swelling behaviour of a high methoxyl pectin gel. *Carbohydr. Res.* 310, 101–107. doi: 10.1016/S0008-6215(98)00172-4
- Tilbrook, J., and Tyerman, S. D. (2009). Hydraulic connection of grape berries to the vine: varietal differences in water conductance into and out of berries, and potential for backflow. *Funct. Plant Biol.* 36, 541–550. doi: 10.1071/FP09019
- Tyerman, S. D., Tilbrook, J., Pardo, C., Kotula, L., Sullivan, W., and Steudle, E. (2004). Direct measurement of hydraulic properties in developing berries of *Vitis vinifera* L. cv Shiraz and Chardonnay. *Aust. J. Grape Wine Res.* 10, 170–181. doi: 10.1111/j.1755-0238.2004.tb00020.x
- Vallarino, J. G., and Osorio, S. (2012). Signaling role of oligogalacturonides derived during cell wall degradation. *Plant Signal. Behav.* 7, 1447–1449. doi: 10.4161/psb.21779
- van Doorn, W. G., Hiemstra, T., and Fanourakis, D. (2011). Hydrogel regulation of xylem water flow: an alternative hypothesis. *Plant Physiol.* 157, 1642–1649. doi: 10.1104/pp.111.185314
- Verdoucq, L., Grondin, A., and Maurel, C. (2008). Structure-function analysis of plant aquaporin AtPIP2;1 gating by divalent cations and protons. *Biochem. J.* 415, 409–416. doi: 10.1042/BJ20080275
- Vorwerk, S., Somerville, S., and Somerville, C. (2004). The role of plant cell wall polysaccharide composition in disease resistance. *Trends Plant Sci.* 9, 203–209. doi: 10.1016/j.tplants.2004.02.005
- Wang, L., and Ruan, Y. L. (2013). Regulation of cell division and expansion by sugar and auxin signaling. *Front. Plant Sci.* 4:163. doi: 10.3389/fpls.2013.00163
- Wang, W. H., Chen, J., Liu, T. W., Chen, J., Han, A. D., Simon, M., et al. (2014). Regulation of the calcium-sensing receptor in both stomatal movement and photosynthetic electron transport is crucial for water use efficiency and drought tolerance in *Arabidopsis*. *J. Exp. Bot.* 65, 223–234. doi: 10.1093/jxb/ert362
- Wang, W. H., Yi, X. Q., Han, A. D., Liu, T. W., Chen, J., Wu, F. H., et al. (2012). Calcium-sensing receptor regulates stomatal closure through hydrogen peroxide and nitric oxide in response to extracellular calcium in *Arabidopsis*. *J. Exp. Bot.* 63, 177–190. doi: 10.1093/jxb/err259
- Webb, A. A. R., Larman, M. G., Montgomery, L. T., Taylor, J. E., and Hetherington, A. M. (2001). The role of calcium in ABA-induced gene expression and stomatal movements. *Plant J.* 26, 351–362. doi: 10.1046/j.1365-313X.2001.01032.x
- Whalley, H. J., and Knight, M. R. (2013). Calcium signatures are decoded by plants to give specific gene responses. *New Phytol.* 197, 690–693. doi: 10.1111/nph.12087
- White, P. J. (2000). Calcium channels in higher plants. *BBA-Biomembranes* 1465, 171–189. doi: 10.1016/S0005-2736(00)00137-1
- White, P. J. (2001). The pathways of calcium movement to the xylem. *J. Exp. Bot.* 52, 891–899. doi: 10.1093/jexbot/52.358.891
- White, P. J., and Broadley, M. R. (2003). Calcium in plants. *Ann. Bot.* 92, 487–511. doi: 10.1093/aob/mcg164
- Willats, W. G. T., Orfila, C., Limberg, G., Buchholt, H. C., Van Alebeek, G., Voragen, A. G. J., et al. (2001). Modulation of the degree and pattern of methyl-esterification of pectic homogalacturonan in plant cell walls - implications for pectin methyl esterase action, matrix properties, and cell adhesion. *J. Biol. Chem.* 276, 19404–19413. doi: 10.1074/jbc.M011242200
- Yu, X. C., Li, M. J., Gao, G. F., Feng, H. Z., Geng, X. Q., Peng, C. C., et al. (2006). Abscisic acid stimulates a calcium-dependent protein kinase in grape berry. *Plant Physiol.* 140, 558–579. doi: 10.1104/pp.105.074971
- Zhu, S. Y., Yu, X. C., Wang, X. J., Zhao, R., Li, Y., Fan, R. C., et al. (2007). Two calcium-dependent protein kinases, CPK4 and CPK11, regulate abscisic acid signal transduction in *Arabidopsis*. *Plant Cell* 19, 3019–3036. doi: 10.1105/tpc.107.050666
- Zsivanovits, G., Macdougall, A. J., Smith, A. C., and Ring, S. G. (2004). Material properties of concentrated pectin networks. *Carbohydr. Res.* 339, 1317–1322. doi: 10.1016/j.carres.2004.02.027
- Zwieniecki, M. A., Melcher, P. J., and Holbrook, N. M. (2001). Hydrogel control of xylem hydraulic resistance in plants. *Science* 291, 1059–1062. doi: 10.1126/science.1057175

Conflict of Interest Statement: The authors declare that the research was conducted in the absence of any commercial or financial relationships that could be construed as a potential conflict of interest.

Copyright © 2016 Hocking, Tyerman, Burton and Gillham. This is an open-access article distributed under the terms of the Creative Commons Attribution License (CC BY). The use, distribution or reproduction in other forums is permitted, provided the original author(s) or licensor are credited and that the original publication in this journal is cited, in accordance with accepted academic practice. No use, distribution or reproduction is permitted which does not comply with these terms.



Identification of Peach NAP Transcription Factor Genes and Characterization of their Expression in Vegetative and Reproductive Organs during Development and Senescence

Fang Li, Jinjin Li, Ming Qian, Mingyu Han, Lijun Cao, Hangkong Liu, Dong Zhang and Caiping Zhao *

OPEN ACCESS

Edited by:

Mario Pezzotti,
University of Verona, Italy

Reviewed by:

Claudio Bonghi,
University of Padova, Italy

Athanasis Tsafaris,

Centre for Research and Technology
Hellas (C.E.R.T.H), Greece

***Correspondence:**

Caiping Zhao
zhcc@nwauaf.edu.cn.

Specialty section:

This article was submitted to
Plant Physiology,
a section of the journal
Frontiers in Plant Science

Received: 09 September 2015

Accepted: 28 January 2016

Published: 16 February 2016

Citation:

Li F, Li J, Qian M, Han M, Cao L, Liu H, Zhang D and Zhao C (2016)
Identification of Peach NAP Transcription Factor Genes and Characterization of their Expression in Vegetative and Reproductive Organs during Development and Senescence.
Front. Plant Sci. 7:147.
doi: 10.3389/fpls.2016.00147

The NAP (NAC-like, activated by AP₃/P₁) transcription factor belongs to a subfamily of the NAC transcription factor family, and is believed to have an important role in regulating plant growth and development. However, there is very little information about this subfamily in Rosaceous plants. We identified seven NAP genes in the peach genome. *PpNAP2* was categorized in the NAP I group, and contained a conserved transcription activation region. The other *PpNAP* genes belonged to the NAP II group. The expression patterns of the *PpNAP* genes differed in various organs and developmental stages. *PpNAP1* and *PpNAP2* were highly expressed in mature and senescing flowers, but not in leaves, fruits, and flower buds. *PpNAP3* and *PpNAP5* were only expressed in leaves. The *PpNAP4* expression level was high in mature and senescing fruits, while *PpNAP6* and *PpNAP7* expression was up-regulated in mature and senescent leaves and flowers. During the fruit development period, the *PpNAP4* and *PpNAP6* expression levels rapidly increased during the S1 and S4 stages, which suggests these genes are involved in the first exponential growth phase and fruit ripening. During the fruit ripening and softening period, the *PpNAP1*, *PpNAP4*, and *PpNAP6* expression levels were high during the early storage period, which was accompanied by a rapid increase in ethylene production. *PpNAP1*, *PpNAP4*, and *PpNAP6* expression slowly increased during the middle or late storage periods, and peaked at the end of the storage period. Additionally, abscisic acid (ABA)-treated fruits were softer and produced more ethylene than the controls. Furthermore, the *PpNAP1*, *PpNAP4*, and *PpNAP6* expression levels were higher in ABA-treated fruits. These results suggest that *PpNAP1*, *PpNAP4*, and *PpNAP6* are responsive to ABA and may regulate peach fruit ripening.

Keywords: *Prunus persica*, NAP subfamily, fruit, development, ripening

INTRODUCTION

The development and maturation of plant tissues involve complex processes regulated by genetic, hormonal, and environmental factors (Wang, 2008). The NAP transcription factor is a member of a subfamily of the plant-specific NAC (NAM, ATAF1, 2.CUC2) transcription factor family, which is important in many vital biological processes during plant growth and development (Sablowski and Meyerowitz, 1998; Fernandez et al., 2006; Fan et al., 2015). Sablowski and Meyerowitz (1998) determined that AtNAP is associated with cell expansion in specific *Arabidopsis thaliana* flower organs, while Guo and Gan (2006) reported that AtNAP is important for leaf senescence. This was further supported by a study that revealed AtNAP regulates leaf senescence processes by directly binding to the promoter of *SAG113* to form an ABA-AtNAP-SAG113 PP2C regulatory chain that controls stomatal movement and water loss in senescent leaves (Zhang and Gan, 2012). Other studies have demonstrated that NAP affects leaf senescence in bamboo (Chen et al., 2011), crocus (Kalivas et al., 2010), *Festuca arundinacea* (Guo et al., 2010), *Asarina procumbens* (Fan and Zhao, 2014), and rice (Ooka et al., 2003). Kou et al. (2012) reported that AtNAP expression increased during siliques senescence in *A. thaliana*. Fernandez et al. (2006) observed that VvNAP may be important for grapevine flower and fruit development. In *Citrus sinensis* (L.) Osbeck, CitNAC expression was detected only in the fruit peel and pulp during the fruit ripening or senescence stages (Liu et al., 2009). Additionally, recent studies showed that the NAP subfamily is also important for regulating plant senescence and response to abiotic stresses (Meng et al., 2009; Zhang and Gan, 2012; Huang et al., 2013). The NAP transcription factor has been identified in various plant species, including rice (Ooka et al., 2003), bamboo (Chen et al., 2011), wheat (Cristobal et al., 2006), cotton (Meng et al., 2009), grape (Fernandez et al., 2006), maize (Fan et al., 2014), and soybean (Meng et al., 2007). However, the effect of NAP on the development of Rosaceae plants has not been studied.

Peach (*Prunus persica*) is an economically important crop, whose typical climacteric fruit undergoes a program of enhanced ethylene production and an associated increase in respiration rate at the onset of ripening (Barry and Giovannoni, 2007). Therefore, peach fruit softening and senescence rapidly occur after harvest, which makes storage and transport difficult. This limits peach production. A more thorough characterization of the physiological basis of peach fruit growth and ripening will enable the development of effective strategies to regulate these processes. Furthermore, peach, as a stone fruit, exhibits a typical double sigmoid growth pattern during fruit development, with distinct growth stages (S1–S4). The S1 stage corresponds to the first exponential growth phase, and is characterized by a rapid increase in cell division and elongation. In the S2 stage, which proceeds more slowly than S1, most of the dry matter is involved in pit hardening and seed and embryo growth. The S3 stage represents the second exponential growth phase, during which the fruit

rapidly increases in size. Fruit ripening occurs in the final stage (S4) (Li et al., 1989; Tonutti et al., 1997; Soto et al., 2013).

In this study, we identified seven members of the peach NAP subfamily and analyzed their expression during leaf, flower, and fruit development and senescence. We revealed that members of this subfamily may function in the development and maturation of flowers and fruits, and regulate fruit softening.

MATERIALS AND METHODS

Plant Materials

Peach tree (*P. persica* cv. 'Qinguang 8') samples were collected from the Experimental Station of the College of Horticulture at the Northwest A & F University in Yangling, Shaanxi, China. Samples included flowers, leaves, and fruits. Flower samples consisted of flower buds, blooming flowers, and flowers 2 days after full bloom. Young leaves were those that had just unfolded, and were collected from new shoots, while mature and senescent leaves were collected from the middle sections of new shoots. Young, mature, and senescent fruits were collected 42, 107, and 131 days after full bloom (DAFB), respectively. For fruit development analyses, young fruits were hand-picked 25 DAFB, and samples were collected every 15 days until the fruits reached commercial maturity (i.e., fruits with light green or partially red peels and slightly hard flesh). At least 20 fruits at each developmental stage were used to determine fruit weight, diameter, and gene expression.

For storage analyses, fruits with no visible defects were randomly hand picked at commercial maturity and divided into two groups. One group was soaked with 100 mM abscisic acid (ABA) for 10 min at 25 ± 1°C. The other group was soaked with water and served as the control group. Each group consisted of 120 fruits, which were kept in individual plastic bags at 25 ± 1°C. During the storage period, fruit samples were collected every 2 days, until the flesh fully softened. All samples were frozen with liquid nitrogen and stored at –80°C.

RNA Extraction and Reverse Transcription

Total RNA was extracted using cetyltrimethylammonium bromide (Chang et al., 1993), and reverse transcription was completed using the PrimeScript RT Reagent Kit with gDNA Eraser (Takara).

Identification of Peach NAP Subfamily Members

Arabidopsis thaliana, *Vitis vinifera*, and *Solanum lycopersicum* NAP gene sequences were used to search the peach genome database¹ with the NCBI BLASTp tool to identify peach genes that were highly homologous to NAP subfamily genes.

¹www.rosaceae.org/species/prunus_persica/genome_v1.0

TABLE 1 | Peach NAP genes identified in this study.

Gene name	Gene locus	Chromosome no.	Genbank accession no.	Deduced polypeptide			Signal peptide
				Length (aa)	MW(kDa)	PI	
PpNAP1	ppa007445m	7	EMJ03289	383	42.91	8.23	—
PpNAP2	ppa009530m	1	EMJ 24523	288	33.19	7.01	—
PpNAP3	ppa020620m	4	EMJ15685	385	44.51	6.37	—
PpNAP4	ppa007577m	4	EMJ 12674	363	40.35	7.78	—
PpNAP5	ppa017586m	6	EMJ 09136	348	39.83	8.18	—
PpNAP6	ppa007314m	4	EMJ 12652	373	41.07	8.45	—
PpNAP7	ppa015363m	6	EMJ07423	356	40.46	8.25	—

Gene locus corresponds to annotation ID from peach (*Prunus persica*) genome data.

Multiple Sequence Alignment, Phylogenetic Analysis, and Exon/Intron Structure Determination

The NCBI BLAST tool² was used to assess sequence similarities. The open reading frames of *PpNAP* genes were analyzed using the NCBI Open Reading Frame Finder tool³. Multiple sequence alignment analyses were conducted using the DNAMAN program, and graphical annotations of consensus sequences were completed using the Weblogo online tool⁴. A phylogenetic tree was generated using the NJ method (with 1,000 repeats) of the MEGA 6.06 software. Genetic structure investigations were conducted using the Gene Structure Display Server online tool⁵. Signal peptides were analyzed with the SignalP program⁶ (version 3.0; Bendtsen et al., 2004). Protein molecular weights and pIs were calculated using the ExPASy Compute pI/Mw tool⁷.

Molecular Cloning of Peach NAP Subfamily Members

To clone the *PpNAP* genes, Primer Premier 6.0 was used to design gene-specific primer pairs according to the peach genome sequence (Table 1). Using cDNA templates, PCR was completed with the Phanta Super-Fidelity DNA Polymerase (Vazyme) according to the manufacturer's recommended procedure. The PCR products were isolated and purified with the MiniBEST Agarose Gel DNA Extraction Kit Ver. 4.0 (Takara). Purified products were inserted into the pMD-19T vector (Takara). Positive clones were confirmed by blue/white plaque assays. Primers for cloning and quantitative reverse transcription (qRT)-PCR were synthesized by Sangon Biotech (Shanghai) Co., Ltd, which also completed all DNA sequencing reactions.

²<http://www.ncbi.nlm.nih.gov/BLAST/>

³<http://www.ncbi.nlm.nih.gov/gorf/gorf.html>

⁴<http://weblogo.berkeley.edu/logo.cgi>

⁵<http://gsds.cbi.pku.edu.cn>

⁶<http://www.cbs.dtu.dk/services/SignalP/>

⁷http://web.expasy.org/compute_pi/

Quantitative Reverse Transcription PCR Assays

The qRT-PCR was conducted using the iQ5 real-time PCR system (Bio-Rad). The gene-specific primers (Table 1) were designed using the Beacon Designer 8.0 software (Premier Biosoft International). Each primer pair (T_m 60°C) was designed to amplify an approximately 200-bp fragment. For each sample, 1 μ L cDNA, 1 μ L each primer, 2 μ L double-distilled water, and 5 μ L 2x SYBR Premix ExTaq II (Takara) were used in a total volume of 10 μ L. The two-step RT-PCR was completed using the manufacturer's recommended program, but the annealing temperature was changed to 60°C. Samples were heated at 95°C for 10 s, cooled to 65°C for 15 s, and finally heated to 95°C at a rate of 0.1°C s^{-1} for melting curve analyses. The specific transcript accumulation was analyzed using the $2^{-\Delta\Delta CT}$ method (Livak and Schmittgen, 2001). Peach 18S ribosomal RNA was used to normalize data. The amplification, melt curve and melt park of 18s ribosomal gene in all samples can be seen in Supplementary Figure S1. Each sample was analyzed in triplicate.

Flesh Firmness and Ethylene Production

Flesh firmness of five randomly selected fruits was measured using the GY-4 firmness meter equipped with a 8-mm diameter probe. A small epicarp segment was peeled from two places of each fruit to enable probe attachment. Three biological replicates were measured. Ethylene production was determined as described by Liguori et al. (2004) using the Trace GC Ultra gas chromatograph (Thermo Fisher Scientific). The oven, injector, and detector temperatures were 90, 110, and 140°C, respectively.

Search for Cis-Acting Elements in the Promoters of Peach NAP Genes

Upstream regions (2000 bp upstream of the transcription start site) of selected peach *NAP* genes were used to search the PlantCARE database for putative *cis*-acting elements (Lescot et al., 2002).

Statistical Analyses

Gene expression levels were subjected to analysis of variance using SAS. Values are provided as the mean \pm standard error

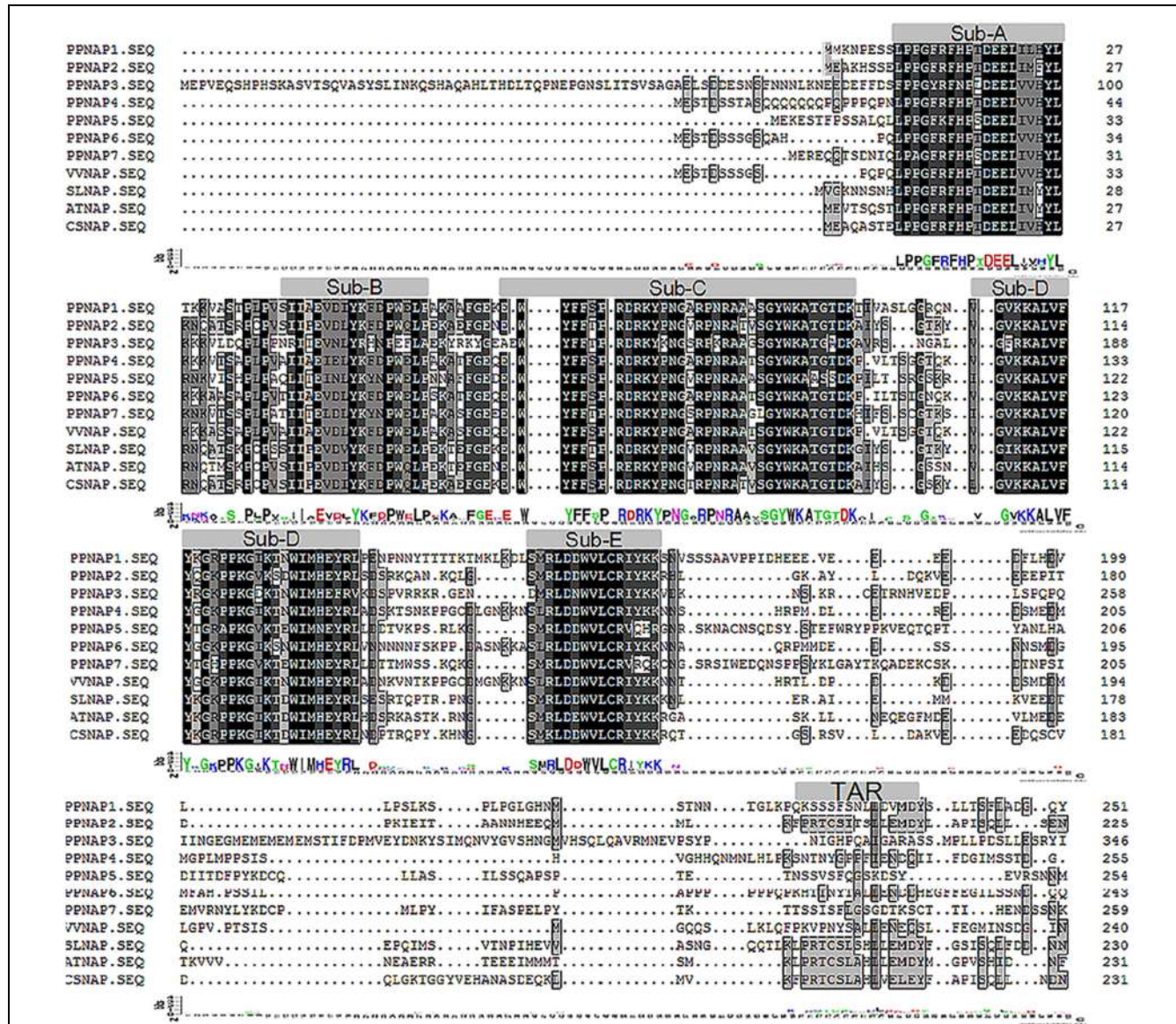


FIGURE 1 | Multiple sequence alignments of PpNAP proteins and NAP proteins from other plants. The accession numbers of the proteins homologous to AtNAP are provided in Supplementary Table S2.

($n = 3$). The overall least significant difference ($p < 0.05$) was calculated and used to separate means.

RESULTS

Identification of Peach NAP Subfamily Members

Seven NAP genes were detected in the peach genome with query IDs of ppa007445m, ppa009530m, ppa020620m, ppa007577m, ppa017586m, ppa007314m, and ppa015363m, which corresponded to *PpNAP1*, *PpNAP2*, *PpNAP3*, *PpNAP4*, *PpNAP5*, *PpNAP6*, and *PpNAP7*, respectively. These peach NAP genes contain a conserved NAC domain structure at the

N-terminus, and the domain can be divided into A, B, C, D, and E subdomains. The conserved amino acid sequences in the A, B, C, D, and E subdomains were LPPGFRFHPTDEELIVHYL, IIAEVDIYKFDPWELP, EWYFFSPRDRKYPNGARP, NRAAVSGYWATGTDK, VGVKKALVFYKGRPPKGYKT-DWIMHEYRL, and SMRLDDWVLCRIYKK, respectively (Figure 1). Furthermore, according to Fan et al. (2015), the NAP subfamily could be divided into two groups (NAP I and NAP II). Because of the presence of the relatively conserved transcription activation region, *PpNAP2* was included in the NAP I group, while the other *PpNAP* genes were included in the NAP II group (Figure 1). The *PpNAP* genes were highly homologous to NAP genes from other species. Similar to other NAP genes, *PpNAP1-6* consisted of three exons and two introns,

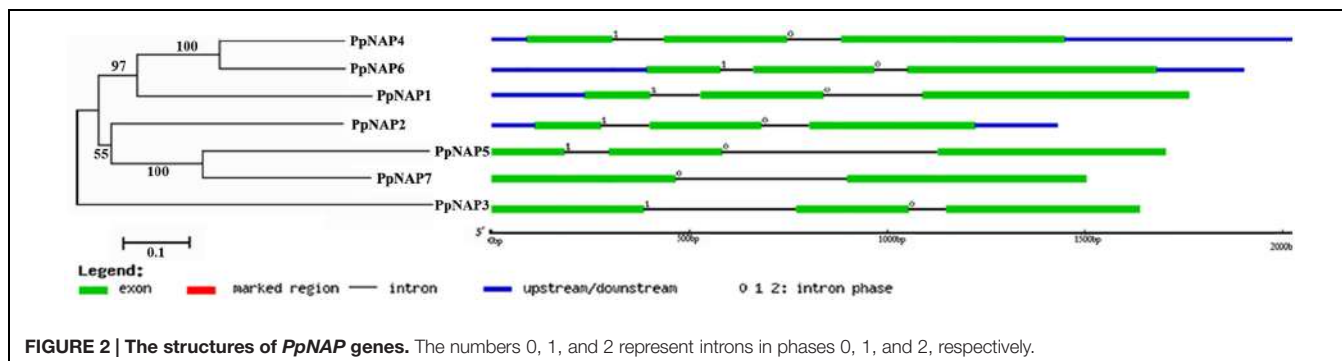


FIGURE 2 | The structures of *PpNAP* genes. The numbers 0, 1, and 2 represent introns in phases 0, 1, and 2, respectively.

while *PpNAP7* contained two exons and one intron (Figure 2). The deduced polypeptide sequences ranged from 288 to 385 amino acids, with predicted molecular weights between 33.19 and 44.51 kDa. The predicted pIs of *PpNAP* genes were from 6.37 to 8.45. None of the identified peach NAP genes contained signal peptide sequences according to SignalP analysis (Table 1).

Phylogenetic Analysis of the Peach NAP Subfamily Members

To evaluate the evolutionary relationships among NAP subfamily members, cluster analyses were completed using the amino acid sequences encoded by the identified *PpNAP* genes and by NAC genes from potato, tomato, pepper, orange, grape, rice, *A. thaliana*, and bamboo using the MEGA 6.06 software. Phylogenetic analyses revealed that all *PpNAPs* are clustered in the NAP subfamily (Figure 3). *PpNAP2* was similar to citrus, *A. thaliana*, and western balsam poplar NAPs, while *PpNAP4* and *PpNAP6* were similar to NAPs from grape and wheat. In contrast, *PpNAP3*, *PpNAP5*, and *PpNAP7* were not particularly similar to NAPs of other plants. Additionally, the deduced amino acid sequences were more highly conserved among *PpNAP4*, *PpNAP5*, *PpNAP6*, and *PpNAP7*, while the similarities among *PpNAP1*, *PpNAP2*, and *PpNAP3* were less than 28%.

PpNAP Gene Expression in Various Organs at Different Developmental Stages

To investigate the potential functions of *PpNAP* genes during peach development, transcription level changes in different organs were analyzed using qRT-PCR. The *PpNAP* expression patterns were different among various organs and developmental stages (Figure 4). The *PpNAP* expression levels in leaves were lower than those in flowers and fruits. The expression of *PpNAP6* and *PpNAP7* rapidly increased in maturing and senescing leaves. The *PpNAP1*, *PpNAP4*, and *PpNAP5* genes were more highly expressed in young and senescent leaves than in mature leaves. In contrast, *PpNAP3* transcript levels were high in mature leaves, while *PpNAP2* expression remained relatively stable and at low levels (Figure 4A).

The expression levels of *PpNAP1* and *PpNAP6* were rapidly up-regulated in blooming and 2 DAFB flowers. *PpNAP2*, *PpNAP4*, and *PpNAP7* were highly expressed in blooming

flowers, but expressed at very low levels in flower buds. Similarly, *PpNAP3* and *PpNAP5* expression were almost undetectable in flowers at all developmental stages (Figure 4B).

The *PpNAP4* and *PpNAP6* expression levels were higher than those of the other *PpNAP* genes in fruits. The higher expression levels were most obvious for *PpNAP4* in mature and senescent fruits and *PpNAP6* in young and senescent fruits. *PpNAP1* and *PpNAP2* were expressed at low levels, while *PpNAP3*, *PpNAP5*, and *PpNAP7* expression was barely detectable (Figure 4C).

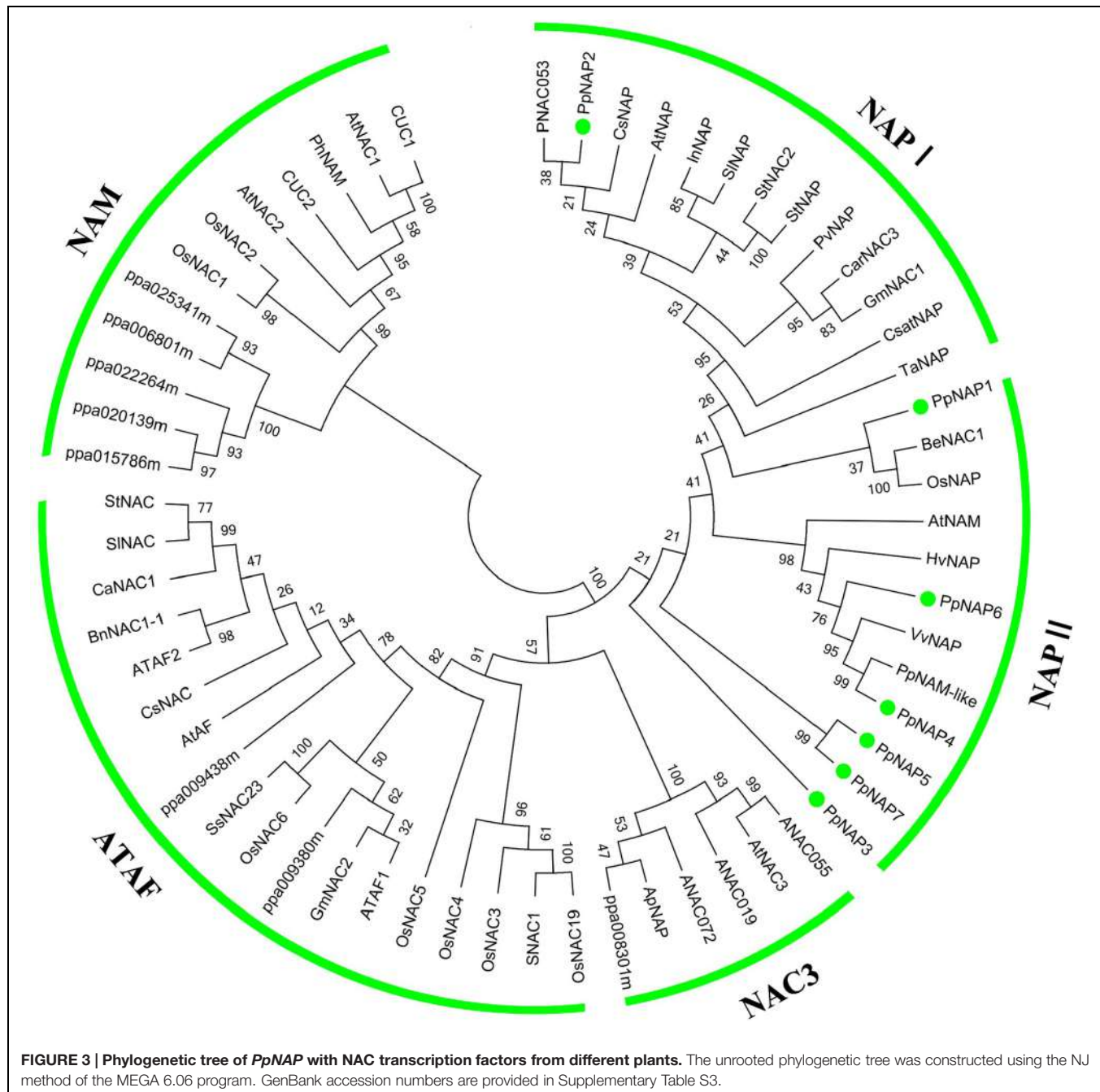
PpNAP Gene Expression Profiles During Fruit Development

To confirm the accuracy of the predicted cDNA sequences and further explore the biological functions of *PpNAP1*, *PpNAP2*, *PpNAP4*, and *PpNAP6* in fruit, we designed specific primer pairs using the peach genome sequence for cloning and expression analyses in mature 'Qinguang 8' fruits. The cDNA sequences of *PpNAP2*, *PpNAP4*, and *PpNAP6* were consistent with the corresponding genome sequences, while that of *PpNAP1* was 48 nucleotides longer than expected (see Supplementary Material). The expression of Pp-ACO1 is strictly related to the transition between the pre-climacteric and climacteric stage. We have analyzed the expression of Pp-ACO1 during developmental stage, and the result showed the obvious enhance of Pp-ACO1 expression at S4 stage (Supplementary Figure S2).

The qRT-PCR results revealed that *PpNAP4* expression in the mesocarp rapidly increased during the S1 fruit development stage (25–55 DAFB; Figures 5A,D), increased slowly during S2 and S3 (55–102 DAFB; Figures 5A,D), and significantly increased during S4, where it was maintained at a high level (102–121 DAFB; Figures 5A,D). In contrast, *PpNAP6* expression rapidly increased during S1, but decreased in S2, remained stable during S3, and increased during S4 (Figures 5A,E). The expression levels of *PpNAP1* and *PpNAP2* were low during fruit development, with elevated expression levels only during S3 (85–100 DAFB) and S1 (25–55 DAFB), respectively (Figures 5A–C).

PpNAP Gene Expression Profiles During Fruit Ripening and Softening

The firmness, ethylene production, and *PpNAP* expression of commercially mature 'Qinguang 8' fruits were measured during



fruit storage. In the first 2 days after harvest (DAH), fruit firmness decreased slowly, while from 2 to 8 DAH, fruit firmness declined rapidly (**Figure 6A**). Ethylene production doubled from 0 to 2 DAH, increased slowly from 2 to 6 DAH, and then decreased considerably (**Figure 6B**).

During storage, the *PpNAP1*, *PpNAP4*, and *PpNAP6* expression levels exhibited similar trends. Expression increased during the early storage period and was highest at 2 DAH, which coincided with the first peak of ethylene release. The expression levels subsequently declined to varying degrees. This was followed by an increasing trend from 4 or 6 DAH to 10 DAH

(**Figures 6C,E,F**). *PpNAP4* and *PpNAP6* expression levels were highest at the end of the storage period (**Figures 6E,F**). In contrast, *PpNAP2* expression was maintained at a low level throughout the storage period, with highest expression levels at 4 DAH (**Figure 6D**).

Effects of ABA Treatment on *PpNAP* Gene Expression, Ethylene Release, and Fruit Firmness

The firmness of the ABA-treated fruits was lower than that of the control fruits in the first 2 DAH, after which the firmness

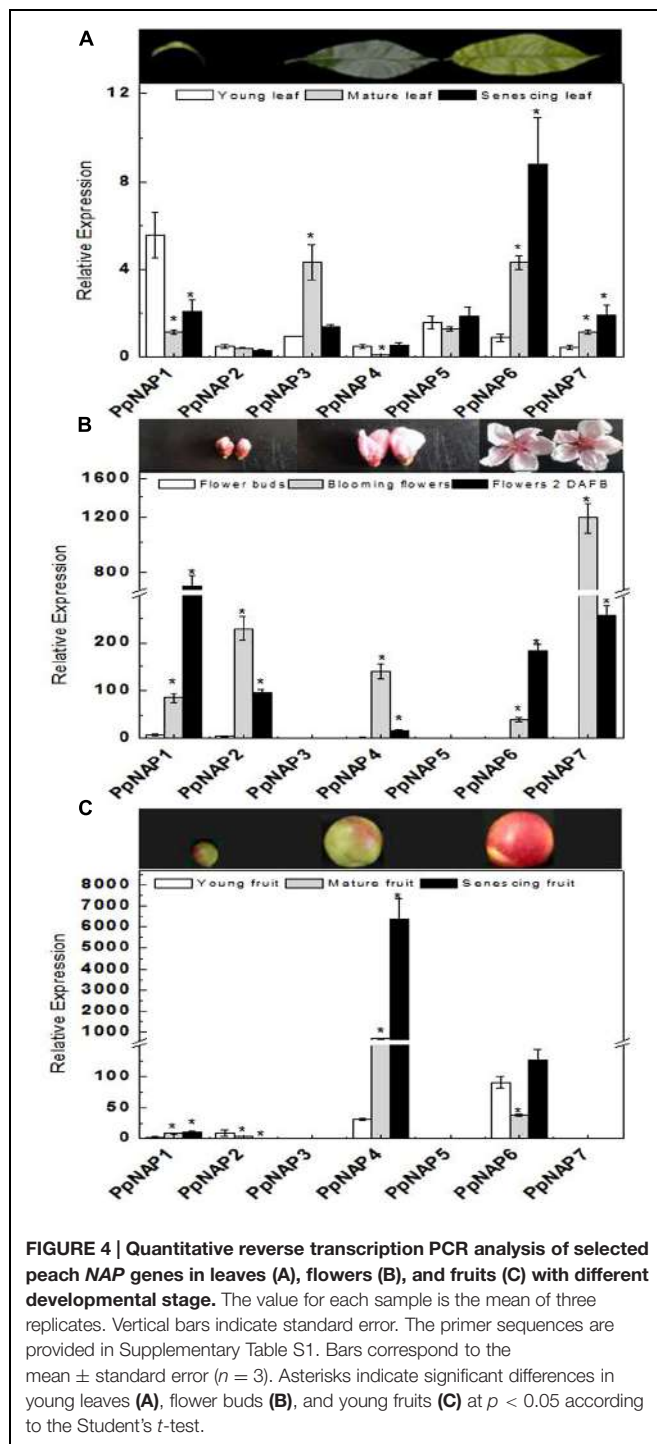


FIGURE 4 | Quantitative reverse transcription PCR analysis of selected peach NAP genes in leaves (A), flowers (B), and fruits (C) with different developmental stage. The value for each sample is the mean of three replicates. Vertical bars indicate standard error. The primer sequences are provided in Supplementary Table S1. Bars correspond to the mean \pm standard error ($n = 3$). Asterisks indicate significant differences in young leaves (A), flower buds (B), and young fruits (C) at $p < 0.05$ according to the Student's *t*-test.

of the treated and control fruits decreased significantly, with treated fruits softening faster. The maximum storage periods for treated and control fruits were 6 and 10 days, respectively (Figure 6A).

After ABA treatment, the release rate of endogenous ethylene sharply increased and peaked at 2 DAH, with higher peak rates for treated fruits than for controls (Figure 6B). The *PpNAP1*, *PpNAP4*, and *PpNAP6* expression levels increased following ABA

treatment for the duration of the storage period (Figures 6E,F). *PpNAP2* expression increased following ABA treatment at 2 and 6 DAH (Figure 6D).

Sequence Analysis of NAP Promoters for Fruit-Specific Expression

PlantCARE database were used to identify *cis*-acting elements in the promoter regions of four NAP genes specifically expressed in fruit. The detected *cis*-acting elements were categorized in the following four classes: (1) involved in the perception of plant hormones, such as ABA, ethylene, methyl jasmonate, salicylic acid, and gibberellic acid; (2) related to expression elements specific to particular tissues, such as endosperm, seed, and shoot; (3) involved in transcription activation and enhancement, such as the TATA-box, CAAT-box, and 5' untranslated region pyrimidine-rich stretch; and (4) associated with responses to environmental and physiological stimuli, such as drought, low temperature, heat stress, anaerobic conditions, light, fungal elicitors, and other stresses (Table 2).

Among the identified *cis*-acting elements associated with hormone-related responses, the ABA-responsive element was present (one to eight copies) in all studied promoters, while the coupling element 3 was detected only in the *PpNAP1* and *PpNAP2* promoters. The CGTCA and TGACG *cis*-acting element motifs responsive to methyl jasmonate were detected (one to four or five copies) in all promoters except for that of *PpNAP1*, while the MADS-domain site CArG-box was present in all promoters (one to three copies).

DISCUSSION

Identified NAP Subfamily Members and Sequence Analyses

The NAP is a transcription factor with crucial roles in many biological processes during plant growth and development (Fan et al., 2015). In this study, we identified seven NAP genes in the peach genome that were homologous to NAP genes from three other plant species. However, Fan et al. (2015) reported that there are four NAP genes in peach, corresponding to the *PpNAP1*, *PpNAP2*, *PpNAP4*, and *PpNAP6* genes identified in our study. We detected three more NAP genes, namely *PpNAP3*, *PpNAP5*, and *PpNAP7*. Multiple sequence alignments revealed that the seven peach NAP proteins contained the five typical NAC subdomains, and were very similar to other NAP proteins (Figure 1). Phylogenetic analyses indicated that all seven *PpNAP* genes clustered in the NAP subfamily, with only *PpNAP2* belonging to the NAP I group, while the others belonged to the NAP II group. This suggests the function of *PpNAP2* may differ from that of the other members.

Tissue-Specific Expression of *PpNAP* Genes

The expression levels of the identified peach NAP genes were measured in leaves, flowers, and fruits, as well as during maturation and senescence. The results indicated the genes had

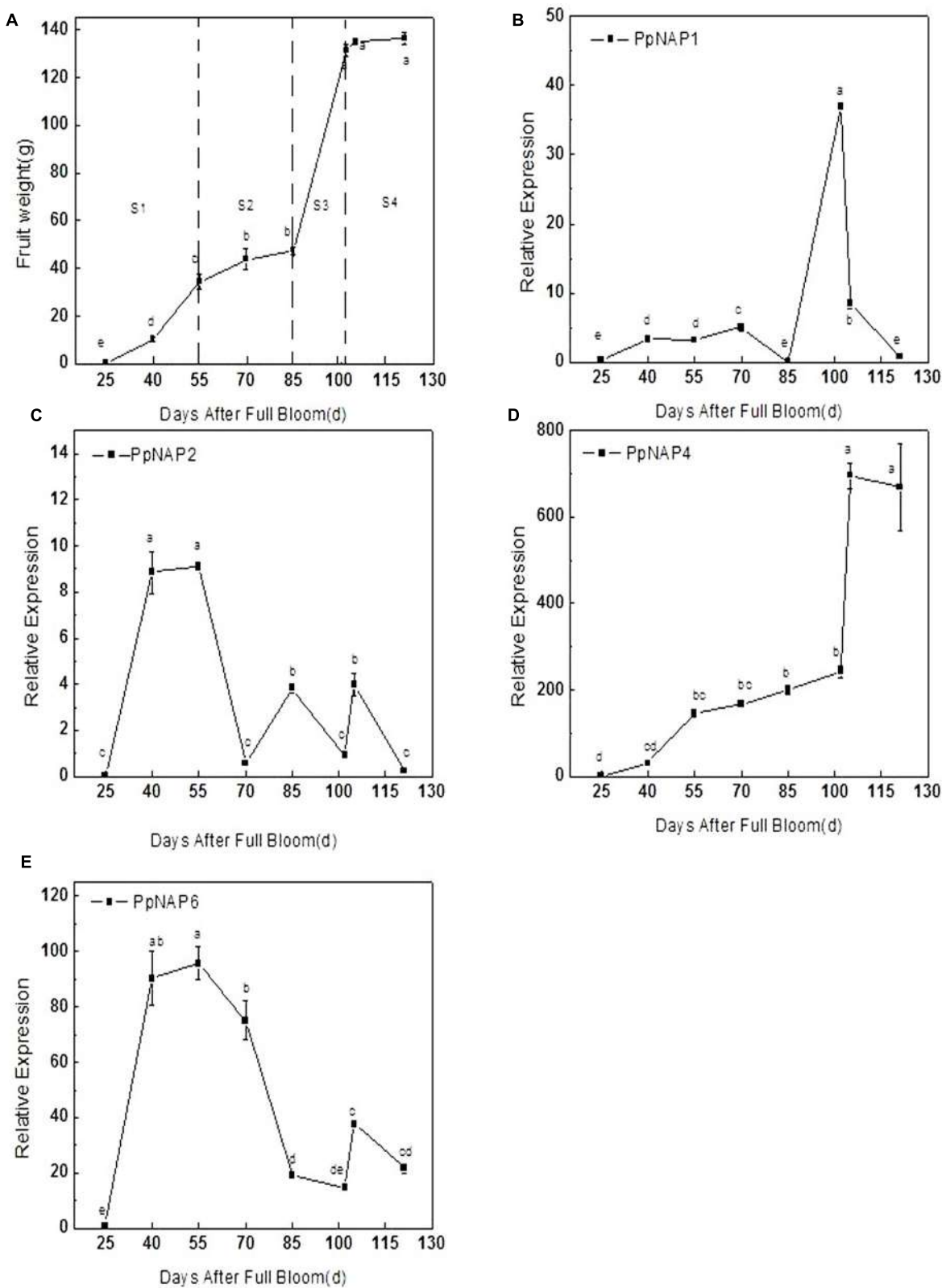


FIGURE 5 | Average fruit weight after full bloom (A), quantitative reverse transcription PCR analysis of selected peach NAP genes during fruit development (B–E). Bars correspond to the mean \pm standard error ($n = 3$). The overall least significant difference ($p < 0.05$) was calculated and used to separate means.

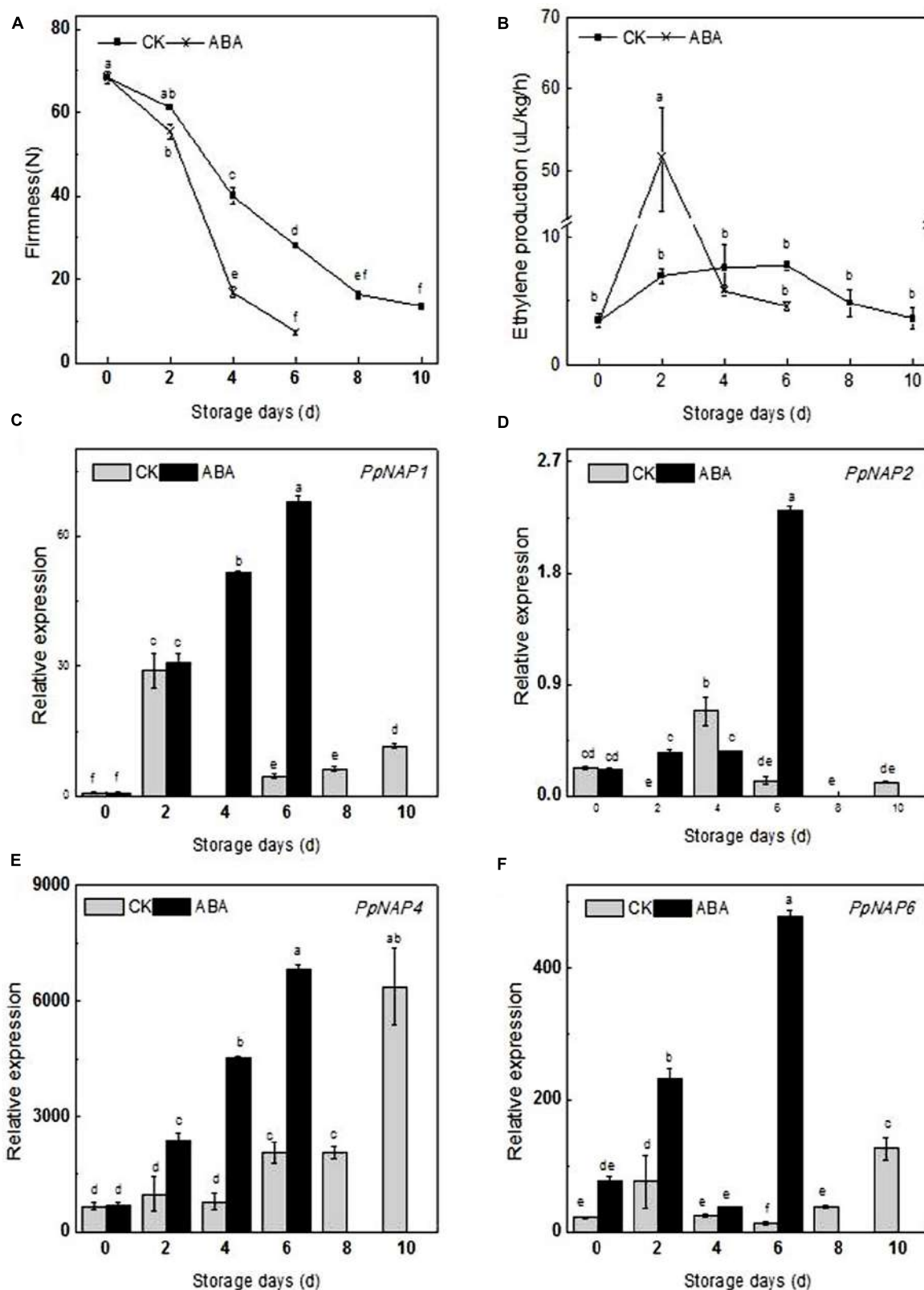


FIGURE 6 | Firmness (A), ethylene production (B) and expression levels of selected peach NAP genes in control and ABA-treated fruits during the storage period (C–F). Bars correspond to the mean \pm standard error ($n = 3$). The overall least significant difference ($p < 0.05$) was calculated and used to separate means.

TABLE 2 | Details of *cis*-acting elements detected in the peach *NAP* gene promoters.

<i>Cis</i> element	Sequence	Number of <i>cis</i> elements				Function
		PpNAP1	PpNAP2	PpNAP4	PpNAP6	
Associated with plant hormones	ABRE	OACGGTG	3	8	1	8
	CE3	GACGCCGTGTC	1	1	0	Cis-acting element involved in the abscisic acid responsiveness
	ERE	ATTTCAAA	1	1	0	Cis-acting element involved in ABA and VP1 responsiveness
	CGTCA-motif	CGTO)	0	5	1	Ethylene-responsive element
	TGACG-motif	TGACG	0	1	1	Cis-acting regulatory element involved in the MeJA-responsiveness
	TCA-element	TCAGAAGAGG	1	2	2	Cis-acting regulatory element involved in the MeJA-responsiveness
	GARE-motif	TCTGTTG	1	0	0	Cis-acting element involved in salicylic acid responsiveness
						Gibberellin-responsive element
Tissue specificity expression elements	Skn1_-motif	GTCAAT	1	3	4	Cis-acting regulatory element required for endosperm expression
	Ry-element	CATGCATG	2	0	0	Cis-acting regulatory element involved in seed-specific regulation
	as-2-box	GATAatGATG	0	0	0	Involved in shoot-specific expression and light responsiveness
Cis transcription functions components	TATA-box	TATA	62	79	49	Core promoter element around -30 of transcription start
	CAAT-box	CAAT	27	43	26	Common cis-acting element in promoter and enhancer regions
	5UTR Py-rich stretch	TTTCTTCTCT	2	0	0	Cis-acting element conferring high transcription levels
Related to physiological and environmental responsiveness	ARE	TGGTTT	4	3	3	Cis-acting regulatory element essential for the anaerobic induction
	LTR	CCGAAA	0	1	1	Cis-acting element involved in low-temperature responsiveness
	CARG-box	CN(AT)6NG	3	2	1	MADS domain site
	HSE	AAAAAAATTTC	3	0	0	Cis-acting element involved in drought-inducibility
	MBS	CAACTG	0	2	2	Cis-acting regulatory element involved in circadian control
	Circadian G-box	CAANNNNATC	1	1	2	Cis-acting regulatory element involved in heat stress responsiveness
	ACE	CACGTG	4	18	6	MYB binding site involved in drought-inducibility
	GTI-motif	ACGIGGA	0	0	1	Cis-acting element involved in light responsiveness
	Box 1	GGTTAA	0	2	3	Light responsive element
	Sp1	TTTCAA	3	1	0	Light responsive element
	Box 4	CC(G/A)CCC	1	3	4	Light responsive element
	ATC-motif	ATTAA	3	3	1	Part of a conserved DNA module involved in light responsiveness
	CATT-motif	GCCATCC	1	2	0	Part of a conserved DNA module involved in light responsiveness
	GAG-motif	GCATTC	1	0	0	Part of a light responsive element
	GATA-motif	GGAGATG	0	2	3	Part of a light responsive element
	TCCC-motif	GATAGGA	1	2	0	Part of a light responsive element
	MRE	TCTCCCT	1	0	3	Part of a light responsive element
	TC-rich repeats	AACCTAA	1	2	0	MYB binding site involved in light responsiveness
	Box-W1	ATTTCCTCA	2	1	0	Cis-acting element involved in defense and stress responsiveness
		TTGACC	0	2	0	Fungal elicitor responsive element

different expression patterns, which suggests they may have different roles in various physiological pathways. *PpNAP1* and *PpNAP2* had relatively high expression levels in blooming flowers and flowers 2 DAFB, but low levels in leaves, fruits, and flower buds (**Figures 4A–C**). Therefore, these genes may be involved in regulating flower maturation and aging. *PpNAP3* and *PpNAP5* expression was observed in leaves, but was almost undetectable in flowers and fruits (**Figures 4A–C**), which indicates they may be associated with leaf development. The expression of *PpNAP4* was rapidly up-regulated and maintained at high levels during fruit maturation and senescence (**Figure 4C**), suggesting that this gene may play a key role in regulating peach fruit ripening and softening. *PpNAP6* and *PpNAP7* expression levels were up-regulated in mature and senescent leaves and flowers (**Figures 4A,B**). Therefore, they may be associated with the maturation and senescence of leaves and flowers. These results suggest that the expression of *PpNAP* genes depends on tissue type, which is supported by the results of related studies in other plants. For example, the expression of *VvNAP* was observed only in grapevine flowers and fruits, and not in vegetative organs such as leaves, shoots, or roots (Fernandez et al., 2006). The expression patterns of *AtNAP* differed among stamens, fertilized flowers, and developing siliques in *A. thaliana* (Sablowski and Meyerowitz, 1998). In *Mikania micrantha*, the *MmNAP* gene was observed to be specifically expressed in stems, petioles, shoots, and leaves, but not in roots (Li et al., 2012).

Possible Roles of NAP Subfamily Members in Fruit Development and Softening

During fruit development, the *PpNAP4* and *PpNAP6* expression levels increased rapidly in stages S1 and S4. However, in the S2 stage, *PpNAP4* expression slowly increased while *PpNAP6* expression levels decreased (**Figure 5**). During the S3 stage, *PpNAP4* and *PpNAP6* expression levels stabilized. Because of the association of the *NAP* gene with cell division and expansion of stamens and petals (Sablowski and Meyerowitz, 1998), our results suggest that *PpNAP4* and *PpNAP6* are likely involved in the first exponential growth phase and fruit ripening.

During the fruit ripening and softening process, the expression of *PpNAP1*, *PpNAP4*, and *PpNAP6* increased considerably in the first 2 DAH, which was accompanied by an increase in ethylene production. Furthermore, the expression of *PpNAP1*, *PpNAP4*, and *PpNAP6* tended to increase during the middle or late storage periods, and was highest at the end of the storage period. These results are consistent with those for *AtNAP* (Kou et al., 2012), *VvNAP* (Fernandez et al., 2006), and *CitNAC* (Liu et al., 2009). Therefore, the functions of *PpNAP1*, *PpNAP4*, and *PpNAP6* are probably similar to those of *AtNAP*, *VvNAP*, and *CitNAC*, and involve activities related to peach fruit ripening and senescence.

The accumulation of ABA plays a key role in the regulation of peach fruit ripening and senescence (Zhang et al., 2009b), and stimulates ethylene biosynthesis and ripening in tomato fruits (Zhang et al., 2009a). Peach fruits treated with ABA during the S4 fruit development stage exhibited accelerated

ripening and up-regulated expression of the ethylene biosynthesis genes *ACS1* and *ACO1* (Soto et al., 2013). Compared with control fruits, ABA-treated fruits softened faster and released more ethylene, ultimately resulting in a shorter maximum storage period. These results are similar to those observed for tomato (Zhang et al., 2009a), and suggest that ABA may stimulate ethylene biosynthesis. Additionally, the expression levels of *PpNAP1*, *PpNAP4*, and *PpNAP6* increased in ABA-treated fruit (**Figures 6A,B**), which was similar to the response of *AtNAP* in ABA-treated siliques (Kou et al., 2012). In rice and *A. thaliana* leaves, *NAP* gene expression was also induced by exogenous ABA (Chen et al., 2014; Yang et al., 2014). Therefore, the ABA-responsive *PpNAP1*, *PpNAP4*, and *PpNAP6* genes may regulate peach fruit ripening and softening. However, the specific regulatory mechanism requires further characterization.

Analysis of Promoter Sequences of Selected Peach NAP Genes

Because of their involvement in regulating transcription, gene promoters contain important *cis*-acting elements (Zhu and Li, 1997). To characterize the possible regulatory mechanisms of *NAP* genes during fruit development, maturation, and softening, we analyzed the promoters of four fruit-specific *NAP* genes. Several motifs associated with responses to phytohormones and environmental factors were detected. These motifs included the ABA-responsive element and coupling element 3, the CGTCA and TGACG motifs associated with responses to methyl jasmonate, and the TCA-element related to responses to salicylic acid (**Table 2**). Exogenous ABA can up-regulate *NAP* expression in *A. thaliana* and rice (Liang et al., 2014; Yang et al., 2014). Zhou et al. (2013) reported that *OsNAP* can regulate leaf senescence by affecting jasmonic acid signaling pathways, and that overexpressing *OsNAP* increases the production of endogenous jasmonic acid in rice. Other studies have demonstrated that hormones, including ABA, jasmonic acid, and salicylic acid, have important regulatory roles during fruit ripening and softening (Creelman and Mullet, 1995; Zhang et al., 2003, 2009a). Therefore, it can be inferred that *PpNAP* genes regulate peach fruit development and softening by influencing specific hormone signal transduction pathways. Moreover, genes containing the MADS-box motif have key roles in flower and fruit development and maturation (Adamczyk and Fernandez, 2009; Smaczniak et al., 2012). We also observed that one to three copies of the MADS-domain site CArG-box were present in the promoters of four *NAP* genes, indicating that *PpNAP* and MADS-box genes may interact to regulate peach fruit development and ripening. However, the specific regulatory mechanisms of *PpNAP* genes that affect peach fruits require further study.

AUTHOR CONTRIBUTIONS

CZ, MH, HL, and DZ: Design and interpretation of all experiments. FL, JL, and MQ: Performed all plant physiological

and biochemical experiments. CZ, FL and LC: Wrote the manuscript.

ACKNOWLEDGMENTS

We wish to thank Minghui Lu for English language modifying. This research was supported by grants from National Science Foundation of China (Grant No. 31572079) and the Natural Science Foundation of Shaanxi Province, China (Grant No. 2015JM3103).

REFERENCES

- Adamczyk, B. J., and Fernandez, D. E. (2009). MIKC* MADS domain heterodimers are required for pollen maturation and tube growth in *Arabidopsis*. *Plant Physiol.* 149, 1713–1723. doi: 10.1104/pp.109.135806
- Barry, C. S., and Giovannoni, J. J. (2007). Ethylene and fruit ripening. *J. Plant Growth Regul.* 26, 143–159. doi: 10.1007/s00344-007-9002-y
- Bendtsen, J. D., Nielsen, H., von Heijne, G., and Brunak, S. (2004). Improved prediction of signal peptides: signalP 3.0. *J. Mol. Biol.* 340, 783–795. doi: 10.1016/j.jmb.2004.05.028
- Chang, S., Puryear, J., and Cairney, J. (1993). A simple and efficient method for isolating RNA from pine trees. *Plant Mol. Biol. Rep.* 11, 113–116. doi: 10.1007/BF02670468
- Chen, X., Wang, Y., Lv, B., Li, J., Luo, L., Lu, S., et al. (2014). The NAC family transcription factor OsNAP confers abiotic stress response through the ABA pathway. *Plant Cell Physiol.* 55, 604–619. doi: 10.1093/pcp/pct204
- Chen, Y., Qiu, K., Kuai, B., and Ding, Y. (2011). Identification of an NAP-like transcription factor BeNAC1 regulating leaf senescence in bamboo (*Bambusa emeiensis* 'Viridisflavus'). *Physiol. Plant.* 142, 361–371. doi: 10.1111/j.1399-3054.2011.01472.x
- Creelman, R. A., and Mullet, J. E. (1995). Jasmonic acid distribution and action in plants: regulation during development and response to biotic and abiotic stress. *Proc. Natl. Acad. Sci. U.S.A.* 92, 4114–4119. doi: 10.1073/pnas.92.10.4114
- Cristobal, U., Assaf, D., Tzion, F., Ann, B., and Jorge, D. (2006). A NAC gene regulating senescence improves grain protein, zinc, and iron content in wheat. *Science* 314, 1298–1301. doi: 10.1126/science.1133649
- Fan, J. P., and Zhao, R. (2014). Cloning and expression pattern analysis of the ApNAP gene in *Asarina procumbens*. *Plant Sci. J.* 32, 251–258.
- Fan, K., Shen, H., Bibi, N., Li, F., Yuan, S., Wang, M., et al. (2015). Molecular evolution and species-specific expansion of the NAP members in plants. *J. Integr. Plant Biol.* 57, 673–687. doi: 10.1111/jipb.12344
- Fan, K., Wang, M., Miao, Y., Ni, M., Bibi, N., Yuan, S., et al. (2014). Molecular evolution and expansion analysis of the NAC transcription factor in *Zea mays*. *PLoS ONE* 9:e111837. doi: 10.1371/journal.pone.0111837
- Fernandez, L., Ageorges, A., and Torregrosa, L. (2006). A putative NAP homolog specifically expressed during grapevine flower and berry development. *Vitis* 45, 51–52.
- Guo, Y., and Gan, S. S. (2006). AtNAP, a NAC family transcription factor, has an important role in leaf senescence. *Plant J.* 46, 601–612. doi: 10.1111/j.1365-313X.2006.02723.x
- Guo, Y., Wei, Q., and Kuai, B. (2010). Cloning and characterization of the AtNAP orthologous in *Festuca arundinacea*. *J. Fudan Univ.* 49, 544–551.
- Huang, G. Q., Li, W., Zhou, W., Zhang, J. M., Li, D. D., Gong, S. Y., et al. (2013). Seven cotton genes encoding putative nac domain proteins are preferentially expressed in roots and in responses to abiotic stress during root development. *Plant Growth Regul.* 71, 101–112. doi: 10.1007/s10725-013-9811-x
- Kalivas, A., Pasentsis, K., Argiriou, A., and Tsafaris, A. S. (2010). Isolation, characterization, and expression analysis of an NAP-like cDNA from *Crocus (Crocus sativus L.)*. *Plant Mol. Biol. Rep.* 28, 654–663. doi: 10.1007/s11105-010-0197-x
- Kou, X., Watkins, C. B., and Gan, S. S. (2012). *Arabidopsis* AtNAP regulates fruit senescence. *J. Exp. Bot.* 63, 6139–6147. doi: 10.1093/jxb/ers266
- Lescot, M., Déhais, P., Thijs, G., Marchal, K., Moreau, Y., Van, de Peer Y., et al. (2002). PlantCARE, a database of plant cis-acting regulatory elements and a portal to tools for in silico analysis of promoter sequences. *Nucleic Acids Res.* 30, 325–327. doi: 10.1093/nar/30.1.325
- Li, D. M., Wang, J. H., Peng, S. L., Zhu, G. F., and Lu, F. B. (2012). Molecular cloning and characterization of two novel NAC genes from *Mikania micrantha* (Asteraceae). *Genet. Mol. Res.* 11, 4383–4401. doi: 10.4238/2012.September.19.3
- Li, S. H., Huguet, J. G., Schoch, P. G., and Orlando, P. (1989). Response of peach tree growth and cropping to soil water deficit at various phenological stages of fruit development. *J. Hortic. Sci.* 64, 541–552.
- Liang, C., Wang, Y., Zhu, Y., Tang, J., Hu, B., Liu, L., et al. (2014). OsNAP connects abscisic acid and leaf senescence by fine-tuning abscisic acid biosynthesis and directly targeting senescence-associated genes in rice. *Proc. Natl. Acad. Sci. U.S.A.* 111, 10013–10018. doi: 10.1073/pnas.1321568111
- Liguori, G., Weksler, A., Zutah, Y., Lurie, S., and Kosto, I. (2004). Effect of 1-methylcyclopropane on ripening of melting flesh peaches and nectarines. *Postharvest Biol. Technol.* 31, 263–268. doi: 10.1016/j.postharvbio.2003.09.007
- Liu, Y. Z., Baig, M. N. R., Fan, R., Ye, J. L., Cao, Y. C., and Deng, X. X. (2009). Identification and expression pattern of a novel NAM, ATAF, and CUC-like gene from *Citrus sinensis* Osbeck. *Plant Mol. Biol. Rep.* 27, 292–297. doi: 10.1007/s11105-008-0082-z
- Livak, K. J., and Schmittgen, T. D. (2001). Analysis of relative gene expression data using real-time quantitative PCR and the 2- $\Delta\Delta CT$ method. *Methods* 25, 402–408. doi: 10.1006/meth.2001.1262
- Meng, C., Cai, C., Zhang, T., and Guo, W. (2009). Characterization of six novel nac genes and their responses to abiotic stresses in *Gossypium hirsutum* L. *Plant Sci.* 176, 352–359. doi: 10.1016/j.plantsci.2008.12.003
- Meng, Q., Zhang, C., Gai, J., and Yu, D. (2007). Molecular cloning, sequence characterization and tissue-specific expression of six NAC-like genes in soybean (*Glycine max* (L.) Merr.). *J. Plant Physiol.* 164, 1002–1012. doi: 10.1016/j.jplph.2006.05.019
- Ooka, H., Satoh, K., Doi, K., Nagata, T., Otomo, Y., Murakami, K., et al. (2003). Comprehensive analysis of NAC family genes in *Oryza sativa* and *Arabidopsis thaliana*. *DNA Res.* 10, 239–247. doi: 10.1093/dnares/10.6.239
- Sablowski, R. W., and Meyerowitz, E. M. (1998). A homolog of no apical meristem is an immediate target of the floral homeotic genes *apetala3/pistillata*. *Cell* 92, 93–103. doi: 10.1016/S0092-8674(00)80902-2
- Smaczniak, C., Immink, R. G., Angenent, G. C., and Kaufmann, K. (2012). Developmental and evolutionary diversity of plant MADS-domain factors: insights from recent studies. *Development* 139, 3081–3098. doi: 10.1242/dev.074674
- Soto, A., Ruiz, K. B., Ravaglia, D., Costa, G., and Torrigiani, P. (2013). Aba may promote or delay peach fruit ripening through modulation of ripening- and hormone-related gene expression depending on the developmental stage. *Plant Physiol. Biochem.* 64, 11–24. doi: 10.1016/j.plaphy.2012.12.011
- Tonutti, P., Bonghi, C., Ruperti, B., and Ramina, A. (1997). "The modulation of ethylene biosynthesis and ACC oxidase gene expression during peach fruit development and fruitlet abscission," in *Biology and Biotechnology of the Plant Hormone Ethylene*, eds A. K. Kanellis, C. Chang, H. Kende, and D. Grierson (Dordrecht: Springer Netherlands), 149–153.
- Wang, Z. (2008). *Plant Physiology*. Beijing: China Agricultural Press, 516–518.

SUPPLEMENTARY MATERIAL

The Supplementary Material for this article can be found online at: <http://journal.frontiersin.org/article/10.3389/fpls.2016.00147>

FIGURE S1 | The amplification (A), melt curve (B) and melt park (C) of 18s ribosomal gene in all samples.

FIGURE S2 | Quantitative reverse transcription PCR analysis of PpACO1genes in fruits with different developmental stage. Arrow indicates the time of harvest(121 DAFB).

- Yang, J., Worley, E., and Udvardi, M. (2014). A NAP-AAO3 regulatory module promotes chlorophyll degradation via ABA biosynthesis in *Arabidopsis* leaves. *Plant Cell* 26, 4862–4867. doi: 10.1105/tpc.114.133769
- Zhang, K., and Gan, S. S. (2012). An abscisic acid-AtNAP transcription factor-SAG113 protein phosphatase 2C regulatory chain for controlling dehydration in senescing *Arabidopsis* leaves. *Plant Physiol.* 158, 961–969. doi: 10.1104/pp.111.190876
- Zhang, M., Leng, P., Zhang, G., and Li, X. (2009a). Cloning and functional analysis of 9-cis-epoxycarotenoid dioxygenase (NCED) genes encoding a key enzyme during abscisic acid biosynthesis from peach and grape fruits. *J. Plant Physiol.* 166, 1241–1252. doi: 10.1016/j.jplph.2009.01.013
- Zhang, M., Yuan, B., and Leng, P. (2009b). The role of ABA in triggering ethylene biosynthesis and ripening of tomato fruit. *J. Exp. Bot.* 60, 1579–1588. doi: 10.1093/jxb/erp026
- Zhang, Y., Chen, K., Zhang, S., and Ferguson, I. (2003). The role of salicylic acid in postharvest ripening of kiwifruit. *Postharvest Biol. Technol.* 28, 67–74. doi: 10.1016/S0925-5214(02)00172-2
- Zhou, Y., Huang, W., Liu, L., Chen, T., Fei, Z., and Lin, Y. (2013). Identification and functional characterization of a rice NAC gene involved in the regulation of leaf senescence. *BMC Plant Biol.* 13:132. doi: 10.1186/1471-2229-13-132
- Zhu, Y. X., and Li, Y. (1997). *Modern Molecular Biology*. Beijing: Higher Education Press.

Conflict of Interest Statement: The authors declare that the research was conducted in the absence of any commercial or financial relationships that could be construed as a potential conflict of interest.

Copyright © 2016 Li, Li, Qian, Han, Cao, Liu, Zhang and Zhao. This is an open-access article distributed under the terms of the Creative Commons Attribution License (CC BY). The use, distribution or reproduction in other forums is permitted, provided the original author(s) or licensor are credited and that the original publication in this journal is cited, in accordance with accepted academic practice. No use, distribution or reproduction is permitted which does not comply with these terms.



Implication of Abscisic Acid on Ripening and Quality in Sweet Cherries: Differential Effects during Pre- and Post-harvest

Verónica Tijerot, Natalia Teribiat, Paula Muñoz and Sergi Munné-Bosch*

Department of Plant Biology, Faculty of Biology, University of Barcelona, Barcelona, Spain

OPEN ACCESS

Edited by:

Mario Pezzotti,
University of Verona, Italy

Reviewed by:

Christoph Martin Geilfus,
Christian-Albrechts-Universität zu Kiel,
Germany

Gianfranco Diretto,
Italian National Agency for New
Technologies, Energy and Sustainable
Economic Development, Italy

*Correspondence:

Sergi Munné-Bosch
smunne@ub.edu

[†]These authors have contributed
equally to this work.

Specialty section:

This article was submitted to
Plant Physiology,
a section of the journal
Frontiers in Plant Science

Received: 11 February 2016

Accepted: 18 April 2016

Published: 04 May 2016

Citation:

Tijero V, Teribia N, Muñoz P
and Munné-Bosch S (2016)
Implication of Abscisic Acid
on Ripening and Quality in Sweet
Cherries: Differential Effects during
Pre- and Post-harvest.
Front. Plant Sci. 7:602.
doi: 10.3389/fpls.2016.00602

Sweet cherry, a non-climacteric fruit, is usually cold-stored during post-harvest to prevent over-ripening. The aim of the study was to evaluate the role of abscisic acid (ABA) on fruit growth and ripening of this fruit, considering as well its putative implication in over-ripening and effects on quality. We measured the endogenous concentrations of ABA during the ripening of sweet cherries (*Prunus avium* L. var. Prime Giant) collected from orchard trees and in cherries exposed to 4°C and 23°C during 10 days of post-harvest. Furthermore, we examined to what extent endogenous ABA concentrations were related to quality parameters, such as fruit biomass, anthocyanin accumulation and levels of vitamins C and E. Endogenous concentrations of ABA in fruits increased progressively during fruit growth and ripening on the tree, to decrease later during post-harvest at 23°C. Cold treatment, however, increased ABA levels and led to an inhibition of over-ripening. Furthermore, ABA levels positively correlated with anthocyanin and vitamin E levels during pre-harvest, but not during post-harvest. We conclude that ABA plays a major role in sweet cherry development, stimulating its ripening process and positively influencing quality parameters during pre-harvest. The possible influence of ABA preventing over-ripening in cold-stored sweet cherries is also discussed.

Keywords: sweet cherry, ABA, ripening, over-ripening, ascorbate, vitamin E, cold storage

INTRODUCTION

In recent decades, sweet cherry has become one of the most important non-climacteric fruits worldwide, with an important distribution to international markets from highly productive countries at origin, such as Turkey, United States, Iran, Italy, and Spain, among others (FAO, 2015). However, both its flavor and nutritional quality is strongly dependent on tree growth conditions at pre-harvest, post-harvest treatments and its consumption at an optimum ripening stage (Ashton, 2007). Over-ripening, which leads to a loss of quality during post-harvest, is associated with fruit darkening, softening and a general loss of organoleptic properties (Meheriuk et al., 1995). Cold treatments are generally used to store them properly during post-harvest in order to avoid fruit quality loss, but the physiological and biochemical mechanisms underlying fruit ripening on the tree and over-ripening during post-harvest are still relatively unknown for sweet cherries.

It has been shown that high concentrations of abscisic acid (ABA) are required for ripening in sweet cherries (Luo et al., 2013; Wang et al., 2015). ABA is a sesquiterpenoid hormone, derived from carotenoids, that is implicated in several physiological processes, from seed dormancy to senescence processes, including plant stress responses and the regulation of fruit development (Nambara and Marion-Poll, 2005; Finkelstein, 2013; Leng et al., 2014). ABA has been shown to play a major role in the ripening process of non-climacteric fleshy fruits, such as cherry fruits, modulating color changes (through modulation of anthocyanin biosynthesis) and sugar accumulation (Kumar et al., 2014; Wang et al., 2015). However, nothing is known about the possible role of ABA in the regulation of fruit quality in terms of vitamin C and E accumulation, or to what extent ABA can affect over-ripening processes in sweet cherries.

Among various quality parameters, the content and composition of water- and lipid-soluble vitamins in edible fleshy fruits is of paramount importance for human health (FAO, 2004). Sweet cherries are rich in vitamin C, which is considered one of the most important water-soluble antioxidants, together with anthocyanins, in this fruit (Serrano et al., 2005). Aside from protecting cells from reactive oxygen species, ascorbate is involved in the regulation of growth processes in plants (Veljovic-Jovanovic et al., 2001), and it plays a role, as a cofactor, in the regulation of 9-cis-epoxycarotenoid dioxygenase (NCED), the key limiting step in the biosynthesis of ABA from carotenoids (Conklin and Barth, 2004). Furthermore, ascorbate recycles oxidized tocopherols (vitamin E), when this lipid-soluble antioxidant reacts with lipid peroxyl radicals in its function of inhibiting the propagation of lipid peroxidation in biological membranes (Munné-Bosch and Alegre, 2002). Although vitamin C has received some attention in the ripening of sweet cherries as a component of organic acids (Serrano et al., 2005), nothing is known about the levels of vitamin E, its possible variations with ripening and regulation by phytohormones in non-climacteric fruits. Only in mango, a climacteric fruit, it has been shown that vitamin E biosynthesis may be modulated by ethylene (Singh et al., 2011).

The aim of this study was to get some insights into the role of ABA in the ripening process of sweet cherries, focusing on the endogenous levels of this phytohormone during fruit development in orchard trees and under different conditions of post-harvest. In addition, to better understand the role of ABA in ripening, as well as the loss of quality during fruit storage, we simultaneously analyzed various parameters associated with the ripening process and the fruit quality, such as fruit biomass, anthocyanin accumulation, and levels of antioxidants, including carotenoids, and vitamins C and E.

MATERIALS AND METHODS

Experimental Design and Sampling

Three independent, complementary experiments were performed using sweet cherries (*Prunus avium* L. var. Prime Giant). The first experiment focused on a study of fruit ripening on the tree followed by an over-ripening process at 23°C, the

second one was performed preventing over-ripening at 4°C, and the third one was performed to test for the tissular location of vitamins in cherry fruits.

For the first experiment, sweet cherries were obtained from trees growing in an exploited orchard at Partida Vall del Sector III (Lleida, NE Spain). Fruits were harvested at various developmental stages on the tree between 23 and 4 days before harvest, and between 3 and 10 days of post-harvest at 23°C, which led to over-ripening (Supplementary Figure S1). First sampling in orchard trees was performed during 30th April 2015 (23 days before harvest), which corresponds to 34 days after full bloom. For the second experiment, 10 kg from the same cherry cultivar and orchard were brought to the laboratory 3 days after commercial harvest. Fruits without visual defects were chosen for experiments. Then, half of the fruits were kept at 23 ± 2°C in the laboratory, while the other half were subject to 4 ± 1°C in a cold chamber. In both cases, fruits were kept in darkness and samples were taken daily during storage for 1 week.

A third experiment was performed to evaluate possible tissue-specific accumulation of vitamins in sweet cherries. The pit, flesh and skin from fruits collected 23 days pre-harvest or 3 days post-harvest were manually separated and immediately immersed in liquid nitrogen for hormone, anthocyanin and vitamins C and E analyses.

All samplings were performed early in the morning (between 9 and 10 a.m. local time) with an average temperature of 10 ± 2°C during pre-harvest and 23 ± 2°C during post-harvest for the first experiment, and with an average temperature of 4 ± 1°C for the second one. Six fruits per tree from eight trees were randomly sampled at each time point during pre-harvest, and six fruits from commercial boxes were randomly sampled daily during post-harvest, for each, 23°C and cold storage. For all experiments, samples were immediately snap frozen in liquid nitrogen and stored at -80°C until analyses.

Endogenous Concentrations of Abscisic Acid

Abscisic acid levels were determined by ultrahigh-performance liquid chromatography coupled to tandem mass spectrometry (UHPLC-MS/MS) as described previously (Müller and Munné-Bosch, 2011). In short, 100 mg per sample were extracted with 200 µL methanol:isopropanol:acetic acid 50:49:1 (v/v/v) using ultrasonication and vortexing (Branson 2510 ultrasonic cleaner, Bransonic, Danbury, CT, USA) for 30 min. Deuterium-labeled ABA was then added, and after centrifugation at 600 g for 15 min at 4°C, the pellet was re-extracted using the same procedure. Supernatants were pooled and filtered through a 0.22 µm PTFE filter (Waters, Milford, MA, USA) before analyses. ABA levels were analyzed by using UHPLC-ESI-MS/MS as described in Müller and Munné-Bosch (2011). Quantification was made considering recovery rates for each sample by using a deuterium-labeled internal standard.

Fruit Quality Parameters

Fruit biomass was estimated by weighing the samples immediately at each sampling time point or after transferring

them to the laboratory in bags (with high humidity to avoid desiccation).

Total anthocyanins were determined spectrophotometrically in methanolic extracts as described (Gitelson et al., 2001). In short, 200 mg per sample were extracted with 1 mL methanol using ultrasonication and vortexing. Extracts were centrifuged at 600 g for 10 min at 4°C and the pellet was re-extracted following the same procedure. Supernatants were pooled and 1% HCl was added. Then, total anthocyanins were measured spectrophotometrically at 530 nm. Total anthocyanins were calculated using the molar extinction coefficient of cyanidin-3-glucoside as a reference, as described (Siegelman and Hendricks, 1958).

Carotenoids levels were estimated by HPLC after extraction with methanol, as described (Munné-Bosch and Alegre, 2000). In short, samples were extracted with methanol, as described for anthocyanins, and separated on a Dupont non-endcapped Zorbax ODS-5 μm column (250 mm long, 4.6 mm i.d.; 20% Carbon, Teknokroma, St. Cugat, Spain) at 30°C for 38 min at a flow rate of 1 mL min⁻¹. The solvent mixture for the gradient consisted of (A) acetonitrile:methanol (85:15, v/v) and (B) methanol:ethyl acetate (68:32, v/v). The gradient used was: 0–14 min 100% A, 0% B; 14–16 min decreasing to 0% A, 100% B; 16–28 min 0% A, 100% B; 28–30 min increasing to 100% A, 0% B; and 30–38 min 100% A, 0% B. Detection was carried out at 445 nm and compounds were identified and quantified as described previously (Munné-Bosch and Alegre, 2000).

The analysis of vitamin C was adapted from Takahama and Oniki (1992) and Queval and Noctor (2007). In short, ascorbic acid and its oxidized form, dehydroascorbic acid were extracted with 6% *m*-phosphoric acid (w/v) and 0.2 mM diethylenetriaminepentaacetic acid, using ultrasonication and vortexing. After centrifugation at 600 g for 10 min at 4°C, the supernatants were collected and the pellet was re-extracted following the same procedure. Their levels were determined spectrophotometrically at 265 nm, using the ascorbate oxidase assay. The oxidized state of ascorbate was calculated as DHA/(AA + DHA) × 100, where AA is ascorbate and DHA is dehydroascorbate.

The analysis of vitamin E was performed as described (Amaral et al., 2005). In short, 200 mg per sample were extracted with methanol, exactly as described for anthocyanins, and then filtered prior to HPLC analyses. The HPLC equipment consisted of an integrated system with a Jasco PU-2089 Plus pump, a Jasco AS-2055 Plus auto-sampler and a FP-1520 fluorescence detector (Jasco, Tokyo, Japan). All tocopherol and tocotrienol forms were separated on an Inertsil 100A (5 μm, 30 × 250 mm, GL Sciences Inc., Tokyo, Japan) normal-phase column, operating at room temperature. The flow rate was 0.7 mL min⁻¹ and the injection volume was 10 μL. The mobile phase was a mixture of *n*-hexane and *p*-dioxane (95.5:4.5, v/v). Detection was carried out at an excitation of 295 nm and emission at 330 nm. Quantification was based on the results obtained from the fluorescence signal and compared to that of a calibration curve made with authentic standards of each compound (Sigma-Aldrich, Steinheim, Germany).

Statistical Analysis

Data were analyzed by using one-way (first experiment) or two-way (second experiment) factorial analysis of variance (ANOVA). Multiple comparisons tests were carried out by using Bonferroni *post-hoc* tests. In all cases, differences were considered significant at a probability level of $P \leq 0.05$. Furthermore, correlation analyses using the Spearman rank's correlation were made. All statistical analyses were performed using the SPSS 20.0 statistical package.

RESULTS

ABA Levels Increase During Ripening on the Tree but Decrease During Over-Ripening

Fruit biomass increased fivefold during ripening on the tree (from 23 days pre-harvest to 3 days post-harvest), to decrease later by 20% due to over-ripening for 1 week (from day 3 to day 10 of post-harvest at 23°C, **Figure 1**). Anthocyanin levels increased from non-detectable values to 95 μg/g fruit during pre-harvest (between 23 and 4 days preharvest), to increase even further up to 582 μg/g fruit at 5 days post-harvest. Then, anthocyanin levels remained relatively constant at high levels during over-ripening until the end of the experiment (10 days post-harvest, **Figure 1**).

Abscisic acid levels increased sharply from 26 ng/g fruit at 23 days pre-harvest to 540 ng/g fruit at 11 days pre-harvest, to keep later constant until 4 days pre-harvest (**Figure 2**). Over-ripening at 23°C led to a depletion of endogenous ABA concentrations in the fruit to attain minimum values of 142 ng/g fruit at 10 days post-harvest. It is noteworthy that ABA increases preceded anthocyanin accumulation during pre-harvest. In contrast, ABA did not change in parallel with anthocyanin accumulation during post-harvest (**Figures 1** and **2**).

Levels of carotenoids decreased sharply during fruit ripening on the tree (**Table 1**). Violaxanthin, an ABA precursor, decreased from 0.58 mg/g FW at 23 days to non-detectable values at 4 days pre-harvest (**Table 1**), which occurred in parallel with increases of ABA levels during fruit ripening on the trees (**Figure 2**). Lutein and zeaxanthin levels also decreased progressively down to non-detectable values during fruit ripening on the tree, while fruits at 4 days pre-harvest still kept 0.17 mg/g FW of β-carotene. The amounts of this antioxidant expressed per fruit unit increased during ripening, attaining maximum levels of 3 mg per fruit unit at 4 days pre-harvest (**Table 1**). Carotenoids were not detected during post-harvest (data not shown).

Total ascorbate levels increased during pre-harvest to decrease later during post-harvest, both when expressed on a fresh weight and a fruit unit basis (**Figure 3**). Interestingly, ascorbate levels showed a biphasic response during post-harvest, with minimum ascorbate levels at 5 and 10 days post-harvest. It is noteworthy that the oxidation state of ascorbate kept constant, both, during pre- and post-harvest, but decreased sharply from around 40% to levels below 20% just after harvest (**Figure 3**).

Vitamin E levels were much lower than those of ascorbate, with maximum levels of 3.5 μg/g fruit being attained at 15 and

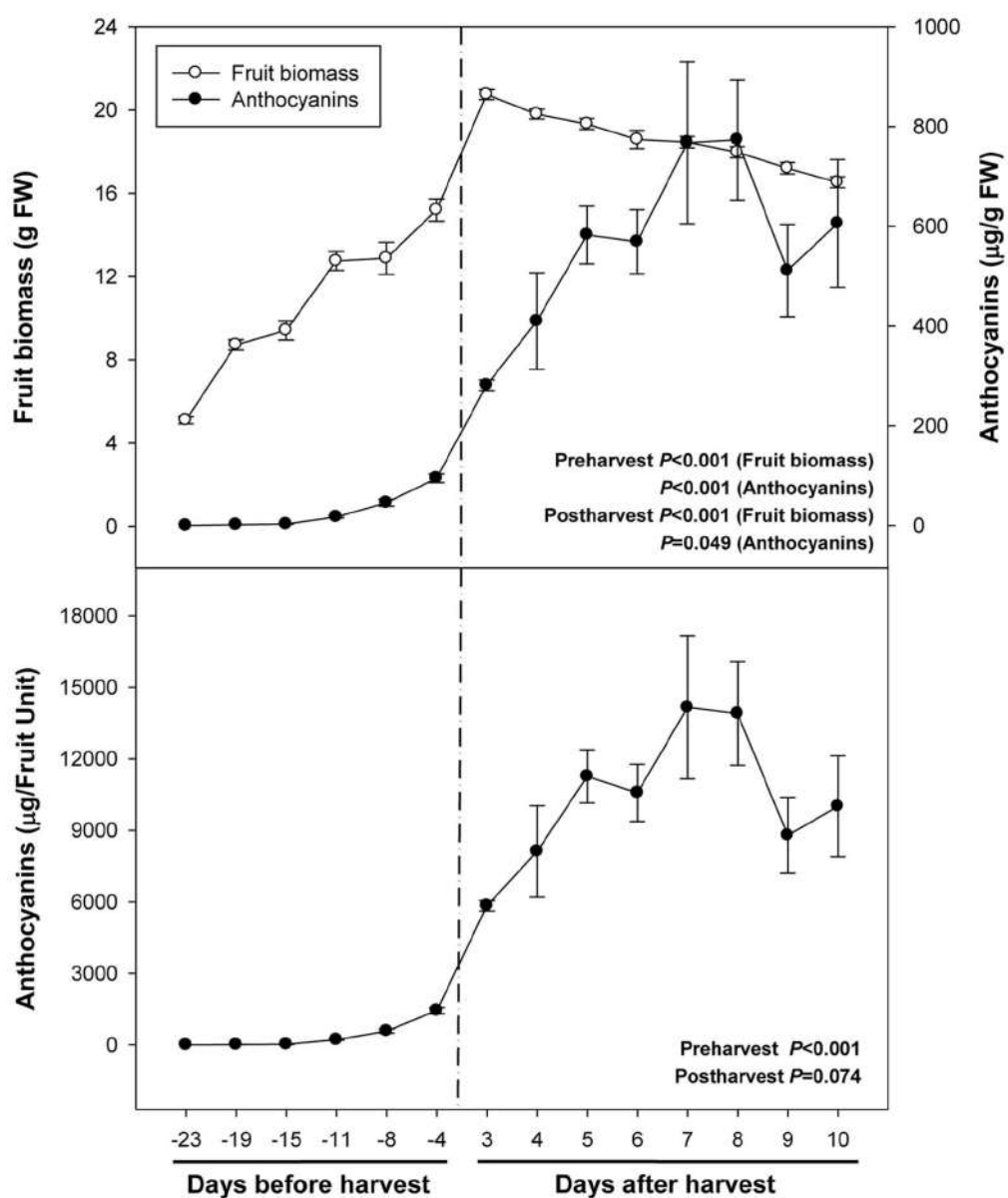


FIGURE 1 | Fruit biomass and levels of total anthocyanins during ripening on the tree (pre-harvest) and during over-ripening at 23°C (post-harvest).

Data are the mean \pm SE of $n = 8$ (pre-harvest) and $n = 3$ (post-harvest) for anthocyanins, and $n = 8$ (pre-harvest) and $n = 6$ (post-harvest) for fruit biomass.

Statistical analyses were performed by one-way ANOVA to test for the effects of time during pre- and post-harvest. Results of statistics are shown in the inlets.

Differences were considered significant when $P \leq 0.05$. NS, not significant. Anthocyanin levels are given both per fresh weight (FW) and per fruit unit. Harvest (time 0 in the X axis) corresponds to 57 days after full bloom.

11 days pre-harvest and at the end of the experiment (**Figure 4**). Sharp fluctuations in total vitamin E levels were mainly due to those of α -tocopherol, the major vitamin E form present in fruits (Supplementary Figure S1). γ -Tocopherol levels were lower but also more stable than those of α -tocopherol. Vitamin E levels tended to increase during ripening, an effect that was particularly observed for γ -tocopherol (Supplementary Figure S1) and when results were expressed on a fruit unit basis (**Figure 4**). Neither vitamin E levels nor those of α - and γ -tocopherol were altered during post-harvest either when expressed per g fruit or per fruit

unit (**Figure 4**; Supplementary Figure S2). β - and δ -tocopherols, and tocotrienols were not detected in cherry fruits.

Variations in ABA Levels during Cold Storage

Cold storage prevented over-ripening, as observed with the maintenance of visual fruit firmness (Supplementary Figure S2), biomass and anthocyanin levels (**Figure 5**). Cold treatment prevented anthocyanin accumulation, an effect that was already

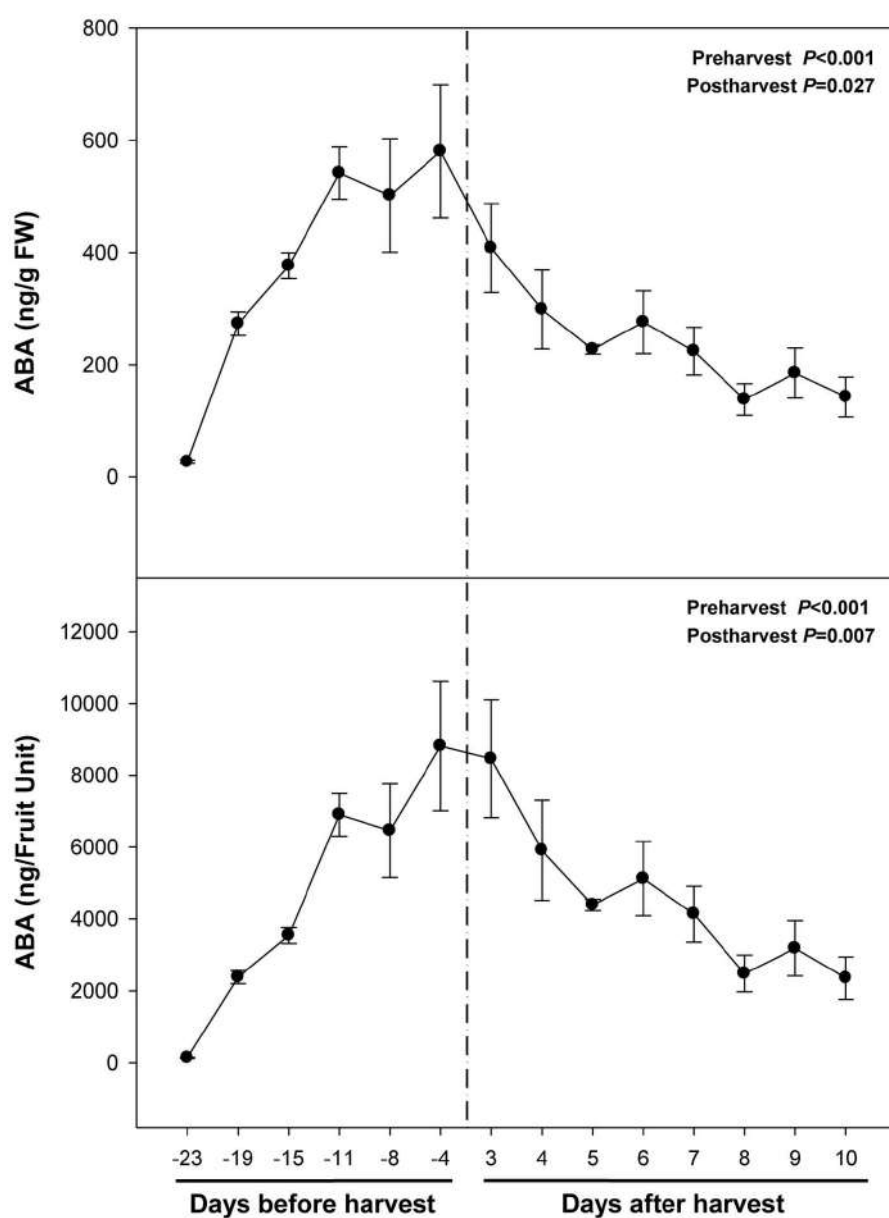


FIGURE 2 | Endogenous concentrations of abscisic acid (ABA) during ripening on the tree (pre-harvest) and during over-ripening at 23°C (post-harvest). Data are the mean \pm SE of $n = 8$ (pre-harvest) and $n = 3$ (post-harvest). Statistical analyses were performed by one-way ANOVA to test for the effects of time during pre- and post-harvest. Results of statistics are shown in the inlets. Differences were considered significant when $P \leq 0.05$. NS, not significant. ABA levels are given both per FW and per fruit unit. Harvest (time 0 in the X axis) corresponds to 57 days after full bloom.

observed at 2 days of cold storage. ABA levels increased in response to cold storage, with an increment at 2 days of treatment (**Figure 6**). Thereafter, ABA levels in cold-stored fruits did not increase further but kept always at higher levels compared to fruits stored at 23°C. In this case, ABA levels inversely correlated, or simply did not correlate with those of anthocyanins. During over-ripening at 23°C, ABA levels decreased, while those of anthocyanins increased. When over-ripening was prevented by cold storage, enhanced ABA levels did not lead to changes in anthocyanin accumulation.

Cold storage did not alter total ascorbate levels, but affected its oxidation state. The ascorbate oxidation state increased in response to cold treatment, but differences were small and *post hoc* analyses did not reveal significant difference at any time point (**Figure 7**). In contrast, ABA levels correlated with vitamin E levels in cold-stored fruits, those of total vitamin E were increasing in parallel with ABA, during the first days of cold treatment (**Figure 8**). The levels of α - and γ -tocopherol were not significantly altered by cold treatment when analyzed separately (Supplementary Figure

TABLE 1 | Carotenoid levels during sweet cherry ripening on the tree.

Days pre-harvest	Violaxanthin	Lutein	Zeaxanthin	β -carotene
Carotenoids (mg/g FW)				
23	0.58 ± 0.18 ^a	3.35 ± 0.25 ^a	0.43 ± 0.05 ^a	0.49 ± 0.10 ^a
15	0.14 ± 0.03 ^b	0.73 ± 0.11 ^b	0.29 ± 0.05 ^a	0.20 ± 0.06 ^{ab}
4	ND ^b	ND ^c	ND ^b	0.17 ± 0.08 ^b
Carotenoids (mg/g Fruit unit)				
23	0.47 ± 0.15 ^a	2.74 ± 0.20 ^a	0.35 ± 0.04 ^a	0.40 ± 0.08 ^a
15	1.34 ± 0.30 ^b	6.86 ± 1.04 ^b	2.74 ± 0.47 ^b	1.65 ± 0.75 ^{ab}
4	ND ^a	ND ^c	ND ^a	3.06 ± 0.91 ^b

Levels of violaxanthin, lutein, zeaxanthin and β -carotene are given at 23, 15, and 4 days pre-harvest, both on a fresh weight (FW) and fruit unit basis. ND, not detected. Different letters indicate significant differences between time points using Bonferroni post hoc tests (ANOVA, $P < 0.05$).

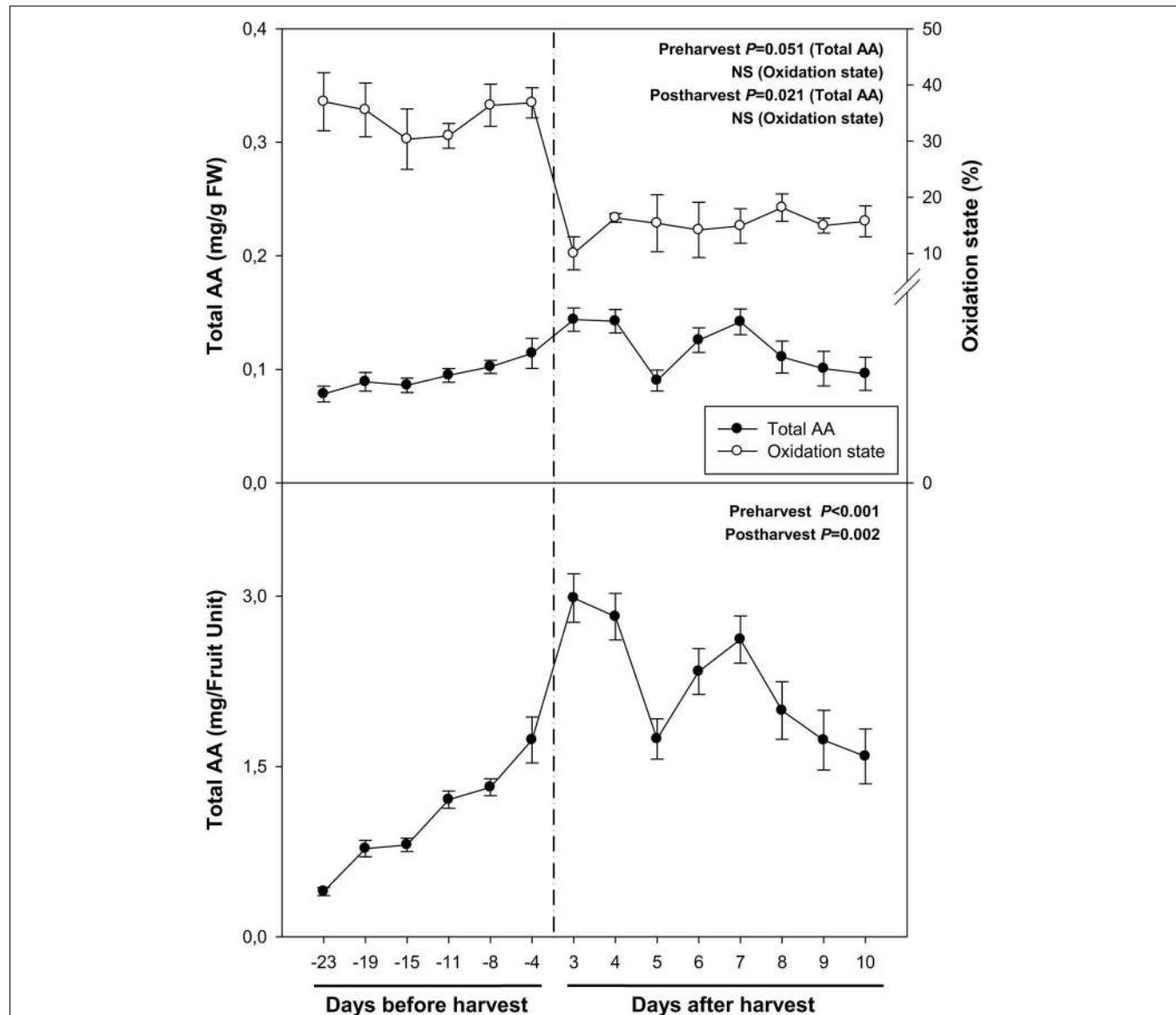


FIGURE 3 | Total ascorbate (AA) and its oxidation state during ripening on the tree (pre-harvest) and during over-ripening at 23°C (post-harvest). Data are the mean \pm SE of $n = 8$ (pre-harvest) and $n = 3$ (post-harvest). Statistical analyses were performed by one-way ANOVA to test for the effects of time during pre- and post-harvest. Results of statistics are shown in the insets. Differences were considered significant when $P \leq 0.05$. NS, not significant. AA levels are given both per FW and per fruit unit. Oxidation state was calculated as oxidized ascorbate per total ascorbate. Harvest (time 0 in the X axis) corresponds to 57 days after full bloom.

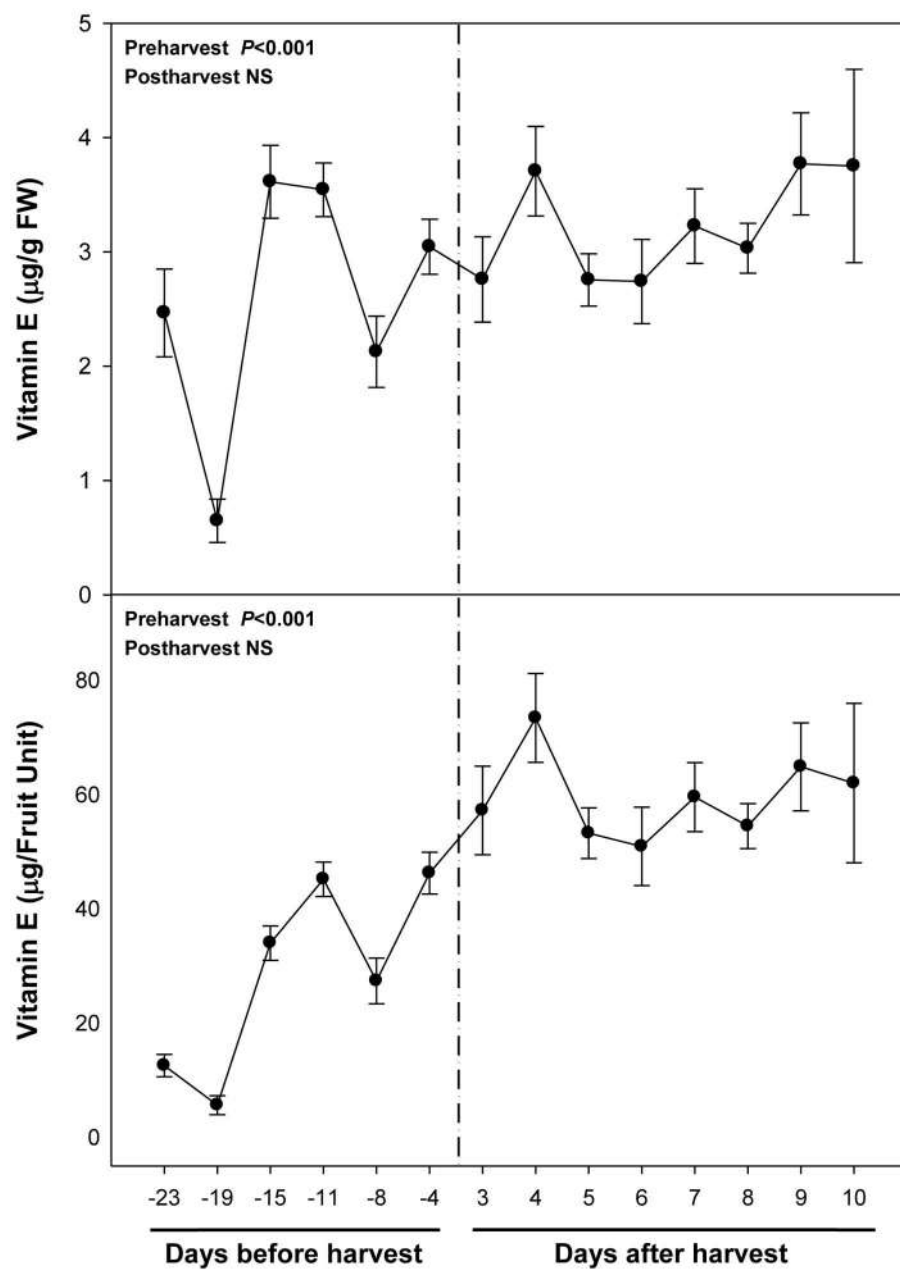


FIGURE 4 | Total vitamin E levels during ripening on the tree (pre-harvest) and during over-ripening at 23°C (post-harvest). Data are the mean \pm SE of $n = 8$ (pre-harvest) and $n = 3$ (post-harvest). Statistical analyses were performed by one-way ANOVA to test for the effects of time during pre- and post-harvest. Results of statistics are shown in the inlets. Differences were considered significant when $P \leq 0.05$. NS, not significant. Vitamin E levels are given both per FW and per fruit unit. Harvest (time 0 in the X axis) corresponds to 57 days after full bloom.

S3), thus indicating that cold effects on total vitamin E levels (Figure 8) were cumulative. It is noteworthy that α - and γ -tocopherol followed a completely different tissue-specific accumulation, with γ -tocopherol accumulating, almost exclusively (>99%), in the pit (Figure 9). In contrast, α -tocopherol, anthocyanins, ascorbate and ABA were all detected in the pit, flesh and skin during both pre- and post-harvest (Figure 9).

DISCUSSION

Sweet cherry is a non-climacteric fruit, which ripening is known to be promoted by ABA (Setha et al., 2005). Its ethylene concentration is low and has no direct effect in the ripening of sweet cherries (Hartmann, 1992; Kondo and Gemma, 1993), although it may influence anthocyanin accumulation (Kondo and Inoue, 1997). ABA is, however, the phytohormone that plays

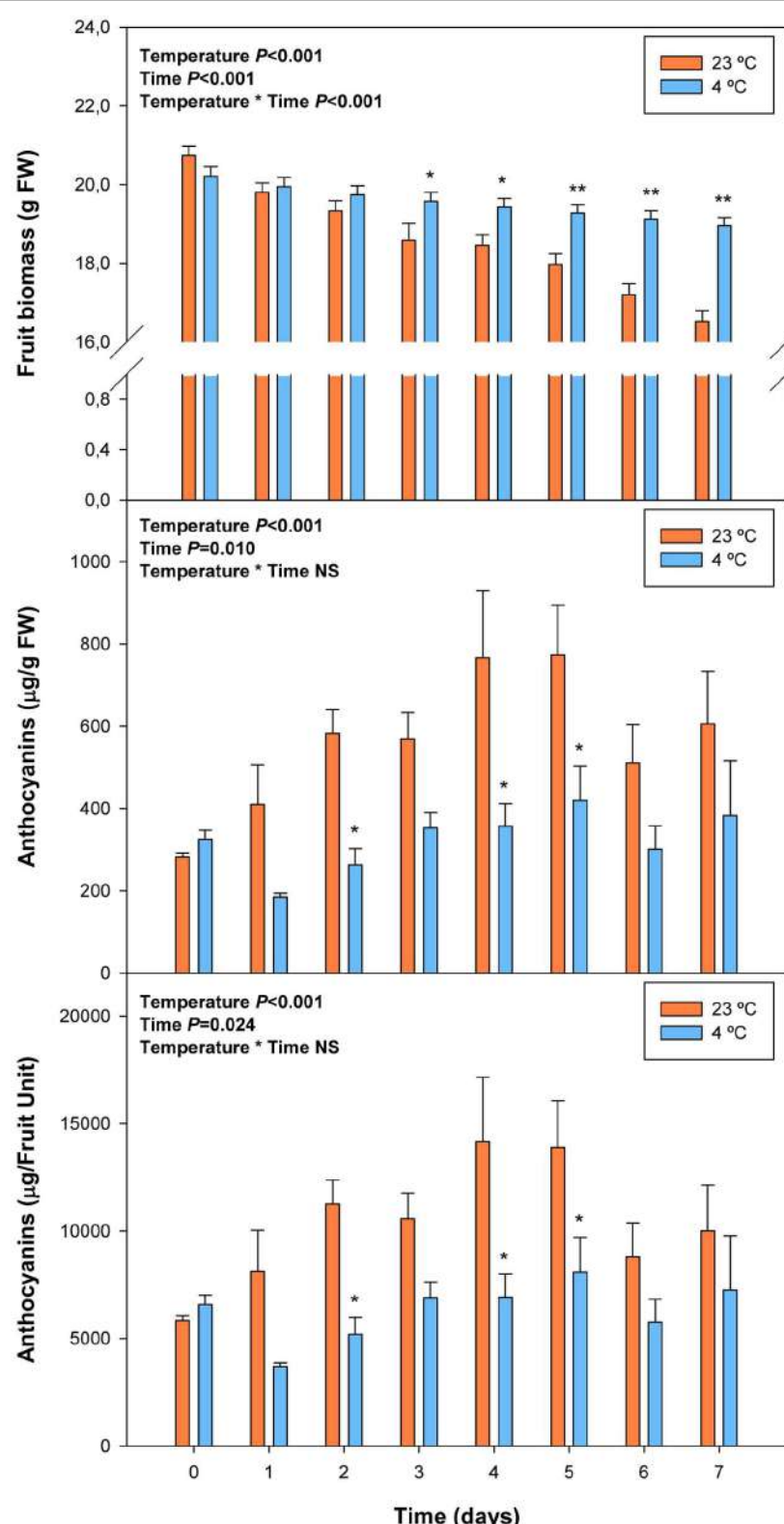


FIGURE 5 | Effects of cold storage on fruit biomass and levels of total anthocyanins during post-harvest. Data are the mean \pm SE of $n = 3$ for anthocyanins and $n = 6$ for fruit biomass. Statistical analyses were performed by two-way ANOVA to test for the effects of treatment and time. Results of statistics are shown in the inlets. One or two asterisks are shown when differences between treatments are significant or highly significant ($P \leq 0.05$ and 0.001 , respectively, Bonferroni post hoc test) at any given time point. NS, not significant. Anthocyanin levels are given both per FW and per fruit unit.

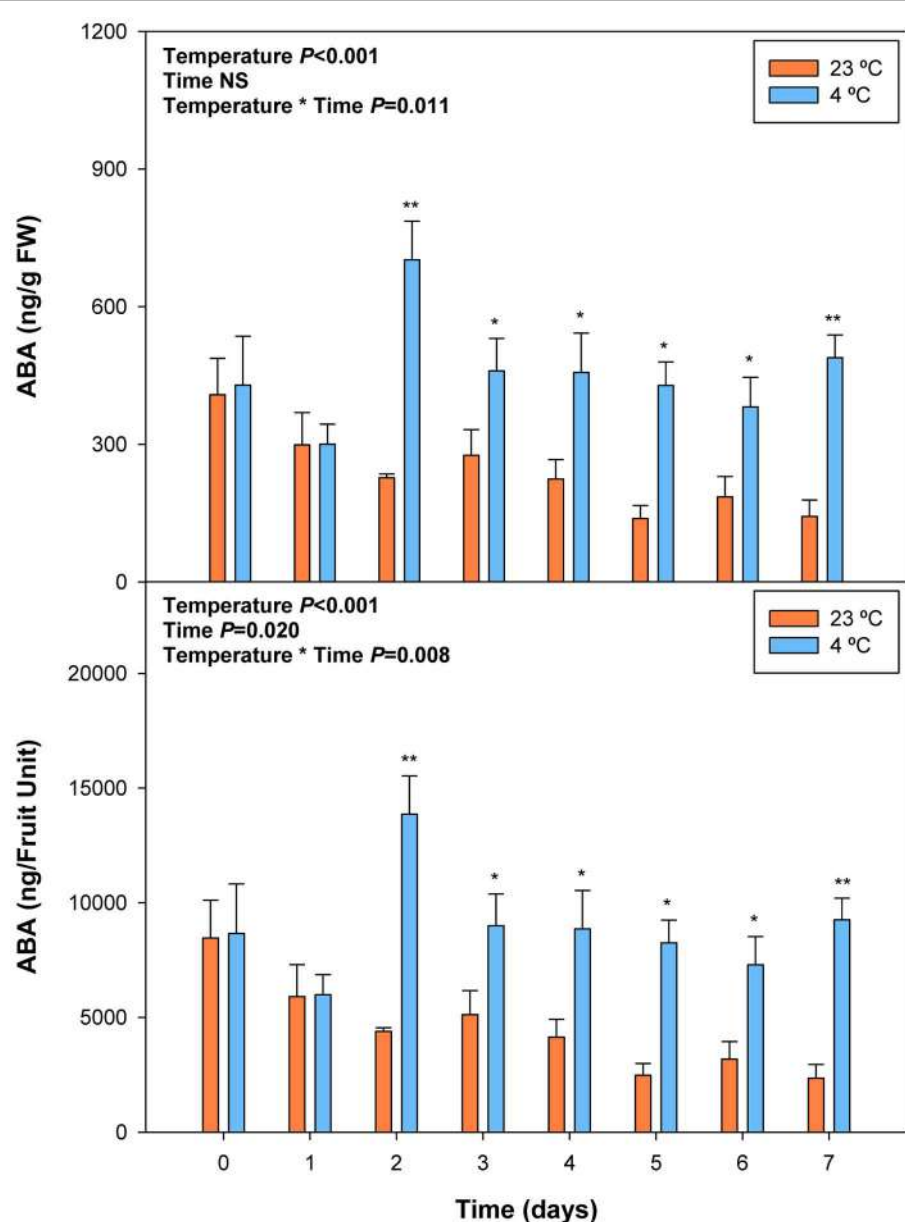


FIGURE 6 | Effects of cold storage on the endogenous concentrations of ABA during post-harvest. Data are the mean \pm SE of $n = 3$. Statistical analyses were performed by two-way ANOVA to test for the effects of treatment and time. Results of statistics are shown in the inlets. One or two asterisks are shown when differences between treatments are significant or highly significant ($P \leq 0.05$ and 0.001 , respectively, Bonferroni post hoc test) at any given time point. NS, not significant. ABA levels are given both per FW and per fruit unit.

a major role in the regulation of anthocyanin accumulation and organoleptic sweet cherries properties, such as the ratio of total soluble sugars to total acidity (Kondo and Gemma, 1993; Kondo and Inoue, 1997; Luo et al., 2013). Studies in other non-climacteric fruits, such as grapes, have also shown that ABA not only modulates color development and sugar accumulation, but it may also be implicated in the control of softening during the ripening process (Castellarin et al., 2016). Here, we provide correlative evidence supporting a role for ABA in the regulation of both anthocyanin and vitamin E

accumulation during pre-harvest, but not during post-harvest, in sweet cherries “Prime Giant.” Furthermore, results suggest that ABA may help prevent over-ripening during post-harvest at 4°C.

We found that ABA levels strongly and positively correlate with anthocyanin accumulation during ripening of fruits on the tree (Table 2), which is in agreement with previous studies (Luo et al., 2013). However, a strong negative correlation was observed between endogenous concentrations of ABA and anthocyanin levels during post-harvest (Table 2). Over-ripening

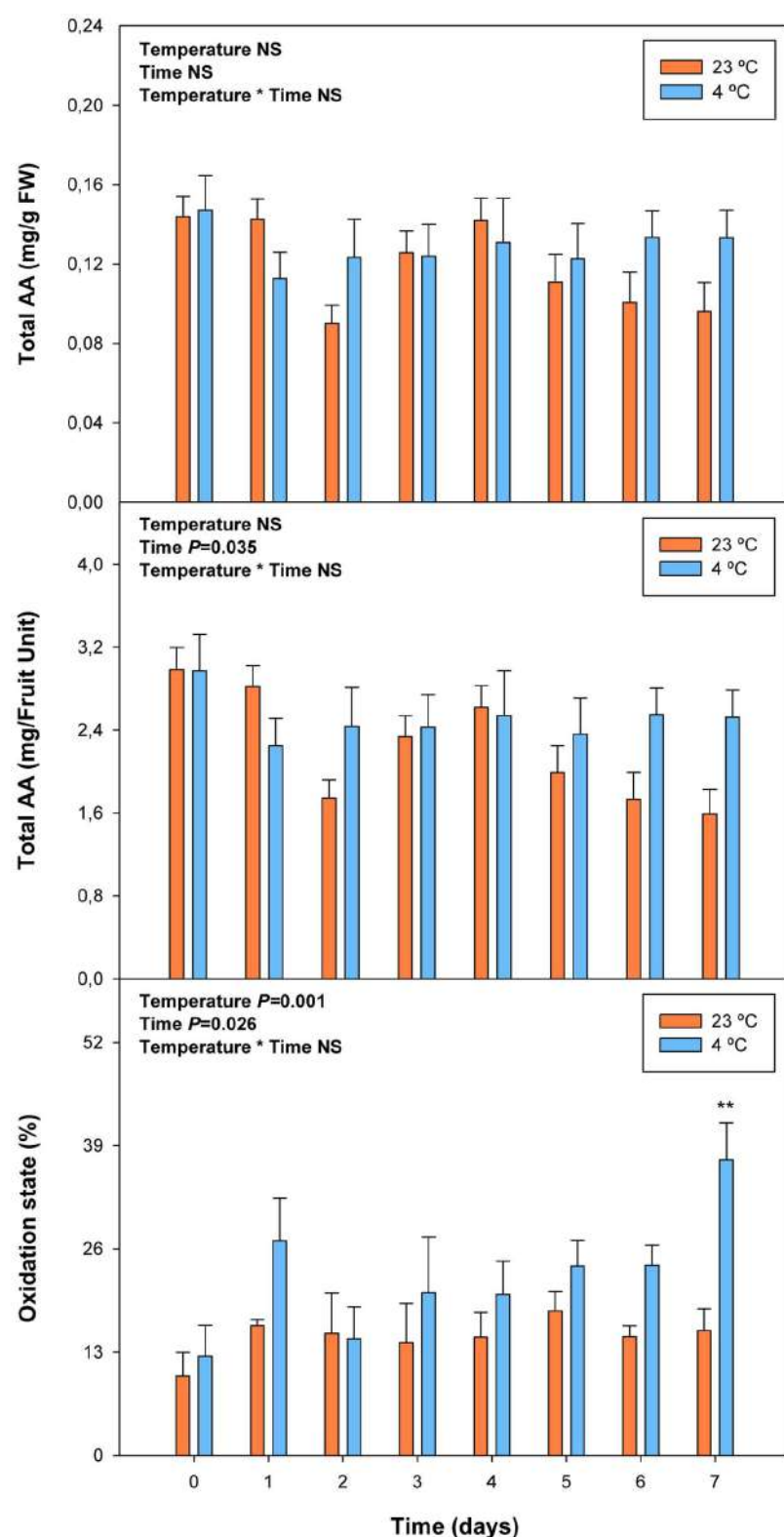


FIGURE 7 | Effects of cold storage on total ascorbate (AA) and its oxidation state during post-harvest. Data are the mean \pm SE of $n = 3$. Statistical analyses were performed by two-way ANOVA to test for the effects of treatment and time. One or two asterisks are shown when differences between treatments are significant or highly significant ($P < 0.05$ and 0.001 , respectively, Bonferroni *post hoc* test). Results of statistics are shown in the inlets. Differences were considered significant when $P \leq 0.05$. NS, not significant. AA levels are given both per FW and per fruit unit. Oxidation state was calculated as oxidized ascorbate per total ascorbate.

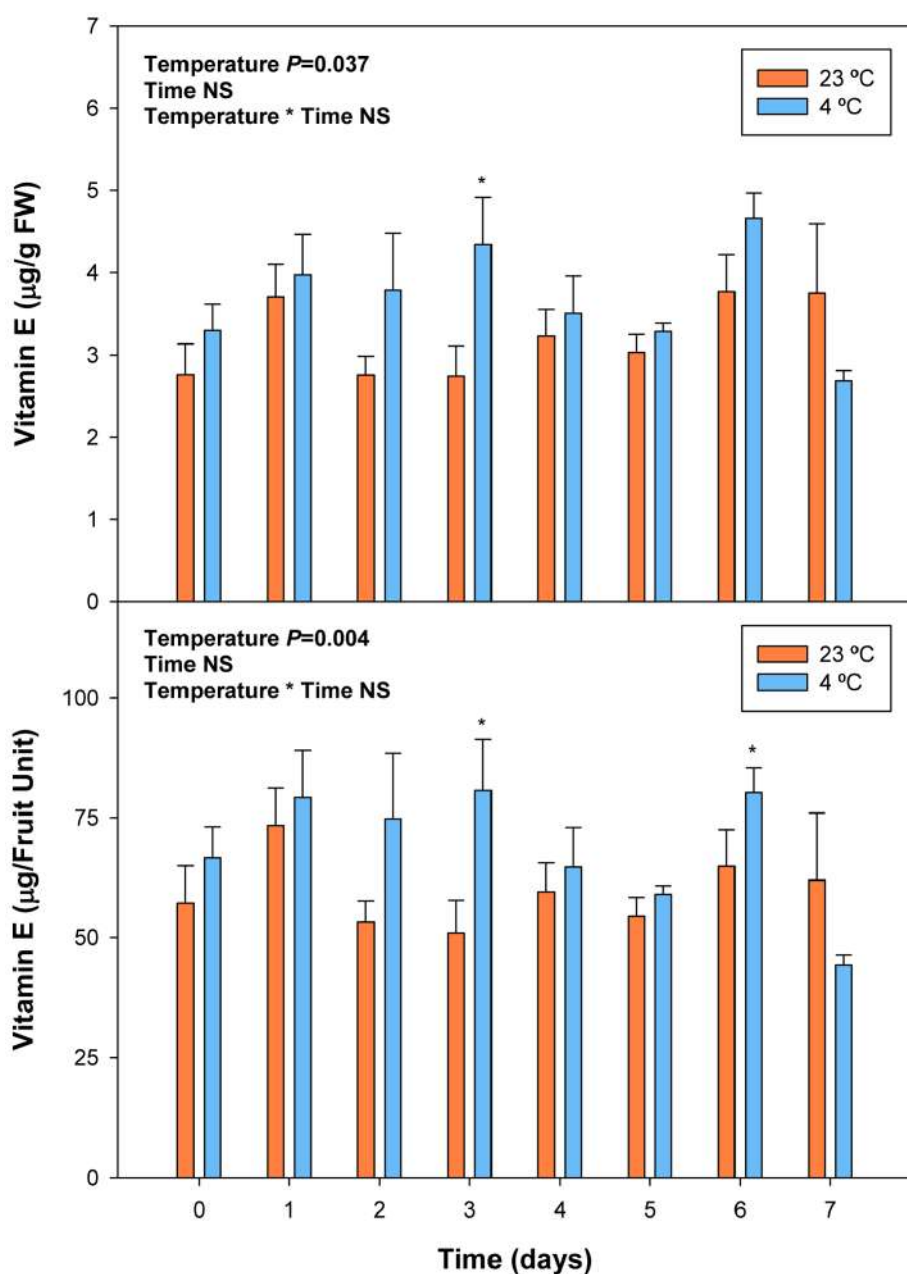


FIGURE 8 | Effects of cold storage on total vitamin E levels during post-harvest. Data are the mean \pm SE of $n = 3$. Statistical analyses were performed by two-way ANOVA to test for the effects of treatment and time. Results of statistics are shown in the insets. One or two asterisks are shown when differences between treatments are significant or highly significant ($P \leq 0.05$ and 0.001 , respectively, Bonferroni *post hoc* test) at any given time point. NS, not significant. Vitamin E levels are given both per FW and per fruit unit.

at 23°C led to progressive decreases in ABA concentrations, while anthocyanin accumulation kept at high levels, thus suggesting an inhibitory role for ABA in over-ripening (Figures 1 and 2). Furthermore, ABA levels increased after 2 days of cold storage, while anthocyanin levels kept at lower levels at 4°C relative to 23°C (Figures 5 and 6), thus suggesting ABA might prevent over-ripening in cold-stored fruits. The role of ABA in over-ripening has been poorly studied to date,

particularly in non-climacteric fruits. However, the application of antitranspirants, such as ABA, in rambutan, a non-climacteric fruit, has been shown to be effective in preventing over-ripening (Siriphollakul et al., 2006), thus supporting further the idea that ABA helps promote ripening in fruits on the tree, but delays over-ripening in detached fruits during post-harvest. This indicates that ABA does not act alone but together with other signaling compounds in the regulation of the ripening

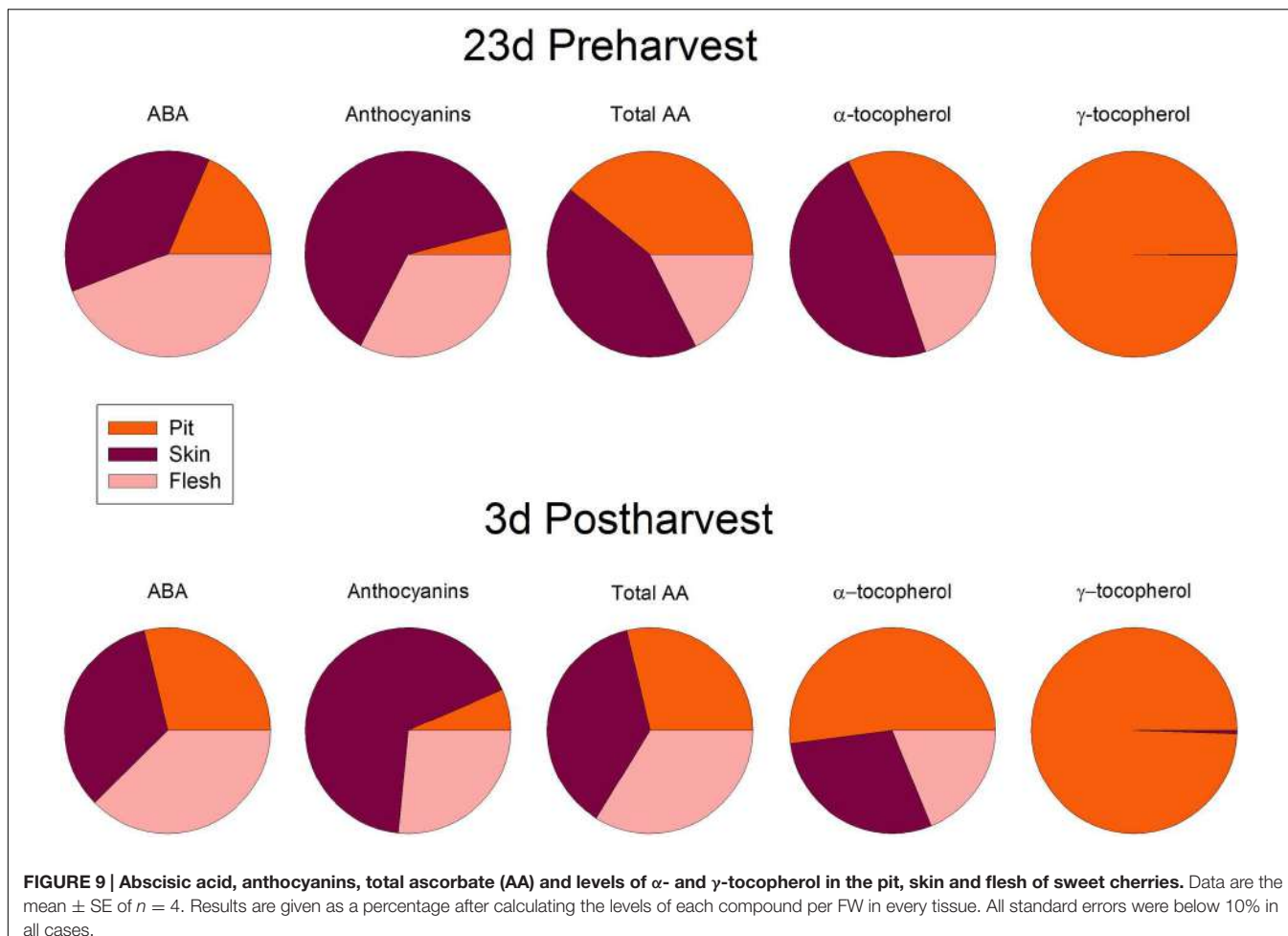


TABLE 2 | Results of Spearman's rank correlation analyses between endogenous concentrations of ABA and quality parameters during pre- and post-harvest.

Parameters	Experiments 1 and 2 (All data)	Experiment 1	Pre-harvest	Post-harvest	Experiment 2
Anthocyanins	0.009	0.033	0.703**	-0.354	-0.531**
Total AA	0.147	0.064	0.219	0.290	0.239
Oxidation state	0.132	0.169	-0.133	-0.287	0.251
Vitamin E	0.196*	0.124	0.282*	-0.137	0.130
α -tocopherol	0.155	0.041	0.176	-0.046	0.147
γ -tocopherol	0.186	0.180	0.367*	-0.179	-0.001

Correlation coefficients values are given followed by one or two asterisks when the correlation is significant or highly significant ($P \leq 0.05$ and 0.001 , respectively). Significant correlations with coefficients above 0.35 are shown in bold. Absence of an asterisk indicates the correlation was not significant. Data was analyzed altogether, and also separately (for each experiment, differentiating also pre- and post-harvest data for Experiment 1).

process in fruits on the tree, an aspect that warrants further investigations.

Aside from its role in the regulation of the ripening process of fruits on the tree, by modulating softening, sugar accumulation and color development (though the modulation of anthocyanin accumulation, Luo et al., 2013; Wang et al., 2015; Castellarin et al., 2016), nothing is known about the possible effects of ABA on vitamin accumulation in sweet cherries or other non-climacteric fruits. Vitamin C is a water-soluble compound that

acts as a cofactor for many iron and copper hydroxylases and dioxygenases involved in key physiological processes in humans, such as in the production of collagen and the synthesis of carnitine (Bender, 2003; Johnston et al., 2007). That is the reason why the frequent intake of foods rich in bioactive compounds, such as vitamin C, is associated with a healthy diet (Arrigoni and De Tullio, 2002). In addition, this compound is considered as one of the most important antioxidants for plant growth and defense (Foyer and Noctor, 2011), which is present in

many plant cell compartments, such as mitochondria, plastids, peroxisomes and the apoplast (Smirnoff, 2000; Foyer, 2001). Moreover, ascorbate is the principal non-enzymatic water-soluble antioxidant that is able to eliminate reactive oxygen species (Cadenas and Packer, 2002). Vitamin C is especially vulnerable to oxidative and enzymatic degradation in raw fruits and vegetables (Redmond et al., 2003). Some studies have reported a loss of vitamin C in many fruits stored under non-optimal conditions after harvest (Munyaka et al., 2010; Neves et al., 2015). Although correlation analyses did not reveal any significant relationship between endogenous concentrations of ABA and vitamin C levels during ripening, over-ripening or cold treatment (Table 2), the present study confirmed that this vitamin is present at high amounts in sweet cherries, attaining maximum levels of 3 mg per fruit unit just after harvest, and it was found that its oxidation increases after 7 days of cold storage. Furthermore, ascorbate is known to act as a cofactor of 9-cis-epoxycarotenoid dioxygenase (NCED), the key limiting step in the biosynthesis of ABA from carotenoids, particularly neoxanthin and/or violaxanthin (Conklin and Barth, 2004). In the present study, violaxanthin levels decreased concomitantly with increases of ABA levels during ripening of fruits on the trees, which is consistent with a role for violaxanthin as a precursor of ABA in sweet cherries (Luo et al., 2013).

On the other hand, vitamin E, a lipid-soluble antioxidant in cell membranes, also with health-promoting effects (Booth et al., 2004), is found at high concentrations in some fruits, such as kiwis or avocados (Chun et al., 2006), but it has received little consideration in sweet cherries, mainly due to their low levels in the fruit, at least, compared to other antioxidants, such as anthocyanins or vitamin C. Among vitamin E compounds, both α - and β -tocopherol were previously shown to be present in sweet cherries, being α -tocopherol the most abundant with amounts around 1 $\mu\text{g/g}$ fruit (Bastos et al., 2015), which is similar to the amounts obtained in the present study (Supplementary Figure S3). However, we did not detect β - but, instead, γ -tocopherol in sweet cherries, which accumulated particularly in the pit (Figure 9). Most importantly, we found a positive correlation between endogenous concentrations of ABA and vitamin E accumulation in sweet cherries, particularly at pre-harvest (Table 2). Interestingly, endogenous concentrations of ABA correlated more strongly with γ - than with α -tocopherol levels. Previous studies have shown the presence of an ABA-responsive element (ABRE) in the promoter region of HYDROXYPHENYL PYRUVATE DIOXYGENASE (HPPD), which encodes for the enzyme responsible of the formation of homogentisate, needed for the biosynthesis of all vitamin E compounds (Chaudhary and Khurana, 2009; Falk and Munné-Bosch, 2010). Therefore, our data supports the contention that ABA is implicated in the biosynthesis of

vitamin E compounds in sweet cherries, as it has been shown in leaves of plants exposed to various abiotic stresses (Chaudhary and Khurana, 2009; Munné-Bosch et al., 2009). It is noteworthy that the correlative evidence obtained in the present study supporting a link between ABA and vitamin E biosynthesis was observed in fruits that were ripening on the tree during pre-harvest, but not during post-harvest at 23°C. Furthermore, enhanced vitamin E levels were preceded by ABA increases during cold storage, thus suggesting ABA may also regulate tocopherol accumulation in response to cold stress in sweet cherries. This may indeed be a defensive response, since both ABA and tocopherols are known to be needed to combat cold-induced reactive oxygen production in plants (El Kayal et al., 2006).

CONCLUSION

The ABA plays a major role in the control of the ripening process in sweet cherries, particularly stimulating this process during pre-harvest and positively influencing quality parameters, such as the accumulation of anthocyanins and vitamin E. Further research is, however, needed to better understand the mechanisms underlying the regulation of vitamin E biosynthesis by ABA during pre-harvest and cold storage, as well as the inhibitory role of ABA in the over-ripening of sweet cherries, beyond its possible function as an antitranspirant.

AUTHOR CONTRIBUTIONS

VT and SM-B conceived and designed the experiments with the help of NT. VT, NT, and PM performed the experiments. SM-B wrote the manuscript with the help of VT; all authors contributed to the discussion, revised and approved the final manuscript.

FUNDING

Research was supported by the Generalitat de Catalunya through the ICREA Academia prize given to SM-B.

ACKNOWLEDGMENTS

We are very grateful to Maren Müller and Serveis Científico-tècnics (University of Barcelona) for their help with ABA analyses. We also thank Josep Maria Gilart for giving us the opportunity to sample the fruits in his orchard.

SUPPLEMENTARY MATERIAL

The Supplementary Material for this article can be found online at: <http://journal.frontiersin.org/article/10.3389/fpls.2016.00602>

REFERENCES

- Amaral, J. S., Casal, S., Torres, D., Seabra, R. M., and Oliveira, B. P. P. (2005). Simultaneous determination of tocopherols and tocotrienols in hazelnuts by a normal phase liquid chromatographic method. *Anal. Sci.* 21, 1545–1548. doi: 10.2116/analsci.21.1545
- Arrigoni, O., and De Tullio, M. C. (2002). Ascorbic acid: much more than just an antioxidant. *Biochim. Biophys. Acta* 1569, 1–9. doi: 10.1016/S0304-4165(01)00235-5
- Ashton, R. W. (2007). *Sweet Cherries for Southern Orchards*. London: Third Millennium Publishing.
- Bastos, C., Barros, L., Dueñas, M., Calhelha, R. C., Queiroz, M. J. R. P., Santos-Buelga, C., et al. (2015). Chemical characterization and bioactive properties of *Prunus avium* L.: the widely studied fruits and the unexplored stems. *Food Chem.* 173, 1045–1053. doi: 10.1016/j.foodchem.2014.10.145
- Bender, D. A. (2003). “Vitamin C (ascorbic acid),” in *Nutritional Biochemistry of the Vitamins*, 2nd Edn, ed. D. A. Bender (Cambridge: Cambridge University Press), 357–384.
- Booth, S. L., Golly, I., Sacheck, J. M., Roubenoff, R., Dallal, G. E., Hamada, K., et al. (2004). Effect of vitamin E supplementation on vitamin K status in adults with normal coagulation status. *Am. J. Clin. Nutr.* 80, 143–148.
- Cadenas, E., and Packer, L. (2002). *Handbook of Antioxidants*, 2nd Edn. New York, NY: Marcel Dekker.
- Castellarin, S. D., Gambetta, G. A., Wada, H., Krasnow, M. N., Cramer, G. R., Peterlunger, E., et al. (2016). Characterization of major ripening events during softening in grape: turgor, sugar accumulation, abscisic acid metabolism, colour development, and their relationship with growth. *J. Exp. Bot.* 67, 709–722. doi: 10.1093/jxb/erv483
- Chaudhary, N., and Khurana, P. (2009). Vitamin E biosynthesis genes in rice: molecular characterization, expression profiling and comparative phylogenetic analysis. *Plant Sci.* 177, 479–491. doi: 10.1016/j.plantsci.2009.07.014
- Chun, J., Leeb, J., Yea, L., Exlerc, J., Ronald, R., and Eitenmiller, R. R. (2006). Tocopherol and tocotrienol contents of raw and processed fruits and vegetables in the United States diet. *J. Food Comp. Anal.* 19, 196–204. doi: 10.1016/j.jfca.2005.08.001
- Conklin, P. L., and Barth, C. (2004). Ascorbic acid, a familiar small molecule intertwined in the response of plants to ozone, pathogens, and the onset of senescence. *Plant Cell Environ.* 17, 959–970. doi: 10.1111/j.1365-3040.2004.01203.x
- El Kayal, W., Keller, G., Debayles, C., Kumar, R., Weier, D., Teulieres, C., et al. (2006). Regulation of tocopherol biosynthesis through transcriptional control of tocopherol cyclase during cold hardening in *Eucalyptus gunnii*. *Physiol. Plant.* 126, 212–223. doi: 10.1111/j.1399-3054.2006.00614.x
- Falk, J., and Munné-Bosch, S. (2010). Tocochromanol functions in plants: antioxidation and beyond. *J. Exp. Bot.* 61, 1549–1566. doi: 10.1093/jxb/erq030
- FAO (2004). *Vitamin and Mineral Requirements in Human Nutrition*. World Health Organization and Food and Agriculture Organization of the United Nations. Available at: <http://apps.who.int/iris/bitstream/10665/42716/1/9241546123.pdf> [accessed on 2 February, 2016].
- FAO (2015). *The Statistical Division (FAOSTAT) of the Food and Agriculture Organization of the United Nations (FAO)*. Available at: http://www.novagrim.com/Pages/2000_2011_cherry_statistics_EN.aspx [accessed on 2 February, 2016].
- Finkelstein, R. (2013). *Abscisic acid Synthesis and Response. The Arabidopsis Book*. Rockville, MD: American Society of Plant Biologists.
- Foyer, C. H. (2001). Prospects of enhancement of the soluble antioxidants, ascorbate and glutathione. *BioFactors* 15, 75–78. doi: 10.1002/biof.5520150204
- Foyer, C. H., and Noctor, G. (2011). Ascorbate and glutathione: the heart of the redox hub. *Plant Physiol.* 155, 2–18. doi: 10.1104/pp.110.167569
- Gitelson, A. A., Merzlyak, M. N., and Chivkunova, O. B. (2001). Optical properties and non-destructive estimation of anthocyanin content in plant leaves. *Photochem. Photobiol.* 74, 38–45. doi: 10.1562/0031-8655(2001)074
- Hartmann, C. (1992). Biochemical changes in harvested cherries. *Post-Harvest Biol. Technol.* 258, 89–96.
- Johnston, C. S., Steinberg, F. M., and Rucker, R. B. (2007). *Ascorbic Acid. Handbook of Vitamins*, 4th Edn. (Boca Raton, FL: CRC Press), 489–520.
- Kondo, S., and Gemma, H. (1993). Relationship between abscisic acid (ABA) content and maturation of the sweet cherry. *J. Japan Soc. Hort. Sci.* 62, 63–68. doi: 10.2503/jjshs.62.63
- Kondo, S., and Inoue, K. (1997). Abscisic acid (ABA) and 1-aminocyclopropane-I-carboxylic acid (ACC) content during growth of ‘Satohnishiki’ cherry fruit, and the effect of ABA and ethephon application on fruit quality. *J. Hort. Sci.* 72, 221–227.
- Kumar, R., Khurana, A., and Sharma, A. K. (2014). Role of plant hormones and their interplay in development and the ripening of fleshy fruits. *J. Exp. Bot.* 16, 4561–4575. doi: 10.1093/jxb/eru277
- Leng, P., Yuan, B., and Guo, Y. (2014). The role of abscisic acid in fruit ripening and responses to abiotic stress. *J. Exp. Bot.* 65, 4577–4588. doi: 10.1093/jxb/eru204
- Luo, H., Dai, S. J., Ren, J., Zhang, C. X., Ding, Y., Li, Z., et al. (2013). The role of ABA in the maturation and post-harvest life of a non-climacteric sweet cherry fruit. *J. Plant Growth Regul.* 33, 373–383. doi: 10.1007/s00344-013-9388-7
- Meheriuk, M., Girard, B., Moys, L., Beveridge, H. J. T., McKenzie, D.-L., Harrison, J., et al. (1995). Modified atmosphere packaging of ‘Lapins’ sweet cherry. *Food Res. Int.* 28, 239–244. doi: 10.1016/0963-9969(95)00003-5
- Müller, M., and Munné-Bosch, S. (2011). Rapid and sensitive hormonal profiling of complex plant samples by liquid chromatography coupled to electrospray ionization tandem mass spectrometry. *Plant Method* 7:37. doi: 10.1186/1746-4811-7-37
- Munné-Bosch, S., and Alegre, L. (2000). Changes in carotenoids, tocopherols and diterpenes during drought and recovery, and the biological significance of chlorophyll loss in *Rosmarinus officinalis* plants. *Planta* 210, 925–931. doi: 10.1007/s004250050699
- Munné-Bosch, S., and Alegre, L. (2002). The function of tocopherols and tocotrienols in plants. *Crit. Rev. Plant Sci.* 21, 31–57. doi: 10.1080/0735260294179
- Munné-Bosch, S., Falara, V., Pateraki, I., López-Carbonell, M., Cela, J., and Kanellis, A. K. (2009). Physiological and molecular responses of the isoprenoid biosynthetic pathway in a drought-resistant Mediterranean shrub, *Cistus creticus* exposed to water deficit. *J. Plant Physiol.* 166, 136–145. doi: 10.1016/j.jplph.2008.02.011
- Munyaka, A. W., Makule, E. E., Oey, I., Loey, A. V., and Hendrickx, M. (2010). Thermal stability of L-ascorbic and ascorbic acid oxidase in broccoli (*Brassica oleracea* var. *italica*). *J. Food Sci.* 75, 336–340. doi: 10.1111/j.1750-3841.2010.01573.x
- Nambara, E., and Marion-Poll, A. (2005). Abscisic acid biosynthesis and catabolism. *Annu. Rev. Plant Biol.* 56, 165–185. doi: 10.1146/annurev.arplant.56.032604.144046
- Neves, L. C., Tosin, J. M., Benedette, R. M., and Cisneros-Zevallos, L. (2015). Post-harvest nutraceutical behaviour during ripening and senescence of 8 highly perishable fruit species from the Northern Brazilian Amazon region. *Food Chem.* 174, 188–196. doi: 10.1016/j.foodchem.2014.10.111
- Queval, G., and Noctor, G. (2007). A plate reader method for measurement of NAD, NADP, glutathione, and ascorbate in tissue extracts: application to redox profiling during *Arabidopsis* rosette development. *Anal. Biochem.* 363, 58–69. doi: 10.1016/j.ab.2007.01.005
- Redmond, G. A., Decaze, A. M., Gormley, T. R., and Butler, F. (2003). The vitamin C status of freeze-chilled mashed potato. *J. Food Eng.* 56, 219–221. doi: 10.1016/S0260-8774(02)00255-8
- Serrano, M., Guillén, F., Martínez-Romero, D., Castillo, S., and Valero, D. (2005). Chemical constituents and antioxidant activity of sweet cherry at different ripening stages. *J. Agric. Food Chem.* 53, 2741–2745. doi: 10.1021/jf0479160
- Setha, S., Kondo, S., Hirai, N., and Ohigashi, H. (2005). Quantification of ABA and its metabolites in sweet cherries using deuterium-labeled internal standards. *Plant Growth Regul.* 45, 183–188. doi: 10.1007/s10725-005-3088-7
- Siegelman, H. W., and Hendricks, S. B. (1958). Photocontrol of anthocyanin synthesis in apple skin. *Plant Physiol.* 33, 185–190. doi: 10.1104/pp.33.6.409
- Singh, R. K., Ali, S. A., Nath, P., and Sane, V. A. (2011). Activation of ethylene-responsive p-hydroxyphenylpyruvate dioxygenase leads to increased tocopherol levels during ripening in mango. *J. Exp. Bot.* 62, 3375–3385. doi: 10.1093/jxb/err006
- Siriphollakul, P., Niyomlao, W., and Kanlayanarat, S. (2006). Antitranspirants maintain freshness and improve storage life of rambutan

- (*Nephelium lappaceum* L.) fruit. *Acta Hortic.* 712, 611–616. doi: 10.17660/ActaHortic.2006.712.74
- Smirnoff, N. (2000). Ascorbic acid: metabolism and functions of a multi-faceted molecule. *Curr. Opin. Plant Biol.* 3, 229–235. doi: 10.1016/S1369-5266(00)00069-8
- Takahama, U., and Oniki, T. (1992). Regulation of peroxidase-dependent oxidation of phenolics in the apoplast of spinach leaves by ascorbate. *Plant Cell Physiol.* 33, 379–387.
- Veljovic-Jovanovic, S. D., Pignocchi, C., Noctor, G., and Foyer, C. H. (2001). Low ascorbic acid in the vtc-1 mutant of *Arabidopsis* is associated with decreased growth and intracellular redistribution of the antioxidant system. *Plant Physiol.* 127, 426–435. doi: 10.1104/pp.010141
- Wang, Y., Chen, P., Sun, L., Li, Q., Dai, S., Sun, Y., et al. (2015). Transcriptional regulation of PaPYLs, PaPP2Cs and PaSnRK2s during sweet cherry fruit development and in response to abscisic acid and auxin at onset of fruit ripening. *Plant Growth Regul.* 75, 455–464. doi: 10.1007/s10725-014-0006-x

Conflict of Interest Statement: The authors declare that the research was conducted in the absence of any commercial or financial relationships that could be construed as a potential conflict of interest.

Copyright © 2016 Tijero, Teribia, Muñoz and Munné-Bosch. This is an open-access article distributed under the terms of the Creative Commons Attribution License (CC BY). The use, distribution or reproduction in other forums is permitted, provided the original author(s) or licensor are credited and that the original publication in this journal is cited, in accordance with accepted academic practice. No use, distribution or reproduction is permitted which does not comply with these terms.



Structural and Functional Analysis of the GRAS Gene Family in Grapevine Indicates a Role of GRAS Proteins in the Control of Development and Stress Responses

OPEN ACCESS

Edited by:

Richard Sayre,
New Mexico Consortium at Los
Alamos National Labs, USA

Reviewed by:

Vasileios Fotopoulos,
Cyprus University of Technology,
Cyprus
Cordelia Bolle,
Ludwig Maximilian University,
Germany

*Correspondence:

Ana M. Fortes
amfortes@fc.ul.pt

Specialty section:

This article was submitted to
Plant Physiology,
a section of the journal
Frontiers in Plant Science

Received: 03 December 2015

Accepted: 07 March 2016

Published: 30 March 2016

Citation:

Grimplet J, Agudelo-Romero P, Teixeira RT, Martinez-Zapater JM and Fortes AM (2016) Structural and Functional Analysis of the GRAS Gene Family in Grapevine Indicates a Role of GRAS Proteins in the Control of Development and Stress Responses. *Front. Plant Sci.* 7:353.
doi: 10.3389/fpls.2016.00353

Jérôme Grimplet¹, Patricia Agudelo-Romero², Rita T. Teixeira²,
Jose M. Martinez-Zapater¹ and Ana M. Fortes^{2,3*}

¹ Instituto de Ciencias de la Vid y del Vino (Consejo Superior de Investigaciones Científicas-Universidad de La Rioja-Gobierno de La Rioja), Logroño, Spain, ² Faculdade de Ciências de Lisboa, BiolSI, Universidade de Lisboa, Lisboa, Portugal, ³ Instituto de Tecnología de Química Biológica, Biotecnología de Células Vegetais, Oeiras, Portugal

GRAS transcription factors are involved in many processes of plant growth and development (e.g., axillary shoot meristem formation, root radial patterning, nodule morphogenesis, arbuscular development) as well as in plant disease resistance and abiotic stress responses. However, little information is available concerning this gene family in grapevine (*Vitis vinifera* L.), an economically important woody crop. We performed a model curation of GRAS genes identified in the latest genome annotation leading to the identification of 52 genes. Gene models were improved and three new genes were identified that could be grapevine- or woody-plant specific. Phylogenetic analysis showed that GRAS genes could be classified into 13 groups that mapped on the 19 *V. vinifera* chromosomes. Five new subfamilies, previously not characterized in other species, were identified. Multiple sequence alignment showed typical GRAS domain in the proteins and new motifs were also described. As observed in other species, both segmental and tandem duplications contributed significantly to the expansion and evolution of the GRAS gene family in grapevine. Expression patterns across a variety of tissues and upon abiotic and biotic conditions revealed possible divergent functions of GRAS genes in grapevine development and stress responses. By comparing the information available for tomato and grapevine GRAS genes, we identified candidate genes that might constitute conserved transcriptional regulators of both climacteric and non-climacteric fruit ripening. Altogether this study provides valuable information and robust candidate genes for future functional analysis aiming at improving the quality of fleshy fruits.

Keywords: abiotic stress, biotic stress, fruit ripening, grapevine, GRAS gene family, transcription factor

INTRODUCTION

Transcription factors play an important role in the regulation of plant development and disease response. Among them, the plant gene family of GRAS transcription factors was defined based on nuclear localization, DNA binding and transcriptional activation features (Silverstone et al., 1998; Itoh et al., 2002; Morohashi et al., 2003). In addition, *in vivo* association of specific GRAS proteins with promoter regions of several putative GRAS target genes was confirmed by chromatin immunoprecipitation (Zentella et al., 2007). The name GRAS derives from its first three identified members, namely, gibberellic acid insensitive (GAI), repressor of GA1 (RGA), and scarecrow (SCR; Pysh et al., 1999; Bolle, 2004). Moreover, the Arabidopsis GRAS Protein SCL14 was shown to be essential for the activation of stress-inducible promoters (Fode et al., 2008).

Genome-wide analysis performed in nearly 30 plant species from more than 20 genera revealed that this gene family is widely distributed in the plant kingdom (Tian et al., 2004), reviewed by Hirsch and Oldroyd (2009) and it is likely to have emerged first in bacteria (Zhang et al., 2012). GRAS proteins are typically 400–700 amino acids in length and exhibit considerable sequence homology among each other in their C-terminus, where five conserved motifs, namely LHR I, VHIID, LHR II, PFYRE, and SAW are located (Pysh et al., 1999; Tian et al., 2004). The VHIID domain of a GRAS protein from *Brassica napus* interacts with a histone deacetylase, supporting the notion that GRAS proteins regulate gene expression at the level of transcription (Gao et al., 2004).

The amino acid sequences of GRAS proteins are highly variable at the N-terminus, which may be responsible for the specificity of their regulatory functions (Tian et al., 2004). For example, a subgroup of GRAS proteins, which function in several plant species as repressors of gibberellin signaling, share in their N-terminal region the amino acid sequence DELLA and are thus referred as DELLA proteins (Silverstone et al., 1998).

The GRAS protein family groups into eight well-known subfamilies: DELLA, HAM, LISCL, PAT1, LAS, SCR, SHR, and SCL3. However, in between 8 and 13 distinct clades can be discriminated in different studies (Huang et al., 2015; Bolle, 2016). Several GRAS genes from plant species such as Arabidopsis, rice, and barley have been functionally characterized, including *CIGR* (PAT subfamily), *GAI*, *RGL*, *RGA*, and *SLN1* (DELLA subfamily), *MOC1* (LAS subfamily) as well as other genes from SCR, SHR, LISCL, SCL, and HAM subfamilies (Fu et al., 2002; Stuurman et al., 2002; Day et al., 2004), reviewed by Bolle (2016). They have been involved in many processes of plant growth and development such as gibberellins signal transduction (Peng et al., 1997; Ikeda et al., 2001), axillary meristem initiation (Greb et al., 2003; Li et al., 2003), shoot meristem maintenance (Stuurman et al., 2002), radial organization of the root (Helariutta et al., 2000), phytochrome A signal transduction (Bolle et al., 2000), and male gametogenesis (Morohashi et al., 2003). GRAS genes have also been connected with plant disease resistance and abiotic stress response (Mayrose et al., 2006; Ma et al., 2010; Cui, 2012). Furthermore, in the model legume species *Medicago truncatula*

and *Lotus japonicus* two GRAS proteins were shown to be required for nodule morphogenesis (Kalo et al., 2005; Heckmann et al., 2006). Recently, the GRAS transcription factor RAM1 and the novel GRAS protein RAD1 were reported to be involved in arbuscule development (Xue et al., 2015). The formation of multicomponent GRAS transcription factor complexes with other proteins was suggested to be a prerequisite for elicitation of nodulation or mycorrhization (Oldroyd, 2013). Genes coding for GRAS transcription factors were also identified as targets of miRNAs during tomato fruit development and ripening (Moxon et al., 2008; Karlova et al., 2013).

So far, various *in silico* genome analyses have predicted the existence of 33, 57 and 48 GRAS genes in the whole genome of Arabidopsis, rice and Chinese cabbage, respectively (Tian et al., 2004; Song et al., 2014). As more species have their complete reference genome sequenced, additional GRAS genes can be identified as it is the case of *Vitis vinifera*.

Due to its economic relevance, much research in grapevine genomics has been carried out during the last decade. Among these studies, the release of the whole grapevine genome sequence in 2007 represented a breakthrough to promote its molecular genetics analysis (Jaillon et al., 2007). Based on the published sequence data, comprehensive analysis of a given gene family can be performed to uncover its molecular functions, evolution, and gene expression profiles. These analyses can contribute to the understanding of how genes in gene families control traits at a genome-wide level.

Previous comparative analysis with Chinese cabbage genome predicted 43 GRAS transcription factors in *V. vinifera* (Song et al., 2014). In this work, we update this number to 52, a very similar number of GRAS genes to the 53 recently reported in tomato (Huang et al., 2015). Furthermore, we provide a detailed analysis of the GRAS transcription factors relationships among several plant species through comparative genomics together with the identification, structural analysis, and mapping of the GRAS transcription factors onto the grapevine chromosomes. Finally, expression analyses based on microarray and RNAseq data suggest that GRAS proteins play an important role in grape ripening and in response to abiotic and biotic stresses.

MATERIALS AND METHODS

Identification of GRAS Genes

Genes previously identified as encoding GRAS proteins in (Grimplet et al.) were blasted (blastp and tblastn) against the grapevine genome 12x2 (<https://urgi.versailles.inra.fr/Species/Vitis/Data-Sequences/Genome-sequences>), the non-redundant list of genes in (Grimplet et al., 2012) and the COST annotation gene set available at the ORCAE website (<http://bioinformatics.psb.ugent.be/orcae/>). Results from different analysis were manually cross-checked to identify new potential loci corresponding to GRAS genes in the grapevine genome. The UGene software (Okonechnikov et al., 2012) was used to design the gene models on the grapevine genome and test their structure.

Gene Structure Analysis

The potential coding DNA sequences (CDS) were blasted (blastx) against the NCBI public database to compare the structures with other known GRAS genes in other species and the NCBI Refseq predictions of the grapevine genes. When discrepancies were observed, gene models were corrected using the UGene software. Loci bearing genes that were not functional were eliminated from the list. A GFF file with the GRAS genes was designed, uploaded into the IGV software and the RNAseq data available (shoot tips, leaves, flower inflorescences and seed tissues) in the laboratory were used to double-check the exon structure of the genes. Final models were uploaded in the *V. vinifera* ORCAE database (Sterck et al., 2012; Grimplet et al., 2014).

Sequence Alignment and Phylogenetic Analysis

Sequence information on previously reported GRAS proteins of *Arabidopsis thaliana* was retrieved from the Arabidopsis Information Resource (<https://www.arabidopsis.org/browse/genefamily/GRAS.jsp>). Evolutionary analyses were conducted in MEGA6 (Tamura et al., 2013). Multiple sequence alignment was inferred using MUSCLE (Edgar, 2004). The evolutionary history was inferred by using the Maximum Likelihood method based on the JTT matrix-based model (Jones et al., 1992). The bootstrap consensus tree inferred from 100 replicates was taken to represent the evolutionary history of the taxa analyzed (Felsenstein, 1985). Branches corresponding to partitions reproduced in less than 30% of bootstrap replicates were collapsed. Initial trees for the heuristic search were obtained automatically by applying Neighbor-Join and BioNJ algorithms to a matrix of pairwise distances estimated using a JTT model, and then selecting the topology with superior log likelihood value. The coding data was translated assuming a Standard genetic code table. All positions with less than 95% site coverage were eliminated. The genes were named according to Grimplet et al. (2014) based on the distance homology with *Arabidopsis* genes.

The alignment file between *Arabidopsis* and grapevine sequences was uploaded to the Jalview and UGene software for manual adjustment of the alignment and manual motif editing. Motifs identified in Tian et al. (2004) were flagged and labeled for the grapevine genes; additional motifs of high homology were also identified (at least 50% homology within the members of the subfamily on at least 10 amino acids) among grapevine sequences.

Expression Analysis

Expression data were retrieved from three different microarray platforms (Affymetrix Genchip (16k probesets) GrapeGen (21k probesets), Vitis Nimblegen array (29k probesets), and from our in-house RNAseq projects. Data normalization was performed on all the array of each platform (RMA normalization). After retrieving the values for the probesets corresponding to each gene, the values for the 3 or 4 replicates of the same condition were averaged to obtain a total of 256 conditions (organ, cultivar, treatment, platform). Based on expression data of the grapevine gene expression atlas (Fasoli et al., 2012), a plant ontology ID

was attributed to each gene if expression intensity in a tissue was above a defined threshold of absolute log₂ value of 8 or absolute value of 256. The same data were used for the co-expression analysis with the whole set of genes available on the Nimblegen platform. Hierarchical clustering with Pearson correlation as metric and average linkage cluster method was performed. Genes considered as having the same profile should present a distance threshold between each other lower than 0.2.

For further evaluation of gene expression samples corresponding to several stages of grapevine development and ripening and several abiotic and biotic stress conditions were used (Cramer et al., 2007; Deluc et al., 2007; Espinoza et al., 2007; Grimplet et al., 2007; Pilati et al., 2007; Tattersall et al., 2007; Fung et al., 2008; Lund et al., 2008; Albertazzi et al., 2009; Pontin et al., 2010; Sreekantan et al., 2010; Carvalho et al., 2011; Fortes et al., 2011; Tillett et al., 2011; Vega et al., 2011; Diaz-Riquelme et al., 2012; Fasoli et al., 2012; Lijavetzky et al., 2012; Carbonell-Bejerano et al., 2013; Agudelo-Romero et al., 2015). Heat maps were performed with the ComplexHeatmap R package (<https://github.com/jokergoo/ComplexHeatmap>).

Comparison to Other Plant Species

We performed a sequence comparison using the GRAS genes from 16 plant species (*A. thaliana*, *Brassica rapa*, *Carica papaya*, *Eucalyptus grandis*, *Citrus sinensis*, *Malus domestica*, *Prunus persica*, *Fragaria vesca*, *Glycine max*, *M. truncatula*, *Cucumis melo*, *Populus trichocarpa*, *Solanum lycopersicum*, *Zea mays*, *Sorghum bicolor*, *Oryza sativa*) retrieved at <http://plantfdb.cbi.pku.edu.cn>. We identified orthologous genes in genomes from the sixteen species following what was performed in Jaillon et al. (2007). Each pair of predicted gene sets was aligned with the BLASTp algorithm, and alignments with an e-value lower than $1e^{-20}$ and sequence homology higher than 40% were retained. If a comparison is above that value, the two genes were considered homologs. Two genes, A from *Vitis* genome GV and B from genome GX, were considered orthologs one-to-one if B was the best match for gene A in GX and A was the best match for B in GV. A phylogenetic tree was constructed with the GRAS genes from these species with the same parameters as before.

RESULTS

Identification and Structural Annotation of the GRAS Genes

Genes that were previously identified as GRAS in the grapevine genome (Grimplet et al., 2012) were used to perform sequence comparison analyses, either against the most up to date gene predictions from CRIBI V1 and V2, the NCBI refseq (on the 12Xv1 of the genome assembly) and the VCOST (on the 12Xv2 of the genome assembly) as well as directly against the reference genome sequence to check whether any potential gene could have been missed by these predictions. In this way, we identified 80 genome regions that shared homology with at least one of the genes.

Gene models were curated using the data collected from gene structure comparisons using different databases as well as

the available RNAseq data from our laboratory (Royo et al., 2016) to validate actually expressed exons. This data also allowed evaluating the expression of newly detected genes, not represented in microarray data, by redoing the bioinformatics analysis of original RNAseq data with an updated GFF file. A total of 52 GRAS genes with a functional structure were identified in the grapevine genome (Table 1). Data relative to the detection of GRAS genes in previous genome annotations or gene-sets are summarized in Supplementary Table 1. Three additional genes were detected compared to the automatic annotation CRIBI V1, one was not seen in the V1, but was known in the annotation from the 8x genome (Table 1). The structure of 14 genes CRIBI annotated genes was curated in our work.

Exon/intron structure is highly conserved amongst GRAS genes in grapevine and most of them presented only one exon which is a common feature of this gene family observed in many plant species (Song et al., 2014; Huang et al., 2015; Lu et al., 2015). Only six genes contained introns (Table 1). Five of them contained two exons while *VviLISCL7* contained four. No subfamily showed a specific intron/exon structure (Supplementary Table 1) while the size of GRAS genes varied greatly, ranging from 294 nucleotides (*VviSCL3b*) to 2349 nucleotides (*VviSCR1*). Forty-one genes (79%) had a length longer than 1400 bp.

Phylogenetic Analysis, Nomenclature, and Motif Analysis

For gene nomenclature, a phylogenetic tree of the GRAS protein coding genes in *V. vinifera* and *Arabidopsis* was constructed (Figure 1) as recommended by the Super-Nomenclature Committee for Grape Gene Annotation (sNCGGA; Grimplet et al., 2014). This analysis identified the eight subfamilies previously described in other plant species: DELLA, HAM, LISCL, PAT, LS, SCR, SHR, and SCL3. Furthermore, five additional groups were detected that could not be assigned to any of those subfamilies (Figure 1). Interestingly, 13 groups were also recently found in tomato (Huang et al., 2015). For individual gene nomenclature, we attributed gene symbols/names using preferentially those previously used when they fit the recommendations of the sNCGGA. If a gene was not described before and had an *Arabidopsis* ortholog, the corresponding *Arabidopsis* gene name was used. In addition, to distinguish different subfamily members, names were composed by the subfamily symbol followed by a number or a letter (when the subfamily symbol ended with a number). Among the new detected subfamilies, two showed an *Arabidopsis* homolog that had not been previously described in a subfamily. These were labeled SCL26 and GRAS8. The 3 remaining new subfamilies were labeled GRASV1, GRASV2 and GRASV3.

Five characteristic conserved motifs were identified in the C-terminus of the GRAS proteins, namely LHRI, VHIID, LHRII, PFYRE, and SAW (summarized by subfamilies in Figure 2 and detailed in Supplementary Image 1). The LHRI motif presented two units (A and B). Leucine repeats found in Unit A were found to be conserved in all GRAS proteins (Figure 2 and Supplementary Image 1) as previously reported (Tian et al.,

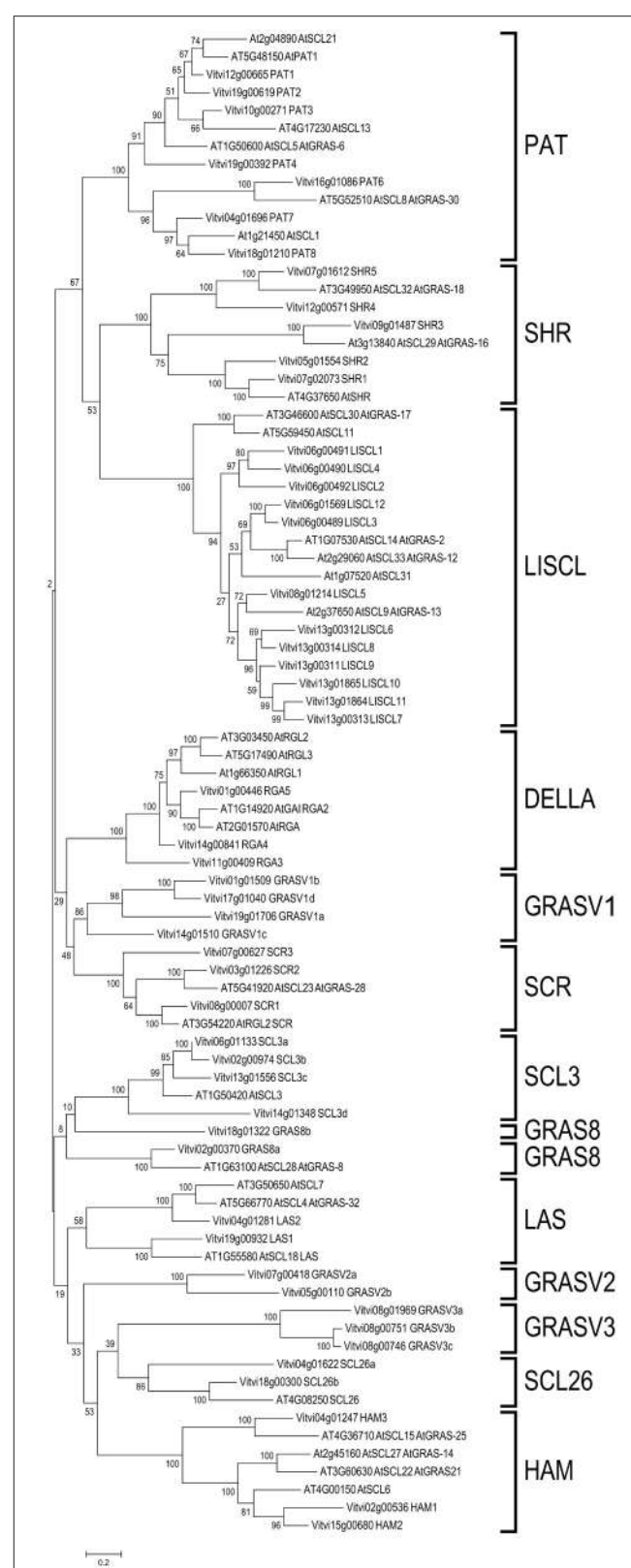


FIGURE 1 | Molecular phylogenetic analysis of grapevine and *Arabidopsis* GRAS genes. Thirteen sub families were identified in grapevine: the known DELLA, HAM, LISCL, PAT, LS, SCR, SHR, and SCL3 and five new subfamilies GRAS8, GRASV1, GRASV2, GRASV3, and SCL26.

TABLE 1 | Genome localization of the 52 grapevine GRAS genes.

Locus ID	Short name	Strand	Position v2	Locus ID	Short name	Strand	Position v2
Vitvi12g00665	PAT1	—	8738265–8739902	Vitvi11g00409	RGA3	—	3959545–3961143
Vitvi19g00619	PAT2	—	7772106–7773743	Vitvi01g01509	GRASV1b	+	20426662–20428254
Vitvi10g00271	PAT3	—	2802206–2803843	Vitvi17g01040	GRASV1d	—	12688373–12689932
Vitvi19g00392	PAT4	—	5276148–5277899	Vitvi19g01706	GRASV1a	+	23595896–23597488
Vitvi16g01086	PAT6	+	19383904–19385748	Vitvi14g01510	GRASV1c	—	25316395–25317516, 25317604–25318488
Vitvi04g01696	PAT7	—	23747087–23748793	Vitvi07g00627	SCR3	+	6996793–6998256
Vitvi18g01210	PAT8	+	13411198–13412895	Vitvi03g01226	SCR2	+	19152243–19153571
Vitvi07g01612	SHR5	+	21912240–21913607	Vitvi08g00007	SCR1	—	115793–116261, 116647–117596
Vitvi12g00571	SHR4	+	7509331–7510668	Vitvi06g01133	SCL3a	+	15915179–15916597
Vitvi09g01487	SHR3	—	910682–912319	Vitvi02g00974	SCL3b	+	13518884–13519177
Vitvi05g01554	SHR2	+	23894334–23895644	Vitvi13g01556	SCL3c	—	24957576–24959012
Vitvi07g02073	SHR1	—	21633666–21635150	Vitvi14g01348	SCL3d	+	23412635–23413888
Vitvi06g00491	LISCL1	+	5938487–5940601	Vitvi18g01322	GRAS8b	+	14926630–14927997
Vitvi06g00490	LISCL4	+	5930838–5932814	Vitvi02g00370	GRAS8a	+	3323726–3325756
Vitvi06g00492	LISCL2	+	5942791–5944119	Vitvi04g01281	LAS2	+	18563606–18565456
Vitvi06g01569	LISCL12	+	5918887–5921169	Vitvi19g00932	LAS1	+	10747971–10749212
Vitvi06g00489	LISCL3	+	5925910–5928204	Vitvi07g00418	GRASV2a	—	4408615–4410429
Vitvi08g01214	LISCL5	+	14792851–14795082	Vitvi05g00110	GRASV2b	—	1038770–1039128, 1039236–1039324, 1039452–1040602
Vitvi13g00312	LISCL6	+	3256665–3258887	Vitvi08g00751	GRASV3a	—	9219561–9220028, 9220132–9221151
Vitvi13g00314	LISCL8	+	3283478–3285724	Vitvi08g00746	GRASV3b	—	9152326–9153933
Vitvi13g00311	LISCL9	+	3251727–3254009	Vitvi08g01969	GRASV3c	+	9227520–9229388
Vitvi13g01865	LISCL10	+	3279518–3281677	Vitvi04g01622	SCL26a	+	22393173–22394627
Vitvi13g01864	LISCL11	+	3274050–3274663, 3274680–3276222	Vitvi18g00300	SCL26b	—	3254592–3256064
Vitvi13g00313	LISCL7	+	3270544–3270684, 3270692–3271508, 3271694–3271929, 3271938–3272162	Vitvi04g01247	HAM3	—	18244582–18246198
Vitvi01g00446	RGA5	—	4895406–4897178	Vitvi02g00536	HAM1	+	5144861–5147299
Vitvi14g00841	RGA4	+	14807005–14808846	Vitvi15g00680	HAM2	—	14397074–14399326

Bold IDs correspond to genes which CDS structure was curated regarding v1 annotation. **Italics** indicate the gene is new when compared to v1 annotation. Genes *VviSCL3d*, *VviGRASV3a*, and *VviGRASV3b* correspond to newly detected genes compared to V1. *VviSCL3d* was already known in the 8x genome. The 14 CRIBI annotated genes with curated structure in this work are in bold.

2004). Unit B contained a putative nuclear localization signal (NLS). The canonical NLS was present in the cluster of DELLA proteins in the phylogenetic tree (**Figure 1**) though it appeared degenerated in *VviRGA3* (**Supplementary Image 1**).

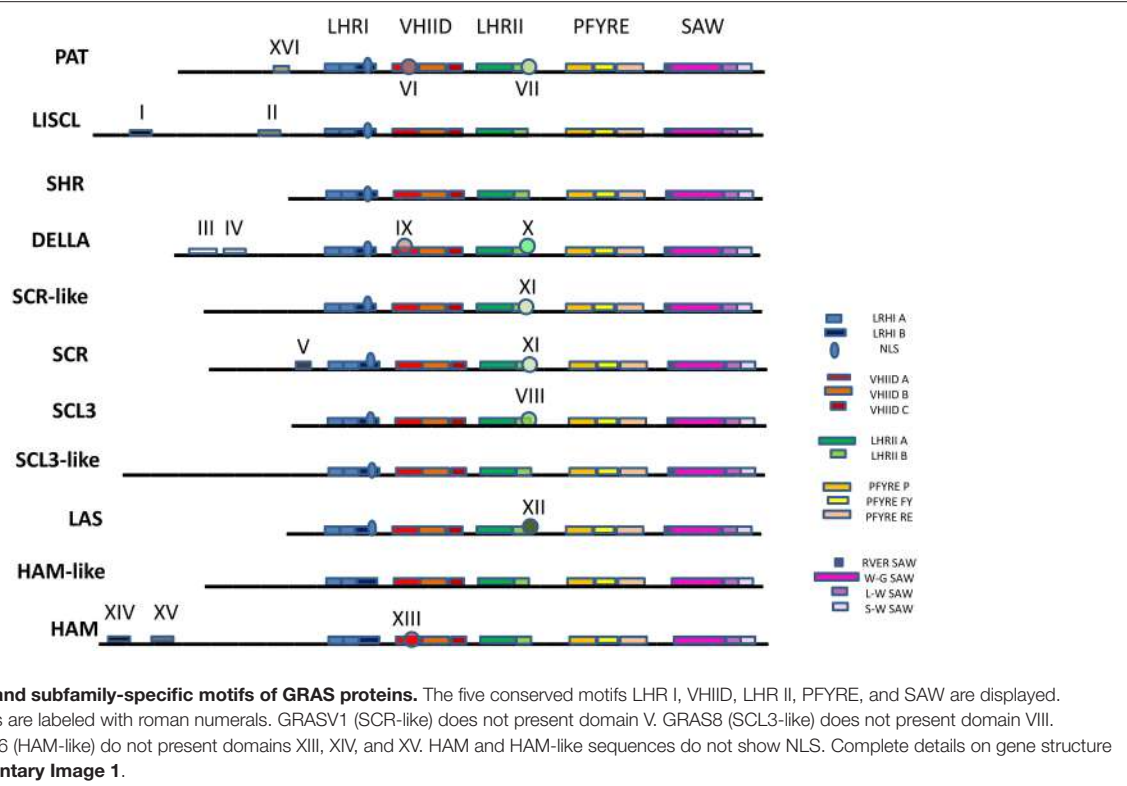
The VHIID motif contained three units (A, B, and C). GRAS proteins could be divided into several distinct groups based on conservation of Unit A. Groups such as PAT, DELLA, and HAM presented high conservation of amino acids (VI, IX, and XIII respectively, **Figure 2**). Unit B was extremely conserved and the C unit had a conserved pattern of LRITG (Pysh et al., 1999; Tian et al., 2004). The L was substituted by I or V and in the case of DELLA proteins by F unit.

The LHRII motif embraced units A and B. In Unit A, three regularly spaced leucine heptad repeats (LX6LX6L) could be found followed by several irregularly spaced leucine repeats. In Unit B, many GRAS proteins had a conserved LXXLL pattern

(DELLA, SCL3, and LS groups) as previously described (Tian et al., 2004; **Figure 2** and subgroups X, VIII, and XII). The PAT1 and SCR groups presented different conserved patterns (VII and XI).

The PFYRE motif could be divided into three units: P, FY, and RE. On the other hand, the SAW motif was composed of two units, RVER and W-W-W (**Figure 2**). RVER could be noticed in many but not all GRAS proteins. Members in the HAM subfamily lacked the RVER domain in their C-termini as well as some members of the SHR group (**Figure 2** and **Supplementary Image 1**). The W-W-W unit included three subunits: W-G, L-W, and S-W (**Figure 2**).

In the N-terminus several units were found, in accordance with previous reports (Tian et al., 2004). Units I and II of the LISCL group, units III and IV of DELLA proteins, and unit V of SCR group (**Figure 2**). Only one sequence in Arabidopsis



(AtRGL2) and its ortholog in *V. vinifera* presented domain V in the SCR group. The TVHYNP domain is characteristic of DELLA proteins (unit IV). In two *V. vinifera* sequences (VviLISCL2 and VviLISCL7) the domains I and/or II of LISCL proteins were missing due to the fact that the N-terminus is too short (**Supplementary Image 1**). The N region was much conserved in LISCL. The N-terminus of SHR proteins was also very short. Furthermore, in HAM subfamily we identified two new motifs named XIV and XV and in PAT subfamily a new motif named XVI (**Figure 2**). The consensus sequences for the new motifs are for XIV: TSVLDTRRSPSPPTSTSTSTL+SS++GGG; and for XV: ++EQS+L+WI+GDV+DPS+G; XVI: RELE+ALLGPDDDD).

Besides these eight known groups, five new additional groups were identified. A new *V. vinifera* group (formed by four proteins- VviGRAS V1a-Vd) showed similarity with SCR proteins but lacked the SCR motif (**Figures 1, 2**). This new subfamily was not present in Arabidopsis and was named GRASV1, with V for *Vitis*. However, this subfamily is apparently only absent in Arabidopsis and Brassica as observed in a comprehensive phylogenetic analysis that includes grapevine and fifteen other plant species (**Supplementary Image 2**).

A subgroup of proteins with much similarity to the SCL group did not present VIII domain including *AtGRAS8* and its ortholog in *V. vinifera* (VviGRAS8). Roman numeric nomenclature for subfamilies as used in Lu et al. (2015) was considered confounding since it was also used to label the motifs, so this subfamily was renamed as VviGRAS8, following the name of the Arabidopsis gene.

Based on the original phylogenetic analysis (**Figure 1**) we detected a third subfamily apparently related to the Arabidopsis gene *SCL26* but the broad species analysis (**Supplementary Image 2**) revealed that this subfamily should be split in 3 distinct subfamilies since only two genes were grouped with *SCL26* in the species analysis. All these proteins were also phylogenetically related to the HAM subfamily but lacking the XIII domain, a reason why they were not included in the HAM group. Furthermore, we identified GRASV2 and GRASV3 subfamilies within the HAM-like group. Both gene subfamilies had representative genes in other species (**Supplementary Image 2**).

From the alignment of predicted GRAS domain sequences we identified members containing partial GRAS domains with missing motifs (**Supplementary Image 1**). The gene *VviSCL3b* seemed severely truncated, it presented a premature stop codon lacking the motifs PFYRE and SAW). Interestingly, this gene whose predicted protein has 98 aminoacids is homologous to *SIGRAS35* which only contains 85 aminoacids Huang et al., 2015.

As mentioned previously we analyzed the orthologous relationships of GRAS genes in *V. vinifera* and other species (**Figure 3** and **Supplementary Image 2**). The orthologous relationships were classified into three categories: (i) genes present in grapevine and absent in a given species; (ii) grapevine genes showing a one-to-one relationship with one gene from a given species; (iii) grapevine genes having homologs in a given species, but without no clear putative ortholog (**Figure 3**). When grapevine genes were compared only to *Arabidopsis*, 18 genes

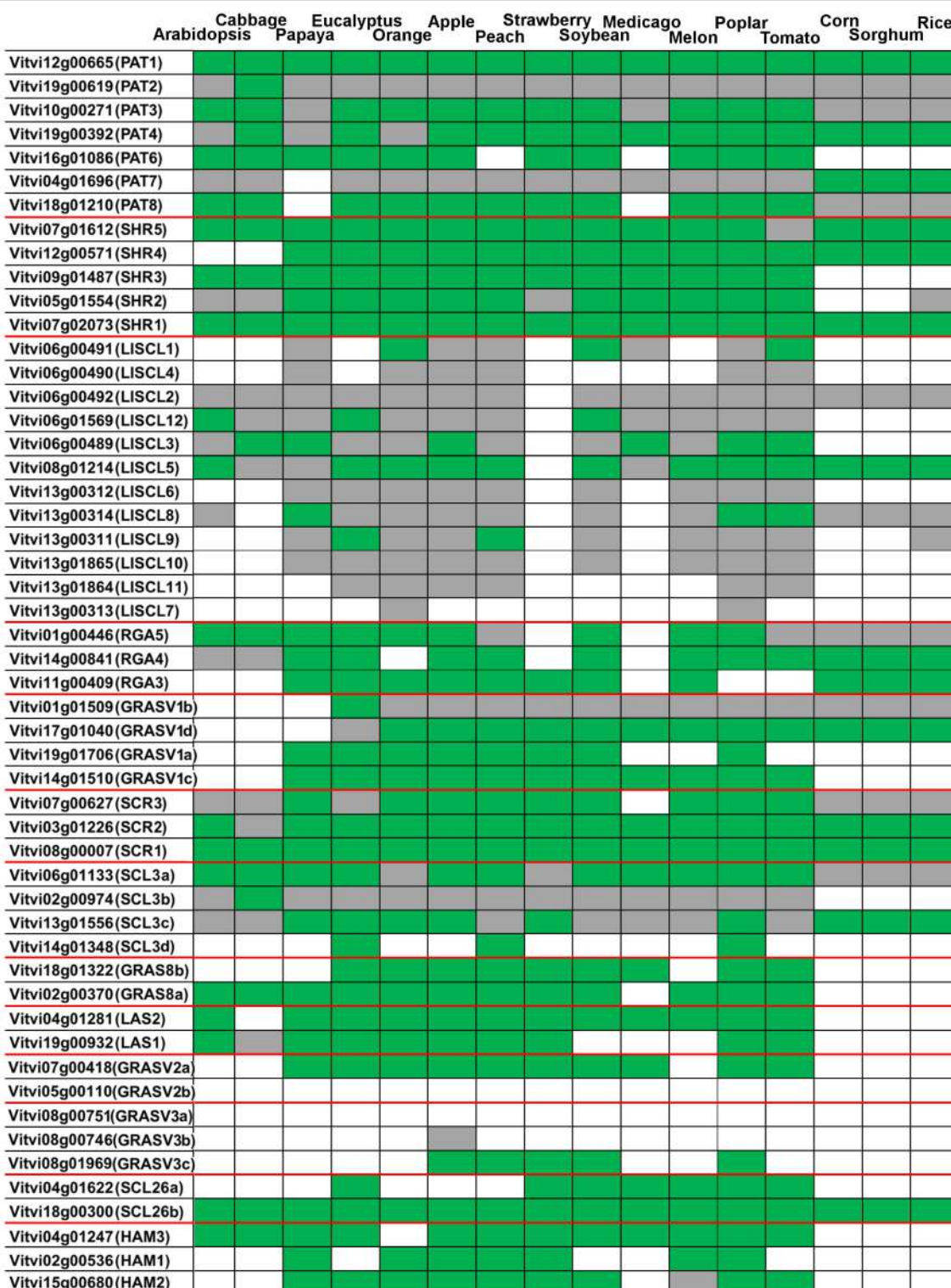


FIGURE 3 | Grapevine GRAS genes orthology against plant species with sequenced genome. Green: a one-to-one ortholog in the species (ortholog one-to-one = best match in the species that has the grapevine deduced protein as the best match in grapevine.). Gray: the grapevine deduced protein has homology in the species genome but no one-to-one ortholog was detected (the best match do not have the grapevine deduced protein as best match). White: no match in the species.

showed a one-to-one ortholog relationship with an *Arabidopsis* gene, a value slightly higher to the 15 obtained in the comparative analysis performed between *Prunus mume* and *Arabidopsis* (Lu et al., 2015). These genes likely correspond to well-conserved functions between both species. Eleven grapevine genes had homologs in *Arabidopsis* but no one-to-one relationship could be found. On the other hand, 23 genes do not have homologs in *Arabidopsis*.

A phylogenetic tree considering several mono and dicotyledonous species together with a sequence comparison were performed to identify genes with widely conserved functions among species (**Figure 3**). Genes that might represent evolutionary conserved functions were *VviPAT1*, *VviSHRI*, *VviSCR1*, and *VviSCL26g* since orthologs were found in all the species analyzed (**Figure 3**).

GRAS gene family has considerably evolved since the divergence of monocot and eudicot plants as determined by the orthologous relationship of GRAS genes in several species. The phylogenetic analysis of LISCL, HAM, PAT, and SCL groups revealed independent clusters with many members from only monocotyledonous species (**Supplementary Image 2**). On the other hand, *E. grandis* and *P. trichocarpa* putative specific subgroups were also noticed. GRAS family expanded significantly in these fast-growing woody tree species. According to Liu and Widmer (2014) there are 106 and 94 GRAS genes in *Populus* and *Eucalyptus*, respectively. In *V. vinifera* no species-specific subgroup was found.

Regarding the new *V. vinifera* subfamilies, the results indicated that group comprising *VviGRASV1a-Vd*, existed before the divergence of dicots and monocots and were lost in *Arabidopsis* and *B. rapa* (**Figure 3** and **Supplementary Image 2**). However, *VviGRASV1c* and *VviGRASV1d* did not appear in monocots.

The genes *VviGRASV2a-* and *VviGRASV3c* also presented orthologs in some species but not in *Arabidopsis* and *B. rapa*. The gene *VviGRASV2a* is homologous to two genes from tomato (**Supplementary Image 2**); therefore they may eventually play similar functional roles in fleshy fruits such as grapevine and tomato. Orthologs of *VviGRASV2a* can be found in many other species whereas for *VviGRASV2b* no ortholog was detected (**Figure 3**).

Regarding the GRAS8 subfamily, gene *VviGRAS8a* was included in a large cluster with *AtSCL28* and homologous genes in tomato and rice. It has orthologs in several species including tomato but not in rice. *VviGRAS8b* has homologs in several mono and dicotyledonous species but not in *Arabidopsis* and *B. rapa*. Orthologs were not found in *Arabidopsis* and monocots.

VviSCL26b clustered with *AtSCL26* and several other species whereas *VviSCL26a* did not have homologs/orthologs in *Arabidopsis*. As expected, since they were never described before in other species, the genes from the new families' shared little homology with genes from *Arabidopsis*.

Chromosomal Location of the GRAS Genes

GRAS genes were distributed unevenly among the nineteen chromosomes of the grapevine genome though they were mapped to all the chromosomes (**Figure 4**). The highest number

of GRAS genes was found on chr 6 and 13, with 6 and 7 genes respectively. The high number of GRAS sequences in these two chromosomes is mainly due to the presence of repeats of genes belonging to the same group (LISCL). On the other hand, chr 3, 9, 10, 11, 15, 16, and 17 only bore one gene. GRAS genes belonging to the same group were located in chromosomal regions that may represent paralogous segments resulting from ancestral polyploidization events (Jaillon et al., 2007; Velasco et al., 2007). LISCL genes were located in chr 6, 8, and 13 (although most of the LISCL in chr 13 were located just beside the presumed paralogous segment) and PAT genes located in chr 10, 12, and 19.

Concerning LISCL genes, the tandem repetition of almost identical coding sequences (e.g., *VviLISCL7* and *VviLISCL11*) suggests that these duplication events in the grapevine genome are quite recent (Licausi et al., 2010). There is also tandem repetition of genes belonging to different groups such as *VviLISCL5* and *VviGRASV3c-e* as well as *VviSCL3a*, and *VviLISCL1-4*). Interestingly, clusters in chr 6 and 13 presented similar sequence string within 4 LISCL genes followed by one SCL3.

Tandem repeats mainly in the LISCL group were also observed in *P. mume* (Lu et al., 2015).

Interestingly, the new *V. vinifera* group comprising *VviGRAS Va-Vd* was distributed in four different chromosomes (1, 14, 17, and 19). Three of them were in paralogous regions in chr 1, 14, and 17.

Therefore, segmental duplication and tandem duplications contributed significantly to the expansion and evolution of the GRAS gene family.

Expression Analysis of Grapevine GRAS Genes

Three distinct approaches were performed to characterized GRAS genes expression in grapevine. First, we constructed an atlas of expression of the GRAS genes based on the absolute value of gene expression in public data. The results of this study are presented in **Figure 5** that displays the data extracted from the published grapevine gene expression atlas (Fasoli et al., 2012). When a gene was clearly expressed in a given tissue a Plant Ontology (PO) was attributed to the gene and reported in the ORCAE database.

Second, we performed a co-expression analysis based on the same original data using the relative values of expression of all the genes, centered on the average expression. The objective here was to determine expression patterns and to identify genes that were following the same pattern of expression as the GRAS genes and that could be under the same regulatory elements, or under the regulation of the GRAS gene itself. The results are presented in **Table 2** and **Supplementary Table 2**. Nine genes showed a correlation with other genes with a Pearson Correlation Coefficient (PCC) threshold of 0.2. Finding the optimal PCC threshold to retrieve functionally related genes was affected by the method of gene expression database construction and the target gene function (Obayashi and Kinoshita, 2009), but the PCC that was chosen was very stringent.

TABLE 2 | Co-expression analysis of GRAS genes.

Unique_ID/nimblegen probeset	Functional_annotation	Functional categories
VIT_02s0025g04000	VviGRAS8a	GRAS family transcription factor
VIT_14s0068g02000	Ribonucleotide reductase R2	Nucleotide metabolism. Purine metabolism
VIT_11s0016g03750	Myb-related protein 3R-1 (Plant c-MYB-like protein 1)	Cellular process. Cell growth and death
VIT_18s0001g07550	Kinesin family member 4/7/21/27	Microtubule-driven movement
VIT_13s0064g00560	DNA topoisomerase, ATP-hydrolyzing	Nucleic acid metabolism. DNA metabolism
VIT_18s0122g00550	Cyclin-dependent kinase B2;1	Cell growth and death; Regulation of cell cycle
VIT_14s0108g00710	Chromosome condensation protein	DNA metabolism. DNA replication
VIT_11s0016g02970	MAP kinase kinase 6	Signaling pathway. Protein kinase. MAPK cascade
VIT_13s0067g03250	CENP-E like kinetochore protein	Cellular process. Cell growth and death
VIT_13s0067g01420	Cyclin 1b (CYC1b)	Cell growth and death; Regulation of cell cycle
VIT_06s0004g05870	Tubulin beta-3 chain	Microtubule organization and biogenesis
VIT_18s0001g02060	Cyclin A1	Cell growth and death; Regulation of cell cycle
VIT_07s0005g01030	Cellulose synthase CSLD5	Cell wall biosynthesis. Cellulose biosynthesis
VIT_01s0010g02430	Mitotic spindle checkpoint protein (MAD2)	MAPK cascade; Regulation of cell cycle
VIT_12s0057g00500	Thymidine kinase	Nucleotide metabolism. Pyrimidine metabolism
VIT_13s0019g02710	Rho guanyl-nucleotide exchange factor ROPGEF5	Signaling pathway. G-protein signaling pathway
VIT_04s0008g01080	Calmodulin-binding region IQD6	Calcium sensors and Signaling
VIT_14s0068g00270	Hydroxyproline-rich glycoprotein	Cell wall organization and biogenesis
VIT_10s0003g05680	CHUP1 (chloroplast unusual positioning 1)	Cytoskeleton. Actin organization and biogenesis
VIT_04s0023g01660	VviLAS2	GRAS family transcription factor
VIT_12s0059g00230	Epoxide hydrolase 2	Epoxide hydrolase family; Biotic stress response
VIT_12s0059g00220	Epoxide hydrolase	Epoxide hydrolase family; Biotic stress response
VIT_08s0007g02240	Calcium/proton exchanger CAX3	Electrochemical Potential-driven Transporters. Porters. Ca ²⁺ :Cation Antiporter
VIT_05s0020g03380	WNK1 (with no lysine (K) 1)	Signaling pathway. Circadian clock Signaling
VIT_14s0108g01420	DEFENSE NO death 1	Biotic stress response. Plant-pathogen interaction
VIT_12s0035g00970	Evolutionarily conserved C-terminal region 11 ECT11	RNA processing. mRNA processing. mRNA splicing
VIT_02s0025g04120	Calmodulin binding protein	Signaling pathway. Calcium sensors and Signaling
VIT_04s0023g01170	Unknown protein	Unknown
VIT_03s0180g00140	Acetyl xylan esterase AxeA	Unknown
VIT_10s0003g02780	Unknown protein	Unknown
VIT_05s0020g00870	UbiE/COQ5 methyltransferase	Biosynthesis of derivatives of dehydroquinic acid, shikimic acid and chorismic acid
VIT_01s0244g00140	Aspartate kinase	Amino acid. Glycine, serine, and threonine metabolism
VIT_07s0005g03700	VviSCR3	GRAS family transcription factor
VIT_15s0046g00930	Zinc finger (C3HC4-type ring finger)	Transcription factor. Zinc finger C3HC4 family transcription
VIT_07s0129g00030	VViSHR1	GRAS family transcription factor
VIT_08s0007g04820	Pectate lyase	Cell wall catabolism. Pectin catabolism
VIT_07s0129g01070	Leucine-rich repeat protein kinase	Signaling. Signaling pathway. Protein kinase
VIT_02s0025g02700	Glutaredoxin family protein	Response to stimulus. Stress response. Abiotic stress
VIT_18s0001g09920	Cyclin delta-3 (CYCD3_1)	Cytokinin-mediated Signaling pathway
VIT_12s0059g01900	Unknown protein	Unknown
VIT_01s0026g01420	Wall-associated kinase 4	Signaling. Signaling pathway. Protein kinase
VIT_01s0137g00720	Lipase GDSL	Unclear
VIT_07s0005g00740	Endo-1,4-beta-glucanase	Cell wall catabolism. Cellulose catabolism
VIT_09s0002g00450	Subtilase	Subtilase-mediated proteolysis
VIT_05s0077g02270	Unknown protein	Unknown
VIT_18s0001g07340	Aspartic proteinase nepenthesin-1 precursor	Proteolysis. Peptidase-mediated proteolysis
VIT_03s0038g02180	Glycosyl hydrolase family 10 protein	Cell wall catabolism. Xylan catabolism

(Continued)

TABLE 2 | Continued

Unique_ID/nimblegen probeset	Functional_annotation	Functional categories
VIT_14s0030g01870	NIMA protein kinase	Signaling. Signaling pathway. Protein kinase
VIT_01s0010g01660	Receptor protein kinase	Signaling. Signaling pathway. Protein kinase
VIT_08s0056g00050	VViSCR1	GRAS family transcription factor
VIT_18s0001g10380	Heat shock transcription factor B4	HSP-mediated protein folding; Temperature stress response
VIT_09s0002g01540	Unknown protein	Unknown
VIT_04s0044g01100	Invertase/pectin methylesterase inhibitor	Cell wall organization and biogenesis
VIT_11s0016g04630	VViRGA3	GRAS family transcription factor
VIT_08s0007g02760	IAA-amino acid hydrolase 1 (ILR1)	Auxin activation by conjugation hydrolysis
VIT_13s0019g01780	VViLISCL11	GRAS family transcription factor
VIT_10s0003g02350	SRG1 (senescence-related gene 1) oxidoreductase	Unclear
VIT_13s0019g01810	VViLISCL8	GRAS family transcription factor
VIT_07s0005g05640	Unknown protein	Unknown
VIT_18s0001g03310	VViSCL26b	GRAS family transcription factor
VIT_13s0067g01190	Cellulase	Cell wall catabolism. Cellulose catabolism
VIT_03s0088g00890	Pathogenesis related protein 1 precursor [<i>Vitis vinifera</i>]	Jasmonate-mediated Signaling pathway; Biotic stress response. Plant-pathogen interaction
VIT_05s0094g01310	Polygalacturonase GH28	Cell wall modification. Pectin modification
VIT_10s0092g00070	Taxane 13-alpha-hydroxylase	Diterpenoid biosynthesis
VIT_08s0105g00170	Dof zinc finger protein DOF3.5	C2C2-DOF family transcription factor
VIT_05s0124g00210	Peptidase S26A, signal peptidase I	Proteolysis. Peptidase-mediated proteolysis
VIT_05s0062g00690	Heat shock protein 81-2 (HSP81-2)	HSP-mediated protein folding; Biotic stress response. Plant-pathogen interaction
VIT_15s0021g01590	RKL1 (Receptor-like kinase 1)	Signaling. Signaling pathway. Protein kinase
VIT_03s0091g00890	Endoxylanase	Cell wall organization and biogenesis
VIT_12s0055g00980	Peroxidase precursor	Phenylalanine biosynthesis; Abiotic stress response. Oxidative stress response

The list of co-expressed genes is complete except for *VViGRAS8a* and *VViSCL26b*. Further details are presented in **Supplementary Table 2**. The list of co-expressed genes are highlighted in bold.

Third, we mined public expression data to identify the behavior of GRAS genes during berry ripening (**Figure 6**) and upon abiotic and biotic stresses (**Figures 7, 8**) not only in *V. vinifera* but also in other *Vitis* species (**Supplementary Table 3**). **Figures 6–8** presented the expression values among the experiments where difference in expression of GRAS genes was detected.

Out of the 52 genes analyzed, six were not detected in any analyzed tissue. The rest of the genes mostly showed a general pattern; they were either highly expressed or lightly expressed in all tissues considered. Nevertheless, about one third of the genes showed some tissue-specific expression. Pollen stands out as a different tissue in terms of GRAS genes expression. Differential expression of some GRAS genes among different tissues was previously shown for tomato and *Populus* (Liu and Widmer, 2014; Huang et al., 2015). Furthermore, differential expression was clearly noticed during grape ripening and stress response.

PAT Subfamily

Expression studies of *VViPAT* genes showed that most of them were expressed in all the tissues, including berry, seed, inflorescence, flower and rachis, among others (**Figure 5**). *VViPAT6* seemed to be more abundant in reproductive organs

(flower, stamen, tendril and berry). *VViPAT7* was expressed only in seedling and root. *VViPAT* genes generally seemed to respond to abiotic stress specifically *VViPAT3*, *VViPAT4*, and *VViPAT6* were up-regulated after prolonged exposure (**Figure 8**). *VViPAT3* and *VViPAT4* also seemed to respond to photoperiod and showed a stronger expression under UV light. *VViPAT4* was up-regulated in grapevine response to *Botrytis cinerea*, leaf response to powdery mildew and inflorescence response to *Bois Noir* suggesting that it could be an important regulator of biotic stress responses (**Figure 8**). *VViPAT3*, *VViPAT4*, and *VViPAT6* were expressed along grape ripening (**Figure 6**) although differences could be noticed among cultivars and ripening stages (**Supplementary Table 3**). Data on the evolution during ripening confirmed that their expression seems dependent of environmental factors since expression did not seem reproducible over the years in Pinot Noir. However, their expression clearly increased in ripe fruit suggesting that these genes might be related to ripening control.

SHR Subfamily

Concerning SHR subfamily, *VViSHR1*, *VViSHR2*, and *VViSHR3* tended to be expressed in all tissues excepted in some floral organs and pollen (**Figure 5**). *VViSHR4* and *VViSHR5* seemed to

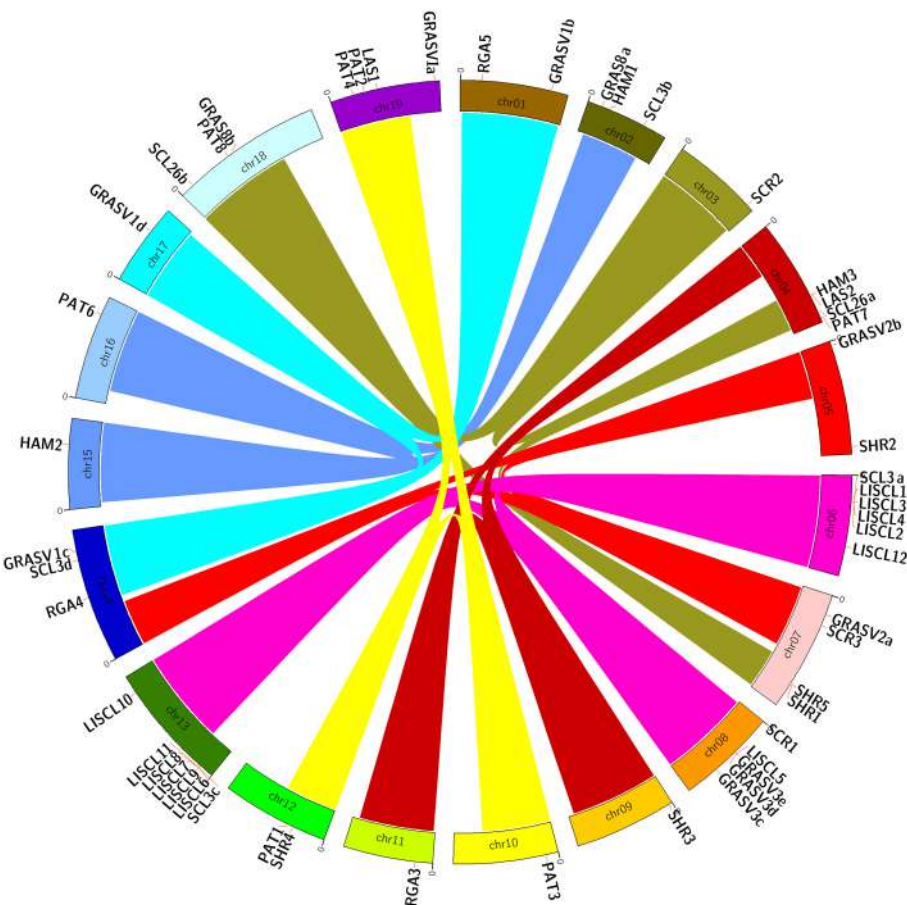


FIGURE 4 | Chromosomal location of grapevine GRAS genes. Links with the same colors in different chromosomes show paralogous regions as previously defined (Jaillon et al., 2007).

be expressed only in specific vegetative tissues. *VviSHR4* showed expression in seedling and *VviSHR2* in stem and root. *VviSHR3* showed the strongest expression in seedling, root and berry. This gene together with *VviSHR5*, an ortholog of AtSCL32, was up-regulated in berries upon *Botrytis cinerea* infection (Figure 8).

VviSHR4 responded positively to *Bois Noir* attack. *VviSHR1* was expressed in several reproductive and vegetative tissues ranging from reproductive tissues (inflorescence and carpel) to root, among others. *VviSHR1* presented co-expression with a cluster of 15 genes that included genes involved in cell wall catabolism, defense, and signaling pathways (Table 2). During ripening, its expression appeared higher during the earlier stages and seemed to be lower at *véraison*. In post-harvest berries this gene was also down-regulated.

LISCL Subfamily

Members of the LISCL subfamily showed distinctive expression patterns. *VviLISCL3*, *VviLISCL5*, *VviLISCL8*, and *VviLISCL12* were expressed in all tissues but pollen, while *VviLISCL2*, *VviLISCL7*, *VviLISCL10* were expressed in almost none tissue (Figure 5). Among them, *VviLISCL2* expression seemed

restricted to older tissues since it was only detected in post-harvest fruit, senescent leave and woody stem. The other genes presented a tissues-specific expression. Expression of *VviLISCL4* was predominant in male reproductive tissues (stamen and pollen).

VviLISCL3 and *VviLISCL12* originated from a duplication event and have high sequence similarity, which resulted in not having a specific probeset for each of them in the GeneChips array. However, their expression seemed to be affected by ripening with the lowest expression around or after *véraison* and the highest expression in ripe or overripe stages (Figure 6). They showed high expression under prolonged abiotic stress and upon virus infection, but distinction between both genes could not be made. Nevertheless, UV light surely affected their expression positively. *VviLISCL1* was also over-expressed after 16 days under water deficit and salt stress (Figure 7).

Interestingly, *VviLISCL7*, whose expression was not detected in most tissues, showed slight over-expression upon *Botrytis* infection (Figure 8). Although *VviLISCL7* presented a short N-terminal lacking domain I, it might be still functional because it looked expressed in some particular conditions, with motifs II, LHRI, VHIID, LHRII, PFYRE, SAW, and RVER (unit B of

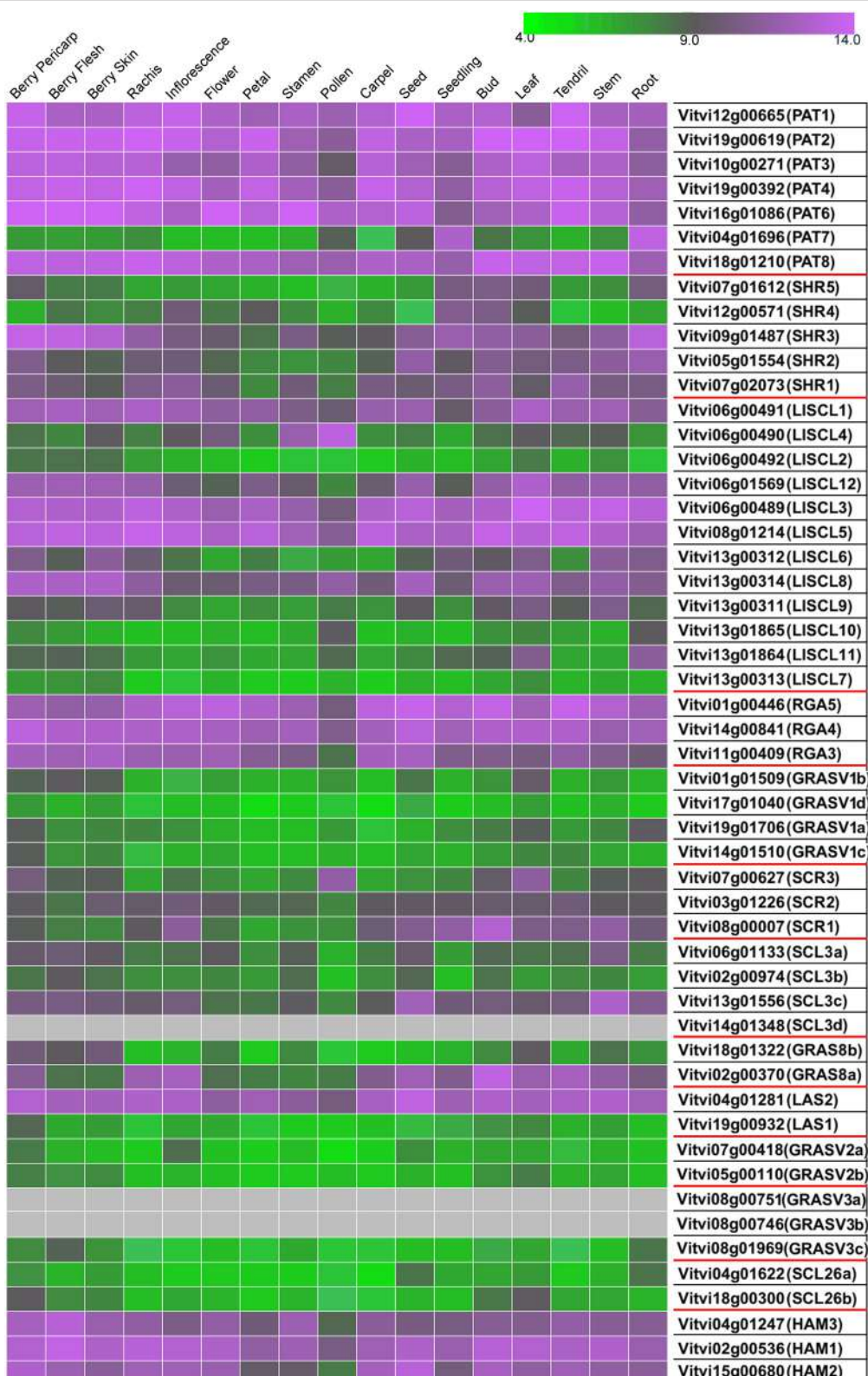
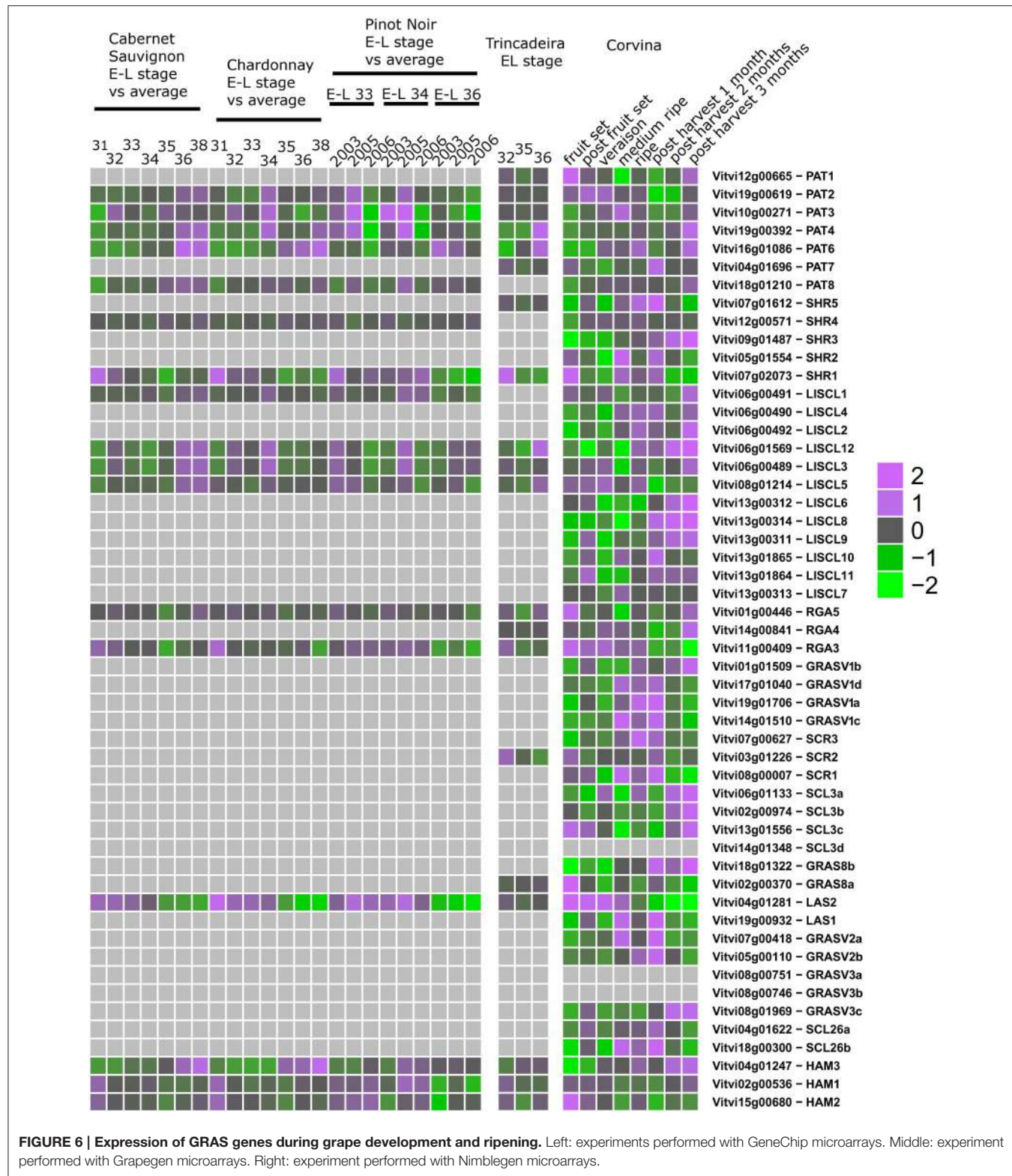


FIGURE 5 | Expression of GRAS genes in grapevine tissues. Gradient color is expressed in RMA-normalized intensity value on the Nimblegen microarray. The value for each tissue corresponds to the condition where the highest expression was reported.



LHRII was also missing). *VviLISCL2* also presented a short N-terminal lacking domain I and II; therefore some motifs may not be essential for functionality. *VviLISCL11* showed coexpression with a senescence-related gene (Table 2) and was over expressed in post-harvest berries.

DELLA Subfamily

Genes *VviRGA3*, *VviRGA4*, and *VviRGA5* were expressed in all tissues (Figure 5). *VviRGA3* and *VviRGA5* were up-regulated in the earliest stages of fruit development, at fruit set and might be involved in the transition from inflorescence to flower.



FIGURE 7 | Expression of GRAS genes upon abiotic stress. Left: experiments performed with GeneChip microarrays. Right: experiment performed with Grapegen microarrays.

VviRGA3 was also down-regulated under abiotic stresses namely salt, water stress, ABA exposure and high light (Figure 7). *VviRGA3* co-expressed with an auxin biosynthesis-related coding for gene IAA-amino acid hydrolase (Table 2), and might be a key regulator of this enzyme. Moreover, their highest expression was detected in plant tissues commonly responsible for auxin production such as seed and flower. *VviRGA5* was up-regulated in berries infected with Botrytis at green stage but its expression severely dropped at véraison so it might participate only in the early response (Figure 8).

SCR Subfamily

The gene *VviSCR3* showed peaks of expression in pollen, ripe berries and senescing leaves (Figure 5) and co-expressed with a Zinc finger transcription factor (C3HC4 family). Interestingly, *VviSCR2*, an ortholog of *AtSCL23*, was down-regulated during ripening in both Trincadeira and Corvina (Figure 6). *VviSCR1*, an ortholog of *AtRGL2*, was expressed only in some vegetative tissues (seedling, bud and stem) but was slightly up-regulated in green berries upon Botrytis infection and showed a dramatic shift of expression between véraison and medium ripe stage in

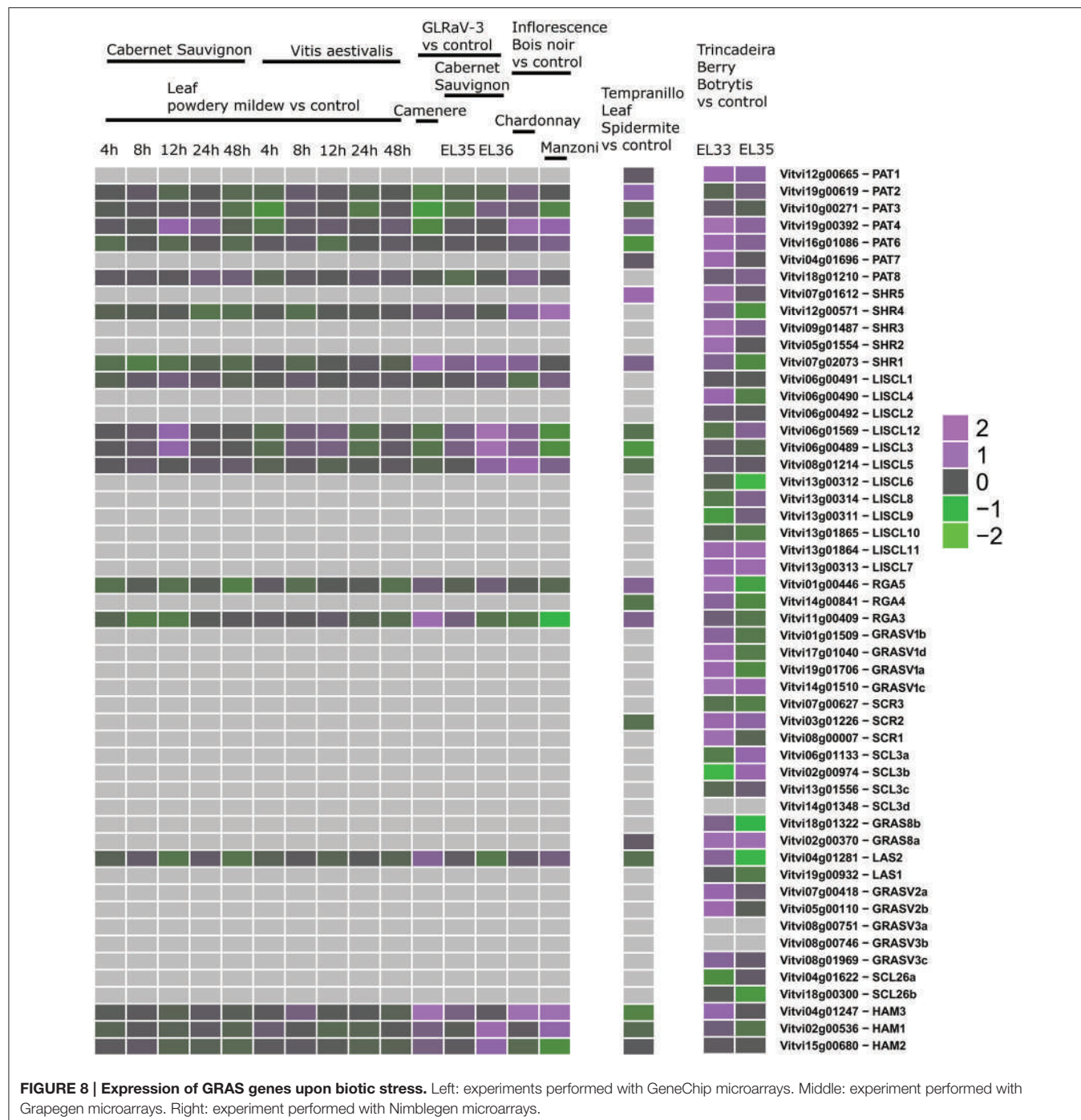


FIGURE 8 | Expression of GRAS genes upon biotic stress. Left: experiments performed with GeneChip microarrays. Middle: experiment performed with Grapegen microarrays. Right: experiment performed with Nimblegen microarrays.

Corvina. This gene co-expressed with a heat shock transcription factor and an invertase/pectin methylesterase inhibitor (**Table 2**).

SCL3 Subfamily

Three SCL3 genes (*VviSCL3a*, *VviSCL3b*, *VviSCL3c*) showed similar expression patterns (**Figure 5**). They were predominantly expressed in the stem, seed and berry flesh. Particularly, *VviSCL3c* might be involved in seed development. The three genes were also up-regulated in late post-harvest withering stages (**Figure 6**). Furthermore, *VviSCL3b* was up-regulated upon Botrytis infection

in Trincadeira grapes at *véraison* stage (**Figure 8**). No expression was found for *VviSCL3d* which only had orthologs in papaya and peach. This gene could be a pseudogene that lost its function during the evolution of the gene subfamily.

GRAS8 Subfamily

In this subfamily, *VviGRAS8a*, an ortholog of *AtSCL28/GRAS8*, exhibited detectable expression in several tissues ranging from inflorescence to tendril and stem (**Figure 5**). *VviGRAS8a* was down-regulated during grape ripening in Corvina, while no

differences were observed in Trincadeira (**Figure 6**). In a general manner, *VviGRAS8a* was more abundant in young tissues (leaf, stem, tendril, rachis, bud) with the only exception of seed. This gene was co-expressed with a large set of genes (79 genes); most of them annotated as genes involved in cell cycle, microtubule organization, nucleotide metabolism or signaling (**Table 2** and **Supplementary Table 2**). This suggests that it might play a role in cell growth and differentiation. It was also over-expressed at ripening and slightly up-regulated upon Botrytis infection in Trincadeira grapes. On the contrary, *VviGRAS8b* was expressed in older tissues (increased expression during post-harvest stages of ripening, leaf, stem, winter bud). As for *VviGRAS8a*, the exception was in the seed where no difference between young and old tissues was noticed.

LAS Subfamily

Genes *VviLAS1* and *VviLAS2* presented quite a different expression profile with *VviLAS1* not being expressed in most tissues (**Figure 5**). *VviLAS2* appeared to be more abundant at the beginning of fruit development, with consistency among varieties. *VviLAS1* was over expressed in mature berries but not in over-ripe berries (**Figure 6**). *VviLAS2* expression also decreased upon Botrytis infection (**Figure 8**) and co-expressed with 11 genes, some of them possibly involved in biotic stress response (**Table 2** and **Supplementary Table 2**).

GRASV1, GRASV2, GRASV3, and SCL26 Subfamilies

Expression of genes belonging to these new subfamilies was low. For some of them, their possible expression could not be confirmed (*VviGRASV1d*, *VviGRASV3a*, *VviGRASV3b*, although for the latter two we only had RNAseqdata for expression validation). The *VviGRASV1* genes shared a similar expression profile during Corvina ripening, peaking at the medium-ripe or ripe stage and showing expression in the first post-harvest stage (**Figure 6**). *VviGRASV2* genes also showed this profile. Interestingly, *VviGRASV1* and *VviGRASV2* genes might also play a role during Botrytis attack (**Figure 8**).

VviGRASV3c was mostly expressed in post-harvest berries. In addition, these 2 subfamilies did not show expression in other tissues, with the exception for *VviGRASV3c* in root and *VviGRASV2a* in young inflorescence.

The SCL26 genes showed a reduced expression level in various tissues. Most notably *VviSCL26b* seemed more abundant in berries at ripe stage (**Figure 6**). *VviSCL26b* co-expressed with genes involved in the pathogen response and in cell wall metabolism but the function of many of the co-expressed genes was unknown (**Table 2**, **Supplementary Table 2**). The expression profile of these genes was intriguing since little consistency was observed among replicates of the same condition. This inconsistency might be caused by a response to unidentified factors during sampling, which appears in experiments performed by independent laboratories.

HAM Subfamily

This subfamily is present in all tissues with notable lower values in pollen (**Figure 5**). *VviHAM3* was up-regulated during ripening, upon *Bois Noir* attacks, and in response to drought in the

seed and shoot tip (**Figures 6–8**). *VviHAM1* and *VviHAM2* were down-regulated in all the cultivars during ripening; they might play a role in early stages of fruit development.

DISCUSSION

The availability of sequenced genomes, expression data and associated bioinformatics tools enable the study of the genomic information to predict the putative function of a gene family in developmental processes and in stress response. In general, transcription regulators belonging to the same taxonomic group exhibit common evolutionary origins and specific conserved motifs related to molecular functions, making their genome-wide analysis an effective and practical method to predict unknown protein functions.

We have performed an exhaustive analysis of GRAS genes on the 12x grapevine genome sequence based on the isolation of the complete set of genes identified in PN40024. Chromosome localization, gene structure analyses, phylogenetic analyses with other genome sequenced species and expression analysis allowed to propose an extended characterization of the GRAS gene family in grapevine and to draw hypotheses on the function of newly described genes.

Expansion of GRAS Family in Grapevine

The grapevine GRAS gene family was greatly expanded by segment/chromosomal duplications as it occurred in other species belonging to different taxonomic groups (Liu and Widmer, 2014; Huang et al., 2015; Lu et al., 2015). Duplicated genes might show functional redundancy and their identification may contribute to decipher gene functions, the evolutionary consequences of gene duplication and their contribution to evolutionary change. Duplicated genes face one of these fates: nonfunctionalization, neofunctionalization (evolving novel functions), or subfunctionalization (partition of gene functions; Prince and Pickett, 2002). The process of non-functionalization can occur when a redundant gene degenerates to a pseudogene or is lost from the genome due to the vagaries of chromosomal remodeling, locus deletion or point mutation (Prince and Pickett, 2002). Likely candidate pseudogenes are some of the outliers in our sequence alignments such as gene *VviSCL3b* which presents only 294 nucleotides and a premature stop codon and lacks motifs PFYRE and SAW. Interestingly, this gene showed an ortholog only in cabbage (**Figure 3**). However, this gene was found to be expressed suggesting that it could still maintain some functionality. No expression was found for *VviSCL3d* which may also be a pseudogene that lost its function during the evolution of the gene family.

We have also identified duplicated grapevine genes such as *VviLISCL7* and *VviLISCL11* whose expression analysis with specific probes might indicate they have evolved into distinct functions. Expression divergence in duplicated GRAS gene was previously detected in several plant species (Wu et al., 2014). Furthermore, no GRAS genes were coexpressed together, reflecting a wide diversity of the functions, or specialization. Unlike other species, tandem duplication events in grapevine seemed mainly restricted to the LISCL subfamily which

contained tandem repeated genes with the highest homology. However, other genes from specific subfamilies were in paralogous areas of the genome resulting from polyploidization event (Jaillon et al., 2007). Amongst them, the PAT subfamily had members in chr 10, 12, and 19 (**Figure 4**), GRASV1 in chr 1, 14, and 17, LISCL in chr 6, 8, 10, and GRASV2 in chr 5 and 7 (only two genes). Although *V. vinifera* has a smaller size genome than *S. lycopersicum* (487 and 760 Mb, respectively), it contained a similar number of GRAS genes (52 and 53 genes, respectively). In addition, *P. mume* with a genome size of 280 Mb, almost half the size of the *V. vinifera* genome, contained 46 GRAS genes, a close number to the 52 *V. vinifera* genes (Lu et al., 2015). Therefore, the density of GRAS genes varies greatly among plant species (Song et al., 2014; Huang et al., 2015; Lu et al., 2015).

The exon-intron organization analysis showed that 88.46% (46 out of 52) of *VviGRAS* genes were intronless in grapevine, the highest percentage found so far, though similar to *P. mume* (82.2%) (Lu et al., 2015). Interestingly, this percentage is much smaller in *Populus* (54.7%) where the GRAS family greatly expanded (Liu and Widmer, 2014). Horizontal gene transfer of plant GRAS genes that originated from prokaryotic genomes has been proposed (Zhang et al., 2012). This prokaryotic origin followed by extensive duplication events in their evolutionary history might explain the abundance of intronless genes within the GRAS gene family. The grapevine GRAS genes also exhibited a highly variable N-terminal domain, as in other species, indicating the functional versatility of this gene family in grapevine. By contrast, highly conserved C-terminal domains (GRAS domain) were observed in all non-truncated proteins.

GRAS Family Members are Putatively Involved in Grapevine Development and Defense

Expression Patterns across a Variety of Tissues Revealed Divergent Functions

GRAS genes showed broad expression patterns across a variety of tissues, as previously observed in *Populus* and *P. mume* (Liu and Widmer, 2014; Lu et al., 2015). For example, *VviSCR1* was highly expressed in the bud whereas the other *VviSCR* genes were not detected in this tissue. In Arabidopsis, *SCR* was located downstream of *SHR*, and both genes were required for stem cell maintenance of the root meristem to ensure its indeterminate growth (Lee et al., 2008). In *V. vinifera*, *VviSHR3* was the gene from SCR and SHR subfamilies presenting highest expression in the root. Its tomato ortholog (*SIGRAS16*) also displayed its highest expression in the root comparing to several tissues and organs tested and was also predicted to be involved in root development (Huang et al., 2015).

VviSCR1, ortholog of *AtSCR*, co-expressed with an invertase/pectin methylesterase inhibitor putatively involved in cell wall organization and biogenesis. *VviSHR1* was expressed in several reproductive and vegetative tissues and was co-expressed with a cluster of genes putatively involved in cell wall biogenesis (pectate lyase, endo-1,4-beta-glucanase, glycosyl hydrolase family 10 protein) and signaling mechanisms (leucine-rich repeat protein kinase, receptor protein kinase, wall-associated

kinase 4). Previous analysis of a short-root (*shr*) mutant showed that the AtSHR protein is also involved in root and shoot radial patterning (Helariutta et al., 2000). These transcription factors are likely to play a role in cell wall reorganization and signaling events during cell growth and differentiation in grapevine. *SHR* and *SCR* were referred to be expressed in leaves, in young leaf primordia, in developing leaf vascular tissue, and bundle sheet cells (reviewed by Bolle, 2016). Recently, *AtSHR*, *AtSCR*, and *AtSCL23* were described to control bundle sheath cell fate and function in *A. thaliana* and this developmental pathway seemed to be evolutionarily conserved (Cui et al., 2014). *AtSCR* was identified as primarily involved in sugar transport whereas *AtSCL23* might play a role in mineral transport. Their expression seemed regulated by *SHR* protein. Their orthologs in *V. vinifera* (*VviSHR1*, *VviSCR1*, and *VviSCR2*, respectively) might play similar cellular functions. The tomato genes *SIGRAS25* and *SIGRAS15* (respective orthologs of *VviSHR1* and *VviSCR1*) in addition to *SIGRAS39*, ortholog of another *SHR* gene, *VviSHR2*, showed high mRNA expression levels in root and stem (Huang et al., 2015), suggesting conserved functions with their homologous gene *AtSHR* (Cui et al., 2007), and *AtSCR* (Helariutta et al., 2000) which are involved in root and shoot radial patterning in *Arabidopsis*. These genes had orthologs in most species (**Figure 3**) indicating that their function might also be conserved in grapevine.

GRAS proteins have also been involved in axillary meristem development. Knock-out *Arabidopsis* plants for *AtLAS/SCL18* are unable to form lateral shoots during vegetative development (Greb et al., 2003). In tomato, mutant plants for the ortholog lateral suppressor (*LeLs*) were blocked in the initiation of axillary meristems and showed lower number of flowers per inflorescence, absence of petals, reduced fertility, and altered hormone levels (Schumacher et al., 1999). The grapevine ortholog (*VviLAS1*) was not expressed in most tissues, except for berry pericarp, mature berry and leaf; however the other member of this subfamily, *VviLAS2*, showed tissue expression that could be more in accordance to the role described for *LeLs*. The ortholog of *VviLAS2* in tomato (*GRAS17*) is also differentially expressed from mature green stage fruits to breaker stage fruits (Huang et al., 2015).

In grapevine, *VviHAM1* is strongly expressed during fruit set and in several tissues such as bud, leaf, and stem. In the petunia mutant hairy meristem (ham) shoot apical meristems fail to retain their undifferentiated character (Stuurman et al., 2002). In *Arabidopsis*, the GRAS proteins from the HAM branch (*SCL6*, 22, and 27) are also involved in leaf development (Wang et al., 2010). *VviHAM1* may be involved in the regulation of meristematic activity in growing tissues.

Many *VviPAT* genes showed expression in a wide range of tissues and might be involved in several developmental processes, through the regulation of phytochrome signaling mechanisms, as in *Arabidopsis* (Bolle, 2004, 2016). PAT genes *PAT1*, *SCL5*, *SCL21* are positive regulators of phytochrome-A signal transduction while *SCL13* is mainly involved in phytochrome-B signal transduction (Bolle et al., 2000; Torres-Galea et al., 2006, 2013). The grapevine PAT subfamily showed the weakest expression in the less photosynthetic tissues (pollen,

roots), with the exception of *VviPAT7* that displayed an opposite expression profile. *VviPAT7* was also one of the few PAT genes with no orthology in other species, except in monocots.

DELLA genes presented a wide range of expression patterns among tissues consistent with their role as negative regulators of gibberellin signal transduction (Peng et al., 1997; Silverstone et al., 1998; Zentella et al., 2007). They interfere with a variety of growth and developmental processes such as stem elongation, flower development, and seed germination (Bolle, 2004). In addition, DELLA proteins integrate not only gibberellin-signaling pathways but also jasmonate, auxin, brassinosteroid, and ethylene pathways, constituting a main signaling hub (Wild et al., 2012; Bolle, 2016). *VviRGA5*, a one-to-one ortholog of *AtRGA/AtGAI*, was highly expressed in seed, flower and stem supporting a role in developmental processes.

The rice DLT gene modulates brassinosteroid-related gene expression (Tong et al., 2009). The homologous gene in Arabidopsis is *AtSCL28* and in *V. vinifera* *VviGRAS8a*. Interestingly, this gene co-expressed with a large set of genes involved in cell cycle, nucleotide metabolism or signaling. In general, the transcripts of this gene were more abundant in young tissues (leaves, stem tendril, rachis, bud) and in inflorescence which is not surprising since brassinosteroids promote growth (reviewed by Fortes et al., 2015). The tomato ortholog *SIGRAS41* was suggested to be involved in flower-fruit transition with a potential role in fruit development by modulating brassinosteroid signaling (Huang et al., 2015). A role that is likely to be played by *VviGRAS8a* in grapevine eventually through an involvement in mechanisms of cell division and differentiation.

As previously mentioned, expression of GRAS genes in pollen tissue differed from other tissues. *VviLISCL4* was almost specifically expressed in the stamen and particularly in pollen. Interestingly, a *LISCL* gene has been shown to be involved in transcriptional regulation during microsporogenesis in the lily anther (Morohashi et al., 2003). Future functional analysis of *VviLISCL4* gene during pollen development is required to confirm the importance of this GRAS gene in grapevine reproduction.

Several GRAS genes (*VviLISCL2*, *VviGRASV2b*) showed higher expression in senescent tissues (senescent leaves, woody stem, post-harvest berries) than in younger tissues, including ripe/mature tissues. In this way, a wheat *LISCL* gene, *TaSCL14*, was identified as promoting senescence in leaves (Chen et al., 2015). *VviGRASV2b* seemed completely grapevine-specific and its potential involvement in senescence has yet to be clarified.

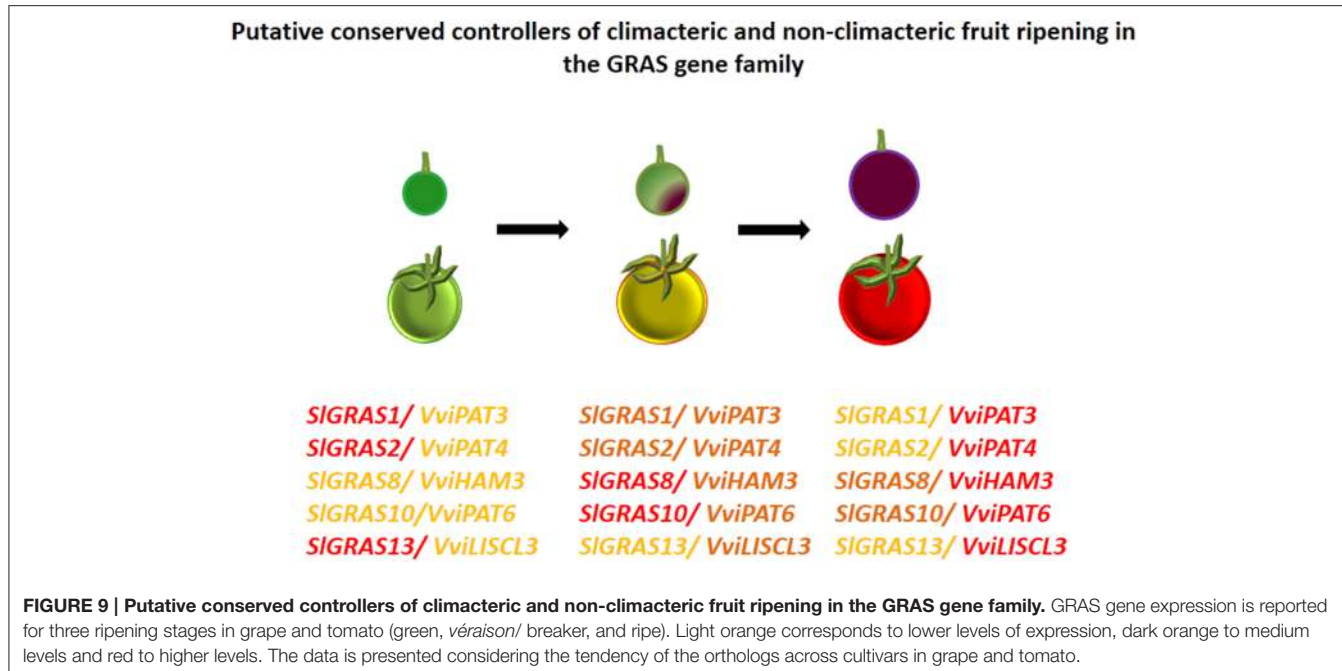
GRAS are Likely to Play a Role in Berry Development and Ripening

Several grapevine GRAS genes showed differential expression among berry ripening stages (Fortes et al., 2011; Agudelo-Romero et al., 2013) namely *VviLISCL3/12*, *VviLISCL11*, *VviPAT3*, *VviPAT4*, *VviPAT6*, *VviSCR3*, *VviGRAS8b*, *VviLAS1*, *VviHAM3*, *VviSCL26b* (up-regulated), *VviHAM1*, *VviHAM2*, *VviRGA3*, *VviSHR1*, *VviLAS2* (down-regulated). Genes *VviHAM1*, *VviHAM2*, *VviRGA3*, *VviSHR1*, and *VviLAS2* seemed to be involved in fruit set and in the early stages of fruit

development when there is intense cell division activity and sugar transport. During these stages, the levels of phytohormones such as auxins, cytokins, gibberellins, and jasmonic acid also peaked (reviewed by Fortes et al., 2015), that might be related to the up-regulation of *RGA3* since DELLA proteins integrate several phytohormone-signaling pathways (Bolle, 2016). Furthermore, *RGA3* co-expressed with a gene coding for IAA-amino acid hydrolase 1 involved in auxin metabolism (auxin activation by conjugation hydrolysis) supporting the role of *VviRGA3* in hormonal regulation.

VviLISCL3/VviLISCL12, *VviPAT4*, *VviPAT6*, and *VviHAM3* were up-regulated at mature stages (ripe, harvest, and post-harvest) whereas *VviSCR3* was up-regulated in medium ripe and ripe berries and co-expressed with a gene coding for a Zinc finger protein (C3HC4-type ring finger). These transcription factors have been previously described as being modulated during grape ripening (Fortes et al., 2011). *VviGRAS8b* was over-expressed at post-harvest stages and *VviLAS1* and *VviSCL26b* at medium ripe, ripe and initial post-harvest stage. The gene *VviSCL26b* co-expressed with genes involved in pathogen response (pathogenesis related protein 1 precursor, heat shock protein 81-2, peroxidase precursor) and cell wall metabolism (endoxyylanase, polygalacturonase GH28, cellulase). This could be associated to the activation of genes that are related to biotic stress response as well as cell wall rearrangements taking place during grape ripening (Fortes et al., 2011). *VviLISCL11* was over expressed in post-harvest berries and might be linked to the regulation of cell wall degradation processes. In agreement with this hypothesis, it was co-expressed with a senescence related gene.

Altogether, these observations could suggest the relevance of GRAS genes as regulators of the different stages of grape berry development. GRAS transcription factors have been previously associated with the control of tomato fruit ripening (Fujisawa et al., 2012). Authors suggested that *SIGRAS38* gene could play a role in fruit ripening due to its ripening-specific expression and direct transcriptional regulation by RIN. In tomato, a typical climacteric fruit, the MADS-box transcription factor RIN is one of the earliest-acting ripening regulators, required for both ethylene-dependent and ethylene-independent pathways. By contrast, *VviSH4*, the grapevine ortholog of *SIGRAS38*, did not seem to be involved in grapevine ripening. Since grape is a non-climacteric fruit in which ethylene does not play a central role in the regulation of ripening (reviewed by Fortes et al., 2015), a different transcriptional regulatory pathway of ripening could be expected. Still, common aspects between ripening pathways in both type of fruits can be observed. Grapevine *VviPAT3*, *VviPAT4*, and *VviPAT6* have expression patterns consistent with their involvement in berry ripening and their tomato orthologs, *SIGRAS1*, *SIGRAS2*, and *SIGRAS10* (respectively) were differentially expressed from mature green stage fruits to breaker stage fruits (Huang et al., 2015). The same holds true for *VviHAM3* and its tomato ortholog *SIGRAS8* as well as *VviLISCL3* and its ortholog *SIGRAS13* (Huang et al., 2015). Therefore, these grapevine GRAS genes (**Figure 9**) could likely be conserved and represent pivotal transcriptional regulators of fruit ripening in both climacteric and non-climacteric species.



Grapevine GRAS Genes are Putatively Involved in Stress and Defense Responses

Several GRAS proteins have been associated with a role in stress signaling (reviewed by Bolle, 2016). Arabidopsis *scr* and *shr* loss of function mutants were found to be hypersensitive to abscisic acid (ABA) and to high levels of glucose but were not affected by high salinity or osmotic stress (Cui, 2012). In grapevine *VviSHR1* expression seemed to be affected by ABA but not by salt (Figure 7). Interestingly, expression of *VviSHR1* decreased during grape ripening when glucose levels significantly increased. Moreover, *VviSHR1* may be involved in grapevine response against virus whereas *VviSCR1* was up-regulated in green berries upon Botrytis infection. In fact, GRAS genes seem to be expressed upon abiotic and biotic factors (reviewed by Bolle, 2016). Furthermore, *VviSHR1* co-expressed with genes involved in stress response (glutaredoxin family protein, subtilase). A poplar GRAS gene showing the highest identity to Arabidopsis *SCL7*, conferred salt and drought tolerance to this plant (Ma et al., 2010). The duplicated gene of *AtSCL7*, *AtSCL4*, is orthologous of the grapevine *VviLAS2* which was down-regulated in response to salt but up-regulated upon UV light and long day exposure. *VviLAS2* expression also decreased upon Botrytis and co-expressed with up to 11 genes possibly involved in biotic stress response (epoxide hydrolase 2, DEFENSE NO death 1). *VviLAS2* might be a negative regulator of expression of these genes.

Other grapevine GRAS genes were found to show differential stress responses. *VviRGA5* was recently shown to be up-regulated in grape berries at initial stage of fungal infection (Agudelo-Romero et al., 2015) and *VviRGA3* was down-regulated under abiotic stresses such as salt, water stress, ABA exposure, and high light. Inhibition of growth by DELLA subfamily genes has been proposed as a response to environmental variability (Harberd

et al., 2009) so these transcription factors may play an important role in the regulation of abiotic and biotic stress response pathways by regulating growth. Furthermore, DELLA proteins control plant immune responses by modulating the balance of jasmonic acid and salicylic acid signaling (Navarro et al., 2008; Wild et al., 2012), growth regulators which involvement in stress responses is well-known.

The Arabidopsis GRAS protein *SCL14* was shown to be essential for the activation of stress-inducible promoters (Fode et al., 2008). The closest grapevine homologs are *VviLISCL12* and *VviLISCL3* that were also up-regulated after biotic stress. *VviLISCL12* was recently shown to be up-regulated upon guazatine treatment, an inhibitor of polyamine catabolism (Agudelo-Romero et al., 2014). In rice, *OsGRAS2*, the ortholog of *AtSCL14* is involved in the regulation of drought stress response (Xu et al., 2015). Other grapevine *LISCL* genes could likely be involved in abiotic stress response namely *VviLISCL1* which was over-expressed after long exposure to water deficit and salt stress (Figure 7).

The *Brassica oleracea* gene *BoGRAS*, was up-regulated under heat stress (Park et al., 2013) and its grapevine ortholog, *VviPAT3*, was also over-expressed during biotic stress. The ortholog of *VviPAT3* in tomato, *SiGRAS1*, was also referred to be involved in biotic stress response (Mayrose et al., 2006). Moreover, *VviPAT4* might be a good candidate in regulating abiotic and biotic stress responses in grapevine since it was up-regulated under both conditions. In tomato *SiGRAS2*, the *VviPAT4* ortholog, was involved in hormone signaling and abiotic stress response (Huang et al., 2015). *VviHAM3* was also up-regulated during ripening, upon *Bois Noir* attacks, and in response to drought in the seed and shoot tip. Therefore, *VviHAM3* exhibited expression patterns that indicate a role in broad stress responses.

Altogether, the expression of several grapevine *GRAS* genes in response to several stress treatments highlights the wide involvement of this gene family in environmental adaptation, showing diverse responses under different environmental conditions and treatments (Huang et al., 2015). The same results were observed in tomato for the expression of many *SIGRAS* genes.

CONCLUSIONS

GRAS transcription factors have been characterized in several species and were proven to be involved in diverse developmental processes and stress responses. However, their involvement in fruit ripening is only now starting to be disclosed. Grape berry development and ripening could be under control of *GRAS* genes, since the expression of many of them is modulated during this process. The involvement of grapevine *GRAS* genes in stress responses was also confirmed in this study. Both ripening and stress responses involved genes from new *GRAS* subfamilies identified in grapevine (GRASV1, GRASV2, GRASV3, SCL26, and GRAS8). Robust candidates for further functional analysis were established and compared with the results of a similar analysis recently performed in tomato, another fleshy fruit. Altogether this data may contribute to the improvement of fruit quality and resilience to biotic and abiotic stresses.

AUTHOR CONTRIBUTIONS

AF and JG designed the study. JG, PA, RT, and AF analyzed the data. AF wrote the manuscript with valuable input from JG and JM. All the authors revised and approved the manuscript.

REFERENCES

- Agudelo-Romero, P., Ali, K., Choi, Y. H., Sousa, L., Verpoorte, R., Tiburcio, A. F., et al. (2014). Perturbation of polyamine catabolism affects grape ripening of *Vitis vinifera* cv. *Trincadeira*. *Plant Physiol. Biochem.* 74, 141–155. doi: 10.1016/j.plaphy.2013.11.002
- Agudelo-Romero, P., Erban, A., Rego, C., Carbonell-Bejerano, P., Nascimento, T., Sousa, L., et al. (2015). Transcriptome and metabolome reprogramming in *Vitis vinifera* cv. *Trincadeira* berries upon infection with *Botrytis cinerea*. *J. Exp. Bot.* 66, 1769–1785. doi: 10.1093/jxb/eru517
- Agudelo-Romero, P., Erban, A., Sousa, L., Pais, M. S., Kopka, J., and Fortes, A. M. (2013). Search for transcriptional and metabolic markers of grape pre-ripening and ripening and insights into specific aroma development in three Portuguese cultivars. *PLoS ONE* 8:e60422. doi: 10.1371/journal.pone.0060422
- Albertazzi, G., Milc, J., Caffagni, A., Francia, E., Roncaglia, E., Ferrari, F., et al. (2009). Gene expression in grapevine cultivars in response to Bois Noir phytoplasma infection. *Plant Sci.* 176, 792–804. doi: 10.1016/j.plantsci.2009.03.001
- Bolle, C. (2004). The role of *GRAS* proteins in plant signal transduction and development. *Planta* 218, 683–692. doi: 10.1007/s00425-004-1203-z
- Bolle, C. (2016). “Functional aspects of *GRAS* family proteins,” in *Plant Transcription Factors, Evolutionary, Structural, and Functional Aspects*, ed D. H. Gonzalez (Cambridge: Elsevier), 295–311.
- Bolle, C., Koncz, C., and Chua, N. H. (2000). PAT1, a new member of the *GRAS* family, is involved in phytochrome A signal transduction. *Genes Dev.* 14, 1269–1278. doi: 10.1101/gad.14.10.1269
- Carbonell-Bejerano, P., Santa Maria, E., Torres-Perez, R., Royo, C., Lijavetzky, D., Bravo, G., et al. (2013). Thermotolerance responses in ripening berries of *Vitis vinifera* L. cv *Muscat Hamburg*. *Plant Cell Physiol.* 54, 1200–1216. doi: 10.1093/pcp/pct071
- Carvalho, L. C., Vilela, B. J., Mullineaux, P. M., and Amancio, S. (2011). Comparative transcriptomic profiling of *Vitis vinifera* under high light using a custom-made array and the Affymetrix GeneChip. *Mol. Plant* 4, 1038–1051. doi: 10.1093/mp/ssr027
- Chen, K., Li, H., Chen, Y., Zheng, Q., Li, B., and Li, Z. (2015). TaSCL14, a novel wheat (*Triticum aestivum* L.) *GRAS* gene, regulates plant growth, photosynthesis, tolerance to photooxidative stress, and senescence. *J. Genet. Genomics* 42, 21–32. doi: 10.1016/j.jgg.2014.11.002
- Cramer, G. R., Ergul, A., Grimplet, J., Tillett, R. L., Tattersall, E. A., Bohlman, M. C., et al. (2007). Water and salinity stress in grapevines: early and late changes in transcript and metabolite profiles. *Funct. Integr. Genomics* 7, 111–134. doi: 10.1007/s10142-006-0039-y
- Cui, H. (2012). Killing two birds with one stone: transcriptional regulators coordinate development and stress responses in plants. *Plant Signal. Behav.* 7, 701–703. doi: 10.4161/psb.20283
- Cui, H., Kong, D., Liu, X., and Hao, Y. (2014). SCARECROW, SCR-LIKE 23 and SHORT-ROOT control bundle sheath cell fate and function in *Arabidopsis thaliana*. *Plant J.* 78, 319–327. doi: 10.1111/tpj.12470
- Cui, H., Levesque, M. P., Vernoux, T., Jung, J. W., Paquette, A. J., Gallagher, K. L., et al. (2007). An evolutionarily conserved mechanism delimiting SHR movement defines a single layer of endodermis in plants. *Science* 316, 421–425. doi: 10.1126/science.1139531

ACKNOWLEDGMENTS

Funding was provided by the Portuguese Foundation for Science and Technology (SFRH/BPD/100928/2014, UID/MULTI/04046/2013 and PEst-OE/BIA/UI4046/2014) and is integrated in the COST (European Cooperation in Science and Technology) Action FA1106 “Quality fruit.” JG was supported by the Ramon y Cajal program (RYC-2011-07791) and the AGL2014-59171-R project from the Spanish MINECO.

SUPPLEMENTARY MATERIAL

The Supplementary Material for this article can be found online at: <http://journal.frontiersin.org/article/10.3389/fpls.2016.00353>

Supplementary Image 1 | Structure and subfamily-specific motifs of *GRAS* proteins. The size varies within the subfamily. Several proteins such as VviSCL2 and VviSCL7 present shorter N-terminal sequences. The protein VviSCL3b lacks the motifs PFYRE and SAW.

Supplementary Image 2 | Molecular phylogenetic analysis by Maximum Likelihood method between Grapevine and 15 plant species.

Lineage-specific groups can be noticed for *Populus* and *Eucalyptus* whereas *Arabidopsis* putatively lacks specific subgroups.

Supplementary Table 1 | Complete annotation of the grapevine *GRAS* genes. Alternative Names correspond to previous annotation (8X and 12X0). The probesets ID for microarray platform are given for Genechips, Grapegen and Nimblegen. The Nimblegen ID is also the 12Xv1 ID.IEP: evidence code inferred by expression pattern. Positions are given for both the 12X v1 and v2 genome.

Supplementary Table 2 | List of genes co-expressed with *GRAS* genes. *GRAS* genes are highlighted in yellow.

Supplementary Table 3 | *GRAS* genes expression in experiments related to ripening, abiotic stress and biotic stress.

- Day, R. B., Tanabe, S., Koshioka, M., Mitsui, T., Itoh, H., Ueguchi-Tanaka, M., et al. (2004). Two rice GRAS family genes responsive to N-acetylchitooligosaccharide elicitor are induced by phytoactive gibberellins: evidence for cross-talk between elicitor and gibberellin signaling in rice cells. *Plant Mol. Biol.* 54, 261–272. doi: 10.1023/B:PLAN.0000028792.72343.ee
- Deluc, L. G., Grimplet, J., Wheatley, M. D., Tillett, R. L., Quilici, D. R., Osborne, C., et al. (2007). Transcriptomic and metabolite analyses of Cabernet Sauvignon grape berry development. *BMC Genomics* 8:429. doi: 10.1186/1471-2164-8-429
- Diaz-Riquelme, J., Grimplet, J., Martinez-Zapater, J. M., and Carmona, M. J. (2012). Transcriptome variation along bud development in grapevine (*Vitis vinifera* L.). *BMC Plant Biol.* 12:181. doi: 10.1186/1471-2229-12-181
- Edgar, R. C. (2004). MUSCLE: multiple sequence alignment with high accuracy and high throughput. *Nucleic Acids Res.* 32, 1792–1797. doi: 10.1093/nar/gkh340
- Espinosa, C., Vega, A., Medina, C., Schlauch, K., Cramer, G., and Arce-Johnson, P. (2007). Gene expression associated with compatible viral diseases in grapevine cultivars. *Funct. Integr. Genomics* 7, 95–110. doi: 10.1007/s10142-006-0031-6
- Fasoli, M., Dal Santo, S., Zenoni, S., Tornielli, G. B., Farina, L., Zamboni, A., et al. (2012). The grapevine expression atlas reveals a deep transcriptome shift driving the entire plant into a maturation program. *Plant Cell* 24, 3489–3505. doi: 10.1105/tpc.112.100230
- Felsenstein, J. (1985). Confidence limits on phylogenies: an approach using the bootstrap. *Evolution* 39, 783–791. doi: 10.2307/2408678
- Fode, B., Siemsen, T., Thurow, C., Weigel, R., and Gatz, C. (2008). The Arabidopsis GRAS protein SCL14 interacts with class II TGA transcription factors and is essential for the activation of stress-inducible promoters. *Plant Cell* 20, 3122–3135. doi: 10.1105/tpc.108.058974
- Fortes, A. M., Agudelo-Romero, P., Silva, M. S., Ali, K., Sousa, L., Maltese, F., et al. (2011). Transcript and metabolite analysis in Trincadeira cultivar reveals novel information regarding the dynamics of grape ripening. *BMC Plant Biol.* 11:149. doi: 10.1186/1471-2229-11-149
- Fortes, A. M., Teixeira, R. T., and Agudelo-Romero, P. (2015). Complex interplay of hormonal signals during grape berry ripening. *Molecules* 20, 9326–9343. doi: 10.3390/molecules20059326
- Fu, X., Richards, D. E., Ait-Ali, T., Hynes, L. W., Ougham, H., Peng, J., et al. (2002). Gibberellin-mediated proteasome-dependent degradation of the barley DELLA protein SLN1 repressor. *Plant Cell* 14, 3191–3200. doi: 10.1105/tpc.006197
- Fujisawa, M., Shima, Y., Higuchi, N., Nakano, T., Koyama, Y., Kasumi, T., et al. (2012). Direct targets of the tomato-ripening regulator RIN identified by transcriptome and chromatin immunoprecipitation analyses. *Planta* 235, 1107–1122. doi: 10.1007/s00425-011-1561-2
- Fung, R. W., Gonzalo, M., Fekete, C., Kovacs, L. G., He, Y., Marsh, E., et al. (2008). Powdery mildew induces defense-oriented reprogramming of the transcriptome in a susceptible but not in a resistant grapevine. *Plant Physiol.* 146, 236–249. doi: 10.1104/pp.107.108712
- Gao, M. J., Parkin, I., Lydiate, D., and Hannoufa, A. (2004). An auxin-responsive SCARECROW-like transcriptional activator interacts with histone deacetylase. *Plant Mol. Biol.* 55, 417–431. doi: 10.1007/s11103-004-0892-9
- Greb, T., Clarenz, O., Schafer, E., Muller, D., Herrero, R., Schmitz, G., et al. (2003). Molecular analysis of the LATERAL SUPPRESSOR gene in Arabidopsis reveals a conserved control mechanism for axillary meristem formation. *Genes Dev.* 17, 1175–1187. doi: 10.1101/gad.260703
- Grimplet, J., Adam-Blondon, A.-F., Bert, P.-F., Bitz, O., Cantu, D., Davies, C., et al. (2014). The grapevine gene nomenclature system. *BMC Genomics* 15:1077. doi: 10.1186/1471-2164-15-1077
- Grimplet, J., Deluc, L. G., Tillett, R. L., Wheatley, M. D., Schlauch, K. A., Cramer, G. R., et al. (2007). Tissue-specific mRNA expression profiling in grape berry tissues. *BMC Genomics* 8:187. doi: 10.1186/1471-2164-8-187
- Grimplet, J., Van Hemert, J., Carbonell-Bejerano, P., Diaz-Riquelme, J., Dickerson, J., Fennell, A., et al. (2012). Comparative analysis of grapevine whole-genome gene predictions, functional annotation, categorization and integration of the predicted gene sequences. *BMC Res. Notes* 5:213. doi: 10.1186/1756-0500-5-213
- Harberd, N. P., Belfield, E., and Yasumura, Y. (2009). The angiosperm gibberellin-GID1-DELLA growth regulatory mechanism: how an “inhibitor of an inhibitor” enables flexible response to fluctuating environments. *Plant Cell* 21, 1328–1339. doi: 10.1105/tpc.109.066969
- Heckmann, A. B., Lombardo, F., Miwa, H., Perry, J. A., Bunnewell, S., Parniske, M., et al. (2006). *Lotus japonicus* nodulation requires two GRAS domain regulators, one of which is functionally conserved in a non-legume. *Plant Physiol.* 142, 1739–1750. doi: 10.1104/pp.106.089508
- Helariutta, Y., Fukaki, H., Wysocka-Diller, J., Nakajima, K., Jung, J., Sena, G., et al. (2000). The SHORT-ROOT gene controls radial patterning of the Arabidopsis root through radial signaling. *Cell* 101, 555–567. doi: 10.1016/S0092-8674(00)80865-X
- Hirsch, S., and Oldroyd, G. E. (2009). GRAS-domain transcription factors that regulate plant development. *Plant Signal. Behav.* 4, 698–700. doi: 10.4161/psb.4.8.9176
- Huang, W., Xian, Z., Kang, X., Tang, N., and Li, Z. (2015). Genome-wide identification, phylogeny and expression analysis of GRAS gene family in tomato. *BMC Plant Biol.* 15:209. doi: 10.1186/s12870-015-0590-6
- Ikeda, A., Ueguchi-Tanaka, M., Sonoda, Y., Kitano, H., Koshioka, M., Futsuhara, Y., et al. (2001). slender rice, a constitutive gibberellin response mutant, is caused by a null mutation of the SLR1 gene, an ortholog of the height-regulating gene GAI/RGA/RHT/D8. *Plant Cell* 13, 999–1010. doi: 10.1105/tpc.13.5.999
- Itoh, H., Ueguchi-Tanaka, M., Sato, Y., Ashikari, M., and Matsuoka, M. (2002). The gibberellin signaling pathway is regulated by the appearance and disappearance of SLENDER RICE1 in nuclei. *Plant Cell* 14, 57–70. doi: 10.1105/tpc.013019
- Jaillon, O., Aury, J. M., Noel, B., Policriti, A., Clepet, C., Casagrande, A., et al. (2007). The grapevine genome sequence suggests ancestral hexaploidization in major angiosperm phyla. *Nature* 449, 463–467. doi: 10.1038/nature06148
- Jones, D. T., Taylor, W. R., and Thornton, J. M. (1992). The rapid generation of mutation data matrices from protein sequences. *Bioinformatics* 8, 275–282. doi: 10.1093/bioinformatics/8.3.275
- Kalo, P., Gleason, C., Edwards, A., Marsh, J., Mitra, R. M., Hirsch, S., et al. (2005). Nodulation signaling in legumes requires NSP2, a member of the GRAS family of transcriptional regulators. *Science* 308, 1786–1789. doi: 10.1126/science.1110951
- Karlova, R., van Haarst, J. C., Maliepaard, C., van de Geest, H., Bovy, A. G., Lamers, M., et al. (2013). Identification of microRNA targets in tomato fruit development using high-throughput sequencing and degradome analysis. *J. Exp. Bot.* 64, 1863–1878. doi: 10.1093/jxb/ert049
- Lee, M. H., Kim, B., Song, S. K., Heo, J. O., Yu, N. I., Lee, S. A., et al. (2008). Large-scale analysis of the GRAS gene family in *Arabidopsis thaliana*. *Plant Mol. Biol.* 67, 659–670. doi: 10.1007/s11103-008-9345-1
- Li, X., Qian, Q., Fu, Z., Wang, Y., Xiong, G., Zeng, D., et al. (2003). Control of tillering in rice. *Nature* 422, 618–621. doi: 10.1038/nature01518
- Licausi, F., Giorgi, F. M., Zenoni, S., Osti, F., Pezzotti, M., and Perata, P. (2010). Genomic and transcriptomic analysis of the AP2/ERF superfamily in *Vitis vinifera*. *BMC Genomics* 11:719. doi: 10.1186/1471-2164-11-719
- Lijavetzky, D., Carbonell-Bejerano, P., Grimplet, J., Bravo, G., Flores, P., Fenoll, J., et al. (2012). Berry flesh and skin ripening features in *Vitis vinifera* as assessed by transcriptional profiling. *PLoS ONE* 7:e39547. doi: 10.1371/annotation/fd93800a-3b3c-484d-97a9-190043309e4b
- Liu, X., and Widmer, A. (2014). Genome-wide comparative analysis of the GRAS gene family in populus, Arabidopsis and rice. *Plant Mol. Biol. Rep.* 32, 1129–1145. doi: 10.1007/s11105-014-0721-5
- Lu, J., Wang, T., Xu, Z., Sun, L., and Zhang, Q. (2015). Genome-wide analysis of the GRAS gene family in *Prunus mume*. *Mol. Genet. Genomics* 290, 303–317. doi: 10.1007/s00438-014-0918-1
- Lund, S. T., Peng, F. Y., Nayar, T., Reid, K. E., and Schlosser, J. (2008). Gene expression analyses in individual grape (*Vitis vinifera* L.) berries during ripening initiation reveal that pigmentation intensity is a valid indicator of developmental staging within the cluster. *Plant Mol. Biol.* 68, 301–315. doi: 10.1007/s11103-008-9371-z
- Ma, H. S., Liang, D., Shuai, P., Xia, X. L., and Yin, W. L. (2010). The salt- and drought-inducible poplar GRAS protein SCL7 confers salt and drought tolerance in *Arabidopsis thaliana*. *J. Exp. Bot.* 61, 4011–4019. doi: 10.1093/jxb/erq217
- Mayrose, M., Ekengren, S. K., Melech-Bonfil, S., Martin, G. B., and Sessa, G. (2006). A novel link between tomato GRAS genes, plant disease resistance and mechanical stress response. *Mol. Plant Pathol.* 7, 593–604. doi: 10.1111/j.1364-3703.2006.00364.x
- Morohashi, K., Minami, M., Takase, H., Hotta, Y., and Hiratsuka, K. (2003). Isolation and characterization of a novel GRAS gene that regulates meiosis-associated gene expression. *J. Biol. Chem.* 278, 20865–20873. doi: 10.1074/jbc.M301712200

- Moxon, S., Jing, R., Szitty, G., Schwach, F., Rusholme Pilcher, R. L., Moulton, V., et al. (2008). Deep sequencing of tomato short RNAs identifies microRNAs targeting genes involved in fruit ripening. *Genome Res.* 18, 1602–1609. doi: 10.1101/gr.080127.108
- Navarro, L., Bari, R., Achard, P., Lison, P., Nemri, A., Harberd, N. P., et al. (2008). DELLA control plant immune responses by modulating the balance of jasmonic acid and salicylic acid signaling. *Curr. Biol.* 18, 650–655. doi: 10.1016/j.cub.2008.03.060
- Obayashi, T., and Kinoshita, K. (2009). Rank of correlation coefficient as a comparable measure for biological significance of gene coexpression. *DNA Res.* 16, 249–260. doi: 10.1093/dnare/dsp016
- Okonechnikov, K., Golosova, O., Fursov, M., and team, U. (2012). Uniprot UGEME: a unified bioinformatics toolkit. *Bioinformatics* 28, 1166–1167. doi: 10.1093/bioinformatics/bts091
- Oldroyd, G. E. (2013). Speak, friend, and enter: signalling systems that promote beneficial symbiotic associations in plants. *Nat. Rev. Microbiol.* 11, 252–263. doi: 10.1038/nrmicro2990
- Park, H. J., Jung, W. Y., Lee, S. S., Song, J. H., Kwon, S. Y., Kim, H., et al. (2013). Use of heat stress responsive gene expression levels for early selection of heat tolerant cabbage (*Brassica oleracea* L.). *Int. J. Mol. Sci.* 14, 11871–11894. doi: 10.3390/ijms140611871
- Peng, J., Carol, P., Richards, D. E., King, K. E., Cowling, R. J., Murphy, G. P., et al. (1997). The *Arabidopsis* GAI gene defines a signaling pathway that negatively regulates gibberellin responses. *Genes Dev.* 11, 3194–3205. doi: 10.1101/gad.11.23.3194
- Pilati, S., Perazzolli, M., Malossini, A., Cestaro, A., Dematte, L., Fontana, P., et al. (2007). Genome-wide transcriptional analysis of grapevine berry ripening reveals a set of genes similarly modulated during three seasons and the occurrence of an oxidative burst at veraison. *BMC Genomics* 8:428. doi: 10.1186/1471-2164-8-428
- Pontin, M. A., Piccoli, P. N., Francisco, R., Bottini, R., Martinez-Zapater, J. M., and Lijavetzky, D. (2010). Transcriptome changes in grapevine (*Vitis vinifera* L.) cv. Malbec leaves induced by ultraviolet-B radiation. *BMC Plant Biol.* 10:224. doi: 10.1186/1471-2229-10-224
- Prince, V. E., and Pickett, F. B. (2002). Splitting pairs: the diverging fates of duplicated genes. *Nat. Rev. Genet.* 3, 827–837. doi: 10.1038/nrg928
- Pysh, L. D., Wysocka-Diller, J. W., Camilleri, C., Bouchez, D., and Benfey, P. N. (1999). The GRAS gene family in *Arabidopsis*: sequence characterization and basic expression analysis of the SCARECROW-LIKE genes. *Plant J.* 18, 111–119. doi: 10.1046/j.1365-313X.1999.00431.x
- Royo, C., Carbonell-Bejerano, P., Torres-Perez, R., Nebish, A., Martinez, O., Rey, M., et al. (2016). Developmental, transcriptome, and genetic alterations associated with parthenocarpy in the grapevine seedless somatic variant Corinto bianco. *J. Exp. Bot.* 67, 259–273. doi: 10.1093/jxb/erv452
- Schumacher, K., Schmitt, T., Rossberg, M., Schmitz, G., and Theres, K. (1999). The Lateral suppressor (Ls) gene of tomato encodes a new member of the VHIID protein family. *Proc. Natl. Acad. Sci. U.S.A.* 96, 290–295. doi: 10.1073/pnas.96.1.290
- Silverstone, A. L., Ciampaglio, C. N., and Sun, T. (1998). The *Arabidopsis* RGA gene encodes a transcriptional regulator repressing the gibberellin signal transduction pathway. *Plant Cell* 10, 155–169. doi: 10.1105/tpc.10.2.155
- Song, X. M., Liu, T. K., Duan, W. K., Ma, Q. H., Ren, J., Wang, Z., et al. (2014). Genome-wide analysis of the GRAS gene family in Chinese cabbage (*Brassica rapa* ssp. *pekinensis*). *Genomics* 103, 135–146. doi: 10.1016/j.ygeno.2013.12.004
- Sreekantan, L., Mathiason, K., Grimplet, J., Schlauch, K., Dickerson, J. A., and Fennell, A. Y. (2010). Differential floral development and gene expression in grapevines during long and short photoperiods suggests a role for floral genes in dormancy transitioning. *Plant Mol. Biol.* 73, 191–205. doi: 10.1007/s11103-010-9611-x
- Sterck, L., Billiau, K., Abeel, T., Rouze, P., and Van de Peer, Y. (2012). ORCAE: online resource for community annotation of eukaryotes. *Nat. Methods* 9:1041. doi: 10.1038/nmeth.2242
- Stuurman, J., Jaggi, F., and Kuhlemeier, C. (2002). Shoot meristem maintenance is controlled by a GRAS-gene mediated signal from differentiating cells. *Genes Dev.* 16, 2213–2218. doi: 10.1101/gad.230702
- Tamura, K., Stecher, G., Peterson, D., Filipski, A., and Kumar, S. (2013). MEGA6: molecular evolutionary genetics analysis version 6.0. *Mol. Biol. Evol.* 30, 2725–2729. doi: 10.1093/molbev/mst197
- Tattersall, E. A., Grimplet, J., DeLuc, L., Wheatley, M. D., Vincent, D., Osborne, C., et al. (2007). Transcript abundance profiles reveal larger and more complex responses of grapevine to chilling compared to osmotic and salinity stress. *Funct. Integr. Genomics* 7, 317–333. doi: 10.1007/s10142-007-0051-x
- Tian, C., Wan, P., Sun, S., Li, J., and Chen, M. (2004). Genome-wide analysis of the GRAS gene family in rice and *Arabidopsis*. *Plant Mol. Biol.* 54, 519–532. doi: 10.1023/B:PLAN.0000038256.89809.57
- Tillet, R. L., Ergul, A., Albion, R. L., Schlauch, K. A., Cramer, G. R., and Cushman, J. C. (2011). Identification of tissue-specific, abiotic stress-responsive gene expression patterns in wine grape (*Vitis vinifera* L.) based on curation and mining of large-scale EST data sets. *BMC Plant Biol.* 11:86. doi: 10.1186/1471-2229-11-86
- Tong, H., Jin, Y., Liu, W., Li, F., Fang, J., Yin, Y., et al. (2009). DWARF AND LOW-TILLERING, a new member of the GRAS family, plays positive roles in brassinosteroid signaling in rice. *Plant J.* 58, 803–816. doi: 10.1111/j.1365-313X.2009.03825.x
- Torres-Galea, P., Hirtreiter, B., and Bolle, C. (2013). Two GRAS proteins, SCARECROW-LIKE21 and PHYTOCHROME A SIGNAL TRANSDUCTION1, function cooperatively in phytochrome A signal transduction. *Plant Physiol.* 161, 291–304. doi: 10.1104/pp.112.206607
- Torres-Galea, P., Huang, L. F., Chua, N. H., and Bolle, C. (2006). The GRAS protein SCL13 is a positive regulator of phytochrome-dependent red light signaling, but can also modulate phytochrome A responses. *Mol. Genet. Genomics* 276, 13–30. doi: 10.1007/s00438-006-0123-y
- Vega, A., Gutierrez, R. A., Pena-Neira, A., Cramer, G. R., and Arce-Johnson, P. (2011). Compatible GLRaV-3 viral infections affect berry ripening decreasing sugar accumulation and anthocyanin biosynthesis in *Vitis vinifera*. *Plant Mol. Biol.* 77, 261–274. doi: 10.1007/s11103-011-9807-8
- Velasco, R., Zharkikh, A., Troggio, M., Cartwright, D. A., Cestaro, A., Pruss, D., et al. (2007). A high quality draft consensus sequence of the genome of a heterozygous grapevine variety. *PLoS ONE* 2:e1326. doi: 10.1371/journal.pone.0001326
- Wang, L., Mai, Y. X., Zhang, Y. C., Luo, Q., and Yang, H. Q. (2010). MicroRNA171c-targeted SCL6-II, SCL6-III, and SCL6-IV genes regulate shoot branching in *Arabidopsis*. *Mol. Plant* 3, 794–806. doi: 10.1093/mp/ssq042
- Wild, M., Daviere, J. M., Cheminant, S., Regnault, T., Baumberger, N., Heintz, D., et al. (2012). The *Arabidopsis* DELLA RGA-LIKE3 is a direct target of MYC2 and modulates jasmonate signaling responses. *Plant Cell* 24, 3307–3319. doi: 10.1101/tpc.112.101428
- Wu, N., Zhu, Y., Song, W., Li, Y., Yan, Y., and Hu, Y. (2014). Unusual tandem expansion and positive selection in subgroups of the plant GRAS transcription factor superfamily. *BMC Plant Biol.* 14:373. doi: 10.1186/s12870-014-0373-5
- Xu, K., Chen, S., Li, T., Ma, X., Liang, X., Ding, X., et al. (2015). OsGRAS23, a rice GRAS transcription factor gene, is involved in drought stress response through regulating expression of stress-responsive genes. *BMC Plant Biol.* 15:141. doi: 10.1186/s12870-015-0532-3
- Xue, L., Cui, H., Buer, B., Vijayakumar, V., Delaux, P. M., Junkermann, S., et al. (2015). Network of GRAS transcription factors involved in the control of arbuscule development in *Lotus japonicus*. *Plant Physiol.* 167, 854–871. doi: 10.1104/pp.114.255430
- Zentella, R., Zhang, Z. L., Park, M., Thomas, S. G., Endo, A., Murase, K., et al. (2007). Global analysis of della direct targets in early gibberellin signaling in *Arabidopsis*. *Plant Cell* 19, 3037–3057. doi: 10.1105/tpc.107.054999
- Zhang, D., Iyer, L. M., and Aravind, L. (2012). Bacterial GRAS domain proteins throw new light on gibberellin acid response mechanisms. *Bioinformatics* 28, 2407–2411. doi: 10.1093/bioinformatics/bts464
- Conflict of Interest Statement:** The authors declare that the research was conducted in the absence of any commercial or financial relationships that could be construed as a potential conflict of interest.
- Copyright © 2016 Grimplet, Agudelo-Romero, Teixeira, Martinez-Zapater and Fortes. This is an open-access article distributed under the terms of the Creative Commons Attribution License (CC BY). The use, distribution or reproduction in other forums is permitted, provided the original author(s) or licensor are credited and that the original publication in this journal is cited, in accordance with accepted academic practice. No use, distribution or reproduction is permitted which does not comply with these terms.**



Evolutionary Recycling of Light Signaling Components in Fleshy Fruits: New Insights on the Role of Pigments to Monitor Ripening

Briardo Llorente*, Lucio D'Andrea and Manuel Rodríguez-Concepción*

Centre for Research in Agricultural Genomics (CRAG) CSIC-IRTA-UAB-UB, Barcelona, Spain

OPEN ACCESS

Edited by:

Antonio Granell,
Consejo Superior de Investigaciones
Científicas, Spain

Reviewed by:

Cornelius Barry,
Michigan State University, USA
María Jesús Rodrigo,
Instituto de Agroquímica y Tecnología
de Alimentos – Consejo Superior
de Investigaciones Científicas, Spain

***Correspondence:**

Briardo Llorente
briardo.llorente@cragenomica.es;
Manuel Rodríguez-Concepción
manuel.rodriguez@cragenomica.es

Specialty section:

This article was submitted to
Plant Physiology,
a section of the journal
Frontiers in Plant Science

Received: 26 November 2015

Accepted: 19 February 2016

Published: 07 March 2016

Citation:

Llorente B, D'Andrea L and Rodríguez-Concepción M (2016)
Evolutionary Recycling of Light Signaling Components in Fleshy Fruits: New Insights on the Role of Pigments to Monitor Ripening.
Front. Plant Sci. 7:263.
doi: 10.3389/fpls.2016.00263

Besides an essential source of energy, light provides environmental information to plants. Photosensory pathways are thought to have occurred early in plant evolution, probably at the time of the Archaeplastida ancestor, or perhaps even earlier. Manipulation of individual components of light perception and signaling networks in tomato (*Solanum lycopersicum*) affects the metabolism of ripening fruit at several levels. Most strikingly, recent experiments have shown that some of the molecular mechanisms originally devoted to sense and respond to environmental light cues have been re-adapted during evolution to provide plants with useful information on fruit ripening progression. In particular, the presence of chlorophylls in green fruit can strongly influence the spectral composition of the light filtered through the fruit pericarp. The concomitant changes in light quality can be perceived and transduced by phytochromes (PHYs) and PHY-interacting factors, respectively, to regulate gene expression and in turn modulate the production of carotenoids, a family of metabolites that are relevant for the final pigmentation of ripe fruits. We raise the hypothesis that the evolutionary recycling of light-signaling components to finely adjust pigmentation to the actual ripening stage of the fruit may have represented a selective advantage for primeval fleshy-fruited plants even before the extinction of dinosaurs.

Keywords: photosensory pathways, light, fleshy fruits, ripening, evolution

INTRODUCTION

Light has a dual role in plants as an essential source of energy for driving photosynthesis and, on the other hand, as an environmental cue that modulates many aspects of plant biology such as photomorphogenesis, germination, phototropism, and entrainment of circadian rhythms (Chen et al., 2004; Jiao et al., 2007). The ability to perceive and respond to light changes is mediated by a set of sophisticated photosensory pathways capable of discriminating the quality (spectral composition), intensity (irradiance), duration (including day length), and direction of light (Moglich et al., 2010). In particular, plants perceive light through at least five types of sensory photoreceptors that are distinct from photosynthetic components and detect specific regions of the electromagnetic spectrum. Cryptochromes (CRYs), phototropins, and Zeitlupe family members function in the blue (390–500 nm) and ultraviolet-A (320–390 nm) wavelengths, while the

photoreceptor UVR-8 operates in the ultraviolet-B (280–315 nm) region. Phytochromes (PHYs), which are probably the best studied photoreceptors, function in a dynamic photoequilibrium determined by the red (R, ca. 660 nm) to far-red (FR, ca. 730 nm) ratio in land plants and throughout the visible spectrum (blue, green, orange, red, and far-red) in different algae (Moglich et al., 2010; Rizzini et al., 2011; Rockwell et al., 2014). The photonic information gathered by these photoreceptors is then transduced into changes in gene expression that ultimately promote optimal growth, development, survival and reproduction (Jiao et al., 2007).

Photosensory pathways are thought to have occurred early in plant evolution, probably at the time of the Archaeplastida ancestor (i.e., the last common ancestor of glaucophyte, red algae, green algae and land plants) or perhaps even earlier, before the occurrence of the endosymbiotic event that gave rise to photosynthetic eukaryotes over more than a billion years ago (Duanmu et al., 2014; Mathews, 2014; Fortunato et al., 2015). Through the ages, these mechanisms diverged to play particular roles in different branches of the plant lineage, ranging from presumably acclimative roles in algae (Duanmu et al., 2014; Rockwell et al., 2014) to resource competition functions in land plants (Jiao et al., 2007). In particular, the ability of PHYs to detect changes in the R/FR ratio allows land plants to detect the presence of nearby vegetation that could potentially compete for light. Light filtered or reflected by neighboring leaves (i.e., shade) has a distinctive spectral composition that is characterized by a decreased R/FR ratio due to a preferential absorption of R light by chlorophyll (Casal, 2013). Low R/FR ratios reduce PHY activity, allowing PHY-interacting transcription factors (PIFs) to bind to genomic regulatory elements that tune the expression of numerous genes (Casal, 2013; Leivar and Monte, 2014). Oppositely, high R/FR ratios enhance PHY activity, causing the inactivation of PIF proteins mainly by proteasome-mediated degradation (Bae and Choi, 2008; Leivar and Monte, 2014). Carotenoid biosynthesis represents a rather well characterized example of this regulation. In *Arabidopsis thaliana*, shade decreases the production of carotenoids in photosynthetic tissues (Roig-Villanova et al., 2007; Bou-Torrent et al., 2015) in part by promoting the accumulation of PIF proteins that repress the expression of the gene encoding phytoene synthase (PSY), the main rate-determining enzyme of the carotenoid pathway (Roig-Villanova et al., 2007; Toledo-Ortiz et al., 2010; Bou-Torrent et al., 2015). De-repression of PSY under sunlight induces carotenoid biosynthesis, which in turn maximizes light harvesting and protects the photosynthetic machinery from harmful oxidative photodamage caused by intense light (Sundstrom, 2008).

Light signals in general and PHYs in particular also modulate the genetic programs associated to fruit development and ripening. Here we will revise current and emerging knowledge on this area based on work carried out in tomato (*Solanum lycopersicum*), which is the main model system for fleshy fruits, that is, fruits containing a juicy fruit pulp. Further, we will discuss potential selection pressures that might account for the evolutionary recycling of light-signaling components in fleshy fruits.

FLESHY FRUIT RIPENING: THE CASE OF TOMATO

Fleshy fruits are differentiated floral tissues that evolved 80–90 million years ago (Ma), i.e., relatively recently in the history of plants (Givnish et al., 2005; Eriksson, 2014), as an adaptive characteristic promoting the animal-assisted dissemination of viable seeds (Tiffney, 2004; Seymour et al., 2013; Duan et al., 2014). After seed maturation, fleshy fruits typically undergo a ripening process that involves irreversible changes in organoleptic characteristics such as color, texture, and flavor, all of which result in the production of an appealing food to frugivorous animals. In this manner, the ripening process orchestrates the mutualistic relationship between fleshy-fruited plants and seed-disperser animals (Tiffney, 2004; Seymour et al., 2013; Duan et al., 2014).

Upon fertilization, the development of fleshy fruits such as tomato can be divided into three distinct phases: cell division, cell expansion, and ripening (Gillaspy et al., 1993; Seymour et al., 2013). These different stages are characterized by hormonal, genetic, and metabolic shifts that have been reviewed in great detail elsewhere (Carrari and Fernie, 2006; Klee and Giovannoni, 2011; Seymour et al., 2013; Tohge et al., 2014). Before ripening occurs, tomato fruits have a green appearance due to the presence of chloroplasts that contain the whole photosynthetic machinery. The transition to ripening is characterized by a loss of chlorophylls, cell wall softening, accumulation of sugars, and drastic alterations in the profile of volatiles and pigments. Most distinctly, chlorophyll degradation is accompanied by a conversion of chloroplasts into chromoplasts that progressively accumulate high levels of the health-promoting carotenoids β-carotene (pro-vitamin A) and lycopene (Tomato Genome Consortium, 2012; Fantini et al., 2013; Seymour et al., 2013). These carotenoid pigments give the characteristic orange and red colors to ripe tomatoes. A large number of other fruits (including bananas, oranges, or peppers) also lose chlorophylls and accumulate carotenoids during ripening, resulting in a characteristic pigmentation change (from green to yellow, orange or red) that acts as a visual signal informing animals when the fruit is ripe and healthy (Klee and Giovannoni, 2011).

THE EFFECT OF LIGHT SIGNALING COMPONENTS ON FRUIT RIPENING

Multiple lines of evidence have exposed the relevance of fruit-localized photosensory pathways as important players in the regulation of fruit ripening and the potential of their manipulation to improve the nutritional quality of tomatoes (Azari et al., 2010). Among many light-signaling mutants displaying altered fruit phenotypes, the tomato high pigment (*hp*) mutants *hp1* and *hp2* are two of the best characterized. These mutants owe their name to a deep fruit pigmentation derived from an increment in the number and size of plastids, which in turn result in elevated levels of carotenoids such as lycopene (Yen et al., 1997; Mustilli et al., 1999; Levin

et al., 2003). Detailed characterization of the *hp1* and *hp2* mutants, which also show increased levels of extraplastidial metabolites such as flavonoids, revealed that the mutated genes encode tomato homologs of the previously described light signal transduction proteins DAMAGED DNA BINDING PROTEIN 1 (DDB1) and DEETIOLATED1 (DET1), respectively (Mustilli et al., 1999; Schroeder et al., 2002; Levin et al., 2003; Liu et al., 2004) (Figure 1). Other components that participate in the same light-signaling pathway that HP1 and HP2 have also been shown to impact tomato fruit metabolism. For instance, silencing the tomato E3 ubiquitin-ligase CUL4, which directly interacts with HP1, also produces highly pigmented fruits (Wang et al., 2008). Another example is the E3 ubiquitin-ligase CONSTITUTIVELY PHOTOMORPHOGENIC 1 (COP1), which specifically promotes the degradation of the light-signaling effector ELONGATED HYPOCOTYL 5 (HY5) (Schwechheimer and Deng, 2000) (Figure 1). Transgenic plants with downregulated transcripts of COP1 and HY5 produce tomato fruits with increased and reduced levels of carotenoids, respectively (Liu et al., 2004).

Work with photoreceptors (Figure 1) has also shed light on the subject. Tomato plants overexpressing the blue light photoreceptor cryptochrome 2 (CRY2) produce fruits with increased levels of flavonoids and carotenoids (Giliberto et al., 2005). PHYs have been found to control different aspects of tomato fruit ripening as well. Activation of fruit-localized PHYs with R light treatments promotes carotenoid biosynthesis, while subsequent PHY inactivation by irradiation with FR light reverts it (Alba et al., 2000; Schofield and Paliyath, 2005). Furthermore, preventing light exposure from the very early stages of fruit set and development results in white fruits completely devoid of pigments (Cheung et al., 1993), a phenotype that resembles that of *phyA phyB1 phyB2* PHY triple mutant plants (Weller et al., 2000). In addition to regulating carotenoid levels in tomato fruits, PHYs seem to regulate the timing of phase transition during ripening (Gupta et al., 2014).

A MECHANISM TO MONITOR RIPENING BASED ON SELF-SHADING AND LIGHT SIGNALING

Although light signaling components have long been known to modulate fruit ripening, another important piece of the puzzle was revealed recently. In tomato, fruit pericarp cells are morphologically similar to leaf palisade cells (Gillaspy et al., 1993). Thus, fruits can be viewed as modified leaves that, besides enclosing the seeds, have suffered a change in organ geometry, namely, a shift from a nearly planate conformation to an expanded three-dimensional anatomy. This anatomy imposes spatial constraints coercing light to pass through successive cell layers, so that the quality of the light that reaches inner sections of the fruit is influenced by the cells of outer pericarp sections (Figure 2). Another key difference between tomato leaves and fruits is the cuticle, which is far more pronounced in the fruit. While a potential role of the cuticle in altering the spectral properties of the light that reaches the pericarp cells remains to

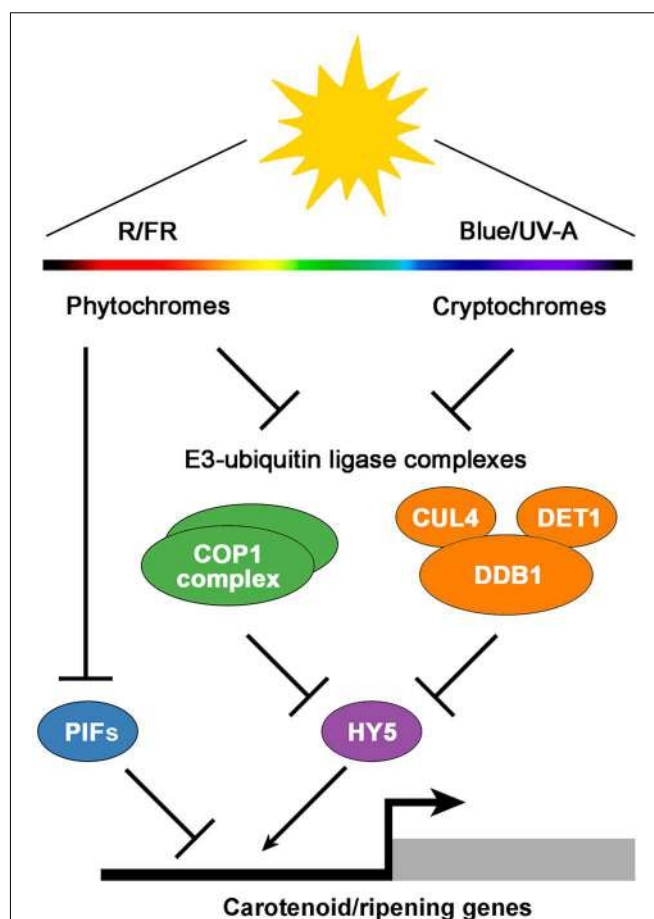
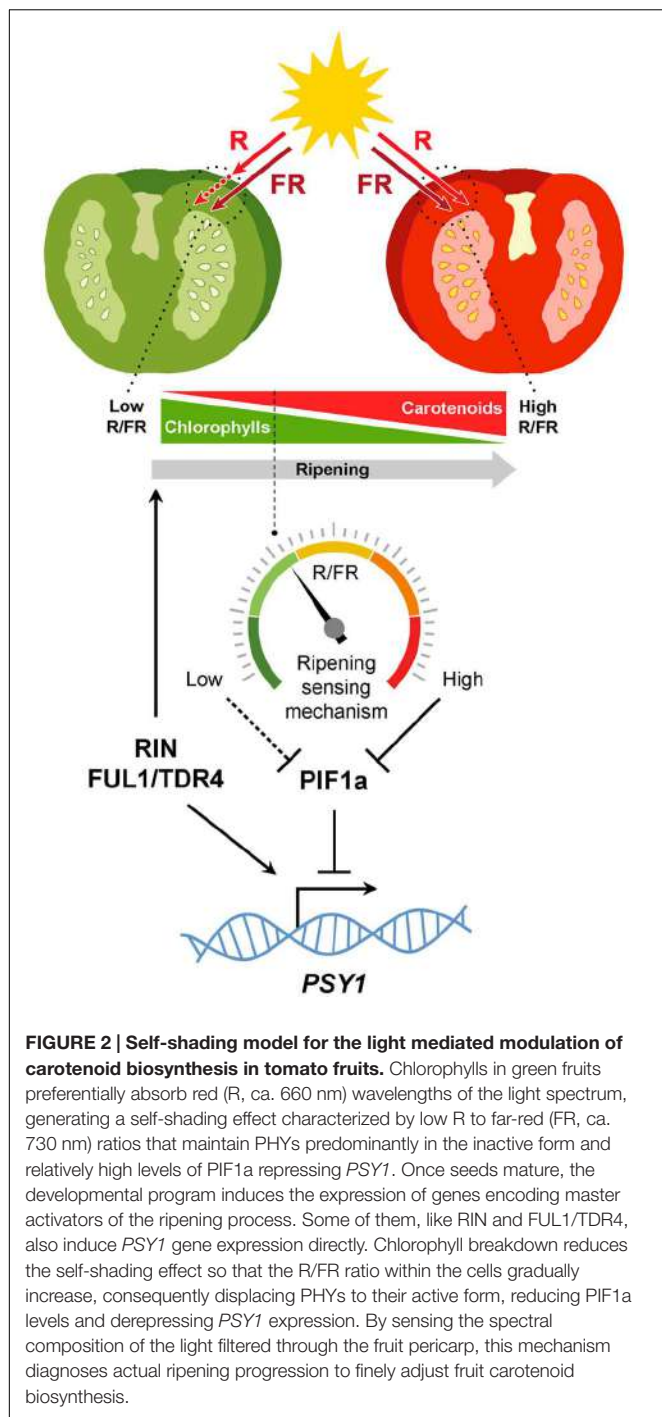


FIGURE 1 | A simplified model of light signaling components involved in the regulation of tomato fruit pigmentation and ripening. Fruit-localized phytochrome and cryptochrome photoreceptors regulate the activity of the downstream E3-ubiquitin ligase COP1 and CUL4-DDB1-DET1 complexes, which in turn mediate the degradation of the transcriptional activator HY5. In addition, active phytochromes reduce the activity of transcriptional repressors such as PIFs. The balance between activators and repressors finally modulates the expression of carotenoid and ripening-associated genes. R, red light; FR, far-red light; Blue, blue light; UV-A, ultraviolet-A light.

be investigated, it is now well established that the occurrence of chlorophyll in fruit chloroplasts significantly reduces the R/FR ratio of the light filtered through the fruit fresh (Alba et al., 2000; Llorente et al., 2015). A reduction in R/FR ratio (also referred to as shade) normally informs plants about the proximity of surrounding vegetation (Casal, 2013). In tomato fruit, however, changes in R/FR ratio can inform of the ripening status. As a consequence of self-shading, it is proposed that a relatively high proportion of PHYs remain inactive in green fruit. This condition stabilizes the tomato PIF1a transcription factor, that binds to a PBE-box located in the promoter of the gene encoding the PSY isoform that controls the metabolic flux to the carotenoid pathway during fruit ripening, *PSY1*. PIF1a binding directly represses *PSY1* expression (Figure 2). Chlorophyll breakdown at the onset of ripening reduces the self-shading effect, consequently



promoting PHY activation, degradation of PIF1a, derepression of PSY1, and eventually carotenoid biosynthesis (Figure 2). In this manner, the genetically controlled expression of PSY1 (and hence the production of carotenoid pigments) is fine-tuned to the actual progression of ripening (Llorente et al., 2015).

Translation of molecular insights from tomato to other fleshy-fruited plants has indicated that many regulatory networks are conserved across a wide range of species (Seymour et al., 2013).

Thus, given the ubiquitous nature of PHYs in land plants and the widespread occurrence of ripening-associated fruit pigmentation changes that typically involve the substitution of an initially chlorophyll-based green color with distinctive non-green (i.e., non-R-absorbing) eye-catching colors, it is possible that similar self-shading regulatory mechanisms might operate in other plant species to inform on the actual stage of ripening (based on the pigment profile of the fruit at every moment) and thus finely coordinate fruit color change. However, the composition of the cuticle or even the anatomy of the most external layer of the pericarp (i.e., the exocarp) might also impact the quality and quantity of light that penetrates the fruit flesh. The self-shading mechanism is expected to be irrelevant in fleshy fruits with a thick skin or exocarp that prevents light to pass through and reach more internal fruit layers.

FRUIT COLORS AS RIPENING SIGNALS IN AN EVOLUTIONARY CONTEXT

Fleshy fruits are considered to have first appeared in the Late Cretaceous (circa 90 Ma) (Givnish et al., 2005; Eriksson, 2014), at a time when the Earth's vegetation was dense and exuberant, and where most ecological niches were taken over by angiosperms (Lidgard and Crane, 1988; Berendse and Scheffer, 2009). The plentiful surplus of nutritious food gave rise to a huge explosion in the Cretaceous fauna, bringing about the coexistence of numerous herbivorous and omnivorous reptiles (dinosaurs, pterosaurs, lizards), birds and mammals (Lloyd et al., 2008; Prentice et al., 2011; Vullo et al., 2012; Wilson et al., 2012; Jones et al., 2013; Jarvis et al., 2014). With such an abundance of plant-eating animals, being able to display a change in fruit color when ripe probably represented a valuable trait among early fleshy-fruited plants to call the attention of these various potential seed dispersers.

Although deep time co-evolutionary scenarios may be difficult to support, this idea gains plausibility if we consider that the same strategy had been successfully implemented beforehand by gymnosperms, which had already evolved fleshy fruit-like structures by the Early Cretaceous, at least some 20–30 million years before the first fleshy fruits (Yang and Wang, 2013). Several gymnosperms (e.g., *Ginkgo biloba*, *Taxus baccata*, and *Ephedra distachya*) produce fleshy colorful tissues around their seeds and, similar to that occurring in angiosperms, these fruit-like structures undergo a ripening process that also serves as a visual advertisement for animals to eat them and disperse their seeds. Recent evidence supports the hypothesis that the main molecular networks underlying the formation of the fleshy fruit were originally established in gymnosperms (Lovisotto et al., 2012, 2015), thus suggesting that the ripening phenomenon was first selected as an ecological adaptation in gymnosperms and that angiosperms merely exploited it afterwards. If correct, this would imply that Cretaceous plant-eater animals would have already been used to feeding on color-changing fleshy fruit-like tissues by the time that angiosperm fleshy-fruited plants evolved, something that may have facilitated the establishment of the latter.

Another relevant fact is that the dominant land animals during the Cretaceous period, the dinosaurs, as well as pterosaurs, lizards, and birds, had highly differentiated color vision, much superior to that of most mammals (Rowe, 2000; Chang et al., 2002; Bowmaker, 2008). Differentiated color vision, or tetrachromacy, is a basal characteristic of land vertebrates derived from the presence of four spectrally distinct retinal cone cells that allow discriminating hues ranging from ultraviolet to red (Bowmaker, 2008; Koschowitz et al., 2014). Turtles, alligators, lizards and birds, are all known to have tetrachromatic color vision, a shared trait inherited from their common reptilian ancestry (Rowe, 2000; Bowmaker, 2008). We have recently come to know that some dinosaurs even sported plumage color patterns and flamboyant cranial crests that may have served for visual display purposes (Li et al., 2010, 2012; Zhang et al., 2010; Bell et al., 2014; Foth et al., 2014; Koschowitz et al., 2014). Altogether, these insights suggest that color cues were likely an important means of signaling among dinosaurs. Although purely speculative at the moment, it is reasonable to assume that there could have also been dinosaurs that, analogously to several birds and reptiles nowadays (Svensson and Wong, 2011), consumed fleshy fruits within their diet as a source of carotenoid pigments used for ornamental coloration. Even though the relevance of, now extinct, Cretaceous megafauna as biological vectors involved in the seed dispersal of primeval fleshy-fruited plants remains speculative and controversial (Tiffney, 2004; Butler et al., 2009; Seymour et al., 2013), it is clear that they certainly had fleshy fruit available to eat during the last 25–35 million years of their existence, until the occurrence of the Cretaceous-Paleogene mass extinction event (65 Ma).

Fruit color change meets the criteria of a classical signal, which can be defined as a cue that increases the fitness of the sender (i.e., fleshy-fruited plants) by altering the behavior of the receivers (i.e., seed-disperser animals) (Maynard Smith and Harper, 1995). Importantly, besides visibility conditions and the visual aptitude

of the receiver, the detectability of a visual signal is determined by its contrast against the background, that is, the conspicuousness of the signal (Schmidt et al., 2004). Ripe fruits displaying a distinct coloration against the foliage leaves are more conspicuous for animals than green fruits and there is no evidence to consider that it was any different to Cretaceous animals. In fact, the invention of fruit fleshiness took place along with expanding tropical forests, suggesting it may have evolved as an advantageous trait related to changes in vegetation from open to more closed environments (Seymour et al., 2013; Eriksson, 2014). In this context, light signaling pathways already established in land plants may have had the chance to evolutionary explore novel phenotypic space in fleshy fruits. Subsequent adaptations under selection in the fruit may have then integrated these pathways as modulatory components of the pigmentation process during ripening. For instance, the self-shading regulation of the tomato fruit carotenoid pathway (Llorente et al., 2015) (**Figure 2**) might have evolved by co-option of components from the preexisting shade-avoidance responses (Mathews, 2006; Casal, 2013). This evolutionary recycling of light-signaling components in fleshy fruits might therefore be a legacy from the time when dinosaurs walked the earth.

AUTHOR CONTRIBUTIONS

BL, LA, and MR-C searched and discussed the literature and wrote the article.

ACKNOWLEDGMENTS

We acknowledge the support of grants from EC (CarotenActors, 300862), CYTED (Ibercarot, 112RT0445), MINECO (FPDI-2013-018882, BIO2011-23680, BIO2014-59092-P), MEC (AP2012-0189), and AGAUR (2014SGR-1434).

REFERENCES

- Alba, R., Cordonnier-Pratt, M. M., and Pratt, L. H. (2000). Fruit-localized phytochromes regulate lycopene accumulation independently of ethylene production in tomato. *Plant Physiol.* 123, 363–370. doi: 10.1104/pp.123.1.363
- Azari, R., Tadmor, Y., Meir, A., Reuveni, M., Evenor, D., Nahon, S., et al. (2010). Light signaling genes and their manipulation towards modulation of phytonutrient content in tomato fruits. *Biotechnol. Adv.* 28, 108–118. doi: 10.1016/j.biotechadv.2009.10.003
- Bae, G., and Choi, G. (2008). Decoding of light signals by plant phytochromes and their interacting proteins. *Annu. Rev. Plant Biol.* 59, 281–311. doi: 10.1146/annurev.arplant.59.032607.092859
- Bell, P. R., Fanti, F., Currie, P. J., and Arbour, V. M. (2014). A mummified duck-billed dinosaur with a soft-tissue cock's comb. *Curr. Biol.* 24, 70–75. doi: 10.1016/j.cub.2013.11.008
- Berendse, F., and Scheffer, M. (2009). The angiosperm radiation revisited, an ecological explanation for Darwin's 'abominable mystery'. *Ecol. Lett.* 12, 865–872. doi: 10.1111/j.1461-0248.2009.01342.x
- Bou-Torrent, J., Toledo-Ortiz, G., Ortiz-Alcaide, M., Cifuentes-Esquivel, N., Halliday, K. J., Martinez-García, J. F., et al. (2015). Regulation of carotenoid biosynthesis by shade relies on specific subsets of antagonistic transcription factors and cofactors. *Plant Physiol.* 169, 1584–1594. doi: 10.1104/pp.15.00552
- Bowmaker, J. K. (2008). Evolution of vertebrate visual pigments. *Vis. Res.* 48, 2022–2041. doi: 10.1016/j.visres.2008.03.025
- Butler, R. J., Barrett, P. M., Kenrick, P., and Penn, M. G. (2009). Diversity patterns amongst herbivorous dinosaurs and plants during the Cretaceous: implications for hypotheses of dinosaur/angiosperm co-evolution. *J. Evol. Biol.* 22, 446–459. doi: 10.1111/j.1420-9101.2008.01680.x
- Carrari, F., and Fernie, A. R. (2006). Metabolic regulation underlying tomato fruit development. *J. Exp. Bot.* 57, 1883–1897. doi: 10.1093/jxb/erj020
- Casal, J. J. (2013). Photoreceptor signaling networks in plant responses to shade. *Annu. Rev. Plant Biol.* 64, 403–427. doi: 10.1146/annurev-arplant-050312-120221
- Chang, B. S., Jonsson, K., Kazmi, M. A., Donoghue, M. J., and Sakmar, T. P. (2002). Recreating a functional ancestral archosaur visual pigment. *Mol. Biol. Evol.* 19, 1483–1489. doi: 10.1093/oxfordjournals.molbev.a004211
- Chen, M., Chory, J., and Fankhauser, C. (2004). Light signal transduction in higher plants. *Annu. Rev. Genet.* 38, 87–117. doi: 10.1146/annurev.genet.38.072902.092259
- Cheung, A. Y., McNellis, T., and Piekos, B. (1993). Maintenance of chloroplast Components during chromoplast differentiation in the tomato mutant green flesh. *Plant Physiol.* 101, 1223–1229.

- Consortium. (2012). The tomato genome sequence provides insights into fleshy fruit evolution. *Nature* 485, 635–641. doi: 10.1038/nature1119
- Duan, Q., Goodale, E., and Quan, R. C. (2014). Bird fruit preferences match the frequency of fruit colours in tropical Asia. *Sci. Rep.* 4:5627. doi: 10.1038/srep05627
- Duanmu, D., Bachy, C., Sudek, S., Wong, C. H., Jimenez, V., Rockwell, N. C., et al. (2014). Marine algae and land plants share conserved phytochrome signaling systems. *Proc. Natl. Acad. Sci. U.S.A.* 111, 15827–15832. doi: 10.1073/pnas.1416751111
- Eriksson, O. (2014). Evolution of angiosperm seed disperser mutualisms: the timing of origins and their consequences for coevolutionary interactions between angiosperms and frugivores. *Biol. Rev. Camb. Philos. Soc.* 91, 168–186. doi: 10.1111/brv.12164
- Fantini, E., Falcone, G., Frusciante, S., Giliberto, L., and Giuliano, G. (2013). Dissection of tomato lycopene biosynthesis through virus-induced gene silencing. *Plant Physiol.* 163, 986–998. doi: 10.1104/pp.113.224733
- Fortunato, A. E., Annunziata, R., Jaubert, M., Bouly, J. P., and Falciatore, A. (2015). Dealing with light: the widespread and multitasking cryptochrome/photolyase family in photosynthetic organisms. *J. Plant Physiol.* 172, 42–54. doi: 10.1016/j.jplph.2014.06.011
- Foth, C., Tischlinger, H., and Rauhut, O. W. (2014). New specimen of Archaeopteryx provides insights into the evolution of pennaceous feathers. *Nature* 511, 79–82. doi: 10.1038/nature13467
- Giliberto, L., Perrotta, G., Pallara, P., Weller, J. L., Fraser, P. D., Bramley, P. M., et al. (2005). Manipulation of the blue light photoreceptor cryptochrome 2 in tomato affects vegetative development, flowering time, and fruit antioxidant content. *Plant Physiol.* 137, 199–208. doi: 10.1104/pp.104.051987
- Gillaspy, G., Ben-David, H., and Gruissem, W. (1993). Fruits: a developmental perspective. *Plant Cell* 5, 1439–1451. doi: 10.1105/tpc.5.10.1439
- Givnish, T. J., Pires, J. C., Graham, S. W., McPherson, M. A., Prince, L. M., Patterson, T. B., et al. (2005). Repeated evolution of net venation and fleshy fruits among monocots in shaded habitats confirms a priori predictions: evidence from an ndhf phylogeny. *Proc. R. Soc. B.* 272, 1481–1490. doi: 10.1098/rspb.2005.3067
- Gupta, S. K., Sharma, S., Santisree, P., Kilambi, H. V., Appenroth, K., Sreelakshmi, Y., et al. (2014). Complex and shifting interactions of phytochromes regulate fruit development in tomato. *Plant Cell Environ.* 37, 1688–1702. doi: 10.1111/pce.12279
- Jarvis, E. D., Mirarab, S., Aberer, A. J., Li, B., Houde, P., Li, C., et al. (2014). Whole-genome analyses resolve early branches in the tree of life of modern birds. *Science* 346, 1320–1331. doi: 10.1126/science.1253451
- Jiao, Y., Lau, O. S., and Deng, X. W. (2007). Light-regulated transcriptional networks in higher plants. *Nat. Rev. Genet.* 8, 217–230. doi: 10.1038/nrg2049
- Jones, M. E., Anderson, C. L., Hipsley, C. A., Muller, J., Evans, S. E., and Schoch, R. R. (2013). Integration of molecules and new fossils supports a Triassic origin for Lepidosauria (lizards, snakes, and tuatara). *BMC Evol. Biol.* 13:208. doi: 10.1186/1471-2148-13-208
- Klee, H. J., and Giovannoni, J. J. (2011). Genetics and control of tomato fruit ripening and quality attributes. *Annu. Rev. Genet.* 45, 41–59. doi: 10.1146/annurev-genet-110410-132507
- Koschowitz, M. C., Fischer, C., and Sander, M. (2014). Beyond the rainbow. *Science* 346, 416–418. doi: 10.1126/science.1258957
- Leivar, P., and Monte, E. (2014). PIFs: systems integrators in plant development. *Plant Cell* 26, 56–78. doi: 10.1105/tpc.113.120857
- Levin, I., Frankel, P., Gilboa, N., Tanny, S., and Lalazar, A. (2003). The tomato dark green mutation is a novel allele of the tomato homolog of the DEETIOLATED1 gene. *Theor. Appl. Genet.* 106, 454–460.
- Li, Q., Gao, K. Q., Meng, Q., Clarke, J. A., Shawkey, M. D., D’Alba, L., et al. (2012). Reconstruction of Microraptor and the evolution of iridescent plumage. *Science* 335, 1215–1219. doi: 10.1126/science.1213780
- Li, Q., Gao, K. Q., Vinther, J., Shawkey, M. D., Clarke, J. A., D’Alba, L., et al. (2010). Plumage color patterns of an extinct dinosaur. *Science* 327, 1369–1372. doi: 10.1126/science.1186290
- Lidgard, S., and Crane, P. R. (1988). Quantitative-analyses of the early angiosperm radiation. *Nature* 331, 344–346. doi: 10.1038/331344a0
- Liu, Y., Roof, S., Ye, Z., Barry, C., van Tuinen, A., Vrebalov, J., et al. (2004). Manipulation of light signal transduction as a means of modifying fruit nutritional quality in tomato. *Proc. Natl. Acad. Sci. U.S.A.* 101, 9897–9902. doi: 10.1073/pnas.0400935101
- Llorente, B., D’Andrea, L., Ruiz-Sola, M. A., Botterweg, E., Pulido, P., Andilla, J., et al. (2015). Tomato fruit carotenoid biosynthesis is adjusted to actual ripening progression by a light-dependent mechanism. *Plant J.* 85, 107–119. doi: 10.1111/tpj.13094
- Lloyd, G. T., Davis, K. E., Pisani, D., Tarver, J. E., Ruta, M., Sakamoto, M., et al. (2008). Dinosaurs and the Cretaceous terrestrial revolution. *Proc. R. Soc. B* 275, 2483–2490. doi: 10.1098/rspb.2008.0715
- Lovisotto, A., Baldan, B., Pavanello, A., and Casadore, G. (2015). Characterization of an AGAMOUS gene expressed throughout development of the fleshy fruit-like structure produced by *Ginkgo biloba* around its seeds. *BMC Evol. Biol.* 15:139. doi: 10.1186/s12862-015-0418-x
- Lovisotto, A., Guzzo, F., Tadiello, A., Toffali, K., Favretto, A., and Casadore, G. (2012). Molecular analyses of MADS-box genes trace back to Gymnosperms the invention of fleshy fruits. *Mol. Biol. Evol.* 29, 409–419. doi: 10.1093/molbev/msr244
- Mathews, S. (2006). Phytochrome-mediated development in land plants: red light sensing evolves to meet the challenges of changing light environments. *Mol. Ecol.* 15, 3483–3503. doi: 10.1111/j.1365-294X.2006.03051.x
- Mathews, S. (2014). Algae hold clues to eukaryotic origins of plant phytochromes. *Proc. Natl. Acad. Sci. U.S.A.* 111, 15608–15609. doi: 10.1073/pnas.1417990111
- Maynard Smith, J., and Harper, D. G. C. (1995). Animal signals: models and terminology. *J. Theor. Biol.* 177, 305–311. doi: 10.1006/jtbi.1995.0248
- Moglich, A., Yang, X., Ayers, R. A., and Moffat, K. (2010). Structure and function of plant photoreceptors. *Annu. Rev. Plant Biol.* 61, 21–47. doi: 10.1146/annurev-arplant-042809-112259
- Mustilli, A. C., Fenzi, F., Ciliento, R., Alfano, F., and Bowler, C. (1999). Phenotype of the tomato high pigment-2 mutant is caused by a mutation in the tomato homolog of DEETIOLATED1. *Plant Cell* 11, 145–157. doi: 10.1105/tpc.11.2.145
- Prentice, K. C., Ruta, M., and Benton, M. J. (2011). Evolution of morphological disparity in pterosaurs. *J. Syst. Palaeontol.* 9, 337–353. doi: 10.1080/14772019.2011.565081
- Rizzini, L., Favory, J. J., Cloix, C., Faggionato, D., O’Hara, A., Kaiserli, E., et al. (2011). Perception of UV-B by the *Arabidopsis* UVR8 protein. *Science* 332, 103–106. doi: 10.1126/science.1200660
- Rockwell, N. C., Duanmu, D., Martin, S. S., Bachy, C., Price, D. C., Bhattacharya, D., et al. (2014). Eukaryotic algal phytochromes span the visible spectrum. *Proc. Natl. Acad. Sci. U.S.A.* 111, 3871–3876. doi: 10.1073/pnas.1401871111
- Roig-Villanova, I., Bou-Torrent, J., Galstyan, A., Carretero-Paulet, L., Portoles, S., Rodriguez-Concepcion, M., et al. (2007). Interaction of shade avoidance and auxin responses: a role for two novel atypical bHLH proteins. *EMBO J.* 26, 4756–4767. doi: 10.1038/sj.emboj.7601890
- Rowe, M. P. (2000). Inferring the retinal anatomy and visual capacities of extinct vertebrates. *Palaeontol. Electron.* 3, 3–43.
- Schmidt, V., Schaefer, H. M., and Winkler, H. (2004). Conspicuousness, not colour as foraging cue in plant–animal signalling. *Oikos* 106, 551–557. doi: 10.1111/j.0030-1299.2004.12769.x
- Schofield, A., and Paliyath, G. (2005). Modulation of carotenoid biosynthesis during tomato fruit ripening through phytochrome regulation of phytoene synthase activity. *Plant Phys. Biochem.* 43, 1052–1060. doi: 10.1016/j.plaphy.2005.10.006
- Schroeder, D. F., Gahrtz, M., Maxwell, B. B., Cook, R. K., Kan, J. M., Alonso, J. M., et al. (2002). De-etiolated 1 and damaged DNA binding protein 1 interact to regulate *Arabidopsis* photomorphogenesis. *Curr. Biol.* 12, 1462–1472. doi: 10.1016/S0960-9822(02)01106-5
- Schwechheimer, C., and Deng, X. W. (2000). The COP/DET/FUS proteins—regulators of eukaryotic growth and development. *Semin. Cell Dev. Biol.* 11, 495–503. doi: 10.1006/scdb.2000.0203
- Seymour, G. B., Ostergaard, L., Chapman, N. H., Knapp, S., and Martin, C. (2013). Fruit development and ripening. *Annu. Rev. Plant Biol.* 64, 219–241. doi: 10.1146/annurev-arplant-050312-120057
- Sundstrom, V. (2008). Femtobiology. *Annu. Rev. Phys. Chem.* 59, 53–77. doi: 10.1146/annurev.physchem.59.032607.093615
- Svensson, P. A., and Wong, B. B. M. (2011). Carotenoid-based signals in behavioural ecology: a review. *Behaviour* 148, 131–189. doi: 10.1163/000579510X548673

- Tiffney, B. H. (2004). Vertebrate dispersal of seed plants through time. *Annu. Rev. Ecol. Evol. S* 35, 1–29. doi: 10.1146/annurev.ecolsys.34.011802.132535
- Tohge, T., Alseekh, S., and Fernie, A. R. (2014). On the regulation and function of secondary metabolism during fruit development and ripening. *J. Exp. Bot.* 65, 4599–4611. doi: 10.1093/jxb/ert443
- Toledo-Ortiz, G., Huq, E., and Rodriguez-Concepcion, M. (2010). Direct regulation of phytoene synthase gene expression and carotenoid biosynthesis by phytochrome-interacting factors. *Proc. Natl. Acad. Sci. U.S.A.* 107, 11626–11631. doi: 10.1073/pnas.0914428107
- Vullo, R., Marugan-Lobon, J., Kellner, A. W., Buscalioni, A. D., Gomez, B., de la Fuente, M., et al. (2012). A new crested pterosaur from the Early Cretaceous of Spain: the first European tapejarid (Pterodactyloidea: Azhdarchoidea). *PLoS ONE* 7:e38900. doi: 10.1371/journal.pone.0038900
- Wang, S., Liu, J., Feng, Y., Niu, X., Giovannoni, J., and Liu, Y. (2008). Altered plastid levels and potential for improved fruit nutrient content by downregulation of the tomato DDB1-interacting protein CUL4. *Plant J.* 55, 89–103. doi: 10.1111/j.1365-313X.2008.03489.x
- Weller, J. L., Schreuder, M. E., Smith, H., Koornneef, M., and Kendrick, R. E. (2000). Physiological interactions of phytochromes A, B1 and B2 in the control of development in tomato. *Plant J.* 24, 345–356. doi: 10.1046/j.1365-313x.2000.00879.x
- Wilson, G. P., Evans, A. R., Corfe, I. J., Smits, P. D., Fortelius, M., and Jernvall, J. (2012). Adaptive radiation of multituberculate mammals before the extinction of dinosaurs. *Nature* 483, 457–460. doi: 10.1038/nature10880
- Yang, Y., and Wang, Q. (2013). The earliest fleshy cone of Ephedra from the early cretaceous Yixian Formation of northeast China. *PLoS ONE* 8:e53652. doi: 10.1371/journal.pone.0053652
- Yen, H. C., Shelton, B. A., Howard, L. R., Lee, S., Vrebalov, J., and Giovannoni, J. J. (1997). The tomato high-pigment (hp) locus maps to chromosome 2 and influences plastome copy number and fruit quality. *Theor. Appl. Genet.* 95, 1069–1079. doi: 10.1007/s001220050664
- Zhang, F., Kearns, S. L., Orr, P. J., Benton, M. J., Zhou, Z., Johnson, D., et al. (2010). Fossilized melanosomes and the colour of Cretaceous dinosaurs and birds. *Nature* 463, 1075–1078. doi: 10.1038/nature08740

Conflict of Interest Statement: The authors declare that the research was conducted in the absence of any commercial or financial relationships that could be construed as a potential conflict of interest.

Copyright © 2016 Llorente, D'Andrea and Rodríguez-Concepción. This is an open-access article distributed under the terms of the Creative Commons Attribution License (CC BY). The use, distribution or reproduction in other forums is permitted, provided the original author(s) or licensor are credited and that the original publication in this journal is cited, in accordance with accepted academic practice. No use, distribution or reproduction is permitted which does not comply with these terms.



In silico Transcriptional Regulatory Networks Involved in Tomato Fruit Ripening

Stilianos Arhondakis, Craita E. Bita, Andreas Perrakis, Maria E. Manioudaki,
Afrodi Krokida, Dimitrios Kaloudas and Panagiotis Kalaitzis *

Department of Horticultural Genetics and Biotechnology, Mediterranean Agronomic Institute of Chania, Chania, Greece

Tomato fruit ripening is a complex developmental programme partly mediated by transcriptional regulatory networks. Several transcription factors (TFs) which are members of gene families such as MADS-box and ERF were shown to play a significant role in ripening through interconnections into an intricate network. The accumulation of large datasets of expression profiles corresponding to different stages of tomato fruit ripening and the availability of bioinformatics tools for their analysis provide an opportunity to identify TFs which might regulate gene clusters with similar co-expression patterns. We identified two TFs, a SIWRKY22-like and a SIER24 transcriptional activator which were shown to regulate modules by using the LeMoNe algorithm for the analysis of our microarray datasets representing four stages of fruit ripening, breaker, turning, pink and red ripe. The WRKY22-like module comprised a subgroup of six various calcium sensing transcripts with similar to the TF expression patterns according to real time PCR validation. A promoter motif search identified a *cis acting* element, the W-box, recognized by WRKY TFs that was present in the promoter region of all six calcium sensing genes. Moreover, publicly available microarray datasets of similar ripening stages were also analyzed with LeMoNe resulting in TFs such as SIERF.E1, SIERF.C1, SIERF.B2, SIERF.A2, SIWRKY24, SLWRKY37, and MADS-box/TM29 which might also play an important role in regulation of ripening. These results suggest that the SIWRKY22-like might be involved in the coordinated regulation of expression of the six calcium sensing genes. Conclusively the LeMoNe tool might lead to the identification of putative TF targets for further physiological analysis as regulators of tomato fruit ripening.

OPEN ACCESS

Edited by:

Mario Pezzotti,
University of Verona, Italy

Reviewed by:

Xinguang Zhu,
University of Chinese Academy of
Sciences, China
Uener Kolukisaoglu,
University of Tübingen, Germany

*Correspondence:

Panagiotis Kalaitzis
panagiot@maich.gr

Specialty section:

This article was submitted to
Plant Physiology,
a section of the journal
Frontiers in Plant Science

Received: 27 February 2016

Accepted: 03 August 2016

Published: 30 August 2016

Citation:

Arhondakis S, Bita CE, Perrakis A,
Manioudaki ME, Krokida A,
Kaloudas D and Kalaitzis P (2016) In
silico Transcriptional Regulatory
Networks Involved in Tomato Fruit
Ripening. *Front. Plant Sci.* 7:1234.
doi: 10.3389/fpls.2016.01234

INTRODUCTION

Fleshy fruit development and ripening is a complex developmental process which is regulated by hormones and plethora of transcription factors (TFs) (Seymour et al., 2013). The evolution of this process requires the action of intricate regulatory networks of TFs (Seymour et al., 2013). In tomato fruit ripening, several TFs were demonstrated to play a central regulatory role such as the MADS box proteins RIPENING INHIBITOR (RIN) (Vrebalov et al., 2002), TOMATO AGAMOUS-LIKE1 (TAGL1) (Vrebalov et al., 2009) and FUL1/TDR4 and FUL2/MBP7 (Bemer et al., 2012). Additional classes of TFs were also shown to regulate tomato ripening such as the COLORLESS NON-RIPENING (CNR) which is a SBP TF (Manning et al., 2006), the NON-RIPENING (NOR) which was identified as a NAC domain TF (Martel et al., 2011) as well as the large class of ETHYLENE RESPONSE FACTORS (ERFs) which

belong to the AP2/ERF family mediating mostly ethylene-dependent gene expression (Pirrello et al., 2012). Alterations in the expression of these TFs results in phenotypes with alterations in all aspects of fruit ripening including carotenoids and flavonoids biosynthesis, fruit softening, fruit size and shape, chloroplast degradation and chromoplast development (Klee and Giovannoni, 2014).

The physiological significance of other families of TFs such as the members of the WRKY gene family has not been investigated in tomato fruit development and ripening despite the fact that several of them are expressed in the fruit during various developmental stages (Huang et al., 2012). It was recently reported that five WRKY genes were upregulated in post-climacteric Chinese pear fruits suggesting association with fruit ripening development (Huang et al., 2014).

Despite the significant progress in the elucidation of the roles and interactions of the transcriptional regulators during tomato fruit ripening there are still unknown regulatory TFs and interactions which need to be investigated (Karlová et al., 2014). In this context, *in silico* analysis of large gene expression datasets has been used in the recent years in order to construct gene regulatory networks (Pan et al., 2013; Clevenger et al., 2015).

A tomato fruit gene regulatory network comprising TF gene expression profiles was generated using artificial network inference analysis to analyze Affymetrix GeneChip transcriptomic data from two different developmental and ripening stages, Mature Green (MG) and Breaker + 7 (Pan et al., 2013). A novel and fruit-related regulator of pigment accumulation in tomato was identified and its function was validated in transgenic plants indicating the significance of network analysis on the identification of regulatory TFs (Pan et al., 2013). In another report, transcriptome analysis of tomato fruit tissues expressing the tomato fruit shape gene SUN resulted in shifts of transcript profiles and metabolites according to gene regulatory network analysis and networks of metabolite correlations (Clevenger et al., 2015). The gene regulatory network analysis was based on the clustering of differentially expressed genes based on the \log_2 fold change using fuzzy C means (Clevenger et al., 2015). It was found that the main node represented genes related to calcium-regulated processes indicating involvement in calcium signaling.

Calcium signals are decoded by several types of Ca^{2+} sensor proteins that contain a high-affinity Ca^{2+} binding motif, the “EF-hand” motif. The three classes of Ca^{2+} sensors include the Calmodulin (CaM), the calcium-dependent protein kinase (CDPK) and the calcineurin B-like protein (CBL) (Kim et al., 2009). It was demonstrated that these Ca^{2+} sensors are involved in transcriptional regulation either directly by binding to TFs and ensuing modulation of their functions or indirectly by modulating posttranslational modification of TFs (Kim et al., 2009).

Recently, a reverse engineering algorithm, LeMoNe (Learning Module Networks) (Joshi et al., 2009) was used to predict gene regulatory networks in soybean nodulation (Zhu et al., 2013), salinity response of two olive cultivars (Bazakos et al., 2012), response of *Arabidopsis* under oxidative stress (Vermeirissen et al., 2014) as well as investigation of fruit acidity in diverse

apples (Bai et al., 2015). LeMoNe is a software package that uses probabilistic, ensemble-based optimization techniques (Joshi et al., 2008, 2009) to extract ensemble transcription regulatory networks of co-expression (Michoel et al., 2007). Genes are first partitioned into co-expression modules and regulators are assigned to modules based on how well they explain the condition-dependent expression behavior of the module (Joshi et al., 2008, 2009).

The goal of this study was to generate gene regulatory networks by analyzing Affymetrix GeneChip expression datasets from four different stages of tomato fruit ripening, Breaker (Br), Turning (Tu), Pink (Pk) and Red Ripe (RR) with the LeMoNe algorithm in order to identify co expression modules and their putative regulatory TFs. The output was compared with the gene regulatory networks which were identified with a similar LeMoNe algorithm analysis of publicly available Affymetrix GeneChip datasets from similar stages of fruit ripening. Further analysis of the modules resulted in the identification of putative regulatory TFs such as a WRKY and an ERF and a subset of calcium signaling genes such as Calcium-binding EF hand family protein (CBF), Calmodulin-like protein, Calcium dependent protein kinase, Calmodulin-binding heat-shock protein and Calcineurin B-like protein kinase. The expression patterns of these TFs and of the calcium signaling subset of genes were determined using real time PCR. The findings provide possible TF targets for further investigation of their role during fruit ripening through regulation of calcium signaling.

MATERIALS AND METHODS

RNA Extraction and cDNA Synthesis

Total RNA was isolated from 200 mg fruit tissue at the stage of breaker (BR), turning (TU), pink (PK) and red ripe (RR) from wild type tomato cv. Ailsa-Craig (*S. lycopersicum*) ground in liquid nitrogen and purified using RNeasy[®] plant mini kit (QIAGEN). Progress of ripening was broadly defined on the basis of skin color and development. 30 μg aliquots were fractionated on a denaturing 1.2% (wt/vol) agarose gel containing formaldehyde to verify RNA quality. First-strand cDNA was performed from 200 ng of the DNase-treated RNA according to the manufacturer's instructions using SuperScriptTM II RNase H-Reverse Transcriptase (Invitrogen, Carlsbad, CA).

qRT-PCR Analyses

Gene expression analysis was performed using a 48-well StepOnePlusTM Real-Time PCR System (ThermoFisher Scientific). Standard dilution curves were performed for each gene fragment. For normalization α -actin primers were chosen instead of Ubiquitin and GAPDH, as they exhibited higher expression stability and uniform efficiency as tested by qPCR and analyzed by Bestkeeper Software. Primers were designed using the Primer Express v2.0 software (<http://bioinfo.ut.ee/primer3/>) based on two different exons of the gene of interest; the sequences of the primers are listed in the **Supplementary Table 1**. A serial dilution of 0.5, 5, 50, and 250 ng of each studied gene was used to determine the amplification efficiency for each target and housekeeping gene. The qRT-PCR reaction (20 μl) mix consisted

of gene specific primers, SYBR® Green PCR Master Mix (ThermoFisher Scientific) and the template on three biological and technical replicates. The thermal cycling conditions were 50°C for 2 min, 95°C for 10 min followed by 95°C for 15 s, 60°C for 30 s and 72°C for 30 s for 40 cycles. For negative control, RT reaction mix without reverse transcriptase was used as a template. At the end, the melting temperature of the product was determined to verify the specificity of the amplified fragment. Data were analyzed using the 2– $\Delta\Delta CT$ method (Livak and Schmittgen, 2001) and presented as relative levels of gene expression.

Microarray Hybridization

We used the custom designed TomGene ST 1.1 array strips and the Affymetrix GeneAtlas Personal Microarray System to monitor differences in gene expression of abscission zones of tomato fruits in different ripening stages. The array design is based on the most recent genomic content and offers the highest probe coverage (up to 25 probes selected across the entire gene). This allows for accurate detection for whole-transcriptome microarray analysis and provides higher resolution and accuracy than other microarray solutions on the market. The tomato GeneChip® genome array contains 22,821 probe sets including 9 tomato housekeeping genes with 19 probe sets, 22,714 tomato EST assembly sequences, 43 public tomato sequence not in assembly and 45 Affymetrix control probe sets. In sum, there are 22,776 probe sets for tomato genes. Each probe set contains 11 pairs of perfect-match and mismatch probes for cross-hybridization control. Probe sequence selection is based toward the 3'-end of the ORF. Among 22,714 tomato EST assembly sequences, 16,800 probe sets with description using cutoff *e*-value as 1.00E-04, 5914 probe sets are with no description. It was estimated that there are 35,000 genes comprising the tomato genome (Tomato Genome Consortium, 2012). Therefore, the GeneChip genome array covers approximately 65% of the tomato genome.

For target preparation, 500 nanograms of total RNA was used as starting material and single stranded cDNA was prepared using the Affymetrix GeneChip WT Plus Reagent Kit according to the relevant Manual Target Preparation for GeneChip Whole Transcript Expression Arrays (No. 703174 Rev. 2). The single stranded cDNA was then fragmented and labeled, then hybridized to the probe array for 20 h at 48°C using the Hybridization station of the Affymetrix system. Immediately after hybridization, the array strips underwent an automated washing and staining protocol on the GeneAtlas Fluidics station using the GeneChip® Hybridization, Wash, and Stain Kit, then imaging on the GeneAtlas scanner. In total, the 9 samples were hybridized. The CEL files of these experiments are available in Gene Expression Omnibus (GEO; accession GSE78733; <http://www.ncbi.nlm.nih.gov/geo/query/acc.cgi?token=wfktmcukfvkpav&acc=GSE78733>).

The probe array was then washed and stained in the Fluidics Station, and scanned on the Imaging Station. Specific experimental information was defined using Affymetrix GeneChip Operating Software (GCOS) on a personal computer-compatible workstation. The array strip scan was also controlled

by the GCOS software to define the probe cells and to compute the intensity for each cell. Two independent biological replicates were assessed for each of the 4 developmental stages assessed.

Microarray Analysis

Imaging of each array strip resulted in a.CEL file that contained the results of the intensity calculations on the pixel values corresponding to each probe on the array. This file was then imported in the Expression Console software to perform gene-level normalization and signal summarization as well as the quality control of the files using default parameter settings and output the.CHP files for further processing. These files were then imported in Affymetrix Transcriptome Analysis Console v.2.0 to obtain the bi-weight average signal of each pair of biological replicate. Afterwards, between each comparison the statistically significant differentially expressed genes were assessed (Fold-Change > ±2, *p* < 0.05).

All procedures for probe preparation, hybridization, washing, staining, and scanning of the TomGene Affymetrix microarray strips, as well as data collection and interpretation were performed at the Horticultural Genetics and Biotechnology Department, MAICH, Chania, Greece.

Network Analysis

The differential expression transcriptomes of Turning, Pink and Red Ripe compared to Breaker were generated, and the interacting relations among transcription factors and target transcripts were identified. In order to infer the module networks for the three pairs, Turning vs. Breaker, Pink vs. Breaker, and Red Ripe vs. Breaker, the LeMoNe algorithm (Michoel et al., 2007; Bonnet et al., 2010a) was used. LeMoNe uses ensemble based probabilistic optimization techniques to identify clusters of co-expressed transcripts as well as their regulators (Bonnet et al., 2010b). First it searches for clusters of co-expressed transcripts and subsequently defines a regulatory program for each cluster. Local optima traps in the first step are avoided using a Gibbs sampling approach for two-way clustering of both transcripts and conditions (Bonnet et al., 2010a). The algorithm receives as input the expression profiles of transcripts across the experimental conditions as well as a list of potential regulators.

In this study the fold-change (Stage/Breaker) of ~6.100 transcripts found to be differentially expressed (Fold Change > ±2, *p* < 0.05) either in Turning, Pink or Red Ripe vs. Breaker was used as transcript expression input. In order to infer the co-expressed modules for the ~6.100 DEGs, fold-change data were clustered based on the Gibbs sampler method (Joshi et al., 2008). To identify reliable clusters we performed 10 independent Gibbs sampler runs with number of clusters half of the amount of genes of the dataset. Finally, clusters were integrated to generate a robust clustering solution, tight clustering, through an ensemble of multiple “ganesh” runs (Bonnet et al., 2015). Afterwards, using a list of ~1700 potential regulators, identified using annotation description as indicated by the terms, “regulators,” “regulation of transcription,” and “transcription regulator activity,” LeMoNe assigned the corresponding regulators in each module characterized by a particular weight (probabilistic score), representing the strength

with which a regulator participates in each module. The significance of those probabilistic scores is determined by comparing the assigned regulators with randomly assigned regulators, using a *t-test* comparing their means. The output is a group of clusters composed of mutually exclusive co-expressed transcripts, with a list of high-scoring regulators attached to each cluster, prioritized according to the corresponding weight. The final set of regulators involved in the regulation of a module, was set by eliminating those with a threshold lower to the threshold of the maximum weight of the randomly assigned regulators.

RESULTS AND DISCUSSION

Construction of Fruit Ripening Regulatory Networks

Expression profiles can be used to infer regulatory networks and key transcription factors (Cramer et al., 2011). We constructed tomato fruit ripening regulatory module networks by analyzing microarray data from different stages of fruit ripening using the LeMoNe algorithm (Michoel et al., 2007; Bonnet et al., 2010a). The output of the algorithm is a set of modules of co-expressed transcripts, with a list of high-scoring transcription factors (TF) regulating the clusters which were prioritized according to their corresponding weight. Specifically, the algorithm assigns sets of TF regulators to each of the modules using a probabilistic scoring, taking into account the profile of the candidate regulator.

Initially, publicly available microarray raw data from tomato fruit ripening stages of Br (Breaker), Br +3, Br + 5, and Br + 7 (Lopez-Gomollon et al., 2012) were retrieved from the GEO database and processed with the Affymetrix Expression Console using the RMA algorithm (Bolstad et al., 2003). This microarray comprised 10,209 probes (Lopez-Gomollon et al., 2012). The expression level (log₂Signa) for each probe was estimated using RMA in the stages of BR, BR+3 (Turning), BR+5 (Pink) and BR+7 (Red Ripe).

The entire dataset of the probes was processed by the LeMoNe algorithm leading to the construction of 107 modules with 770 redundant TFs distributed across the modules. The top 1% TFs (Bonnet et al., 2015) with the higher weight was comprised of seven TFs; two WRKYs, WRKY 24 (Solyc09g066010) and WRKY37 (Solyc01g079360) (Huang et al., 2012); four Ethylene-responsive TFs, SIERF1a (ERF.C1; Solyc05g051200.1.1), SIERF1b (Solyc03g093610), SIERF2b (ERF.E1 or TERF1/JERF2; Solyc09g075420), SIERF5 (ERF.B2; Solyc03g093560) (Pan et al., 2012; Pirrello et al., 2006, 2012) and one MADS-box/TM29 (Solyc02g089200) (**Supplementary Table 2**). These seven TFs were found to regulate five distinct modules (**Figure 1**). The SIERF.C1 and SIERF.A2 co-regulated module M27 which comprised 77 genes, while the SIERF.B2, SIERF.E1 and WRKY24 co-regulated module 32 with 123 genes (**Figure 1**). The WRKY37 regulated two modules, M76 and M79 comprising 119 and 59 genes, respectively (**Figure 1**). Moreover, the MADS box/TM29 regulated module M38 with 88 genes (**Figure 1**).

The WRKY24 and WRKY37 comprise one WRKY domain, a zinc-finger motif and belong to the group II-d and II-e,

respectively according to a phylogenetic tree of WRKY genes among tomato, Arabidopsis and rice (Huang et al., 2012). The group II-e represents a unique WRKY gene expansion event that occurred only in Solanaceae species (Huang et al., 2012). The involvement of WRKYS in tomato fruit ripening has not been investigated extensively although a recent report showed that five WRKY genes were up-regulated in the post-climacteric stages of Chinese Pear (*Pyrus ussuriensis*) fruits (Huang et al., 2014).

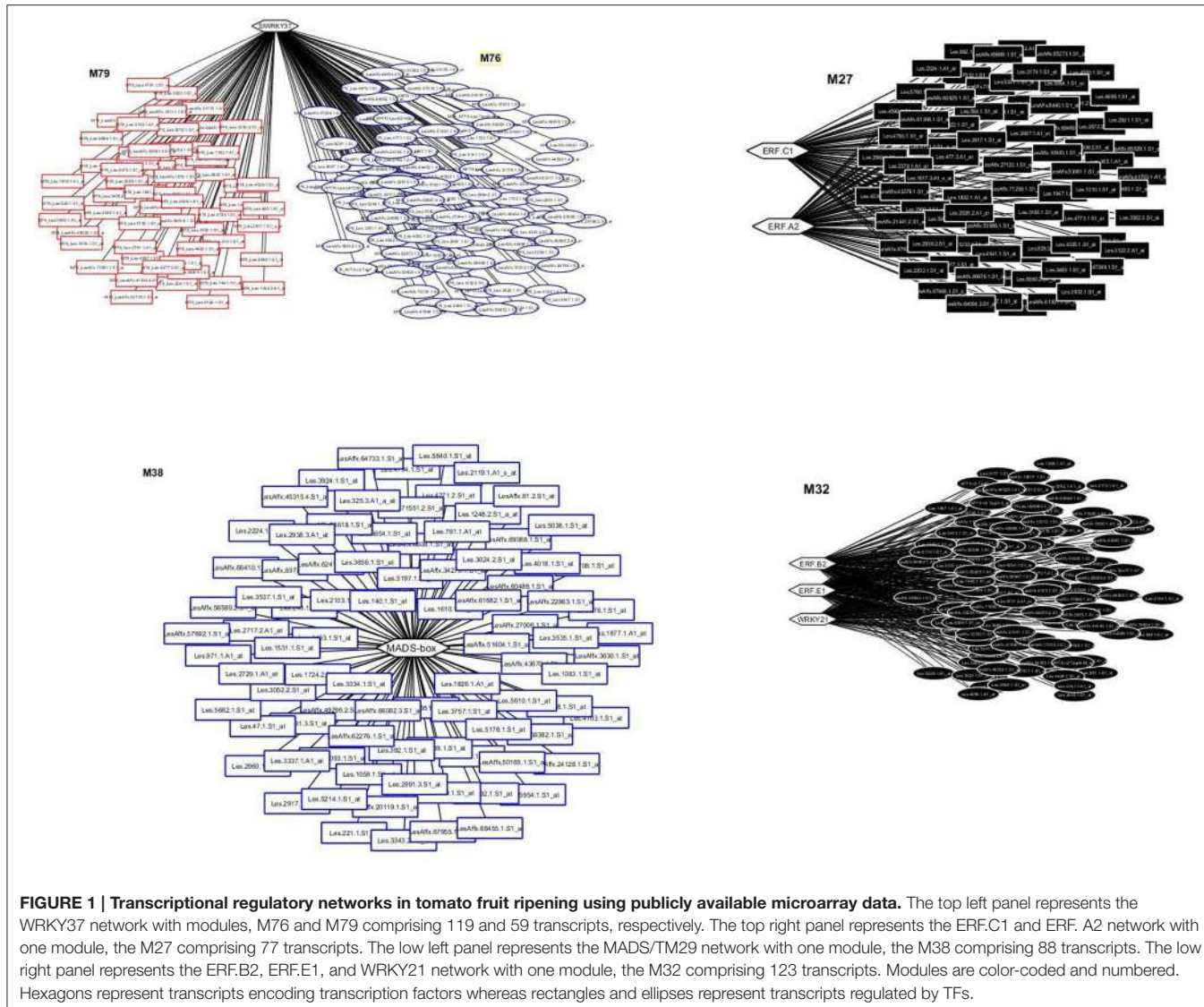
The SIERF.C1, SIERF.E1, SIERF.B2, SIERF.A2 are members of the tomato ERF family (Liu et al., 2016). The SIERF.E1 is considered one of the main ripening-associated genes among all tomato ERFs due to the significant up-regulation at the onset of ripening as well as the dramatic down-regulation in the ripening mutants *rin*, *Nr* and *nor* (Liu et al., 2016). Moreover, the SIERF.E1 was shown to be induced by ethylene while RIN was demonstrated to act as positive regulator of the promoter activity of SIERF.E1 (Liu et al., 2016). The SIERF.C1 and the SIERF.B2 are also considered among the 19 ERF best candidates for regulating the ripening process based on their ripening-related pattern and high expression levels (Liu et al., 2016). The SIERF.B2 is also among only three ERFs which are consistently induced in the *rin*, *Nr* and *nor* ripening mutants suggesting that reduced expression levels at the onset of ripening might be required for progression of this process (Liu et al., 2016). In addition, the SIERF.B2 was found to promote adaptation to drought and salt tolerance in tomato (Pan et al., 2012). The SIERF.A2 seems to have the lower importance for fruit ripening considering that is strongly down-regulated during this process while exhibiting high expression in roots, leaves and immature fruits (Liu et al., 2016).

The MADS-box/TM29 is a tomato SEPALLATA homolog which was shown to be involved in parthenocarpic fruit development and floral reversion (Ampomah-Dwamena et al., 2002). Moreover, it was also considered as a putative FRUITFULL1 (FUL1) interacting partner due to their strong expression in ripening fruits (Fujisawa et al., 2014).

The LeMoNe algorithm resulted in the identification of seven TFs as putative regulators of five modules according to their co-expression patterns (**Figure 1**). Three ERFs, SIERF.E1, SIERF.B2, and SIERF.C1, as well as one MADS-box/TM29 are considered to play a role in fruit ripening suggesting that this algorithm might be used to identify TFs with putative regulatory function. The involvement of the WRKYS remains to be determined.

Analysis of Fruit Ripening Regulatory Networks and Modules

A microarray experiment was performed with four fruit ripening stages, breaker, turning, pink and red ripe and the expression data were analyzed using the LeMoNe algorithm. The Affymetrix microarray comprised 37,897 probes compared to the 10,209 probes of the previous analysis. The expression data suggested that most of the changes in expression occurred at turning and pink stages with genes undergoing a massive down-regulation (**Supplementary Figures 1–4** and **Supplementary Table 3**). Contrary, an up-regulation of the majority of genes was observed at the red ripe stage (**Supplementary Figures 1–4** and **Supplementary Table 3**).



Analysis of the microarray data resulted in the identification of 6,100 Differentially Expressed Genes (Fold Change $> \pm 2$, $p < 0.05$) either in Turning, Pink or Red Ripe vs. breaker. The DEGs and a list of putative transcription factors were analyzed using the LeMoNe algorithm resulting in 193 modules (M0 to M192; **Supplementary Table 4**).

The 193 modules are associated with 1052 TFs representing 196 unique TFs. The redundancy in TFs is explained by the fact that one TF can regulate more than one module while most of the modules comprise TFs. Only two TFs had a weight higher than the random threshold after using two different clustering procedures for the partition of the DEGs into modules of co-expressed genes with the LeMoNe tool. The Affymetrix microarray datasets of Lopez-Gomollon et al. (2012) comprised 10,209 probes and were analyzed using the entire expression data. We used the TomGene ST 1.1 Affymetrix microarray and analyzed only the DEGs. The

TomGene ST 1.1 comprises 37,897 *Solanum lycopersicum* probes. This probably justifies the different output of LeMoNe algorithm after analysis of microarray data from similar developmental stages of fruit ripening. It is worth mentioning that WRKY22-like and ER24 probes were not present in the 10,209 probe-microarray.

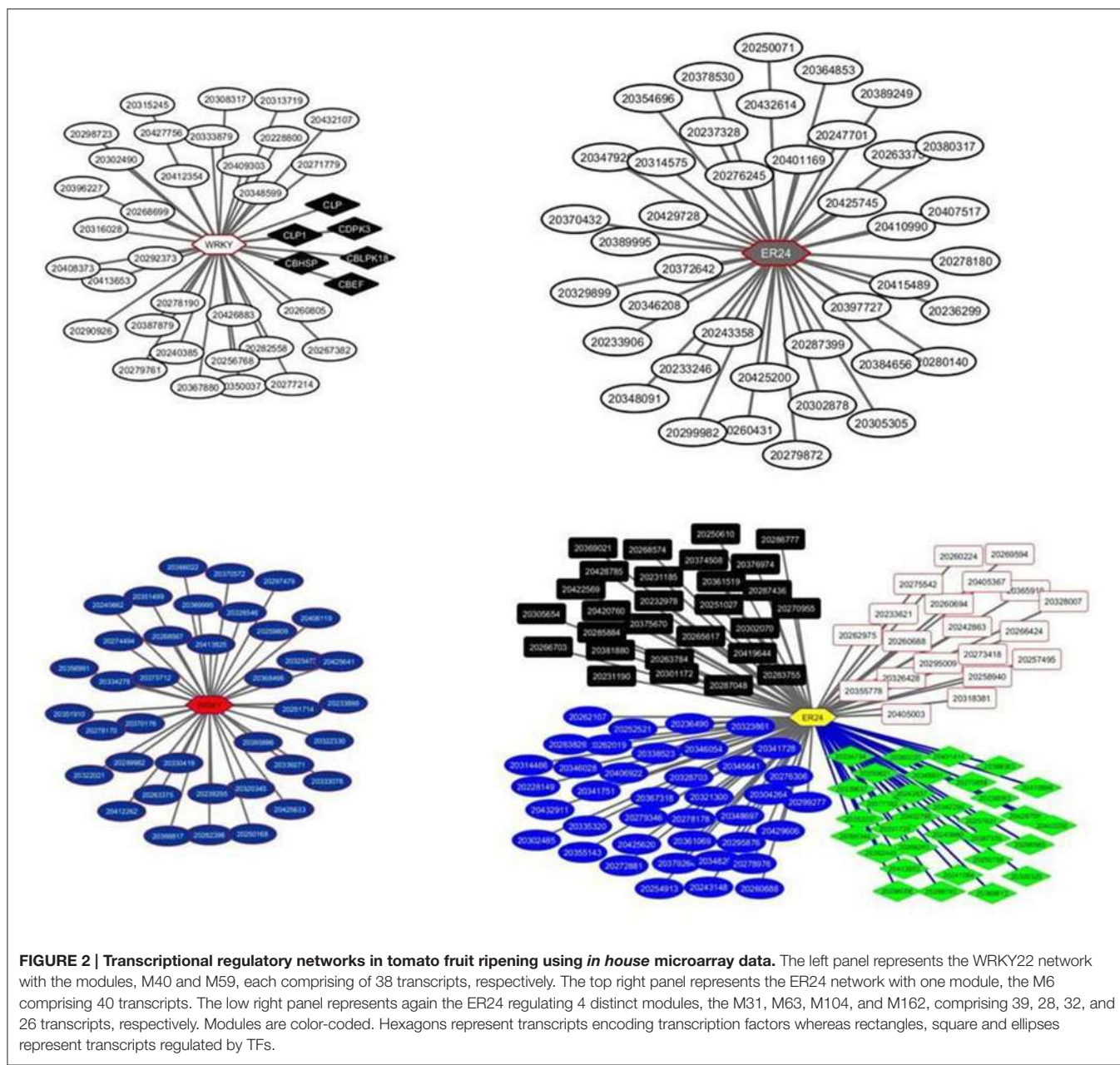
The two TFs are the WRKY TF 22-like (Solyc05g050050.1.1) and an Ethylene-responsive transcriptional coactivator (ER24) (Solyc01g104740.2.1). The WRKY regulates the module M40 comprising 38 transcripts while the ER24 regulates the module 6 comprising 40 transcripts (**Figure 2**). Both modules showed similar expression patterns with a significant down regulation in the turning and pink stages and an upregulation in the red ripe stage to the initial breaker stage levels (**Figure 3**). It is interesting to note that the expression patterns of the two TFs are similar but still slightly divergent from the pattern of the genes comprising the module (**Figure 4** and **Supplementary Figure 5**).

The same microarray datasets were analyzed again with LeMoNe using different clustering parameters such as the level of the number of initial clusters (50% of the genes in the matrix) and the number of runs of the Gibbs sampler (10 runs). This analysis resulted in 191 modules and 1040 potential TFs, representing 161 non redundant TFs. Only five among those TFs had a weight higher to the maximum threshold of the random weight, representing two non-redundant TFs, the WRKY22 and ER24. The same exactly TFs were identified in the previous analysis of the expression datasets by the LeMoNe algorithm suggesting a level of output consistency. However, changes were observed in the number of modules regulated by the two TFs. The WRKY22 was found to regulate again one module, the M59, containing 38 transcripts while the ER24 was found to be

involved in the regulation of four modules, the M31, M63, M104, and M162, containing, 39, 28, 32, and 26 transcripts, respectively (**Figure 2**).

Real time PCR was used to further validate the expression levels of both TFs. The expression of WRKY significantly decreased in the turning and red ripe stage while slight down regulation was also observed in the pink stage (**Figure 5**). The ER24 showed gradual up regulation in the turning and pink stage by 14- and 28-fold, respectively which was not sustained in the red ripe stage (**Figure 5**). These patterns of expression can be considered almost similar to those observed in the microarray analysis (**Figures 3, 4** and **Supplementary Figure 5**).

The WRKY 22 comprises one WRKY domain, a zinc-finger motif and belongs to the Group II-e according to a phylogenetic



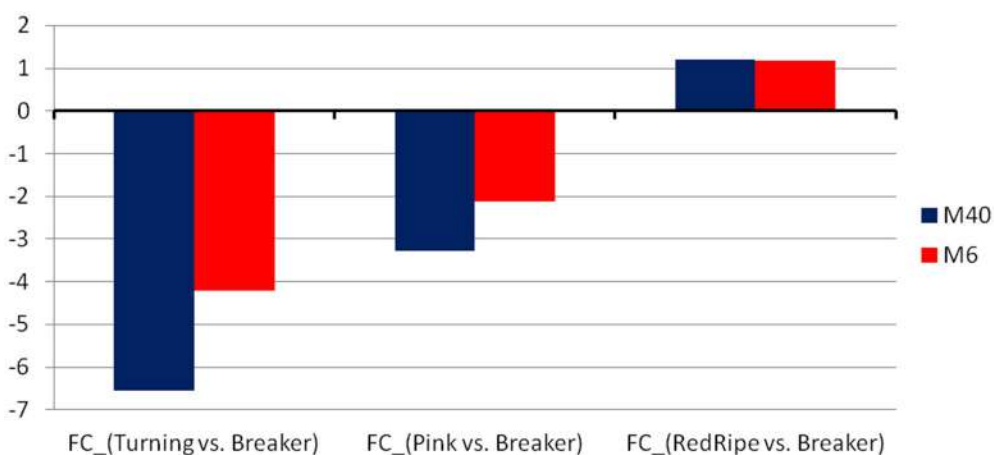


FIGURE 3 | The average fold-change of the two modules, M40 and M6, found to be regulated by the WRKY and the ER24 TFs, respectively.

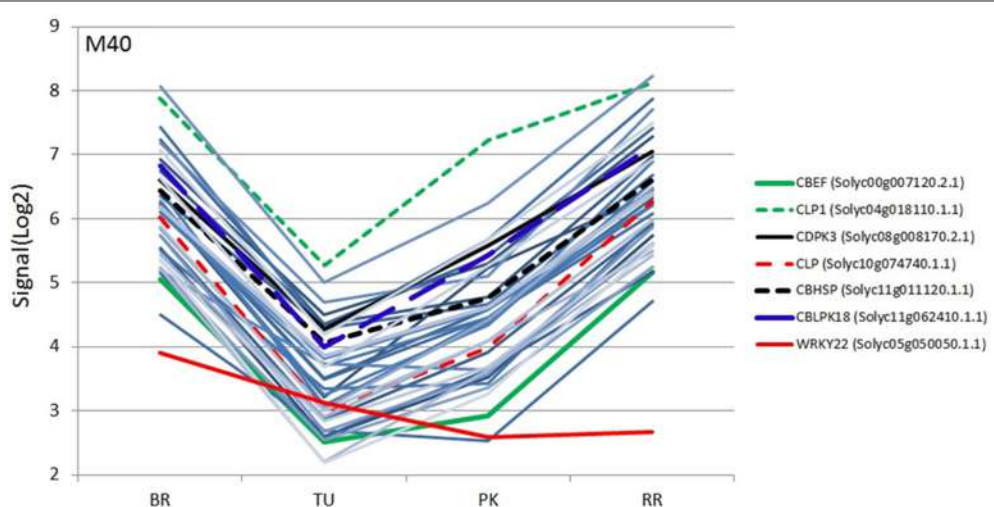


FIGURE 4 | Expression profiles (SignalLog2) of module M40 transcripts and WRKY22 TF in BR (Breaker), TU (Turning), PK (Pink) and RR (Red Ripe) stages based on the microarray data. The expression profiles of the WRKY22 and the six calcium signaling transcripts are represented by different colors (see inset) and the other transcripts with the same color lines (light blue).

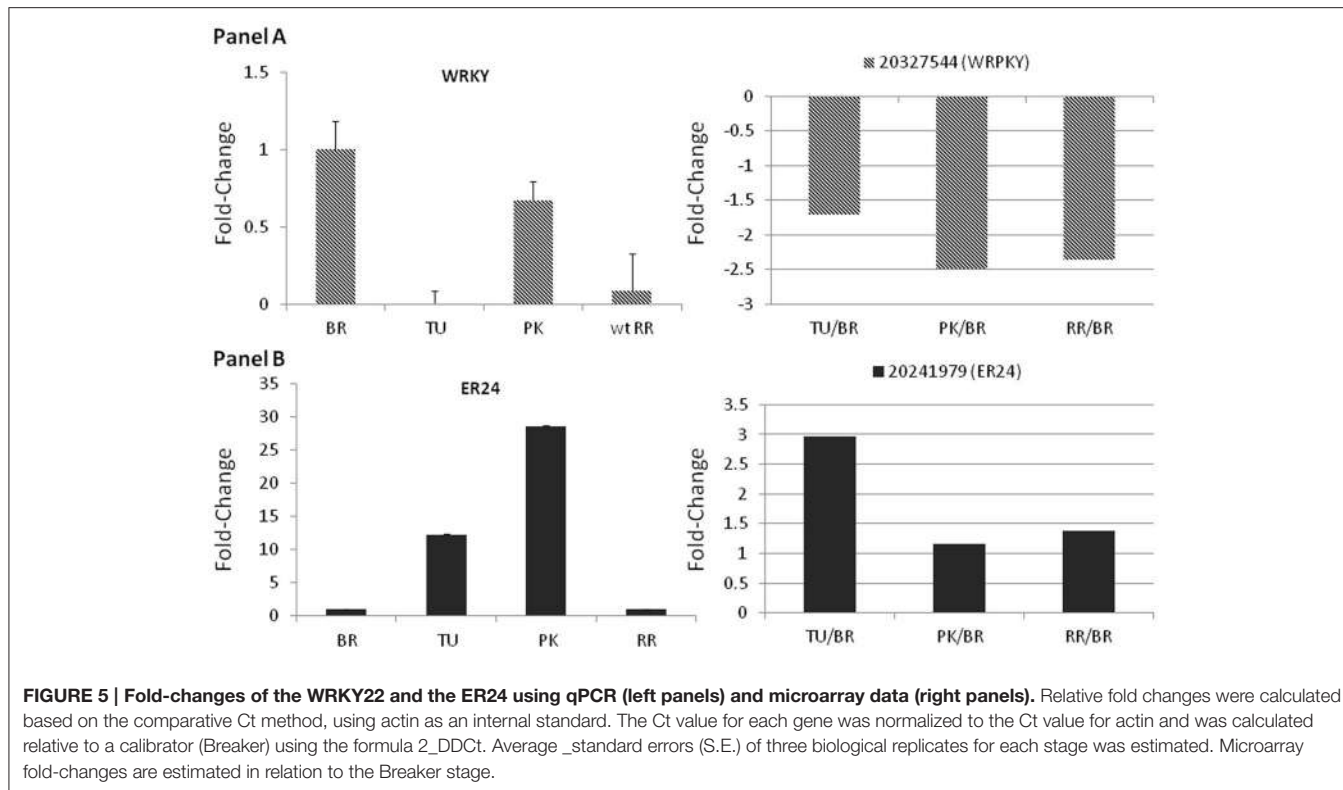
tree of WRKY genes among tomato, Arabidopsis and rice (Huang et al., 2012). The WRKY 22 is one out of eight unique, divergent tomato WRKYS which form a distinct subclade in Group II-e which is considered the result of a distinct gene expansion event (Huang et al., 2012). Moreover, the characterized motif compositions allow Group II-e members in tomato to be divided into distinct subclasses (Huang et al., 2012). A group of WRKY genes, group II-c were suggested to be involved in berry ripening and cold acclimation in grapevine (Wang et al., 2014). However, the physiological significance of WRKYS in tomato fruit ripening needs to be further investigated.

The ER24 is homologous to multi-protein bridging factor MBF1 involved in transcriptional activation and was shown to be strongly induced by ethylene in tomato fruit (Zegzouti et al., 1999). In addition, a gradual increase in expression was observed

during ripening which peaked at the red ripe stage while no expression could be detected in the leaves either before or after ethylene treatment indicating that ER24 is predominantly a fruit ripening-related co-activator (Zegzouti et al., 1999).

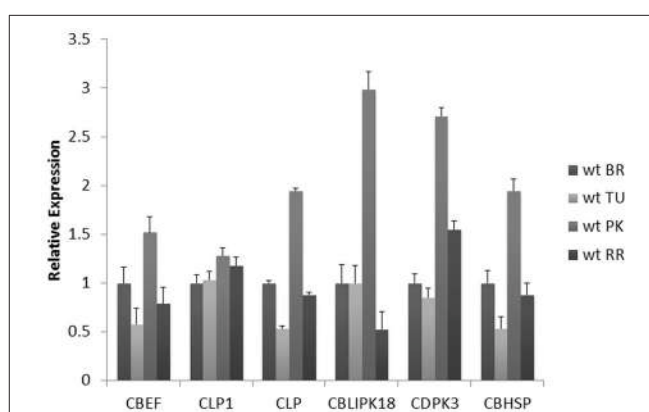
A WRKY22 Module Comprises a Subgroup of Calcium Signaling Genes

The module 40 comprised 38 transcripts including six mRNAs involved in Calcium regulation, 11 uncharacterized, two mRNAs related to protein phosphorylation encoding a Serine/threonine-protein phosphatase 6 regulatory subunit 3 and a Serine/threonine-protein kinase-like protein, two mRNAs involved in protein and peptides degradation such as an Oligopeptidase A and an Ubiquitin carboxyl-terminal hydrolase (**Supplementary Table 5**).



Further analysis was focused on the Calcium homeostasis-related group of six mRNAs. This group comprised of a Calcium-binding EF hand family protein (CBEF) (*Solyc00g007120.2.1*), Calcium-binding EF (CBEF), Calmodulin-like protein (CLP) (*Solyc10g074740.1.1*), Calmodulin-like protein 1 with an EF-Hand type domain (CLP1) (*Solyc04g018110.1.1*), Calcium dependent protein kinase 3 (CDPK3) (*Solyc08g008170.2.1*), Calmodulin-binding heat-shock protein (CBHSP) (*Solyc11g011120.1.1*) and a Calcineurin B-like (CBL)-interacting protein kinase 18 (CBLPK18) (*Solyc11g062410.1.1*). These six genes might have similar co-expression patterns during fruit ripening considering that they are members of the same module. Therefore, their expression was determined during the four stages of ripening using real time PCR to further validate this assumption (Figure 6). The CBEF, CLP1, CLP, CBLPK18, and CBHSP have identical patterns of expression characterized by a decrease in the turning followed by an up-regulation in the pink and return to lower levels in the red ripe stage (Figure 6). The only exception is the expression pattern of CDPK3 which showed a gradual increase up to the pink stage followed by down regulation in the red ripe stage (Figure 6). However, the pattern of CDPK3 expression can only be considered slightly different compared to the other five transcripts (Figure 6).

The promoter sequences of the six calcium related genes were extracted from Sol Genomics and the presence of functional motifs was determined using ScanWM-PL (<http://www.softberry.com/berry.phtml>). Approximately 100 motifs were identified which were distributed across the 6 genes



(Supplementary Table 6). The analysis indicated the presence of a W-box regulatory element in the promoter sequence of all six genes which represents a binding factor for the WRKY family.

These results suggest that the WRKY22-like TF might bind to the promoter of the six calcium signaling genes in order to regulate their expression.

The function of calmodulin remains elusive for fleshy fruit development while expression studies during tomato fruit development and ripening suggest a dual role (Yang et al., 2014). Down regulation during the pre-climacteric stage might be critical to initiate ripening while at the climacteric stage might be involved in ripening coordination (Yang et al., 2014). In tomato, only four CDPK genes were characterized suggesting involvement in wounding, heat stress and hormones (Chang et al., 2009; Kamiyoshihara et al., 2010).

CONCLUSIONS

The analysis of two microarray datasets representing the expression profiles of similar stages of tomato fruit ripening using the LeMoNe algorithm resulted in the identification of putative regulatory TFs belonging to either the WRKY family or to the ERF family and ER24, an ethylene induced transcriptional activator, suggesting a level of consistency in the identification of regulatory TFs. As a result of network analysis, the WRKY22-like module comprised a subgroup of calcium signaling transcripts with expression patterns similar to their regulatory TF as determined by qPCR analysis. Moreover, this subgroup contains a W- box motif in their promoter sequences, known as a WRKY binding factor, validating to a certain extend transcriptional regulation by this TF. Therefore, the WRKY22-like might be involved in the coordinated regulation of expression of the six genes suggesting that alterations in the TF expression might result in expression changes of the six calcium signaling genes. Conclusively, the LeMoNe tool might provide putative TF targets for further physiological analysis as regulators of tomato fruit ripening.

AUTHOR CONTRIBUTIONS

PK conceived and designed the work. PK, SA, CB, MM, AP, AK, and DK, were involved in the acquisition, analysis, and interpretation of the data. PK, SA, CB, MM, AP, AK, and DK were involved in drafting the work. All authors revised and approved the final version.

FUNDING

This research has been co-financed by the European Union (European Social Fund) and Greek National funds, through NSRF 2007-2013 - Program "Excellence II."

REFERENCES

- Ampomah-Dwamena, C., Morris, B. A., Sutherland, P., Veit, B., and Yao, J. L. (2002). Down-regulation of TM29, a tomato SEPALLATA homolog, causes parthenocarpic fruit development and floral reversion. *Plant Physiol.* 130, 605–617. doi: 10.1104/pp.005223
- Bai, Y., Dougherty, L., Cheng, L., Zhong, G. Y., and Xu, K. (2015). Uncovering co-expression gene network modules regulating fruit acidity in diverse apples. *BMC Genomics* 16:612. doi: 10.1186/s12864-015-1816-6
- Bazakos, C., Dulger, A. O., Tevfik, U. A., Spaniolas, S., Spano, T., and Kalaitzis, P. (2012). A SNP-based PCR-RFLP capillary electrophoresis analysis for the identification of the varietal origin of olive oils. *Food Chem.* 134, 2411–2418. doi: 10.1016/j.foodchem.2012.04.031
- Bemer, M., Karlova, R., Ballester, A. R., Tikunov, Y. M., Bovy, A. G., Wolters-Arts, M., et al. (2012). The tomato FRUITFULL homologs TDR4/FUL1 and

ACKNOWLEDGMENTS

This work benefited from the networking activities within the European funded COST ACTION FA1106 "Qualityfruit."

SUPPLEMENTARY MATERIAL

The Supplementary Material for this article can be found online at: <http://journal.frontiersin.org/article/10.3389/fpls.2016.01234>

Supplementary Figure 1 | The % of differentially expressed genes (DEGs) for each comparison, Turning vs. Breaker, Pink vs. Breaker, and Red Ripe vs. Breaker.

Supplementary Figure 2 | The average fold-change for each comparison, Turning vs. Breaker, Pink vs. Breaker, and Red Ripe vs. Breaker.

Supplementary Figure 3 | The % of up- (red) and down-regulated (green) DEGs in each comparison, Turning vs. Breaker, Pink vs. Breaker, and Red Ripe vs. Breaker. The table below, reports the absolute numbers of up- and down-regulated DEGs genes, and the total number of DEGs for each comparison.

Supplementary Figure 4 | Venn diagram showing overlap between DEGs in the three comparisons.

Supplementary Figure 5 | Expression profiles (SignalLog2) of module M6 transcripts and ER24 TF in BR (Breaker), TU (Turning), PK (Pink), and RR (Red Ripe) stages based on the microarray data. The expression profile of the ER24 is represented by a red color line, and the other transcripts with the same color lines (light blue).

Supplementary Table 1 | List of qRT-PCR Primers used for the gene expression analysis.

Supplementary Table 2 | Details of the top 1% transcription factors regulating the modules. First column reports the Affymetrix Transcript cluster ID, the 2nd the number of the module, and the 3rd column the Sol Genomics accession. The remaining columns report the description of each TF as established from three different resources: (i) the plant transcription factors database (PlantTFDB), (ii) the sol genomics, and (iii) the NCBI.

Supplementary Table 3 | Table with the top 10 up- and down-regulated genes for each comparison, Turning vs. Breaker, Pink vs. Breaker, Red Ripe vs. Breaker. Blue cells reflect the genes that rank with the top 10 DEGs, while green cells those with a significant differential expression but not within the top 10. No colored cells denote genes with no significant change in their expression.

Supplementary Table 4 | The 193 modules detected in our data.

Supplementary Table 5 | Table with the co-expressed transcripts in the M40. The first column reports the Affymetrix ID, the 2nd the Gene Symbol, the 3rd a brief description, and the last column the Public Gene IDs.

Supplementary Table 6 | Promoter motif analysis of the six calcium signaling genes. The Table denotes starting from right to left: the accession of the regulatory element (RE), the name of the RE, the binding Transcription Factor (BF), the calcium signaling genes, the cumulative number for each motif found in the genes. The plus symbol (+) indicates presence of the motif for the calcium signaling genes.

- MBP7/FUL2 regulate ethylene-independent aspects of fruit ripening. *Plant Cell* 24, 4437–4451. doi: 10.1105/tpc.112.103283
- Bolstad, B. M., Irizarry R. A., Åstrand, M., and Speed, T. P. (2003). A comparison of normalization methods for high density oligonucleotide array data based on bias and variance. *Bioinformatics* 19, 185–193. doi: 10.1093/bioinformatics/19.2.185
- Bonnet, E., Calzone, L., and Michoel, T. (2015). Integrative multi-omics module network inference with Lemon-Tree. *PLoS Comput. Biol.* 11:e1003983. doi: 10.1371/journal.pcbi.1003983
- Bonnet, E., Michoel, T., and Van de Peer, Y. (2010b). Prediction of a gene regulatory network linked to prostate cancer from gene expression, microRNA and clinical data. *Bioinformatics* 26, i638–i644. doi: 10.1093/bioinformatics/btq395
- Bonnet, E., Tatari, M., Joshi, A., Michoel, T., Marchal, K., Berx, G., et al. (2010a). Module network inference from a cancer gene expression data set identifies microRNA regulated modules. *PLoS ONE* 5:e10162. doi: 10.1371/journal.pone.0010162
- Chang, W. J., Su, H. S., Li, W. J., and Zhang, Z. L. (2009). Expression profiling of a novel calcium-dependent protein kinase gene, LeCPK2, from tomato (*Solanum lycopersicum*) under heat and pathogen-related hormones. *Biosci. Biotech. Biochem.* 73, 2427–2431. doi: 10.1271/bbb.90385
- Clevenger, J. P., Houten, J. V., Blackwood, M., Rodriguez, G. R., Jikumaru, Y., Kamiya, Y., et al. (2015). Network analyses reveal shifts in transcript profiles and metabolites that accompany the expression of SUN and an elongated tomato fruit. *Plant Physiol.* 168, 1164–1178. doi: 10.1104/pp.15.00379
- Cramer, G. R., Urano, K., Delrot, S., Pezzotti, M., and Shinozaki, K. (2011). Effects of abiotic stress on plants: a systems biology perspective. *BMC Plant Biol.* 11:163. doi: 10.1186/1471-2229-11-163
- Fujisawa, M., Shima, Y., Nakagawa, H., Kitagawa, M., Kimbara, J., Nakano, T., et al. (2014). Transcriptional regulation of fruit ripening by tomato FRUITFULL homologs and associated MADS box proteins. *Plant Cell* 26, 89–101. doi: 10.1105/tpc.113.119453
- Huang, G., Li, T., Li, X., Tan, D., Jiang, Z., Wei, Y., et al. (2014). Comparative transcriptome analysis of climacteric fruit of Chinese pear (*Pyrus ussuriensis*) reveals new insights into fruit ripening. *PLoS ONE* 9:e107562. doi: 10.1371/journal.pone.0107562
- Huang, X., Qian, K., Yang, J., Zhang, J., Li, L., Yu, C., et al. (2012). Functional nanoporous graphene foams with controlled pore sizes. *Adv. Mater.* 24, 4419–4423. doi: 10.1002/adma.201201680
- Joshi, A., De Smet, R., Marchal, K., Van de Peer, Y., and Michoel, T. (2009). Module networks revisited: computational assessment and prioritization of model predictions. *Bioinformatics* 25, 490–496. doi: 10.1093/bioinformatics/btn658
- Joshi, A., Van de Peer, Y., and Michoel, T. (2008). Analysis of a Gibbs sampler method for model-based clustering of gene expression data. *Bioinformatics* 24, 176–182. doi: 10.1093/bioinformatics/btm562
- Kamiyoshihara, Y., Iwata, M., Fukaya, T., Tatsuki, M., and Mori, H. (2010). Turnover of LeACS2, a wound-inducible 1-aminocyclopropane-1-carboxylic acid synthase in tomato, is regulated by phosphorylation/dephosphorylation. *Plant J.* 64, 140–150. doi: 10.1111/j.1365-313X.2010.04316.x
- Karlová, R., Chapman, N., David, K., Angenent, G. C., Seymour, G., and Maagd, R. A. (2014). Transcriptional control of fleshy fruit development and ripening. *J. Exp. Bot.* 65, 4527–4541. doi: 10.1093/jxb/eru316
- Kim, C. M., Chung, S. W., Yun, D.-J., and Cho, M. J. (2009). Calcium and Calmodulin-mediated regulation of gene expression in plants. *Mol. Plant* 2, 13–21. doi: 10.1093/mp/ssn091
- Klee, H. J., and Giovannoni, J. J. (2014). Genetics and control of tomato fruit ripening and quality attributes. *Annu. Rev. Genet.* 45, 41–59. doi: 10.1146/annurev-genet-110410-132507
- Liu, M., Gomes, B. L., Mila, I., Purgatto, E., Peres, L. E. P., Frasse, P., et al. (2016). Comprehensive profiling of Ethylene Response Factors expression identifies ripening-associated *ERF* genes and their link to key regulators of fruit ripening in tomato (*Solanum lycopersicum*). *Plant Physiol.* 170, 1732–1744. doi: 10.1104/pp.15.01859
- Livak, K. J., and Schmittgen, T. D. (2001). Analysis of relative gene expression data using real-time quantitative PCR and the $2^{-\Delta\Delta CT}$ Method. *Methods* 25, 402–408. doi: 10.1006/meth.2001.1262
- Lopez-Gomollon, S., Mohorianu, I., Szittyá, G., Moulton, V., and Dalmau, T. (2012). Diverse correlation patterns between microRNAs and their targets during tomato fruit development indicates different modes of microRNA actions. *Planta* 236, 1875–1887. doi: 10.1007/s00425-012-1734-7
- Manning, K., Tör, M., Poole, M., Hong, M., Thompson, A. J., King, G. J., et al. (2006). A naturally occurring epigenetic mutation in a gene encoding an SBP-box transcription factor inhibits tomato fruit ripening. *Nat. Genet.* 38, 948–952. doi: 10.1038/ng1841
- Martel, C., Vrebalov, J., Tafelmeyer, P., and Giovannoni, J. J. (2011). The tomato MADS-Box transcription factor RIPENING INHIBITOR interacts with promoters involved in numerous ripening processes in a COLORLESS NONRIPENING-dependent manner. *Plant Physiol.* 157, 1568–1579. doi: 10.1104/pp.111.181107
- Michoel, T., Maere, S., Bonnet, E., Joshi, A., Saeys, Y., Van den Bulcke, T., et al. (2007). Validating module network learning algorithms using simulated data. *BMC Bioinformatics* 8(Suppl 2):S5. doi: 10.1186/1471-2105-8-S2-S5
- Pan, Y., Bradley, G., and Pyke, K. (2013). Network inference analysis identifies an APRR2-like gene linked to pigment accumulation in tomato and pepper fruits. *Plant Physiol.* 161, 1476–1485. doi: 10.1104/pp.112.212654
- Pan, Y., Seymour, G. B., Lu, C., Hu, Z., Chen, X., and Chen, G. (2012). An ethylene response factor (ERF5) promoting adaptation to drought and salt tolerance in tomato. *Plant Cell Rep.* 31, 349–360. doi: 10.1007/s00299-011-1170-3
- Pirrello, J., Jaimes-Miranda, F., Sanchez-Ballesta, M. T., Tournier, B., Khalil-Ahmad, Q., Regad, F., et al. (2006). Sl-ERF2, a tomato ethylene response factor involved in ethylene response and seed germination. *Plant Cell Physiol.* 47, 1195–1205. doi: 10.1093/pcp/pjc084
- Pirrello, J., Prasad, B. C. N., Zhang, W., Chen, K., Mila, I., Zouine, M., et al. (2012). Functional analysis and binding affinity of tomato ethylene response factors provide insight on the molecular bases of plant differential responses to ethylene. *BMC Plant Biol.* 12:190. doi: 10.1186/1471-2229-12-190
- Seymour, G. B., Østergaard, L., Chapman, N. H., Knapp, S., and Martin, C. (2013). Fruit development and ripening. *Annu. Rev. Plant Biol.* 64, 219–224. doi: 10.1146/annurev-aplant-050312-120057
- Tomato Genome Consortium (2012). The tomato genome sequence provides insights into fleshy fruit evolution. *Nature* 485, 635–641. doi: 10.1038/nature11119
- Vermeirissen, V., De Clercq, I., Van Parry, T., Van Breusegem, F., and Van de Peer, Y. (2014). Arabidopsis ensemble reverse-engineered gene regulatory network discloses interconnected transcription factors in oxidative stress. *Plant Cell Prev.* 26, 4656–4679. doi: 10.1105/tpc.114.131417
- Vrebalov, J., Pan, I. L., and Arroyo, A. J. M. (2009). Fleshy fruit expansion and ripening are regulated by the tomato SHATTERPROOF gene TAGL1. *Plant Cell* 21, 3041–3062. doi: 10.1105/tpc.109.066936
- Vrebalov, J., Ruezinsky, D., Padmanabhan, V., White, R., Medrano, D., Drake, R., et al. (2002). A MADS-box gene necessary for fruit ripening at the tomato ripening-inhibitor (rin) locus. *Science* 296, 343–346. doi: 10.1126/science.1068181
- Wang, L., Zhu, W., Fang, L., Sun, X., Su, L., and Liang, Z. (2014). Genome-wide identification of WRKY family genes and their response to cold stress in *Vitis vinifera*. *BMC Plant Biol.* 14:103. doi: 10.1186/1471-2229-14-103
- Yang, T., Peng, H., and Bauchan, G. R. (2014). Functional analysis of tomato calmodulin gene family during fruit development and ripening. *Horticult. Res.* 1:14057. doi: 10.1038/hortres.2014.57
- Zegzouti, H., Jones, B., Frasse, P., Marty, C., Maitre, B., Latch, A., et al. (1999). Ethylene-regulated gene expression in tomato fruit: characterization of novel ethylene-responsive and ripening-related genes isolated by differential display. *Plant J.* 18, 589–600. doi: 10.1046/j.1365-313X.1999.00483.x
- Zhu, M., Dahmen, J. L., Stacey, G., and Cheng, J. (2013). Predicting gene regulatory networks of soybean nodulation from RNA-Seq transcriptome data. *BMC Bioinformatics* 14:278. doi: 10.1186/1471-2105-14-278
- Conflict of Interest Statement:** The authors declare that the research was conducted in the absence of any commercial or financial relationships that could be construed as a potential conflict of interest.
- Copyright © 2016 Arhondakis, Bita, Perrakis, Manioudaki, Krokida, Kaloudas and Kalaitzis. This is an open-access article distributed under the terms of the Creative Commons Attribution License (CC BY). The use, distribution or reproduction in other forums is permitted, provided the original author(s) or licensor are credited and that the original publication in this journal is cited, in accordance with accepted academic practice. No use, distribution or reproduction is permitted which does not comply with these terms.**



OPEN ACCESS

Edited by:

Mario Pezzotti,
University of Verona, Italy

Reviewed by:

Chi-Kuang Wen,
Shanghai Institutes for Biological Sciences (CAS), China
Vasileios Fotopoulos,
Cyprus University of Technology,
Cyprus

***Correspondence:**

Rameshwar Sharma
rameshwar.sharma@gmail.com

†Present Address:

Suresh K. Gupta,
Department of Ornamental Plants and Agricultural Biotechnology, Institute of Plant Sciences, Agricultural Research Organization Volcani Center, Rishon LeZion, Israel;
Pinjari O. Basha,

Department of Genetics and Genomics, Yogi Vemana University, Kadapa, India;
Kannabiran Sakthivel, Vegetable Research Station, Tamilnadu Agricultural University, Palur, India

[‡]These authors have contributed equally to this work.

Specialty section:

This article was submitted to
Plant Physiology,
a section of the journal
Frontiers in Plant Science

Received: 16 May 2016

Accepted: 31 October 2016

Published: 28 November 2016

Citation:

Bodanapu R, Gupta SK, Basha PO, Sakthivel K, Sadhana, Sreelakshmi Y and Sharma R (2016) Nitric Oxide Overproduction in Tomato *shr* Mutant Shifts Metabolic Profiles and Suppresses Fruit Growth and Ripening. *Front. Plant Sci.* 7:1714.
doi: 10.3389/fpls.2016.01714

Nitric Oxide Overproduction in Tomato *shr* Mutant Shifts Metabolic Profiles and Suppresses Fruit Growth and Ripening

Reddaiah Bodanapu[‡], Suresh K. Gupta ^{†‡}, Pinjari O. Basha [†], Kannabiran Sakthivel [†], Sadhana, Yellamaraju Sreelakshmi and Rameshwar Sharma ^{*}

Repository of Tomato Genomics Resources, Department of Plant Sciences, School of Life Sciences, University of Hyderabad, Hyderabad, India

Nitric oxide (NO) plays a pivotal role in growth and disease resistance in plants. It also acts as a secondary messenger in signaling pathways for several plant hormones. Despite its clear role in regulating plant development, its role in fruit development is not known. In an earlier study, we described a *short root* (*shr*) mutant of tomato, whose phenotype results from hyperaccumulation of NO. The molecular mapping localized *shr* locus in 2.5 Mb region of chromosome 9. The *shr* mutant showed sluggish growth, with smaller leaves, flowers and was less fertile than wild type. The *shr* mutant also showed reduced fruit size and slower ripening of the fruits post-mature green stage to the red ripe stage. Comparison of the metabolite profiles of *shr* fruits with wild-type fruits during ripening revealed a significant shift in the patterns. In *shr* fruits intermediates of the tricarboxylic acid (TCA) cycle were differentially regulated than WT indicating NO affected the regulation of TCA cycle. The accumulation of several amino acids, particularly tyrosine, was higher, whereas most fatty acids were downregulated in *shr* fruits. Among the plant hormones at one or more stages of ripening, ethylene, Indole-3-acetic acid and Indole-3-butryric acid increased in *shr*, whereas abscisic acid declined. Our analyses indicate that the retardation of fruit growth and ripening in *shr* mutant likely results from the influence of NO on central carbon metabolism and endogenous phytohormones levels.

Keywords: tomato, nitric oxide, fruit ripening, metabolites, molecular mapping

INTRODUCTION

Nitric oxide (NO) is a bioactive gaseous molecule that participates in a plethora of plant development responses right from seed germination to plant senescence. It acts as a multifunctional signaling molecule regulating a range of developmental processes in conjunction with almost all major phytohormones (Freschi, 2013). Several evidences have indicated that the interplay between auxin and NO regulates cucumber adventitious roots development (Pagnussat et al., 2003), tomato lateral root formation (Correa-Aragunde et al., 2004). Similarly, cytokinin (CK) and NO synergistically and antagonistically regulate several developmental processes of plants (Liu et al., 2013). It is reported that NO and gibberellic acid (GA) interact in seed germination (Bethke et al., 2007) and hypocotyl growth during de-etiolation process (Lozano-Juste and León, 2011), wherein NO acts upstream to GA. During seed germination, NO appears to negate abscisic acid

(ABA) effects and enhance germination by activation of transcription of ABA catabolism gene CYP707A2 and NO sensing gene ERFVII (Liu et al., 2009; Gibbs et al., 2014). On the contrary, NO also participates in many ABA signaling events particularly G protein-coupled signaling cascades (Wang et al., 2001).

During recent years, many studies reported that cold stress can increase the production of NO in seeds (Bai et al., 2012), leaves (Zhao et al., 2009; Cantrel et al., 2011) and fruits (Xu et al., 2012). Considering that NO signaling operates during cold stress, the fumigation of fruits with NO gas has been used to prevent chilling injury during cold storage (Singh et al., 2009; Zaharah and Singh, 2011). Studies on NO fumigation to fruits also indicated its involvement in the ripening of both climacteric and non-climacteric fruits. The prevention of chilling injury by NO has been attributed to several factors including delay in climacteric phase by antagonizing ethylene synthesis (Manjunatha et al., 2012), protecting fruits from pathogens and impeding ripening and/or senescence (Singh et al., 2013). The NO treatment delayed the ripening by suppressed respiration rate, reduced ethylene biosynthesis and chilling injury, delayed development of browning disorders, disease incidence, and skin color changes, flesh softening and reduced activity of softening enzymes (Lessem and Pinchasov, 2000; Manjunatha et al., 2010).

Currently information about the influence of NO on molecular processes regulating fruit ripening is largely restricted to post-harvest fruits stored in cold (Manjunatha et al., 2014). NO fumigation of cold-stored mango fruits increased the levels of tartaric acid and shikimic acids (Zaharah and Singh, 2011). NO treatment of peach fruits increased palmitoleic, oleic, and linolenic acids, while decreased linoleic acid levels (Zhu and Zhou, 2006). The softening of banana fruits was retarded by NO by lowering the activity of cell wall degrading enzymes pectin methylesterase (PME) and β -1-4-endoglucanase (Cheng et al., 2009). In peach and kiwi fruits NO upregulated the activity of enzymes involved in quenching of reactive oxygen species such as catalase, peroxidases and superoxide dismutase (SOD) (Flores et al., 2008; Zhu et al., 2008). Exogenous NO delayed tomato ripening via transcriptional suppression of ethylene biosynthesis genes ACC synthase (ACS) and ACC oxidase (ACO) (Eum et al., 2009). In pepper fruits, ripening is associated with an increase in the nitration of proteins and exogenous treatment of NO delayed ripening by blocking protein nitration (Chaki et al., 2015).

Most studies examining the role of NO in plant development including fruit ripening are largely confined to exogenous application of NO and its agonists and antagonists. This is related to the dearth of mutants affected in NO levels in the higher plants. The paucity of mutants may be related to the multiplicity of pathways for NO generation in plants depending on the tissue and ambient conditions (Gupta et al., 2011). Characterization of *Arabidopsis* NO mutants revealed that the *in-vivo* level of NO is reportedly regulated by mutations in diverse genes. The mutation in the *cGTPase* gene in *nos1/noa1* mutant (Guo et al., 2003; Moreau et al., 2008) lowered NO levels and stimulated early flowering. In contrast mutation in *CUE1* gene encoding a chloroplast phosphoenolpyruvate/phosphate translocator enhanced NO levels and delayed flowering (He

et al., 2004). The null alleles of *HOT5* locus encoding S-nitrosoglutathione reductase (GSNOR) display decreased tolerance to temperature stress associated with increase in levels of nitrate, NO and nitroso species (Lee et al., 2008). An increase in NO level in arginase negative mutants stimulated lateral roots while reduction in NO level in prohibitin (*PHB3*) gene mutant reduced auxin-induced lateral root formation (Wang et al., 2010).

Considering that exogenous NO influences post-harvest fruit ripening it would be of interest to examine how endogenous NO regulates fruit ripening and associated cellular metabolism. In this study, we compared fruit ripening in the *short root* (*shr*) mutant of tomato that hyperaccumulates NO (Negi et al., 2010, 2011) with its wild type (WT) progenitor. We report that *shr* mutation prominently affects the fruit growth and delays ripening probably through its effect on cellular homeostasis. Profiling of plant hormones in *shr* and wild-type fruits revealed changes in accumulation patterns of ABA, indole-3-acetic acid (IAA) and indole-3-butryric acid (IBA) that may have influenced the observed metabolic shifts. We also mapped *shr* locus on chromosome nine of tomato. However, its identity remained elusive.

MATERIALS AND METHODS

Plant Materials

The *shr* mutant of *Solanum lycopersicum* cv Ailsa Craig (wild type- WT) was isolated from a γ -irradiated M₂ population of tomato as described in Negi et al. (2010). *S. pennellii* [LA 716] and *S. pimpinellifolium* [LA1589] (SP) seeds were obtained from Tomato Genetics Resource Center (UC, Davis, USA). The plants were grown in the greenhouse at Hyderabad under natural photoperiod (12–14 h day, 10–12 h night) at 28 ± 1°C during the day and ambient temperature (14–18°C) in the night. The RH in the greenhouse ranged from 45–70%.

A F₂ mapping population consisting of 69 plants was generated, segregating for short root phenotype, from an interspecific F₁ hybrid (*S. lycopersicum* *shr/shr* x *S. pennellii* *SHR/SHR*). Owing to self-incompatibility, the F₁ plants were selfed by manual sib mating. A second F₂ mapping population was generated which consist of 769 plants, segregating for short root phenotype, from an interspecific F₁ hybrid (*S. lycopersicum* *shr/shr* x *S. pimpinellifolium* *SHR/SHR*). The F₂ seedlings were scored for root length and NO levels as described in Negi et al. (2010). For NO determination detached roots were submerged in 10 μ M of DAF-2 DA fluorescent probe in 10 mM MES-KCl (pH 7.0) buffer for 20 min. Thereafter the roots were washed with 10 mM MES-KCl (pH 7.0) buffer for 15 min. The NO level was examined by epi-fluorescence using the U-MWIB2 mirror unit (excitation 495 nm, emission 515 nm) in the Olympus BX-51 Microscope (Negi et al., 2010).

After scoring the seedling phenotypes, seedlings were transferred to the pots and plants were grown in the greenhouse. Wherever possible, F₃ seedlings were used to confirm the phenotype of F₂ plants. Chi-square tests were performed to determine the goodness of fit between the Mendelian ratio of the F₂ mapping population and the segregation data for the short root (*shr*) and the molecular markers.

Estimation of Ethylene, Pigments, Brix and Fruit Firmness

For estimation of ethylene, fruits were harvested at different ripening stages viz., mature green (MG), breaker (BR) and red ripe (RR) stage. The ethylene emission from the harvested fruits was measured using a previously described procedure (Kilambi et al., 2013). Chlorophylls and carotenoids were extracted from leaves from 7–8 internodes of 45-day-old plants in 80% (v/v) acetone using the protocol of Makeen et al. (2007) and their amounts were calculated using the equation of Lichtenthaler (1987). Carotenoids were extracted from the pericarp of MG, BR and RR fruits using the procedure of Gupta et al. (2015). To avoid photooxidation, the entire procedure was performed under dim light. The carotenoids amount from the fruit tissue was calculated by comparing the peak area with the peak area obtained using pure standards of each carotenoid. For determination of sugars, the entire pericarp of fruit was homogenized, and values were recorded using PAL-1 refractometer. The firmness of fruits was measured three times at equatorial plane using Durofel DFT 100 (Gupta et al., 2014).

Determination of Endogenous NO Levels in Fruits

The endogenous levels of NO at MG and RR stage of fruits was determined by using EPR spectroscopy, and also the fruits cells were examined for DAF-2 DA fluorescence following the protocols described in Negi et al. (2010). However, both methods could not detect the NO indicating that NO level in fruits was below the limit of detection.

Extraction of Primary Metabolites and GC-MS Data Processing

The metabolite profiling of fruits of WT and *shr* was essentially carried out by following the protocol of Roessner et al. (2000). The fruits from MG, BR, and RR stage were ground to a fine powder in liquid nitrogen. A 100 mg fresh weight of fruit powder was mixed with 1.4 mL 100% methanol and 60 µL of internal standard ribitol (0.2 mg/ml, w/v). After mixing, the sample was shaken at 70°C in a thermomixer for 15 min at 950 rpm. After that, 1.4 mL MilliQ water was added and after thorough mixing the sample was transferred in GL-14 Schott Duran glass vial and centrifuged at 2200 g for 15 min. An aliquot of polar phase (150 µL) was transferred in fresh Eppendorf tube and dried by vacuum centrifugation for 3–4 h. The dried sample was derivatized; first, it was dissolved in 80 µL of methoxyamine hydrochloride (20 mg/mL) and incubated at 37°C for 90 min at 600 rpm. Thereafter, 80 µL of MSTFA was added, and incubation was carried out at 37°C for 30 min at 600 rpm. The derivatized sample was transferred to a GC-MS injection vial and analyzed by Leco-PEGASUS GCXGC-TOF-MS system (Leco Corporation, USA) equipped with 30 m Rxi-5 ms column with 0.25 mm i.d. and 0.25 µm film thickness (Restek, USA). The injection temperature, interface, and ion source were set at 230°, 250°, and 200°C respectively. For the proper separation of groups of metabolites, the run program was set as following; isothermal heating at 70°C for 5 min, followed by 5°C min⁻¹

oven temperature ramp to 290°C and then final heating at 290°C for 5 min. The carrier gas (helium gas) flow rate was set to 1.5 mL/min. A 1 µL of sample was injected in split less mode and mass spectra were recorded at 2 scans/sec within a mass-to-charge ratio range 70–600.

The raw data were processed by ChromaTOF software 2.0 (Leco Corporation, USA) and further analyzed using the MetaAlign software package (Lommen and Kools, 2012; www.metalign.nl) with a signal to noise ratio of ≥ 2, for base line correction, noise estimation, alignment and extraction of ion-wise mass signal. The mass signals that were present in less than three samples were discarded. The Metaalign results were processed with MSClust software for reduction of data and compound mass extraction (Tikunov et al., 2012). The mass spectra extracted by MSClust were opened in NIST MS Search v 2.2 software for the identification of compound name within the NIST (National Institute of Standard and Technology) Library, and Golm Metabolome Database Library. The compound hits which showed maximum matching factor (MF) value (>600) and least deviation from the retention index (RI) was used for metabolite identity. The data was analyzed by normalizing with the internal standard ribitol.

Extraction of Phytohormones and LC-MS Analysis

The phytohormone extraction from the fruit sample of WT and *shr* was performed as described in Pan et al. (2004). A 100 mg homogenized powder from fruit sample was mixed with 500 µL of pre-chilled extraction solvent consisting of 2-propanol: MilliQ water: concentrated HCL in the ratio of 2:1:0.002 (v/v/v) respectively. After mixing, the extraction was carried out by shaking the sample for 30 min at 4°C at 500 rpm. Thereafter, 1 mL of dichloromethane (DCM) was added to the sample mix, and the incubation was continued for 30 min at 4°C at 500 rpm. After centrifugation at 13,000 g for 15 min at 4°C, the supernatant (~ 900 µL) was transferred to a fresh Eppendorf tubes and dried completely using the Speedvac (Thermo Scientific, USA). Before injection, the dried residue was dissolved in 70 µL of precooled 100% methanol followed by centrifugation at 13,000 g for 5 min.

The sample was transferred to an injection vial and analyzed using UPLC/ESI-MS (Waters, Milford, MA USA). The system consists of an Aquity UPLC™ System, quaternary pump, and autosampler. For separation of hormones, the sample was analyzed on a Hypercil GOLD C₁₈ (Thermo Scientific) column (2.1 × 75 mm, 2.7 µm). A gradient elution program was performed using two solvents system, solvent A- containing ultrapure water with 0.1% (v/v) formic acid, solvent B-containing acetonitrile with 0.1% (v/v) formic acid and run for 9 min at 20°C. The abscisic acid (ABA), jasmonic acid (JA), and salicylic acid (SA) detection was performed on Exactive™ Plus Orbitrap mass spectrometer (Thermo Fisher Scientific, USA) in all ion fragmentation (AIF) mode (range of m/z 50–450) equipped with heated electrospray ionization (ESI) in negative ion mode. The zeatin, IAA, IBA, epibrassinosteroids (Epi-BR) and methyl jasmonate (MeJA) were analyzed in positive ion mode. For both modes, the following instruments setting were

used, capillary temperature -350°C , sheath gas flow (N_2) 35 (arbitrary units), AUX gas flow rate (N_2) 10 (arbitrary units), collision gas (N_2) 4 (arbitrary units) and the capillary voltage 4.5 kV under ultra-high vacuum 4e^{-10} mbar. The hormones were analyzed from the >5 different fruits harvested from ripening stages viz. MG, BR, and RR of WT and *shr*. The quantification of each hormone was carried out by comparing the peak areas with those obtained for the respective hormone standards.

Principal Component Analysis (PCA)

To obtain the overall clustering of the samples, we performed PCA using Metaboanalyst 3.0 (Xia et al., 2015; <http://www.metaboanalyst.ca/>). Firstly, we took the average of metabolites from at least three replicates and analyzed the differences in metabolites accumulation across the ripening stages in both WT and *shr* and then the results were presented in a two-dimensional graphical display.

Construction of Primary Metabolite Pathways

All the metabolites measured using the GC-MS methods were mapped to the general metabolic pathways as described in the KEGG (Kyoto Encyclopedia of Genes and Genomes, <http://www.genome.jp/kegg>) and Lycocyc (Sol Genomic networks, <http://solcyc.solgenomics.net/>). To compare levels of each metabolite across the ripening stages (MG, BR, and RR), we performed all pairwise multiple comparison procedures (Student-Newman-Keuls Method) by One-Way ANOVA using Sigma Plot version 11 with a significance threshold $P \leq 0.05$ to highlight patterns of change across the ripening stages in *shr* compared to WT. Average fold change of metabolites occurring across the ripening stages in *shr* fruits compared to WT was shown on a primary metabolite pathway as presented in Do et al. (2010). A log₂ fold of 0 means no difference, a log₂-fold of 0.5 means 1or higher fold changes (equal to average means 1.5-fold) 1 means 2-fold or higher, a log₂-fold of two means 4-fold or higher, and so on.

Metabolites and Hormones Correlation Networks Creation

Networks for both WT and *shr* were created using Cytoscape software package (<http://www.cytoscape.org/>; Cline et al., 2007). Nodes represent the metabolites (circle), hormones (hexagon shape) and edges represent connectivity between the two metabolites. The connectivity between two nodes is drawn if the Pearson's Correlation Coefficient (PCC) value is larger than 0.9 either in positive or negative mode. New correlations in the *shr* network, which were insignificant in WT at all ripening stages were considered as new associations in *shr* or vice-versa.

DNA Extraction

Genomic DNA was isolated from young leaves (80–100 mg/well) in 96 well deepwell plates using a DNA extraction protocol developed for tomato (Sreelakshmi et al., 2010). The DNA was quantified using Nanodrop (ND-1000) spectrophotometer and DNA samples were diluted to final concentration of 5 ng/ μL .

Screening for Polymorphic Markers

For mapping *shr* locus, we selected 129 SSR and 6 InDel markers that were evenly distributed across twelve chromosomes of the tomato. These markers were selected from the Solanaceae Genome Network (<http://solgenomics.net/>) and Tomato Mapping Resource Database (<http://www.tomatomap.net/>, Last accessed in 2013) and chosen based on their polymorphisms between tomato cultivar Ailsa Craig, *S. pimpinellifolium* and *S. pennellii* (**Supplementary Table 1**, for marker details). First, the location of mutation was determined to chromosome nine. Thereafter chromosome 9 was genotyped with 24 SSR and 7 CAPS markers. PCR amplification was in total volume of 20 μL containing 20 ng of genomic DNA, 1 \times PCR buffer (10 mM Tris, 5 mM KCl, 1.5 mM MgCl₂, 0.1% (w/v) gelatin, 0.005% (v/v) Tween-20, 0.005% (v/v) Np-40, pH 8.8, 0.2 mM dNTPs, 1 μL Taq polymerase and 5 pmoles each of forward and reverse primers. The cycling conditions for amplification were 94°C-5 min, followed by 35 cycles of 94°C-30 s, 57°C-30 s, 72°C-1 min, finally an extension step 72°C-8 min, and held at 4°C. The PCR products were size separated on 3.5% (w/v) agarose gels and gel images were collected with Alpha Imager™ gel documentation system.

Bulk Segregant Analysis (BSA) and Genotyping

Selected individuals of F₂ mapping populations of *shr* x *S. pimpinellifolium* and *shr* x *S. pennellii* were screened for polymorphism between bulks. DNA from fifteen *shr* and fifteen long root plants from *shr* x *S. pimpinellifolium* population, and twelve *shr* and twelve long root plants from *shr* x *S. pennellii* population were selected for bulks preparation. Short root and long root DNA bulks were prepared by pooling equivalent amount of DNA from each plant with specific phenotypic segregant of the F₂ mapping population. The parent lines and the bulks DNA were then subjected to BSA analysis for the identification of the tightly linked marker (Michelmore et al., 1991). Markers which corresponded to short root bulk and short root mutant and differed in the size of the PCR product with both long root parents (*S. pennellii* and *S. pimpinellifolium*) and long root bulks were considered to co-segregate with *shr* phenotype. Markers that were specific between bulks were assessed on debulks along with their parents.

Screening of Additional Markers

For saturation of the *shr* locus, 14 SSR markers from Kazusa DNA Research Institute (<http://www.kazusa.or.jp/tomato/>, Shirasawa et al., 2010a,b), 10 SSR markers from Veg Marks a DNA marker database for vegetables (<http://vegmarks.nivat.afrc.go.jp>, Last accessed in 2013) and 7 CAPS markers viz., At3g63190, C2_At4g02580, C2_At2g29210, C2_At4g02680, C2_At1g02910, C2_At4g03200, and U228448 (<http://solgenomics.net>) that were specific to chromosome 9 were selected and screened for polymorphism between the parental lines of mapping population (**Supplementary Tables 2–4** for marker details). For amplification of CAPS region, 30 ng genomic DNA, 1 μL of 5 pM/ μL primer, 1X PCR buffer (10 mM Tris, 5 mM KCl, 1.5 mM MgCl₂, 0.1% (w/v) gelatin, 0.005% (v/v) Tween-20, 0.005%

(v/v) Np-40, pH 8.8, 0.2 mM dNTPs and 1 μL Taq polymerase were used. After confirming PCR amplification for CAPS locus by agarose gel electrophoresis, the PCR amplicons of the CAPS markers were digested using *ApoI*, *HinfI*, *DraI* and *MspI* (Fermentas) enzymes. Digestion reactions performed according to the supplier's manual and the products were separated on 3.5% (w/v) agarose gels.

Map Construction and Linkage Analysis

Markers that showed bulk specific segregation along with *shr* phenotype were used for molecular mapping of the *shr* locus. Given the availability of the higher number of F₂ segregating progeny, we selected *shr* x *S. pimpinellifolium* mapping population for map construction for *shr* locus. Four SSR markers and one CAPS marker were chosen for molecular mapping of the *shr* locus. Total 769 F₂ plants of *shr* x *S. pimpinellifolium* were genotyped and analyzed by Chi-square test. Map construction was carried out using the MAPMAKER/EXE V.3.0 (Lander et al., 1987; Lincoln and Lander, 1992) program following Kosambi Function (Kosambi, 1943). Linkage groups were determined using "group" and "error detection on" commands with a LOD score of 3.0 and a recombination fraction of 0.5. The "compare" and "order" commands in Mapmaker were used to identify the most probable marker order within a linkage group. The "ripple" command was used to verify and confirm marker order as determined by multipoint analysis. Recombination frequencies were converted into map distances centi-Morgans (cM) using the Kosambi mapping function (Kosambi, 1943), and the linkage group maps were drawn using the MapChartv. 2.1 software (Voorrips, 2002).

Genome Analysis and Candidate Gene Prediction

The tomato genome, ITAG version 2.3 (SGN: http://solgenomics.net/gb2/gbrowse/ITAG2.3_genomic/) was used for overlaying the closest markers encompassing the *shr* locus. The predicted genes in the region encompassing *shr* locus were searched. The information on expression of the predicted genes was found by BLASTN searching of Tomato Expression Database (<http://solgenomics.net/ted>).

RESULTS

Inheritance of *shr* Locus

We crossed *shr* mutant with *S. pimpinellifolium*, a red fruited wild relative of tomato for mapping of the *shr* gene, and also compared the phenotypes of *shr* mutant plants and the parental lines at the different stages of development. Both light and dark grown seedlings of *shr* mutant showed extremely short roots compared to parental lines (Figures 1A–D). The F₁ seedlings of *shr* x *S. pimpinellifolium* grown in both light and dark conditions displayed elongated roots like WT and *S. pimpinellifolium*. Examination of root length of F₂ segregation mapping populations suggested that *shr* locus is encoded by a monogenic recessive locus (Supplementary Table 5). While seedlings of *S. pimpinellifolium* did not form lateral roots, however, light-grown seedlings of F₁ cross of *shr* x *S. pimpinellifolium* displayed lateral roots like WT (Figure 1A). The

etiolated seedlings of WT lacked lateral roots and consequently etiolated seedlings of F₁ cross of *shr* x *S. pimpinellifolium* roots did not display lateral roots (Figures 1B,D). Interestingly, the lateral root formation in the F₂ population of *shr* x *S. pimpinellifolium* showed opposite segregation pattern of 1:3, indicating the presence of a locus in *S. lycopersicum* controlling lateral root initiation independently of *shr* locus (Supplementary Table 6).

The shortening of root in the *shr* mutant is associated with hyperaccumulation of NO; therefore, cosegregation of short root phenotype and accumulation of NO was examined by staining the primary root tip with NO-sensitive fluorophore 4, 5-diaminofluorescein diacetate (DAF-2DA) (Correa-Aragunde et al., 2004). *In vivo* imaging of NO levels in parental lines and *shr* mutant showed stronger fluorescence of DAF-2DA in *shr* mutant root tips, while the level of DAF-2 DA fluorescence in root tips of parental lines was nearly similar. The F₁ plants of *shr* x *S. pimpinellifolium* showed DAF-2 DA fluorescence level that was similar to parental lines indicating the recessive nature of *shr* locus. The imaging of F₂ population of *shr* x *S. pimpinellifolium* showed DAF-2 DA fluorescence pattern consistent with above results, showing a 3:1 segregation pattern in root tips. The segregation pattern of NO accumulation as visualized by DAF-2 DA fluorescence in F₂ mapping population was consistent with *shr* phenotype and indicated the cosegregation of NO hyperaccumulation with the short root locus (Figure 1E).

The F₁ seedlings of *shr* x *S. pimpinellifolium* were slightly taller and had longer internodes than either WT or *S. pimpinellifolium* (Supplementary Figures 1A,B). Similarly, the leaf of F₁ plant was longer than *shr* mutant and possessed chlorophylls and carotenoids similar to WT and *S. pimpinellifolium* (Supplementary Figures 1C,D). However, F₁ plants showed an intermediate phenotype than either of its progenitors in the number of flowers and the shape of inflorescence (Figure 1F). On the contrary, the RR fruits of F₁ hybrid (*shr* x *S. pimpinellifolium*) emitted less ethylene (3.18 ± 0.2120 nL/h/g FW) than *S. pimpinellifolium* (14.59 ± 1.11 nL/h/g FW) and *shr* fruits.

Mapping of *shr* Locus

To map the *shr* gene, the SSR markers described in Tomato Mapping Resource Database (<http://www.tomatomap.net>, Last accessed in 2013) and Solanaceae Genome Network (<http://solgenomics.net>) were screened using the bulk segregation analysis (BSA). Out of 135 markers used, only 69 were polymorphic between the *shr* and *S. pimpinellifolium*. These 69 polymorphic markers were used for BSA of *shr* x *S. pimpinellifolium* populations. Among these, two markers, SSR19, and SSR110 showed polymorphism and mapping results indicated that the *shr* locus was located in a region intervening between SSR19-SSR110 on chromosome 9 of tomato. To develop high-resolution molecular map and saturate the region around the *shr* locus, additional markers for chromosome 9 were selected and analyzed for polymorphism between *shr* mutant and *S. pimpinellifolium* (Ohyama et al., 2009; Shirasawa et al., 2010a). The bulk segregation analysis with TGS0213 and C2_At3g63190 markers showed strong linkage with *shr* locus, and these were used for genotyping of entire mapping population (Supplementary Figures 2A–C).

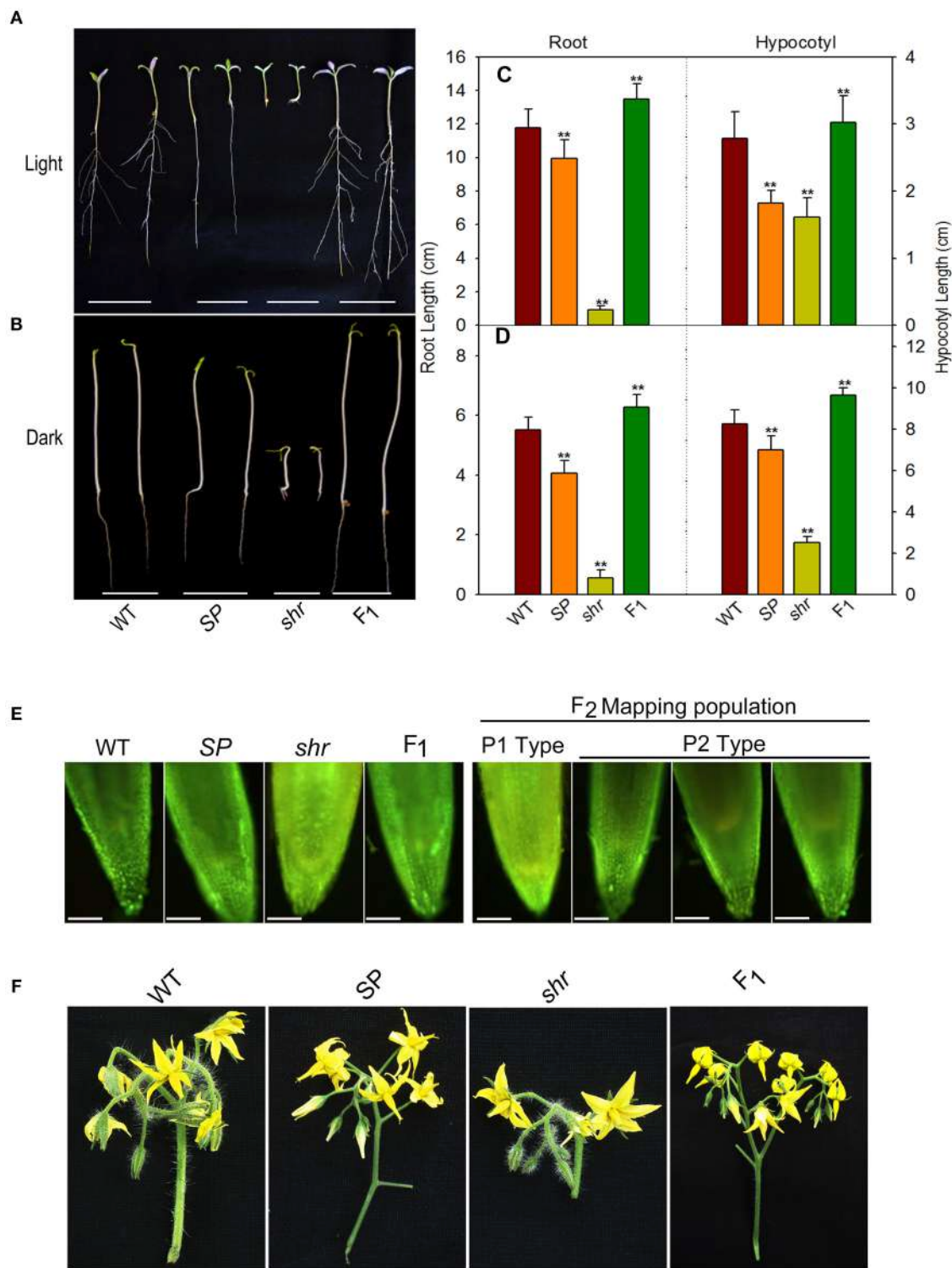


FIGURE 1 | Genetic segregation of phenotypic traits in *shr* mutant. Seedling phenotype (**A,B**), root and hypocotyl length (**C,D**) of Ailsa Craig (WT), *S. pimpinellifolium* (SP), short root (*shr*) mutant and F₁ seedlings grown in light (**A,C**- 9-day old seedlings) and darkness (**B,D**- 5-day old seedlings). (**E**) NO levels in root tips of 9-day old light-grown seedlings of parent plants (left panel) and mapping population (right panel) using NO-sensitive dye DAF-2DA. In F₂ mapping population, short-root seedlings showed NO staining similar to *shr* mutant parent(P1 type) and long-root seedlings showed NO staining similar to SP parent (P2 type). (**F**) Inflorescence morphology of WT, SP, *shr* and F₁ plants. The values are the mean \pm SD ($n = 79$ seedlings). Asterisk indicates statistically significant difference between WT and SP, *shr*, and F₁ (One-Way ANOVA; ** $P < 0.001$). In fluorescence microscopic picture of the root, scale bar corresponds to 10x zoom micro scale, Olympus BX51.

A total of six polymorphic markers around *shr* locus, including one CAPS (C2_At3g63190), one InDel (CosI52) and four SSRs (SSR19, SSR110, SSR383, TGS0213) markers, were genotyped on 769 F₂*shr* x *S. pimpinellifolium* mapping population. Out of these, five markers showed satisfactorily expected ratio for the co-dominant inheritance of 1:2:1 and were used for mapping the *shr* locus (**Supplementary Table 7**). Using MAPMAKER3.0 program, the *shr* locus was mapped at 0.2 cM from TGS0213 and 2.8 cM from C2_At3g63190, on chromosome 9 (**Figure 2**). To identify the candidate gene encoding *shr* locus, the sequence of SSR markers tightly linked to *shr* was searched with BLAST against the tomato genome sequence release ITAG 2.3 Release SL2.40ch09:54045071..58939091(http://solgenomics.net/gb2/gbrowse/ITAG2.3_genomic). The genomic region flanked by two markers was about 4.89 Mb (4894020 bp) and contained 197 genes, which were examined as candidate genes for NO hyperaccumulation. However, the above genomic region is not completely sequenced and consists of two major gaps of size 35116 bp (SL2.40ch09:56426627...56461743) and 31568 bp (SL2.40ch09:56795954...56827522). Currently, it is not known whether these two gaps also harbors functional genes or consist of repetitive DNA sequences. Out of the 197 genes, 139 genes showed high to low expression in tomato root and remaining showed no expression (**Supplementary Table 8**).

Out of 139 genes showing root specific expression, only three genes were reported to be associated with modulation of cellular NO levels; alcohol dehydrogenase III (ADH3)/GSNO reductase (GSNOR1/HOT5/PAR2, Solyc09g064370 alcohol dehydrogenase III gene), CUE domain containing protein 2 (Solyc09g064860CUE domain containing protein), and glutathione S-transferase (Solyc09g063150 Glutathione S-transferase) (Li et al., 2008; Chen et al., 2009; Lok et al., 2012). The presence of the *shr* mutation in these three genes was examined by amplifying complete ORF of genes from WT and *shr* mutant using PCR and detection of mutation in heteroduplexed DNA using mismatch endonuclease assay (Seelakshmi et al., 2010). However, no mutation was detected in any of these three genes, thus ruling them out as candidate genes.

***shr* Mutant Shows Reduced Fruit Growth and Delayed Ripening**

The *shr* mutant shows sluggish growth, prolonged life cycle (*shr*-150 ± 10 days, WT-110 ± 10 days) and a diminutive phenotype with pale green leaves with reduced level of photosynthetic pigments compared to WT (Negi et al., 2010; **Supplementary Figure 1D**). The pleiotropic effect of *shr* mutation also manifests during reproductive phase. Compared to WT, the initiation of the first inflorescence in the mutant was delayed by nearly 3 weeks (**Figures 3A,B**). The *shr* mutant made fewer inflorescences with smaller flowers and inflorescence had ca. 50% less flowers than the WT (**Figures 3C–F**).

The influence of *shr* mutation was examined on the chronological development of fruit from anthesis (days post anthesis- DPA) to RR stage. Analogous to delayed inflorescence initiation, the fruit development was slower, and the ripened *shr* fruits were smaller in size than WT (**Figures 4A,B**). In addition,

the *shr* mutation influenced the transition phases of ripening. The time period to reach the MG stage was longer in *shr* fruits (35–37 days *shr*, 30–33 days WT) (**Figure 4C**). The transition from MG to RR Stage was 7–8 days slower in *shr* fruits than WT. Though *shr* fruits were smaller in size at RR stage, they emitted nearly two-fold higher ethylene than WT (**Figure 7**). Among *shr* and WT fruits, no obvious difference was found in TSS level (Brix) except at RR stage (**Supplementary Figure 3A**). During ripening, the loss of firmness in *shr* fruits was similar to WT (**Supplementary Figure 3B**). The pH of WT and *shr* fruits was almost similar (**Supplementary Figure 3C**). Unlike reduced photosynthetic pigments in *shr* leaves, the accumulation of lycopene and β-carotene in *shr* fruits was only mildly affected. However, the level of carotenoids precursors, phytoene and phytofluene were higher in *shr* fruits than WT (**Supplementary Table 9**).

***shr* Mutation Alters the Cellular Metabolism during the Fruit Ripening**

A total of 96 metabolites were identified in WT and *shr* fruits at three ripening stages, MG, BR, and RR. The levels of several metabolites in *shr* fruits were significantly different from WT at one or more stages (**Supplementary Table 10**). Principal component analysis (PCA) and the correlation variances explained by the two principal components clearly revealed two clusters of WT and *shr* metabolites (**Figure 5**). Based on chemical nature the metabolites were grouped as amino acids and amines, sugars, organic acids, fatty acids, and miscellaneous (**Supplementary Table 10**). Only those metabolites which showed up-regulation or down-regulation >1.5-fold (Log₂ *shr*/WT value 0.5) in *shr* fruits than WT were mapped on the metabolic networks (**Figure 6**, **Supplementary Figures 4A–E**).

***shr* Mutation Preferentially Stimulates Tyrosine Accumulation in Fruits**

In *shr* fruits, only 14 out of 25 amino acids/amines were differentially regulated at one or more stages. Among these, tyrosine was detected only in *shr* fruits, and its levels progressively declined during ripening. The upregulation of asparagine, tryptophan, alanine 3-cyano, and ornithine 1-5-lactam in *shr* fruits was discernible at all stages with maxima at BR (**Figure 6**, **Supplementary Table 10**). The glutamine level in *shr* fruits was significantly higher at MG and BR but was similar to WT at RR. Contrastingly, glutamate was downregulated in *shr* fruits, most significantly at MG and RR (**Figure 6**, **Supplementary Table 10**). The hydroxylamine consistently showed higher levels in *shr* fruits. The amino acids derived from the 3-phosphoglycerate and pyruvate showed no or little change in *shr* fruits. Polyamine, putrescine showed significantly high level at MG stage. Considering tyrosine, asparagine, and glutamine showed substantial upregulation (~10-fold) and glutamate showed downregulation, these amino acids may have a key role in cellular homeostasis of *shr* fruits.

A total of 27 sugars and their derivatives were identified in *shr* and WT fruits; however only a few were up- or down-regulated in *shr* fruit (**Figure 6**, **Supplementary Table 10**). The glucose

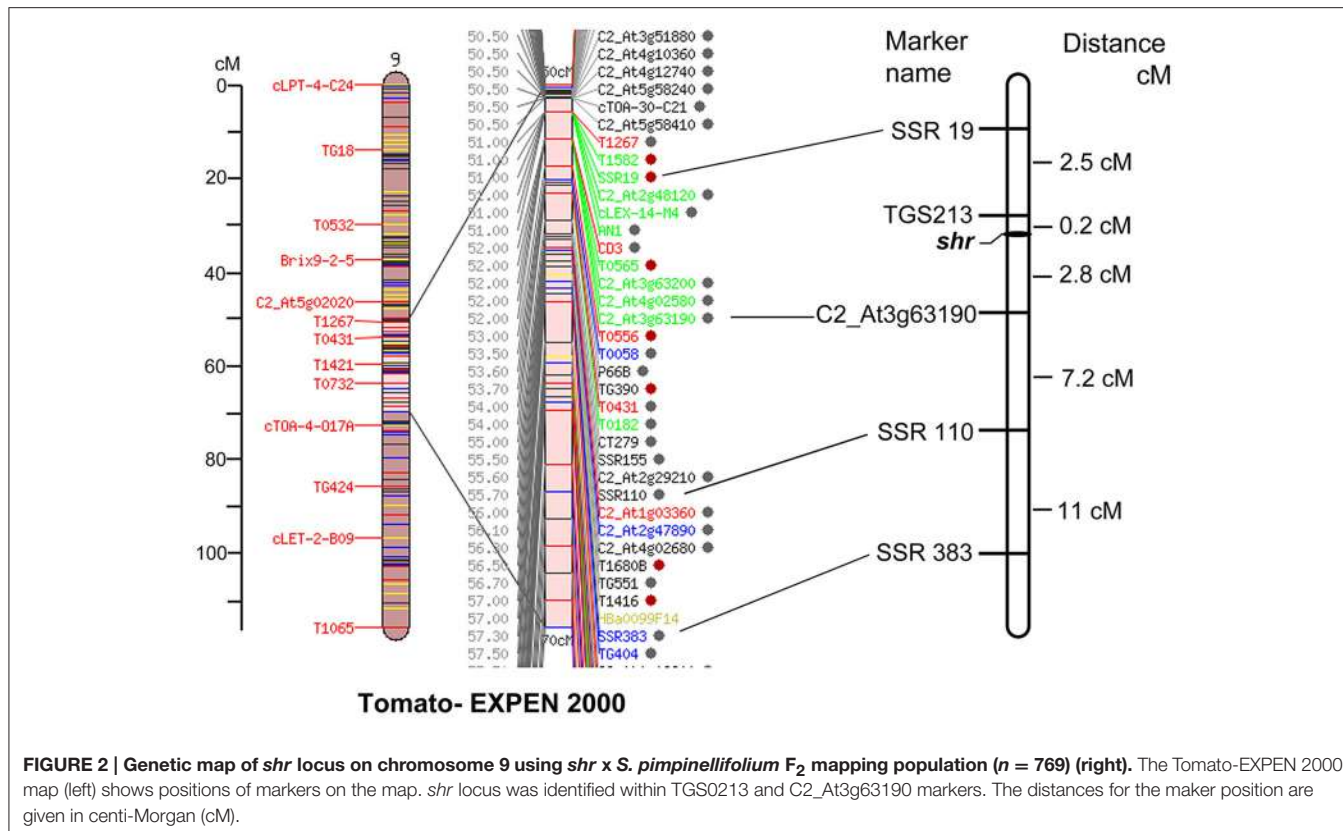


FIGURE 2 | Genetic map of *shr* locus on chromosome 9 using *shr* x *S. pimpinellifolium* F₂ mapping population (*n* = 769) (right). The Tomato-EXPEN 2000 map (left) shows positions of markers on the map. *shr* locus was identified within TGS0213 and C2_At3g63190 markers. The distances for the marker position are given in centi-Morgan (cM).

6-phosphate derived metabolite ribofuranose was downregulated at all stages in *shr* fruits. Similarly, arabinopyranose and threose (immediate precursor glycerol-3-phosphate) were downregulated in *shr* fruits. While glucopyranose levels were high at BR and RR in *shr* fruits, it was undetectable in WT at same stages.

***shr* Mutation Upregulates Tricarboxylic Acid (TCA) Pathway Metabolites**

In *shr* fruits, out of 6 TCA cycle components, citrate and cis-aconitate were upregulated while succinate and methyl succinate were downregulated at all stages. Isocitrate at BR, RR, and malate at RR were upregulated, and fumarate was downregulated at BR. Lactate increased considerably at MG and BR. Acetyl-CoA derived compound- acetate significantly declined during ripening (Figure 6). Interestingly, dehydroascorbate dimer and tartarate were upregulated at all stages. Caffeate (a chlorogenic acid metabolites) and nicotinate, derived from the shikimate pathway considerably increased at all stages. In addition to TCA cycle components nucleic acid metabolites; guanidine and adenosine were also upregulated at MG-RR and BR-RR stage respectively (Figure 6, Supplementary Table 10).

***shr* Mutation Retards Fatty Acid Metabolism during Ripening**

Interestingly in *shr* fruits, all fatty acids were significantly downregulated at MG and BR except myristate that was

downregulated at all stages. Only linolate exhibited no alterations in *shr* compared to WT. During ripening, free fatty acid metabolites in WT progressively declined from a high level at MG, while in *shr* though the level was half of WT, it remained unchanged during ripening.

***shr* Mutation Regulates Ripening by Modulating Auxin and Abscisic Acid Level**

Among the plant hormones, GA and Epi-BR were below the detectable level, and SA, zeatin, MeJA, and JA levels were similar in WT and *shr* fruits. In *shr* fruits, ABA level was low at MG and BR but attained level similar to WT at RR (Figure 7). Conversely, IAA content was high at BR and RR whereas IBA was high at MG in *shr* fruits. The *shr* fruits also emitted higher ethylene at RR (Figure 7). These results indicated that *shr* mutation influenced the temporal changes in ethylene, auxins, and ABA during ripening.

Metabolites and Hormones Regulatory Network Analysis

The regulatory network involved in *shr* fruit ripening was identified by constructing correlation network of significantly different (*P* < 0.05) metabolites and hormones at all stages. The network comprised of 28 metabolites and 2 hormones (ABA and JA) for WT and 16 metabolites and hormone JA for *shr*. In both WT and *shr* network, 3

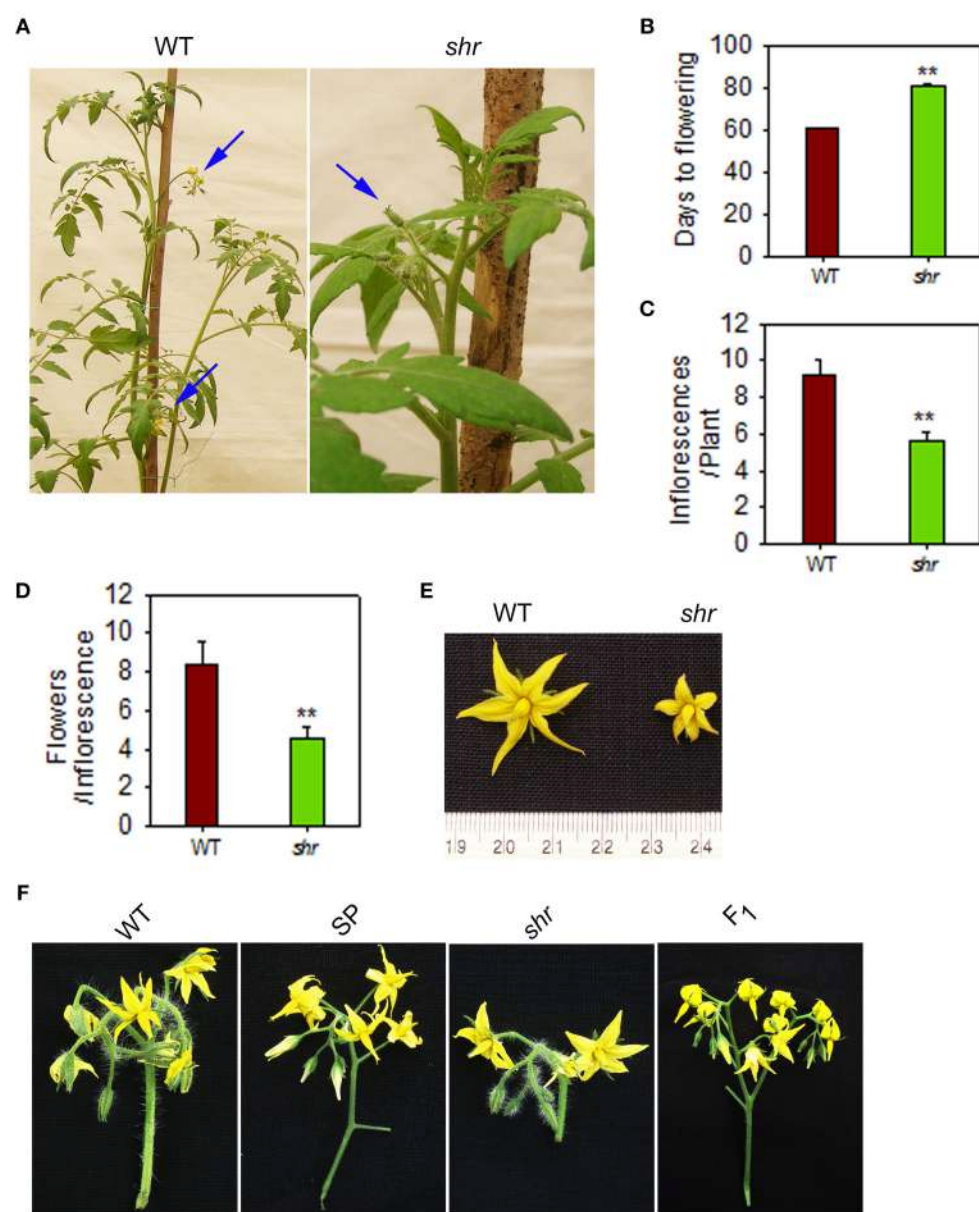


FIGURE 3 | Inflorescence and floral morphology of *shr* mutant plants. (A) Inflorescence(s) in WT and *shr* mutant plants. The blue arrow points that WT plant (60-day old) bears two inflorescences whereas *shr* mutant (80-day old) bear only one inflorescence with unopened flowers. **(B)** Days from sowing for the onset of the flowering. **(C)** Number of inflorescences per plant. **(D)** Number of flowers per inflorescence. **(E)** Floral morphology of WT and *shr* mutant. **(F)** Inflorescence morphology of WT, *S. pimpinellifolium* (SP), *shr* and F1. Note: The peduncle of the inflorescence of *shr* mutant was short and bore less number of flowers compared to WT. The values are the mean \pm SD ($n = 5$). Asterisk indicates statistically significant difference between WT and *shr* (One-Way ANOVA; ** $P < 0.001$).

clusters (I, II, and III) could be distinguished (Figure 8) of which cluster II was most dense with a maximum node connectivity while cluster I and III were sparse with less connectivity.

The PCA of *shr* and WT revealed that the collective complement of metabolites in *shr* fruits was distinctly different from the WT at all stages of fruit ripening. Consistent with this the correlation network of *shr* fruits was distinctly different from WT. First, the network density in *shr* fruits (0.65)

was less than the WT (0.71) (Supplementary Table 11). The number of interactions in *shr* was about 1/4th of the WT. Unlike in WT where positive and negative interactions were about 329 and 170 respectively, these were nearly equal in *shr* (+37 and -41). Most importantly there was only a little overlap in the interactions between WT and *shr*. Among 78 interactions that were present in *shr* only 14 were common with WT and positive to the WT. Moreover, WT network showed 31 unique nodes and had only 9 nodes common with *shr*.

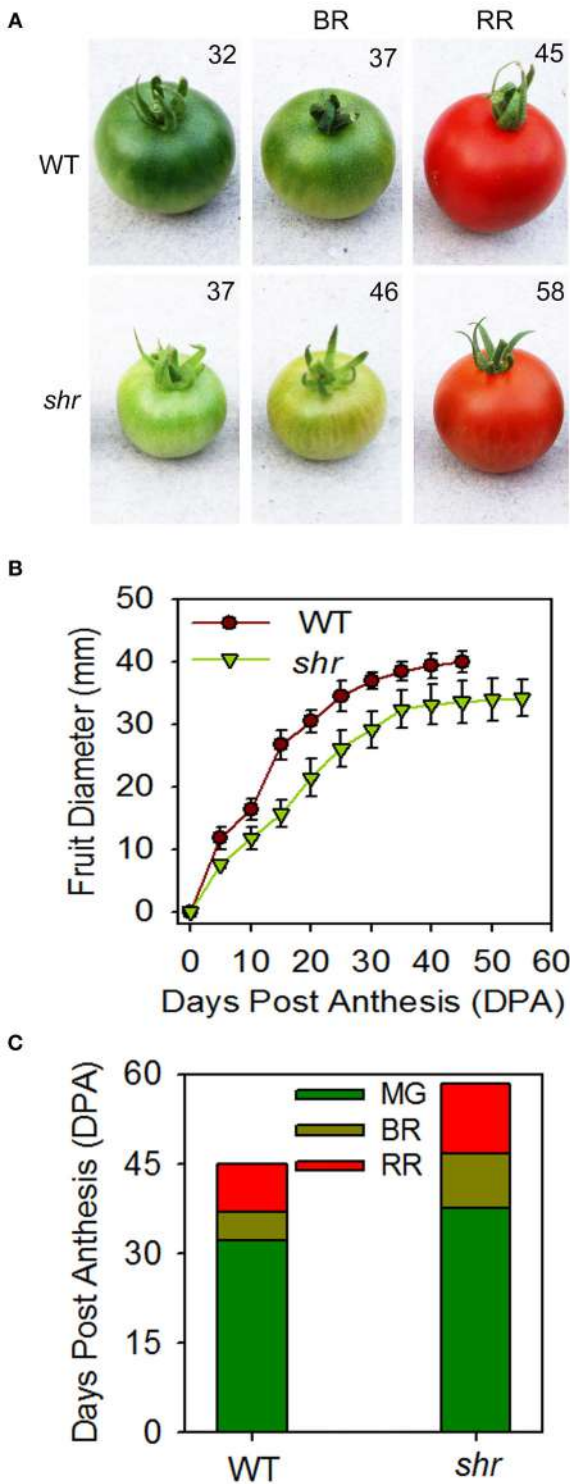


FIGURE 4 | Fruit development and ripening of *shr* fruits. **(A)** WT and *shr* fruits harvested at different days from anthesis. **(B)** Time course of fruit development in WT and *shr* mutant from the day of anthesis to RR stage. **(C)** Duration of different ripening phases of WT and *shr* mutant fruits. The values are the mean \pm SD ($n = 5$). All the data point statistically significantly different between WT and *shr* were determined through One-Way ANOVA ($P < 0.001$).

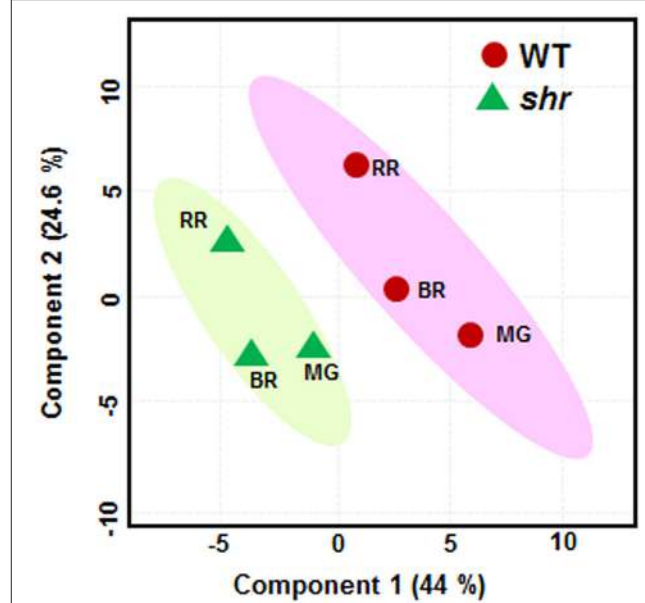
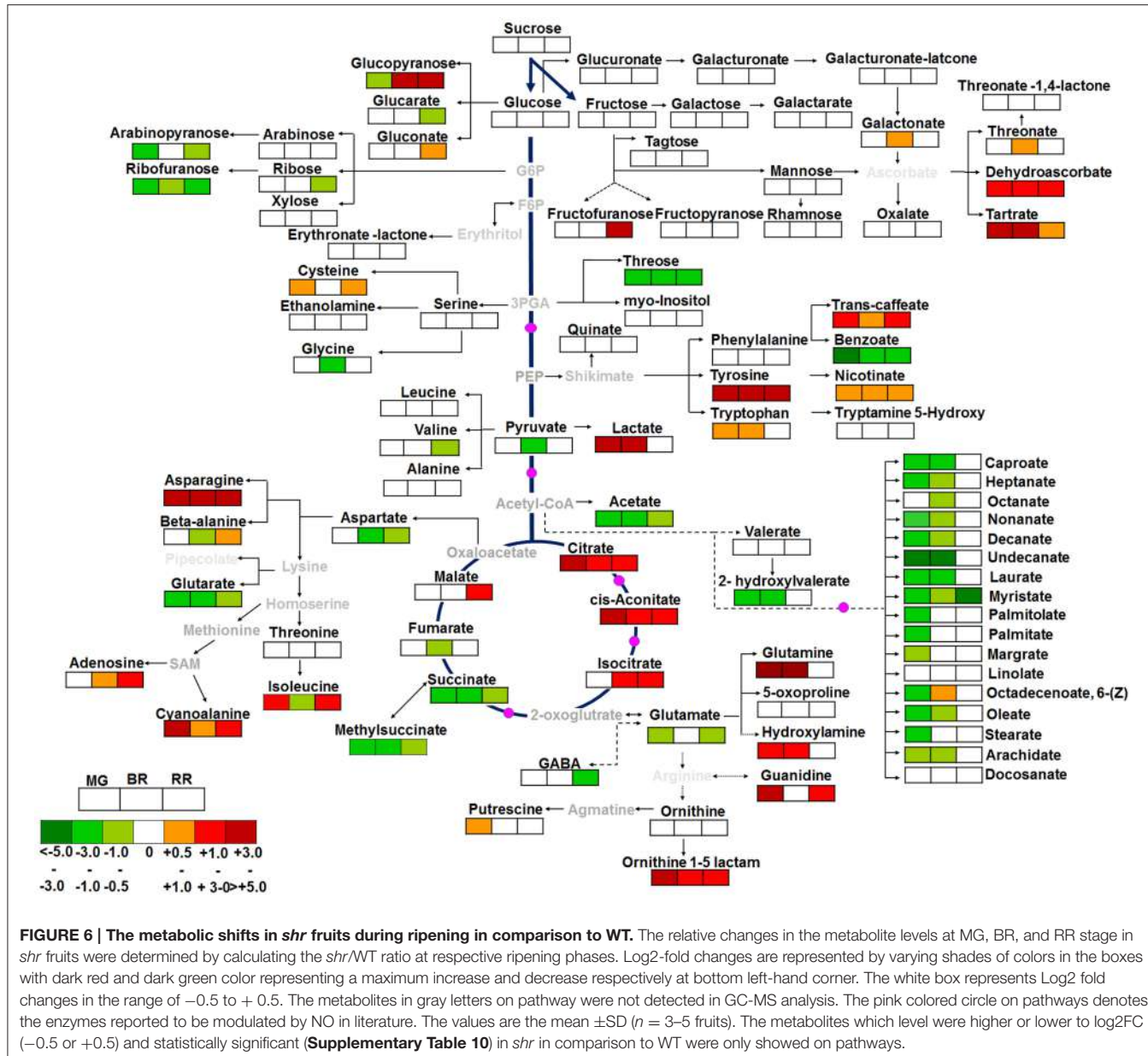


FIGURE 5 | Principle component analysis (PCA) of metabolic profiles. The WT and *shr* mutant fruits were analyzed at MG, BR, and RR stage. The PCA was constructed using the MetaboAnalyst 3.0. The variance of PC1 and PC2 component is given within parentheses.

Similarly, *shr* also showed 8 unique nodes in its correlation network.

These differences between WT and *shr* indicate that the *shr* mutation causes a massive shift in metabolic interaction during the fruit ripening. Most of the interactions that were present in WT were not observed in *shr*. In addition, *shr* showed several unique interactions that were not present in WT. For several metabolites, the interactions were opposite in nature, for example, the interaction of tyrosine with other metabolites (Supplementary Table 11). Interestingly, most of the fatty acids metabolites showed negative interaction with group I (citrate and cis-Aconitate) and positive interaction with group II (acetate, methylsuccinate, and succinate) in WT network, while none of the fatty acids metabolites showed interaction with group I and II metabolites in the *shr* network. These results indicated the metabolites were regulated in a different fashion in *shr* fruits than in the WT.

Examination of WT and *shr* network revealed that TCA pathway metabolites (citrate, cis-aconitate, succinate, methylsuccinate, and acetate) were interconnected and also had maximum connectivity with the other metabolites mostly positioned in cluster II (Figure 8, Supplementary Table 11). On the basis of interactions, two groups were discernible in WT and *shr*. In WT the group I (citrate and cis-acetocinate) positively correlated with each other and negatively correlated with group II (succinate, methylsuccinate, and acetate) and vice-versa. Similarly, in *shr* the group I (citrate) negatively correlated with group II (succinate, and acetate)



and vice-versa. The phytohormones ABA and JA showed maximum connectivity with cluster II (Figure 8). In WT, ABA, and JA positively correlated with group II and negatively correlated with group I. Similarly in *shr*, JA negatively correlated with the group I and positively with group II.

In both WT and *shr*, the cluster I and III were populated with few metabolites. The tyrosine amino acid that specifically is accumulated at a high level in *shr* fruits was positioned in cluster III and it positively correlated with aspartate (Figure 8, Supplementary Table 11). However, tyrosine negatively correlated with most metabolites in *shr* fruit. In addition, several significantly different out-class metabolites were identified that were present only in *shr* network. Taken together the network

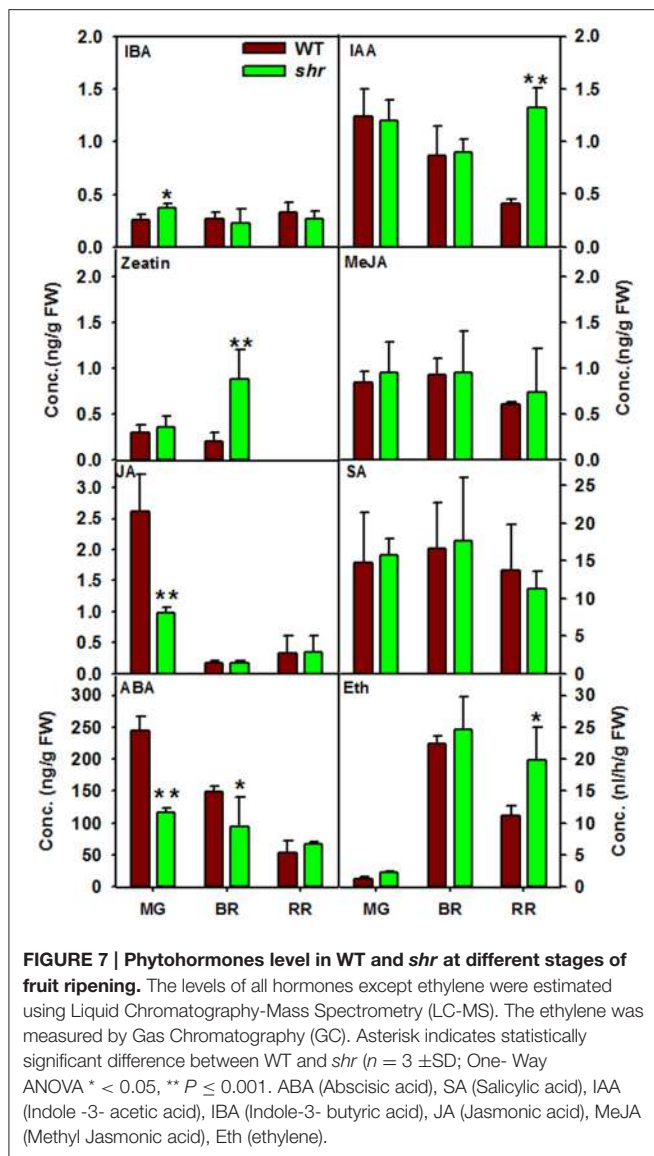
analysis indicated that the *shr* mutation distinctly influences the regulation of metabolites during fruit ripening.

DISCUSSION

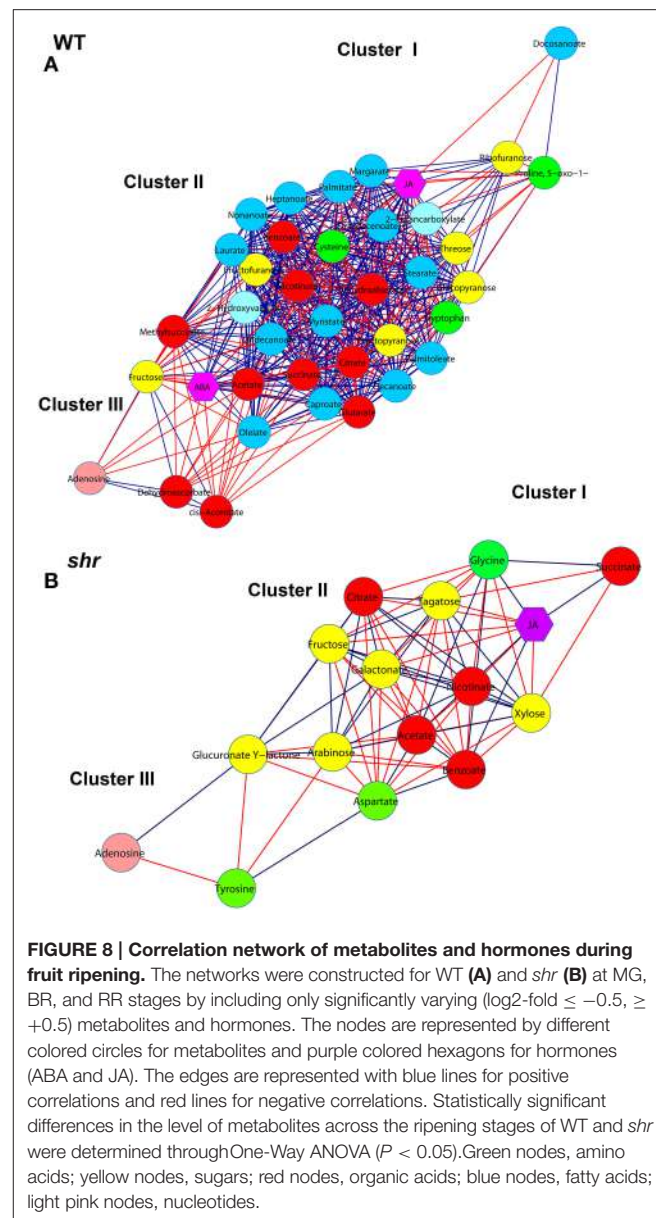
Mapping of *shr* Locus and Candidate Gene Prediction

The genetic analysis of *shr* segregation indicated that the *shr* locus is encoded by a single recessive gene located on chromosome nine and it co-segregates with hyperaccumulation of NO.

Using the advantage of the availability of the complete genome sequence of tomato, we overlaid the *shr* locus on to the tomato physical map. The *shr* locus was located within 4.89 Mb (4894020



bp) region of genome scaffold SL2.40ch09:54045071..58939091 (http://solgenomics.net/gb2/gbrowse/ITAG2.3_genomic). Among the known genes regulating NO levels in plants, only one gene was found in the region encompassing *shr* locus. In Arabidopsis, the null alleles of the *HOT5* locus (GSNOR1/HOT5/PAR2) show increase in *in vivo* levels of NO (Lee et al., 2008; Chen et al., 2009). Based on their reported role in regulating NO level in the mammalian system, glutathione S-transferase (Lok et al., 2012) and CUE domain containing protein (Li et al., 2008) were also examined as potential candidate genes. However, these three most obvious candidate genes did not show a mutation in their respective ORFs. Considering that the tomato genome sequence encompassing *shr* locus region has two major unfilled gaps of 35116 bp and 31568 bp size, it could be possible that these gaps may have additional genes and one of them may be encoding for *shr* mutation. Since *shr* mutant was obtained from γ -irradiated population, the possibility remains



that rather than a single gene mutation, the chromosomal rearrangement, and/or deletion may have contributed to the phenotype attributed to *shr* locus.

shr Mutation Retards Growth and Development

Although the source of *in vivo* NO production (Domingos et al., 2015) remains to be fully deciphered, endogenous NO regulates several facets of higher plant development. The observed diminutive size, sluggish growth and delayed life cycle of the *shr* mutant is consistent with the reports that high endogenous NO level reduces the growth and prolongs the life cycle (Morot-Gaudry-Talarmain et al., 2002). One distinct effect of *shr* locus was on the onset and progression of the reproductive phase. In Arabidopsis, NO overproducer mutant, *nox1* shows

delayed flowering (He et al., 2004) whereas NO under-producer mutant *nos1/noa1* shows earlier flowering (Guo et al., 2003). Consistent with this, *shr* mutant displayed delayed development of inflorescence(s) with smaller and fewer flowers than the parental WT.

Delayed Ripening of *shr* Fruits May Be Due to Alteration in Phytohormone Levels

Compared to vegetative development, little is known about the role of endogenous NO in fruit development and quality. So far the information is largely derived by the application of exogenous NO donors to detached fruits with an aim to extend the postharvest shelf life (Manjunatha et al., 2010; Lai et al., 2011). Post-anthesis, the fruit development in *shr* was sluggish with 5–7 days delay in attaining MG stage than the WT. Consistent with the reduction in root and leaf size due to high endogenous NO levels, the MG fruits of *shr* mutant too were half in size than the WT. Even post-MG stage, the transition to different ripening stages was much slower in *shr* fruits than the WT. Attainment of RR stage in *shr* fruit was delayed by ca. 9 days compared to WT. Though hyperaccumulation of NO slowed ripening of fruits, the on vine shelf life of *shr* fruit post-RR stage was similar to WT. Considering that the carotenoids levels, firmness, and brix of *shr* fruits were similar to WT, it can be assumed that these responses were not affected by NO hyperaccumulation.

Tomato being a climacteric fruit, its ripening is strongly enhanced by the emission of the plant hormone ethylene before the onset of the ripening. The reduction in ethylene biosynthesis by transgenic means also delays tomato ripening (Oeller et al., 1991). Considering that *shr* fruits emitted a higher amount of ethylene than WT, the post MG-delay in ripening is apparently not linked to ethylene biosynthesis. Moreover, our results are not in conformity with the reports that NO downregulates ethylene biosynthesis (Eum et al., 2009; Lai et al., 2011), presumably by S-nitrosylation-mediated inhibition of enzymes regulating ethylene synthesis (Abat and Deswal, 2009). Conversely, our results indicate that higher endogenous NO likely extends the shelf life by delaying the ripening process from MG to RR stage. In several species such as banana, tomato, and strawberries, the application of NO donor SNP (sodium nitroprusside) to detached fruits extended postharvest life (Manjunatha et al., 2010, 2012; Lai et al., 2011). It can be surmised that exogenous NO donors may be extending the fruit shelf life by delaying the overall ripening process.

Apart from their antagonistic interactions in several developmental processes of plants, ethylene and ABA, synergistically promote the ripening process in climacteric fruits (Sun et al., 2012). ABA acts as a principal signal for the onset of ripening, and a decline in ABA levels precedes the climacteric ethylene production in tomato fruit. Considering that the *shr* mutation upregulated ethylene emission at RR stage, it may have affected the endogenous ABA levels. Consistent with this ABA levels in *shr* fruit at MG and BR stages were lower than the WT. The smaller size of *shr* fruits appears to be related to lower ABA levels as ABA deficiency in tomato leads to a reduction in fruit size (Galpaz et al., 2008; Nitsch et al., 2012;

Sun et al., 2012). Tomato fruits harvested at the pink stage from ABA deficient plants showed significantly extended shelf life (Sun et al., 2012). Analogously, the slower development of *shr* fruits and prolonged post-MG ripening period is likely related to reduced ABA levels. However, unlike ABA-deficient plants (Galpaz et al., 2008; Sun et al., 2012), carotenoids levels and firmness is not higher in *shr* fruits. Thus, the observed effects of NO on above processes can also arise from a mechanism other than ABA.

In tomato fruits, the endogenous level of free IAA massively declines before the onset of ripening at MG stage followed by a minor rise at RR stage (Böttcher et al., 2010). Contrarily IAA level declined in WT fruits post-MG stage, whereas in *shr* fruits it increased at RR stage. Conversely, *shr* fruits showed higher IBA levels at MG stage than WT. While the role of IBA *per se* is not yet established in fruit ripening, it is well established that auxin-mediated gene expression strongly influences the ripening process, and excess auxin levels cause parthenocarpy in tomato fruits (de Jong et al., 2009). Tomato WT/35S::IPT plants showed 1.5-2 fold higher zeatin levels in ripe fruit accompanied with higher fruit weight (Ghanem et al., 2011). Though *shr* fruit had 4-fold higher levels of zeatin than WT, it had no effect on fruit weight. While MeJA level in *shr* was nearly similar to WT, it had nearly 4-fold less JA level at MG stage. Though JA-deficient tomato mutants show a reduction in lycopene level (Liu et al., 2012), *shr* fruit showed no such decline in lycopene. It remains to be established how *shr* mutation affected multiple hormonal responses during ripening. However, the observed changes may result from cross talk between NO and phytohormone(s) as NO is the part of signal transduction chain triggered by several hormones. Such a cross talk has been recently reported in developing tomato fruits where AUXIN RESPONSE FACTOR 2A homodimerizes with ABA STRESS RIPENING (ASR1) protein, thus linking ABA and ethylene-dependent ripening. (Breitel et al., 2016).

The *shr* Mutation Likely Affects Metabolome by Modulating TCA Cycle

Tricarboxylic acid (TCA) cycle, at the center of cellular metabolism, is interconnected to wider metabolic network contributing to a plethora of pathways such as amino acid biosynthesis (Mackenzie and McIntosh, 1999), regulation of carbon/nitrogen balance (Noguchi and Terashima, 2006), isoprenoid synthesis (Fatland et al., 2005) and cellular redox control (Scheibe et al., 2005) etc. The profiling of proteins from capsicum fruit exposed to NO revealed nitrosylation of a substantial number of enzymes involved in photosynthesis, glycolysis, oxidative/redox metabolism, amino acid biosynthesis, and proteolysis (Chaki et al., 2015). Therefore, it can be presumed that the increased level of NO in *shr* mutant alters the cellular homeostasis by modifying the activity of enzymes involved in metabolic pathways, consequently affecting the fruit size and prolonging the ripening of fruits. This presumption is in consonance with a previous report wherein enhanced levels of central carbon metabolites are

associated with reduced fruit size in tomato (Schauer et al., 2006).

Considering that the observed shifts in metabolite levels may arise from multiple factors, we focused only on those metabolites that were significantly different in *shr* from WT at all three stages of fruit development. In *shr* fruits among the intermediates of TCA cycle, the citrate and cis-aconitate levels were high and succinate and its derivative, methylsuccinate were low. In tobacco leaf extracts addition of a NO donor inhibited aconitase activity by forming a metal-nitrosyl complex with the Fe-S cluster of the enzyme (Navarre et al., 2000). The higher levels of TCA cycle intermediates in *shr* fruits appears to be related to NO-mediated inhibition of aconitase activity. The leaves of aconitase deficient mutant of *Lycopersicon pennellii* (*Solanum pennellii*) show a similar increase in citrate levels (Carrari et al., 2003). Likewise, hypoxia induced NO accumulation in *Arabidopsis* roots concomitantly reduced aconitase activity and increased the citrate and malate levels (Gupta et al., 2012). Similarly, a reduction in aconitase activity in a tomato introgression line increased citrate levels and reduced succinate level in fruits (Morgan et al., 2013). Thus, it can be assumed that enhanced citrate and reduced succinate levels in *shr* fruit may have resulted from inhibition of aconitase. Considering that the tomato non-ripening mutants *rin*, *Nr*, and *nor* also display reduced level of succinate during ripening (Osorio et al., 2011), the reduced succinate level in *shr* may be linked to prolonged ripening period. However, nitric oxide also affects the activity of other TCA cycle constituents; succinate dehydrogenase (Simonin and Galina, 2013) and cytochrome C oxidase (Millar and Day, 1996). The observed shift in TCA cycle intermediates and ensuing metabolome may thus represent a cumulative effect of NO on a plethora of enzymes and proteins. From the foregoing, it is apparent that the reduction in fruit size and prolonged ripening of *shr* fruits may have a relationship with alteration in central carbon metabolism.

The Cellular Aminome Is Altered in *shr* Fruits

The *shr* mutation had a broad spectrum effect on the cellular aminome eliciting significant changes in levels of several amino acids during fruit ripening. The NO-mediated aconitase inhibition reportedly activates the alternate oxidase pathway and shifts the metabolism toward upregulation of amino acids (Gupta et al., 2012). Among the upregulated amino acids, the high level of hydroxylamine in *shr* fruits may have a relationship to NO biosynthesis as tobacco cell suspensions reportedly convert hydroxylamine to NO (Rümer et al., 2009). Little is known about the role of 3-cyanoalanine in fruit ripening except that it is a byproduct in detoxification of HCN produced during ethylene emission from fruits. Though ornithine,1-5 lactam levels were higher in *shr* fruits, it had no significant effect on polyamines levels which are implicated for longer shelf life of fruits (Mehta et al., 2002), except putrescine at MG stage.

The strong upregulation of tyrosine in *shr* fruit is intriguing. The increased level of tyrosine may signify a block in its downstream metabolism or strong upregulation of its biosynthesis. Considering that the activity of arogenate dehydrogenase that converts arogenate to tyrosine is strongly inhibited by tyrosine (Rippert and Matringe, 2002), the upregulation of biosynthesis is unlikely. Alternately tyrosine can be synthesized from prephenate by the action of prephenate dehydrogenase which lacks feedback regulation by tyrosine via 4-hydroxyphenylpyruvate (Schenck et al., 2015). However, this pathway is reported only in legumes. Nonetheless, upregulation of tyrosine level represents a very specific modulation of a metabolite level by *shr* mutation.

Considering that asparagine is derived from glutamine and aspartate, the high level of glutamine may have correspondingly increased the asparagine levels, indicating a co-ordinated upregulation of these two amino acids. This is also corroborated by the reduced level of aspartate in *shr* fruits. In tomato, arbuscular mycorrhizal association specifically upregulates asparagine and glutamine levels in fruits, presumably by promoting their transport from root to the fruits (Salvioli et al., 2012). Considering that *shr* mutation strongly influences the root phenotype, it may have also influenced the mobilization of these amino acids to the fruit. The reduced level of the glutamate may have a relationship with the prolonged period of ripening of *shr* fruit. A comparison of glutamate levels in *rin* and *nor* non-ripening mutants of tomato with a normal cultivar revealed a significant negative correlation between fruit glutamate levels and shelf life, with lower glutamate levels being associated with a longer shelf life (Pratta et al., 2004). Thus, the lower level of glutamate in *shr* fruit is consistent with its slower ripening.

The progression of fruit ripening in tomato is associated with a steady decline in the fatty acid levels. However, in *shr* fruits, the levels of most fatty acids were much lower even at MG stage and for some even at BR stage. By RR stage, due to a continual decline in fatty acids levels in WT, their levels became nearly equal to *shr* fruits. In leaves of *Arabidopsis ssi2* mutant, the reduction in oleic acid (18:1) level has been shown to induce NO production in chloroplast (Mandal et al., 2012). Considering that level of oleate in *shr* fruits is lower it may have a linkage with the *shr* mutation.

shr Mutation Shifts Cellular Homeostasis

The sizable shift in metabolomic interactions, loss of nodes present in WT and appearance of new nodes in *shr* likely reflects a broad spectrum action of *shr* mutation. A large number of proteins regulating a range of metabolic and developmental processes are known to be targets of NO (Hu et al., 2015). Assuming that the observed shift is related to hyperaccumulation of NO in *shr* mutant, it is plausible that it may have affected the activity of several key proteins regulating cellular metabolism. This presumption is consistent with the report that exogenous application of NO to pepper fruits delayed fruit ripening which may be related to protein nitration of key enzymes (Chaki et al., 2015). One of the distinct responses related to protein nitrosylation pertains to ABA signaling. Plants deficient in NO are hypersensitive to ABA and tyrosine nitration of ABA receptor by NO inhibits ABA signaling (Castillo et al., 2015). The absence

of ABA in the correlation network of *shr* fruits may reflect such a negative effect of the *shr* mutation on ABA-triggered signal transduction. The effect of NO was not restricted to ABA alone. Though JA mapped on the *shr* network, it interacted with a different metabolite sets than in WT.

Currently, little is known how developmental mutants regulate the metabolic shifts. Similar to *shr* mutant, tomato *sun* mutant also showed massive shifts in metabolite interactions, with the loss of several interactions and appearance of unique interactions compared to WT (Clevenger et al., 2015). While *shr* had 64 unique interaction pairs and lost 485 interaction pairs present in the WT, *sun* fruits had 151 unique interaction pairs and lost 273 interaction pairs. Consistent with SUN being a protein with calmodulin recruitment domains, the mutation in it affects the calcium related processes; the major metabolic shifts in *sun* mutant were related to calcium signaling (Clevenger et al., 2015). Likewise, it can be assumed that analogous to *sun* mutant, the metabolic shifts in *shr* mutant may be related to its modulation of NO level. The shift in *shr* correlation networks probably stems from a requirement to sustain the metabolomic homeostasis affected by the *shr* mutation. The altered interactions between different metabolites likely arise from the need to maintain the cellular homeostasis to continue the normal process of ripening (Fares, 2015; Ho and Zhang, 2016), though the overall duration of ripening in *shr* is prolonged. While it can be presumed that the observed loss and gain of metabolite interactions in *shr* represents the process of metabolic compensation, the mechanisms underlying this process are yet to be deciphered.

In summary, the characterization of *shr* mutant indicated that hyperaccumulation of NO slows the on-vine process of fruit ripening in tomato, possibly by altering the overall cellular homeostasis. Our results have an implication for increasing the shelf life of tomato, as selective manipulation of NO levels during ripening can keep the fruits fresh for a longer duration.

AUTHORS CONTRIBUTIONS

The crosses for mapping were made by KS. The mapping analysis of F₂ plants was done by RB and PB. The fruit and seedling phenotyping and metabolic characterization were done by RB and SG. The candidate gene prediction was done by RS and YS. Overall conceptualization of work was done by RS. RB, SG, YS, and RS were involved in writing of manuscript. S and SG made the correlation networks. All authors read and approved the manuscript.

ACKNOWLEDGMENTS

This work was supported by DBT, New Delhi (BT/PR/6803/PBD/16/621/2005; BT/PR/5275/AGR/16/465/2004; BT/PR11671/PBD/16/828/2008) to RS and YS; IAEA, Vienna (15632/R0) to RS). The research fellowship support from CSIR, New Delhi (SG) is gratefully acknowledged. We thank Erika Asamizu, University of Tsukuba, Japan for providing marker information and A. Chandrasekhar, Yogi Vemana

University, Kadapa, India for assistance with Mapmaker software.

SUPPLEMENTARY MATERIAL

The Supplementary Material for this article can be found online at: <http://journal.frontiersin.org/article/10.3389/fpls.2016.01714/full#supplementary-material>

Supplementary Figure S1 | The *shr* mutant plants showed sluggish growth. 45-day-old greenhouse grown *shr*, WT, *S. pimpinellifolium* (*SP*), and F₁ plants were compared **(A)** Morphology of plants. **(B)** Internode (5–6th) length (*upper panel*) and height (*lower panel*). **(C)** Variation in leaf size and morphology. The leaves were harvested from the 7th node of respective plants. **(D)** Chlorophylls and carotenoids levels. Asterisk indicates statistically significant difference between WT and *SP*, *shr* and F₁. The values are the mean ± SD (*n* = 5). Asterisk indicates statistically significant difference between WT and *SP*, *shr*, and F₁ (One Way ANOVA * <0.05, ** *P* < 0.001).

Supplementary Figure S2 | Bulk segregant analysis (BSA) and genotyping of F₂ mapping lines. PCR amplification profile of bulk segregants with the TGS0213 **(A)** and C2_At3g63190 markers **(B)**. P1, short root parent; P2, *S. pimpinellifolium*; B1, short root DNA bulk; B2, long root DNA bulk. **(C)** PCR-based genotyping of TGS0123 marker using *shr* × *S. pimpinellifolium* F₂ mapping population. The lanes 1–22 are F₂ mapping population individuals. Lanes 1–6 are *shr* individuals, and lanes 7–22 are other than short root. The lanes 7–9, 11, 13–15, and 17–20 are heterozygotes. The lanes 10, 12, 16, and 21–22 are long root individuals. The PCR products were electrophoresed on 3.5% (w/v) agarose gel. M- 100-bp DNA ladder.

Supplementary Figure S3 | Ripening induced changes in WT and *shr* mutant at different stages of ripening. **(A)** Brix content. **(B)** Fruit firmness. **(C)** Fruit pH at RR stage. Asterisk indicates statistically significant difference between WT and *shr* mutant (mean ± SD; *n* = 5, Student's *t*-test * *P* ≤ 0.05).

Supplementary Figure S4 | Relative levels of different metabolites in *shr* and WT. The relative level of metabolites was obtained by dividing the peak area of ribitol, the internal standard. Data are the mean value of *n* ≥ 3 ± S.D. (One Way ANNOVA * *P* < 0.05, ** *P* ≤ 0.001). Only most significant metabolites are presented here, the list of total metabolites is given in **Supplementary Table 10**. **(A)**, organic acids; **(B)**, Amino acids; **(C)**, Sugars; **(D)**, Fatty acids; **(E)**, miscellaneous compounds. MG, mature green; BR,breaker; RR, red ripe.

Supplementary Table S1 | The details of SSR and Indel markers used for mapping of *shr* locus. (<http://solgenomics.net/> and <http://www.tomatomap.net/>, Last accessed in 2013).

Supplementary Table S2 | List of additional Simple Sequence Repeats (SSR) markers selected from Kazusa DNA research institute (<http://marker.kazusa.or.jp/tomato>).

Supplementary Table S3 | List of additional Simple Sequence Repeats (SSR) markers selected from Veg Marks, a DNA marker database for vegetables (<http://vegmarks.nivat.affrc.go.jp>, Last accessed in 2013).

Supplementary Table S4 | List of Cleaved Amplified Polymorphic Sequences (CAPS) markers used to map *shr* locus on the chromosome (<http://solgenomics.net>).

Supplementary Table S5 | The genetic segregation of short root phenotype. The segregation was analyzed in the progeny of *shr* × *S. pimpinellifolium* and WT × *shr*. The seedlings were grown under white light and segregation of short root, and long root phenotype in F₁ and F₂ generation was analyzed 7–9 days after germination.

Supplementary Table S6 | The segregation of lateral root phenotype in the progeny of *shr* × *S. pimpinellifolium*. The seedlings were grown under white light and segregation of lateral root, and no lateral root phenotype in F₁ and F₂ generation was analyzed 7–9 days after germination. The identical segregation ratio for lateral root was obtained for another tomato mutant in Ailsa Craig background that was crossed with *S. pimpinellifolium* (data not shown) indicating

that lateral root gene was contributed by *S. lycopersicum* and was unrelated to *shr* locus.

Supplementary Table S7 | Genotype frequency for molecular markers on chromosome 9 in the mapping population derived from *shr* x *S. pimpinellifolium*.

Supplementary Table S8 | List of genes between SSR marker TGS0213 and CAPS marker C2_At3g6310

(http://solgenomics.net/gb2/gbrowse/ITAG2.3_genomic/). Expression of genes was retrieved from Tomato Genome Consortium (2012).

REFERENCES

- Abat, J. K., and Deswal, R. (2009). Differential modulation of S-nitrosoproteome of *Brassica juncea* by low temperature: change in S-nitrosylation of Rubisco is responsible for the inactivation of its carboxylase activity. *Proteomics* 9, 4368–4380. doi: 10.1002/pmic.200800985
- Bai, X. G., Chen, J. H., Kong, X. X., Todd, C. D., Yang, Y. P., Hu, X. Y., et al. (2012). Carbon monoxide enhances the chilling tolerance of recalcitrant *Baccharis ramiflora* seeds via nitric oxide-mediated glutathione homeostasis. *Free Radic. Biol. Med.* 53, 710–720. doi: 10.1016/j.freeradbiomed.2012.05.042
- Bethke, P. C., Libourel, I. G., Aoyama, N., Chung, Y. Y., Still, D. W., and Jones, R. L. (2007). The *Arabidopsis* aleurone layer responds to nitric oxide, gibberellin, and abscisic acid and is sufficient and necessary for seed dormancy. *Plant Physiol.* 143, 1173–1188. doi: 10.1104/pp.106.093435
- Böttcher, C., Keyzers, R. A., Boss, P. K., and Davies, C. (2010). Sequestration of auxin by the indole-3-acetic acid-amido synthetase GH3-1 in grape berry (*Vitis vinifera* L.) and the proposed role of auxin conjugation during ripening. *J. Exp. Bot.* 61, 3615–3625. doi: 10.1093/jxb/erq174
- Breitel, D. A., Chappell-Maor, L., Meir, S., Panizel, I., Puig, C. P., Hao, Y., et al. (2016). AUXIN RESPONSE FACTOR 2 intersects hormonal signals in the regulation of tomato fruit ripening. *PLoS Genet.* 12:e1005903. doi: 10.1371/journal.pgen.1005903
- Cantral, C., Vazquez, T., Puyaubert, J., Rezé, N., Lesch, M., Kaiser, W. M., et al. (2011). Nitric oxide participates in cold-responsive phospholipid formation and gene expression in *Arabidopsis thaliana*. *New Phytol.* 189, 415–427. doi: 10.1111/j.1469-8137.2010.03500.x
- Carrari, F., Nunes-Nesi, A., Gibon, Y., Lytovchenko, A., Loureiro, M. E., and Fernie, A. R. (2003). Reduced expression of aconitase results in an enhanced rate of photosynthesis and marked shifts in carbon partitioning in illuminated leaves of wild species tomato. *Plant Physiol.* 133, 1322–1335. doi: 10.1104/pp.103.026716
- Castillo, M. C., Lozano-Juste, J., González-Guzmán, M., Rodriguez, L., Rodriguez, P. L., and León, J. (2015). Inactivation of PYR/PYL/RCAR ABA receptors by tyrosine nitration may enable rapid inhibition of ABA signaling by nitric oxide in plants. *Sci. Signal.* 8, ra89. doi: 10.1126/scisignal.aaa7981
- Chaki, M., De Morales, P. Á., Ruiz, C., Begara-Morales, J. C., Barroso, J. B., Corpas, F. J., et al. (2015). Ripening of pepper (*Capsicum annuum*) fruit is characterized by an enhancement of protein tyrosine nitration. *Ann. Bot.* 116, 637–647. doi: 10.1093/aob/mcv016
- Chen, R., Sun, S., Wang, C., Li, Y., Liang, Y., An, F., et al. (2009). The *Arabidopsis* PARAQUAT RESISTANT2 gene encodes an S-nitrosoglutathione reductase that is a key regulator of cell death. *Cell Res.* 19, 1377–1387. doi: 10.1038/cr.2009.117
- Cheng, G., Yang, E., Lu, W., Jia, Y., Jiang, Y., and Duan, X. (2009). Effect of nitric oxide on ethylene synthesis and softening of banana fruit slice during ripening. *J. Agric. Food Chem.* 57, 5799–5804. doi: 10.1021/jf901173n
- Clevenger, J. P., Van Houten, J., Blackwood, M., Rodríguez, G. R., Jikumaru, Y., Kamiya, Y., et al. (2015). Network analyses reveal shifts in transcript profiles and metabolites that accompany the expression of SUN and an elongated tomato fruit. *Plant Physiol.* 168, 1164–1178. doi: 10.1104/pp.15.00379
- Cline, M. S., Smoot, M., Cerami, E., Kuchinsky, A., Landys, N., Workman, C., et al. (2007). Integration of biological networks and gene expression data using Cytoscape. *Nat. Protoc.* 2, 2366–2382. doi: 10.1038/nprot.2007.324
- Correa-Aragunde, N., Graziano, M., and Lamattina, L. (2004). Nitric oxide plays a central role in determining lateral root development in tomato. *Planta* 218, 900–905. doi: 10.1007/s00425-003-1172-7
- de Jong, M., Mariani, C., and Vriezen, W. H. (2009). The role of auxin and gibberellin in tomato fruit set. *J. Exp. Bot.* 60, 1523–1532. doi: 10.1093/jxb/erp094
- Do, P. T., Prudent, M., Sulpice, R., Causse, M., and Fernie, A. R. (2010). The influence of fruit load on the tomato pericarp metabolome in a *Solanum chmielewskii* introgression line population. *Plant physiol.* 154, 1128–1142. doi: 10.1104/pp.110.163030
- Domingos, P., Prado, A. M., Wong, A., Gehring, C., and Feijo, J. A. (2015). Nitric oxide: a multitasked signaling gas in plants. *Mol. Plant* 8, 506–520. doi: 10.1016/j.molp.2014.12.010
- Eum, H. L., Kim, H. B., Choi, S. B., and Lee, S. K. (2009). Regulation of ethylene biosynthesis by nitric oxide in tomato (*Solanum lycopersicum* L.) fruit harvested at different ripening stages. *Eur. Food Res. Technol.* 228, 331–338. doi: 10.1007/s00217-008-0938-3
- Fares, M. A. (2015). The origins of mutational robustness. *Trends Genet.* 31, 373–381. doi: 10.1016/j.tig.2015.04.008
- Fatland, B. L., Nikolau, B. J., and Wurtele, E. S. (2005). Reverse genetic characterization of cytosolic acetyl-CoA generation by ATP-citrate lyase in *Arabidopsis*. *Plant Cell* 17, 182–203. doi: 10.1105/tpc.104.026211
- Flores, F. B., Sánchez-Bel, P., Valdenegro, M., Romojoar, F., Martínez-Madrid, M. C., and Egea, M. I. (2008). Effects of a pretreatment with nitric oxide on peach (*Prunus persica* L.) storage at room temperature. *Eur. Food Res. Technol.* 227, 1599–1611. doi: 10.1007/s00217-008-0884-0
- Freschi, L. (2013). Nitric oxide and phytohormone interactions: current status and perspectives. *Front. Plant Sci.* 4:398. doi: 10.3389/fpls.2013.00398
- Galpaz, N., Wang, Q., Menda, N., Zamir, D., and Hirschberg, J. (2008). Abscisic acid deficiency in the tomato mutant high-pigment 3 leading to increased plastid number and higher fruit lycopene content. *Plant J.* 53, 717–730. doi: 10.1111/j.1365-313X.2007.03362.x
- Ghanem, M. E., Albacete, A., Smigocki, A. C., Frébort, I., Pospíšilová, H., Martínez-Andújar, C., et al. (2011). Root-synthesized cytokinins improve shoot growth and fruit yield in salinized tomato (*Solanum lycopersicum* L.) plants. *J. Exp. Bot.* 62, 125–140. doi: 10.1093/jxb/erq266
- Gibbs, D. J., Isa, N. M., Movahedi, M., Lozano-Juste, J., Mendiondo, G. M., Berckhan, S., et al. (2014). Nitric oxide sensing in plants is mediated by proteolytic control of group VII ERF transcription factors. *Mol. Cell* 53, 369–379. doi: 10.1016/j.molcel.2013.12.020
- Guo, F. Q., Okamoto, M., and Crawford, N. M. (2003). Identification of a plant nitric oxide synthase gene involved in hormonal signaling. *Science* 302, 100–103. doi: 10.1126/science.1086770
- Gupta, K. J., Fernie, A. R., Kaiser, W. M., and Van Dongen, J. T. (2011). On the origins of nitric oxide. *Trends Plant Sci.* 16, 160–168. doi: 10.1016/j.tplants.2010.11.007
- Gupta, K. J., Shah, J. K., Brotman, Y., Jahnke, K., Willmitzer, L., Kaiser, W. M., et al. (2012). Inhibition of aconitase by nitric oxide leads to induction of the alternative oxidase and to a shift of metabolism towards biosynthesis of amino acids. *J. Exp. Bot.* 63, 1773–1784. doi: 10.1093/jxb/ers053
- Gupta, P., Sreelakshmi, Y., and Sharma, R. (2015). A rapid and sensitive method for determination of carotenoids in plant tissues by high performance liquid chromatography. *Plant Methods* 11, 1. doi: 10.1186/s13007-015-0051-0
- Gupta, S. K., Sharma, S., Santisree, P., Kilambi, H. V., Appenroth, K., Sreelakshmi, Y., et al. (2014). Complex and shifting interactions of phytochromes regulate fruit development in tomato. *Plant Cell Environ.* 37, 1688–1702. doi: 10.1111/pce.12279

- He, Y., Tang, R.-H., Hao, Y., Stevens, R. D., Cook, C. W., Ahn, S. M., et al. (2004). Nitric oxide represses the *Arabidopsis* floral transition. *Science* 305, 1968–1971. doi: 10.1126/science.1098837
- Ho, W.-C., and Zhang, J. (2016). Adaptive genetic robustness of *Escherichia coli* metabolic fluxes. *Mol. Biol. Evol.* 33, 1164–1176. doi: 10.1093/molbev/msw002
- Hu, J., Huang, X., Chen, L., Sun, X., Lu, C., Zhang, L., et al. (2015). Site-specific nitrosoproteomic identification of endogenously S-nitrosylated proteins in *Arabidopsis*. *Plant Physiol.* 167, 1731–1746. doi: 10.1104/pp.15.00026
- Kilambi, H. V., Kumar, R., Sharma, R., and Sreelakshmi, Y. (2013). Chromoplast-specific carotenoid-associated protein appears to be important for enhanced accumulation of carotenoids in hp1 tomato fruits. *Plant Physiol.* 161, 2085–2101. doi: 10.1104/pp.112.212191
- Kosambi, D. D. (1943). The estimation of map distances from recombination values. *Ann. Eugen.* 12, 172–175. doi: 10.1111/j.1469-1809.1943.tb0231x
- Lai, T., Wang, Y., Li, B., Qin, G., and Tian, S. (2011). Defense responses of tomato fruit to exogenous nitric oxide during postharvest storage. *Postharvest Biol. Technol.* 62, 127–132. doi: 10.1016/j.postharvbio.2011.05.011
- Lander, E. S., Green, P., Abrahamson, J., Barlow, A., Daly, M. J., Lincoln, S. E., et al. (1987). MAPMAKER: an interactive computer package for constructing primary genetic linkage maps of experimental and natural populations. *Genomics* 1, 174–181. doi: 10.1016/0888-7543(87)90010-3
- Lee, U., Wie, C., Fernandez, B. O., Feelisch, M., and Vierling, E. (2008). Modulation of nitrosative stress by S-nitrosoglutathione reductase is critical for thermotolerance and plant growth in *Arabidopsis*. *Plant Cell* 20, 786–802. doi: 10.1105/tpc.107.052647
- Leshem, Y. Y., and Pinchasov, Y. (2000). Non-invasive photoacoustic spectroscopic determination of relative endogenous nitric oxide and ethylene content stoichiometry during the ripening of strawberries *Fragaria ananassa* (Duch.) and avocados *Persea americana* (Mill.). *J. Exp. Bot.* 51, 1471–1473. doi: 10.1093/jexbot/51.349.1471
- Li, H. Y., Liu, H., Wang, C. H., Zhang, J. Y., Man, J. H., Gao, Y. F., et al. (2008). Deactivation of the kinase IKK by CUEDC2 through recruitment of the phosphatase PP1. *Nat. Immunol.* 9, 533–541. doi: 10.1038/ni.1600
- Lichtenthaler, H. K. (1987). Chlorophyll and carotenoids: pigments of photosynthetic biomembranes. *Meth. Enzymol.* 148, 350–382. doi: 10.1016/0076-6879(87)48036-1
- Lincoln, S. E., and Lander, E. S. (1992). Systematic detection of errors in genetic linkage data. *Genomics* 14, 604–610. doi: 10.1016/S0888-7543(05)80158-2
- Liu, L., Wei, J., Zhang, M., Zhang, L., Li, C., and Wang, Q. (2012). Ethylene independent induction of lycopene biosynthesis in tomato fruits by jasmonates. *J. Exp. Bot.* 63, 5751–5751. doi: 10.1093/jxb/ers224
- Liu, W. Z., Kong, D. D., Gu, X. X., Gao, H. B., Wang, J. Z., Xia, M., et al. (2013). Cytokinins can act as suppressors of nitric oxide in *Arabidopsis*. *Proc. Natl. Acad. Sci. U.S.A.* 110, 1548–1553. doi: 10.1073/pnas.1213235110
- Liu, Y., Shi, L., Ye, N., Liu, R., Jia, W., and Zhang, J. (2009). Nitric oxide-induced rapid decrease of abscisic acid concentration is required in breaking seed dormancy in *Arabidopsis*. *New Phytol.* 183, 1030–1042. doi: 10.1111/j.1469-8137.2009.02899.x
- Lok, H. C., Rahmanto, Y. S., Hawkins, C. L., Kalinowski, D. S., Morrow, C. S., Townsend, A. J., et al. (2012). Nitric oxide storage and transport in cells are mediated by glutathione S-transferase P1-1 and multidrug resistance protein 1 via dinitrosyl iron complexes. *J. Biol. Chem.* 287, 607–618. doi: 10.1074/jbc.M111.310987
- Lommen, A., and Kools, H. J. (2012). MetAlign 3.0: performance enhancement by efficient use of advances in computer hardware. *Metabolomics* 8, 719–726. doi: 10.1007/s11306-011-0369-1
- Lozano-Juste, J., and León, J. (2011). Nitric oxide regulates DELLA content and PIF expression to promote photomorphogenesis in *Arabidopsis*. *Plant Physiol.* 156, 1410–1423. doi: 10.1104/pp.111.177741
- Mackenzie, S., and McIntosh, L. (1999). Higher plant mitochondria. *Plant Cell* 11, 571–585. doi: 10.1105/tpc.11.4.571
- Makeen, K., Babu, S. G., Lavanya, G., and Grard, A. (2007). Studies of chlorophyll content by different methods in black gram (*Vigna mungo* L.). *Int. J. Agric. Res.* 2, 651–654. doi: 10.3923/ijar.2007.651.654
- Mandal, M. K., Chandra-Shekara, A., Jeong, R. D., Yu, K., Zhu, S., Chanda, B., et al. (2012). Oleic acid-dependent modulation of NITRIC OXIDE ASSOCIATED protein levels regulates nitric oxide-mediated defense signaling in *Arabidopsis*. *Plant Cell* 24, 1654–1674. doi: 10.1105/tpc.112.096768
- Manjunatha, G., Gupta, K. J., Lokesh, V., Mur, L., and Neelwarne, B. (2012). Nitric oxide counters ethylene effects on ripening fruits. *Plant Signal. Behav.* 7, 476–483. doi: 10.4161/psb.19523
- Manjunatha, G., Lokesh, V., and Neelwarne, B. (2010). Nitric oxide in fruit ripening: trends and opportunities. *Biotechnol. Adv.* 28, 489–499. doi: 10.1016/j.biotechadv.2010.03.001
- Manjunatha, G., Lokesh, V., Neelwarne, B., Singh, Z., and Gupta, K. J. (2014). Nitric oxide applications for quality enhancement of horticulture produce. *Hortic. Rev.* 42, 121–156. doi: 10.1002/9781118916827.ch02
- Mehta, R. A., Cassol, T., Li, N., Ali, N., Handa, A. K., and Mattoo, A. K. (2002). Engineered polyamine accumulation in tomato enhances phytonutrient content, juice quality, and vine life. *Nat. Biotechnol.* 20, 613–618. doi: 10.1038/nbt0602-613
- Michelmore, R. W., Paran, I., and Kesseli, R. (1991). Identification of markers linked to disease-resistance genes by bulked segregant analysis: a rapid method to detect markers in specific genomic regions by using segregating populations. *Proc. Natl. Acad. Sci. U.S.A.* 88, 9828–9832. doi: 10.1073/pnas.88.21.9828
- Millar, A. H., and Day, D. A. (1996). Nitric oxide inhibits the cytochrome oxidase but not the alternative oxidase of plant mitochondria. *FEBS Lett.* 398, 155–158. doi: 10.1016/S0014-5793(96)01230-6
- Moreau, M., Lee, G. I., Wang, Y., Crane, B. R., and Klessig, D. F. (2008). AtNOS/AtNOA1 is a functional *Arabidopsis thaliana* cGTPase and not a nitric-oxide synthase. *J. Biol. Chem.* 283, 32957–32967. doi: 10.1074/jbc.M804838200
- Morgan, M. J., Osorio, S., Gehl, B., Baxter, C. J., Kruger, N. J., Ratcliffe, R. G., et al. (2013). Metabolic engineering of tomato fruit organic acid content guided by biochemical analysis of an introgression line. *Plant Physiol.* 161, 397–407. doi: 10.1104/pp.112.209619
- Morot-Gaudry-Talarmain, Y., Rockel, P., Moureaux, T., Quilleré, I., Leydecker, M., Kaiser, W., et al. (2002). Nitrite accumulation and nitric oxide emission in relation to cellular signaling in nitrite reductase antisense tobacco. *Planta* 215, 708–715. doi: 10.1007/s00425-002-0816-3
- Navarre, D. A., Wendehenne, D., Durner, J., Noad, R., and Klessig, D. F. (2000). Nitric oxide modulates the activity of tobacco aconitase. *Plant Physiol.* 122, 573–582. doi: 10.1104/pp.122.2.573
- Negi, S., Kharshiing, E. V., and Sharma, R. (2011). NO way! *Plant Signal. Behav.* 6, 1049–1052. doi: 10.4161/psb.6.7.15633
- Negi, S., Santisree, P., Kharshiing, E. V., and Sharma, R. (2010). Inhibition of the ubiquitin–proteasome pathway alters cellular levels of nitric oxide in tomato seedlings. *Mol. Plant* 3, 854–869. doi: 10.1093/mp/ssq033
- Nitsch, L., Kohlen, W., Oplaat, C., Charnikhova, T., Cristescu, S., Michieli, P., et al. (2012). ABA-deficiency results in reduced plant and fruit size in tomato. *J. Plant Physiol.* 169, 878–883. doi: 10.1016/j.jplph.2012.02.004
- Noguchi, K., and Terashima, I. (2006). Responses of spinach leaf mitochondria to low N availability. *Plant Cell Environ.* 29, 710–719. doi: 10.1111/j.1365-3040.2005.01457.x
- Oeller, P. W., Lu, M., Taylor, L. P., Pike, D. A., and Theologis, A. (1991). Reversible inhibition of tomato fruit senescence by antisense RNA. *Science* 254, 437–439. doi: 10.1126/science.1925603
- Ohyama, A., Asamizu, E., Negoro, S., Miyatake, K., Yamaguchi, H., Tabata, S., et al. (2009). Characterization of tomato SSR markers developed using BAC-end and cDNA sequences from genome databases. *Mol. Breed.* 23, 685–691. doi: 10.1007/s11032-009-9265-z
- Osorio, S., Alba, R., Damasceno, C. M., Lopez-Casado, G., Lohse, M., Zanor, M. I., et al. (2011). Systems biology of tomato fruit development: combined transcript, protein, and metabolite analysis of tomato transcription factor (nor, rin) and ethylene receptor (Nr) mutants reveals novel regulatory interactions. *Plant Physiol.* 157, 405–425. doi: 10.1104/pp.111.175463
- Pagnussat, G. C., Lanteri, M. L., and Lamattina, L. (2003). Nitric oxide and cyclic GMP are messengers in the indole acetic acid-induced adventitious rooting process. *Plant Physiol.* 132, 1241–1248. doi: 10.1104/pp.103.022228
- Pan, X., Welti, R., and Wang, X. (2004). Quantitative analysis of major plant hormones in crude plant extracts by high-performance liquid chromatography–mass spectrometry. *Nat. Protoc.* 5, 986–992. doi: 10.1038/nprot.2010.37

- Pratta, G., Zorzoli, R., Boggio, S., Picardi, L., and Valle, E. (2004). Glutamine and glutamate levels and related metabolizing enzymes in tomato fruits with different shelf-life. *Sci. Hortic.* 100, 341–347. doi: 10.1016/j.scienta.2003.08.004
- Rippert, P., and Matringe, M. (2002). Purification and kinetic analysis of the two recombinant arogenate dehydrogenase isoforms of *Arabidopsis thaliana*. *Eur. J. Biochem.* 269, 4753–4761. doi: 10.1046/j.1432-1033.2002.03172.x
- Roessner, U., Wagner, C., Kopka, J., Trethewey, R. N., and Willmitzer, L. (2000). Simultaneous analysis of metabolites in potato tuber by gas chromatography-mass spectrometry. *Plant J.* 23, 131–142. doi: 10.1046/j.1365-313x.2000.00774.x
- Rümer, S., Gupta, K. J., and Kaiser, W. M. (2009). Plant cells oxidize hydroxylamines to NO. *J. Exp. Bot.* 60, 2065–2072. doi: 10.1093/jxb/erp077
- Salvioli, A., Zouari, I., Chalot, M., and Bonfante, P. (2012). The arbuscular mycorrhizal status has an impact on the transcriptome profile and amino acid composition of tomato fruit. *BMC Plant Biol.* 12:44. doi: 10.1186/1471-2229-12-44
- Schauer, N., Semel, Y., Roessner, U., Gur, A., Balbo, I., Carrari, F., et al. (2006). Comprehensive metabolic profiling and phenotyping of interspecific introgression lines for tomato improvement. *Nat. Biotechnol.* 24, 447–454. doi: 10.1038/nbt1192
- Scheibe, R., Backhausen, J. E., Emmerlich, V., and Holtgrefe, S. (2005). Strategies to maintain redox homeostasis during photosynthesis under changing conditions. *J. Exp. Bot.* 56, 1481–1489. doi: 10.1093/jxb/eri181
- Schenck, C. A., Chen, S., and Siehl, D. L. (2015). Maeda, H. A. Non-plastidic, tyrosine-insensitive prephenate dehydrogenases from legumes. *Nat. Chem. Biol.* 11, 52–57. doi: 10.1038/nchembio.1693
- Shirasawa, K., Asamizu, E., Fukuoka, H., Ohyama, A., Sato, S., Nakamura, Y., et al. (2010a). An interspecific linkage map of SSR and intronic polymorphism markers in tomato. *Theor. Appl. Genet.* 121, 731–739. doi: 10.1007/s00122-010-1344-3
- Shirasawa, K., Isobe, S., Hirakawa, H., Asamizu, E., Fukuoka, H., Just, D., et al. (2010b). SNP discovery and linkage map construction in cultivated tomato. *DNA Res.* 17, 381–391. doi: 10.1093/dnarecs/dsq024
- Simonin, V., and Galina, A. (2013). Nitric oxide inhibits succinate dehydrogenase-driven oxygen consumption in potato tuber mitochondria in an oxygen tension-independent manner. *Biochem. J.* 449, 263–273. doi: 10.1042/BJ20120396
- Singh, S., Singh, Z., and Swinny, E. (2009). Postharvest nitric oxide fumigation delays fruit ripening and alleviates chilling injury during cold storage of Japanese plums (*Prunus salicina* Lindell). *Postharvest Biol. Technol.* 53, 101–108. doi: 10.1016/j.postharvbio.2009.04.007
- Singh, Z., Khan, A. S., Zhu, S., and Payne, A. D. (2013). Nitric oxide in the regulation of fruit ripening: challenges and thrusts. *Stewart Postharvest Rev.* 9, 1–11. doi: 10.2212/spr.2013.4.3
- Sreelakshmi, Y., Gupta, S., Bodanapu, R., Chauhan, V. S., Hanjabam, M., Thomas, S., et al. (2010). NEATTILL: A simplified procedure for nucleic acid extraction from arrayed tissue for TILLING and other high-throughput reverse genetic applications. *Plant Methods* 6:3. doi: 10.1186/1746-4811-6-3
- Sun, L., Sun, Y., Zhang, M., Wang, L., Ren, J., Cui, M., et al. (2012). Suppression of 9-cis-epoxycarotenoid dioxygenase, which encodes a key enzyme in abscisic acid biosynthesis, alters fruit texture in transgenic tomato. *Plant Physiol.* 158, 283–298. doi: 10.1104/pp.111.186866
- Tikunov, Y., Laptenok, S., Hall, R., Bovy, A., and De Vos, R. (2012). MSClust: a tool for unsupervised mass spectra extraction of chromatography-mass spectrometry ion-wise aligned data. *Metabolomics* 8, 714–718. doi: 10.1007/s11306-011-0368-2
- Voorrips, R. (2002). MapChart: software for the graphical presentation of linkage maps and QTLs. *J. Hered.* 93, 77–78. doi: 10.1093/jhered/93.1.77
- Wang, X. Q., Ullah, H., Jones, A. M., and Assmann, S. M. (2001). G protein regulation of ion channels and abscisic acid signaling in *Arabidopsis* guard cells. *Science* 292, 2070–2072. doi: 10.1126/science.1059046
- Wang, Y., Ries, A., Wu, K., Yang, A., and Crawford, N. M. (2010). The *Arabidopsis* prohibitin gene PHB3 functions in nitric oxide-mediated responses and in hydrogen peroxide-induced nitric oxide accumulation. *Plant Cell* 22, 249–259. doi: 10.1105/tpc.109.072066
- Xia, J., Sinelnikov, I. V., Han, B., and Wishart, D. S. (2015). MetaboAnalyst 3.0—making metabolomics more meaningful. *Nucleic Acids Res.* 43, W251–W257. doi: 10.1093/nar/gkv380
- Xu, M., Dong, J., Zhang, M., Xu, X., and Sun, L. (2012). Cold-induced endogenous nitric oxide generation plays a role in chilling tolerance of loquat fruit during postharvest storage. *Postharvest Biol. Technol.* 65, 5–12. doi: 10.1016/j.postharvbio.2011.10.008
- Zaharah, S. S., and Singh, Z. (2011). Postharvest nitric oxide fumigation alleviates chilling injury, delays fruit ripening and maintains quality in cold-stored ‘Kensington Pride’ mango. *Postharvest Biol. Technol.* 60, 202–210. doi: 10.1016/j.postharvbio.2011.01.011
- Zhao, M.-G., Chen, L., Zhang, L.-L., and Zhang, W.-H. (2009). Nitric reductase-dependent nitric oxide production is involved in cold acclimation and freezing tolerance in *Arabidopsis*. *Plant Physiol.* 151, 755–767. doi: 10.1104/pp.109.140996
- Zhu, S., Sun, L., Liu, M., and Zhou, J. (2008). Effect of nitric oxide on reactive oxygen species and antioxidant enzymes in kiwifruit during storage. *J. Sci. Food Agric.* 88, 2324–2331. doi: 10.1002/jsfa.3353
- Zhu, S., and Zhou, J. (2006). Effects of nitric oxide on fatty acid composition in peach fruits during storage. *J. Agric. Food Chem.* 54, 9447–9452. doi: 10.1021/jf062451u

Conflict of Interest Statement: The authors declare that the research was conducted in the absence of any commercial or financial relationships that could be construed as a potential conflict of interest.

Copyright © 2016 Bodanapu, Gupta, Basha, Sakthivel, Sadhana, Sreelakshmi and Sharma. This is an open-access article distributed under the terms of the Creative Commons Attribution License (CC BY). The use, distribution or reproduction in other forums is permitted, provided the original author(s) or licensor are credited and that the original publication in this journal is cited, in accordance with accepted academic practice. No use, distribution or reproduction is permitted which does not comply with these terms.



On the Developmental and Environmental Regulation of Secondary Metabolism in *Vaccinium* spp. Berries

Katja Karppinen^{1,2}, Laura Zoratti¹, Nga Nguyenquynh¹, Hely Häggman¹ and Laura Jaakola^{2,3*}

¹ Genetics and Physiology Unit, University of Oulu, Oulu, Finland, ² Climate laboratory Holt, Department of Arctic and Marine Biology, UiT the Arctic University of Norway, Tromsø, Norway, ³ NIBIO, Norwegian Institute of Bioeconomy Research, Ås, Norway

OPEN ACCESS

Edited by:

Antonio Granell,
Consejo Superior de Investigaciones
Científicas, Spain

Reviewed by:

Shan Lu,
Nanjing University, China
Andrea Matros,
IPK-Gatersleben, Germany

*Correspondence:

Laura Jaakola
laura.jaakola@uit.no

Specialty section:

This article was submitted to
Plant Physiology,
a section of the journal
Frontiers in Plant Science

Received: 12 February 2016

Accepted: 28 April 2016

Published: 18 May 2016

Citation:

Karppinen K, Zoratti L, Nguyenquynh N, Häggman H and Jaakola L (2016) On the Developmental and Environmental Regulation of Secondary Metabolism in *Vaccinium* spp. Berries. *Front. Plant Sci.* 7:655.
doi: 10.3389/fpls.2016.00655

Secondary metabolites have important defense and signaling roles, and they contribute to the overall quality of developing and ripening fruits. Blueberries, bilberries, cranberries, and other *Vaccinium* berries are fleshy berry fruits recognized for the high levels of bioactive compounds, especially anthocyanin pigments. Besides anthocyanins and other products of the phenylpropanoid and flavonoid pathways, these berries also contain other metabolites of interest, such as carotenoid derivatives, vitamins and flavor compounds. Recently, new information has been achieved on the mechanisms related with developmental, environmental, and genetic factors involved in the regulation of secondary metabolism in *Vaccinium* fruits. Especially light conditions and temperature are demonstrated to have a prominent role on the composition of phenolic compounds. The present review focuses on the studies on mechanisms associated with the regulation of key secondary metabolites, mainly phenolic compounds, in *Vaccinium* berries. The advances in the research concerning biosynthesis of phenolic compounds in *Vaccinium* species, including specific studies with mutant genotypes in addition to controlled and field experiments on the genotype × environment (G×E) interaction, are discussed. The recently published *Vaccinium* transcriptome and genome databases provide new tools for the studies on the metabolic routes.

Keywords: anthocyanins, bilberry, blueberry, carotenoids, flavonoids, fruits, light, temperature

INTRODUCTION

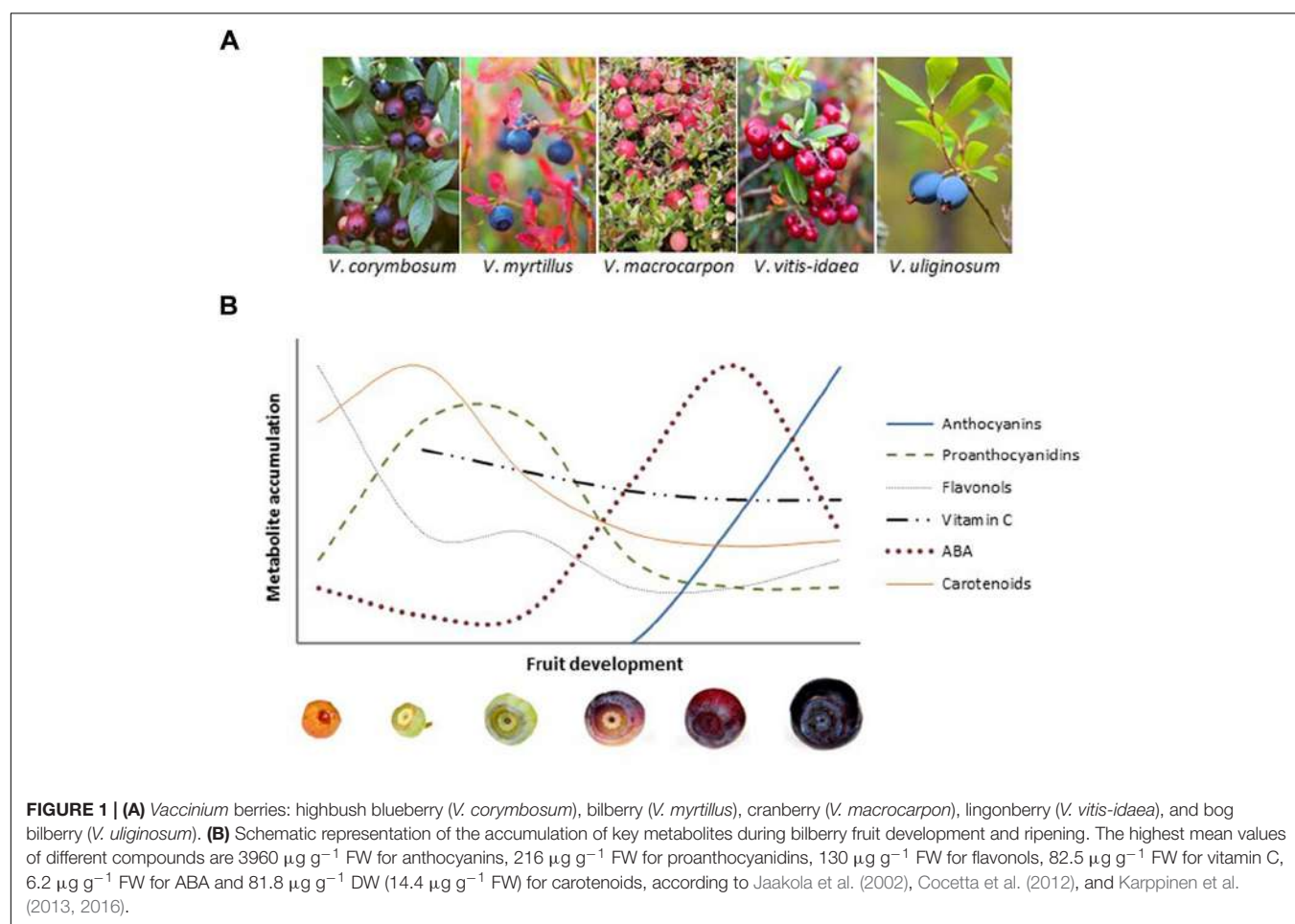
Genus *Vaccinium* includes over 450 deciduous or evergreen species distributed in cool temperate regions and mountains of the northern and southern hemispheres. The genus contains economically important cultivated and wild berry species, such as blueberries (e.g., *Vaccinium corymbosum*, *V. angustifolium*), bilberry (*V. myrtillus*), cranberries (*V. macrocarpon*, *V. oxycoccus*), and lingonberry (*V. vitis-idaea*; **Figure 1A**). Numerous studies have given evidence on the beneficial health effects of these berries, for instance in reducing risk of metabolic syndrome and various microbial and degenerative diseases (Kolehmainen et al., 2012; Blumberg et al., 2013; Norberto et al., 2013; Patel, 2014). These health-benefits are mostly attributed to the various phenolic compounds. *Vaccinium* berries are rich with flavonoids, including anthocyanins, flavonols, and proanthocyanidins (Määttä-Riihinne et al., 2004; Rodrigues-Mateos et al., 2012;

Ancillotti et al., 2016), which are linked to many biological activities such as anti-inflammatory, antimutagenic, antimicrobial, anticancer, antiobesity, and antioxidant properties (Szajdeka and Borowska, 2008; He and Giusti, 2010; Nile and Park, 2014). However, these berries also contain other valuable compounds, such as carotenoids and their derivatives, other flavor compounds and vitamins. This review covers the current knowledge on the developmental and environmental regulation of the biosynthesis of key metabolites in *Vaccinium* berries. Most studies in this topic have been performed on flavonoids but other compounds, such as other phenylpropanoids, carotenoid derivatives, and vitamin C are also covered.

DEVELOPMENTAL REGULATION

Development and ripening of fleshy fruits include major changes in fruit structure and in overall metabolism. At the metabolic level, development of *Vaccinium* berries is characterized by the production of high amounts of flavonoids, especially red/blue-pigmented anthocyanins coloring the ripe fruits (**Figure 1A**). At the early stages of berry development, proanthocyanidins, flavonols, and hydroxinnamic acids are the major phenolic compounds in these berries, and the

accumulation of anthocyanins begins at the onset of ripening (Jaakola et al., 2002; Vvedenskaya and Vorsa, 2004; Castrejón et al., 2008; Zifkin et al., 2012; Gibson et al., 2013; **Figure 1B**). However, the flavonoid profiles vary between *Vaccinium* berries most of which accumulate anthocyanins only in the skin at ripening. Bilberry, which is recognized as one of the richest source of anthocyanins, accumulates these compounds also in flesh of ripe fruits with 15 different major anthocyanin glycosides identified (Jaakola et al., 2002; Zoratti et al., 2014b). The profile of anthocyanins in ripe bilberries and blueberries comprises glycosides of cyanidin, delphinidin, peonidin, petunidin, and malvidin anthocyanidins (Lohachoompol et al., 2008; Zoratti et al., 2014b). In red-colored *Vaccinium* berries, the profile of anthocyanins is less diverse, cyanidin glycosides being the major anthocyanins in ripe lingonberries, in addition to peonidins in ripe cranberries (Lee and Finn, 2012; Grace et al., 2014; Česonienė et al., 2015). However, proanthocyanidin content in ripe berries is typically higher in red-colored *Vaccinium* berries compared with blueberries. The proanthocyanidin profile of ripe *Vaccinium* berries includes procyanidins with rare A-type linkages (Määttä-Riihinen et al., 2005; Lähti et al., 2011; Grace et al., 2014). In addition to the role of anthocyanins in seed dispersal, the variation in flavonoid profile during berry development is considered to be related in defense responses.



For instance, the astringent proanthocyanidins are suggested to provide protection against predation in unripe berries (Harborne, 1997).

Fleshy fruits are traditionally defined as either climacteric or non-climacteric according to the differences in respiration rate and production of ethylene at ripening (Gapper et al., 2013; McAtee et al., 2013; Osorio et al., 2013). In recent years, regulatory role of abscisic acid (ABA) has been established at molecular level in ripening initiation as well as in control of ripening-related anthocyanin biosynthesis of non-climacteric fruits (Jia et al., 2011; Li et al., 2011; Shen et al., 2014; Kadomura-Ishikawa et al., 2015), which includes *Vaccinium* berries. The increase in ABA levels at fruit ripening has been demonstrated in several non-climacteric fruits (Wheeler et al., 2009; Jia et al., 2011; Luo et al., 2014), also in bilberry (Karppinen et al., 2013; **Figure 1B**) and highbush blueberry (Zifkin et al., 2012), suggesting a role for ABA in ripening regulation in *Vaccinium* berries.

The flavonoid biosynthetic routes in plants are well understood and they are known to be regulated mainly through transcriptional control of structural genes (Hichri et al., 2011). The flavonoid pathway has been intensively studied also in *Vaccinium* berries, especially in bilberries and blueberries. The main structural genes have been isolated from bilberry (Jaakola et al., 2002), highbush blueberry (Zifkin et al., 2012), cranberry (Polashock et al., 2002; Sun et al., 2015), and bog bilberry (*V. uliginosum*; Primetta et al., 2015). The studies have indicated the increase in transcription levels of especially chalcone synthase (CHS), dihydroflavonol 4-reductase (DFR), anthocyanidin synthase (ANS), and UDP-glucose flavonoid 3-O-glucosyltransferase (UFGT) at the ripening stage leading to anthocyanin accumulation.

The key regulators of the flavonoid pathway have been characterized as R2R3 MYB transcription factors, MYC-like basic helix-loop-helix (bHLH) and WD40-repeat proteins, which comprise so called MBW-complex (Ferreira et al., 2012; Xu et al., 2015). In *Vaccinium* species, potential R2R3 MYB genes involved in flavonoid biosynthesis have been identified in bilberry (Jaakola et al., 2010), highbush blueberry (Li X. et al., 2012; Zifkin et al., 2012; Gupta et al., 2015), and bog bilberry (Primetta et al., 2015). However, the upstream signaling network behind flavonoid biosynthesis is still unclear. At least part of the regulatory network controlling fleshy fruit ripening seems to be conserved during the evolution throughout climacteric and non-climacteric fruits (Seymour et al., 2013). In bilberry, a link between anthocyanin biosynthesis and one of the key regulators of fruit development, a SQUAMOSA-class MADS-box transcription factor, has been demonstrated (Jaakola et al., 2010). However, there are indications that the regulation of anthocyanin biosynthesis might differ in genus *Vaccinium* compared with other species studied so far. In a recent study, white berry mutants of bog bilberry and bilberry deficient in anthocyanins were demonstrated to have a down-regulated MYBPA1-type transcription factor (Primetta et al., 2015), which has been indicated as the key regulator of proanthocyanidin biosynthesis in other fruit species. During recent years, several transcriptome and genome databases of *Vaccinium* berries have been published

(Li X. et al., 2012; Rowland et al., 2012; Zifkin et al., 2012; Polashock et al., 2014; Gupta et al., 2015; Sun et al., 2015). From these databases, different families of transcription factors with potential roles in flavonoid biosynthesis have been identified. The databases will serve as an important tool in revealing signaling network involved in regulation of flavonoid biosynthesis and other metabolites in *Vaccinium* species.

Due to the high accumulation of anthocyanins in skin at ripening, carotenoids do not serve as the main pigments attracting seed dispersers in *Vaccinium* berries. However, among fruits *Vaccinium* berries can be considered as good sources of carotenoids, especially lutein and β-carotene (Marinova and Ribarova, 2007; Bunea et al., 2012; Lashmanova et al., 2012; Karppinen et al., 2016). Our recent study on carotenoid biosynthesis has shown that carotenoid content in bilberry fruit is modified during berry development with decreasing trend from small green berry toward ripening berries (Karppinen et al., 2016; **Figure 1B**). This trend is likely to reflect the variable roles of carotenoids during berry development and ripening. In unripe fruits, carotenoids are primarily involved in photosynthesis, whereas during ripening the carotenoid metabolism can turn toward enzymatic degradation to produce apocarotenoids, such as ABA and flavor compounds (McQuinn et al., 2015). Based on study in bilberry, transcriptional regulation of the both key biosynthetic and cleavage genes plays a role in the determination of carotenoid content during berry development and ripening (Karppinen et al., 2016). This indicates coordinately regulated interplay with ABA and carotenoid biosynthetic routes and, furthermore, anthocyanin biosynthesis at bilberry ripening.

Many berries accumulate carotenoid derived volatile flavor compounds at ripening (Beekwilder et al., 2008; García-Limones et al., 2008). However, reports concerning the regulation of formation of these compounds during development and ripening of *Vaccinium* berries are still scant (Rohloff et al., 2009; Gilbert et al., 2013). The aroma of ripe fruits is a complex combination of various flavor compounds, sugars and acids, and variations in these can be high even between the cultivars of the same species (El Hadi et al., 2013). Cultivar-specific differences in volatile profiles have been reported among *Vaccinium* species and highbush blueberry cultivars (Hirvi and Honkanen, 1983; Baloga et al., 1995; Horvat et al., 1996; Forney et al., 2012). The most critical volatiles for the blueberry aroma are considered to be linalool, *trans*-2-hexenol, *trans*-2-hexenal, hexanal, and 1-penten-3-ol, which show increasing trend in highbush blueberries toward fruit maturity (Du et al., 2011; Gilbert et al., 2013).

Fruits and berries are recognized as dietary sources of vitamins. Among berries, *Vaccinium* species have shown to be low or moderate sources of vitamin C with the levels of 0.1–27 mg 100 g⁻¹ FW (Bushway et al., 1983; Klein, 2005; Walker et al., 2006; Brown et al., 2012). In bilberry, the levels of vitamin C have shown to be relatively stable during the berry development and ripening (Cocetta et al., 2012; **Figure 1B**), whereas more decrease during berry development was detected in highbush blueberry cultivars (Liu et al., 2015). Moreover, low to moderate levels of other vitamins are reported in *Vaccinium* fruits (Mazza, 2005; Chun et al., 2006). So far, studies on the upstream regulation of

vitamin C biosynthesis during berry development in *Vaccinium* spp. species are lacking.

ENVIRONMENTAL REGULATION

Environmental factors have a substantial role in the regulation of secondary metabolism in fruits. In general, genetic background determines the secondary metabolite profile of species, whereas environmental factors can cause prominent qualitative and quantitative changes to the metabolite composition. In addition to temperature and light conditions, nutritional status, water balance, diseases and other stresses have been shown to affect the production of secondary metabolites in fruits and berries (Ferrandino and Lovisolo, 2014; Zoratti et al., 2014a; Koshita, 2015). The environmental effects on berry secondary metabolism have been studied widely also in genus *Vaccinium* (**Table 1**). Many studies have focused on the influence of growth conditions on the content of anthocyanins and other phenolic compounds in berries of both wild and cultivated species.

Light conditions have a significant role in the flavonoid metabolism in fruits (Zoratti et al., 2014a), including *Vaccinium* berries, in which especially content and composition of anthocyanins is affected. However, the effect of light on the accumulation of flavonoids in *Vaccinium* berries seems to be regulated in a species-specific manner. Many of the wild *Vaccinium* berries, such as bilberry and lingonberry, grow in shaded habitats and do not require high light for induction of anthocyanin biosynthesis. In these berries, light conditions appear to have merely fine-tuning effects on flavonoid biosynthesis. Recently, it was reported that bilberries grown in sites with higher photosynthetic active radiation contained higher levels of anthocyanins, flavonols, hydroxycinnamic acids, and total phenolics (Mikulic-Petkovsek et al., 2015). The positive effect of light on total phenolics and anthocyanin was also apparent in bilberries grown under sunlight versus shadowed habitats in Montenegro (Jovančević et al., 2011). Although blueberries are also shade-adapted species they seem to require higher solar exposure for normal ripening and anthocyanin accumulation (Zoratti et al., 2015b). In a postharvest study, light had also positive effect on the accumulation of anthocyanins in cranberries (Zhou and Singh, 2004).

In addition to intensity, light effect can be transmitted through perception of other attributes, such as light quality and day length (Zoratti et al., 2014a). Longer days seem to be associated with more intense flavonoid production than shorter days (Jaakola and Hohtola, 2010; Mazur et al., 2014). In bilberry, the effect of photoperiod appears to be one reason for more rapid accumulation and higher concentrations of anthocyanins at northern latitudes compared to southern growth conditions (Uleberg et al., 2012; **Table 1**).

Higher plants utilize multiple photoreceptors to detect different wavelengths of light from ultraviolet (UV)-B to far-red (Möglich et al., 2010; Casal, 2013). In a recent study, a short exposure to specific portions of light spectrum during the early development of bilberry fruit affected the final flavonoid profile in ripe berry (Zoratti et al., 2014b). Especially blue

wavelengths increased the accumulation of more hydroxylated anthocyanins; delphinidins, petunidins and malvidins, but not cyanidins and peonidins. Earlier, short treatments with red wavelengths increased anthocyanin accumulation in cranberries compared to white light- or dark-treated berries (Zhou and Singh, 2002). Postharvest studies with UV-B and UV-C light induced anthocyanin accumulation in blueberries (Perkins-Veazie et al., 2008; Wang et al., 2009; Nguyen et al., 2014). However, the signaling pathway from different photoreceptors to flavonoid accumulation and induction of R2R3 MYB transcription factors is not well understood. It is generally accepted that CONSTITUTIVE PHOTOMORPHOGENIC 1 (COP1) acts as a major center of light signaling directly interacting with photoreceptors (Jang et al., 2010; Galvão and Fankhauser, 2015). The MdCOP1 was shown to interact with MdMYB1, a positive regulator of anthocyanin biosynthesis, in apple (Li Y.Y. et al., 2012). A recent study in non-climacteric strawberry fruit revealed that light regulates anthocyanin biosynthesis and related R2R3 MYB transcription factors independently from ABA (Kadomura-Ishikawa et al., 2015). In accordance, additive effect on anthocyanin accumulation was observed under combined light and ABA treatments.

Temperature also affects the composition of secondary metabolites in fruits. In general, cooler temperatures favor biosynthesis of phenolic compounds and vitamin C (Lee and Kader, 2000; Koshita, 2015), whereas both lower and higher temperatures have been shown to decrease the carotenoid biosynthesis in tomatoes and other carotenoid accumulating fruits (Gross, 1991). In *Vaccinium* berries, the temperature effect has been most intensively studied in regards to formation of phenolic compounds. Many studies have concerned the optimal postharvest storage temperature for the stability of phenolic compounds in blueberries and cranberries (Wang and Stretch, 2001; Connor et al., 2002a; Schotmans et al., 2007). Moreover, Uleberg et al. (2012) showed in a controlled experiment that bilberries produced higher levels of flavonols and hydroxycinnamic acids in 12°C than in 18°C, whereas contents of all anthocyanins, except delphinidin glycosides, were higher in 18°C. Zoratti et al. (2015b) compared the effect of light-temperature combinations contemporary on bilberry and highbush blueberry (cv. Brigitta Blue). For both species, lower temperatures favored the accumulation of anthocyanins in berries. In bilberry, decrease in temperature from 25 to 10°C increased the more hydroxylated forms of anthocyanins in ripening fruits. Similarly, a higher accumulation of anthocyanins was detected in blueberries ripened at 25°C compared to 30°C. However, temperatures below 25°C delayed the ripening of blueberries leading to a slight decrease in all anthocyanins (Zoratti et al., 2015a,b).

Genotype × environment (G×E) interaction related with the formation of secondary metabolites has been studied in many *Vaccinium* species. Connor et al. (2002b) reported significant variation in anthocyanin content among highbush blueberry cultivars across different locations in US, as well as within years in each location indicating a considerable G×E interaction in regulation of anthocyanin content. The G×E interaction was observed also in bilberries affecting especially to accumulation of

TABLE 1 | Main responses of secondary metabolites to environmental effects in *Vaccinium* berries.

Species	Metabolite	Experimental condition	Response	Reference
<i>Vaccinium corymbosum</i> (highbush blueberry)	Phenolic compounds	Year/season	Affects significantly the accumulation of total phenolic content and anthocyanins in different cultivars.	Connor et al., 2002b
		Location	Affects significantly the accumulation of total phenolic content and anthocyanins in different cultivars.	Prior et al., 1998; Connor et al., 2002b; Spinardi et al., 2009; Jovančević et al., 2011; Može et al., 2011; Zoratti et al., 2015a
		Light	Anthocyanin accumulation is dependent from high solar radiation.	Zoratti et al., 2015b
		Temperature	The accumulation of anthocyanins is favored at 25°C compared to 30°C. Temperatures lower than 25°C retard ripening and anthocyanin accumulation.	Zoratti et al., 2015a,b
		Post-harvest UV light	UV-B and UV-C increase accumulation of anthocyanins, flavonols, and phenolic acids.	Perkins-Veazie et al., 2008; Wang et al., 2009; Eichholz et al., 2011; Nguyen et al., 2014
	Volatile compounds	Year/season	1-Hexenol, E2-hexanal, and hexanoic acid are the most variable compounds in six cultivars.	Gilbert et al., 2015
<i>V. myrtillus</i> (bilberry)		Location	Significant effect on volatile accumulation depending on the cultivar.	Du et al., 2011; Gilbert et al., 2015
		Post-harvest UV light	In cv. Blucrop, UV-B increases the accumulation of terpenes, ketones, and aldehydes after 2 h of high irradiance whereas alcoholic compounds increased after 24 h.	Eichholz et al., 2011
		Post-harvest visible light	In cv. Scintilla, hexanal and trans-2-hexenal are increased after 8 h treatment under red and far-red light compared to white light.	Colquhoun et al., 2013
	Phenolic compounds	Year/season	Affects significantly anthocyanins in bilberry individuals grown in the same location.	Åkerström et al., 2010; Zoratti et al., 2015a
		Location	The accumulation of anthocyanins increases progressively with increasing latitude and altitude.	Lähti et al., 2008; Rieger et al., 2008; Åkerström et al., 2010; Zoratti et al., 2015a,b
		Light	High light increases content of anthocyanins, flavonols, hydroxycinnamic acids, and total phenolics. Blue, red, and far-red light increase the accumulation of anthocyanins and flavonols under controlled temperature conditions.	Jovančević et al., 2011; Zoratti et al., 2014b; Mikulic-Petkovsek et al., 2015
<i>V. macrocarpon</i> (cranberry)	Phenolic compounds	Photoperiod	Photoperiod of 24 h increases the accumulation of phenolic compounds compared to 12 h day/night.	Uleberg et al., 2012
		Temperature	Higher levels of flavonols and hydroxycinnamic acids in 12°C vs. 18°C. Lower temperatures (10–15°C) favor the accumulation of delphinidins.	Uleberg et al., 2012; Zoratti et al., 2015a,b
	Phenolic compounds	Light	Visible light increases accumulation of anthocyanins. The highest increase was observed under red light wavelengths.	Zhou and Singh, 2002
		Post-harvest visible light	Increases accumulation of anthocyanins.	Zhou and Singh, 2004

anthocyanins in relation to differences in latitude and altitude, in which the variation of climatic factors such as temperature, day length, and spectral composition of sunlight are closely correlated (Zoratti et al., 2015a,b). Especially latitude has been shown to influence the accumulation of anthocyanins in *Vaccinium* berries, as a clear increasing trend in anthocyanin content toward north has been reported for North European populations of both bilberry and bog bilberry (Lätti et al., 2008, 2010; Åkerström et al., 2010). Bilberries of the northernmost clones contained not only higher yields of anthocyanins but also a higher proportion of delphinidins whereas more cyanidins accumulated in the berries grown in southern latitudes.

In *Vaccinium* berries, only few studies on the production of secondary metabolites have specifically focused on the effect of increasing altitudes, which are characterized by progressive decrease in temperature and increase in the intensity of visible light. In Northern Italy, higher levels of anthocyanins and ascorbic acid were found in blueberries grown at 600 m a.s.l. compared with 450 m a.s.l. (Spinardi et al., 2009). The same trend in anthocyanin accumulation in bilberries and blueberries was detected along an altitudinal gradient in the Alps of Italy (Zoratti et al., 2015a) as well as in accumulation of anthocyanins and total phenolics in bilberries grown in different altitudes in Montenegro (Jovančević et al., 2011). In the study of Zoratti et al. (2015a), six natural bilberry populations between 1166 and 1829 m a.s.l. showed a clear positive trend in anthocyanin accumulation with increasing elevation, in a 2-year study. In the same study, highbush blueberries showed variation in the anthocyanin accumulation in relation to growth location at different altitude levels, although it resulted to be mostly dependent on the season and particularly temperature. Seasonal differences might explain the results of a 2-year study in Austria (Rieger et al., 2008), where decreasing bilberry anthocyanin contents were found along with increasing altitude (from 800 to 1500 m a.s.l.).

Moreover, environmental factors affect other metabolites in *Vaccinium* berries. In blueberry, G×E interaction was detected in the accumulation of volatile compounds of blueberry aroma profile. Eichholz et al. (2011) and Colquhoun et al. (2013) reported that the accumulation of volatile compounds is affected by light quality, especially UV and red/far-red wavelengths (Table 1). The variation of triterpenoid compounds has been

studied in bilberry and lingonberry (Szakiel et al., 2012a,b). In lingonberry, dependence of the metabolite levels on geographical origin was detected and considered to be related to length of the growing season and thickness of snow cover.

FUTURE PROSPECTS

Vaccinium berries are among economically the most important fleshy berry fruits worldwide, and the interest in utilization of both cultivated and wild berries of the genus has been showing an increasing trend. The studies reviewed here show that environmental factors can modify the content and composition of secondary metabolites in *Vaccinium* berries, which is important to consider when using these berries in industrial applications. The recent and upcoming data from transcriptome and genome databases along with more accurate tools for metabolite and metabolomics analyses are opening a new era in studies concerning regulation of secondary metabolism in *Vaccinium* species. New methods allow more in depth studies at species and cultivar level and they will increase our understanding on the role of complicated G×E interactions in the regulation of formation of the health-beneficial secondary compounds.

AUTHOR CONTRIBUTIONS

All authors (KK, LZ, NN, HH, and LJ) have participated in preparation of the manuscript and have accepted the final version of the manuscript.

ACKNOWLEDGMENTS

This work was financially supported by the Finnish Cultural Foundation, Niemi Foundation and Osk. Huttunen Foundation to KK, and Centre for International Mobility (CIMO, Finland) to NN. For the photographs in Figure 1A, we thank Ilkka Jaakola (*V. corymbosum*, *V. myrtillus*, *V. vitis-idaea*, and *V. uliginosum*) and Dr. Marge Starast (*V. macrocarpon*).

REFERENCES

- Åkerström, A., Jaakola, L., Bång, U., and Jäderlund, A. (2010). Effects of latitude-related factors and geographical origin on anthocyanin concentrations in fruits of *Vaccinium myrtillus* L. (bilberries). *J. Agric. Food Chem.* 58, 11939–11945. doi: 10.1021/jf102407n
- Ancillotti, C., Ciofi, L., Pucci, D., Sagona, E., Giordani, E., Biricolti, S., et al. (2016). Polyphenolic profiles and antioxidant and antiradical activity of Italian berries from *Vaccinium myrtillus* L. and *Vaccinium uliginosum* L. subsp. *gaultherioides* (Bigelow) S.B. Young. *Food Chem.* 204, 176–184. doi: 10.1016/j.foodchem.2016.02.106
- Baloga, D. W., Vorsa, N., and Lawter, L. (1995). “Dynamic headspace gas chromatography-mass spectrometry analysis of volatile flavor compounds from wild diploid blueberry species,” in *Fruit Flavors: Biogenesis, Characterization and Authentication*. ACS Symposium Series 596, eds R. L. Rousseff and M. M. Leahy (Oxford: Oxford University Press), 235–247.
- Beekwilder, J., van der Meer, I. M., Simic, A., Uitdewilligen, J., van Arkel, J., de Vos, R. C. H., et al. (2008). Metabolism of carotenoids and apocarotenoids during ripening of raspberry fruit. *Biofactors* 34, 57–66.
- Blumberg, J. B., Camesano, T. A., Cassidy, A., Kris-Etherton, P., Howell, A., Manach, C., et al. (2013). Cranberries and their bioactive constituents in human health. *Adv. Nutr.* 4, 618–632. doi: 10.3945/an.113.004473
- Brown, P. N., Turi, C. E., Shipley, P. R., and Murch, S. J. (2012). Comparisons of large (*Vaccinium macrocarpon* Ait.) and small (*Vaccinium oxycoccus* L., *Vaccinium vitis-idaea* L.) cranberry in British Columbia by phytochemical determination, antioxidant potential, and metabolomic profiling with chemometric analysis. *Planta Med.* 78, 630–640. doi: 10.1055/s-0031-1298239
- Bunea, A., Rugină, D., Pintea, A., Andrei, S., Bunea, C., Pop, R., et al. (2012). Carotenoid and fatty acid profiles of bilberries and cultivated blueberries from Romania. *Chem. Pap.* 66, 935–939. doi: 10.2478/s11696-012-0162-2

- Bushway, R. J., Mc Gann, D. F., Cook, W. P., and Bushway, A. A. (1983). Mineral and vitamin content of lowbush blueberries (*Vaccinium angustifolium* Ait.). *J. Food Sci.* 48:1878. doi: 10.1111/j.1365-2621.1983.tb05109.x
- Casal, J. J. (2013). Photoreceptor signaling networks in plant responses to shade. *Ann. Rev. Plant Biol.* 64, 403–427. doi: 10.1146/annurev-arplant-050312-120221
- Castrejón, A. D. R., Eichholz, I., Rohn, S., Kroh, L. W., and Huyskens-Keil, S. (2008). Phenolic profile and antioxidant activity of highbush blueberry (*Vaccinium corymbosum* L.) during fruit maturation and ripening. *Food Chem.* 109, 564–572. doi: 10.1016/j.foodchem.2008.01.007
- Česoniènè, L., Daubaras, R., Jasutienè, I., Miliauskienè, I., and Zych, M. (2015). Investigations of anthocyanins, organic acids, and sugars show great variability in nutritional and medicinal value of European cranberry (*Vaccinium oxycoccus*) fruit. *J. Appl. Bot. Food Qual.* 88, 295–299. doi: 10.5073/JABFQ.2015.088.042
- Chun, J., Lee, J., Ye, L., Exler, J., and Eitenmiller, R. R. (2006). Tocopherol and tocotrienol contents of raw and processed fruits and vegetables in the United States diet. *J. Food Compos. Anal.* 19, 196–204. doi: 10.1016/j.jfca.2005.08.001
- Coccetta, G., Karppinen, K., Suokas, M., Hohtola, A., Häggman, H., Spinardi, A., et al. (2012). Ascorbic acid metabolism during bilberry (*Vaccinium myrtillus* L.) fruit development. *J. Plant Physiol.* 169, 1059–1065. doi: 10.1016/j.jplph.2012.03.010
- Colquhoun, T. A., Schwieterman, M. L., Gilbert, J. L., Jaworski, E. A., Langer, K. M., Jones, C. R., et al. (2013). Light modulation of volatile organic compounds from petunia flowers and select fruits. *Postharvest Biol. Technol.* 86, 37–44. doi: 10.1016/j.postharvbio.2013.06.013
- Connor, A. M., Luby, J. J., Hancock, J. F., Berkheimer, S., and Hanson, E. J. (2002a). Changes in fruit antioxidant activity among blueberry cultivars during cold-temperature storage. *J. Agric. Food Chem.* 50, 893–898. doi: 10.1021/jf011212y
- Connor, A. M., Luby, J. J., Tong, C. B. S., Finn, C. E., and Hancock, J. F. (2002b). Genotypic and environmental variation in antioxidant activity, total phenolic content, and anthocyanin content among blueberry cultivars. *J. Am. Soc. Hort. Sci.* 127, 89–97.
- Du, X., Plotto, A., Song, M., Olmstead, J., and Rouseff, R. (2011). Volatile composition of four southern highbush blueberry cultivars and effect of growing location and harvest date. *J. Agric. Food Chem.* 59, 8347–8357. doi: 10.1021/jf201184m
- Eichholz, I., Huyskens-Keil, S., Keller, A., Ulrich, D., Kroh, L. W., and Rohn, S. (2011). UV-B-induced changes of volatile metabolites and phenolic compounds in blueberries (*Vaccinium corymbosum* L.). *Food Chem.* 126, 60–64. doi: 10.1016/j.foodchem.2010.10.071
- El Hadi, M. A. M., Zhang, F. J., Wu, F. F., Zhou, C. H., and Tao, J. (2013). Advances in fruit aroma volatile research. *Molecules* 18, 8200–8229. doi: 10.3390/molecules18078200
- Ferrandino, A., and Lovisolo, C. (2014). Abiotic stress effects on grapevine (*Vitis vinifera* L.): focus on abscisic acid-mediated consequences on secondary metabolism and berry quality. *Environ. Exp. Bot.* 103, 138–147. doi: 10.1016/j.envexpbot.2013.10.012
- Ferreyya, M. L. F., Rius, S. P., and Casati, P. (2012). Flavonoids: biosynthesis, biological functions, and biotechnological applications. *Front. Plant Sci.* 3:222. doi: 10.3389/fpls.2012.00222
- Forney, C. F., Kalt, W., and Vander Kloet, S. P. (2012). Comparison of berry composition of selected *Vaccinium* species (Ericaceae) with *Gaylussacia dumosa*. *Botany* 90, 355–363. doi: 10.1139/B11-098
- Galvão, V. C., and Fankhauser, C. (2015). Sensing the light environment in plants: photoreceptors and early signaling steps. *Curr. Opinion Neurobiol.* 34, 46–53. doi: 10.1016/j.conb.2015.01.013
- Gapper, N. E., McQuinn, R. P., and Giovannoni, J. J. (2013). Molecular and genetic regulation of fruit ripening. *Plant Mol. Biol.* 82, 575–591. doi: 10.1007/s11103-013-0050-3
- García-Limones, C., Schnäbele, K., Blanco-Portales, R., Bellido, M. L., Caballero, J. L., Schwab, W., et al. (2008). Functional characterization of FaCCD1: a carotenoid cleavage dioxygenase from strawberry involved in lutein degradation during fruit ripening. *J. Agric. Food Chem.* 56, 9277–9285. doi: 10.1021/jf801096t
- Gibson, L., Rupasinghe, H. P. V., Forney, C. F., and Eaton, L. (2013). Characterization of changes in polyphenols, antioxidant capacity and physico-chemical parameters during lowbush blueberry fruit ripening. *Antioxidants* 2, 216–229. doi: 10.3390/antiox2040216
- Gilbert, J. L., Guthart, M. J., Gezan, S. A., de Carvalho, M. P., Schwieterman, M. L., Colquhoun, T. A., et al. (2015). Identifying breeding priorities for blueberry flavor using biochemical, sensory, and genotype by environment analyses. *PLoS ONE* 10:e0138494. doi: 10.1371/journal.pone.0138494
- Gilbert, J. L., Schwieterman, M. L., Colquhoun, T. A., Clark, D. G., and Olmstead, J. W. (2013). Potential for increasing southern highbush blueberry flavor acceptance by breeding for major volatile components. *Hortscience* 48, 835–843.
- Grace, M. H., Esposito, D., Dunlap, K. L., and Lila, M. A. (2014). Comparative analysis of phenolic content and profile, antioxidant capacity, and anti-inflammatory bioactivity in wild Alaskan and commercial *Vaccinium* berries. *J. Agric. Food Chem.* 62, 4007–4017. doi: 10.1021/jf403810y
- Gross, J. (1991). *Pigments in Vegetables. Chlorophylls and Carotenoids*. New York, NY: Springer Science + Business Media.
- Gupta, V., Estrada, A. D., Blakley, I., Reid, R., Patel, K., Meyer, M. D., et al. (2015). RNA-Seq analysis and annotation of a draft blueberry genome assembly identifies candidate genes involved in fruit ripening, biosynthesis of bioactive compounds, and stage-specific alternative splicing. *Gigascience* 4:5. doi: 10.1186/s13742-015-0046-9
- Harborne, J. B. (1997). "Phytochemistry of fruits and vegetables: an ecological overview," in *Phytochemistry of Fruits and Vegetables*, eds F. A. Tomás-Barberán and R. J. Robins (New York, NY: Oxford University Press), 335–367.
- He, J., and Giusti, M. M. (2010). Anthocyanins: natural colorants with health-promoting properties. *Annu. Rev. Food Sci. Technol.* 1, 163–187. doi: 10.1146/annurev.food.080708.100754
- Hichri, I., Barrieu, F., Bogs, J., Kappel, C., Delrot, S., and Lauvergeat, V. (2011). Recent advances in the transcriptional regulation of the flavonoid biosynthetic pathway. *J. Exp. Bot.* 62, 2465–2483. doi: 10.1093/jxb/erq442
- Hirvi, T., and Honkanen, E. (1983). The aroma of blueberries. *J. Sci. Food Agric.* 34, 992–996. doi: 10.1002/jsfa.2740340916
- Horvat, R. J., Schlotzhauer, W. S., Chortyk, O. T., Nottingham, S. F., and Payne, J. A. (1996). Comparison of volatile compounds from rabbiteye blueberry (*Vaccinium ashei*) and deerberry (*V. stamineum*) during maturation. *J. Essent. Oil Res.* 8, 645–648. doi: 10.1080/10412905.1996.9701033
- Jaakola, L., and Hohtola, A. (2010). Effect of latitude on flavonoid biosynthesis in plants. *Plant Cell Environ.* 33, 1239–1247. doi: 10.1111/j.1365-3040.2010.02154.x
- Jaakola, L., Määttä, K., Pirttilä, A. M., Törrönen, R., Kärenlampi, S., and Hohtola, A. (2002). Expression of genes involved in anthocyanin biosynthesis in relation to anthocyanin, proanthocyanidin, and flavonol levels during bilberry fruit development. *Plant Physiol.* 130, 729–739. doi: 10.1104/pp.006957
- Jaakola, L., Poole, M., Jones, M. O., Kämäräinen-Karppinen, T., Koskimäki, J. J., Hohtola, A., et al. (2010). A SQUAMOSA MADS box gene involved in the regulation of anthocyanin accumulation in bilberry fruits. *Plant Physiol.* 153, 1619–1629. doi: 10.1104/pp.110.158279
- Jang, I. C., Henriquez, R., Seo, H. S., Nagatani, A., and Chua, N. H. (2010). *Arabidopsis* PHYTOCHROME INTERACTING FACTOR proteins promote phytochrome B polyubiquitination by COP1 E3 ligase in the nucleus. *Plant Cell* 22, 2370–2383. doi: 10.1101/tpc.109.072520
- Jia, H. F., Chai, Y. M., Li, C. L., Lu, D., Luo, J. J., Qin, L., et al. (2011). Abscisic acid plays an important role in the regulation of strawberry fruit ripening. *Plant Physiol.* 157, 188–199. doi: 10.1104/pp.111.177311
- Jovančević, M., Balijagić, J., Menković, N., Šavikin, K., Zdunić, G., Janković, T., et al. (2011). Analysis of phenolic compounds in wild populations of bilberry (*Vaccinium myrtillus* L.) from Montenegro. *J. Med. Plants Res.* 5, 910–914.
- Kadomura-Ishikawa, Y., Miyawaki, K., Takahashi, A., Masuda, T., and Noji, S. (2015). Light and abscisic acid independently regulated FaMYB10 in *Fragaria × ananassa* fruit. *Planta* 241, 953–965. doi: 10.1007/s00425-014-2228-6
- Karppinen, K., Hirvelä, E., Nevala, T., Sipari, N., Suokas, M., and Jaakola, L. (2013). Changes in the abscisic acid levels and related gene expression during fruit development and ripening in bilberry (*Vaccinium myrtillus* L.). *Phytochemistry* 95, 127–134. doi: 10.1016/j.phytochem.2013.06.023
- Karppinen, K., Zoratti, L., Sarala, M., Carvalho, E., Hirsimäki, J., Mentula, H., et al. (2016). Carotenoid metabolism during bilberry (*Vaccinium myrtillus* L.) fruit

- development under different light conditions is regulated by biosynthesis and degradation. *BMC Plant Biol.* 16:95. doi: 10.1186/s12870-016-0785-5
- Klein, M. A. (2005). "Cranberry (*Vaccinium macrocarpon*) Aiton," in *Encyclopedia of Dietary Supplements*, eds P. M. Coates, M. R. Blackman, G. M. Cragg, M. Levine, J. Moss, and J. D. White (New York, NY: Marcel Dekker), 143–149. doi: 10.1081/E-EDS2-130002026
- Kolehmainen, M., Mykkänen, O., Kirjavainen, P. V., Leppänen, T., Moilanen, E., Adriaens, M., et al. (2012). Bilberries reduce low-grade inflammation in individuals with features of metabolic syndrome. *Mol. Nutr. Food Res.* 56, 1501–1510. doi: 10.1002/mnfr.201200195
- Koshita, Y. (2015). "Effect of temperature on fruit color development," in *Abiotic Stress Biology in Horticultural Plants*, eds Y. Kanayama and A. Kochetov (Berlin: Springer), 47–58.
- Lashmanova, K. A., Kuzivanova, O. A., and Dymova, O. V. (2012). Northern berries as a source of carotenoids. *Acta Biochim. Pol.* 59, 133–134.
- Lähti, A. K., Jaakola, L., Riihinne, K. R., and Kainulainen, P. S. (2010). Anthocyanin and flavonol variation in bog bilberries (*Vaccinium uliginosum* L.) in Finland. *J. Agric. Food Chem.* 58, 427–433. doi: 10.1021/jf903033m
- Lähti, A. K., Riihinne, K. R., and Jaakola, L. (2011). Phenolic compounds in berries and flowers of a natural hybrid between bilberry and lingonberry (*Vaccinium × intermedium* Ruthe). *Phytochemistry* 72, 810–815. doi: 10.1016/j.phytochem.2011.02.015
- Lähti, A. K., Riihinne, K. R., and Kainulainen, P. S. (2008). Analysis of anthocyanin variation in wild populations of bilberry (*Vaccinium myrtillus* L.) in Finland. *J. Agric. Food Chem.* 56, 190–196. doi: 10.1021/jf072857m
- Lee, J., and Finn, C. E. (2012). Lingonberry (*Vaccinium vitis-idaea* L.) grown in the Pacific Northwest of North America: anthocyanin and free amino acid composition. *J. Funct. Foods* 4, 213–218. doi: 10.1016/j.jff.2011.10.007
- Lee, S. K., and Kader, A. A. (2000). Preharvest and postharvest factors influencing vitamin C content of horticultural crops. *Postharvest Biol. Technol.* 20, 207–220. doi: 10.1016/S0925-5214(00)00133-2
- Li, C., Jia, H., Chai, Y., and Shen, Y. (2011). Abscisic acid perception and signaling transduction in strawberry. *Plant Signal. Behav.* 6, 1950–1953. doi: 10.4161/psb.6.12.18024
- Li, X., Sun, H., Pei, J., Dong, Y., Wang, F., Chen, H., et al. (2012). De novo sequencing and comparative analysis of the blueberry transcriptome to discover putative genes related to antioxidants. *Gene* 511, 54–61. doi: 10.1016/j.gene.2012.09.021
- Li, Y. Y., Mao, K., Zhao, C., Zhao, X. Y., Zhang, H. L., Shu, H. R., et al. (2012). MdCOP1 ubiquitin E3 ligases interact with MdMYB1 to regulate light-induced anthocyanin biosynthesis and red fruit coloration in apple. *Plant Physiol.* 160, 1011–1022. doi: 10.1104/pp.112.199703
- Liufu, F., Wang, L., Gu, L., Zhao, W., Su, H., and Cheng, X. (2015). Higher transcription levels in ascorbic acid biosynthetic and recycling genes were associated with higher ascorbic acid accumulation in blueberry. *Food Chem.* 188, 399–405. doi: 10.1016/j.foodchem.2015.05.036
- Lohachoompol, V., Mulholland, M., Srzednicki, G., and Craske, J. (2008). Determination of anthocyanins in various cultivars of highbush and rabbiteye blueberries. *Food Chem.* 111, 249–254. doi: 10.1016/j.foodchem.2008.03.067
- Luo, H., Dai, S., Ren, J., Zhang, C., Ding, Y., Li, Z., et al. (2014). The role of ABA in the maturation and postharvest life of a nonclimacteric sweet cherry fruit. *J. Plant Growth Regul.* 33, 373–383. doi: 10.1007/s00344-013-9388-7
- Määttä-Riihinne, K. R., Kähkönen, M. P., Törrönen, A. R., and Heinonen, I. M. (2005). Catechins and procyanidins in berries of *Vaccinium* species and their antioxidant activity. *J. Agric. Food Chem.* 53, 8485–8491. doi: 10.1021/jf050408l
- Määttä-Riihinne, K. R., Kamal-Eldin, A., Mattila, P. H., González-Paramás, A. M., and Törrönen, A. R. (2004). Distribution and contents of phenolic compounds in eighteen Scandinavian berry species. *J. Agric. Food Chem.* 52, 4477–4486. doi: 10.1021/jf049595y
- Marinova, D., and Ribarova, F. (2007). HPLC determination of carotenoids in Bulgarian berries. *J. Food Composit. Anal.* 20, 370–374. doi: 10.1016/j.jfca.2006.09.007
- Mazur, S. P., Sønsteby, A., Wold, A. B., Foito, A., Freitag, S., Verrall, S., et al. (2014). Post-flowering photoperiod has marked effects on fruit chemical composition in red raspberry (*Rubus idaeus*). *Ann. Appl. Biol.* 165, 454–465. doi: 10.1111/aab.12153
- Mazza, G. (2005). Compositional and functional properties of saskatoon berry and blueberry. *Int. J. Fruit Sci.* 5, 101–120. doi: 10.1300/J492v05n03_10
- McAtee, P., Karim, S., Schaffer, R., and David, K. (2013). A dynamic interplay between phytohormones is required for fruit development, maturation, and ripening. *Front. Plant Sci.* 4:79. doi: 10.3389/fpls.2013.00079
- McQuinn, R. P., Giovannoni, J. J., and Pogson, B. J. (2015). More than meets the eye: from carotenoid biosynthesis, to new insights into apocarotenoid signaling. *Curr. Opin. Plant Biol.* 27, 172–179. doi: 10.1016/j.pbi.2015.06.020
- Mikulic-Petkovsek, M., Schmitzer, V., Slatnar, A., Stampar, F., and Veberic, R. (2015). A comparison of fruit quality parameters of wild bilberry (*Vaccinium myrtillus* L.) growing at different locations. *J. Sci. Food Agric.* 95, 776–785. doi: 10.1002/jsfa.6897
- Möglich, A., Yang, X., Ayers, R. A., and Moffat, K. (2010). Structure and function of plant photoreceptors. *Annu. Rev. Plant Biol.* 61, 21–47. doi: 10.1146/annurev-arplant-042809-112259
- Može, S., Polak, T., Gašperlin, L., Koron, D., Vanžo, A., Poklar Ulrich, N., et al. (2011). Phenolics in Slovenian bilberries (*Vaccinium myrtillus* L.) and blueberries (*Vaccinium corymbosum* L.). *J. Agric. Food Chem.* 59, 6998–7004. doi: 10.1021/jf200765n
- Nguyen, C. T. T., Kim, J., Yoo, K. S., Lim, S., and Lee, E. J. (2014). Effect of prestorage UV-A, -B, and -C radiation on fruit quality and anthocyanin of 'Duke' blueberries during cold storage. *J. Agric. Food Chem.* 62, 12144–12151. doi: 10.1021/jf504366x
- Nile, S. H., and Park, S. W. (2014). Edible berries: bioactive components and their effect on human health. *Nutrition* 30, 134–144. doi: 10.1016/j.nut.2013.04.007
- Norberto, S., Silva, S., Meireles, M., Faria, A., Pintado, M., and Calhau, C. (2013). Blueberry anthocyanins in health promotion: a metabolic overview. *J. Funct. Foods* 5, 1518–1528. doi: 10.1016/j.jff.2013.08.015
- Osorio, S., Scossa, F., and Fernie, A. R. (2013). Molecular regulation of fruit ripening. *Front. Plant Sci.* 4:198. doi: 10.3389/fpls.2013.00198
- Patel, S. (2014). Blueberry as functional food and dietary supplement: the natural way to ensure holistic health. *Med. J. Nutri. Metab.* 7, 133–143. doi: 10.3233/MNM-140013
- Perkins-Veazie, P., Collins, J. K., and Howard, L. (2008). Blueberry fruit response to postharvest application of ultraviolet radiation. *Postharvest Biol. Technol.* 47, 280–285. doi: 10.1016/j.postharvbio.2007.08.002
- Polashock, J., Zelzion, E., Fajardo, D., Zalapa, J., Georgi, L., Bhattacharya, D., et al. (2014). The American cranberry: first insights into the whole genome of a species adapted to bog habitat. *BMC Plant Biol.* 14:165. doi: 10.1186/1471-2229-14-165
- Polashock, J. J., Griesbach, R. J., Sullivan, R. F., and Vorsa, N. (2002). Cloning of a cDNA encoding the cranberry dihydroflavonol-4-reductase (DFR) and expression in transgenic tobacco. *Plant Sci.* 163, 241–251. doi: 10.1016/S0168-9452(02)00087-0
- Primetta, A. K., Karppinen, K., Riihinne, K. R., and Jaakola, L. (2015). Metabolic and molecular analyses of white mutant *Vaccinium* berries show down-regulation of MYBPA1-type R2R3 MYB regulatory factor. *Planta* 242, 631–643. doi: 10.1007/s00425-015-2363-8
- Prior, R. L., Cao, G., Martin, A., Sofic, E., McEwen, J., O'Brien, C., et al. (1998). Antioxidant capacity as influenced by total phenolic and anthocyanin content, maturity, and variety of *Vaccinium* species. *J. Agric. Food Chem.* 46, 2686–2693. doi: 10.1021/jf980145d
- Rieger, G., Müller, M., Guttenberger, H., and Bucar, F. (2008). Influence of altitudinal variation on the content of phenolic compounds in wild populations of *Calluna vulgaris*, *Sambucus nigra*, and *Vaccinium myrtillus*. *J. Agric. Food Chem.* 56, 9080–9086. doi: 10.1021/jf801104e
- Rodrigues-Mateos, A., Cifuentes-Gomez, T., Tabatabaei, S., Lecras, C., and Spencer, J. P. E. (2012). Procyanidin, anthocyanin, and chlorogenic acid contents of highbush and lowbush blueberries. *J. Agric. Food Chem.* 60, 5772–5778. doi: 10.1021/jf203812w
- Rohloff, J., Nestby, R., Nes, A., and Martinussen, I. (2009). Volatile profiles of European blueberry: few major players, but complex aroma patterns. *Latvian J. Agron.* 12, 98–103.
- Rowland, L. J., Alkharouf, N., Darwish, O., Ogden, E. L., Polashock, J. J., Bassil, N. V., et al. (2012). Generation and analysis of blueberry transcriptome sequences from leaves, developing fruit, and flower buds from cold acclimation through deacclimation. *BMC Plant Biol.* 12:46. doi: 10.1186/1471-2229-12-46
- Schotsmans, W., Molan, A., and MacKay, B. (2007). Controlled atmosphere storage of rabbiteye blueberries enhances postharvest quality aspects. *Postharvest Biol. Technol.* 44, 277–285. doi: 10.1016/j.postharvbio.2006.12.009

- Seymour, G. B., Østergaard, L., Chapman, N. H., Knapp, S., and Martin, C. (2013). Fruit development and ripening. *Annu. Rev. Plant Biol.* 64, 219–241. doi: 10.1146/annurev-arplant-050312-120057
- Shen, X., Zhao, K., Liu, L., Zhang, K., Yuan, H., Liao, X., et al. (2014). A role for PacMYBA in ABA-regulated anthocyanin biosynthesis in red-colored sweet cherry cv. Hong Deng (*Prunus avium* L.). *Plant Cell Physiol.* 55, 862–880. doi: 10.1093/pcp/pcu013
- Spinardi, A., Mignani, I., Folini, L., and Beghi, R. (2009). Quality and nutraceutical content of blueberries (*Vaccinium corymbosum*) grown at two different altitudes (450 and 650 m above sea level). *Acta Hort.* 810, 817–822. doi: 10.17660/ActaHortic.2009.810.108
- Sun, H., Liu, Y., Gai, Y., Geng, J., Chen, L., Liu, H., et al. (2015). De novo sequencing and analysis of the cranberry fruit transcriptome to identify putative genes involved in flavonoid biosynthesis, transport and regulation. *BMC Genomics* 16:652. doi: 10.1186/s12864-015-1842-4
- Szajdek, A., and Borowska, E. J. (2008). Bioactive compounds and health-promoting properties of berry fruits: a review. *Plant Foods Hum. Nutr.* 63, 147–156. doi: 10.1007/s11130-008-0097-5
- Szakiel, A., Pączkowski, C., and Huttunen, S. (2012a). Triterpenoid content of berries and leaves of bilberry *Vaccinium myrtillus* from Finland and Poland. *J. Agric. Food Chem.* 60, 11839–11849. doi: 10.1021/jf3046895
- Szakiel, A., Pączkowski, C., Koivuniemi, H., and Huttunen, S. (2012b). Comparison of the triterpenoid content of berries and leaves of lingonberry *Vaccinium vitis-idaea* from Finland and Poland. *J. Agric. Food Chem.* 60, 4994–5002. doi: 10.1021/jf300375b
- Uleberg, E., Rohloff, J., Jaakola, L., Tröst, K., Junntila, O., Häggman, H., et al. (2012). Effects of temperature and photoperiod on yield and chemical composition of northern and southern clones of bilberry (*Vaccinium myrtillus* L.). *J. Agric. Food Chem.* 60, 10406–10414. doi: 10.1021/jf302924m
- Vvedenskaya, I. O., and Vorsa, N. (2004). Flavonoid composition over fruit development and maturation in American cranberry, *Vaccinium macrocarpon*. *Ait. Plant Sci.* 167, 1043–1054. doi: 10.1016/j.plantsci.2004.06.001
- Walker, P. G., Gordon, S. L., Brennan, R. M., and Hancock, R. D. (2006). A high-throughput monolithic HPLC method for rapid vitamin C phenotyping of berry fruit. *Phytochem. Anal.* 17, 284–290. doi: 10.1002/pca.916
- Wang, C. Y., Chen, C. T., and Wang, S. Y. (2009). Changes of flavonoid content and antioxidant capacity in blueberries after illumination with UV-C. *Food Chem.* 117, 426–431. doi: 10.1016/j.foodchem.2009.04.037
- Wang, S. Y., and Stretch, A. W. (2001). Antioxidant capacity in cranberry is influenced by cultivar and storage temperature. *J. Agric. Food Chem.* 49, 969–974. doi: 10.1021/jf001206m
- Wheeler, S., Loveys, B., Ford, C., and Davies, C. (2009). The relationship between the expression of abscisic acid biosynthesis genes, accumulation of abscisic acid and the promotion of *Vitis vinifera* L. berry ripening by abscisic acid. *Aust. J. Grape Wine Res.* 15, 195–204. doi: 10.1111/j.1755-0238.2008.00045.x
- Xu, W., Dubos, C., and Lepiniec, L. (2015). Transcriptional control of flavonoid biosynthesis by MYB-bHLH-WDR complexes. *Trends Plant Sci.* 20, 176–185. doi: 10.1016/j.tplants.2014.12.001
- Zhou, Y., and Singh, B. R. (2002). Red light stimulates flowering and anthocyanin biosynthesis in American cranberry. *Plant Growth Regul.* 38, 165–171. doi: 10.1023/A:1021322418740
- Zhou, Y., and Singh, B. R. (2004). Effect of light on anthocyanin levels in submerged, harvested cranberry fruit. *J. Biomed. Biotechnol.* 5, 259–263. doi: 10.1155/S1110724304403027
- Zifkin, M., Jin, A., Ozga, J. A., Zaharia, L. I., Schernthaner, J. P., Gesell, A., et al. (2012). Gene expression and metabolite profiling of developing highbush blueberry fruit indicates transcriptional regulation of flavonoid metabolism and activation of abscisic acid metabolism. *Plant Physiol.* 158, 200–224. doi: 10.1104/pp.111.180950
- Zoratti, L., Jaakola, L., Häggman, H., and Giorgio, L. (2015a). Anthocyanin profile in berries of wild and cultivated *Vaccinium* spp. along altitudinal gradients in the Alps. *J. Agric. Food Chem.* 63, 8641–8650. doi: 10.1021/acs.jafc.5b02833
- Zoratti, L., Jaakola, L., Häggman, H., and Giorgio, L. (2015b). Modification of sunlight radiation through colored photo-selective nets affects anthocyanin profile in *Vaccinium* spp. berries. *PLoS ONE* 10:e0135935. doi: 10.1371/journal.pone.0135935
- Zoratti, L., Karppinen, K., Luengo Escobar, A., Häggman, H., and Jaakola, L. (2014a). Light-controlled flavonoid biosynthesis in fruits. *Front. Plant Sci.* 5:534. doi: 10.3389/fpls.2014.00534
- Zoratti, L., Sarala, M., Carvalho, E., Karppinen, K., Martens, S., Giorgio, L., et al. (2014b). Monochromatic light increases anthocyanin content during fruit development in bilberry. *BMC Plant Biol.* 14:377. doi: 10.1186/s12870-014-0377-1

Conflict of Interest Statement: The authors declare that the research was conducted in the absence of any commercial or financial relationships that could be construed as a potential conflict of interest.

Copyright © 2016 Karppinen, Zoratti, Nguyenquynh, Häggman and Jaakola. This is an open-access article distributed under the terms of the Creative Commons Attribution License (CC BY). The use, distribution or reproduction in other forums is permitted, provided the original author(s) or licensor are credited and that the original publication in this journal is cited, in accordance with accepted academic practice. No use, distribution or reproduction is permitted which does not comply with these terms.



Phenylpropanoids Accumulation in Eggplant Fruit: Characterization of Biosynthetic Genes and Regulation by a MYB Transcription Factor

Teresa Docimo^{1*}, Gianluca Francese², Alessandra Ruggiero¹, Giorgia Batelli¹, Monica De Palma¹, Laura Bassolino³, Laura Toppino³, Giuseppe L. Rotino³, Giuseppe Mennella² and Marina Tucci^{1*}

¹ Consiglio Nazionale delle Ricerche, Istituto di Bioscienze e Biorisorse, UOS Portici, Italy, ² Consiglio per la Ricerca in Agricoltura e l'Analisi dell'Economia Agraria, Centro di Ricerca per l'Orticoltura, Pontecagnano, Italy, ³ Consiglio per la Ricerca in Agricoltura e l'Analisi dell'Economia Agraria, Unità di Ricerca per l'Orticoltura, Montanoso Lombardo, Italy

OPEN ACCESS

Edited by:

Mario Pezzotti,
University of Verona, Italy

Reviewed by:

Weiqi Li,
Chinese Academy of Sciences, China
Alessandro Vannozzi,
University of Padova, Italy

*Correspondence:

Marina Tucci
mtucci@unina.it;
Teresa Docimo
teresdocimo@gmail.com

Specialty section:

This article was submitted to
Plant Physiology,
a section of the journal
Frontiers in Plant Science

Received: 14 October 2015

Accepted: 19 December 2015

Published: 28 January 2016

Citation:

Docimo T, Francese G, Ruggiero A, Batelli G, De Palma M, Bassolino L, Toppino L, Rotino GL, Mennella G and Tucci M (2016) Phenylpropanoids Accumulation in Eggplant Fruit: Characterization of Biosynthetic Genes and Regulation by a MYB Transcription Factor. *Front. Plant Sci.* 6:1233. doi: 10.3389/fpls.2015.01233

Phenylpropanoids are major secondary metabolites in eggplant (*Solanum melongena*) fruits. Chlorogenic acid (CGA) accounts for 70–90% of total phenolics in flesh tissues, while anthocyanins are mainly present in the fruit skin. As a contribution to the understanding of the peculiar accumulation of these health-promoting metabolites in eggplant, we report on metabolite abundance, regulation of CGA and anthocyanin biosynthesis, and characterization of candidate CGA biosynthetic genes in *S. melongena*. Higher contents of CGA, Delphinidin 3-rutinoside, and rutin were found in eggplant fruits compared to other tissues, associated to an elevated transcript abundance of structural genes such as *PAL*, *HQT*, *DFR*, and *ANS*, suggesting that active *in situ* biosynthesis contributes to anthocyanin and CGA accumulation in fruit tissues. Putative orthologs of the two CGA biosynthetic genes *PAL* and *HQT*, as well as a variant of a *MYB1* transcription factor showing identity with group six MYBs, were isolated from an Occidental *S. melongena* traditional variety and demonstrated to differ from published sequences from Asiatic varieties. *In silico* analysis of the isolated *SmPAL1*, *SmHQT1*, *SmANS*, and *SmMyb1* promoters revealed the presence of several Myb regulatory elements for the biosynthetic genes and unique elements for the TF, suggesting its involvement in other physiological roles beside phenylpropanoid biosynthesis regulation. Transient overexpression in *Nicotiana benthamiana* leaves of *SmMyb1* and of a C-terminal *SmMyb1* truncated form (*SmMyb1Δ9*) resulted in anthocyanin accumulation only of *SmMyb1* agro-infiltrated leaves. A yeast two-hybrid assay confirmed the interaction of both *SmMyb1* and *SmMyb1Δ9* with an anthocyanin-related potato bHLH1 TF. Interestingly, a doubled amount of CGA was detected in both *SmMyb1* and *SmMyb1Δ9* agro-infiltrated leaves, thus suggesting that the N-terminal region of *SmMyb1* is sufficient to activate its synthesis. These data suggest that a deletion of the C-terminal region of *SmMyb1* does not limit its capability to regulate CGA accumulation, but impairs anthocyanin biosynthesis. To our knowledge, this is the first study reporting a functional elucidation of the role of the C-term conserved domain in MYB activator proteins.

Keywords: *S. melongena*, chlorogenic acid, RACE, qRT-PCR, gene regulation, genome walking

INTRODUCTION

Eggplant, also known as brinjal, is a berry-producing vegetable belonging to the large Solanaceae family and, similarly to other popular and important Solanaceous crop such as tomato, potato, and pepper, is cultivated across all continents. Eggplant is represented by three cultivated species, *Solanum macrocarpon* L. and *S. aethiopicum* L., which are indigenous to a vast area of Africa and are locally cultivated, and the worldwide cultivated *S. melongena* L., which was domesticated in multiple locations of the Asian continent (Knapp et al., 2013). Thus, opposite to the other widely cultivated Solanaceae, tomato, potato, and pepper, which are native of the New World (Fukuoka et al., 2010; Albert and Chang, 2014; Hirakawa et al., 2014), eggplant has a phylogenetic uniqueness, due to its exclusive Old World origin.

In the Solanaceae family, eggplant is the second most consumed fruit crop after tomato. Although generally considered as a “low-calorie vegetable,” the nutritional value of its fruits is comparable to most common vegetables, and they are also rich in important phytonutrients like phenolic compounds and flavonoids, many of which have antioxidant activities (Raigón et al., 2008), conferring to this vegetable a high nutritional value and extraordinary health-promoting effects (Stommel and Whitaker, 2003). As basic ingredient of the Eastern cuisine, it has been shown that daily eggplant dietary intake appears to be linked to a reduction of chronic disease risks (McCullough et al., 2002). In fact, eggplant has been used in traditional medicine; its tissue extracts have been considered useful for the treatment of asthma, bronchitis, cholera, and dysuria, beneficial in lowering blood cholesterol and showed also antimutagenic properties (Khan, 1979; Hinata, 1986; Kalloo, 1993; Collonnier et al., 2001; Kashyap et al., 2003).

Chlorogenic acid (CGA) is the main phenylpropanoid metabolite in the Solanaceae (Niggeweg et al., 2004). Growing interest for this molecule is due to its many beneficial properties for the treatment of various metabolic and cardiovascular diseases (Dos Santos et al., 2006; Cho et al., 2010; Plazas et al., 2013a). Moreover, CGA is highly stable at high temperatures, and its bioavailability in eggplant increases after cooking compared to the raw product (Lo Scalzo et al., 2010, 2016). CGA is accumulated in all plant tissues, reaching the highest amount in fruits, ranging from 75 to 90% of total phenolics. Other phenylpropanoid compounds include the purple and red anthocyanic pigments (D3R and Nasunin) and the flavonols, which are reported to be the major antioxidant constituents in eggplant fruit skin (Mennella et al., 2010). Along with CGA, anthocyanins and flavonols display considerable health-promoting effects due also to their ability to modulate mammalian cell signaling pathways (Meiers et al., 2001; Lamy et al., 2006). The three initial reactions of the phenylpropanoid pathway are catalyzed by phenylalanine ammonia lyase (PAL), cinnamate 4-hydroxylase (C4H) and 4-coumaroyl CoA ligase (4CL), to provide the high energy intermediate Coumaroyl-CoA

ester. In eggplant, 4-Coumaroyl CoA is esterified with quinic acid by the hydroxycinnamoyl CoA-quinate transferase (HQT) enzyme to form CGA, and is also the substrate for the chalcone synthase (CHS) enzyme to form naringenin, the entry molecule of the flavonoid pathway (Vogt, 2010).

In several fruits and vegetables, such as apple, tomato, onion, and potato, skin and flesh tissues are often characterized by a distinct metabolite composition or content (Vrhovsek et al., 2004; Takos et al., 2006; Mintz-Oron et al., 2008; Stushnoff et al., 2010). This is also true for eggplant, whose phenylpropanoid profile differs between skin and fruit flesh, indicating that their degree of accumulation is tightly regulated (Mennella et al., 2010, 2012; Plazas et al., 2013b).

The production of phenylalanine-derived compounds in plants is mostly regulated by R2R3-MYB proteins, which are the largest class of secondary metabolism modulators (Stracke et al., 2007). A number of 222, 138, 118, 244 R2R3-MYB proteins have been reported in apple, *Arabidopsis thaliana*, grapevine, and soybean, respectively (Matus et al., 2008; Wilkins et al., 2009; Du et al., 2012; Katiyar et al., 2012; Cao et al., 2013), and more than a hundred seems to be present in eggplant (The Italian Eggplant Genome Consortium, unpublished).

Functional redundancy has been often reported for this class of MYB TFs, since several structurally related MYB TFs have been shown to activate identical gene subsets by interacting with the same *cis* elements in their gene promoters (Hartmann et al., 2005; Stracke et al., 2007). Differently, structural genes controlling the late steps of the anthocyanin biosynthetic pathway are regulated by a ternary transcriptional complex composed by members of the R2R3-MYB family (like, in *Arabidopsis*, *Myb114*, *Myb111*, *PAP1*, and *PAP2*), in combination with bHLH TFs (*TT8*, *GL3*, and *EGL3*) and WD40 repeat proteins such as *TTG1* (Dare et al., 2008; Petroni and Tonelli, 2011; Laursen et al., 2015).

Albeit several MYB R2R3-TFs seem to regulate the same activation program, localization and expression studies indicate major differences in their spatial and temporal expression pattern, thus suggesting that their recruitment is indeed selective (Feller et al., 2011). Moreover, endogenous signals, such as cell or tissue specificity, as well as exogenous stimuli, operate to fine tuning this network, thus making phenylpropanoid pathway regulation extremely accurate (Hahlbrock et al., 2003; Wilkins et al., 2009). In this regard, it has been reported that heterologous expression of several MYB TFs induces the biosynthesis of phenylpropanoids in a species-specific manner (Docimo et al., 2013), even in closely related species. For example, the *A. thaliana* and tobacco flavonol regulator *AtMyb12*, when heterologously over-expressed in tomato plants, leads to the activation of off-target genes, determining an increase of CGA content, thus indicating that target genes transactivation might differ between different plant species (Luo et al., 2008).

Despite the phenylpropanoid pathway and its regulation, as well as the members of the MYBs-WRD40-bHLH complex, have been extensively studied in many plant species including Solanaceae (Spelt et al., 2000; Thorup et al., 2000; Pattanaik et al., 2010; Povero et al., 2011; D’Amelia et al., 2014; Kiferle et al., 2015; Montefiori et al., 2015) the peculiar high production of CGA in eggplant has been investigated to a

Abbreviations: bHLH, basic helix-loop-helix; DNA, deoxyribonucleic acid; LC-MS, liquid chromatography-mass spectrometry; qRT-PCR, quantitative real time-polymerase chain reaction; RNA, ribonucleic acid; TF, transcription factor.

lesser extent. Genetic studies pointed to the understanding of quantitative traits loci (QTL) affecting either CGA or anthocyanin content, in order to address breeding programs toward the improvement of these quality traits (Barchi et al., 2011; Plazas et al., 2013b; Gramazio et al., 2014). Gramazio et al. (2014) mapped candidate CGA biosynthetic genes on a interspecific map (*S. melongena* × *S. incanum*) on chromosomes E01, E03, E06, E07, and E09. More recently, a QTL study for the metabolic content of anti-nutritional and flavor and health-related metabolites performed on a intra-specific map of eggplant already described by Barchi et al. (2011, 2012) allowed the localization of two conserved major/minor QTLs for CGA on chromosomes E04 and E06 (Toppino et al., unpublished).

The recently published draft genome of the Asian eggplant cv. ‘Nakate-Shinkuro’ (Hirakawa et al., 2014) and a rich ESTs collection (Fukuoka et al., 2010) are providing valuable information on the accumulation of metabolites of interest for eggplant. Mining of the eggplant draft genome revealed a single HQT gene, but multiple copies of putative CH3 genes, belonging to the CYP family, and their comparison with tomato and potato genes suggested that the CGA biosynthetic pathway might have encountered a different evolution in eggplant compared to these two species, possibly to grant a higher metabolic rate (Fukuoka et al., 2010; Hirakawa et al., 2014). Besides, two *Myb-like* genes were also identified, supposedly involved in controlling anthocyanin accumulation in the flower (Hirakawa et al., 2014), while the *SmMYB1* gene, isolated from a cultivar with purple fruits, was able to drive anthocyanin accumulation in over-expressing shoots (Zhang et al., 2014). A few more studies addressed the biosynthesis of flavonoids or the regulatory mechanisms responsible for the high presence and accumulation of anthocyanins in eggplant, and indicate that domestication of *S. melongena* might have affected the accumulation of phenolic compounds (Meyer et al., 2015), as well as altered the regulation of some anthocyanin target genes (Doganlar et al., 2002). Hence, the presence of multiple copies of structural genes and the redundancy of different regulatory proteins suggest that evolutionary mechanisms affected qualitative and quantitative accumulation of CGA and anthocyanins.

Further studies on metabolite distribution and relevant gene expression along with the isolation and characterization of structural and regulatory genes are needed to better explain the peculiar accumulation of metabolites in eggplant.

To this aim, we investigated phenylpropanoid accumulation in several tissues and organs of the Occidental eggplant cv. ‘Lunga Napoletana’ by LC-MS analysis, and characterized the spatial and temporal expression of the relative structural and potential regulatory genes by qRT-PCR. We report here our independent isolation of *SmPAL* and *SmHQT* key genes for CGA biosynthesis and of a genetic variant of the recently isolated MYB TF *SmMyb1* (Zhang et al., 2014). Although pathway genes are fully represented in the eggplant draft genome¹, in this study we provide further indication of the genetic diversity between *S. melongena* varieties. To expand our understanding of the regulatory mechanisms underlying phenylpropanoid

accumulation, we also isolated *SmANS* (Anthocyanidin synthase) and *SmMyb1* promoter sequences, whose *in silico* analysis for *cis*-acting elements highlighted common regulatory motifs, suggesting a possible coordinated regulation. On the contrary, comparison with other anthocyanins and phenolic acids-related TFs revealed distinctive regulatory motifs of the isolated eggplant *SmMyb1* promoter.

Finally, to assess the function of *SmMyb1*, both the entire coding sequence and a truncated C-terminal form were transiently over expressed in tobacco leaves and their effects were evaluated by molecular and biochemical analysis. In addition, the ability of *SmMyb1* to interact with a bHLH partner was assessed by yeast two hybrid assay. To our knowledge this is the first time that the function of the C-terminal domain in MYB activator proteins is reported.

Our results indicate that the regulatory function of the isolated genetic variant of *SmMyb1* is not limited to the activation of anthocyanin biosynthesis but might also have a role in regulation of CGA accumulation.

MATERIALS AND METHODS

Plant Material

Solanum melongena cultivar “Lunga Napoletana” with purple-black oblong fruits, was cultivated in the greenhouse of the CNR-IBBR, UOS Portici, (Italy). Samples were all harvested when fruits reached a commercially ripe stage (Mennella et al., 2012). Flowers, leaves in two stages (young and mature), stem, roots and fruits (skin and flesh) were simultaneously collected for biochemical and molecular analyses. Samples from three different plants were frozen in liquid nitrogen and stored for further molecular and biochemical analysis.

Nicotiana benthamiana plants for transient transformation assays were grown in growth chamber of CNR-IBBR, UOS Portici, (Italy) at the temperature of 22°C with a photoperiod of 16 h light/8 h dark. After 1 month, youngest leaves were used for transient assays. Leaf samples were collected in liquid nitrogen and stored at -80°C for further biochemical and molecular analyses.

LC-MS Analysis of Phenylpropanoids

Anthocyanins, flavonoids and CGA were analyzed by mass spectrometry in different tissues and organs of the *S. melongena* cultivar “Lunga Napoletana” and in *N. benthamiana* leaves. Metabolic analysis of *N. benthamiana* agro-infiltrated leaves was carried out on three independent replicates collected for each infiltration.

Phenylpropanoids were extracted according to the following protocol. Briefly, 5 and 25 mg of lyophilized samples, respectively, for eggplant and *N. benthamiana*, were extracted in 1.5 ml of 75% (v/v) methanol containing 0.05% (v/v) trifluoroacetic acid (TFA). After homogenization, the samples were stirred for 40 min and centrifuged at 19,000 × g for 10 min. The extracts were filtered through 0.2 μm polytetrafluoroethylene filters. For each tissue and/or genotype, three biological replicates (each in two technical replicates) were prepared. All the extracts were analyzed

¹<http://eggplant.kazusa.or.jp/>

through reversed phase liquid chromatography coupled to a photodiode array detector and to an ion trap mass spectrometry (LC-PDA-MS) system. Such a system consisted of an ultra-performance liquid chromatography (UPLC) DIONEX Ultimate 3000 model coupled to a LTQ XL mass spectrometer (Thermo Fisher Scientific). A 5 μ L aliquot of sample was injected on a Luna C18 (100 mm \times 2.0 mm, 2.5 μ m particle size) column equipped with a Security Guard column (3.0 mm \times 4.0 mm) from Phenomenex. The separations were carried out using a binary gradient of ultrapure water (A) and acetonitrile (B), both acidified with 0.1% (v/v) formic acid, with a flow rate of 0.22 mL/min.

The initial solvent composition consisted of 95% (v/v) of A and 5% (v/v) of B; increased linearly to 25% A and 75% B in 25 min and maintained for 1 min; returned to 95% of A in 1 min. The column was equilibrated to 95% A and 5% B for 11 min before the next injection. The analysis lasted for 38 min and the column temperature was set to 40°C. Mass spectra were obtained in positive ion mode over the range m/z 70–1,400. The capillary voltages were set at 9.95 V and the source temperature was 34°C. Quantitative determination of compounds was conducted by comparison with dose-response curves based on m/z data from authentic, distinct and appropriately diluted standard solutions of D3R (Polyphenols Laboratories AS, Sandnes, Norway), CGA and rutin (Sigma-Aldrich, St. Louis, MO, USA). Xcalibur software (Thermo Fisher Scientific) was used to control all instruments and for data acquisition and data analysis.

RNA Isolation and qRT-PCR

Total RNA was extracted from 100 mg of eggplant tissues and organs using an RNAsy kit (Qiagen, Valencia, CA, USA). Using a Super ScriptII™ kit (Life Technologies, Carlsbad, CA, USA), first-strand cDNA was synthesized by reverse transcription (RT) with oligo-dT primers following the manufacturer's instructions. Gene expression was analyzed using qRT-PCR, which was performed using an ABI7900 HT (Life Technologies, Carlsbad, CA, USA). To amplify the gene fragments, 1 μ L of 1:25 diluted cDNA was used as a template in a 20 μ L PCR reaction with 10 μ L SYBR Green, and 0.4 μ M of each primer. The PCR reaction was conducted as follows: 50°C for 2 min, followed by incubation for 30 s at 95°C and denaturation for 15 s at 95°C, annealing for 20 s at 60°C, and 40 cycles of elongation at 72°C for 20 s. The analysis was done on three biological replicates and in technical triplicate. A relative standard curve for each gene was developed using fourfold serial diluted cDNA and included in all runs to relate to quantitative data. PCR efficiency of primer pairs was optimized to be between 79 and 97% with R^2 -values of 0.985. PCR product melting curves were analyzed for the presence of a single peak, showing that only one PCR product is formed. PCR products were cloned and sequenced to verify that all primer pairs targeted the desired RNA. Adenine phosphoribosyltransferase (APRT) was used as internal reference gene since its expression was found stable in all the analyzed tissues as also reported by Gantasala et al. (2013). Results were analyzed using the $\Delta\Delta Ct$ method (Pfaffl, 2001, 2004) and reported as relative expression levels, compared to young leaves as internal calibrator.

Expression analysis on *N. benthamiana* was performed on RNA extracted from 5 days post agro-infiltration leaves. The

results were expressed in the form of relative expression through the $\Delta\Delta Ct$ method, by using tobacco wild type leaves as internal calibrator tissue. Normalization was performed by using α -Tubulin as housekeeping gene, since its expression was stable as reported by Pattanaik et al. (2010).

A list of the analyzed genes, accession numbers, and primer sequences can be found in Supplementary Table S1. For tobacco qPCR primers, the sequences used in this study are identical to primer pair sequences reported by Pattanaik et al. (2010).

***SmPAL*, *SmHQT*, and *SmMyb1* Genes Isolation and Cloning**

Gene isolation from the Occidental traditional eggplant cv. 'Lunga Napoletana' was initially attempted by using degenerate primers designed on *PAL*, *HQT*, and *Myb* nucleotidic sequences from other Solanaceae, which however, amplified several unspecific fragments. Therefore, 5' RACE strategy was used for gene isolation. Sequences available for *PAL* and *HQT* from Solanaceae were used to BLAST search orthologs in a *S. melongena* ESTs collection (Fukuoka et al., 2010). Gene specific primers were designed on ESTs FS058603.1 and FS083932.1 for *PAL* and *HQT*, respectively. For *Myb1* isolation, primers designed on the *S. melongena* FS084890 EST were used for 3'-5' end RACE. Total RNA extracted from *S. melongena* fruit tissues was used as a template to amplify the *SmPAL*, *SmHQT*, and *SmMyb1*cDNAs. Both 3'-RACE (3'-RACE System, Life Technologies, Carlsbad, CA, USA) and 5'-RACE (Smart Race Kit, Clontech, Mountain View, CA, USA) were performed, following the manufacturers' instructions. Two groups of two gene-specific primers, 3'GSP1, 3'GSP2, and 5'GSP1, 5'GSP2, (Supplementary Table S1) were used for 3'-RACE and 5'-RACE, for *SmPAL* and *SmHQT*, respectively. Touchdown-PCR reactions were performed as follows: 3 min pre-denaturation at 94°C, followed by 94°C for 30 s, 68°C for 30 s, and 72°C for 1 min in the first cycle, then decreasing the annealing temperature by 1°C/cycle for 11 cycles, followed by 94°C for 30 s, 57°C for 30 s, and 72°C for 1 min for 19 cycles and ending with 7 min of elongation at 72°C. Amplified cDNA fragments were ligated to the TOPO TA vector (Life Technologies, Carlsbad, CA, USA) following the manufacturer's instructions. Recombinant bacteria growing on kanamycin selective media were screened and verified by PCR. All sequences were confirmed by DNA sequencing (Primm s.r.l. laboratories, Milan, Italy²).

Genomic DNA was extracted from eggplant leaves using the "DNAsy Plant mini kit" (Qiagen, Valencia, CA, USA). *SmMYB1* was amplified by PCR starting from genomic DNA isolated from eggplant leaves using *Phusion* DNA polymerase (Thermo Fisher Scientific, Waltham, MA, USA) and specific primers (Supplementary Table S1). The amplified *SmMYB1* was cloned into TOPO-TA vectors and verified by sequencing as above reported.

Bioinformatics and Statistical Analyses

The ORF finder program of Vector NTII was used to search for open reading frames in the putative full-length cDNAs of

²<http://www.primmbiotech.com>

S. melongena PAL (KT259041), HQT (KT259042), and Myb1 (KT259043). The fundamental properties and structural features of the proteins were analyzed via ScanProsite³. Alignments of multiple amino acid sequences were carried out using ClustalW⁴. Phylogenetic trees of the SmPAL, SmHQT, and SmMYB1 proteins were produced by Neighbor Joining matrix (Saitou and Nei, 1987) with 1,000 bootstrap trials using MEGA6 (Tamura et al., 2013). The evolutionary distances were computed using the p-distance method and are in the units of the number of amino acid differences per site (Nei and Kumar, 2000).

Analysis of variance (ANOVA) on qPCR Δ Ct data was carried out using SigmaPlot version 12.0, from Systat Software Inc., San Jose, CA, USA⁵. Duncan's test was performed to compare mean values. Pearson product moment correlation coefficients (*r*-values) were calculated by Systat Software using the means of metabolite concentrations or relative gene expression values.

Promoter Cloning and Regulatory Elements Analysis

Promoter sequences for the SmANS and SmMyb1 genes of the cv. 'Lunga Napoletana' were amplified by the Genome walking strategy (Clontech, Mountain View, CA, USA) by using gene specific primers (Supplementary Table S1) designed in order to amplify the 5'UTR region. Promoter regions longer than 1 Kb were isolated, cloned into TOPO-TA vectors (Life Technologies, Carlsbad, CA, USA) and sequenced. Putative promoter sequences for SmPAL and SmHQT were also obtained by Genome Walking, but sequence mining of the genome sequenced by the Italian Eggplant Consortium revealed that they in fact belonged to another PAL isoform and to a putative HCT highly similar to *S. tuberosum* (personal communication). Since the ANS and MYB1 upstream sequences isolated from 'Lunga Napoletana' (this work) were found identical to the sequences from the genome of the Italian Eggplant Genome Consortium, we used the latter PAL and HQT promoters for further studies, after verifying sequence identity. Promoter sequences corresponding to *S. lycopersicum* ANT1, *S. tuberosum* AN1, *S. tuberosum* CA1, and *Vitis vinifera* cultivar Pinot Noir VvMybA1 were retrieved from the respective publicly available genomic sources. Analysis of *cis*-regulatory elements was performed through the Genomatix platform⁶.

SmMyb1 Transient Expression in *Nicotiana benthamiana*

SmMyb1 cds was *Pfu* amplified with primers designed for pENTR-D-TOPO cloning vector (Life Technologies, Carlsbad, CA, USA). SmMyb1 gene from the entry clone was cloned in the 35SCaMV expression cassette of pGWB411 (Nakagawa et al., 2009) using the Gateway recombination technology (Invitrogen, Carlsbad, CA, USA). Spectinomycin positive colonies were sequenced and used to transform *Agrobacterium tumefaciens* LBA4404.

³<http://www.expasy.ch/tools/scanprosite/>

⁴<http://www.genome.jp/tools/clustalw/>

⁵www.sigmaplot.com

⁶<https://www.genomatix.de>

Nicotiana benthamiana plants were grown until they had six leaves and the youngest leaves over 1 cm long were infiltrated with *A. tumefaciens* LBA4404. Bacteria were cultured on Lennox agar (Life Technologies, Carlsbad, CA, USA) supplemented with 50 μ g ml⁻¹ kanamycin (Sigma-Aldrich, St. Louis, MO, USA) and incubated at 28°C. A 10 μ l loop of confluent bacteria were re-suspended in 10 ml of infiltration media (10 mM MgCl₂, 0.5 μ M acetosyringone), to an OD₆₀₀ of 0.3, and incubated at room temperature without shaking for 2 h before infiltration. Infiltrations were performed according to the method of Voinnet et al. (2003). Approximately 300 μ l of the *Agrobacterium* suspension were infiltrated into a young leaf of *N. benthamiana* and transient expression was assayed 5 days post inoculation.

Yeast Two-Hybrid Assay

For yeast two-hybrid experiments, the prey plasmid pGADT7 (Clontech, Mountain View, CA, USA) was used. The full-length coding sequence of SmMyb1 and a truncated form lacking the last nine amino acids (SmMyb1Δ9) were PCR amplified and cloned in frame into pGADT7 between EcoRI and XbaI restriction sites. Plasmids were sequenced to rule out PCR-induced mutations. The bait plasmid StbHLH1pGBKT7 was previously described (D'Amelia et al., 2014). The bait and prey plasmids were transformed into the yeast strain AH109 (Clontech, Mountain View, CA, USA) using the Lithium acetate/Polyethylene glycol method (Bai and Elledge, 1997). The self-activation test was performed prior to the testing of combinations of interest. In particular an equal amount of cells transformed with the prey plasmid pGADT7 containing SmMyb1 or SmMyb1Δ9 was spotted on medium lacking leucine and medium lacking adenine, histidine, leucine. The same was done for the bait plasmid StbHLH1 pGBKT7, that was grown on medium lacking tryptophan and medium lacking adenine, histidine, and tryptophan. After verifying that the bait and prey plasmids when transformed alone conferred ability to grow on tryptophan or leucine, respectively, indicating presence of the plasmid, but not on media lacking three amino acids, which would have indicated self-activation, co-transformations to verify interactions were performed. Transformed colonies containing bait and prey plasmids were selected on synthetic drop-out medium lacking leucine and tryptophan (-W/-L). Co-transformants were grown overnight in liquid culture lacking leucine and tryptophan (-W/-L). For the interaction between bait and prey, an equal amount of cells was spotted on medium lacking adenine, histidine, leucine and tryptophan (-W/-L/-H/-A). Positive and negative controls were also performed as indicated in the legend of Figure 6.

Accession Numbers

The cloned sequences for SmPAL (KT259041), SmHQT (KT259042), SmMyb1 (KT259043) CDS, SmMyb1 genomic and promoter sequence (KT727965) and ANS promoter (KT727965) sequences were submitted to the GenBank/EMBL database. Promoter sequences for SmPAL (KT591485) and SmHQT (KT591484) were kindly provided by the Italian Eggplant Genome Consortium. The genomic localization of

the analyzed promoters were Chr10: 64468200...64466701 for *SIANT1*, 219865...218366 for *StANI*; Ch9: 163301...161802 for *StCAI*; Ch2: 14242103...14240604 for *VvMybA1*. Sequences used for phylogenetic analyses are reported in **Figure 3** and Supplementary Figures S1–S3.

RESULTS

Phenylpropanoid Content in *S. melongena* Cultivar “Lunga Napoletana”

The patterns of accumulation of the major phenylpropanoid metabolites of *S. melongena*, namely the anthocyanin D3R, the phenolic acid CGA and the flavonoid rutin were investigated in several tissues and organs of the eggplant cultivar “Lunga Napoletana,” namely two leaf stages (young and mature), stems, flowers, roots, and fruit skin and flesh.

As expected, the D3R content mirrored anthocyanic pigmentation in all the considered tissues. A concentration of about 200 µg/100 mg dw was detected in flowers, while a six times higher amount (~1200 µg/100 mg dw) was measured in the eggplant fruit skin (**Figure 1**). CGA was detected in all the tissues, and its amount ranged from 1300 to 1800 µg/100 mg dw in leaves and flowers to more than 3000 µg/100 mg dw in fruits. The lowest content was detected in stems and roots, with 600 and 250 µg/100 mg dw, respectively (**Figure 1**).

The flavonoid rutin was detected only in leaves at both stages, stems and fruit skin and its amount in the green tissues ranged from 1 µg in stems and young leaves to 3 µg/100 mg dw in mature leaves, while about a three times higher content was detected in the fruit skin.

Overall, the fruits showed the highest content of CGA, D3R, and rutin.

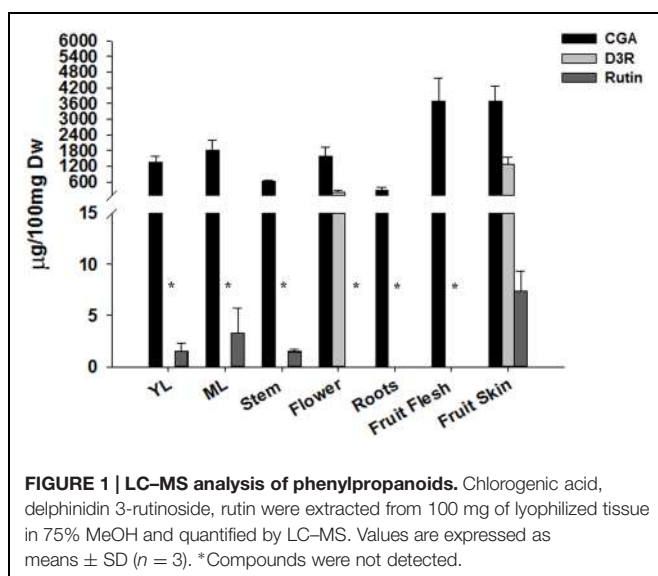


FIGURE 1 | LC-MS analysis of phenylpropanoids. Chlorogenic acid, delphinidin 3-rutinoside, rutin were extracted from 100 mg of lyophilized tissue in 75% MeOH and quantified by LC-MS. Values are expressed as means ± SD ($n = 3$). *Compounds were not detected.

Expression Analysis of Phenylpropanoid Biosynthetic Genes

Quantitative expression analyses were performed in the same tissues sampled for accumulation of metabolites. The transcript abundance of both the early genes, i.e., *PAL*, *C4H*, and *4CL*, and the late genes of the phenylpropanoid pathway encoding for enzymatic steps leading to CGA, D3R, and rutin biosynthesis, namely hydroxycinnamoyl-CoA quinate transferase (*HQT*), dehydroflavonol reductase (*DFR*), and anthocyanidin synthase (*ANS*) were analyzed (**Figure 2**).

PAL, *C4H*, and *4CL* transcripts were detected in all the tissues, with a lower transcript abundance being observed in green tissues (young and mature leaves and stem) than in flowers, roots and fruits, where the expression levels were overall higher. Expression levels were notably high in fruits, where *PAL* transcripts were 1 to 2 orders of magnitude more abundant than in the other tissues. Expression of *HQT*, the key biosynthetic gene in CGA formation, was strongest in both fruit skin and flesh, while showing low expression levels in the other tissues.

Anthocyanin and flavonoid common biosynthetic genes for D3R and rutin formation were also examined. *DFR* and *ANS* transcripts showed a similar pattern of accumulation, with higher expression levels detected in anthocyanin-pigmented tissues, i.e., in flowers and fruit skin. Interestingly, the expression of the two genes was almost 25 and 35 times higher in fruit skin than in flowers, respectively. On the contrary, transcripts levels were significantly lower in non-anthocyanin pigmented tissues.

PAL and *HQT* Genes Isolation

Our biochemical and gene expression results indicated that a high accumulation of CGA mainly occurs in fruits, due to the up-regulation of its biosynthetic genes at the transcriptional level. Therefore, isolation of *PAL* and *HQT* encoding genes was achieved through RACE PCR starting from fruit tissues mRNA. Since at the time of the experiments the eggplant draft genome was not available yet, we used conserved *PAL* and *HQT* sequences from tomato and potato to mine an eggplant ESTs collection through BlastN. Gene specific primers designed on the two *S. melongena* ESTs FS058603.1 and FS083932.1, corresponding to putative *SmPAL* and *SmHQT*-encoding sequences, respectively, amplified single products by 5' 3' RACE PCR. Regarding *SmPAL*, a 2712 bp fragment was cloned and confirmed by sequencing to contain a full length ORF of 2430 bp, encoding for a 724 aa protein of 78.7 kD molecular mass and isoelectric point at 6.4 pH. The sequence isolated from ‘Lunga Napoletana’ was blasted in the eggplant draft genome, and several partial sequences were found. Sequence comparison showed a similarity of 89% with Sme2.5_03336.1_g00008.1, an eggplant sequence annotated as *PAL1* (Supplementary Figure S1A). On the contrary, higher similarity was found with orthologous *PAL* members from other Solanaceae, 93% with *Capsicum annuum* and *Solanum tuberosum* and 92% with *Solanum lycopersicum* (Supplementary Figure S1A). Prosite scan revealed that *S. melongena* *PAL*, similarly to all the other *PAL* proteins, possesses the typical features of an Histidine Lyase protein with the conserved active site

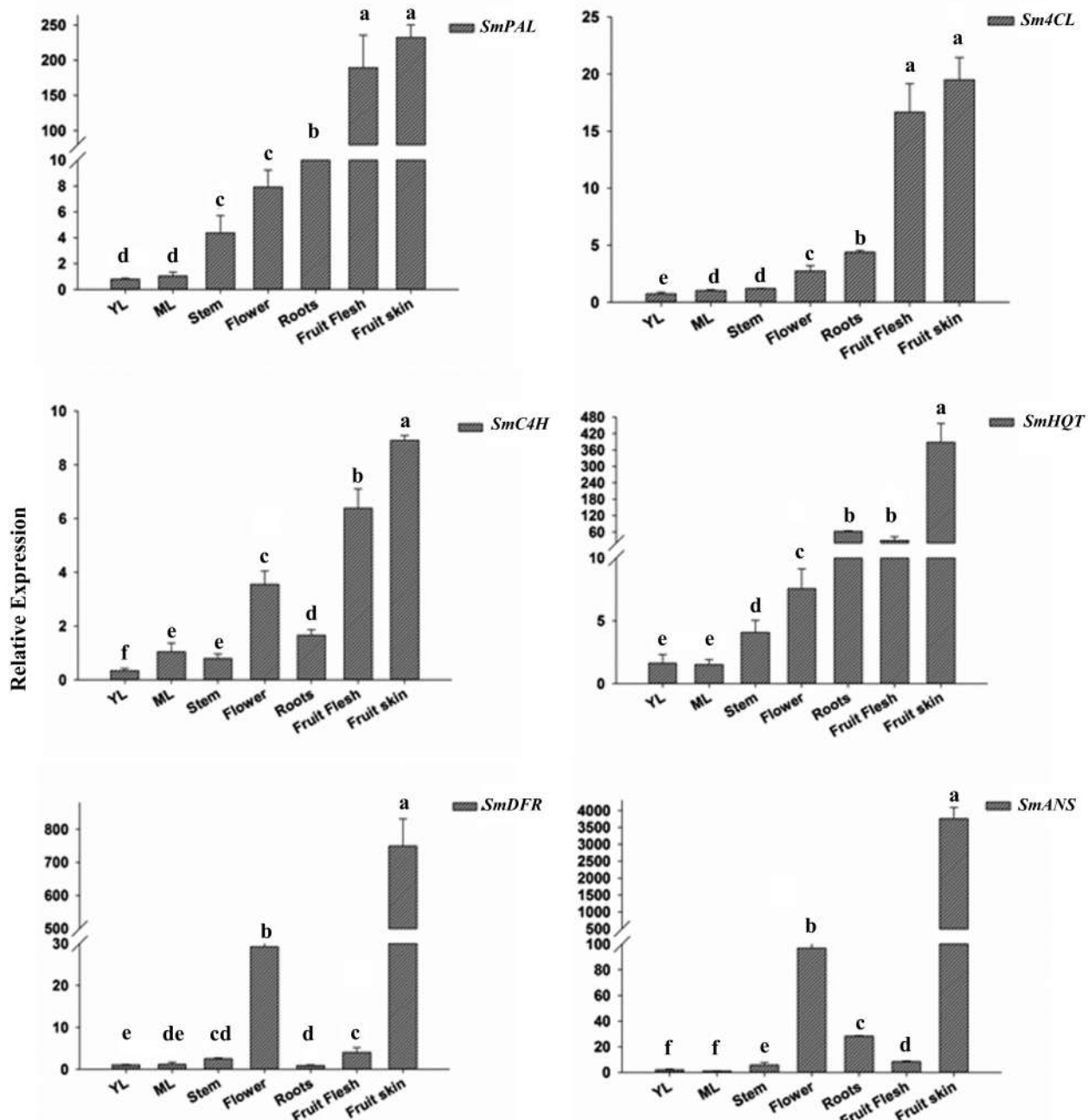
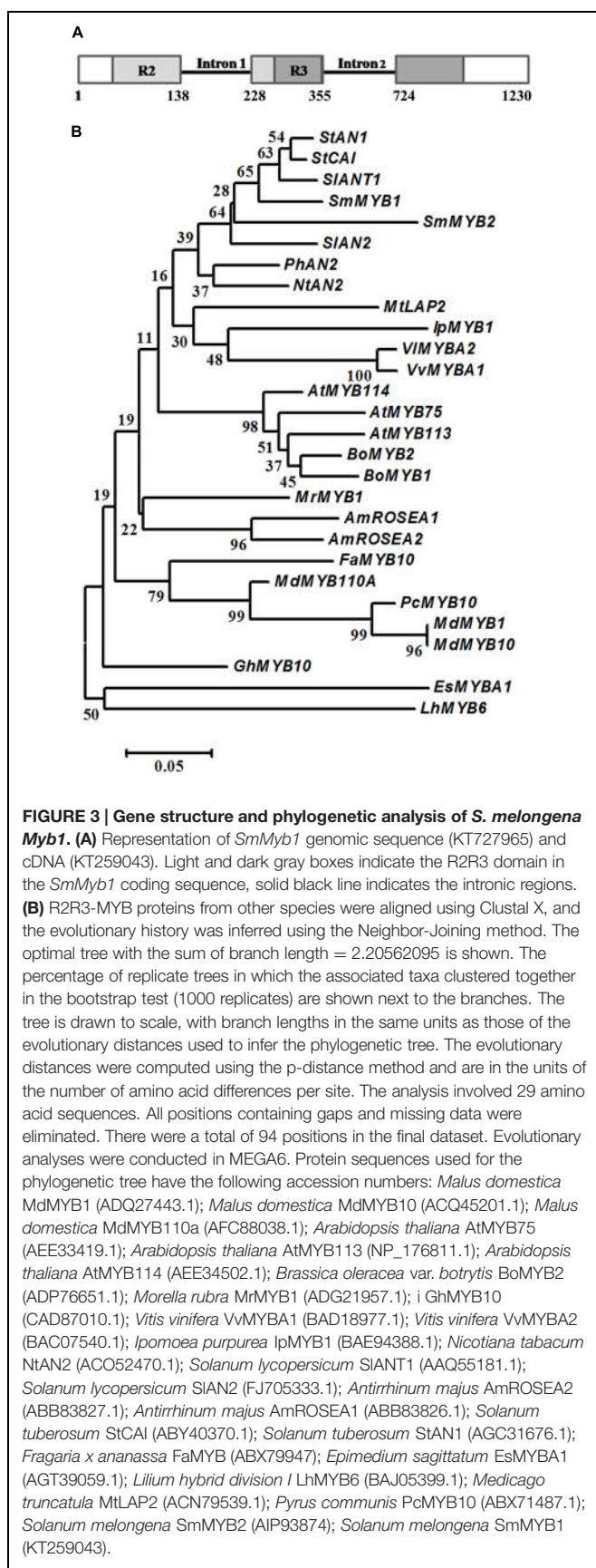


FIGURE 2 | Relative transcript levels of *SmPAL*, *SmC4H*, *Sm4CL*, *SmHQT*, *SmDFR*, and *SmANS* in various *Solanum melongena* organs and at two leaf development stages (YL, young leaves and ML, mature leaves). The results were analyzed using the $\Delta\Delta Ct$ method and presented as fold changes compared with the young leaves, used as internal calibrator. Data are reported as means \pm SD. Means denoted by the same letter did not differ significantly at $p \leq 0.05$ according to Duncan's multiple range test.

(GTITASGDLVPLSYIA), including the Ala-Ser-Gly motif at position 206–208, which autocatalytically forms the methylidene-4h-imidazol-4-one (MIO) prosthetic group (MacDonald and D'Cunha, 2007) by cyclization and dehydration. Moreover, the residues involved in the modulation of PAL activities, i.e., Gly501 in the active site pocket, and Thr556 in the post transcriptional

phosphorylation site are also conserved, thus suggesting that *SmPAL* is a functionally active protein.

Sequence analysis of the cloned 5' and 3' RACE-PCR *SmHQT* fragment identified a 1694 bp full length sequence containing an ORF of 1284 bp, encoding for a putative protein of 428 aa, with 47.6 kD molecular mass and isoelectric point at 6.4 pH.



The predicted eggplant HQT from cv. ‘Lunga Napoletana’ was blasted in the eggplant draft genome, and a 96% similarity was found with Sme2.5_00673.1_g00011.1, an HQT-like gene lacking the N-terminal portion. Then *SmHQT* was aligned to other dicot members encoding HQT protein, and a high degree of similarity was found with other Solanaceous HQTs (89% to *Solanum lycopersicum*, 88% to *Solanum tuberosum*, and 87% to *Nicotiana tabacum*). *SmHQT* possesses the characteristic HTLSD peptide of acyltransferase proteins from position 153, corresponding to the conserved sequence motif HXXXXDG, and the DFGWG block from position 383, observed in other plant acyltransferases belonging to the BAHD family (St-Pierre and De Luca, 2000; D’Auria et al., 2002; Supplementary Figure S2A).

The results for *S. melongena* PAL and HQT protein sequences were used to construct phylogenetic trees using the Neighbor Joining method and illustrate their evolutionary relationships with respect to the related enzymes from other plants. Notably, eggplant proteins encoded by the *SmPAL* and *SmHQT* genes isolated in this study cluster within the same clade with other Solanaceae (tomato, potato, and tobacco) characterized enzymes, as shown in Supplementary Figures S1B and S2B.

Myb1 Isolation and Characterization

In search for a MYB TF responsible for the activation of the phenylpropanoid pathway in eggplant, the eggplant ESTs database was searched by BLAST with the CDS of *S. tuberosum* Chlorogenate inducer (CAI; EU310399), since neither the sequence of the eggplant *SmMyb* TF by Zhang et al. (2014) nor those of the eggplant draft genome were publically available yet. Primers for qRT-PCR were designed on the identified *S. melongena* FS084890 EST and adapted for 5'3' end RACE PCR of eggplant leaf RNA. Cloning and sequencing of the amplified fragments revealed a full length cDNA of 1197 bp containing a 771 bp ORF, which from BLAST analysis was found homologous to a sequence recently isolated from fruits of the Chinese eggplant cv. ‘Zi Chang’ and recorded as *MYB1* (KF727476; Zhang et al., 2014). The *S. melongena* “Lunga Napoletana” *Myb1* variant differed from this sequence for the presence of four SNPs at positions 260, 675, 678, and 737, determining non-synonymous amino acid transitions in position 87 from Aspartate to Glycine and in position 246 from Serine to Phenylalanine. BLAST analysis of this MYB sequence in the draft eggplant genome demonstrated a 98% similarity at the nucleotide level with the sequence Sme2.5_05099.1_g00002.1, annotated as *ANT1*. This eggplant isoform also showed four SNPs, which, however, did not result in amino acid transitions, and therefore encoded a MYB protein identical to the one encoded by our *SmMyb* sequence (Supplementary Figure S3).

Sequence comparison between the cDNA and the genomic sequence of *SmMyb1*, isolated from genomic DNA (KT727965) with specific primers designed on the start and stop codons of the cDNA, revealed that *SmMyb1* contains two introns, located in the R2R3 domain (Figure 3A), as reported for other *Myb* genes (Pattanaik et al., 2010).

Alignment of the encoded MYB1 protein of 258 aa with 12 R2R3-MYB proteins belonging to clade 6 (Liu et al., 2015) and known as anthocyanin and phenolic acids MYB regulators

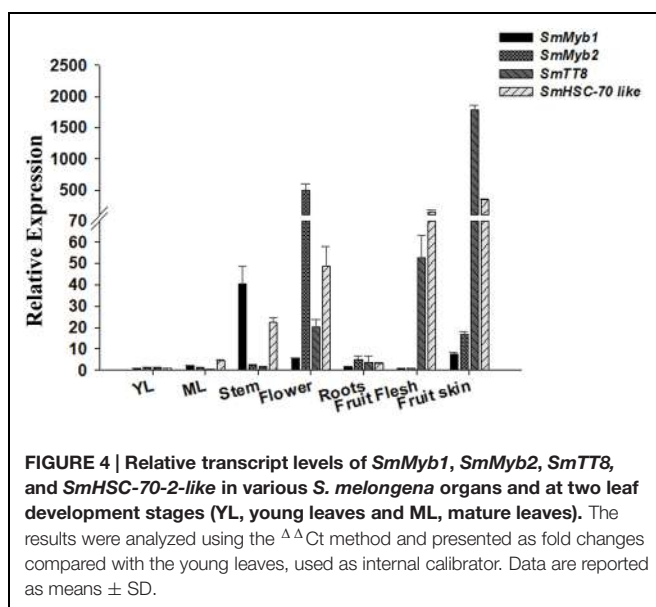


FIGURE 4 | Relative transcript levels of *SmMyb1*, *SmMyb2*, *SmTT8*, and *SmHSC-70-like* in various *S. melongena* organs and at two leaf development stages (YL, young leaves and ML, mature leaves). The results were analyzed using the $\Delta\Delta Ct$ method and presented as fold changes compared with the young leaves, used as internal calibrator. Data are reported as means \pm SD.

demonstrated high sequence homology in the R2R3 domain (Supplementary Figure S3), while less sequence homology is shared in the C-terminal region of all the sequences. *SmMYB1* shares 72 and 71% amino acid identity with *S. lycopersicum* ANT1 and *S. tuberosum* CAI, respectively, while 66, 56, and 47% homology is shared with *S. tuberosum* AN2, *V. vinifera* MYBA1 and *Petunia hybrida* AN2, respectively. A phylogenetic analysis was performed on the alignment of 28 R2R3-MYB protein sequences and the evolutionary history was inferred by using the Neighbor Joining method. The analysis included R2R3-MYB proteins involved not only in the activation of the anthocyanin pathway but also in the regulation of phenolic compounds.

Interestingly, *SmMYB1* clusters more closely to ANT1 from *S. lycopersicum* as well as with AN1 from potato thus suggesting that it may be the homologous protein in *S. melongena*. Noteworthily, *SmMYB1* clusters also with CaiMYB protein from potato (Figure 3B).

Myb1 Expression Analysis in *S. melongena*

In order to further investigate the function of *SmMyb1* as putative regulator of phenylpropanoid accumulation, we performed a qPCR expression analysis of the distribution of *Myb1* transcripts in different *S. melongena* organs and tissues along with other three genes putatively involved in anthocyanin biosynthesis, namely *SmMyb2*, whose sequence mostly resembles the AN2 gene from Solanaceae (Supplementary Figure S4), *SmTT8* (KT591486), a putative homolog of the bHLH TF encoding gene *AtTT8* involved in anthocyanin regulation, and the heat shock cognate 70 protein 2 (*SmHSC70-2-like*, KT591487), which was previously found associated with a *S. melongena* QTL for anthocyanin accumulation mapping on chromosome 10 (Barchi et al., 2012). As shown in Figure 4, *SmMyb1* is expressed in all the tissues at a relatively low level except in stems. In the fruit flesh, both *SmMyb1* and *SmMyb2* show a low expression

level, while *SmTT8* and *SmHSC70-2-like* are highly expressed. In addition, *SmMyb2* resulted to be induced at the highest level in flowers while *SmTT8* is mostly induced in the fruit skin. Interestingly, a higher *SmMyb2*, *SmTT8*, and *SmHSC70-2-like* transcript accumulation was observed in pigmented tissues, thus suggesting a correlation between the expression level of these regulatory genes and the accumulation of D3R (Figures 1–4).

Isolation and *In Silico* Analysis of Phenylpropanoid Biosynthetic Genes and TFs Regulator Promoters

The coordinated expression of the CGA biosynthetic genes in fruit tissues as well as the high expression of late anthocyanin biosynthetic genes in the fruit skin, suggested that in *S. melongena*, as in other Solanaceae fruits, fruit skin and flesh are characterized by different metabolic processes and regulation (Jung et al., 2009). In order to investigate whether CGA and anthocyanin biosynthesis might be differentially regulated in eggplant, *PAL*, *HQT* and *ANS* gene promoters were *in silico* scanned for regulatory elements. MatInspector analysis (Cartharius et al., 2005) of 5' upstream regions of 1546 bp for *SmPAL*, 1500 bp for *SmHQT*, and 1194 bp for *SmANS* showed that they share the presence of common motifs such as auxin, circadian rhythm, light, stress and phytohormone responsive elements, along with several MYB regulatory elements. Moreover, several sugar responsive elements were found in the promoters of *SmPAL*, *SmHQT*, and *SmANS*, whereas sugar starvation or hormone signaling motifs were not found in the *ANS* promoter (Table 1). Along with the structural genes, the isolated promoter region of *S. melongena Myb1* was compared with the promoter regions of other four MYBTF belonging to group 6 (Liu et al., 2015), namely *S. lycopersicum* ANT1, *S. tuberosum* AN1 and CAI, and *V. vinifera* MybA1, whose sequences were retrieved from the respective genomic resources. Interestingly, the comparison between the TFs revealed that only MYBST1, MYBGAH, and MYBAT consensus were present in *SmMyb1*, while all the other putative MYB binding sites corresponding to MYBPLANT (MACCWAMC), MYBPZM (CCWACC), MYCATERD (CATGTGG), and MYBCORE (CNGTTR) were absent (Table 1). Moreover, some distinctive elements, such as elements for cell proliferation and growth, were found only in *SmMyb1* and *VvMybA1* promoters, while phosphate starvation responsive elements were present only in *S. tuberosum* and *S. melongena* TFs. Unique elements were found in the *SmMyb1* promoter, such as the TATCCAT motif, which is required for alpha-amylase expression during sugar starvation, as well as the SURE motif, shared only with *SmPAL* and *SmHQT* structural genes.

Transient Expression in *N. benthamiana*

The role of the isolated *SmMyb1* in the regulation of the phenylpropanoid biosynthetic pathway was investigated through transient transformation of *N. benthamiana* leaves of the full length *SmMyb1* gene. *SmMYB1Δ9*, a truncated mutant obtained

TABLE 1 | List of common *cis*-acting regulatory elements for structural biosynthetic genes, *SmMYB1* and TF from other species.

IUPAC Family	<i>SmANS</i>	<i>SmHQT</i>	<i>SmPAL</i>	<i>SIANT1</i>	<i>StAN1</i>	<i>StCai</i>	<i>VvMYBA1</i>	<i>SmMYB1</i>	Function
PFAM014	1	3	7	3	3	3	3	3	MybSt1
PFAM171	3	0	3	0	4	0	2	0	Myc
P\$FAM003	3	4	4	3	2	3	2	0	MybPLANT
Pfam170	4	0	0	0	0	4	4	0	MybPZM
Pfam266	1	3	1	2	2	5	4	3	MybAT
Pfam325	0	0	2	0	3	1	0	0	MYBCOREATCYCB1
	3	1	1	1	0	0	1	2	Mybgah
PFAM099	0	0	0	0	0	0	0	2	Phytocrome regulation
PFAM08	2	3	4	0	8	1	1	3	Plastid regulation
PFAM302	0	0	0	0	0	0	1	3	Cell proliferation and growth
PFAM234	0	0	0	2	0	1	0	1	Sporamine
									Defense signaling and Wounding
PFAM002	6	1	4	6	17	3	16	4	Wounding stress jasmonateinduction
PFAM010	5	3	5	6	2	3	5	4	WRKY and SalicylicAcid
PFAM322	5	2	3	3	0	1	6	2	Disease
PFAM290	7	8	8	11	0	5	2	12	Pathogen and Salt induced
									Plant stress signaling
PFAM292	1	1	1	0	0	1	1	1	Hypo osmolarity-responsive element
PFAM310	1	3	2	1	0	0	0	3	Cytokinin
PFAM266-026	5	4	1	4	2	7	9	3	Abscisic acid and Aba mediation
PFAM260-170	4	1	2	1	0	0	3	2	Gibberellin responsive
PFAM204	1	1	1	0	0	1	0	1	Gibberellin and abscisic acid
PFAM205	1	4	3	4	2	5	3	3	Gibberellin and sugar repression
PFAM107-273-025	0	1	2	0	0	0	1	3	Sugar starvation and hormone regulation
PFAM272	1	1	0	0	0	0	0	1	Binding amylase
PFAM267-098	16	10	6	2	3	6	5	7	Auxin/Auxine response
PFAM295	0	0	0	0	4	4	0	2	Phosphate starvation response
PFAM311	4	0	3	2	0	1	4	5	Low Co ₂
PFAM124	2	1	2	0	0	0	1	2	Ethylene responsive elements
PFAM305	1	0	1	0	0	2	0	2	Fermentative pathway
									Light responsive <i>cis</i>-acting elements
PFAM012-027	6	17	12	3	4	6	1	5	Light responsiveness /light regulation
PFAM262	2	3	2	2	7	2	1	1	Circadian expression/light
PFAM300	0	2	0	0	1	1	1	4	Sorlip

by deleting nine C-terminal triplets from the *SmMyb1* sequence, was also transformed in *N. benthamiana* leaves to study the functional role of the conserved C-terminal domain. Both the full length and the truncated genes were cloned into the transient expression Gateway vector pGWB411, transfected into *Agrobacterium* and infiltrated into *N. benthamiana* leaves, alongside with the empty vector. Five days post inoculation, *SmMyb1* agro-infiltrated *N. benthamiana* leaves showed an anthocyanic-pigmented phenotype, which was clearly visible due to the lack of anthocyanic pigmentation in wild type tobacco leaves. On the contrary, *SmMyb1Δ9* as well as the empty vector-infiltrated leaves did not show any red pigmentation (**Figure 5A**). Beside visible anthocyanin accumulation, metabolic analysis showed that *SmMyb1* over-expression induces a strong accumulation of D3R (130.21 ± 20.56 µg/100 mg dw), which was barely detectable in *SmMYB1Δ9* agro-infiltrated leaves (14.95 ± 3.04 µg/100 mg dw) and not detectable in the empty vector agro-infiltrated

controls. Interestingly, a CGA content of 835.09 ± 60.06 and 792.00 ± 50.03 µg/100 mg dw was found in *SmMyb1* and *SmMyb1Δ9* agro-infiltrated leaves, respectively, an almost doubled amount in comparison to what was found in the empty vector transformed and in untransformed leaves (464.80 ± 43.71 µg/100 mg dw, 354.67 ± 13.34 µg/100 mg dw, respectively, **Table 2**).

Expression analysis of several key phenylpropanoid biosynthetic genes, i.e. *HQT*, *CHS*, *DFR*, and *ANS*, detected a similar expression level of the *SmHQT* gene in *SmMyb1* and *SmMyb1Δ9* agro-infiltrated leaves, whereas higher levels of expression for *CHS*, *DFR*, and *ANS* were measured in *SmMyb1* leaves in comparison with *SmMyb1Δ9* transformed leaves (**Figure 5B**). In agreement with previous studies (Spelt et al., 2000; Kiferle et al., 2015), a strong induction of the *DFR* gene was detected in *SmMyb1* agro-infiltrated leaves, about 10 and 100 times higher than in *SmMyb1Δ9* agro-infiltrated and control leaves.

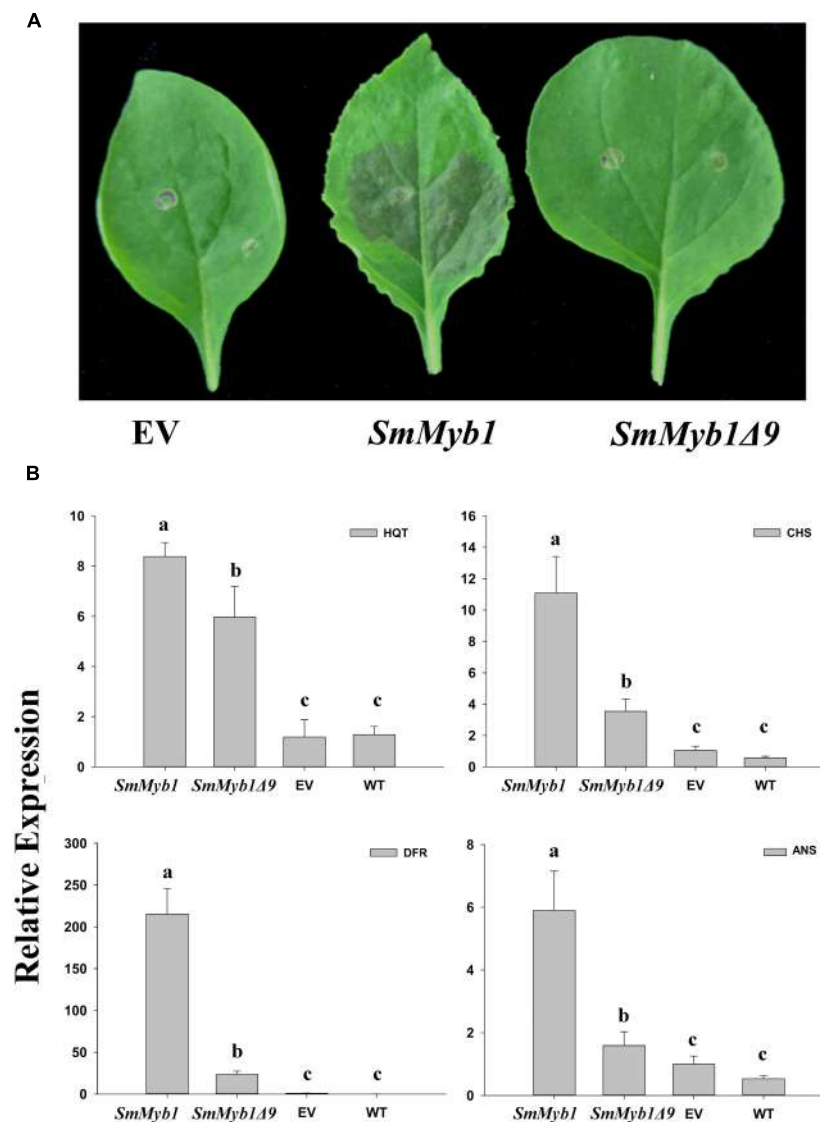


FIGURE 5 | The effects of over-expression of *SmMyb1* in *Nicotiana benthamiana* leaves. **(A)** Leaves of *N. benthamiana* after agro-infiltration with *SmMyb1*, *SmMyb1Δ9*, pGWB411 (empty vector, EV). **(B)** Gene expression analysis of *HQT*, *CHS*, *DFR*, and *ANS* late phenylpropanoid structural genes in agro-infiltrated *N. benthamiana* leaves monitored by qRT-PCR. The results were analyzed using the $\Delta\Delta Ct$ method and presented as fold changes compared with the young leaves, used as internal calibrator. Data are reported as means \pm SD. Means denoted by the same letter did not differ significantly at $p \leq 0.05$ according to Duncan's multiple range test.

Protein–Protein Interaction

The regulatory function of several MYB proteins in anthocyanin biosynthesis depends on their ability to form a regulatory complex with bHLH partners (Lin-Wang et al., 2010; Patta et al., 2010; Albert et al., 2014). To determine the ability of *SmMYB1* to interact with heterologous bHLH proteins, we performed a yeast two-hybrid assay to verify interaction with a previously identified *StbHLH1* from potato. This particular bHLH was selected because its role in anthocyanin regulation is well established both in tubers and leaves of potato (Payyavula et al., 2013; D'Amelia et al., 2014). Because a previous report had shown that fusion of an anthocyanin MYB-type regulator

from petunia with the GAL4 binding domain (GAL4 BD) resulted in auto activation of the reporter genes *HIS* and *ADE*, while fusion with the GAL4 activation domain (GAL4 AD) did not (Quattroccio et al., 2006), we fused *SmMYB1* or a truncated form lacking the last nine amino acids (*SmMyb1Δ9*) with GAL4 AD. After preliminary assessment of the absence of auto-activation of reporter genes for all the used constructs (Supplementary Figure S5), the interaction of *SmMYB1* or *SmMYB1Δ9* with *StbHLH1* fused with GAL4 BD was verified. As shown in Figure 6, yeast cells co-transformed with *SmMyb1* and *StbHLH1* were capable of growing on selective media lacking leucine, tryptophan, histidine, and adenine. Negative controls,

TABLE 2 | Metabolite content in *Nicotiana benthamiana* agro-infiltrated leaves with *SmMyb1*, *SmMyb1Δ9*, EV (Empty Vector), and WT (Wild Type).

<i>N. benthamiana</i> leaves	D3R (μg/100 mg Dw)	CGA (μg/100 mg Dw)
SmMyb1	130.21 ± 20.56	835.09 ± 60.06 ^a
Sm Myb1 Δ9	14.95 ± 3.04	792.00 ± 50.03 ^a
EV	Nd*	464.80 ± 43.71 ^b
WT	Nd*	354.67 ± 13.34 ^c

*Nd, not detected compounds.

Data are reported as means ± SD. Means denoted by the same letter did not differ significantly at $p \leq 0.05$ according to Duncan's multiple range test.

consisting of yeast cells co-transformed with prey plasmids containing *SmMyb1* and empty bait plasmid, as well as the opposite combination, *StbHLH1* combined with empty prey plasmid, did not grow on selective medium, indicating that an interaction between *SmMYB1* and *StbHLH1* does take place in yeast. *SmMYB1Δ9* was still capable of interaction with *StbHLH1*, suggesting that the tested C-term truncation did not interfere with the interaction, as expected by previous reports showing that interaction with bHLH partners requires the N-terminal portion of MYB-type TFs (Plazas et al., 2013a).

DISCUSSION

Solanum melongena is placed in the top rank among the edible Solanaceae and other vegetables with high radical scavenging properties. These beneficial traits are due to the high accumulation of antioxidant polyphenols in eggplant fruit flesh and skin (Plazas et al., 2013a). The most important phytonutrients in this species are CGA, and the anthocyanic pigments, delphinidin 3-rutinoside and/or nasunin (Mennella et al., 2010). Besides the benefits to the human health (Jaganath and Crozier, 2009), these compounds play an active role in the plant defense against biotic and abiotic injuries (Hura et al., 2008) and thus their synthesis must be tightly regulated.

The importance of these specialized metabolites prompted us to investigate phenylpropanoid biosynthesis and its regulation in eggplant. In this study we report our findings on metabolite distribution, transcripts accumulation, along with a characterization of biosynthetic genes and a special focus on a R2R-MYB putatively involved in transcriptional regulation of biosynthetic genes.

Phenylpropanoid Accumulation and Expression Analysis of Structural Genes

Metabolic analysis showed CGA accumulation in all the analyzed tissues of the Occidental eggplant cv. "Lunga Napoletana." The highest content of CGA, of about 4000 μg/100 mg dw, was found in fruit flesh and skin, while almost half the amount was detected in all the other tissues. However, it is roughly 10 and 100 times higher than in tomato and potato, respectively. Although a wide variation of CGA content has been reported in the eggplant gene pool (Plazas et al., 2013b), our data confirm that this vegetable is the best source of CGA among Solanaceous species (Plazas et al., 2013a).

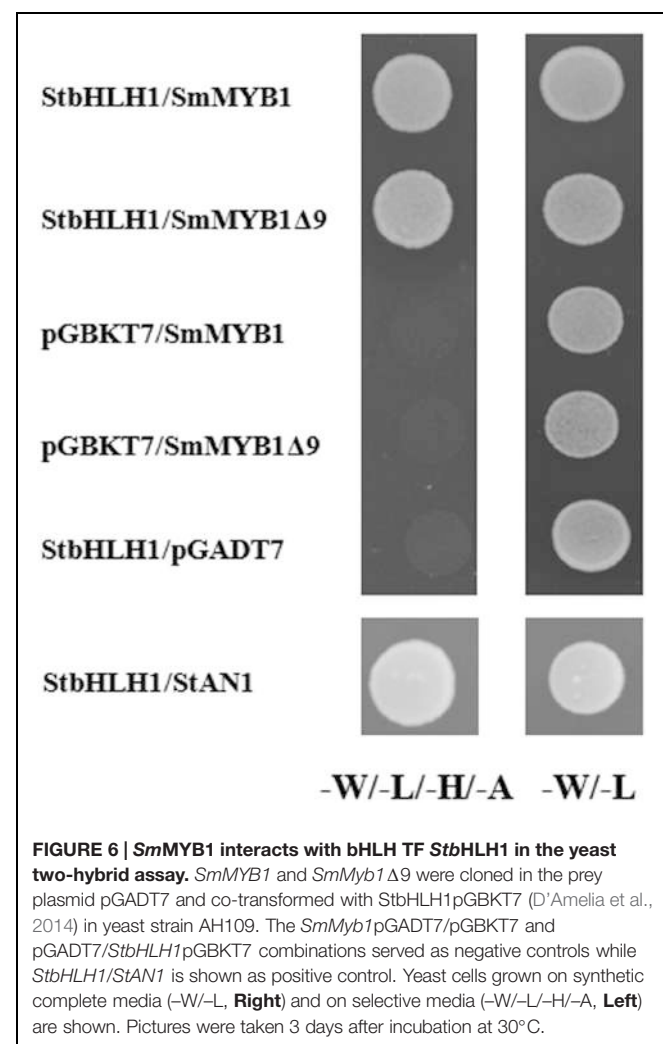


FIGURE 6 | *SmMYB1* interacts with bHLH TF *StbHLH1* in the yeast two-hybrid assay. *SmMYB1* and *SmMyb1Δ9* were cloned in the prey plasmid pGADT7 and co-transformed with *StbHLH1*pGBT7 (D'Amelia et al., 2014) in yeast strain AH109. The *SmMyb1*pGADT7/pGBT7 and pGADT7/*StbHLH1*pGBT7 combinations served as negative controls while *StbHLH1/StAN1* is shown as positive control. Yeast cells grown on synthetic complete media (-W/L, Right) and on selective media (-W/-L/-H/-A, Left) are shown. Pictures were taken 3 days after incubation at 30°C.

The flavonol rutin was barely detectable in leaves at two developmental stages and in stems, and slightly higher in the fruit skin, where D3R was found in high amounts, similarly to flowers, another pigmented tissue. The D3R content detected in the fruit skin of our eggplant cultivar is consistent with the amounts reported by Mennella et al. (2012) for non-Japanese genotypes.

Overall, our metabolic analysis indicates the eggplant fruit, and in particular the fruit skin, as the major accumulator of nutraceutical compounds.

Transcription profiles of flavonoid and CGA structural genes supported metabolic analyses. Early genes of the phenylpropanoid pathway were found expressed in all tissues, with higher transcript levels detected in fruits. However, *SmPAL* and the late gene *SmHQT* showed an order of magnitude higher expression levels in the fruit skin than *C4H* and *4CL*, which mirrored the higher accumulation of CGA in this tissue. This result may reflect the different functions of these genes. PAL, C4H, and 4CL enzymes, as initial committed steps in phenylpropanoid formation, can play multiple functions by providing phenylalanine-derived units for the different

branches of the pathway, while HQT is specifically responsible for CGA biosynthesis. However, the coordinated expression (correlation coefficient $r = 0.756$, $p < 0.05$) of the eggplant *PAL* and *HQT* genes isolated in this paper may account for the high accumulation of CGA in eggplant, similarly to what was demonstrated for specific *HQT* and *PAL* isoforms in tobacco and tomato (Niggeweg et al., 2004; Payyavula et al., 2014). In pigmented tissues, like fruit skin and flowers, extremely high expression levels were detected for the flavonoid structural genes, *DFR* and *ANS*, which correlated with the D3R content ($r = 0.991$, $p < 0.05$, and $r = 0.992$, $p < 0.05$, respectively). As shown in tomato, the fruit surface accumulates a vast array of secondary metabolites, which are necessary for the fruit survival (Mintz-Oron et al., 2008), but whether metabolite accumulation in the fruit peel is the result of *de novo* biosynthesis or of active transport remains unclear. The correlation between accumulation of key structural gene transcripts and of the corresponding metabolites in the eggplant fruit skin suggest that this tissue might have an active role in their biosynthesis, although more accurate studies, e.g., isotope labeling (Docimo et al., 2012) or epidermis cell enrichment by laser dissection technologies combined with transcriptomic and metabolic profiling, would be necessary to definitively clarify this point.

Isolation of CGA Biosynthetic Genes and of a MYB Regulatory Gene

To gain knowledge on the accumulation of CGA, we firstly searched for the candidate biosynthetic genes, whose sequences were not publically available from the eggplant draft genome at the time of these experiments. Besides, draft genomes are known to be less complete than finished genomes, and to be prone to misassembling and sequencing errors. Therefore, the full length cDNA sequences of *SmPAL* and *SmHQT* were isolated by conventional 3' 5' RACE from eggplant fruit flesh tissue. The *PAL* protein is encoded by a multi gene family, which encountered extensive duplications during evolution. About 18 and 13 *PAL* sequences are found in the potato and tomato genomes, respectively (Albert and Chang, 2014). Blast analysis in the draft genome indicated that several *PAL* partial sequences were present, which, however, showed a relatively low similarity level in respect to homologous sequences from "sister species," confirming the extensive genetic variation already reported in eggplant varieties (Li et al., 2010). According to our phylogenetic analysis (Supplementary Figure S1) performed on homologous sequences from other plant species including Solanaceae, *SmPAL* is closely related to the *C. annuum*, *S. tuberosum*, and *S. lycopersicum* ones, and its structure mostly resembles a *PAL1*-like protein (Joos and Hahlbrock, 1992). Similarly, *SmHQT* resulted phylogenetically grouped with *S. tuberosum* HQT, *S. lycopersicum* HQT, and *N. tabacum* HQT (Supplementary Figure S2). Although from the sequence similarity it is not possible to predict whether shikimate or quinate might be the preferential substrate for this enzyme, shikimate esters were not detectable in our analyses, thus indicating this eggplant HQT as a true HQT (Comino et al., 2009; Sonnante et al., 2010; Lallemand et al., 2012; Pardo Torre et al., 2013). Unlike potato tubers (Payyavula et al., 2012), *SmHQT* expression in eggplant

correlates with CGA accumulation, suggesting that the major route for CGA formation in eggplant might be through HQT, as reported in tomato and tobacco (Niggeweg et al., 2004). Deeper comparative analysis would be necessary to evaluate the level of conservation among the sequences isolated in this work in respect to those of the eggplant draft genome. Nevertheless, it is worth noting that the presence of several SNPs might underlie that eggplant lines geographically unrelated (Asian cvs. versus Occidental cvs.) have encountered a different evolutionary program.

Along with CGA, also the high anthocyanin content contributes to the sensorial and nutraceutical properties of eggplant fruits, as well as to improved plant tolerance to biotic and abiotic stresses. Correlation between fruit color and improved quality has been reported for many species, and it is known that higher anthocyanins content in tomato fruits reduces pathogen susceptibility (Bassolino et al., 2013; Zhang et al., 2013). Therefore, knowledge of the factors controlling the production and distribution of CGA and anthocyanins is of great moment for genetic improvement of plant species.

To provide insights into the regulation of phenylpropanoid production in eggplant, we searched for a MYB TF homologous to *S. tuberosum* CAI, which was shown to be a regulator of CGA and flavonoids biosynthesis (Rommens et al., 2008). We isolated a MYBTF from the *S. melongena* cv. 'Lunga Napoletana,' which resulted to contain four SNPs in respect to *SmMYB1* from the cv. 'Zi Chang' (Zhang et al., 2014), determining two non-synonymous amino acid transitions, possibly affecting the function of the encoded protein. Interestingly, also the draft eggplant genome contains a nucleotide sequence with four SNPs, encoding a protein identical to our sequence, which was annotated as ANT1 (Hirakawa et al., 2014).

Similarly to several R2R3-MYB proteins-encoding genes, such as *PhAN2*, *NtAN2*, and *PAP1*, also *SmMyb1* shares a conserved intron/exons organization, thus supporting the idea that they might have a common evolutionary origin (Quattroccio et al., 1999; Borevitz et al., 2000; Pattanaik et al., 2010).

The alignment with 12 highly similar R2R3-MYB TF showed that *SmMYB1* shares all the typical features of a MYB anthocyanin biosynthesis activator (Supplementary Figure S3), a bHLH interaction domain, a ANDV domain, as well as the conserved sequence KPRPRS/TF at the end of the R3 domain (Stracke et al., 2014). As most MYB proteins of this class, *SmMYB1* retains the residues FXXXDLVS at the C-terminal, whose function, contrarily to MYB repressor proteins (Dubos et al., 2008, 2010; Matsui et al., 2008; Albert et al., 2014; Xu et al., 2014) has been investigated to a lesser extent.

Further, we investigated the phylogenetic relationships of *SmMYB1* with 28 related R3R2-MYB proteins involved in the activation of phenylpropanoids. Neighbor Joining analysis placed *SmMYB1* in a clade with other sequences from Solanaceae, namely *S. tuberosum* Chlorogenate inducer CAI, *S. tuberosum* AN1 and *S. lycopersicum* ANT1, suggesting that *SmMyb1* is an eggplant homologous of *SlANT1*. Moreover, a BLAST analysis of *SmMyb2* (Zhang et al., 2014) onto the tomato genome indicated that this gene is located, together with the Heat Shock-encoding gene *SmHsp70-2-like* and with several candidate

genes for anthocyanin accumulation, on chromosome 10, in a QTL controlling anthocyanin pigmentation (Doganol et al., 2002; Barchi et al., 2012; Fukuoka et al., 2012), and is syntenic with *SIAN2* (Tomato Genome Consortium, 2012). Consistently, *SmMYB2* clusters closely to AN2 from *S. lycopersicum* and *S. tuberosum*, thus suggesting a possible distinct regulatory role from *SmMYB1*. Eggplant R2R3-MYB TFs homologous to *SIANT1* and *SIAN2* were recognized as main regulators of anthocyanin pigmentation (Kiferle et al., 2015). Nevertheless, the *SIANT1*-homologous potato gene *StAN1* was also shown to have a key role in phenylpropanoid accumulation, namely in regulating CGA synthesis in potato (Payyavula et al., 2014). To determine the involvement of *SmMYB1* in the regulation of phenylpropanoid accumulation, we measured the expression levels of *SmMyb1*, *SmMyb2*, *SmTT8* and *SmHsp70-2-like*. Except for stems, *SmMyb1* expression was overall low in all tissues, while *SmMyb2* transcripts accumulated at high levels in anthocyanic tissues, and especially in flowers, confirming previous data on *SIANT1* and *SIAN2*, respectively, in tomato (Kiferle et al., 2015). The bHLH-encoding *TT8* and *HSC70-2-like* genes resulted to be highly expressed in stems and flowers, and even more in the fruit flesh and skin, where their expression levels were about 10 to 100 times higher than the analyzed MYBs. These results strongly supported the involvement of these two genes in anthocyanin accumulation.

Anthocyanins are known to contribute to stress resistance in plants (Chalker-Scott, 1999; Lev-Yadun and Gould, 2009). During heat stress, anthocyanins are produced to decrease leaf osmotic potential and prevent loss of water, while bHLH proteins participate to heat-related mechanisms and hormone signaling (Leivar and Quail, 2011) and heat shock proteins function in avoiding protein misfolding (Bita and Gerats, 2013). It is tempting to speculate that *TT8*, *HSC70-2* like and anthocyanins take part to protective mechanisms toward the gradual increase in temperature experienced by ripening fruits. However, elucidation of the functions that *TT8*, *HSC70-2* like and anthocyanins may play during eggplant development or stress response requires further investigation. Our biochemical and expression data, together with the sequence homology between *SmMyb1* and *SIANT1* suggest that the TF gene isolated in this study is somehow involved in the control of anthocyanin pigmentation by taking part in the MBW complex, although with a more marginal role than hypothesized by Zhang et al. (2014), and in accordance to the recent reports on *SIANT1* in tomato (Kiferle et al., 2015).

Since CGA and anthocyanin production is modulated by biotic and abiotic factors, we searched the promoter regions of *SmPAL*, *SmHQT*, *SmANS*, and *SmMyb1* for relevant *cis*-acting elements. Multiple *cis*-acting elements, including fundamental and special elements associated with defense signaling and hormone regulation were found in the *SmMyb1*, *PAL*, *HQT*, and *ANS* promoters. The presence of the same light, circadian rhythm and sucrose responsive elements in *S. melongena* phenylpropanoid genes and *SmMyb1* promoters suggests they may be coordinately expressed and supports the idea that in eggplant CGA and anthocyanins accumulation is controlled by the same environmental factors as in potato tubers (Payyavula et al., 2013). This is consistent with the CGA and anthocyanin

role in plant biotic interactions (Dixon, 2001; Del Campo et al., 2013), and their abundance in eggplant tissues suggests that this specialized metabolites might actively participate in inducible defenses, either by triggering plant resistance to pathogens or functioning as donor of structural elements for cell wall formation in case of damage (Malinovsky et al., 2014). A BLAST analysis of the 'Lunga Napoletana' promoter sequences in the draft genome of the Asian cv. 'Nakate-Shinkuro' highlighted that, beside the *ANS* promoter, all the other 5' upstream regions have a lower level of similarity (data not shown), thus suggesting that general phenylpropanoid gene regulation may be influenced by distinct regulatory signals in the two eggplant varieties.

Extension of the comparative analysis to the promoters of other anthocyanins and phenolic acids-related TFs, *SIANT1*, *StAN1*, *StCAI*, and *VvMybA1*, detected distinctive regulatory motifs in the *SmMyb1* promoter. Several elements for ethylene, cytokinin and gibberellin responsiveness were found, which were scarcely represented or absent in *SIANT1* and in the potato *AN1* and *CAI* TFs promoters, thus suggesting that this eggplant TF might sense hormone signaling and mediate phenylpropanoids production as an active response to abiotic and biotic stresses (Croteau et al., 2000; Gális et al., 2006). Moreover, the presence of additional and distinctive elements involved in the response to phosphate/sugar starvation, phytochrome/plastid regulation, sporamine formation and cell proliferation and growth gives an indication that the activation of this TF is induced by different factors than the other TFs and that it may play various and different physiological roles in eggplant.

The functional role of *SmMyb1* in phenylpropanoid biosynthesis regulation was further tested by transient overexpression in *N. benthamiana* leaves. It is known that sequence variability at the conserved C-terminal region of *PhAN2-like*, as well as *C1* from maize, is tolerated without affecting protein functionality, while mutation or nucleotide variation determining premature stop codon results in a complete loss of activity (Goff et al., 1992; Quattrocchio et al., 1999). However, the function of this domain has not been elucidated so far. To address this point, we performed functional analysis of a *SmMyb1* C-terminal truncated form. Opposite to *SmMyb1Δ9* and empty vector-transformed leaves, *SmMyb1* over-expression determined a red pigmentation of tobacco leaves, which normally accumulate very low amounts of anthocyanins. The red leaf phenotype correlated both with a high expression level of the late anthocyanin biosynthetic gene *DFR* and with a higher content of the D3R pigment. Additionally, the normal phenotype of the tobacco leaves carrying the MYBTF truncated form was consistent with the lower expression of the *DFR* gene and with a barely detectable D3R content. These results confirmed that anthocyanin regulation by *SmMyb1* proceeds thorough the activation of *DFR* transcription, as it was shown for *SIANT1* and *SIAN2* (Kiferle et al., 2015). Interestingly, *SmMyb1* and *SmMyb1Δ9* transformed leaves also showed higher expression of *CHS*, *HQT*, and *ANS*, along with a doubled content of CGA. These results suggest that, similarly to *StAN1*, *SmMyb1* may have a direct involvement in CGA biosynthesis and that a deletion at the C-terminal determines a loss of activity on anthocyanin biosynthesis. Therefore, we may speculate that the

C-terminal domain in *SmMYB1* is essential for transcriptional activation of anthocyanin genes, though its regulatory function on the production of other metabolites, like CGA, is not compromised by the mutation.

Remarkably, we found a high accumulation of *HSC70-2* like and *TT8* in both anthocyanic and non-anthocyanic eggplant tissues, thus suggesting that these anthocyanin-related genes (Barchi et al., 2011) are not the limiting factor for anthocyanin accumulation, but require parallel MYBs expression to promote their synthesis via the MBW complex in *S. melongena* flower and fruit skin.

Two-hybrid interaction indicated that the *SmMyb1* and its truncated form are both able to interact with a heterologous bHLH, but results of the transient overexpression of *SmMyb1* without bHLH suggests that the eggplant TF is able to recruit a tobacco endogenous partner (Quattrochio et al., 1998; Pattaik et al., 2010). Moreover, these results indicate that the *SmMyb1* TF alone is sufficient to trigger anthocyanin accumulation

CONCLUSION

We have improved our knowledge on the behavior of phenylpropanoid genes in eggplant, and demonstrated the role of *SmMyb1* in controlling both anthocyanin and CGA synthesis in *S. melongena* tissues. Besides, for the first time, we propose a functional role of the C-terminal domain of this TF. Our results may thus contribute at facilitating and improving the design of targeted breeding strategies and metabolic engineering approaches to increase accumulation

REFERENCES

- Albert, N. W., Davies, K. M., Lewis, D. H., Zhang, H., Montefiori, M., Brendolise, C., et al. (2014). A conserved network of transcriptional activators and repressors regulates anthocyanin pigmentation in eudicots. *Plant Cell* 26, 962–980. doi: 10.1105/tpc.113.122069
- Albert, V. A., and Chang, T.-H. (2014). Evolution of a hot genome. *Proc. Natl. Acad. Sci. U.S.A.* 111, 5069–5070. doi: 10.1073/pnas.1402378111
- Bai, C., and Elledge, S. J. (1997). Gene identification using the yeast two-hybrid system. *Methods Enzymol.* 283, 141–156. doi: 10.1016/S0076-6879(97)83013-3
- Barchi, L., Lanteri, S., Portis, E., Acquadro, A., Valè, G., Toppino, L., et al. (2011). Identification of SNP and SSR markers in eggplant using RAD tag sequencing. *BMC Genomics* 12:304. doi: 10.1186/1471-2164-12-304
- Barchi, L., Lanteri, S., Portis, E., Valè, G., Volante, A., Pulcini, L., et al. (2012). A RAD tag derived marker based eggplant linkage map and the location of QTLs determining anthocyanin pigmentation. *PLoS ONE* 7:e43740. doi: 10.1371/journal.pone.0043740
- Bassolino, L., Zhang, Y., Schoonbeek, H. J., Kiferle, C., Perata, P., and Martin, C. (2013). Accumulation of anthocyanins in tomato skin extends shelf life. *New Phytol.* 200, 650–655. doi: 10.1111/nph.12524
- Bita, C. E., and Gerats, T. (2013). Plant tolerance to high temperature in a changing environment: scientific fundamentals and production of heat stress-tolerant crops. *Front. Plant Sci.* 4:273. doi: 10.3389/fpls.2013.00273
- Borevitz, J. O., Xia, Y., Blount, J., Dixon, R. A., and Lamb, C. (2000). Activation tagging identifies a conserved MYB regulator of phenylpropanoid biosynthesis. *Plant Cell* 12, 2383–2394. doi: 10.1105/tpc.12.12.2383
- Cao, Z. H., Zhang, S. Z., Wang, R. K., Zhang, R. F., and Hao, Y. J. (2013). Genome Wide Analysis of the Apple MYB transcription factor family allows the identification of MdoMYB121 gene conferring abiotic stress tolerance in plants. *PLoS ONE* 8:e69955. doi: 10.1371/journal.pone.0069955
- Cartharius, K., Frech, K., Grote, K., Klocke, B., Haltmeier, M., Klingenhoff, A., et al. (2005). MatInspector and beyond: promoter analysis based on transcription factor binding sites. *Bioinformatics* 21, 2933–2942. doi: 10.1093/bioinformatics/bti473
- Chalker-Scott, L. (1999). Environmental significance of anthocyanins in plant stress responses. *Photochem. Photobiol.* 70, 1–9. doi: 10.1111/j.1751-1097.1999.tb01944.x
- Cho, A. S., Jeon, S. M., Kim, M. J., Yeo, J., Seo, K. I., Choi, M. S., et al. (2010). Chlorogenic acid exhibits anti-obesity property and improves lipid metabolism in high-fat diet-induced-obese mice. *Food Chem. Toxicol.* 48, 937–943. doi: 10.1016/j.fct.2010.01.003
- Collonnier, C., Fock, I., Kashyap, V., Rotino, G. L., Daunay, M. C., Lian, Y., et al. (2001). Applications of biotechnology in eggplant. *Plant Cell Tissue Organ. Cult.* 65, 91–107
- Comino, C., Hehn, A., Moglia, A., Menin, B., Bourgaud, F., Lanteri, S., et al. (2009). The isolation and mapping of a novel hydroxycinnamoyltransferase in the globe artichoke chlorogenic acid pathway. *BMC Plant Biol.* 9:30. doi: 10.1186/1471-2229-9-30
- Croteau, R., Kutchan, T. M., and Lewis, N. G. (2000). Secondary Metabolites. *Biochem. Mol. Biol. Plants* 7, 1250–1318. doi: 10.1016/j.phytochem.2011.10.011
- D'Amelia, V., Aversano, R., Batelli, G., Caruso, I., Castellano Moreno, M., Castro-Sanz, A. B., et al. (2014). High AN1 variability and interaction with basic helix-loop-helix co-factors related to anthocyanin biosynthesis in potato leaves. *Plant J.* 80, 527–540. doi: 10.1111/tpj.12653

of specific antioxidant and color-related phenolics in target species.

AUTHOR CONTRIBUTIONS

TD and MT designed research; TD, AR, GB, and MDP performed research; GM and GF designed and performed biochemical analyses; TD, GB, and MT analyzed data; LB, LT, and GR provided bio-informatic analyses and critical suggestions; TD and MT wrote the paper.

FUNDING

This work was partially supported by a research grant from the Italian Ministry of Education, University and Research, project GenHORT, PON02_00395_3082360.

ACKNOWLEDGMENTS

We thank Dr. Contaldi Felice and Dr. Andolfo Giuseppe for helpful support in promoter sequence search in *V. vinifera*, *S. tuberosum*, and *S. lycopersicum* genomes, and Dr. Cappetta Elisa and Sannino Lorenza for assistance with plant care.

SUPPLEMENTARY MATERIAL

The Supplementary Material for this article can be found online at: <http://journal.frontiersin.org/article/10.3389/fpls.2015.01233>

- Dare, A. P., Schaffer, R. J., Lin-Wang, K., Allan, A. C., and Hellens, R. P. (2008). Identification of a cis-regulatory element by transient analysis of co-ordinately regulated genes. *Plant Methods* 4:17. doi: 10.1186/1746-4811-4-17
- D'Auria, J. C., Feng, C., and Pichersky, E. (2002). Characterization of an acyltransferase capable of synthesizing benzylbenzoate and other volatile esters in flowers and damaged leaves of *Clarkia breweri*. *Plant Physiol.* 130, 466–476. doi: 10.1104/pp.006460
- Del Campo, M. L., Halitschke, R., Short, S. M., Lazzaro, B. P., and Kessler, A. (2013). Dietary plant phenolic improves survival of bacterial infection in *Manduca sexta* caterpillars. *Entomol. Exp. Appl.* 146, 321–331. doi: 10.1111/eea.12032
- Dixon, R. A. (2001). Natural products and plant disease resistance. *Nature* 411, 843–847. doi: 10.1038/35081178
- Docimo, T., Mattana, M., Fasano, R., Consonni, R., de Tommasi, N., Coraggio, I., et al. (2013). Ectopic expression of the Osmyb4 rice gene enhances synthesis of hydroxycinnamic acid derivatives in tobacco and clary sage. *Biol. Plant.* 57, 179–183. doi: 10.1007/s10535-012-0257-1
- Docimo, T., Reichelt, M., Schneider, B., Kai, M., Kunert, G., Gershenson, J., et al. (2012). The first step in the biosynthesis of cocaine in *Erythroxylum coca*: the characterization of arginine and ornithine decarboxylases. *Plant Mol. Biol.* 78, 599–615. doi: 10.1007/s11103-012-9886-1
- Doganlar, S., Frary, A., Daunay, M. C., Lester, R. N., and Tanksley, S. D. (2002). Conservation of gene function in the Solanaceae as revealed by comparative mapping of domestication traits in eggplant. *Genetics* 161, 1713–1726.
- Dos Santos, M. D., Almeida, M. C., Lopes, N. P., and de Souza, G. E. P. (2006). Evaluation of the anti-inflammatory, analgesic and antipyretic activities of the natural polyphenol chlorogenic acid. *Biol. Pharm. Bull.* 29, 2236–2240. doi: 10.1248/bpb.29.2236
- Du, H., Feng, B.-R., Yang, S.-S., Huang, Y.-B., and Tang, Y.-X. (2012). The R2R3-MYB transcription factor gene family in Maize. *PLoS ONE* 7:e37463. doi: 10.1371/journal.pone.0037463
- Dubos, C., Le Gourrierec, J., Baudry, A., Huep, G., Lanet, E., Debeaujon, I., et al. (2008). MYBL2 is a new regulator of flavonoid biosynthesis in *Arabidopsis thaliana*. *Plant J.* 55, 940–953. doi: 10.1111/j.1365-313X.2008.03564.x
- Dubos, C., Stracke, R., Grotewold, E., Weisshaar, B., Martin, C., and Lepiniec, L. (2010). MYB transcription factors in *Arabidopsis*. *Trends Plant Sci.* 15, 573–581. doi: 10.1016/j.tplants.2010.06.005
- Feller, A., MacHemer, K., Braun, E. L., and Grotewold, E. (2011). Evolutionary and comparative analysis of MYB and bHLH plant transcription factors. *Plant J.* 66, 94–116. doi: 10.1111/j.1365-313X.2010.04459.x
- Fukuoka, H., Miyatake, K., Nunome, T., Negoro, S., Shirasawa, K., Isobe, S., et al. (2012). Development of gene-based markers and construction of an integrated linkage map in eggplant by using *Solanum orthologous* (SOL) gene sets. *Theor. Appl. Genet.* 125, 47–56. doi: 10.1007/s00122-012-1815-9
- Fukuoka, H., Yamaguchi, H., Nunome, T., Negoro, S., Miyatake, K., and Ohyama, A. (2010). Accumulation, functional annotation, and comparative analysis of expressed sequence tags in eggplant (*Solanum melongena* L.), the third pole of the genus *Solanum species* after tomato and potato. *Gene* 450, 76–84. doi: 10.1016/j.gene.2009.10.006
- Gális, I., Šimek, P., Narisawa, T., Sasaki, M., Horiguchi, T., Fukuda, H., et al. (2006). A novel R2R3 MYB transcription factor NtMYBJ1 is a methyl jasmonate-dependent regulator of phenylpropanoid-conjugate biosynthesis in tobacco. *Plant J.* 46, 573–592. doi: 10.1111/j.1365-313X.2006.02719.x
- Gantasala, N. P., Papolu, P. K., Thakur, P. K., Kamaraju, D., Sreevathsa, R., and Rao, U. (2013). Selection and validation of reference genes for quantitative gene expression studies by real-time PCR in eggplant (*Solanum melongena* L.). *BMC Res.* 6:312. doi: 10.1186/1756-0500-6-312
- Goff, S. A., Cone, K. C., and Chandler, V. L. (1992). Functional analysis of the transcriptional activator encoded by the maize B gene: evidence for a direct functional interaction between two classes of regulatory proteins. *Genes Dev.* 6, 864–875. doi: 10.1101/gad.6.5.864
- Gramazio, P., Prohens, J., Plazas, M., Andújar, I., Herráiz, F. J., Castillo, E., et al. (2014). Location of chlorogenic acid biosynthesis pathway and polyphenol oxidase genes in a new interspecific anchored linkage map of eggplant. *BMC Plant Biol.* 14:350. doi: 10.1186/s12870-014-0350-z
- Hahlbrock, K., Bednarek, P., Ciolkowski, I., Hamberger, B., Heise, A., Liedgens, H., et al. (2003). Non-self recognition, transcriptional reprogramming, and secondary metabolite accumulation during plant/pathogen interactions. *Proc. Natl. Acad. Sci. U.S.A.* 100(Suppl. 2), 14569–14576. doi: 10.1073/pnas.0831246100
- Hartmann, U., Sagasser, M., Mehrten, F., Stracke, R., and Weisshaar, B. (2005). Differential combinatorial interactions of cis-acting elements recognized by R2R3-MYB, BZIP, and BHLH factors control light-responsive and tissue-specific activation of phenylpropanoid biosynthesis genes. *Plant Mol. Biol.* 57, 155–171. doi: 10.1007/s11103-004-6910-6910
- Hinata, H. (1986). "Eggplant (*Solanum melongena* L.)" in *Biotechnology in Agriculture and Forestry*, Vol. 2, *Crop I*, ed. Y. P. S. Bajaj (Berlin: Springer), 363–370.
- Hirakawa, H. I., Shirasawa, K. E., Miyatake, K. O. J. I., Nunome, T. S., Negoro, S. A., Ohyama, A. K. I. O., et al. (2014). Draft genome sequence of eggplant (*Solanum melongena* L.): the representative solanum species indigenous to the old world. *DNA Res.* 21, 649–660. doi: 10.1093/dnares/dsu027
- Hura, T., Hura, K., and Grzesiak, S. (2008). Contents of total phenolics and ferulic acid, and PAL activity during water potential changes in leaves of maize single-cross hybrids of different drought tolerance. *J. Agron. Crop Sci.* 194, 104–112. doi: 10.1111/j.1439-037X.2008.00297.x
- Jaganath, I. B., and Crozier, A. (2009). "Dietary flavonoids and phenolic compounds," in *Plant Phenolics and Human Health: Biochemistry, Nutrition, and Pharmacology*, ed. C. G. Fraga (Hoboken, NJ: John Wiley and Sons, Inc.). doi: 10.1002/9780470531792.ch1
- Joos, H.-J., and Hahlbrock, K. (1992). Phenylalanine ammonia-lyase in potato (*Solanum tuberosum* L.). Genomic complexity, structural comparison of two selected genes and modes of expression. *Eur. J. Biochem.* 204, 621–629. doi: 10.1111/j.1432-1033.1992.tb16675.x
- Jung, C. S., Griffiths, H. M., De Jong, D. M., Cheng, S., Bodis, M., Kim, T. S., et al. (2009). The potato developer (D) locus encodes an R2R3 MYB transcription factor that regulates expression of multiple anthocyanin structural genes in tuber skin. *Theor. Appl. Genet.* 120, 45–57. doi: 10.1007/s00122-009-1158-3
- Kalloo, G. (ed.). (1993). "Eggplant (*Solanum melongena*)" in *Genetic Improvement of Vegetable Crops* (Oxford: Pergamon Press), 587–604.
- Kashyap, V., Vinod Kumar, S., Collonnier, C., Fusari, F., Haicour, R., Rotino, G. L., et al. (2003). Biotechnology of eggplant. *Sci. Hortic.* 97, 1–25. doi: 10.1016/S0304-4238(02)00140-1
- Katiyar, A., Smita, S., Lenka, S. K., Rajwanshi, R., Chinnusamy, V., and Bansal, K. C. (2012). Genome-wide classification and expression analysis of MYB transcription factor families in rice and *Arabidopsis*. *BMC Genomics* 13:544. doi: 10.1186/1471-2164-13-544
- Khan, R. (1979). "Solanum melongena and its ancestral forms," in *The Biology and Taxonomy of the Solanaceae*, eds J. G. Hawkes, R. N. Lester, and A. D. Skelding (London: Academic Press), 629–638.
- Kiferle, C., Fantini, E., Bassolino, L., Povero, G., Spelti, C., Butti, S., et al. (2015). Tomato R2R3-MYB Proteins SLANT1 and SLAN2: same protein activity, different roles. *PLoS ONE* 10:e0136365. doi: 10.1371/journal.pone.0136365
- Knapp, S., Vorontsova, M. S., and Prohens, J. (2013). Wild Relatives of the Eggplant (*Solanum melongena* L.: Solanaceae): new understanding of species names in a complex group. *PLoS ONE* 8:e57039. doi: 10.1371/journal.pone.0057039
- Lallemand, L. A., Zubietta, C., Lee, S. G., Wang, Y., Acaljaoui, S., Timmins, J., et al. (2012). A structural basis for the biosynthesis of the major chlorogenic acids found in coffee. *Plant Physiol.* 160, 249–260. doi: 10.1104/pp.112.202051
- Lamy, S., Blanchette, M., Michaud-Levesque, J., Lafleur, R., Durocher, Y., Moghrabi, A., et al. (2006). Delphinidin, a dietary anthocyanidin, inhibits vascular endothelial growth factor receptor-2 phosphorylation. *Carcinogenesis* 27, 989–996. doi: 10.1093/carcin/bgi279
- Laursen, T., Møller, B. L., and Bassard, J.-E. (2015). Plasticity of specialized metabolism as mediated by dynamic metabolons. *Trends Plant Sci.* 20, 20–32. doi: 10.1016/j.tplants.2014.11.002
- Leivar, P., and Quail, P. H. (2011). PIFs: pivotal components in a cellular signaling hub. *Trends Plant Sci.* 16, 19–28. doi: 10.1016/j.tplants.2010.08.003
- Lev-Yadun, S., and Gould, K. S. (2009). "Role of anthocyanins in plant defence," in *Anthocyanins: Biosynthesis, Functions, and Applications*, eds K. Gould, K. Davies, and C. Winefield (New York: Springer), 21–48.
- Li, H., Chen, H., Zhuang, T., and Chen, J. (2010). Analysis of genetic variation in eggplant and related *Solanum species* using sequence-related amplified polymorphism markers. *Sci. Hortic. (Amsterdam)* 125, 19–24. doi: 10.1016/j.scienta.2010.02.023

- Lin-Wang, K., Bolitho, K., Grafton, K., Kortstee, A., Karunairetnam, S., McGhie, T. K., et al. (2010). An R2R3 MYB transcription factor associated with regulation of the anthocyanin biosynthetic pathway in Rosaceae. *BMC Plant Biol.* 10:50. doi: 10.1186/1471-2229-10-50
- Liu, J., Osbourn, A., and Ma, P. (2015). MYB transcription factors as regulators of phenylpropanoid metabolism in plants. *Mol. Plant* 8, 689–708. doi: 10.1016/j.molp.2015.03.012
- Lo Scalzo, R., Fibiani, M., Francese, G., D'Alessandro, A., Rotino, G. L., Conte, P., et al. (2016). Cooking influence on physico-chemical fruit characteristics of eggplant (*Solanum melongena* L.). *Food Chem.* 194, 835–842. doi: 10.1016/j.foodchem.2015.08.063
- Lo Scalzo, R., Fibiani, M., Mennella, G., Rotino, G. L., Dal Sasso, M., Culici, M., et al. (2010). Thermal treatment of eggplant (*Solanum melongena* L.) increases the antioxidant content and the inhibitory effect on human neutrophil burst. *J. Agric. Food Chem.* 58, 3371–3379. doi: 10.1021/jf903881s
- Luo, J., Butelli, E., Hill, L., Parr, A., Niggeweg, R., Bailey, P., et al. (2008). AtMYB12 regulates caffeoyl quinic acid and flavonol synthesis in tomato: expression in fruit results in very high levels of both types of polyphenol. *Plant J.* 56, 316–326. doi: 10.1111/j.1365-313X.2008.03597.x
- MacDonald, M. J., and D'Cunha, G. B. (2007). A modern view of phenylalanine ammonia lyase. *Biochem. Cell Biol.* 85, 273–282. doi: 10.1139/o07-147
- Malinovsky, F. G., Fangel, J. U., and Willats, W. G. T. (2014). The role of the cell wall in plant immunity. *Front. Plant Sci.* 5:178. doi: 10.3389/fpls.2014.00178
- Matsui, K., Umemura, Y., and Ohme-Takagi, M. (2008). AtMYBL2, a protein with a single MYB domain, acts as a negative regulator of anthocyanin biosynthesis in *Arabidopsis*. *Plant J.* 55, 954–967. doi: 10.1111/j.1365-313X.2008.03565.x
- Matus, J. T., Aquea, F., and Arce-Johnson, P. (2008). Analysis of the grape MYB R2R3 subfamily reveals expanded wine quality-related clades and conserved gene structure organization across *Vitis* and *Arabidopsis* genomes. *BMC Plant Biol.* 8:83. doi: 10.1186/1471-2229-8-83
- McCullough, M. L., Feskanich, D., Stampfer, M. J., Giovannucci, E. L., Rimm, E. B., Hu, F. B., et al. (2002). Diet quality and major chronic disease risk in men and women: moving toward improved dietary guidance. *Am. J. Clin. Nutr.* 76, 1261–1271.
- Meiers, S., Kemény, M., Weyand, U., Gastpar, R., von Angerer, E., and Marko, D. (2001). The anthocyanidins cyanidin and delphinidin are potent inhibitors of the epidermal growth-factor receptor. *J. Agric. Food Chem.* 49, 958–962. doi: 10.1021/jf0009100
- Mennella, G., Lo Scalzo, R., Fibiani, M., D'Alessandro, A., Francese, G., Toppino, L., et al. (2012). Chemical and bioactive quality traits during fruit ripening in eggplant (*S. melongena* L.) and allied species. *J. Agric. Food Chem.* 60, 11821–11831. doi: 10.1021/jf3037424
- Mennella, G., Rotino, G. L., Fibiani, M., D'Alessandro, A., Francese, G., Toppino, L., et al. (2010). Characterization of health-related compounds in eggplant (*Solanum Melongena* L.) lines derived from introgression of allied species. *J. Agric. Food Chem.* 58, 7597–7603. doi: 10.1021/jf101004z
- Meyer, R. S., Whitaker, B. D., Little, D. P., Wu, S.-B., Kennelly, E. J., Long, C.-L., et al. (2015). Parallel reductions in phenolic constituents resulting from the domestication of eggplant. *Phytochemistry* 115, 194–206. doi: 10.1016/j.phytochem.2015.02.006
- Mintz-Oron, S., Mandel, T., Rogachev, I., Feldberg, L., Lotan, O., Yativ, M., et al. (2008). Gene expression and metabolism in tomato fruit surface tissues. *Plant Physiol.* 147, 823–851. doi: 10.1104/pp.108.116004
- Montefiori, M., Brendolise, C., Dare, A. P., Lin-Wang, K., Davies, K. M., Hellens, R. P., et al. (2015). In the Solanaceae, a hierarchy of bHLHs confer distinct target specificity to the anthocyanin regulatory complex. *J. Exp. Bot.* 66, 1427–1436. doi: 10.1093/jxb/eru494
- Nakagawa, T., Ishiguro, S., and Kimura, T. (2009). Gateway vectors for plant transformation. *Plant Biotechnol.* 26, 275–284. doi: 10.5511/plantbiotechnology.26.275
- Nei, M., and Kumar, S. (2000). *Molecular Evolution and Phylogenetics*. Oxford: Oxford University Press.
- Niggeweg, R., Michael, A. J., and Martin, C. (2004). Engineering plants with increased levels of the antioxidant chlorogenic acid. *Nat. Biotechnol.* 22, 746–754. doi: 10.1038/nbt966
- Pardo Torre, J. C., Schmidt, G. W., Paetz, C., Reichelt, M., Schneider, B., Gershenson, J., et al. (2013). The biosynthesis of hydroxycinnamoyl quinate esters and their role in the storage of cocaine in *Erythroxylum coca*. *Phytochemistry* 91, 177–186. doi: 10.1016/j.phytochem.2012.09.009
- Pattanaik, S., Kong, Q., Zaitlin, D., Werkman, J. R., Xie, C. H., Patra, B., et al. (2010). Isolation and functional characterization of a floral tissue-specific R2R3 MYB regulator from tobacco. *Planta* 231, 1061–1076. doi: 10.1007/s00425-010-1108-y
- Payavula, R. S., Navarre, D. A., Kuhl, J. C., Pantoja, A., and Pillai, S. S. (2012). Differential effects of environment on potato phenylpropanoid and carotenoid expression. *BMC Plant Biol.* 12:39. doi: 10.1186/1471-2229-12-39
- Payavula, R. S., Shakya, R., Sengoda, V. G., Munyaneza, J. E., Swamy, P., and Navarre, D. A. (2014). Synthesis and regulation of chlorogenic acid in potato: rerouting phenylpropanoid flux in HQT-silenced lines. *Plant Biotechnol.* 15, 14743–14752. doi: 10.1111/pbi.12280
- Payavula, R. S., Singh, R. K., and Navarre, D. A. (2013). Transcription factors, sucrose, and sucrose metabolic genes interact to regulate potato phenylpropanoid metabolism. *J. Exp. Bot.* 64, 5115–5131. doi: 10.1093/jxb/ert303
- Petroni, K., and Tonelli, C. (2011). Recent advances on the regulation of anthocyanin synthesis in reproductive organs. *Plant Sci.* 181, 219–229. doi: 10.1016/j.plantsci.2011.05.009
- Pfaffl, M. W. (2004). “Quantification strategies in real-time PCR,” in *The Real-Time PCR Encyclopedia A-Z of Quantitative PCR*, ed. S. A. Bustin (La Jolla, CA: International University Line), 87–120.
- Pfaffl, M. W. (2001). A new mathematical model for relative quantification in real-time RT-PCR. *Nucleic Acids Res.* 29:e45. doi: 10.1093/nar/29.9.e45
- Plazas, M., Andújar, I., Vilanova, S., Hurtado, M., Gramazio, P., Herreraiz, F. J., et al. (2013a). Breeding for chlorogenic acid content in eggplant: interest and prospects. *Not. Bot. Hortic. Agrobot. Cluj Napoca* 41, 26–35.
- Plazas, M., López-Gresa, M. P., Vilanova, S., Torres, C., Hurtado, M., Gramazio, P., et al. (2013b). Diversity and relationships in key traits for functional and apparent quality in a collection of eggplant: fruit phenolics content, antioxidant activity, polyphenol oxidase activity, and browning. *J. Agric. Food Chem.* 61, 8871–8879. doi: 10.1021/jf402429k
- Povero, G., Gonzali, S., Bassolino, L., Mazzucato, A., and Perata, P. (2011). Transcriptional analysis in high-anthocyanin tomatoes reveals synergistic effect of *Aft* and *atv* genes. *J. Plant Physiol.* 168, 270–279. doi: 10.1016/j.jplph.2010.07.022
- Quattroccchio, F., Verweij, W., Kroon, A., Spelt, C., Mol, J., and Koes, R. (2006). PH4 of petunia is an R2R3 MYB protein that activates vacuolar acidification through interactions with basic-helix-loop-helix transcription factors of the anthocyanin pathway. *Plant Cell* 18, 1274–1291. doi: 10.1105/tpc.105.034041
- Quattroccchio, F., Wing, J., van der Woude, K., Souer, E., de Vetten, N., Mol, J., et al. (1999). Molecular analysis of the anthocyanin2 gene of petunia and its role in the evolution of flower color. *Plant Cell* 11, 1433–1444. doi: 10.1105/tpc.5.11.1497
- Quattroccchio, F., Wing, J. F., Van der Woude, K., Mol, J. N. M., and Koes, R. (1998). Analysis of bHLH and MYB domain proteins: Species-specific regulatory differences are caused by divergent evolution of target anthocyanin genes. *Plant J.* 13, 475–488. doi: 10.1046/j.1365-313X.1998.00046.x
- Rraigón, M. D., Prohens, J., Muñoz-Falcón, J. E., and Nuez, F. (2008). Comparison of eggplant landraces and commercial varieties for fruit content of phenolics, minerals, dry matter and protein. *J. Food Compos. Anal.* 21, 370–376. doi: 10.1016/j.jfca.2008.03.006
- Rommens, C. M., Richael, C. M., Yan, H., Navarre, D. A., Ye, J., Krucker, M., et al. (2008). Engineered native pathways for high kaempferol and caffeoylquinate production in potato. *Plant Biotechnol. J.* 6, 870–886. doi: 10.1111/j.1467-7652.2008.00362.x
- Saitou, N., and Nei, M. (1987). The neighbor-joining method: a new method for reconstructing phylogenetic trees. *Mol. Biol. Evol.* 4, 406–425.
- Sonnante, G., D'Amore, R., Blanco, E., Pierri, C. L., De Palma, M., Luo, J., et al. (2010). Novel hydroxycinnamoyl-coenzyme A quinate transferase genes from artichoke are involved in the synthesis of chlorogenic acid. *Plant Physiol.* 153, 1224–1238. doi: 10.1104/pp.109.150144
- Spelt, C., Quattroccchio, F., Mol, J. N., and Koes, R. (2000). Anthocyanin1 of petunia encodes a basic helix-loop-helix protein that directly activates transcription of structural anthocyanin genes. *Plant Cell* 12, 1619–1632. doi: 10.1105/tpc.12.9.1619

- Stommel, J. R., and Whitaker, B. D. (2003). Phenolic acid content and composition of eggplant fruit in a germplasm core subset. *J. Am. Soc. Hortic. Sci.* 128, 704–710.
- St-Pierre, B., and De Luca, V. (2000). “Evolution of acyltransferase genes: origin and diversification of the BAHD superfamily of acyltransferases involved in secondary metabolism,” in *Recent Advances in Phytochemistry: Evolution of Metabolic Pathways*, Vol. 34, eds J. T. Romeo, R. Ibrahim, L. Varin, and V. De Luca (Amsterdam: Elsevier Science), 285–315. doi: 10.1016/S0079-9920(00)80010-6
- Stracke, R., Holtgräwe, D., Schneider, J., Pucker, B., Rosleff Sørensen, T., and Weisshaar, B. (2014). Genome-wide identification and characterisation of R2R3-MYB genes in sugar beet (*Beta vulgaris*). *BMC Plant Biol.* 14:249. doi: 10.1186/s12870-014-0249-8
- Stracke, R., Ishihara, H., Huep, G., Barsch, A., Mehrtens, F., Niehaus, K., et al. (2007). Differential regulation of closely related R2R3-MYB transcription factors controls flavonol accumulation in different parts of the *Arabidopsis thaliana* seedling. *Plant J.* 50, 660–677. doi: 10.1111/j.1365-313X.2007.03078.x
- Stushnoff, C., Ducreux, L. J. M., Hancock, R. D., Hedley, P. E., Holm, D. G., McDougall, G. J., et al. (2010). Flavonoid profiling and transcriptome analysis reveals new gene-metabolite correlations in tubers of *Solanum tuberosum* L. *J. Exp. Bot.* 61, 1225–1238. doi: 10.1093/jxb/erp394
- Takos, A. M., Jaffé, F. W., Jacob, S. R., Bogs, J., Robinson, S. P., and Walker, A. R. (2006). Light-induced expression of a MYB gene regulates anthocyanin biosynthesis in red apples. *Plant Physiol.* 142, 1216–1232. doi: 10.1104/pp.106.088104
- Tamura, K., Stecher, G., Peterson, D., Filipski, A., and Kumar, S. (2013). MEGA6: Molecular evolutionary genetics analysis version 6.0. *Mol. Biol. Evol.* 30, 2725–2729. doi: 10.1093/molbev/mst197
- Thorup, T. A., Tanyolac, B., Livingstone, K. D., Popovsky, S., Paran, I., and Jahn, M. (2000). Candidate gene analysis of organ pigmentation loci in the Solanaceae. *Proc. Natl. Acad. Sci. U.S.A.* 97, 11192–11197. doi: 10.1073/pnas.97.21.11192
- Tomato Genome Consortium (2012). The tomato genome sequence provides insights into fleshy fruit evolution. *Nature* 485, 635–641. doi: 10.1038/nature11119
- Vogt, T. (2010). Phenylpropanoid biosynthesis. *Mol. Plant* 3, 2–20. doi: 10.1093/mp/ssp106
- Voinnet, O., Rivas, S., Mestre, P., and Baulcombe, D. (2003). An enhanced transient expression system in plants based on suppression of gene silencing by the p19 protein of tomato bushy stunt virus. *Plant J.* 33, 949–956. doi: 10.1046/j.1365-313X.2003.01676.x
- Vrhovsek, U., Rigo, A., Tonon, D., and Mattivi, F. (2004). Quantitation of polyphenols in different apple varieties. *J. Agric. Food Chem.* 52, 6532–6538. doi: 10.1021/jf049317z
- Wilkins, O., Nahal, H., Foong, J., Provart, N. J., and Campbell, M. M. (2009). Expansion and diversification of the *Populus* R2R3-MYB family of transcription factors. *Plant Physiol.* 149, 981–993. doi: 10.1104/pp.108.132795
- Xu, F., Ning, Y., Zhang, W., Liao, Y., Li, L., Cheng, H., et al. (2014). An R2R3-MYB transcription factor as a negative regulator of the flavonoid biosynthesis pathway in *Ginkgo biloba*. *Funct. Integr. Genomics* 14, 177–189. doi: 10.1007/s10142-013-0352-1
- Zhang, Y., Butelli, E., De Stefano, R., Schoonbeek, H. J., Magusin, A., Pagliarani, C., et al. (2013). Anthocyanins double the shelf life of tomatoes by delaying overripening and reducing susceptibility to gray mold. *Curr. Biol.* 23, 1094–1100. doi: 10.1016/j.cub.2013.04.072
- Zhang, Y., Hu, Z., Chu, G., Huang, C., Tian, S., Zhao, Z., et al. (2014). Anthocyanin accumulation and molecular analysis of anthocyanin biosynthesis associated genes in eggplant (*Solanum melongena* L.). *J. Agric. Food Chem.* 62, 2906–2912. doi: 10.1021/jf404574c

Conflict of Interest Statement: The authors declare that the research was conducted in the absence of any commercial or financial relationships that could be construed as a potential conflict of interest.

Copyright © 2016 Docimo, Francese, Ruggiero, Batelli, De Palma, Bassolino, Toppino, Rotino, Mennella and Tucci. This is an open-access article distributed under the terms of the Creative Commons Attribution License (CC BY). The use, distribution or reproduction in other forums is permitted, provided the original author(s) or licensor are credited and that the original publication in this journal is cited, in accordance with accepted academic practice. No use, distribution or reproduction is permitted which does not comply with these terms.



Metabolic and Molecular Changes of the Phenylpropanoid Pathway in Tomato (*Solanum lycopersicum*) Lines Carrying Different *Solanum pennellii* Wild Chromosomal Regions

Maria Manuela Rigano¹, Assunta Raiola¹, Teresa Docimo², Valentino Ruggieri¹, Roberta Calafiore¹, Paola Vitaglione¹, Rosalia Ferracane¹, Luigi Frusciante¹ and Amalia Barone^{1*}

¹ Department of Agricultural Sciences, University of Naples Federico II, Naples, Italy, ² Istituto di Bioscienze e BioRisorse, UOS Portici, Consiglio Nazionale delle Ricerche, Naples, Italy

OPEN ACCESS

Edited by:

Ana Margarida Fortes,
University of Lisbon, Portugal

Reviewed by:

Christoph Martin Geilfus,
University of Kiel, Germany
Robert David Hall,
Wageningen University and Research
Centre, Netherlands

*Correspondence:

Amalia Barone
ambarone@unina.it

Specialty section:

This article was submitted to
Plant Physiology,
a section of the journal
Frontiers in Plant Science

Received: 30 May 2016

Accepted: 20 September 2016

Published: 04 October 2016

Citation:

Rigano MM, Raiola A, Docimo T, Ruggieri V, Calafiore R, Vitaglione P, Ferracane R, Frusciante L and Barone A (2016) Metabolic and Molecular Changes of the Phenylpropanoid Pathway in Tomato (*Solanum lycopersicum*) Lines Carrying Different *Solanum pennellii* Wild Chromosomal Regions. *Front. Plant Sci.* 7:1484.
doi: 10.3389/fpls.2016.01484

Solanum lycopersicum represents an important dietary source of bioactive compounds including the antioxidants flavonoids and phenolic acids. We previously identified two genotypes (IL7-3 and IL12-4) carrying loci from the wild species *Solanum pennellii*, which increased antioxidants in the fruit. Successively, these lines were crossed and two genotypes carrying both introgressions at the homozygous condition (DHO88 and DHO88-SL) were selected. The amount of total antioxidant compounds was increased in DHOs compared to both ILs and the control genotype M82. In order to understand the genetic mechanisms underlying the positive interaction between the two wild regions pyramided in DHO genotypes, detailed analyses of the metabolites accumulated in the fruit were carried out by colorimetric methods and LC/MS/MS. These analyses evidenced a lower content of flavonoids in DHOs and in ILs, compared to M82. By contrast, in the DHOs the relative content of phenolic acids increased, particularly the fraction of hexoses, thus evidencing a redirection of the phenylpropanoid flux toward the biosynthesis of phenolic acid glycosides in these genotypes. In addition, the line DHO88 exhibited a lower content of free phenolic acids compared to M82. Interestingly, the two DHOs analyzed differ in the size of the wild region on chromosome 12. Genes mapping in the introgression regions were further investigated. Several genes of the phenylpropanoid biosynthetic pathway were identified, such as one 4-coumarate:CoA ligase and two UDP-glycosyltransferases in the region 12-4 and one chalcone isomerase and one UDP-glycosyltransferase in the region 7-3. Transcriptomic analyses demonstrated a different expression of the detected genes in the ILs and in the DHOs compared to M82. These analyses, combined with biochemical analyses, suggested a central role of the 4-coumarate:CoA ligase in redirecting the phenylpropanoid pathways toward the biosynthesis of phenolic acids in the pyramided lines. Moreover, analyses here carried out suggest the presence in the introgression regions of novel regulatory proteins, such as one Myb4 detected on chromosome 7 and one bHLH detected in chromosome 12. Overall our data indicate that structural and regulatory genes identified in this study might have a key role for the manipulation of the phenylpropanoid metabolic pathway in tomato fruit.

Keywords: phenolic acids, chlorogenic acid, flavonoids, pyramided lines, introgression lines

INTRODUCTION

Tomato (*Solanum lycopersicum*) is the second most consumed vegetable in the world; indeed, tomato consumption reaches 40–45 kg *pro capita per year* in several European countries (FAO database). Consumption of tomato fruits is associated with a reduced risk of some types of cancer and of several chronic non-communicable diseases (CNCDs), such as diabetes, hypertension, and obesity (Raiola et al., 2014). These health benefits are mainly attributed to the occurring of hydrophilic and lipophilic phytochemicals (polyphenols, ascorbic acid, carotenoids, and tocopherols) in the fruits. Among these, polyphenols are very active compounds that in humans are able to reduce DNA oxidation and to control inflammation and cell proliferation and differentiation (Lodovici et al., 2001; Visioli et al., 2011). In plants these secondary metabolites are implicated in UV-B tolerance, plant response toward biotic and abiotic stimuli, growth control and developmental processes (Vogt, 2010; Tohge et al., 2015). In the first step of the general phenylpropanoid biosynthetic pathway, the phenylalanine is deaminated by the enzyme PAL (phenylalanine ammonia lyase) to form cinnamic acid that is then hydroxylated to generate coumaric acid (Figure 1). The enzyme 4-coumarate:CoA ligase (4CL) catalyzes the last step of the general phenylpropanoid pathway. The enzyme 4CL converts coumaric acid and other substituted cinnamic acids (caffeoic, ferulic, and sinapic acids) into corresponding CoA esters that are then used for the biosynthesis of flavonoids, isoflavonoids, lignins, coumarins, and other phenolics (Alberstein et al., 2012; Sun et al., 2013; Li et al., 2015; Pandey et al., 2015). It is thought that the substrate specificity of 4CL determines the direction of the metabolic flux in the downstream reactions (Alberstein et al., 2012). In tomato, flavonoids are located mostly in the skin and are involved in the pigmentation and aroma of the fruit; they include naringenin, quercetin, rutin, kampferol, and catechin and show a protective action against intestinal inflammation and rheumatoid arthritis (Kauss et al., 2008; González et al., 2011; Raiola et al., 2014). Phenolic acids are responsible for the astringent taste of tomato fruits and consist mainly of gallic, chlorogenic, and ferulic acids (Moco et al., 2007). Hydroxycinnamates, due to their antioxidant capacity, have important beneficial health effects: they can limit LDL (low-density lipid) oxidation, prevent carcinogenesis and are potential therapeutic agents for neurodegenerative diseases, such as Alzheimer and Parkinson and for the prevention of cardiovascular disease and diabetes (Niggeweg et al., 2004; Calvenzani et al., 2015; Tohge et al., 2015).

The cultivated tomato varieties generally do not contain high amounts of phenolic compounds in the fruit (Tohge et al., 2015). This is also due to tomato domestication that resulted in the loss of about 95% of the chemical diversity of wild relatives (Perez-Fons et al., 2014). For example, domestication in *S. lycopersicum* has led to poor tasting tomatoes also due to reduced formation of volatile compounds (Bolger et al., 2014). Several strategies have been previously used to increase the content of antioxidants in tomato fruits. One strategy considers screening wild genetic resources for quality traits, such as antioxidant content, that could be introduced into modern varieties (Gur and Zamir, 2004; Schauer et al., 2006). Around 20 years ago nearly isogenic

lines were generated to effectively reintroduce unused genetic variation from wild species into cultivated varieties and to facilitate the mapping of traits originating from wild donors (Gur and Zamir, 2015). Introgression lines (ILs) include single marker-defined introgressed genomic regions from the wild species into the genomic background of the cultivated variety *S. lycopersicum* (M82). *Solanum pennellii* ILs were produced and were used to map several QTLs associated with traits related to tomato fruit quality (Eshed and Zamir, 1995; Rousseaux et al., 2005). We previously identified two introgression lines (IL7-3 and IL12-4) carrying loci from the wild species *S. pennellii* that increase antioxidants in the fruit (Sacco et al., 2013). Successively, these lines were crossed and genotypes carrying both introgressions at the homozygous condition were selected (Rigano et al., 2014). When we examined their nutritional quality we found that the amount of total antioxidant compounds was increased in the pyramided lines compared to the parental lines and the cultivated control genotype M82. Additional metabolic analyses revealed significant increase of total polyphenols in the pyramided lines compared to the parental lines and to M82 and a concomitant reduction of flavonoids (Rigano et al., 2014). In this study, two pyramided lines with a different *S. pennellii* introgression region in chromosome 12 were selected and analyzed in order to better investigate the genetic mechanisms underlying the interaction between the two wild regions. The integration of genomic, transcriptomic, metabolic and biochemical analyses was carried out and allowed us to define the role of different wild *S. pennellii* genes in redirecting the phenylpropanoid pathways toward the biosynthesis of phenolic acids in the pyramided lines.

MATERIALS AND METHODS

Chemical and Reagents

Phenylalanine, cinnamic, ferulic, caffeoic, *p*-coumaric, chlorogenic and gallic acids, rutin, and quercetin standard were purchased from Sigma (Italy), naringenin from Aldrich (Italy), naringenin-7-O-glucoside from Infodine (USA). Methanol, formic acid, and water HPLC grade were obtained from Merck (Darmstadt, Germany). Deionized water was obtained from a Milli-Q water purification system (Millipore, Bedford, MA, USA). Chromatographic solvents were degassed for 20 min using a Branson 5200 (Branson Ultrasonic Corp., USA) ultrasonic bath.

Plant Material and Growth Conditions

Seeds from IL12-4 (LA4102), IL7-3 (LA4066) and their parental line M82 (LA3475) were kindly provided by the Tomato Genetics Resource Centre (TGRC)¹. Genotypes DHO88 and DHO88-SL were selected from F₂ genotypes previously obtained by intercrossing IL12-4 and IL7-3 (Sacco et al., 2013). The F₂ genotypes were selfed for two generations and then screened by species-specific markers. During the years 2014 and 2015, the double-homozygous plants of the F₄ progenies and their parents were grown in an experimental field located in Acerra

¹<http://tgrc.ucdavis.edu/>

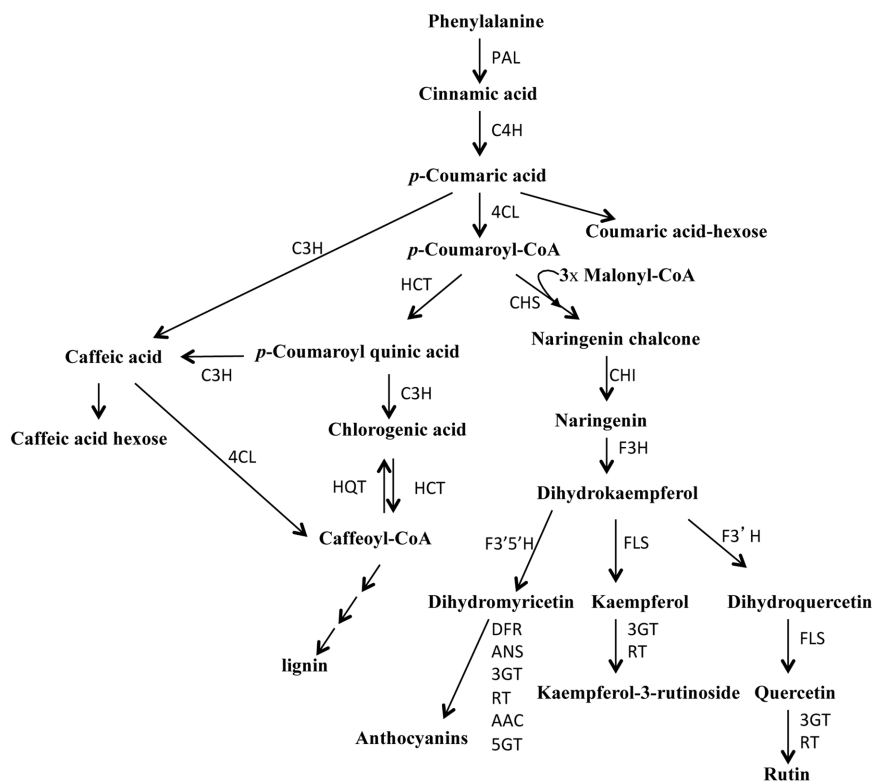


FIGURE 1 | Schematic overview of the phenylpropanoid pathway in tomato. PAL, phenylalanine-ammonia-lyase; C4H, cinnamate 4-hydroxylase; 4CL, 4-coumarate:CoA ligase; HCT, cinnamoyl-CoA shikimate/quinate transferase; C3H, *p*-coumaroyl ester 3-hydroxylase; HQT, hydroxycinnamoyl-CoA quinate transferase; CHS, chalcone synthase; CHI, chalcone isomerase; F3H, flavanone-3-hydroxylase; F3'H, flavonoid-3'-hydroxylase; FLS, flavonol synthase; 3GT, flavonoid-3-O-glucosyltransferase; RT, flavonoid 3-O-glucoside-rhamnosyltransferase; F3'5'H, flavonoid-3'-5'-hydroxylase; DFR, dihydroflavonol reductase; ANS, anthocyanidin synthase; AAC, anthocyanin acyltransferase; 5GT, flavonoid 5-glucosyltransferase.

(Naples, Italy), according to a completely randomized design with three replicates (10 plants/replicate). The physico-chemical properties of the soil have been reported in Supplementary Table S1. Seeds were first germinated in Petri dishes on water-soaked filter paper and subsequently transferred in peat on a seed tray and incubated in a growth chamber at 22°C and 16 h/8 h light/dark. Plants were transplanted at the four leaf-stage. Before transplanting urea phosphate fertilizer (40 kg ha⁻¹) was applied to the soil. Tillage treatments included plowing followed by one or two milling. Successively, weeding and ridging were carried out. Plants were irrigated as required (2–3 times *per* week in absence of rain). Recommended levels of N (190 kg ha⁻¹), P (25 kg ha⁻¹), and K (20 kg ha⁻¹) were applied during cultivation *via* fertirrigation. During the growing season, the insecticides and fungicides were applied according to general local practices and recommendations. In the two growing seasons we recorded temperatures and precipitation in the seasonal media for the Campania region, even though in 2014 rainfall was slightly heavier than in 2015, whereas in the latter year the temperatures were slightly higher than in 2014.

Samples of about 20 full mature red fruits *per* plot were collected. Tomato fruits were chopped, ground in liquid nitrogen in a blender (FRI150, Fimar) to a fine powder, and kept at -80°C

until the subsequent metabolic, molecular, and enzymatic analyses were performed.

Chemical Extractions

For the metabolic analyses, each sample consisted of 20-pooled fruits *per* plot. The extraction of the polyphenolic fraction was carried out according to the procedure reported by Choi et al. (2011) with some changes. Briefly, frozen tomato powder (3 g) was weighed, placed into a 50 ml Falcon tube, and extracted with 15 ml of 70% methanol into an ultrasonic bath (Branson 5200, Ultrasonic, Corp.) for 30 min at 30°C. The mixture was centrifuged at 20000 g for 10 min at 4°C, and the supernatant was collected, while the pellet was re-extracted for the second time as previously described. An aliquot (500 µl) of the methanolic extract was stored at -20°C until further analyses, while 25 ml of extract were dried by rotary evaporator (Buchi R-210, Milan, Italy) at 30°C for 10 min and dissolved in 70% methanol (2 ml). Then, the extract was transferred in a glass tube and was further dried by using a SpeedVac (Thermo Scientific, Savant, SPD131DDA SpeedVac Concentrator, Waltham, MA, USA). The dried extract was dissolved in 70% methanol (500 µl) obtaining a final concentration of 5 g fresh weight (FW)/ml. The extract was passed through a 0.45 µm Millipore nylon filter (Merck Millipore,

Bedford, MA, USA) and stored at -20°C until LC/MS/MS analysis.

Total Flavonoids

Total flavonoids were quantified by the aluminum chloride colorimetric test reported by Marinova et al. (2005) with slight modifications. An aliquot (500 μl) of methanolic extract (see Chemical Extractions) was added to 5% NaNO₂ (30 μl) and, after an incubation of 5 min, 10% AlCl₃ (30 μl) was added. After 6 min 1 M NaOH (200 μl) and H₂O (240 μl) were added and the absorbance of the resulting solution was measured at 510 nm. Total flavonoids content was expressed as mg quercetin equivalent (QE)/100 g FW. Three biological replicates and three technical assays for each biological repetition were analyzed.

LC/MS/MS Analysis of Polyphenols

Chromatographic separation was performed using an HPLC apparatus equipped with two Micropumps Series 200 (PerkinElmer, Shelton, CT, USA), a UV/VIS series 200 detector (PerkinElmer, Shelton, CT, USA) set at 330 nm and a Prodigy ODS3 100 Å column (250 mm \times 4.6 mm, particle size 5 μm ; Phenomenex, CA, USA).

The eluents were: A water 0.2% formic acid; B acetonitrile/methanol (60:40, v/v). The gradient program was as follows: 20–30% B (6 min), 30–40% B (10 min), 40–50% B (8 min), 50–90% B (8 min), 90–90% B (3 min), 90–20% B (3 min) at a constant flow of 0.8 ml/min. The LC flow was split and 0.2 ml/min was sent to the mass spectrometry. Injection volume was 20 μl . Mass spectrometer analyses were performed on an API 3000 triple quadrupole (Applied Biosystems, Canada) equipped with a TurboIonSpray source working in the negative ion mode. The analyses were performed in MRM (multiple reaction monitoring), using the following settings: drying gas (air) was heated to 400°C, capillary voltage (IS) was set to 4000 V. The MS/MS characteristics of phenolic compounds identified in extracts are reported in Supplementary Table S2. Example of a chromatogram of phenolic compounds in M82 detected at 330 nm is reported in Supplementary Figure S1.

The compounds were identified comparing retention times and MS/MS fragments with standards data. Identification of compounds that were not available as standards was obtained comparing their MS and MS/MS spectra with the literature data (Moco et al., 2006; Vallverdú-Queralt et al., 2011).

Molecular Marker Analyses

In order to define the wild region size of the DHO lines, polymorphic markers previously selected in our laboratory and spanning the introgression regions 7-3 and 12-4 were used (Ruggieri et al., 2015; Calafiore et al., 2016). Total genomic DNA was extracted from leaves using the PureLinkTM Genomic DNA Kit (Invitrogen). PCR DNA amplification was carried out in 50 μl reaction volume containing 50 ng DNA, 1X reaction buffer, 0.2 mM each dNTP, 1.0 mM primer and 1.25 U GoTaq polymerase (Promega). The restriction endonuclease reaction was performed in 50 μl of reaction volume containing 20 μl PCR product, 5 μl 10X reaction buffer and 1 μl of the selected

restriction enzyme (10 u/ml). Digested fragments were separated by electrophoresis on 2% agarose gel in 1X TAE buffer.

Identification and Expression of Candidate Genes

The search for candidate genes (CG) mapping in the regions 7-3 and 12-4 of chromosomes 7 and 12 and potentially associated with phenolics metabolism was conducted by exploring the annotations and the Gene Ontology terms of genes included in the two regions. The number of CGs was then reduced by selecting only those expressed in the fruit at different developmental stages in the reference cv. Heinz, as reported in the Tomato Functional Genomic Database (TED²). RNA-Seq data from the red fruit of *S. pennellii* ILs and of *S. lycopersicum* cv. M82 were also retrieved from the TED.

The expression of CGs in the ILs fruit compared to that in M82 was verified by Real-Time PCR amplification. Total RNA was isolated from tomato fruit of lines M82, IL7-3, IL12-4, DHO88, and DHO88-SL by using the TRIzol[®] reagent (Invitrogen, Carlsbad, CA, USA) and treated with RNase-free DNase (Invitrogen, Carlsbad, CA, USA; Madison, WI, USA) according to the method reported by the manufacturer (Invitrogen). Total RNA (1 μg) was treated by the Transcriptor High Fidelity cDNA Synthesis Kit (Roche) and cDNA was stored at -20°C until RT-PCR analysis. For each RT-PCR reaction, 1 μl of cDNA diluted 1:10 was mixed with 12.5 μl SYBR Green PCR master mix (Applied) and 5 pmol each of forward and reverse primers (Supplementary Table S3) in a final volume of 25 μl . The reaction was carried out by using the 7900HT Fast-Real Time PCR System (Applied Biosystems). The amplification program was carried out according to the following steps: 2 min at 50°C, 10 min at 95°C, 0.15 min at 95°C and 60°C for 1 min for 40 cycles. In order to verify the amplification specificity, the amplification program was followed by the thermal denaturing step (0.15 min at 95°C, 0.15 min at 60°C, 0.15 min at 95°C) to generate the dissociation curves. All reactions were run in triplicate for each of the three biological replicates and a housekeeping gene coding for the elongation factor 1-alpha (*Ef 1- α* – Solyc06g005060) was used as reference gene (Calafiore et al., 2016). The expression levels relative to the reference gene were calculated using the formula $2^{-\Delta CT}$, where $\Delta CT = (CT_{\text{RNAtarget}} - CT_{\text{reference RNA}})$ (Schmittgen et al., 2004). Comparison of RNA expression was based on a comparative CT method (ΔCT) and the relative expression was quantified and expressed according to $\log_2 RQ$, where RQ was calculated as $2^{-\Delta\Delta CT}$ and where $\Delta\Delta CT = (CT_{\text{RNAtarget}} - CT_{\text{reference RNA}}) - (CT_{\text{calibrator}} - CT_{\text{reference RNA}})$ (Winer et al., 1999; Livak and Schmittgen, 2001). M82 was selected as calibrator. Quantitative results were expressed as the mean value \pm SE.

Phylogenetic Analysis

All known and reported 4CL and UDP-glycosyltransferase protein-coding sequences were retrieved from the National Center for Biotechnology Information (NCBI). In total, 34 4CL protein sequences and 38 UDP-glycosyltransferases from

²www.ted.bti.cornell.edu

several dicots and monocots species were collected and accession numbers are reported in Supplementary Table S4. The 4CL and UDP amino acid alignments were performed using ClustalW implemented in MEGA 6 (Tamura et al., 2013) and non-rooted phylogenetic trees were constructed using the Maximum Likelihood method and the Jones-Taylor-Thornton (JTT) model using default parameters. Initial trees for the heuristic search were obtained by applying the Neighbor-Joining method to a matrix of pairwise distances estimated using a JTT model. All positions containing gaps and missing data were eliminated. Bootstrap-supported consensus trees were inferred from 500 replicates. Branches with <50% bootstrap support were collapsed.

Enzymatic Assays

Enzyme extractions were performed at 4°C following the method described in Weitzel and Petersen (2010) with slight modifications. Tomato frozen powder (0.3 g) was ground with 0.1 M potassium phosphate buffer pH 7.5 containing 1 mM DTT, 0.1 mM EDTA, 5 mM ascorbic acid, 1 mM PMSF, 0.15% w/v PVP. Then the homogenate was centrifuged at 12000 g for 20 min at 4°C and the supernatant was used as a source of crude enzymes for assaying PAL and 4CL activities. Protein concentration was evaluated by the method of Bradford (1976).

Phenylalanine ammonia lyase activity was determined spectrophotometrically. The reaction mixture contained 50 mM Tris-HCl buffer pH 8.9, 3.6 mM NaCl, 10 mM phenylalanine and 50 µl protein extract. The reaction was incubated at 37°C for 1 h and stopped by adding 150 µl 6 M HCl. The tubes were centrifuged for 10 min at 12000 g. The absorbance was read at 290 nm using as control a reaction without phenylalanine. The rate of appearance of cinnamic acid was taken as a measure of enzyme activity using an increase of 0.01 A₂₉₀ equal to 3.09 nmol of cinnamic acid formed (Saunders and McClure, 1975).

4CL enzyme activity was measured spectrophotometrically. The reaction mixture contained 0.1 M potassium phosphate buffer, pH 7.5, 2.5 mM ATP, 2.5 mM MgCl₂, 1 mM DTT, 50 µl protein preparation and 0.5 mM substrate. The reaction was started by the addition of 0.3 mM CoA and incubated for 1 h at 40°C. The formation of the respective CoA thioesters was measured at different path length depending on the used substrate: 311 nm (cinnamic acid), 333 nm (4-coumaric acid), 346 nm (caffeic acid), and 345 nm (ferulic acid). The extinction coefficient of these esters was used to calculate enzyme activity (Lee et al., 1997; Chen et al., 2006).

Statistical Analyses

In Real-time q-PCR analyses, differences of expression of CGs among samples were determined by using SPSS (Statistical Package for Social Sciences) Package 6, version 15.0. Significant different expression levels were determined by comparing the genotypes through a Student's *t*-test at a significance level of 0.05. In metabolic analyses, quantitative results were expressed as the mean value ± SD. Differences among analyzed genotypes were determined by using SPSS (Statistical Package for Social Sciences) Package 6, version 15.0 (SPSS, Inc., Chicago, IL, USA). Significant different metabolite levels were determined by comparing mean values through a factorial analysis of variance (ANOVA) with

Duncan *post hoc* test at a significance level of 0.05. Enzymatic data were subjected to ANOVA statistical analyses and means were compared using the Tukey HSD test ($p \leq 0.05$) by using SigmaPlot software.

The percentage of variations of quantitative parameters compared to M82 was calculated by using the following formula:

$$\text{Increase or Decrease (\%)} =$$

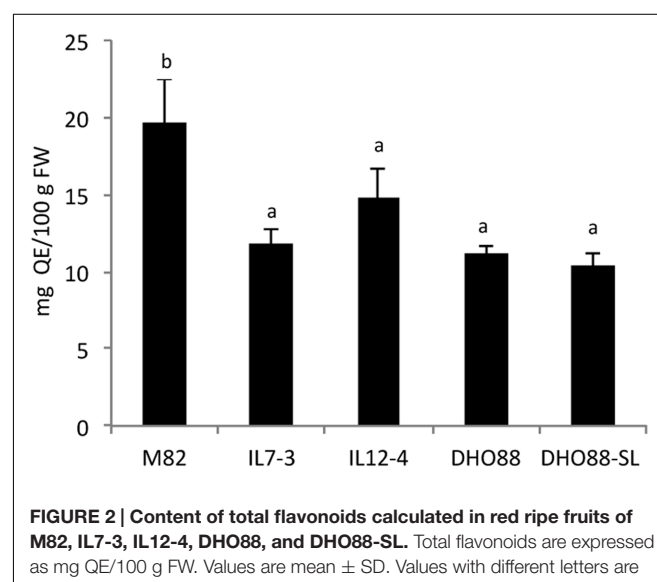
$$\left[\frac{\text{value of tested genotype} - \text{value of M82}}{\text{value of M82}} \right] * 100.$$

RESULTS

Phenolic Compounds in Introgression and Pyramided Lines

Metabolic analyses were performed on mature red fruits of the cultivated genotype M82, of the ILs 7-3 and 12-4 and of two selected pyramided lines (DHO88 and DHO88-SL) obtained by crossing the two introgression lines (IL7-3 × IL12-4). The cultivated genotype M82 contained a mean concentration of flavonoids of 19.70 ± 2.74 mg/100 g FW that was reduced by 40.2% in IL7-3 and by 25.1% in IL12-4 (Figure 2). A significant decrease of total flavonoids in the pyramided genotypes compared to the cultivated genotype M82 was also recorded and was comparable to that calculated in the parental lines IL7-3 and IL12-4.

Results from LC/MS/MS analysis of polyphenols are reported in Supplementary Table S5 and Figure 3. Data showed that chlorogenic acid, coumaric acid hexose, caffeic acid hexose, rutin, naringenin glucoside, and chalconaringenin were the main polyphenols present in all the samples. Considering the parental lines, the amount of chlorogenic acid, the most abundant compound among free phenolic acids in the analyzed lines,



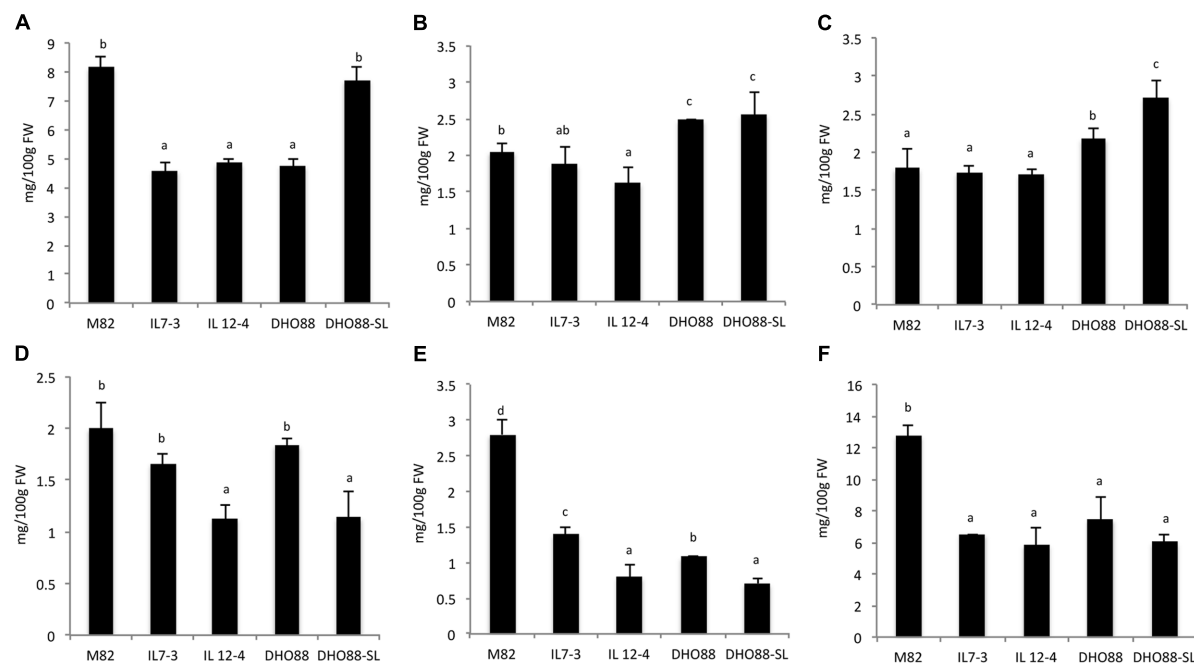


FIGURE 3 | Phenolic compounds amount (mg/100 g FW) calculated in red ripe fruits from M82, IL7-3, IL12-4, DHO88, and DHO88-SL quantified by LC/MS/MS: (A) chlorogenic acid; (B) coumaric acid hexose; (C) caffeic acid hexose; (D) rutin; (E) naringenin glucoside; (F) chalconaringenin. Values are mean \pm SD. Values with different letters are significantly different ($p < 0.05$).

significantly decreased both in IL7-3 (-43.6%), and in IL12-4 (-40.5%) compared to M82. A decrease of caffeic acid in IL12-4 (-31.25%) compared to M82 was also detected (Supplementary Table S5). Regarding the fraction of hexoses, the amount of coumaric acid hexose decreased in IL12-4 compared to M82, while the concentrations of caffeic acid hexose were comparable in both the ILs and in M82. The amount of detected flavonoids was significantly different in the genotypes analyzed. In particular, the compound rutin decreased of 43.5% in IL12-4 compared to M82. A significant decrease of naringenin glucoside and of chalconaringenin was detected both in IL7-3 and in IL12-4 compared to M82.

As for the pyramided lines, the amount of chlorogenic acid exhibited a significant decrease (-41.5%) only in DHO88 compared to M82. By contrast, this acid significantly increased in DHO88-SL compared to the ILs and to the pyramided line DHO88. As for the content of caffeic acid, no significant differences were detected in DHO88 compared to M82, whereas a significant increase was found in DHO88-SL compared to the cultivated line and to the parental lines. Both coumaric acid hexose and caffeic acid hexose were significantly higher in DHO88 and DHO88-SL than in M82 and in the ILs. Overall, in the DHO lines the content of phenolic acids increased compared to the parental line IL7-3 and IL12-4, above all the fraction of hexoses.

As for the flavonoids, the amount of rutin detected in DHO88 was comparable to that found in M82 and IL7-3. In contrast, in DHO88-SL it decreased compared to M82 and was comparable to the amount recorded in IL12-4.

Lower levels of naringenin glucoside and chalconaringenin were found in both the pyramided lines compared to M82. The amount of chalconaringenin detected in the pyramided lines was comparable to the amount found in the ILs.

Genomic Characterization of DHO Lines

In order to understand which genetic mechanisms might explain the interactions between the two wild *S. pennellii* regions pyramided in DHO genotypes in influencing the phenylpropanoid metabolism, the introgression regions borders were precisely defined by using molecular markers reported in Ruggieri et al. (2015) and Calafiore et al. (2016) (Table 1). In both genotypes DHO88 and DHO88-SL the wild region 7-3 stretches from marker N27 to marker N17, spanning the same 6.6 Mbp region of IL7-3. By contrast, the wild region of chromosome 12 has different size in DHO88 and DHO88-SL. In particular, in DHO88 this stretches from marker M1 to marker M18, whereas from marker M10 to marker M18 in the line DHO88-SL, thus reducing in the latter the *S. pennellii* genome to 2.1 Mbp. Consequently, the number of wild alleles at potential CGs for phenylpropanoid accumulation varied in the two lines. Out of 725 genes mapping in the region 7-3 (Calafiore et al., 2016), four CGs involved in the flavonoid biosynthetic pathway were identified, that are Solyc07g062030 annotated as a chalcone-flavonone isomerase (CHI) and three genes coding for UDP-glucosyltransferase (UGT). Out of 480 genes mapping in the region 12-4 (Ruggieri et al., 2015), DHO88 line shares with IL12-4 the same wild alleles for 14

TABLE 1 | Candidate genes mapping in the introgressed regions 7-3 and 12-4.

Candidate gene	Gene identifier (Solyc ID)	Gene position (release SL2.50) bp	Expression level (RPKM)
Chromosome 7			
N27			
Myb family transcription factor-like	Solyc07g049640	59978797–59979255	0.00
Myb-related transcription factor	Solyc07g052300	60797135–60800394	0.00
Myb family transcription factor	Solyc07g052490	61003154–61004234	0.00
Glycosyltransferase-like protein	Solyc07g052630	61096621–61100859	0.00
Glycosyltransferase-like protein	Solyc07g052650	61109726–61111909	0.00
Transcription factor (Fragment)	Solyc07g052670	61115970–61120548	0.55
bHLH transcription factor-like	Solyc07g052930	61324832–61326734	0.30
Myb like-4	Solyc07g053230	61699380–61700488	1.97
Myb like-4	Solyc07g053240	61710088–61711189	0.18
Myb like	Solyc07g053630	62062717–62066811	0.00
Myb transcription factor	Solyc07g054840	63019149–63020392	0.00
Myb-related transcription factor	Solyc07g054960	63121625–63123021	0.00
Myb-related transcription factor	Solyc07g054980	63133145–63137020	0.00
Myb like-4	Solyc07g055000	63145852–63147956	0.36
Glycosyltransferase	Solyc07g055930	63851843–63858435	38.33
Myb transcription factor	Solyc07g056120	63983586–63986633	5.06
Chalcone-flavonone isomerase	Solyc07g062030	64874570–64877582	6.41
Transcription factor bHLH126	Solyc07g062200	64999668–65002971	0.00
N17			
Chromosome 12			
M1			
4-Coumarate-CoA ligase	Solyc12g094520	64739117–64737891	26.05
M10			
UDP-glucosyltransferase family 1 protein	Solyc12g096080	65151226–65150412	0.00
N-hydroxycinnamoyl/benzoyltransferase 5	Solyc12g096250	65264285–65263439	0.06
Hydroxycinnamoyl CoA quinate transferase	Solyc12g096770	65547985–65549310	0.00
Hydroxycinnamoyl CoA quinate transferase	Solyc12g096790	65568543–65567197	0.00
Hydroxycinnamoyl CoA quinate transferase	Solyc12g096800	65570588–65569209	0.00
UDP-glucosyltransferase family 1 protein	Solyc12g096820	65586813–65587528	0.25
UDP-glucosyltransferase family 1 protein	Solyc12g096830	65589413–65590134	8.56
N-acetyltransferase	Solyc12g096840	65599970–65599549	0.00
UDP-glucosyltransferase 1	Solyc12g096870	65622881–65624341	0.10
Chalcone synthase	Solyc12g098090	65743943–65744925	0.00
UDP-glucosyltransferase family 1 protein	Solyc12g098580	66045023–66043754	1.02
UDP-glucosyltransferase family 1 protein	Solyc12g098590	66047542–66048121	0.00
UDP-glucosyltransferase family 1 protein	Solyc12g098600	66049474–66050865	0.00
bHLH	Solyc12g098620	66065713–66066266	5.95
WD-repeat protein-like	Solyc12g098690	66118366–66118781	36.47
Myb transcription factor	Solyc12g099120	66392195–66392661	0.15
Myb transcription factor	Solyc12g099130	66395992–66396421	0.38
Myb transcription factor	Solyc12g099140	66404232–66404530	0.56
M18			

For each Solyc the position on the chromosome is reported in bp. RPKM: expression values as those reported in the Tomato Functional Genomic Database.

CGs involved in the phenylpropanoid metabolism, that are one *4-coumarate:CoA ligase* (4CL), seven *UDP-glucosyltransferase*, three *hydroxycinnamoyl-CoA quinate transferase* (HCT), one *N-hydroxycinnamoyl/benzoyltransferase*, one *N-acetyltransferase*, and one *chalcone synthase*. Due to its reduced introgression region size, line DHO88-SL included wild alleles for 13 CGs,

the most consistent difference between DHO88 and DHO88-SL being the lack of the *4-coumarate:CoA ligase* wild allele in line DHO88SL. Interestingly, all the genes for the biosynthesis of flavonoids were located in the lower part of the introgressed region 12-4. In addition, several transcription factors (TFs), such as the TFs Myb, WD-40 and bHLH, were identified in

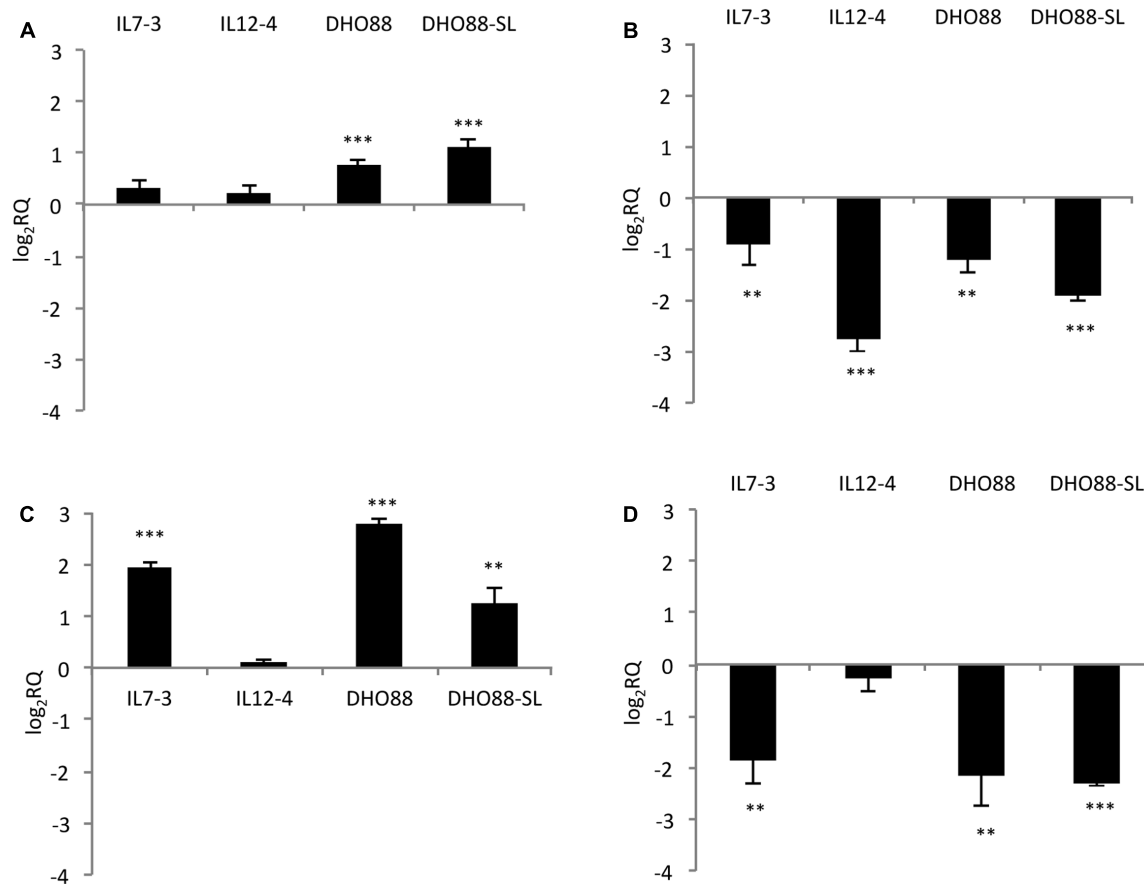


FIGURE 4 | Real-time qPCR analysis of expression of the CGs mapping in the introgressed region 7-3 in the fruit of IL7-3, IL12-4, DHO88, and DHO88-SL. The expression levels of (A) Solyc07g062030 (CHI); (B) Solyc07g055930 (UGT); (C) Solyc07g053230 (Myb 4-like); (D) Solyc07g056120 (Myb) are reported in comparison to those observed in M82. Asterisks indicate statistically significant differences of each genotype compared to M82 (** $p < 0.01$, *** $p < 0.001$).

both introgressed regions. Among the identified TFs, three Myb like-4 mapped in the introgressed region 7-3. Myb4 TFs are known to be able to negatively regulate the expression of several genes of the phenylpropanoids pathway such as *cinnamate 4-hydroxylase* and *dihydroflavonol 4-reductase* (Preston et al., 2004). Out of the 37 CGs and TFs identified in the introgressed regions 7-3 and 12-4, 28 genes are not expressed in tomato fruit, as reported in the Tomato Functional Genomics Database (Table 1). These genes were eliminated from subsequent analyses.

Expression Variability of Selected Candidate Genes

We studied the modulation in expression of nine selected CGs in ripe fruits of M82, ILs and pyramided lines DHO88 and DHO88-SL through real-time q-PCR. As for the introgressed region 7-3, we analyzed the expression of two selected genes involved in the biosynthetic pathways and of two genes coding for TFs (Figure 4). The gene coding for one chalcone isomerase (CHI – Solyc07g062030) demonstrated a higher expression only in the lines DHO88 and DHO88-SL compared to

M82. A drop in the expression of the gene coding for one UDP-glucosyltransferase (UGT- Solyc07g055930) was demonstrated in all the genotypes tested compared to M82. The expression of the gene coding for the TF Myb4-like Solyc07g053230 was higher in IL7-3 and in the two pyramided lines compared to M82. Finally, the gene coding for the Myb Solyc07g056120 showed a lower expression level in IL7-3 and in the two pyramided lines compared to M82.

As for genes mapping on the introgressed region 12-4 (Figure 5), the gene Solyc12g094520 coding for one 4-coumarate:CoA ligase and located in the upper part of the introgression region 12-4 displayed lower mRNA levels in ripe fruits of IL12-4 and DHO88 compared to M82. The expression of the gene Solyc12g096830 coding for one UDP-glucosyltransferase (UGT) did not change in the lines here tested (data not shown). A drop in expression of the gene Solyc12g098580 coding for another UDP-glucosyltransferase family 1 (UGT) protein and located in the lower part of the introgressed region 12-4 was instead recorded in IL12-4 and in both the pyramided lines. Interestingly, a down-regulation of the gene Solyc12g098620

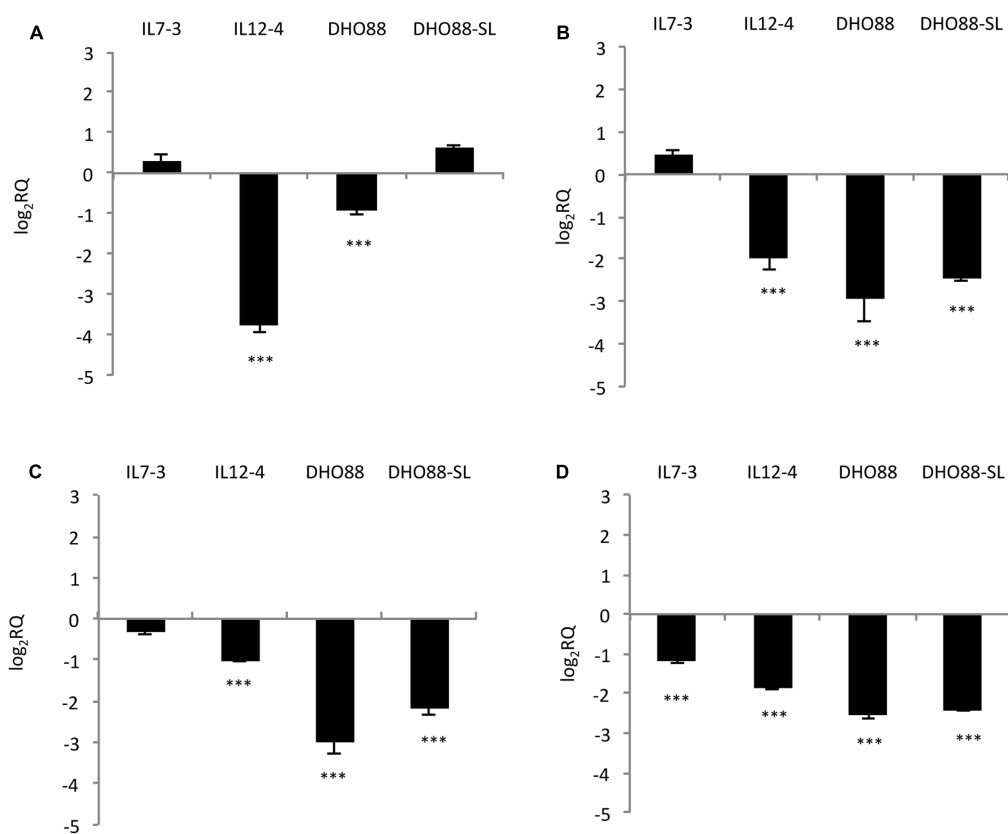


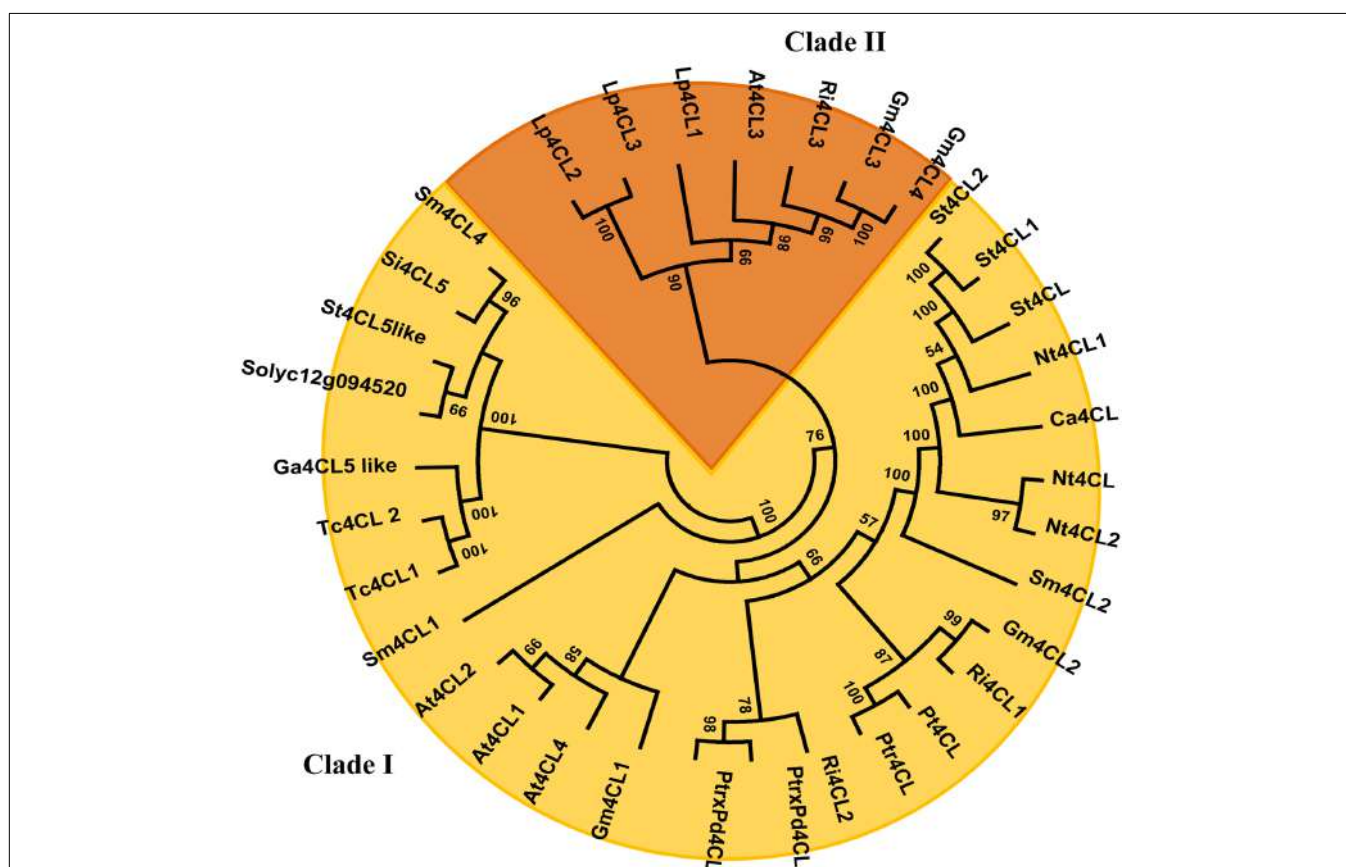
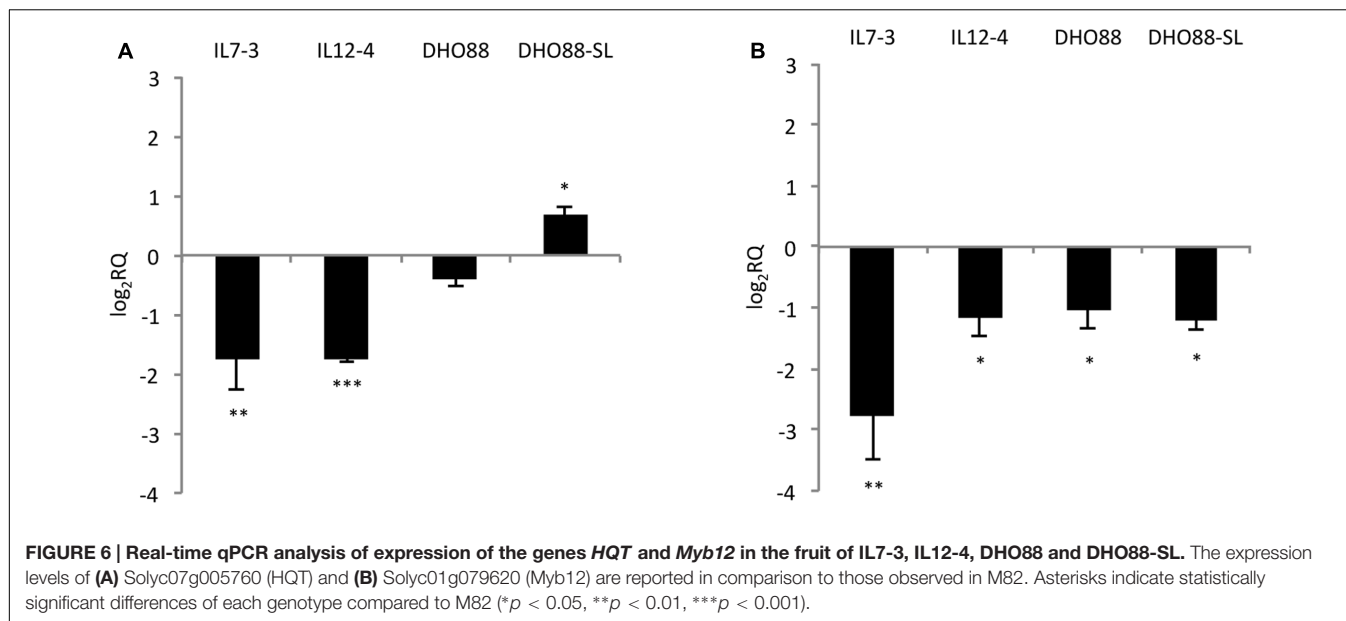
FIGURE 5 | Real-time qPCR analysis of expression of the CGs mapping in the introgressed region 12-4 in the fruit of IL7-3, IL12-4, DHO88, and DHO88-SL. The expression levels of (A) Solyc12g094520 (4CL); (B) Solyc12g098580 (UGT); (C) Solyc12g098620 (bHLH); (D) Solyc12g098690 (WD40) are reported in comparison to those observed in M82. Asterisks indicate statistically significant differences of each genotype compared to M82 (**p < 0.001).

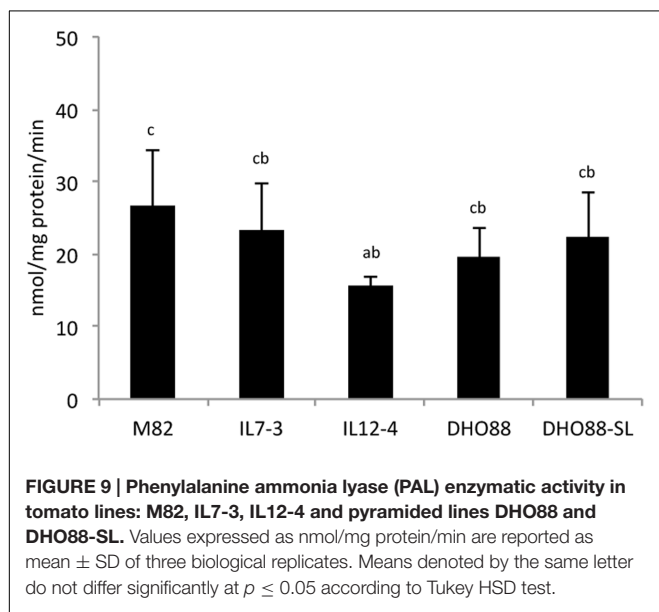
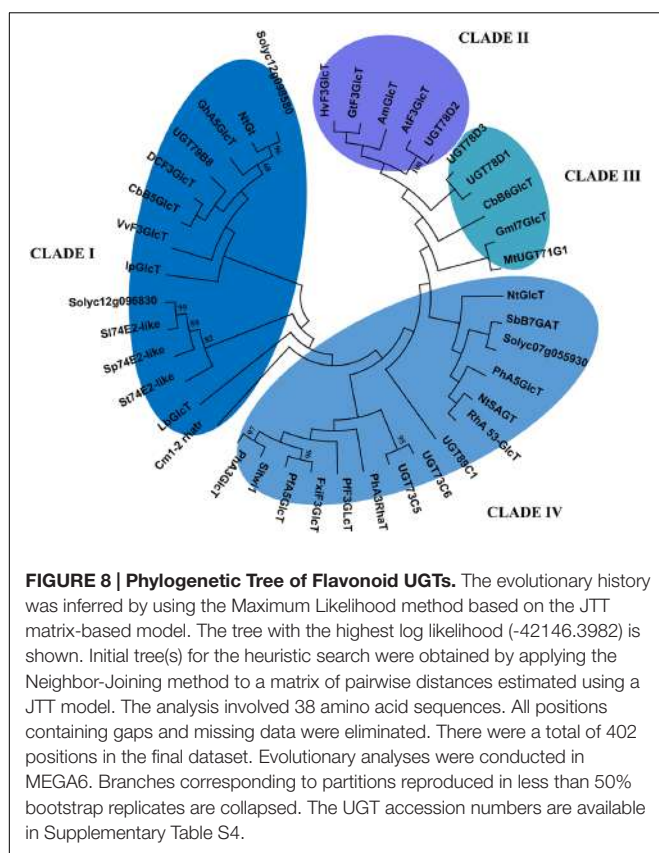
coding for one bHLH protein and of the gene Solyc12g098690 coding for one WD40 protein was recorded in IL12-4 and in both pyramided lines. A lower expression of the gene Solyc12g098690 was recorded also in the introgression line IL7-3. Interestingly, the genes coding for the TFs bHLH and WD40 were located next to the gene Solyc12g098580 coding for one UGT.

Additionally, we tested the expression of two genes located outside of the introgressed regions (Figure 6). We tested the expression levels of the genes *HQT* (*hydroxycinnamoyl-CoA quinate hydroxycinnamoyl transferase*) Solycg07g005760 that is the central gene for the production of chlorogenic acid in tomato fruit (Moglia et al., 2014). Indeed, this gene catalyzes the formation of chlorogenic acid from caffeoyl CoA and quinic acid (Niggeweg et al., 2004). We also analyzed the expression levels of the gene Solyc01g079620 coding for the Myb12, a TF that regulates the production of flavonones and in particular of naringenin chalcone in tomato fruit (Ballester et al., 2010). We demonstrated that the gene *HQT* was down-regulated in IL7-3 and in IL12-4. A slightly higher expression for this gene was detected in DHO88-SL compared to M82. A drop in the expression of the gene coding for Myb12 was instead detected in the red ripe fruit of all the genotypes here tested compared to M82.

Phylogenetic Analyses of Candidate Genes

Phylogenetic analyses were performed on the CGs 4CL and UGTs identified in the introgressed regions 12-4 and 7-3. Since 4CL converts 4-coumaric acid and other cinammic acids (such as caffeic and ferulic acids) into corresponding CoA thiolesters then used for the biosynthesis of flavonoids, lignins, isoflavonoids, suberins, coumarins and wall-bound phenolics (Sun et al., 2013), members of the 4CL family have overlapping yet distinct roles in phenylpropanoid metabolism. A phylogenetic analysis of the 4CL superfamily was carried out exploiting the amino acid sequences of 34 4CL available from different plant species and allowed to generate a Maximum Likelihood (ML) tree. As shown in Figure 7 class I and class II clades (Alberstein et al., 2012; Li et al., 2015) are distinctly defined, and Solyc12g094520 is closely linked to other 4CLs of class I, which have been previously associated with the biosynthesis of lignin and structurally related phenylpropanoid derivatives (Docimo et al., 2013). Instead, flavonoid biosynthesis has been mostly associated to Class II enzymes (Alberstein et al., 2012; Li et al., 2015). Therefore, albeit experimental studies are necessary for functional assignments, this preliminary analysis suggested that the tomato 4CL encoded by Solyc12g094520 could be mostly involved into channeling





hydroxicinnamic acids into lignin synthesis rather than in flavonoid formation.

It is also known that the transfer from nucleoside diphosphate-activated sugars to aglycon substrates is catalyzed by glycosyltransferase enzymes; however, the substrate specificity of these enzymes includes several class of molecules, such as flavonoids,

coumarins, terpenoids, and cyanohydrins (Shao et al., 2005). Therefore, since several UDP-glycosyltransferases mapped into the introgressed regions, we wanted to evaluate the relatedness of the identified tomato glycosyltransferases to other UGTs with different function. In order to predict a substrate specificity for the identified tomato UGT enzymes, a phylogenetic tree was constructed for Solyc07g055930, Solyc12g098580, and Solyc12g09683 along with other characterized UGTs from other plant families (Figure 8). The phylogenetic tree constructed on 39 UGT members highlighted the formation of four clusters. The two tomato glycosyltransferases from chromosome 12 clustered in the clade I, where mostly are grouped UGTs involved in the 3-O- and 5-O-glycosilation of flavonoids, whereas clusters II and III mostly include enzymes characterized by flavonoid 5-O-glycosyltransferase and flavonoid 7-O-glycosyltransferase activity, respectively (Shao et al., 2005). Cluster III also contains glycosyltransferases that are unrelated to flavonoid biosynthesis and Cluster IV contains GTs that catalyze glycosyl transfer to sugar moieties of flavonoid glycosides. In this latter Cluster, the Solyc07g055930 was located more closely related to SbB7GAT an UGT involved in 7-O-glucuronosylation of baicalein in *Scutellaria baicalensis* and to PhA5GlcT, which is responsible for 5-O-glycosilation of anthocyanin in *Petunia hybrida*.

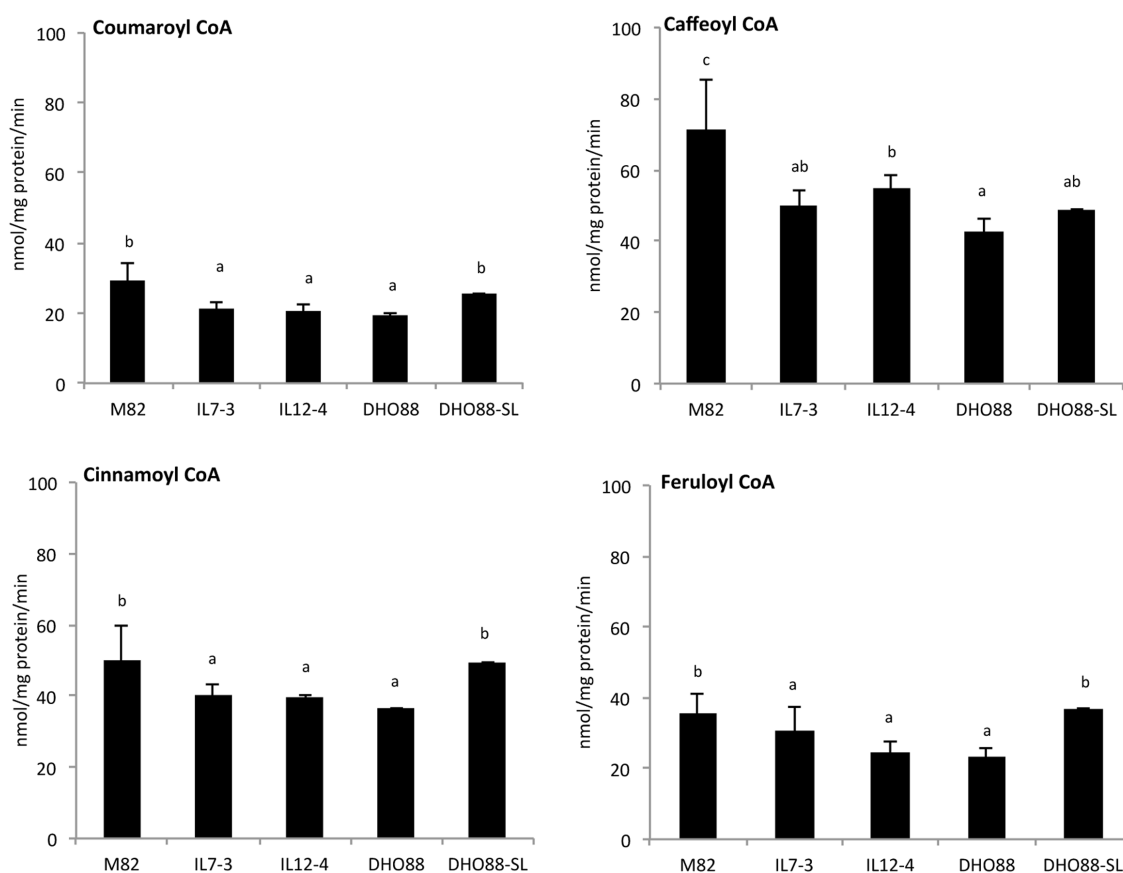
Enzyme Activity in Pyramided Lines

Finally, we investigated the early steps of phenylpropanoid biosynthesis by measuring the enzymatic activities of PAL and 4CL enzymes in red ripe fruits of the tomato lines here analyzed. These analyses were performed in order to understand whether M82, the ILs and the pyramided lines showed a different ability to produce CoA activated molecules. We demonstrated that PAL activity was similar in M82, in IL7-3 and in the pyramided lines (Figure 9), whereas in the line IL12-4 the amount of cinnamoylCoA recorded was significantly lower than in M82.

In addition, we assayed 4CL enzyme activity using four substrates: coumaric acid, ferulic acid, cinnamic acid, and caffeic acid (Figure 10). Overall, highest 4CL enzyme activity was found toward caffeic and ferulic acids, whereas a lower activity was detected for cinnamic and coumaric acids. Interestingly, for all the substrates, the 4CL enzyme activity recorded in IL7-3, IL12-4 and DHO88 was lower than the activity recorded in M82. On the contrary, the 4CL activity toward coumaric acid, ferulic acid, cinnamic acid was similar in M82 and in DHO88-SL. Only the 4CL activity toward caffeic acid was lower in DHO88-SL compared to M82.

DISCUSSION

Wild species are important sources of novel alleles for improving quality traits, such as antioxidant content, that could be introgressed into modern varieties by using traditional and innovative breeding approaches (Gur and Zamir, 2004, 2015; Schauer et al., 2006). In this regard, the production of ILs from wild species can help to facilitate the mapping of valuable traits originating from wild donors and to introduce unused alleles



that were neglected during domestication (Gur and Zamir, 2015). Here, detailed analyses of metabolites accumulated in the fruit of two introgression lines (IL7-3 and IL12-4), of two pyramided lines obtained by crossing the two ILs (DHO88 and DHO88-SL) and of the cultivated line M82 were carried out. Metabolic analyses evidenced a lower content of flavonoids (naringenin glucoside and chalconaringenin) and phenolic acids (such as chlorogenic acid) in the red ripe fruits of both the introgression lines IL12-4 and IL7-3 compared to the control M82.

In the introgression lines IL7-3 the lower levels of phenylpropanoids detected were apparently caused by the down-regulation of one flavonoid biosynthetic gene, the *UGT* Solyc07g055930, and to the altered expression level of positive and negative regulators detected in the introgressed region 7-3. In particular, the lower expression of the Myb Solyc07g056120, putatively involved in the activation of the phenylpropanoid biosynthetic pathways, together with the higher expression of the Myb4-like Solyc07g053230, might have caused in the introgression line IL7-3 a block of the metabolic flux at the branch point represented by the 4-coumarate:CoA ligase. Several *Myb4-like* genes have been previously described as negative regulators of hydroxycinnamic acid biosynthesis in a group of

plant species, directly repressing genes such as *cinnamate-4-hydrolase* and *4-coumarate:CoA ligase* (Perez-Diaz et al., 2016). Accordingly, in IL7-3 we detected a lower 4CL enzyme activity and a PAL activity that was comparable to that detected in M82. Moreover, in IL7-3 real time PCR demonstrated a lower expression of the gene *HQT*, a key gene for the biosynthesis of chlorogenic acid (Moglia et al., 2014), and of the TF Myb12, a TF that regulates the production of naringenin chalcone in the fruit (Ballester et al., 2010). These results further suggest a reduction in this IL of the flux through the hydroxycinnamate and flavonoid biosynthetic pathways. Moreover, the different expression levels observed for the *HQT* gene suggest the presence of regulatory proteins present in the introgression region that may control, directly or indirectly, the transcription of the *HQT* gene.

A lower level of phenolic acids and flavonoids was also detected in IL12-4 compared to the cultivated line M82. These results correlated well with the lower PAL and 4CL enzyme activity measured in this line compared to the cultivated line. These analyses indicate that in the introgression line IL12-4 a lower amount of precursors was available for chlorogenic acid, phenolic acids conjugated and flavonoids formation compared to M82. Accordingly, a lower expression level of the *HQT* gene and

of the TF Myb12 was detected in IL12-4. Our hypothesis is that in the IL12-4 this altered metabolic flux was caused primarily by the down-regulation of one gene of the general phenylpropanoid pathway, the *4CL* gene identified in the upper part of the region 12-4. Additionally, the reduced flavonoid biosynthesis in IL12-4 may be caused by the down-regulation of the wild gene Solyc12g098580 coding for one UDP-glycosyltransferase and located in the lower part of the introgressed region 12-4. Phylogenetic analysis indicated that the protein encoded by this gene is closely related to GhA5GlcT and St74E2-like, and therefore possibly involved in 5-and 3-O glycosylation of flavonoids. In the fruits of several plant species (peach, apple, and grape), UDP-glucosyltransferase gene transcription is controlled by the involvement of different TFs, such as regulatory complexes composed by Myb, bHLH, and WD40 (Ravaglia et al., 2013). Two TFs, bHLH and WD40 (encoded by Solyc12g098620 and Solyc12g098690, respectively), putatively involved in regulating genes of the flavonoid pathway and located next to the gene Solyc12g098580 coding for the UDP-glucosyltransferase, were identified in the introgressed region 12-4. Interestingly, our transcriptional analyses demonstrated that these TFs were both down-regulated in IL12-4 and in both DHOs.

Considering the genetic background of IL7-3 and IL12-4, the pyramided lines DHO88 and DHO88-SL showed a peculiar accumulation of metabolites in their fruits. Indeed, in both the DHOs the content of phenolic acids increased, particularly the fraction of hexoses. In addition, a contrasting behavior was observed between the two different DHO genotypes here analyzed when the amount of free phenolic acids (such as chlorogenic acid) was considered. In particular, the line DHO88 exhibited a lower content of this fraction compared to M82, whereas the line DHO88-SL showed an accumulation level comparable to M82. These results are justified by the different size of the wild region carried on chromosome 12 in the two DHOs.

In the line DHO88, carrying the entire introgressions 7-3 and 12-4, we speculated that the lower levels of chlorogenic acid and flavonoids detected were primarily caused by the down-regulation of the wild *4CL* gene identified in IL12-4 and of the *UGTs* detected in both ILs. The lower amount of phenylpropanoids detected in this line was likely also due to the influence of regulatory protein coded by genes present in both the introgressed regions. Surprisingly, in DHO88, which carries the wild *4CL*, we could not detect any differences in the expression levels of the *HQT* gene compared to M82 and the PAL enzyme activity was not altered. However, a lower expression level of the TF Myb12 was demonstrated and a lower 4CL enzyme activity was also recorded in this line toward all the substrates tested. The phylogenetic study carried out indicated that the 4CL isoform encoded by the Solyc12g094520 could be mostly involved into channeling hydroxycinnamic derivatives for lignin formation (Alberstein et al., 2012; Sun et al., 2013). Indeed, the 4CL isoform here identified clustered with type I 4CLs, as well as the 4CL identified in *Salvia miltiorrhiza* (Sm4CL4, accession number AGW27194), which are reported to be involved in lignin biosynthesis (Alberstein et al., 2012; Sun et al., 2013).

Therefore, the higher levels of phenolic acid hexose detected in DHO88 could indicate that the pool of precursors left unused by the flavonoid biosynthetic pathway and also by the lignin biosynthetic pathway had been reallocated to the synthesis of other phenolic compounds. Indeed, recent work carried out in *Arabidopsis thaliana* and in tomato demonstrated that, if downstream branches of the phenylpropanoid pathway are less active, this could lead to the reorientation of the carbon flux with a consequent accumulation of various classes of hexosylated phenylpropanoids (van der Rest et al., 2006; Vanholme et al., 2012).

In the line DHO88-SL, carrying the entire introgression 7-3 and the lower part of the introgression region 12-4, a reduced content of flavonoids (rutin, naringenin glucoside, and chalconaringenin) was also found compared to M82. The lower expression level of the *UGTs* Solyc12g098580 and Solyc07g055930, together with the additional influence of regulatory proteins present in both the introgressed regions 7-3 and 12-4, might reduce the levels of flavonoids detected. As expected, the expression of the TFs Myb12 was lower in DHO88-SL compared to M82. Interestingly, the level of phenolic acids hexoses was higher in DHO88-SL compared to the parental lines IL7-3 and IL12-4 and also to the pyramided line DHO88. In addition a higher level of chlorogenic acid compared to the parental lines and to the pyramided line DHO88 was demonstrated. These results correlated well with the results obtained with the biochemical analyses that demonstrated that the 4CL activity toward coumaric acid, ferulic acid and cinnamic acid was similar in DHO88-SL compared to M82 and was higher compared to the parental lines and to DHO88. Accordingly, real-time PCR analyses demonstrated that the expression level of the gene *HQT* was slightly higher in DHO88-SL compared to M82. Therefore we concluded that in the pyramided line DHO88-SL, that carries the cultivated allele for *4CL* in the homozygous state, a major accumulation of cinnamic acid intermediates remained available for hexose conjugation but also for chlorogenic acid formation, thus indicating the presence of an enzymatic machinery correctly working (van der Rest et al., 2006; Vanholme et al., 2012). This result confirmed the central role of the *4CL* gene identified in IL12-4 in the redirection of the phenylpropanoid biosynthetic pathways in the pyramided lines DHO88 and DHO88-SL.

Hydroxycinnamates that accumulated in high amount in the lines here described have several beneficial health activity including very potent antioxidant activity and hepatoprotective, hypoglycaemic and antiviral activities (Tohge et al., 2015). Consequently, there is an increasing interest in the production of alternative dietary sources that are rich in these phenolic compounds (Tohge et al., 2015). Results obtained in this study suggest that pathway rerouting may be a valid strategy in order to produce tomatoes with a higher amount of hydroxycinnamic acids in the fruit. Altogether, results obtained in this work highlighted that, in order to design an efficient pyramiding strategy for increasing tomato nutritional quality, detailed information on the possible interaction effects between QTLs are necessary.

CONCLUSION

Here, we integrated genomic, transcriptomic and biochemical analyses to identify CGs controlling phenylpropanoid accumulation in the fruits of pyramided lines obtained by crossing two *S. pennellii* introgression lines (IL12-4 and IL7-3). One pyramided genotype (DHO88-SL) was demonstrated to contain a higher amount of phenolic acids and phenolic acids hexose in the fruits compared to the parental lines. This increase was due to changes in the formation and/or availability of compounds in the different branches of the phenylpropanoid biosynthetic pathway caused by the combined effects of the two introgressed regions 12-4 and 7-3. In fact, a repression of flavonoid synthesis in the pyramided line DHO88-SL was accompanied by an increased synthesis of products from other branches of the phenylpropanoid pathway such as caffeic acid hexose. Moreover, analyses carried out in this paper highlighted the central role of one 4-coumarate:CoA ligase identified in the region 12-4, in the perturbation of the phenylpropanoid biosynthetic pathways in the pyramided lines DHO88 and DHO88-SL. Now, experiments involving reverse genetic approaches are underway in order to unveil the functional role of the CGs here detected to better define their role in tomato fruits.

REFERENCES

- Alberstein, M., Eisenstein, M., and Abeliovich, H. (2012). Removing allosteric feedback inhibition of tomato 4-coumarate:CoA ligase by direct evolution. *Plant J.* 69, 57–69. doi: 10.1111/j.1365-313X.2011.04770.x
- Ballester, A., Molthoff, J., de Vos, R., te Lintel Hekkert, B., Orzaez, D., Fernandez-Moreno, J., et al. (2010). Biochemical and molecular analysis of pink tomatoes: deregulated expression of the genes encoding transcription factor SLMYB12 leads to pink tomato fruit color. *Plant Physiol.* 152, 71–84. doi: 10.1104/pp.109.147322
- Bolger, A., Scossa, F., Bolger, M. E., Lanz, C., Maumus, F., Tohge, T., et al. (2014). The genome of the stress-tolerant wild tomato species *Solanum pennellii*. *Nat. Genet.* 46, 1034–1038. doi: 10.1038/ng.3046
- Bradford, M. M. (1976). A rapid and sensitive method for the quantitation of microgram quantities of protein utilizing the principle of protein dye binding. *Anal. Biochem.* 72, 248–254. doi: 10.1016/0003-2697(76)90527-3
- Calafiori, R., Ruggieri, V., Raiola, A., Rigano, M. M., Sacco, A., Hassan, M. I., et al. (2016). Exploiting genomics resources to identify candidate genes underlying antioxidants content in tomato fruits. *Front. Plant Sci.* 7:397. doi: 10.3389/fpls.2016.00397
- Calvenzani, V., Castagna, A., Ranieri, A., Tonelli, C., and Petroni, K. (2015). Hydroxycinnamic acids and UV-B depletion: profiling and biosynthetic gene expression in flesh and peel of wild-type and hp-1. *J. Plant Physiol.* 181, 75–82. doi: 10.1016/j.jplph.2015.04.008
- Chen, J.-Y., Wen, P.-F., Kong, W.-F., Pan, Q.-H., Wan, S.-B., and Huang, W.-D. (2006). Changes and subcellular localizations of the enzymes involved in phenylpropanoid metabolism during grape berry development. *J. Plant Physiol.* 163, 115–127. doi: 10.1016/j.jplph.2005.07.006
- Choi, S. H., Kim, H. R., Kim, H. J., Lee, I. S., Kozukue, N., Levin, C. E., et al. (2011). Free amino acid and phenolic contents and antioxidative and cancer cell-inhibiting activities of extracts of 11 greenhouse-grown tomato varieties and 13 tomato-based foods. *J. Agric. Food Chem.* 59, 12801–12814. doi: 10.1021/jf100162j
- Docimo, T., Consonni, R., Coraggio, I., and Mattana, M. (2013). Early phenylpropanoid biosynthetic steps in *Cannabis sativa*: link between genes and metabolites. *Int. J. Mol. Sci.* 14, 13626–13644. doi: 10.3390/ijms140713626
- Eshed, Y., and Zamir, D. (1995). An introgression line population of *Lycopersicon pennellii* in the cultivated tomato enables the identification and fine mapping of yield-associated QTL. *Genetics* 141, 1147–1162.
- González, R., Ballester, I., López-Pozadas, R., Suárez, M. D., Zarzuelo, A., Martínez-Augustin, O., et al. (2011). Effects of flavonoids and other polyphenols on inflammation. *Crit. Rev. Food Sci. Nutr.* 51, 331–362. doi: 10.1080/10408390903584094
- Gur, A., and Zamir, D. (2004). Unused natural variation can lift yield barriers in plant breeding. *PLoS Biol.* 2:e245. doi: 10.1371/journal.pbio.0020245
- Gur, A., and Zamir, D. (2015). Mendelizing all components of a pyramid of three yield QTL in tomato. *Front. Plant Sci.* 6:1096. doi: 10.3389/fpls.2015.01096
- Kauss, T., Moynet, D., and Rambert, J. (2008). Rutoside decreases human macrophage-derived inflammatory mediators and improves clinical signs in adjuvant-induced arthritis. *Arthritis Res. Ther.* 10:R19. doi: 10.1186/ar2372
- Lee, D., Meyer, K., Chapple, C., and Douglas, C. J. (1997). Antisense suppression of 4-coumarate:coenzyme A ligase activity in *Arabidopsis* leads to altered lignin subunit composition. *Plant Cell* 9, 1985–1998. doi: 10.1105/tpc.9.11.1985
- Li, Y., Kim, J. I., Pysh, L., and Chapple, C. (2015). Four Isoforms of *Arabidopsis* 4-coumarate:CoA ligase have overlapping yet distinct roles in phenylpropanoid metabolism. *Plant Physiol.* 169, 2409–2421. doi: 10.1104/pp.15.00838
- Livak, K. J., and Schmittgen, T. D. (2001). Analysis of relative gene expression data using real-time quantitative PCR and the 2 $^{-\Delta\Delta CT}$ method. *Methods* 25, 402–408. doi: 10.1006/meth.2001.1262
- Lodovici, M., Guglielmi, F., Meoni, M., and Dolara, P. (2001). Effect of natural phenolic acids on DNA oxidation in vitro. *Food Chem. Toxicol.* 39, 1205–1210. doi: 10.1016/S0278-6915(01)00067-9
- Marinova, D., Ribarova, F., and Atanassova, M. (2005). Total phenolics and total flavonoids in bulgarian fruits and vegetables. *J. Univ. Chem. Technol. Metall.* 40, 255–260.
- Moco, S., Bino, R. J., Vorst, O., Verhoeven, H. A., de Groot, J., van Beek, T. A., et al. (2006). A liquid chromatography-mass spectrometry-based metabolome database for tomato. *Plant Physiol.* 141, 1205–1218. doi: 10.1104/pp.106.078428
- Moco, S., Capanoglu, E., Tikunov, Y., Bino, R. J., Boyacioglu, D., Hall, R. D., et al. (2007). Tissue specialization at the metabolite level is perceived during the development of tomato fruit. *J. Exp. Bot.* 58, 4131–4146. doi: 10.1093/jxb/erm271

AUTHOR CONTRIBUTIONS

MR, AR, TD, VR contributed to metabolic, biochemical and transcriptomic analyses, to the experimental analyses carried out to identify CGs, and to draft the manuscript; RC contributed to molecular marker analysis and to grow materials; PV and RF contributed to metabolic analysis and critically revised the manuscript; LF contributed to the conception of the experiment and critically revised the manuscript; AB contributed to the experiment design, to data analysis and interpretation, to draft the manuscript.

FUNDING

This research was supported by the Italian Ministry of University and Research (MIUR; grant MIUR-PON02-GenoPOMpro).

SUPPLEMENTARY MATERIAL

The Supplementary Material for this article can be found online at: <http://journal.frontiersin.org/article/10.3389/fpls.2016.01484>

- Moglia, A., Lanteri, S., Comino, C., Hill, L., Knevitt, D., Caglier, C., et al. (2014). Dual catalytic activity of hydroxycinnamoyl-Coenzyme A quinate transferase from tomato allows it to moonlight in the synthesis of both mono- and dicaffeoylquinic acids. *Plant Physiol.* 166, 1777–1787. doi: 10.1104/pp.114.251371
- Niggeweg, R., Michael, A. J., and Martin, C. (2004). Engineering plants with increased levels of the antioxidant chlorogenic acid. *Nat. Biotechnol.* 22, 746–754. doi: 10.1038/nbt966
- Pandey, A., Misra, P., Choudhary, D., Yadav, R., Goel, R., Bhambhani, S., et al. (2015). AtMYB12 expression in tomato leads to large scale differential modulation in transcriptome and flavonoid content in leaf and fruit tissues. *Sci. Rep.* 5:12412. doi: 10.1038/srep12412
- Perez-Diaz, J. R., Perez-Diaz, J. P., Madrid-Espenoza, J., Gonzalez-Villanueva, E., Moreno, Y., and Ruiz-Lara, S. (2016). New member of the R2R3-Myb transcription factors family in grapevine suppresses the anthocyanin accumulation in the flowers of transgenic tobacco. *Plant Mol. Biol.* 90, 63–76. doi: 10.1007/s11103-015-0394-y
- Perez-Fons, L., Wells, T., Corol, D. I., Ward, J. L., Gerrish, C., Beale, M. H., et al. (2014). A genome-wide metabolomics resource for tomato fruit from *Solanum pennellii*. *Sci. Rep.* 4:3859. doi: 10.1038/srep03859
- Preston, J., Wheeler, J., Haezelwood, J., Feng Li, S., and Parish, R. W. (2004). AtMYB32 is required for normal pollen development in *Arabidopsis thaliana*. *Plant J.* 40, 979–995. doi: 10.1111/j.1365-313X.2004.02280.x
- Raiola, A., Rigano, M. M., Calafio, R., Frusciante, L., and Barone, A. (2014). Enhancing the health-promoting effects of tomato fruit for biofortified food. *Mediators Inflamm.* 2014:139873. doi: 10.1155/2014/139873
- Ravaglia, D., Esplay, R. V., Henry, R. A., Andreotti, C., Ziosi, V., Hellens, R. P., et al. (2013). Transcriptional regulation of flavonoid biosynthesis in nectarine (*Prunus persica*) by a set of R2R3 Myb transcription factors. *BMC Plant Biol.* 13:68. doi: 10.1186/1471-2229-13-68
- Rigano, M. M., Raiola, A., Tenore, G. C., Monti, D. M., Del Giudice, R., Frusciante, L., et al. (2014). Quantitative trait loci pyramiding can improve the nutritional potential of tomato (*Solanum lycopersicum*) fruits. *J. Agric. Food Chem.* 62, 11519–11527. doi: 10.1021/jf502573n
- Rousseaux, M. C., Jones, C. M., Adams, D., Chetelat, R., Bennett, A., and Powell, A. (2005). QTL analysis of fruit antioxidants in tomato using *Lycopersicon pennellii* introgression lines. *Theor. Appl. Genet.* 111, 1396–1408. doi: 10.1007/s00122-005-0071-7
- Ruggieri, V., Sacco, A., Calafio, R., Frusciante, L., and Barone, A. (2015). Dissecting a QTL into candidate genes highlighted the key role of pectinesterases in regulating the ascorbic acid content in tomato fruit. *Plant Genome* 8, 1–10. doi: 10.3835/plantgenome2014.08.0038
- Sacco, A., Di Matteo, A., Lombardi, N., Trotta, N., Punzo, B., Mari, A., et al. (2013). Quantitative trait loci pyramiding for fruit quality traits in tomato. *Mol. Breed.* 31, 217–222. doi: 10.1007/s11032-012-9763-2
- Saunders, J. A., and McClure, J. W. (1975). Phytochrome controlled phenylalanine ammonia lyase activity in *Hordeum vulgare* plastids. *Phytochemistry* 14, 1285–1289. doi: 10.1016/S0031-9422(00)98612-6
- Schauer, N., Semel, Y., Roessner, U., Gur, A., Balbo, I., Carrari, F., et al. (2006). Comprehensive metabolic profiling and phenotyping of interspecific introgression lines for tomato improvement. *Nat. Biotechnol.* 24, 447–454. doi: 10.138/nbt1192
- Schmittgen, T. D., Jiang, J., Liu, Q., and Yang, L. (2004). A high-throughput method to monitor the expression of microRNA precursors. *Nucleic Acids Res.* 32, 43. doi: 10.1093/nar/gnh040
- Shao, H., He, X., Blount, J. W., Dixon, R. A., and Wang, X. (2005). Crystal structures of a multifunctional triterpene/flavonoid glycosyltransferase from *Medicago truncatula*. *Plant Cell* 17, 3141–3154. doi: 10.1105/tpc.105.035055
- Sun, H., Li, Y., Feng, S., Zou, W., Guo, K., Fan, C., et al. (2013). Analysis of five rice 4-coumarate:coenzyme ligase enzyme activity and stress response for potential roles in lignin and flavonoid biosynthesis in rice. *Biochem. Biophys. Res. Commun.* 430, 1151–1156. doi: 10.1016/j.bbrc.2012.12.019
- Tamura, K., Stecher, G., Peterson, D., Filipski, A., and Kumar, S. (2013). MEGA6: molecular evolutionary genetics analysis version 6.0. *Mol. Biol. Evol.* 30, 2725–2729. doi: 10.1093/molbev/mst197
- Tohge, T., Zhang, Y., Peterek, S., Matros, A., Rallapalli, G., Tandron, Y. A., et al. (2015). Ectopic expression of snapdragon transcription factors facilitates the identification of genes encoding enzymes of anthocyanin decoration in tomato. *Plant J.* 83, 686–704. doi: 10.1111/tpj.12920
- Vallverdú-Queralt, A., Jáuregui, O., Di Lecce, G., Andrés-Lacueva, C., and Lamuela-Raventós, R. M. (2011). Screening of the polyphenol content of tomato-based products through accurate-mass spectrometry (HPLC-ESI-QTOF). *Food Chem.* 129, 877–883. doi: 10.1016/j.foodchem.2011.05.038
- van der Rest, B., Danoun, S., Bouhet, A., and Rochange, S. F. (2006). Down-regulation of cinnamoyl-CoA reductase in tomato (*Solanum lycopersicum* L.) induces dramatic changes in soluble phenolic pools. *J. Exp. Bot.* 57, 1399–1411. doi: 10.1093/jxb/erj120
- Vanholme, R., Storme, V., Vanholme, B., Sundin, L., Christensen, J. H., Goeminne, G., et al. (2012). A system biology view of responses to lignin biosynthesis perturbations in *Arabidopsis*. *Plant Cell* 24, 3506–3529. doi: 10.1105/tpc.112.102574
- Visioli, F., De La Lastra, C. A., Andres-Lacueva, C., Aviram, M., Calhau, C., Cassano, A., et al. (2011). Polyphenols and human health: a prospectus. *Crit. Rev. Food Sci. Nutr.* 51, 524–546. doi: 10.1080/10408391003698677
- Vogt, T. (2010). Phenylpropanoid biosynthesis. *Mol. Plant* 3, 2–20. doi: 10.1093/mp/ssp106
- Weitzel, C., and Petersen, M. (2010). Enzyme of phenylpropanoid metabolism in the important medicinal plant *Melissa officinalis* L. *Planta* 232, 731–742. doi: 10.1007/s00425-010-1206-x
- Winer, J., Jung, C. K., Shackel, I., and Williams, P. M. (1999). Development and validation of real-time quantitative reverse transcriptase-polymerase chain reaction for monitoring gene expression in cardiac myocytes in vitro. *Anal. Biochem.* 270, 41–49. doi: 10.1006/abio.1999.4085

Conflict of Interest Statement: The authors declare that the research was conducted in the absence of any commercial or financial relationships that could be construed as a potential conflict of interest.

Copyright © 2016 Rigano, Raiola, Docimo, Ruggieri, Calafio, Vitaglione, Ferracane, Frusciante and Barone. This is an open-access article distributed under the terms of the Creative Commons Attribution License (CC BY). The use, distribution or reproduction in other forums is permitted, provided the original author(s) or licensor are credited and that the original publication in this journal is cited, in accordance with accepted academic practice. No use, distribution or reproduction is permitted which does not comply with these terms.



Exploiting Genomics Resources to Identify Candidate Genes Underlying Antioxidants Content in Tomato Fruit

Roberta Calafiore^{1†}, Valentino Ruggieri^{1†}, Assunta Raiola¹, Maria M. Rigano¹, Adriana Sacco¹, Mohamed I. Hassan², Luigi Frusciante¹ and Amalia Barone^{1*}

¹ Department of Agricultural Sciences, University of Naples Federico II, Portici, Italy, ² Department of Genetics, Faculty of Agriculture, Assiut University, Assiut, Egypt

OPEN ACCESS

Edited by:

Antonio Granell,
Consejo Superior de Investigaciones
Científicas, Spain

Reviewed by:

Angelos K. Kanellis,
Aristotle University of Thessaloniki,
Greece
Lorenzo Zacarias,
Consejo Superior de Investigaciones
Científicas, Spain

*Correspondence:

Amalia Barone
ambarone@unina.it

[†]These authors have contributed
equally this work.

Specialty section:

This article was submitted to
Plant Physiology,
a section of the journal
Frontiers in Plant Science

Received: 14 January 2016

Accepted: 14 March 2016

Published: 08 April 2016

Citation:

Calafiore R, Ruggieri V, Raiola A, Rigano MM, Sacco A, Hassan MI, Frusciante L and Barone A (2016) Exploiting Genomics Resources to Identify Candidate Genes Underlying Antioxidants Content in Tomato Fruit.

Front. Plant Sci. 7:397.

doi: 10.3389/fpls.2016.00397

The tomato is a model species for fleshy fruit development and ripening, as well as for genomics studies of others Solanaceae. Many genetic and genomics resources, including databases for sequencing, transcriptomics and metabolomics data, have been developed and are today available. The purpose of the present work was to uncover new genes and/or alleles that determine ascorbic acid and carotenoids accumulation, by exploiting one *Solanum pennellii* introgression lines (IL7-3) harboring quantitative trait loci (QTL) that increase the content of these metabolites in the fruit. The higher ascorbic acid and carotenoids content in IL7-3 was confirmed at three fruit developmental stages. The tomato genome reference sequence and the recently released *S. pennellii* genome sequence were investigated to identify candidate genes (CGs) that might control ascorbic acid and carotenoids accumulation. First of all, a refinement of the wild region borders in the IL7-3 was achieved by analyzing CAPS markers designed in our laboratory. Afterward, six CGs associated to ascorbic acid and one with carotenoids metabolism were identified exploring the annotation and the Gene Ontology terms of genes included in the region. Variants between the sequence of the wild and the cultivated alleles of these genes were investigated for their functional relevance and their potential effects on the protein sequences were predicted. Transcriptional levels of CGs in the introgression region were extracted from RNA-Seq data available for the entire *S. pennellii* introgression lines collection and verified by Real-Time qPCR. Finally, seven IL7-3 sub-lines were genotyped using 28 species-specific markers and then were evaluated for metabolites content. These analyses evidenced a significant decrease in transcript abundance for one 9-cis-epoxycarotenoid dioxygenase and one *L*-ascorbate oxidase homolog, whose role in the accumulation of carotenoids and ascorbic acid is discussed. Comprehensively, the reported results demonstrated that combining genetic and genomic resources in tomato, including bioinformatics tools, was a successful strategy to dissect one QTL for the increase of ascorbic acid and carotenoids in tomato fruit.

Keywords: ascorbic acid, total carotenoids, *Solanum pennellii*, wild alleles, introgression sub-lines, *L*-ascorbate oxidase, 9-cis-epoxycarotenoid dioxygenase

INTRODUCTION

In recent years increasing attention has been given to the nutritional properties of plant antioxidant compounds, since their consumption has demonstrated to be associated with a reduced risk of cancer, inflammation and cardiovascular diseases. A great contribute to these health effects is attributed to secondary metabolites, including ascorbic acid (AsA, vitamin C) and carotenoids (precursors of Vitamin A) (Canene-Adams et al., 2005; Raiola et al., 2014). Besides their critical role in human nutrition, these compounds have major roles in several plant biological processes, such as photoreception and photoprotection, hormone signaling, cell cycle, cell expansion, plant development, responses to biotic and abiotic stresses. The biosynthetic pathway of carotenoids has been extensively studied and most metabolic key-steps that control their accumulation in plants has been identified (Giuliano, 2014). Plants produce AsA through several biosynthetic pathways, including the D-mannose-L-galactose as the main pathway, even though the role of the L-gulose, the D-galacturonate, and the *myo*-inositol pathways has also been suggested (Valpuesta and Botella, 2004); in addition the recycling pathway can contribute to the regulation of AsA accumulation (Chen et al., 2003). Finally, since AsA doesn't diffuse through lipid bilayers because of its negatively charged form at physiological pH values, a class of transporters (Nucleobase Ascorbate Transporter, NAT) may be involved in the mechanisms of AsA accumulation (Badejo et al., 2012; Cai et al., 2014). The level of antioxidants in plants is highly influenced by environmental conditions, and this can explain why in recent years many scientific efforts were focused on better understanding the genetic architecture of this complex trait in various plant species (Davey et al., 2006; Stevens et al., 2007; Hayashi et al., 2012; Fantini et al., 2013; Kandianis et al., 2013; Lisko et al., 2014). Indeed, even though the biosynthesis of carotenoids and AsA in plants is well characterized, their gene regulation and their accumulation in fruits still remain elusive.

Humans are unable to synthesize AsA and carotenoids, and their dietary intake mainly derives from fruit and vegetables. Among these, tomato is the second most consumed vegetable in the world, thus being one of main sources of antioxidants. Indeed, tomato consumption reaches 40–45 kg *pro capita* per year in countries such as Spain, Italy, or USA (source: FAO databases); used as fresh product or processed (paste, juice, sauce and powder), its antioxidant content may protect against cancer, inflammation and cardiovascular diseases (Canene-Adams et al., 2005; Friedman, 2013).

Tomato is also a reference species for genetic and genomic studies in the Solanaceae family, due to its diploid genome with relative small size (950 Mbp), its short generation time, efficient transformation technologies, high synteny with various Solanaceae and numerous genetic and genomics resources already available (Mueller et al., 2005; Barone et al., 2008). Information data on gene function, genetic diversity and evolution in tomato and in other Solanaceae species are available since the year 2012 when the tomato genome was completely sequenced (Tomato Genome Consortium, 2012). Since then, high-throughput datasets and bioinformatics

platforms extremely useful for the Solanaceae plant research community were newly generated or implemented. The Sol Genomics Network¹ is a clade-oriented database for the Solanaceae family and its close relatives, which hosts genotypic and phenotypic data and analysis tools. The tomato genome resources database (TGRD²) is a resource that allows investigations on genes, quantitative trait loci (QTL), miRNA, transcription factors (TFs), single sequence repeat (SSR) and SNPs. Other specific databases, generated before the release of the tomato genome, are the SolEST, miSolRNA, Tomatoma, KaTomics, Tomato Functional Genomics Database (TFGD) and several others recently reviewed in Suresh et al. (2014).

Some of these resources might be extremely useful to dissect genetic complex traits into quantitative trait loci, especially when combined with the exploitation of genetic resources, such as the introgression lines (IL). These lines contain a defined homozygous segment of wild genome in a cultivated genetic background and, taken all together, represent a genomic library of the wild species (Eshed and Zamir, 1995). IL populations have been obtained from various wild tomato species, such as *Solanum pennellii*, *S. habrochaites*, *S. pimpinellifolium*, *S. lycopersicoides*, *S. chmielewskii*, and *S. sitiens* (Fernie et al., 2006) and they are useful to identify genes involved in QTLs regulation thus helping the detection of favorable wild alleles controlling the trait under study. The *S. pennellii* IL population is the most exhaustive; it consists of 76 lines with overlapping wild segments in the cultivated genetic background of the variety M82. These ILs have been widely used to map QTLs (Lippman et al., 2007), have been characterized at genomic and transcriptomic level (Chitwood et al., 2013) and, recently, Alseekh et al. (2013, 2015) carried out their high-dense genotyping and detailed metabolic profiling.

In this work we integrated genomic and transcriptomic data to identify candidate genes (CGs) controlling antioxidant metabolite accumulation in the fruit of *S. pennellii* IL7-3, which has been previously selected in our laboratory since it harbors a positive QTL for AsA and carotenoids content in the fruit (Sacco et al., 2013; Rigano et al., 2014). In addition, in order to restrict the number of CGs, we selected sub-lines of IL7-3 by the aid of species-specific CAPS markers and evaluated their metabolites content. This allowed us to identify one gene that might control carotenoids levels in the fruit. In addition, we could locate the genes controlling AsA content in a restricted part of the introgressed region 7-3, focusing on the role of one gene involved in AsA recycling pathway. These findings can provide valuable tools for improving the nutritional value of tomato and may represent a focus for future investigations.

MATERIALS AND METHODS

Plant Material

Plant material consisted of one *S. pennellii* in *S. lycopersicum* introgression line (IL7-3, accession LA4102) and the cultivated

¹<https://solgenomics.net/>

²<http://59.163.192.91/tomato2/>

genotype M82 (accession LA3475). The accessions were kindly provided by the Tomato Genetics Resources Centre³. Sub-lines of the region 7-3 (genotypes coded from R200 to R207) were selected from F₂ genotypes previously obtained by intercrossing two ILs (IL12-4 × IL7-3; Sacco et al., 2013). The F₂ genotypes were selfed for two generations and then screened by species-specific markers in order to select sub-lines carrying different wild regions at the homozygous condition. Additional IL7-3 sub-lines (genotypes coded from R176 to R182) were kindly provided by Dr. Dani Zamir (Hebrew University, Israel). All genotypes were grown in open-field conditions in the years 2014 and 2015 in a randomized complete block design with three replicates *per* genotype and 10 plants *per* replicate. Fruits were collected at three developmental stages (MG: mature green, BR: breaker stage, MR: mature red). Seeds and columella were subsequently removed, and fruits were ground in liquid nitrogen and stored at -80°C until analyses.

Phenotypic Evaluations

Ascorbic Acid Determination

Ascorbic acid determination was carried out by a colorimetric method (Stevens et al., 2006) with modifications reported by Rigano et al. (2014). Briefly, 500 mg of frozen powder were extracted with 300 µl of ice cold 6% TCA. The mixture was vortexed, incubated for 15 min on ice and centrifuged at 14000 rpm for 20 min at 4°C. Twenty microliters of supernatant were placed in an eppendorf tube with 20 µl of 0.4 M phosphate buffer (pH 7.4) and 10 µl of double distilled (dd) H₂O. Then, 80 µl of color reagent solution were prepared by mixing solution A [31% H₃PO₄, 4.6% (w/v) TCA and 0.6% (w/v) FeCl₃] with solution B [4% 2,2'-dipyridil (w/v)]. The mixture was incubated at 37°C for 40 min and measured at 525 nm by a NanoPhotometer™ (Implen). Three separated biological replicates for each sample and three technical assays for each biological repetition were measured. The concentration was expressed in nmol of AsA according to the standard curve, designed over a range of 0–70 nmol; then the values were converted into mg/100 g of fresh weight (FW).

Carotenoids Determination

The extraction of carotenoids was carried out according to the method reported by Zouari et al. (2014) with minor modifications. Briefly, one gram of frozen powder was extracted with a solution of acetone/hexane (40/60, v/v) for 15 min. The mixture was centrifuged at 4000 rpm for 10 min and the absorbance of surnatant was measured at 663, 645, 505, and 453 nm. Total carotenoids were determined by the equation reported by Wellburn (1994). Results were expressed as mg *per* 100 g FW. All biological replicates *per* sample were analyzed in triplicate.

Molecular Marker Analysis

In order to define the wild region size of IL sub-lines, polymorphic markers spanning the introgression region 7-3 were searched for by exploring the Sol Genomics Network

database⁴. Some markers were retrieved from the database, others markers instead were designed by searching for polymorphisms between the reference tomato sequence (release SL2.50) and the *S. pennellii* genome (Bolger et al., 2014) using the Tomato Genome Browser⁵. The primer pairs used to amplify the genomic region were designed using the Primer3web⁶. Total genomic DNA was extracted from leaves using the PureLink™ Genomic DNA Kit (Invitrogen). PCR DNA amplification was carried out in 50 µl reaction volume containing 50 ng DNA, 1X reaction buffer, 0.2 mM each dNTP, 1.0 mM primer and 1.25 U GoTaq polymerase (Promega). Discriminating restriction enzymes were identified using the CAPS Designer tool available at the Sol Genomics Network⁷. The restriction endonuclease reaction was made in 50 µl of reaction volume containing 20 µl PCR product, 5 µl 10X reaction buffer and 1 µl of the selected restriction enzyme (10 u/ml). Digested fragments were separated by electrophoresis on 2% agarose gel in TAE buffer.

Bioinformatic Identification of Candidate Genes

The search for CGs associated with ascorbic acid and carotenoids metabolism was conducted by exploring the annotations and the Gene Ontology terms of the genes included in the region 7-3 of the tomato chromosome 7 (Alseekh et al., 2013). Due to the preliminary annotation of *S. pennellii* genome (Bolger et al., 2014), the genes of the wild parent were computationally re-annotated by Blast2Go program (version 3⁸; Conesa and Götz, 2008), to better characterize the gene set and collect additional information on their function. BlastX algorithm (e-value < 1E⁻⁶) and NCBI nr protein database were considered for Blast2Go analysis, while the annotation of all the sequences was performed by using default parameters (e-value < 1E⁻⁵). The 'Augment Annotation by ANNEX' function was also used to refine annotations (implemented in Blast2Go and described in Zdobnov and Apweiler, 2001).

Variants between *S. lycopersicum* and *S. pennellii* for all the CGs were obtained by extracting information from the Tomato Variant Brower (Aflitos et al., 2014). In addition, in order to validate the structural variants, the gene sequences were aligned using the genomic sequence information available for both cultivated *S. lycopersicum* and wild *S. pennellii* species. The effects of these variants and the prediction on their functional impact on the protein were analyzed using SnpEff v4.2 (Cingolani et al., 2012). The program performs a simple estimation of putative deleteriousness of the variants, classifying them in four classes (HIGH, MODERATE, LOW, MODIFIER, for detailed information refer to the documentation at http://snpeff.sourceforge.net/SnpEff_manual.html). Variants with high impact cause a stop codon or a frame shift; those with moderate impact are missense variants, whereas those with low impact are synonymous SNPs. The potential

⁴<https://solgenomics.net/>

⁵<http://www.tomatogenome.net/VariantBrowser>

⁶<http://primer3.ut.ee/>

⁷http://solgenomics.net/tools/caps_designer/caps_input.pl

⁸<https://www.blast2go.com/>

³<http://tgrc.ucdavis.edu/>

effect of these polymorphisms on the protein sequence was also cross-validated with the PROVEAN protein tool (publicly available from the J. Craig Venter Institute at http://provean.jcvi.org/seq_submit.php). According to the author's guideline, we considered a "deleterious" effect of the variant if the PROVEAN score was equal or below -2.5.

The Tomato Functional Genomic Database (TED⁹), which reports RNA-seq data from the red fruit of *S. pennellii* ILs, was exploited to verify the expression of the identified CGs in tomato fruits and to estimate their differential expression in M82 and IL7-3. Finally, the TFs mapping in the introgression region were identified by investigating the 2505 TFs present in the Tomato Genomic Resources Database¹⁰ and the 1845 TFs categorized in the Plant Transcription Factor Database¹¹. CGs and TFs with an RPKM value <3 in the RNA-seq database were excluded from further analyses and genes/TFs with Log₂ ratio (IL7-3/M82) >1.5 or <-1.5 were considered to be differentially expressed, following the thresholds reported by Ye et al. (2015).

Real-Time PCR Amplification of Candidate Genes

Total RNA was isolated from tomato fruit at the three stages of ripening (MG, BR, MR) by TRIzol[®] reagent (Invitrogen, Carlsbad, CA, USA) and treated with RNase-free DNase (Invitrogen, Carlsbad, CA, USA; Madison, WI, USA) according to the method reported by the manufacturer (Invitrogen). Total RNA (1 µg) was treated by the Transcriptor High Fidelity cDNA Synthesis Kit (Roche) and cDNA was stored at -20°C until RT-PCR analysis. For each PCR reaction, 1 µL of cDNA diluted 1:10 was mixed with 12.5 µL SYBR Green PCR master mix (Applied Biosystems) and 5 pmol each of forward and reverse primers (Supplementary Table S1) in a final volume of 25 µL. The reaction was carried out by using the 7900HT Fast-Real Time PCR System (Applied Biosystems). The amplification program was carried out according to the following steps: 2 min at 50°C, 10 min at 95°C, 0.15 min at 95°C, and 60°C for 1 min for 40 cycles, and followed by a thermal denaturing step (0.15 min at 95°C, 0.15 min at 60°C, 0.15 min at 95°C) to generate the dissociation curves in order to verify the amplification specificity. All the reactions were run in triplicate for each of the three biological replicates and a housekeeping gene coding for the elongation factor 1-α (*Ef 1-α*)

⁹<http://ted.bti.cornell.edu/>

¹⁰59.163.192.91/tomato2/tfs.html

¹¹plantfdb.cbi.pku.edu.cn

was used as reference gene. The level of expression relative to the reference gene has been calculated using the formula $2^{-\Delta CT}$, where $\Delta CT = (CT_{RNA \ target} - CT_{reference \ RNA})$ (Schmittgen et al., 2004). Comparison of RNA expression was based on a comparative CT method ($\Delta \Delta CT$) and the relative expression has been quantified and expressed according to $\log_2 RQ$, where RQ was calculated as $2^{-\Delta \Delta CT}$, and $\Delta \Delta CT = (CT_{RNA \ target} - CT_{reference \ RNA}) - (CT_{calibrator} - CT_{reference \ RNA})$ (Winer et al., 1999; Livak and Schmittgen, 2001). M82 MG, BR, and MR were selected as calibrators for the three analyzed stages of ripening. Quantitative results were expressed as the mean value ± SE. Differences among samples were determined by using Statistical Package for Social Sciences (SPSS) Package 6, version 15.0. Significance was determined by comparing the genotypes for each stage of ripening through a *t*-Student's test at a significance level of 0.05.

RESULTS

Phenotypic Evaluation of Parental Lines

In order to confirm the presence of one positive QTL for AsA and carotenoids in the region 7-3, metabolic analyses were performed for two consecutive years on mature red fruits of the cultivated genotype M82 and of IL7-3 grown in open fields (Table 1). In both years, IL7-3 accumulated a significant higher level of AsA and carotenoids in the fruit compared to M82, confirming data previously reported in our laboratory (Di Matteo et al., 2010; Sacco et al., 2013; Rigano et al., 2014). The metabolites content was also estimated in three different ripening stages (mature green – MG, breaker – BR, and mature red – MR) as shown in Figure 1. In M82, the AsA level increased from MG to BR and then decreased from BR to MR; accordingly, in IL7-3 the AsA level increased in the first ripening stages but did not decrease in MR. The total carotenoids content deeply increased in both genotypes from BR to MR as expected, and was higher in IL7-3.

Identification of Candidate Genes (CGs)

In order to identify CGs controlling AsA and carotenoids content in IL7-3, we firstly better defined the introgression region size. At this purpose, we selected species-specific molecular markers at the two region borders, referring to those reported in the Sol Genomics Network database¹² and taking into account the

¹²solgenomics.net

TABLE 1 | Evaluation of metabolite content (ascorbic acid, and total carotenoids, mean and standard error) in mature red fruit of genotypes M82 and IL7-3 in the years 2014 and 2015.

Genotype	Ascorbic acid (mg/100 g FW)		Total carotenoids (mg/100 g FW)	
	2014	2015	2014	2015
M82	14.62 ± 1.02	21.38 ± 2.13	10.62 ± 0.44	9.49 ± 0.61
IL7-3	28.32 ± 0.10***	31.28 ± 1.71***	15.88 ± 0.43 ***	11.36 ± 0.62**

Asterisks indicate statistically significant differences compared to M82 (Student's *t*-test, ***P* < 0.01, ****P* < 0.001).

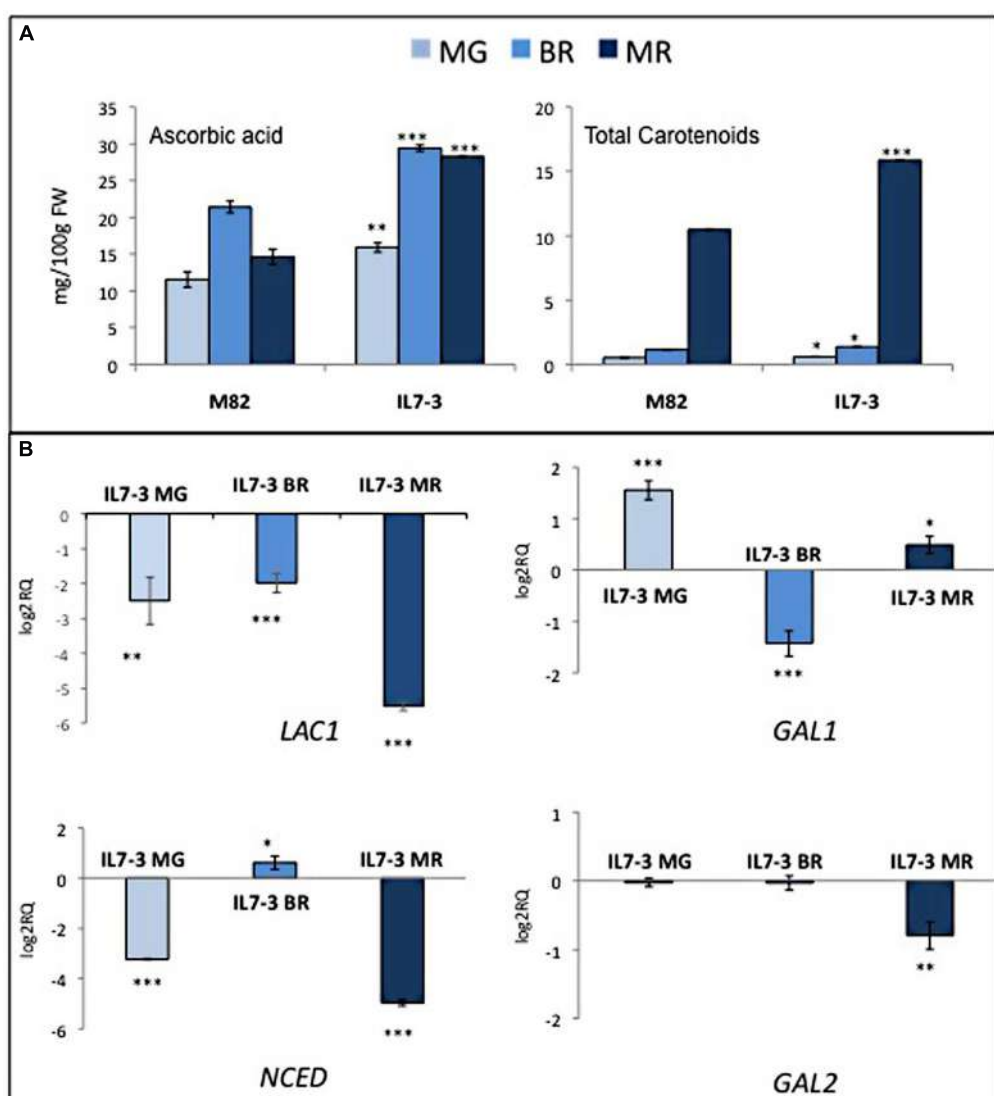


FIGURE 1 | Phenotypic and molecular evaluation of the parental genotypes M82 and IL7-3. (A) Metabolite content (AsA and total carotenoids) at three different ripening stages (MG, mature green; BR, breaker; MR, mature red); **(B)** Expression level of four selected CGs (*LAC1*: laccase-22/L-ascorbate-oxidase homolog; *GAL1* and *GAL2*: β -1-3-galactosyltransferase; *NCED*: 9-cis-epoxycarotenoid dioxygenase) in IL7-3 at different ripening stages. Asterisks indicate statistically significant differences of each ripening stage to the corresponding M82 stage (* $P < 0.05$, ** $P < 0.01$, *** $P < 0.001$).

information on *S. pennellii* ILs reported in Chitwood et al. (2013) regarding the chromosomal positions of ILs boundaries. By testing ten markers (from N22 to N28 at the upper border, and from N12 to N30 at the lower border, Table 2) on the parental genotypes M82 and on IL7-3, we ascertained that the wild region stretches from marker N27 (corresponding to Solyc07g048030 at 59,218,716 bp) to marker N17 (corresponding to Solyc07g063330 at 65,816,155 bp), covering about 6.6 Mbp. This region includes 725 genes (Supplementary Table S2), 120 (16.5%) were annotated as unknown proteins, whereas 94 (13.0%) were TFs. Among the remaining 511 annotated genes, we searched for those related to AsA and carotenoids accumulation. Six CGs putatively involved in determining AsA content were detected (Table 3), but none of them belong to the main biosynthetic galactose pathway. The

identified genes were: one *polygalacturonase* (Solyc07g056290, *POLYGAL*), two *beta-1-3-galactosyltransferase* (Solyc07g052320 and Solyc07g062590, *GAL1* and *GAL2*, respectively), two *laccase-22/L-ascorbate-oxidase homolog* (Solyc07g052230 and Solyc07g052240, *LAC1* and *LAC2*, respectively), and one *nucleobase-ascorbate transporter* (Solyc07g049320, *NAT*). The investigation of the SolCyc biochemical pathways database¹³ allowed confirming the involvement of the gene *POLYGAL* in the galacturonate AsA biosynthetic pathway (enzymatic step EC 3.2.1.15), and of *GAL1* and *GAL2* in enzymatic reactions (EC 2.1.4-) potentially regulating myo-inositol content, that might feed the glucuronate biosynthetic pathway. *LAC1*

¹³solcyc.solgenomics.net

and *LAC2* might enter the recycling pathway of AsA by reducing L-ascorbate into monodehydroascorbate (EC 1.10.3.3), whereas the NAT might have a role in transporting AsA among the different intracellular compartments. In addition, in the introgression region one *9-cis-epoxycarotenoid dioxygenase* (Solyc07g056570, *NCED*) was also mapped that, entering the carotenoids pathway, determines the carotenoids oxidative cleavage with consequent production of apocarotenoids, the direct substrates for abscisic acid (ABA) synthesis. The latter gene was included into the group of those to be further investigated.

Sequence Variation and Expression Variability of Selected CGs

In order to better define which CGs determine the different metabolites content between M82 and IL7-3 fruit, differences in their sequence and/or in their expression level were investigated. The impact of polymorphisms between *S. lycopersicum* and *S. pennellii* was estimated for the 117 variations identified in CGs mapping in the introgression region (**Table 3**). No case of high impact polymorphism was detected, and *NAT* and *GAL1* did not even exhibit any variants with moderate impact effect. For the other genes, the number of variants with moderate impact varied from two (*LAC2*) to seven (*POLYGAL*), and a deleterious effect at the protein level investigated by PROVEAN was predicted for genes *LAC1* and *POLYGAL*.

The RNA-seq data available for M82 and IL7-3 in the TFGD (Fei et al., 2010) allowed to ascertain that three CGs for AsA were not expressed or expressed at very low levels in the red fruit (**Table 3**): *NAT*, *LAC2* and *POLYGAL*. By contrast, *GAL1*, *GAL2*, *LAC1* and *NCED* showed a lower expression level in IL7-3 compared to M82. The expression of all CGs was analyzed by qRT-PCR in three developmental stages of M82 and IL7-3 fruits. This analysis allowed confirming the lack of expression of *NAT*, *LAC2* and *POLYGAL*. The different expression levels of *LAC1* and/or *GAL2* detected here well correlate with the different trend of AsA accumulation in M82 and IL7-3 in the three developmental fruit stages (**Figure 1**), even though also the down-regulation of *GAL1* at BR stage could be relevant. Finally, the significant lower expression of the gene *NCED* at the MR stage well correlated with the higher level of total carotenoids observed in IL7-3.

Besides the identified CGs, TFs mapping in the introgression region 7-3 might play a role in increasing antioxidants. Indeed, if differentially expressed or polymorphic between M82 and IL7-3, they could *trans*-regulate the expression of genes involved in AsA or carotenoids biosynthesis and accumulation mapping in the introgression or in other regions of the genome. Sequence variations with deleterious effects on the protein functionality were found in 27 TFs (Supplementary Table S3), but in most cases (85%) the polymorphic TFs were not expressed in the fruit (Supplementary Table S4). The ten TFs selected for their significant differential expression between IL7-3 and M82 (Supplementary Table S3) did not show any sequence variation that cause deleterious effect as predicted by PROVEAN. Most of them exhibited a lower expression in IL7-3, except for one *MYB* (Solyc07g053240), one *GRAS* (Solyc07g052960) and one

storekeeper protein (Solyc07g052870), but none corresponded to the TFs identified by Ye et al. (2015) for their correlation with expression of genes involved in high AsA and carotenoids in tomato fruit. The availability of the whole transcriptome of M82 and IL7-3 in the TED database allowed also investigating the expression of all the genes involved in AsA and carotenoids biosynthetic pathways, which were annotated in the tomato genome (Supplementary Table S5). No differentially expressed gene among these was identified. When looking at the whole transcriptome, an unbalance of ascorbate-oxidase activity could be hypothesized in IL7-3 compared to M82. Indeed, besides the gene *LAC1* of the introgression 7-3, two other *laccases-22/L-ascorbate-oxidase*, mapping on chromosomes 2 and 8, showed a decreased expression in IL7-3. They could exert an additive action to that of the wild *LAC1* in increasing AsA content in the fruit. Finally, two *myo-inositol phosphate synthase* (Solyc04g050820 and Solyc05g051850) were over-expressed in IL7-3, and they could affect the *myo*-inositol pathway, as well as the two *GAL1* and *GAL2* that map into the introgression.

Selection and Phenotyping of IL7-3 Sub-lines

In order to reduce the number of CGs potentially responsible for the higher antioxidant content in the IL7-3 red ripe fruit, introgression sub-lines of the wild region were selected through the analysis of 28 polymorphic markers mapping within this region. Comprehensively, we identified seven distinct sub-lines showing a reduced wild region compared to IL7-3 and carrying different combinations of wild alleles for four CGs (**Figure 2**). Only two sub-lines, R182 (from marker N27 to N14) and R181 (from marker N7 to N17), had no wild alleles for the CGs, even though they carried different introgressed wild regions. Four sub-lines carried two wild CGs for AsA (*LAC1* and *GAL1*) but differed for the presence (R201, R202) or absence (R176, R178) of the wild allele for *NCED* gene. Finally, one sub-line (R179) carried wild alleles for *GAL2* and *NCED* genes. All the sub-lines were grown in open field and were evaluated for AsA and carotenoids content in the fruit (**Table 4**). The carotenoids level of the three sub-lines carrying the wild allele for *NCED* (R179, R201, R202) was higher than in M82; sub-lines carrying the cultivated allele showed a level of carotenoids comparable to M82. As for AsA, it was evident that two sub-lines (R179 and R181) exhibited levels of AsA comparable to that of the control genotype M82, whereas all the others showed AsA content significantly higher than M82 and similar to IL7-3. Therefore, considering the different combinations of wild CGs carried by the sub-lines, it is possible to exclude the role of *GAL2* wild allele in increasing AsA content in IL7-3. By contrast, the wild alleles of both *LAC1* and *GAL1* might be involved in increasing AsA in IL7-3 and in a group of sub-lines, even though the qRT-PCR results evidenced that the action of *GAL1* occurs earlier at BR. The expression level of the selected CGs *NCED* and *LAC1* was verified in the sub-lines (**Figure 3**) to better ascertain their role in affecting carotenoids and AsA, respectively. Surprisingly, a higher expression of *NCED* compared to M82 and a concurrent higher level of AsA were observed in R182, a sub-line with a reduced

TABLE 2 | CAPS molecular markers used to define the whole introgression region 7-3 and the sub-lines obtained from this region.

Marker code	Position on Chromosome 7 SL2.5 (bp)	Primer sequence 5'-3'	Expected PCR product size (bp)	Restriction enzyme	M82 fragment size (bp)	IL7-3 fragment size (bp)
N22	58,951,964	F:ATGTGCTTGCCATGTGTCG R:AAGAGATGGAGCGTTGGGA	507	TaqI	290 + 217	507
N23	58,963,247	F:TGACCACTGCCATAATGCTT R:GCTGATGAAGTGAGGAACCC	526	HaeIII	288 + 238	526
N24	59,131,334	F:CACAGTCATCTCAGCAATGTG R:CTTGTCTTCCCATAAGCTGCG	444/481	RsaI	90 + 391	90 + 348 + 43
N26	59,184,600	F:GATGGTAGTTTATGCGGATCA R:GTCACCTGCTAACCTCAGT	378	TaqI	296 + 47 + 35	343 + 35
N27	59,218,716	F:TGGGACACAATGAAGAGCG R:ACTGTGGATGCTAAACCTCCA	610	TaqI	610	291 + 319
N28	59,240,752	F:CAGCAATAACCAGATTTCGCA R:CCAGCAACACAGCACCAT	402	HaeIII	402	268 + 134
N25	59,289,774	F:TGTCACTGGTCCCTCATCAAC R:GCGGAAAGGCACAACTCCAAA	612	TaqI	417 + 195	612
N14	59,523,504	F:TCCGCTTTCATCATCTGTTG R:TCCAATTCCATCCGATTG	492	TaqI	492	399 + 93
N18	59,578,421	F:GCCATTAACATTGGGACTCG R:AGCTTACATCTGATCCGCC	440	Scal	223 + 217	440
N15	59,926,751	F:TGACATGCCGATAGTGTTCAC R:TGTGATGGTGTGACTGGG	489	RsaI	489	176 + 313
N16	60,507,445	F:CGCTTGCCTTGTAAATCCA R:ACTGGTGGGACGTATACTTTGT	869	RsaI	57 + 483 + 173 + 156	57 + 483 + 329
N33	60,724,902	F:ACAGTGTGAGTCCCTTCACT R:AATTGCCCCATTCACCAGG	650	AluI	650	257 + 393
N10	60,874,313	F:GATTGCTGGTCTACGCTTGC R:ACAAGAAGCCAGCAAAGACG	303	TaqI	263 + 40	56 + 96 + 111 + 40
N11	61,065,289	F:GCTTCCTCAAGACACCCAGA R:CAGTTGTTCAATTCTCAGGT	458	HaeIII	458	304 + 154
N4	61,181,115	F:CAATGAGATATACTGGTACACG R:ACGTGCAGAGAACAAAGTTGAG	782	TaqI	414 + 176 + 192	590 + 192
N1	62,747,850	F:TGACCGATAAACCTTGAGCAGCAC R:ATAACCTAGCTCCCTCTATGGTGT	300	TaqI	300	300 + 100
N8	63,198,615	F:GGTGGCAATTAGGGTGACA R:TCAAAATCCACCGTACACCA	767	HaeIII	518 + 251	767
N19	64,147,505	F:GGATGGACAAGGTGCTGTTG R:TTCTGTTCATATCCGTCGTTCA	824	Scal/RsaI	139 + 685	824
N9	64,214,216	F:GCACGAAACCCACCAATT R:GCAATCTCAGTAGTATGTGAG	743/-	-	743	-
N2	64,340,348	F:TCACTCTTGATTTGTGAG R:AGTGCCTTATGTTAACGCTTAT	650	TaqI	420 + 150 + 80	500 + 150
N5	64,734,536	F:TAGAGGACGGGAATGGACC R:AGGAGGGAAAGGGCTTGT	854	AluI	854	586 + 268
N6	65,022,435	F:GTCGAAACCTGATTTACCTGG R:GACTGACATATGCTCTGCTTC	967/947	-	967	947
N7	65,309,240	F:ACAGGGTGGTGGTAGATGG R:TCACCATGCGTGTATTAGCA	609	TaqI	609	422 + 187
N3	65,598,163	F:TTGGTCTATTGCAATATTGATGG R:AATCAATATGGCTGTAACAGCAGTTG	370	AluI	370	230 + 140
N12	65,699,488	F:GGGATCGTTGCTGGTTC R:GCCATTGCTCACCGAGCT	301	HaeIII	301	168 + 133

(Continued)

TABLE 2 | Continued

Marker code	Position on Chromosome 7 SL2.5 (bp)	Primer sequence 5'-3'	Expected PCR product size (bp)	Restriction enzyme	M82 fragment size (bp)	IL7-3 fragment size (bp)
N17	65,816,155	F:CCAATCCTAGTATACTCCAGCA R:TGAATATGCCATGCGAAGTTGT	413	EcoRI	413	241 + 172
N29	65,969,635	F:AGATGAGCAGTTGGTAGTCC R:CCAAAAGCCATCAGTTGCCT	450	TaqI	270 + 180	450
N30	66,061,621	F:AGTAGAACAGAGGATAGGGAAC R:GGAGTAGAGGCAGCAATGGA	520	TaqI	297 + 223	520

Markers are ordered following their crescent map position (bp) on chromosome 7. For each marker are reported: the primer sequences, the PCR product size, the restriction enzymes used, the polymorphic fragment size between M82 and IL7-3. In bold: markers that are borders of the introgression region.

introgression size of 200 kb, where no wild allele for any CGs and no differentially expressed or polymorphic TFs was retained. A total of 24 genes map in this region, including two unknown genes.

DISCUSSION

The exploitation of wild *Solanum* species has driven the improvement of tomato varieties for several traits by using traditional and innovative breeding approaches (Bai and Lindhout, 2007). The wild species are precious sources of new alleles for improving specific traits, most of which are quantitatively inherited and therefore highly influenced by environmental conditions and by multiple interactions among a consistent number of genes. In this view, the production of ILs from tomato wild species helped to dissect many complex traits into major QTLs (Lippman et al., 2007), which might be then transferred into improved varieties. This genetic effort is boosted by the availability of genomic tools and resources, which may have a deep impact on the success of this breeding strategy.

The *S. pennellii* IL7-3 has been selected in our laboratory for its higher antioxidant properties compared to the cultivated variety M82 (Sacco et al., 2013; Rigano et al., 2014). It exhibited stable performances in different years and we could therefore assume that these properties depend on a strong genetic basis. By integrating data coming from many genomics resources publicly available, we exploited this genetic resource with the aim of identifying CGs and their wild alleles, which may contribute to increase AsA and total carotenoids in the fruit. One CG was identified that might affect carotenoids accumulation: the *NCED* gene, which controls a key-enzyme in ABA biosynthesis (Zhang et al., 2009). The lower expression of this gene in IL7-3 might reduce the metabolic flux toward ABA production, pushing the upstream metabolic pathway and thus feeding carotenoids accumulation, as proposed by Sun et al. (2012), who observed an increase of carotenoids level and a reduction of ABA when the gene *SINCED1* was silenced in tomato fruit. Also in our case, a concurrent increase of carotenoids and decrease of ABA was observed in IL7-3 compared to M82 (data not shown), thus supporting the role attributed to the wild allele of *NCED*. In addition, even though no deleterious impact on proteins was detected by PROVEAN when comparing the wild and

cultivated alleles of *NCED*, the alteration of amino acid sequences may result in enzymes with modified activities (Yuan et al., 2015).

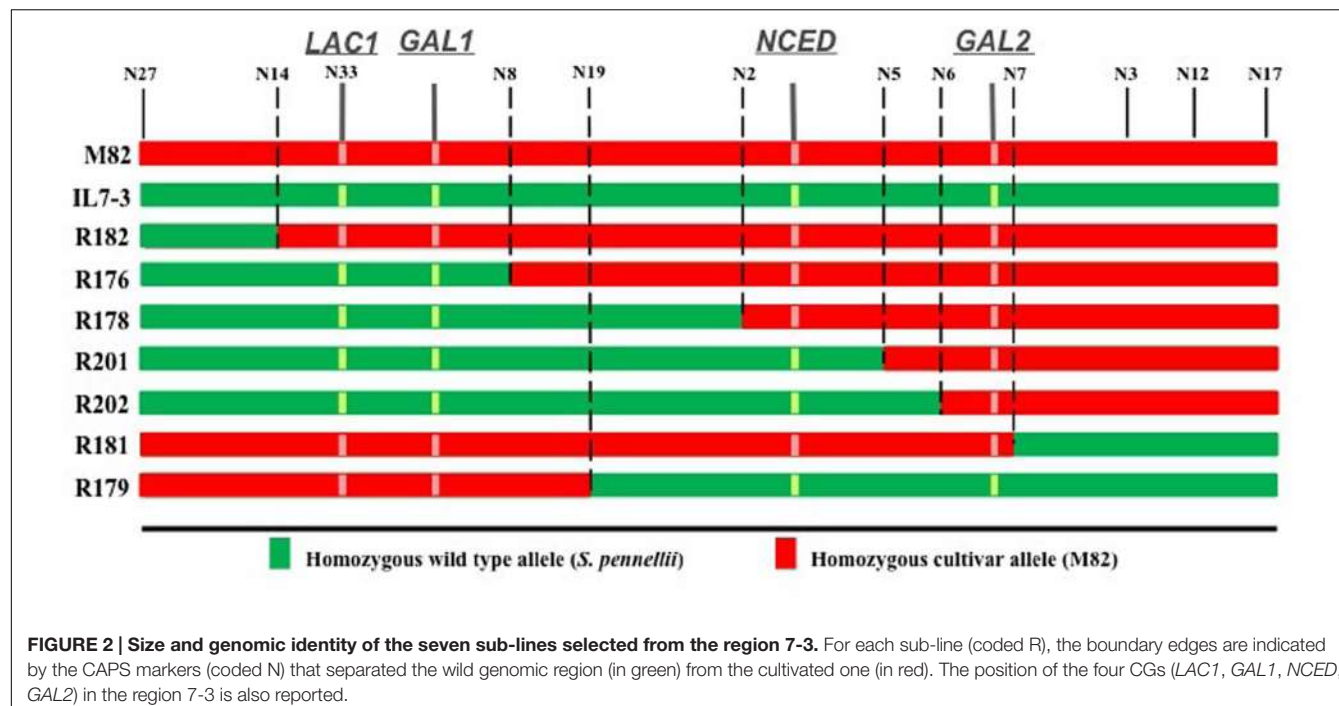
Understanding the genetic control of the higher AsA content in IL7-3 fruit was more complicated. Out of six CGs identified in the introgressed region, which might be involved in the synthesis and accumulation of AsA, only three were expressed in the fruit. Among these, the gene *LAC1* was expressed only in traces in IL7-3 fruits respect to M82, as retrieved from available RNAseq data in the TED database, and confirmed in our work using three primer pairs for Real Time PCR targeting different regions of this gene. In addition, a deleterious missense variant (-6.337 PROVEAN score) has been detected in *LAC1* when comparing the sequences of *S. lycopersicum* and *S. pennellii*. This caused a substitution of a glycine in glutamic acid at position 194 (G194E), which affects the cupredoxin domain. The deleterious alteration of the protein in that position might be crucial for its correct functionality. The two *GAL* genes mapping in the introgression exhibited both a slight lower expression in IL7-3, and might contribute to enhance AsA content in the fruit. Finally, the wild allele of *NCED* might be indirectly related to the increased level of AsA, since an intricate relationship between ABA biosynthesis and AsA metabolism has been already hypothesized in different species, including *Arabidopsis*, strawberry, tomato, and *Ocimum* (Ghassemian et al., 2008; Nair et al., 2009; Lima-Silva et al., 2012; Dongdong et al., 2015). However, in some cases the correlation occurred between ABA content and ascorbate oxidase expression level without any modifications of *NCED* expression (Lopez-Carbonell et al., 2006; Fotopoulos et al., 2008). Therefore, the AsA increase in IL7-3 might be also attributed to variations of ABA content determined by the reduced activity of *NCED*, *LAC1* or both the enzymes.

Since the introgressed region 7-3 has a large size (6.6 Mbp), we analyzed sub-lines of the region, which allowed focusing on a restricted number of CGs. The selected sub-lines carried only two or three CGs, or even no CG at all. The phenotypic characterization of the sub-lines led us to draw some conclusions on the potential role of the CGs. Firstly, the carotenoids content well-reflected the presence/absence of the wild allele for *NCED*, even though its specific action should be further investigated, since the lower expression of *NCED* is correlated to a higher carotenoids content only in three out of four sub-lines (R179, R201, and R202). Therefore, approaches of gene replacement

TABLE 3 | Candidate genes for ascorbic acid and carotenoids, and transcription factors mapping in the introgressed region 7-3, all selected for their \log_2 fold change <-1.5 or >1.5 .

Gene function	Gene identifier (SOLyc ID)	Gene position (SL2.50) bp	Expression level RPKM ¹	Log ₂ fold change		Prediction by SNPeff		Prediction by PROVEAN	
				M82	IL7-3	Variants with HIGH impact No.	Variants with MODERATE impact No.	Variants with LOW impact No.	Deleterious variants No.
Candidate genes									
Nucleobase ascorbate transporter (NAT)	SOLyc07g049320	59577405...59581995	0.04	0.02	-1	0	0	10	-
Laccase-22L-ascorbate oxidase homolog (LAC1)	SOLyc07g052230	60723150...60729170	9.43	0.02	-8.8811	0	6	13	1
Laccase-22L-ascorbate oxidase homolog (LAC2)	SOLyc07g052240	60726910...60730555	0.04	0.00	ND	0	2	25	0
β -1,3-galactosyltransferase (GAL1)	SOLyc07g052320	60816826...60820674	9.43	3.48	-1.4382	0	0	11	-
Polygalacturonase (POLYGA1)	SOLyc07g056290	64146906...64150487	0.00	0.00	ND	0	7	9	1
9-cis-epoxycarotenoid dioxygenase (NCED)	SOLyc07g056570	64361346...64363163	97.58	19.77	-2.3033	0	4	19	0
β -1,3-galactosyltransferase (GAL2)	SOLyc07g062590	65282118...65288822	7.35	2.54	-1.5329	0	4	7	0
Transcription factors									
Storekeeper protein	SOLyc07g052870	61299858...61301426	1.54	4.45	1.5308	0	2	1	0
GRAS family transcription factor	SOLyc07g052960	61367195...61368484	451.9	1421.77	1.6533	0	3	7	0
CONSTANS-like zinc finger protein	SOLyc07g053140	61593135...61594431	35.64	6.53	-2.4483	0	6	5	0
Myb-related transcription factor	SOLyc07g053240	61710098...61711189	0.08	4.08	5.6724	1	8	4	0
Ethylene-responsive transcription factor 4	SOLyc07g053740	62167919...62168596	222.36	15.85	-3.8103	0	0	11	-
Ethylene responsive transcription factor 2a	SOLyc07g054220	62574142...62575314	1.37	0.43	-1.6717	0	10	6	0
WRKY transcription factor 5	SOLyc07g055280	63369004...63372627	5.26	0.56	-3.2315	0	2	4	0
BHL transcription factor	SOLyc07g062950	65585877...65588912	2.55	0.62	-2.0401	0	1	3	0
Squamosa promoter binding-like protein	SOLyc07g082980	65599440...65600609	55.86	2.15	-4.6894	0	2	2	0
DNA-binding WRKY VQ	SOLyc07g063070	65649614...65650315	10.77	3.45	-1.6423	0	2	5	0

For each SOLyc the position on the chromosome is reported in bp. The number of sequence variants of wild alleles classified for their impact/deleteriousness following SNEff and PROVEAN are reported. ¹RPKM expression values are those reported in the Tomato Functional Genomic Database (<http://ted.tbi.com/ledu>).



between the wild and the cultivated allele will be undertaken to verify that the presence of the wild allele may be effectively correlated to higher levels of carotenoids content. Secondly, the wild allele of *NCED* is not essential for determining the higher AsA content in IL7-3, even though it can contribute to increase it, as discussed above. Thirdly, the down-regulation of *GAL2* is not correlated to the higher AsA content in IL7-3 and in sub-lines.

Unfortunately, it was not possible to disrupt the linkage between the two CGs *LAC1* and *GAL1*, and then clearly identify if only one or both of them control the AsA increase. However, it is expected that more genes mapping in one QTL contribute to affect one phenotype, and therefore in our case it may be assumed that both *LAC1* and *GAL1* might have a determinant role in increasing AsA, and this could confirm the existence of polygenes in the QTL under study. In particular, the down-regulation of *GAL1* at BR stage would reduce the metabolic flux

toward the *myo*-inositol biosynthetic pathway. Moreover, it is worth saying that, when the whole transcriptome of IL7-3 was analyzed in comparison to that of M82, two genes annotated as *inositol-3-phosphate synthase* were over-expressed in IL7-3, with a potential contrasting action on the *myo*-inositol pathway respect to *GAL1*. Since the involvement of the latter pathway in the AsA biosynthesis in plants is still controversial (Endres and Tenhaken, 2009; Torabinejad et al., 2009; Gallie, 2013), we did not focus further attention on *GAL1*.

The role of *LAC1* is supported by its down-regulation in IL7-3 MR fruit and in the sub-lines that exhibited a high level of AsA (R176, R178, R201, R202). Indeed, the ascorbate oxidase is an apoplastic enzyme that catalyzes the reversible oxidation of ascorbate to dehydroascorbate, through the formation of monodehydroascorbate, with the concomitant reduction of molecular oxygen to water. Transgenic plants over-expressing or under-expressing this gene have shed light on its role in

TABLE 4 | Phenotyping and genotyping of the seven *S. pennellii* introgression sub-lines: for each sub-line the higher content of ascorbic acid (AsA) and total carotenoids respect to M82 is reported, together with the presence of wild alleles for four candidate genes (CG), and the number of genes classified as unknown and transcription factors (TF), which map in the introgressed region.

Sub-line	Border Markers	AsA ¹	Carotenoids ¹	Wild CGs	Unknown	TFs
R182	N27-N14	+	-	-	2	0
R176	N27-N8	+	-	<i>LAC1</i> - <i>GAL1</i>	65	6
R178	N27-N2	+	-	<i>LAC1</i> - <i>GAL1</i>	85	7
R201	N27-N5	+	+	<i>LAC1</i> - <i>GAL1</i> - <i>NCED</i>	91	7
R202	N27-N6	+	+	<i>LAC1</i> - <i>GAL1</i> - <i>NCED</i>	100	7
R179	N19-N17	-	+	<i>GAL2</i> - <i>NCED</i>	36	3
R181	N7-N17	-	-	-	12	3

¹Ascorbic acid (AsA) and carotenoids content in the sub-line significantly higher (+) than M82.

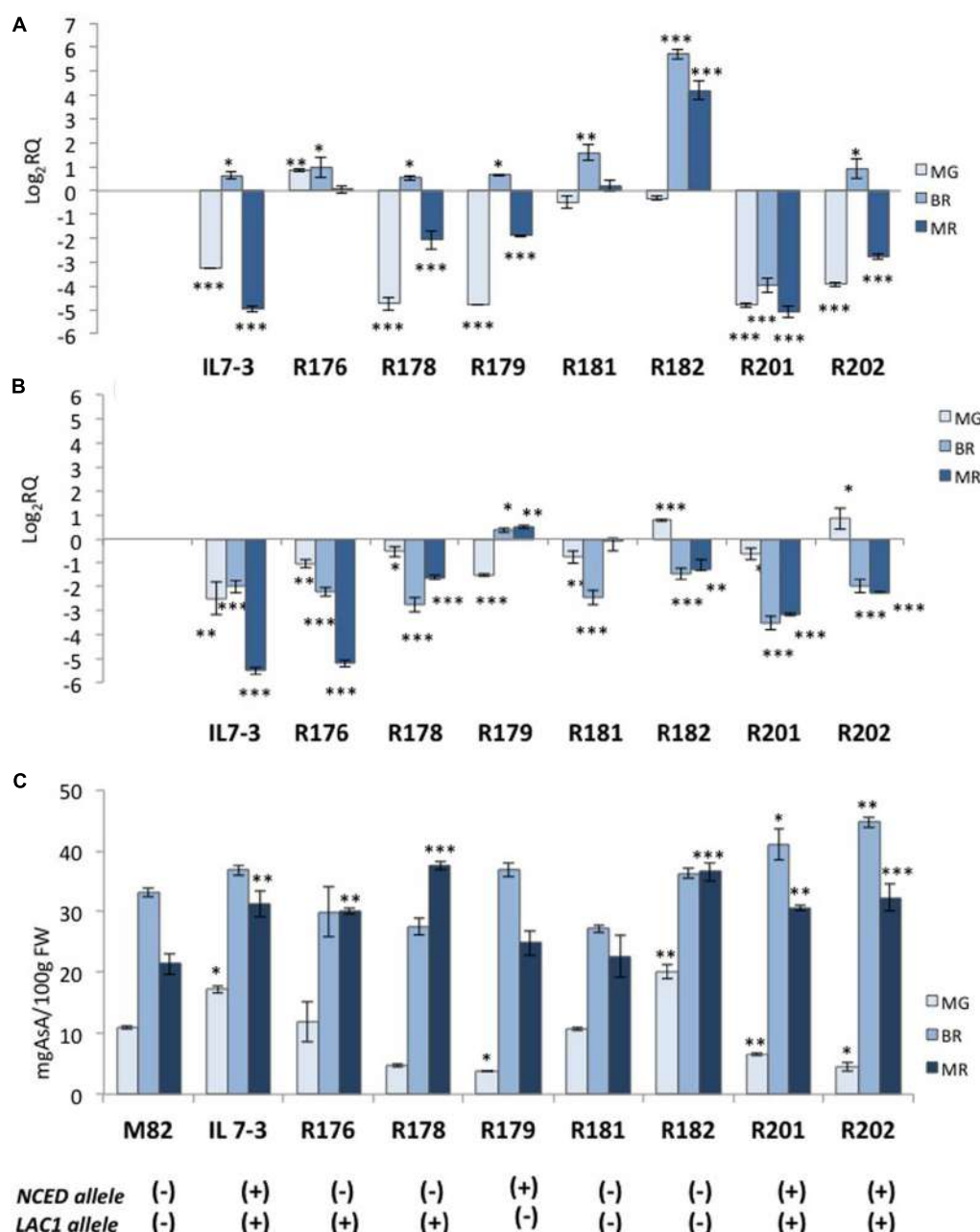


FIGURE 3 | Gene expression of two CGs (NCED and LAC1) and ascorbic acid (AsA) content in the fruit of the seven sub-lines of the region 7-3. The expression level of NCED (A) and LAC1 (B) in the parental IL7-3 and its sub-lines is reported in comparison to that observed in the parental M82 at three different ripening stages, together with the AsA content (C) in the fruit evaluated at the same stages for all genotypes. Asterisks indicate statistically significant differences of each ripening stage to the corresponding M82 stage (* $P < 0.05$, ** $P < 0.01$, *** $P < 0.001$). The presence of the wild (+) or cultivated (-) alleles of NCED and LAC1 genes for each genotype is reported at the bottom.

regulating the apoplastic ascorbate pool (Pignocchi et al., 2003; Sanmartin et al., 2003), and therefore the ascorbate redox state, thus also influencing the perception of environmental stresses (Yamamoto et al., 2005; Fotopoulos et al., 2006, 2008; Gachery et al., 2013). In our case, the down-regulation of the wild *laccase-22/L-ascorbate oxidase LAC1* might have an effect comparable to that described in RNAi lines with reduced ascorbate oxidase

activity (Zhang et al., 2011), which exhibited high ascorbic acid accumulation in tomato fruit. This effect could explain the significantly higher Asa level observed in IL7-3 and in the sub-lines with respect to the control M82. In the future, the potential correlation between the down-regulation of LAC1 in our tomato genotypes and their improved response to agents imposing oxidative stress will be also investigated.

Finally, in the sub-line R182 the increased level of AsA detected in the red ripe fruits should be further investigated, but it confirms that the IL7-3 AsA QTL consists of more than one CG. Among the 24 genes mapping in the small introgressed region of R182, two annotated as unknown were detected, whereas no TFs was differentially expressed in tomato fruit. In the future, the functional role of all these 24 genes in modulating AsA in tomato fruit will be further investigated by using reverse genetic approaches to clearly define their specific role in controlling AsA content in the tomato mature fruit.

It is also worth saying that the existence in the 7-3 region of several genes annotated as unknown proteins paves the way to other hypotheses. Indeed, besides the differential expression and the structural variants affecting enzyme activity, additional transcriptional and translational interactions may occur and contribute to influence it. Recently, regulators of AsA biosynthesis in plants have been described (reviewed in Zhang, 2012). In *Arabidopsis* it has been demonstrated that light regulates AsA synthesis through the interaction between a photomorphogenetic factor and the enzyme GDP-mannose pyrophosphorylase (Wang et al., 2013), as well as that a feedback regulation of AsA biosynthesis occurs following the interaction between ascorbate and an Open Reading Frame (ORF) in the long 5' UTR (untranslated region) of the GDP-L-galactose phosphorylase gene (Laing et al., 2015). Now, it will be crucial to demonstrate if similar mechanisms or others may operate in tomato fruit and, therefore, influence AsA concentration in IL7-3.

CONCLUSION

Results reported in the present work clearly demonstrated that exploiting the genetic and genomic resources nowadays available for tomato, including bioinformatics tools, was a successful strategy to dissect one positive QTL for the increase of AsA and carotenoids in the mature fruit. In particular, two CGs for improving these metabolites were detected in the wild region 7-3 introgressed from the species *S. pennellii*. These were one *L-ascorbate oxidase* (*LAC1*) and one *9-cis-epoxycarotenoid dioxygenase* (*NCED*), whose wild alleles, exhibiting polymorphisms and/or differential transcript levels,

might increase AsA and total carotenoids content. The first CG favors the accumulation of reduced ascorbate controlling the redox state of ascorbate in the apoplast. The action of the second CG still needs to be elucidated, even though the presence of the wild allele for *NCED* was correlated to higher carotenoids content. Finally, the latter gene might also indirectly contribute to increase AsA content, as revealed by the sub-line R182, which showed a high expression of the cultivated allele for *NCED* combined with high AsA content. A group of 24 genes mapping in the wild introgression of the sub-line R182 will be further investigated in the future to better understand their role in the architecture of the QTL that positively influences the level of antioxidants in the investigated region of the chromosome 7.

AUTHOR CONTRIBUTIONS

RC and VR contributed to bioinformatic and experimental analyses carried out to identify CGs and the introgression sub-lines, and to draft the manuscript; AR contributed to metabolic and transcriptomic analyses; MR contributed to metabolic analysis and critically revised the manuscript; AS contributed to the bioinformatic analysis and drafted the manuscript; MH contributed to molecular marker analysis and to grow materials; LF contributed to the conception of the experiment and critically revised the manuscript; AB contributed to the experiment design, to data analysis and interpretation, to draft the manuscript.

FUNDING

This research was supported by the Italian Ministry of University and Research (MIUR) [grant MIUR-PON02-GenoPOMpro].

SUPPLEMENTARY MATERIAL

The Supplementary Material for this article can be found online at: <http://journal.frontiersin.org/article/10.3389/fpls.2016.00397>

REFERENCES

- Aflitos, S. A., Schijlen, E., de Jong, H., de Ridder, D., Smit, S., Finkers, R., et al. (2014). Exploring genetic variation in the tomato (*Solanum* section *Lycopersicon*) clade by whole-genome sequencing. *Plant J.* 80, 136–148. doi: 10.1111/tpj.12616
- Alseekh, S., Ofner, I., Pleban, T., Tripodi, P., Di Dato, F., Cammareri, M., et al. (2013). Resolution by recombination: breaking up *Solanum pennellii* introgressions. *Trends Plant Sci.* 8, 536–538. doi: 10.1016/j.tplants.2013.08.003
- Alseekh, S., Tohge, T., Wendenberg, R., Scossa, F., Omranian, N., Li, J., et al. (2015). Identification and mode of inheritance of quantitative trait loci for secondary metabolite abundance in tomato. *Plant Cell* 27, 485–512. doi: 10.1105/tpc.114.132266
- Badejo, A. A., Wada, K., Gao, Y., Maruta, T., Sawa, Y., Shigeoka, S., et al. (2012). Translocation and the alternative D-galacturonate pathway contribute to increasing the ascorbate level in ripening tomato fruits together with the D-mannose/L-galactose pathway. *J. Exp. Bot.* 63, 229–239. doi: 10.1093/jxb/err275
- Bai, Y., and Lindhout, P. (2007). Domestication and breeding of tomatoes: what have we gained and what can we gain in the future? *Ann. Bot.* 100, 1085–1094. doi: 10.1093/aob/mcm150
- Barone, A., Chiusano, M. L., Ercolano, M. R., Giuliano, G., Grandillo, S., and Frusciante, L. (2008). Structural and functional genomics of tomato. *Int. J. Plant Genomics* 2008:820274. doi: 10.1155/2008/820274
- Bolger, A., Scossa, F., Bolger, M. E., Lanz, C., Maumus, F., and Tohge, T. (2014). The genome of the stress-tolerant wild tomato species *Solanum pennellii*. *Nat. Genet.* 46, 1034–1038. doi: 10.1038/ng.3046
- Cai, X., Ye, J., Hu, T., Zhang, Y., and Ye, Z. (2014). Genome-wide classification and expression analysis of nucleobase-ascorbate transporter (NAT) gene family in tomato. *Plant Growth Regul.* 73, 19–30. doi: 10.1007/s10725-013-9864-x
- Canene-Adams, K., Campbell, J. K., Zaripheh, S., Jeffery, E. H., and Erdman, J. W. Jr. (2005). The tomato as a functional food. *J. Nutr.* 135, 1226–1230.

- Chen, Z., Young, T. E., Ling, J., Chang, S. C., and Gallie, D. R. (2003). Increasing vitamin C content of plants through enhanced ascorbate recycling. *Proc. Natl. Acad. Sci. U.S.A.* 100, 3525–3530. doi: 10.1073/pnas.0635176100
- Chitwood, D. H., Kumar, R., Headland, L. R., Ranjan, A., Covington, M. F., Ichihashi, Y., et al. (2013). A quantitative genetic basis for leaf morphology in a set of precisely defined tomato introgression lines. *Plant Cell* 25, 2465–2481. doi: 10.1105/tpc.113.112391
- Cingolani, P., Platts, A., Wang le, L., Coon, M., Nguyen, T., Wang, L., et al. (2012). A program for annotating and predicting the effects of single nucleotide polymorphisms, SnpEff: SNPs in the genome of *Drosophila melanogaster* strain w1118; iso-2; iso-3. *Fly* 6, 80–92. doi: 10.4161/fly.19695
- Conesa, A., and Götz, S. (2008). Blast2GO: a comprehensive suite for functional analysis in plant genomics. *Int. J. Plant Genomics* 2008:619832. doi: 10.1155/2008/619832
- Davey, M. W., Kenis, K., and Keulemans, J. (2006). Genetic control of fruit vitamin C contents. *Plant Physiol.* 142, 343–351. doi: 10.1104/pp.106.083279
- Di Matteo, A., Sacco, A., Anacletia, M., Pezzetti, M., Delledonne, M., Ferrarini, A., et al. (2010). The ascorbic acid content of tomato fruits is associated with the expression of genes involved in pectin degradation. *BMC Plant Biol.* 10:163. doi: 10.1186/1471-2229-10-163
- Dongdong, L., Li, L., Luo, Z., Mou, W., Mao, L., and Yieng, T. (2015). Comparative transcriptomic analysis reveals the influence of abscisic acid on the metabolism of pigments, ascorbic acid and folic acid during strawberry fruit ripening. *PLoS ONE* 10:e0130037. doi: 10.1371/journal.pone.0130037
- Endres, S., and Tenhaken, R. (2009). Myoinositol oxygenase controls the level of myoinositol in *Arabidopsis*, but does not increase ascorbic acid. *Plant Physiol.* 149, 1042–1049. doi: 10.1104/pp.108.130948
- Eshed, Y., and Zamir, D. (1995). An introgression line population of *Lycopersicon pennellii* in the cultivated tomato enables the identification and fine mapping of yield-associated QTL. *Genetics* 141, 1147–1162.
- Fantini, E., Falcone, G., Frusciante, S., Giliberto, L., and Giuliano, G. (2013). Dissection of tomato lycopene biosynthesis through virus-induced gene silencing. *Plant Physiol.* 163, 986–998. doi: 10.1104/pp.113.224733
- Fei, Z., Joung, J. G., Tang, X., Zheng, Y., Huang, M., Lee, J. M., et al. (2010). Tomato functional genomics database: a comprehensive resource and analysis package for tomato functional genomics. *Nucleic Acids Res.* 39, D1156–D1163. doi: 10.1093/nar/gkq991
- Fernie, A. R., Tadmor, Y., and Zamir, D. (2006). Natural genetic variation for improving crop quality. *Curr. Opin. Plant Biol.* 9, 196–202. doi: 10.1016/j.pbi.2006.01.010
- Fotopoulos, V., De Tullio, M. C., Barnes, J., and Kanellis, A. K. (2008). Altered stomatal dynamics in ascorbate oxidase over-expressing tobacco plants suggest a role for dehydroascorbate signalling. *J. Exp. Bot.* 59, 729–737. doi: 10.1093/jxb/erm359
- Fotopoulos, V., Sanmartin, M., and Kanellis, A. K. (2006). Effect of ascorbate oxidase over-expression on ascorbate recycling gene expression in response to agents imposing oxidative stress. *J. Exp. Bot.* 57, 3933–3943. doi: 10.1093/jxb/erl147
- Friedman, M. (2013). Anticarcinogenic, cardioprotective, and other health benefits of tomato compounds lycopene, α -tomatine, and tomatidine in pure form and in fresh and processed tomatoes. *J. Agric. Food Chem.* 61, 9534–9550. doi: 10.1021/jf402654e
- Gallie, D. R. (2013). L-Ascorbic acid: a multifunctional molecule supporting plant growth and development. *Scientifica* 2013:795964. doi: 10.1155/2013/795964
- Garchery, C., Gest, N., Do, P. T., Alhagdow, M., Baldet, P., Menard, G., et al. (2013). A diminution in ascorbate oxidase activity affect carbon allocation and improves yield in tomato under water deficit. *Plant Cell Environ.* 36, 159–175. doi: 10.1111/j.1365-3040.2012.02564.x
- Ghassemian, M., Lutes, J., Chang, H. S., Lange, I., Chen, W., Zhu, T., et al. (2008). Abscisic acid-induced modulation and redox control pathways in *Arabidopsis thaliana*. *Phytochemistry* 69, 2899–2911. doi: 10.1016/j.phytochem.2008.09.020
- Giuliano, G. (2014). Plant carotenoids: genomics meets multi-gene engineering. *Curr. Opin. Plant Biol.* 19, 111–117. doi: 10.1016/j.pbi.2014.05.006
- Hayashi, E., You, Y., Lewis, R., Calderon, M. C., Wan, G., and Still, D. W. (2012). Mapping QTL, epistasis and genotype \times environment interaction of antioxidant activity, chlorophyll content and head formation in domesticated lettuce (*Lactuca sativa*). *Theor. Appl. Genet.* 124, 1487–1502. doi: 10.1007/s00122-012-1803-0
- Kandianis, C. B., Stevens, R., Liu, W., Palacios, N., Montgomery, K., Pixley, K., et al. (2013). Genetic architecture controlling variation in grain carotenoid composition and concentrations in two maize populations. *Theor. Appl. Genet.* 126, 2879–2895. doi: 10.1007/s00122-013-2179-5
- Laing, W. A., Martinez-Sanchez, M., Wright, M. A., Bulley, S. M., Brewster, D., Dare, A. P., et al. (2015). An upstream Open Reading Frame is essential for feedback regulation of ascorbate biosynthesis in *Arabidopsis*. *Plant Cell* 27, 772–786. doi: 10.1105/tpc.114.133777
- Lima-Silva, V., Rosado, A., Amorim-Silva, V., Muñoz-Mérida, A., Pons, C., Bombarely, A., et al. (2012). Genetic and genome-wide transcriptomic analyses identify co-regulation of oxidative response and hormone transcript abundance with vitamin C content in tomato fruit. *BMC Genomics* 13:187. doi: 10.1186/1471-2164-13-187
- Lippman, Z. B., Semel, Y., and Zamir, D. (2007). An integrated view of quantitative trait variation using tomato interspecific introgression lines. *Curr. Opin. Genet. Dev.* 17, 545–552. doi: 10.1016/j.gde.2007.07.007
- Lisko, K. A., Aboobucker, S. I., Torres, R., and Lorence, A. (2014). “Engineering elevated vitamin C content in plants to improve their nutritional content, growth, and tolerance to abiotic stress,” in *Phytochemicals-Biosynthesis, Function and Application, Recent Advances in Phytochemistry* 44, ed. R. Jetter (Berlin: Springer International Publishing Switzerland), 109–128.
- Livak, K. J., and Schmittgen, T. D. (2001). Analysis of relative gene expression data using real-time quantitative PCR and the $2^{-\Delta \Delta CT}$. *Methods* 25, 402–408. doi: 10.1006/meth.2001.1262
- Lopez-Carbonell, M., Munné-Bosch, S., and Alegre, L. (2006). The ascorbate-deficient vtc-1 *Arabidopsis* mutant shows altered ABA accumulation in leaves and chloroplast. *J. Plant Growth Regulat.* 25, 137–144. doi: 10.1007/s00344-005-0119-6
- Mueller, L. A., Solow, T., Taylor, N., Skwarecki, B., Buels, R., Binns, J., et al. (2005). The SOL Genomics Network. A comparative resource for Solanaceae biology and beyond. *Plant Physiol.* 138, 1310–1317. doi: 10.1104/pp.105.060707
- Nair, V. D., Cheruth, A. J., Gopi, R., Gomathinayagam, M., and Panneerselvam, R. (2009). Antioxidant potential of *Ocimum sanctum* under growth regulator treatments. *Eur. Asian J. Biosci.* 3, 1–9. doi: 10.5053/ejobios.2009.3.0.1
- Pignocchi, C., Fletcher, J. M., Wilkinson, J. E., Barnes, J. D., and Foyer, C. H. (2003). The function of ascorbate oxidase in tobacco. *Plant Physiol.* 132, 1631–1641. doi: 10.1104/pp.103.022798
- Raiola, A., Rigano, M. M., Calafiole, R., Frusciante, L., and Barone, A. (2014). Enhancing the health-promoting effects of tomato fruit for biofortified food. *Mediat. Inflamm.* 2014, 1–16. doi: 10.1155/2014/139873
- Rigano, M. M., Raiola, A., Tenore, G. C., Monti, D. M., Del Giudice, R., Frusciante, L., et al. (2014). Quantitative trait loci pyramiding can improve the nutritional potential of tomato (*Solanum lycopersicum*) fruits. *J. Agric. Food Chem.* 62, 11519–11527. doi: 10.1021/jf502573n
- Sacco, A., Di Matteo, A., Lombardi, N., Trotta, N., Punzo, B., Mari, A., et al. (2013). Quantitative trait loci pyramiding for fruit quality traits in tomato. *Mol. Breed.* 31, 217–222. doi: 10.1007/s11032-012-9763-2
- Sanmartin, M., Drogoudi, P. A., Lyons, T., Pateraki, I., Barnes, J., and Kanellis, A. K. (2003). Over-expression of ascorbate oxidase in the apoplast of transgenic tobacco results in altered ascorbate and glutathione redox states and increased sensitivity to ozone. *Planta* 216, 918–928.
- Schmittgen, T. D., Jiang, J., Liu, Q., and Yang, L. (2004). A high-throughput method to monitor the expression of microRNA precursors. *Nucleic Acids Res.* 32, 43. doi: 10.1093/nar/gnh040
- Stevens, R., Buret, M., Duffe, P., Garchery, C., Baldet, P., Rothan, C., et al. (2007). Candidate genes and Quantitative Trait Loci affecting fruit ascorbic acid content in three tomato populations. *Plant Physiol.* 143, 1943–1953. doi: 10.1104/pp.106.091413
- Stevens, R., Buret, M., Garchery, C., Carretero, Y., and Causse, M. (2006). Technique for rapid small-scale analysis of vitamin C levels in fruit and application to a tomato mutant collection. *J. Agric. Food Chem.* 54, 6159–6165. doi: 10.1021/jf061241e
- Sun, L., Yuan, B., Zhang, M., Wang, L., Cui, M., Wang, Q., et al. (2012). Fruit-specific RNAi-mediated suppression of SINCED1 increases both lycopene and β -carotene contents in tomato fruit. *J. Exp. Bot.* 63, 3097–3108. doi: 10.1093/jxb/ers026
- Suresh, B. V., Roy, R., Sahu, K., Misra, G., and Chattopadhyay, D. (2014). Tomato Genomic Resources Database: an integrated repository of useful

- tomato genomic information for basic and applied research. *PLoS ONE* 9:86387. doi: 10.1371/journal.pone.0086387
- Tomato Genome Consortium (2012). The tomato genome sequence provides insight into fleshy tomato. *Nature* 485, 635–641. doi: 10.1038/nature11119
- Torabinejad, J., Donahue, J. L., Gunesekera, B. N., Allen-Daniels, M. J., and Gillaspy, G. E. (2009). VTC4 is a bifunctional enzyme that affects myoinositol and ascorbate biosynthesis in plants. *Plant Physiol.* 150, 951–961. doi: 10.1104/pp.108.135129
- Valpuesta, V., and Botella, M. A. (2004). Biosynthesis of L-ascorbic acid in plants: new pathways for an old antioxidant. *Trends Plant Sci.* 9, 573–577. doi: 10.1016/j.tplants.2004.10.002
- Wang, J., Yu, Y., Zhang, Z., Quan, R., Zhang, H., Ma, L., et al. (2013). Arabidopsis CSN5B interacts with VTC1 and modulates ascorbic acid synthesis. *Plant Cell* 25, 626–636. doi: 10.1105/tpc.112.106880
- Wellburn, A. R. (1994). The spectral determination of chlorophylls a and b, as well as total carotenoids, using various solvents with spectrophotometers of different resolution. *J. Plant Physiol.* 144, 307–313. doi: 10.1016/S0176-1617(11)81192-2
- Winer, J., Jung, C. K., Shackel, I., and Williams, P. M. (1999). Development and validation of real-time quantitative reverse transcriptase-polymerase chain reaction for monitoring gene expression in cardiac myocytes in vitro. *Anal. Biochem.* 270, 41–49. doi: 10.1006/abio.1999.4085
- Yamamoto, A., Bhuiyan, M. N., Waditee, R., Tanaka, Y., Esaka, M., Oba, K., et al. (2005). Suppressed expression of the apoplastic ascorbate oxidase gene increases salt tolerance in tobacco and *Arabidopsis* plants. *J. Exp. Bot.* 56, 1785–1796. doi: 10.1093/jxb/eri167
- Ye, J., Hu, T., Yang, C., Li, H., Yang, M., Ijaz, R., et al. (2015). Transcriptome profiling of tomato fruit development reveals transcription factors associated with ascorbic acid, carotenoid and flavonoid biosynthesis. *PLoS ONE* 10:e0130885. doi: 10.1371/journal.pone.0130885
- Yuan, H., Zhang, J., Nageswaran, D., and Li, L. (2015). Carotenoid metabolism and regulation in horticultural crops. *Hort. Res.* 2, 15036. doi: 10.1038/hortres.2015.36
- Zdobnov, E. M., and Apweiler, R. (2001). InterProScan—an integration platform for the signature-recognition methods in InterPro. *Bioinformatics* 17, 847–848. doi: 10.1093/bioinformatics/17.9.847
- Zhang, M., Yuan, B., and Leng, P. L. (2009). The role of ABA in triggering ethylene biosynthesis and ripening of tomato fruit. *J. Exp. Bot.* 60, 1579–1588. doi: 10.1093/jxb/erp026
- Zhang, Y. (2012). *Ascorbic Acid in Plants: Biosynthesis, Regulation and Enhancement*. Berlin: Springer Science & Business Media.
- Zhang, Y., Li, H., Shu, W., Zhang, C., Zhang, W., and Ye, Z. (2011). Suppressed expression of ascorbate oxidase gene promotes ascorbic acid accumulation in tomato fruit. *Plant Mol. Biol. Rep.* 29, 638–645. doi: 10.1007/s11105-010-0271-4
- Zouari, I., Salvioli, A., Chialva, M., Novero, M., Miozzi, L., Tenore, G. C., et al. (2014). From root to fruit: RNA-Seq analysis shows that arbuscular mycorrhizal symbiosis may affect tomato fruit metabolism. *BMC Genomics* 15:221. doi: 10.1186/1471-2164-15-221

Conflict of Interest Statement: The authors declare that the research was conducted in the absence of any commercial or financial relationships that could be construed as a potential conflict of interest.

Copyright © 2016 Calafiore, Ruggieri, Raiola, Rigano, Sacco, Hasson, Frusciante and Barone. This is an open-access article distributed under the terms of the Creative Commons Attribution License (CC BY). The use, distribution or reproduction in other forums is permitted, provided the original author(s) or licensor are credited and that the original publication in this journal is cited, in accordance with accepted academic practice. No use, distribution or reproduction is permitted which does not comply with these terms.



Exploring New Alleles Involved in Tomato Fruit Quality in an Introgression Line Library of *Solanum pimpinellifolium*

Walter Barrantes^{1,2}, Gloria López-Casado³, Santiago García-Martínez⁴, Aranzazu Alonso⁴, Fernando Rubio⁴, Juan J. Ruiz⁴, Rafael Fernández-Muñoz³, Antonio Granell¹ and Antonio J. Monforte^{1*}

¹ Instituto de Biología Molecular y Celular de Plantas, Consejo Superior de Investigaciones Científicas, Polytechnic University of Valencia, Valencia, Spain, ² Estación Experimental Agrícola Fabio Baudrit Moreno, Universidad de Costa Rica, Alajuela, Costa Rica, ³ Instituto de Hortofruticultura Subtropical y Mediterránea "La Mayora", Consejo Superior de Investigaciones Científicas, University of Málaga, Algarrobo-Costa, Spain, ⁴ Departamento de Biología Aplicada, Escuela Politécnica Superior de Orihuela, Universidad Miguel Hernández, Orihuela, Spain

OPEN ACCESS

Edited by:

Soren K. Rasmussen,
University of Copenhagen, Denmark

Reviewed by:

Andrea Mazzucato,
Tuscia University, Italy
Paul Christiaan Struik,
Wageningen University and Research
Centre, Netherlands

***Correspondence:**

Antonio J. Monforte
amonforte@ibmcp.upv.es

Specialty section:

This article was submitted to
Crop Science and Horticulture,
a section of the journal
Frontiers in Plant Science

Received: 23 March 2016

Accepted: 21 July 2016

Published: 17 August 2016

Citation:

Barrantes W, López-Casado G, García-Martínez S, Alonso A, Rubio F, Ruiz JJ, Fernández-Muñoz R, Granell A and Monforte AJ (2016) Exploring New Alleles Involved in Tomato Fruit Quality in an Introgression Line Library of *Solanum pimpinellifolium*. *Front. Plant Sci.* 7:1172.
doi: 10.3389/fpls.2016.01172

We have studied a genomic library of introgression lines from the *Solanum pimpinellifolium* accession TO-937 into the genetic background of the "Moneymaker" cultivar in order to evaluate the accession's breeding potential. Overall, no deleterious phenotypes were observed, and the plants and fruits were phenotypically very similar to those of "Moneymaker," which confirms the feasibility of translating the current results into elite breeding programs. We identified chromosomal regions associated with traits that were both vegetative (plant vigor, trichome density) and fruit-related (morphology, organoleptic quality, color). A trichome-density locus was mapped on chromosome 10 that had not previously been associated with insect resistance, which indicates that the increment of trichomes by itself does not confer resistance. A large number of quantitative trait loci (QTLs) have been identified for fruit weight. Interestingly, fruit weight QTLs on chromosomes 1 and 10 showed a magnitude effect similar to that of QTLs previously defined as important in domestication and diversification. Low variability was observed for fruit-shape-related traits. We were, however, able to identify a QTL for shoulder height, although the effects were quite low, thus demonstrating the suitability of the current population for QTL detection. Regarding organoleptic traits, consistent QTLs were detected for soluble solid content (SSC). Interestingly, QTLs on chromosomes 2 and 9 increased SSC but did not affect fruit weight, making them quite promising for introduction in modern cultivars. Three ILs with introgressions on chromosomes 1, 2, and 10 increased the internal fruit color, making them candidates for increasing the color of modern cultivars. Comparing the QTL detection between this IL population and a recombinant inbred line population from the same cross, we found that QTL stability across generations depended on the trait, as it was very high for fruit weight but low for organoleptic traits. This difference in QTL stability may be due to a predominant additive gene action for QTLs involved in fruit weight, whereas epistatic and genetic background interactions are most likely important for the other traits.

Keywords: quantitative trait loci (QTL), germplasm, wild species, mapping, genotype by environment interaction

INTRODUCTION

Cultivated tomato, *Solanum lycopersicum* L., has undergone two domestication steps during its history (Blanca et al., 2012, 2015). The first domestication occurred early on in Ecuador and northern Peru, and was most likely carried out by ancient farmers on *Solanum pimpinellifolium* L. and/or *S. lycopersicum* var. *cerasiforme*. The second step most likely took place in Mesoamerica due to migrated pre-domesticated tomatoes. Spanish conquistadors brought the tomato from Mesoamerica to Europe, and from there it was spread all around the world. One consequence of this process was dramatic genetic erosion, caused especially by the bottleneck during the migration from the Andean regions to Mesoamerica. Early research (Williams and Clair, 1993) showed a much higher diversity in Andean *S. pimpinellifolium* and *S. lycopersicum* var. *cerasiforme* populations than among Mesoamerican cultivars, and this has been supported by recent high density single nucleotide polymorphism (SNP) variability analysis (Blanca et al., 2015). Therefore, accessions originating anywhere from the Andes to Mesoamerica will most certainly prove to be an important source of useful genetic diversity for tomato breeding.

After the introduction of tomato into Europe, intense breeding efforts were carried out in order to increase yield, adaptation, stability, and disease resistance (Bai and Lindhout, 2007). Despite these common objectives, the breeding goals changed over time due to the requirements of specific markets and uses. During the 1970 and 1980s, one of the most important breeding objectives, especially for fresh-market tomatoes, was to increase yield and shelf life. Both breeding objectives resulted in improved external quality, although at the expense of internal fruit quality. During the following decade, taste became the main breeding objective. Sugars, acids and more than 30 volatile compounds are known to influence tomato flavor (Tieman et al., 2012; Rambla et al., 2014). Organoleptic quality is a very complex trait as it depends on the evolving preferences of the market. Even so, significant improvement in tomato flavor seems possible by increasing the fruit sugar and acid contents and by modifying the balance between the two (Stevens et al., 1977). Wild species have mostly been used to introduce resistance genes, thus increasing the genetic diversity of modern cultivars compared to vintage cultivars (Sim et al., 2009, 2011, 2012).

The complex polygenic control of tomato fruit quality traits involves multiple quantitative trait loci (QTLs; Labate et al., 2007). Interestingly, favorable effects on fruit quality have been identified in wild species, such as *S. pimpinellifolium*, *Solanum pennellii*, *Solanum cheesmaniae*, and *Solanum habrochaites* (Eshed and Zamir, 1995; Bernacchi et al., 1998; Monforte et al., 2001; Fulton et al., 2002; Lippman et al., 2007), even though the fruits of these species are not usually consumed by humans. The exploitation of these QTLs in practical breeding has been very limited because of the inherent difficulties in implementing marker-assisted selection (MAS) for QTLs (Collard and Mackill, 2008) in addition to deleterious linkage drag. Nevertheless, a few successful studies have been reported (Gur and Zamir, 2004).

Both advanced backcross and introgression lines (ILs) may be used to facilitate the incorporation of genetic variability from wild species (Eshed and Zamir, 1995; Tanksley et al., 1996). ILs are developed by MAS and contain a unique chromosome fragment from a donor genotype (usually a wild species or unadapted germplasm) in a uniform elite genetic background. These collections are also called “genomic libraries of ILs” when the whole genome of the donor genotype is represented among the introgressions.

In tomato, ILs have been developed from *S. pennellii* LA0716 (Eshed and Zamir, 1994), *S. habrochaites* LA1777 (Monforte and Tanksley, 2000a), *Solanum lycopersicoides* LA 2951 (Chetelat and Meglic, 2000; Canady et al., 2005), *S. habrochaites* LA0407 (Francis et al., 2001) and *S. habrochaites* LYC4 (Finkers et al., 2007). In addition, a small number of ILs have been developed for the *S. pimpinellifolium* accessions LA1589 (Tanksley et al., 1996; Bernacchi et al., 1998) and LA2093 (Kinkade and Foolad, 2013). IL collections are extremely useful for identifying QTLs (Eshed and Zamir, 1995; Rousseaux et al., 2005), verifying QTL effects (Tanksley et al., 1996), studying QTL x environmental, QTL x genetic background and QTL x QTL interactions (Monforte et al., 2001), QTL fine mapping (Eshed and Zamir, 1996; Ku et al., 2000; Monforte and Tanksley, 2000b; Ashrafi et al., 2012) and introducing new genetic variability from wild species into elite germplasm (Tanksley and McCouch, 1997; Zamir, 2001; Gur and Zamir, 2004). IL analysis is also a powerful tool for genomics research, as it facilitates the study of the genetic basis of metabolome (Schauer et al., 2006), transcriptome and its correlation with metabolome (Lee et al., 2012), enzyme activity (Steinhauser et al., 2011) and QTL cloning (Frary et al., 2000; Fridman et al., 2000; Liu et al., 2002). The most widely used IL collection is the *S. pennellii* LA 0716 collection, which has facilitated the identification of more than 2,700 QTLs involved in agronomical important characters (Lippman et al., 2007).

The development of IL collections has traditionally required intense effort spanning several years (Eshed and Zamir, 1994; Eduardo et al., 2005). Barrantes et al. (2014) applied high-throughput genotyping in an IL breeding program, demonstrating that IL libraries can now be produced with far less effort at a lower cost. The IL population thus produced was derived from a cross between the cultivar Moneymaker (*S. lycopersicum*) and the *S. pimpinellifolium* accession TO-937. This accession is from Peru, i.e., the region where the tomato most likely underwent its first domestication step. It is therefore a quite suitable accession for introducing new genetic variability into the cultivated tomato genetic pool. Previous works have demonstrated that TO-937 harbors genetic variability that is of interest for breeding purposes, such as enhancing ascorbic acid (Lima-Silva et al., 2012), sugar, organic acid and carotenoid fruit content (Capel et al., 2015), as well as modifying aroma volatile compounds (Rambla et al., 2014) and resistance to pests (Fernández-Muñoz et al., 2000; Silva et al., 2014). Furthermore, populations derived from this accession were used to map the *Uniform ripening* (*U*) locus (Powell et al., 2012). In the current report, we present a thorough phenotypic characterization of this IL library, focusing mainly on fruit traits and the characterization

of QTLs involved in fruit quality as the first step in introducing new genetic variability into the elite tomato gene pool.

MATERIALS AND METHODS

Plant Material

A complete genomic library of 54 ILs derived from a cross between the wild *S. pimpinellifolium* (SP) accession TO-937 as a donor parent, obtained from the Instituto de Hortofruticultura Subtropical y Mediterránea “La Mayora” (IHSM-UMA-CSIC) germplasm bank, and the cultivar “Moneymaker” (*S. lycopersicum*) as recurrent parent (hereafter referred to as MM, Barrantes et al., 2014) were studied in the current report. In brief, each IL contains an average of 3.7% of the SP genome (range: 0.5–7.7%), altogether covering 98.8% of the donor parent genome, with an average introgression size of 25 Mb (ranging from 0.7 to 75 Mb). IL evaluation was performed during the spring-summer of 2013 at three locations in Spain: Alginet, Valencia (Agricultural Cooperative Alginet Coagri), School of Engineering of Orihuela, Alicante (Miguel Hernández University) and Algarrobo-Costa, Málaga (IHSM-UMA-CSIC). All three locations are on the Mediterranean coast of Spain, and, therefore, have similar weather conditions. ILs were grown in plastic greenhouses following a randomized complete block design with eight blocks, each containing one replicate per IL and six replicates of MM. In the first through seventh blocks, each replicate had a single plant, whereas in the eighth block each replicate consisted of three plants. The eighth block was used to better distinguish categorical traits between the ILs and MM.

Phenotypic Analysis

Traits were classified into two categories: descriptive and quantitative traits. Descriptive traits were only evaluated in block 8, as each replicate consisted of three plants, which made it easier to observe the differences between the ILs and MM categorically. This group of traits included: vigor (VIG), as the height of the plant at first fruit set expressed in cm; purple (PURP), as the presence or absence of anthocyanin coloration in branches and stems; trichomes (TRI), visually observed long trichome density on stems with a scale of: 0 = absence, 1 = low, 2 = medium, and 3 = high; and earliness (EAR), as days from transplanting to first ripe fruit and presence/absence of dark green shoulder (GS) on breaker fruit. Quantitative fruit traits were evaluated on four fruits harvested at light-red stage, selected from a large sample of fruits for being the most representative as regards homogeneity in maturity and size. A single sample per plant was obtained for blocks 1–7, whereas a pooled sample of three plants was obtained in block 8. Each fruit was weighted (FW in grams) and the external color (EC) was recorded at three points in the equatorial region of the tomato fruit using a Minolta Chroma Meter model CR-400 (Konica Minolta, Inc., Tokyo, Japan), applying the CIE Lab color space, where higher +a* indicates red and lower -a* indicates green, whereas higher b* indicates yellow and lower b* green. The color space is three-dimensional, where

the third axis, L*, represents black to white and the a*-b* plane may be visualized as a color wheel that is lighter or darker depending on the level of L*. Lower L* values represent a darker color. Chroma (C*), a measure of color saturation, was calculated using the formula: $(a^{*2}+b^{*2})^{1/2}$. Hue-angle (H), in degrees, is the measurement of an object's color in the a*-b* plane and was calculated as $(180/p) \cdot \cos^{-1}(a^*/C^*)$ for the positive values of b* obtained. Perception of hue angle differences depends on the chroma, with the differences being more detectable at higher chroma (Sacks and Francis, 2001). After longitudinal cutting, fruits were scanned at 300 dots per inch (dpi). The images were saved as jpeg files and imported into Tomato Analyzer 3.0 software for automated phenotypic analysis¹. Fruit morphology descriptors were following Brewer et al. (2006): maximum diameter (FD, in cm), max length (FL, in cm) fruit shape: fruit shape index (FS), fruit shape circular (CIR), shoulder height (PSH, that is a measurement of the indentation of peduncle scar at the proximal end of the fruit). For internal color (IC), the Tomato Analyzer color module was calibrated with a scanned X-Rite Color Checker card. Images were previously processed with Photoshop CS5 v. 12. (Adobe Systems Incorporated, San Jose, CA, USA) in order to save an image of the same fragment of pericarp tissue in each fruit. Finally, CIELab color parameters were obtained using Tomato Analyzer (Darrigues et al., 2008). The organoleptic traits, such as soluble solid content (SSC), pH (PH), and titratable acidity (TA) were analyzed from tomato pericarp tissue from four fruits ground and stored at -20°C. Samples were thawed and centrifuged at 3500 rpm for 10 min, an aliquot of supernatant was used for measuring SSC (expressed in °Brix) using a digital refractometer (Atago CO LTD, Tokyo, Japan) and PH and TA (expressed in percentage of citric acid) were determined from 1 ml of the supernatant homogenized juice with the electronic analyzer PH-Matic23 (CRISON, Barcelona, Spain).

Statistical Analyses

For each trait, the genetic (G), location (L) and interaction (G-x-L) effects were estimated by two-way ANOVA. Heritability was estimated by one-way ANOVA in each locality (G-x-L was significant for nearly all traits, see below) as $h^2 = V_g/V_t$ (where V_g represents genetic variance, estimated as the variance among genotypes, and V_t represents total variance). Pearson's correlation coefficients among traits were calculated in each location. IL and control MM means were compared by a Dunnet's test at $p < 0.05$. Only ILs that were significantly different from MM in at least two locations were considered for QTL assignment. QTLs were mapped in the chromosome regions that were covered by the TO-937 introgressions in the ILs that showed significant effects on the trait under study. In those cases where the means of two ILs with overlapping introgressions were significantly different from MM, a contrast test was performed between those ILs. When IL means were not different, the QTL was assumed to be located in the overlapping regions; when the means were different, two QTLs were assumed. All statistical

¹<http://oardc.ohio-state.edu/vanderknaap/>

analyses were performed with JMP v. 11 (SAS Institute, Cary, NC, USA).

RESULTS

Recurrent Parent (MM)

The trait means and standard deviations of parental MM at the three locations are presented in Supplementary Table S1. No significant differences in FW were found between locations, with the average being 98.1 g, whereas other fruit dimension traits such as FL and FD showed significant differences ($p \leq 0.01$), with higher values in Málaga. Shape-related traits showed statistically significant differences among locations ($p \leq 0.01$), except for FS. Significant differences for organoleptic traits (SSC, PH, and TA) and color traits (IC and EC) were also found among locations.

Introgression Lines and QTL Mapping

In general, the phenotypes of both plant and fruit were very similar to the phenotypes of the recurrent MM. Only in very few cases did we observe extreme phenotypes. A thorough description of the phenotypes and the QTL mapping can be found below. In Supplementary Table S2, a summary of the comparison of each IL with MM across all locations is also shown.

Descriptive Traits

During the cultivation of the IL collection, several phenotypic characteristics that were consistent in at least two locations were clearly observed (Supplementary Figure S1). ILs SP_2-4 and SP_2-5 showed fast vegetative growth, defining a locus for plant vigor (*vig2.1*). SP_3-1, on the other hand, suffered such a drastic reduction of plant growth that it did not set fruits in two locations, which, in turn, permitted to define another locus (*vig3.1*). Furthermore, SP_5-2 and SP_5-3 displayed purple shoots, probably due to anthocyanin accumulation (*purp5.1*). SP_10-3, meanwhile, had denser trichomes (*tri10.1*) than MM. IL_2-5 set the first ripe fruit 8 days earlier than MM (*ear2.1*), whereas, IL_11-4 produced the first ripe fruit 8–13 days after MM (*ear11.1*). IL_10-1 and IL_10-2 had fruits with dark GSs at the breaker stage (*gs10.1*).

Fruit Size

The average FW of the whole IL collection across trials was 11.3% lower than MM (around 98 g per fruit, **Table 1**). The range was between 47.81 and 117.86 g (SP_3-3 and SP_12-5, respectively). FW was strongly correlated with its trait components: fruit length (FL) and fruit diameter (FD; $r > 0.5$, Supplementary Table S3). The effect of the genotype (G) was 35% of total variance; whereas the effects of the location (L) and the interaction (G-x-L) were lower than G effects, 19 and 5%, respectively (**Table 1**). FW was the trait with higher heritability (h^2 range: 0.62–0.45, Supplementary Table S4). As a general rule, introgressions from SP had a negative effect on FW, except for SP_12-5, which increased FW 20% (**Figure 1**; Supplementary Figure S2). Three ILs (SP_1-2, SP_2-5, and SP_3-3) showed the most consistent effects among locations, and, on average, reduced FW by up to more than 40% in some locations. Fourteen additional ILs with

consistent effects on FW allowed us to define a total of 12 QTLs: *fw1.1*, *fw1.2*, *fw2.1*, *fw2.2*, *fw3.1*, *fw3.2*, *fw4.1*, *fw4.2*, *fw7.1*, *fw10.1*, *fw11.1*, and *fw12.1* (**Table 2**).

Fruit Shape-Related Traits

The fruit shape index (FS) showed a relatively modest variability in the IL collection, as the fruits were nearly round, just like MM (both the IL population and MM had the same mean value of FS = 0.89), ranging from 0.82 (SP_6-2) to 0.93 (SP_4-2), being the G effect 23% of total variance (**Table 1**). FS was negatively correlated with FD ($r = -0.35$, Supplementary Table S3) and positively with FL, but to a lesser extent ($r = 0.27$), indicating that FD is the most important determinant of the variation in FS in this population. Heritability ranged from 0.48 to 0.29 (Supplementary Table S4). SP_6-2, SP_4-2, and SP_10-5 showed consistent effects on FS. Three QTLs were defined with opposite effects: *fs6.1* and *fs10.1*, which induced flattened fruits, and *fs4.1*, which induced more elongated fruits (**Figure 2**; **Table 2**).

The variability of circular fruit shape (CIR) was also low, being G effect 26% of total variance (**Table 1**), with an average value of 0.06 for the IL collection (the same value as MM, **Table 1**), ranging from 0.04 to 0.08 (SP_2-5 and SP_10-5, respectively). CIR clearly showed a high correlation (Supplementary Table S3) with FD ($r = 0.48$) but not with FL ($r = -0.02$), which supports the previous observation that FD is the principal determinant of FS variability in this population. Heritability was similar to FS, ranging from 0.47 to 0.35 (Supplementary Table S4). Additionally, SP_6-2 also increased CIR, making a total of three QTLs: *cir2.1* induced up to 26% rounder fruit, while *cir6.1* and *cir10.1* induced 42% less round fruit on average (**Figure 2**; **Table 2**).

PSH averages were the same for both the ILs and MM (0.06), with a very low G effect and the L effect being the most important one, 6 and 27% of total variance, respectively (**Table 1**). Heritability was also a little bit lower than previous fruit shape traits, ranging from 0.30 to 0.35 (Supplementary Table S4). Despite the low G effect, ILs SP_1-2 and SP_3-3 showed statistically significant differences as compared to MM in all three locations, reducing PSH by as much as 42% (**Table 2**). Two stable QTLs were defined as a result: *psh1.1* and *psh3.1* (**Figure 2**).

Organoleptic Related Characters

The average SSC in the IL collection was similar to that of MM (4.48 ° Brix), although the range was wide, from 3.85° to 5.1 Brix° (SP_4-3 and SP_10-6, respectively). The G effect was 29% of total variance, whereas L effect and G-x-L interaction represented 9% of total variance both of them (**Table 1**). Interestingly, correlations between SSC and fruit size and other fruit morphology-related traits were very low and non-significant ($r < 0.1$, Supplementary Table S3). Heritability was near 0.5 (Supplementary Table S4). SP_3-3 increased SSC in all three trials, whereas four additional ILs increased it in two trials (**Figure 1**; **Table 2**). On the other hand, SP_4-3 and SP_5-2 decreased SSC by 13 and 8%, respectively. A total of six consistent QTLs were defined with opposite effects: *ssc2.1*, *ssc2.2*, *ssc3.1*, and *ssc9.1* increased SSC by up to 13%, whereas *ssc4.1* and *ssc5.1* decreased SSC by up to 12% (**Table 2**; **Figure 2**).

TABLE 1 | Trait mean values [fruit weight (FW), diameter (FD), length (FL), shape (FS), circular shape (CIR), shoulder height (PSH), soluble solid content (SSC), pH (PH), titrable acidity (TA)] and the internal and external CIELab color system variables L*, a*, b*, C* and H for the whole Introgression Line (IL) collection and the recurrent parent Moneymaker (MM).

*	Trait acronyms	Means		Effects (%)		
		ILs	MM	Genotype	Location	Genotype-x-location
Size	FW (g)	86.23	98.18	35**	19**	5**
	FD (cm)	5.71	5.99	30**	26**	5*
	FL (cm)	5.05	5.29	35**	20**	5*
Shape	FS	0.89	0.88	23**	9**	9**
	CIR	0.06	0.06	26**	15**	Ns
	PSH	0.04	0.04	6**	57**	4**
Organoleptic	SSC (°Brix)	4.48	4.45	29**	9**	9**
	PH	4.23	4.42	7**	58**	3**
	TA (% citric acid)	0.29	0.29	12**	44**	5**
External color	L	40.06	40.04	6**	59**	4**
	a	22.22	22.45	20**	37**	8**
	b	23.76	23.81	15**	24**	8**
	C	32.71	32.98	16**	38**	7**
	H	46.85	46.71	22**	7**	12**
Internal color	L	39.2	39.52	11**	26**	12**
	a	24.72	24.16	7**	50**	7**
	b	27.41	27.5	14**	1**	13**
	C	37.08	36.81	10**	37**	9**
	H	48.42	49.07	7**	42**	7**

The genetic (G) and location (L) effects and their interaction (G-x-L) were estimated by two-way ANOVA and expressed as a percentage (%) of the total variance, with ns being non-significant, and * $p < 0.05$ and ** $p < 0.001$, respectively.

The average TA and PH of the fruits of the IL collection were similar to those of MM (0.29 and 4.6, respectively). For both traits, the G effect was 12%, whereas L effect was the most important (44%, **Table 1**), indicating a low genetic variability for this trait in the current population. Correlations with other traits were generally low, except for SSC, which was relatively important ($r = 0.44$, Supplementary Table S3). Heritability ranged from 0.2 to 0.48 (Supplementary Table S4). Only SP_2-4 showed a significant TA decrease of 17% compared with MM in all three trials, defining the QTL *ta2.1* on chromosome 2 (**Figures 1 and 2; Table 2**).

Fruit Color

External color average values were very similar between the ILs and MM. The G effect was low for L*, b* and C* (6–16%), moderate for a* and H (>20%, **Table 1**), and the L effect was important in most of them (>24% of total variance, $p < 0.001$). Meanwhile, interaction G-x-L was generally lower than 12% of total variance. EC positively correlated moderately with fruit size ($r \sim 0.2$, $p = 0.004$, Supplementary Table S3) and negatively with the organoleptic traits SSC and TA ($r < 0.4$, $p = 0.004$). Heritability ranged from 0.23 to 0.55 (Supplementary Table S4). Three ILs, SP_2-1, SP_2-3 and SP_7-3, showed significant differences in the a* color component, defining the QTLs *ec_a*2.1* and *ec_a*7.1* (**Figure 1**), associated in both cases with a reduction of the color red (**Figure 2; Table 2**).

Internal color average values were very similar between the ILs and MM, except for the components C* and H, which were

slightly higher or slightly lower in the IL collection, respectively. The G effects represented between 7 and 14 of the total variance, being the L effect was higher in most cases (>26%), with the exception of b* (**Table 1**). The interaction G-x-L for IC components ranged from 7 to 13% of total variance (**Table 1**). No high correlation values between IC and the other traits were detected (Supplementary Table S3). ILs SP_1-2, SP_5-2, SP_10-2 increased the H, L* and a* components, respectively, whereas SP_2-5 decreased L* (**Figure 1**). Heritability ranged from 0.23 to 0.44 (Supplementary Table S4). A total of four QTLs were defined: *ic_a*2.1* and *ic_a*10.1*, associated with an increased red-colored fruit, and *ic_H1.1* and *ic_L*5.1*, which reduced red coloration (**Figure 2; Table 2**).

In summary, a total of 33 QTLs with consistent effects in at least two locations were defined (**Figure 2**). These QTLs were mapped and covered different regions in all chromosomes, except chromosome 8, where no QTL was detected. The distribution of QTLs was not homogeneous among chromosomes, with the largest number of QTLs (8) being found in chromosome 2. Chromosomes 1, 3, 4, and 10 had four QTLs and the rest of the chromosomes showed fewer QTLs.

DISCUSSION

QTLs Detected in the IL Population

To the best of our knowledge, the current work reports the first thoroughly evaluated IL collection with an *S. pimpinellifolium*

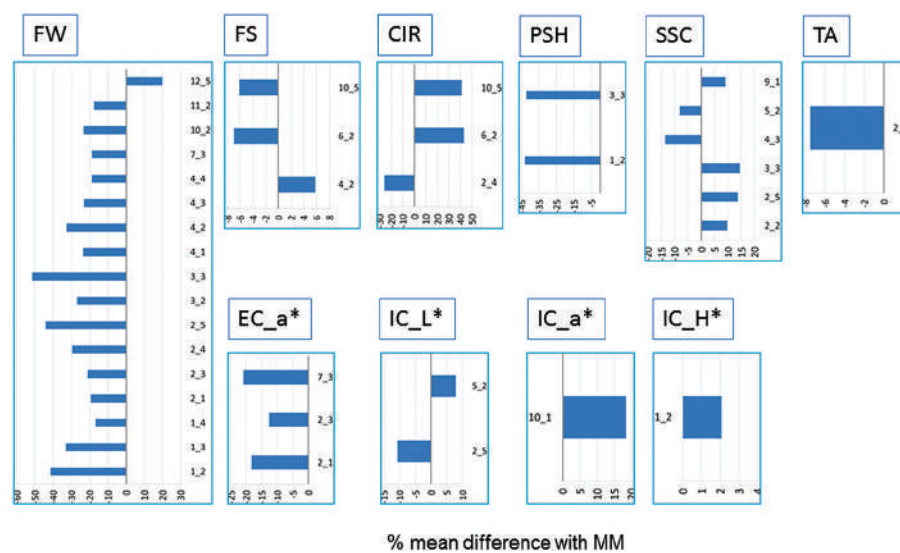


FIGURE 1 | Differences between IL means and Moneymaker (MM) across the three locations expressed in percentage (%) from the MM mean. Only ILs showing significant mean differences with MM at $p < 0.05$ according to the Dunnett's test in at least two locations are shown. Trait abbreviators are: fruit weight (FW), shape (FS), circular shape (CIR), shoulder height (PSH), soluble solid content (SSC), titrable acidity (TA) and internal and external color (EC; ICOL, ECOL) based on CIELab color system variables a*, b*, L*, H, C*.

accession as donor. SP is the phylogenetically closest wild species to the cultivated tomato, which could explain why, in general, the phenotypes of the ILs were so similar to MM, especially compared with other IL collections derived from more distant wild species (Eshed and Zamir, 1995; Bernacchi et al., 1998; Monforte et al., 2001). As a result, deleterious linkage drag effects are minimized in this collection, which facilitates the exploitation of this genetic resource in plant breeding. Furthermore, MM is a fresh-market variety, in contrast to the processing cultivars more widely used as genetic background (Eshed and Zamir, 1995; Monforte and Tanksley, 2000a).

A few extreme phenotypes were observed in the population, some of which affected general plant growth and architecture. SP_3-1 showed severe plant growth impairment, limiting fruit production drastically. This phenotype is very similar to the one caused by the *pauper* mutation, which maps on the short arm of chromosome 3 (tgrc.ucdavis.edu), so *vig3.1* could represent an allele of the *pau* gene. As neither MM nor TO-937 showed any growth impairment, it is unlikely that a new mutation on *pau* would have occurred during IL development. We think that the effect can most likely be attributed to interactions between TO-937 alleles (*pau* or other genes) within the SP_3-1 introgression and other genes in MM genetic background. Another classical mutant, *pro* or *procera* (tgrc.ucdavis.edu), which exhibits a more rapid growth rate, produces tall, slender, weak plants and elongated internodes, and co-locates with the earliness QTL *ear11.1* in IL SP_11-4.

SP_5-2 and SP_5-3 displayed the color purple on both primary and axillary shoots, indicating anthocyanin over-accumulation. The *Af* gene (*anthocyanin free*, tgrc.ucdavis.edu) is involved in the accumulation of anthocyanins as mutations (*af*) in this gene, and produces plants that do not accumulate anthocyanin in all

tissues (Burdick, 1958). This gene is located in the short arm of chromosome 5 and encodes a chalcone isomerase enzyme (CHI) that catalyzes the synthesis of 2(S)-naringenin, a key intermediate in the flavonoid pathway, which is required for flavonoid production (Kang et al., 2014). This means that *purp5.1* may be allelic to *Af*. As in the previous example, neither MM nor TO-937 displayed anthocyanin accumulation under normal non-stress conditions, suggesting that epistatic interactions between TO-937 alleles at CHI and with MM genetic background likely induced an expression of CHI, which would explain the resulting anthocyanin accumulation.

SP_10-3 displayed a much higher trichome density than MM, with long type-I trichomes (Luckwill, 1943) densely covering leaves and stems. Yang et al. (2011) isolated the *Woolly* gene (*Wo*), essential for trichome formation in all vegetative parts. This gene is located in the long arm of chromosome 2, meaning that SP_10-3 most likely contains a novel gene involved in trichome development. Trichomes have been associated with insect resistance (Guo et al., 1993; Blauth et al., 1998; Maluf et al., 2010). Salinas et al. (2013) mapped two QTLs in chromosome 2 from the wild tomato TO-937 that control resistance against the two-spotted spider mite (*Tetranychus cinnabarinus* Koch) and which is based on short, glandular, type-IV trichomes that produce acylsucroses (Alba et al., 2009). However, no gene or QTL involved in insect resistance has been mapped in chromosome 10 so far, which suggests that the increase of trichome density induced by *tric10.1* is not related to disease resistance. Since the *h* gene (hairs absent, tgrc.ucdavis.edu) produces absence of long trichomes (except on hypocotyl) and is located in the long arm of chromosome 10, it is likely that *tric10.1* is allelic to *h*. No candidate gene is known for this gene.

TABLE 2 | Summary of the quantitative trait loci (QTLs) detected in the population of introgression lines for the analyzed traits [FW, FS, CIR, PSH, soluble solid content (SSC), TA, external (EC) and internal (IC) color the last two are based on CIELab color system variables L*, a*, b*, C*, H].

Trait	QTL	Chr	QTL genetic position (cM)	QTL physical position (Mb)	Localities detected	Differences with MM (%)
FW	<i>fw1.1</i>	1	57–75	74–78	3	−25
	<i>fw1.2</i>	1	77–128	78–90	2	−17
	<i>fw2.1</i>	2	47–69	38–40	2	−25
	<i>fw2.2</i>	2	69–138	42–50	3	−19
	<i>fw3.1</i>	3	51–111	7–58	3	−27
	<i>fw3.2</i>	3	111–124	58–62	2	−24
	<i>fw4.1</i>	4	0–30	0–4	2	−13
	<i>fw4.2</i>	4	30–135	4–62	2	−18
	<i>fw7.1</i>	7	39–77	60–64	2	−19
	<i>fw10.1</i>	10	0–84	0–61	2	−23
	<i>fw11.1</i>	11	69–93	49–50	2	−17
	<i>fw12.1</i>	12	94–133	62–65	2	20
CIR	<i>cir2.1</i>	2	69–86	36–42	2	−26
	<i>cir6.1</i>	6	17–56	3–35	3	43
	<i>cir10.1</i>	10	104–115	64–65	3	41
FS	<i>fs4.1</i>	4	41–94	3–35	2	6
	<i>fs6.1</i>	6	17–56	3–35	3	−7
	<i>fs10.1</i>	10	104–115	64–65	2	−6
PSH	<i>psh1.1</i>	1	50–135	3.8–70	3	−43
	<i>psh3.1</i>	3	11–124	58–62	3	−42
SSC	<i>ssc2.1</i>	2	46–63	0–36	2	10
	<i>ssc2.2</i>	2	86–139	42–49	2	14
	<i>ssc3.1</i>	3	11–124	58–62	3	14
	<i>ssc4.1</i>	4	41–94	4–57	2	−13
	<i>ssc5.1</i>	5	4–32	0–0.5	2	−8
	<i>ssc9.1</i>	9	13–92	4–57	2	9
TA	<i>ta2.1</i>	2	46–63	36–42	2	−16
EC	<i>ec_a*2.1</i>	2	1–46	28–35	2	−15
	<i>ec_a*7.1</i>	7	77–100	60–63	2	−20
IC	<i>ic_L*2.1</i>	2	63–86	42–50	2	−11
	<i>ic_L*5.1</i>	5	4–84	0–0.5	2	8
	<i>ic_a*10.1</i>	10	27–31	0–2.8	2	18
	<i>ic_H1.1</i>	1	50–135	5–78	2	2

The intervals of the QTL positions are listed in genetic and physical units following Barrantes et al. (2014). The number of locations where the QTL was significant is also indicated. The effect of the QTLs is shown as the mean difference between the locations of ILs with significant effects and recurrent parent Moneymaker (MM), expressed as a percentage with respect to MM.

Regarding fruit quality traits, in general no important deleterious phenotypes were observed. SP_10-1 and SP_10-2 yielded dark green-shouldered fruits as a consequence of the allelic replacement of the *uniform ripening* (*u*) gene that is located in the introgressions presented by the ILs and which corresponds to the reconstitution of the function of the *GLK-2* gene involved in chloroplast development in fruit (Powell et al., 2012).

Fruit weight showed the highest genetic variability and heritability as well as the largest number of detected QTLs. The striking phenotypic differences between parental lines explain these results. The increase in FW is an important domestication and diversification trait. Major QTLs involved in this trait have been isolated in the last few years (Monforte et al., 2014), and some QTLs detected in the current report provide additional

evidence for them: *fw2.2* (Frary et al., 2000), *fw3.2* (Chakrabarti et al., 2013) FAB, FIN (Xu et al., 2015), which are most likely responsible for the FW QTLs reported herein in chromosomes 2, 3, 4, and 11, respectively. These QTLs are involved in either domestication or improvement (Lin et al., 2014), together with other loci in chromosomes 5, 7, 9, and 12. The current population revealed additional FW QTLs on chromosomes 1 (SP_1-2, SP1_3, and SP_1-4) and 10 (SP_10-2), with effects of a comparable magnitude (Figure 1) to those previously described, even though they have not been previously associated to either domestication or improvement. These QTLs have not been found in other mapping populations derived from SP accessions, although they may be orthologous to FW QTLs from other wild tomato species, such as *S. pennellii* (Eshed and Zamir, 1995). Also worthy of note are the transgressive effects of IL_12-5 that increase FW.

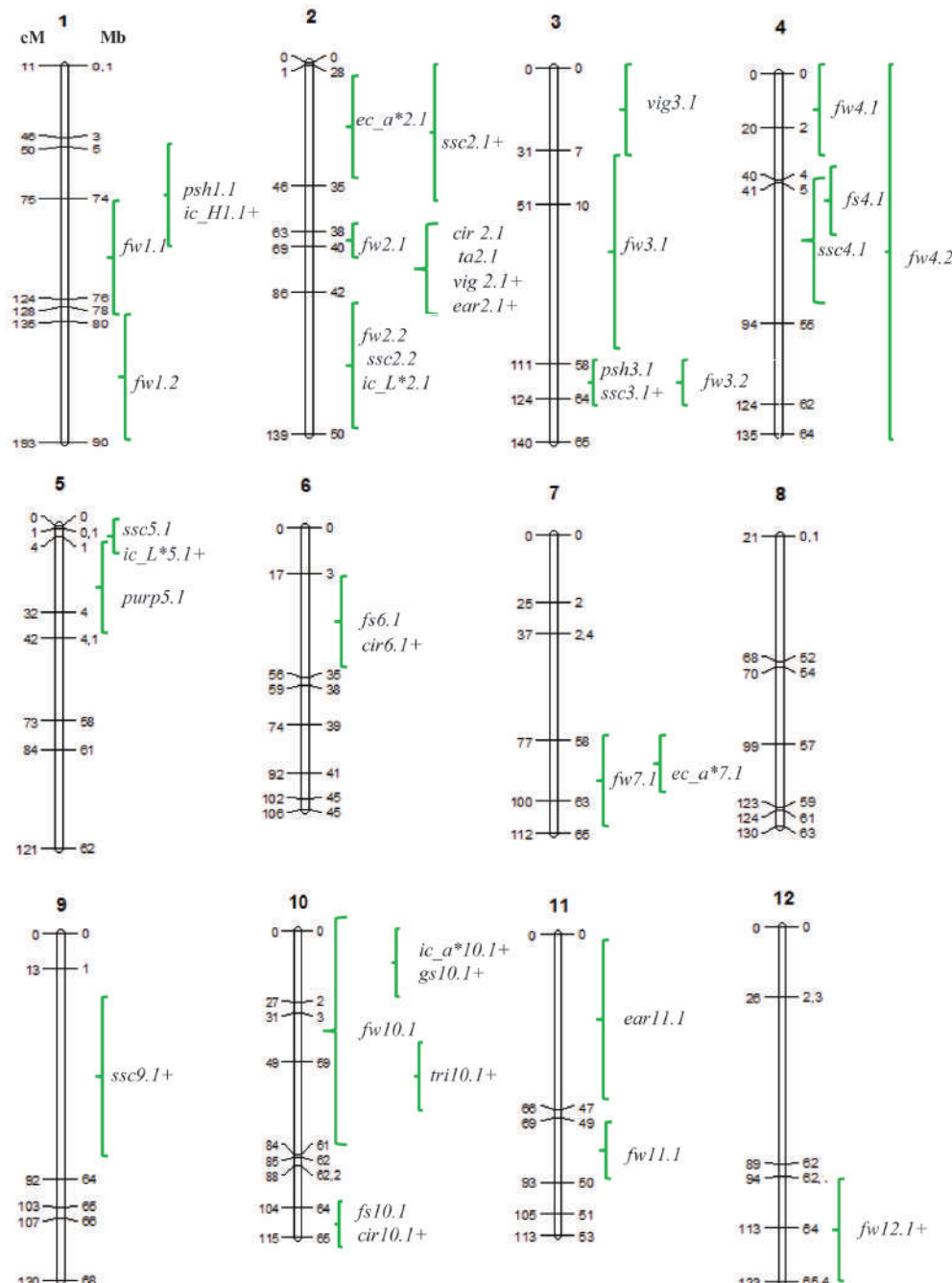


FIGURE 2 | Quantitative trait loci (QTL) positions on the tomato map. Genetic distances (cM) are shown on the left of the chromosome drawings, and physical distances (Mb), according to the tomato genome version SL2.40, on the right. QTLs are named using an abbreviation of the trait: plant vigour (VIG), earliness (EA), presence or absence of anthocyanin coloration in branches and stems (PURP); trichome density (TRI), green shoulder on the fruit (GS), FW, FS, circular shape (CIR), shoulder height (PSH), soluble solid content (SSC), TA and internal and EC (ICOL, ECOL, respectively) based on CIELab color system variables a^* , b^* , L^* , H, C*, followed by the chromosome on which they map and a digit indicating the number of the QTL within the chromosome. (*) Indicates that the TO-937 wild allele increases the trait value.

QTLs involved in FW have been mapped in this region, either increasing (Causse et al., 2004) or decreasing (Fulton et al., 2000; Prudent et al., 2009; Xu et al., 2013), indicating that there must be allelic variability for this QTL in the wild species germplasm

that was probably not selected during domestication into the cultivated gene pool.

With respect to FS, the genetic variability observed in the current IL population was modest. At the same time, the number

of detected QTLs was small and their effects were low. The QTL *cir2.1*, responsible for 26% of fruit round shape variability likely corresponds to QTLs detected in previous SP-derived populations (Grandillo and Tanksley, 1996; Tanksley et al., 1996; Bernacchi et al., 1998; van der Knaap and Tanksley, 2003). The physical position coincides with *ovate*, so *cir2.1* could be a weak allele of the ovate gene (Liu et al., 2002). QTLs *cir6.1* and *cir10.1*, mapped in chromosomal regions previously associated with FS on chromosomes 6 (Bernacchi et al., 1998; van der Knaap and Tanksley, 2003) and 10 (Chen et al., 1999) in SP-derived populations, are most likely allelic QTLs.

Shoulder height QTLs were mapped for the first time by Brewer et al. (2007) in chromosomes 1, 2, and 7. In the current study, *psh1.1* and *psh3.1* were mapped, with *psh1.1* located at the same position previously defined by Brewer et al. (2007) on chromosome 1. The appearance of shoulder height in tomato fruit is restricted to cultivated tomato, which is probably a consequence of domestication. It seems unlikely that ancient farmers would have selected for this trait intentionally. One possible explanation is a pleiotropic effect of fruit size increase; in fact, SP_1-2 and SP_3-3 decreased both FW and PSH, although other ILs that reduced FW did not show any effects on PSH. An alternative explanation is that the pleiotropic effect could be QTL-specific. SSC is one of the primary quality traits of tomato fruits. The amount of genetic variability in the current population was higher than it was for FS, with a total of five QTLs with opposite effects being detected (three increasing, two decreasing). No correlation was found between SSC and FW. SP_2-2 and SP_9-1 increased SSC but did not decrease FW, making those QTLs an appropriate choice for increasing SSC without negative effects on FW. QTLs on ILs SP_3-3, SP_4-3, and SP_5-1 have been detected in a very limited number of previous works (Tanksley et al., 1996; Chen et al., 1999), whereas QTLs on SP_2-2, SP_2-5, and SP_9-1 have been detected more frequently (Grandillo and Tanksley, 1996; Tanksley et al., 1996; Chen et al., 1999; Doganlar et al., 2002; Causse et al., 2004; Chaïb et al., 2006; Xu et al., 2013; Pereira da Costa et al., 2013). The QTL on SP_2-5 is likely a pleiotropic effect of *fw2.2* (Frary et al., 2000), whereas the effect on SP_9-1 could be due to the apoplastic invertase *Lin5* (Fridman et al., 2004). This difference in SSC QTL detection among different mapping populations most likely reflects a high genetic variability for this trait in both cultivated and wild germplasm.

Fruit color is also an important quality trait as it is associated with lycopene accumulation. Both EC and IC components showed a moderate genetic variance in this population, indicating low allelic diversity between MM and TO-937. Correlations between EC and IC components were low and non-significant, confirming a different genetic control for these traits (Monforte et al., 2001). All EC QTLs from TO-937 reduced red coloration, an unexpected result since TO-937 fruits are redder than MM fruits. On the other hand, SP_1-2, SP_2-5, and SP_10-1 displayed a more intense red IC, whereas SP_5-2 showed a diminished red IC, which makes those first ILs promising for the improvement of the nutritional quality of tomatoes. *Phytoene synthase 2 (psy2)* is located in the SP_2-5 introgression (Bartley and Scolnik, 1993), and is a strong candidate gene. QTLs for IC have been detected

previously in the same genomic region, which expands the introgression of SP_1-2 (Grandillo and Tanksley, 1996; Bernacchi et al., 1998; Liu et al., 2003). Since the *high pigment-2 (hp-2)* locus maps in the same region (van Tuinen et al., 1997), it is likely that the current QTL is an allele of *hp-2* with weaker effects. The loci on SP_5-2 and SP_10-1 are the most promising ones, although the introgressions still harbor a large number of genes that may turn out to be candidate genes.

Comparison of QTL Detection between RIL and IL Populations

A RIL population derived from the same parents as the current IL library was recently used to map QTLs involved in FW, SSC, TA and PH, among other traits (Capel et al., 2015), which gave us the opportunity to assess the effect of the genetic structure of the mapping population on QTL detection. In general, the fruits of the RIL population were smaller than those of the IL population, which was probably due to the accumulation of FW QTLs from SP in the RIL genomes. However, FW showed a similar range of phenotypic variation to the ILs in absolute values for FW (1.51–58.24 g among RILs, compared to 47.81–117.86 g among the ILs), while a higher range was observed for SSC, TA, and PH among RILs than the ILs. These differences in the range of variation suggest that additive gene action is common for FW, whereas, for the other traits, epistatic interactions among QTLs are significant contributors to the genetic variance.

Several FW QTLs were detected in both the RIL and IL populations on the same regions of chromosomes 1, 2, 7, and 11. Two additional QTLs were detected on other regions of chromosome 7 in the RILs, whereas FW QTLs on chromosomes 3, 4, 10, and 12 were only detected with the ILs. Moreover, QTLs on chromosomes 1 and 2 were separated as two linked QTLs with the ILs. Therefore, most of the QTLs detected in the RIL population were verified with the ILs, and further QTLs were also detected, which reflects a high consistency of FW QTLs across generations. This is compatible with the previous hypothesis on the additive effects of FW QTLs and the efficacy of ILs in detecting FW QTLs.

Of the seven SSC QTLs reported in the RIL population and the six SSC QTLs in the IL population, only two mapped in the same chromosomal region on chromosomes 2 and 3. Despite the lower consistency between generations found for TA, none of the TA QTLs detected in the RILs could be verified with the ILs, and the only QTL detected in the ILs (*ta2.1*) was not present in the RIL QTL map.

The stability of QTL effects over generations is a crucial issue when implementing MAS. The lack of this stability is one of the major factors that could explain the limited use of MAS for QTLs (Collard and Mackill, 2008). In tomato, what is probably the most thorough study on QTL effect stability over generations was carried out by Chaïb et al. (2006), where they found that, out of 10 QTLs detected in an RIL population, five were detected in BC3S1 and eight in BC3S3 populations, indicating a good stability.

In the current report, we have found that QTL stability depends on the trait in question, as it is high for FW, low for SSC and absent for TA. The discrepancy in QTL detection among

generations can be attributed to experimental (environmental) and biological factors. Interaction with genetic background must have an important role; the fact that different traits show different levels of stability can be explained by differences in the importance of genetic background interactions in the expression of the QTLs, i.e., the prevalence of additive gene action versus epistasis. Of note is the fact that the comparison of trait distributions between the RILs and the ILs indicated that epistatic interactions most likely have an important role in SSC and TA traits, as all show a low QTL stability. Another factor could be the pleiotropic effects of fruit size on SSC and TA, as RIL fruits are much smaller than IL fruits.

The differences in QTL stability across generations observed in the current work reinforce the necessity of developing populations in the proper genetic background, depending on the objectives of the study. Transferring QTLs to different genetic backgrounds will always be a challenge, and it will probably always depend on each particular case. ILs are the populations of choice, especially for applied MAS, as the QTLs of interest can be evaluated in the final genetic background.

AUTHOR CONTRIBUTIONS

WB: was involved in data acquisition, analysis, interpretation of the data, and drafted the manuscript; GL-C, SG-M, AA, and JR: was involved in data acquisition and critical review of the manuscript; RF-M: was involved in the design of the work, data acquisition, and critical review of the manuscript; AG: was

involved in the design of the work, data acquisition and critical review of the manuscript; AM: was involved in the design of the work, data acquisition, analysis, and drafted the manuscript. All authors approve this version of the manuscript and agree to be accountable for all aspects of the work.

ACKNOWLEDGMENTS

The authors want to thank Soledad Casal, Teresa León, Erika Moro, Teresa Caballero, Rafael Martínez, Silvia Presa, Adrián Grau, José Joaquín García, Javier Vives, Alberto Lara, Antonio Núñez, Luís Rodríguez, Rafael Gómez, Agricultural Cooperative Alginet Coagri and the Metabolomics Service of the IBMCP for their help in the field experiments and phenotyping, the funding from grant AGL2015-65246-R (Spanish MINECO, co-financed by European Union FEDER programme) and the EU Framework Program Horizon 2020 COST Action FA1106 Quality Fruit for networking activities. WB was supported by a fellowship granted by the Universidad de Costa Rica and CSIC-Spain by way of a collaboration agreement between CSIC/UCR. GL-C was supported by a JAE-Doc contract by CSIC co-funded by the European Social Fund (ESF).

SUPPLEMENTARY MATERIAL

The Supplementary Material for this article can be found online at: <http://journal.frontiersin.org/article/10.3389/fpls.2016.01172>

REFERENCES

- Alba, J. M., Montserrat, M., and Fernández-Muñoz, R. (2009). Resistance to the two-spotted spider mite (*Tetranychus urticae*) by acylsucroses of wild tomato (*Solanum pimpinellifolium*) trichomes studied in a recombinant inbred line population. *Exp. Appl. Acarol.* 47, 35–47. doi: 10.1007/s10493-008-9192-4
- Ashrafi, H., Kinkade, M. P., Merk, H., and Foolad, M. R. (2012). Identification of novel QTLs for increased lycopene content and other fruit quality traits in a tomato RIL population. *Mol. Breed.* 30, 549–567. doi: 10.1007/s11032-011-9643-1
- Bai, Y., and Lindhout, P. (2007). Domestication and breeding of tomatoes: what have we gained and what can we gain in the future? *Ann. Bot.* 100, 1085–1094. doi: 10.1093/aob/mcm150
- Barrantes, W., Fernández-del-Carmen, A., López-Casado, G., González-Sánchez, M. A., Fernández-Muñoz, R., Granel, A., et al. (2014). Highly efficient genomics-assisted development of a library of introgression lines of *Solanum pimpinellifolium*. *Mol. Breed.* 34, 1817–1831. doi: 10.1007/s11032-014-0141-0
- Bartley, G. E., and Scolnik, P. A. (1993). cDNA cloning, expression during development, and genome mapping of PSY2, a second tomato gene encoding phytoene synthase. *J. Biol. Chem.* 268, 25718–25721.
- Bernacchi, D., Beck-Bunn, T., Emmatty, D., Eshed, Y., Inai, S., Lopez, J., et al. (1998). Advanced backcross QTL analysis of tomato. II Evaluation of near-isogenic lines carrying single-donor introgressions for desirable wild QTL alleles derived from *Lycopersicon hirsutum* and *Lycopersicon pimpinellifolium*. *Theor. Appl. Genet.* 97, 170–180. doi: 10.1007/s001220051009
- Blanca, J., Cañizares, J., Cordero, L., Pascual, L., Diez, M. J., and Nuez, F. (2012). Variation revealed by SNP genotyping and morphology provides insight into the origin of the tomato. *PLoS ONE* 7:e48198. doi: 10.1371/journal.pone.0048198
- Blanca, J., Montero-Pau, J., Sauvage, C. H., Bauchet, G., Illa, E., Diez, M. J., et al. (2015). Genomic variation in tomato, from wild ancestors to contemporary breeding accessions. *BMC Genomics* 16:257. doi: 10.1186/s12864-015-1444-1
- Blauth, S. L., Churchill, G. A., and Mutschler, M. A. (1998). Identification of quantitative trait loci associated with acylsugar accumulation using intraspecific populations of the wild tomato, *Lycopersicon pennellii*. *Theor. Appl. Genet.* 96, 458–467. doi: 10.1007/s001220050762
- Brewer, M. T., Lang, L., Fujimura, K., Dujmovic, N., Gray, S., and van der Knaap, E. (2006). Development of a controlled vocabulary and software application to analyze fruit shape variation in tomato and other plant species. *Plant. Physiol.* 141, 15–25. doi: 10.1104/pp.106.077867
- Brewer, M. T., Moyseenko, J. B., Monforte, A. J., and van der Knaap, E. (2007). Morphological variation in tomato: a comprehensive study of Quantitative Trait Loci controlling fruit shape and development. *J. Exp. Bot.* 58, 1339–1349. doi: 10.1093/jxb/erl301
- Burdick, A. (1958). New mutants. *Tomato Genet. Coop. Rep.* 8, 9–11.
- Canady, M. A., Meglic, V., and Chetelat, R. (2005). A library of *Solanum lycopersicoides* introgression lines in cultivars tomato. *Genome* 48, 685–697. doi: 10.1139/g05-032
- Capel, C., Fernández del Carmen, A., Alba, J. M., Lima-Silva, V., Hernández-Gras, F., Salinas, et al. (2015). Wide-genome QTL mapping of fruit quality traits in a tomato RIL population derived from the wild-relative species *Solanum pimpinellifolium* L. *Theor. Appl. Genet.* 128, 2019–2035. doi: 10.1007/s00122-015-2563-4
- Causse, M., Duffe, P., Gomez, M. C., Buret, M., Damidaux, R., Zamir, D., et al. (2004). A genetic map of candidate genes and QTLs involved in tomato fruit size and composition. *J. Exp. Bot.* 55, 1671–1685. doi: 10.1093/jxb/erh207
- Chaib, J., Lecomte, L., Buret, M., and Causse, M. (2006). Stability over genetic backgrounds, generations and years of quantitative trait locus (QTLs) for organoleptic quality in tomato. *Theor. Appl. Genet.* 112, 934–944. doi: 10.1007/s00122-005-0197-7

- Chakrabarti, M., Zhang, N. A., Sauvage, C. H., Munos, S., Blanca, J., Cañizares, J., et al. (2013). A cytochrome P450 regulates a domestication trait in cultivated tomato. *Proc. Natl. Acad. Sci. U.S.A.* 110, 17125–17130. doi: 10.1073/pnas.1307313110
- Chen, F. Q., Foolad, M. R., Hyman, J., St. Clair, D. A., and Beelaman, R. B. (1999). Mapping of QTLs for lycopene and other fruit traits in a *Lycopersicon esculentum* x *L. pimpinellifolium* cross and comparison of QTLs across tomato species. *Mol. Breed.* 5, 283–299. doi: 10.1023/A:1009656910457
- Chetelat, R. T., and Meglic, V. (2000). Molecular mapping of chromosome segments introgressed from *solanum lycopersicoides* into cultivated tomato (*Lycopersicum esculentum*). *Theor. Appl. Genet.* 100, 232–241. doi: 10.1007/s001220050031
- Collard, B. C., and Mackill, D. J. (2008). Marker-assisted selection: an approach for precision plant breeding in the twenty-first century. *Philos. Trans. R. Soc. B Biol. Sci.* 363, 557–572. doi: 10.1098/rstb.2007.2170
- Darrigues, A., Hall, J., van der Knaap, E., and Francis, D. M. J. (2008). Tomato Analyzer-Color Test: a new tool for efficient digital phenotyping. *Am. Soc. Hortic. Sci.* 133, 579–586.
- Doganlar, S., Frary, A., Ku, H. M., and Tanksley, S. D. (2002). Mapping quantitative trait loci in inbred backcross lines of *Lycopersicon pimpinellifolium* (LA1589). *Genome* 45, 1189–1202. doi: 10.1139/g02-091
- Eduardo, I., Arus, P., and Monforte, A. J. (2005). Development of a genomic library of near isogenic lines (NILs) in melon (*Cucumis melo* L.) from the exotic accession PI161375. *Theor. Appl. Genet.* 112, 139–148. doi: 10.1007/s00122-005-0116-y
- Eshed, Y., and Zamir, D. (1994). Introgressions from *Lycopersicon pennellii* can improve the solute-solids yield of tomato hybrids. *Theor. Appl. Genet.* 88, 891–897. doi: 10.1007/BF01254002
- Eshed, Y., and Zamir, D. (1995). An introgression line population of *Lycopersicon pennellii* in the cultivated tomato enables the identification and fine mapping of yield-associated QTL. *Genetics* 141, 1147–1162.
- Eshed, Y., and Zamir, D. (1996). Less-than-additive epistatic interactions of quantitative trait loci in tomato. *Genetics* 143, 1807–1817.
- Fernández-Muñoz, R., Domínguez, E., and Cuartero, J. (2000). A novel source of resistance to the two-spotted spider mite in *Lycopersicon pimpinellifolium* Just Mill.: its genetics as affected by interplot interference. *Euphytica* 111, 169–173. doi: 10.1023/A:1003893432676
- Finkers, R., Heusden, A. W., Dekens-Meijer, F., Kan, J. A., Maris, P., and Lindhout, P. (2007). The construction of a *Solanum habrochaites* LYC4 introgression line population and the identification of QTLs for resistance to *Botrytis cinerea*. *Theor. Appl. Genet.* 112, 1360–1373.
- Francis, D. M., Kabelka, E., Bell, J., Franchino, B., and St. Clair, D. (2001). Resistance to bacterial canker in tomato (*Lycopersicon hirsutum* LA407) and its progeny derived from crosses to *L. esculentum*. *Plant. Dis.* 85, 1171–1176. doi: 10.1094/PDIS.2001.85.11.1171
- Frary, A., Nesbitt, T. C., Grandillo, S., van der Knaap, E., Cong, B., Liu, J., et al. (2000). Cloning and transgenic expression of fw2.2: a quantitative trait locus key to the evolution of tomato fruit. *Science* 289, 85–87. doi: 10.1126/science.289.5476.85
- Fridman, E., Carrari, F., Liu, Y. S., and Zamir, D. (2004). Zooming in on a quantitative trait for tomato yield using interspecific introgressions. *Science* 305, 1786–1789. doi: 10.1126/science.1101666
- Fridman, E., Pleban, T., and Zamir, D. (2000). A recombination hotspot delimits a wild-species quantitative trait locus for tomato sugar content to 484pb within an invertase gene. *Proc. Natl. Acad. Sci. U.S.A.* 97, 4718–4723. doi: 10.1073/pnas.97.9.4718
- Fulton, T. M., Bucheli, P., Voirol, E., López, J., Pétiard, V., and Tanksley, S. D. (2002). Quantitative trait loci (QTL) affecting sugars, organics acids and other biochemical properties possibly contributing to flavor, identified in four advanced backcross populations of tomato. *Euphytica* 127, 163–177. doi: 10.1023/A:1020209930031
- Fulton, T. M., Grandillo, S., Beck-Bun, T., Fridman, E., Frampton, A., Lopez, J., et al. (2000). Advanced backcross QTL analysis of a *Lycopersicon esculentum* x *Lycopersicon parviflorum* cross. *Theor. Appl. Genet.* 100, 1025–1042. doi: 10.1007/s001220051384
- Grandillo, S., and Tanksley, S. D. (1996). QTL Analysis of horticultural traits differentiating the cultivated tomato from the closely related species *Lycopersicon pimpinellifolium*. *Theor. Appl. Genet.* 92:935. doi: 10.1007/BF00224033
- Guo, Z., Weston, P. A., and Snyder, J. C. (1993). Repellency to two-spotted spider mite *Tetranychus urticae* Koch, as related to leaf surface chemistry of *Lycopersicon hirsutum* accessions. *J. Chem. Ecol.* 19, 2965–2979. doi: 10.1007/BF00980596
- Gur, A., and Zamir, D. (2004). Unused natural variation can lift yield barriers in plant breeding. *PLoS Biol.* 2:e245. doi: 10.1371/journal.pbio.0020245
- Kang, J. H., McRoberts, J., Shi, F., Moreno, J. E., Jones, A. D., and Howe, G. A. (2014). The flavonoid biosynthetic enzyme chalcone isomerase modulates terpenoid production in glandular trichomes of tomato. *Plant. Phys.* 164, 1161–1174. doi: 10.1104/pp.113.233395
- Kinkade, M. P., and Foolad, M. R. (2013). Validation and fine mapping of lyc12.1, a QTL for increased tomato fruit lycopene content. *Theor. Appl. Genet.* 126, 2163–2175. doi: 10.1007/s00122-013-2126-5
- Ku, H. M., Grandillo, S., and Tanksley, S. D. (2000). fs8.1, a major QTL, sets the pattern of tomato carpel shape well before anthesis. *Theor. Appl. Genet.* 101, 873–878. doi: 10.1007/s001220051555
- Labate, J. A., Grandillo, S., Fulton, T., Muños, S., Caicedo, A. L., Peralta, I., et al. (2007). “Tomato,” in *Genome Mapping and Molecular Breeding in Plants Vol. 5: Vegetables*, ed. C. Kole (Berlin: Springer), 1–96.
- Lee, J. M., Joung, J. G., McQuinn, R., Chung, M. Y., Fei, Z., Tieman, D., et al. (2012). Combined transcriptome genetic diversity and metabolite profiling in tomato fruit reveals that the ethylene response factor SIERF6 plays an important role in ripening and carotenoid accumulation. *Plant. J.* 70, 191–204. doi: 10.1111/j.1365-313X.2011.04863.x
- Lima-Silva, V., Rosado, A., Amorim-Silva, V., Muñoz-Merida, A., Pons, C., Bombarely, A., et al. (2012). Genetic genome-wide transcriptomic analyses identify co-regulation of oxidative response and hormone transcript abundance with vitamin C content in tomato fruit. *BMC Genomics* 13:187. doi: 10.1186/1471-2164-13-187
- Lin, T., Zhu, G., Zhang, J., Xu, X., Yu, A., Zheng, Z., et al. (2014). Genomic analyses provide insights into the history of tomato breeding. *Nat. Genet.* 46, 1220–1226. doi: 10.1038/ng.3117
- Lippman, Z. B., Semel, Y., and Zamir, D. (2007). An integrated view of quantitative trait variation using tomato interspecific introgression lines. *Curr. Opin. Genet. Dev.* 17, 545–552. doi: 10.1016/j.gde.2007.07.007
- Liu, J. P., van Eck, J., Cong, B., and Tanksley, S. D. (2002). A new class of regulatory genes underling the cause of pear-shaped tomato fruit. *Proc. Natl. Acad. Sci. U.S.A.* 99, 813302–813306. doi: 10.1073/pnas.162485999
- Liu, Y.-S., Gur, A., Ronen, G., Causse, M., Damidaux, R., Buret, M., et al. (2003). There is more to tomato fruit colour than candidate carotenoid genes. *Plant Biotechnol. J.* 1, 195–207. doi: 10.1046/j.1467-7652.2003.00018.x
- Luckwill, L. C. (1943). *The Genus Lycopersicon. An Historical, Biological, and Taxonomic Survey of the Wild and Cultivated Tomatoes*. Aberdeen: Aberdeen University Press.
- Maluf, W. R., Maciel, G. M., Gomes, L. A., Cardoso, M. D. G., and Goncalves, L. D. (2010). Broad-spectrum arthropod resistance in hybrids between high- and low-acylsugar tomato lines. *Crop Sci.* 50, 439–450. doi: 10.2135/cropsci2009.01.0045
- Monforte, A. J., Diaz, A., Caño-Delgado, A., and van der Knaap, E. (2014). The genetic basis of fruit morphology in horticultural crops: lessons from tomato and melon. *J. Exp. Bot.* 65, 4625–4637. doi: 10.1093/jxb/eru017
- Monforte, A. J., Friedman, E., Zamir, D., and Tanksley, S. D. (2001). Comparison of set of allelic QTL_NILs for chromosome 4 of tomato deducions about natural variation and implications for germplasm utilization. *Theor. Appl. Genet.* 102, 572–590. doi: 10.1007/s001220051684
- Monforte, A. J., and Tanksley, S. D. (2000a). Development of a set of near isogenic and backcross recombinant inbred lines containing most of the *Lycopersicon hirsutum* genome in a *L. esculentum* genetic background: a tool for gene mapping and gene discovery. *Genome* 43, 803–813. doi: 10.1139/g00-043
- Monforte, A. J., and Tanksley, S. D. (2000b). Fine mapping of a quantitative trait locus (QTL) from *Lycopersicon hirsutum* chromosome 1 affecting fruit characteristics and agronomic traits: breaking linkage among QTLs affecting different traits and dissection of heterosis for yield. *Theor. Appl. Genet.* 100, 471–479. doi: 10.1007/s001220050061
- Pereira da Costa, J. H., Rodriguez, R. G., Pratta, R. G., Picardi, A. L., and Zorzoli, R. (2013). QTL detection for fruit shelf life and quality traits

- across segregating populations of tomato. *Sci. Hortic.* 156, 47–53. doi: 10.1016/j.scienta.2013.03.015
- Powell, A., Nguyen, C., Hill, T., Cheng, K. L., Figueira, R., Aktos, H., et al. (2012). Uniform ripening encodes a golden 2-like transcription factor science regulating tomato fruit chloroplast development. *Science* 336, 1711–1715. doi: 10.1126/science.1222218
- Prudent, M., Causse, M., Genard, M., Tripodi, P., Grandillo, S., and Bertin, N. (2009). Genetic and physiological analysis of tomato fruit weight and composition: influence of carbon availability on QTL detection. *J. Exp. Bot.* 60, 923–937. doi: 10.1093/jxb/ern338
- Rambla, J. L., Tikunov, Y. M., Monforte, A. J., Bovy, A. G., and Granell, A. (2014). The expanded tomato fruit volatile landscape. *J. Exp. Bot.* 65, 4613–4623. doi: 10.1093/jxb/eru128
- Rousseaux, M. C., Jones, C. M., Adams, D., Chetelat, R., Bennett, A., and Powell, A. (2005). QTL analysis of fruit antioxidants in tomato using *Lycopersicon pennellii* introgression lines. *Theor. Appl. Genet.* 111, 1396–1408. doi: 10.1007/s00122-005-0071-7
- Sacks, E. J., and Francis, D. M. (2001). Genetic and environmental variation for flesh color of tomato fruit in a population of modern breeding lines. *J. Am. Soc. Hortic. Sci.* 126, 221–226.
- Salinas, M., Capel, C., Alba, J. M., Mora, B., Cuartero, J., Fernández-Muñoz, R., et al. (2013). Genetic mapping of two QTL from the wild tomato *Solanum pimpinellifolium* L. controlling resistance against two-spotted spider mite (*Tetranychus urticae* Koch). *Theor. Appl. Genet.* 126, 83–92. doi: 10.1007/s00122-012-1961-0
- Schauer, N., Semel, Y., Roessner, U., Gur, A., Balbo, I., Carrari, F., et al. (2006). Comprehensive metabolic profiling and phenotyping of interspecific introgression lines for tomato improvement. *Nat. Biotechnol.* 24, 447–454. doi: 10.1038/nbt1192
- Silva, F., Michereff-Filho, M., Fonseca, E. N. M., Silva-Filho Texeira, C. A. A., Moita, W. A., Torres, B. J., et al. (2014). Resistance to *Bemisia tabaci* biotype B of *Solanum pimpinellifolium* is associated with higher densities of type IV glandular trichomes and acylsugar accumulation. *Entomol. Exp. Appl.* 151, 218–230. doi: 10.1111/eea.12189
- Sim, S.-C., Durstewitz, G., Plieske, J., Wieseke, R., Ganal, M. W., and Van Deynze, A. (2012). Development of a large SNP genotyping array and generation of high-density genetic maps in tomato. *PLoS ONE* 7:e40563. doi: 10.1371/journal.pone.0040563
- Sim, S.-C., Robbins, M. D., Chilcott, C., Zhu, T., and Francis, D. M. (2009). Oligonucleotide array discovery of polymorphisms in cultivated tomato (*Solanum lycopersicum* L.) reveals patterns of SNP variation associated with breeding. *BMC Genomics.* 10:466. doi: 10.1186/1471-2164-10-466
- Sim, S.-C., Robbins, M. D., Van Deynze, A., Michel, A. P., and Francis, D. M. (2011). Population structure and genetic differentiation associated with breeding history and selection in tomato (*Solanum lycopersicum* L.). *Heredity* 106, 927–935. doi: 10.1038/hdy.2010.139
- Steinhauser, M. C., Steinhäuser, D., Gibon, Y., Bolger, M., Arrivault, S., Usadel, B., et al. (2011). Identification of enzyme activity quantitative trait loci in a *Solanum lycopersicum* × *Solanum pennellii* introgression line population. *Plant. Physiol.* 157, 998–1014. doi: 10.1104/pp.111.181594
- Stevens, M. A., Kader, A. A., Albright-Holton, M., and Alga, M. (1977). Genotypic variation on flavor and composition in fresh market tomatoes. *J. Am. Soc. Hortic. Sci.* 102:680.
- Tanksley, S. D., Grandillo, S., Fulton, T. M., Zamir, D., Eshed, Y., Petiard, V., et al. (1996). Advanced backcross QTL analysis in a cross between an elite processing line of tomato and its wild relative *L. pimpinellifolium*. *Theor. Appl. Genet.* 92, 213–224. doi: 10.1007/BF00223378
- Tanksley, S. D., and McCouch, S. R. (1997). Seed banks molecular maps: unlocking genetic from the wild. *Science* 277, 1063–1066. doi: 10.1126/science.277.5329.1063
- Tieman, D., Bliss, P., McLatitude, L. M., Blondon-ubeda, A., Bies, D., Odabasi, A. Z., et al. (2012). The chemical interactions underlying tomato flavor preferences. *Curr. Biol.* 22, 1035–1039. doi: 10.1016/j.cub.2012.04.016
- van der Knaap, E., and Tanksley, S. D. (2003). The making of a bell pepper-shaped tomato fruit: identification of loci controlling fruit morphology in yellow stuffer tomato. *Theor. Appl. Genet.* 107, 139–147.
- van Tuinen, A., Cordonnier-Pratt, M. M., Pratt, L. H., Verkerk, R., Zabel, P., and Koornneef, M. (1997). The mapping of phytochrome genes and photomorphogenic mutants of tomato. *Theor. Appl. Genet.* 94, 115–122. doi: 10.1007/s001220050389
- Williams, C. E., and Clair, D. A. (1993). Phenetic relationships and levels of variability detected by restriction fragment length polymorphism and random amplified polymorphic DNA analysis of cultivated and wild accessions of *Lycopersicon esculentum*. *Genome* 36, 619–630. doi: 10.1139/g93-083
- Xu, C., Liberatore, K. L., MacAlister, C. A., Huang, Z., Chu, Y.-H., Jiang, K., et al. (2015). A cascade of arabinosyltransferases controls shoot meristem size in tomato. *Nat. Genet.* 47, 784–792. doi: 10.1038/ng.3309
- Xu, J., Ranc, N., Muñoz, E., Rolland, S., Bouchet, J. P., Desplat, N., et al. (2013). Phenotypic diversity and association mapping for fruit quality traits in cultivated tomato and related species. *Theor. Appl. Genet.* 126, 567–581. doi: 10.1007/s00122-012-2002-8
- Yang, C. H., Li, H., Zhang, J., Wang, T., and Ye, Z. (2011). Fine-mapping of the woolly gene controlling multicellular trichome formation and embryonic development in tomato. *Theor. Appl. Genet.* 123, 625–633. doi: 10.1007/s00122-011-1612-x
- Zamir, D. (2001). Improving plant breeding with exotic genetic libraries. *Nat. Rev. Genet.* 2, 983–989. doi: 10.1038/nrg1101-983

Conflict of Interest Statement: The authors declare that the research was conducted in the absence of any commercial or financial relationships that could be construed as a potential conflict of interest.

Copyright © 2016 Barrantes, López-Casado, García-Martínez, Alonso, Rubio, Ruiz, Fernández-Muñoz, Granell and Monforte. This is an open-access article distributed under the terms of the Creative Commons Attribution License (CC BY). The use, distribution or reproduction in other forums is permitted, provided the original author(s) or licensor are credited and that the original publication in this journal is cited, in accordance with accepted academic practice. No use, distribution or reproduction is permitted which does not comply with these terms.



Identification of Loci Affecting Accumulation of Secondary Metabolites in Tomato Fruit of a *Solanum lycopersicum* × *Solanum chmielewskii* Introgression Line Population

OPEN ACCESS

Edited by:

Ana Margarida Fortes,
University of Lisbon, Portugal

Reviewed by:

Roy Navarre,
United States Department
of Agriculture, USA
Juan Capel,
University of Almería, Spain

*Correspondence:

Arnaud G. Bovy
arnaud.bovy@wur.nl

†Present address:

Ana-Rosa Ballester,
Instituto de Agroquímica y Tecnología
de Alimentos, Consejo Superior
de Investigaciones Científicas,
Valencia, Spain

Specialty section:

This article was submitted to
Plant Physiology,
a section of the journal
Frontiers in Plant Science

Received: 22 April 2016

Accepted: 07 September 2016

Published: 28 September 2016

Citation:

Ballester A-R, Tikunov Y, Molthoff J, Grandillo S, Viquez-Zamora M, de Vos R, de Maagd RA, van Heusden S and Bovy AG (2016) Identification of Loci Affecting Accumulation of Secondary Metabolites in Tomato Fruit of a *Solanum lycopersicum* × *Solanum chmielewskii* Introgression Line Population. *Front. Plant Sci.* 7:1428.
doi: 10.3389/fpls.2016.01428

Ana-Rosa Ballester^{1†}, Yury Tikunov¹, Jos Molthoff¹, Silvana Grandillo²,
Marcela Viquez-Zamora¹, Ric de Vos¹, Ruud A. de Maagd¹, Sjaak van Heusden¹ and
Arnaud G. Bovy^{1,3*}

¹ Wageningen University and Research Centre, Wageningen, Netherlands, ² Institute of Biosciences and Bioresources, National Research Council of Italy, Portici, Italy, ³ Centre for Biosystems Genomics, Wageningen, Netherlands

Semi-polar metabolites such as flavonoids, phenolic acids, and alkaloids are very important health-related compounds in tomato. As a first step to identify genes responsible for the synthesis of semi-polar metabolites, quantitative trait loci (QTLs) that influence the semi-polar metabolite content in red-ripe tomato fruit were identified, by characterizing fruits of a population of introgression lines (ILs) derived from a cross between the cultivated tomato *Solanum lycopersicum* and the wild species *Solanum chmielewskii*. By analyzing fruits of plants grown at two different locations, we were able to identify robust metabolite QTLs for changes in phenylpropanoid glycoconjugation on chromosome 9, for accumulation of flavonol glycosides on chromosome 5, and for alkaloids on chromosome 7. To further characterize the QTLs we used a combination of genome sequencing, transcriptomics and targeted metabolomics to identify candidate key genes underlying the observed metabolic variation.

Keywords: tomato (*Solanum lycopersicum*), QTL analysis, flavonoids, alkaloids, introgression lines

INTRODUCTION

Tomato (*Solanum lycopersicum*) is one of the most important vegetable crops worldwide with more than 160 million tons produced in 2013 (FAOSTAT, 2015)¹. This crop has served as a model organism for fleshy fruit plants and the complete genome sequence of one reference genome and up to 500 re-sequenced accessions is now available through the Solanaceae Genome Network (SGN)² (Tomato Genome Consortium, 2012). As with many other crop plants, tomato has been subjected to intensive domestication and breeding activities, which reduced the genetic variability in commercial materials. Domestication has been focused on yield, disease resistance, color and shape, while taste and nutritional value have long been neglected (Lin et al., 2014). Currently,

¹<http://faostat3.fao.org/>

²<http://solgenomics.net>

there is a growing demand to introduce novel genetic variation in commercial tomato in order to improve quality traits such as flavor and nutritional value. This genetic variation can be found in mutagenized populations, in core collections and in wild species and in introgression lines (ILs) derived from those. The potential of wild species as sources for genetic improvement of crops is increasingly recognized. A major goal of modern tomato breeding is to screen crossable wild *Solanum* species, such as *Solanum lycopersicoides*, *Solanum pennelli*, *Solanum habrochaites*, *Solanum chmielewskii*, *Solanum pimpinellifolium*, *Solanum neorickei*, *Solanum peruvianum*, and *Solanum cheesmanii* for valuable traits, such as resistance against various biotic and abiotic stresses (Légnani et al., 1996; Frankel et al., 2003), primary metabolites (Schauer et al., 2005) and secondary metabolites (Alseekh et al., 2015). Wild species have been used as a source to develop ILs in *S. lycopersicum*, resulting in a set of lines each carrying a single or a few well-defined chromosome segments from the exotic germplasm source. These populations can be used to identify quantitative trait loci (QTLs) that improve crop quality once introgressed into an elite genetic background (Zamir, 2001). In addition to desirable traits, wild species also carry many agriculturally undesirable traits. Molecular genetic studies can identify the genetic and physical position of the underlying QTLs and introgression breeding can transfer the desirable traits into commercial varieties, while selecting against the undesirable ones.

The quality of tomato, in terms of nutritional value, taste, fragrance and appearance is essentially determined by its biochemical composition. To improve the quality of the crop, currently much research is devoted to the elucidation of the pathways and mechanisms that lead to the synthesis and accumulation of quality-related metabolites. The identification of QTLs that influence the chemical composition of ripe fruit, by screening IL populations, is an effective first step toward the identification of the underlying key genes that influence the nutritional quality of tomatoes. One of the best examples of this approach is the use of the founder tomato IL population, derived from a cross between the cultivated *S. lycopersicum* cv M82 and the green fruited wild species *S. pennelli* LA0716 (Eshed and Zamir, 1995). This population has been used to identify QTLs for primary metabolites, volatile compounds, as well as semi-polar secondary metabolites, such as flavonoids and alkaloids (Schauer et al., 2006; Semel et al., 2006; Tieman et al., 2006; Mathieu et al., 2009; Toubiana et al., 2012; Alseekh et al., 2015). These analyses also led to the identification of candidate genes involved in specific QTLs (Fridman et al., 2001; Causse et al., 2004; Stevens et al., 2007; Bermudez et al., 2008), some of which have been shown to be the key gene underlying a specific QTL by reverse genetics studies (Zanor et al., 2009), while for others this still remains to be demonstrated. Despite the large number of studies related to primary metabolites and yield-associated traits, far less is known about QTLs determining secondary metabolites, such as flavonoids and alkaloids.

Flavonoids represent a large family of low molecular weight polyphenolic secondary metabolites that are widespread over the plant kingdom. To date, more than 6000 different flavonoids

have been described and the number is still growing (Koes et al., 1994). Based on their aglycone structure they can be grouped into several classes, such as chalcones, flavanones, flavonols, anthocyanins, and others. Flavonoids are involved in a diverse range of biological processes, such as pigmentation to attract pollinators and seed dispersers, protection against damage from ultraviolet light and pathogen resistance. In addition, they are associated with human health-promoting properties (Harborne and Williams, 2000; Tapas et al., 2008). In tomato fruits, accumulation of flavonoids is restricted to the peel (Bovy et al., 2002, 2010; Schijlen et al., 2008). The main flavonoids present in tomato fruit peel are the chalcone naringenin-chalcone and various sugar conjugates of the flavonols quercetin and kaempferol. The structural information available about flavonoids and other semi-polar metabolites present in tomato increased substantially in the past decade, thanks to advances made in metabolomics tools, such as liquid chromatography and mass spectrometry (Moco et al., 2006, 2007; Iijima et al., 2008; Mintz-Oron et al., 2008). However, our understanding of the genetic network regulating the accumulation of these compounds in tomato fruit is still incomplete. As indicated above, QTL analyses in interspecific IL populations can be used as a tool to identify key genes of this network in two ways: (i) qualitative and quantitative variation within and between metabolites, established by metabolic profiling of the complete set of ILs, can be used to determine the functional nature of the underlying key genes and (ii) precise knowledge of map positions of introgressions and the tomato genome sequence could facilitate the molecular cloning of these candidate genes. Previously, we demonstrated the success of this approach, by using an IL population derived from a cross between the commercial tomato cultivar *S. lycopersicum* cv. Moneyberg and the wild species *S. chmielewskii* (accession LA1840) to unravel the molecular and biochemical basis underlying the *y* mutation in tomato, which leads to pink-colored tomato fruits (Ballester et al., 2010).

Alkaloids are generally considered as anti-nutritional factors in our diet. Their biological effects in humans range from highly toxic, such as α -solanine and α -chaconine in potato tubers, to bitter tasting, such as α -tomatine in tomato. Domestication and breeding efforts have focused on reducing the levels of these anti-nutrients, but the success has been limited and some of these substances still remain in our daily diet (Friedman, 2002, 2006). In recent years, significant progress has been made in the elucidation of the steroidial glycoalkaloid pathway in Solanaceae species (Iijima et al., 2008, 2013; Mintz-Oron et al., 2008; Itkin et al., 2011, 2013; Cárdenas et al., 2016). In fruit of the cultivated tomato, the bitter tasting α -tomatine is present at high levels in early developmental stages and its levels decrease upon ripening due to its conversion into the acetyl glucosylated forms lycoperoside G, F or esculeoside A, which are not bitter. Putative intermediates in this conversion are hydroxytomatine (also called lycoperoside H), lycoperoside A, B, or C and hydroxyllycoperoside A, B, or C, resulting from subsequent hydroxylation, acetylation and a second hydroxylation reactions. Fruits of many wild tomato species accumulate mostly the early, bitter, type of alkaloids (Iijima et al., 2013).

In the current study, we used the *S. chmielewskii* IL population to identify genomic regions controlling the production of semi-polar secondary metabolites, such as alkaloids, flavonoids and other phenylpropanoids, in tomato fruit. By combining biochemical pathway knowledge and genomic information, several candidate genes were identified. Further analysis of a major QTL on chromosome 5 for flavonols revealed the flavonoid pathway gene *chalcone isomerase 1* (*CHI1*) as the key gene underlying the variation in quercetin- and kaempferol glycosides.

MATERIALS AND METHODS

Plant Material and Growth Conditions

The IL population is composed of 34 indeterminate lines containing single or multiple introgressions from the wild species *Solanum chmielewskii* (LA1840) in the background of the commercial tomato variety *Solanum lycopersicum* cv. Moneyberg. The 34 ILs were grown in two greenhouses located in Avignon (Southern France) and Wageningen (The Netherlands) during spring and summer of 2007. From them, 25 were grown in both locations, five only in Avignon and four only in Wageningen. The day/night temperature set points were 25/15°C and 21/19°C in Avignon and Wageningen, respectively. At least nine plants were grown per each IL and each biological replicate consisted of at least six ripe fruit obtained from three different plants. Whole fruit was sampled from the plants grown in Wageningen, while fruit pericarp from plants grown in Avignon. After harvesting and sampling, the fruit material was immediately frozen in liquid nitrogen, ground to a fine frozen powder using an analytical electric mill and stored at -80°C until used for further analyses.

Selected ILs were grown again during the spring and summer of 2008 in Wageningen (The Netherlands). Samples were harvested at four stages of ripening (mature green (G), breaker (B), turning (T), and red (R)), which were judged by the fruit appearance and firmness. Subsequently, the fruit peel was carefully separated from the rest of the fruit (the flesh tissue) using a scalpel. Both flesh and peel tissues were immediately frozen in liquid nitrogen and stored at -80°C until used. Each biological replicate consisted of at least six fruit of the same ripening stage obtained from two different plants.

IL Genotyping

Illumina® infinium bead array was used for a high resolution mapping of the IL population. This analysis was performed as described in Viquez-Zamora et al. (2013) according to the Illumina® Infinium® HD Assay protocol: (Illumina® Infinium® HD Assay Ultra Protocol Guide. California, USA: © Illumina, Inc; 2009. pp. 1–224. Catalog #WG-901-4007). The complete information of the SNP markers used is available at <http://www.plantbreeding.wur.nl/Publications/SNP/4072SNP-Sequences.xlsx>.

In addition, a set of PCR-based markers consisting of 130 COSII markers (Wu et al., 2006) and three simple sequence

repeats (Frary et al., 2005), previously mapped in the tomato genome and covering all 12 tomato chromosomes, were used to genotype the *S. chmielewskii* IL population (Prudent et al., 2009; Do et al., 2010). Sequences of the primers are available on the Solanaceae Genomics Network Web site.

For the COSII markers, amplicon size differences between the two parents were detected in 12% of the cases and were used to genotype the IL population directly; in the other cases, the amplicons were digested with different restriction enzymes (*TaqI*, *HinfI*, *AluI*, *DraI*, *RsaI*, and *MseI*) to identify polymorphisms. Where no polymorphisms were detected, single-band amplicons were purified and sequenced. Amplicon sequences were aligned and examined for polymorphisms using the program CAPSdesigner³. Thereafter, the IL population was genotyped via cleaved-amplified polymorphic sequence assays (Konieczny and Ausubel, 1993).

Analysis of Semi-polar Metabolites by LC-PDA-QTOF-MS

Semi-polar metabolites were extracted according to Moco et al. (2006). Briefly, 500 mg of fresh weight tissue were extracted with 1.5 mL pure methanol (final methanol concentration in the extract approximately 75%). The samples were sonicated for 15 min, filtered through 0.2 µm inorganic membrane filter and 5 µL were used for the analysis.

Liquid chromatography quadrupole time of flight-mass spectrometry analyses (LC-PDA-QTOF-MS) were carried out according to Bino et al. (2005). The detected flavonoid compounds were identified using authentic standards and accurate mass liquid chromatography mass spectrometry analysis using public databases (Moco et al., 2006; Iijima et al., 2008).

RNA Isolation and qRT-PCR Gene Expression Analysis

Total RNA was isolated from 150 mg of tomato fruit tissue using 1.50 mL of Trizol reagent (Invitrogen) according to the manufacturer's instructions. Before cDNA synthesis, total RNA was treated with DNase-I Amplification Grade (Invitrogen) and purified with an RNeasy Mini Kit (Qiagen). And aliquot of 1 µg of total RNA was used for cDNA synthesis using the iScript cDNA synthesis kit (Bio-Rad Laboratories) in a 20-µL final volume according to the manufacturer. Expression levels of each gene were measured in duplicate reactions, performed with the same cDNA pool, in the presence of fluorescent dye (iQ SYBR Green Supermix) using an iCycler iQ instrument (Bio-Rad Laboratories) with specific primer pairs (Supplementary Table 5) (Ballester et al., 2010). The constitutively expressed mRNA encoding ubiquitin was used as internal reference. Expression levels were determined relative to the internal reference and multiplied by a factor 10. Calculations of each sample were carried out according to the comparative Ct method.

³https://solgenomics.net/tools/caps_designer/caps_input.pl

Microarray Analysis

The transcript profiling analysis was done using whole fruit tissue. Three biological replicates – pools of at least six fruit per plant were analyzed. Total RNA was extracted as described for real-time quantitative PCR. The 100 ng of total RNA was used to synthesize cDNA using Ambion WT expression kit (Applied Biosystems/Life Technologies, Nieuwekerk a/d IJssel, The Netherlands), which was subsequently labeled with biotin using the Affymetrix GeneChip WT Terminal Labeling Kit (Affymetrix, Santa Clara, CA, USA) and hybridized to Affymetrix EUTOM3 tomato exon arrays (Affymetrix). The microarray signals were determined using MadMax microarray analysis software⁴. The raw data can be found in Supplementary Data Sheet 1. Further analysis was performed using Genemath XT microarray data analysis software (Applied Maths)⁵. Prior to analysis, the data were normalized using 2log transformation and subsequently scaled by subtraction of the mean (for each compound over the samples).

Student's *t*-test was performed in Genemath XT, the Pearson correlation coefficients were calculated using the corresponding function of Microsoft Office Excel 2010.

Cloning, Sequencing, and Mapping of CHI1 Gene

Full-length cDNA sequences were amplified from ripe whole fruit of cv. Moneyberg, IL5b and IL7d using the SMART RACE cDNA amplification kit (Clontech Laboratories). Genomic DNA was amplified from leaves of the parental lines *S. lycopersicum* cv. Moneyberg and *S. chmielewskii* LA1840 using the GenomeWalker kit (Clontech Laboratories). The amplified sequences of both full-length cDNAs and genomic DNAs were cloned into pGEM-T-Easy vector (Promega) and sequenced.

RESULTS

Physical Mapping of the *S. lycopersicum* × *S. chmielewskii* IL Population

The objective of this study was to discover genetic and genomic regions of *S. chmielewskii* LA1840 that affect accumulation of secondary metabolites in fruits of the commercial tomato *S. lycopersicum* cv. Moneyberg, as a first step toward discovering genes acting in the related metabolic pathways. For this purpose we analyzed a population of 25 *S. chmielewskii* LA1840 ILs. For 20 of them the first linkage maps, based on COSII and SSR markers, were presented in Prudent et al. (2009) and Do et al. (2010). According to these data, 14 ILs each carried a single wild chromosomal introgression. In our study a high resolution genome wide SNP array, consisting of 5,528 SNP markers (Viquez-Zamora et al., 2013) was used to determine physical boundaries of the ILs. 1,660 markers were found to be

polymorphic between *S. chmielewskii* LA1840 and *S. lycopersicum* cv. Moneyberg. As a result, out of the 25 ILs analyzed, 15 ILs were found to carry a single, homozygous *S. chmielewskii* introgression and 10 ILs carried two or more introgressions in one or in multiple chromosomes (Figure 1; Supplementary Table 1). Four major heterozygous introgressions were found on chromosomes 1, 3, 7, and 12.

Metabolic Profiling of the *S. chmielewskii* ILs Using Liquid Chromatography Coupled to Mass Spectrometry (LC-MS)

The *S. chmielewskii* IL population was grown at two different locations, Wageningen (The Netherlands) and Avignon (France), and ripe fruits were harvested. Three biological replicates were created by pooling fruit material of three independent plants per replicate. Semi-polar metabolites of ripe fruits were profiled using LC-MS. A total of 126 compounds were putatively identified in tomato fruit based on public mass spectral databases (Moco et al., 2006; Iijima et al., 2008). The mass spectra and the retention times were compared with authentic chemical standards when available (Supplementary Table 2). Different biochemical families of secondary metabolites were identified, including alkaloids, flavonoids (flavanones, flavones, and flavonols) and other phenylpropanoids.

Analysis of variance (ANOVA) showed that the content of 56 compounds was significantly affected ($p < 0.05$) in fruits of the ILs compared to fruits of cv. Moneyberg in both growing locations (Figure 2; Supplementary Table 3). Glycosylated volatile organic compounds (VOCs), alkaloids, and flavonoids were the most representative – 18, 17, and 14 compounds, respectively. Introgression in chromosomes 9 (IL9d) and 7 (IL7d) appeared to have the largest effects on the accumulation of different types of glycosylated VOCs and alkaloids, respectively. Two introgressions, on chromosomes 4 (IL4d) and 5 (IL5b), had a major effect on the accumulation of tomato fruit flavonols.

Introgression 5b in Chromosome 5 Increases the Accumulation of Kaempferol and Quercetin Glycosides

The result from the IL screening showed that the largest quantitative changes in levels of flavonols in ripe fruits were due to the presence of the IL5b introgression (Figure 2; Supplementary Table 3). To further investigate the accumulation of kaempferol and quercetin glycosides in tomato fruit, metabolic profiling was performed in different ripening stages (mature green (G), breaker (B), turning (T), and ripe (R)) of IL5b fruits and the control cv. Moneyberg. Since flavonoids normally accumulate in the fruit peel only (Muir et al., 2001; Bovy et al., 2002; Colliver et al., 2002), we decided to focus the LC-MS analyses on methanolic extracts of the peel of IL5b and cv. Moneyberg fruits to increase the sensitivity of the measurements. An increase in the flavonols quercetin- and kaempferol-3-O-rutinoside (denoted as Q3R and K3R, respectively), quercetin- and kaempferol-3-O-rutinoside-7-O-glucoside (Q3R7G and K3R7G) and quercetin/kaempferol-3-O-glucose (Q3G and K3G) was observed in the fruit peel of

⁴<https://madmax.bioinformatics.nl>

⁵<http://www.applied-maths.com/genemath-xt>

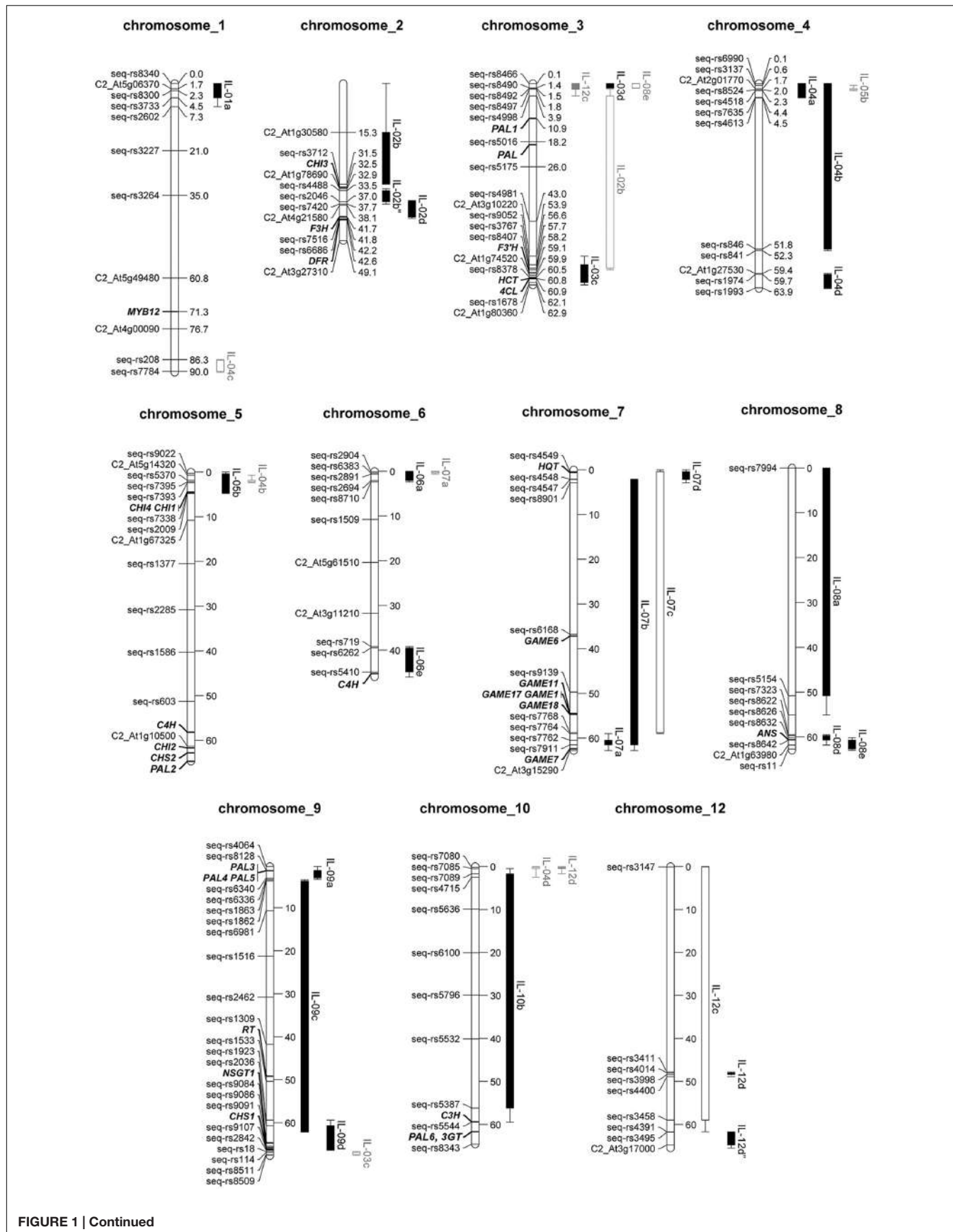


FIGURE 1 | Continued

FIGURE 1 | Physical map of the subset of *S. lycopersicum* × *S. chmielewskii* introgression lines used in this study. Markers flanking introgressions and candidate genes are shown on the left side of chromosomes and their physical positions (in Mbp) – on the right side. Homozygous and heterozygous introgressions are depicted by filled and empty rectangles, respectively, on the right side of chromosomes. Whiskers indicate a distance between *S. chmielewskii* and *S. lycopersicum* alleles of markers flanking introgressions, therefore showing how far introgressions could possibly stretch. Introgressions depicted in gray are minor introgressions, which are detected in an IL carrying a major introgression in a different chromosome. For precise genomic marker positions see Supplementary Table 1.

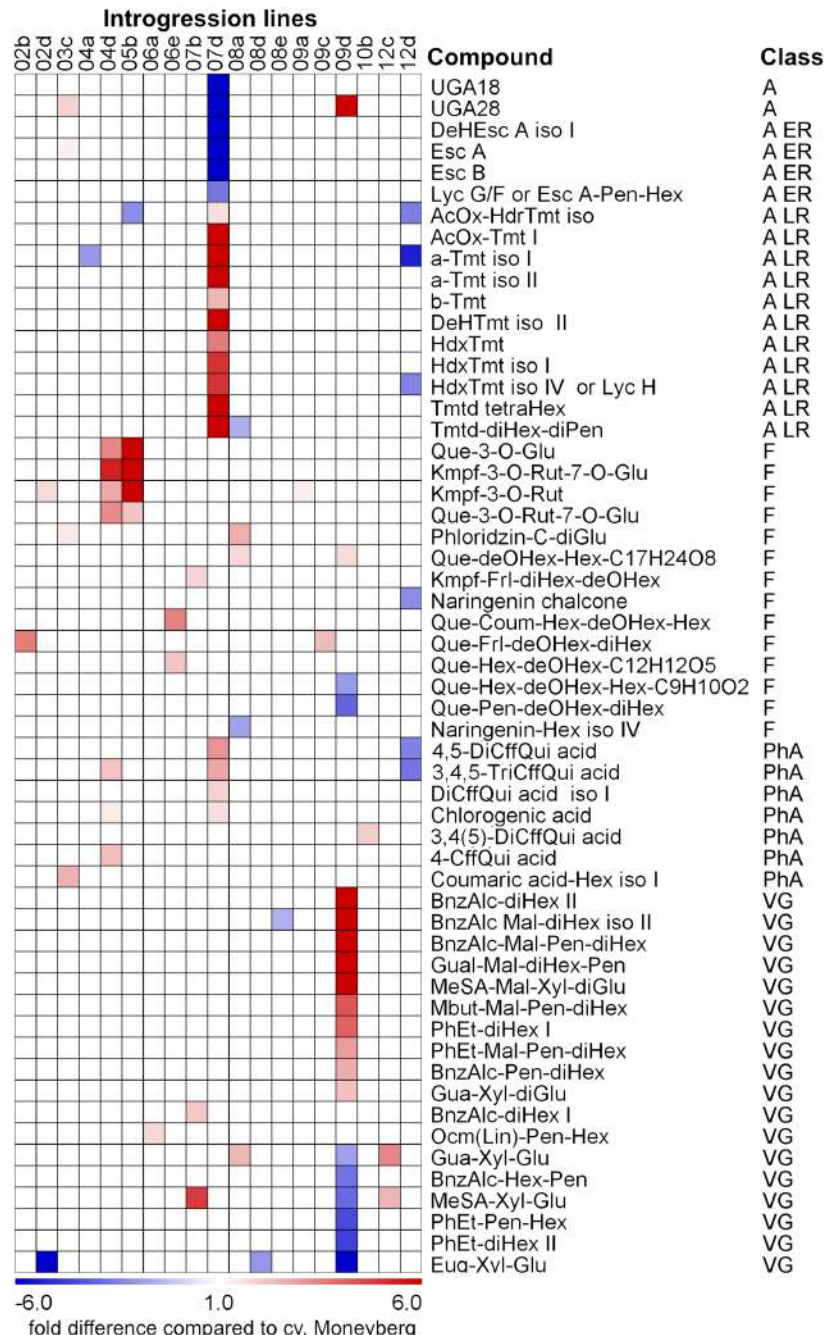


FIGURE 2 | Heat map of fold differences in accumulation of non-volatile secondary metabolites between ripe fruits of the *S. chmielewskii* ILs compared to fruits of the recipient parent *S. lycopersicum* cv. Moneyberg. The differences represented in the heat map were significant ($p < 0.05$) in both the geographical locations where fruits of the ILs were harvested. Compound classes: A – alkaloids; A ER – alkaloids, which are present at early ripening stage of *S. lycopersicum* fruits; A LR - alkaloids, which are present at a later ripening stage of *S. lycopersicum* fruits; F – flavonoids; PhA – phenolic acids; VG – glycosylated volatile compounds. For the exact ratio values see Supplementary Table 3.

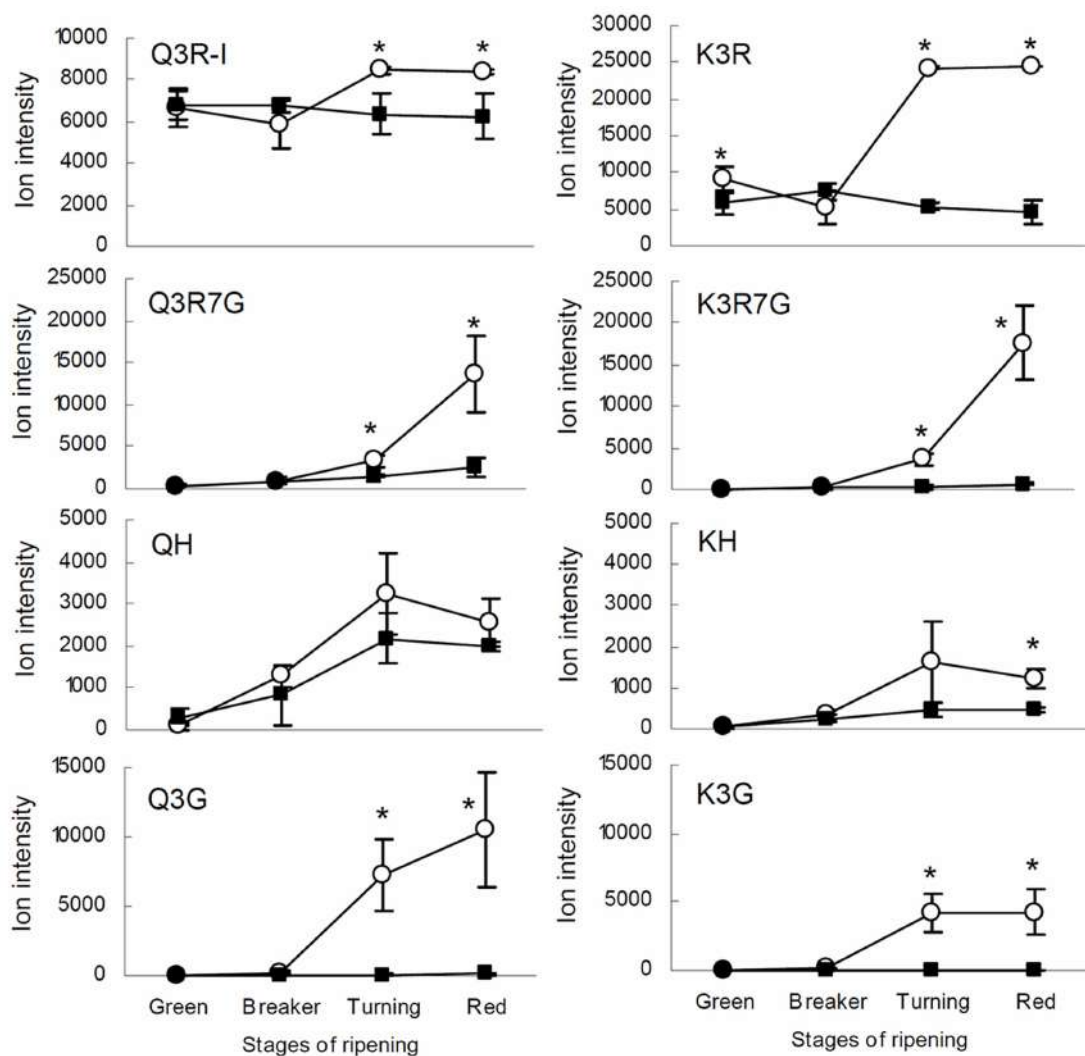


FIGURE 3 | Flavonol glycosides in tomato fruit. Ion intensity of the quercetin and kaempferol glycosides in the peel of tomato fruit of IL5b (white circles) and cv. Moneyberg (black squares) during four stages of ripening: green, breaker, turning and red. Values are the average of three biological replicates, including the standard deviation. Stars (*) indicate significant changes based on a *t*-test ($p < 0.05$).

IL5b compared to cv. Moneyberg, although the extent of the differences appeared to be compound-dependent (Figure 3). In order to unravel the genetic factors associated with the different patterns of accumulation of quercetin and kaempferol glycosides caused by the introgression in IL5b, a transcriptomics analysis of the ripening fruits (G, B/T, and R) was performed using the EU-TOM3 Affymetrix microarray. A total of 511 genes predicted by the International Tomato Annotation Group (ITAG) (Tomato Genome Consortium, 2012) were located in the chromosomal region corresponding to the IL5b introgression. Expression levels of 17 genes in the IL5b introgression region were found to be upregulated threefold or higher in turning fruits of IL5b compared to turning fruits of cv. Moneyberg (Supplementary Table 4). Among them, one gene – *CHALCONE ISOMERASE 1* (*CHI1*) (Solyc05g010320) is directly involved in the flavonoid biosynthesis pathway (Bovy et al., 2002). To

corroborate the results from the microarray experiments, the expression of a set of known fruit-expressed biosynthetic genes involved in the phenylpropanoid/flavonoid pathway (Ballester et al., 2010) (Supplementary Table 5) was analyzed also in ripening fruit peel samples of IL5b and cv. Moneyberg, using qRT-PCR (Figure 4). Furthermore, we tested the expression of three additional putative *CHI* genes, which we denoted as *CHI2* (Solyc05g052240), *CHI3* (Solyc02g067870, BQ505699), and *CHI4* (Solyc05g010310). Most of the genes tested showed a similar ripening-correlated pattern of expression in both IL5b and cv. Moneyberg: expression levels of phenylalanine ammonia-lyase (*PAL*), coumaroyl-4-hydroxylase (*C4H*), 4-coumarate ligase (*4CL*), chalcone synthases (*CHS1* and *CHS2*), chalcone isomerases 2 and 3 (*CHI2* and *CHI3*), flavonoid-3-hydroxylase (*F3H*), flavonoid-3'-hydroxylase (*F3'H*), flavonol synthase (*FLS*), flavonoid-3-O-glucosyltransferase (*3GT*) and

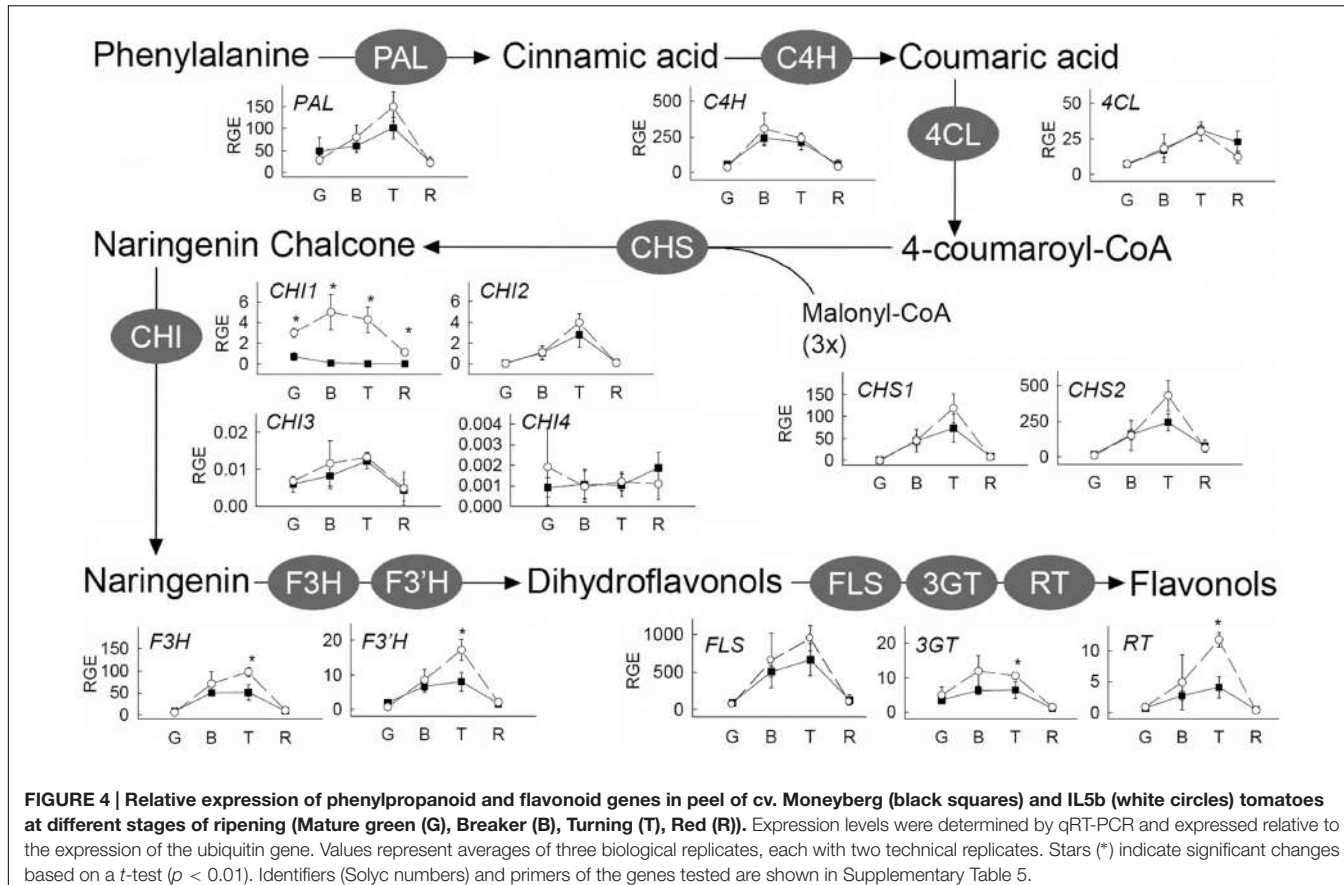


FIGURE 4 | Relative expression of phenylpropanoid and flavonoid genes in peel of cv. Moneyberg (black squares) and IL5b (white circles) tomatoes at different stages of ripening (Mature green (G), Breaker (B), Turning (T), Red (R)). Expression levels were determined by qRT-PCR and expressed relative to the expression of the ubiquitin gene. Values represent averages of three biological replicates, each with two technical replicates. Stars (*) indicate significant changes based on a *t*-test ($p < 0.01$). Identifiers (Solyc numbers) and primers of the genes tested are shown in Supplementary Table 5.

flavonoid 3-O-glucoside-rhamnosyltransferase (*RT*) increased during ripening, peaked at B/T stage and decreased in ripe fruits. In contrast, the ripening-regulated pattern of *CHI1* expression in cv. Moneyberg was opposite to the other genes in the phenylpropanoid/flavonoid pathway. This gene showed a low expression at G stage, which decreased even more at the later stages of ripening. This confirmed earlier observations (Muir et al., 2001; Bovy et al., 2002) that low expression of *CHI1* is a major bottleneck in the biosynthesis of flavonols in fruits of cultivated tomatoes, such as cv. Moneyberg. In line with the microarray results, *CHI1* expression in IL5b was significantly increased compared to cv. Moneyberg at G, B and T stages, suggesting that *CHI1* expression relieves the block of the pathway in fruits of IL5b, which makes it the primary candidate gene for the flavonoid QTL mapped on IL5b.

Although all other flavonoid pathway genes did not show such a dramatic difference in expression as *CHI1*, in general, they tended to be expressed at higher levels in breaker and/or turning fruits of IL5b compared to cv. Moneyberg. This suggests that differences in flavonoid content between IL5b and cv. Moneyberg might also be due to coordinate control of flavonoid gene expression during ripening. The MYB12 transcription factor has previously been shown to regulate flavonol biosynthesis in tomato fruit (Adato et al., 2009; Ballester et al., 2010). Another MYB family transcription factor (Solyc05g009720) was found among the genes up-regulated in fruits of IL5b and

physically located in the introgression region – at 3.93 Mb on chromosome 5. However, no significant correlation of expression was observed between this MYB gene and the 14 biosynthetic genes involved in the phenylpropanoid/flavonoid pathway present on the microarray (Supplementary Table 6). Analysis of two near-isogenic tomato lines only differing for a *S. chmielewskii* introgression in chromosome 5 that starts downstream of the MYB gene, but covers the *CHI1* gene, confirmed the high-flavonoid fruit phenotype caused by the presence of the *S. chmielewskii* introgression (results not shown). This supports our conclusion that *CHI1* is the primary candidate gene underlying the flavonoid QTL on chromosome 5.

Full length cDNAs of *CHI1* (Solyc05g010320) were isolated from ripe fruit of both cv. Moneyberg and IL5b using Rapid Amplification of cDNA Ends (RACE). The derived protein sequences differ at only 2 amino acid positions (N35S and D137N in cv. Moneyberg→IL5b, Figure 5A). We cannot exclude that these two amino acid differences affect the function of the protein, but consider it unlikely that they account for the changes seen in *CHI1* gene expression.

A genome walking approach was used to analyze and compare the genomic structure of *CHI1* in the parental lines cv. Moneyberg and *S. chmielewskii*. The genomic sequence between both cv. Moneyberg and *S. chmielewskii* showed the presence of three introns, with the highest sequence variation observed in the first intron (Figure 5B). Deletions of 16, 38, 14, and 17 bp and an

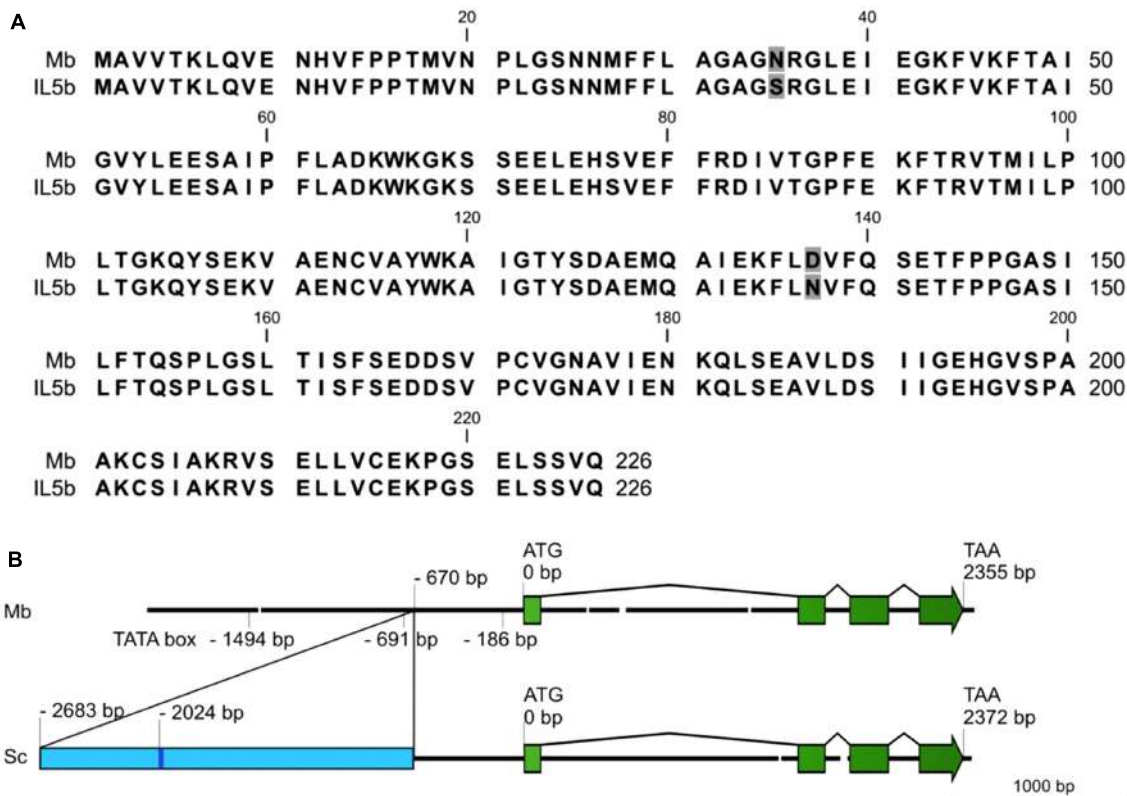


FIGURE 5 | (A) Alignment of deduced amino acid sequences of *CHI1* alleles, including the sequences of *S. lycopersicum* cv. Moneyberg (Mb) and the *S. chmielewskii* introgressed line 5b (IL5b). Different amino acids between the sequences are boxed in gray. **(B)** Schematic overview of the genomic structures of the *CHI1* gene in Moneyberg (Mb) and *S. chmielewskii* (Sc). The *CHI1* gene consists of four exons (boxes in green) and three introns. The blue box represents part of ToRTL1, a *Ty1/Copia* long terminal repeat (LTR) retroelement observed in the promoter region of *S. chmielewskii* *CHI1* gene.

insertion of 17 bp were observed in cv. Moneyberg compared to *S. chmielewskii*. Comparison of the promoter regions, using the TSSP/Prediction of PLANT Promoters tool at the RegSite Plant DB (Softberry Inc.), revealed an insertion in the promoter region of *S. chmielewskii* at \sim 670 bp of the transcription start site, with a size of at least 2,063 bp. The insertion sequence was searched for homology to transposon-like sequences in RepBase (Jurka et al., 2005). In this insertion several fragments were found with 68 to 91% similarity to (from 5' to 3') (i) twice a Copia-38_ST Long Terminal Repeat fragment from potato, (ii) a 34 nt sequence with high similarity (91%) to the polypurine tract containing region of ToRTL1, (iii) a *Ty1/Copia* long terminal repeat (LTR) retroelement (Daraselia et al., 1996), and (iv) to 3' and 5' sequences, respectively, of a hAT-like DNA transposon from potato (Jurka and Kohany, 2006).

IL7d Affects Accumulation of Alkaloids in Tomato Fruit

According to the marker data IL7d carried a *S. chmielewskii* introgression in the top of chromosome 7 (0–2.86 Mb) (Figure 1; Supplementary Table 1). This introgression affected accumulation of two groups of alkaloids in fruits of this IL (Figure 2; Supplementary Table 3). α -tomatine, hydroxytomatine

(lycoperoside H) and lycoperoside A/B/C had higher levels in fruits of IL7d compared to the control cv. Moneyberg (Figure 6), whereas the amounts of esculeoside A and lycoperoside F/G in fruits of this introgression line were reduced by up to 45-fold (Figure 6). According to the proposed tomato alkaloid biosynthetic pathway (Mintz-Oron et al., 2008; Itkin et al., 2013) α -tomatine undergoes a number of ripening-induced hydroxylation and glycosylation modifications to produce the esculeoside type glycoalkaloids. Therefore, the accumulation of the green fruit-type alkaloids in fruits of IL7d suggests that this genomic region harbors a genetic factor which prevents or blocks the ripening-dependent glycoalkaloid modification (Figure 6). Accumulation of putative intermediates in the proposed pathway, such as hydroxy-lycoperoside A, B, or C, which after glycosylation produce the esculeoside type alkaloids, was not observed in fruits of IL7d. This suggests that the pathway is most likely interrupted at the step of hydroxylation of acetoxytomatine. Hydroxylation of alkaloids and other secondary metabolites is often mediated by enzymes of the cytochrome P450 family.

Three P450s were found to be located in the IL7d introgression region: Solyc07g006140, Solyc07g006890, and Solyc07g007460. Of these three genes, Solyc07g006890 was the most highly

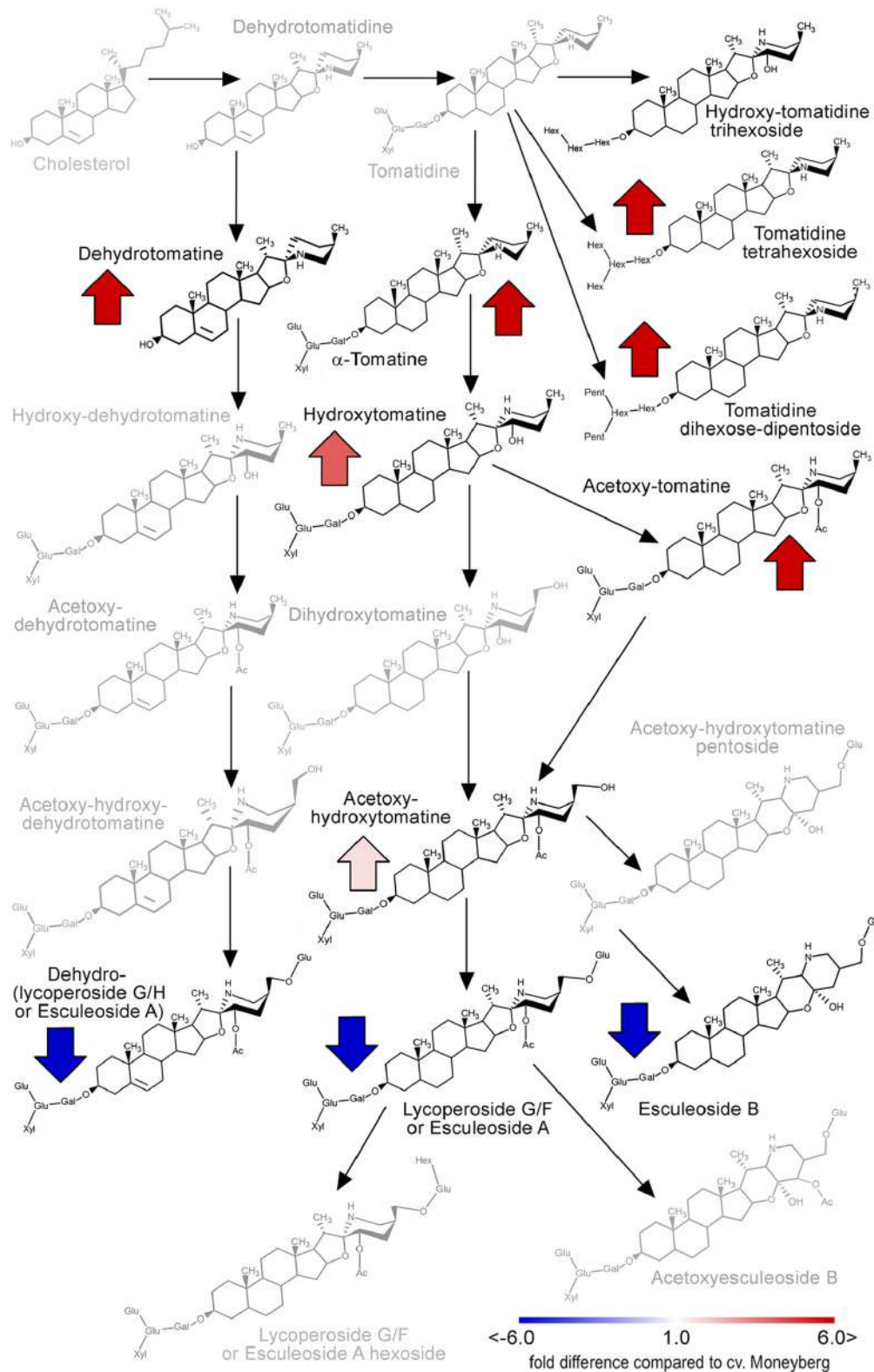


FIGURE 6 | Alterations in the tomato fruit alkaloid pathway caused by the IL7d introgression (adapted from Itkin et al., 2011). The intensity of red and blue arrows indicate the extent of quantitative changes of alkaloids compared to their amounts in fruit of cv. Moneyberg. Gray colored compounds were not detected in this study.

expressed in fruits and its transcript level increased during ripening. In ripe fruits of IL7d this gene showed a moderate threefold decrease in expression compared to its average expression observed in fruits of cv. Moneyberg and of IL5b (Supplementary Table 7).

IL9d Affects the Accumulation of Volatile Glycosides

The introgression 9d in chromosome 9 affected the accumulation of different glycoconjugate forms of volatile compounds, such as guaiacol, methyl salicylate (MeSA), and eugenol (**Figure 2**; Supplementary Table 3). IL9d led to the conversion of xylosyl-glucopyranoside forms of these volatiles into the corresponding xylosyl-diglucopyranoside forms. This conversion was shown to be mediated by the Non-Smoky Glycosyltransferase 1 gene (*NSGT1*), located within the IL9d introgression (**Figure 1**) (Tikunov et al., 2013) and suggests that *S. chmielewskii* carries a functional version of *NSGT1*. Indeed, re-sequencing of the *S. chmielewskii* LA1840 genome using a next generation sequencing approach revealed a gene with 96% homology to *NSGT1* (Supplementary Image 1). In addition to glycosides of guaiacol, MeSA and eugenol, our data revealed that diglycosides of the aroma volatiles benzyl alcohol, 2-phenylethanol, and 2- or 3-methylbutanol were modified in the same manner (**Figure 2**; Supplementary Table 3).

DISCUSSION

Many metabolite QTLs (mQTLs) have been described in ILs derived from the wild tomato relatives *S. pennellii* or *S. habrochaites* (Schauer et al., 2006; Tieman et al., 2006; Mathieu et al., 2009; Steinhauser et al., 2011; Toubiana et al., 2012; Alseekh et al., 2015). *S. chmielewskii* is another wild species crossable with cultivated tomato, with smaller, green fruits. The influence of the fruit load on the accumulation of dry matter and sugars in tomato fruit and on primary metabolites have been described recently in tomatoes derived from the *S. chmielewskii* IL population (Prudent et al., 2009; Do et al., 2010). In this paper, we used a combination of genomic and metabolomics approaches to identify mQTLs and candidate genes controlling the synthesis of semi-polar compounds in tomato fruit. For this, ripe fruits harvested from the *S. chmielewskii* IL population were analyzed for variation in semi-polar secondary metabolites, using LC-PDA-QTOF-MS. By growing the plants at two different locations we could select for robust mQTLs. The screening revealed quantitative and qualitative changes in metabolites accumulating in specific ILs. The major mQTLs were found in ILs 4d, 5b, 7d, and 9d (**Figure 2**).

Accumulation of Specific Flavonol Glycosides in Tomato Fruit Related to an Increase in *CHI* Gene Expression

Our metabolic analyses revealed a major ripening-dependent increase of several flavonol glycosides in peel of IL5b compared to cv. Moneyberg (**Figure 3**). Absolute quantification of the main

flavonols revealed an increase in quercetin-3-O-rutinoside from 30 to 260 mg/kg FW and of kaempferol-3-O-rutinoside from 3 to 35 mg/kg FW in peel of ripe IL5b compared to cv. Moneyberg fruits (Supplementary Image 2). Compared to the levels of these compounds found among a collection of 94 cultivated tomato hybrids (Bovy et al., 2010), the IL9d introgression upgrades Moneyberg tomatoes from a low-flavonol to a high-flavonol round tomato type, with levels comparable to those in cherry tomatoes, which are generally regarded as a much better source of flavonols than round/beef tomatoes.

Chalcone synthase (CHS) is the first enzyme involved in the phenylpropanoid/flavonoid pathway leading to the formation of these semi-polar compounds, most of which are present in a glycosylated form. Most of the biosynthetic genes involved in the flavonoid pathway and also transcription factors involved in the regulation of the biosynthetic genes have been identified (Schijlen et al., 2004; Adato et al., 2009; Ballester et al., 2010) and, due to the availability of the tomato genome sequence (Tomato Genome Consortium, 2012), their physical position and chromosomal location is known (**Figure 1**; Supplementary Table 8). However, due to the complexity of flavonoid modification and the presence of more than 500 different forms of flavonoids in tomato (Moco et al., 2006; Iijima et al., 2008; Grennan, 2009), further analysis is still needed to understand the flavonoid pathway to its full extent.

Most plants do not accumulate chalcones, the first class of flavonoids at the top of the biosynthetic pathway. After its formation, naringenin chalcone is usually rapidly isomerized by chalcone isomerase (CHI) to form the flavanone naringenin, a process that may also occur spontaneously in the absence of active CHI. However, in tomato fruit, low expression of *CHI* is rate-limiting and naringenin chalcone is the predominant yellow pigment that accumulates in the peel (Muir et al., 2001; Bovy et al., 2002). Four different putative *CHI* genes have been annotated in tomato, which share at most 75% identity at the amino acid level. The first one (Solyc05g010320), *CHI1*, has been described by Bovy et al. (2002) and its expression was low in ripe tomato fruit, explaining the accumulation of the CHI substrate naringenin chalcone. *CHI2* (Solyc05g052240) expression and CHI activity was increased in *Del/Ros1* transgenic plants accumulating anthocyanins (GenBank acc. no. ES893795) (Butelli et al., 2008), and the expression of the third one, here called *CHI3* (Solyc02g067870, BQ505699), was up-regulated in transgenic plants overexpressing the MYB transcription factor *ANT1* leading to anthocyanin pigmentation in the fruit (Mathews et al., 2003). The expression of the fourth one (Solyc05g010310, here called *CHI4*), is very low compared to the other *CHI* genes (**Figure 4**). Based on the genome annotation, *CHI1*, *CHI2* and *CHI4* are located on chromosome 5, while *CHI3* is located on chromosome 2 (**Figure 1**).

There are two major arguments supporting the conclusion that *CHI1* is the key gene underlying the flavonoid QTL on chromosome 5. Firstly, after analyzing the expression of the biosynthetic flavonoid genes in tomato, *CHI1* showed the highest expression increase in IL5b compared to cv. Moneyberg and was the only gene whose expression was significantly increased in IL5b compared to cv. Moneyberg at all stages of fruit ripening (**Figure 4**; Supplementary Table 4). The increase of the expression

of this gene might redirect the flux of the pathway toward the formation of flavonol glycosides, as shown in the results of semi-polar metabolites detected in the fruits of IL5b and in line with results found in transgenic plants overexpressing the petunia *CHI1* gene (Muir et al., 2001). Secondly, *CHI1* is located within the IL5b introgression and is among the 17 genes (out of 511) mapping in this region with an expression level at least threefold higher in turning IL5b fruits relative to cv. Moneyberg fruits (Supplementary Table 4).

IL5b is not a pure line in the sense that a small (<0.5 Mb) additional introgression region in chromosome 4 was also detected in this IL (Figure 1). However, within the subset of the *S. chmielewskii* population analyzed in this study, there are several other ILs with introgressions overlapping with the region in this chromosome. None of these lines showed an increase of flavonol glycosides compared to cv. Moneyberg and therefore we consider it unlikely that genes of this introgressed fragment might be responsible for the IL5b flavonoid QTL. In addition, NILs only differing in a chromosome 5 introgression showed a contrasting flavonoid accumulation pattern (results not shown), supporting that the flavonoid QTL is indeed due to the chromosome 5 introgression.

The lack of *CHI1* gene expression in cultivated tomato might be due to (i) a mutation in a promoter regulatory sequence (*cis*-effect) and/or (ii) a mutation in a transcription factor responsible for expression of *CHI* (Willits et al., 2005) (*trans*-effect). We cannot completely exclude the latter possibility and, in this respect, we found a possible candidate *MYB* TF gene in the IL5b QTL region, which was upregulated in T stage fruit of IL5b. However, the expression pattern of this *MYB* gene during ripening was not correlated with the expression of *CHI1*, nor with the expression of the other flavonoid genes tested, which argues against a causal role for this candidate gene. After analyzing the genomic structure of the *CHI1* gene, our results revealed the presence of several repetitive sequences related to transposons and retrotransposons of tomato and potato. Many examples exist of (retro-)transposon insertions influencing expression of downstream genes such as, in tomato, retrotransposon ToRTL1 driving high expression of the 3-hydroxy-3-methylglutaryl coenzyme A reductase gene 2 (HMG2) (Daraselia et al., 1996). A possible influence of the upstream transposon-like sequences of *CHI1* on its expression, however, remains to be demonstrated.

Accumulation of α -Tomatine and Lycoperosides in Tomato Fruit

In our study, fruits of IL7d showed an accumulation of α -tomatine, hydroxytomatine and lycoperoside A, B, or C, while levels of lycoperoside G, F and esculeoside A were low compared with cv. Moneyberg fruit. None of the above-mentioned intermediates could be detected in fruits of IL5b or cv. Moneyberg.

A cluster of alkaloid biosynthesis genes has been previously discovered at the bottom of tomato and potato chromosome 7 (Itkin et al., 2013). Our genetic and metabolic data showed that there might be another genetic factor(s) at the top of this chromosome. The accumulation of the compounds from the first steps of the putative alkaloid pathway could be due

to (i) a mutation of a gene involved in the hydroxylation of lycoperoside A, B, or C, or (ii) a mutation in regulatory element, such as a transcription factor (TF), responsible for the expression of the hydroxylation gene(s). An example of TF-mediated regulation of alkaloid biosynthesis has been recently shown by Cárdenas et al. (2016). Cytochrome P450s can catalyze aromatic hydroxylations, aliphatic hydroxylations and skeleton formation in secondary metabolite pathways in plants (Ayabe and Akashi, 2006), and therefore CYP's would be good candidates for further studies. The evaluation of the genomic region of the IL7d introgression region revealed the presence of three cytochrome P450 genes: Solyc07g006140 (SL2.40ch07: 984510-988395 bp), Solyc07g006890 (SL2.40ch07: 1747021-1748529 bp), and Solyc07g007460 (SL2.40ch07: 2165949-2167526 bp). Further functional analysis of these candidate genes is currently underway.

Glycosylation of Tomato Fruit Volatiles

Our results indicate that the IL9d introgression carries a functional version of the *NSGT1* gene, which mediates the conversion of xylosyl-glucopyranosides of the phenylpropanoid volatiles guaiacol, methyl salicylate and eugenol into the corresponding xylosyl-diglucopyranosides. This conversion affected the release of the corresponding volatiles and subsequently the fruit aroma (Tikunov et al., 2010, 2013). In addition to glycosides of guaiacol, MeSA and eugenol, the present data showed that glycosides of other volatile compounds which play a role in tomato fruit aroma, such as benzyl alcohol, 2-phenylethanol, and 2- or 3-methylbutanol were modified in the same manner. This suggests that these diglycosides may be used as a substrate of the *NSGT1* enzyme as well. This hypothesis could indeed be confirmed by metabolic analysis of transgenic *NSGT1* fruits (Tikunov et al., 2013) (Supplementary Image 3). In contrast to phenylpropanoid volatiles, the changes in glycosylation pattern of the other volatiles did not affect their release, neither in IL9d fruits (Supplementary Image 4), nor in transgenic *NSGT1* fruits (Tikunov et al., 2013). This suggests that, in addition to *NSGT1*-mediated glycosylation of the third sugar, the identity of the first two sugar conjugates and the interaction with putative glycoside hydrolases are important determinants for the release of aroma volatiles. We are currently aiming to get a better understanding of the various aspects of volatile “logistics” in tomato fruit and explore the opportunities to influence tomato fruit aroma by manipulating the volatile glycosylation status and thereby the release of these volatiles.

CONCLUSION

We identified a number of mQTLs involved in the production of semi-polar metabolites, by examining an IL population derived from a cross between *S. lycopersicum* cv. Moneyberg and *S. chmielewskii* LA1840. The use of specific *S. chmielewskii* ILs in combination with the knowledge gained on these mQTLs and the underlying candidate genes can be used to breed for tomatoes with improved quality. Reverse genetics is required to further elucidate the function of specific candidate genes, in order to gain

a better understanding of the biosynthetic pathways leading to the synthesis and accumulation of health-related compounds.

AUTHOR CONTRIBUTIONS

A-RB carried out the research and wrote the manuscript. YT was responsible for the metabolomics analyses. JM was involved in the research, SG was involved in writing and correcting the manuscript, MV-Z and SH were involved in the marker analyses, RM was involved in manuscript preparation and data analysis, AB was involved in supervising the project, data analysis, and writing.

FUNDING

This work was carried out with support of the FP7 project EU-SOL (FOOD-CT-2006-016214), the Dutch genomics initiative

Centre for Biosystems Genomics (CBSG) and the COST action Quality fruit (FA1106).

ACKNOWLEDGMENTS

We thank Keygene Netherlands for kindly providing the *S. chmielewskii* IL population as well as Mr. Paul Dijkhuis, and Mrs. Fien Meijer-Dekens for excellent greenhouse management and plant cultivation. We thank Bert Schipper for assistance with the LC-PDA-QTOF-MS.

SUPPLEMENTARY MATERIAL

The Supplementary Material for this article can be found online at: <http://journal.frontiersin.org/article/10.3389/fpls.2016.01428>

REFERENCES

- Adato, A., Mandel, T., Mintz-Oron, S., Venger, I., Levy, D., Yativ, M., et al. (2009). Fruit-surface flavonoid accumulation in tomato is controlled by a SlMYB12-regulated transcriptional network. *PLoS Genet.* 5:e1000777. doi: 10.1371/journal.pgen.1000777
- Alseekh, S., Tohge, T., Wendenberg, R., Scossa, F., Omranian, N., Li, J., et al. (2015). Identification and mode of inheritance of quantitative trait loci for secondary metabolite abundance in tomato. *Plant Cell* 27, 485–512. doi: 10.1105/tpc.114.132266
- Ayabe, S.-i., and Akashi, T. (2006). Cytochrome P450s in flavonoid metabolism. *Phytochem. Rev.* 5, 271–282. doi: 10.1007/s11101-006-9007-3
- Ballester, A. R., Molthoff, J., de Vos, R., Hekkert, B. T., Orzaez, D., Fernandez-Moreno, J.-P., et al. (2010). Biochemical and molecular analysis of pink tomatoes: deregulated expression of the gene encoding transcription factor SlMYB12 leads to pink tomato fruit color. *Plant Physiol.* 152, 71–84. doi: 10.1104/pp.109.147322
- Bermudez, L., Urias, U., Milstein, D., Kamenetzky, L., Asis, R., Fernie, A. R., et al. (2008). A candidate gene survey of quantitative trait loci affecting chemical composition in tomato fruit. *J. Exp. Bot.* 59, 2875–2890. doi: 10.1093/jxb/ern146
- Bino, R. J., De Vos, C. H. R., Lieberman, M., Hall, R. D., Bovy, A., Jonker, H. H., et al. (2005). The light-hyperresponsive high pigment-2dg mutation of tomato: alterations in the fruit metabolome. *New Phytol.* 166, 427–438. doi: 10.1111/j.1469-8137.2005.01362.x
- Bovy, A., De Vos, R., Kemper, M., Schijlen, E., Almenar Pertejo, M., Muir, S., et al. (2002). High-flavonol tomatoes resulting from the heterologous expression of the maize transcription factor genes LC and C1. *Plant Cell* 14, 2509–2526. doi: 10.1105/tpc.004218
- Bovy, A. G., Gomez-Roldan, V., and Hall, R. D. (2010). “Strategies to optimize the flavonoid content of tomato fruit,” in *Recent Advances in Polyphenol Research*, Vol II, eds C. Santos Buelga, M. T. Escrivano-Bailón, and V. Lattanzio (Oxford: Wiley-Blackwell Publishing).
- Butelli, E., Titta, L., Giorgio, M., Mock, H.-P., Matros, A., Peterek, S., et al. (2008). Enrichment of tomato fruit with health-promoting anthocyanins by expression of select transcription factors. *Nat. Biotechnol.* 26, 1301–1308. doi: 10.1038/nbt.1506
- Cárdenas, P. D., Sonawane, P. D., Pollier, J., Vanden Bossche, R., Dewangan, V., Weithorn, E., et al. (2016). GAME9 regulates the biosynthesis of steroidal alkaloids and upstream isoprenoids in the plant mevalonate pathway. *Nat. Commun.* 7:10654. doi: 10.1038/ncomms10654
- Causse, M., Duffe, P., Gomez, M. C., Buret, M., Damidaux, R., Zamir, D., et al. (2004). A genetic map of candidate genes and QTLs involved in tomato fruit size and composition. *J. Exp. Bot.* 55, 1671–1685. doi: 10.1093/jxb/erh207
- Colliver, S., Bovy, A., Collins, G., Muir, S., Robinson, S., De Vos, C. H. R., et al. (2002). Improving the nutritional content of tomatoes through reprogramming their flavonoid biosynthetic pathway. *Phytochem. Rev.* 1, 113–123. doi: 10.1023/A:1015848724102
- Daraselia, N. D., Tarchevskaya, S., and Narita, J. O. (1996). The promoter for tomato 3-hydroxy-3-methylglutaryl coenzyme A reductase gene 2 has unusual regulatory elements that direct high-level expression. *Plant Physiol.* 112, 727–733. doi: 10.1104/pp.112.2.727
- Do, P. T., Prudent, M., Sulpice, R., Causse, M., and Fernie, A. R. (2010). The influence of fruit load on the tomato pericarp metabolome in a *Solanum chmielewskii* introgression line population. *Plant Physiol.* 154, 1128–1142. doi: 10.1104/pp.110.163030
- Eshed, Y., and Zamir, D. (1995). An introgression line population of *Lycopersicon pennellii* in the cultivated tomato enables the identification and fine mapping of yield-associated QTL. *Genetics* 141, 1147–1162.
- FAOSTAT (2015). *Food and Agriculture Organization of the United Nations, FAOSTAT Database*. Available at: <http://faostat3.fao.org/>
- Frankel, N., Hasson, E., Iusem, N. D., and Rossi, M. S. (2003). Adaptive evolution of the water stress-induced gene Asr2 in *Lycopersicon* species dwelling in arid habitats. *Mol. Biol. Evol.* 20, 1955–1962. doi: 10.1093/molbev/msg214
- Frary, A., Xu, Y., Liu, J., Mitchell, S., Tedeschi, E., and Tanksley, S. (2005). Development of a set of PCR-based anchor markers encompassing the tomato genome and evaluation of their usefulness for genetics and breeding experiments. *Theor. Appl. Genet.* 111, 291–312. doi: 10.1007/s00122-005-2023-7
- Fridman, E., Liu, Y. S., Carmel-Goren, L., Gur, A., Shores, M., Pleban, T., et al. (2001). Two tightly linked QTLs modify tomato sugar content via different physiological pathways. *Mol. Genet. Genomics* 266, 821–826.
- Friedman, M. (2002). Tomato glycoalkaloids: role in the plant and in the diet. *J. Agric. Food Chem.* 50, 5751–5780. doi: 10.1021/jf020560c
- Friedman, M. (2006). Potato glycoalkaloids and metabolites: roles in the plant and in the diet. *J. Agric. Food Chem.* 54, 8655–8681. doi: 10.1021/jf061471t
- Grennan, A. K. (2009). MoTo DB: a metabolic database for tomato. *Plant Physiol.* 151, 1701–1702. doi: 10.1104/pp.109.900308
- Harborne, J. B., and Williams, C. A. (2000). Advances in flavonoid research since 1992. *Phytochemistry* 55, 481–504. doi: 10.1016/S0031-9422(00)00235-1
- Iijima, Y., Nakamura, Y., Ogata, Y., Tanaka, K., Sakurai, N., Suda, K., et al. (2008). Metabolite annotations based on the integration of mass spectral information. *Plant J.* 54, 949–962. doi: 10.1111/j.1365-313X.2008.03434.x
- Iijima, Y., Watanabe, B., Sasaki, R., Takenaka, M., Ono, H., Sakurai, N., et al. (2013). Steroidal glycoalkaloid profiling and structures of glycoalkaloids in wild tomato fruit. *Phytochemistry* 95, 145–157. doi: 10.1016/j.phytochem.2013.07.016
- Itkin, M., Heinig, U., Tzfadia, O., Bhide, A. J., Shinde, B., Cardenas, P. D., et al. (2013). Biosynthesis of antinutritional alkaloids in solanaceous

- crops is mediated by clustered genes. *Science* 341, 175–179. doi: 10.1126/science.1240230
- Itkin, M., Rogachev, I., Alkan, N., Rosenberg, T., Malitsky, S., Masini, L., et al. (2011). GLYCOALKALOID METABOLISM1 is required for steroid alkaloid glycosylation and prevention of phytotoxicity in tomato. *Plant Cell* 23, 4507–4525. doi: 10.1105/tpc.111.088732
- Jurka, J., Kapitonov, V. V., Pavlicek, A., Klonowski, P., Kohany, O., and Walichiewicz, J. (2005). Repbase update, a database of eukaryotic repetitive elements. *Cytogenet. Genome Res.* 110, 462–467. doi: 10.1159/000084979
- Jurka, J., and Kohany, O. (2006). hAT-2_SD hAT transposon from *Solanum demissum*. *Repbase Rep.* 6, 492–492.
- Koes, R. E., Quattrocchio, F., and Mol, J. N. M. (1994). The flavonoid biosynthetic pathway in plants: function and evolution. *Bioessays* 16, 123–132. doi: 10.1002/bies.950160209
- Konieczny, A., and Ausubel, F. M. (1993). A procedure for mapping *Arabidopsis* mutations using co-dominant ecotype-specific PCR-based markers. *Plant J.* 4, 403–410. doi: 10.1046/j.1365-313X.1993.04020403.x
- Légnani, R., Gognalons, P., Gébré Sélassié, K., Marchoux, G., Moretti, A., and Laterrot, H. (1996). Identification and characterization of resistance to tobacco etch virus in *Lycopersicon* species. *Plant Dis.* 80, 306–309. doi: 10.1094/PD-80-0306
- Lin, T., Zhu, G., Zhang, J., Xu, X., Yu, Q., Zheng, Z., et al. (2014). Genomic analyses provide insights into the history of tomato breeding. *Nat. Genet.* 46, 1220–1226. doi: 10.1038/ng.3117
- Mathews, H., Clendennen, S. K., Caldwell, C. G., Liu, X. L., Connors, K., Mattheis, N., et al. (2003). Activation tagging in tomato identifies a transcriptional regulator of anthocyanin biosynthesis, modification, and transport. *Plant Cell* 15, 1689–1703. doi: 10.1105/tpc.012963
- Mathieu, S., Cin, V. D., Fei, Z., Li, H., Bliss, P., Taylor, G., et al. (2009). Flavour compounds in tomato fruits: identification of loci and potential pathways affecting volatile composition. *J. Exp. Bot.* 60, 325–337. doi: 10.1093/jxb/ern294
- Mintz-Oron, S., Mandel, T., Rogachev, I., Feldberg, L., Lotan, O., Yativ, M., et al. (2008). Gene expression and metabolism in tomato fruit surface tissues. *Plant Physiol.* 147, 823–851. doi: 10.1104/pp.108.116004
- Moco, S., Bino, R. J., Vorst, O., Verhoeven, H. A., de Groot, J., van Beek, T. A., et al. (2006). A liquid chromatography-mass spectrometry-based metabolome database for tomato. *Plant Physiol.* 141, 1205–1218. doi: 10.1104/pp.106.078428
- Moco, S., Capanoglu, E., Tikunov, Y., Bino, R. J., Boyacioglu, D., Hall, R. D., et al. (2007). Tissue specialization at the metabolite level is perceived during the development of tomato fruit. *J. Exp. Bot.* 58, 4131–4146. doi: 10.1093/jxb/erm271
- Muir, S. R., Collins, G. J., Robinson, S., Hughes, S., Bovy, A., Ric de Vos, C. H., et al. (2001). Overexpression of petunia chalcone isomerase in tomato results in fruit containing increased levels of flavonols. *Nat. Biotechnol.* 19, 470–474. doi: 10.1038/88150
- Prudent, M., Causse, M., Génard, M., Tripodi, P., Grandillo, S., and Bertin, N. (2009). Genetic and physiological analysis of tomato fruit weight and composition: Influence of carbon availability on QTL detection. *J. Exp. Bot.* 60, 923–937. doi: 10.1093/jxb/ern338
- Schauer, N., Semel, Y., Roessner, U., Gur, A., Balbo, I., Carrari, F., et al. (2006). Comprehensive metabolic profiling and phenotyping of interspecific introgression lines for tomato improvement. *Nat. Biotechnol.* 24, 447–454. doi: 10.1038/nbt1192
- Schauer, N., Zamir, D., and Fernie, A. R. (2005). Metabolic profiling of leaves and fruit of wild species tomato: a survey of the *Solanum lycopersicum* complex. *J. Exp. Bot.* 56, 297–307. doi: 10.1093/jxb/eri057
- Schijlen, E. G. W. M., Beekwilder, J., Hall, R. D., and Meer, I. M. (2008). Boosting beneficial phytochemicals in vegetable crop plants. *CAB Rev.* 3, 1–21. doi: 10.1079/PAVSNNR20083025
- Schijlen, E. G. W. M., De Vos, C. H. R., Van Tunen, A. J., and Bovy, A. G. (2004). Modification of flavonoid biosynthesis in crop plants. *Phytochemistry* 65, 2631–2648. doi: 10.1016/j.phytochem.2004.07.028
- Semel, Y., Nissenbaum, J., Menda, N., Zinder, M., Krieger, U., Issman, N., et al. (2006). Overdominant quantitative trait loci for yield and fitness in tomato. *Proc. Natl. Acad. Sci. U.S.A.* 103, 12981–12986. doi: 10.1073/pnas.0604635103
- Steinhauser, M.-C., Steinhäuser, D., Gibon, Y., Bolger, M., Arrivault, S., Usadel, B., et al. (2011). Identification of enzyme activity quantitative trait loci in a *Solanum lycopersicum* x *Solanum pennellii* introgression line population. *Plant Physiol.* 157, 998–1014. doi: 10.1104/pp.111.181594
- Stevens, R., Buret, M., Duffe, P., Garchery, C., Baldet, P., Rothan, C., et al. (2007). Candidate genes and quantitative trait loci affecting fruit ascorbic acid content in three tomato populations. *Plant Physiol.* 143, 1943–1953. doi: 10.1104/pp.106.091413
- Tapas, A. R., Sakarkar, D. M., and Kakde, R. B. (2008). Flavonoids as nutraceuticals: a review. *Trop. J. Pharm. Res.* 7, 1089–1099. doi: 10.4314/tjpr.v7i3.14693
- Tieman, D. M., Zeigler, M., Schmelz, E. A., Taylor, G., Bliss, P., Kirst, M., et al. (2006). Identification of loci affecting flavour volatile emissions in tomato fruits. *J. Exp. Bot.* 57, 887–896. doi: 10.1093/jxb/erj074
- Tikunov, Y. M., de Vos, R. C. H., Gonzalez Paramas, A. M., Hall, R. D., and Bovy, A. G. (2010). A role for differential glycoconjugation in the emission of phenylpropanoid volatiles from tomato fruit discovered using a metabolic data fusion approach. *Plant Physiol.* 152, 55–70. doi: 10.1104/pp.109.146670
- Tikunov, Y. M., Molthoff, J., de Vos, R. C. H., Beekwilder, J., van Houwelingen, A., van der Hooft, J. J., et al. (2013). Non-smoky GLYCOSYLTRANSFERASE1 prevents the release of smoky aroma from tomato fruit. *Plant Cell* 25, 3067–3078. doi: 10.1105/tpc.113.114231
- Tomato Genome Consortium (2012). The tomato genome sequence provides insights into fleshy fruit evolution. *Nature* 485, 635–641. doi: 10.1038/nature11119
- Toubiana, D., Semel, Y., Tohge, T., Beleggia, R., Cattivelli, L., Rosental, L., et al. (2012). Metabolic profiling of a mapping population exposes new insights in the regulation of seed metabolism and seed, fruit, and plant relations. *PLoS Genet.* 8:e1002612. doi: 10.1371/journal.pgen.1002612
- Viquez-Zamora, M., Vosman, B., van de Geest, H., Bovy, A. G., Visser, R. G. F., Finkers, R., et al. (2013). Tomato breeding in the genomic era: insights from a SNP array. *BMC Genet.* 14:354. doi: 10.1186/1471-2164-14-354
- Willits, G., Kramer, C. M., Prata, R. T. N., De Luca, V., Potter, B. G., Stephens, J. C., et al. (2005). Utilization of the genetic resources of wild species to create a nontransgenic high flavonoid tomato. *J. Agric. Food Chem.* 53, 1231–1236. doi: 10.1021/jf0493551
- Wu, F., Mueller, L. A., Crouzillat, D., Petiard, V., and Tanksley, S. D. (2006). Combining bioinformatics and phylogenetics to identify large sets of single copy, orthologous genes (COSII) for comparative, evolutionary and systematic studies: a test case in the eudicot plant clade. *Genetics* 174, 1407–1420. doi: 10.1534/genetics.106.062455
- Zamir, D. (2001). Improving plant breeding with exotic genetic libraries. *Nat. Rev. Genet.* 2, 983–989. doi: 10.1038/nrg1101-983
- Zanor, M. I., Osorio, S., Nunes-Nesi, A., Carrari, F., Lohse, M., Usadel, B., et al. (2009). RNA interference of LIN5 in tomato confirms its role in controlling brix content, uncovers the influence of sugars on the levels of fruit hormones, and demonstrates the importance of sucrose cleavage for normal fruit development and fertility. *Plant Physiol.* 150, 1204–1218. doi: 10.1104/pp.109.136598

Conflict of Interest Statement: The authors declare that the research was conducted in the absence of any commercial or financial relationships that could be construed as a potential conflict of interest.

Copyright © 2016 Ballester, Tikunov, Molthoff, Grandillo, Viquez-Zamora, de Vos, de Maagd, van Heusden and Bovy. This is an open-access article distributed under the terms of the Creative Commons Attribution License (CC BY). The use, distribution or reproduction in other forums is permitted, provided the original author(s) or licensor are credited and that the original publication in this journal is cited, in accordance with accepted academic practice. No use, distribution or reproduction is permitted which does not comply with these terms.



Metabolite Profiling of Italian Tomato Landraces with Different Fruit Types

Svetlana Baldina¹, Maurizio E. Picarella¹, Antonio D. Troise^{2,3}, Anna Pucci¹, Valentino Ruggieri³, Rosalia Ferracane³, Amalia Barone³, Vincenzo Fogliano² and Andrea Mazzucato^{1*}

¹ Department of Agricultural and Forestry Sciences, University of Tuscia, Viterbo, Italy, ² Food Quality Design Group, Wageningen University, Wageningen, Netherlands, ³ Department of Agricultural Sciences, University of Naples "Federico II", Napoli, Italy

OPEN ACCESS

Edited by:

Ana Margarida Fortes,
Faculdade de Ciências da
Universidade de Lisboa, Portugal

Reviewed by:

Gad Galili,
The Weizmann Institute of Science,
Israel
Jaime Prohens,
Universitat Politècnica de València,
Spain

*Correspondence:

Andrea Mazzucato
mazz@unitus.it

Specialty section:

This article was submitted to
Plant Physiology,
a section of the journal
Frontiers in Plant Science

Received: 12 February 2016

Accepted: 29 April 2016

Published: 19 May 2016

Citation:

Baldina S, Picarella ME, Troise AD, Pucci A, Ruggieri V, Ferracane R, Barone A, Fogliano V and Mazzucato A (2016) Metabolite Profiling of Italian Tomato Landraces with Different Fruit Types. *Front. Plant Sci.* 7:664.
doi: 10.3389/fpls.2016.00664

Increased interest toward traditional tomato varieties is fueled by the need to rescue desirable organoleptic traits and to improve the quality of fresh and processed tomatoes in the market. In addition, the phenotypic and genetic variation preserved in tomato landraces represents a means to understand the genetic basis of traits related to health and organoleptic aspects and improve them in modern varieties. To establish a framework for this approach, we studied the content of several metabolites in a panel of Italian tomato landraces categorized into three broad fruit type classes (flattened/ribbed, pear/oxheart, round/elongate). Three modern hybrids, corresponding to the three fruit shape typologies, were included as reference. Red ripe fruits were morphologically characterized and biochemically analyzed for their content in glycoalkaloids, phenols, amino acids, and Amadori products. The round/elongate types showed a higher content in glycoalkaloids, whereas flattened types had higher levels of phenolic compounds. Flattened tomatoes were also rich in total amino acids and in particular in glutamic acid. Multivariate analysis of amino acid content clearly separated the three classes of fruit types. Making allowance of the very low number of genotypes, phenotype-marker relationships were analyzed after retrieving single nucleotide polymorphisms (SNPs) among the landraces available in the literature. Sixty-six markers were significantly associated with the studied traits. The positions of several of these SNPs showed correspondence with already described genomic regions and QTLs supporting the reliability of the association. Overall the data indicated that significant changes in quality-related metabolites occur depending on the genetic background in traditional tomato germplasm, frequently according to specific fruit shape categories. Such a variability is suitable to harness association mapping for metabolic quality traits using this germplasm as an experimental population, paving the way for investigating their genetic/molecular basis, and facilitating breeding for quality-related compounds in tomato fruits.

Keywords: Amadori products, amino acids, glycoalkaloids, landraces, metabolites, phenolics, quality, tomato

INTRODUCTION

Over the past half century nutrient content and flavor of intensively bred crops has dropped because breeding efforts focused mainly on yield, stress resistance and agronomic, and technological properties of the edible product. Tomato (*Solanum lycopersicum* L.) is a good example of this trend: yield has remarkably increased but its taste has worsened according to consumers (Zanor et al., 2009; Causse et al., 2010; Tieman et al., 2012; Klee and Tieman, 2013). Compared to traditional varieties, modern cultivars are thought to have fewer of the most important contributors to flavor (sugars, acids, free amino acids, and volatiles).

The cultivated tomato is a model for the study of fruit development and a major crop being the second most cultivated and consumed vegetable worldwide. Domesticated in Tropical America, tomato was introduced in the Old World at the beginning of the Sixteenth-century. Only one century later the species began to be appreciated for its edible product and its cultivation spread through Europe, with greater success in the Mediterranean countries, including Spain, and Italy (Soressi, 1969; Esquinas-Alcazar and Nuez, 1995; Andreakis et al., 2004; García-Martínez et al., 2013). Due to its success in cultivation and to the wide environmental variability, tomato found in Italy a secondary center of diversification and several landraces developed in different regions according to human selection and adaptation to local climatic and edaphic conditions (Siviero, 2001; Mazzucato et al., 2008). This led to the establishment of landraces with different typologies of the fruit, including flat angled and ribbed tomatoes as well as pear-shaped, heart-shaped, extremely elongated, and cherry and plum forms. All these landraces have been cultivated for centuries and are still common in the local markets (Soressi, 1969; Acciari et al., 2007). Flattened-ribbed tomatoes were mainly diffused in Northern (“Costoluto Genovese”, “Riccio di Parma”, “Ladino di Pannocchia”) and Central (“Costoluto fiorentino”, “Pantano romanesco”, “Scatolone di Bolsena”, “Spagnoletta di Gaeta e Formia”) Italy. Differently, varieties with elongate (“San Marzano”, “Corbarino”), or oval/round (“Piennolo”, “Pizzutello”) fruit shape were mainly found in the Southern regions of the country (Soressi, 1969; Andreakis et al., 2004). Whereas few of these varieties are found in the official registers of varieties, many of them are only listed in voluntary regional catalogs and in registers for conservation varieties.

Although these traditional types usually lack good agronomic performances in terms of yield, resistance and shelf-life of the product, they usually show good adaptation to local environments and outstanding organoleptic qualities. Therefore, it is thought that traditional varieties represent a vault of genes with great interest for improving health- and flavor-related compounds in tomato (Rodríguez-Burrueto et al., 2005; Tieman et al., 2012; Figàs et al., 2015a,b). A strategy to valorize this genetic treasure is to unravel the extent of genetic variability for primary and secondary metabolites in traditional tomato germplasm and to establish correlations between the composition of the fruit, its genetic basis, and the consumer preferences (Hurtado et al., 2014).

Including in a broad sense health and flavor aspects, tomato quality is mainly determined by morphological traits (size, shape, absence of defects) and by the content in products of the primary (sugars, acids, free amino acids) and of the secondary (carotenoids, flavonoids, volatiles) metabolism. Several studies have addressed the identification of genetic factors (quantitative trait loci, QTLs) underlying important traits related to quality in tomato, including morphology, and proximate traits (Shirasawa et al., 2013; Ruggieri et al., 2014; Sacco et al., 2015). Other studies addressed the identification of QTLs related to metabolic traits (mQTLs) with a focus on primary metabolism (Saliba-Colombani et al., 2001; Causse et al., 2002, 2004; Fulton et al., 2002; Schauer et al., 2008; Xu et al., 2013). Among secondary metabolites, most attention has been payed to carotenoids (Rousseaux et al., 2005; Panthee et al., 2013) and volatiles (Mathieu et al., 2009; Zanor et al., 2009; Tieman et al., 2012; Zhang et al., 2015). Fewer studies have addressed the variation in amino acids, among primary (Schauer et al., 2006, 2008; Sauvage et al., 2014), and in alkaloids and phenolic compounds among secondary metabolites (Rousseaux et al., 2005; Alseekh et al., 2015). In addition, no specific analysis has been carried out to search for mQTL associated with Amadori products, a class of compounds formed by the interaction between reducing sugars and amino acids or proteins, that increase with ripening due to the high concentration of sugars, free amino groups, and the acidic environment (Meitinger et al., 2014; Troise et al., 2015).

Due to the wide variability for chemical composition traits described in traditional tomato germplasm (Martínez-Valverde et al., 2002; Rodríguez-Burrueto et al., 2005; Carli et al., 2011; Tieman et al., 2012; Panthee et al., 2013; Cortés-Olmos et al., 2014; Figàs et al., 2015b), the adoption of collections of landraces as experimental populations has been regarded as a promising strategy to associate genetic regions to phenotypic traits of interest (Mazzucato et al., 2008; Panthee et al., 2013; Ruggieri et al., 2014; Sacco et al., 2015). To investigate the potentialities of Italian traditional varieties in association studies involving quality-related compounds, we set up to study the content of several metabolites in a panel of landraces representing three broad fruit typology classes (flattened/ribbed, pear/oxheart, and round/elongate). This characterization paves the way for investigating the genetic/molecular basis for such a variation and for breeding tomatoes with improved fruit quality.

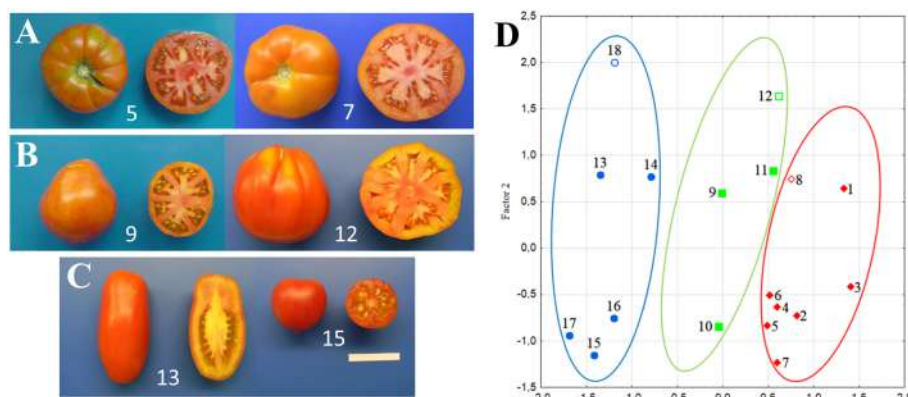
MATERIALS AND METHODS

Plant Materials

Fourteen Italian and one French tomato landraces and three modern F₁ hybrids were adopted for this study (Table 1). Seven landraces belonged to the category of tomatoes with flattened/ribbed fruits, three to pear/oxheart (globose) types, and five to the round/elongate category (Figures 1A–C). Three modern hybrids corresponding to the flat (Marinda, Nunhems), pear (Tomawak, Syngenta), and elongated (Pozzano, Enza Zaden) fruit category were chosen for comparison and purchased from the market. Seeds of landraces were obtained from the tomato collection held by the authors at the University of

TABLE 1 | Landraces (L) and hybrids (H) used in the analyses, their origin, classification into fruit shape classes, and group means for selected phenotypic traits.

Code	Name	Varietal type	Region/Company of origin	Fruit shape class	Phenotypic traits ^c		
					Pericarp index	Dry weight (%)	Brix value
1	Mezzo tempo	L	Abruzzo	Flattened/ribbed	0.74 b	4.76 b	4.31 b
2	Spagnola	L	Latium				
3	Stella	L	Tuscany				
4	Costoluto fiorentino	L	Tuscany				
5	Scatolone di Bolsena	L	Latium				
6	Pantano romanesco	L	Latium				
7	Marmalade	L	France				
8	Marinda	H	Nunhems				
9	Cuor di bue di Albenga	L	Liguria	Pear/oxheart	0.81 b	5.02 b	4.56 ab
10	Cuor di bue	L	Italy ^b				
11	Pera d'Abruzzo	L	Abruzzo				
12	Tomawak	H	Syngenta				
13	San Marzano	L	Campania	Round/elongate	1.18 a	6.09 a	5.20 a
14	Allungato ^a	L	Umbria				
15	Principe Borghese	L	Campania				
16	Ovale Puglia	L	Puglia				
17	Ovale Campania	L	Campania				
18	Pozzano	H	Enza Zaden				

^aAnalyzed as belonging to the "Pear/oxheart" group after genotypic analysis.^bLandrace diffused in several regions.^cMeans within a column followed by the same lowercase letter are not significantly different for $P \leq 0.05$.**FIGURE 1 | Examples of tomato genotypes studied and their distribution according to multivariate Factor Analysis.** Flattened/ribbed (A), pear/oxheart (B), and round/elongate (C) fruits produced by six of the varieties included in the experiments. Separation of the 18 studied varieties according to the first two factors based on morphological traits (D). Circles group accession with flattened/ribbed (red), pear/oxheart (green) and round/elongate (blue) fruits; open symbols refer to hybrids. In all panels, numbers refer to the accession codes given in Table 1.

Tuscia. A field trial was established with the above-described seed stocks at Viterbo, Italy ($42^{\circ}25'07''$ N, $12^{\circ}06'34''$ E). The accessions were arranged in a randomized block design with two replicates and eight plants per elementary experimental unit. Plants were grown in open field with the standard agronomic practices adopted for genotypes with indeterminate growth. F_2 progenies ($n = 18$) of the hybrids included in the study were grown to maturity in the subsequent season to

check for the eventual segregation of alleles conferring delayed ripening.

Morphological Characterization

On a single plant basis, 15 morpho-physiological traits were scored or calculated as detailed in Table S1. Briefly, the growth habit (GH), plant height (PH), inflorescence type (IT), and green shoulder (GS) were scored during plant growth. At the maturity

of the second truss, four representative fruits per plant were used to measure or score fruit polar (PD, mm) and equatorial (ED, mm) diameter, stem-end shape (SES, score), blossom-end shape (BES, score), number of fruit locules (LN), pericarp thickness (PT, mm), puffiness (PUF, score), fruit weight (FW, g) and fruit-shape cross section (FSC, score). Two further traits were calculated; the fruit-shape index [FS, (PD/PE)] and the pericarp thickness index [PI, (PT/((PD + PE)/2))]. These descriptors largely conform to the guidelines of Bioversity International for tomato (<http://www.bioversityinternational.org/e-library/publications/detail/descriptors-for-tomato-lycopersicon-spp/>).

Six fruits per genotype were cut and the soluble solids content was measured as refractive index at 20°C (Brix) in the juice obtained after extracting the seeds using a digital refractometer (MA871, Milwaukee, Milwaukee Instruments, Inc., NC, USA) on a single fruit basis. Dry matter content was calculated as the percentage of dry weight (DW) over fresh weight (FW). Total solid content determination was carried out by gravimetric method according to AOAC International (1995).

Chemicals

Acetonitrile and water for liquid chromatography high resolution mass spectrometry (LC/HRMS) analysis were obtained from Merck (Darmstadt, Germany). L-Amino acids standards, perfluoropentanoic acid (NFPA), acetic acid, and formic acid were obtained from Sigma-Aldrich (St. Louis, MO). Amadori products (APs) were synthesized according to the procedure described in Troise et al. (2015). The calibration solutions (see “Liquid chromatography/high resolution mass spectrometry” Section) were obtained from Thermo Fisher Scientific (Bremen, Germany).

Genotypic Data Retrieval

Genotypic data of the landraces adopted here were available from the study of a wider collection of tomato germplasm using the SolCAP single nucleotide polymorphism (SNP) array (Sacco et al., 2015). Raw data were retrieved and markers with more than 10% missing genotypes were removed. After discarding sites with Minor Allele Frequency (MAF)<15%, levels of observed heterozygosity (H_O) were calculated and a neighbor-joining tree was generated using TASSEL 5.0 (Bradbury et al., 2007).

Liquid Chromatography/High Resolution Mass Spectrometry LC-HRMS Analyses

Twenty representative vine-ripened fruits were harvested for all the genotypes from eight plants per accession and the concentration of amino acids and APs, glycoalkaloids, and phenolic acids (63 markers in total) was monitored by liquid chromatography high resolution mass spectrometry (LC-HRMS). Each sample was extracted twice and analyzed in duplicate ($n = 4$). Data were reported as mg/kg FW.

Amino acids and APs were analyzed according to Troise et al. (2015). Briefly, tomato samples were ground in a knife mill Grindomix 200 (Retsch, Haan, Germany) and 100 mg were mixed with 0.3 mL of deionized water and centrifuged (14,800 rpm, 20 min, 4°C). The supernatants were filtered using regenerated cellulose filters (RC 0.45 μm, Phenomenex, Torrance, CA).

For the chromatographic separation of amino acids and their respective APs, the mobile phases consisted of 5 mM NFPA (solvent A) and 5 mM NFPA in acetonitrile (solvent B). The following linear gradient of solvent B (min/%B): (0/2), (2/2), (5/50), (7/50), (9/50) was used. The flow rate was set to 200 μL/min and the injection volume was 5 μL. Chromatographic separation of amino acids and APs was achieved through a thermostated (30°C) core-shell C-18 column (Kinetex 2.6 μm, 100 × 2.1 mm, Phenomenex, Torrance, CA). The Accela 1250 UPLC system (Thermo Fisher Scientific, Bremen, Germany) was directly interfaced to an Exactive Orbitrap high resolution mass spectrometer (Thermo Fisher Scientific, Bremen, Germany). Analytes were detected through a heated electrospray interface (HESI) operating in the positive mode and scanning the ions in the m/z range of 60–500. The resolving power was set to 50,000 full width at half maximum (FWHM, m/z 200) resulting in a scan time of 1 s. The automatic gain control was used in balanced mode (1×10^6 ions); maximum injection time was 50 ms. The interface parameters were as follows: spray voltage 3.8 kV, capillary voltage 10 V, skimmer voltage 15 V, capillary temperature 275°C, heater temperature 200°C, sheath gas flow 30, and auxiliary gas flow 3 arbitrary units.

The same simplified extraction procedure was used for antioxidants compounds. Phenolic acids and glycoalkaloids were analyzed according to Troise et al. (2014). Chromatographic separation was carried out on a Gemini C18 column (5 μm, 150 × 2.0 mm Phenomenex, Torrance, CA) thermostated at 30°C while mobile phases were 0.1% formic acid (solvent A) and 0.1% formic acid in acetonitrile (solvent B). The following linear gradient of solvent B (min/%B): (0/10), (8/90), (10/90) was used. The flow rate was set to 200 μL/min and the injection volume was 10 μL. The UPLC was directly interfaced to the Orbitrap equipped with HESI interface. Mass analyzer operated in the full spectra acquisition mode and positive and negative ionization mode was simultaneously used in the mass range of m/z 65–1300. The resolving power was set to 50,000 (FWHM, m/z 200) resulting in a scan time of 1 s. The automatic gain control was used (ultimate mass accuracy mode, 5×10^5 ions) and maximum injection time was 100 ms. The interface parameters were as follows: the spray voltage was 3.5 and –3.0 kV in positive and negative ion mode, respectively; the tube lens was at 100 V (–100 V in negative ion), the capillary voltage was 30 V (–50 V in negative ion), the capillary temperature was 275°C, and a sheath and auxiliary gas flow of 30 and 15 arbitrary units were used. The instrument was externally calibrated by infusion with a positive ions solution that consisted of caffeine, Met-Arg-Phe-Ala (MRFA), Ultramark 1621, and acetic acid in a mixture of acetonitrile/methanol/water (2:1:1, v/v/v), then with a negative ions solutions that consisted of sodium dodecyl sulfate, sodium taurocholate, Ultramark 1621, and acetic acid in a mixture methanol/water (1:1 v/v). Reference mass (lock mass) of diisooctyl phthalate ($[M + H]^+$, exact mass = 391.28429) was used as recalibrating agent for positive ion detection. To optimize the mass spectrometer conditions and the mass accuracy, the calibration procedure was performed each day both in positive and negative mode. The analytical performances, i.e., mass error,

linearity, reproducibility, repeatability, LOD, and LOQ were in line with those previously reported.

Data Analysis

Analysis of variance (ANOVA) for differences among fruit shape groups was carried out adopting the General Linear Model (GLM) using the SAS software (SAS Institute, 2004). Significant differences were estimated by Duncan multiple range test. A Pearson correlation matrix was developed to ascertain the correlation coefficient (r) between all studied parameters and a heatmap obtained by Gitoools software version 2.2.2 (Perez-Llamas and Lopez-Bigas, 2011). Standardized morphological and metabolic data were statistically analyzed by Factor Analysis (FA) using “Statistica 10” (StatSoft Inc., Tulsa, OK, USA). Hierarchical clustering (Ward’s method) of the 15 landraces and the three hybrids under study, based on the content of 63 analyzed metabolites, was carried out by Past 3.11 (Hammer et al., 2001).

To assess the genetic relationships within the investigated collection, the population structure was determined by using STRUCTURE 2.3.4 software (Pritchard et al., 2000), with no a priori information regarding population origin. The degree of admixture was estimated by setting for both burn-in period and Markov Chain Monte Carlo iterations a value of 100,000 for each run. Seven independent runs across a range of K -values ($K = 1\text{--}12$) were made. The best number of clusters (K) was obtained using STRUCTURE HARVESTER program (Earl and vonHoldt, 2012) based on the method of Evanno (Evanno et al., 2005). Genome-Wide Association Study (GWAS) between traits and DNA polymorphisms was performed using the GLM model with Q matrix as implemented in TASSEL 5.0 (Bradbury et al., 2007). P -values were corrected following the standard Bonferroni procedure. Significant associations were detected with corrected p value lower than $5.2E^{-5}$ ($0.05/954$). A physical map of the tomato genome showing the position of the SNP markers significantly associated with the traits was constructed using Map Chart 2.2 (Voorrips, 2002).

RESULTS

Phenotyping of Morphological Traits

All the measured morphological traits, including plant and fruit characters, showed a large range of phenotypic variation among the 15 tomato landraces and three market F₁ hybrids. With the exception of GH, PH, GS, BES, PT, and PUF, all the phenotypic traits showed significant differences among fruit type groups (Table S2). In addition to obvious differences in traits related to fruit shape (PD, ED, FS), ANOVA indicated that round/elongated types were differentiated for the simple inflorescence, the flat stem end shape, the lower number of locules and lower fruit weight (Table S2). Types with round/elongate fruits also showed higher PI, DW and Brix values (Table 1). The two first FA components explained 56% of the phenotypic variation and distinguished the genotypes according to these phenotypes (Figure 1D). Factor 1 was mainly loaded by FS and LN, whereas Factor 2 mainly by PD.

Several morphological traits were significantly correlated; in addition to trivial correlations (e.g., LN with ED and FWE),

plants producing fruits with high LN (flattened/ribbed types) showed also compound IT and depressed SES (Figure S1). DW was highly correlated with Brix. Plant traits (GH and PH) together with GS, PI and PUF were rather independent. In agreement with the previously assumed information, the three hybrids used, when progeny tested in the F₂ generation, showed no segregation of genes for delayed ripening (not shown).

Genotyping

SolCAP data for the 15 landraces retrieved from the literature (Sacco et al., 2015) included 7719 readable SNP sites of which 2022 resulted polymorphic in the studied material. Sites filtered for MAF < 15% resulted in 954 polymorphic SNPs, that offered a whole coverage of the tomato genome, ranging from a minimum of 54 (Chr6 and Chr10) to a maximum of 155 (Chr3) SNPs per chromosome. All genotypes showed low levels of Ho, ranging between 0.064 and 0.088, with the exception of genotypes #10 and #14 that showed higher values (0.430 and 0.362 respectively, data not show).

The Neighbor-joining dendrogram separated genotypes with flat and globose fruits from those with round/elongated berry types (Figure 2). The landrace #14 (Allungato), that was initially classified among the round/elongated types due to the shape index of the fruit (Table 1), clustered among globose types. Therefore, also on the basis of the similar fruit structure (higher number of locules and higher proportion of flesh than in round/elongate types), this genotype was included in the pear/oxheart group in all the further analyses.

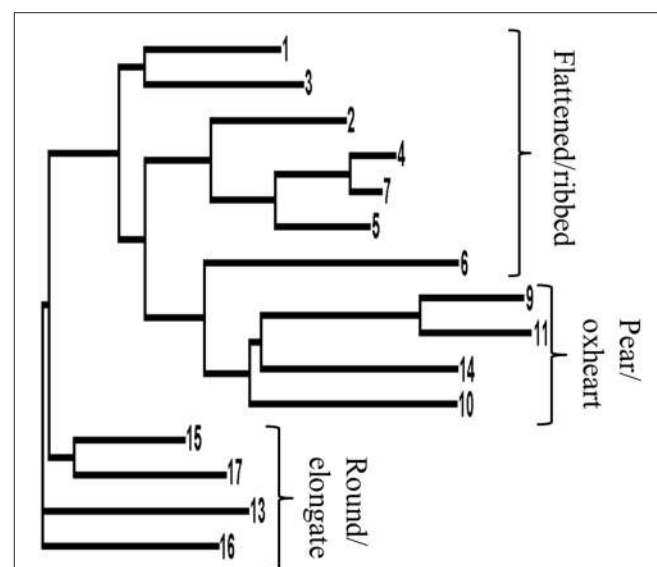


FIGURE 2 | Neighbor-joining dendrogram based on genetic distances among the 15 landraces for which SNP data were retrieved (Sacco et al., 2015). The dendrogram is based on 954 SNP sites polymorphic among the 15 tomato landrace accessions. Numbers indicating each branch refer to the accession code as reported in Table 1.

Biochemical Analysis

In total, 63 fruit metabolites belonging to the glycoalkaloid, phenolic, free amino acid, and AP classes have been analyzed in the studied genotypes. Detailed data on these analyses are reported in Tables S3–S6.

With the exception of dehydro-tomatine, all the glycoalkaloids showed significant differences among tomato fruit types (Table S3). The total alkaloid content was very variable among the genotypes; the variety with highest content (#15, Principe Borghese) showed an amount of total glycoalkaloids that was almost eight-fold that recorded in the lowest one (#11, Pera d'Abruzzo). α -tomatine and tomatoside-A were the most represented analytes accounting for more than 50% of total glycoalkaloids. Round/elongate types showed contents significantly higher than the other types both for single analytes and for total alkaloid content (Figure 3A; Table S3). Being higher in tomato plants with round/elongate fruits, glycoalkaloid content was positively correlated with FS, PI, DW and Brix (Figure S1), which are all traits with higher values in round/elongated types. In addition, all the single analytes and the total content showed high reciprocal positive correlations (Figure S1).

Chlorogenic acid together with caffeic acid hexoside were on average the most represented phenolic compounds in tomato ripe fruits, accounting for about 55% of the total average content (Table S4). Variation in total phenolics was lower than that for

glycoalkaloids, the highest value being barely two-folds the lowest one. The analyte with highest genotypic variation was Naringin that in the flat type #3 (Stella Pisa) had levels about 34-fold higher than in the pear-shaped genotype #9 (Cuor di bue di Albenga). There were no differences among groups of varieties for the phenolic compounds, with the exception of pentosyl rutin, that showed lower levels in flat tomatoes and total phenolics that were lower in pear/oxheart cultivars (Figure 3B; Table S4).

The most represented amino acids in tomato fruits resulted glutamic acid (Glu) and glutamine (Gln), accounting for up to 70% of the total amino acid content. The accession means showed a wide variation for amino acid composition and several fold differences were observed between the minimum and maximum value. The highest differences were observed for valine (Val), tyrosine (Tyr), and arginine (Arg; Table S5). ANOVA showed significant differences among typologies for 11 amino acids (Table S5), but highly significant ($P \leq 0.01$) variations were only recorded for Val, serine (Ser), Glu, and total amino acid content (Figures 3C,D). Glu was on average more than two-fold higher in flattened/ribbed varieties than in the other groups of genotypes (Figure 3D).

All amino acids, with the exception of Val, phenylalanine (Phe), Tyr, methionine (Met) and proline (Pro), were strongly positively correlated among them. The content of (at least) 12 amino acids was positively correlated with FWE and negatively correlated with Brix. Glu content was significantly correlated with eight out

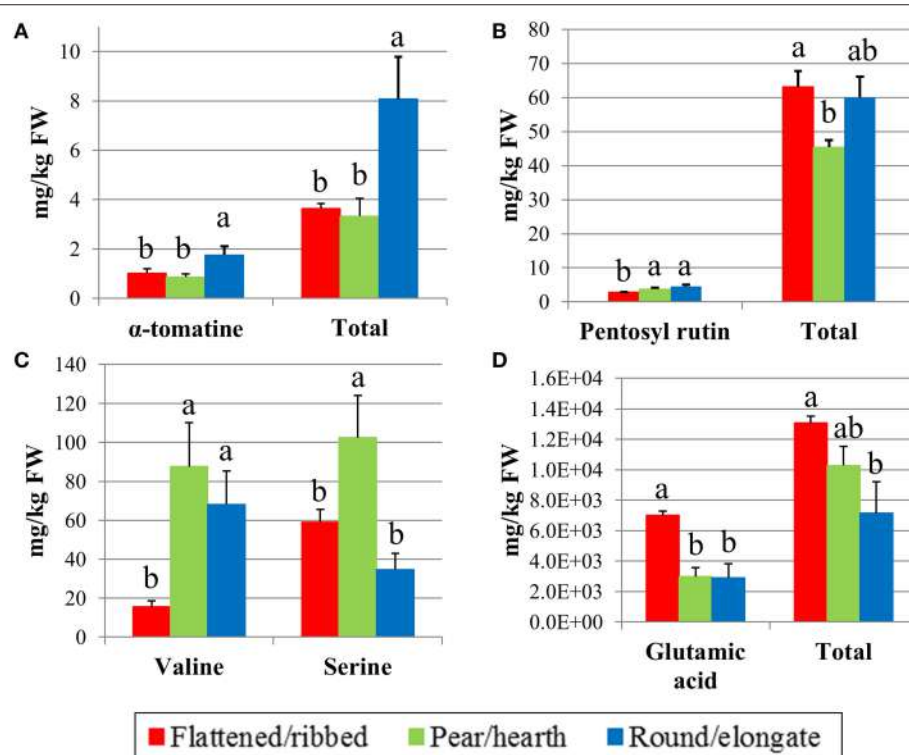


FIGURE 3 | Significant variation in selected metabolites in the 18 tomato varieties analyzed according to their classification in different fruit typologies. Content in α -tomatine and total glycoalkaloids (A), pentosyl rutin and total phenolics (B), valine and serine (C), glutamic acid, and total free amino acids (D). Mean values indicated by different letters are significantly different for $P \leq 0.01$.

of 15 morphological variables (Figure S1), indicating that this analyte is strictly related to specific plant and fruit types.

Multivariate analysis of amino acid content yielded the two first components that explained 72.8% of the total variation. Metabolite contribution to Factor 1 was high and negative for leucine (Leu), isoleucine (Ile), threonine (Thr), asparagine (Asn), Gln, and histidine (His); Factor 2 was positively charged by Phe and negatively by Glu (not shown). The analysis revealed that amino acids clearly separated the three fruit types; the flattened/ribbed types grouped together, whereas the other types were also differentiated with only few exceptions (Figure 4). As supported by genotypic analysis, the elongate type #14 was more related to pear/oxheart shaped tomatoes than to elongate types. On the contrary, the pear-shaped hybrid (#12) was rather distant from landraces of the same typology according to amino acid content (Figure 4). Genotype #16 (Ovale Puglia) also showed in the plot a position distant from the group of varieties with similar fruit type, due to its very high amino acid content (Table S5).

The difference from the highest and the lowest value for total APs was about five-fold; considering single analytes the highest variations were found for Fru-Arg, Fru-Lys and Fru-Gly (Table S6). Fru-Ser was by far the most relevant glycosylated amino acid form, accounting on average for about 75% of the total in mature fruits. Differently from the free amino acids, APs showed less variation among the tomato types analyzed; highly significant differences were only reported for Fru-Leu and Fru-Ile (highest in round/elongate types) and for Fru-Asn (higher in flattened types; Table S6). As for free amino acids, several APs showed a

positive correlation with FWE and related morphological traits (Figure S1).

Hierarchical clustering based on 63 metabolites showed that fruit composition is similar in genotypes having similar fruit type (Figure S2). However, hybrids did not always follow this behavior. Whereas the hybrid with elongate fruit (#18, Pozzano) grouped within landraces with the same fruit type, the hybrids representing oxheart and flattened types were misplaced and did not show a metabolic composition parallel to that shown by landraces with similar fruits (Figure S2).

Molecular Analysis and Comparison with Morphological and Biochemical Traits

Making allowance for the very small number of genotypes sampled, we crossed morphological and biochemical data with molecular polymorphisms. To improve the reliability of such attempt, the structure of the population has been taken into account and the Bonferroni correction applied to a level of significance below $P < 5.2E-05$. The Evanno test (Evanno et al., 2005) indicated that the best number of clusters to divide the population was three (Figure S3A), in parallel with the a priori division on fruit typologies. Model-based groups represented in the plot of ancestry estimates (Figure S3B) confirmed the genetic relatedness of types with round/elongate fruits, with the exception of accession #14 that was more similar to pear/oxheart types. Among flat-fruited tomatoes, #6 (Pantano Romanesco) also showed relatedness to pear/oxheart types, as already indicated by hierarchical clustering (Figure 2).

GWAS yielded a total of 66 markers (involving 56 genes) significantly associated with the morphological traits and the four categories of analytes on 11 tomato chromosomes (Table 2). No association was reported on Chr9. A relatively low number of associations was highlighted for each category of traits analyzed; the position in the tomato genome of the markers significantly associated with morphological and metabolic traits is mapped in Figure S4.

Among morphological traits, high numbers of associations were reported for ED (9) and LN (13). For glycoalkaloids, only the total content of showed positive associations, indicating two regions of the genome, one on the short arm of Chr8 and the second on the long arm of Chr10 (Table 2). Two phenolic compounds, coumaric acid hexoside and naringin, showed associations; remarkably, coumaric acid hexoside had eight associated markers spanning a wide region of the long arm of Chr3. Four amino acids yielded significant hits, alanine (Ala) on six different chromosomes and Asn, Glu and Pro, each one on a single chromosome. For Glu, significant markers were found on both the short and long arm of Chr10 (Table 2; Figure S4).

DISCUSSION

A deep characterization of tomato germplasm used in traditional cultivations, including morphological, agronomic, nutritional, and organoleptic traits, is desirable for several reasons. This phenotypic information, coupled with deep genotypic analysis, can be helpful to characterize and distinguish landraces for

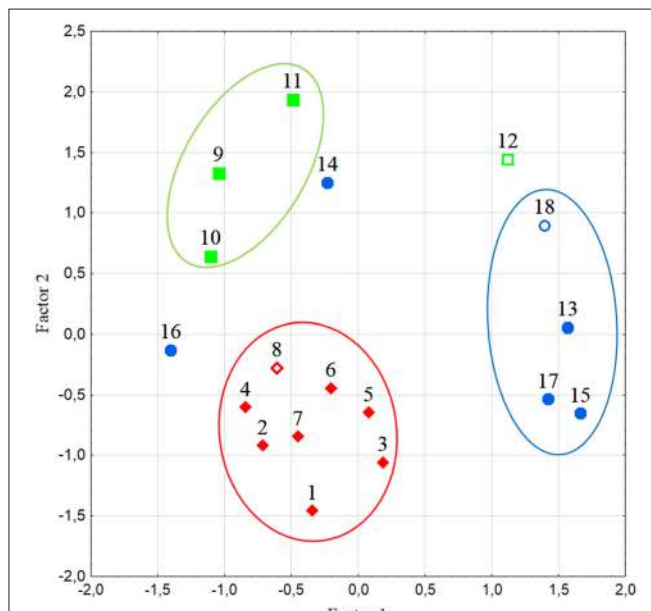


FIGURE 4 | Distribution of the studied tomato varieties according to the first two factors in multivariate analysis of the amino acid content. Numbers refer to the accession codes given in Table 1. Circles group accessions with flattened/ribbed (red), pear/oxheart (green), and round/elongate (blue) fruits. Open symbols refer to hybrids.

TABLE 2 | SNP Markers associated to morphological and biochemical traits in Italian tomato landraces.

Phenotypic class	Trait^a	SolCap ID^b	Chr^c	Position	Solyc ID	p-value
Morphological traits	ED	5624	02	47148187	Solyc02g083900.2.1	2.82E-05
		5625	02	47218361	Solyc02g083990.2.1	5.07E-05
		4597	02	52417091	Solyc02g090960.1.1	4.47E-06
		7584	03	64512996	Solyc03g114560.2.1	5.31E-06
		2501(2)	04	1170841	Solyc04g007500.1.1	2.82E-05
		2020	06	41163560	Solyc06g065720.1.1	2.82E-05
		6943	07	62062707	_d	3.77E-05
		112	12	66795414	Solyc12g099800.1.1	2.82E-05
	GS	1722	07	64287991	Solyc07g056430.2.1	4.36E-05
		7583	03	64588871	Solyc03g114690.2.1	2.12E-05
	LN	518	01	730154	Solyc01g006050.2.1	1.40E-06
		2557	02	40887642	Solyc02g071440.2.1	9.13E-07
		5731	02	45515428	Solyc02g081640.2.1	3.71E-07
		2994	02	45761358	Solyc02g082030.2.1	3.71E-07
		7465	03	62386150	Solyc03g111740.2.1	1.45E-06
		6980	04	1163761	Solyc04g007490.2.1	3.71E-07
		5963	07	57927159	Solyc07g044870.2.1	2.51E-07
		1981	10	58672684	Solyc10g074950.1.1	8.30E-08
		3617	11	54854070	Solyc11g071340.1.1	1.45E-06
		2076 (2)	11	54970033	Solyc11g071530.1.1	1.45E-06
		3534	11	55072385	Solyc11g071660.1.1	9.13E-07
		504	11	55074586	Solyc11g071670.1.1	1.45E-06
Glycoalkaloids	Total	377	08	230545	Solyc08g005300.1.1	3.80E-05
		1745	10	51335068	_	3.80E-05
		7469	10	51524389	Solyc10g051110.1.1	3.80E-05
		5993 (3)	10	54449604	Solyc10g054010.1.1	3.80E-05
		5984 (2)	10	54518281	Solyc10g054030.1.1	3.80E-05
		1982	10	58189616	_	3.80E-05
Phenolics	Coumaric acid hexoside	1678	03	52079075	Solyc03g080190.2.1	4.68E-06
		7575	03	65365147	_	5.20E-07
		2374	03	66796966	Solyc03g117760.2.1	5.68E-06
		2373	03	66806264	Solyc03g117770.2.1	5.18E-05
		2372 (2)	03	66807096	Solyc03g117780.2.1	5.18E-05
		4652	03	70262451	Solyc03g123390.2.1	6.96E-06
		4651	03	70365262	Solyc03g123530.2.1	7.32E-06
		2193	10	57397425	Solyc10g055760.1.1	5.68E-06
		7535	10	64340240	Solyc10g084990.1.1	5.68E-06
		7534	10	64340314	_	5.68E-06
	Naringin	2099	04	7569869	Solyc04g017610.2.1	6.35E-06
		6122	04	36996123	Solyc04g047750.2.1	6.35E-06
		1875	08	63328385	Solyc08g079900.1.1	6.35E-06
Amino acids	Ala	7498	02	39605044	Solyc02g069780.2.1	3.51E-05
		7499 (2)	02	39617885	Solyc02g069780.2.1	3.51E-05
		6407	03	54696154	Solyc03g093400.2.1	1.45E-05
		1572	05	3898119	Solyc05g009700.2.1	2.71E-05
		2915	05	3947680	Solyc05g009740.1.1	2.71E-05

(Continued)

TABLE 2 | Continued

Phenotypic class	Trait ^a	SolCap ID ^b	Chr ^c	Position	Solyc ID	p-value
		1327	06	37080820	Solyc06g054270.2.1	4.73E-05
		7664	10	4260136	Solyc10g011960.1.1	8.55E-06
		7122	11	12993630	–	3.41E-05
	Asn	1106	11	55733112	–	1.60E-05
	Glu	3340	10	6769606	Solyc10g018140.1.1	5.20E-05
		531	10	7464111	Solyc10g018340.1.1	5.20E-05
		1983	10	58003053	Solyc10g074470.1.1	5.20E-05
	Pro	3455	10	58307818	Solyc10g074700.1.1	5.20E-05
		1918 (4)	07	2870461	Solyc07g008160.2.1	3.30E-05
		1914	07	2883786	Solyc07g008170.2.1	3.30E-05

For each marker the position in bp on the related chromosome is reported, together with the corresponding gene (Solyc ID) according to SL2.50 and the p-value.

^aAbbreviation as detailed in Materials and Methods.

^bNumbers in brackets indicate multiple significant markers within the same gene.

^cChromosome.

– Not in gene region.

their quality related traits in fresh (Mazzucato et al., 2010; Figàs et al., 2015a and refs therein) and processed (Andreakis et al., 2004; Caramante et al., 2011) products, to improve the traditional varieties without losing those peculiar traits (Acciarri et al., 2007) and for breeding quality improvement alleles into more productive and modern backgrounds (Rodríguez-Burrueto et al., 2005; Tieman et al., 2012; Sacco et al., 2015). Finally, landrace germplasm can be adopted to discover structural and regulatory genes important in tuning plant primary and secondary metabolism, as suitable targets for metabolic engineering strategies (Bovy et al., 2007).

In this work, we pursued the analysis of a set of Italian tomato landraces representing the major fruit typologies in order to describe the degree of variation in metabolite concentration in comparison with modern hybrids belonging to the same fruit shape classes. Selected hybrids were confirmed to lack genes affecting ripening [such as *ripening inhibitor* (*rin*) and *non-ripening* (*nor*)] which could have influenced the metabolic composition of red ripe fruits (Osorio et al., 2011). Our analysis evidenced the wide variation of several metabolites in different genotypes and overall in groups with different fruit types, in agreement with description of large diversity in tomato germplasm autochthonous of different geographic regions (Rodríguez-Burrueto et al., 2005; Cortés-Olmos et al., 2014; Figàs et al., 2015b).

Content of Quality-Related Metabolites in Tomatoes with Different Fruit Shape

A wide variation among varieties and types was found for glycoalkaloid compounds, the round/elongate varieties having up to eight-fold the content showed by other genotypes, in agreement with previous estimations on cherry and elongate tomatoes (Leonardi et al., 2000). However, the content of alkaloids found in Italian landraces belonging to this category are higher than those reported in the literature (Friedman, 2002).

As round/elongate varieties also show higher values of Brix and DW, these two correlated traits (Carli et al., 2009, 2011; Figàs et al., 2015b; this work) showed a strong correlation with all the alkaloid analytes. Although alkaloids are regarded as potentially toxic compounds, many health-beneficial effects of tomatine have also been described. In addition, the content in alkaloids may affect the degree of resistance to pathogens and parasites, and the alkaloid-correlated traits Brix and DW are positively correlated with fruit taste (Figàs et al., 2015b). Thus, selecting new tomato varieties with beneficial total glycoalkaloid content could be an important breeding objective in the future.

The tomato fruit contains also a considerable amount of phenolic compounds, among which chlorogenic acid and quercetin are the most represented (Martínez-Valverde et al., 2002). It was reported that phenolics give the major contribution to antioxidant capacity (Toor and Savage, 2005). In our analysis, flattened types showed a concentration of total phenolics higher than pear/oxheart types, whereas round/elongate tomatoes were intermediate. Because a taste index showed positive correlation with total phenolics (Figàs et al., 2015b), the improvement in this class of compounds will also be important to breed tomatoes with improved both nutritional and organoleptic quality (Kaushik et al., 2015).

Free amino acids form about 2–2.5% of the total dry matter of tomatoes. In addition to represent a source of nitrogen in the diet, amino acids play a role in organoleptic qualities deeply affecting fruit flavor (Choi et al., 2014). The content of several amino acids showed a strong positive reciprocal correlation in the material analyzed, confirming that these metabolites share high interconnection (Schauer et al., 2006; Carli et al., 2009). The most abundant amino acid found in the tomato fruits analyzed was Glu, followed by Gln; these two forms comprised on average 70% of the total free amino acids confirming previous reports (Kader et al., 1978; Sorreiqueta et al., 2010; Pratta et al., 2011; Choi et al., 2014). High variation in Glu content

among cultivars with different fruit size was also reported in the literature (Zushi and Matsuzoe, 2011). Glu, commonly referred to as “glutamate” because it is present in its anionic form at physiological pH, plays diverse biological roles in organisms (Forde and Lea, 2007). In fruits, it represents a taste-enhancing compound, known to be sensed as the fifth basic taste (umami), which evokes a savory feeling; this property has been related to an adaptive role in attracting mammal predators (Chaudhari et al., 2009). Average content in Glu in tomato fruits found in literature ranges between 1000 and 2000 mg/kg FW (Kader et al., 1978; Pratta et al., 2011; Zushi and Matsuzoe, 2011), reaching a maximum of 3500 in a cherry green-fruited variety (Choi et al., 2014). The average concentration of Glu detected in Italian flattened/ribbed genotypes (6871 mg/kg FW), as well as that in the French cultivar Marmande (7565 mg/kg FW), are the highest ever reported being about two-fold those measured in other tomato types.

Amadori compounds increase in the tomato paste during processing due to the Maillard reaction. Due to their processing-induced nature, APs are found in raw fruits at level several folds lower than free amino acids. Despite processing-induced APs in foods have historically been related with mostly negative health effects, a few individual analytes have been associated with antioxidant activity and other positive biological properties. The activity of Fru-His as a potent copper chelator indicated possible antioxidant activity (Mossine and Mawhinney, 2007). If the positive correlation between Fru-His in the fresh fruit and in the processed tomato will be demonstrated, the significant differences in Fru-His detected in the material studied here could be a basis to obtain fortified tomatoes as a consequence of the antioxidant potential of Fru-His and the inhibitory activity of Fru-His/lycopene against prostate cancer cell proliferation (Mossine et al., 2008).

Molecular Analysis and Comparison with Morphological and Biochemical Traits

GWAS strategies rely on the development of large volumes of phenotypic and genotypic data, that can be analyzed together to unravel QTLs and candidate genes involved in the control of complex traits of interest. Although only the analysis of large sets of genotypes may indicate reliable associations, the possibility that a limited sampling can be adopted to obtain useful insights into gene-phenotype relationships and networks has been proposed (Carli et al., 2009, 2011). Even if based on a minimal number of genotypes, the trait-marker relationships reported here are considered to represent a reliable indication of functional genomic regions because of their relatively low number and their frequent coincidence with associations previously reported using biparental populations or GWAS with a wider array of genotypes. Such insights represent a useful basis to extend GWAS on biochemical traits using traditional tomato germplasm.

Several associations with morphological phenotypic traits evidenced here corresponded to already characterized genomic regions. For instance, association of the correlated traits LN and ED with markers of Chr2, Chr10, and Chr11 coincided with those reported by others (Shirasawa et al., 2013; Xu et al., 2013; Sacco et al., 2015) being tightly close to the *Locule number* (*Lc*; Solyc02g083940 or 950), *SUN1* (Solyc10g079240),

and *FASCIATED* (*FAS*; Solyc11g071819) gene respectively. In this study, seven out of 12 markers linked to LN and three out of eight markers linked to ED corresponded to polymorphisms previously associated with these traits (Sacco et al., 2015). In addition, the marker associated with Brix with higher probability, that was not described in detail because it did not reach the significance threshold ($P = 0.0148$), was located on Chr10 at position 62.5 Mbp (not shown) in tight proximity to a marker associated with the same trait at position 60.3 Mbp (Xu et al., 2013).

Of the six markers associated with total glycoalkaloids, five mapped on a 7 Mbp region on the long arm of Chr10. This region well-corresponded to that involved in the introgression lines IL10-2 and IL10-3 (Eshed and Zamir, 1995) where QTLs for the content of lycoperoside G and F or esculeoside A were positioned (Alseekh et al., 2015). A gene candidate to underlie these QTLs has been identified in an uncharacterized UDP-glycosyltransferase involved in glycoalkaloids biosynthesis (Solyc10g085230; Itkin et al., 2013; Alseekh et al., 2015). This gene, whose product catalyzes the conversion of esculeoside A to esculeoside A+exose, is compatible with the distalmost QTL position found in our analysis.

Ten markers linked to coumaric acid hexoside were detected on the long arm of Chr3 and Chr10. A QTL involved in coumaric acid-exoside compatible with this latter position was recently described and genes candidate have been proposed as five UDP-glycosyltransferase 1 family genes (*UGT1*; Solyc10g085730, Solyc10g085860, Solyc10g085870, Solyc10g085880, and Solyc10g086240) and one phenylalanine ammonia lyase gene (*PAL*; Solyc10g086180; Alseekh et al., 2015). These genes span positions from 64.81 to 65.10 Mbp, whereas our closest marker mapped at 64.34 Mbp. Three markers linked to the content of naringin were found on Chr4 and Chr8; this represents the first report of markers linked to this metabolite and their consistence will need further investigation.

Out of 15 markers linked to amino acid content, eight showed association with Ala; six of them indicated positions on Chr2, Chr3, Chr5, and Chr10 compatible with previously reported QTLs (Schauer et al., 2006). The same held for the markers linked to Pro content on Chr7. Four markers significantly associated with Glu were arranged on Chr10, two on the short and two on the long arm. The latter position corresponded to a described QTL for Glu content (Fulton et al., 2002). As these markers were remarkably coincident with those linked to total glycoalkaloids, it remains to be ascertained if they actually reflect the position of different genes or are the consequence of the negative correlation existing between total glycoalkaloids and Glu content. However, the markers linked with Glu, spanning a region between Solyc10g074470 and Solyc10g074700 (57.33–57.63 Mbp), were in close proximity to one of the four glutamate dehydrogenase 1 (*GDH1*) genes annotated in tomato (Solyc10g078550, position 59.66 Mbp; Ferraro et al., 2012). *GDH1* encodes an enzyme that converts alpha oxoglutarate to glutamate (Forde and Lea, 2007), an important reaction in glutamate metabolism. Moreover, GDH protein content and activity were highly induced in ripe fruits paralleling the increase in the relative content of Glu at ripening; *GDH1* is thus a good candidate for determining Glu levels in tomato fruits (Sorrieta et al., 2010).

Perspectives for Improving and Valorize Italian Tomato Landraces

Taking into consideration all the metabolites analyzed, the study indicates that modern hybrids that are selected for particular fruit type categories may not present similar composition and consequently organoleptic qualities as the traditional tomatoes with similar fruit shape (Figure S2). The results also showed that metabolic profiling of tomato landraces can indicate which metabolites contribute more to the quality of specific variety and, once this information will be associated with a sensorial analysis, it will be clear which metabolites contribute more to consumer acceptance.

As an example, the group of flattened/ribbed tomatoes was relatively homogeneous for metabolic composition; however, the Scatolone di Bolsena landrace emerged as having, within this group, the highest Brix value, α -tomatine content and sweetness score according to a non-professional panel test assessment (not shown). This association was in agreement with reports of these traits as positively correlated (Figàs et al., 2015b). The hybrid Marinda, that was misplaced in the hierarchical clustering based on all metabolites, scored lowest values among flat types for all the three traits. Thus it is possible to argue that the fruit composition of this hybrid does not represent that of traditional flat-fruited tomatoes, although Marinda showed other positive properties as high scores for juiciness (not shown).

The content in Glu, a compound directly related to organoleptic quality, was discriminant of genotypes with different fruit types, being high in all flat types and intermediate or low in pear/oxheart and in round/elongate types. One exception was the landrace #16 (Ovale Puglia, a genotype with elongate fruit and high Glu level). Interestingly, at all the four SNP positions linked to Glu content this genotype carried the same allele as the flat tomatoes, giving a good marker and a candidate gene to pursue Glu content improvement. On the contrary, the pear-shaped hybrid Tomawak showed a very low Glu value in comparison with tomatoes with similar fruit types. As it was shown by multivariate analysis of all the analytes, this hybrid showed a different position compared with similar varieties (Figure S2), possibly reflecting different organoleptic qualities. The detection of mQTLs for important metabolites as those exemplified above will give valuable tools to improve traditional tomato varieties by assisted breeding without losing general and specific quality traits.

CONCLUSIONS

Overall the data supported the idea that significant changes in quality-related metabolites occur not only according to the ripening process but also depending on the genetic background (Carli et al., 2011). Consequently, metabolic profiling and the association of metabolic profiles with variation at specific genomic regions may represent a useful tool to characterize traditional varieties with functional markers in order to establish new criteria for distinctiveness and protection (Vallverdú-Queralt et al., 2011). The reported analysis indicated the

reliability of the described association; turning these information into markers efficient for selection or into candidates for cloning the genes underlying mQTLs will need the study of a much wider germplasm collection, endowed with wider phenotypic diversity.

In the past decade, the platforms for genotyping plant genomes at high density have increased considerably due to resequencing (Shirasawa et al., 2013; Ercolano et al., 2014; Lin et al., 2014) and genotyping by sequencing (Deschamps et al., 2012) approaches. In parallel, opportunities for efficiently analyzing a large number of genotypes for phenotypic as well as biochemical traits are becoming more affordable (Klee and Tieman, 2013). This scenario paves the way for investigating the genetic/molecular basis of organoleptic trait variation and breeding for quality-related compounds in tomato fruits. Network analysis demonstrated that the complex control of organoleptic quality in fresh tomato can be dissected into few strong relationships between sensory perception and specific biochemical data (Carli et al., 2009). This achievement supports the possibility of unraveling main genetic determinants of tomato quality and improving the crop by breeding a limited number of favorable alleles into elite germplasm.

AUTHOR CONTRIBUTIONS

AM and VF designed the study. SB, MP, AP carried out the morphological characterization. AT and RF performed the biochemical analyses. VR, AB, and AM carried out the analysis of data and drafted the manuscript. All authors corrected and approved the final version.

FUNDING

This work was supported by the Italian Ministry for Economic Development (MiSE), PROGRAMMA INDUSTRIA 2015, "Made in Italy", TEMA A6, project title "Approcci TEcnologici Nuovi per l'Aumento della shelf-life e del contenuto di servizio nei prodotti qualificanti il modello alimentare mediterraneo" (ATENA). We are finally grateful to the COST Action FA1106 QualityFruit, supported by COST (European Cooperation in Science and Technology) for support to mobility.

ACKNOWLEDGMENTS

The authors thank Fabrizio Ruiu and Aurelia Buccellato for helpful discussion during the experiments, Gianplacido Di Rosa, and Valentino Ferrari for help with seed supply and Marena Torelli for excellent assistance in growing the plants. Two reviewers who helped improving the manuscript with constructive comments and suggestions are also truly acknowledged.

SUPPLEMENTARY MATERIAL

The Supplementary Material for this article can be found online at: <http://journal.frontiersin.org/article/10.3389/fpls.2016.00664>

REFERENCES

- Acciari, N., Rotino, G. L., Voltattorni, S., Mennella, G., Nigro, C., Cerbino, D., et al. (2007). Recupero, caratterizzazione e valorizzazione di varietà locali italiane di pomodoro da mensa. *Italus Hortus* 14, 74–84.
- Alseekh, S., Tohge, T., Wendenberg, R., Scossa, F., Omranian, N., Li, J., et al. (2015). Identification and mode of inheritance of quantitative trait loci for secondary metabolite abundance in tomato. *Plant Cell* 27, 485–512. doi: 10.1101/tpc.114.132266
- Andreakis, N., Giordano, I., Pentangelo, A., Fogliano, V., Graziani, G., Monti, L. M., et al. (2004). DNA fingerprinting and quality traits of Corbarino cherry-like tomato landraces. *J. Agric. Food Chem.* 52, 3366–3371. doi: 10.1021/jf049963y
- AOAC International (1995). *Official Methods of Analysis*, Arlington, VA, AOAC International.
- Bovy, A., Schijlen, E., and Hall, R. D. (2007). Metabolic engineering of flavonoids in tomato (*Solanum lycopersicum*): the potential for metabolomics. *Metabolomics* 3, 399–412. doi: 10.1007/s11306-007-0074-2
- Bradbury, P. J., Zhang, Z., Kroon, D. E., Casstevens, T. M., Ramdoss, Y., and Buckler, E. S. (2007). TASSEL: software for association mapping of complex traits in diverse samples. *Bioinformatics* 23, 2633–2635. doi: 10.1093/bioinformatics/btm308
- Caramante, M., Corrado, G., Monti, L. M., and Rao, R. (2011). Simple Sequence Repeats are able to trace tomato cultivars in tomato food chains. *Food Control* 22, 549–554. doi: 10.1016/j.foodcont.2010.10.002
- Carli, P., Arima, S., Fogliano, V., Tardella, L., Frusciante, L., and Ercolano, M. R. (2009). Use of network analysis to capture key traits affecting tomato organoleptic quality. *J. Exp. Bot.* 60, 3379–3386. doi: 10.1093/jxb/erp177
- Carli, P., Barone, A., Fogliano, V., Frusciante, L., and Ercolano, M. (2011). Dissection of genetic and environmental factors involved in tomato organoleptic quality. *BMC Plant Biol.* 11, 58. doi: 10.1186/1471-2229-11-58
- Causse, M., Duffe, P., Gomez, M. C., Buret, M., Damidaux, R., Zamir, D., et al. (2004). A genetic map of candidate genes and QTLs involved in tomato fruit size and composition. *J. Exp. Bot.* 55, 1671–1685. doi: 10.1093/jxb/erh207
- Causse, M., Friguet, C., Coiret, C., Lépicier, M., Navez, B., Lee, M., et al. (2010). Consumer preferences for fresh tomato at the European scale: a common segmentation on taste and firmness. *J. Food Sci.* 75, S531–S541. doi: 10.1111/j.1750-3841.2010.01841.x
- Causse, M., Saliba-Colombani, V., Lecomte, L., Duffé, P., Rousselle, P., and Buret, M. (2002). QTL analysis of fruit quality in fresh market tomato: a few chromosome regions control the variation of sensory and instrumental traits. *J. Exp. Bot.* 53, 2089–2098. doi: 10.1093/jxb/erf058
- Chaudhari, N., Pereira, E., and Roper, S. D. (2009). Taste receptors for umami: the case for multiple receptors. *Am. J. Clin. Nutr.* 90, 738S–742S. doi: 10.3945/ajcn.2009.27462H
- Choi, S. H., Kim, D.-S., Kozukue, N., Kim, H.-J., Nishitani, Y., Mizuno, M., et al. (2014). Protein, free amino acid, phenolic, β -carotene, and lycopene content, and antioxidative and cancer cell inhibitory effects of 12 greenhouse-grown commercial cherry tomato varieties. *J. Food Comp. Anal.* 34, 115–127. doi: 10.1016/j.jfca.2014.03.005
- Cortés-Olmos, J., Leiva-Brondo, M., Roselló, J., Raigón, M. D., and Cebolla-Cornejo, J. (2014). The role of traditional varieties of tomato as sources of functional compounds. *J. Sci. Food Agric.* 94, 2888–2904. doi: 10.1002/jsfa.6629
- Deschamps, S., Llaca, V., and May, G. D. (2012). Genotyping-by-sequencing in plants. *Biology* 1, 460–483. doi: 10.3390/biology1030460
- Earl, D., and vonHoldt, B. (2012). STRUCTURE HARVESTER: a website and program for visualizing STRUCTURE output and implementing the Evanno method. *Conserv. Genet. Res.* 4, 359–361. doi: 10.1007/s12686-011-9548-7
- Ercolano, M. R., Sacco, A., Ferriello, F., D'Alessandro, R., Tononi, P., Traini, et al. (2014). Patchwork sequencing of tomato San Marzano and Vesuviano varieties highlights genome-wide variations. *BMC Genomics* 15:138. doi: 10.1186/1471-2164-15-138
- Eshed, Y., and Zamir, D. (1995). An introgression line population of *Lycopersicon pennellii* in the cultivated tomato enables the identification and fine mapping of yield-associated QTL. *Genetics* 141, 1147–1162.
- Esquinas-Alcázar, J., and Nuez, V. F. (1995). “Situación taxonómica, domesticación y difusión del tomate”, in *El Cultivo del Tomate*, ed. F. Nuez Viñals (Madrid: Mundiprensa), 15–43.
- Evanno, G., Regnaut, S., and Goudet, J. (2005). Detecting the number of clusters of individuals using the software STRUCTURE: a simulation study. *Mol. Ecol.* 14, 2611–2620. doi: 10.1111/j.1365-294X.2005.02553.x
- Ferraro, G., Bortolotti, S., Mortera, P., Schlereth, A., Stitt, M., Carrari, F., et al. (2012). Novel glutamate dehydrogenase genes show increased transcript and protein abundances in mature tomato fruits. *J. Plant Physiol.* 169, 899–907. doi: 10.1016/j.jplph.2012.02.002
- Figàs, M. R., Prohens, J., Raigón, M. D., Fernández-de-Córdoba, P., Fita, A., and Soler, S. (2015a). Characterization of a collection of local varieties of tomato (*Solanum lycopersicum* L.) using conventional descriptors and the high-throughput phenomics tool Tomato Analyzer. *Genet. Res. Crop Evol.* 62, 189–204. doi: 10.1007/s10722-014-0142-1
- Figàs, M. R., Prohens, J., Raigón, M. D., Fita, A., García-Martínez, M. D., Casanova, C., et al. (2015b). Characterization of composition traits related to organoleptic and functional quality for the differentiation, selection and enhancement of local varieties of tomato from different cultivar groups. *Food Chem.* 187, 517–524. doi: 10.1016/j.foodchem.2015.04.083
- Forde, B. G., and Lea, P. J. (2007). Glutamate in plants: metabolism, regulation, and signalling. *J. Exp. Bot.* 58, 2339–2358. doi: 10.1093/jxb/erm121
- Friedman, M. (2002). Tomato glycoalkaloids: role in the plant and in the diet. *J. Agric. Food Chem.* 50, 5751–5780. doi: 10.1021/jf020560c
- Fulton, T. M., Bucheli, P., Voirol, E., López, J., Pétard, V., and Tanksley, S. D. (2002). Quantitative trait loci (QTL) affecting sugars, organic acids and other biochemical properties possibly contributing to flavor, identified in four advanced backcross populations of tomato. *Euphytica* 127, 163–177. doi: 10.1023/A:1020209930031
- García-Martínez, S., Corrado, G., Ruiz, J. J., and Rao, R. (2013). Diversity and structure of a simple of traditional Italian and Spanish tomato accessions. *Genet. Resour. Crop Evol.* 60, 789–798. doi: 10.1007/s10722-012-9876-9
- Hammer, Ø., Harper, D. A. T., and Ryan, P. D. (2001). PAST: Paleontological statistics software package for education and data analysis. *Palaeontol. Electron.* 4, 9.
- Hurtado, M., Vilanova, S., Plazas, M., Gramazio, P., Andújar, I., Herraiz, F. J., et al. (2014). Enhancing conservation and use of local vegetable landraces: the *Almagro* eggplant (*Solanum melongena* L.) case study. *Genet. Resour. Crop Evol.* 61, 787–795. doi: 10.1007/s10722-013-0073-2
- Itkin, M., Heinig, U., Tzafadia, O., Bhide, A. J., Shinde, B., Cardenas, P. D., et al. (2013). Biosynthesis of antinutritional alkaloids in solanaceous crops is mediated by clustered genes. *Science* 341, 175–179. doi: 10.1126/science.1240230
- Kader, A. A., Stevens, M. A., Albright, M., and Morris, L. L. (1978). Amino-acid composition and flavor of fresh market tomatoes as influenced by fruit ripeness when harvested. *J. Am. Soc. Hort. Sci.* 103, 541–544.
- Kaushik, P., Andújar, I., Vilanova, S., Plazas, M., Gramazio, P., Herraiz, F., et al. (2015). Breeding vegetables with increased content in bioactive phenolic acids. *Molecules* 20, 18464–18481. doi: 10.3390/molecules201018464
- Klee, H. J., and Tieman, D. M. (2013). Genetic challenges of flavor improvement in tomato. *Trends Genet.* 29, 257–262. doi: 10.1016/j.tig.2012.12.003
- Leonardi, C., Ambrosino, P., Esposito, F., and Fogliano, V. (2000). Antioxidative activity and carotenoid and tomatine contents in different typologies of fresh consumption tomatoes. *J. Agric. Food Chem.* 48, 4723–4727. doi: 10.1021/jf000225t
- Lin, T., Zhu, G., Zhang, J., Xu, X., Yu, Q., Zheng, Z., et al. (2014). Genomic analyses provide insights into the history of tomato breeding. *Nat. Genet.* 46, 1220–1226. doi: 10.1038/ng.3117
- Martínez-Valverde, I., Periago, M. J., Provan, G., and Chesson, A. (2002). Phenolic compounds, lycopene and antioxidant activity in commercial varieties of tomato (*Lycopersicum esculentum*). *J. Sci. Food Agric.* 82, 323–330. doi: 10.1002/jsfa.1035
- Mathieu, S., Cin, V. D., Fei, Z., Li, H., Bliss, P., Taylor, M. G., et al. (2009). Flavour compounds in tomato fruits: identification of loci and potential pathways affecting volatile composition. *J. Exp. Bot.* 60, 325–337. doi: 10.1093/jxb/ern294
- Mazzucato, A., Ficcadenti, N., Caioni, M., Mosconi, P., Piccinini, E., Sanampudi, V. R. R., et al. (2010). Genetic diversity and distinctiveness in tomato (*Solanum lycopersicum* L.) landraces: the Italian case study of ‘a pera Abruzzese’. *Sci. Hortic.* 125, 55–62. doi: 10.1016/j.scientia.2010.02.021
- Mazzucato, A., Papa, R., Bitocchi, E., Mosconi, P., Nanni, L., Negri, V., et al. (2008). Genetic diversity, structure and marker-trait associations in a collection

- of Italian tomato (*Solanum lycopersicum* L.) landraces. *Theor. Appl. Genet.* 116, 657–669. doi: 10.1007/s00122-007-0699-6
- Meitinger, M., Hartmann, S., and Schieberle, P. (2014). Development of stable isotope dilution assays for the quantitation of Amadori compounds in foods. *J. Agric. Food Chem.* 62, 5020–5027. doi: 10.1021/jf501464g
- Mossine, V. V., Chopra, P., and Mawhinney, T. P. (2008). Interaction of tomato lycopene and ketosamine against rat prostate tumorigenesis. *Cancer Res.* 68, 4384–4391. doi: 10.1158/0008-5472.CAN-08-0108
- Mossine, V. V., and Mawhinney, T. P. (2007). N-alpha-(1-DeOXY-D-fructos-1-yl)-L-histidine (“D-fructoseL-histidine”): a potent copper chelator from tomato powder. *J. Agric. Food Chem.* 55, 10373–10381. doi: 10.1021/jf072092i
- Osorio, S., Alba, R., Damasceno, C. M. B., Lopez-Casado, G., Lohse, M., Zanor, M. I. S., et al. (2011). Systems biology of tomato fruit development: combined transcript, protein, and metabolite analysis of tomato transcription factor (*nor*, *rin*) and ethylene receptor (*Nr*) mutants reveals novel regulatory interactions. *Plant Physiol.* 157, 405–425. doi: 10.1104/pp.111.175463
- Panthee, D. R., Labate, J. A., McGrath, M. T., Breksa, A. P. III, and Robertson, L. D. (2013). Genotype and environmental interaction for fruit quality traits in vintage tomato varieties. *Euphytica* 193, 169–182. doi: 10.1007/10681-013-0895-1
- Perez-Llamas, C., and Lopez-Bigas, N. (2011). Gitools: analysis and visualisation of genomic data using interactive heat-maps. *PLoS ONE* 6:e19541. doi: 10.1371/journal.pone.0019541
- Pratta, G. R., Rodríguez, G. R., Zorzoli, R., Picardi, L. A., and Valle, E. M. (2011). Biodiversity in a tomato germplasm for free amino acid and pigment content of ripening fruits. *Am. J. Plant Sci.* 2, 255–261. doi: 10.4236/ajps.2011.22027
- Pritchard, J. K., Stephens, M., and Donnelly, P. (2000). Inference of population structure using multilocus genotype data. *Genetics* 155, 945–959.
- Rodríguez-Burruzeo, A., Prohens, J., Roselló, S., and Nuez, F. (2005). ‘Heirloom’ varieties as sources of variation for the improvement of fruit quality in greenhouse-grown tomatoes. *J. Hortic. Sci. Biotechnol.* 80, 453–460. doi: 10.1080/14620316.2005.11511959
- Rousseaux, M. C., Jones, C. M., Adams, D., Chetelat, R., Bennett, A., and Powell, A. (2005). QTL analysis of fruit antioxidants in tomato using *Lycopersicon pennellii* introgression lines. *Theor. Appl. Genet.* 111, 1396–1408. doi: 10.1007/s00122-005-0071-7
- Ruggieri, V., Francese, G., Sacco, A., D’Alessandro, A., Rigano, M. M., Parisi, M., et al. (2014). An association mapping approach to identify favourable alleles for tomato fruit quality breeding. *BMC Plant Biol.* 14:337. doi: 10.1186/s12870-014-0337-9
- Sacco, A., Ruggieri, V., Parisi, M., Festa, G., Rigano, M. M., Picarella, M. E., et al. (2015). Exploring a tomato landraces collection for fruit-related traits by the aid of a high-throughput genomic platform. *PLoS ONE* 10:e0137139. doi: 10.1371/journal.pone.0137139
- Saliba-Colombani, V., Causse, M., Langlois, D., Philouze, J., and Buret, M. (2001). Genetic analysis of organoleptic quality in fresh market tomato. 1. Mapping QTLs for physical and chemical traits. *Theor. Appl. Genet.* 102, 259–272. doi: 10.1007/s001220051643
- SAS Institute (2004). *SAS Language and Procedure: Usage, version 8.1*. Cary, NC: SAS Institute Inc.
- Sauvage, C., Segura, V., Bauchet, G., Stevens, R., Do, P. T., Nikoloski, Z., et al. (2014). Genome-wide association in tomato reveals 44 candidate loci for fruit metabolic traits. *Plant Physiol.* 165, 1120–1132. doi: 10.1104/pp.114.241521
- Schauer, N., Semel, Y., Balbo, I., Steinfath, M., Repsilber, D., Selbig, J., et al. (2008). Mode of inheritance of primary metabolic traits in tomato. *Plant Cell* 20, 509–523. doi: 10.1105/tpc.107.056523
- Schauer, N., Semel, Y., Roessner, U., Gur, A., Balbo, I., Carrari, F., et al. (2006). Comprehensive metabolic profiling and phenotyping of interspecific introgression lines for tomato improvement. *Nat. Biotechnol.* 24, 447–454. doi: 10.1038/nbt1192
- Shirasawa, K., Fukuoka, H., Matsunaga, H., Kobayashi, Y., Kobayashi, I., Hirakawa, H., et al. (2013). Genome-wide association studies using single nucleotide polymorphism markers developed by re-sequencing of the genomes of cultivated tomato. *DNA Res.* 20, 593–603. doi: 10.1093/dnar/esd033
- Siviero, P. (2001). “Le tipologie presenti in Italia,” in *Il Pomodoro da Mensa in Italia*, ed G. Setti (Bologna, Calderini Edagricole), 9–44.
- Soressi, G. P. (1969). *Il Pomodoro. Trattato di Genetica Agraria Speciale*. Bologna: Agricole.
- Sorrequita, A., Ferraro, G., Boggio, S. B., and Valle, E. M. (2010). Free amino acid production during tomato fruit ripening: a focus on l-glutamate. *Amino Acids* 38, 1523–1532. doi: 10.1007/s00726-009-0373-1
- Tieman, D., Bliss, P., McIntyre, L. M., Blandon-Ubeda, A., Bies, D., Odabasi, A. Z., et al. (2012). The chemical interactions underlying tomato flavor preferences. *Curr. Biol.* 22, 1035–1039. doi: 10.1016/j.cub.2012.04.016
- Toor, R. K., and Savage, G. P. (2005). Antioxidant activities in different fractions of tomato. *Food Res. Intl.* 38, 487–494. doi: 10.1016/j.foodres.2004.1.016
- Troise, A. D., Ferracane, R., Palermo, M., and Fogliano, V. (2014). Targeted metabolite profile of food bioactive compounds by Orbitrap high resolution mass spectrometry: the “FancyTiles” approach. *Food Res. Int.* 63, 139–146. doi: 10.1016/j.foodres.2014.01.001
- Troise, A. D., Fiore, A., Roviello, G., Monti, S. M., and Fogliano, V. (2015). Simultaneous quantification of amino acids and Amadori products in foods through ion-pairing liquid chromatography-high-resolution mass spectrometry. *Amino Acids* 47, 111–124. doi: 10.1007/s00726-014-1845-5
- Vallverdú-Queralt, A., Medina-Remón, A., Martínez-Huélamo, M., Jáuregui, O., Andres-Lacueva, C., and Lamuela-Raventos, R. M. (2011). Phenolic profile and hydrophilic antioxidant capacity as chemotaxonomic markers of tomato varieties. *J. Agric. Food Chem.* 59, 3994–4001. doi: 10.1021/jf104400g
- Voorrips, R. E. (2002). MapChart: software for the graphical presentation of linkage maps and QTLs. *J. Hered.* 93, 77–78. doi: 10.1093/jhered/93.1.77
- Xu, J., Ranc, N., Muñoz, S., Rolland, S., Bouchet, J.-P., Desplat, N., et al. (2013). Phenotypic diversity and association mapping for fruit quality traits in cultivated tomato and related species. *Theor. Appl. Genet.* 126, 567–581. doi: 10.1007/s00122-012-2002-8
- Zanor, M. I., Rambla, J.-L., Chaib, J., Steppa, A., Medina, A., Granell, A., et al. (2009). Metabolic characterization of loci affecting sensory attributes in tomato allows an assessment of the influence of the levels of primary metabolites and volatile organic contents. *J. Exp. Bot.* 60, 2139–2154. doi: 10.1093/jxb/erp086
- Zhang, J., Zhao, J., Xu, Y., Liang, J., Chang, P., Yan, F., et al. (2015). Genome-wide association mapping for tomato volatiles positively contributing to tomato flavor. *Front. Plant Sci.* 6:1042. doi: 10.3389/fpls.2015.01042
- Zushi, K., and Matsuzoe, N. (2011). Utilization of correlation network analysis to identify differences in sensory attributes and organoleptic compositions of tomato cultivars grown under salt stress. *Sci. Hortic.* 129, 18–26. doi: 10.1016/j.scientia.2011.02.011

Conflict of Interest Statement: The authors declare that the research was conducted in the absence of any commercial or financial relationships that could be construed as a potential conflict of interest.

Copyright © 2016 Baldina, Picarella, Troise, Pucci, Ruggieri, Ferracane, Barone, Fogliano and Mazzucato. This is an open-access article distributed under the terms of the Creative Commons Attribution License (CC BY). The use, distribution or reproduction in other forums is permitted, provided the original author(s) or licensor are credited and that the original publication in this journal is cited, in accordance with accepted academic practice. No use, distribution or reproduction is permitted which does not comply with these terms.



The Relationship between *CmADHs* and the Diversity of Volatile Organic Compounds of Three Aroma Types of Melon (*Cucumis melo*)

Hao Chen¹, Songxiao Cao¹, Yazhong Jin^{1,2}, Yufan Tang¹ and Hongyan Qi^{1*†}

¹ Key Laboratory of Protected Horticulture of Ministry of Education and Liaoning Province, College of Horticulture, Shenyang Agricultural University, Shenyang, China, ² Department of Horticulture, College of Agriculture, Heilongjiang Bayi Agricultural University, Daqing, China

OPEN ACCESS

Edited by:

Mario Pezzotti,
University of Verona, Italy

Reviewed by:

Uener Kolukisaoglu,
University of Tübingen, Germany

Hao Peng,
Washington State University, USA

*Correspondence:

Hongyan Qi
hyqiaaa@126.com;
syauhongyan@hotmail.com

†Present Address:

Hongyan Qi,
College of Horticulture, Shenyang
Agricultural University,
Shenyang, China

Specialty section:

This article was submitted to
Plant Physiology,
a section of the journal
Frontiers in Physiology

Received: 10 April 2016

Accepted: 10 June 2016

Published: 28 June 2016

Citation:

Chen H, Cao S, Jin Y, Tang Y and Qi H (2016) The Relationship between *CmADHs* and the Diversity of Volatile Organic Compounds of Three Aroma Types of Melon (*Cucumis melo*). *Front. Physiol.* 7:254.
doi: 10.3389/fphys.2016.00254

Alcohol dehydrogenase (ADH) plays an important role in aroma volatile compounds synthesis of plants. In this paper, we tried to explore the relationship between *CmADHs* and the volatile organic compounds (VOCs) in oriental melon. Three different aroma types of melon were used as materials. The principle component analysis of three types of melon fruit was conducted. We also measured the *CmADHs* expression level and enzymatic activities of ADH and alcohol acyl-transferase (AAT) on different stages of fruit ripening. An incubation experiment was carried out to investigate the effect of substrates and inhibitor (4-MP, 4-methylpyrazole) on *CmADHs* expression, ADH activity, and the main compounds of oriental melon. The results illustrated that ethyl acetate, hexyl acetate (E,Z)-3,6-nonadien-1-ol and 2-ethyl-2hexen-1-ol were the four principal volatile compounds of these three types of melon. AAT activity was increasing with fruit ripening, and the AAT activity in CH were the highest, whereas ADH activity peaked on 32 DAP, 2 days before maturation, and the ADH activity in CB and CG were higher than that in CH. The expression pattern of 11 *CmADH* genes from 24 to 36 day after pollination (DAP) was found to vary in three melon varieties. *CmADH4* was only expressed in CG and the expression levels of *CmADH3* and *CmADH12* in CH and CB were much higher than that in CG, and they both peaked 2 days before fruit ripening. Ethanol and 4-MP decreased the reductase activity of ADH, the expression of most *CmADHs* and ethyl acetate or hexyl acetate contents of CB, except for 0.1 mM 4-MP, while aldehyde improved the two acetate ester contents. In addition, we found a positive correlation between the expression of *CmADH3* and *CmADH12* and the key volatile compound of CB. The relationship between *CmADHs* and VOCs synthesis of oriental melon was discussed.

Keywords: volatiles organic compounds, alcohol dehydrogenase, oriental melon, fruit ripening, gene expression

INTRODUCTION

Oriental melon (*Cucumis melo* var. *makuwa* makino) is a species of thin-pericarp melon, and it has extensive cultivated varieties and the largest plantation in China. The oriental melon has a sweet and crisp taste, juicy flesh and an edible rind, especially intense volatile aromas compound that is one of the most attractive qualities (Liu et al., 2012). Most volatile aroma compounds,

as a sign of fruit maturity, are produced and released during the maturation period (Visai and Vanoli, 1997; Goff and Klee, 2006). To date, more than 2000 types of volatile compounds have been detected in various plants, including melons, apples, strawberries, pears, tomatoes, and bananas (Dixon and Hewett, 2000; Maul et al., 2000; Urruty et al., 2002; Li et al., 2014, 2016). In different melon varieties, ~240 volatile compounds have been found, including volatile alcohols, aldehydes, terpene, especially abundant esters (Kourkoutas et al., 2006; Khanom and Ueda, 2008; Obando-Ulloa et al., 2010). Specifically, the contents of aromatic compounds vary drastically according to the melon variety. In climacteric melon varieties, volatile esters are prominent, together with short-chain alcohols, aldehydes and terpenes, while non-aromatic varieties often have much lower levels of total volatiles, lacking the volatile esters (Gonda et al., 2010). Tang also found that ester, especially straight-chain esters were important VOCs in oriental melon (Tang et al., 2015). As the most abundant aroma in climacteric melon, esters are mainly produced from two ways, namely the amino acid way, producing the branched-chain esters and the lipoxygenase (LOX) way synthesizing the straight-chain esters (Zhang et al., 2014; Tang et al., 2015).

The lipoxygenase (LOX) pathway may be the most critical way for aroma foundation because of the high straight-chain esters content of oriental melon. The LOX way consist of four enzymes, including LOX, HPL (Hydroperoxide lyase), ADH (Alcohol dehydrogenase, EC1.1.1.1), and AAT (Alcohol acetyltransferase). As the last two steps in the foundation of volatile esters, some ADH and AAT have been extensively investigated, both in melons and in other plants. These steps involve alcohol dehydrogenase and alcoholacetyl transferase activities that convert volatile aldehydes to their respective alcohols and esters, and these activities are related to climactericity (Gonda et al., 2010).

The classic ADHs are Z-binding enzymes, relying on an NAD(P) co-factor to interconvert ethanol and acetaldehyde (and other short linear alcohol/aldehyde pairs). In petunia, *PhADH2* and *PhADH3* were involved in floral scent from the lipoxygenase pathway (Garabagi and Strommer, 2004). Previous reports also showed that ADHs were expressed in a developmentally-regulated manner, particularly during fruit ripening (Salas and Sánchez, 1998; Speirs et al., 2002; Lara et al., 2003; Manríquez et al., 2006). Over-expression of *LeADH2* in tomato led to increasing the level of alcohols, particularly Z-3-hexenol of the fruit (Salas and Sánchez, 1998). The specific down-regulation of *SlscADH1* in tomato fruit did not alter the aldehyde/alcohol balance of the volatiles compounds, but made higher concent of C5 and C6 volatile compounds from the lipoxygenase pathway (Moummou et al., 2012). However, there were few reports on ADHs, participating in aroma synthesis, in oriental melon which has the extensive cultivated varieties and the largest plantation in China.

As our previous works, 12 *CmADH* genes (*CmADH1-12*) have been identified in the melon genome (<http://melonomics.net/>) and bioinformatics analyzed. We have also investigated the response of 12 *CmADHs* to ethylene in oriental melon (Jin et al., 2016), but the function of most members were far from clear,

except for *CmADH1* and *CmADH2* in Countloup melon. The key *CmADH* gene participating in the accumulation of various volatile organic compounds (VOCs) in different aroma types of melon and the regulation of *CmADHs* family in the process of aroma foundation in oriental melon are still unknown. In this paper, to explore the potential *CmADH* genes participating in the key aroma compounds production, we analyzed the VOCs and investigated the activities and expression of ADH and AAT in ripening fruits of three different aroma types of melon. Simultaneously, a fruit disk incubation experiment was conducted to investigate the influence of substrates (ethanol and aldehyde) or inhibitor on ADH activity, *CmADHs* expression and VOCs productions in oriental melons.

MATERIALS AND METHODS

Plant Materials

Three different aromatic oriental melon varieties were used, including strong- aromatic melon (*C. melo* var. *makuwa* Makino) cultivar “Cai Hong” (CH), less-aromatic melon (*C. melo* var. *makuwa* Makino) cultivar “Cui Bao” (CB), and non-aromatic melon “Cai Gua” (CG) which is called as snake melon (*C. melo* L var. *flexuosus* Naud) in China. They were grown in pots (volume of 25 L and soil: peat: compost = 1: 1: 1) in a greenhouse under standard cultural practices for fertilization and pesticide treatments at Shenyang Agricultural University(Shenyang, China) from March to June in 2014. Female flowers were pollinated with “Fengchanji 2” to increase the rate of fruit set, and tagged on the day of bloom. Melons were harvested on 24, 26, 28, 30, 32, 34, 36 days after pollination (DAP).

Fruit Firmness, Soluble Solids Content (SSC) Evaluation

The firmness of melon fruit was measured with a hardness tester (FHM-1, Takemura, Japan) according to the method of Tijskens (Tijskens et al., 2009). The soluble solids content of melon fresh was determined by a digital refractometer (DBR45, Huixia, Fujian, China) described by Liu (Liu et al., 2012). A CR-400/410 spectrophotometer (Konica Minolta, Japan) was used to detect the rind color of melons. Six readings were taken from equatorial zone of each fruit (Liu et al., 2012). The firmness and SSC experiment was performed in triplicate.

ADH Enzyme Activity Assay

Reductase and dehydrogenase activities of ADH were evaluated by CARY 100 scan ultraviolet (UV)/visible spectrophotometer (Varian, USA). The method was optimized on the foundation of Longhurst et al. (1990) and Manríquez et al. (2006). Approximately 3 g fresh melon was ground into powder in liquid nitrogen using mortar and pestle, then mixed with 6 ml pre-cooling extract buffer [4°C, 100 mM MES-Tris (pH 6.5), 2 mM DTT (dithiothreitol), 1% PVP (polyvinyl pyrrolidone) (m/v)]. The ground slurry was centrifuged at 15,000 g for 30 min at 4°C, and the supernatant was collected for ADH activity analyzing as crude enzyme. Reductase activity was measured in 1 ml total volume containing 200 µl crude protein, 5 mM aldehyde, 0.25 mM NADH, or NADPH and 50 mM sodium

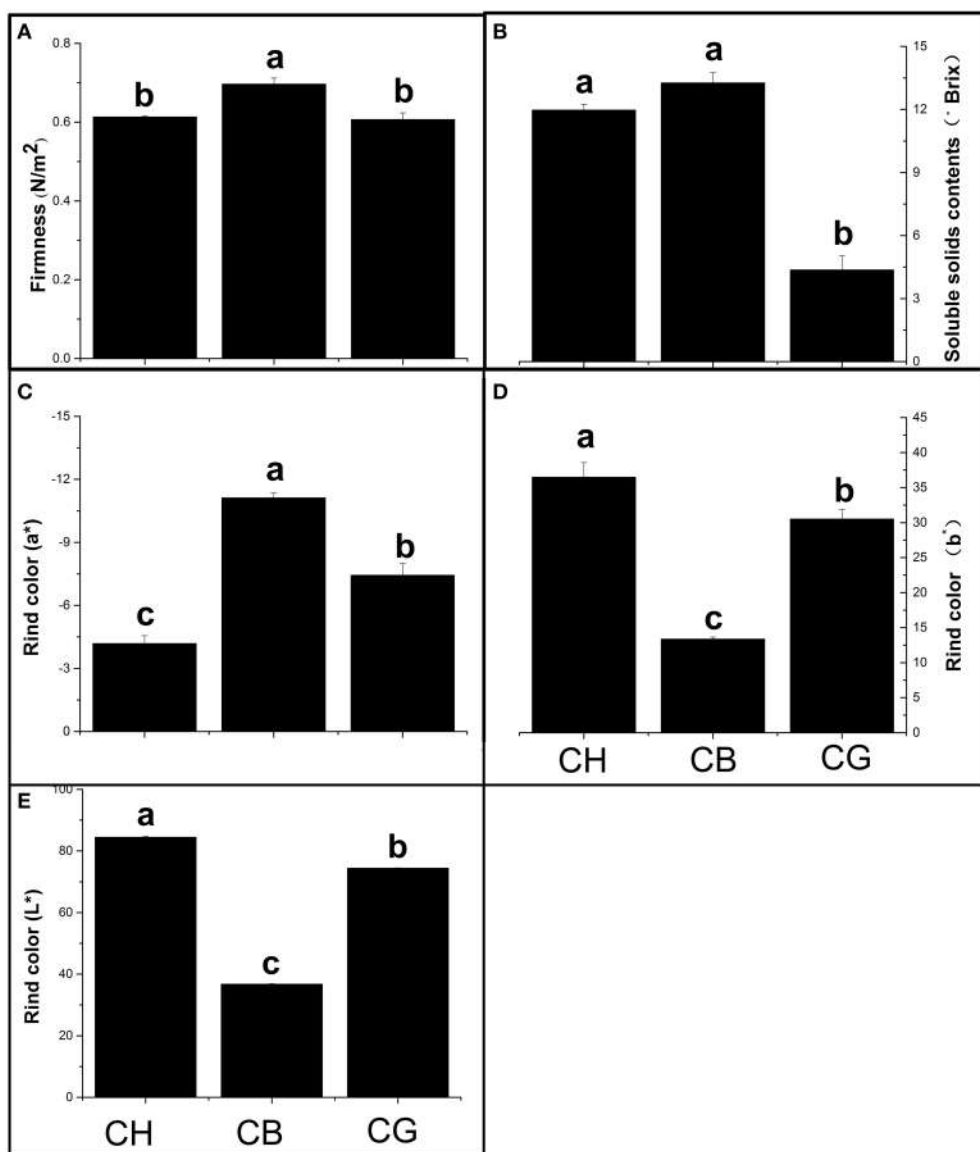


FIGURE 1 | Different physiological characteristics of three types of melon at their maturity. (A) Firmness, **(B)** Soluble solids contents of melon flesh, **(C–E)** Pericarp color (a^* means the red/green ratio and b^* represents the yellow/blue ratio, L^* represents the brightness of rind). Duncan's multiple range tests have been performed with different letters above the columns represent significant differences ($P < 0.05$) between different types of melon.

phosphate buffer (pH 5.8). Dehydrogenase activity was assayed in solution contained 5 mM ethanol, 0.25 mM NAD or NADP and glycine-NaOH buffer pH 9.4 in 1 ml. Reductase/dehydrogenase activity was measured by the increase/decrease in absorbance at 340 nm due to change of NAD(P). The reaction was initiated by the addition of ethanol or aldehyde and the rate of absorbance change without ethanol or aldehyde was subtracted to give the substrate dependent rate.

AAT Enzyme Activity

AAT activity was measured according to Shalit (Shalit et al., 2001). Total protein was extracted from 3 g melon fruit without peel and macerated with 6 ml 0.1 M sodium phosphate buffer

(pH = 0.8) at 4°C. The supernatant was collected as the crude enzyme for AAT activity analyzing after the mixture was centrifuged at 16,000 g for 30 min at 4°C. The reaction system consisted of 2.5 ml 5 M MgCl₂, 50 µl 0.5 mM acetyl CoA, 50 µl 200 mM butanol and 0.6 ml crude enzyme. 150 µl 5,5-disulfide double nitro benzoic acid (DTNB) was added into the mixture after 15 min. The AAT activity was determined by the changes of A412 measured by spectrophotometer and each measurement was repeated three times.

Protein Content

Total proteins were quantified with modifications (BioRad Protein Assay Kit, Bio-Rad, USA) according to the method of

coomassie brilliant blue G-250 described by Bradford (Bradford, 1976).

Volatile Organic Compounds Analysis

The VOCs of different melons were detected under the procedure of headspace (HP)-solid phase micro extraction (SPME)-gas chromatography-mass spectrometry (GC-MS), as Liu and Tang was used (Liu et al., 2012; Tang et al., 2015). About 100 g frozen melon flesh were thawed and squeezed into juice. 1-octanol (50 μ l, 59.5 mg/l) were added into 10 ml juice samples as an internal standard. SPME needle was from Supelco (57347-U, Bellefonte, PA, USA), and GC-MS was from Thermo Scientific

(Trace GC Ultra-ITQ 900, Waltham MA 02454). The GC system was equipped with a 30 m*0.25 mm*0.25 um thickness capillary column (Thermo TR-5 ms SQC, USA).

For incubation experiment, a 1 g aliquot of the melon powder was placed in a 10 ml glass vial containing 0.7 g of solid NaCl, 2 ml of a 20 % (w/v) NaCl solution (Gonda et al., 2010) and 10 μ l of a 59.5 mg/l 1-octanol used as internal standard. Then, the sample was measured with the method mentioned above.

Incubation Experiments

Melon cubes (4 g) from CB mature fruit were put in sterile petri dish plates and 500 μ l of a solution of 5 mM ethanol or 5 mM aldehyde and different concentrations of ADH inhibitor (4-methylpyrazole, 4-MP. 0.1, 1, and 5 mM) were applied on top of each cube, and distilled water was taken as control. The plate was covered and incubated overnight at room temperature. Then, each cube was frozen in liquid nitrogen and stored at -80° C (Gonda et al., 2010).

Real-Time Quantitative (qPCR) Analysis

The total RNA was isolated with TRIzol Reagent (Takara, Japan). DNase I (Promega, USA) was used to remove genomic DNA. cDNA template was obtained by reverse transcriptase(Invitrogen, Thermo fisher scientific, USA) with random primer. The PCR program parameters consisted of a preliminary step of 3 min at 95° C followed by 45 cycles at 95° C for 15 s and at 60° C for 30 s, finally, 68° C 30 s. The template cDNA was amplified in a 20

TABLE 1 | Total and different classes of volatile compounds and their concentrations in different aromatic melon types.

Volatile compounds (μ g.g $^{-1}$ FW)	Different types of melon		
	CH	CB	CG
Total esters	207.83 \pm 17.21 ^a	127.16 \pm 16.75 ^b	5.29 \pm 1.82 ^c
Total alcohols	30.24 \pm 2.48 ^b	23.68 \pm 1.87 ^b	136.85 \pm 4.85 ^a
Total acids	15.73 \pm 5.28 ^a	8.14 \pm 2.62 ^b	9.31 \pm 3.97 ^b
Others	54.15 \pm 20.01 ^a	10.07 \pm 1.32 ^b	6.14 \pm 1.21 ^b

Duncan's multiple range tests were performed, and different letters represent significant differences ($P < 0.05$) between different types of melon.

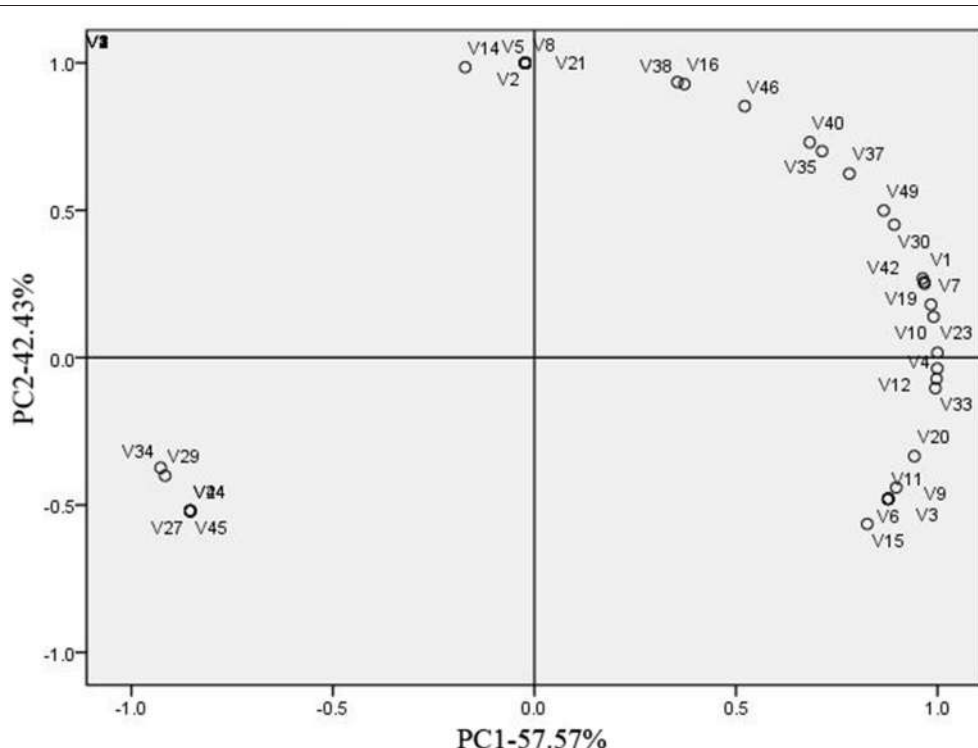


FIGURE 2 | Principal component analysis (PCA) of aroma volatiles identified in three types of melon at mature period. Loading plots of the two main PCA of the aroma volatiles identified in three types of melon at mature period. One hundred percent of the variability in the volatile compounds in the melon cultivars could be explained by two principal PCs. PC1 explained 57.57% of the variability, while PC2 explained 42.43% of the variability. Each sample consisted of three replicates. Codes were corresponding to the volatile compounds number in Table S1.

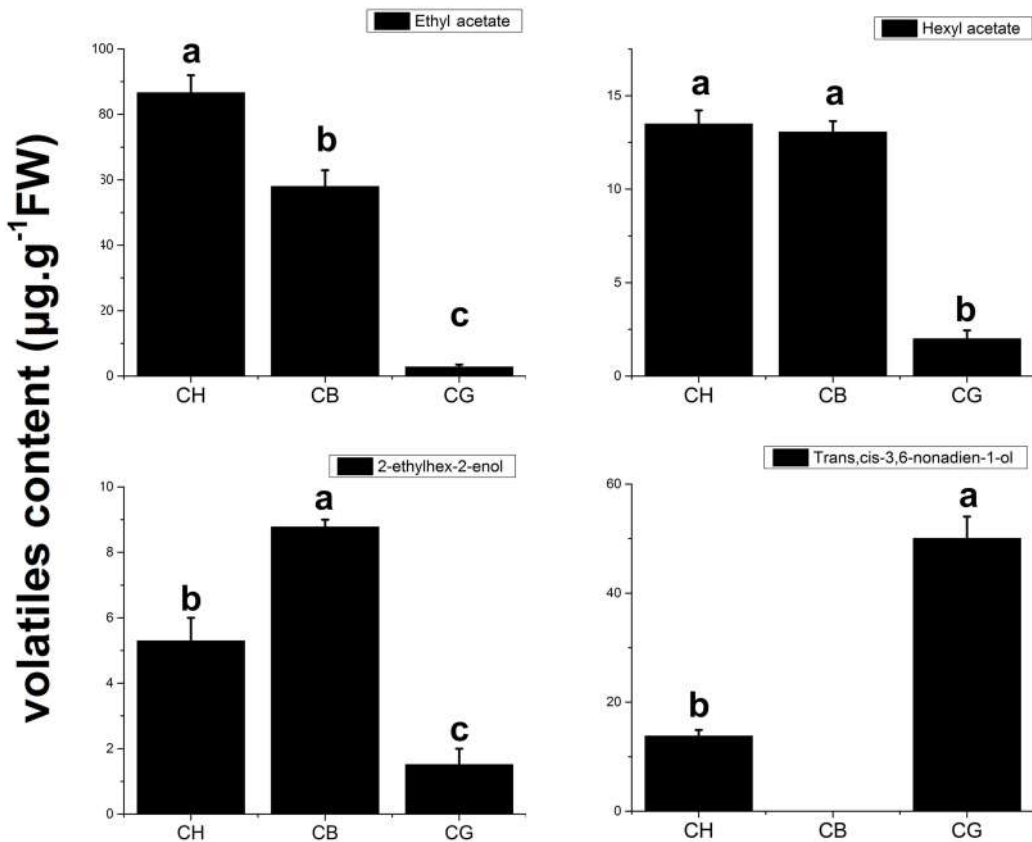


FIGURE 3 | Four principal volatile compounds of three types of melon at mature period. All of the data for volatile compounds are means \pm SE value of three replicates.

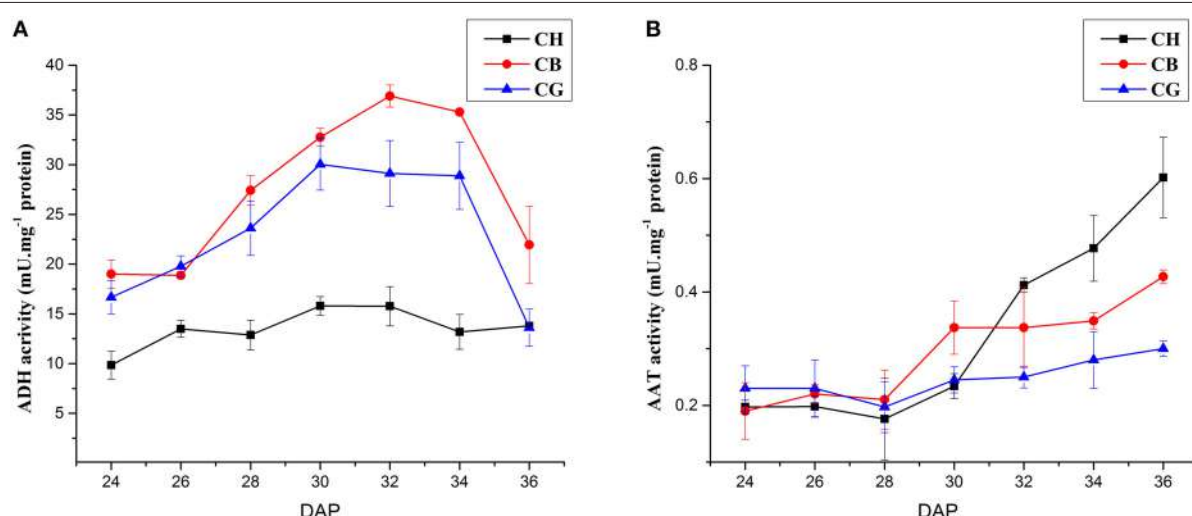


FIGURE 4 | ADH and AAT activities in three aroma types of melon at different DAP. **(A)** ADH activities in three types of melon. **(B)** AAT activities in three types of melon. Each experiment was performed in triplicate and the means \pm SE value of their activities were shown in the line chart.

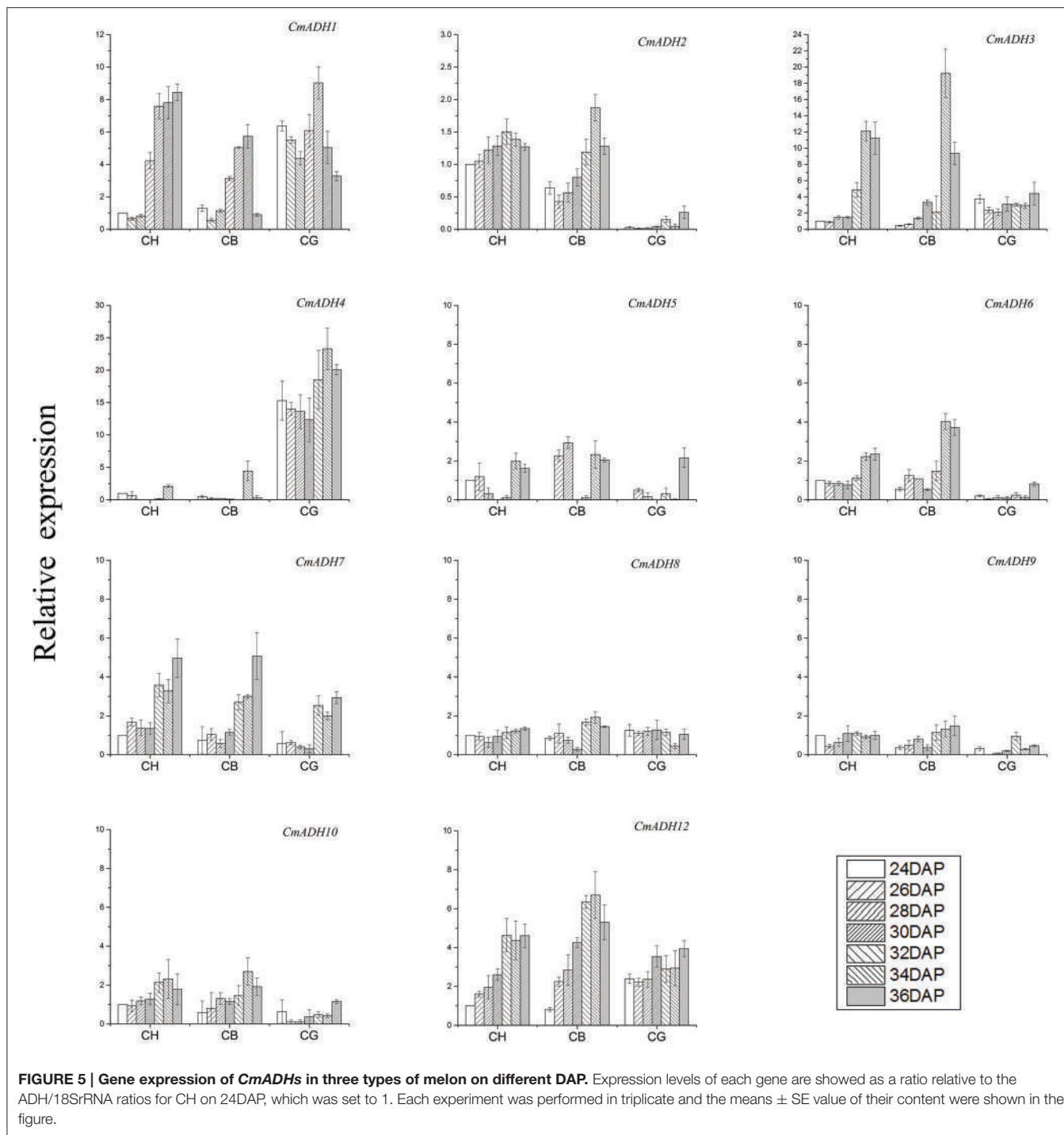


FIGURE 5 | Gene expression of *CmADHs* in three types of melon on different DAP. Expression levels of each gene are showed as a ratio relative to the ADH/18SrRNA ratios for CH on 24DAP, which was set to 1. Each experiment was performed in triplicate and the means \pm SE value of their content were shown in the figure.

μ l reaction (2xSYBR Green PCR Master Mix, Tiangen Biotech Co. Ltd. Beijing, China) on an ABI 7500 sequence detection system. All qPCR experiments were performed in triplicate with different cDNA template. The ADH/18s rRNA ration for samples were related to the ratio for CH in **Figure 5** and for CB in **Figure 8** which were set to 1, respectively. The $2^{-\Delta\Delta Ct}$ method was used to calculate relative genes expression of the *CmADH* genes produced by real time PCR.

Statistical Analysis

A principal component analysis (PCA) was employed to identify the key aroma compounds of the three aromatic melon varieties according to their VOCs by the SPSS 20.0. And significant analysis was conducted by a one-way ANOVA following Duncan's multiple range tests for experiment at a $p < 0.05$ level. The figures were produced by Origin 9.0.

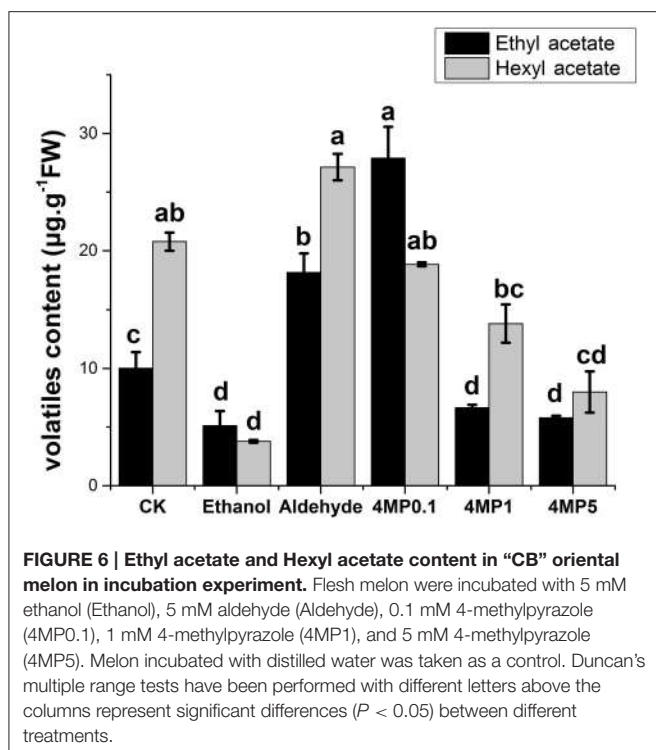


FIGURE 6 | Ethyl acetate and Hexyl acetate content in “CB” oriental melon in incubation experiment. Flesh melon were incubated with 5 mM ethanol (Ethanol), 5 mM aldehyde (Aldehyde), 0.1 mM 4-methylpyrazole (4MP0.1), 1 mM 4-methylpyrazole (4MP1), and 5 mM 4-methylpyrazole (4MP5). Melon incubated with distilled water was taken as a control. Duncan’s multiple range tests have been performed with different letters above the columns represent significant differences ($P < 0.05$) between different treatments.

RESULTS

Firmness, Soluble Solids Content (SSC), and Rind Color

In order to determine the maturation period, SSCs of the three types of melon was chosen for the signal of fruit maturation (Tang et al., 2015). We chose DAP34 as the maturation period of three melon, due to the directly relationship between SSCs and fruit development of melons. The SSC of three types of melon nearly reached the highest concentration at the same time at 34 DAP (Figure S1). The firmness of CH and CG were similar and lower than that of “CB” (Figure 1A). Both CH and CB fruit had higher SSCs than CG (Figure 1B). In terms of rind color, CH and CG were brighter or yellow, CB were dark green (Figures 1C–E; Figure S2). Moreover, CH, CB, and CG fruits also exhibited various morphological and physical characteristics, implying the ripening of different type melons.

Volatile Organic Compounds of Three Types of Melon

We had detected 49 VOCs, including esters, alcohols, acids, and other aroma in three types melons (Table S1). Esters were the most abundant volatiles in CH and CB ($\sim 207.83 \mu\text{g.g}^{-1}\text{FW}$ and $127.16 \mu\text{g.g}^{-1}\text{FW}$, respectively). On the other hand, alcohol contributed the aroma of CG. We also found that the content of esters or total aroma accumulated in CH was nearly twice of those in CB, although esters was the main compounds in both of them (Table 1).

To further distinguish the variety of aroma in three types of melon, PCA of aroma volatiles identified in three types of melon at mature period was conducted (Figure 2). It was clearly that CG was separated from the others in account of V29 [(E,Z)-3,6-nonadien-1-ol], V24 (z-6-nonenal), V27 (3-carene), V34 (2-octyn-1-ol), V44 [Stearic acid, 3-(octadecyloxy) propyl ester], and V45 (10,12-Octadecadiynoic acid; Figure 2), and (E,Z)-3,6-Nonadien-1-ol was the representative volatile compound of CG considering the content (Table S1). V1 (ethyl acetate), V23 (hexyl acetate), and V20 (2-ethyl-2hexen-1-ol) were three principal contributors to PC1, when their abundance were taking into account (Figure 2, Table S1). We regarded ethyl acetate, hexyl acetate, (E, Z)-3, 6-nonadien-1-ol and 2-ethyl-2hexen-1-ol as four principal volatile compounds of these three types of melon. In Figure 3, it was obvious that acetate esters made “CH” or “CB” be separated from “CG.”

Reductase Activity of ADH and AAT Activity in Three Types of Melon at Different DAP

During fruit development from 24 to 36 DAP, reductase activity of ADH in three types of melon showed a trend of increasing at first and decreasing subsequently, which reached a peak at 32 DAP. ADH activity was higher in flesh of CB and CG than that of CH from 24 to 36 DAP, but the change of ADH activity in flesh of CH was smaller than that of CB and CG (Figure 4A).

Figure 4B shows that AAT activity in flesh of CH significantly increased after 32 DAP and peaked on day 36. AAT activity in flesh of CB shows the similar change to CH, which increased after 30 DAP and peaked at 36 DAP, although the AAT activity in flesh of CB was lower than that of CH from 32 to 36 DAP. The AAT activity in CG did not change significantly and the level of enzyme activity in CG was the lowest among three melons from 32 to 36 DAP.

CmADHs Expression in Three Types of Melon during Fruit Ripening

A total of 11 CmADHs were expressed during ripening of melon (Figure 5), as CmADH11 was not detected during our experiment. Transcript analysis indicate that these 11 CmADH genes were specifically expressed in ripening fruit of three aroma types of melon. CmADH2 and CmADH6 were specifically expressed in strong-aromatic melon CH and less-aromatic melon CB and CmADH4 was only expressed in non-aromatic melon CG. The expression of CmADH3, CmADH7, and CmADH12 in CH and CB were higher than that in CG, and most of the genes were consistently expressed with an increase in transcript abundance and reached the peak at 34 DAP or 36 DAP in CH and CB. In addition, the expression level of CmADH5, CmADH8, CmADH9, CmADH10 were either not expressed or maintained a low level during fruit ripening.

Volatile Aroma Compounds of CB in Incubation Experiment

Production of ethyl acetate and hexyl acetate in CB were significantly affected by substrates or inhibitor (Figure 6). Both ethyl acetate and hexyl acetate abundance reduced after ethanol

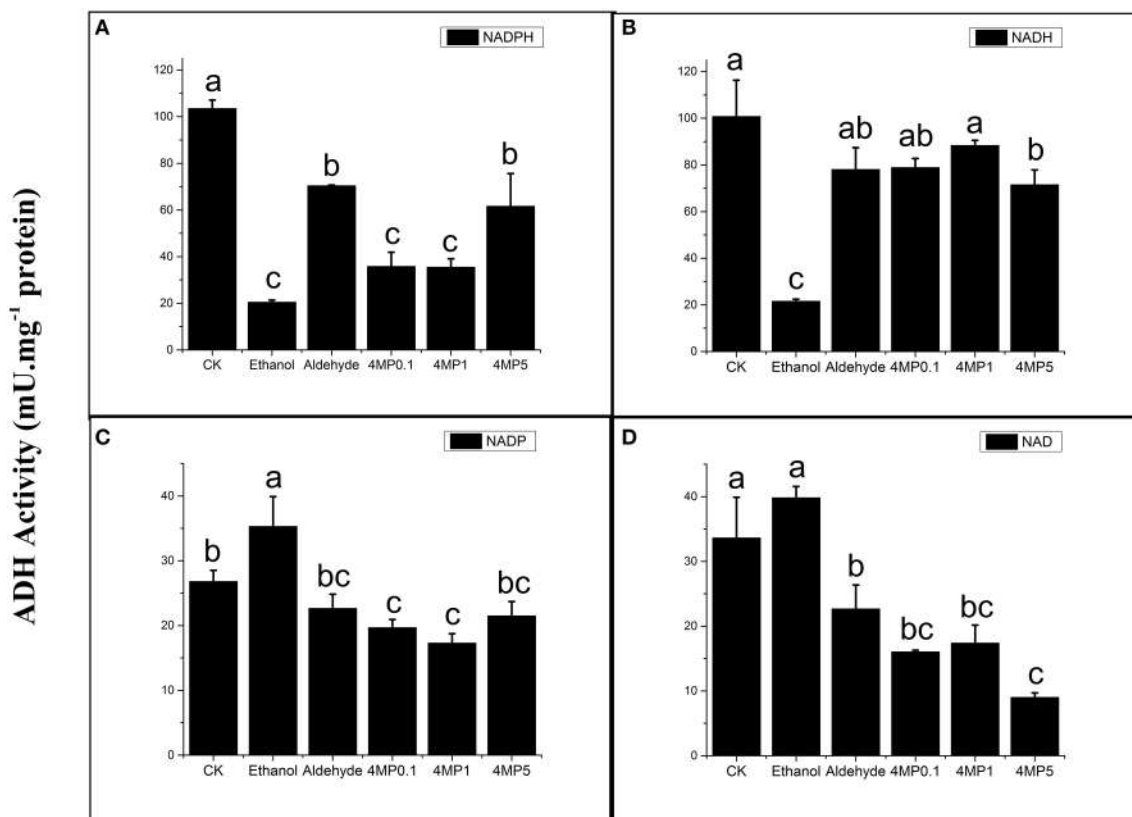


FIGURE 7 | ADH activities depended on four co-factors (0.25 mM NADPH/NADP and NADH/NAD) of CB flesh melon incubated with multiple solutions, including 5 mM ethanol (Ethanol), 5 mM aldehyde (Aldehyde), 0.1 mM 4-methylpyrazole (4MP0.1), 1 mM 4-methylpyrazole (4MP1), and 5 mM 4-methylpyrazole (4MP5) (**A–D**). **(A)** ADH activity depended on 0.25 mM NADPH. **(B)** ADH activity depended on 0.25 mM NADH. **(C)** ADH activity depended on 0.25 mM NADP. **(D)** ADH activity depended on 0.25 mM NAD. Flesh melon incubated with distilled water were used as control. Duncan's multiple range tests have been performed with different letters above the columns represent significant differences ($P < 0.05$) between different treatments.

treatment. Aldehyde only facilitated the production of ethyl acetate. The level of hexyl acetate was up-regulated, but it was not significant. For 4-methylpyrazole (4-MP), the inhibitor of ADH, it seems that the effect of 4-MP on melon acetate production was dose-dependent manner to some extent. Medium and high dose of 4-MP decreased the production of two acetates, while Low dose of 4-MP increased the ethyl acetate content (Figure 6).

ADH Activity in Incubation Experiment

In incubation experiment, the ADH reductase activity was suppressed by ethanol, a production of ADH in melon, regardless of NADH or NADPH was used and ethanol showed a stronger suppression than 4-MP (Figures 7A,B). The dehydrogenase activity were increased by ethanol treatment, though activity change was more significant when the co-factor was NADP. 4-MP also worked as an inhibitor, but it depended on co-factor and its concentration (Figures 7C,D). Aldehyde did not promoted the ADH reductase activity, but it significantly inhibited the dehydrogenase activity when the co-factor was NAD (Figure 7D).

CmADHs Expression in Incubation Experiment

Based on the incubation experiment, 11 *CmADH* genes were expressed in oriental melon “CB” (Figure 8). *CmADH1*, *CmADH4*, *CmADH9*, and *CmADH12* were up-regulated following the addition of aldehyde, while *CmADH2*, *CmADH3*, and *CmADH7* seemed to not response to aldehyde. Most of *CmADHs* genes were down-regulated under ethanol treatment except *CmADH4*, *CmADH7*, and *CmADH9*. Different dose of 4-MP (0.1, 1, and 5 mM) reduced the levels of most *CmADHs* except *CmADH4*, *CmADH7*, *CmADH9*, and *CmADH12* (Figure 8).

DISCUSSION

Aroma was an important quality of ripe fruit, and it differed between varieties of the same species, which was found in many plants (Poll, 1981; Visai and Vanoli, 1997; Kourkoutas et al., 2006; Goulet et al., 2012). For example, esters and alcohols were the main aroma volatiles of Cantalope melon, sulfur esters and straight-chain compounds of six-carbon or nine-carbon were

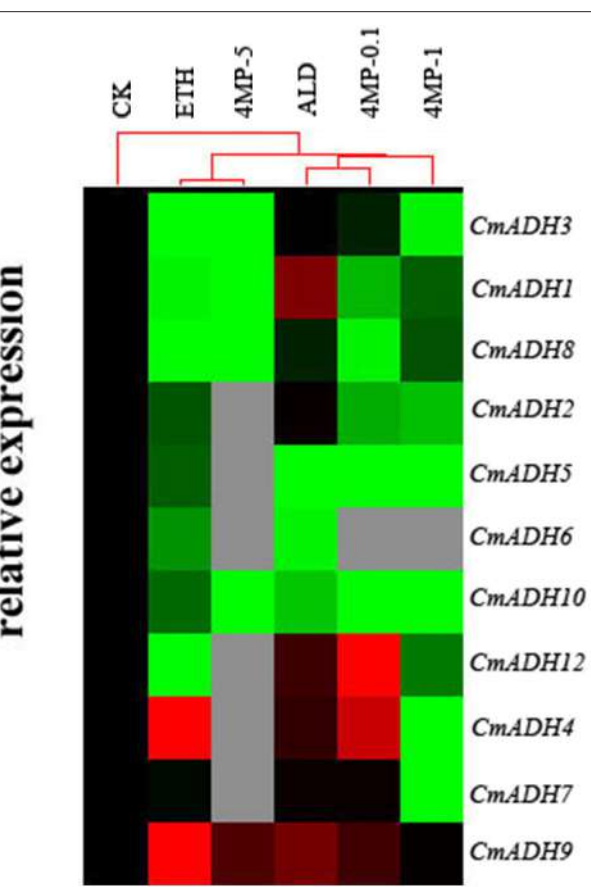


FIGURE 8 | *CmADHs* gene expression in the incubation experiment of oriental melon “CB” flesh fruit. Expression levels of each gene are showed as a ratio relative to the ADH/18SrRNA ratios for CK, which was set to black. The red cube means transcript level was up-regulated and the green cube means down-regulated on the contrary. All of the data for ADH gene expression are means of three replicates.

abundant, while E, Z-2,6-nonadienal was the principle aroma compound of honeydew melon fruit, and methyl esters were the main volatiles of Galia melon (Kourkoutas et al., 2006). Similar results were showed in high-aromatic melon Arava and less-aromatic melon Rochet; Acetate esters were abundant in Arava, while Rochet had high level of volatiles, such as alcohols and aldehydes (Shalit et al., 2001). In our study, unsurprisingly, except for soluble solids content and rind color, three types of melon showed diverse physiological characteristics in flavor, the aroma content of CH is the most abundant, either the total VOCs concentration or esters and CB content less esters than CH, but esters were still the most abundant volatile in CB flesh melon as well as CH; There were little esters in CG flesh melon, on the contrary, alcohols were the principle volatile of non-aromatic melon. Ethyl acetate and hexyl acetate were found to be the principle aroma compounds of CH and CB by PCA analysis combined with their content in ripening fruit, which was consistent with previous conclusion that volatile esters, especially straight-chain esters, were important VOCs in aromatic melon (Tang et al., 2015). In contrast, (E, Z)-3,6-nonadien-1-ol was the

most abundant volatile in CG. These results illustrated that there were differences on the primary VOCs among different aroma types of melon and esters, especially ethyl esters were important aromatic compounds in oriental melons (Li et al., 2011; Liu et al., 2012).

The synthesis of straight-chain ethyl ester, such as hexyl acetate and butyl acetate, was directly correlated with the main enzymes activity in LOX pathway (Senesi et al., 2002; Echeverría et al., 2004; Altisent et al., 2009; Paige and Sheryl, 2012). ADH, as one of the key enzymes in LOX pathway, plays an important role in diverse volatile compounds synthesis in many plants. In olive, ADH activity may account for the diversity in aldehydes and alcohols of two cultivars, Carolea, and Coratina (Iaria et al., 2012). The high expression of *PuADH3* in pear during fruit ripening also indicated the relationship between *PuADHs* and aroma (Li et al., 2014). *CmADH1* and *CmADH2* were involved in fruit development due to their highly expression in Cantaloupe melon and ethylene-induced regulation. Particular substances preferences of two ADHs indicated their particular functions in the formation of various flavor of melon (Manríquez et al., 2006). But ADH is not the final step of LOX pathway, some alcohols produced by ADH would convert into esters under the function of AAT. So that there may be a complex relationship between ADH, AAT and volatiles: During the development of apricot fruit, the expression levels of *PaADH* and *PaLOX* stayed constant at all stages, however *PaAAT* levels showed a sharp increase in the late harvest stages, with the changes observed in ester levels (González-Agüero et al., 2009); Silencing *SlsCADH1*, a specifically expressing gene in tomato fruit, resulted in the accumulation of C5 and C6 compounds rather than the alternation of alcohols/aldehydes balance (Moummou et al., 2012). In our study, ADH activity of all cultivars increased slightly first and raised up to several fold 2 days before the fruits ripened. There was no obvious difference between Less-aromatic melon CB with high esters content and non-aromatic CG with low esters content on ADH activity during fruit development, indicating that ADH activity might not be a key regulator of esters abundance in oriental melon. Increase of AAT activity was detected during ripening of fruit in CH and CB, but there was no significant change about AAT activity in non-aromatic melon CG. It seems there was no direct correlation between the total ADH activity and the total content of VOCs or the alcohols, and the AAT activity was positively correlated with the content of esters in oriental melons. The gene expression pattern of *CmADHs* also various in three cultivars during fruit ripening (Figure 5). The specific *CmADH* genes expression might be an important reason for the diversity of alcohols and follow-up ester components in oriental melon considering that different ADH had particular preferences for various substrates (Manríquez et al., 2006; Moummou et al., 2012) and further more studies are needed to prove the speculation.

We cannot analysis the specific substrate preference of each *CmADH* using crude enzyme, but the change of expression of every *CmADH* caused by some substrate could be detected in incubation experiment. Ethanol was immediate precursor of ethyl acetate, the most abundant characteristic aroma compound in oriental melon. Ethanol and aldehyde could be converted

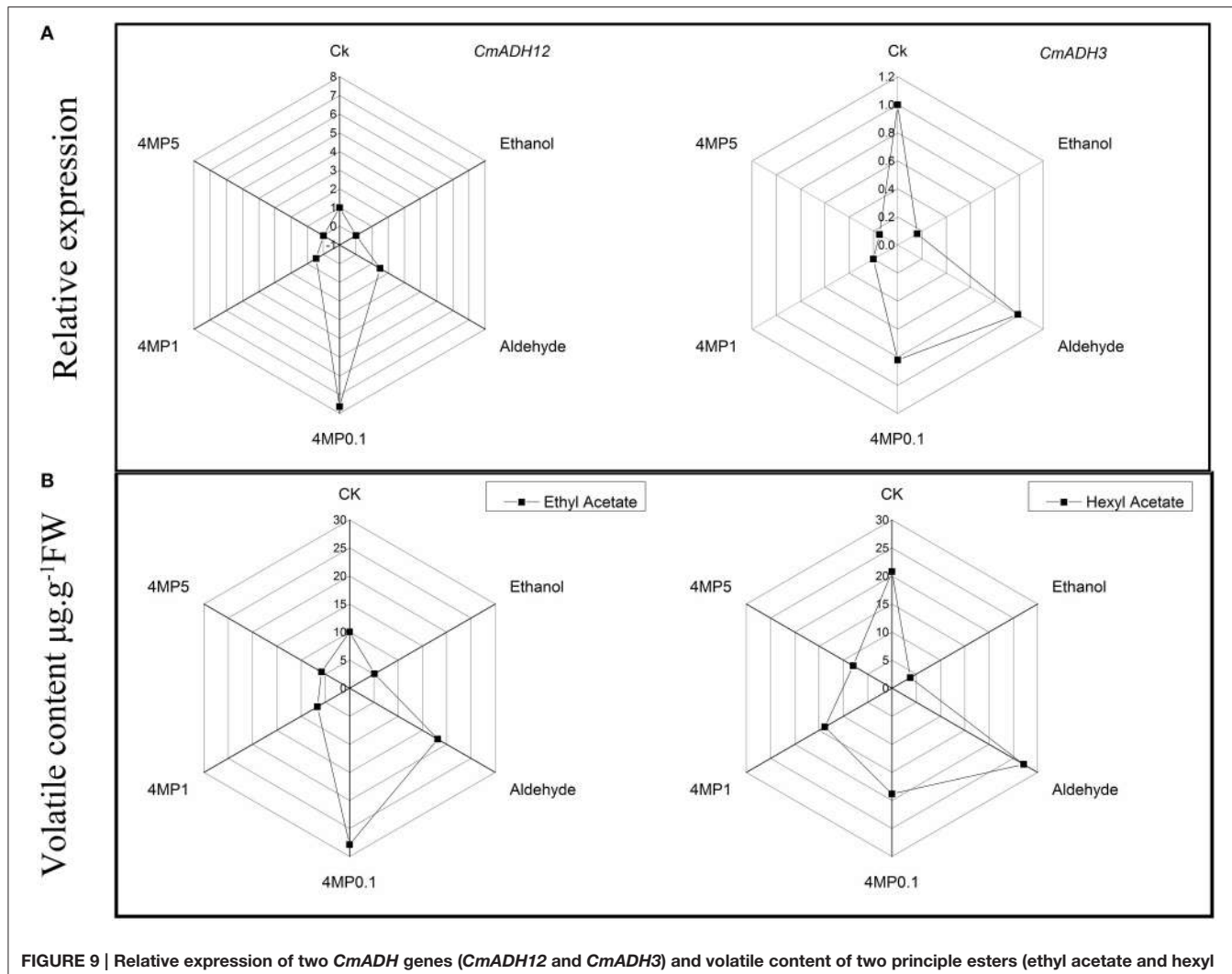


FIGURE 9 | Relative expression of two *CmADH* genes (*CmADH12* and *CmADH3*) and volatile content of two principle esters (ethyl acetate and hexyl acetate) in incubation experiment. **(A)** *CmADH12* and *CmADH3* relative expressions in CB melon incubated with multiple treatments. **(B)** Volatile content of ethyl acetate and hexyl acetate in CB melon incubated with multiple treatments. The treatments were ethanol (Ethanol), aldehyde (Aldehyde), 0.1mM 4-MP (4MP0.1), 1mM 4-MP (4MP1), and 5mM 4-MP (4MP5). All of the data for ADH gene expression and volatile contents are means of three replicates.

into each other by ADH through oxidation or reduction. Previous study showed that the exogenous application of ethanol could delay the maturation of oriental melon and increase the accumulation of aroma volatile compounds within a short time without influencing the ADH activity (Liu et al., 2012). Our study demonstrated ethanol significantly inhibited the activity of ADH enzyme of oriental fresh melon in incubation experiment, just like high concentration of 4-MP, the competitive inhibitor which could inhibit 40 to 60% of the *in vivo* activity of ADH in tomato (Beaulieu et al., 1997) or prevent the formation of ethanol (Kato-Noguchi and Yasuda, 2007), and the levels of most *CmADHs* expression were down-regulated with the reduction of esters. The confliction with former studies may be due to the concentration of ethanol treatment and the treatment time. Dehydrogenase activities of *CmADH* were slight deduced by aldehyde, but increase of reduction activities which we suspected were not found. The expression levels of *CmADH1*, *CmADH4*, *CmADH9*, and *CmADH12* in acetaldehyde treatment were improved, along

with the production of ethyl acetate and hexyl acetate, suggesting their potential function in aroma volatile or ester synthesis. The results suggested that substrates were not the mainly regulator of *CmADHs* expression and ADH activity in oriental melon, and similar result was found in grapevine (Tesniere et al., 2004). Perhaps there was a complex regulation of ADH and enzymatic activity in oriental melon.

So far, 12 *CmAdh* genes were found from the melon genome website and the function of most members were far from clear, except for *CmADH1* and *CmADH2* in Countloup melon. By bioinformatic analysis, we found that high homology appeared between *CmADH2* and *CmADH12* in spite of the low homology of the ADH gene family, and functional domains checked via NCBI's Conserved Domain Database suggested that *CmADH12* might have the same catalytic function as short-chain dehydrogenases (Strommer, 2011; Jin et al., 2016). In addition, we were surprised to find the correlation among *CmADH3* or *CmADH12* gene expression pattern in our experiment, the ADH

reductase activity when NADPH acted as the co-factor, and the accumulation of hexyl acetate or ethyl acetate in incubation experiment (**Figure 9**), although the *CmADHs* gene expression and the changes of enzyme activity would not directly affect the synthesis of esters in theory. It hinted *CmADH3* and *CmADH12* might involve in synthesis of aroma compounds of oriental melon. Considering that their expression levels were up-regulated by ethylene in our previous study (Jin et al., 2016). The recombinant protein or the transgenic plants were needed to obtain more information about the role of certain *CmADHs* in oriental melon aroma formation.

CONCLUSIONS

In this paper, volatile esters, especially ethyl acetate, and hexyl acetate, as the primary aroma were identified in strong and less aromatic oriental melons, and alcohols, (E, Z)-3, 6-nonadien-1-ol, as the principle volatile, were also identified in non-aromatic melon. We found that the specific *CmADH* genes expression might be an important reason for the diversity of alcohols and follow-up ester components in three types of melon. ADH activity, *CmADH* genes expression and the content of two principle esters were significantly inhibited by ethanol, and the 4-MP, a kind of competitive inhibitor of ADH enzyme. While affection of aldehyde on *CmADH* activity or *CmADH* expression depended on co-factors or genes. We also found the relationship between *CmADH3*, *CmADH12* and the characteristic volatile, namely ethyl acetate or hexyl acetate. In conclusion, our study provide some evidences for the relationship between *CmADHs* and volatile compounds of oriental melon, and more studies are needed to make it clear.

REFERENCES

- Altisent, R., Echeverría, G., Graell, J., López, L., and Lara, I. (2009). Lipoxygenase activity is involved in the regeneration of volatile ester-synthesizing capacity after ultra-low oxygen storage of “Fuji” apple. *J. Agric. Food Chem.* 57, 4305–4312. doi: 10.1021/jf803930j
- Beaulieu, J. C., Peiser, G., and Saltveit, M. E. (1997). Acetaldehyde is a causal agent responsible for ethanollnduced ripening inhibition in tomato fruit. *Plant Physiol.* 113, 431–439.
- Bradford, M. M. (1976). A rapid and sensitive method for the quantitation of microgram quantities of protein utilizing the principle of protein-dye binding. *Anal. Biochem.* 72, 248–254. doi: 10.1016/0003-2697(76)90527-3
- Dixon, J., and Hewett, E. W. (2000). Factors affecting apple aroma/flavour volatile concentration: a review. *N. Z. J. Crop Hortic. Sci.* 28, 155–173. doi: 10.1080/01140671.2000.9514136
- Echeverría, G., Graell, J., López, M. L., and Lara, I. (2004). Volatile production, quality and aroma-related enzyme activities during maturation of “Fuji” apples. *Postharvest Biol. Technol.* 31, 217–227. doi: 10.1016/j.postharvbio.2003.09.003
- Garabagi, F., and Strommer, J. (2004). Distinct genes produce the alcohol dehydrogenases of pollen and maternal tissues in *Petunia hybrida*. *Biochem. Genet.* 42, 199–208. doi: 10.1023/B:BIGI.0000026634.69911.2e
- Goff, S. A., and Klee, H. J. (2006). Plant volatile compounds: sensory cues for health and nutritional value? *Science* 311, 815–819. doi: 10.1126/science.1112614
- Gonda, I., Bar, E., Portnoy, V., Lev, S., Burger, J., Schaffer, A. A., et al. (2010). Branched-chain and aromatic amino acid catabolism into aroma volatiles in *Cucumis melo* L. fruit. *J. Exp. Bot.* 61, 1111–1123. doi: 10.1093/jxb/erp390
- González-Agüero, M., Troncoso, S., Gudenschwager, O., Campos-Vargas, R., Moya-León, M. A., and Defilippi, B. G. (2009). Differential expression levels of aroma-related genes during ripening of apricot (*Prunus armeniaca* L.). *Plant Physiol. Biochem.* 47, 435–440. doi: 10.1016/j.plaphy.2009.01.002
- Goulet, C., Mageroy, M. H., Lam, N. B., Floystad, A., Tieman, D. M., and Klee, H. J. (2012). Role of an esterase in flavor volatile variation within the tomato clade. *Proc. Natl. Acad. Sci. U.S.A.* 109, 19009–19014. doi: 10.1073/pnas.1216515109
- Iaria, D. L., Bruno, L., Macchione, B., Tagarelli, A., Sindona, G., Giannino, D., et al. (2012). The aroma biogenesis-related *Olea europaea* ALCOHOL DEHYDROGENASE gene is developmentally regulated in the fruits of two *O. europaea* L. cultivars. *Food Res. Int.* 49, 720–727. doi: 10.1016/j.foodres.2012.09.004
- Jin, Y., Zhang, C., Liu, W., Tang, Y., Qi, H., and Chen, H. (2016). The alcohol dehydrogenase gene family in melon (*Cucumis melo* L.): bioinformatic analysis and expression patterns. *Front. Plant Sci.* 7:670. doi: 10.3389/fpls.2016.00670
- Kato-Noguchi, H., and Yasuda, Y. (2007). Effect of low temperature on ethanolic fermentation in rice seedlings. *J. Plant Physiol.* 164, 1013–1018. doi: 10.1016/j.jplph.2006.06.007
- Khanom, M. M., and Ueda, Y. (2008). Bioconversion of aliphatic and aromatic alcohols to their corresponding esters in melons (*Cucumis melo* L. cv. Prince melon and cv. Earl's favorite melon). *Postharvest Biol. Technol.* 50, 18–24. doi: 10.1016/j.postharvbio.2008.02.015
- Kourkoutas, D., Elmore, J. S., and Mottram, D. S. (2006). Comparison of the volatile compositions and flavour properties of cantaloupe, Galia and honeydew muskmelons. *Food Chem.* 97, 95–102. doi: 10.1016/j.foodchem.2005.03.026
- Lara, I., Miró, R. M., Fuentes, T., Sayez, G., Graell, J., and López, M. L. (2003). Biosynthesis of volatile aroma compounds in pear fruit stored under long-term controlled-atmosphere conditions. *Postharvest Biol. Technol.* 29, 29–39. doi: 10.1016/S0925-5214(02)00230-2

AUTHOR CONTRIBUTIONS

HC and HQ designed research; HC performed research; HC analyzed data; HC and HQ wrote the paper; SC, YJ, and YT helped to revise the paper.

FUNDING

First level of Liaoning high school Talent support program, LR2014020.

SUPPLEMENTARY MATERIAL

The Supplementary Material for this article can be found online at: <http://journal.frontiersin.org/article/10.3389/fphys.2016.00254>

Table S1 | Volatile compounds and their concentrations (μg.g-1FW) in different aroma types of the melon ripe fruit. Include “Cai Hong” (CH), “Cui Bao” (CB) and “Cai Gua” (CG). Each experiment was performed in triplicate and the mean value of their concentrations were shown in this table.

Figure S1 | The SSC of three types of melon at different days after pollination (DAP). The three aroma types melon are CH (short for “Cai Hong”), CB (short for “Cui Bao”), and CG (short for “Cai Gua”). Each experiment was performed in triplicate and the means ± SE value of their content were shown in the line chart.

Figure S2 | Different appearance of three types of melon (*Cucumis melo*). (A) Oriental melon (*C. melo* var. *makuwa* Makino) cultivar “Chai Hong” (CH). (B) Oriental melon (*C. melo* var. *makuwa* Makino) cultivar “Chai Hong” (CH). (B) Oriental melon (*C. melo* var. *makuwa* Makino) cultivar “Cui Bao” (CB). (C) Snake melon (*C. melo* L. var. *flexuosus* Naud) “Cai Gua” (CG).

- Li, G., Jia, H., Li, J., Wang, Q., Zhang, M., and Teng, Y. (2014). Emission of volatile esters and transcription of ethylene- and aroma-related genes during ripening of "Pingxiangli" pear fruit (*Pyrus ussuriensis* Maxim). *Sci. Hortic.* 170, 17–23. doi: 10.1016/j.scientia.2014.03.004
- Li, Y., Qi, H., Jin, Y., Tian, X., Sui, L., and Qiu, Y. (2016). Role of ethylene in biosynthetic pathway of related-aroma volatiles derived from amino acids in oriental sweet melons (*Cucumis melo* var. *makuwa* Makino). *Sci. Hortic.* 201, 24–35. doi: 10.1016/j.scientia.2015.12.053
- Li, Y., Qi, H. Y., Liu, Y. F., and Guan, X. C. (2011). Effects of ethephon and 1-methylcyclopropene on fruit ripening and the biosynthesis of volatiles in oriental sweet melon (*Cucumis melo* var. *makuwa* Makino). *J. Hortic. Sci. Biotechnol.* 86, 517–526. doi: 10.1080/14620316.2011.11512798
- Liu, W. W., Qi, H. Y., Xu, B. H., Li, Y., Tian, X. B., Jiang, Y. Y., et al. (2012). Ethanol treatment inhibits internal ethylene concentrations and enhances ethyl ester production during storage of oriental sweet melons (*Cucumis melo* var. *makuwa* Makino). *Postharvest Biol. Technol.* 67, 75–83. doi: 10.1016/j.postharvbio.2011.12.015
- Longhurst, T. J., Tung, H. F., and Brady, C. J. (1990). Developmental regulation of the expression of alcohol dehydrogenase in ripening tomato fruits. *J. Food Biochem.* 14, 421–433. doi: 10.1111/j.1745-4514.1990.tb00804.x
- Manríquez, D., El-Sharkawy, I., Flores, F. B., El-Yahyaoui, F., Regad, F., Bouzayen, M., et al. (2006). Two highly divergent alcohol dehydrogenases of melon exhibit fruit ripening-specific expression and distinct biochemical characteristics. *Plant Mol. Biol.* 61, 675–685. doi: 10.1007/s11103-006-0040-9
- Maul, F., Sargent, S. A., Sims, C. A., Baldwin, E. A., Balaban, M. O., and Huber, D. J. (2000). Tomato flavor and aroma quality as affected by storage temperature. *J. Food Sci.* 65, 1228–1237. doi: 10.1111/j.1365-2621.2000.tb10270.x
- Moummou, H., Tonfack, L. B., Chervin, C., Benichou, M., Youmbi, E., Ginies, C., et al. (2012). Functional characterization of *SlsCADH1*, a fruit-ripening-associated short-chain alcohol dehydrogenase of tomato. *J. Plant Physiol.* 169, 1435–1444. doi: 10.1016/j.jplph.2012.06.007
- Obando-Ulloa, J. M., Ruiz, J., Monforte, A. J., and Fernández-Trujillo, J. P. (2010). Aroma profile of a collection of near-isogenic lines of melon (*Cucumis melo* L.). *Food Chem.* 118, 815–822. doi: 10.1016/j.foodchem.2009.05.068
- Paige, T., and Sheryl, B. (2012). Influence of lipid content and lipoxygenase on flavor volatiles in the tomato peel and flesh. *J. Food Sci.* 77, C830–C837. doi: 10.1111/j.1750-3841.2012.02775.x
- Poll, L. (1981). Evaluation of 18 apple varieties for their suitability for juice production. *J. Sci. Food Agric.* 32, 1081–1090. doi: 10.1002/jsfa.2740321107
- Salas, J. J., and Sánchez, J. (1998). Alcohol dehydrogenases from olive (*Olea europaea*) fruit. *Phytochemistry* 48, 35–40. doi: 10.1016/S0031-9422(97)01097-2
- Senesi, E., Scalzo, R. L., Prinzivalli, C., and Testoni, A. (2002). Relationships between volatile composition and sensory evaluation in eight varieties of netted muskmelon (*Cucumis melo* L. var. *reticulatus* Naud). *J. Sci. Food Agric.* 82, 655–662. doi: 10.1002/jsfa.1087
- Shalit, M., Katzir, N., Tadmor, Y., Larkov, O., Burger, Y., Shalekhet, F., et al. (2001). Acetyl-CoA: alcohol acetyltransferase activity and aroma formation in ripening melon fruits. *J. Agric. Food Chem.* 49, 794–799. doi: 10.1021/jf001075p
- Speirs, J., Correll, R., and Cain, P. (2002). Relationship between ADH activity, ripeness and softness in six tomato cultivars. *Sci. Hortic.* 93, 137–142. doi: 10.1016/S0304-4238(01)00316-8
- Strommer, J. (2011). The plant ADH gene family. *Plant J.* 66, 128–142. doi: 10.1111/j.1365-313X.2010.04458.x
- Tang, Y., Zhang, C., Cao, S., Wang, X., and Qi, H. (2015). The effect of CmLOXs on the production of volatile organic compounds in four aroma types of melon (*Cucumis melo*). *PLoS ONE* 10:e0143567. doi: 10.1371/journal.pone.0143567
- Tesniere, C., Pradal, M., El-Kereamy, A., Torregrosa, L., Chatelet, P., Roustan, J. P., et al. (2004). Involvement of ethylene signalling in a non-climacteric fruit: new elements regarding the regulation of ADH expression in grapevine. *J. Exp. Bot.* 55, 2235–2240. doi: 10.1093/jxb/erh244
- Tijskens, L. M. M., Dos-Santos, N., Jowkar, M. M., Obando-Ulloa, J. M., Moreno, E., Schouten, R. E., et al. (2009). Postharvest firmness behaviour of near-isogenic lines of melon. *Postharvest Biol. Technol.* 51, 320–326. doi: 10.1016/j.postharvbio.2008.06.001
- Urruty, L., Giraudel, J. L., Lek, S., Roudeillac, P., and Montury, M. (2002). Assessment of strawberry aroma through SPME/GC and ANN methods. *Classification and discrimination of varieties*. *J. Agric. Food Chem.* 50, 3129–3136. doi: 10.1021/jf0116799
- Visai, C., and Vanoli, M. (1997). Volatile compound production during growth and ripening of peaches and nectarines. *Sci. Hortic.* 70, 15–24. doi: 10.1016/S0304-4238(97)00032-0
- Zhang, C., Jin, Y., Liu, J., Tang, Y., Cao, S., and Qi, H. (2014). The phylogeny and expression profiles of the lipoxygenase (LOX) family genes in the melon (*Cucumis melo* L.) genome. *Sci. Hortic.* 170, 94–102. doi: 10.1016/j.scientia.2014.03.005

Conflict of Interest Statement: The authors declare that the research was conducted in the absence of any commercial or financial relationships that could be construed as a potential conflict of interest.

Copyright © 2016 Chen, Cao, Jin, Tang and Qi. This is an open-access article distributed under the terms of the Creative Commons Attribution License (CC BY). The use, distribution or reproduction in other forums is permitted, provided the original author(s) or licensor are credited and that the original publication in this journal is cited, in accordance with accepted academic practice. No use, distribution or reproduction is permitted which does not comply with these terms.



Gene-Metabolite Networks of Volatile Metabolism in Airen and Tempranillo Grape Cultivars Revealed a Distinct Mechanism of Aroma Bouquet Production

José L. Rambla^{1,2†}, Almudena Trapero-Mozos^{1†}, Gianfranco Doretto³,
Angela Rubio-Moraga¹, Antonio Granell², Lourdes Gómez-Gómez¹ and
Oussama Ahrazem^{1,4*}

¹ Facultad de Farmacia, Instituto Botánico, Universidad de Castilla-La Mancha, Albacete, Spain, ² Instituto de Biología Molecular y Celular de Plantas, CSIC-Universidad Politécnica de Valencia, Valencia, Spain, ³ Italian National Agency for New Technologies, Energy, and Sustainable Development, Casaccia Research Centre, Rome, Italy, ⁴ Fundación Parque Científico y Tecnológico de Castilla-La Mancha, Albacete, Spain

OPEN ACCESS

Edited by:

Steven Carl Huber,
Agricultural Research Service (USDA),
USA

Reviewed by:

Encarna Gómez-Plaza,
University of Murcia, Spain
Andreas P.M. Weber,
University of Düsseldorf, Germany

*Correspondence:

Oussama Ahrazem
Oussama.ahrazem@uclm.es

[†]These authors have contributed
equally to this work.

Specialty section:

This article was submitted to
Plant Physiology,
a section of the journal
Frontiers in Plant Science

Received: 11 December 2015

Accepted: 13 October 2016

Published: 27 October 2016

Citation:

Rambla JL, Trapero-Mozos A, Doretto G, Rubio-Moraga A, Granell A, Gómez-Gómez L and Ahrazem O (2016) Gene-Metabolite Networks of Volatile Metabolism in Airen and Tempranillo Grape Cultivars Revealed a Distinct Mechanism of Aroma Bouquet Production. *Front. Plant Sci.* 7:1619.
doi: 10.3389/fpls.2016.01619

Volatile compounds are the major determinants of aroma and flavor in both grapes and wine. In this study, we investigated the emission of volatile and non-volatile compounds during berry maturation in two grape varieties (Airén and Tempranillo) throughout 2010 and 2011. HS-SPME coupled to gas chromatography and mass spectrometry was applied for the identification and relative quantitation of these compounds. Principal component analysis was performed to search for variability between the two cultivars and evolution during 10 developmental stages. Results showed that there are distinct differences in volatile compounds between cultivars throughout fruit development. Early stages were characterized in both cultivars by higher levels of some apocarotenoids such as β -cyclocitral or β -ionone, terpenoids (E)-linalool oxide and (Z)-linalool oxide and several furans, while the final stages were characterized by the highest amounts of ethanol, benzenoid phenylacetaldehyde and 2-phenylethanol, branched-amino acid-derived 3-methylbutanol and 2-methylbutanol, and a large number of lipid derivatives. Additionally, we measured the levels of the different classes of volatile precursors by using liquid chromatography coupled to high resolution mass spectrometry. In both varieties, higher levels of carotenoid compounds were detected in the earlier stages, zeaxanthin and α -carotene were only detected in Airén while neoxanthin was found only in Tempranillo; more variable trends were observed in the case of the other volatile precursors. Furthermore, we monitored the expression of homolog genes of a set of transcripts potentially involved in the biosynthesis of these metabolites, such as some glycosyl hydrolases family 1, lipoxygenases, alcohol dehydrogenases hydroperoxide lyases, O-methyltransferases and carotenoid cleavage dioxygenases during the defined developmental stages. Finally, based on Pearson correlation analyses, we explored the metabolite-metabolite fluctuations within VOCs/precursors during the berry development; as well as tentatively linking the formation of some metabolites

detected to the expression of some of these genes. Our data showed that the two varieties displayed a very different pattern of relationships regarding the precursor/volatile metabolite-metabolite fluctuations, being the lipid and the carotenoid metabolism the most distinctive between the two varieties. Correlation analysis showed a higher degree of overall correlation in precursor/volatile metabolite-metabolite levels in Airén, confirming the enriched aroma bouquet characteristic of the white varieties.

Keywords: volatile organic compounds, precursors, aroma, expression analysis, *Vitis vinifera*

INTRODUCTION

Secondary metabolites of grapes (*Vitis vinifera L.*) play a key role in wine quality. The phenolic components of the skin and seeds are the main source of the color of wine and its structural properties (Ribereau-Gayon and Glories, 1986), while volatile organic compounds (VOCs) are the major determinants of aroma and flavor in wine (Zoeklein et al., 1998).

The final aroma of wine is determined by several hundreds of volatile compounds of varying chemical nature. Among these compounds, alcohols, esters, aldehydes, ketones, and hydrocarbons have been characterized, all at very low concentrations with a human threshold detection ranging between 10^{-4} and 10^{-12} g/L (Koundouras et al., 2009). The concentration of these compounds in the final product depends on factors associated with grape variety, cultivation (climate, irrigation, etc.) as well as the fermentation process (pH, temperature, nutrients and microflora) and posterior management involving factors such as filtration, clarification or aging. The characteristics and intensity of aroma may vary depending on the grape variety used, and also the geographical and climatic conditions where the grapes were grown. The volatile compounds that contribute to the aroma of the grape are mainly esters of acetic acid and modified monoterpenoids such as linalool, geraniol, nerol, citronellol, α -terpineol, and hotrienol (Rapp and Mandery, 1986). Other groups of volatile aromatic compounds playing an important role in aroma are aldehydes such as (E)-2-hexenal and hexanal, ketones, e.g., 2- and 3-alkanones; and alcohol compounds including n-alcohols from 4 to 11 carbon atoms, unsaturated alcohols and short-chain branched and aromatic alcohols such as benzyl alcohol. Furthermore, it should be noted that a large amount of compounds responsible for the aroma have been described in grape in glycosylated non-volatile form (Winterhalter and Skouroumounis, 1997). The most abundant included within this group are modified terpenes, particularly monoterpenes.

The existence of a non-volatile and odorless grape fraction that can be revealed by chemical or enzymatic pathways was first demonstrated by Cordonier and Bayonove (1974).

During the past two decades, a growing number of studies have shown that the glycosides represent a natural reservoir of volatile compounds in a high number of fresh or processed fruits (Buttery et al., 1990; Marlatt et al., 1992; Buttery, 1993; Krammer et al., 1994; Sakho et al., 1997; Boulanger and Crouzet, 2001; Aubert et al., 2003; Lalel et al., 2003; Osorio et al., 2003; Tikunov et al., 2010, 2013), in grapes and wine (Williams,

1993; Baek and Cadwallader, 1999; Genovés et al., 2003; Sarry and Günata, 2004), and also in flowers and plants and their derivatives (Loughrin et al., 1992; Straubinger et al., 1998; Wang et al., 2001; Watanabe et al., 2001; Nonier et al., 2005). The enzymatic and acid hydrolysis of glycosylated precursors release the volatile aglycones, thus changing the flavor (Williams, 1993). Enzymatic hydrolysis is catalyzed by glycosidases. This is a large group of biologically important enzymes, both biomedical and industrial, which are found in plants and microorganisms, mainly yeasts, and filamentous fungi (Pogorzelski and Wilkowska, 2007). Although, endogenous glycosidic activities increased in the fruit during the ripening process, no evidence of their relationship with the hydrolysis of glycosylated precursors of volatile compounds has been proved so far (Lecas et al., 1991; Kumar and Ramón, 1996; Manzanares et al., 2001; Mizutani et al., 2002; Sarry and Günata, 2004; Wei et al., 2004; Tsuruhami et al., 2006).

As stated before, in grape berries there are hundreds of compounds that potentially contribute to the aroma and flavor of wine. The nature of these metabolites shows a large chemical diversity and belongs to different metabolic pathways producing mainly fatty acids, amino acids, esters and terpenoid derivatives.

Volatiles derived from fatty acids are a class of compounds which includes one of the most important volatiles produced in many fruits. These compounds are classified as green leaf volatiles due to their characteristic “green” fresh aroma of cut grass, since high amounts of lipid-derived C₆ aldehydes and alcohols are released from vegetative tissues when disrupted (Klee, 2010; Rambla et al., 2014). The initial step in the biosynthesis of these compounds is still not completely understood. Due to their toxicity free fatty acids are rapidly catabolized mainly by means of the lipoxygenase pathway which includes the sequential activity of lipoxygenase (LOX) and hydroperoxide lyase (HPL) enzymes (Tieman et al., 2012). The aldehydes produced from this LOX pathway can be reduced to alcohols by means of alcohol dehydrogenases (ADHs), enzymes catalyzing their reversible interconversion (Speirs et al., 1998a,b; Tesniere et al., 2006).

A variety of compounds are derived from the amino acid phenylalanine, such as 2-phenylethanol, phenylacetaldehyde and benzaldehyde, some of which provide a floral aroma (Baldwin et al., 2008; Tzin et al., 2013). The main biosynthesis of these compounds is started by means of a phenylalanine ammonia-lyase (PAL) producing (E)-cinnamic acid, while the last steps of the biosynthesis of some of these compounds are catalyzed by an O-methyltransferase (Mageroy et al., 2012).

Other important volatile compounds are terpenoids, which can be classified into two groups: monoterpenoids (C_{10}) and sesquiterpenoids (C_{15}). They are both synthesized from the five-carbon precursors isopentenyl diphosphate (IPP) and dimethylallyl diphosphate (DMAPP). The carotenoid derived volatiles, such as the C_{13} ketones β -ionone or β -damascenone, are synthesized by the oxidative cleavage of double bonds in carotenoids carried out by carotenoid cleavage dioxygenases (CCDs) (El Hadi et al., 2013; Granell and Rambla, 2013; Frusciante et al., 2014; Rubio-Moraga et al., 2014; Ahrazem et al., 2016).

Many of the volatiles are not preformed but produced by action of enzymes on precursors or conjugated substrates. To see to what extent the variability in volatile production from berries of two grape cultivars Airén (white) and Tempranillo (red) is in part due to differences in precursors levels or precursor availability to the volatile pathway, we study the profiles of volatiles and non-volatiles metabolites and investigated the correlations among the level of volatile compounds and their precursors and the expression of some genes potentially involved in their formation. A positive correlation between precursors and final volatile products will help us to exploit biotechnologically their potential to increase volatiles by selecting varieties with more precursors or conjugated forms of volatiles.

MATERIAL AND METHODS

Plant Material

Grapevine berries and leaves of healthy *Vitis vinifera* L. from Tempranillo and Airén varieties were sampled in Tarazona de la Mancha, Spain, during 2010 and 2011. The two genotypes are cultivated in neighboring vineyards thus they are under the same climatic, microclimatic and stress impacts. Vineyard management was carried out to provide optimum plant growth and yield including fertilization, plant protection treatment, irrigation and canopy management according to local viticulture standards.

For every 10 plants, three bunches of grapes were sampled over a 10-week period from the end of July to early October. A total of 10 samples corresponding to 10 different stages were inspected visually before sampling and only intact and healthy bunches were taken. The weekly samples corresponding to the phenology of the two cultivars is shown in Supplementary Figure 1. After collection, all samples were immediately frozen in liquid nitrogen and stored at -80°C until required.

Volatile Detection and Quantification

For volatile analysis, three biological replicates were processed and analyzed independently for each developmental stage. Each biological replicate consisted in a pool of about 500 g of whole berries in the same developmental stage. Samples were cooled with liquid nitrogen, ground with mortar and pestle, and stored at -80°C until analysis. Prior to the analysis of volatile compounds, frozen fruit powder (1 g fresh weight) from each sample was weighed in a 7 mL vial, closed, and incubated at 30°C for 10 min. Then, 2.2 g of $\text{CaCl}_2 \cdot 2\text{H}_2\text{O}$ and 1 mL of EDTA 100 mM were added, shaken gently and sonicated for 5 min,

and 1.5 mL of the homogenized mixture was transferred into a 10 ml screw cap headspace vial, where volatiles were collected from.

Volatile compounds were extracted by headspace solid-phase microextraction (HS-SPME) by means of a 65 μm PDMS/DVB fiber (Supelco). Initially, headspace vials were tempered at 50°C for 10 min. Then, the volatiles were extracted by exposing the fiber to the vial headspace for 30 min under continuous agitation and heating at 50°C . The extracted volatiles were desorbed in the GC injection port for 1 min at 250°C in splitless mode. Incubation of the vials, extraction and desorption were performed automatically by a CombiPAL autosampler (CTC Analytics). Chromatography was performed on a 6890N gas chromatograph (Agilent Technologies) with a DB-5ms (60 m \times 0.25 mm \times 1 μm) column (J&W Scientific) with Helium as carrier gas at a constant flow of 1.2 mL/min. Oven temperature conditions were: 40°C for 2 min, $5^{\circ}\text{C}/\text{min}$ ramp until 250°C and then held at 250°C for 5 min. Mass spectra were recorded in scan mode in the 35–250 m/z range by a 5975B Mass Spectrometer (Agilent Technologies) at an ionization energy of 70 eV and a scanning speed of 6 scans/s. MS source temperature was 230°C . Chromatograms and spectra were recorded and processed using the Enhanced ChemStation software (Agilent Technologies).

For GC-MS, compounds were unequivocally identified by comparison of both mass spectrum and retention time to those of pure standards (SIGMA-Aldrich), except those labeled with an asterisk, which were tentatively identified by comparison of their mass spectra with those in the NIST05 library. For quantification, peak areas of selected specific ions were integrated for each compound and normalized by comparison with the peak area of the same compound in a reference sample injected regularly in order to correct for variations in detector sensitivity and fiber aging. The reference sample consisted in a homogeneous mixture of all the samples analyzed. Data for a particular sample were expressed as the relative content of each metabolite compared to those in the reference.

Precursors Detection and Quantification by LC-MS

Carotenoids and chlorophylls have been analyzed and quantified by LC-DAD-APCI-HRMS as previously described (Liu et al., 2014) (Su et al., 2015) with slight modifications. Forty milligram of freeze-dried berry powder have been used for each extraction, and APCI-MS settings were as following: sheath and auxiliary gas, set to 30 and 12 units, respectively; the vaporizer temperature and the capillary temperature were set to 270 and 220°C , respectively, while the discharge current was set to 3.5 μA , and the capillary voltage and tube lens settings were 25 V and 80 V. Identification was performed using literature data (Mendes-Pinto et al., 2004; Crupi et al., 2010; Kamffer et al., 2010), and on the basis of the m/z accurate masses, as reported on Pubchem (<http://pubchem.ncbi.nlm.nih.gov/>) or ChemsSpider (<http://www.chemsSpider.com>). Linoleic and linolenic acids have been analyzed using the same experimental

conditions, confirmed by using authentic standards, and have been relatively quantified as fold on the internal standard (α -tocopherol acetate) level. For each experimental point, at least 4 independent extractions have been used.

LC-ESI(+)-HRMS analysis of semi-polar precursors of volatiles (amino acids, phenylpropanoids, terpene glucosides) has been performed as previously described (De Vos et al., 2007; Iijima et al., 2008) with slight modifications. 20 mg of freeze-dried grape berry powder were extracted with 0.75 mL cold 75% (v/v) methanol, 0.1% (v/v) formic acid, spiked with 10 μ g/ml formononetin. After shaking for 40' at 20 Hz using a Mixer Mill 300 (Qiagen), samples were centrifuged for 15 min at 20,000 g at 4°C. 0.6 mL of supernatant was removed and transfer to HPLC tubes. For each genotype/stage, at least five independent extractions have been carried out. LC-MS analyses were carried out using a LTQ-Orbitrap Discovery mass spectrometry system (Thermo Fisher Scientific) operating in positive electrospray ionization (ESI), coupled to an Accela U-HPLC system (Thermo Fisher Scientific, Waltham, MA). Liquid chromatography was carried out using a Phenomenex C18 Luna column (150 \times 2.0 mm, 3 μ m) and mobile phase was composed by water –0.1% Formic Acid (A) and acetonitrile –0.1% Formic Acid (B). The gradient was: 95%A:5%B (1 min), a linear gradient to 25%A:75%B over 40 min, 2 min isocratic, before going back to the initial LC conditions in 18 min. Ten microliter of each sample were injected and a flow of 0.2 mL was used during the whole LC runs. Detection was carried out continuously from 230 to 800 nm with an online Accela Surveyor photodiode array detector (PDA, Thermo Fischer Scientific, Waltham, MA). All solvents used were LC-MS grade quality (CHROMASOLV® from Sigma-Aldrich). Metabolites were quantified in a relative way by normalization on the internal standard amounts. ESI-MS ionization was performed using the following parameters: capillary voltage and temperature were set at 10V and 285°C; sheath and aux gas flow rate at, respectively, 40 and 10. Spray voltage was set to 6 kV and tube lens at 60 V. Metabolite identification was performed by through comparing chromatographic and spectral properties with authentic standards and reference spectra, literature data, and on the basis of the m/z accurate masses, as reported on Pubchem database (<http://pubchem.ncbi.nlm.nih.gov/>) for monoisotopic masses identification, or on Metabolomics Fiehn Lab Mass Spectrometry Adduct Calculator (<http://fiehnlab.ucdavis.edu/staff/kind/Metabolomics/MS-Adduct-Calculator/>) in case of adduct ion detection.

RNA Extraction and Quantitative Real-Time PCR Analysis

The same batch of material used for RNA extraction was used for volatiles analysis. Total RNA extractions were performed as reported (Gómez-Gómez et al., 2012). The quantitative RT-PCR was carried out on cDNA from three biological replicates; reactions were set up in GoTaq[®] qPCR Master Mix (Promega, Madison WI, USA) according to manufacturer's instructions, with gene-specific primers (0.125 μ M) in a final volume of 25 μ L. The grapevine Genoscope database was used to identify sequences

related to GH, CCD, LOX, HPL, ADH, and OMT genes (<http://www.genoscope.cns.fr/externe/GenomeBrowser/Vitis/>). The Primer design was performed using Primer3 program (<http://frodo.wi.mit.edu/>) (Rozen and Skaletsky, 2000). Primer sequences are listed in Supplementary Table 1. Transcripts were normalized to a reference number derived from transcript levels of the constitutively expressed 18rRNA. The cycling parameters of qPCR consisted of an initial denaturation at 94°C for 5 min; 40 subsequent cycles of denaturation at 94°C for 20 s, annealing at 58°C for 20 s and extension at 72°C for 20 s; and final extension at 72°C for 5 min. Assays were conducted with a StepOneTM Thermal Cycler (Applied Biosystems, California, USA) and analyzed using StepOne software v2.0 (Applied Biosystems, California, USA). Analyses of qRT-PCR data used the classic $(1 + E)^{-\Delta\Delta CT}$ method (C_T is the threshold cycles of one gene, E is the amplification efficiency). ΔCT is equal to the difference in threshold cycles for target (X) and reference (R) ($C_{T,X} - C_{T,R}$), while the $\Delta\Delta CT$ is equal to the difference of ΔCT for stage 1 (C) and the other stages (T) ($\Delta C_{T,T} - \Delta C_{T,C}$) for each variety. The amplification system (e.g., primer and template concentrations) was properly optimized, and the efficiency was close to 1. So the amount of target, normalized to an endogenous reference and relative to a calibrator, is given by: Amount of target = $2^{-\Delta\Delta CT}$. The qPCR products were separated on a 1.0% agarose gel and, then, were sequenced to confirm their identity using an automated DNA sequencer (ABI PRISM 3730xl, Perkin Elmer) from Macrogen Inc. (Seoul, Korea). Additionally, subsequent reactions for DNA melt curves were created for each primer combination to confirm the presence of a single product.

Statistical and Bioinformatics Analysis

For Principal Component Analysis (PCA), the complete dataset including all replicates was considered. The ratio of the signal relative to a reference consisting in a homogeneous mixture of all the samples was used, after log2 transformation. PCA was performed by means of the program SIMCA-P version 11 (Umetrics, Umea, Sweden) with Unit Variance normalization.

Pearson correlation coefficients were calculated with SPSS version 15.0 software (SPSS Inc., Chicago, USA) with the relative target quantity in samples based on the comparative C_T ($\Delta\Delta CT$) method of each gene and the log 2 transformed levels of the average ratio of each volatile/precursor metabolite for each variety and developmental stage. A Hierarchical Cluster Analysis (HCA) was performed with the resulting correlation values using the Acuity 4.0 program (Axon Instruments), with the distance measures based on Pearson correlation. Data from the correlation matrix were represented as a heatmap or correlation network by means of the Acuity 4.0 program.

Gene and metabolite data were transformed in linear fold change and Pearson correlation coefficients ($|\rho|$) were calculated using the PAST software (<http://folk.uio.no/ohammer/past/>). Subsequently, gene-metabolite correlation heat maps and matrices were built and colored using the GENE-E software (<http://www.broadinstitute.org/cancer/software/GENE-E/>). Finally, correlation networks were performed as previously described (Diretto et al., 2010).

RESULTS AND DISCUSSION

Volatile Profiling

Airén and Tempranillo, sourced from Castilla-La Mancha (Spain), represent important commercial varieties in this region. A study was carried out over a 2-year period to determine the evolution of the volatile fractions and also some of their precursors during grape development. In addition, we have tentatively associated some of the genes potentially involved in their formation expressions and the metabolites found in different stages of development in both varieties.

Many studies have sought to analyse and characterize wine VOCs in Tempranillo (Rosillo et al., 1999; Hermosín Gutiérrez, 2003; González et al., 2007; Izquierdo Cañas et al., 2008; López et al., 2008; Cynkar et al., 2010) and Airén (Gonzalez-Viñas et al., 1996; Pérez-Coello et al., 1999; Rosillo et al., 1999; Pérez-Coello et al., 2000; Castro Vázquez et al., 2002; Hernández-Orte et al., 2005). However, few studies have been dedicated to the aroma of grape juices in Tempranillo (González-Mas et al., 2009) or Airén (García et al., 2003).

There are clear and distinct aroma differences between grape cultivars, which are due to differences in their profile of volatile compounds. These variations are mostly attributed to differences in the levels of the substances that constitute the aroma of grape rather than to qualitative differences in the volatile compounds produced. Headspace solid phase microextraction (HS-SPME) technique was chosen for the acquisition of volatiles due to its high sensitivity and low manipulation required.

A total of 55 compounds were identified in the volatile fraction of both Airén and Tempranillo. Forty-eight of these metabolites were unequivocally identified by both mass spectra and retention index with those of authentic standards. For the other 7 compounds, a tentative identification based on their mass spectra similarity was proposed.

The volatiles identified are detailed in **Table 1**, which also shows the nature of the compounds detected in the 10 developmental stages analyzed for the two cultivars (Airén and Tempranillo) and their classification into different metabolic pathways: phenylpropanoids, terpenoids, lipid derivatives, branched-chain amino acid and other amino acid derivatives and norisoprenoids. Most of the VOCs shown in **Table 1** had been previously detected in these varieties (González-Mas et al., 2009; Cejudo-Bastante et al., 2011). The complete results obtained for the analysis of volatiles of all the samples are shown in Supplementary Table 2.

Principal Component Analysis (PCA) was performed in order to unravel the main features of the differences in volatile compounds among the samples. The score plot of the first two principal components, explaining 24.2 and 18.2% of the total variability respectively, separates the two varieties throughout the different stages based on their distinct volatile profiles. It can also be appreciated that there is a parallel evolution of the volatile levels during most of the developmental stages in both varieties, with the exception of the latest stages in Tempranillo, when a dramatic change is developed and a characteristic profile appears (**Figure 1**).

The volatile profile of Tempranillo was characterized by higher levels of branched-chain amino acid-derived compounds such as 3-methylbutanol, 2-methylbutanol, 2-methyl-2-propanol and 2-methyl-2-butanol, C₅ lipid derivatives pentanal, 1-pentanol, 1-penten-3-ol and (E)-2-pentenal, other lipid derivatives such as 1-hexanol, heptanal (only detected in this variety), (E)-2-heptenal, (E,E)-2,4-heptadienal, 1-octen-3-ol, (E)-2-octenal and (E)-2-nonenal, phenylpropanoids methyl salicylate, salicylaldehyde, benzylalcohol, phenylacetaldehyde, and 2-phenylethanol, which has been reported to be important in the flavor of Noble muscadine wine, and also other compounds such as 2-pentylfuran, acetaldehyde, ethyl ether, and ethyl acetate.

On the other hand, white variety Airén showed higher levels of norisoprenoids (β-damascenone, β-ionone, β-cyclocitral, and an unknown compound at 33.56 min with a norisoprenoid structure), monoterpenoids (linalool, terpineol and (Z)- and (E)-linalool oxide isomers), sesquiterpenes (ylangene and two unidentified compounds at 39.38 and 39.96 min only detected in this variety), C₆ lipid-derived aldehydes ((Z)-3-hexenal, (E)-2-hexenal and (E,E)-2,4-hexadienal) and also a few other compounds characteristic of early developmental stages (**Figure 2**).

Regarding the contribution to aroma of apocarotenoids, we know from the sensory work done that β-damascenone and β-ionone have a very low perception threshold. Thus, β-ionone confers intense fruity and floral aromas with violet notes (Silva Ferreira and Guedes De Pinho, 2004). The main characteristics of these volatile profiles, with minor variations, were consistent in the 2 years of sampling.

Lipid derivatives are generated by the enzymatic degradation of lipids when cellular tissue breakdown occurs (Baldwin et al., 1998), while their level in the intact fruit is minimal (Riley and Thompson, 1998). This applies, for example, to C₆ aldehydes (hexanal and (Z)-3-hexenal) responsible for the “green” flavor note, cut grass aroma and fruity notes of grapes (Vilanova et al., 2010). Hexanal and (Z)-3-hexenal are formed, respectively, from linoleic and linolenic acids, after the action of a lipoxygenase (LOX) followed by a hydroperoxide lyase (HPL) (Granell and Rambla, 2013). Hexanal and (Z)-3-hexenal can then be reduced to their corresponding alcohols, 1-hexanol and (Z)-3-hexenol, respectively, by the action of an alcohol dehydrogenase (ADH) (Galliard et al., 1977). The instability of (Z)-3-hexenal has been described in many papers (Buttery et al., 1987, 1988), and especially its broad isomerization to (E)-2-hexenal (Galliard et al., 1977; Buttery, 1993; Riley and Thompson, 1998; Gray et al., 1999).

Norisoprenoids are obtained from the degradation of carotenoids such as β-carotene or lycopene (Stevens, 1970; Simkin et al., 2004; Lewinsohn et al., 2005b). These reactions take place only in the fruit, and in some cases occur after cellular tissue breakdown. However, the biochemical nature of these degradative oxidation mechanisms, and the enzymes and genes involved should be reviewed in each case (Lewinsohn et al., 2005a).

Compounds which originate from amino acids can be subsequently converted into aldehydes, alcohols and esters, via

TABLE 1 | Volatile compounds detected in Tempranillo and Airén fruit juice.

ID	Compound	Identification	Compound nature	Metabolic pathway
1	Acetaldehyde	Unequivocal	Aldehyde	
2	Ethanol	Unequivocal	Alcohol	
3	Acetone	Unequivocal	Ketone	
4	2-propanol	Unequivocal	Alcohol	
5	Ethyl ether	Unequivocal	Ether	
6	2-methyl-2-propanol	Unequivocal	Alcohol	BAA?
7	Ethyl acetate	Unequivocal	Ester	
8	2-methyl-2-butanol	Unequivocal	Alcohol	BAA?
9	1-butanol	Unequivocal	Alcohol	
10	1-penten-3-ol	Unequivocal	Alcohol	L
11	Pentanal	Unequivocal	Aldehyde	L
12	2-ethylfuran	Unequivocal	Furan	L?
13	3-methylbutanol	Unequivocal	Alcohol	BAA
14	2-methylbutanol	Unequivocal	Alcohol	BAA
15	(E)-2-pentenal	Unequivocal	Aldehyde	L
16	1-pentanol	Unequivocal	Alcohol	L
17	(Z)-3-hexenal	Unequivocal	Aldehyde	L
18	Hexanal	Unequivocal	Aldehyde	L
19	(E)-2-hexenal	Unequivocal	Aldehyde	L
20	(E)-2-hexen-1-ol	Unequivocal	Alcohol	L
21	1-hexanol	Unequivocal	Alcohol	L
22	Heptanal	Unequivocal	Aldehyde	L
23	(E,E)-2,4-hexadienal	Unequivocal	Aldehyde	L
24	(E)-2-heptenal	Unequivocal	Aldehyde	L
25	1-octen-3-ol	Unequivocal	Alcohol	L
26	2-pentyfuran	Unequivocal	Furan	L?
27	2-octanol	Unequivocal	Alcohol	L
28	(E,E)-2,4-heptadienal	Unequivocal	Aldehyde	L
29	Limonene	Unequivocal	Monoterpene	T
30	Benzylalcohol	unequivocal	Alcohol/phenolic	Ph
31	Unknown 25.22 (furan)	Tentative	Furan	
32	Phenylacetaldehyde	Unequivocal	Aldehyde/phenolic	AA
33	(E)-2-octenal	Unequivocal	Aldehyde	L
34	Salicylaldehyde	Unequivocal	Aldehyde/phenolic	Ph
35	1-octanol	Unequivocal	Alcohol	L
36	(Z)-linalool oxide	Unequivocal	Monoterpoid	T
37	(E)-linalool oxide	Unequivocal	Monoterpoid	T
38	2-ethylhexanoic acid	Unequivocal	Organic acid	
39	Linalool	Unequivocal	Monoterpoid	T
40	2-phenylethanol	Unequivocal	Alcohol/phenolic	AA
41	(E)-2-nonenal	Unequivocal	Aldehyde	L
42	3-ethylbenzaldehyde	Unequivocal	Aldehyde/phenolic	Ph?
43	2-ethylbenzaldehyde	Unequivocal	Aldehyde/phenolic	Ph?
44	Terpineol	Unequivocal	Monoterpoid	T
45	Methyl salicylate	Unequivocal	Ester/phenolic	Ph
46	β-cyclocitral	Unequivocal	Norisoprenoid	C
47	Nonanoic acid	Unequivocal	Organic acid	L
48	Unkown 33.56 (apocarotenoid)	Tentative	Norisoprenoid	C
49	2, 6-diisocyanatotoluene	Tentative	Phenolic	
50	beta-damascenone	Unequivocal	Norisoprenoid	C

(Continued)

TABLE 1 | Continued

ID	Compound	Identification	Compound nature	Metabolic pathway
51	Ylangene	Tentative	Sesquiterpene	T
52	β -ionone	Unequivocal	Norisoprenoid	C
53	Unknown 39.38 (sesquiterpene)	Tentative	Sesquiterpene	T
54	1-(2,3,6-trimethylphenyl)-3-buten-2-one	Tentative	Ketone/phenolic	
55	Unknown 39.96 (sesquiterpene)	Tentative	Sesquiterpene	T

BAA, branched-amino acid derivative; L, lipid derivative; Ph, phenylpropanoid; AA, other amino acid derivatives; T, terpenoid; C, apocarotenoid. A question mark indicates some degree of uncertainty about the metabolic pathway.

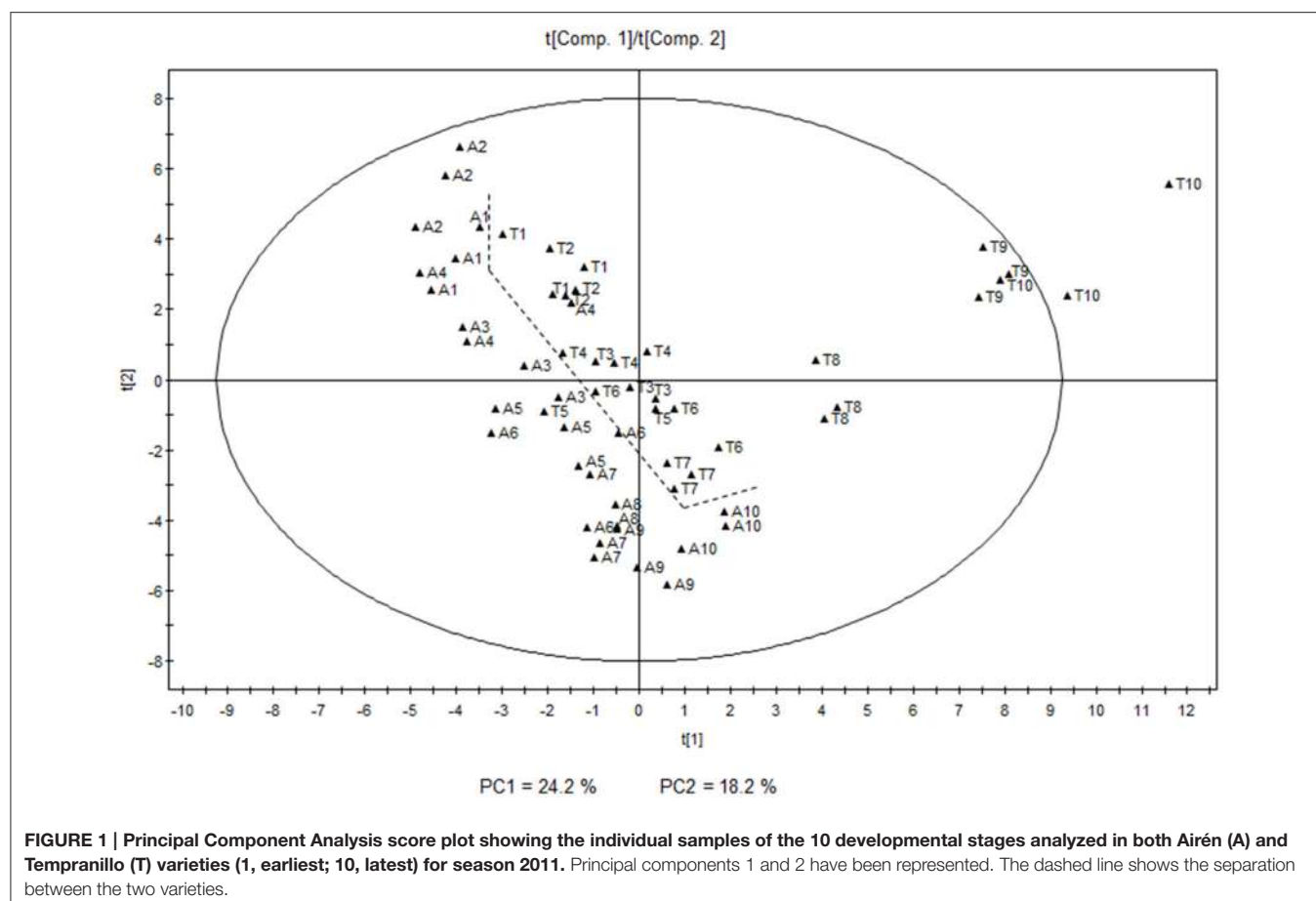


FIGURE 1 | Principal Component Analysis score plot showing the individual samples of the 10 developmental stages analyzed in both Airén (A) and Tempranillo (T) varieties (1, earliest; 10, latest) for season 2011. Principal components 1 and 2 have been represented. The dashed line shows the separation between the two varieties.

various steps including deamination, decarboxylation, reduction and esterification (Crouzett, 1992). Phenylpropanoid volatile compounds such as 2-phenylethanol, methyl salicylate, or benzaldehyde are primarily derived from phenylalanine. The synthesis of some of these compounds requires the shortening of the carbon skeleton side chain by a C₂ unit, which can potentially occur via either the β -oxidative pathway or non-oxidatively (Dudareva et al., 2004; Orlova et al., 2006; Pichersky et al., 2006).

C₆ aldehydes are partially responsible for the green, herbaceous and sometimes bitter aromas of wine. Volatile phenolic compounds such as phenylacetaldehyde figure as one of the substances responsible for the hyacinth and rose-like odor described in the French-Romanian Admira grape variety (Wang

and Kays, 2000), while terpenoid and norisoprenoid compounds are responsible for the floral and fruity aroma of wine made from these varieties.

As previously mentioned, a clear evolution in the volatile profile throughout grape development was also observed. This was markedly parallel in both varieties, except for the last ripening stages in Tempranillo, where a dramatic change was detected between stages 7 and 8–10. The score plot shows the existence of four different stages for both cultivars corresponding to immature, unripe, ripe and overripe. Higher levels of carotenoid derivatives were characteristic of the earlier stages of development in both varieties with higher levels of some apocarotenoids such as β -cyclocitral

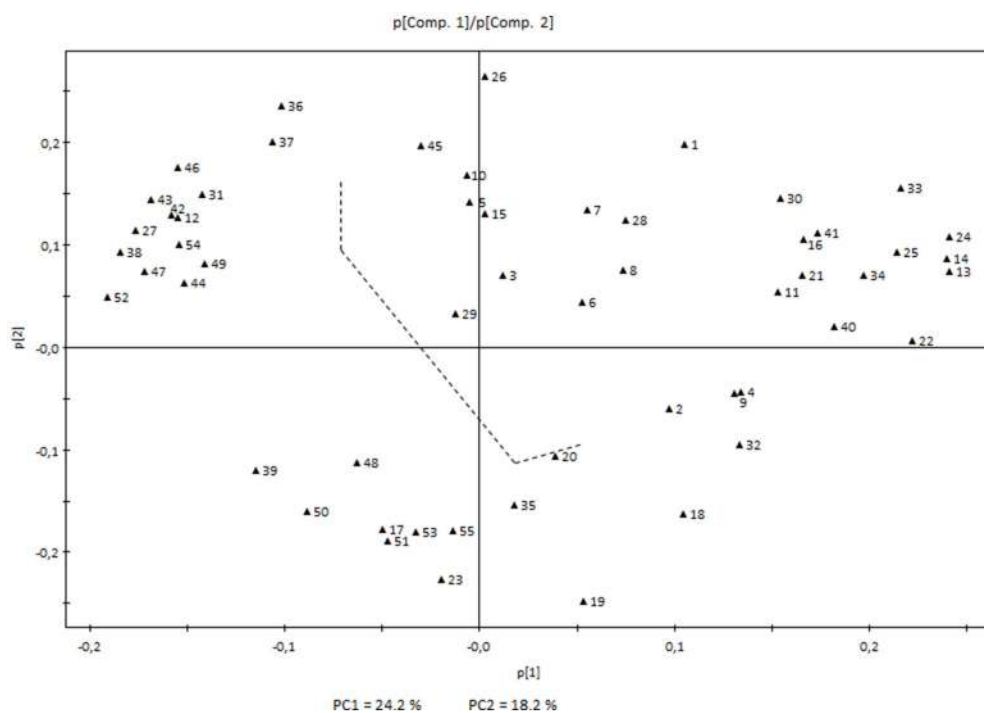


FIGURE 2 | Principal Component Analysis loading plot showing the volatile compounds determining the first two principal components. The two components represented and the dashed line correspond to those in the score plot (Figure 1). Each number corresponds to a volatile compound as indicated in Table 1 and Supplementary Table 2.

or β -ionone, and monoterpenoids (E)-linalool oxide, (Z)-linalool oxide, and terpineol. Higher levels of other compounds such as 2-ethylbenzaldehyde, 3-ethylbenzaldehyde, 1-(2,3,6-trimethylphenyl)-3-buten-2-one, 2-octanol, and 2-ethylhexanoic acid were also characteristic in these stages. Carotenoids may undergo breakdown reactions that generate C₁₃ norisoprenoid compounds involved in the typical aromas of some grapevine cultivars (Baumes et al., 2002). Apocarotenoids are mostly generated by the cleavage of a carotenoid molecule by enzymes of the CCD family.

In the last stages of development in Tempranillo (T8-T10), a dramatic change in the volatile profile was observed, characterized by a significant increase in the levels of branched-chain amino acid-derived alcohols 3-methylbutanol and 2-methylbutanol, a set of lipid-derived aldehydes ((E)-2-heptenal, (E)-2-octenal, (E)-2-nonenal, heptanal, and pentanal) and alcohols (1-octen-3-ol, 1-hexanol, and 1-pentanol), and some phenylpropanoid compounds (salicylaldehyde, benzyl alcohol, and 2-phenylethanol).

The last stages of development were not characterized by such a dramatic change in Airén volatiles; although a significant increase in lipid-derived compounds such as hexanal, (E)-2-hexenal, (E)-2-hexen-1-ol, and 1-octanol was observed (Figure 2).

Volatile Precursors Profiling

In order to search for possible volatile precursors, we carried out LC-HRMS analyses of the non-volatile fractions (both polar and

non-polar by, respectively, ESI- and APCI-MS) in both varieties. A total of 56 compounds were identified in the Airén and Tempranillo samples, belonging to different metabolic pathways. Forty-eight of these metabolites were unequivocally identified by retention index and maximal absorption wavelength with those of authentic standards. Eight compounds were annotated as unknown from which 6 were carotenoids and 2 were chlorophylls (Tables 2A,B).

A strong relationship has been reported between the amino acid profile of grape varieties and the relative levels of the higher alcohols in wine and therefore the final aroma in wine (Hernández-Orte et al., 2002). The four amino acids detected in Airén and Tempranillo varieties were isoleucine, leucine, valine, and phenylalanine. Phenylalanine was the most abundant amino acid in grapes from both cultivars. This aromatic amino acid has been reported to produce aromatic alcohols such as 2-phenylethanol (Rossouw et al., 2009), which has a characteristic honey/spice/rose/lilac aroma (Francis and Newton, 2005) and is considered to play an important role in white wine aroma (López et al., 2003). Different accumulation patterns were observed in red and white varieties. In Tempranillo, higher levels were detected at T8 stage for isoleucine, leucine and valine, while phenylalanine had its maximum accumulation at T3 stage, whereas in Airén, isoleucine and phenylalanine were higher at the earlier stages of maturation decreasing later on, and leucine and valine were abundant in both earlier and latest stages. These patterns were in agreement with those obtained by (Garde-CerdáN et al., 2009) where higher accumulation at the end of

TABLE 2A | Volatile precursors detected in Airén throughout maturation stages.

Metabolites	λ_{max}	RT	A1	A2	A3	A4	A5	A6	A7	A8	A9	A10
AMINO ACIDS												
Isoleucine		1.29	0.0171	0.0166	0.0036	0.0096	0.0094	0.0065	0.0116	0.0036	0.0061	0.0103
Leucine		1.82	0.0327	0.0378	0.0140	0.0313	0.0369	0.0296	0.0404	0.0175	0.0300	0.0453
Phenylalanine*		2.77	0.0624	0.1002	0.0688	0.2004	0.1131	0.0722	0.1144	0.0628	0.0753	0.1733
Valine		1.25	0.0138	0.0134	0.0034	0.0089	0.0090	0.0092	0.0056	0.0054	0.0091	0.0132
LIPIDS												
Linoleic Acid		0.90	0.0064	0.0037	0.0059	0.0051	0.0072	0.0044	0.0060	0.0053	0.0032	0.0041
Linolenic Acid		0.70	0.0452	0.0464	0.0559	0.0426	0.0284	0.0313	0.0235	0.0215	0.0159	0.0258
CAROTENOIDS												
Unknown carotenoid (1)	(375) 400, 421, 441	1.15	0.0604	0.0131	0.0006	0.0022	NF	NF	NF	NF	NF	NF
Unknown carotenoid (2)	(375) 400, 421, 441	1.34	0.0944	0.0877	0.0001	0.0017	NF	NF	NF	NF	NF	NF
Unknown carotenoid (3)	398, 422, 444	1.52	0.0213	0.0095	0.0016	NF	0.0005	NF	NF	0.0004	NF	NF
Unknown carotenoid (4)	421, 444, 470	1.70	0.1252	0.0093	NF	0.0023	NF	NF	NF	NF	NF	NF
Unknown carotenoid (5)	(375) 400, 421, 441	1.83	0.0843	0.0335	0.0000	0.0008	0.0023	NF	NF	NF	NF	NF
Neochrome-like structure	400, 421, 445	2.00	0.0364	0.0100	0.0015	NF	NF	0.0005	0.0091	0.0008	NF	0.0001
Neochrome a	401, 419, 446	2.27	0.0334	0.0144	0.0044	0.0113	0.0009	0.0016	NF	0.0021	0.0010	0.0016
Neoxanthin	420, 440, 466	2.40	NF									
Neochrome b	402, 421, 447	2.63	0.0062	0.0071	0.0054	0.0177	NF	NF	0.0055	0.0041	0.0016	0.0035
Luteoxanthin isomer	402, 421, 447	2.84	0.0115	0.0269	0.0106	0.0201	0.0044	0.0046	0.0209	0.0087	0.0053	NF
All-trans-violaxanthin	416, 442, 463	2.87	NF									
9-cis-violaxanthin	438, 462	2.91	NF	NF	NF	NF	0.0148	0.0431	0.0050	0.0010	0.0096	0.0166
Luteoxanthin	421, 444, 465	3.05	NF									
Auroxanthin	403, 425, 444	3.13	0.0033	0.0054	0.0023	0.0047	0.0020	0.0315	0.0072	0.0003	0.0018	0.0051
Flavoxanthin	(375), 402, 423, 446	3.47	0.0115	0.0068	0.0028	0.0510	NF	0.0132	0.0200	0.0048	0.0006	0.0015
All-trans-lutein	445, 472	4.09	0.3771	0.9528	1.1306	0.9413	0.1485	0.5769	0.6059	0.1842	0.2535	0.1136
Zeaxanthin	450, 476	4.77	0.4398	0.2700	0.2641	0.0000	0.0786	0.0656	0.1452	NF	0.1565	0.0739
13Z or 13Z' lutein	442, 468	4.87	NF	0.0128	0.0091	0.0601	0.0046	0.0060	0.0022	0.0775	0.0072	0.0066
9Z or 9Z' lutein	438, 467	4.98	NF	NF	NF	0.0022	NF	NF	0.0020	0.0026	0.0007	0.0013
Lutein-like structure	424, 446, 473	5.14	0.0605	0.0695	NF							
9Z or 9Z' lutein-like structure	440, 468	5.45	NF	NF	0.0120	0.0821	0.0107	0.0143	0.0241	0.0276	0.0209	0.0053
Lutein-like structure	424, 446, 473	5.50	0.2215	0.2220	0.0288	0.0249	0.0238	NF	0.0472	NF	0.0154	0.0059
5, 8-epoxy- β -carotene	406, 426, 450	6.29	0.0639	0.0879	0.0225	0.0762	0.0179	0.0180	0.0115	NF	NF	0.0119
All-trans- α -carotene	444, 470	6.42	0.0349	0.0495	0.0117	0.0373	0.0224	0.0142	0.0038	0.0153	0.0123	0.0167
All-trans- β -carotene	452, 477	7.01	0.1263	0.3116	0.3068	0.2428	0.0698	0.1008	0.2784	0.0908	0.1184	0.0616
9-cis- β -carotene	423, 447, 473	7.13	0.0655	0.0991	0.0762	0.0660	0.0250	0.0230	0.0478	0.0208	0.0365	0.0275
Unknown carotenoid (6)	422, 446	7.75	0.0056	0.0100	0.0101	NF	NF	NF	0.0091	NF	NF	NF
All-trans- δ -carotene	453	8.02	0.0572	0.0295	0.0046	NF	NF	NF	0.0110	NF	NF	NF
TOTAL			1.9402	2.3385	1.9058	1.6446	0.4263	0.9134	1.2561	0.4412	0.6413	0.3528
CHLOROPHYLLS												
Pyropheophorbide b	436, 655	2.08	NF									
Pyropheophorbide a	410, 665	2.22	0.0010	NF	0.0003							
Chlorophyll b	469, 651	3.73	NF	NF	NF	NF	0.1866	0.0530	0.1466	NF	0.1687	0.2337
Chlorophyll a	432, 665	5.05	NF									
Unknown chlorophyll derivative (1)	401	5.64	0.3015	0.4567	0.0850	0.0805	0.0445	NF	0.0940	NF	0.0024	NF
Unknown chlorophyll derivative (2)	402	6.04	0.0222	0.0080	0.0050	0.0048	0.0031	0.0055	0.0117	0.0065	0.0038	NF
Pheophytin a-like (1)	410	6.12	0.1240	0.0854	0.0589	0.0047	NF	NF	NF	NF	NF	NF
Pheophytin a-like (2)	415, 445, 665	6.39	0.0168	0.0135	0.0141	0.0066	NF	0.0015	0.0045	0.0011	NF	0.0007

(Continued)

TABLE 2A | Continued

Metabolites	λ_{max}	RT	A1	A2	A3	A4	A5	A6	A7	A8	A9	A10
Pheophytin b-like	419, 436, 656	6.52	0.0286	0.0107	0.0048	0.0059	NF	NF	0.0071	0.0139	NF	NF
Pheophytin b	432, 654	6.89	0.5318	0.8759	0.4672	0.7853	0.0533	0.1730	0.2664	0.3316	0.1672	0.1702
Pheophytin a	408, 666	6.91	0.6346	0.9565	0.1426	0.1744	0.1006	0.1075	0.2378	0.3304	0.0841	0.0347
TOTAL			1.6604	2.4068	0.7776	1.0622	0.3881	0.3406	0.7681	0.6835	0.4262	0.4396
OTHERS												
α -tocopherol	290	2.74	1.0555	4.4248	3.1581	6.5971	2.0164	0.9774	3.6324	1.0689	1.9921	0.7909
Ubiquinone	296	5.89	9.3522	7.8888	4.0349	4.9211	2.6044	1.6224	6.2746	3.6986	5.0433	2.7090
Unknown	255	6.28	5.0114	12.8318	1.0207	10.8884	27.9940	5.7073	5.4368	4.9682	22.1602	4.9485
TOTAL			15.4192	25.1455	8.2137	22.4066	32.6148	8.3071	15.3438	9.7357	29.1956	8.4484
PHENYLPROPANOIDES												
Benzoic acid		10.84	0.0033	0.0054	0.0005	0.0005	0.0007	0.0005	0.0005	0.0001	0.0003	0.0002
Caffeic acid		7.36	0.0001	0.0001	NF							
Cinnamic acid		13.45	0.0001	0.0002	0.0002	0.0005	0.0003	0.0002	0.0003	0.0002	0.0002	0.0005
Coniferyl acetate		18.20	0.0005	0.0005	0.0005	0.0006	0.0005	0.0007	0.0264	0.0016	0.0008	0.0010
Coniferyl alcohol		0.72	0.0009	0.0008	0.0004	0.0004	0.0004	0.0004	0.0005	0.0004	0.0003	0.0004
Coniferyl aldehyde		10.56	0.0005	0.0005	NF							
Coumaric acid		8.86	0.0040	0.0040	0.0012	0.0011	0.0017	0.0018	0.0022	0.0015	0.0017	0.0020
Ferulic acid		10.59	0.0002	0.0003	NF							
Hydroxyconiferyl alcohol		6.56	0.0002	0.0002	NF	NF	NF	NF	0.0002	NF	NF	NF
Sinapyl alcohol		0.80	NF									
TERPENES												
α -terpinol-[xylosyl-(1->6)-glucoside]		7.25	0.0005	0.0002	0.0001	0.0001	0.0001	0.0001	0.0003	0.0001	0.0001	0.0002
α -terpinol-beta-d-glucoside		9.00	0.0002	0.0001	NF							
L-Linalool 3-[xylosyl-(1->6)-glucoside]		9.76	0.0012	0.0010	0.0003	0.0002	0.0002	0.0002	0.0005	0.0002	0.0001	0.0003
Limonene-arabinofuranose		11.83	0.0001	0.0002	0.0001	0.0002	0.0001	0.0001	0.0002	0.0002	0.0001	0.0002
Limonene-arabinofuranose-glucoside		15.62	0.0000	0.0000	0.0000	0.0001	NF	0.0000	0.0001	0.0001	0.0000	0.0001
Linalool-arabinofuranose		10.09	0.0001	0.0001	NF							
Linalyl-beta-d-glucoside		9.20	0.0004	0.0003	NF							
E-/Z-linalool oxide-arabinofuranose1**		9.00	0.0010	0.0006	NF							
E-/Z-linalool oxide-arabinofuranose2**		11.78	0.0001	0.0001	NF							
E-/Z-linalool oxide-arabinofuranose-glucoside1**		9.71	0.0013	0.0010	0.0003	0.0002	0.0002	0.0002	0.0004	0.0001	0.0001	0.0003
E-/Z-linalool oxide-arabinofuranose-glucoside2**		10.09	0.0007	0.0006	0.0001	0.0001	0.0001	0.0001	0.0003	0.0001	0.0000	0.0001
E-/Z-linalool oxide-glucoside1**		7.80	0.0002	0.0002	NF		NF	NF	0.0001	NF	NF	0.0001
E-/Z-linalool oxide-glucoside2**		9.00	0.0002	0.0001	NF							
E-/Z-linalool oxide-rhamnopyranose1**		8.10	0.0004	0.0003	NF	0.0000	NF	NF	NF	NF	NF	NF
E-/Z-linalool oxide-rhamnopyranose2**		9.50	0.0002	0.0001	NF							

(Continued)

TABLE 2A | Continued

Metabolites	λ_{max}	RT	A1	A2	A3	A4	A5	A6	A7	A8	A9	A10
E-/Z-linalool oxide-Rhamnopyranoside-glucoside**		12.08	0.0001	0.0002	0.0001	NF	0.0001	0.0000	0.0001	NF	NF	NF
E-/Z-linalool oxide-Rhamnopyranoside-glucoside2**		12.65	0.0000	0.0000	0.0000	NF	0.0000	0.0000	0.0000	NF	NF	0.0000

Isoprenoids (carotenoids, chlorophylls, ubiquinone, and α -tocopherol) were identified and quantified by LC-DAD-APCI-MS and data are expressed as $\mu\text{g}/\text{mg}$ DW. Other metabolite precursors were detected and relatively quantified by LC-APCI-MS (lipids) and LC-ESI-MS (amino acids, phenylpropanoids, terpene glucosides) and data are expressed as fold on the internal standard level (APCI, α -tocopherol acetate; ESI, formononetin). For more details, see materials and methods.

*Also involved in phenylpropanoid-derived volatiles.

**Not possible discriminating the E- and Z-isomers.

ripening of amino acids were found in red varieties (Monastrell organic, Syrah, and Merlot grapes), whereas in the white grape Petit Verdot it diminished at the same stage.

The C₆ aldehydes and alcohols derived from fatty acids constitute the major aroma derivatives responsible for the “green” aroma and are generally formed by the action of lipoxygenase (LOX), hydroperoxide lyase (HPL), (3Z)-(2E) enal isomerase, and alcohol dehydrogenase (ADH) enzymes when the grape is crushed (Baldwin, 2002; Schwab et al., 2008). Lipidic precursors linoleic and linolenic acids were detected in all the samples. Linoleic acid was detected at very low levels in Airén, while its levels in Tempranillo were about 25-fold higher. Linolenic acid was more abundant than linoleic acid in both varieties, and its levels were slightly higher in Tempranillo. In Airén, both fatty acids showed their higher levels in earlier stages, decreasing thereafter. A different pattern was observed in Tempranillo, with a sharp increase at stage T8, particularly dramatic in the case of linolenic acid. It is known that the phenolic content of grape is dependent on grape variety and maturity but is also influenced by variations in water and nutrient availability, light and temperature environment, and changes in predation and disease stresses (Downey et al., 2006; Cohen and Kennedy, 2010; Robinson et al., 2014). Phenylpropanoid precursors levels were found to be higher in Tempranillo than in Airén. In both varieties, benzoic acid and coumaric acid were found to be the predominant phenolic acids and were detected at the earlier stages. Benzoic acid is the precursor of several common hydroxybenzoic acids usually found in wine, such as gallic acid, gentisic acid, p-hydroxybenzoic acid, protocatechuic acid (3,4-dihydroxybenzoic acid), syringic acid, salicylic acid and vanillic acid (Peña et al., 2000; Pozo-Bayón et al., 2003; Monagas et al., 2005), whereas coumaric acid is a polyphenol precursor, especially for flavonoids, flavones and flavonols (Hrazdina et al., 1984). The latter acid is equally a crucial substrate for enzymes to create resveratrol (Goldberg et al., 1998). Sinapyl alcohol, one of the substrates necessary for the polymerization reactions that produce lignin, was only detected in Tempranillo, while caffeic acid was only found in Airén. The majority of phenylpropanoid precursors have a double sigmoid curve accumulation pattern with higher contents at the earlier and latest stages, a patterns which had been found for a variety of Semillon as well as for the flesh of Muscat Gordo Blanco berries (Francis et al., 1992).

Despite the diverse range of structures that have been isolated from natural sources, few carotenoids have been detected in grapes, 85% of the total carotenoids are β -carotene and lutein, with neochrome, neoxanthin, violaxanthin, luteoxanthin, flavoxanthin, lutein-5,6-epoxide and zeaxanthin, cis isomers of lutein and α -carotene the next most abundant (Mendes-Pinto, 2009). In both varieties, the carotenoids precursors were detected mainly at the earlier stages, with some exception where the metabolites were detected in all stages as all-trans lutein. Some of these metabolites were variety specific as the unknown carotenoid (2), all-tran- α -carotene, zeaxanthin and neochrome which were detected only in Airén, whereas neoxanthin, all-trans-violaxanthin and luteoxanthin were identified in Tempranillo. The concentration of some of these metabolites was higher in one of the varieties than the other; this is the case of the unknown carotenoid (4), which appears to be 4-fold higher in the red cultivar. Our data are in concordance with numerous studies on the evolution of carotenoids during grape development that pointed out that levels of β -carotene, lutein, flavoxanthin, and neoxanthin decrease drastically after veraison until maturation (Razungles et al., 1996; Bureau et al., 1998; Yuan and Qian, 2016). Processes of bioconversion of these compounds into others have been reported as, for example, the formation of violaxanthin from β -carotene as a consequence of the activation of the xanthophylls cycle at the end of maturation (Düring, 1999). Violaxanthin, lutein 5,6-epoxide and luteoxanthin only appear when higher concentration of sugar is reached, while neochrome is characteristic of green grapes (Guedes De Pinho et al., 2001; Grimplet et al., 2007; Deluc et al., 2009).

Regarding chlorophyll metabolites, chlorophyll a was absent under our analysis conditions, which could be due to the coefficient response of chlorophyll a, which is 4 times lower than the coefficient response of chlorophyll b, whereas pyropheophorbide b was only detected in Tempranillo. Higher concentrations of chlorophyll metabolites were detected in Tempranillo than in Airén. Chlorophyll-derived compounds are degraded more quickly than lutein or α -carotene. No chlorophyll-derived compounds are present in wines; grapes with a high content of these compounds are transformed into wines with a higher aromatic complexity (Winterhalter and Rouseff, 2002; Mendes-Pinto et al., 2005).

TABLE 2B | Volatile precursors detected in Tempranillo throughout maturation stages.

Metabolites	λ_{max}	RT	T1	T2	T3	T4	T5	T6	T7	T8	T9	T10
AMINO ACIDS												
Isoleucine			0.0054	0.0045	0.0128	0.0016	0.0083	0.0033	0.0020	0.0228	0.0104	0.0032
Leucine			0.0167	0.0173	0.0519	0.0072	0.0443	0.0175	0.0102	0.1005	0.0596	0.0153
Phenylalanine*			0.0478	0.0578	0.1588	0.0255	0.1013	0.0457	0.0404	0.1215	0.1178	0.0368
Valine			0.0128	0.0097	0.0230	0.0039	0.0138	0.0066	0.0039	0.0364	0.0220	0.0059
LIPIDS												
Linoleic Acid			0.0098	0.0089	0.0086	0.0057	0.0056	0.0076	0.0076	0.0112	0.0064	0.0056
Linolenic Acid			0.0444	0.0850	0.0767	0.0286	0.0822	0.0232	0.0344	0.4349	0.0582	0.0372
CAROTENOIDS												
Unknown carotenoid (1)	(375) 400, 421, 441	1.15	0.0786	0.0457	0.1030	NF						
Unknown carotenoid (2)	(375) 400, 421, 441	1.34	NF	NF	NF	NF	NF	NF	NF	NF	NF	NF
Unknown carotenoid (3)	398, 422, 444	1.52	0.0561	0.0595	0.0569	0.0244	0.0188	0.0131	0.0064	NF	NF	NF
Unknown carotenoid (4)	421, 444, 470	1.70	0.0175	NF	NF	NF	NF	NF	NF	NF	NF	NF
Unknown carotenoid (5)	(375) 400, 421, 441	1.83	NF	NF	0.0300	0.0284	0.0182	0.0165	0.0049	NF	0.1232	NF
Neochrome-like structure	400, 421, 445	2.00	0.1990	NF	NF	NF	NF	NF	NF	0.0189	0.1600	NF
Neochrome a	401, 419, 446	2.27	NF	NF	NF	NF	NF	NF	NF	NF	NF	NF
Neoxanthin	420, 440, 466	2.40	NF	NF	NF	NF	NF	NF	0.1006	NF	0.1230	NF
Neochrome b	402, 421, 447	2.63	0.0867	0.0686	0.0503	NF	NF	NF	NF	NF	0.0115	0.0709
Luteoxanthin isomer	402, 421, 447	2.84	0.3063	0.2396	0.0970	0.3509	0.0790	NF	NF	NF	0.0689	NF
All-trans-violaxanthin	416, 442, 463	2.87	NF	NF	NF	NF	NF	0.2267	0.2435	NF	NF	NF
9-cis-violaxanthin	438, 462	2.91	NF	0.1184	NF	NF	NF	0.1511	NF	NF	NF	NF
Luteoxanthin	421, 444, 465	3.05	NF	NF	0.0299	0.0247	0.0137	0.0554	0.1522	NF	0.3048	1.2015
Auroxanthin	403, 425, 444	3.13	0.3277	0.1742	0.0646	NF	NF	NF	NF	0.0619	0.1520	NF
Flavoxanthin	(375), 402, 423, 446	3.47	0.7499	0.2313	0.1284	NF	NF	NF	NF	0.1691	0.1482	NF
All-trans-lutein	445, 472	4.09	9.9916	7.6905	4.9760	4.4097	2.2627	2.9679	2.8582	1.9456	2.6001	2.7767
Zeaxanthin	450, 476	4.77	NF	NF	NF	NF	NF	NF	NF	NF	NF	NF
13Z or 13Z' lutein	442, 468	4.87	0.9707	0.2728	0.1881	0.4108	0.0538	0.2203	NF	0.1092	0.1751	1.0202
9Z or 9Z' lutein	438, 467	4.98	0.0866	0.1354	0.2069	0.0162	NF	0.1210	NF	NF	NF	NF
Lutein-like structure	424, 446, 473	5.14	0.0352	NF	NF	NF	NF	NF	NF	NF	NF	NF
9Z or 9Z' lutein-like structure	440, 468	5.45	0.5244	0.6207	0.7687	0.6037	0.2918	0.1278	0.1456	0.2171	0.3323	0.5097
Lutein-like structure	424, 446, 473	5.50	0.3054	NF	NF	NF	NF	NF	NF	NF	NF	NF
5,8-epoxy- β -carotene	406, 426, 450	6.29	0.9041	0.5826	0.5256	0.3810	0.0945	0.2507	0.1520	0.1829	0.1075	NF
All-trans- α -carotene	444, 470	6.42	NF	NF	NF	NF	NF	NF	NF	NF	NF	NF
All-trans- β -carotene	452, 477	7.01	4.9373	3.8749	0.6841	1.4960	0.8937	1.3463	1.5620	0.9064	0.9788	0.2520
9-cis- β -carotene	423, 447, 473	7.13	1.7399	1.1741	0.6765	0.5374	0.2493	0.3821	0.3580	0.2368	0.3233	NF
Unknown carotenoid (6)	422, 446	7.75	0.0771	0.0364	0.0296	NF						
All-trans- δ -carotene	453	8.02	0.0279	0.0426	0.0164	NF						
TOTAL			21.4219	15.3672	8.6320	8.2832	3.9756	5.8788	5.5834	3.8481	5.6087	5.8310
CHLOROPHYLLS												
Pyropheophorbide b	436, 655	2.08	NF	NF	NF	NF	NF	NF	NF	0.0192	NF	NF
Pyropheophorbide a	410, 665	2.22	NF	NF	NF	NF	NF	NF	NF	0.0276	0.0912	NF
Chlorophyll b	469, 651	3.73	NF	2.6581	NF	2.7103	0.9423	3.1888	3.6151	NF	1.0158	2.2874
Chlorophyll a	432, 665	5.05	NF	NF	NF	NF	NF	0.0474	0.4265	NF	NF	NF
Unknown chlorophyll derivative (1)	401	5.64	1.0691	0.2496	0.3093	NF	NF	NF	0.0205	NF	NF	NF
Unknown chlorophyll derivative (2)	402	6.04	0.1963	0.0974	0.1222	NF	NF	NF	0.0186	0.0705	0.0444	NF
Pheophytin a-like (1)	410	6.12	0.1168	0.0516	0.1256	NF	0.0577	NF	NF	0.0256	0.0258	0.0198
Pheophytin a-like (2)	415, 445, 665	6.39	0.0698	NF	0.0585	NF	0.0390	NF	NF	NF	NF	NF

(Continued)

TABLE 2B | Continued

Metabolites	λ_{max}	RT	A1	A2	A3	A4	A5	A6	A7	A8	A9	A10
Pheophytin b-like	419, 436, 656	6.52	0.8094	0.4350	0.8440	0.2006	0.1131	NF	NF	0.2263	0.1325	NF
Pheophytin b	432, 654	6.89	14.1734	7.8599	11.3427	3.8593	3.0228	0.4781	0.4265	2.3711	3.3644	1.4385
Pheophytin a	408, 666	6.91	5.3704	3.2120	3.4230	2.0915	1.0261	1.0585	0.7032	0.6567	1.1197	0.5704
TOTAL			21.8052	14.5636	16.2253	8.8616	5.2010	4.7727	5.2103	3.3968	5.7939	4.3161
OTHERS												
α-tocopherol	290	2.74	45.1689	28.6563	12.3871	22.0931	13.4224	21.0568	19.4971	19.3449	25.3264	11.9777
Ubiquinone	296	5.89	27.9983	25.4948	18.1442	8.6920	NF	21.2234	13.5892	6.9020	19.9027	NF
Unknown	255	6.28	119.4096	NF	93.9746	NF	NF	NF	NF	54.0751	NF	NF
TOTAL			192.5768	54.1511	124.5060	30.7851	13.4224	42.2802	33.0863	80.3219	45.2291	11.9777
PHENYLPROPANOIDES												
Benzoic acid			0.0095	0.0053	0.0034	0.0006	0.0002	0.0002	0.0002	0.0001	0.0001	0.0001
Caffeic acid			NF									
Cinnamic acid			0.0001	0.0001	0.0005	0.0001	0.0003	0.0001	0.0001	0.0004	0.0004	0.0001
Coniferyl acetate			0.0008	0.0006	0.0006	0.0006	0.0006	0.0007	0.0007	0.0006	0.0006	0.0005
Coniferyl alcohol			0.0006	0.0003	0.0003	0.0001	NF	0.0004	NF	NF	NF	NF
Coniferyl aldehyde			0.0016	0.0007	0.0002	0.0003	0.0001	0.0004	0.0003	0.0001	NF	NF
Coumaric acid			0.0040	0.0030	0.0021	0.0017	0.0012	0.0013	0.0009	0.0014	0.0012	0.0010
Ferulic acid			0.0018	0.0009	NF	0.0003	NF	NF	NF	NF	NF	NF
Hydroxyconiferyl alcohol			0.0003	0.0002	0.0001	0.0001	0.0001	0.0001	0.0001	0.0001	NF	NF
Sinapyl alcohol			0.0007	0.0003	NF	0.0001	NF	NF	0.0002	NF	NF	NF
TERPENES												
α-terpinol-[xylosyl-(1->6)-glucoside]			0.0003	0.0002	0.0001	0.0002	0.0001	0.0002	0.0002	0.0001	0.0002	0.0002
α-terpinol-beta-d-glucoside			NF									
L-Linalool 3-[xylosyl-(1->6)-glucoside]			0.0003	0.0002	0.0001	0.0000	0.0000	0.0002	0.0000	0.0000	0.0000	0.0000
Limonene-arabinofuranose			0.0000	0.0002	0.0001	0.0001	0.0001	0.0001	0.0003	0.0002	0.0001	0.0002
Limonene-arabinofuranose-glucoside			NF									
Linalool-arabinofuranose			NF									
Linalyl-beta-d-glucoside			NF									
E-/Z-linalool oxide-arabinofuranose1**			0.0007	0.0004	NF							
E-/Z-linalool oxide-arabinofuranose2**			0.0002	0.0002	NF							
E-/Z-linalool oxide-arabinofuranose-glucoside1**			0.0004	0.0002	0.0001	0.0001	0.0000	0.0002	0.0000	NF	NF	NF
E-/Z-linalool oxide-arabinofuranose-glucoside2**			0.0002	0.0001	0.0001	NF						
E-/Z-linalool oxide-glucoside1**			NF									
E-/Z-linalool oxide-glucoside2**			NF									
E-/Z-linalool oxide-rhamnopyranose1**			NF									

(Continued)

TABLE 2B | Continued

Metabolites	λ_{max}	RT	A1	A2	A3	A4	A5	A6	A7	A8	A9	A10
E-/Z-linalool oxide-rhamnopyranose2**			NF	NF	NF	NF	NF	NF	NF	NF	NF	NF
E-/Z-linalool oxide-Rhamnopyranoside-glucoside**		0.0001	0.0000	0.0001	0.0000	NF	0.0000	0.0000	0.0000	0.0000	0.0000	0.0000
E-/Z-linalool oxide-Rhamnopyranoside-glucoside2**		0.0000	NF	0.0000	0.0000	NF	0.0000	NF	NF	0.0000	0.0000	0.0000

Isoprenoids (carotenoids, chlorophylls, ubiquinone, and α -tocopherol) were identified and quantified by LC-DAD-APCI-MS and data are expressed as $\mu\text{g}/\text{mg DW}$; other metabolite precursors were detected and relatively quantified by LC-APCI-MS (lipids) and LC-ESI-MS (amino acids, phenylpropanoids, terpene glucosides) and data are expressed as fold on the internal standard level (APCI, α -tocopherol acetate; ESI, formononetin). For more details, see materials and methods.

*Also involved in phenylpropanoid-derived volatiles.

**Not possible discriminating the E- and Z-isomers.

Other metabolites such as α -tocopherol, ubiquinone and an unknown metabolite with a maximum absorption at 290, 296, and 255, respectively, have been detected in both varieties and were present during all maturation stages. α -tocopherol is the main tocopherol detected in grape berries compared to γ and δ -tocopherols, while β -tocopherol was not found in the berries. Among the tocopherols present in foods, the α -homolog shows the highest vitamin E activity, thus making it the most important for human health and biological activity (Baydar, 2006; El Gengaihi et al., 2013).

Monoterpenes and sesquiterpenes play important roles in a number of different grape varieties as contributors to the overall aroma. Red grapes are not characterized by high levels of terpenes; however some terpenes are usually present at low levels (Canuti et al., 2009).

A total number of 17 glycosylated terpenes were detected in the samples analyzed. The total amounts of glycosylated terpenes were higher in Airén than in Tempranillo and 8 of these precursors were detected only in the white variety. In general, precursors with a disaccharide remained mainly constant throughout the maturation stages in both varieties while the precursors with one linked sugar were only found in stages 1 and 2, with the exception of limonene-arabinofuranose which was detected throughout all the stages in Airén.

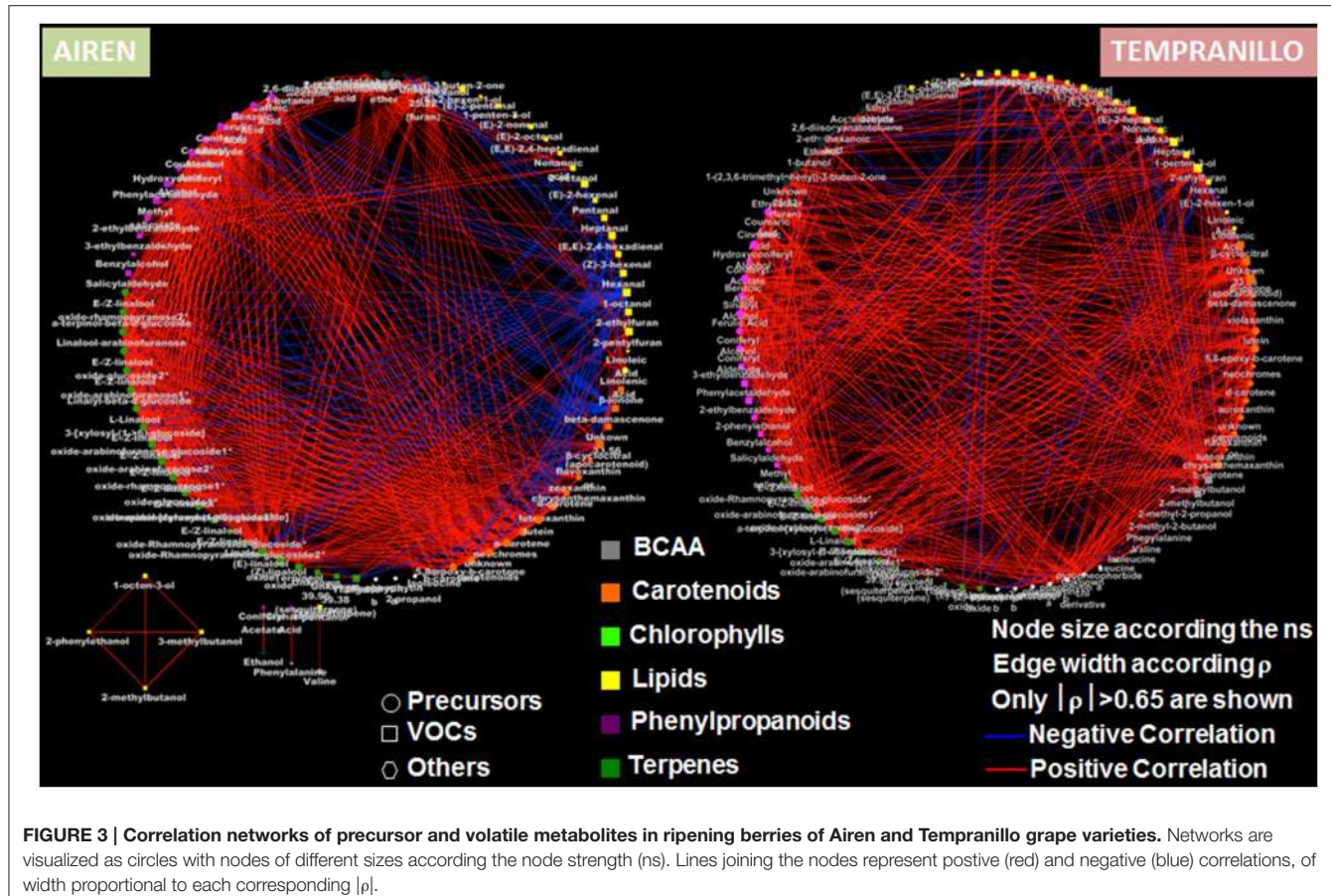
The data obtained for glycosylated terpenes and carotenoids are in accordance with the levels detected for related volatile compounds, showing the highest levels of terpenoid and apocarotenoid volatiles in early stages and in the white variety Airén. On the contrary, the abundance of branched-chain amino acids and fatty acids do not seem to be in accordance to the levels observed for their related volatile compounds, likely due to the cell demand for keeping high contents in primary metabolites involved in a broad range of reactions and metabolic pathways.

Metabolite-Metabolite and Metabolite-Gene Correlation Analyses

In order to explore precursor/volatile metabolite-metabolite fluctuations during the ripening of the Airén and Tempranillo berries, we generated two correlation matrices (Supplementary Figure 2) by calculating the Pearson correlation coefficients

for each data pair. Overall, the two varieties displayed a very different extent of relationships, stronger in Airén compared to Tempranillo. However, for both varieties we could identify a common “positive correlation core,” represented by the precursor/volatile metabolites involved in secondary pathways: phenylpropanoids, carotenoids, terpenes, and chlorophyll. This finding suggests the existence of a metabolic co-regulation during berry ripening, implying a general decrease in compounds which are exploited as volatile precursors, or are associated to early developmental stages. Oppositely, primary metabolism, particularly in lipids, exhibited a very distinct attitude between the two varieties: Airén berries showed a general negative correlation between lipids against the secondary metabolites, which was not observed in the Tempranillo matrix, indicating a different contribution of the lipid metabolism in the generation of the berry aroma bouquet.

Furthermore, we used correlative analyses to build two correlation networks, a different approach to investigate relationships among the different metabolic pathways, as well as within the same metabolism (Figure 3). In agreement with what was previously observed, the two varieties mainly differentiate at the lipid level, yielding a negative correlation region in the Airén berries. Additionally, we observed the presence of areas of high positive correlations (e.g., number of nodes belonging to the same metabolic pathways harvesting a large number of correlations $>|0.65|$) like the terpene and carotenoid pathways (for Airén) and the phenylpropanoid metabolism (both varieties, but with a greater number of correlations in Airén compared to Tempranillo). The distinct pattern of the lipid precursors and volatiles with respect to the other metabolic classes and between the two varieties prove that the volatile evolution in the Tempranillo berries occurs through a concerted process in which metabolites from the different pathways move together (general presence of positive correlations). On the contrary, Airén berries display a “metabolite imbalance” between the primary (lipids, negatively correlated toward all the other pathways) and the secondary (phenylpropanoids, carotenoids, terpenes, which are positively correlated) metabolism. Finally, the evaluation of the “node strength” (ns) (Diretto et al., 2010) which is the average of all the $|\rho|$ of a node, demonstrates that, with the exception of the



primaries as well as some other random metabolite, in general all the compounds under investigation take part with the same “weight” in the metabolic shift arising during berry ripening.

To gain insights into the biological roles played by *V. vinifera* GH Family 1, LOX, HPL, OMT, ADH, and CCD, a set of primers have been designed based on the full length sequences obtained at the Genoscope database with the exception of ADH and LOX, where only 3 sequences per gene were selected (Supplementary Table 1) for OMT. Using these primers, qRT-PCR analyses were carried out to determine the expression pattern in both Tempranillo and Airén cultivars, using tissues from the 10 stages.

Taking together the expression analyses and the metabolite compound levels throughout the different stages, for each variety we have built three heat maps referring to lipid, carotenoid and phenylpropanoid metabolism (Figures 4–6, respectively). To achieve this, we used Pearson correlation analysis, a best-fit approach that creates a mathematical simulation of expression values using the available experimental data. Significant correlation does not necessarily mean that there is a cause-effect relationship between genes and metabolites; although it allowed us to suggest possible candidates for a gene function, and also to discard genes as unrelated to metabolites.

For each pathway, elements are placed according to the following order: non-volatile precursors, genes (LOX, HPL, CCD, and OMT) and volatile compounds. Using this approach, it is

possible to identify metabolites and transcripts whose levels show a concordant or opposite evolution, resulting in, respectively, positive and negative correlations. Since GH 1 and ADH proteins have low substrate affinities, we have built a correlation network for assessing their putative activities (Supplementary Figure 3).

Overall correlation values between volatile, non-volatile levels and gene expression were higher in the Airén variety than in Tempranillo (Supplementary Tables 3–5).

Regarding the lipid metabolism as shown in Figure 4, linolenic acid showed a higher significant positive relationship with some volatiles than linoleic acid as (E,E)-2,4-heptadienal (0.75), 1-penten-3-ol (0.80), 2-ethylfuran (0.84), (E)-2-pentenol (0.75), nonanoic acid (0.81), 2-pentylfuran (0.80), and 2-octanol (0.75) while both fatty acids correlated negatively with (E)-2-hexen-1-ol (-0.68). GSVIVP00014710001 (HPL2) and GSVIVP00036457001 (HPL6) correlated positively between each other (0.90) and with LOXD (0.85, 0.91), respectively; LOXA correlated positively with (Z)-3-hexenal (0.70) and negatively with 2-pentylfuran (-0.70), whereas LOXC and LOXD were strongly correlated to each other (0.87). LOXC correlated strongly with GSVIVP00014710001 (HPL2) (0.69), GSVIVP00036456001 (HPL5) (0.71) and GSVIVP00036457001 (HPL6) (0.81).

In Tempranillo, more correlations among the volatile compounds were found than with the precursors or HPL and LOX genes, for example (E,E)-2,4-hexadienal and (Z)-3-hexenal

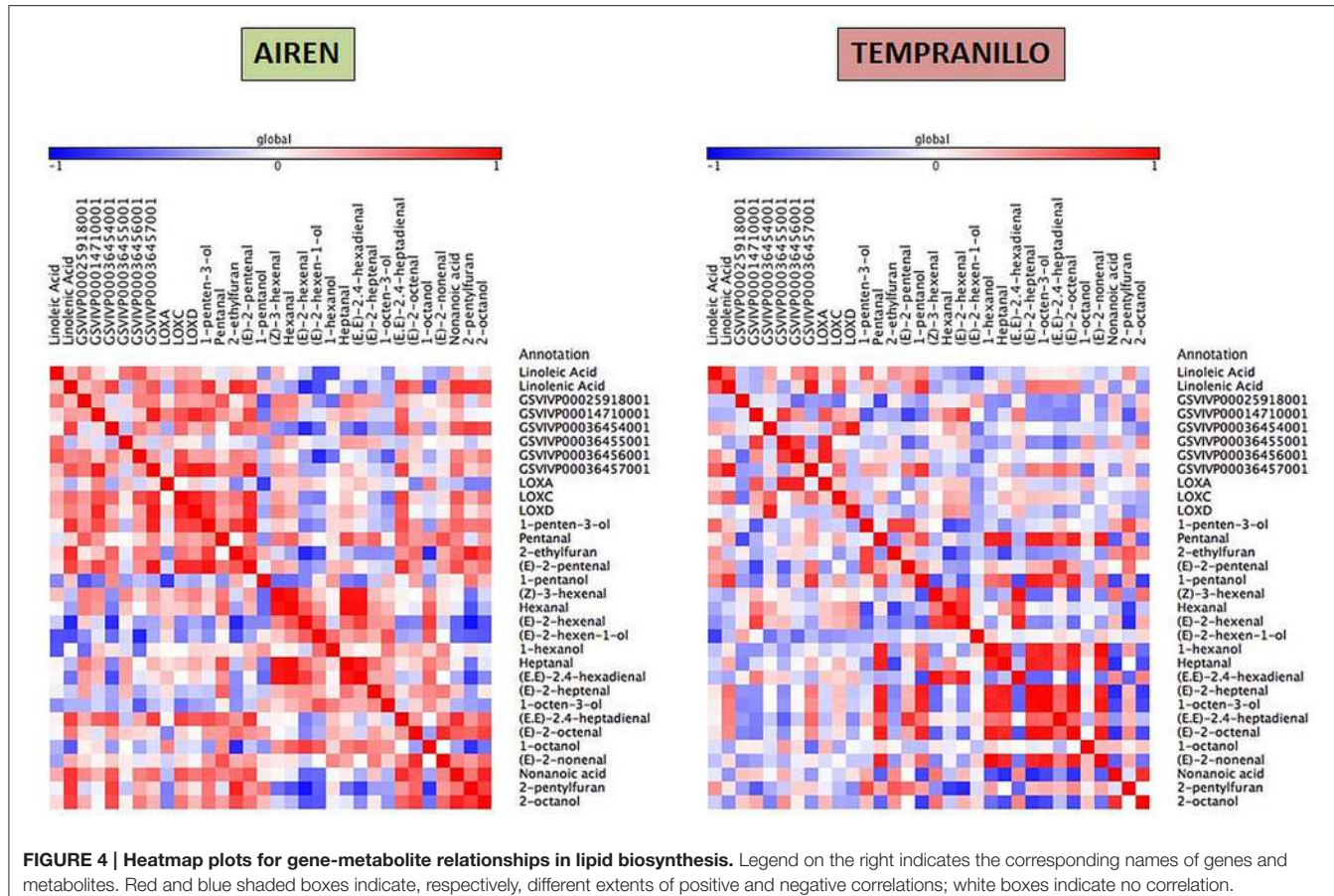


FIGURE 4 | Heatmap plots for gene-metabolite relationships in lipid biosynthesis. Legend on the right indicates the corresponding names of genes and metabolites. Red and blue shaded boxes indicate, respectively, different extents of positive and negative correlations; white boxes indicate no correlation.

have a strong correlation (0.98) with each other. Only linoleic acid correlated positively with GSVIVP00036457001 (HPL6) (0.70). A low relationship was obtained between (E)-2-hexenal and GSVIVP00014710001 (HPL2) (0.67) and between (E)-2-pentenal and LOXA. Transcript levels of LOXD and HPL6 correlate negatively with linolenic acid (-0.74) and positively with linoleic acid (0.76), respectively.

Four LOX genes VvLOXA, VvLOXO, VvLOXC, and VvLOXD from the white grape cultivar Sauvignon Blanc have been isolated and characterized (Podolyan et al., 2010). The recombinant LOXA-TP and LOXO-TP proteins have been expressed and both enzymes were able to convert LnA into 13(S)-hydroperoxyoctadecatrienoic acid and LA into 13(S)-hydroperoxyoctadecadienoic acid. During berry development for three seasons, transcripts from VvLOXA exhibited an initial decrease in early stages of development, followed by an increase in expression around veraison. LOX enzymes generate some derivatives that can be catalyzed by hydroperoxide lyase to produce aldehydes. Our data suggested that linoleic and linolenic are catalyzed by LOXA and HPL2, producing (E)-2-hexenal and (E)-2-pentenal, while it is possible that HPL6 could also be involved in this pathway.

Correlations from carotenoid metabolism exhibited more relationships among the precursors and volatile compounds than CCD expression genes. Different patterns were found

in Airén and Tempranillo. In the white grape cultivar, β -cyclocitral positively correlated with neochromes (0.70), lutein (0.81), β -carotene (0.82), and α -carotene (0.83). β -damascenone correlated with GSVIVP00028786001 (CCD1) (0.86) and also, to a lesser extent with GSVIVP00032423001 (CCD1-1) (0.73).

In the red grape cultivar, looking at the relationships between precursors and VOCs, positive correlations were found among the unknown 33.56 apocarotenoid (0.91, 0.77), β -cyclocitral (0.87, 0.82), and β -ionone (0.92, 0.68) with lutein and 5,8-epoxy- β -carotene respectively. β -damascenone showed a low correlation with neochromes (0.71). On the other hand, positive correlations between gene expressions and precursors were found only between δ -carotene and GSVIVP00001163001 (CCD4a) (0.81) and between neochromes.

Our data showed a relationship among CCD1, lutein, β -ionone, β -cyclocitral, β -damascenone, and the unknown 33.56 apocarotenoid. It is known that CCD1 enzymes are involved in the cleavage of the 5,6 (5',6') (Vogel et al., 2008); 7,8 (7',8') (Ilg et al., 2009) and 9,10 (9',10') (Schwartz et al., 2001) double bonds to produce a variety of volatiles. In grape, VvCCD1 is able to produce 3-hydroxy- β -ionone from zeaxanthin (Mathieu et al., 2005), pseudoionone from lycopene, β -ionone from β -carotene and 6-methyl-5-heptene-2-one (6MHO) from lutein (Lashbrooke et al., 2013). β -damascenone is generated from multiple grape glycoconjugated precursors as lutein (Pineau et al.,

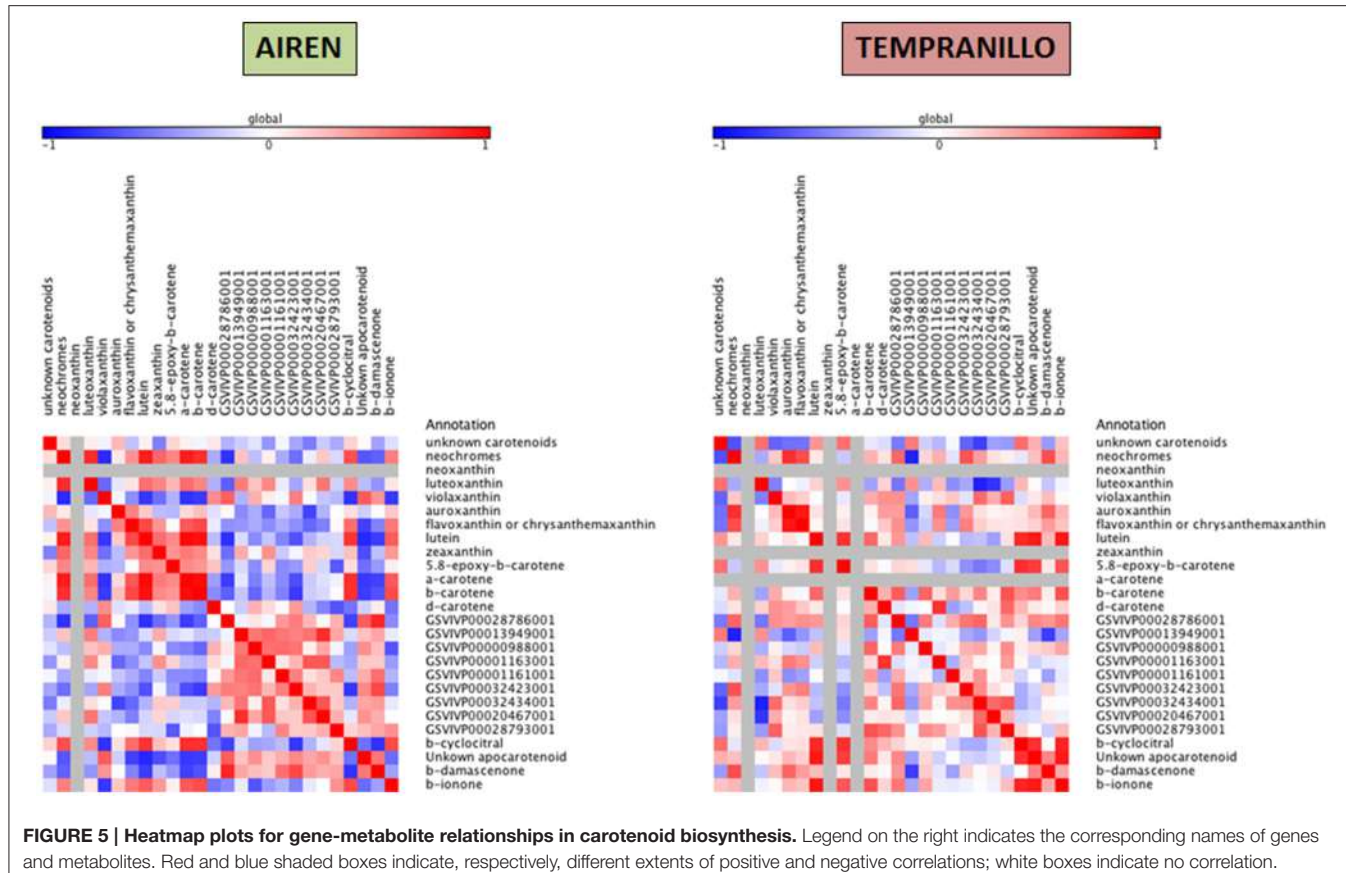


FIGURE 5 | Heatmap plots for gene-metabolite relationships in carotenoid biosynthesis. Legend on the right indicates the corresponding names of genes and metabolites. Red and blue shaded boxes indicate, respectively, different extents of positive and negative correlations; white boxes indicate no correlation.

2007). *In vitro* enzyme assay was carried out by (Mathieu et al., 2005) using VvCCD1 from *V. vinifera* L. cv Shiraz catalyzed only the cleavage of zeaxanthin and lutein to produce 3-hydroxy-β-ionone but not β-carotene as a substrate. However VvCCD1 isolated from *V. vinifera* L. cv Pinotage by (Lashbrooke et al., 2013), was capable of catalyzing the cleavage of lycopene, β-carotene and ε-carotene, but not neurosporene and ζ-carotene. Recent studies suggest that apocarotenoids instead of carotenoids act as the major substrates of CCD1 in plant (Floss et al., 2008; Ilg et al., 2010; Rubio-Moraga et al., 2014).

No clear associations were found among the precursors and the CCD4 genes in either the white or in the red cultivars. The CCD4 family contains at least two forms of genes with different structure and genome position (Ahrazem et al., 2010). The main group contains enzymes with a 9,10 (9',10') double bond cleavage activity (Rubio et al., 2008; Huang et al., 2009) and a second clade with 5,6 (5',6') activity as CCD4a and b enzymes from *V. vinifera* (Lashbrooke et al., 2013). A new CCD4 from citrus was recently isolated and has the ability to cleave asymmetrically at the 7',8' double bond in zeaxanthin and β-cryptoxanthin (Rodrigo et al., 2013). In grape, VvCCD4a and VvCCD4b were able to produce α-ionone from ε-carotene and geranylacetone from neurosporene, also VvCCD4a and VvCCD4b were capable of releasing 6-MHO from lycopene and geranylacetone from ζ-carotene (Lashbrooke et al., 2013). Despite the low correlation among lutein and the CCD4 a and b, the plastidial location of these CCDs and the

characterization of an orthologue from saffron CsCCD4c, with a restricted expression in stigmas, having activity 9,10 (9',10') over lutein (Rubio-Moraga et al., 2014) suggest that these enzymes might use lutein as a substrate.

The fact that β-cyclocitral was detected in both cultivars indicate the presence of a CCD4 which cleaves at the 7',8' double bond in zeaxanthin or lutein. Two more VvCCD4c and d were described in *Vitis* showing a 97% of identity in nucleotides between each other and were related to CcCCD4b from citrus and PtCCD4c and d from *Populus truncata* (Ahrazem et al., 2010). Even though the expression of the VvCCD4c could not be detected in any of the tissues analyzed by (Lashbrooke et al., 2013), these enzymes seem to be candidates to release β-cyclocitral from zeaxanthin or lutein by an asymmetric cleavage.

Concerning the phenylpropanoid pathway, different patterns were obtained in both cultivars. In Airén, a cluster formed by benzoic acid, coniferyl alcohol (0.73) and coumaric acid (0.72) correlated positively among each other and also with the volatiles 3- and 2-benzaldehyde (0.76 and 0.79). Coniferyl acetate showed strong positive and negative correlations with hydroxyconiferyl alcohol (0.95) and methyl salicylate (-0.92) respectively. OMT1 has a relatively high correlation with phenylacetaldehyde (0.74) and in a lesser extent with 2-phenylethanol (0.69), OMT4 has a negative association with benzylalcohol (-0.70). Some volatiles showed relationships among each other as benzylalcohol and 3- and 2-ethylbenzaldehyde (0.76 and 0.76).

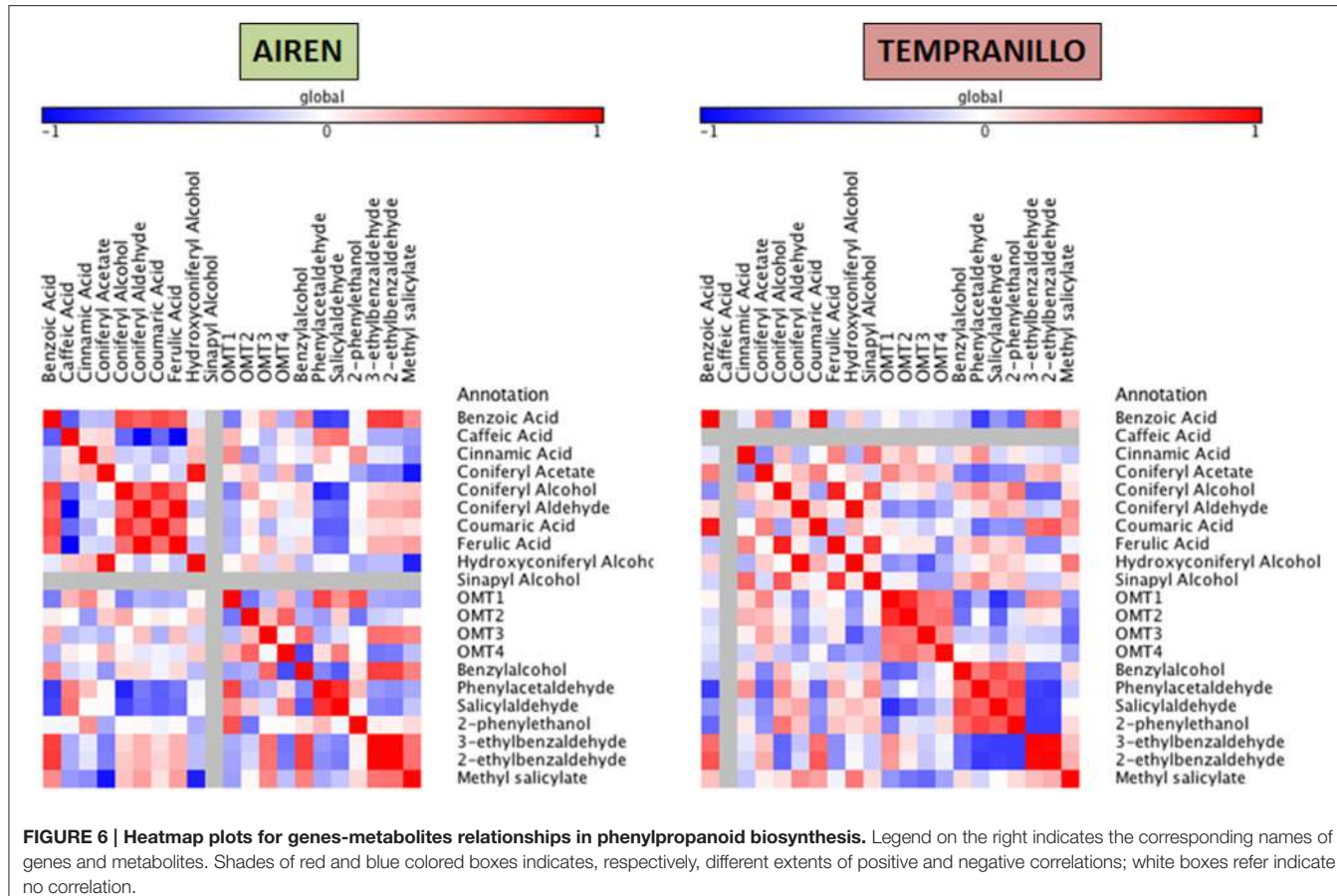


FIGURE 6 | Heatmap plots for genes-metabolites relationships in phenylpropanoid biosynthesis. Legend on the right indicates the corresponding names of genes and metabolites. Shades of red and blue colored boxes indicates, respectively, different extents of positive and negative correlations; white boxes refer indicate no correlation.

A strong positive relation was found between benzoic acid and coumaric acid (0.93) with 2-ethylbenzaldehyde (0.68). Another cluster is formed by coniferyl alcohol, ferulic acid and sinapyl alcohol, which are all strongly correlated among themselves (up to 0.88). High positive correlation was also found between coniferyl aldehyde and hydroxyconiferyl alcohol (0.97). OMT1 and OMT2 were related to each other and were also negatively associated with salicylaldehyde (0.81). We were not able to establish any relationship among the OMTs studied and the VOC compounds.

Regarding branched-chain amino acids and the volatile compounds related to them, no significant correlation appeared either in Airén or in Tempranillo.

In relation to GH 1 (Supplementary Table 5 and Supplementary Figure 3), a cluster formed by GS6, GS21, and GS25 showed a positive correlation among each other and showed the same pattern against the metabolites involved in the amino acid metabolism (precursors: Isoleucine, leucine, and valine; volatiles: 2-methyl-2-propanol, 3-methylbutanol and 2-methylbutanol) and against two lipids [linolenic acid and (Z)-3-hexenal] and a terpene (Unknown 39.38 (sesquiterpene)], suggesting a putative role in the generation of these volatiles. Similarly, GS9 also exhibited a broad set of significant correlations toward metabolites of the lipid pathway, positive with linoleic acid (0.66), 1-penten-3-ol (0.77), and

2-ethylfuran (0.74), and negative with Hexanal and (E)-2-hexenal (-0.68 each), which could, thus, let hypothesize a function in the evolution of the lipid-derived volatiles.

GS10, GS15, GS24, and GS28 placed, together with the already mentioned GS9, in the most crowded region of the network, and showed significant positive correlations with almost all the phenylpropanoid precursors detected with score values ranging from 0.91 (Coniferyl Aldehyde) to 0.67 (Coniferyl Alcohol) and also with some terpene glucosides (α -terpinol-[xylosyl-(1 \rightarrow 6)-glucoside] (0.82); L-Linalool 3-[xylosyl-(1 \rightarrow 6)-glucoside] (0.78); E-/Z-linalool oxide-arabinofuranose1* (0.82); E-/Z-linalool oxide-arabinofuranose-glucoside1* (0.84); E-/Z-linalool oxide-arabinofuranose-glucoside2* (0.88)). Surprisingly, these transcripts also displayed significant positive correlations with carotenoid precursors and apocarotenoid compounds [for instance, auroxanthin (0.92) and flavoxanthin (0.84) in the former, and b-ionone and the Unknown 33.56 (apocarotenoid) (0.82 each)].

Transcript levels of glycosidases GS1, GS5, GS12, GS16, GS20, GS22, and GS26 showed no significant correlation with any volatile compound. Therefore, the proteins encoded by these genes would not be expected to be involved in the production of any of the volatile compounds identified, at least in the wide range of developmental stages studied, or unless their activities would be mostly regulated at translational or post-translational

level. The rest of glycosidases not mentioned above have few correlations with the metabolites detected (for instance, GS8 with limonene or GS23 with (E)-2-pentenal), indicating either a very specialized activity, or that these glycosidases should produce a minor effect in the generation of the final bouquet.

In the classic model of volatile emission, the occurrence of significant negative correlations between the precursor metabolite and the genes coding for volatile-producing enzymes would be expected, along with a positive correlation between the latter and the volatiles. However, this simplified model does not take into consideration regulation phenomena at protein/enzymatic activity level (as mentioned above). Additionally, it must be remarked that some precursors (especially the ones involved in primary metabolism) are needed at high constitutive levels for a series of additional functions in cell metabolism, or are accumulated as sink (as in the case of the terpene glucosides). In this complex framework, we believe that the presence of significant correlations, although with an opposite sign with respect to the expected, could be biologically relevant, and could reflect the presence of specific metabolic tunings.

ADH1 exhibited only a few correlations with (E)-2-hexen-1-ol (0.67) and, contrary to the expectation, with the pyropheophorbide a (0.71), while ADH2 and ADH3 displayed almost the same pattern against the metabolites and showed high correlative power toward lipid derivatives (Supplementary Table 5). However, ADH3 showed higher scores than ADH2 and more relationships with other metabolites such as (E)-2-hexenal (0.67), 3-ethylbenzaldehyde (0.84), 2-ethylbenzaldehyde (0.74), terpeniol (0.73) and 2,6-diisocyanotoluene (0.82). It has been shown that grape ADH1 gene expression was detected in the first phase of fruit development, while ADH2 has been described as a berry ripening-related isogene, with data suggesting that transcriptional regulation of these genes and ADH enzyme activity could partially be related to the ethylene signaling pathway (Cirilli et al., 2012).

Our data allow a general and extensive view of the evolution of volatile and non-volatile compounds from the early formation of the berry to the post ripening stages, along with their relationships with some transcripts involved in their biosynthesis (Figure 3). Differences between the two varieties regarding VOCs were found, even though these variations were mostly attributed to differences in the levels of the substances that constitute grape aroma rather than to qualitative differences in the volatile compounds produced. The results obtained provide potential glycosidase candidates that could participate in the final aroma of Airén and Tempranillo, such as GS9, GS10, GS15, GS16, GS21, GS24, and GS25. In relation to lipid metabolism, data showed the possible involvement of LOXA and HPL2 to generate (E)-2-hexenal and (E)-2-pentenal. At

the carotenoid metabolism level, volatiles exhibited a higher extent of correlations toward their precursors compared to the biosynthetic genes; although a notable exception was represented by CCD1, which was related mainly with the production of β -ionone and CCD4c, and seems to be the candidate for the release of β -cyclocitral from zeaxanthin or lutein by an asymmetric cleavage. Concerning phenylpropanoid and branched-chain amino acid pathways, no clear relationships were found among the metabolites and gene expression. Interestingly, the white variety showed a higher "metabolite imbalance" between primary (lipids, negatively correlated toward all the other pathways) and secondary (phenylpropanoids, carotenoids, terpenes, which are positively correlated among each other) metabolism than the red variety. Furthermore, correlation analysis also showed a higher degree of overall correlation in precursor/volatile metabolite-metabolite levels in Airén, which confirms a distinct mechanism of the white varieties for producing an enriched aroma bouquet compared to the red ones.

AUTHOR CONTRIBUTIONS

OA, LG conceived and designed the experiments with the help of AG, GD, JR, AT performed the volatile detection and quantification experiments. AT, AR, and LG contributed to the preparation of the RNA samples and performed the qRT-PCR experiments. GD, AG performed the precursors detection and quantification analyses. OA, JR, and GD achieved the *in silico*, statistical, and bioinformatics analyses. OA, GD, JR, and LG wrote the manuscript and all authors contributed to the discussion and approved the final manuscript.

ACKNOWLEDGMENTS

We thank J. Argandoña (Instituto Botánico, Universidad de Castilla-La Mancha, Albacete, Spain) for excellent technical support, and K.A. Walsh for language revision. This work was supported by the "Junta de comunidades de Castilla-La Mancha" (JCCM) [PPII-10-0062-7718] and benefited from the networking activities within the European Cooperation in Science and Technology Action CA15136 (EUROCAROTEN). GD was supported by short-term fellowships of the Quality Fruit (FA1106) European Cooperation in Science and Technology actions. OA was funded by FPCYTCLM through the INCRECYT Programme.

SUPPLEMENTARY MATERIAL

The Supplementary Material for this article can be found online at: <http://journal.frontiersin.org/article/10.3389/fpls.2016.01619/full#supplementary-material>

REFERENCES

- Ahrazem, O., Rubio-Moraga, A., Berman, J., Capell, T., Christou, P., Zhu, C., et al. (2016). The carotenoid cleavage dioxygenase CCD2 catalysing the synthesis of

- crocetin in spring crocuses and saffron is a plastidial enzyme. *New Phytol.* 209, 650–663. doi: 10.1111/nph.13609
 Ahrazem, O., Trapero, A., Gómez, M., Rubio-Moraga, A., and Gómez-Gómez, L. (2010). Genomic analysis and gene structure of the plant carotenoid

- dioxygenase 4 family: a deeper study in *Crocus sativus* and its allies. *Genomics* 96, 239–250. doi: 10.1016/j.ygeno.2010.07.003
- Aubert, C., Ambid, C., Baumes, R., and Günta, Z. (2003). Investigation of bound aroma constituents of Yellow-Freshed nectarines (*Prunus persica* L. cv Springbright). Changes in bound aroma profile during maturation. *J. Agric. Food Chem.* 51, 6280–6286. doi: 10.1021/jf034613h
- Baek, H. H., and Cadwallader, K. R. (1999). Contribution of free and glycosidically bound volatile compounds to the aroma of Muscadine Grape Juice. *J. Food Sci.* 64, 441–444. doi: 10.1111/j.1365-2621.1999.tb15059.x
- Baldwin, E. A. (2002). “Fruit flavor, volatile metabolism and consumer perceptions,” in *Fruit Quality and its Biological Basis*, ed M. Knee (Boca Raton, FL: CRC Press), 89–106.
- Baldwin, E. A., Goodner, K., and Plotto, A. (2008). Interaction of volatiles, sugars, and acids on perception of tomato aroma and flavor descriptors. *J. Food Sci.* 73, S294–S307. doi: 10.1111/j.1750-3841.2008.00825.x
- Baldwin, E. A., Scott, J. W., Einstein, M. A., Malundo, M. M., Carr, B. T., Shewfelt, R. L., et al. (1998). Relationship between sensory and instrumental analysis for tomato flavor. *J. Am. Soc. Hortic. Sci.* 123, 906–915.
- Baumes, R., Wirth, J., Bureau, S., Gunata, Z., and Razungles, A. (2002). Biogeneration of C13-norisoprenoid compounds: experiments supportive for an apo-carotenoid pathway in grapevines. *Anal. Chim. Acta* 458, 3–14. doi: 10.1016/S0003-2670(01)01589-6
- Baydar, N. G. (2006). Organic acid, tocopherol, and phenolic compositions of some Turkish grape cultivars. *Chem. Nat. Comp.* 42, 156–159. doi: 10.1007/s10600-006-0066-x
- Boulanger, R., and Crouzet, J. (2001). Changes on volatile compounds during heating of Bacuri pulp. *J. Agric. Food Chem.* 49, 5911–5915. doi: 10.1021/jf010894m
- Bureau, S. M., Razungles, A., Baumes, R., and Bayonove, C. (1998). Effect of vine or bunch shading on the carotenoid composition in *Vitis Vinifera* L. berries. I. Syrah grapes. *Wein Wissenschaft* 53, 64–71.
- Buttery, R. G. (1993). “Quantitative and sensory aspects of flavor of tomato and other vegetables and fruits,” in *Flavor Science: Sensible Principles and Techniques*, eds T.E. Acree and R. Teranishi (Washington, DC: American Chemistry Society), 259–281.
- Buttery, R. G., Takeoka, G., Teranishi, R., and Ling, L. C. (1990). Tomato aroma components: identification of glycoside hydrolysis volatiles. *J. Agric. Food Chem.* 38, 2050–2053. doi: 10.1021/jf00101a010
- Buttery, R. G., Teranishi, R., and Ling, L. C. (1987). Fresh tomato aroma volatiles: a quantitative study. *J. Agric. Food Chem.* 35, 540–544. doi: 10.1021/jf00076a025
- Buttery, R. G., Teranishi, R., Ling, L. C., Flath, R. A., and Stern, D. J. (1988). Quantitative studies on origins of fresh tomato aroma volatiles. *J. Agric. Food Chem.* 36, 1247–1250. doi: 10.1021/jf00084a030
- Canutti, V., Conversano, M., Calzì, M. L., Heymann, H., Matthews, M. A., and Ebeler, S. E. (2009). Headspace solid-phase microextraction–gas chromatography–mass spectrometry for profiling free volatile compounds in Cabernet Sauvignon grapes and wines. *J. Chromatogr. A* 1216, 3012–3022. doi: 10.1016/j.chroma.2009.01.104
- Castro Vázquez, L., Pérez-Coello, M. S., and Cabezudo, M. D. (2002). Effects of enzyme treatment and skin extraction on varietal volatiles in Spanish wines made from Chardonnay, Muscat, Airén, and Macabeo grapes. *Anal. Chim. Acta* 458, 39–44. doi: 10.1016/S0003-2670(01)01521-5
- Cejudo-Bastante, M. J., Castro-Vázquez, L., Hermosín-Gutiérrez, I., and Pérez-Coello, M. S. (2011). Combined effects of prefermentative skin maceration and oxygen addition of must on color-related phenolics, volatile composition, and sensory characteristics of Airén white wine. *J. Agric. Food Chem.* 59, 12171–12182. doi: 10.1021/jf202679y
- Cirilli, M., Bellincontro, A., De Santis, D., Botondi, R., Colao, M. C., Muleo, R., et al. (2012). Temperature and water loss affect ADH activity and gene expression in grape berry during postharvest dehydration. *Food Chem.* 132, 447–454. doi: 10.1016/j.foodchem.2011.11.020
- Cohen, S. D., and Kennedy, J. A. (2010). Plant metabolism and the environment: implications for managing phenolics. *Crit. Rev. Food Sci. Nutr.* 50, 620–643. doi: 10.1080/10408390802603441
- Cordonier, R., and Bayonove, C. (1974). Mise en évidence dans la baie de raisin, variété Muscat d’Alexandrie, de monoterpenes liés révélateurs par une ou plusieurs enzymes du fruit. *Compt. Rend. l’Acad. Sci.* 278, 3397–3390.
- Crouzett, J. (1992). “La biogénèse des arômes,” in *Les Arômes Alimentaires*, eds H. Richard and J. L. Multon (Paris: TEC and DOC - LAVOISIER), 80–97.
- Crupi, P., Milella, R. A., and Antonacci, D. (2010). Simultaneous HPLC-DAD-MS (ESI+) determination of structural and geometrical isomers of carotenoids in mature grapes. *J. Mass Spectrom.* 45, 971–980. doi: 10.1002/jms.1794
- Cynkar, W., Damberg, R., Smith, P., and Cozzolino, D. (2010). Classification of Tempranillo wines according to geographic origin: combination of mass spectrometry based electronic nose and chemometrics. *Anal. Chim. Acta* 660, 227–231. doi: 10.1016/j.aca.2009.09.030
- De Vos, R. C., Moco, S., Lommen, A., Keurentjes, J. J., Bino, R. J., and Hall, R. D. (2007). Untargeted large-scale plant metabolomics using liquid chromatography coupled to mass spectrometry. *Nat. Protoc.* 2, 778–791. doi: 10.1038/nprot.2007.95
- Deluc, L. G., Quilici, D. R., Decendit, A., Grimplet, J., Wheatley, M. D., Schlauch, K. A., et al. (2009). Water deficit alters differentially metabolic pathways affecting important flavor and quality traits in grape berries of Cabernet Sauvignon and Chardonnay. *BMC Genomics* 10:212. doi: 10.1186/1471-2164-10-212
- Diretto, G., Al-Babili, S., Tavazza, R., Scossa, F., Papacchioli, V., Migliore, M., et al. (2010). Transcriptional-metabolic networks in β-carotene-enriched potato tubers: the long and winding road to the Golden phenotype. *Plant Physiol.* 154, 899–912. doi: 10.1104/pp.110.159368
- Downey, M. O., Dokoozlian, N. K., and Krstic, M. P. (2006). Cultural practice and environmental impacts on the flavonoid composition of grapes and wine: a review of recent research. *Am. J. Enol. Vitic.* 57, 257–268.
- Dudareva, N., Pichersky, E., and Gershenson, J. (2004). Biochemistry of plant volatiles. *Plant Physiol.* 135, 1893–1902. doi: 10.1104/pp.104.049981
- Düring, H. (1999). Photoprotection in leaves of grapevines: responses of the xanthophyll cycle to alterations of light intensity. *Vitis* 38, 21–24.
- El Gengaihi, S., Ella, F. M. A., Hassan, E. M., Shalaby, E. A., and Baker, D. H. A. (2013). Phytochemical investigation and radical scavenging activity of wastes of some grape varieties grown in Egypt. *Glob. J. Pharmacol.* 7, 465–473. doi: 10.5829/idosi.gjp.2013.7.4.1115
- El Hadi, M. A., Zhang, F.-J., Wu, F.-F., Zhou, C.-H., and Tao, J. (2013). Advances in fruit aroma volatile research. *Molecules* 18, 8200–8229. doi: 10.3390/molecules18078200
- Floss, D. S., Schliemann, W., Schmidt, J., Strack, D., and Walter, M. H. (2008). RNA interference-mediated repression of MtCCD1 in mycorrhizal roots of *Medicago truncatula* causes accumulation of C27 apocarotenoids, shedding light on the functional role of CCD1. *Plant Physiol.* 148, 1267–1282. doi: 10.1104/pp.108.125062
- Francis, I. L., Sefton, M. A., and Williams, P. J. (1992). Sensory descriptive analysis of the aroma of hydrolysed flavour precursor fractions from Semillon, Chardonnay, and Sauvignon blanc grape juices. *J. Sci. Food Agric.* 59, 511–520. doi: 10.1002/jsfa.2740590414
- Francis, I., and Newton, J. (2005). Determining wine aroma from compositional data. *Aust. J. Grape Wine Res.* 11, 114–126. doi: 10.1111/j.1755-0238.2005.tb00283.x
- Frusciante, S., Diretto, G., Bruno, M., Ferrante, P., Pietrella, M., Prado-Cabrero, A., et al. (2014). Novel carotenoid cleavage dioxygenase catalyzes the first dedicated step in saffron crocin biosynthesis. *Proc. Natl. Acad. Sci. U.S.A.* 111, 12246–12251. doi: 10.1073/pnas.1404629111
- Galliard, T., Matthew, J. A., Wright, A. J., and Fishwick, J. (1977). The enzymic breakdown of lipids to volatile and non-volatile carbonyl fragments in disrupted tomato fruits. *J. Sci. Food Agric.* 28, 863–868. doi: 10.1002/jsfa.2740280915
- García, E., Chacón, J. L., Martínez, J., and Izquierdo, P. M. (2003). Changes in volatile compounds during ripening in grapes of Airén, Macabeo and Chardonnay white varieties grown in La Mancha Region (Spain). *Food Sci. Technol. Int.* 9, 33–39. doi: 10.1177/108201320309001006
- Garde-CerdáN, T., Lorenzo, C.N., Lara, J.F., Pardo, F., Ancín-Azpilicueta, C., and Salinas, M.R. (2009). Study of the evolution of nitrogen compounds during grape ripening. Application to differentiate grape varieties and cultivated systems. *J. Agric. Food Chem.* 57, 2410–2419. doi: 10.1021/jf8037049
- Genovés, S., Gil, J. V., Manzanares, P., Aleixandre, J. L., and Vallés, S. (2003). Candida molischiana β-glucosidase production by *Saccharomyces cerevisiae* and its application in winemaking. *J. Food Microbiol. Safety* 68, 2096–2100. doi: 10.1111/j.1365-2621.2003.tb07025.x

- Goldberg, D. M., Tsang, E., Karumanchiri, A., and Soleas, G. J. (1998). Quercetin and p-coumaric acid concentrations in commercial wines. *Am. J. Enol. Vitic.* 49, 142–151.
- Gómez-Gómez, L., Trapero-Mozos, A., Gomez, M. D., Rubio-Moraga, A., and Ahrazem, O. (2012). Identification and possible role of a MYB transcription factor from saffron (*Crocus sativus*). *J. Plant Physiol.* 169, 509–515. doi: 10.1016/j.jplph.2011.11.021
- González, S. S., Gallo, L., Climent, M. D., Barrio, E., and Querol, A. (2007). Enological characterization of natural hybrids from *Saccharomyces cerevisiae* and *S. kudriavzevii*. *Int. J. Food Microbiol.* 116, 11–18. doi: 10.1016/j.ijfoodmicro.2006.10.047
- González-Mas, M. C., García-Ria-o, L. M., Alfaro, C., Rambla, J. L., Padilla, A. I., and Gutierrez, A. (2009). Headspace-based techniques to identify the principal volatile compounds in red grape cultivars. *Int. J. Food Sci. Technol.* 44, 510–518. doi: 10.1111/j.1365-2621.2008.01779.x
- Gonzalez-Viñas, M. A., Perez-Coello, M. S., Salvador, M. D., Cabezudo, M. D., and Martin-Alvarez, P. J. (1996). Changes in gas-chromatographic volatiles of young Airen wines during bottle storage. *Food Chem.* 56, 399–403. doi: 10.1016/0308-8146(95)00207-3
- Granell, A., and Rambla, J. L. (2013). “Biosynthesis of volatile compounds,” in *The Molecular Biology and Biochemistry of Fruit Ripening*, eds G. Seymour, G.A. Tucker, M. Poole and J.J. Giovannoni (Oxford: Wiley-Blackwell), 135–161.
- Gray, D. A., Prestage, S., Linforth, R. S. T., and Taylor, A. J. (1999). Fresh tomato specific fluctuations in the composition of lipoxygenase-generated C6 aldehydes. *Food Chem.* 64, 149–155. doi: 10.1016/S0308-8146(98)00163-0
- Grimplet, J., Deluc, L. G., Tillett, R. L., Wheatley, M. D., Schlauch, K. A., Cramer, G. R., et al. (2007). Tissue-specific mRNA expression profiling in grape berry tissues. *BMC Genomics* 8:187. doi: 10.1186/1471-2164-8-187
- Guedes De Pinho, P., Silva Ferreira, A. C., Mendes Pinto, M., Benitez, J. G., and Hogg, T. A. (2001). Determination of carotenoid profiles in grapes, musts, and fortified wines from Douro varieties of *Vitis vinifera*. *J. Agric. Food Chem.* 49, 5484–5488. doi: 10.1021/jf010515p
- Hermosín Gutiérrez, I. (2003). Influence of ethanol content on the extent of copigmentation in a Cencibel young red wine. *J. Agric. Food Chem.* 51, 4079–4083. doi: 10.1021/jf021029k
- Hernández-Orte, P., Cacho, J. F., and Ferreira, V. (2002). Relationship between varietal amino acid profile of grapes and wine aromatic composition. Experiments with model solutions and chemometric study. *J. Agric. Food Chem.* 50, 2891–2899. doi: 10.1021/jf011395o
- Hernández-Orte, P., Ibarz, M. J., Cacho, J., and Ferreira, V. (2005). Effect of the addition of ammonium and amino acids to musts of Airen variety on aromatic composition and sensory properties of the obtained wine. *Food Chem.* 89, 163–174. doi: 10.1016/j.foodchem.2004.02.021
- Hrazdina, G., Parsons, G. G., and Mattick, L. R. (1984). Physiological and biochemical events during development and maturation of grape berries. *Am. J. Oenol. Vitic.* 35, 220–227.
- Huang, F. C., Molnár, P., and Schwab, W. (2009). Cloning and functional characterization of carotenoid cleavage dioxygenase 4 genes. *J. Exp. Bot.* 60, 3011–3022. doi: 10.1093/jxb/erp137
- Iijima, Y., Nakamura, Y., Ogata, Y., Tanaka, K. I., Sakurai, N., Suda, K., et al. (2008). Metabolite annotations based on the integration of mass spectral information. *Plant J.* 54, 949–962. doi: 10.1111/j.1365-313X.2008.03434.x
- Ilg, A., Beyer, P., and Al-Babili, S. (2009). Characterization of the rice carotenoid cleavage dioxygenase 1 reveals a novel route for geranyl biosynthesis. *FEBS J.* 276, 736–747. doi: 10.1111/j.1742-4658.2008.06820.x
- Ilg, A., Yu, Q., Schaub, P., Beyer, P., and Al-Babili, S. (2010). Overexpression of the rice carotenoid cleavage dioxygenase 1 gene in Golden Rice endosperm suggests apocarotenoids as substrates in planta. *Planta* 232, 691–699. doi: 10.1007/s00425-010-1205-y
- Izquierdo Cañas, P. M., García Romero, E., Gómez Alonso, S., and Palop Herreros, M. L. L. (2008). Changes in the aromatic composition of Tempranillo wines during spontaneous malolactic fermentation. *J. Food Compos. Anal.* 21, 724–730. doi: 10.1016/j.jfca.2007.12.005
- Kamffer, Z., Bindon, K. A., and Oberholster, A. (2010). Optimization of a method for the extraction and quantification of carotenoids and chlorophylls during ripening in grape berries (*Vitis vinifera* cv. Merlot). *J. Agric. Food Chem.* 58, 6578–6586. doi: 10.1021/jf1004308
- Klee, H. J. (2010). Improving the flavor of fresh fruits: genomics, biochemistry, and biotechnology. *New Phytol.* 187, 44–56. doi: 10.1111/j.1469-8137.2010.03281.x
- Koundouras, S., Hatzidimitriou, E., Karamolegkou, M., Dimopoulos, E., Kallithraka, S., Tsialtas, J. T., et al. (2009). Irrigation and rootstock effects on the phenolic concentration and aroma potential of *Vitis vinifera* L. cv. cabernet sauvignon grapes. *J. Agric. Food Chem.* 57, 7805–7813. doi: 10.1021/jf901063a
- Krammer, G. E., Takeoka, G. R., and Buttery, R. G. (1994). Isolation and identification of 2,5-dimethyl-4-hydroxy-3(2H)-furanone glucoside from tomatoes. *J. Agric. Food Chem.* 42, 1595–1597. doi: 10.1021/jf00044a001
- Kumar, S., and Ramón, D. (1996). Purification and regulation of the synthesis of a β -xylosidase from *Aspergillus nidulans*. *FEMS Microbiol. Lett.* 135, 287–293. doi: 10.1016/0378-1097(95)00468-8
- Lalel, H. J. D., Singh, Z., and Tan, S. C. (2003). Glycosidically-bound aroma volatile compounds in the skin and pulp of “Kensington Pride” mango fruit at different stages of maturity. *Postharvest Biol. Technol.* 29, 205–218. doi: 10.1016/S0925-5214(02)00250-8
- Lashbrooke, J. G., Young, P. R., Dockrill, S. J., Vasanth, K., and Vivier, M. A. (2013). Functional characterisation of three members of the *Vitis vinifera* L. carotenoid cleavage dioxygenase gene family. *BMC Plant Biol.* 13:156. doi: 10.1186/1471-2229-13-156
- Lecas, M., Günata, Z. Y., Sapis, J. C., and Bayonove, C. L. (1991). Purification and partial characterization of β -glucosidase from grape. *Phytochemistry* 30, 451–454. doi: 10.1016/0031-9422(91)83702-M
- Lewinsohn, E., Sitrit, Y., Bar, E., Azulay, Y., Ibdah, M., Meir, A., et al. (2005a). Not just colors- carotenoid degradation as a link between pigmentation and aroma in tomato and watermelon fruit. *Trends Food Sci. Technol.* 16, 407–415. doi: 10.1016/j.tifs.2005.04.004
- Lewinsohn, E., Sitrit, Y., Bar, E., Azulay, Y., Meir, A., Zamir, D., et al. (2005b). Carotenoid pigmentation affects the volatile composition of tomato and watermelon fruits, as revealed by comparative genetic analyses. *J. Agric. Food Chem.* 53, 3142–3148. doi: 10.1021/jf047927t
- Liu, M., Diretto, G., Pirrello, J., Roustan, J. P., Li, Z., Giuliano, G., et al. (2014). The chimeric repressor version of an Ethylene Response Factor (ERF) family member, SL-ERF_B3, shows contrasting effects on tomato fruit ripening. *New Phytol.* 203, 206–218. doi: 10.1111/nph.12771
- López, N., Puertolas, E., Condón, S., Álvarez, I., and Raso, J. (2008). Effects of pulsed electric fields on the extraction of phenolic compounds during the fermentation of must of Tempranillo grapes. *Innov. Food Sci. Emerg. Technol.* 9, 477–482. doi: 10.1016/j.ifset.2007.11.001
- López, R., Ortín, N., Pérez-Trujillo, J. P., Cacho, J., and Ferreira, V. (2003). Impact odorants of different young white wines from the Canary Islands. *J. Agric. Food Chem.* 51, 3419–3425. doi: 10.1021/jf026045w
- Loughrin, J. H., Hamilton-Kemp, T. R., Burton, H. R., Andersen, R. A., and F., H. D. (1992). Glycosidically bound volatile components of *Nicotiana sylvestris* and *N. aveolens* flowers. *Phytochemistry* 31, 1537–1540. doi: 10.1016/0031-9422(92)83101-4
- Mageroy, M. H., Tieman, D. M., Floystad, A., Taylor, M. G., and Klee, H. J. (2012). A *Solanum lycopersicum* catechol-O-methyltransferase involved in synthesis of the flavor molecule guaiacol. *Plant J.* 69, 1043–1051. doi: 10.1111/j.1365-313X.2011.04854.x
- Manzanares, P., Van Den Broeck, H. C., H, D.G. L., and Visser, J. (2001). Purification and characterisation of two different α -L-rhamnosidases, RhaA and RhaB, from *Aspergillus aculeatus*. *Appl. Environ. Microbiol.* 67, 2230–2234. doi: 10.1128/AEM.67.5.2230-2234.2001
- Marlatt, C., Ho, C., and Chien, M. (1992). Studies of aroma constituents bound as glycosides in tomato. *J. Agric. Food Chem.* 40, 249–252. doi: 10.1021/jf00014a016
- Mathieu, S., Terrier, N., Procureur, J., Bigey, F., and Gunata, Z. (2005). A carotenoid cleavage dioxygenase from *Vitis vinifera* L.: functional characterization and expression during grape berry development in relation to C13-norisoprenoid accumulation. *J. Exp. Bot.* 56, 2721–2731 doi: 10.1093/jxb/eri265
- Mendes-Pinto, M. (2009). Carotenoid breakdown products the - norisoprenoids- in wine aroma. *Arch. Biochem. Biophys.* 483, 236–245. doi: 10.1016/j.abb.2009.01.008

- Mendes-Pinto, M. M., Ferreira, A. S., Oliveira, M. B. P., and Guedes De Pinho, P. (2004). Evaluation of some carotenoids in grapes by reversed-and normal-phase liquid chromatography: a qualitative analysis. *J. Agric. Food Chem.* 52, 3182–3188. doi: 10.1021/jf0499469
- Mendes-Pinto, M. M., Silva Ferreira, A. C., Caris-Veyrat, C., and Guedes De Pinho, P. (2005). Carotenoid, chlorophyll, and chlorophyll-derived compounds in grapes and Port wines. *J. Agric. Food Chem.* 53, 10034–10041. doi: 10.1021/jf0503513
- Mizutani, M., Nakanishi, H., Ema, J., Ma, S. J., Noguchi, E., Inohara-Ochiai, M., et al. (2002). Cloning of β -primeverosidase from tea leaves, a key enzyme in tea aroma formation. *Plant Physiol.* 130, 2164–2176. doi: 10.1104/pp.102.011023
- Monagas, M., Suárez, R., Gómez-Cordovés, C., and Bartolomé, B. (2005). Simultaneous determination of nonanthocyanin phenolic compounds in red wines by HPLC-DAD/ESI-MS. *Am. J. Enol. Vitic.* 56, 139–147.
- Nonier, M. F., Vivas De Gaulejac, N., Vivas, N., and Vitry, C. (2005). Glycosidically bound flavour compounds in *Quercus petraea* Liebl. wood. *Flavour Fragrance J.* 20, 567–572. doi: 10.1002/ff.1488
- Orlova, I., Marshall-Colón, A., Schnepf, J., Wood, B., Varbanova, M., Fridman, E., et al. (2006). Reduction of benzenoid synthesis in petunia flowers reveals multiple pathways to benzoic acid and enhancement in auxin transport. *Plant Cell* 18, 3458–3475. doi: 10.1105/tpc.106.046227
- Osorio, C., Duque, C., and Batista-Viera, F. (2003). Studies on aroma generation in lulo (*Solanum quitoense*): enzymatic hydrolysis of glycosides from leaves. *Food Chem.* 80, 333–340. doi: 10.1016/S0308-8146(02)00427-2
- Peña, A., Hernández, T., García-Vallejo, C., Estrella, I., and Suárez, J. (2000). A survey of phenolic compounds in Spanish wines from different geographical origins. *Eur. Food Res. Technol.* 210, 445–448. doi: 10.1007/s00217-005-0579
- Pérez-Coello, M. S., Briones Pérez, A. I., Ubeda Iranzo, J. F., and Martin Alvarez, P. J. (1999). Characteristics of wines fermented with different *Saccharomyces cerevisiae* strains isolated from the La Mancha region. *Food Microbiol.* 16, 563–573. doi: 10.1006/fmic.1999.0272
- Pérez-Coello, M. S., Sánchez, M. A., García, E., González-Vi-as, M. A., Sanz, J., and Cabezudo, M. D. (2000). Fermentation of white wines in the presence of wood chips of American and French oak. *J. Agric. Food Chem.* 48, 885–889. doi: 10.1021/jf990884+
- Pichersky, E., Noel, J. P., and Dudareva, N. (2006). Biosynthesis of plant volatiles: nature's diversity and ingenuity. *Science* 311, 808–811. doi: 10.1126/science.1118510
- Pineau, B., Barbe, J. C., Van Leeuwen, C., and Dubourdieu, D. (2007). Which impact for beta-damascenone on red wines aroma? *J. Agric. Food Chem.* 55, 4103–4108. doi: 10.1021/jf070120r
- Podolyan, A., White, J., Jordan, B., and Winefield, C. (2010). Identification of the lipoxygenase gene family from *Vitis vinifera* and biochemical characterisation of two 13-lipoxygenases expressed in grape berries of Sauvignon Blanc. *Funct. Plant Biol.* 37, 767–784. doi: 10.1071/FP09271
- Pogorzelski, E., and Wilkowska, A. (2007). Flavour enhancement through the enzymatic hydrolysis of glycosidic aroma precursors in juices and wine beverages: a review. *Flavour Fragrance J.* 22, 251–254. doi: 10.1002/ff.1784
- Pozo-Bayón, M. Á., Hernández, M. T., Martín-Álvarez, P. J., and Polo, M. C. (2003). Study of low molecular weight phenolic compounds during the aging of sparkling wines manufactured with red and white grape varieties. *J. Agric. Food Chem.* 51, 2089–2095. doi: 10.1021/jf021017z
- Rambla, J. L., Tikunov, Y. M., Monforte, A. J., Bovy, A. G., and Granell, A. (2014). The expanded tomato fruit volatile landscape. *J. Exp. Bot.* 65, 4613–4623. doi: 10.1093/jxb/eru128
- Rapp, A., and Mandery, H. (1986). Wine aroma. *Esperientia* 42, 873–884. doi: 10.1007/BF01941764
- Razungles, A. J., Babic, I., Sapis, J. C., and Bayonove, C. L. (1996). Particular behavior of epoxy xanthophylls during veraison and maturation of grape. *J. Agric. Food Chem.* 44, 3821–3825. doi: 10.1021/jf960260t
- Ribereau-Gayon, P., and Glories, Y. (1986). "Phenolics in grape and wines," in *Proceedings of the Sixth Australian Wine Industry Technical Conference*, ed T. Lee (Adelaide), 247–256.
- Riley, J. C. M., and Thompson, J. E. (1998). Ripening-induced acceleration of volatile aldehyde generation following tissue disruption in tomato fruit. *Physiol. Plant.* 104, 571–576. doi: 10.1034/j.1399-3054.1998.1040408.x
- Robinson, A. L., Boss, P. K., Solomon, P. S., Trengove, R. D., Heymann, H., and Ebeler, S. E. (2014). Origins of grape and wine aroma. Part 1. Chemical components and viticultural impacts. *Am. J. Enol. Vitic.* 65, 1–24. doi: 10.5344/ajev.2013.12070
- Rodrigo, M. J., Alquezar, B., Alos, E., Medina, V., Carmona, L., Bruno, M., et al. (2013). A novel carotenoid cleavage activity involved in the biosynthesis of Citrus fruit-specific apocarotenoid pigments. *J. Exp. Bot.* 64, 4461–4478. doi: 10.1093/jxb/ert260
- Rosillo, L., Salinas, M., Garijo, J., and Alonso, G.L. (1999). Study of volatiles in grapes by dynamic headspace analysis: application to the differentiation of some *Vitis vinifera* varieties. *J. Chromatogr. A* 847, 155–159. doi: 10.1016/S0021-9673(99)00036-9
- Rossouw, D., Olivares-Hernandes, R., Nielsen, J., and Bauer, F. F. (2009). Comparative transcriptomic approach to investigate differences in wine yeast physiology and metabolism during fermentation. *Appl. Environ. Microbiol.* 75, 6600–6612. doi: 10.1128/AEM.01251-09
- Rozen, S., and Skaletsky, H. J. (2000). "Primer3 on the WWW for general users and for biologist programmers," in *Bioinformatics Methods and Protocols: Methods in Molecular Biology*, eds S. Krawetz and S. Misener. (Totowa NJ: Humana Press), 365–386.
- Rubio, A., Rambla, J. L., Santaella, M., Gomez, M. D., Orzaez, D., Granell, A., et al. (2008). Cytosolic and plastoglobule-targeted carotenoid dioxygenases from *Crocus sativus* are both involved in beta-ionone release. *J. Biol. Chem.* 283, 24816–24825. doi: 10.1074/jbc.M804000200
- Rubio-Moraga, A., Rambla, J. L., Fernández-De Carmen, A., Traperero-Mozos, A., Ahrazem, O., Orzáez, D., et al. (2014). New target carotenoids for CCD4 enzymes are revealed with the characterization of a novel stress-induced carotenoid cleavage dioxygenase gene from *Crocus sativus*. *Plant Mol. Biol.* 86, 555–569. doi: 10.1007/s11103-014-0250-5
- Sakho, M., Chassangne, D., and Crouzet, J. (1997). African mango glycosidically bound volatile compounds. *J. Agric. Food Chem.* 45, 883–888. doi: 10.1021/jf960277b
- Sarry, J. E., and Günata, Z. (2004). Plant and microbial glycoside hydrolases: volatile release from glycosidic aroma precursors. *Food Chem.* 87, 509–521. doi: 10.1016/j.foodchem.2004.01.003
- Schwab, W., Davidovich-Rikanati, R., and Lewinsohn, E. (2008). Biosynthesis of plant-derived flavor compounds. *Plant J.* 54, 712–732. doi: 10.1111/j.1365-313X.2008.03446.x
- Schwartz, S., Qin, X., and Zeevaart, J. (2001). Characterization of a novel carotenoid cleavage dioxygenase from plants. *J. Biol. Chem.* 276, 25208–25211. doi: 10.1074/jbc.M102146200
- Silva Ferreira, A. C., and Guedes De Pinho, P. (2004). Nor-isoprenoids profile during port wine ageing: influence of some technological parameters. *Anal. Chim. Acta* 513, 169–176. doi: 10.1016/j.aca.2003.12.027
- Simkin, A. J., Schwartz, S. H., Auldridge, M., Taylor, M. G., and Klee, H. J. (2004). The tomato carotenoid cleavage dioxygenase 1 genes contribute to the formation of the flavor volatiles β -ionone, pseudoionone, and geranylacetone. *Plant J.* 40, 882–892. doi: 10.1111/j.1365-313X.2004.02263.x
- Speirs, J., Lee, E., Holt, K., Yong-Duk, K., Scott, N. S., Loveys, B., et al. (1998a). Genetic manipulation of alcohol dehydrogenase levels in ripening tomato fruit affects the balance of some flavor aldehydes and alcohols. *Plant Physiol.* 117, 1047–1058. doi: 10.1104/pp.117.3.1047
- Speirs, J., Lee, E., Holt, K., Yong-Duk, K., Steele Scott, N., Loveys, B., et al. (1998b). Genetic manipulation of alcohol dehydrogenase levels in ripening tomato fruit affects the balance of some flavor aldehydes and alcohols. *Plant Physiol.* 117, 1047–1058. doi: 10.1104/pp.117.3.1047
- Stevens, M. A. (1970). Relationship between polyene-carotene content and volatile compound composition in tomatoes. *J. Am. Soc. Hortic. Sci.* 95, 461–464.
- Straubinger, M., Bau, B., Eckstein, S., Fink, M., and Winterhalter, P. (1998). Identification of novel glycosidic aroma precursors in Saffron (*Crocus sativus* L.). *J. Agric. Food Chem.* 46, 3238–3243. doi: 10.1021/jf980119f
- Su, L., Diretto, G., Purgatto, E., Danoun, S., Zouine, M., Li, Z., et al. (2015). Carotenoid accumulation during tomato fruit ripening is modulated by the auxin-ethylene balance. *BMC Plant Biol.* 15:114. doi: 10.1186/s12870-015-0495-4
- Tesniere, C., Torregrosa, L., Pradal, M., Souquet, J. M., Gilles, C., Dos Santos, K., et al. (2006). Effects of genetic manipulation of alcohol dehydrogenase levels on

- the response to stress and the synthesis of secondary metabolites in grapevine leaves. *J. Exp. Bot.* 57, 91–99. doi: 10.1093/jxb/erj007
- Tieman, D., Bliss, P., McIntyre, L. M., Blandon-Ubeda, A., Bies, D., Odabasi, A. Z., et al. (2012). The chemical interactions underlying tomato flavor preferences. *Curr. Biol.* 22, 1035–1039. doi: 10.1016/j.cub.2012.04.016
- Tikunov, Y. M., de Vos, R. C., Gonzalez Paramas, A. M., Hall, R. D., and Bovy, A. G. (2010). A role for differential glycoconjugation in the emission of phenylpropanoid volatiles from tomato fruit discovered using a metabolic data fusion approach. *Plant Physiol.* 152, 55–70. doi: 10.1104/pp.109.146670
- Tikunov, Y. M., Molthoff, J., De Vos, R. C., Beekwilder, J., Van Houwelingen, A., Van Der Hooft, J. J., et al. (2013). NON-SMOKY GLYCOSYLTRANSFERASE1 Prevents the Release of Smoky Aroma from Tomato Fruit. *Plant Cell* 25, 3067–3078. doi: 10.1105/tpc.113.114231
- Tsuruhami, K., Mori, S., Amarume, S., Saruwatari, S., Murata, T., Hirakake, J., et al. (2006). Isolation and characterization of a β -primeverosidase-like enzyme from *Penicillium multicolor*. *Biosci. Biotechnol. Biochem.* 70, 691–698. doi: 10.1271/bbb.70.691
- Tzin, V., Rogachev, I., Meir, S., Moyal Ben Zvi, M., Masci, T., Vainstein, A., et al. (2013). Tomato fruits expressing a bacterial feedback-insensitive 3-deoxy-D-arabino-heptulosonate 7-phosphate synthase of the shikimate pathway possess enhanced levels of multiple specialized metabolites and upgraded aroma. *J. Exp. Bot.* 64, 4441–4452. doi: 10.1093/jxb/ert250
- Vilanova, M., Genisheva, Z., Masa, A., and Oliveira, J. M. (2010). Correlation between volatile composition and sensory properties in Spanish Albariño wines. *Microchem. J.* 95, 240–246. doi: 10.1016/j.microc.2009.12.007
- Vogel, J. T., Tan, B. C., McCarty, D. R., and Klee, H. J. (2008). The carotenoid cleavage dioxygenase 1 enzyme has broad substrate specificity, cleaving multiple carotenoids at two different bond positions. *J. Biol. Chem.* 283, 11364–11373. doi: 10.1074/jbc.M710106200
- Wang, D., Kubota, K., Kobayashi, A., and Juan, I. M. (2001). Analysis of glycosidically bound aroma precursors in tea Leaves.3. Change in the glycoside content of tea leaves during the Oolong tea manufacturing process. *J. Agric. Food Chem.* 49, 5391–5396. doi: 10.1021/jf010235+
- Wang, Y., and Kays, S. J. (2000). Contribution of volatile compounds to the characteristic aroma of Baked 'Jewel' Sweetpotatoes. *J. Am. Soc. Hortic. Sci.* 125, 638–643.
- Watanabe, S., Hashimoto, I., Hayashi, K., Yagi, K., Asai, T., Knapp, H., et al. (2001). Isolation and identification of 2-phenylethyl disaccharide glycosides and monoglycosides from Rose flowers, and their potential role in scent formation. *Biosci. Biotechnol. Biochem.* 65, 442–445. doi: 10.1271/bbb.65.442
- Wei, S., Marton, I., Dekel, M., Shalitin, D., Lewinsohn, E., Bravdo, B. A., et al. (2004). Manipulating volatile emission in tobacco leaves by expressing *Aspergillus niger* β -glucosidase in different subcellular compartments. *Plant Biotechnol. J.* 2, 341–350. doi: 10.1111/j.1467-7652.2004.00077.x
- Williams, P. J. (1993). "Hydrolytic flavor release in fruit and wines through hydrolysis of non-volatile precursors," in *Flavor Science: Sensible Principles and Techniques*, eds T.E. Acree and R. Teranishi (Washington DC: American Chemical Society), 287–308.
- Winterhalter, P., and Rouseff, R. (2002). Carotenoid derived aroma compounds. *ACS Symposium series*, 802.
- Winterhalter, P., and Skouroumounis, G. K. (1997). "Glycoconjugated aroma compounds: occurrence, role and biotechnological transformation," in *Advances in Biochemical Engineering/Biotechnology* ed T. Scheper (Heidelberg-Berlin: Springer-Verlag), 74–105.
- Yuan, F., and Qian, M. C. (2016). Development of C<inf>13</inf>-norisoprenoids, carotenoids and other volatile compounds in *Vitis vinifera* L. Cv. *Pinot noir* grapes. *Food Chem.* 192, 633–641. doi: 10.1016/j.foodchem.2015.07.050
- Zoecklein, B. W., Wolf, T. K., Duncan, S. E., Marcy, J. E., and Jasinski, Y. (1998). Effect of fruit zone leaf removal on total glycoconjugates and conjugate fraction concentration of Riesling and Chardonnay (*Vitis vinifera* L.) grapes. *Am. J. Enol. Vitic.* 49, 259–265.

Conflict of Interest Statement: The authors declare that the research was conducted in the absence of any commercial or financial relationships that could be construed as a potential conflict of interest.

Copyright © 2016 Rambla, Trapero-Mozos, Diretto, Rubio-Moraga, Granell, Gómez-Gómez and Ahrazem. This is an open-access article distributed under the terms of the Creative Commons Attribution License (CC BY). The use, distribution or reproduction in other forums is permitted, provided the original author(s) or licensor are credited and that the original publication in this journal is cited, in accordance with accepted academic practice. No use, distribution or reproduction is permitted which does not comply with these terms.



How Does Host Carbon Concentration Modulate the Lifestyle of Postharvest Pathogens during Colonization?

Dov B. Prusky^{1*}, Fangcheng Bi², Juan Moral³ and Shiri Barad¹

¹ Department of Postharvest Science of Fresh Produce, Agricultural Research Organization, The Volcani Center, Beit Dagan, Israel, ² Institute of Fruit Tree Research, Guangdong Academy of Agricultural Sciences, Key Laboratory of South Subtropical Fruit Biology and Genetic Resource Utilization, Ministry of Agriculture, Guangzhou, China, ³ Departamento de Agronomía, Universidad de Córdoba, Córdoba, Spain

OPEN ACCESS

Edited by:

Mondher Bouzayen,
Institut National Polytechnique
de Toulouse, France

Reviewed by:

Serge Delrot,
University of Bordeaux, France
Nabil I. Elsheery,
Tanta University, Egypt

***Correspondence:**

Dov B. Prusky
dovprusk@agri.gov.il

Specialty section:

This article was submitted to
Plant Physiology,
a section of the journal
Frontiers in Plant Science

Received: 29 February 2016

Accepted: 15 August 2016

Published: 01 September 2016

Citation:

Prusky DB, Bi F, Moral J and Barad S (2016) How Does Host Carbon Concentration Modulate the Lifestyle of Postharvest Pathogens during Colonization? *Front. Plant Sci.* 7:1306.
doi: 10.3389/fpls.2016.01306

Postharvest pathogens can penetrate fruit by breaching the cuticle or directly through wounds, and they show disease symptoms only long after infection. During ripening and senescence, the fruit undergo physiological processes accompanied by a decline in antifungal compounds, which allows the pathogen to activate a mechanism of secretion of small effector molecules that modulate host environmental pH. These result in the activation of genes under their optimal pH conditions, enabling the fungus to use a specific group of pathogenicity factors at each particular pH. New research suggests that carbon availability in the environment is a key factor triggering the production and secretion of small pH-modulating molecules: ammonia and organic acids. Ammonia is secreted under limited carbon and gluconic acid under excess carbon. This mini review describes our most recent knowledge of the mechanism of activation of pH-secreted molecules and their contribution to colonization by postharvest pathogens to facilitate the transition from quiescence to necrotrophic lifestyle.

Keywords: small effector molecules, pH regulation, pathogenicity, postharvest susceptibility, *colletotrichum*, *penicillium*

INTRODUCTION

The resistance of unripe fruit to pathogen infection and colonization after harvest is considered a dynamic process that is modulated during host maturation and ripening. In many postharvest pathogens, disease symptoms occur long after the initial stages of infection when the pathogen is quiescent. During ripening of the host, the quiescent biotrophic infection resulting from fruit penetration directly or through wounds becomes active and develops into necrotrophic colonization that manipulates the host's physiological response (Denison et al., 1995; Calvo et al., 2002; Caracuel et al., 2003b; O'Meara et al., 2010). For successful colonization, a pathogen must be able to overcome the host's defenses and initiate attack under prevailing physiological and environmental conditions. During this period, the pathogen must trigger pathogenicity factors that macerate host tissues and release the nutrients required to sustain its development. Since both the host and the pathogen are living entities, the conditions imposed by the host are critical to inducing susceptibility and activating the pathogen quiescent stage. While the mechanism of pH modulation by fungal metabolism has been thoroughly reported, no specific studies have indicated the effect of host pH on fungal pathogenicity. Furthermore fruit ripening and host susceptibility is accompanied by significant sugar accumulation, pH change and many other host changes that

affect fungal pathogenicity and have not been independently studied (Prusky, 1996). In this mini review, we analyze the conditions that modulate the pathogen's initial stages of colonization by pH modulation of the host.

POSTHARVEST PATHOGENS AND pH MODULATION

The ability of postharvest pathogens to alter pH locally was initially described for *Colletotrichum gloeosporioides*, and then extended to some other pathogens, such as *Alternaria alternata*, *Botrytis cinerea*, *Penicillium expansum*, *Penicillium digitatum*, *Penicillium italicum*, *Phomopsis mangiferae*, *Monilinia fructicola*, and *Fusarium oxysporum* (Prusky et al., 2001, 2004; Rollins and Dickman, 2001; Eshel et al., 2002a,b; Manteau et al., 2003; Davidzon et al., 2010; Miyara et al., 2010, 2012).

Ambient alkalization by fungi is achieved by their active secretion of ammonia, which results from the activation of proteases followed by deamination of amino acids (Jennings, 1989; Miyara et al., 2010). Ammonium accumulation has been detected in association with pathogenicity of many *Colletotrichum* species, including *C. gloeosporioides*, *C. acutatum*, *C. higginsianum*, *C. graminicola*, and *C. coccodes* (Alkan et al., 2008; Dieguez-Uribeondo et al., 2008; Miyara et al., 2010; O'Connell et al., 2012), *A. alternata* (Eshel et al., 2002a,b), and *F. oxysporum* (Miyara et al., 2012). The ammonium secreted by these species alkalinizes the host tissue, and its concentration can reach approximately 5 mM, as found in decayed avocado, tomato, and persimmon fruit (Eshel et al., 2002a,b; Alkan et al., 2008; Miyara et al., 2010). In each case with *Colletotrichum* spp., increased ammonium accumulation has been related to enhanced pathogenicity (Alkan et al., 2008, 2009; Miyara et al., 2010). In the case of *A. alternata*, ammonium accumulation led to a 2.4 pH unit increase in several hosts—tomato, pepper, melon, and cherry (Eshel et al., 2002a,b). Interestingly, ammonia accumulation and pH increase were not correlated across host species, suggesting that pH increase in each host depends on a complex interaction that involves the buffer capacity of the tissue, nitrogen, and carbon availability, and the fruit's initial pH (Eshel et al., 2002b). Indeed, fruit differ in their buffer capacity and pH. However, low pH has been found to activate higher ammonia production and secretion in *Colletotrichum* spp. (Kramer-Haimovich et al., 2006; Alkan et al., 2008).

In contrast, other pathogenic fungi, such as *P. expansum*, *P. digitatum*, *P. italicum* (Prusky et al., 2004), *Phomopsis mangiferae* (Davidzon et al., 2010), *Aspergillus niger* (Ruijter et al., 1999), *B. cinerea* (Manteau et al., 2003), and *Sclerotinia sclerotiorum* (Bateman and Beer, 1965) use tissue acidification in their attack. Tissue acidification is enhanced by the secretion of organic acids and/or H⁺ excretion. *S. sclerotiorum* and *B. cinerea* decrease host pH by secreting significant amounts of oxalic acid (OA; Rollins and Dickman, 2001; Manteau et al., 2003); gluconic acid (GLA) is secreted by *Phomopsis mangiferae* (Davidzon et al., 2010), and combinations of gluconic and citric acids are mainly secreted by *Penicillium* (Prusky et al., 2004) and *Aspergillus* (Ruijter et al., 1999). In *P. expansum*, reduced GLA

accumulation has been related to reduced pathogenicity (Barad et al., 2014).

In both cases, alkalization or acidification of the environment by the secretion of ammonia by *Colletotrichum* or organic acid by *Penicillium*, respectively, clearly modulates (activating or repressing) pathogenicity factors. *P. expansum* acidifies the host tissue to pH levels of 3.5–4.0, at which polygalacturonase (*pgl*) transcription is significantly enhanced (Prusky et al., 2004). Similarly, in *C. gloeosporioides*, *pelB* (encoding pectate lyase) is expressed and secreted *in vitro* at pH levels higher than 5.7, similar to the pH values present in decaying tissue (Prusky et al., 1989; Yakoby et al., 2000, 2001). Analysis of endoglucanase 1 gene expression in *A. alternata* showed maximal expression at pH levels higher than 6.0, i.e., values similar to those found in the decayed tissue in which maximal virulence was observed (Eshel et al., 2002b). This suggests that postharvest pathogens modulate the expression of genes contributing to pathogenicity according to environmental pH-inducing conditions.

GENE MODULATION OF FUNGAL PATHOGENICITY FACTORS

What is the mechanism governing fungal modulation of pH-responsive genes? PacC is a transcription factor that regulates gene expression under increasing alkaline conditions. Previous work in the model fungal system *Aspergillus* has suggested that PacC responds to external pH to enable fungal survival under varied pH conditions (Penalva et al., 2008; Selvig and Alspaugh, 2011). Moreover, in fruit fungal pathogens, *pacC* knockout significantly reduces pathogenicity (Miyara et al., 2008; Zhang et al., 2013), suggesting that this transcription factor not only modulates genes for fungal survival, but contributes to pathogenicity as well. The reports that the pathogen may modulate pH by increasing or decreasing the pH of the environment, as described in Section "Postharvest Pathogens and pH Modulation," suggest that PacC shows dual regulation of pathogenicity genes (activation and repression) under pH change. Thus, it is likely that fungi with different pH preferences contain an arsenal of both alkaline- and acid-regulated genes to exploit changing pH conditions. Alkan et al. (2013) characterized alkaline- and acid-expressed genes. Those modulated genes encoded transporters, antioxidants and cell wall-degrading enzymes (CWDEs) (Alkan et al., 2013). Transporters, including those involved in sulfate, potassium, carboxylic acid, and ammonium transport, are likely to be controlled by pH due to the direct pH effect on the charge of inorganic or organic acid ions. The upregulation of transporters may compensate for changes in ionic differences between intracellular and extracellular regions to restore fungal homeostasis under changing pH (Bensen et al., 2004). The pH shifts also seem to affect cellular redox status, as exemplified by changes in antioxidants that include catalase activity and hydrogen peroxide catabolic process. Major components of PacC regulation in *C. gloeosporioides* are CWDE pathogenicity factors. Genes that are shown here to be affected by PacC include *pelB*, and those encoding cellulase, α-mannosidase and 1,4-β-xylanase activity. These findings extend the repertoire

of pH-modulated CWDEs from the previously identified PelB in *C. gloeosporioides*, endoglucanases in *Alternaria alternata* (Yakoby et al., 2000; Prusky et al., 2001, 2004; Eshel et al., 2002a), and polygalacturonases *BcpG1–6* in *B. cinerea* (Wubben et al., 2000; ten Have et al., 2001).

What is interesting to note is that gene families with members of similar functionality were both up- and downregulated by PacC (Alkan et al., 2013). This indicated that similar functions might occur under alkaline and acidic conditions, including CWDE activity. The differential pH regulation of genes with similar activities suggests that they are selectively activated on the basis of their optimal enzymatic pH activity, allowing the fungus to cope with variable pH conditions and make optimal use of the available enzymes.

While PacC has been reported as a gene regulator under alkaline conditions, a recent publication by Barad et al. (2016) showed that the *pacC* transcript can be activated under acidic conditions in *P. expansum*. Electrophoretic mobility shift assay (EMSA) of *P. expansum* PacC, together with antibodies against the different cleaved proteins, showed that PePacC is not protected against proteolytic signaling at pH 4.5 compared to pH 7.0. Moreover, Barad et al. (2016) observed that ammonia is not produced only by alkalinizing pathogens, but by acidifying pathogens as well, under specific growth conditions, at reduced carbon levels and at the leading edge of the colonized area (Barad et al., 2016). Ammonia did not further enhance PacC proteolytic cleavage but did enhance activation of *palF* transcript in the PaL pathway under acidic conditions. The PaL pathway represents a key process regulating PacC cleavage (Diez et al., 2002). Ammonia accumulation in the host environment by the pathogen under acid pH may be a regulatory cue for *pacC* activation, toward accumulation of pathogenicity factors. This process has not been investigated in other acidifying pathogens. However, similar processes may be occurring there as well.

The results obtained under acidification and alkalinization conditions are consistent with the observation that Δ *pacC* mutants of *C. gloeosporioides*, *C. acutatum*, *F. oxysporum*, *P. expansum*, and *S. sclerotiorum* are less virulent than the wild type (Caracuel et al., 2003a; Rollins, 2003; You et al., 2007; Miyara et al., 2008; Zhang et al., 2013; Barad et al., 2014). This suggests the importance of gene regulation by PacC in acidifying and alkalinizing pathogens. It indicates that PacC controls enzyme fine-tuning so that the optimum repertoire will be expressed at any given pH. That is probably how transporters and antioxidants maintain homeostasis and expression of pathogenicity factors for orchestration of the genomic arsenal under changing pH. Hence, at each pH, the fungus is likely to express an optimal gene combination. Those acid-expressed genes are crucial for *P. expansum* and *B. cinerea* pathogenicity because the pathogenicity thrives at low pH. Reciprocally, in fungi that alkalinize the environment, such as *C. gloeosporioides* and *A. alternata*, PacC will be activated only after the fungi raise the surrounding pH. Because fungi are likely to encounter a broad spectrum of initial environmental pH, broad conservation of pH responses may be activated to justify a preferred pH for pathogenicity.

MODULATING THE ACTIVATION OF SMALL SECRETED MOLECULES

The pathogens' ability to secrete pH-regulating molecules, on the one hand, and the transcriptome analysis of PacC-modulated genes, on the other, has revealed that pH may regulate the arsenal of pathogenicity factors. However, previous reports in most postharvest pathogens have shown that a given pathogen has a single, specific lifestyle by which it modulates its host pH, and the same pathogen was usually not found to be able to act in the opposite direction (Table 1). The questions are: how specific are the pH-regulating patterns for each particular fungal species during pathogenicity, and what is the signal that may differentially activate the specific pH modulation during colonization?

One of the significant changes observed in fruit during ripening is an increase in sugar content. Sugars are one of the major constituents responsible for tomato fruit quality, accounting for some 50% of the dry matter (Hulme, 1971; Prusky, 1996). In tomato the total sugar content increases progressively during ripening from the mature-green to red-ripe stage. The sucrose content of bananas also changes from a high concentration of starch to a higher concentration of sucrose during ripening (Hulme, 1971; Prusky, 1996).

In a recent work by Bi et al. (2016), it was reported that postharvest pathogens such as *C. gloeosporioides*, *P. expansum*, *Aspergillus nidulans* and *F. oxysporum* can cause either alkalinization or acidification of their environment. The acidification was induced by all pathogens under carbon excess, e.g., 175 mM sucrose; in contrast, alkalinization occurred under conditions of carbon deprivation, e.g., less than 15 mM sucrose. The carbon source was metabolized by glucose oxidase (GOX2) to GLA, contributing to medium acidification, while catalyzed deamination of non-preferred carbon sources, such as the amino acid glutamate, by glutamate dehydrogenase 2 (GDH2) resulted in the secretion of ammonia. Interestingly, this type of response was similar in *C. gloeosporioides*, *P. expansum*, *A. nidulans*, and *F. oxysporum*, suggesting that carbon response is concentration-dependent rather than pathogen-dependent (Bi et al., 2016) (Figure 1).

Can different host nutritional conditions, such as increasing sugar levels during fruit ripening, modulate the type of small effector molecules secreted by fungi to modulate host pH? Fungi

TABLE 1 | Fungal pathogens and small secreted molecules that modulate pH for the activation of pathogenicity factors.

Pathogens	Alkalizers	Acidifiers
<i>Colletotrichum</i>	Ammonia	
<i>Alternaria</i>	Ammonia	
<i>Fusarium</i>	Ammonia	
<i>Penicillium</i>		Gluconic acid
<i>Phomopsis</i>		Gluconic acid
<i>Monilinia</i>		Gluconic acid
<i>Sclerotinia</i>		Oxalic acid
<i>Botrytis</i>		Oxalic acid

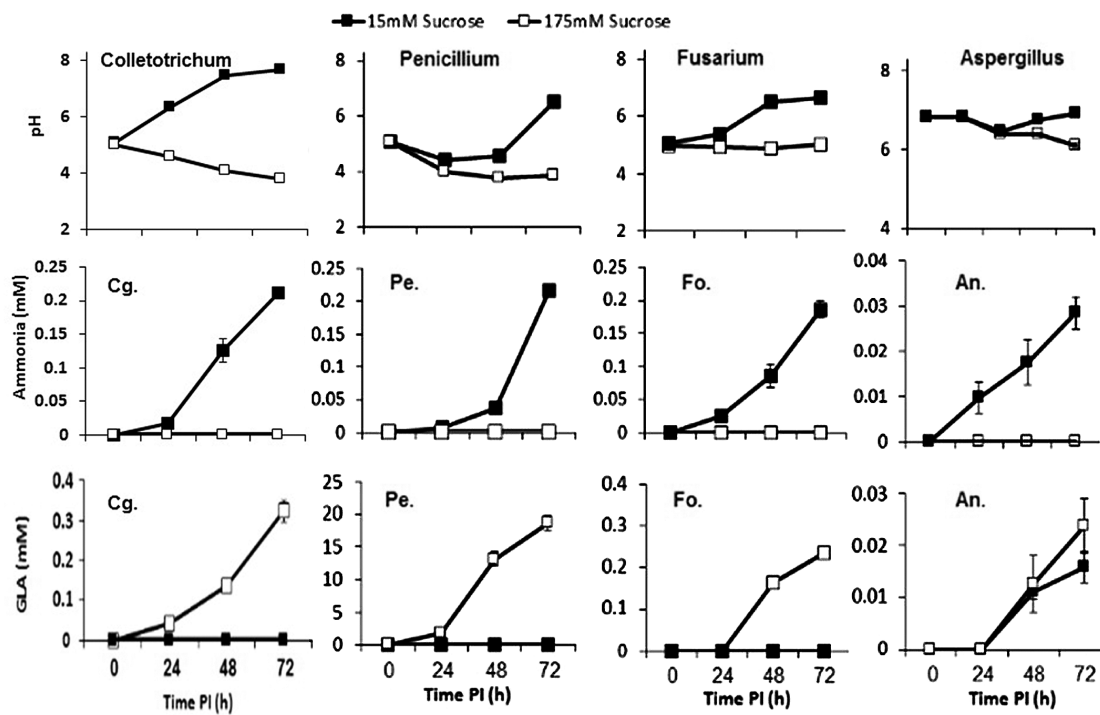


FIGURE 1 | Effects of carbon level on the induction of alkalization or acidification of medium by *Penicillium expansum* (Pe.), *Fusarium oxysporum* (Fo.), *Aspergillus nidulans* (An.), and *Colletotrichum gloeosporioides* (Cg.). Fungal mycelia were grown in primary rich medium for 2–3 days and then transferred to secondary medium containing sucrose at 15 mM (■) or 175 mM (□), adjusted to pH 5, for 72 h (Bi et al., 2016).

possess sensitive gene-regulatory mechanisms to respond to nutrient fluctuations in the environment, as occur in ripening fruit or growing plants. Nutritional availability at the initial stages of germination and growth is certainly different from that during necrotrophic colonization, where nutrients are available in excess (Bi et al., 2016). Lack of nutrient availability at the leading edge of the colonized tissue of ripening fruit induces ammonia accumulation by *C. gloeosporioides* (Miyara et al., 2010). With low sugar concentrations, the importance of glutaminolysis for cell energy supply is clear, and ammonia is generated as a byproduct of the glutaminase and glutamate dehydrogenase synthesis reactions (Newland et al., 1990). Similarly, exposure of *P. expansum* spores to natural acidic conditions on the wounded fruit peel enhances its germination and biomass development (Barad et al., 2012). Under high glucose/sucrose concentrations in ripe fruit, sugar may be oxidized to CO₂ via tricarboxylic acid, with high rates of glycolysis and the production of organic acids that contribute to the secretion of metabolites that decrease host pH (Figure 2). Bi et al. (2016) found accumulation of ammonia by *C. gloeosporioides* and enhanced alkalization during pathogenicity on tomato, whose total sugar content reached 6%. However, in plum fruit, with a sugar concentration of at least 14%, the same pathogen did not accumulate ammonia. On the contrary, in plum, accumulation of GLA by *C. gloeosporioides* was twice as high as in inoculated tomato, suggesting that during host colonization, the balance between ammonia and GLA accumulation by

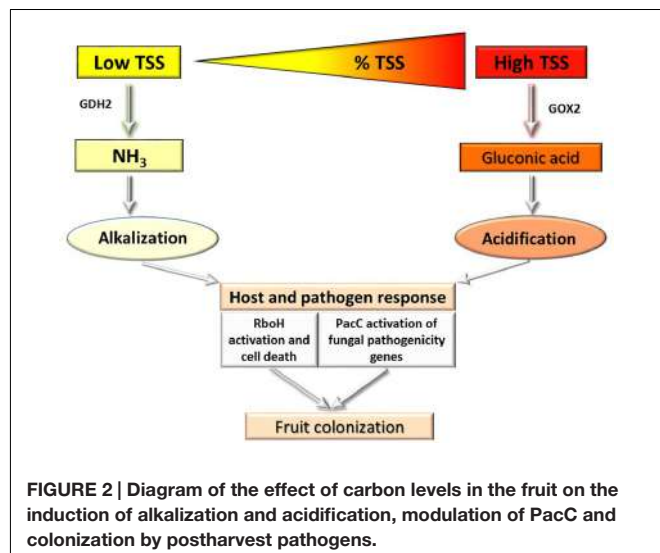


FIGURE 2 | Diagram of the effect of carbon levels in the fruit on the induction of alkalization and acidification, modulation of PacC and colonization by postharvest pathogens.

the same pathogen also determines the final pH of the host environment.

Understanding the genetic pathways that regulate the responses of pathogenic fungi to their environment is paramount to developing effective disease-prevention strategies. Pathogens use specific gene-induction pathways to metabolize a wide range of carbon and nitrogen compounds, but this colonization

is moderated by two global regulatory systems that ensure the preferential utilization of a few favored carbon and nitrogen sources. Carbon catabolite repression (CCR) is a global regulatory mechanism found in a wide range of microbial organisms; it ensures the utilization of preferred carbon sources, such as glucose, over less favorable ones. However, little is known about the components of CCR that interact with pH-modulating nitrogen systems: CCR operates via the negatively acting zinc finger repressor CreA to ensure that glucose is utilized preferentially, by preventing the expression of genes required for the metabolism of less preferred carbon sources (Fernandez et al., 2012, 2014). According to Bi et al. (2016), CreA is induced at high sucrose concentrations where GLA accumulation is induced and ammonia production is repressed. How is this system activated? This question is of high importance for understanding the differential pH response and the consequent expression of genes that modulate

pathogenicity under dynamic pH and colonization conditions (Figure 2).

AUTHOR CONTRIBUTIONS

DP wrote the manuscript and FB contribute to test the effect carbon on *Colletotrichum* and SB contribute to test the effect of carbon on *Penicillium*. JM reviewed and discussed the final revised version.

ACKNOWLEDGMENT

We acknowledge the support of the Binational US–Israel Agricultural Research and Development Fund (BARD and the Israel Science Foundation (ISF) (IS-4773-14)) during several stages of our work.

REFERENCES

- Alkan, N., Davydov, O., Sagi, M., Fluhr, R., and Prusky, D. (2009). Ammonium secretion by *Colletotrichum coccodes* activates host NADPH oxidase activity enhancing host cell death and fungal virulence in tomato fruits. *Mol. Plant Microbe Interact.* 22, 1484–1491. doi: 10.1094/MPMI-22-12-1484
- Alkan, N., Fluhr, R., Sherman, A., and Prusky, D. (2008). Role of ammonia secretion and pH modulation on pathogenicity of *Colletotrichum coccodes* on tomato fruit. *Mol. Plant Microbe Interact.* 21, 1058–1066. doi: 10.1094/MPMI-21-8-1058
- Alkan, N., Meng, X., Friedlander, G., Reuveni, E., Sukno, S., Sherman, A., et al. (2013). Global aspects of pacC regulation of pathogenicity genes in *Colletotrichum gloeosporioides* as revealed by transcriptome analysis. *Mol. Plant Microbe Interact.* 26, 1345–1358. doi: 10.1094/MPMI-03-13-0080-R
- Barad, S., Espeso, E. A., Sherman, A., and Prusky, D. (2016). Ammonia activates pacC and patulin accumulation in an acidic environment during apple colonization by *Penicillium expansum*. *Mol. Plant Pathol.* 17, 727–740. doi: 10.1111/mpp.12327
- Barad, S., Horowitz, S. B., Kobiler, I., Sherman, A., and Prusky, D. (2014). Accumulation of the mycotoxin patulin in the presence of gluconic acid contributes to pathogenicity of *Penicillium expansum*. *Mol. Plant Microbe Interact.* 27, 66–77. doi: 10.1094/MPMI-05-13-0138-R
- Barad, S., Horowitz, S. B., Moscovitz, O., Lichten, A., Sherman, A., and Prusky, D. (2012). A *Penicillium expansum* glucose oxidase-encoding gene, GOX2, is essential for gluconic acid production and acidification during colonization of deciduous fruit. *Mol. Plant Microbe Interact.* 25, 779–788. doi: 10.1094/MPMI-01-12-0002
- Bateman, D., and Beer, S. (1965). Simultaneous production and synergistic action of oxalic acid and polygalacturonase during pathogenesis by *Sclerotium rolfsii*. *Phytopathology* 55, 204–211.
- Bensen, E. S., Martin, S. J., Li, M. C., Berman, J., and Davis, D. A. (2004). Transcriptional profiling in *Candida albicans* reveals new adaptive responses to extracellular pH and functions for Rim101p. *Mol. Microbiol.* 54, 1335–1351. doi: 10.1111/j.1365-2958.2004.04350.x
- Bi, F., Barad, S., Ment, D., Luria, N., Dubey, A., Casado, V., et al. (2016). Carbon regulation of environmental pH by secreted small molecules that modulate pathogenicity in phytopathogenic fungi. *Mol. Plant Pathol.* doi: 10.1111/mpp.12355 [Epub ahead of print].
- Calvo, A. M., Wilson, R. A., Bok, J. W., and Keller, N. P. (2002). Relationship between secondary metabolism and fungal development. *Microbiol. Mol. Biol. Rev.* 66, 447–459. doi: 10.1128/MMBR.66.3.447-459.2002
- Caracuel, Z., Casanova, C., Roncero, M. I., Di Pietro, A., and Ramos, J. (2003a). pH response transcription factor PacC controls salt stress tolerance and expression of the P-Type Na⁺-ATPase Ena1 in *Fusarium oxysporum*. *Eukaryot. Cell* 2, 1246–1252. doi: 10.1128/EC.2.6.1246-1252.2003
- Caracuel, Z., Roncero, M. I., Espeso, E. A., Gonzalez-Verdejo, C. I., Garcia-Maceira, F. I., and Di Pietro, A. (2003b). The pH signalling transcription factor PacC controls virulence in the plant pathogen *Fusarium oxysporum*. *Mol. Microbiol.* 48, 765–779. doi: 10.1046/j.1365-2958.2003.03465.x
- Davidzon, M., Alkan, N., Kobiler, I., and Prusky, D. (2010). Acidification by gluconic acid of mango fruit tissue during colonization via stem end infection by *Phomopsis mangiferae*. *Postharvest Biol. Technol.* 55, 71–77. doi: 10.1016/j.postharvbio.2009.08.009
- Denison, S. H., Orejas, M., and Arst, H. N. Jr. (1995). Signaling of ambient pH in *Aspergillus* involves a cysteine protease. *J. Biol. Chem.* 270, 28519–28522. doi: 10.1074/jbc.270.48.28519
- Dieguez-Uribeondo, J., Forster, H., and Adaskaveg, J. E. (2008). Visualization of localized pathogen-induced pH modulation in almond tissues infected by *Colletotrichum acutatum* using confocal scanning laser microscopy. *Phytopathology* 98, 1171–1178. doi: 10.1094/PHYTO-98-11-1171
- Diez, E., Alvaro, J., Espeso, E. A., Rainbow, L., Suarez, T., Tilburn, J., et al. (2002). Activation of the *Aspergillus* PacC zinc finger transcription factor requires two proteolytic steps. *EMBO J.* 21, 1350–1359. doi: 10.1093/emboj/21.6.1350
- Eshel, D., Lichten, A., Dinoor, A., and Prusky, D. (2002a). Characterization of *Alternaria alternata* glucanase genes expressed during infection of resistant and susceptible persimmon fruits. *Mol. Plant Pathol.* 3, 347–358. doi: 10.1046/j.1364-3703.2002.00127.x
- Eshel, D., Miyara, I., Ailing, T., Dinoor, A., and Prusky, D. (2002b). pH regulates endoglucanase expression and virulence of *Alternaria alternata* persimmon fruit. *Mol. Plant Microbe Interact.* 15, 774–779. doi: 10.1094/MPMI-2002.15.8.774
- Fernandez, J., Marroquin-Guzman, M., and Wilson, R. A. (2014). Mechanisms of nutrient acquisition and utilization during fungal infections of leaves. *Annu. Rev. Phytopathol.* 52, 155–174. doi: 10.1146/annurev-phyto-102313-050135
- Fernandez, J., Wright, J. D., Hartline, D., Quispe, C. F., Madayiputhiya, N., and Wilson, R. A. (2012). Principles of carbon catabolite repression in the rice blast fungus: Tps1, Nmr1-3, and a MATE-family pump regulate glucose metabolism during infection. *PLoS Genet.* 8:e1002673. doi: 10.1371/journal.pgen.1002673
- Hulme, A. C. (1971). *The Biochemistry of Fruits and their Products*. New York, NY: Academic Press.
- Jennings, D. H. (1989). “Some perspectives on nitrogen and phosphorus metabolism in fungi,” in *Nitrogen, Phosphorus and Sulphur Utilization by Fungi*, eds L. Boddy, R. Machant, and D. J. Read (Cambridge: Cambridge University Press), 1–31.
- Kramer-Haimovich, H., Servi, E., Katan, T., Rollins, J., Okon, Y., and Prusky, D. (2006). Effect of ammonia production by *Colletotrichum gloeosporioides* on pelB activation, pectate lyase secretion, and fruit pathogenicity. *Appl. Environ. Microbiol.* 72, 1034–1039. doi: 10.1128/AEM.72.2.1034-1039.2006
- Manteau, S., Abouna, S., Lambert, B., and Legendre, L. (2003). Differential regulation by ambient pH of putative virulence factor secretion by the

- phytopathogenic fungus *Botrytis cinerea*. *FEMS Microbiol. Ecol.* 43, 359–366. doi: 10.1111/j.1574-6941.2003.tb01076.x
- Miyara, I., Shafran, H., Davidzon, M., Sherman, A., and Prusky, D. (2010). pH regulation of ammonia secretion by *Colletotrichum gloeosporioides* and its effect on appressorium formation and pathogenicity. *Mol. Plant Microbe Interact.* 23, 304–316. doi: 10.1094/MPMI-23-3-0304
- Miyara, I., Shafran, H., Haimovich, H. K., Rollins, J., Sherman, A., and Prusky, D. (2008). Multi-factor regulation of pectate lyase secretion by *Colletotrichum gloeosporioides* pathogenic on avocado fruits. *Mol. Plant Pathol.* 9, 281–291. doi: 10.1111/j.1364-3703.2007.00462.x
- Miyara, I., Shnaiderman, C., Meng, X., Vargas, W. A., Diaz-Minguez, J. M., Sherman, A., et al. (2012). Role of nitrogen-metabolism genes expressed during pathogenicity of the alkalinizing *Colletotrichum gloeosporioides* and their differential expression in acidifying pathogens. *Mol. Plant Microbe Interact.* 25, 1251–1263. doi: 10.1094/MPMI-01-12-0017-R
- Newland, M., Greenfield, P. F., and Reid, S. (1990). Hybridoma growth limitations: the roles of energy metabolism and ammonia production. *Cytotechnology* 3, 215–229. doi: 10.1007/BF00365485
- O'Connell, R. J., Thon, M. R., Hacquard, S., Amyotte, S. G., Kleemann, J., Torres, M. F., et al. (2012). Lifestyle transitions in plant pathogenic *Colletotrichum* fungi deciphered by genome and transcriptome analyses. *Nat. Genet.* 44, 1060–1065. doi: 10.1038/ng.2372
- O'Meara, T. R., Norton, D., Price, M. S., Hay, C., Clements, M. F., Nichols, C. B., et al. (2010). Interaction of *Cryptococcus neoformans* Rim101 and protein kinase A regulates capsule. *PLoS Pathog.* 6:e1000776. doi: 10.1371/journal.ppat.1000776
- Penalva, M. A., Tilburn, J., Bignell, E., and Arst, H. N. (2008). Ambient pH gene regulation in fungi: making connections. *Trends Microbiol.* 16, 291–300. doi: 10.1016/j.tim.2008.03.006
- Prusky, D. (1996). Pathogen quiescence in postharvest diseases. *Annu. Rev. Phytopathol.* 34, 413–434. doi: 10.1146/annurev.phyto.34.1.413
- Prusky, D., Gold, S., and Keen, N. T. (1989). Purification and characterization of an endopolysaccharide produced by *Colletotrichum-gloeosporioides*. *Physiol. Mol. Plant Pathol.* 35, 121–133. doi: 10.1016/0885-5765(89)90082-9
- Prusky, D., McEvoy, J. L., Leverentz, B., and Conway, W. S. (2001). Local modulation of host pH by *Colletotrichum* species as a mechanism to increase virulence. *Mol. Plant Microbe Interact.* 14, 1105–1113. doi: 10.1094/MPMI.2001.14.9.1105
- Prusky, D., McEvoy, J. L., Saftner, R., Conway, W. S., and Jones, R. (2004). Relationship between host acidification and virulence of *Penicillium* spp. on apple and citrus fruit. *Phytopathology* 94, 44–51. doi: 10.1094/PHYTO.2004.94.1.44
- Rollins, J. A. (2003). The *Sclerotinia sclerotiorum* pac1 gene is required for sclerotial development and virulence. *Mol. Plant Microbe Interact.* 16, 785–795. doi: 10.1094/MPMI.2003.16.9.785
- Rollins, J. A., and Dickman, M. B. (2001). PH signaling in *Sclerotinia sclerotiorum*: identification of a pacC/RIM1 homolog. *Appl. Environ. Microbiol.* 67, 75–81. doi: 10.1128/AEM.67.1.75-81.2001
- Ruijter, G. J. G., Van De Vondervoort, P. J. I., and Visser, J. (1999). Oxalic acid production by *Aspergillus niger*: an oxalate-non-producing mutant produces citric acid at pH 5 and in the presence of manganese. *Microbiology* 145, 2569–2576. doi: 10.1099/00221287-145-9-2569
- Selvig, K., and Alspaugh, J. A. (2011). pH response pathways in fungi: adapting to host-derived and environmental signals. *Mycobiology* 39, 249–256. doi: 10.5941/MYCO.2011.39.4.249
- ten Have, A., Breuil, W. O., Wubben, J. P., Visser, J., and Van Kan, J. A. L. (2001). *Botrytis cinerea* endopolygalacturonase genes are differentially expressed in various plant tissues. *Fungal Genet. Biol.* 33, 97–105. doi: 10.1006/fgb.2001.1269
- Wubben, J. P., Ten Have, A., Van Kan, J. A. L., and Visser, J. (2000). Regulation of endopolygalacturonase gene expression in *Botrytis cinerea* by galacturonic acid, ambient pH and carbon catabolite repression. *Curr. Genet.* 37, 152–157. doi: 10.1007/s002940050022
- Yakoby, N., Beno-Moualem, D., Keen, N. T., Dinoor, A., Pines, O., and Prusky, D. (2001). *Colletotrichum gloeosporioides* pelB is an important virulence factor in avocado fruit-fungus interaction. *Mol. Plant Microbe Interact.* 14, 988–995. doi: 10.1094/MPMI.2001.14.8.988
- Yakoby, N., Kobiler, I., Dinoor, A., and Prusky, D. (2000). pH regulation of pectate lyase secretion modulates the attack of *Colletotrichum gloeosporioides* on avocado fruits. *Appl. Environ. Microbiol.* 66, 1026–1030. doi: 10.1128/AEM.66.3.1026-1030.2000
- You, B. J., Choquer, M., and Chung, K. R. (2007). The *Colletotrichum acutatum* gene encoding a putative pH-responsive transcription regulator is a key virulence determinant during fungal pathogenesis on citrus. *Mol. Plant Microbe Interact.* 20, 1149–1160. doi: 10.1094/MPMI-20-9-1149
- Zhang, T., Sun, X., Xu, Q., Candelas, L. G., and Li, H. (2013). The pH signaling transcription factor PacC is required for full virulence in *Penicillium digitatum*. *Appl. Microbiol. Biotechnol.* 97, 9087–9098. doi: 10.1007/s00253-013-5129-x

Conflict of Interest Statement: The authors declare that the research was conducted in the absence of any commercial or financial relationships that could be construed as a potential conflict of interest.

Copyright © 2016 Prusky, Bi, Moral and Barad. This is an open-access article distributed under the terms of the Creative Commons Attribution License (CC BY). The use, distribution or reproduction in other forums is permitted, provided the original author(s) or licensor are credited and that the original publication in this journal is cited, in accordance with accepted academic practice. No use, distribution or reproduction is permitted which does not comply with these terms.



Inter-Species Comparative Analysis of Components of Soluble Sugar Concentration in Fleshy Fruits

Zhanwu Dai^{1*}, Huan Wu¹, Valentina Baldazzi², Cornelis van Leeuwen³, Nadia Bertin², Hélène Gautier², Benhong Wu⁴, Eric Duchêne⁵, Eric Gomès¹, Serge Delrot¹, Françoise Lescourret² and Michel Génard²

¹ EGFV, Bordeaux Sciences Agro, INRA, Université de Bordeaux, Villenave d'Ornon, France, ² INRA, UR1115, Plantes et Systèmes de Culture Horticoles, Avignon, France, ³ Bordeaux Sciences Agro, ISVV, UMR 1287 EGFV, Villenave d'Ornon, France, ⁴ Institute of Botany – Chinese Academy of Sciences, Beijing, China, ⁵ INRA, UMR 1131 SVQV, Colmar, France

OPEN ACCESS

Edited by:

Antonio Granell,
Consejo Superior de Investigaciones
Científicas, Spain

Reviewed by:

Li-Qing Chen,
Carnegie Institution for Science,
USA

Manpreet Singh Katari,
New York University, USA

*Correspondence:

Zhanwu Dai
zhanwu.dai@bordeaux.inra.fr

Specialty section:

This article was submitted to
Plant Physiology,
a section of the journal
Frontiers in Plant Science

Received: 12 February 2016

Accepted: 28 April 2016

Published: 19 May 2016

Citation:

Dai Z, Wu H, Baldazzi V, van Leeuwen C, Bertin N, Gautier H, Wu B, Duchêne E, Gomès E, Delrot S, Lescourret F and Génard M (2016) Inter-Species Comparative Analysis of Components of Soluble Sugar Concentration in Fleshy Fruits. *Front. Plant Sci.* 7:649.
doi: 10.3389/fpls.2016.00649

The soluble sugar concentration of fleshy fruit is a key determinant of fleshy fruit quality. It affects directly the sweetness of fresh fruits and indirectly the properties of processed products (e.g., alcohol content in wine). Despite considerable divergence among species, soluble sugar accumulation in a fruit results from the complex interplay of three main processes, namely sugar import, sugar metabolism, and water dilution. Therefore, inter-species comparison would help to identify common and/or species-specific modes of regulation in sugar accumulation. For this purpose, a process-based mathematical framework was used to compare soluble sugar accumulation in three fruits: grape, tomato, and peach. Representative datasets covering the time course of sugar accumulation during fruit development were collected. They encompassed 104 combinations of species (3), genotypes (30), and growing conditions (19 years and 16 nutrient and environmental treatments). At maturity, grape showed the highest soluble sugar concentrations (16.5–26.3 g/100 g FW), followed by peach (2.2 to 20 g/100 g FW) and tomato (1.4 to 5 g/100 g FW). Main processes determining soluble sugar concentration were decomposed into sugar importation, metabolism, and water dilution with the process-based analysis. Different regulation modes of soluble sugar concentration were then identified, showing either import-based, dilution-based, or import and dilution dual-based. Firstly, the higher soluble sugar concentration in grape than in tomato is a result of higher sugar importation. Secondly, the higher soluble sugar concentration in grape than in peach is due to a lower water dilution. The third mode of regulation is more complicated than the first two, with differences both in sugar importation and water dilution (grape vs. cherry tomato; cherry tomato vs. peach; peach vs. tomato). On the other hand, carbon utilization for synthesis of non-soluble sugar compounds (namely metabolism) was conserved among the three fruit species. These distinct modes appear to be quite species-specific, but the intensity of the effect may significantly vary depending on the genotype and management practices. These results provide novel insights into the drivers of differences in soluble sugar concentration among fleshy fruits.

Keywords: dilution, fruit metabolism, grape, peach, sugar importation, tomato

INTRODUCTION

Fresh fruits (such as grape, tomato, and peach) and their processed products (e.g., wine from grape) have a major economical importance. Fresh fruits also play an essential role in the composition of a healthy diet. The composition of fruits largely determines their sensory properties, their nutritional value, and hence, consumer preference and the final profit for fruit growers. Among other compounds, soluble sugars are one of the major determinants of fruit quality. They directly impact the sweetness and taste of fresh fruits and provide precursors for the synthesis of other quality-related compounds, such as organic acids, anthocyanins, and aroma compounds. They affect alcohol content after fermentation in processed products (e.g., wine). For example, consumers prefer peaches with a high (~9.5–10%) value of total soluble solids (TSSs, mainly soluble sugars) rather than fruits with a lower TSS (<8%; Grechi et al., 2008). On the other hand, a too high soluble sugar content (TSS over 30%) in grape leads to a high alcohol level in wines, which may be detrimental for the perception of wine quality and the health of wine consumers (Duchêne and Schneider, 2005). Therefore, modulating fruit sugar concentration to an attractive and desirable level for the consumers has scientific interest and agronomical relevance.

Soluble sugar concentration as well as sugar composition show large variations across species (Coombe, 1976). For example, grape has a very high soluble sugar concentration (~2 mmol/gFW) compared to other fleshy fruits (Coombe, 1992), while peach and tomato has, respectively, moderate (~0.4 mmol/gFW; Quilot et al., 2004) and low (~0.15 mmol/gFW) soluble sugar concentration (Prudent et al., 2011; Biais et al., 2014). The form of soluble sugars stored in fruits can be hexoses (glucose and fructose) dominated with trace sucrose (most of grape and tomato varieties) or sucrose dominated with moderate levels of hexoses (peach and few specific varieties of grape and tomato) and low levels of sorbitol (peach; Desnoues et al., 2014).

Soluble sugar concentration in fruit is the result of several processes. First, photoassimilates are imported into the fruit, following phloem unloading. Different phloem unloading mechanisms exist (Lalonde et al., 2003; Kühn and Grof, 2010) and their coordination follows specific developmental patterns depending on the species (Ruan and Patrick, 1995; Zhang et al., 2006; Zanon et al., 2015). Second, imported photoassimilates are metabolized in apoplasm, symplasm or vacuole and partly used to synthesize cell walls, organic acids or storage compounds (e.g. starch in tomato). Although sugar metabolism shares similar reaction pathways associated with common enzymes, such as sucrose synthase (SuSy), sucrose phosphate synthase (SPS) and invertase (INV), specificities exist for individual species depending on the nature of accumulated soluble sugars (e.g., sorbitol for peach). Moreover, the evolution of enzymes activities over fruit development may significantly differ among species, whereas it appears pretty stable among genotypes of the same species (Biais et al., 2014; Desnoues

et al., 2014). Last but not least, dilution by water also plays an important role in determining the concentration of soluble sugars (Génard et al., 2014) and it is known to be largely affected by environmental conditions or management practices. For example, a negative correlation is usually found between sugar content and irrigation levels (Kobashi et al., 2000; Castellarin et al., 2007; Sadras and McCarthy, 2007; Ripoll et al., 2016). Therefore, any difference in soluble sugar concentration among species or among genotypes within a given species may result from the different contributions of sugar importation, sugar metabolism, and/or dilution, during fruit development.

Considering that the basic processes determining soluble sugar concentration are similar, multispecies comparison may help to understand whether the main control levers of soluble sugar concentration are species-specific or follow a species-overarching manner. However, multispecies comparison among fruits is largely hampered by (a) the complex nature of sugar accumulation as affected by the genotype \times environment interactions and (b) the lack of proper tools to integrate information into a common framework to make comparable the results from different species. Recently, Klie et al. (2014) identified some conserved dynamics of metabolic processes across species during fruit development with a generalized principal component approach (STATIS). STATIS can capture similarities and differences between multiple tables containing metabolite data during different fruit development and ripening stages, providing a way of multispecies comparison of metabolism in fruits (Klie et al., 2014). However, as other statistical analysis approaches, STATIS analyzes the metabolite profiles but cannot provide indications on biological processes that may affect these metabolite profiles.

Process decomposition may serve as an alternative framework for multispecies comparison. It can dissect a complex trait into processes more physiological relevant and stable over changing environments (Bertin et al., 2010). A number of frameworks indeed have been developed that describe the temporal evolution of soluble sugar concentration within the fruit and have been used to evaluate the contributions of sugar importation, metabolism and water dilution on changes in soluble sugar concentration, under contrasted environment or genotypes, for a panel of species (Génard et al., 2003; Quilot et al., 2004; Dai et al., 2009; Prudent et al., 2011). However, inter-species comparison by using this approach has never been attempted so far.

Inspired by these studies, we propose here to use process-based decomposition as a tool for multispecies comparison. Based on experimental data, the contribution of sugar importation, metabolism and water dilution on soluble sugar concentration was computed all over fruit development and used to analyze the drivers causing the inter-species variability in soluble sugar concentration, and to identify similarities and differences among three fruit species. A particular attention was also devoted to investigate genotypic variability and the effect of environment and management practices on the regulation of soluble sugar concentration.

MATERIALS AND METHODS

Data sources

Developmental profiles of fruit flesh fresh weight (FW), dry weight (DW), and soluble sugar concentration (SC) were collected for three fruit species (grape, tomato, and peach) from both published literatures and unpublished data (Supplementary Table S1). In total, there were 104 different sugar accumulation profiles, covering 30 genotypes and various growing conditions (19 years and 17 nutrient and environmental treatments; Supplementary Table S1). Grape and peach datasets were mainly focused on the second rapid growth phase, ranging from 30 to 140 days after flowering (DAF), with 5–12 sampling points at regular intervals of 7–15 days in each profile. Tomato datasets covered the full fruit development stages, ranging from 5 to 70 DAF, with 7–14 sampling points at regular intervals of 5–10 days. Crop load (an agricultural term describing the ratio between leaf surface and number of fruits for a fruit tree) treatments that can modulate the source-sink relationships were imposed to some genotypes of peach and tomato. In addition, the truss (or the bunch) position of fruits within a plant was also included in the analysis for tomato. At least three biological replicates were used at each sampling date. The three fruit species were chosen for the analysis because (1) their data are collected within a long-term collaboration network where protocols and analysis were rather standardized with various genotypes and years; (2) these three fruit species are representative of drupes, berry and fleshy fruits as well as non-climacteric and climacteric fruits, making their comparison meaningful from a biological perspective.

Flesh FW was measured by weighing whole fruit, and then seed weight was excluded for peach (Génard et al., 2003); jelly and seed were excluded for tomato in Prudent et al. (2009) but whole fruit were considered in other studies of cherry tomato and tomato (Bertin et al., 2009); an average proportion of 12.5% of seed and skin weight in grape berry was excluded (Dai et al., 2009). Flesh DW was obtained from FW by subtracting flesh water content (WC). The WC of peach and tomato were obtained by drying a pre-weighed piece of fresh fruit. For grape, the WC was empirically determined as a function of soluble sugar concentration (Garcia de Cortazar-Atauri et al., 2009). Soluble sugars were measured either with enzymatic method (Génard et al., 2003; Prudent et al., 2009) or HPLC method (Wu et al., 2012). For some grape samples, TSSs (^oBrix) were determined using a PAL-1 portable electronic refractometer and an empirical relationship was then applied to transform ^oBrix into hexose concentration (OIV, 2009). Total soluble sugar concentration was obtained by summing up all the sugar forms accumulated in the fruit, including sucrose, glucose, fructose, and sorbitol as described by Quilot et al. (2004). To make data comparable, all FW and DW were expressed in gram, and soluble sugar concentration in g sugar/100 g FW.

Process-Based Comparative Approach

As described in Quilot et al. (2004), carbon arrives into the fruit as sugars, via the phloem. In the flesh, part of this flow of carbon is used as substrates for respiratory pathways. The remaining

carbon is used partly for soluble sugar synthesis and partly for synthesis of other carbohydrate compounds (e.g., starch, acids, structural carbohydrates, and proteins). Accordingly, the variation in soluble sugar concentration (SC) in the fruit results from the balance among three different processes, the net sugar import rate from the plant to the fruit (import rate – respiration rate, u), the rate of metabolic consumption of soluble sugars to synthesize other compounds (m) and the rate of dilution (d) as the volume of the fruit increases:

$$\frac{dSC}{dt} = u(t) + m(t) + d(t) \quad (1)$$

The net sugar uptake rate u (g/100 g/day) can be calculated directly from dry mass variation of the fruit as done by Génard et al. (2003):

$$u = \frac{100\gamma_{DW}}{\gamma_{sugar}FW} \frac{dDW}{dt} \quad (2)$$

where γ_{DW} represents the carbon concentration of the flesh (gC per gram of dry mass) and γ_{sugar} is the mean carbon content of sugars (gC/g sugars).

In an analogous way, the dilution rate d describes the soluble sugar concentration loss caused by fruit volume increases and can be derived from fresh mass variation as in Génard et al. (2003):

$$d = \frac{SC}{FW} \frac{dFW}{dt} \quad (3)$$

Note that both u , m , and d components can be time, genotype and environment dependent.

By integrating all over fruit development, the overall contribution of each process, for a given genotype and environment, can be defined at fruit maturity as:

$$U = \int_{t_0}^{t_m} u(t)dt, M = \int_{t_0}^{t_m} m(t)dt, D = \int_{t_0}^{t_m} d(t)dt \quad (4)$$

By definition,

$$\Delta SC = SC(t_m) - SC_0 = U + M + D$$

where $SC(t_0)$ and $SC(t_m)$ are the total soluble sugar concentrations at the beginning of experiment and at maturity, respectively.

To calculate the three components (U, M, and D), observed developmental curves of FW, DW, and SC were fitted by local regression to compute a daily value. $\frac{dFW}{dt}$ and $\frac{dDW}{dt}$ were then calculated by derivation of daily FW and DW. Once U and D determined from Eq. 4, the total metabolic component M can be computed from the difference $M = SC(t_m) + SC(t_0) - U - D$, providing an estimate of the overall sugar turnover during fruit development.

Statistical Analysis

The data analysis was conducted using the R Statistical Computing Environment (R Development Core Team, 2010). The local regression of FW, DW, and SC were obtained with the “loess” function and the derivation of FW and DW with

the “diff” function. The differential equations were numerically integrated using the Euler method with a 1-day time step.

Statistical methods suitable for unbalanced one-way factorial dataset are needed to determine if one variable is significantly different among fruit species. To this end, “gao_cs” function of “nparcomp” package was applied to conduct a non-parametric multiple comparison (Baudrit et al., 2015). Principal component analysis (PCA) was performed on mean-centered and scaled data with “dudi.pca” function of “ade4” package (Dray and Dufour, 2007), in order to compare three drivers of soluble sugar concentration among fruit species. PCA was first made by using the three drivers of sugar concentration (namely the U, M, D), and then FW, DW, and SC at maturity were projected as non-active variables. In this way, one can assess the discriminations of different fruit species, genotypes, and growth conditions by the three components and compare the prediction quality of the PCs identified from the active dataset in relation to the non-active dataset.

RESULTS

Fruit Size and Soluble Sugar Concentration at Maturity

Based on a pre-analysis, cherry tomato was found to behavior differently from normal tomato in both final sugar concentration and contributions of the three main components. Therefore, cherry tomato was treated separately in the following sections, although it belongs to the same species as tomato. The FW of fruits at maturity varied among fruit species, showing peach \geq tomato > cherry tomato > grape, in the studied dataset (Figure 1). Fruit species also showed a large diversity in soluble sugar concentration at maturity, with grape having the highest soluble sugar concentrations (16.5 to 26.3 g/100 g FW), followed by peach (2.2 to 20 g/100 g FW), cherry tomato (3.5 to 6.1 g/100 g FW), and tomato (1.4 to 5 g/100 g FW; Figure 1). Comparing FW and soluble sugar concentration, it is clear that the smallest fruit species (grape) had the highest soluble sugar concentration. However, peach weight is higher than cherry tomato and tomato but it had a higher concentration of soluble sugars.

Dynamics of Fruit Growth and Soluble Sugar Concentration Over Fruit Development

It is well-known that grape and peach fruits have a double-sigmoid growth curve (DeJong and Goudriaan, 1989; Coombe and McCarthy, 2000), while tomato fruit has a single-sigmoid growth curve (Bertin et al., 2009). In the present dataset, developmental profiles of grape and peach covered mainly the second rapid growth stage, while those of tomato covered almost the full developmental stages (Figure 2). As a consequence, during the studied period, fresh and DWs of all the three fruits exhibited similar dynamics: remaining at low level at beginning, then increasing sharply, and reaching a plateau around maturity (Figures 2A–H). Despite these similarities, soluble sugar concentration showed large differences

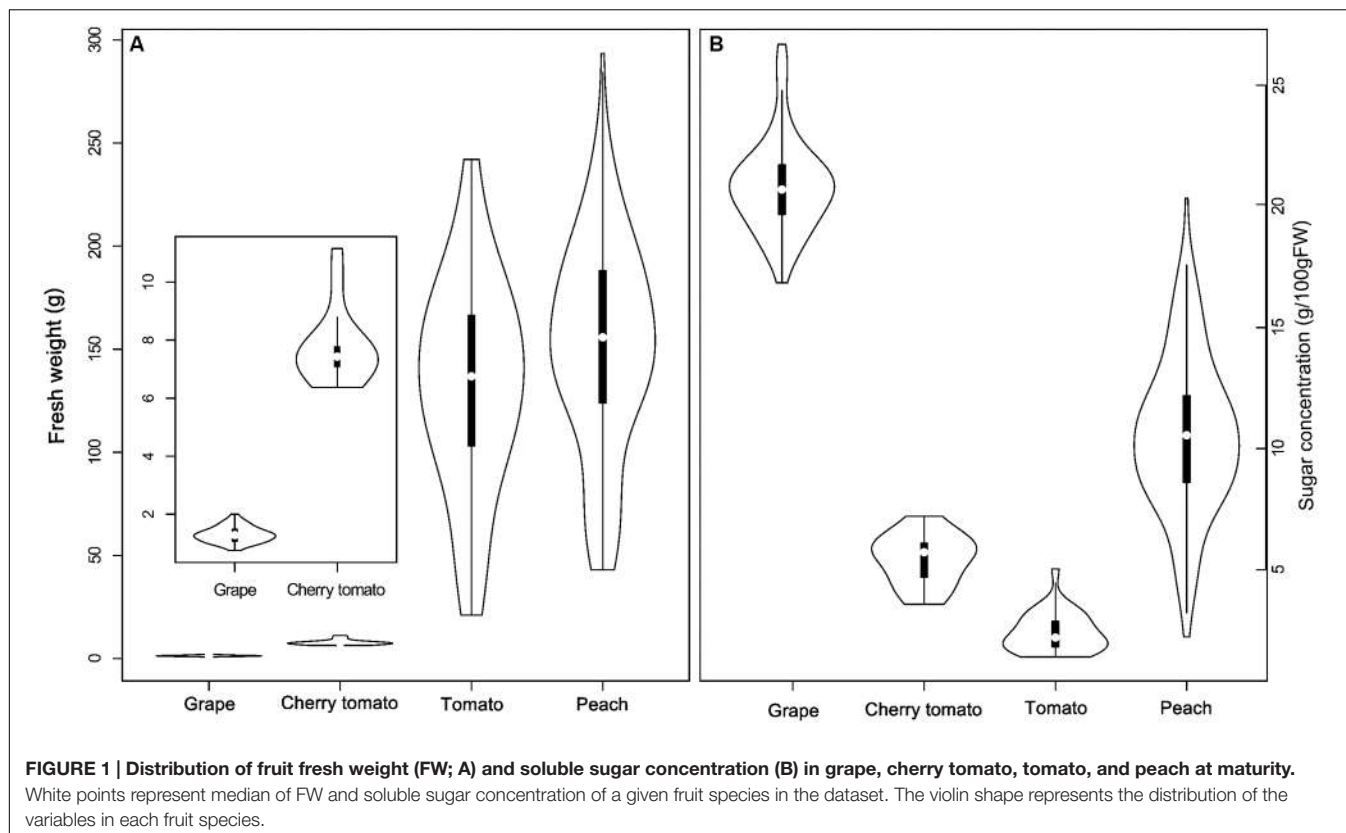
in their developmental dynamics. Soluble sugar concentration of grape increased strongly from veraison on, and reached a plateau approaching maturity (Figure 2I); Cherry tomato showed a continuous and exponential increase in soluble sugar concentration up to the maturity (Figure 2J); tomato and peach had much smaller fluctuations of sugar accumulation, even exhibited decreases in soluble sugar concentration over fruit development (Figures 2K,L).

Contributions of Sugar Importation, Metabolism, and Dilution on Soluble Sugar Concentration among Different Fruit Species

To gain insights into the potential drivers underlying the differences in soluble sugar concentration among the three fruit species (Figure 1), developmental profiles in Figure 2 were subjected into the process-based analysis to decompose soluble sugar concentration into three processes, namely sugar importation, metabolism and water dilution (Figure 3). Moreover, development stages were normalized, with flowering to be 0 and maturity to be 1, to make the developmental profiles comparable among fruit species (Figures 3A–D). After this normalization, it is clear that most of the developmental profiles spanned from 40% maturity to 100% maturity for the three fruit species, and therefore, cumulative contribution of the three processes was calculated over this period (Figures 3E–H). To take into account the variation in duration between 40 and 100% maturity, the cumulative contribution was further divided by the duration (days) of the chosen period for each condition (Figures 3E–H).

Over the considered developmental stages, peach showed a distinct dynamics of sugar importation, metabolism, and water dilution, in comparison with those of grape, cherry tomato, and tomato (Figures 3A–D). In grape, cherry tomato and tomato, higher sugar importation, metabolism, and water dilution were observed at early developmental stages, and they simultaneously approached to zero at maturity (Figures 3A–C). On the other hand, the three processes of peach were low around 40% of maturity, then peaked around 75% of maturity, and approached to zero thereafter (Figure 3D). Interestingly, the metabolism changed from negative value to positive value around maturity, particularly for cherry tomato (Supplementary Figure S1B) and in some cases for the other fruits (Supplementary Figures S1A,C,D). In addition, dilution also changed from negative to positive value around maturity for grape (Supplementary Figure S1A).

The absolute values of mean cumulative contributions of sugar importation, metabolism, and water dilution were of the same order of magnitude regardless of the species over the period of 40% maturity to 100% maturity (Figures 3E–H). The sugar importation was always the most important component with a contribution 2–3 times that of metabolism or dilution. Sugar importation was higher in grape and peach than in cherry tomato and tomato. Metabolism did not show significant differences among the three fruit species. Water dilution was the highest in peach, followed by grape and tomato, and lowest in cherry tomato. Based on these statistical results, the modes causing



differences in soluble sugar concentration among fruit species were then summarized in **Figure 4**. Firstly, the higher soluble sugar concentration in grape than in tomato is a result of higher sugar importation, while metabolism and water dilution were the same in both fruit species. Secondly, the higher soluble sugar concentration in grape than in peach is a result of lower water dilution. The third mode of regulation is more complicated than the first two, with differences both in sugar importation and water dilution (grape vs. cherry tomato; cherry tomato vs. peach; peach vs. tomato). In this mode, a higher sugar importation was always followed with a higher water dilution (grape vs. cherry tomato; peach vs. tomato), and *vice versa* (cherry tomato vs. peach). Therefore, the relative extent of differences in water dilution and sugar importation led to a higher soluble sugar concentration. A fourth potential mode, namely a higher sugar importation with a lower water dilution, was not observed in the present dataset.

PCA of Genotypes and Growing Conditions

In addition to the inter-species variability, genotypic and environmental variability was further analyzed by PCA. Mean cumulative values of sugar importation, metabolism and dilution were used to discriminate different genotypes and growing conditions (**Figure 5**). Results are plotted on the first two axes, which account for more than 90% of variability. The first axis mainly describes the effect of sugar importation and metabolism, whereas the second one deals with water dilution. Results confirm

a reduction of import and, to a less extent, metabolism for cherry tomato, although there is a common tendency in large tomato too, as shown in **Figure 3**. For all species, a strong genotypic and environmental variability is present, especially along the first principal component (metabolism and sugar importation).

A closer look to individual genotypes and growing conditions, for each species, shows that PCA was able to discriminate a few phenotypic classes. White and red grapes were well-separated, with white grapes being characterized by an increased dilution term and a higher importation rate (**Figure 5C**), which is consistent with their larger fresh mass. Red grapes showed a high variability in the metabolic and import component (PC1), with the Cabernet-Sauvignon generally being the less sweet due to low import. Moreover, different genotypes showed varying environmental sensitivity, with Merlot being the most sensitive one to vintages in comparison with Cabernet-Sauvignon and Cabernet franc (**Figure 5C**).

Crop load exerted its effect on soluble sugar concentration using dilution and sugar importation as the main lever in peach (**Figure 5E**). A stable gradient of dilution was visible for Suncrest genotype conducted under three levels of load, in two different years. Interestingly, the dilution effect was stronger at low load but carbon content (and soluble sugar concentration) tended to be higher, meaning that carbon import increases faster than dilution. The same is true for the nectarine Zephir, although in this case the effect on dilution is accompanied by a strong change in sugar importation (**Figure 5E**).

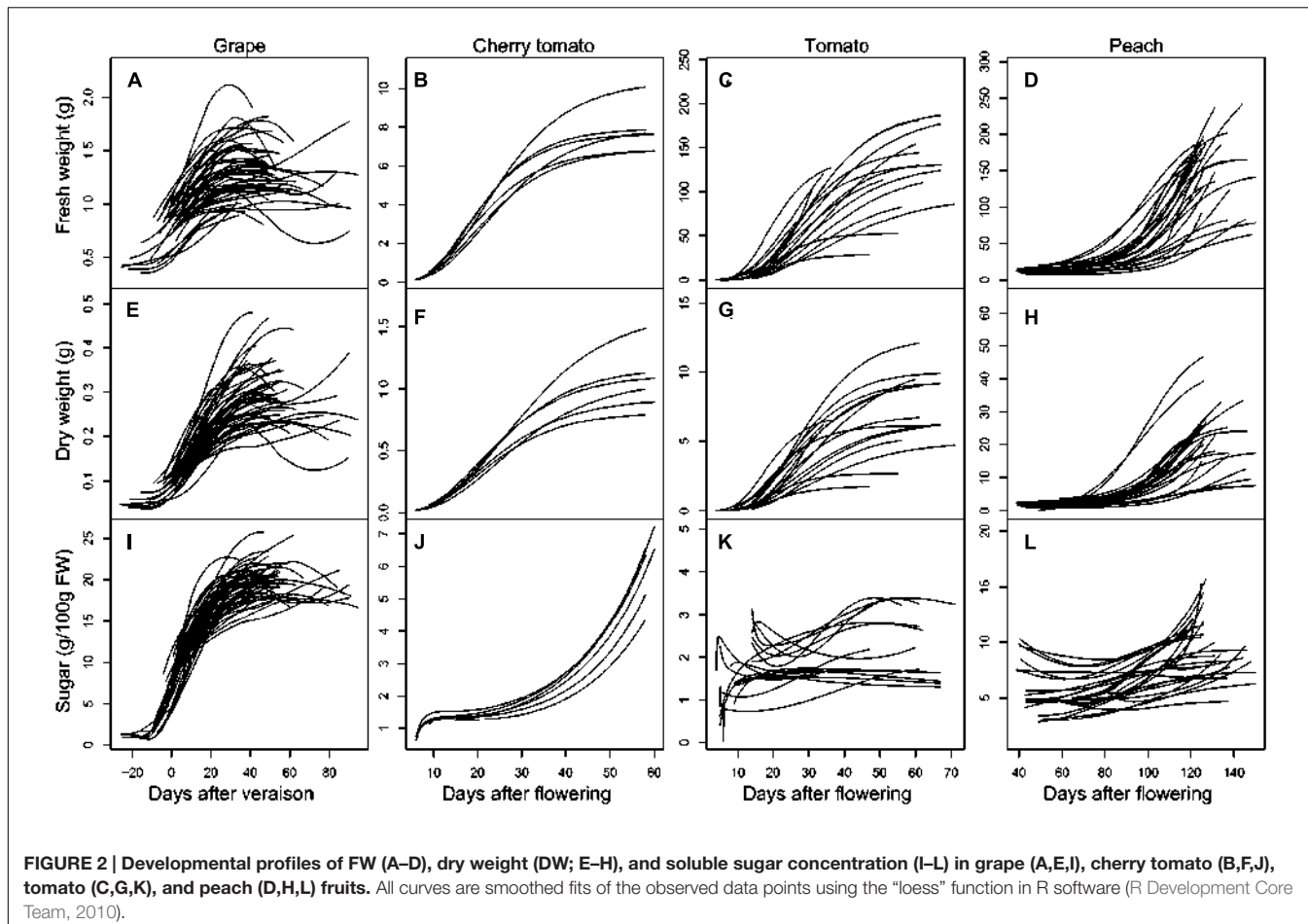


FIGURE 2 | Developmental profiles of FW (A–D), dry weight (DW; E–H), and soluble sugar concentration (I–L) in grape (A,E,I), cherry tomato (B,F,J), tomato (C,G,K), and peach (D,H,L) fruits. All curves are smoothed fits of the observed data points using the “loess” function in R software (R Development Core Team, 2010).

In tomato, as in peach, crop load reduced fruit fresh mass but the mechanism may differ according to genotypes (Figure 5D). In cherry tomatoes, the impact of crop load was small and essentially acted by increasing slightly the metabolism. In large fruit genotypes, on the contrary, the impact of load appeared more important (except for Levovil), increasing dilution or decreasing slightly the metabolism.

DISCUSSION

Inter-species variability in soluble sugar concentration of grape, tomato, and peach was investigated by using a process-based framework, which decomposes soluble sugar concentration into three potential drivers (sugar importation, metabolism, and water dilution). Various datasets were collected and the developmental profiles of FW, DW, and soluble sugar concentration represented well the characteristics of each species described in the literature (Ho et al., 1987; Coombe and McCarthy, 2000; Génard et al., 2003), providing a solid base for our inter-species comparison.

The dynamics of the three processes (namely sugar importation, metabolism, and water dilution) grouped non-climacteric grape and climacteric tomato fruits together and

discriminated them from the climacteric peach fruits (Figure 3). This suggests that the three processes related to soluble sugar concentration are not tightly affected by ethylene-associated events that characterize the two categories of fruits. In fact, Klie et al. (2014) compared the dynamics of metabolite concentration over development in non-climacteric strawberry and pepper fruits as well as climacteric peach and tomato fruits, and they also found that some cultivars of tomato were grouped with non-climacteric fruits and the others with climacteric peach fruit. Despite differences in respiration burst at the onset of ripening, cherry tomato and tomato are different from grape and peach by accumulating transiently starches during early development stages, which are then degraded to form soluble sugars around maturity (Schaffer and Petreikov, 1997; Luengwilai and Beckles, 2009; Petreikov et al., 2009). The transient accumulation of starches in cherry tomato and tomato is most likely reflected by the much higher levels of both sugar importation and metabolism during the early developmental stages (10% maturity to 40% maturity). On the other hand, positive values of metabolism were observed around maturity in cherry tomato and tomato (Figures 3B,C and Supplementary Figures S1B,C), and they may be a result of the starch degradation when approaching maturity. It is also worth noting that a positive value of “water dilution”

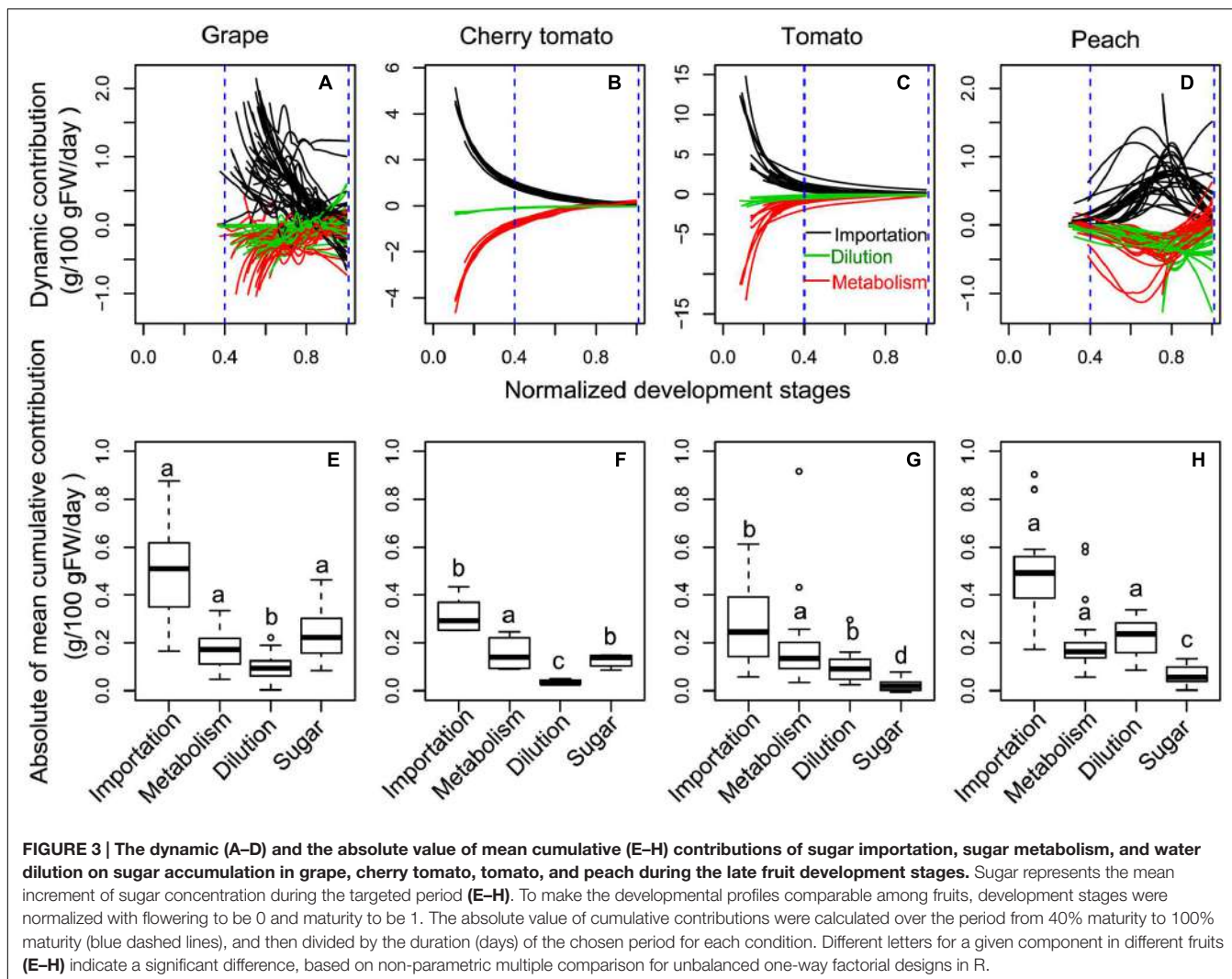
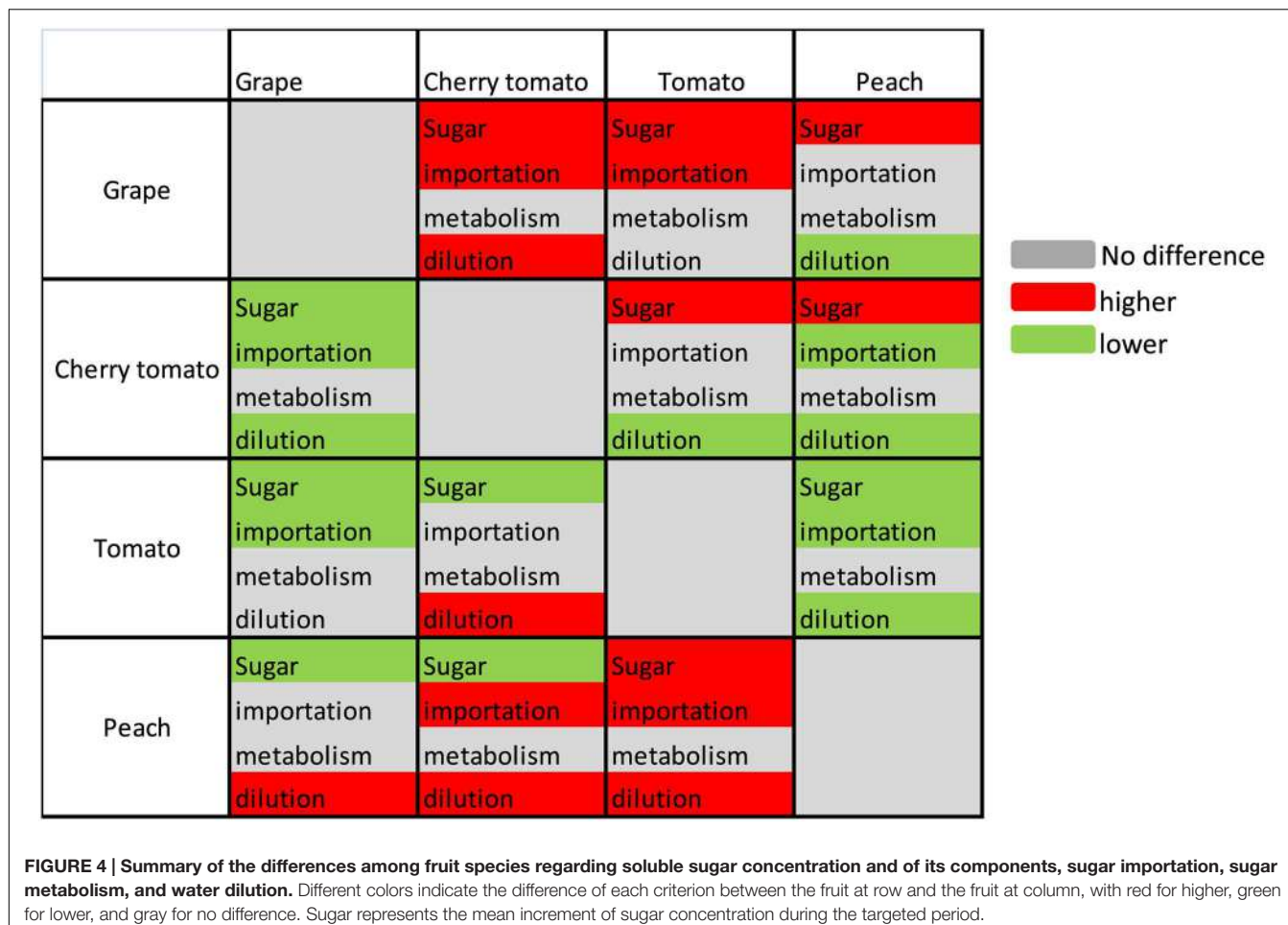


FIGURE 3 | The dynamic (A–D) and the absolute value of mean cumulative (E–H) contributions of sugar importation, sugar metabolism, and water dilution on sugar accumulation in grape, cherry tomato, tomato, and peach during the late fruit development stages. Sugar represents the mean increment of sugar concentration during the targeted period (E–H). To make the developmental profiles comparable among fruits, development stages were normalized with flowering to be 0 and maturity to be 1. The absolute value of cumulative contributions were calculated over the period from 40% maturity to 100% maturity (blue dashed lines), and then divided by the duration (days) of the chosen period for each condition. Different letters for a given component in different fruits (E–H) indicate a significant difference, based on non-parametric multiple comparison for unbalanced one-way factorial designs in R.

indicates a positive effect on soluble sugar concentration due to fruit dehydration and this was evident in most of grape berries (Figure 3A and Supplementary Figure S1A). In fact, grape berries are known to be vulnerable to dehydration around maturity, which concentrates soluble sugar concentration without necessarily modifying total sugar quantity in the berry (Tilbrook and Tyerman, 2009). Based on the dynamic analysis, it is clear that the process-based decomposition can capture inter-species features related to soluble sugar concentration.

Our analysis shows the existence of different patterns for soluble sugar concentration control, either import-based, dilution-based, or import-dilution coupled (Figure 4). On the other hand, conserved metabolic rate was observed among the three fruit species for the consumption of imported carbon for synthesis of other compounds than sugars (e.g., starch, organic acids, structural carbohydrates, and proteins). Sugar importation is well-regulated by sugar transporters and the sugar gradient between phloem and fruits (Lecourieux et al., 2014; Osorio et al., 2014). Jensen et al. (2013) has analyzed the

phloem sugar concentration of 41 species reported in more than 50 experiments and estimated that the optimal concentration for sugar transport in plants is 0.235 g/g. The phloem sugar concentration was estimated to be 0.21 g/g for grape (Dai et al., 2008), 0.11 g/g for tomato (Liu et al., 2007), and 0.38 g/g for peach (Jensen et al., 2013). The lower phloem sugar concentration in tomato might be one potential cause of the lower sugar importation observed for cherry tomato and tomato (Figures 3E–H). In addition, more efforts are needed to compare the activities of sugar transporters among the three fruits to identify the underlying reasons of differences in sugar importation (Lecourieux et al., 2014; Osorio et al., 2014). Another noticeable aspect is that the mean cumulative contribution of each process is also affected by the developmental stage considered. If the early developmental stages were considered, cherry tomato and tomato showed very high levels of sugar importation in concert with high metabolism (Supplementary Figure S2). It will be interesting to quantify the relative contributions of the three processes in grape and peach during the early developmental stages.



Fruit water balance, which affects dilution, is a function of water influxes from xylem and phloem and water effluxes via skin transpiration (Fishman and Génard, 1998; Guichard et al., 2001; Dai et al., 2010). Fruit transpiration is related to environmental conditions (temperature and relative humidity) and skin water permeability that quantifies the permeation coefficient of the fruit surface to water vapor (Fishman and Génard, 1998). Skin water permeability varies largely amongst fruit species (Nobel, 1975), ranging from 26 cm/h for tomato (recalculated from Leonardi et al., 2000), 50–100 cm/h for grapes (Dai et al., 2008; Zhang and Keller, 2015), and 200–800 for peaches (Lescourret et al., 2001). Lescourret et al. (2001) assessed the effect of skin water permeability on peach fruit growth and found that low skin water permeability confers high WC in peach, which results in a higher dilution effect on soluble sugar accumulation. Surprisingly, we found that peach had a higher dilution component than grape, cherry tomato, and tomato (Figure 3), which seems to be the reverse of what can be extrapolated from the analysis of Lescourret et al. (2001). We postulate that differences in dilution among the three fruit species should originate from the water influxes. Therefore, phloem and xylem water conductivities of fruit species seem to be pertinent candidates for further comparative analysis.

Environments, growing conditions, and management practices may influence fruit growth and soluble sugar concentration, with different responses depending on species and genotype (Coombe, 1976; Nookaraju et al., 2010; Beckles et al., 2012; Kromdijk et al., 2014; Kuhn et al., 2014; Soltis and Kliebenstein, 2015). This variability was clearly shown in the PCA analysis of mean cumulative values of sugar importation, metabolism and dilution (Figure 5), confirming the analyses conducted in previous publications (Quilot et al., 2004; Dai et al., 2009; Prudent et al., 2011) where the data were collected. Among the variation factors, such as year, crop load, water supply, and genotype, the same genotypes were often clustered together. This highlights the importance of genotype on determining soluble sugar accumulation in fleshy fruits. Within a given genotype, we compared the contributions of sugar importation, metabolism and dilution in response to crop load modifications between peach and tomato (Figures 5D,E). Crop load manipulation is an effective way to modify the carbon balance between sources and sinks (Kromdijk et al., 2014). Its effect on sugar importation is rather straightforward, as observed in peach. However, not only sugar importation is modified, the dilution component is also largely affected. Higher importation occurs in parallel with higher dilution

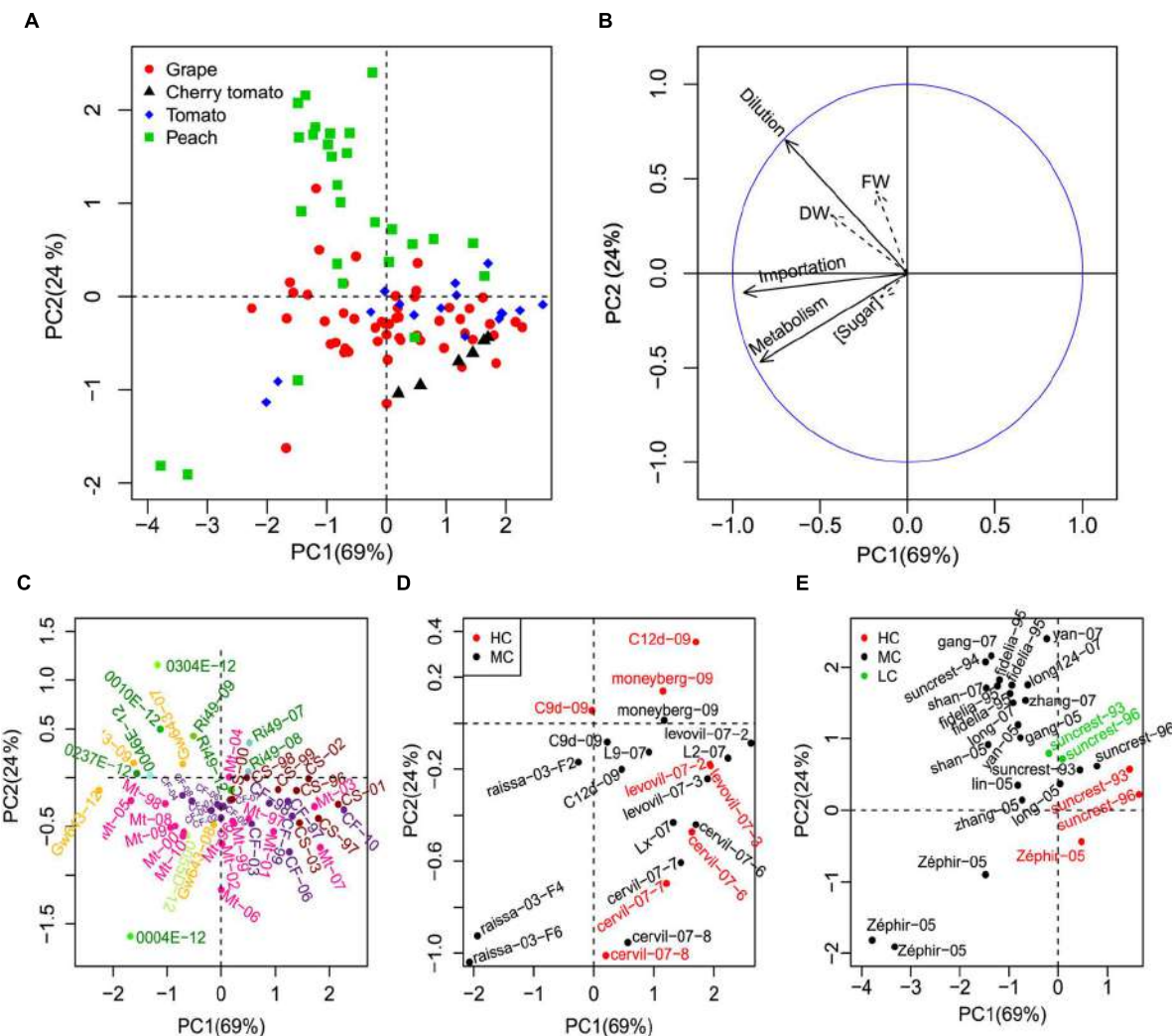


FIGURE 5 | Principal component analysis (PCA) analysis of genotypes and growing conditions of the three fruit species. The three components (importation, metabolism, dilution) were used to make the PCA discriminate the three fruit species (**A**). Soluble sugar concentration, FW, and DW were projected as non-active variables on the first two PCs (**B**). To have a better view of the genotypes and growing conditions, a zooming of the general scatter plot (**A**) was conducted for each fruit (C for grape, D for cherry tomato and tomato, and E for peach). The genotype, year, and truss (for tomato) of the fruits were labeled as “genotype-year-truss.” Mt = Merlot, CS = Cabernet-Sauvignon, CF = Cabernet franc, GW643 = Gewurztraminer, R49 = Riesling in (**C**). Green and yellow dots represent white grape genotypes and pink, violet and brown dots represent red grape genotypes (**C**). HC, MC, and LC represent high, mean and low crop loads, respectively (**D,E**).

in peach under low crop load. Crop load altering fruit water relationship has been reported (McFadyen et al., 1996). This suggests, on the one hand, a strong coordination between carbon and water influxes into fruits (Ho et al., 1987; Fishman and Génard, 1998; Guichard et al., 2001). On the other hand, it highlights the importance of growing conditions on the metabolite patterns in each fruit species (Kromdijk et al., 2014; Soltis and Kliebenstein, 2015) and pinpoints out the necessity of considering dilution effect in metabolic analysis (Génard et al., 2014).

In addition, the results obtained in this study could be useful in agricultural application. By representing biological processes and dissecting a complex trait into processes more physiological

relevant and stable over changing environments (Bertin et al., 2010), the decomposition approach has also been applied to assist QTL identification in relation to sugar levels in tomato fruit (Prudent et al., 2011), evidencing its valuable role in marker-assisted breeding. The inter-species comparison conducted in this study highlighted different control modes of sugar concentration in each species, providing clues for breeding strategies to obtain fruits with targeted sugar levels (Tohge and Fernie, 2015). Moreover, the intra-species variabilities among different cultivars could also provide valuable agricultural implementations. For example, the different sensitivities of grape cultivars to dilution and importation may help to select suitable cultivars sensitive to agronomical factors such as irrigation or fruit load.

CONCLUSION

Our analysis shows the existence of different patterns for soluble sugar concentration control, either import-based, dilution-based, or shared. On the other hand, conserved metabolic rate was observed among the three fruit species for the consumption of imported carbon for synthesis of other compounds than sugars (e.g., starch, organic acids, structural carbohydrates, and proteins). These distinct modes appear to be quite species-specific, with dilution being the main lever in peach, but a strong genotypic variability is present when considering the intensity of the effect. Growing seasons and management practices can further explain genotypic variability within a given species. These results provide novel insights into the drivers of differences in soluble sugar concentration among fleshy fruits and further emphasize the importance of dilution. In addition, the process-based decomposition framework proves to be a suitable tool for conducting inter-species comparison, because of its capability to decompose complex traits and extract stable and conserved information. It can be complementary to the metabolic multispecies comparison of Klie et al. (2014). It should be noted that the comparison presented here mainly focuses on the late developmental stages (40% maturity to 100% maturity), and it warrants more efforts to cover the whole fruit developmental stages for the inter-species comparison. Moreover, the underlying mechanisms of sugar importation and water influxes deserve further investigation for inter-species comparison, for example, by coupling the observed developmental profiles with the virtual fruit model that describes the process of phloem sugar importation and xylem water transport (Lescourret and Génard, 2005; Génard et al., 2007, 2010).

REFERENCES

- Baudrit, C., Perrot, N., Brousset, J. M., Abbal, P., Guillemin, H., Perret, B., et al. (2015). A probabilistic graphical model for describing the grape berry maturity. *Comput. Electron. Agric.* 118, 124–135. doi: 10.1016/j.compag.2015.08.019
- Beckles, D. M., Hong, N., Stamova, L., and Luengwilai, K. (2012). Biochemical factors contributing to tomato fruit sugar content: a review. *Fruits* 67, 49–64. doi: 10.1051/fruits/2011066
- Bertin, N., Causse, M., Brunel, B., Tricon, D., and Génard, M. (2009). Identification of growth processes involved in QTLs for tomato fruit size and composition. *J. Exp. Bot.* 60, 237–248. doi: 10.1093/jxb/ern281
- Bertin, N., Martre, P., Génard, M., Quilot, B., and Salon, C. (2010). Under what circumstances can process-based simulation models link genotype to phenotype for complex traits? Case-study of fruit and grain quality traits. *J. Exp. Bot.* 61, 956–967. doi: 10.1093/jxb/erp377
- Biais, B., Bénard, C., Beauvoit, B., Colombié, S., Prodhomme, D., Ménard, G. N., et al. (2014). Remarkable reproducibility of enzyme activity profiles in tomato fruits grown under contrasting environments provides a roadmap for studies of fruit metabolism. *Plant Physiol.* 164, 1204–1221. doi: 10.1104/pp.113.231241
- Castellarin, S., Matthews, M., Gaspero, G., and Gambetta, G. (2007). Water deficits accelerate ripening and induce changes in gene expression regulating flavonoid biosynthesis in grape berries. *Planta* 227, 101–112. doi: 10.1007/s00425-007-0598-8
- Coombe, B. G. (1976). The development of fleshy fruits. *Annu. Rev. Plant Physiol.* 27, 207–228. doi: 10.1146/annurev.pp.27.060176.001231
- Coombe, B. G. (1992). Research on development and ripening of the grape berry. *Am. J. Enol. Viticul.* 43, 101–110.

AUTHOR CONTRIBUTIONS

MG, VB, and ZD designed and oversaw the research; HW, MG, VB, and ZD performed the research and analyzed data. ZD, VB, and MG drafted the manuscript; CL, NB, HG, FL, BW, and ED contributed to data collection; CL, NB, HG, BW, ED, EG, FL, and SD critically revised the manuscript. All authors read and approved the final manuscript.

FUNDING

This research was supported partly by a grant from the Environment and Agronomy (EA) department of the Institute National de la Recherche Agronomique (INRA), France. It also received funding from the Agence Nationale de la Recherche for the project “Frimouss” (grant no. ANR-15-CE20-0009) and was developed within the framework of COST Action FA 1106 and the EA “Fruit and seed quality” network of INRA.

ACKNOWLEDGMENT

We thank Dr. Yves Gibon for valuable discussions and Agnès Destrac Irvine for help in data collection.

SUPPLEMENTARY MATERIAL

The Supplementary Material for this article can be found online at: <http://journal.frontiersin.org/article/10.3389/fpls.2016.00649>

- Coombe, B. G., and McCarthy, M. G. (2000). Dynamics of grape berry growth and physiology of ripening. *Aust. J. Grape Wine Res.* 6, 131–135. doi: 10.1111/j.1755-0238.2000.tb00171.x
- Dai, Z. W., Vivin, P., Barrieu, F., Ollat, N., and Delrot, S. (2010). Physiological and modelling approaches to understand water and carbon fluxes during grape berry growth and quality development: a review. *Aust. J. Grape Wine Res.* 16, 70–85. doi: 10.1111/j.1755-0238.2009.00071.x
- Dai, Z. W., Vivin, P., and Génard, M. (2008). Modelling the effects of leaf-to-fruit ratio on dry and fresh mass accumulation in ripening grape berries. *Acta Hortic.* 803, 283–291. doi: 10.17660/ActaHortic.2008.803.36
- Dai, Z. W., Vivin, P., Robert, T., Milin, S., Li, S. H., and Génard, M. (2009). Model-based analysis of sugar accumulation in response to source-sink ratio and water supply in grape (*Vitis vinifera*) berries. *Funct. Plant Biol.* 36, 527–540. doi: 10.1071/FP08284
- DeJong, T. M., and Goudriaan, J. (1989). Modeling peach fruit growth and carbohydrate requirements: reevaluation of the double-sigmoid growth pattern. *J. Am. Soc. Hortic. Sci.* 114, 800–804.
- Desnoues, E., Gibon, Y., Baldazzi, V., Signoret, V., Génard, M., and Quilot-Turion, B. (2014). Profiling sugar metabolism during fruit development in a peach progeny with different fructose-to-glucose ratios. *BMC Plant Biol.* 14:336. doi: 10.1186/s12870-014-0336-x
- Dray, S., and Dufour, A. B. (2007). The ade4 package: implementing the duality diagram for ecologists. *J. Stat. Softw.* 22, 1–20. doi: 10.18637/jss.v022.i04
- Duchêne, E., and Schneider, C. (2005). Grapevine and climatic changes: a glance at the situation in Alsace. *Agron. Sustain. Dev.* 25, 93–99. doi: 10.1051/agro:2004057

- Fishman, S., and Génard, M. (1998). A biophysical model of fruit growth: simulation of seasonal and diurnal dynamics of mass. *Plant Cell Environ.* 21, 739–752. doi: 10.1046/j.1365-3040.1998.00322.x
- Garcia de Cortazar-Atauri, I., Brisson, N., Ollat, N., Jacquet, O., and Payan, J. C. (2009). Asynchronous dynamics of grapevine (*Vitis vinifera*) maturation: experimental study for a modelling approach. *J. Int. Sci. Vigne Vin* 43, 83–97.
- Génard, M., Baldazzi, V., and Gibon, Y. (2014). Metabolic studies in plant organs: don't forget dilution by growth. *Front. Plant Sci.* 5:85. doi: 10.3389/fpls.2014.00085
- Génard, M., Bertin, N., Borel, C., Bussières, P., Gautier, H., Habib, R., et al. (2007). Towards a virtual fruit focusing on quality: modelling features and potential uses. *J. Exp. Bot.* 58, 917–928. doi: 10.1093/jxb/erl287
- Génard, M., Bertin, N., Gautier, H., Lescourret, F., and Quilot, B. (2010). Virtual profiling: a new way to analyse phenotypes. *Plant J.* 62, 344–355. doi: 10.1111/j.1365-313X.2010.04152.x
- Génard, M., Lescourret, F., Gomez, L., and Habib, R. (2003). Changes in fruit sugar concentration in response to assimilate supply, metabolism and dilution: a model approach applied to peach fruit (*Prunus persica*). *Tree Physiol.* 23, 373–385. doi: 10.1093/treephys/23.6.373
- Grechi, I., Hilgert, N., Génard, M., and Lescourret, F. (2008). Assessing the peach fruit refractometric index at harvest with a simple model based on fruit growth. *J. Am. Soc. Hortic. Sci.* 133, 178–187.
- Guichard, S., Bertin, N., Leonardi, C., and Gary, C. (2001). Tomato fruit quality in relation to water and carbon fluxes. *Agronomie* 21, 385–392. doi: 10.1051/agro:2001131
- Ho, L. C., Grange, R. I., and Picken, A. J. (1987). An analysis of the accumulation of water and dry matter in tomato fruit. *Plant Cell Environ.* 10, 157–162. doi: 10.1111/j.1365-3040.ep11602110
- Jensen, K. H., Savage, J. A., and Holbrook, N. M. (2013). Optimal concentration for sugar transport in plants. *J. R. Soc. Interface* 10, 20130055. doi: 10.1098/rsif.2013.0055
- Klie, S., Osorio, S., Tohge, T., Drincovich, M. F., Fait, A., Giovannoni, J. J., et al. (2014). Conserved changes in the dynamics of metabolic processes during fruit development and ripening across species. *Plant Physiol.* 164, 55–68. doi: 10.1104/pp.113.226142
- Kobashi, K., Gemma, H., and Iwahori, S. (2000). Abscisic acid content and sugar metabolism of peaches grown under water stress. *J. Am. Soc. Hortic. Sci.* 125, 425–428.
- Kromdijk, J., Bertin, N., Heuvelink, E., Molenaar, J., de Visser, P. H. B., Marcelis, L. F. M., et al. (2014). Crop management impacts the efficiency of quantitative trait loci (QTL) detection and use: case study of fruit load \times QTL interactions. *J. Exp. Bot.* 65, 11–22. doi: 10.1093/jxb/ert365
- Kühn, C., and Grof, C. P. L. (2010). Sucrose transporters of higher plants. *Curr. Opin. Plant Biol.* 13, 287–297. doi: 10.1016/j.pbi.2010.02.001
- Kuhn, N., Guan, L., Dai, Z. W., Wu, B.-H., Lauvergeat, V., Gomès, E., et al. (2014). Berry ripening: recently heard through the grapevine. *J. Exp. Bot.* 65, 4543–4559. doi: 10.1093/jxb/ert395
- Lalonde, S., Tegeder, M., Throne-Holst, M., Frommer, W. B., and Patrick, J. W. (2003). Phloem loading and unloading of sugars and amino acids. *Plant Cell Environ.* 26, 37–56. doi: 10.1046/j.1365-3040.2003.00847.x
- Lecourieux, F., Kappel, C., Lecourieux, D., Serrano, A., Torres, E., Arce-Johnson, P., et al. (2014). An update on sugar transport and signalling in grapevine. *J. Exp. Bot.* 65, 821–832. doi: 10.1093/jxb/ert394
- Leonardi, C., Guichard, S., and Bertin, N. (2000). High vapour pressure deficit influences growth, transpiration and quality of tomato fruits. *Sci. Hortic. (Amsterdam)* 84, 285–296. doi: 10.1016/S0304-4238(99)00127-2
- Lescourret, F., and Génard, M. (2005). A virtual peach fruit model simulating changes in fruit quality during the final stage of fruit growth. *Tree Physiol.* 25, 1303–1315. doi: 10.1093/treephys/25.10.1303
- Lescourret, F., Génard, M., Habib, R., and Fishman, S. (2001). Variation in surface conductance to water vapor diffusion in peach fruit and its effects on fruit growth assessed by a simulation model. *Tree Physiol.* 21, 735–741. doi: 10.1093/treephys/21.11.735
- Liu, H. F., Génard, M., Guichard, S., and Bertin, N. (2007). Model-assisted analysis of tomato fruit growth in relation to carbon and water fluxes. *J. Exp. Bot.* 58, 3567–3580. doi: 10.1093/jxb/erm202
- Luengwilai, K., and Beckles, D. M. (2009). Starch granules in tomato fruit show a complex pattern of degradation. *J. Agric. Food Chem.* 57, 8480–8487. doi: 10.1021/jf901593m
- McFadyen, L. M., Hutton, R. J., and Barlow, E. W. R. (1996). Effects of crop load on fruit water relations and fruit growth in peach. *J. Hortic. Sci.* 71, 469–480. doi: 10.1080/14620316.1996.11515428
- Nobel, P. S. (1975). Effective thickness and resistance of the air boundary layer adjacent to spherical plant parts. *J. Exp. Bot.* 26, 120–130. doi: 10.1093/jxb/26.1.120
- Nookaraju, A., Upadhyaya, C. P., Pandey, S. K., Young, K. E., Hong, S. J., Park, S. K., et al. (2010). Molecular approaches for enhancing sweetness in fruits and vegetables. *Sci. Hortic.* 127, 1–15. doi: 10.1016/j.scienta.2010.09.014
- OIV (2009). *Recueil des Méthodes Internationales D'analyses de Vins et des Moûts*, Vol. 1. Paris: OIV, 35–56.
- Osorio, S., Ruan, Y.-L., and Fernie, A. R. (2014). An update on source-to-sink carbon partitioning in tomato. *Front. Plant Sci.* 5:516. doi: 10.3389/fpls.2014.00516
- Petreikov, M., Yeselson, L., Shen, S., Levin, I., Schaffer, A. A., Efrati, A., et al. (2009). Carbohydrate balance and accumulation during development of near-isogenic tomato lines differing in the AGPase-L1 allele. *J. Am. Soc. Hortic. Sci.* 134, 134–140.
- Prudent, M., Causse, M., Génard, M., Tripodi, P., Grandillo, S., and Bertin, N. (2009). Genetic and physiological analysis of tomato fruit weight and composition: influence of carbon availability on QTL detection. *J. Exp. Bot.* 60, 923–937. doi: 10.1093/jxb/ern338
- Prudent, M., Lecomte, A., Bouchet, J.-P., Bertin, N., Causse, M., and Génard, M. (2011). Combining ecophysiological modelling and quantitative trait locus analysis to identify key elementary processes underlying tomato fruit sugar concentration. *J. Exp. Bot.* 62, 907–919. doi: 10.1093/jxb/erq318
- Quilot, B., Génard, M., Kervella, J., and Lescourret, F. (2004). Analysis of genotypic variation in fruit flesh total sugar content via an ecophysiological model applied to peach. *Theor. Appl. Genet.* 109, 440–449. doi: 10.1007/s00122-004-1651-7
- R Development Core Team (2010). *R: A Language and Environment for Statistical Computing*. Vienna: R Foundation for Statistical Computing.
- Ripoll, J., Urban, L., and Bertin, N. (2016). The potential of the MAGIC TOM parental accessions to explore the genetic variability in tomato acclimation to repeated cycles of water deficit and recovery. *Front. Plant Sci.* 6:1172. doi: 10.3389/fpls.2015.01172
- Ruan, Y. L., and Patrick, J. W. (1995). The cellular pathway of postphloem sugar transport in developing tomato fruit. *Planta* 196, 434–444. doi: 10.1007/BF00203641
- Sadras, V. O., and McCarthy, M. G. (2007). Quantifying the dynamics of sugar concentration in berries of *Vitis vinifera* cv. Shiraz: a novel approach based on allometric analysis. *Aust. J. Grape Wine Res.* 13, 66–71. doi: 10.1111/j.1755-0238.2007.tb00236.x
- Schaffer, A. A., and Petreikov, M. (1997). Sucrose-to-starch metabolism in tomato fruit undergoing transient starch accumulation. *Plant Physiol.* 113, 739–746.
- Soltis, N. E., and Kliebenstein, D. J. (2015). Natural variation of plant metabolism: genetic mechanisms, interpretive caveats, and evolutionary and mechanistic insights. *Plant Physiol.* 169, 1456–1468. doi: 10.1104/pp.15.01108
- Tilbrook, J., and Tyerman, S. D. (2009). Hydraulic connection of grape berries to the vine: varietal differences in water conductance into and out of berries, and potential for backflow. *Funct. Plant Biol.* 36, 541–550. doi: 10.1071/FP09019
- Tohge, T., and Fernie, A. R. (2015). Metabolomics-inspired insight into developmental, environmental and genetic aspects of tomato fruit chemical composition and quality. *Plant Cell Physiol.* 56, 1681–1696. doi: 10.1093/pcp/pcv093
- Wu, B. H., Quilot, B., Génard, M., Li, S. H., Zhao, J. B., Yang, J., et al. (2012). Application of a SUGAR model to analyse sugar accumulation in peach cultivars that differ in glucose-fructose ratio. *J. Agric. Sci.* 150, 53–63. doi: 10.1017/S0021859611000438
- Zanon, L., Falchi, R., Santi, S., and Vizzotto, G. (2015). Sucrose transport and phloem unloading in peach fruit: potential role of two transporters localized in different cell types. *Physiol. Plant.* 154, 179–193. doi: 10.1111/ppl.12304
- Zhang, X.-Y., Wang, X.-L., Wang, X.-F., Xia, G.-H., Pan, Q.-H., Fan, R.-C., et al. (2006). A shift of phloem unloading from symplasmic to apoplasmic pathway is involved in developmental onset of ripening in grape berry. *Plant Physiol.* 142, 220–232. doi: 10.1104/pp.106.081430

Zhang, Y., and Keller, M. (2015). Grape berry transpiration is determined by vapor pressure deficit, cuticular conductance, and berry size. *Am. J. Enol. Viticul.* 66, 454–462. doi: 10.5344/ajev.2015.15038

Conflict of Interest Statement: The authors declare that the research was conducted in the absence of any commercial or financial relationships that could be construed as a potential conflict of interest.

Copyright © 2016 Dai, Wu, Baldazzi, van Leeuwen, Bertin, Gautier, Wu, Duchêne, Gomès, Delrot, Lescourret and Génard. This is an open-access article distributed under the terms of the Creative Commons Attribution License (CC BY). The use, distribution or reproduction in other forums is permitted, provided the original author(s) or licensor are credited and that the original publication in this journal is cited, in accordance with accepted academic practice. No use, distribution or reproduction is permitted which does not comply with these terms.



Insights into molecular and metabolic events associated with fruit response to post-harvest fungal pathogens

Noam Alkan^{1*} and Ana M. Fortes²

¹ Department of Postharvest Science of Fresh Produce, Volcani Center, Agricultural Research Organization, Bet Dagan, Israel, ² Biosystems & Integrative Sciences Institute, Faculdade de Ciências de Lisboa, Universidade de Lisboa, Lisboa, Portugal

OPEN ACCESS

Edited by:

Zuhua He,

Shanghai Institutes for Biological Sciences – Chinese Academy of Sciences, China

Reviewed by:

Wei-Hua Tang,

Shanghai Institute of Plant Physiology and Ecology – Chinese Academy of Sciences, China

Vasileios Fotopoulos,

Cyprus University of Technology, Cyprus

*Correspondence:

Noam Alkan

noamal@volcani.agri.gov.il

Specialty section:

This article was submitted to

Plant Physiology,

a section of the journal

Frontiers in Plant Science

Received: 15 July 2015

Accepted: 07 October 2015

Published: 20 October 2015

Citation:

Alkan N and Fortes AM (2015)

Insights into molecular and metabolic events associated with fruit response to post-harvest fungal pathogens.

Front. Plant Sci. 6:889.

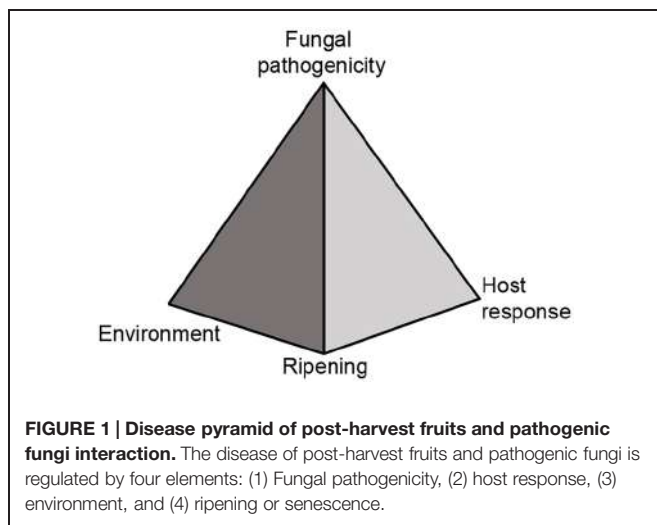
doi: 10.3389/fpls.2015.00889

Due to post-harvest losses more than 30% of harvested fruits will not reach the consumers' plate. Fungal pathogens play a key role in those losses, as they cause most of the fruit rots and the customer complaints. Many of the fungal pathogens are already present in the unripe fruit but remain quiescent during fruit growth until a particular phase of fruit ripening and senescence. The pathogens sense the developmental change and switch into the devastating necrotrophic life style that causes fruit rotting. Colonization of unripe fruit by the fungus initiates defensive responses that limit fungal growth and development. However, during fruit ripening several physiological processes occur that correlate with increased fruit susceptibility. In contrast to plant defenses in unripe fruit, the defense posture of ripe fruit entails a different subset of defense responses that will end with fruit rotting and losses. This review will focus on several aspects of molecular and metabolic events associated with fleshy fruit responses induced by post-harvest fungal pathogens during fruit ripening.

Keywords: post-harvest, ripening, plant response, phytohormones, cuticle, softening, phytoalexin, quiescent

INTRODUCTION

Food waste from the grower to the consumer is an important issue as it depletes natural resources. Recent researches and surveys done by NRDC (Natural Resources Defense Council), USDA (US Department of Agriculture), FAO (Food and Agriculture Organization of the United Nations), and the OECD (Organization for Economic Co-operation and Development) revealed that food losses are estimated to be more than 33% (Gustavsson et al., 2011; Lipinski et al., 2013; Buzby et al., 2014; Okawa, 2014). Post-harvest losses of fruits and vegetables are even higher and are estimated to be 40–50%. Post-harvest fruit rotting are a major cause of those losses and are chiefly caused by fungal pathogens after fruit ripening. In a manner similar to foliar diseases that occur in the field, several factors as: fungal pathogenicity, host response and environment determine the outcome of host resistance or susceptibility. However, in post-harvest diseases fruit ripening is another major component that will determine fruit resistance and must be considered (**Figure 1**).



Post-harvest Disease Development

Fruits infected by post-harvest fungal pathogens develop, in general, disease symptoms after harvest and during storage. Post-harvest fungal pathogens germinate and enter the fruit by breaching the host cuticle (Emery et al., 2000; Alkan et al., 2015). This is achieved by: degrading host cuticle (Rijkenberg et al., 1980), entering through natural openings of the host and wounds (Barkai-Golan, 2001), or by living endophytically in the stem end (Johnson et al., 1992; Prusky et al., 2009). When those particularly insidious pathogens encounter unripe fruit these fungi often remain quiescent and confined to the initial site of introduction. They are unnoticed to visual examination, for as long as months of storage, until the harvested fruit ripen (Prusky et al., 2013). Several species of fungal pathogens, such as *Colletotrichum*, *Alternaria*, *Botrytis*, *Monilinia*, *Lasiodiplodia*, *Phomopsis*, and *Botryosphaeria* have been reported to live quiescently in their hosts until the fruits ripen (Prusky et al., 1981; Adaskaveg et al., 2000; Prins et al., 2000). As fruit ripen, post-harvest fungal pathogens switch to aggressive growth. At this aggressive stage, the fungi are necrotrophs, which kill the host cell and obtain nutrients from the host, leading to decomposed fruit tissue and decay (Prusky, 1996; Prusky et al., 2013). However, before this devastating stage those fungi adopt different types of life styles. Some fungi as *Lasiodiplodia*, *Phomopsis*, *Colletotrichum*, *Alternaria* and others, cause stem-end-rot and colonize the stem-end by adopting endophytic-like lifestyle before fruit ripening (Johnson et al., 1992). Other fungi, e.g., *Colletotrichum* are defined as hemibiotroph, those fungi live quiescently as biotrophs in unripe fruit cells without killing them (O'Connell et al., 2012; Alkan et al., 2015). In a parallel manner, fully necrotrophic fungi as *Botrytis* can infect and live in a restricted 1–3 cells of unripe fruit without damaging the surrounding tissue (Cantu et al., 2008a).

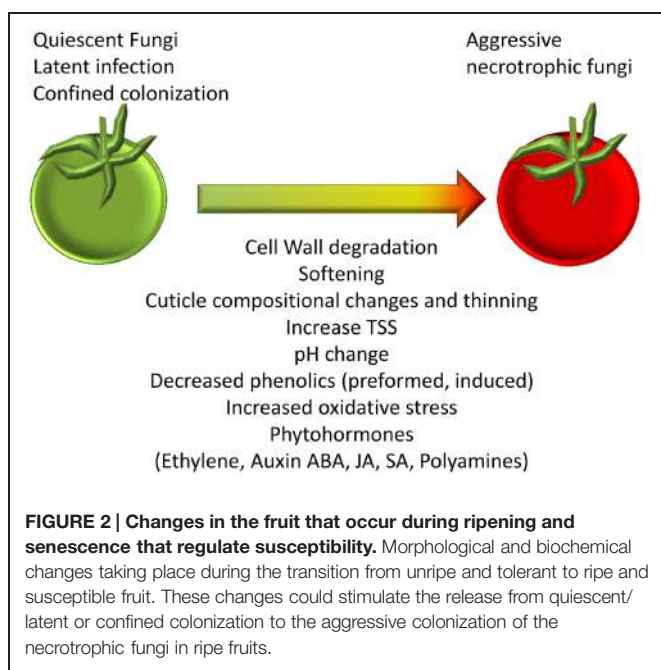
Botrytis and Colletotrichum Model

Due to lack of omics data and in-depth knowledge in the stem-end-rot pathosystems, this review will focus on the better understood *Colletotrichum* (anthracnose) representing

hemibiotrophic fungi and on *Botrytis* (gray mold) as necrotrophic fungi. These fungi are two of the most common post-harvest fruit disease agents that are known to attack many economically important fruits and present problems world-wide (Sutton, 1992; Cannon et al., 2000; Hyde et al., 2009). *Colletotrichum gloeosporioides* causes the anthracnose disease to at least 470 host genera (Sutton, 1980; Hyde et al., 2009) and *Botrytis cinerea* causes the gray mold disease on over 200 species of fruit. On unripe fruit, *Colletotrichum* conidia germinate and develop appressoria which penetrate the fruit cuticle via an infection peg. *C. gloeosporioides* enters the quiescent stage whereupon two distinct structures develop: dendritic-like protrusions which form within the fruit cuticle and swollen hyphae which colonize the first epidermal cell layer but advance no further (Alkan et al., 2015). When *C. gloeosporioides* germinates on the cuticle of ripe fruit it germinates as on green fruit and goes through a short biotrophic stage. Only this time it is much more rapid and the quiescent structures immediately switch to necrotrophic growth. This indicates that hemibiotrophic growth in *C. gloeosporioides* is developmentally cued when encounter with fruit cuticle. On the other hand, *Botrytis* spore germlings tend to penetrate through small wounds or cracks in the epidermis or cuticle of unripe fruit and remain confined within the lumen of the wounds (Williamson et al., 2007; Cantu et al., 2008a). When the hemibiotrophic *C. gloeosporioides* germinates on small wounds of unripe fruits, its colonization skips the biotrophic-like stage and it adopts the necrotrophic strategy, similarly to *B. cinerea* (Alkan et al., 2015). Growth of either pathogen on wounds in unripe fruit is limited for long periods, and upon ripening, both pathogens become necrotrophic, degrade host tissues and produce symptoms of disease (Prusky, 1996; Prusky et al., 2013).

Unripe Fruit Tolerance and Changes Occurring during Ripening

During fruit ripening, significant physiological shifts occur: cell wall remodeling (Brummell et al., 1999; Huckelhoven, 2007), soluble sugar accumulation, decrease in the amount of phytoanticipins and phytoalexins (Prusky, 1996); decline of inducible host defense responses (Beno-Moualem and Prusky, 2000); cuticle biosynthesis (Bargel and Neinhuis, 2005) and changes in the ambient host pH (Prusky et al., 2013; Figure 2). Most of those changes are thought to be governed by complex hormonal signals including ethylene, ABA, jasmonic acid (JA), and salicylic acid (SA), which occur during natural fruit ripening (Giovannoni, 2001; Seymour et al., 2013). Interestingly, similar phytohormones are regulated in the host in response to pathogens (Blanco-Ulate et al., 2013; Alkan et al., 2015). In response to the changes in the host, pathogens alter the enzymes and compounds they produce which allow them to infect and break down or macerate the fruit tissue (Blanco-Ulate et al., 2014; Agudelo-Romero et al., 2015; Alkan et al., 2015). Signals for release from quiescence probably occur during fruit ripening and may include: disassembled cell wall substrates, alterations in cuticle and other signals (Cantu et al., 2008a,b; Mengiste et al., 2012; Figure 2). When the fungi are re-activated they



induce rotting disease that impairs crop quantity, quality and appearance. These aspects will be discussed in the following sections.

HOST FACTORS MODULATING POST-HARVEST FUNGAL DEVELOPMENT

Recently, with the expansion of omics technique several observations elaborated on the involvement of differential response of ripe and unripe fruit to fungal pathogens (Blanco-Ulate et al., 2014; Agudelo-Romero et al., 2015; Alkan et al., 2015).

This review will describe both the changes occurring during fruit ripening and the fruit response to post-harvest fungal pathogens.

Phytohormones: Jasmonate-salicylate Crosstalk and More

Phytohormones are well-known to affect fruit ripening (Burg and Burg, 1965; Alexander and Grierson, 2002) and the defense responses to pathogens (Alkan et al., 2012, 2015; Blanco-Ulate et al., 2013; Agudelo-Romero et al., 2015). Important signaling roles have been ascribed to classical defense hormones SA, JA, abscisic acid (ABA), and ethylene (ET) in molding plant-pathogen interactions (Fujita et al., 2006; Spoel and Dong, 2008). Gibberellic acid (GA), auxin (IAA), brassinosteroids (BRs), and cytokinines (CK) have recently been emerged as important modulators of plant defenses against microorganisms based mostly on vegetative tissues data and on the lifestyle of the infecting pathogen (Robert-Seilantian et al., 2011).

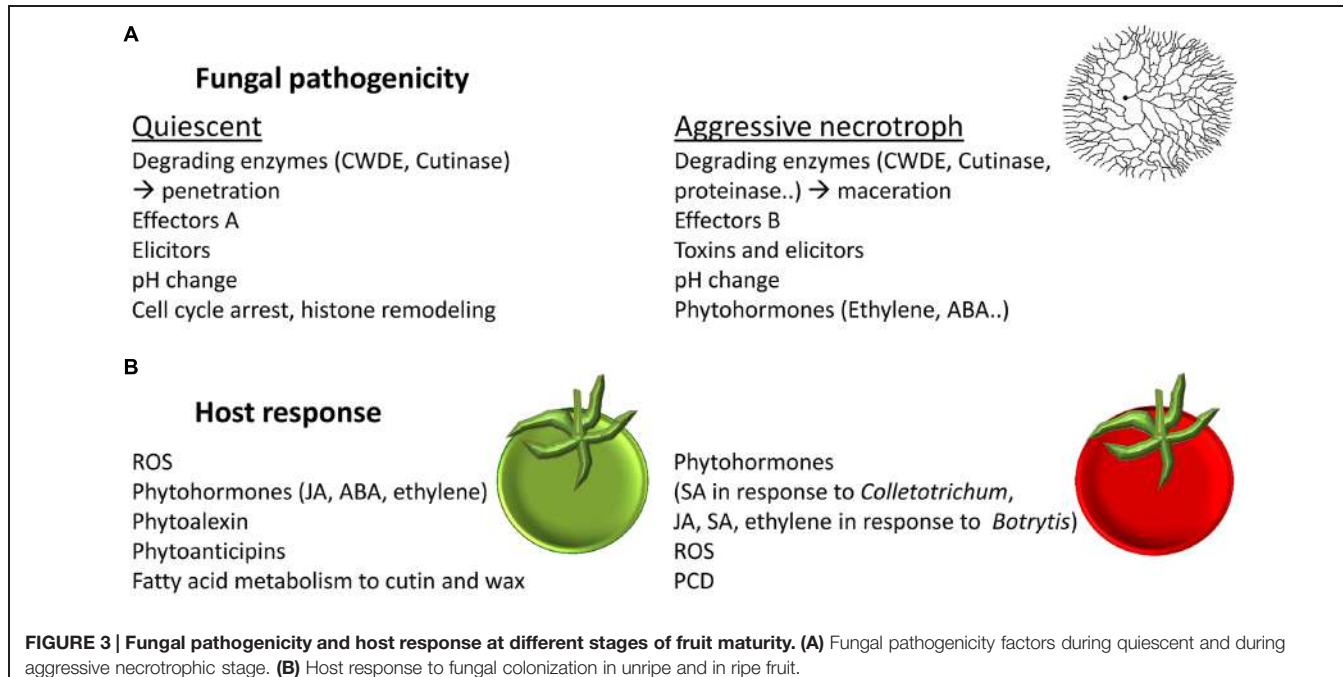
Jasmonate-salicylate Crosstalk

Salicylic acid and JA signaling pathways are generally considered as antagonistic dependent on NPR1 and hormone concentration (Spoel et al., 2007; Spoel and Dong, 2008; Pieterse et al., 2012). This interplay between SA and JA was suggested to optimize host-response to pathogen's lifestyle (Glazebrook, 2005; Spoel et al., 2007; Spoel and Dong, 2008; Pieterse et al., 2012). In vegetative tissue it is commonly postulated that an effective responses to biotrophic pathogens are typically mediated by SA and programmed cell death (PCD; Glazebrook, 2005; Spoel et al., 2007), and responses to necrotrophic pathogens, which benefit from host cell death, involve JA and ethylene signaling (Glazebrook, 2005; Spoel et al., 2007; Figures 3 and 4B).

During normal fruit ripening many phytohormones as ethylene, IAA, ABA, GA, JA, and SA are regulated (Bari and Jones, 2009; Symons et al., 2012; Zaharah et al., 2012; Seymour et al., 2013; Figure 2), which complicate the effective fruit response to pathogens. Indeed, in infections of grapes and tomato fruit with *Botrytis* (Blanco-Ulate et al., 2013; Agudelo-Romero et al., 2015) and tomato fruit infections with *Colletotrichum* (Alkan et al., 2015) several stress hormone responsive pathways including ethylene, ABA, JA, and SA were regulated. In fruit, high levels of ET and ABA, which stimulate senescence/ripening processes, may facilitate colonization by necrotrophs. The balance between SA and JA responses seems to be crucial for fruit resistance (Blanco-Ulate et al., 2013; Alkan et al., 2015).

During the biotrophic-like quiescence stage of *C. gloeosporioides* the resistant unripe fruit mainly responded through activation of JA, ethylene, and ABA (Alkan et al., 2015). However, the ripe tomato is more susceptible to disease and the fungi adopt a necrotrophic mode of host colonization. In the fruit response to necrotrophic infections, SA biosynthetic, signaling and response pathways were activated (Alkan et al., 2015; Figure 3). SA signaling was shown to have an important role in necrotrophic colonization stage of *Colletotrichum* on tomato fruit by inducing cell death and likely as a means to suppress JA mediated defense response (Alkan et al., 2012). The activation of this pathway was dependent on NADPH oxidase activity that was induced by ammonia secreted by the fungus (Alkan et al., 2009). Indeed, JA application leads to increase tolerance and SA application leads to PCD and increased susceptibility to *C. gloeosporioides* at its necrotrophic stage (Alkan et al., 2012). Similarly, ripe *NahG* tomato fruit mutant, lacking SA responses, showed increased tolerance to *C. gloeosporioides*. In a reciprocal manner, the *Spr1* mutant, deficient in JA signaling, showed increased susceptibility (Alkan et al., 2015).

The responses of tomato fruit to *Botrytis* involved several stress hormone responsive pathways including ethylene, ABA, JA, and SA in a complex manner that differ during infections of ripe and unripe tomato fruit. In general, both grape and tomato defense response to *Botrytis* were mainly mediated by JA and ET (Blanco-Ulate et al., 2013; Agudelo-Romero et al., 2015; Figure 3). Similarly, *Arabidopsis* leaves response to *Botrytis* was mediated mainly by JA and ET (AbuQamar et al., 2006). However, in unripe tomato fruit the *NahG* gene showed susceptibility to *Botrytis* (Blanco-Ulate et al., 2013). This result suggests that SA has an important role in unripe fruit resistance to *Botrytis*.



In grapes of susceptible cultivar infected with *B. cinerea*, the pathogen causes shutdown of defenses, which are regulated by SA and are expressed during the normal ripening (Agudelo-Romero et al., 2015). It remains to be established whether SA-mediated defense system is inhibited or not in resistant cultivars.

In climacteric fruit ET and ABA stimulate ripening and may affect the host defense response (Seymour et al., 2013). Thus, resistance of *sittens* mutants at ripe fruit stage to *Botrytis* and ABA elevation in response to *Botrytis* was correlated to susceptibility (Blanco-Ulate et al., 2013). The ethylene and ABA elevation seems to play a dual role, on the one hand it correlated with JA and ethylene resistance response, and on the other hand it induced ripening and increase susceptibility (**Figure 4A**). This assumption will be further discussed below.

Not Only SA and JA Crosstalk

As discussed above, major responses to fungal pathogens are mediated by ethylene, ABA, JA, and SA phytohormones (**Figure 3**). Additional phytohormones and growth regulators such as gibberellin, cytokinins, steroid, polyamines, and BRs were reported to affect fruit response to fungal pathogens. For example gibberellin-treated persimmon fruit had increased resistance of to *Alternaria alternata* by delaying fruit maturation and reducing cuticle cracks (Eshel et al., 2000; Biton et al., 2014). Gibberellin seems to act also in an alternative way, the DELLA transcription factors enable plants to respond to gibberellin; this mechanism seems to maintain transient growth arrest and lead to plant response to biotic and abiotic stress (Harberd et al., 2009). DELLA transcription factors were shown to promote susceptibility to biotrophs and resistance to necrotrophs in leaves (Navarro et al., 2008).

Polyamines may have a role in response to post-harvest pathogens. In fact, genes involved in polyamine biosynthesis are

up-regulated in *Botrytis*-grapes pathosystem (Geny et al., 2003; Agudelo-Romero et al., 2015). Over-expression of ARGAH2 in *Arabidopsis* leads to enhanced resistance to *B. cinerea*, thus suggesting a role for the polyamine arginase in plant resistance (Brauc et al., 2012). Furthermore, polyamines seem to be co-regulated with ethylene biosynthesis and seem to co-work with ABA (Bitrian et al., 2012).

Steroids such as β-sitosterol and stigmasterol have been previously shown to be involved in plant-pathogen interactions (Griebel and Zeier, 2010). Indeed, several genes involved in steroid biosynthesis were also upregulated in grape and tomato response to *Botrytis* (Blanco-Ulate et al., 2013; Agudelo-Romero et al., 2015). Furthermore, BRs play a role in grape ripening (Symons et al., 2006) and are known to change in plants response pathogen infection (Krishna, 2003). BAK1, known for BRs signaling, contributes to pathogen associated molecular pattern-triggered immunity (PAMP) to necrotrophic pathogens (Mengiste et al., 2012). Loss of BAK1 results in increased susceptibility to the necrotrophic fungi (Kemmerling et al., 2007). Several genes coding for BAK1 were down-regulated in grapes infected with *Botrytis* at the onset of ripening (Blanco-Ulate et al., 2013; Agudelo-Romero et al., 2015). Application of BRs reduced *Penicillium expansum* decay in jujube fruit and delayed fruit senescence (Zhu et al., 2010).

Ethylene Dual Role in Ripening and Defense Response

Ethylene is a key post-harvest hormone with a dual role. In climacteric fruit ripening (Giovannoni, 2001; Seymour et al., 2013), the presence of ethylene will lead to susceptibility, however, ethylene could also acts as a defense hormone together with JA (Spoel and Dong, 2008; **Figure 4A**).

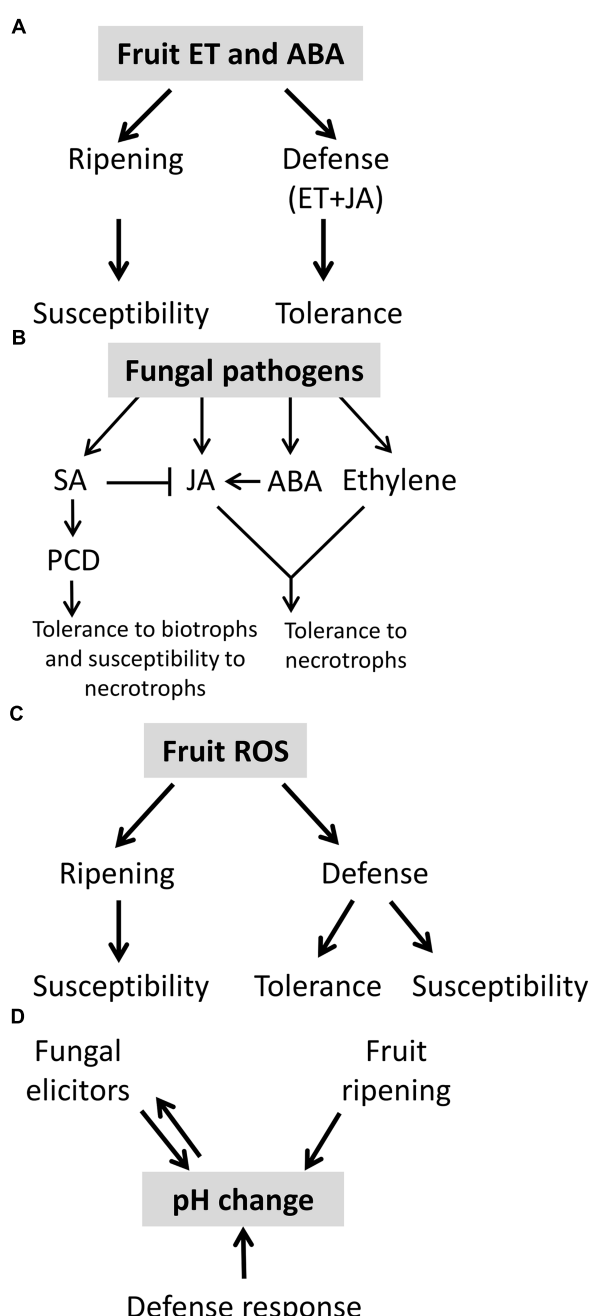


FIGURE 4 | Role of phytohormones, ROS, and pH in post-harvest disease. **(A)** Ethylene and abscisic acid (ABA) activate fruit ripening and susceptibility in fruit but also participate in the defense response to pathogens together with JA. This interplay of hormonal signals can lead to increased tolerance. **(B)** Fruit defense response to fungal pathogens is mediated by phytohormones as salicylic acid (SA), jasmonic acid (JA), ABA, and ethylene. Phytohormones cross-talk can determine fruit tolerance to biotrophic or necrotrophic fungal pathogens. JA and ethylene are classically reported to be involved in tolerance to necrotrophs and SA to biotrophs. **(C)** ROS is one of the components that control fruit ripening and thus susceptibility. ROS also participate in fruit defense response, depending on its relative concentration it could lead to susceptible or tolerant response. **(D)** Fruit ripening, fruit defense response and fungal elicitors modify the pH in the court of host-pathogen interaction.

In tomato, a climacteric fruit, ethylene is known to commence during the breaker stage of fruit ripening (Seymour et al., 2013). Post-harvest fungal pathogen as *B. cinerea* and *C. gloeosporioides* infections induce the ethylene biosynthesis pathway, transcription factors as non-ripening (NOR), ripening-inhibitor (RIN) and never-ripe (NR) and the ethylene-regulated defense genes in both ripe and unripe tomato fruit (Blanco-Ulate et al., 2013; Alkan et al., 2015). Therefore, they enhance the ripening process and hasten the release from quiescence.

The increased susceptibility of ripe fruit to *B. cinerea* depends on the ripening regulator NOR, but not on RIN, and only partially on the fruit's perception of ethylene. The *rin* mutant fruits and those treated with 1-MCP did not ripe but, nevertheless, were susceptible to *B. cinerea* (Cantu et al., 2009; Blanco-Ulate et al., 2013). The differential effect of NOR and RIN indicate the existence of a specific susceptibility factor. Although *nor* and *rin* act together in a cascade for ripening *nor* appears to have a more global effect indicating that it operates upstream of *rin* (Osorio et al., 2011). Inspection of the differential expression of genes in these mutants may point to a source for susceptibility.

Applications of 1-MCP, an inhibitor of ethylene perception, are widely used due to the beneficial effects in delaying fruit senescence and prolonging storage (Watkins, 2006; Watkins and Nock, 2008). Indeed, in apples (Saftner et al., 2003), peaches (Liu et al., 2005), and plums (Menniti et al., 2004) 1-MCP treatment reduced fungal pathogens rotting. However, in tomato (Su and Gubler, 2012; Biswas et al., 2014), avocado (Woolf et al., 2005), custard apple, mango, and papaya (Hofman et al., 2001), citrus (Porat et al., 1999), apples (Janisiewicz et al., 2003) 1-MCP promoted susceptibility to pathogens. It seems that 1-MCP could affect citrus, strawberry, and tomato fruits susceptibility in a concentration dependent manner. At low concentrations it enhances tolerance, but reduces it at high concentrations (Ku et al., 1999; Dou et al., 2005; Blanco-Ulate et al., 2013). Thus, small amounts of endogenous ethylene may be necessary to maintain basic levels of resistance to pathogens due to ethylene involvement in regulation of plant defense genes (Marcos et al., 2005).

These results support the conclusion that ethylene has dual opposing roles: as a ripening hormone it promotes susceptibility (Burg and Burg, 1965) and as a participant in hormone-activated defense responses ethylene provide resistance (Glazebrook, 2005; Spoel et al., 2007). Thus, the timing of ethylene release, perception and the levels of ethylene are likely to be crucial for the outcomes of resistance or susceptibility (**Figure 4A**).

ROS Role in Ripening and Defense Response

Accumulation of reactive oxygen species (ROS) are the result of the balance between ROS production and antioxidant activity. The mitochondria chloroplast and peroxisome are all potential sources for ROS production. ROS and particularly hydrogen peroxide (H_2O_2) and singlet oxygen (1O_2) contribute to fruit ripening and senescence (Brennan and Frenkel, 1977; Lacan and Baccou, 1998; Rogiers et al., 1998; Tian et al., 2013). In grape and tomato, ROS, lipid peroxidation, and protein oxidation

were increased at breaker stage (**Figure 4C**). In many fruits, storage is associated with an increase in ROS, which results either from increased ROS production or from a decrease in antioxidative makeup (Hodges, 2003). Antioxidants inhibit fruit ripening and senescence (Lester, 2003), while, high O₂ or application of H₂O₂ leads to increase ROS and senescence (Tian et al., 2013). Oxidative damage of several mitochondrial proteins, which involved in fruit senescence would result in impairment of mitochondrial function and lead to fruit senescence (Tian et al., 2013).

Many post-harvest fungi can modulate host ROS production. Fungi secrete elicitors, toxins and antioxidants in order to modify the plant ROS production (Aver'yanov et al., 2012; Alkan et al., 2013a). For example, oxalate secreted by *Sclerotinia* generates reducing conditions and inhibited plant oxidative burst at pH 3–4 (Cessna et al., 2000; Williams et al., 2011). In contrast, oxalic acid also induced plant NADPH oxidase and ROS production that correlated with a pH increase to 5–6, that later induced host PCD (Kim et al., 2008). Another example is ammonia that is secreted by *Colletotrichum*, which activated the tomato NADPH oxidase, this resulted in oxidative burst leading to induction of SA mediated defense response, host cell death and enhanced necrotrophic colonization (Alkan et al., 2009, 2012). How these small molecules manipulate the NADPH oxidase is unknown.

Plant ROS can be toxic, e.g., in photo-oxidative stress, but are also known to play an important role in eliciting a wide range of defense mechanisms (Baker and Orlandi, 1995; D'Autréaux and Toledano, 2007; **Figure 4C**). One of the earliest plant cellular responses following successful pathogen recognition is the production of ROS, also called oxidative burst (Torres et al., 2006). ROS also play a central role in redox-dependent defense signaling and in creating toxic environments that induce cell death (Dickman and Fluhr, 2013). In this regard, at the cellular juncture of pathogenesis, NPR1, the master regulator of SA-mediated defense, is actually reduced by thioredoxin, which removes the effect of nitrosylation (Tada et al., 2008). Once reduced, the NPR1 oligomer is disrupted and its monomers enter the nucleus, and activate SA-mediated defense and PCD. It should be noted that in a manner that is not fully understood such signaling can take place even under conditions of cellular oxidative stress.

Reactive oxygen species levels can regulate the host cells fate. High ROS levels in plant cells results in a spreading cell death, which provides nutrients to necrotrophic pathogens. Intermediate concentration of ROS usually results in restricted PCD, and low concentration of ROS can act as a signaling molecule, including the activation of antioxidant enzymes usually leading to host protection against necrotrophs (Dickman and Fluhr, 2013). Mitochondria ROS was shown to be involved in plant PCD in both biotic and abiotic stress responses (Dickman and Fluhr, 2013; Tian et al., 2013). A recent report revealed another ROS, singlet oxygen, which plays a major role in plant response to both biotic and abiotic stress (Mor et al., 2014). Signaling of ROS is important in both the ripening process and defense response (**Figure 4C**). However, the exact roles of ROS can appear counterintuitive and there is a need to better understand their compartmentalization.

Cuticle and Fatty Acid Biosynthesis

Necrotrophic plant pathogens such as *B. cinerea* and *C. gloeosporioides*, at the pathogenic stage, produce cutinases and pectinolytic enzymes to penetrate plant cuticle and epidermal cell wall. Cuticle and cuticular wax are known to regulate fungal cutinase gene expression, leading to the release of cutin monomers from the plant cuticle (Woloshuk and Kolattukudy, 1986). Cutin monomers induce typical PAMP-triggered immunity (PTI) responses including medium alkalization, ethylene production, ROS, and upregulation of defense-related genes (Schweizer et al., 1996; Kauss et al., 1999). Furthermore, treatments with cutin monomers or their production *in vivo* enhances resistance to both biotrophic and necrotrophic fungi (Mengiste et al., 2012). *Arabidopsis* plants expressing a fungal cutinase or mutants with a defective cuticle, such as *long-chain acyl-CoA synthetase2* which is involved in cutin biosynthesis, are surprisingly resistant to *B. cinerea* (Bessire et al., 2007; Chassot et al., 2007). This may be due to faster perception and response to fungal elicitors, easier diffusion of defense signals and antifungal compounds to the infection site and faster oxidative burst (Mengiste et al., 2012). *Bdg* and *lacs2.3* mutants impaired in cutin synthesis are known to display a high level of resistance to *B. cinerea* produced ROS even in the absence of wounding of the leaves (L'Haridon et al., 2011). Moreover, *aba2* and *aba3* mutants together with *bdg* and *lacs2.3* mutants presented increased permeability of the cuticle and enhanced ROS production. In fact, ABA was reported to play an essential role in cuticular permeability, which may influence tomato fruit resistance to *B. cinerea* and may lead to the termination of quiescence (Curvers et al., 2010).

Cuticle related mutants that alter cuticle development and composition were shown to modify plant defenses response and resistance (Voisin et al., 2009). Therefore, the processes of degradation of cuticle and cell wall may have an effect on quiescence. Thus, cell wall and cuticle can constitute valuable targets for improvement of early sensing of pathogen and activation of immune responses accompanied with fruit quality traits. Due to this reason the regulatory mechanisms involved in cuticle deposition have been investigated (Hen-Avivi et al., 2014). The first identified cuticle – associated transcription factor was SHINE1/WAXINDUCER1 (SHN1/WIN; Aharoni et al., 2004; Broun et al., 2004). Recently, it was shown that silencing a tomato ortholog (*SISHN3*) in the fruit resulted in a dramatic reduction in cuticle formation (Shi et al., 2013). It was suggested in this study that *SISHN3* regulates not only the genes involved in cutin metabolism but also controls the expression of regulatory genes associated with epidermal cell patterning including tomato genes similar to *GLABRA2* and *MIXTA* (Shi et al., 2013). Recent data showed that *SIMIXTA-like* is a major transcriptional regulator of cutin biosynthesis, likely acting downstream of *SISHN3*. *SIMIXTA-like* not only promoted conical-type epidermal cell development in tomato fruit but also positively regulated cuticular lipids in particular cutin monomer biosynthesis as well as cuticle assembly (Lashbrooke et al., 2015). Tomato fruit silenced in either *SISHN3* or *SIMIXTA-like* had a significant increase susceptibility to *Colletotrichum* (Shi et al., 2013; Lashbrooke et al., 2015). In another study, leaves of

SISHN3 over-expressing plants were shown to be more resistant to *B. cinerea* than wild-type leaves, highlighting the importance of cuticle in plant-pathogen interactions (Buxdorf et al., 2014).

The thickness and composition of the cuticle has been shown to influence infection of grape berries by *B. cinerea* (Figure 2; Commenil et al., 1997). Hexacosanoic acid, an important component of wax, is present in higher amounts in Touriga Nacional berries than in Trincadeira berries (Agudelo-Romero et al., 2013) and this may be involved in tolerance of Touriga Nacional cultivar to *B. cinerea*. Recently, it was reported that Trincadeira berries infected with *B. cinerea* accumulate saturated long-chain fatty acids which are major constituents of grape waxes accompanied with up-regulation of several acyl-CoA synthetases and wax synthases (Agudelo-Romero et al., 2015). In this study, significant changes were observed in the contents of glycerol and fatty acids such as oleic acid. In addition, a gene encoding a stearyl acyl carrier protein desaturase, which catalyzes the desaturation of stearic acid to oleic acid, was up-regulated in infected berries. It has been shown that a reduction in oleic acid levels results in constitutive activation of the SA-dependent pathway and repression of the JA-dependent pathway (Kachroo and Kachroo, 2009; Kachroo and Robin, 2013). The results in grapes supported these data, since increased oleic acid levels were correlated with activation of JA biosynthesis and signaling in infected berries (Agudelo-Romero et al., 2015). Thus, changes in lipid composition likely represent fruit response to infection.

Interestingly, transcriptome analysis of *C. gloeosporioides* and tomato fruit pathosystem revealed that during appressoria formation and before fungal penetration the tomato fruit host recognizes the fungus and activates fatty acid biosynthesis, elongation, and synthesis of cutin and waxes (Alkan et al., 2015). Specifically, genes involved in synthesis of very long chain fatty acids that are components of cutin and waxes were up-regulated namely 3-ketoacyl CoA synthase and CYP86A cytochrome p450. Interestingly, tomato fruit mutated in CYP86 were much more susceptible to *Colletotrichum* infection (Shi et al., 2013). These genes were also up-regulated in grape berries infected with *B. cinerea* along with a decrease in expression of genes involved in glycerolipid catabolism (Agudelo-Romero et al., 2015). Both pathosystems also reported the induction of β -oxidation fatty acid degradation pathway (Agudelo-Romero et al., 2015; Alkan et al., 2015). This would provide both reducing power and carbon components for metabolism of very long chain fatty acids or alternatively would provide more sugars that might be metabolized by the fungus or serve as precursors of plant secondary metabolites involved in defense. These observations further emphasize the critical role of fatty acids, wax and cutin during infection. This topic deserves further attention, since pathogen and host lipids and lipid metabolites have a critical role in the dynamics of pathogenesis and in plants defense.

Cell Wall Remodeling and Soluble Sugar Accumulation

Cell walls are structurally complex network of polysaccharides, including cellulose, hemicelluloses, and pectin (Cosgrove, 2005). They serve as a physical barrier that limits pathogen access, but

are also involved in pathogen recognition and in the deployment of plant responses to pathogens (Vorwerk et al., 2004; Cantu et al., 2008a,b; Hématy et al., 2009). In order to break down the cell wall barrier pathogens use mechanical force as appressoria (Deising et al., 2000) or release cell wall degrading enzymes (CWDEs), which serve as a pathogenicity factors (Walton, 1994). Also post-harvest pathogens as *Botrytis* (van Kan et al., 1997; Blanco-Ulate et al., 2014) and *Colletotrichum* (Alkan et al., 2013b, 2015) produces CWDEs during pathogenic colonization of tomato fruit. The degradation of the plant cell wall matrix by pathogens may affect the proteins embedded in the cell wall and are likely to activate PAMP-triggered immunity (van Loon et al., 2006; Mengiste, 2012), which often leads to callose deposition at sites of penetration, accumulate phenolic compounds and various toxins in the cell wall and synthesize lignin-like polymers to reinforce the wall (Huckelhoven, 2007).

During natural fleshy fruit ripening the fruit soften as a result of fruit activation of CWDEs as polygalacturonase (PG), pectin methylesterase, pectate lyase, β -galactosidase, cellulase, and expansin (Brummell et al., 1999; Paniagua et al., 2014). Phytohormones as ethylene, ABA, SA and JA, are known to influence the expression of CWDEs which contribute to fruit softening (Huckelhoven, 2007). Because, fruit CWDEs are normally activated during ripening, it was commonly assumed that fruit softening contributes to the transition to susceptibility to pathogens (Figure 2; Paniagua et al., 2014). In tomato, the suppression of softening-associated CWDEs, *SlPG* and *SlExp1*, reduced susceptibility to *B. cinerea* infection during ripening, indicating that PG and Exp support both softening (Brummell et al., 1999, 2002; Kalamaki et al., 2003; Powell et al., 2003) and susceptibility to *B. cinerea* (Cantu et al., 2008a,b). Interestingly, *B. cinerea* infections induce *SlPG* and *SlExp1* expression (GonzalezBosch et al., 1996; Flors et al., 2007), suggesting that *Botrytis* induces similar softening to the softening that occurs during fruit ripening. Endo- β -1,4-glucanase (EGase) is another CWDE that have a role in fruit softening. Tomato fruit EGase antisense had enhanced callose deposition and was more resistant against *Botrytis* infection (Flors et al., 2007). Plants PG inhibiting proteins (PGIPs) reduce the pathogen pectin degradation (De Lorenzo et al., 2001). PGIPs inhibit most of the *Botrytis* PGs during pear pathogenesis (Sharrock and Labavitch, 1994). An over-expression of PGIPs enhances ripe tomato fruit tolerance to *Botrytis* (Powell et al., 2000). To conclude, fruit cell wall is a complex and dynamic barrier which changes during ripening and its interaction with fungal pathogens plays a major role in the defense response against pathogens.

pH Change during Fruit Ripening and Fungal Colonization

The pH change plays an important role in three different aspects of fruit-fungal interaction: (1) the pH change during fruit ripening, (2) fungal-dependent pH modulation of the local infection court, and (3) the local host pH modulation during the activation of defense responses (Figure 4D). The combined pH changes were suggested to trigger defense related processes as ROS and activate cell wall hydrolases in the fruit.

The ratio between sugar and pH are determinants of the fruit taste. During fruit ripening total soluble sugars (TSSs) increase and organic acid usually decreases leading to increase in pH. For instance, the pH of avocado fruit increases from 5.2 to 6.0 during ripening (Yakoby et al., 2000). However, in tomato fruit the apoplastic pH decreases during ripening from 6.7 to 4.4 (Almeida and Huber, 1999).

Also fungal pathogens alter their local pH by secretion of ammonia or organic acids to optimize the environment to each fungus enzymatic arsenal (reviewed in Alkan et al., 2013a). Interestingly, fruit pH greatly affects fungal pathogenicity. Acidified environment induce ammonia secretion in alkalizing fungi as *Colletotrichum* and *Alternaria* (Eshel et al., 2002; Alkan et al., 2008), while alkaline environment activate organic acid secretion in acidifying fungi as *Penicillium* and *Botrytis* (Manteau et al., 2003; Hadas et al., 2007). The pH dependent fungal pathogenicity factors are controlled in filamentous fungi by Pal signaling pathway which activates PACC transcription factor (Penalva et al., 2008). PACC activates transcription of those pathogenicity factors at alkaline pH and the AREB transcription factor, which represses acidic expressed pathogenicity factors at alkaline environment (Alkan et al., 2013b; Ment et al., 2015). In this way, fungi adjust their ambient pH in order to optimize the activity of their enzymatic arsenal.

Changes in apoplastic pH, could lead to oxidative burst (Gao et al., 2004). For example, exposing bean cells to alkaline condition resulted in oxidative burst (Wojtaszek et al., 1995). Medium alkalization activate NADPH oxidase, probably as a result of induced K^+/H^+ exchange, followed by Ca^{2+} influx/ Cl^- efflux (Simon-Plas et al., 1997; Nurnberger and Scheel, 2001; Zhao et al., 2005). Transient extracellular alkalinization is an essential factor in induction of defense response and PCD (Schaller and Oecking, 1999; Clarke et al., 2005; Hano et al., 2008). In this connection, changes in *Arabidopsis thaliana* roots external pH rapidly alter plant gene expression and modulate host responses, similarly to elicitors (Lager et al., 2010). Similarly, tomato fruit apoplastic alkalinization by *Colletotrichum* or application of ammonia lead to activation of fruit NADPH oxidase, oxidative burst and SA mediated defense response that ended with extended cell death (Alkan et al., 2012). *P. expansum* secrets gluconic acid and acidify its ambient pH in apples; this acidification was correlated with oxidative burst (Hadas et al., 2007). Taken together both pathogen and fruit modulate their ambient pH in order to optimize respectively their attack and responses (**Figure 4D**).

Preformed and Inducible Antifungal Resistance

Plants contain preformed secondary metabolites of a defensive nature such as phenolics, sulfur compounds, saponins, cyanogenic glycosides, and glucosinolates. Phenolic compounds play an important role in non-host resistance to fungi. They can either be performed occurring constitutively in healthy plants (phytoanticipins) or synthesized from precursors in response to pathogen attack, being more restricted to the damaged tissue

(phytoalexins). Some antibiotic phenolics are stored in plant cells as inactive bound forms but are readily converted into biologically active antibiotics by plant glycosidases in response to pathogen attack. Since these compounds do not involve *de novo* transcription of gene products they are also considered phytoanticipins (Lattanzio et al., 2006). Concentrations of preformed phytoanticipins and inducible phytoalexins were found to decline during fruit ripening (**Figure 2**) and this occurred more rapidly in susceptible cultivars than in resistant cultivars (Prusky, 1996; Lattanzio et al., 2001; Prusky et al., 2013).

The grape berry cultivar Trincadeira is susceptible to *B. cinerea* and downy mildew. It presents lower phenolics content than the tolerant cultivars Touriga Nacional and Aragonês (Ali et al., 2011). The green and *veraison* stages of Aragonês and Touriga Nacional showed higher levels of quercetin glucoside, catechin and hydroxycinnamic acid derivatives such as caftaric acid and coutaric acid than the ripe grape berry (Ali et al., 2011; Agudelo-Romero et al., 2013). A decrease in caffeic acid was also detected in ripe berries of all the three varieties (Agudelo-Romero et al., 2013). This decline may be related to increased susceptibility of ripe fruits to pathogenic fungi. In fact, caffeic acid presents antimicrobial activity (Widmer and Laurent, 2006). Further, constitutive secondary metabolites of the bitter orange *Citrus aurantium* are the flavanone-naringin and the polymethoxyflavone-tangeretin, which showed antifungal activity against *Penicillium digitatum* (Arcas et al., 2000).

Other widely reported preformed antifungal compounds are the family of mono-, di-, and triene compounds in avocado; the resorcinol derivates in mango; the tannins in banana peel (Prusky, 1996) and tomatine in tomato fruits (Itkin et al., 2011). These compounds were shown to decline dramatically during fruit ripening, thus enabling development of penetrating mycelia (Verhoeff, 1974; Prusky et al., 2013).

Inducible Phenylpropanoid Metabolism

Phytoalexins are generally induced after infection. They accumulate rapidly in response to infection and reach high antimicrobial levels in resistant plants, while there is either lesser or slower accumulation in susceptible plants (Lattanzio et al., 2006). When the accumulation of phytoalexins is either increased or decreased by manipulation of the experimental conditions such as post-harvest stress treatments, the plant and fruit become either more resistant or more susceptible (Lattanzio et al., 2006). Fawe et al. (1998) reported that silicon is involved in the increased resistance of cucumber to powdery mildew by enhancing the antifungal activity due to the presence of metabolites such as flavonol aglycone rhamnetin (3,5,3',4'-tetrahydroxy-7-O-methoxyflavone).

Pathogens often remain quiescent in unripe fruits. During ripening the concentrations of pathogen-induced and pre-formed antifungal phenolics decrease to subtoxic levels (**Figure 2**); this chemical decline occurs more rapidly in susceptible cultivars than in resistant ones (Lattanzio et al., 2006). The principal phenolics in the peach fruit include chlorogenic acid, catechin, and epicatechin. The decline in chlorogenic acid and other endogenous phenolics during fruit

ripening correspond to the transition to susceptibility (Bostock et al., 1999). In immature strawberry fruits with a high content of proanthocyanidins *B. cinerea* remains quiescent. When the inhibitory activity of proanthocyanidins in fruits decreases due to maturation, the quiescent fungus can switch to the necrotrophic stage and progress further into the fruit tissue (Jersch et al., 1989). In addition, inducible antifungal compounds, such as capsicannol in pepper, scoparone in citrus, resveratrol in grapes, and others, have been reported to be activated in unripe fruits but not always in ripe fruits (Prusky, 1996). These compounds were hypothesized to be quiescence modulating factors.

The resistance of *Vitis* sp. to *B. cinerea* infection has been shown to correlate with *trans*-resveratrol content (Gabler et al., 2003). Touriga Nacional is not infected by *B. cinerea* under normal field conditions; this cultivar presents higher content in *trans*-resveratrol than the susceptible cultivar Trincadeira (Agudelo-Romero et al., 2013). Recently, in-field infections of Trincadeira cultivar with *B. cinerea* led to profound alterations in secondary metabolism linked to stress response together with a significant increase in *trans*-resveratrol. Indeed, several genes involved in phytoalexin biosynthesis and coding for stilbene synthase and resveratrol synthase were up-regulated at pre-*veraison* in infected grapes (Agudelo-Romero et al., 2015). Therefore, resveratrol was considered a potential positive metabolic marker of *B. cinerea* infection at this stage. Other identified positive markers of infection were gallic acid and 3,4-dihydroxybenzoic acid which present antifungal properties (Lattanzio et al., 2006). In fact, plant benzoic acids and their derivatives are common and widespread mediators of plant responses to biotic and abiotic stress (Wildermuth, 2006). In another work with grape, flavonoid compounds were only found in botrytized berries of botrytized bunches at harvest stage (Hong et al., 2012).

Trincadeira, a *Botrytis*-susceptible variety, is able to initiate to some extent a basal defense reprogramming of the transcriptome and metabolome that is unable to slow down disease progression (Agudelo-Romero et al., 2015). This can be due to the fact that the pathogen can shut down host defenses. For example, sesquiterpenoid biosynthesis, as measured by genes involved in their synthesis; namely *beta*-amyrin synthase and (-)-germacrene D synthase, was down-regulated at the *veraison* stage. Oleanolic acid, a triterpenoid, decreased in infected grapes at pre-*veraison* and *veraison* stages. Unconjugated triterpenoids, such as oleanolic acid, are often found in the epicuticular waxes of plants serving as a first defense barrier against pathogens (Heinzen et al., 1996). This result suggested that infection renders the fruit to be more susceptible by down-regulating defense compounds.

Recently, it was showed through a combined analysis of the transcriptomes of *C. gloeosporioides* and tomato fruit pathosystem that during the quiescent stage, defense pathways

were up-regulated including the phenypropanoid pathway for phytoalexin and lignin precursors such as cinnamic, cumarayl, coniferyl, caffeoyl, shikimic, quinic, and sinapyl derivatives (Alkan et al., 2015). The authors suggested that phytoalexin biosynthesis and lignification comprise a major ongoing fruit defense pathway employed by the fruit in response to the persistent presence of quiescent fungi. Such host responses may effectively restrain the pathogen. Indeed, the number of infection sites emerging from quiescence appears to be below the potential primary infection sites, indicating successful containment of the infection. In this study, genes involved in the synthesis of sesquiterpenoids (e.g., rishitin) were also down-regulated together with the up-regulation of key steroid glycoalkaloid (e.g., tomatine) transcripts. Previously, α -tomatine was shown to inhibit *Colletotrichum* fungal growth and germination (Itkin et al., 2011). Hence, transcript expression suggests the occurrence of shifts from rishitin to α -tomatine biosynthetic pathway as an effective response to this fungus. All of those antifungal compounds decline in ripe fruits, which may permit emergence of fungi from quiescence (Prusky, 1996).

CONCLUSION

During ripening, fruit undergo major changes such as activation of ethylene synthesis and other phytohormones, pH change, cuticular changes, cell-wall loosening and increase of soluble sugars, decline of antifungal compounds (Figure 2), which release the fungus from its quiescent state and promote a necrotrophic and pathogenic life style. Knowledge on the molecular and metabolic events responsible for the onset of necrotrophic stage, occurring both in the host and in fungi, is important key in order to develop strategies to enhance fruit defense and decrease of fungal virulence that ultimately will result in increased quality of fruits. This knowledge can be considered in breeding programs, pre and post-harvest treatments or alternatively provide a framework for biotechnological approaches.

ACKNOWLEDGMENTS

We thank Professor Robert Fluhr for his critical comments on the manuscript. This manuscript is contribution no. 728/14 from the Agricultural Research Organization, the Volcani Center, P.O. Box 6, Bet Dagan 50250, Israel. This work was developed within BioFig (PEst-OE/BIA/UI4046/2014) and funded by Portuguese FCT (SFRH/BPD/100928/2014). The review is integrated in the COST (European Cooperation in Science and Technology) Action FA1106 ‘Quality fruit’.

REFERENCES

- AbuQamar, S., Chen, X., Dhawan, R., Bluhm, B., Salmeron, J., Lam, S., et al. (2006). Expression profiling and mutant analysis reveals complex regulatory networks

- involved in *Arabidopsis* response to Botrytis infection. *Plant J.* 48, 28–44. doi: 10.1111/j.1365-313X.2006.02849.x
Adaskaveg, J. E., Forster, H., and Thompson, D. F. (2000). Identification and etiology of visible quiescent infections of *Monilinia fructicola* and

- Botrytis cinerea* in sweet cherry fruit. *Plant Dis.* 84, 328–333. doi: 10.1094/PDIS.2000.84.3.328
- Agudelo-Romero, P., Erban, A., Rego, C., Carbonell-Bejerano, P., Nascimento, T., Sousa, L., et al. (2015). Transcriptome and metabolome reprogramming in *Vitis vinifera* cv. *Trincadeira berries* upon infection with *Botrytis cinerea*. *J. Exp. Bot.* 66, 1769–1785. doi: 10.1093/jxb/eru517
- Agudelo-Romero, P., Erban, A., Sousa, L., Pais, M. S., Kopka, J., and Fortes, A. M. (2013). Search for transcriptional and metabolic markers of grape pre-ripening and ripening and insights into specific aroma development in three portuguese cultivars. *PLoS ONE* 8:e60422. doi: 10.1371/journal.pone.0060422
- Aharoni, A., Dixit, S., Jetter, R., Thoenes, E., van Arkel, G., and Pereira, A. (2004). The SHINE clade of AP2 domain transcription factors activates wax biosynthesis, alters cuticle properties, and confers drought tolerance when overexpressed in *Arabidopsis*. *Plant Cell* 16, 2463–2480. doi: 10.1105/tpc.104.022897
- Alexander, L., and Grierson, D. (2002). Ethylene biosynthesis and action in tomato: a model for climacteric fruit ripening. *J. Exp. Bot.* 53, 2039–2055. doi: 10.1093/jxb/erf072
- Ali, K., Maltese, F., Fortes, A. M., Pais, M. S., Choi, Y. H., and Verpoorte, R. (2011). Monitoring biochemical changes during grape berry development in Portuguese cultivars by NMR spectroscopy. *Food Chem.* 124, 1760–1769. doi: 10.1016/j.foodchem.2010.08.015
- Alkan, N., Davydov, O., Sagi, M., Fluhr, R., and Prusky, D. (2009). Ammonium secretion by *Colletotrichum coccodes* activates host NADPH oxidase activity enhancing host cell death and fungal virulence in tomato fruits. *Mol. Plant Microbe* 22, 1484–1491. doi: 10.1094/MPMI-22-12-1484
- Alkan, N., Espeso, E. A., and Prusky, D. (2013a). Virulence regulation of phytopathogenic fungi by pH. *Antioxid. Redox Signal.* 19, 1012–1025. doi: 10.1089/ars.2012.5062
- Alkan, N., Meng, X., Friedlander, G., Reuveni, E., Sukno, S., Sherman, A., et al. (2013b). Global aspects of pacC regulation of pathogenicity genes in *Colletotrichum gloeosporioides* as revealed by transcriptome analysis. *Mol. Plant Microbe* 26, 1345–1358. doi: 10.1094/MPMI-03-13-0080-R
- Alkan, N., Fluhr, R., and Prusky, D. (2012). Ammonium secretion during *Colletotrichum coccodes* infection modulates salicylic and jasmonic acid pathways of ripe and unripe tomato fruit. *Mol. Plant Microbe* 25, 85–96. doi: 10.1094/MPMI-01-11-0020
- Alkan, N., Fluhr, R., Sherman, A., and Prusky, D. (2008). Role of ammonia secretion and pH modulation on pathogenicity of *Colletotrichum coccodes* on tomato fruit. *Mol. Plant Microbe* 21, 1058–1066. doi: 10.1094/MPMI-21-8-1058
- Alkan, N., Friedlander, G., Ment, D., Prusky, D., and Fluhr, R. (2015). Simultaneous transcriptome analysis of *Colletotrichum gloeosporioides* and tomato fruit pathosystem reveals novel fungal pathogenicity and fruit defense strategies. *New Phytol.* 205, 801–815. doi: 10.1111/nph.13087
- Almeida, D. P., and Huber, D. J. (1999). Apoplastic pH and inorganic ion levels in tomato fruit: a potential means for regulation of cell wall metabolism during ripening. *Physiol. Plant.* 105, 506–512. doi: 10.1034/j.1399-3054.1999.105316.x
- Arcas, M. C., Botia, J. M., Ortuno, A. M., and Del Rio, J. A. (2000). UV irradiation alters the levels of flavonoids involved in the defence mechanism of *Citrus aurantium* fruits against *Penicillium digitatum*. *Eur. J. Plant Pathol.* 106, 617–622. doi: 10.1023/A:1008704102446
- Aver'yanov, A. A., Belozerskaya, T. A., and Gessler, N. N. (2012). *Fungus Development and Reactive Oxygen: Phytopathological Aspects, Biocommunication of Fungi* (Berlin: Springer), 261–271.
- Baker, C. J., and Orlandi, E. W. (1995). Active oxygen in plant pathogenesis. *Annu. Rev. Phytopathol.* 33, 299–321. doi: 10.1146/annurev.py.33.090195.001503
- Bargel, H., and Neinhuis, C. (2005). Tomato (*Lycopersicon esculentum* Mill.) fruit growth and ripening as related to the biomechanical properties of fruit skin and isolated cuticle. *J. Exp. Bot.* 56, 1049–1060. doi: 10.1093/jxb/eri098
- Bari, R., and Jones, J. (2009). Role of plant hormones in plant defence responses. *Plant Mol. Biol.* 69, 473–488. doi: 10.1007/s11103-008-9435-0
- Barkai-Golan, R. (2001). *Postharvest Diseases of Fruits and Vegetables: Development and Control*. Amsterdam: Elsevier.
- Beno-Moualem, D., and Prusky, D. (2000). Early events during quiescent infection development by *Colletotrichum gloeosporioides* in unripe avocado fruits. *Phytopathology* 90, 553–559. doi: 10.1094/PHYTO.2000.90.5.553
- Bessire, M., Chassot, C., Jacquat, A. C., Humphry, M., Borel, S., Petétot, J. M. C., et al. (2007). A permeable cuticle in *Arabidopsis* leads to a strong resistance to *Botrytis cinerea*. *EMBO J.* 26, 2158–2168. doi: 10.1038/sj.emboj.7601658
- Biswas, P., East, A., Hewett, E., and Heyes, J. (2014). Ripening delay caused by 1-MCP may increase tomato chilling sensitivity. *N. Z. J. Crop Hortic. Sci.* 42, 145–150. doi: 10.1080/01140671.2013.870218
- Biton, E., Kobiler, I., Feygenberg, O., Yaari, M., Friedman, H., and Prusky, D. (2014). Control of alternaria black spot in persimmon fruit by a mixture of gibberellin and benzyl adenine, and its mode of action. *Postharvest Biol. Technol.* 94, 82–88. doi: 10.1016/j.postharvbio.2014.03.009
- Bitrian, M., Zarza, X., Altabella, T., Tiburcio, A. F., and Alcazar, R. (2012). Polyamines under abiotic stress: metabolic crossroads and hormonal crosstalks in plants. *Metabolites* 2, 516–528. doi: 10.3390/metabo2030516
- Blanco-Ulate, B., Morales-Cruz, A., Amrine, K., Labavitch, J. M., Powell, A., and Cantu, D. (2014). Genome-wide transcriptional profiling of *Botrytis cinerea* genes targeting plant cell walls during infections of different hosts. *Front. Plant Sci.* 5:435. doi: 10.3389/fpls.2014.00435
- Blanco-Ulate, B., Vincenti, E., Powell, A. L. T., and Cantu, D. (2013). Tomato transcriptome and mutant analyses suggest a role for plant stress hormones in the interaction between fruit and *Botrytis cinerea*. *Front. Plant Sci.* 4:142. doi: 10.3389/fpls.2013.00142
- Bostock, R. M., Wilcox, S. M., Wang, G., and Adaskaveg, J. E. (1999). Suppression of *Monilinia fructicola* cutinase production by peach fruit surface phenolic acids. *Physiol. Mol. Plant Pathol.* 54, 37–50. doi: 10.1006/pmpp.1998.0189
- Brauc, S., De Vooght, E., Claeys, M., Geuns, J. M. C., Hofte, M., and Angenon, G. (2012). Overexpression of arginase in *Arabidopsis thaliana* influences defence responses against *Botrytis cinerea*. *Plant Biol.* 14, 39–45. doi: 10.1111/j.1438-8677.2011.00520.x
- Brennan, T., and Frenkel, C. (1977). Involvement of hydrogen peroxide in the regulation of senescence in pear. *Plant Physiol.* 59, 411–416. doi: 10.1104/pp.59.3.411
- Broun, P., Poindexter, P., Osborne, E., Jiang, C. Z., and Riechmann, J. L. (2004). WIN1, a transcriptional activator of epidermal wax accumulation in *Arabidopsis*. *Proc. Natl. Acad. Sci. U.S.A.* 101, 4706–4711. doi: 10.1073/pnas.0305574101
- Brummell, D. A., Harpster, M. H., Civello, P. M., Palys, J. M., Bennett, A. B., and Dunsmuir, P. (1999). Modification of expansin protein abundance in tomato fruit alters softening and cell wall polymer metabolism during ripening. *Plant Cell* 11, 2203–2216. doi: 10.1105/tpc.11.11.2203
- Brummell, D. A., Howie, W. J., Ma, C., and Dunsmuir, P. (2002). Postharvest fruit quality of transgenic tomatoes suppressed in expression of a ripening-related expansin. *Postharvest Biol. Technol.* 25, 209–220. doi: 10.1016/S0925-5214(01)00179-X
- Burg, S. P., and Burg, E. A. (1965). Ethylene action and the ripening of fruits ethylene influences the growth and development of plants and is the hormone which initiates fruit ripening. *Science* 148, 1190–1196. doi: 10.1126/science.148.3674.1190
- Buxdorf, K., Rubinsky, G., Barda, O., Burdman, S., Aharoni, A., and Levy, M. (2014). The transcription factor SISHINE3 modulates defense responses in tomato plants. *Plant Mol. Biol.* 84, 37–47. doi: 10.1007/s11103-013-0117-1
- Buzby, J. C., Wells, H. F., and Hyman, J. (2014). *The Estimated Amount, Value, and Calories of Postharvest Food Losses at the Retail and Consumer Levels in the United States*. USDA EIB-121, US. Department of Agriculture, Economic Research Service. doi: 10.2139/ssrn.2501659
- Cannon, P. F., Bridge, P. D., and Monte, E. (2000). “Linking the past, present, and future of *Colletotrichum* systematics,” in ‘*Colletotrichum: Host Specificity, Pathology, and Host Pathogen Interaction*, eds D. F. S. Prusky and M. B. Dickman (St. Paul, MI: APS Presspp), 1–20.
- Cantu, D., Blanco-Ulate, B., Yang, L., Labavitch, J. M., Bennett, A. B., and Powell, A. L. T. (2009). Ripening-regulated susceptibility of tomato fruit to *Botrytis cinerea* requires NOR but not RIN or ethylene. *Plant Physiol.* 150, 1434–1449. doi: 10.1104/pp.109.138701
- Cantu, D., Vicente, A. R., Greve, L. C., Dewey, F. M., Bennett, A. B., Labavitch, J. M., et al. (2008a). The intersection between cell wall disassembly, ripening, and fruit susceptibility to *Botrytis cinerea*. *Proc. Natl. Acad. Sci. U.S.A.* 105, 859–864. doi: 10.1073/pnas.0709813105

- Cantu, D., Vicente, A. R., Labavitch, J. M., Bennett, A. B., and Powell, A. L. T. (2008b). Strangers in the matrix: plant cell walls and pathogen susceptibility. *Trends Plant Sci.* 13, 610–617. doi: 10.1016/j.tplants.2008.09.002
- Cessna, S. G., Sears, V. E., Dickman, M. B., and Low, P. S. (2000). Oxalic acid, a pathogenicity factor for *Sclerotinia sclerotiorum*, suppresses the oxidative burst of the host plant. *Plant Cell* 12, 2191–2199. doi: 10.1105/tpc.12.1.12191
- Chassot, C., Nawrath, C., and Metraux, J. P. (2007). Cuticular defects lead to full immunity to a major plant pathogen. *Plant J.* 49, 972–980. doi: 10.1111/j.1365-313X.2006.03017.x
- Clarke, A., Mur, L. A. J., Darby, R. M., and Kenton, P. (2005). Harpin modulates the accumulation of salicylic acid by *Arabidopsis* cells via apoplastic alkalization. *J. Exp. Bot.* 56, 3129–3136. doi: 10.1093/jxb/eri310
- Commenil, P., Brunet, L., and Audran, J.-C. (1997). The development of the grape berry cuticle in relation to susceptibility to bunch rot disease. *J. Exp. Bot.* 48, 1599–1607. doi: 10.1093/jexbot/48.313.1599
- Cosgrove, D. J. (2005). Growth of the plant cell wall. *Nat. Rev. Mol. Cell Biol.* 6, 850–861. doi: 10.1038/nrm1746
- Curvers, K., Seifi, H., Mouille, G., de Rycke, R., Asselbergh, B., Van Hecke, A., et al. (2010). Abscisic acid deficiency causes changes in cuticle permeability and pectin composition that influence tomato resistance to *Botrytis cinerea*. *Plant Physiol.* 154, 847–860. doi: 10.1104/pp.110.158972
- D'Autréaux, B., and Toledano, M. B. (2007). ROS as signalling molecules: mechanisms that generate specificity in ROS homeostasis. *Nat. Rev. Mol. Cell Biol.* 8, 813–824. doi: 10.1038/nrm2256
- De Lorenzo, G., D'ovidio, R., and Cervone, F. (2001). The role of polygalacturonase-inhibiting proteins (PGIPs) in defense against pathogenic fungi. *Annu. Rev. Phytopathol.* 39, 313–335. doi: 10.1146/annurev.phyto.39.1.313
- Deising, H. B., Werner, S., and Wernitz, M. (2000). The role of fungal appressoria in plant infection. *Microbes Infect.* 2, 1631–1641. doi: 10.1016/S1286-4579(00)01319-8
- Dickman, M. B., and Fluhr, R. (2013). Centrality of host cell death in plant-microbe interactions. *Annu. Rev. Phytopathol.* 51, 543–570. doi: 10.1146/annurev-phyto-081211-173027
- Dou, H., Jones, S., and Ritenour, M. (2005). Influence of 1-MCP application and concentration on post-harvest peel disorders and incidence of decay in citrus fruit. *J. Hortic. Sci. Biotechnol.* 80, 786–792.
- Emery, K. M., Michailides, T. J., and Scherm, H. (2000). Incidence of latent infection of immature peach fruit by *Monilinia fructicola* and relationship to brown rot in Georgia. *Plant Dis.* 84, 853–857. doi: 10.1094/PDIS.2000.8.4.853
- Eshel, D., Ben-Arie, R., Dinoor, A., and Prusky, D. (2000). Resistance of gibberellin-treated persimmon fruit to *Alternaria alternata* arises from the reduced ability of the fungus to produce endo-1,4-beta-glucanase. *Phytopathology* 90, 1256–1262. doi: 10.1094/PHYTO.2000.90.11.1256
- Eshel, D., Miyara, I., Ailing, T., Dinoor, A., and Prusky, D. (2002). pH regulates endoglucanase expression and virulence of *Alternaria alternata* persimmon fruit. *Mol. Plant Microbe* 15, 774–779. doi: 10.1094/MPMI.2002.15.8.774
- Fawcett, A., Abou-Zaid, M., Menzies, J. G., and Belanger, R. R. (1998). Silicon-mediated accumulation of flavonoid phytoalexins in cucumber. *Phytopathology* 88, 396–401. doi: 10.1094/PHYTO.1998.88.5.396
- Flors, V., Leyva, M. D., Vicedo, B., Finiti, I., Real, M. D., Garcia-Agustin, P., et al. (2007). Absence of the endo-beta-1,4-glucanases Cel1 and Cel2 reduces susceptibility to *Botrytis cinerea* in tomato. *Plant J.* 52, 1027–1040. doi: 10.1111/j.1365-313X.2007.03299.x
- Fujita, M., Fujita, Y., Noutoshi, Y., Takahashi, F., Narusaka, Y., Yamaguchi-Shinozaki, K., et al. (2006). Crosstalk between abiotic and biotic stress responses: a current view from the points of convergence in the stress signaling networks. *Curr. Opin. Plant Biol.* 9, 436–442. doi: 10.1016/j.pbi.2006.05.014
- Gabler, F. M., Smilanick, J. L., Mansour, M., Ramming, D. W., and Mackey, B. E. (2003). Correlations of morphological, anatomical, and chemical features of grape berries with resistance to *Botrytis cinerea*. *Phytopathology* 93, 1263–1273. doi: 10.1094/PHYTO.2003.93.10.1263
- Gao, D., Knight, M. R., Trewavas, A. J., Sattelmacher, B., and Plieth, C. (2004). Self-reporting *Arabidopsis* expressing pH and $[Ca^{2+}]$ indicators unveil ion dynamics in the cytoplasm and in the apoplast under abiotic stress. *Plant Physiol.* 134, 898–908. doi: 10.1104/pp.103.032508
- Geny, L., Darriueumerlou, A., and Doneche, B. (2003). Conjugated polyamines and hydroxycinnamic acids in grape berries during *Botrytis cinerea* disease development: differences between 'noble rot' and 'grey mould'. *Austr. J. Grape Wine Res.* 9, 102–106. doi: 10.1111/j.1755-0238.2003.tb0259.x
- Giovannoni, J. (2001). Molecular biology of fruit maturation and ripening. *Annu. Rev. Plant Phys.* 52, 725–749. doi: 10.1146/annurev.applant.52.1.725
- Glazebrook, J. (2005). Contrasting mechanisms of defense against biotrophic and necrotrophic pathogens. *Annu. Rev. Phytopathol.* 43, 205–227. doi: 10.1146/annurev.phyto.43.040204.135923
- GonzalezBosch, C., Brummell, D. A., and Bennett, A. B. (1996). Differential expression of two endo-1,4-beta-glucanase genes in pericarp and locules of wild-type and mutant tomato fruit. *Plant Physiol.* 111, 1313–1319.
- Griebel, T., and Zeier, J. (2010). A role for beta-sitosterol to stigmasterol conversion in plant-pathogen interactions. *Plant J.* 63, 254–268. doi: 10.1111/j.1365-313X.2010.04235.x
- Gustavsson, J., Cederberg, C., Sonesson, U., van Otterdijk, R., and Meybeck, A. (2011). *Global Food Losses and Food Waste - Extent, Causes and Prevention*. Rome: Food and Agriculture Organization.
- Hadas, Y., Goldberg, I., Pines, O., and Prusky, D. (2007). Involvement of gluconic acid and glucose oxidase in the pathogenicity of *Penicillium expansum* in apples. *Phytopathology* 97, 384–390. doi: 10.1094/PHYTO-97-3-0384
- Hano, C., Addi, M., Fliniaux, O., Bensaddek, L., Duverger, E., Mesnard, F., et al. (2008). Molecular characterization of cell death induced by a compatible interaction between *Fusarium oxysporum* f. sp. lini and flax (*Linum usitatissimum*) cells. *Plant Physiol. Biochem.* 46, 590–600. doi: 10.1016/j.plaphy.2008.02.004
- Harberd, N. P., Belfield, E., and Yasumura, Y. (2009). The angiosperm gibberellin-GID1-DELLA growth regulatory mechanism: how an "Inhibitor" enables flexible response to fluctuating environments. *Plant Cell* 21, 1328–1339. doi: 10.1105/tpc.109.066969
- Heinzen, H., deVries, J. X., Moyna, P., Remberg, G., Martinez, R., and Tietze, L. F. (1996). Mass spectrometry of labelled triterpenoids: thermospray and electron impact ionization analysis. *Phytochem. Anal.* 7, 237–244. doi: 10.1002/(SICI)1099-1565(199609)7:5<237::AID-PCA310>3.0.CO;2-M
- Hématy, K., Cherk, C., and Somerville, S. (2009). Host-pathogen warfare at the plant cell wall. *Curr. Opin. Plant Biol.* 12, 406–413. doi: 10.1016/j.pbi.2009.06.007
- Hen-Avivi, S., Lashbrooke, J., Costa, F., and Aharoni, A. (2014). Scratching the surface: genetic regulation of cuticle assembly in fleshy fruit. *J. Exp. Bot.* 65, 4653–4664. doi: 10.1093/jxb/eru225
- Hodges, D. (2003). *Overview: Oxidative Stress and Postharvest Produce. Postharvest Oxidative Stress in Horticultural Crops* (New York, NY: Food Products Press), 1–12.
- Hofman, P. J., Jobin-Decom, M., Meiburg, G. F., Macnish, A. J., and Joyce, D. C. (2001). Ripening and quality responses of avocado, custard apple, mango and papaya fruit to 1-methylcyclopropene. *Aust. J. Exp. Agric.* 41, 567–572. doi: 10.1071/EA00152
- Hong, Y., Martinez, A., Liger-Belair, G., Jeandet, P., Nuzillard, J., and Cilindre, C. (2012). Metabolomics reveals simultaneous influences of plant defence system and fungal growth in *Botrytis cinerea*-infected *Vitis vinifera* cv. *Chardonnay* berries. *J. Exp. Bot.* 63, 5773–5785. doi: 10.1093/jxb/ers228
- Huckelhoven, R. (2007). Cell wall - associated mechanisms of disease resistance and susceptibility. *Annu. Rev. Phytopathol.* 45, 101–127. doi: 10.1146/annurev.phyto.45.062806.094325
- Hyde, K. D., Cai, L., Cannon, P. F., Crouch, J. A., Crous, P. W., Damm, U., et al. (2009). Colletotrichum - names in current use. *Fungal Divers.* 39, 147–182.
- Itkin, M., Rogachev, I., Alkan, N., Rosenberg, T., Malitsky, S., Masini, L., et al. (2011). GLYCOALKALOID METABOLISM1 is required for steroid alkaloid glycosylation and prevention of phytotoxicity in tomato. *Plant Cell* 23, 4507–4525. doi: 10.1105/tpc.111.088732
- Janisiewicz, W. J., Leverenz, B., Conway, W. S., Saftner, R. A., Reed, A. N., and Camp, M. J. (2003). Control of bitter rot and blue mold of apples by integrating heat and antagonist treatments on 1-MCP treated fruit stored under controlled atmosphere conditions. *Postharvest Biol. Technol.* 29, 129–143. doi: 10.1016/S0925-5214(03)00040-1

- Jersch, S., Scherer, C., Huth, G., and Schlosser, E. (1989). Proanthocyanidins as basis for quiescence of *Botrytis cinerea* in immature strawberry fruits. *Z. Pflanzenk. Pflanzen* 96, 365–378.
- Johnson, G. I., Mead, A. J., Cooke, A. W., and Dean, J. R. (1992). Mango stem end rot pathogens - fruit infection by endophytic colonization of the inflorescence and pedicel. *Ann. Appl. Biol.* 120, 225–234. doi: 10.1111/j.1744-7348.1992.tb03420.x
- Kachroo, A., and Kachroo, P. (2009). Fatty acid-derived signals in plant defense. *Annu. Rev. Phytopathol.* 47, 153–176. doi: 10.1146/annurev-phyto-080508-081820
- Kachroo, A., and Robin, G. P. (2013). Systemic signaling during plant defense. *Curr. Opin. Plant Biol.* 16, 527–533. doi: 10.1016/j.pbi.2013.06.019
- Kalamaki, M. S., Harpster, M. H., Palys, J. M., Labavitch, J. M., Reid, D. S., and Brummell, D. A. (2003). Simultaneous transgenic suppression of LePG and LeExp1 influences rheological properties of juice and concentrates from a processing tomato variety. *J. Agric. Food Chem.* 51, 7456–7464. doi: 10.1021/jf0341641
- Kauss, H., Fauth, M., Merten, A., and Jeblick, W. (1999). Cucumber hypocotyls respond to cutin monomers via both an inducible and a constitutive H₂O₂-generating system. *Plant Physiol.* 120, 1175–1182. doi: 10.1104/pp.120.4.1175
- Kemmerling, B., Schwedt, A., Rodriguez, P., Mazzotta, S., Frank, M., Abu Qamar, S., et al. (2007). The BRI1-associated kinase 1, BAK1, has a Brassinolide-independent role in plant cell-death control. *Curr. Biol.* 17, 1116–1122. doi: 10.1016/j.cub.2007.05.046
- Kim, K. S., Min, J. Y., and Dickman, M. B. (2008). Oxalic acid is an elicitor of plant programmed cell death during *Sclerotinia sclerotiorum* disease development. *Mol. Plant Microbe* 21, 605–612. doi: 10.1094/MPMI-21-5-0605
- Krishna, P. (2003). Brassinosteroid-mediated stress responses. *J. Plant Growth Regul.* 22, 289–297. doi: 10.1007/s00344-003-0058-z
- Ku, V. V. V., Wills, R. B. H., and Ben-Yehoshua, S. (1999). 1-methylcyclopropene can differentially affect the postharvest life of strawberries exposed to ethylene. *Hortscience* 34, 119–120.
- Lacan, D., and Baccou, J.-C. (1998). High levels of antioxidant enzymes correlate with delayed senescence in nonnetted muskmelon fruits. *Planta* 204, 377–382. doi: 10.1007/s004250050269
- Lager, I., Andréasson, O., Dunbar, T. L., Andreasson, E., Escobar, M. A., and Rasmussen, A. G. (2010). Changes in external pH rapidly alter plant gene expression and modulate auxin and elicitor responses. *Plant Cell Environ.* 33, 1513–1528. doi: 10.1111/j.1365-3040.2010.02161.x
- Lashbrooke, J. G., Adato, A., Alkan, N., Tsimbalist, T., Rechav, K., Fernandez, J. P., et al. (2015). The tomato MIXTA-like transcription factor coordinates fruit epidermis conical cell development and cuticular lipid biosynthesis and assembly. *Plant Physiol.* doi: 10.1104/pp.15.01145 [Epub ahead of print].
- Lattanzio, V., Di Venere, D., Linsalata, V., Bertolini, P., Ippolito, A., and Salermo, M. (2001). Low temperature metabolism of apple phenolics and quiescence of *Phlyctaena vagabunda*. *J. Agric. Food Chem.* 49, 5817–5821. doi: 10.1021/jf010255b
- Lattanzio, V., Lattanzio, V. M. T., and Cardinali, A. (2006). “Role of phenolics in the resistance mechanisms of plants against fungal pathogens and insects,” in *Phytochemistry: Advances in Research*, ed. F. Imperato (Kerala: Research Signpost), 23–67.
- Lester, G. (2003). *Oxidative Stress Affecting Fruit Senescence. Postharvest Oxidative Stress in Horticultural Crops* (New York: Food Products Press), 113–129.
- L'Haridon, F., Besson-Bard, A., Binda, M., Serrano, M., Abou-Mansour, E., Balet, F., et al. (2011). A permeable cuticle is associated with the release of reactive oxygen species and induction of innate immunity. *PLoS Pathog.* 7:e1002148. doi: 10.1371/journal.ppat.1002148
- Lipinski, B., Hanson, C., Lomax, J., Kitinoja, L., Raite, W., and Searchinger, T. (2013). *Reducing Food Loss and Waste*. Washington, DC: United Nations Environment Programme.
- Liu, H. X., Jiang, W. B., Zhou, L. G., Wang, B. G., and Luo, Y. B. (2005). The effects of 1-methylcyclopropene on peach fruit (*Prunus persica* L. cv. Jubao) ripening and disease resistance. *Int. J. Food Sci. Technol.* 40, 1–7. doi: 10.1111/j.1365-2621.2004.00905.x
- Manteau, S., Abouna, S., Lambert, B., and Legendre, L. (2003). Differential regulation by ambient pH of putative virulence factor secretion by the phytopathogenic fungus *Botrytis cinerea*. *FEMS Microbiol. Ecol.* 43, 359–366. doi: 10.1111/j.1574-6941.2003.tb01076.x
- Marcos, J. F., González-Candela, L., and Zacarias, L. (2005). Involvement of ethylene biosynthesis and perception in the susceptibility of citrus fruits to *Penicillium digitatum* infection and the accumulation of defence-related mRNAs. *J. Exp. Bot.* 56, 2183–2193. doi: 10.1093/jxb/eri218
- Mengiste, T. (2012). Plant immunity to necrotrophs. *Annu. Rev. Phytopathol.* 50, 267–294. doi: 10.1146/annurev-phyto-081211-172955
- Mengiste, T., VanAlfen, N., Leach, J., and Lindow, S. (2012). Plant immunity to necrotrophs. *Annu. Rev. Phytopathol.* 50, 267–294. doi: 10.1146/annurev-phyto-081211-172955
- Menniti, A. M., Gregori, R., and Donati, I. (2004). 1-methylcyclopropene retards postharvest softening of plums. *Postharvest Biol. Technol.* 31, 269–275. doi: 10.1016/j.postharvbio.2003.09.009
- Ment, D., Alkan, N., Luria, N., Bi, F.-C., Reuveni, E., Fluhr, R., et al. (2015). A role of AREB in the regulation of PACC-dependent acid-expressed-genes and pathogenicity of *Colletotrichum gloeosporioides*. *Mol. Plant Microbe* 28, 154–166. doi: 10.1094/MPMI-09-14-0252-R
- Mor, A., Koh, E., Weiner, L., Rosenwasser, S., Sibony-Benyamin, H., and Fluhr, R. (2014). Singlet oxygen signatures are detected independent of light or chloroplasts in response to multiple stresses. *Plant Physiol.* 165, 249–261. doi: 10.1104/pp.114.236380
- Navarro, L., Bari, R., Achard, P., Lison, P., Nemri, A., Harberd, N. P., et al. (2008). DELLAAs control plant immune responses by modulating the balance of jasmonic acid and salicylic acid signaling. *Curr. Biol.* 18, 650–655. doi: 10.1016/j.cub.2008.03.060
- Nurnberger, T., and Scheel, D. (2001). Signal transmission in the plant immune response. *Trends Plant Sci.* 6, 372–379. doi: 10.1016/S1360-1385(01)0019-2
- O'Connell, R. J., Thon, M. R., Hacquard, S., Amyotte, S. G., Kleemann, J., Torres, M. F., et al. (2012). Lifestyle transitions in plant pathogenic *Colletotrichum* fungi deciphered by genome and transcriptome analyses. *Nat. Genet.* 44, 1060–1065. doi: 10.1038/ng.2372
- Okawa, K. (2014). *Market and Trade Impacts of Food Loss and Waste Reduction* (Paris: Organisation for Economic Co-operation and Development).
- Osorio, S., Alba, R., Damasceno, C. M., Lopez-Casado, G., Lohse, M., Zanor, M. I., et al. (2011). Systems biology of tomato fruit development: combined transcript, protein, and metabolite analysis of tomato transcription factor (nor, rin) and ethylene receptor (Nr) mutants reveals novel regulatory interactions. *Plant Physiol.* 157, 405–425. doi: 10.1104/pp.111.175463
- Paniagua, C., Pose, S., Morris, V. J., Kirby, A. R., Quesada, M. A., and Mercado, J. A. (2014). Fruit softening and pectin disassembly: an overview of nanostructural pectin modifications assessed by atomic force microscopy. *Ann. Bot. Lond.* 114, 1375–1383. doi: 10.1093/aob/mcu149
- Penalva, M. A., Tilburn, J., Bignell, E., and Arst, H. N. (2008). Ambient pH gene regulation in fungi: making connections. *Trends Microbiol.* 16, 291–300. doi: 10.1016/j.tim.2008.03.006
- Pieterse, C. M. J., Van der Does, D., Zamioudis, C., Leon-Reyes, A., and Van Wees, S. C. M. (2012). Hormonal modulation of plant immunity. *Annu. Rev. Cell Dev. Biol.* 28, 489–521. doi: 10.1146/annurev-cellbio-092910-154055
- Porat, R., Weiss, B., Cohen, L., Daus, A., Goren, R., and Droby, S. (1999). Effects of ethylene and 1-methylcyclopropene on the postharvest qualities of ‘Shamouti’ oranges. *Postharvest Biol. Technol.* 15, 155–163. doi: 10.1016/S0925-5214(98)00079-9
- Powell, A. L. T., Kalamaki, M. S., Kurien, P. A., Gurrieri, S., and Bennett, A. B. (2003). Simultaneous transgenic suppression of LePG and LeExp1 influences fruit texture and juice viscosity in a fresh market tomato variety. *J. Agric. Food Chem.* 51, 7450–7455. doi: 10.1021/jf034165d
- Powell, A. L. T., van Kan, J., ten Have, A., Visser, J., Greve, L. C., Bennett, A. B., et al. (2000). Transgenic expression of pear PGIP in tomato limits fungal colonization. *Mol. Plant Microbe* 13, 942–950. doi: 10.1094/MPMI.2000.13.9.942
- Prins, T. W., Tudzynski, P., von Tiedemann, A., Tudzynski, B., ten Have, A., Hansen, M. E., et al. (2000). “Infection strategies of *Botrytis cinerea* and related necrotrophic pathogens,” in *Fungal Pathology*, ed. W. Kronstad (Dordrecht: Kluwer Academic), 33–65. doi: 10.1007/978-94-015-9546-9_2

- Prusky, D. (1996). Pathogen quiescence in postharvest diseases. *Annu. Rev. Phytopathol.* 34, 413–434. doi: 10.1146/annurev.phyto.34.1.413
- Prusky, D., Alkan, N., Mengiste, T., and Fluh, R. (2013). Quiescent and necrotrophic lifestyle choice during postharvest disease development. *Annu. Rev. Phytopathol.* 51, 55–76. doi: 10.1146/annurev.phyto-082712-102349
- Prusky, D., Benarie, R., and Guelfatrich, S. (1981). Etiology and histology of *Alternaria* rot of persimmon fruits. *Phytopathology* 71, 1124–1128. doi: 10.1094/Phyto-71-1124
- Prusky, D., Kobiler, I., Miyara, I., and Alkan, N. (2009). “Fruit diseases,” in *The Mango, Botany, Production and Uses*, 2nd Edn, ed. R. E. Litz (Cambridge: CABI International), 210–231. doi: 10.1079/9781845934897.0210
- Rijkenberg, F., Leeuw, G. D., and Verhoeff, K. (1980). Light and electron microscopy studies on the infection of tomato fruits by *Botrytis cinerea*. *Can. J. Bot.* 58, 1394–1404. doi: 10.1139/b80-170
- Robert-Seilaniantz, A., Grant, M., and Jones, J. D. G. (2011). Hormone crosstalk in plant disease and defense: more than just jasmonate-salicylate antagonism. *Annu. Rev. Phytopathol.* 49, 317–343. doi: 10.1146/annurev.phyto-073009-114447
- Rogiers, S. Y., Kumar, G. N. M., and Knowles, N. R. (1998). Maturation and ripening of fruit of *Amelanchier alnifolia* Nutt are accompanied by increasing oxidative stress. *Ann. Bot. Lond.* 81, 203–211. doi: 10.1006/anbo.1997.0543
- Saftner, R. A., Abbott, J. A., Conway, W. S., and Barden, C. L. (2003). Effects of 1-methylcyclopropene and heat treatments on ripening and postharvest decay in ‘Golden Delicious’ apples. *J. Am. Soc. Hortic. Sci.* 128, 120–127.
- Schaller, A., and Oecking, C. (1999). Modulation of plasma membrane H+-ATPase activity differentially activates wound and pathogen defense responses in tomato plants. *Plant Cell* 11, 263–272.
- Schweizer, P., Felix, G., Buchala, A., Müller, C., and Métraux, J. P. (1996). Perception of free cutin monomers by plant cells. *Plant J.* 10, 331–341. doi: 10.1046/j.1365-313X.1996.10020331.x
- Seymour, G. B., Østergaard, L., Chapman, N. H., Knapp, S., and Martin, C. (2013). Fruit development and ripening. *Annu. Rev. Plant Biol.* 64, 219–241. doi: 10.1146/annurev-aplant-050312-120057
- Sharrock, K. R., and Labavitch, J. M. (1994). Polygalacturonase inhibitors of bartlett pear fruits differential effects on *Botrytis cinerea* polygalacturonase isozymes, and influence on products of fungal hydrolysis of pear cell walls and on ethylene induction in cell culture. *Physiol. Mol. Plant Pathol.* 45, 305–319. doi: 10.1016/S0885-5765(05)80061-X
- Shi, J. X., Adato, A., Alkan, N., He, Y. H., Lashbrooke, J., Matas, A. J., et al. (2013). The tomato SISHINE3 transcription factor regulates fruit cuticle formation and epidermal patterning. *New Phytol.* 197, 468–480. doi: 10.1111/nph.12032
- Simon-Plas, F., Rusterucci, C., Milat, M. L., Humbert, C., Montillet, J. L., and Blein, J. P. (1997). Active oxygen species production in tobacco cells elicited by cryptogein. *Plant Cell Environ.* 20, 1573–1579. doi: 10.1046/j.1365-3040.1997.d01-45.x
- Spoel, S. H., and Dong, X. (2008). Making sense of hormone crosstalk during plant immune responses. *Cell Host Microbe* 3, 348–351. doi: 10.1016/j.chom.2008.05.009
- Spoel, S. H., Johnson, J. S., and Dong, X. (2007). Regulation of tradeoffs between plant defenses against pathogens with different lifestyles. *Proc. Natl. Acad. Sci. U.S.A.* 104, 18842–18847. doi: 10.1073/pnas.0708139104
- Su, H., and Gubler, W. D. (2012). Effect of 1-methylcyclopropene (1-MCP) on reducing postharvest decay in tomatoes (*Solanum lycopersicum* L.). *Postharvest Biol. Technol.* 64, 133–137. doi: 10.1016/j.postharvbio.2011.06.005
- Sutton, B. C. (1980). *The Coelomycetes. Fungi Imperfici with Pycnidia, Acervuli and Stromata*. Kew: Commonwealth Mycological Institute.
- Sutton, B. C. (1992). “The genus *Glomerella* and its anamorph *Colletotrichum*,” in *Colletotrichum: Biology, Pathology and Control*, eds J. A. Bailey and J. M. Jeger (Wallingford: Centre for Biosciences and Agriculture International), 1–26.
- Symons, G., Chua, Y.-J., Ross, J., Quittenden, L., Davies, N., and Reid, J. (2012). Hormonal changes during non-climacteric ripening in strawberry. *J. Exp. Bot.* 63, 4741–4750. doi: 10.1093/jxb/ers147
- Symons, G., Davies, C., Shavrukov, Y., Dry, I., Reid, J., and Thomas, M. (2006). Grapes on steroids. Brassinosteroids are involved in grape berry ripening. *Plant Physiol.* 150–158.
- Tada, Y., Spoel, S. H., Pajerowska-Mukhtar, K., Mou, Z., Song, J., Wang, C., et al. (2008). Plant immunity requires conformational charges of NPR1 via S-nitrosylation and thioredoxins. *Science* 321, 952–956. doi: 10.1126/science.1156970
- Tian, S., Qin, G., and Li, B. (2013). Reactive oxygen species involved in regulating fruit senescence and fungal pathogenicity. *Plant Mol. Biol.* 82, 593–602. doi: 10.1007/s11103-013-0035-2
- Torres, M. A., Jones, J. D., and Dangl, J. L. (2006). Reactive oxygen species signaling in response to pathogens. *Plant Physiol.* 141, 373–378. doi: 10.1104/pp.106.079467
- van Loon, L. C., Rep, M., and Pieterse, C. M. J. (2006). Significance of inducible defense-related proteins in infected plants. *Annu. Rev. Phytopathol.* 44, 135–162. doi: 10.1146/annurev.phyto.44.070505.143425
- van Kan, J. A. L., van't Klooster, J. W., Wagemakers, C. A. M., Dees, D. C. T., and van der Vlugt Bergmans, C. J. B. (1997). Cutinase of *Botrytis cinerea* is expressed, but not essential, during penetration of gerbera and tomato. *Mol. Plant Microbe Interact.* 10, 30–38. doi: 10.1094/MPMI.1997.10.1.30
- Verhoeff, K. (1974). Latent infections by fungi. *Annu. Rev. Phytopathol.* 12, 99–110. doi: 10.1146/annurev.py.12.090174.000531
- Voisin, D., Nawrath, C., Kurdyukov, S., Franke, R. B., Reina-Pinto, J. J., Efremova, N., et al. (2009). Dissection of the complex phenotype in cuticular mutants of *Arabidopsis* reveals a role of SERRATE as a mediator. *PLoS Genet.* 5:e1000703. doi: 10.1371/journal.pgen.1000703
- Vorwerk, S., Somerville, S., and Somerville, C. (2004). The role of plant cell wall polysaccharide composition in disease resistance. *Trends Plant Sci.* 9, 203–209. doi: 10.1016/j.tplants.2004.02.005
- Walton, J. D. (1994). Deconstructing the cell wall. *Plant Physiol.* 104, 1113–1118.
- Watkins, C. B. (2006). The use of 1-methylcyclopropene (1-MCP) on fruits and vegetables. *Biotechnol. Adv.* 24, 389–409. doi: 10.1016/j.biotechadv.2006.01.005
- Watkins, C. B., and Nock, J. F. (2008). Effects of delayed controlled atmosphere storage of apples after rapid 1-MCP treatment. *Hortscience* 43, 1087–1087.
- Widmer, T. L., and Laurent, N. (2006). Plant extracts containing caffeic acid and rosmarinic acid inhibit zoospore germination of *Phytophthora* spp. pathogenic to *Theobroma cacao*. *Eur. J. Plant Pathol.* 115, 377–388. doi: 10.1007/s10658-006-9024-5
- Wildermuth, M. C. (2006). Variations on a theme: synthesis and modification of plant benzoic acids. *Curr. Opin. Plant Biol.* 9, 288–296. doi: 10.1016/j.pbi.2006.03.006
- Williams, B., Kabbage, M., Kim, H. J., Britt, R., and Dickman, M. B. (2011). Tipping the balance: *Sclerotinia sclerotiorum* secreted oxalic acid suppresses host defenses by manipulating the host redox environment. *PLoS Pathog.* 7:e1002107. doi: 10.1371/journal.ppat.1002107
- Williamson, B., Tudzynski, B., Tudzynski, P., and van Kan, J. A. L. (2007). *Botrytis cinerea*: the cause of grey mould disease. *Mol. Plant Pathol.* 8, 561–580. doi: 10.1111/j.1364-3703.2007.00417.x
- Wojtaszek, P., Trethowan, J., and Bolwell, G. P. (1995). Specificity in the immobilization of cell-wall proteins in response to different elicitor molecules in suspension-cultured cells of french bean (*Phaseolus-vulgaris* L.). *Plant Mol. Biol.* 28, 1075–1087. doi: 10.1007/BF00032668
- Woloshuk, C. P., and Kolattukudy, P. E. (1986). Mechanism by which contact with plant cuticle triggers cutinase gene-expression in the spores of *Fusarium-solani* F-Sp Pisi. *Proc. Natl. Acad. Sci. U.S.A.* 83, 1704–1708. doi: 10.1073/pnas.83.6.1704
- Woolf, A. B., Requejo-Tapia, C., Cox, K. A., Jackman, R. C., Gunson, A., Arpaia, M. L., et al. (2005). 1-MCP reduces physiological storage disorders of ‘Hass’ avocados. *Postharvest Biol. Technol.* 35, 43–60. doi: 10.1016/j.postharvbio.2004.07.009
- Yakoby, N., Kobiler, I., Dinoor, A., and Prusky, D. (2000). pH regulation of pectate lyase secretion modulates the attack of *Colletotrichum gloeosporioides* on avocado fruits. *Appl. Environ. Microbiol.* 66, 1026–1030. doi: 10.1128/AEM.66.3.1026–1030.2000
- Zaharah, S. S., Singh, Z., Symons, G. M., and Reid, J. B. (2012). Role of brassinosteroids, ethylene, abscisic acid, and indole-3-acetic acid in mango fruit ripening. *J. Plant Growth Regul.* 31, 363–372. doi: 10.1007/s00344-011-9245-5
- Zhao, J., Davis, L. C., and Verpoorte, R. (2005). Elicitor signal transduction leading to production of plant secondary metabolites. *Biotechnol. Adv.* 23, 283–333. doi: 10.1016/j.biotechadv.2005.01.003

Zhu, Z., Zhang, Z. Q., Qin, G. Z., and Tian, S. P. (2010). Effects of brassinosteroids on postharvest disease and senescence of jujube fruit in storage. *Postharvest Biol. Technol.* 56, 50–55. doi: 10.1016/j.postharvbio.2009.11.014

Conflict of Interest Statement: The authors declare that the research was conducted in the absence of any commercial or financial relationships that could be construed as a potential conflict of interest.

Copyright © 2015 Alkan and Fortes. This is an open-access article distributed under the terms of the Creative Commons Attribution License (CC BY). The use, distribution or reproduction in other forums is permitted, provided the original author(s) or licensor are credited and that the original publication in this journal is cited, in accordance with accepted academic practice. No use, distribution or reproduction is permitted which does not comply with these terms.



Field-Grown Grapevine Berries Use Carotenoids and the Associated Xanthophyll Cycles to Acclimate to UV Exposure Differentially in High and Low Light (Shade) Conditions

Chandré Joubert¹, Philip R. Young^{1,2}, Hans A. Eyéghé-Bickong^{1,2,3} and Melané A. Vivier^{1,2*}

¹ Department of Viticulture and Oenology, Stellenbosch University, Stellenbosch, South Africa, ² Institute for Wine Biotechnology, Stellenbosch University, Stellenbosch, South Africa, ³ Institute for Grape and Wine Sciences, Stellenbosch University, Stellenbosch, South Africa

OPEN ACCESS

Edited by:

Ana Margarida Fortes,
Faculdade de Ciências da
Universidade de Lisboa, Portugal

Reviewed by:

Simone Diego Castellarin,
The University of British Columbia,
Canada
Hernâni Gerós,
Universidade do Minho, Portugal

*Correspondence:

Melané A. Vivier
mav@sun.ac.za

Specialty section:

This article was submitted to
Plant Physiology,
a section of the journal
Frontiers in Plant Science

Received: 12 February 2016

Accepted: 22 May 2016

Published: 10 June 2016

Citation:

Joubert C, Young PR, Eyéghé-Bickong HA and Vivier MA (2016) Field-Grown Grapevine Berries Use Carotenoids and the Associated Xanthophyll Cycles to Acclimate to UV Exposure Differentially in High and Low Light (Shade) Conditions. *Front. Plant Sci.* 7:786.
doi: 10.3389/fpls.2016.00786

Light quantity and quality modulate grapevine development and influence berry metabolic processes. Here we studied light as an information signal for developing and ripening grape berries. A *Vitis vinifera* Sauvignon Blanc field experiment was used to identify the impacts of UVB on core metabolic processes in the berries under both high light (HL) and low light (LL) microclimates. The primary objective was therefore to identify UVB-specific responses on berry processes and metabolites and distinguish them from those responses elicited by variations in light incidence. Canopy manipulation at the bunch zone via early leaf removal, combined with UVB-excluding acrylic sheets installed over the bunch zones resulted in four bunch microclimates: (1) HL (control); (2) LL (control); (3) HL with UVB attenuation and (4) LL with UVB attenuation. Metabolite profiles of three berry developmental stages showed predictable changes to known UV-responsive compound classes in a typical UV acclimation (versus UV damage) response. Interestingly, the berries employed carotenoids and the associated xanthophyll cycles to acclimate to UV exposure and the berry responses differed between HL and LL conditions, particularly in the developmental stages where berries are still photosynthetically active. The developmental stage of the berries was an important factor to consider in interpreting the data. The green berries responded to the different exposure and/or UVB attenuation signals with metabolites that indicate that the berries actively managed its metabolism in relation to the exposure levels, displaying metabolic plasticity in the photosynthesis-related metabolites. Core processes such as photosynthesis, photo-inhibition and acclimation were maintained by differentially modulating metabolites under the four treatments. Ripe berries also responded metabolically to the light quality and quantity, but mostly formed compounds (volatiles and polyphenols) that have direct antioxidant and/or “sunscreening” abilities. The data presented for the green berries and those for the ripe berries conform to what is known for UVB and/or light stress in young, active leaves and older, senescing tissues respectively and provide scope for further evaluation of the sink/source status of fruits in relation to photosignalling and/or stress management.

Keywords: UVB radiation, solar radiation, climate change adaptation, acclimation, berry development

INTRODUCTION

Plants not only use solar light to drive photosynthesis and energy production, they also use it as a source of information about their environment. New information regarding the impact of the different spectral components of solar light (visible, UVA and UVB) are emerging, causing paradigm shifts with regards to the interpretation of existing and new results, the methods of experimentation, as well as the development of hypothesis and models to understand the intricate modulating effects versus the stress responses evoked by light components (Hidieg et al., 2013). In the study of UV effects, it is now established that under ecological/field conditions, plants rarely display the classical UV damage phenotypes that have been established. Instead, a more complex picture is emerging showing that low ecologically relevant doses of UV are used by plants to acclimate and to modulate core processes to remain productive and thriving (Hidieg et al., 2013; Li et al., 2013).

UVB (280–315 nm) is an intrinsic part of solar radiation and is no longer considered a generic abiotic stress factor, but has been demonstrated to be a specific modulator. This is supported by the fact that UVB radiation is required for photomorphogenic responses (including acclimation) and is essential in the formation of the UVB photoreceptor, UVR8. In the absence of UVB radiation, UVR8 occurs as an inactive dimer (homo-dimers connected by salt bridges). UVB radiation causes a rapid accumulation of the active monomeric form of UVR8 in the nucleus, where the protein directly binds chromatin via histones. UVB radiation neutralizes the salt bridges (connecting the UVR8 homodimers) resulting in the release of the active UVR8 monomers. The UVR8 monomers subsequently conjugate with COP1, and this UVR8-COP1 conjugate activates the transcription of HY5. HY5, a bZIP transcription factor, subsequently regulates numerous light-responsive genes (>100 in *Arabidopsis*) involved in photomorphogenesis (Favery et al., 2009). In the absence of UVB radiation, UVR8 monomer dimerization is catalyzed by WD40-repeat proteins RUP1 and RUP2 (in *Arabidopsis thaliana*). Photomorphogenic responses to UVB radiation in leaves include reduced leaf expansion, increased leaf thickness, accumulation of phenolic compounds (predominantly flavonoids) and cuticular waxes (Tilbrook et al., 2013). These responses are comprehensively described for a number of plant species and specifically in photosynthetic organs (predominantly leaves), but data from fruit acclimation suggest that fruit in the early developmental stages, when chloroplasts are still functionally photosynthesizing, react in much the same way as leaves (via photo-protective mechanisms with the purpose of maintaining photosynthesis) (Blanke and Lenz, 1989).

Grapes are fleshy fruits grown in temperate areas of the world where a large proportion of similar cultivated varieties are produced under vastly different environmental conditions. The different climatic zones in viticultural production areas have been extensively characterized, particularly considering the potential impacts of climate change on berry metabolism and consequent quality. The responses of field-grown plants (including grapevine) to biotic and abiotic stress are complex.

Plants are typically exposed to multiple stresses and their responses are dynamic and overlapping and are classified as elastic (reversible) or plastic (irreversible) responses (reviewed in Cramer et al., 2011). Changes in the environment necessitate the alteration of the plant's phenotype in order to adapt to external environmental factors. This is referred to as phenotypic plasticity and is deemed the foremost method employed by plants to cope with environmental changes. *Vitis vinifera* has been shown to display phenotypic plasticity under these diverse conditions, particularly evidenced in berry transcripts and metabolites (Dal Santo et al., 2013; Young et al., 2016).

The limited research on grapevine berries and UV exposure in natural settings have shown that cultivated varieties are relatively well adapted to ambient UV exposure and typically show acclimation and not UV stress responses. Similarly, studies on other fruits and crops have revealed that acclimation responses to natural UVB levels involve the production of UVB absorbing flavonoids and phenolics. It has been shown that in some instances these compounds can act as UVB screens directly (Kolb et al., 2003), whereas in other occasions and/or locations, the inherent antioxidant capacity of the same compounds rather contributes to acclimation responses (Carbonell-Bejerano et al., 2014). The current understanding of UV effects on grapevine organs conforms to what is known for other species, i.e., with regards to the regulating aspects of UV stimuli, the phenylpropanoid pathway has been strongly linked to UV exposure. The observation that the attenuation of UVB reduces the accumulation of UVB absorbing compounds is not unique to grapevine and has been shown in a number of other fruits, including: apple (Arakawa et al., 1985; Ubi et al., 2006), tomato (Calvenzani et al., 2010) and blackcurrant (Huyskens-Keil et al., 2012).

Several studies have focused on UV effects on grapevine berries (Gregan et al., 2012; Gil et al., 2013; Carbonell-Bejerano et al., 2014), with some reports on vegetative and/or whole plant physiological performance (Pontin et al., 2010; Martínez-Lüscher et al., 2013). It has been demonstrated that the flavonoid biosynthetic pathway is transcriptionally regulated by UVB radiation in the skin of berries (Downey et al., 2004; Carbonell-Bejerano et al., 2014). Interestingly, a recent study on Sauvignon Blanc berries under different light and UV regimes lends support to the notion that in grapevine berries the biosynthesis of flavonols are increased through the classical low fluence UVB response pathway (Tian et al., 2015). Moreover, in the ripe berry stages putative terpenoid biosynthetic genes encoding for linalool and eucalyptol were upregulated in *V. vinifera* L. cv. Tempranillo in response to UVB radiation (Carbonell-Bejerano et al., 2014). Although these studies have identified possible regulatory genes and stress pathways that could be involved in UVB stress/acclimation, significant gaps still exist in our understanding of the mechanisms (and biological drivers) behind the observed responses. Additional motivation exists to clarify the effects of UV and general solar radiation on berry (and fruits in general) composition, since it is accepted to impact berry and wine quality.

The hypothesis of this study was that under field conditions high/low photosynthetically active radiation (PAR) and high/low UV exposures contribute in different ways to the response of berries to solar exposure. Our primary objective was to distinguish between UV and PAR-specific responses on berry metabolites. To this end we evaluated Sauvignon Blanc berries in a high-altitude (moderately characterized) vineyard where an experimental system to study berry metabolism under low and high (PAR) light exposure in the bunch zones was validated previously (Young et al., 2016). It was reported that specific metabolites responded to increased solar exposure [PAR + UV = High Light (HL)] in a metabolically plastic pattern in a likely process of antioxidant homeostasis, involving different metabolites depending on the developmental stage of the berries and when compared to the low light (LL) control. This characterized HL and LL experimental system provided an excellent opportunity to evaluate the specific responses and/or contribution of UV exposure to the metabolic responses. UV exclusion sheets were used to attenuate UVB light exposure (>99% reduction) on the berries under these two light regimes. In the first two seasons of the study, we found a strong light (PAR) and UV effect on specific berry carotenoid pigments, prompting a comprehensive analysis of the carotenoids and their derivatives (norisoprenoids) in subsequent seasons. Apart from two earlier studies by Schultz et al. (1998) (reporting total carotenoids and zeaxanthin in Riesling) and Steel and Keller (2000) (β -carotene and lutein in Cabernet Sauvignon), the impact of UV exposure on the photosynthetic pigments in berries is still relatively poorly described (compared to e.g., polyphenolics in red cultivars). Our results extend the current understanding of UV impacts in grapevine fruits (and fruits in general) by showing that specific carotenoids involved in photoprotection are responsive to levels of solar radiation (exposure), but that the UVB component in this light signal is required for the typical photo-protective response linked to the violaxanthin cycle under HL, as well as the accumulation of lutein epoxide under LL conditions. The ripe berry stages in particular displayed the accumulation of volatile compounds, but the profiles and levels depended on the specific level of exposure and UVB presence/absence. The results are discussed within the context of fruit metabolism in reaction to light as a source of information to modulate core processes.

MATERIALS AND METHODS

Vineyard Treatment, Experimental Design, and Berry Sampling

A model *Vitis vinifera* L. cv. Sauvignon Blanc vineyard established in a commercial vineyard situated in the Elgin area of South Africa was used for the experiment. The vines were orientated in a north-west, south-east row direction and trained on a vertical shoot positioned (VSP) trellis system. Spur pruning to two buds was employed during winter and diligent canopy management occurred throughout the growing season. No water constraints were noted due to the high moisture content of the deep shale soils, as was confirmed by stem water potential

measurements in the same vineyard and reported in Young et al. (2016).

The experimental plot included three rows from which 16 panels were selected. Two controls and two treatments were applied randomly over the 16 panels with each control/treatment being repeated four times. Each panel consisted of four consecutive vines and represented a single biological repeat (**Supplementary Figure S1** shows a diagram of the plot layout as well as images of the treatments).

Canopy manipulation via basal leaf and lateral shoot removal in the bunch zone (30–40 cm above the cordon) resulted in an altered exposure of the grape berries to light, thereby creating two distinctive bunch microclimates (with reference to exposure). This was done only on the East-facing side of the canopy, namely the side which was exposed to sunlight in the morning. A full characterization of the leaf removal treatment was recently reported in Young et al. (2016) that delivered a validated exposed versus a shaded bunch microclimate. UV light manipulation was achieved by installing UV-excluding acrylic sheets (Perspex® South Africa) over the bunch zone. The following four scenarios were therefore created in the vineyard: (1) complete leaf and lateral shoot removal in the bunch zone (30–40 cm above the cordon) on the morning side of the canopy (East side), generating the High Light control (HLcontrol); (2) a similar scenario to the first with the addition of a UVB excluding acrylic sheet installed over the bunch zone, generating the High Light-UVB (HL-UVB) treatment; (3) no leaf or lateral shoot removal, constituting a fully shaded situation, generating the Low Light control (LLcontrol); (4) and a similar scenario to the third with the addition of a UVB excluding sheet over the bunch zone, generating the Low Light-UVB (LL-UVB) treatment.

Leaf and lateral removal as well as the installation of the UV-excluding sheets were carried out when the berries reached peppercorn size according to the Eichhorn and Lorenz (EL) system (EL 29) (Eichhorn and Lorenz, 1977). Sampling of the berries occurred at pea-sized berries (EL31), véraison (EL35), and ripe (corresponding to the harvest date; EL38) to yield samples that covered the full growing and ripening season. The stages corresponded to 26, 67, and 107 DAA (days after anthesis) in the 2011/2012 season and 25, 66, and 96 DAA in the 2014/2015 season. Berry sampling was carried out at each of the phenological stages on a per panel basis and therefore comprised of four biological repeats per treatment. Each sample consisted of 48–50 berries. Representative bunches on the exposed side (east-facing) of the canopy were selected from which to sample. Care was taken to select only berries from the exposed side of the selected bunches. Samples were frozen immediately after being picked in the field using liquid nitrogen and then transported to the laboratory. The seeds were removed and the remaining tissue milled in liquid nitrogen, after which they were stored at -80°C until analyzed.

The trial was conducted over multiple seasons (2011/2012; 2013/2014; 2014/2015), but metabolite profiling mainly occurred in the first and last season and will be presented in the results section.

Climatic Measurements

Climatic monitoring (meso-and micro-) occurred in the vineyard to quantify the main abiotic factors which could influence grapevine growth and development in response to the treatments. Various loggers and sensors were placed in the vineyard to measure climatic variables.

Temperature was measured at the mesoclimatic level via Tinytag® loggers (TinyTag Plus 2 – TGP-4500., Gemini Data Loggers (UK) Ltd., Chichester, United Kingdom) installed above the canopy. Similar loggers were placed within the canopy to measure temperature on a microclimatic scale. Bunch temperatures were monitored using dual channel temperature data loggers to which two thermistor flying lead probes were attached (TinyTag Plus 2 – TGP-4520). These probes were positioned within selected bunches from each of the controls and treatments. With regard to light measurements, both solar radiation (including PAR) and UV radiation were monitored. Solar radiation sensors (Vantage Pro2™ solar radiation sensors Davis Instruments, Hayward, CA, USA) were also installed inside and outside the canopy. The outer unit measured the ambient solar radiation while the internal sensors measured the solar radiation which penetrated the canopy and reached the bunch zone. A solar sensor was placed in the bunch zone of each of the four light environments to determine the degree of light penetration in each case. UV radiation was measured using sensors (Apogee SU-100 UV sensors. Apogee Instruments Inc., Logan, UT, USA) which were positioned similarly to the solar radiation sensors; one externally to measure ambient UV and one placed in the bunch zone of each created light environment. The solar and UV sensors were attached to two loggers (DataTaker DT82E data logger, Thermo Fisher Scientific Australia Pty Ltd, Melbourne, VIC, Australia) which recorded measurements throughout berry development.

Analysis of Major Sugars and Organic Acid Concentrations

The major sugars and organic acids of the berries were extracted and analyzed using HPLC as described in Eyéghé-Bickong et al. (2012).

Analysis of Photosynthetic Pigment Concentrations

The carotenoids and chlorophylls of the berries were extracted and analyzed using UPLC as described in Lashbrooke et al. (2010) and Young et al. (2016) respectively. The de-epoxidation state (DEPS) of the xanthophylls were calculated as $(\text{zeaxanthin} + 0.5\text{antheraxanthin}) / (\text{violaxanthin} + \text{zeaxanthin} + \text{antheraxanthin})$ as described in Thayer and Björkman (1990).

Analysis of Volatile Aroma Compounds

All authentic standards for volatile analysis were purchased from Sigma Aldrich (Steinheim, Germany): 6-methyl-6-heptan-2-one, trans-2-hexanol, 2-octenal, d-anisol, trans-2-heptanal, geranylacetone, eucalyptol, limonene, trans-linalool-oxide, *cis*-linalool-oxide, linalool, 4-terpineol, citronellol, nerol, geraniol, β -damascenone, α -ionone, β -ionone and pseudo-ionone,

β -damascone and α -terpineol. Tartaric acid, ascorbic acid, sodium chloride (NaCl), sodium azide (NaN₃) and methanol were also acquired from Sigma Aldrich. For extraction of volatiles from grape berry tissue, approximately 1 g of ground, frozen tissue was weighed into a 20 mL GC vial and 2 mL of tartaric acid buffer (2 g.L⁻¹ tartrate, 2.1 g.L⁻¹ ascorbic acid and 0.8 mg.L⁻¹ L⁻¹ sodium azide; pH 3) was added to each vial. Volatiles were extracted by head space (HS) solid phase microextraction (SPME) using a 50/30 μm divinylbenzene/carboxen/polydimethylsiloxane (DVB/CAR/PDMS) fiber (2 cm gray fiber from Supelco, Bellefonte, PA, USA) (Barros et al., 2012). Prior to use, the fiber was conditioned at 270°C for 60 min in the GC injection port according to the manufacturer's specifications.

The samples were equilibrated at 60°C for 5 min in a heating chamber (with constant agitation at 250 rpm). After equilibration, the SPME fiber was inserted through the vial septa and exposed to the sample at 60°C for 30 min with constant agitation at 250 rpm. The bound analytes were thermally desorbed from the fiber in the GC injection port. After desorption, the fiber was maintained for 20 min in the injection port for cleaning in order to prevent potential carryover between samples.

GC analysis was carried out on an Agilent 6890N gas chromatograph (Agilent, Palo Alto, CA, USA) system coupled to a CTC CombiPal Analytics auto-sampler and an Agilent 5975B inert XL EI/CI MSD mass spectrometer detector through a transfer line. Analysis was done using a Zebron 7HG-G009-11 capillary column (30 m \times 250 μm ID, 0.25 μm). Desorption of analytes from the SPME fiber was performed in the injection port at 250°C by pulsed splitless mode for 1 min. The purge flow was 30 mL.min⁻¹ (for 2 min). The column operating head pressure was raised from 111 kPa to obtain a pulse pressure of 300 kPa for 1 min. Helium was used as carrier gas with a constant flow rate of 1 mL.min⁻¹. The oven parameters were as follows: initial temperature of 40°C (2 min), a linear increase to a final temperature of 240°C (at a rate of 10°C.min⁻¹), and the temperature was held at 240°C for a final 2 min. The total run time was 28 min. The transfer line temperature was maintained at 250°C. The MS detector was operated in scan and selected ion monitoring (SIM) modes. The scan parameters were set ranging from 35 to 350 m/z. The dwell time for each ion in a group was set to 100 ms. The software used was MSD ChemStation (G1701-90057, Agilent).

For quantification, external standard calibration was done by plotting standard curves using the ratio of the peak area of each authentic standard relative to that of the internal standard, versus the standard concentration (see **Supplementary Table S1** for calibration parameters). Volatiles in samples were identified according to their elution times and masses compared to those of the respective authentic standards and quantified using the calibration parameters. Compounds without available authentic standard were identified by matching their mass spectrum with the Wiley 275 mass spectral library (Wiley, New York, NY, USA) and quantified. The resulted concentrations in $\mu\text{g/L}$ were then divided by the berry fresh weight and multiplied by the sample volume (2 mL) to obtain the content (in ng/g FW).

The selected ions used for the integration of peak areas of the respective compounds of interest, their retention time on the Zebron column, and quantifier molecules are summarized in **Supplementary Table S2**.

Analysis of Polyphenolics

Total polyphenolic acids were analyzed by HPLC on an Agilent 1200 at the Oxidative Stress Research Centre, Cape Peninsula University of Technology, Bellville, South Africa.

Statistical Analysis

The resulting datasets were evaluated statistically, and were subjected to multivariate data analyses to integrate the different data layers. Microsoft Excel and Statistica (version 12) were utilized for standard statistical analysis. The responses of the various compounds to the individual treatments were tested for significance using a pairwise *t*-test. Testing was conducted on a “per developmental stage” basis. The contrasts examined were separated into HL and LL comparisons, thereby allowing for the examination of the effects of UV in a HL environment [HLcontrol (HL + ambient UV) versus HL-UVB] as well as a LL environment [LLcontrol (LL + ambient UV) versus LL-UVB]. Analysis of variance (ANOVA) was conducted on those pairwise contrasts with a *p*-value of <0.05. Linear models were fitted to the contrasts showing significant variation in order to visualize the actual concentrations of the relevant compounds during berry development. Similar testing was conducted on the climate data to identify the main treatment effect(s).

Furthermore, a repeated measures ANOVA was conducted on the data in order to rank the significance of each compound in response to the three main experimental factors (i.e., development, light exposure and UVB radiation) individually and in combination. A repeated measures ANOVA was used to test for potential cause-effect relationships between the measured compounds and the main experimental factors. The results of the ANOVA are reported as *F*-values. The higher the *F*-value is, the lower the *p*-value, and the greater the significance will be. Fisher LSD Post Hoc tests were used to confirm which compounds reacted statistically significantly to the specified factors (adjusted *p*-value, *q*-value).

Multivariate data analysis was conducted using SIMCA (version 12.0.3.0 from MKS Data Analytics and Solutions). The data was analyzed using orthogonal partial least squares – discriminant analysis (OPLS-DA). These models are used to relate the data matrix (*X*, the measured metabolites) to a specified qualitative vector (*Y*, class, e.g., developmental stage, exposure or UV). The use of supervised OPLS-DA models assisted in the visualization of the complex datasets which consisted of multiple variables and helped to identify putative correlations within the dataset. The score plots are related to the individual observations which are grouped into similar patterns. The corresponding loading plots are used to relate the observed patterns in the OPLS-DA to the measured variables. Coefficient plots are displayed here in lieu of loading plots as they give an indication of direction. The X-variables are scaled and centered and the regression coefficients displayed are related to these values, thereby allowing for the comparison between coefficients. The size of the coefficient

factor gives an indication of how strongly the Y-variable (i.e., development, light exposure or UVB radiation) is correlated to each of the X-variables (i.e., metabolites) (BioPAT SIMCA user manual).

RESULTS

Characterization of the Microclimates in the Canopy and Bunch Zones

The characterization of the vineyard was performed according to the field-omics approach as explained in Alexandersson et al. (2014). Detailed monitoring was performed in the vineyard and the climatic data are summarized in **Table 1**, indicating that the targeted parameters for this study, namely solar radiation (including PAR) and UVB exposure significantly differed in the microclimates generated for this study (**Figure 1**; **Supplementary Figure S2**). The specifications of the acrylic sheets used stated that they would be able to block out 99% of UV light. This was confirmed by measuring the UV radiation behind and in front of the sheets. Further specification of these sheets can be seen in **Figure 1A**, indicating that the UV-excluding sheets would block UVB (280–315 nm) since it attenuated wavelengths between 280 and 350 nm. When evaluating the HL and LL environments separately, ANOVA plots furthermore showed that the HLcontrol and HL-UVB treatment (and similarly the LLcontrol and LL-UVB treatment) had similar solar radiation exposure levels, confirming that the UV-excluding sheets did not change the solar radiation further (**Figure 1B**). The data confirmed that the UV-excluding-sheets effectively attenuated UVB radiation reaching the bunch zone (**Figure 1C**). The leaf removal and

TABLE 1 | A characterization of all the microclimatic climatic data collected in the 2014/2015 season on the sampling days during the sampling window (09h00 – 11h00).

		HLcontrol	HL-UVB	LLcontrol	LL-UVB
EL-31	Canopy temperature (°C)	24.4 ^a	23.4 ^a	24.3 ^a	24.2 ^a
	Bunch temperature (°C)	25.2 ^a	25.4 ^a	24.1 ^b	23.7 ^b
	Solar radiation (W/m ²)	643.8 ^a	707.8 ^a	86.0 ^b	86.8 ^b
	UV (W/m ²)	6.5 ^a	0.4 ^b	0.7 ^c	0.0 ^d
	Humidity (%)	57.1 ^a	48.5 ^b	59.1 ^c	60.7 ^c
EL-35	Canopy temperature (°C)	23.4 ^a	22.8 ^a	23.6 ^a	23.6 ^a
	Bunch temperature (°C)	29.9 ^a	29.8 ^a	23.7 ^b	23.0 ^b
	Solar radiation (W/m ²)	998.7 ^a	855.1 ^a	201.3 ^b	198.0 ^b
	UV (W/m ²)	8.6 ^a	0.6 ^b	0.8 ^c	0.0 ^d
	Humidity (%)	48.8 ^a	39.0 ^b	49.4 ^a	53.0 ^c
EL-38	Canopy temperature (°C)	19.0 ^a	18.5 ^a	19.0 ^a	19.0 ^a
	Bunch temperature (°C)	21.1 ^a	22.0 ^a	18.6 ^b	18.7 ^b
	Solar radiation (W/m ²)	168.2 ^a	156.7 ^a	71.7 ^b	68 ^b
	UV (W/m ²)	12.8 ^a	0.2 ^b	1.0 ^c	0.0 ^d
	Humidity (%)	71.9 ^a	62.0 ^b	68.6 ^c	70.0 ^a

The table shows the mean values calculated over the sampling window per stage for each climatic variable and each individual light environment. Different superscripted letters indicate significant differences between variables: *p*-value < 0.001^a; 0.001 < *p*-value < 0.01^b; 0.01 < *p*-value < 0.05^c and insignificant^d.

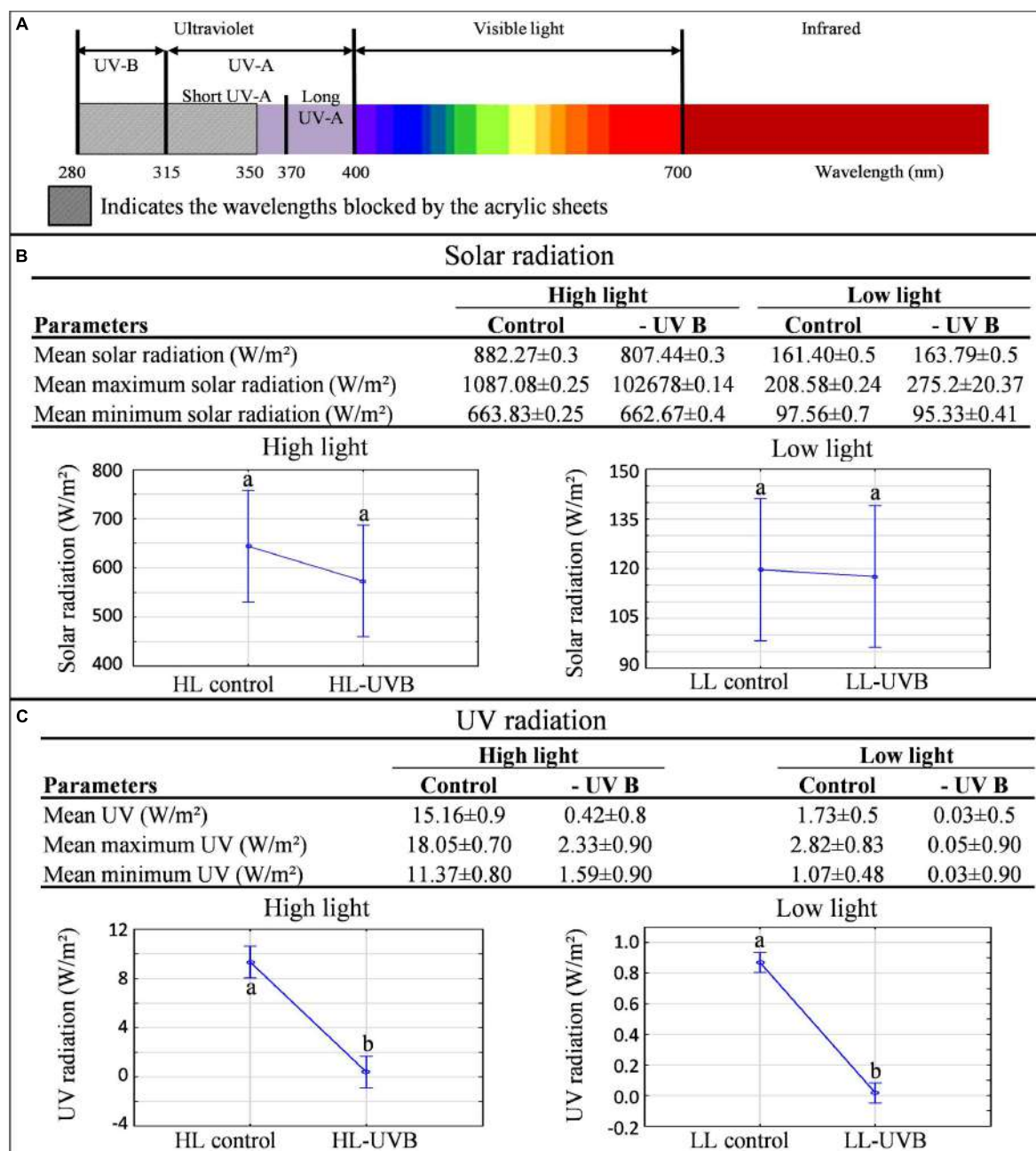


FIGURE 1 | A characterization of the light microclimates created by the four treatments in the 2014/2015 season (A). The electromagnetic spectrum showing the wavelengths blocked by the acrylic sheets used in the experiment. **(B)** The mean(\pm SD), mean maximum(\pm SD) and mean minimum(\pm SD) bunch solar radiation values **(B)** and bunch UV radiation values **(C)** calculated for each light environment over the sampling window (9h00–11h00) and their corresponding ANOVA plots; different letters indicate significant difference ($p \leq 0.05$).

increased exposure lead to differences in the bunch temperature between the HL and LL microclimates, but the UV-excluding sheets did not lead to additional differences in temperature within the HL (i.e., HLcontrol versus HL-UVB) or LL microclimates (**Figure 2; Supplementary Figure S3**). The canopy temperatures were similar between all four the experimental scenarios.

Developmental and Treatment Impacts on Berry Metabolites

The ripening parameters showed typical developmental curves for grapevine berries (**Supplementary Figure S4**) with some variation in the total acids between seasons and samples at the earlier time-points.

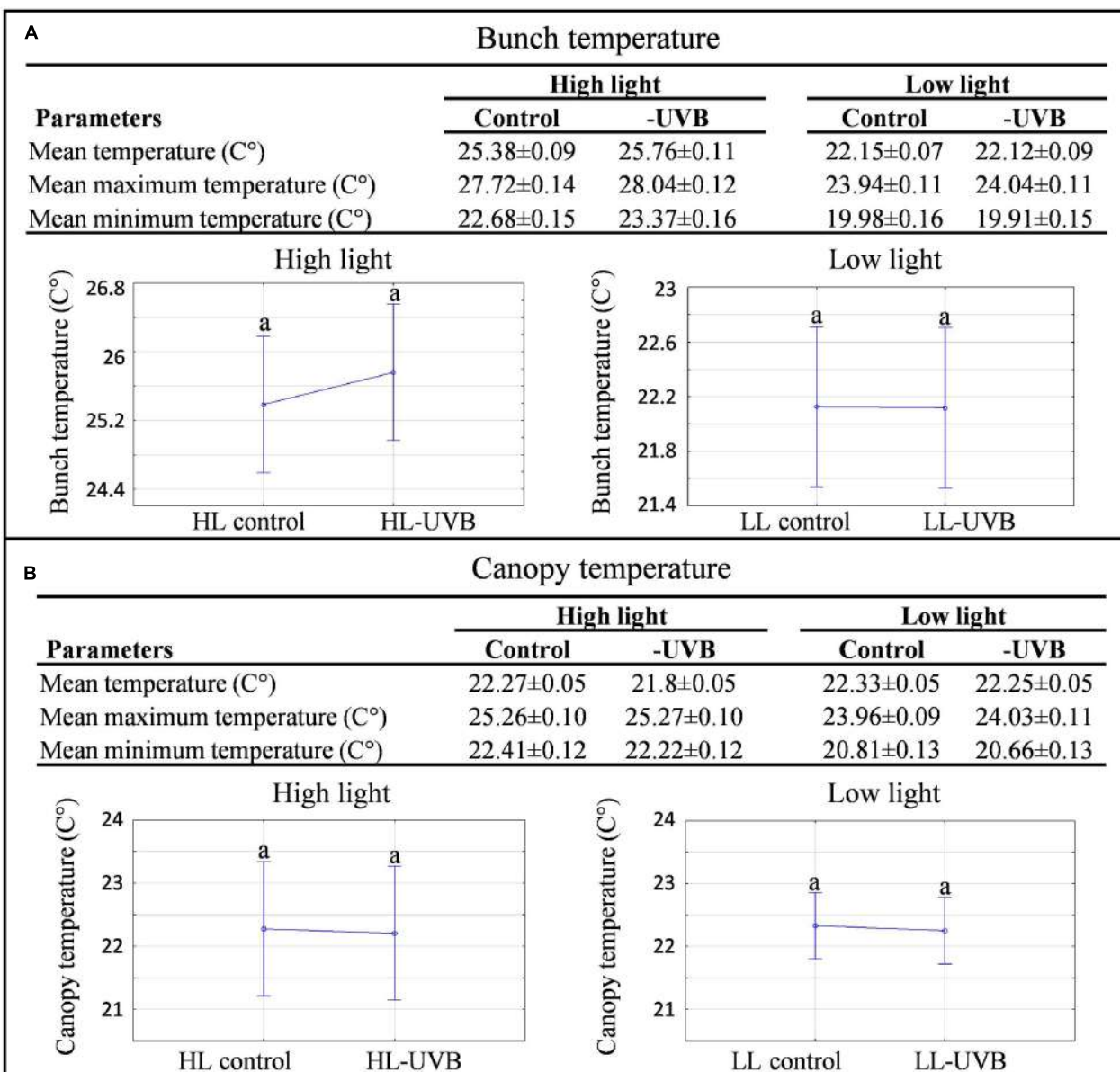


FIGURE 2 | A characterization of the temperature data collected in each microclimate in the 2014/2015 season. The mean(\pm SD) mean maximum(\pm SD) and mean minimum(\pm SD) bunch (A) and canopy (B) temperatures measured on the sampling days during the sampling window (9h00 – 11h00) with the corresponding ANOVA plots for both high light and low light environments are shown; different letters indicate significant difference ($p \leq 0.05$).

When analyzing the berry metabolites from the first season of study using a repeated measures ANOVA (Supplementary Table S3), developmental stage had the strongest effect on chlorophyll, carotenoid and xanthophyll pool sizes, and the latter two pools were also significantly affected by both the exposure of the berries, as well as UVB attenuation. These results prompted a more in-depth analysis in a subsequent season on the photosynthetically related pigments, as well as volatile compounds in reaction to UVB attenuation. All the metabolite data measured over the two seasons in the green, véraison and ripe berries sampled from the four microclimates

(HLcontrol, HL-UVB, LLcontrol, and LL-UVB) are provided in Supplementary Table S4.

Orthogonal partial least squares – discriminant analysis plots using developmental stage (Supplementary Figure S5A) or light exposure (Supplementary Figure S5B) as Y- variables, and the corresponding coefficient plots of compounds that contributed most to the models, highlighted metabolites that responded to the two factors. Separation in the samples was observed according to developmental stage with both primary and secondary metabolites contributing, in varying degrees, to the observed separation. Similarly, variation in light exposure also resulted in

a clear separation between samples, confirming the influence of a HL and LL environment on berry metabolism (**Supplementary Figure S5B**). The metabolites mainly responsible for the separation, the xanthophylls, were similar to those previously reported by Young et al. (2016).

To better elucidate the subtle effects of UVB attenuation, OPLS-DA plots were created for the early and late stages of development separately. It was clear that different metabolites contributed to the separation in the green (**Supplementary Figure S6A**) versus ripe berries (**Supplementary Figure S6B**). The corresponding coefficient plots of compounds that contributed most to the models, highlighted specific xanthophylls and volatile aroma compounds that responded to UVB radiation/attenuation. The results of the OPLS-DA were further statistically validated by multifactor analysis (repeated measures ANOVA) in order to rank the significance of each compound in response to the three main experimental factors (i.e., development, light exposure and UVB radiation) individually, and in combination (**Table 2**). To simplify and visualize the data according to the main focus of the study (“What is the impact of UVB on berry metabolites and how is it different from exposure?”); compounds that responded to the variation in light exposure and/or UVB-attenuation were used to create Venn diagrams per developmental stage (**Figure 3**). Fisher LSD Post Hoc tests were used to identify statistically significant changes. Interestingly, in the pre-ripening stages, all compounds that responded to exposure, also responded to UVB attenuation. These compounds therefore differed in amplitude, and not in presence or absence. In the ripening stage, however, compounds were identified that responded only to UVB attenuation.

Specific Xanthophylls Responded to UVB Attenuation in Predominantly the Green Photosynthetically Active Berry Stages

During the early stages of development, the xanthophylls zeaxanthin and lutein epoxide were identified as being the most responsive to UVB attenuation. Interestingly, the responses to UVB attenuation differed between the HL and LL environments. The attenuation of UVB in the HL environment resulted in a statistically significant decrease in zeaxanthin (**Figure 4**). This in turn resulted in a smaller xanthophyll pool size (violaxanthin, antheraxanthin, zeaxanthin) and a consequent lowered de-epoxidation state (DEPS ratio) in those samples (**Figure 4**). Although this was particularly obvious at the green berry stage, the lower xanthophyll pool, and consequent lower DEPS ratio, was consistently seen throughout berry development in the HL-UVB microclimate, but decreasing with developmental stage progression. Furthermore, the attenuation of UVB in the LL environment also resulted in a decreased V + A + Z pool and a lowered DEPS ratio in the green stage (**Figure 4**), although the effect was less pronounced compared to HL.

A significant difference in the levels of lutein epoxide between the LLcontrol and LL-UVB contrasts was also confirmed, clearly showing that UVB exposure in LL conditions is involved in the metabolism of lutein epoxide. Since lutein levels did not change,

the Lx:L ratio was consequently significantly affected in the green developmental stage and to a lesser degree at the harvest stage (**Figure 4**).

In the Ripe Berry Stages Specific Volatiles Responded to UVB Attenuation

UVB attenuation was shown to affect specific volatile compounds in the ripe developmental stage (EL-38). These included monoterpenes, carotenoid-derived norisoprenoids and certain C₆ compounds. In the HL environment, certain monoterpenes and norisoprenoids were decreased by UVB attenuation, leading to larger monoterpene and norisoprenoid pools in the HL control samples (**Figure 5**) and confirming that UVB exposure stimulates volatile organic compounds (VOCs) in exposed berries. Under LL conditions, however, both the monoterpene and norisoprenoids pools were decreased relative to the HL microclimate and UVB attenuation resulted in no further statistically significant differences between the LLcontrol and LL-UVB microclimates.

Interestingly, under LL conditions, different VOC profiles as well as contents of individual volatile compounds were observed when comparing the LLcontrol with the UVB attenuated microclimate (LL-UVB) in ripe berry samples. Certain straight chain aldehydes and ketones (e.g., 1-octen-3-one, 2-heptanal and trans-2,4-heptadienal), decreased with UVB attenuation. Conversely, a significantly higher concentration of C₆ compounds, including trans-2-hexenal and N-hexanal were observed when UVB was attenuated in the LL environment. This is the opposite of the scenario in HL, where the HLcontrol had more total C₆ compounds than the HL-UVB (**Figure 5**).

Furthermore, to control for well-known metabolite responses to UV, samples were also analyzed for polyphenols. As expected, total polyphenolics, and specifically the flavonol quercetin-glucoside, was significantly reduced with UVB attenuation in the HL microclimate, most notably in the early developmental stages (**Figure 6A**), although this pattern followed through to harvest (**Figure 6B**). No statistical significances were seen in the LL microclimate (LLcontrol versus LL-UVB) in either the early or late developmental stages.

DISCUSSION

A number of studies have shown that increased exposure (including UV) of grape berries, leads to the increased accumulation of polyphenolic compounds (Tardaguila et al., 2010; Diago et al., 2012; Song et al., 2015), as well as changes to varietal aroma compounds (Bureau et al., 2000; Zhang et al., 2014; Song et al., 2015). The increase in phenolic compounds, including anthocyanins, proanthocyanidins and flavonols, have been attributed to the increased expression of a number genes involved in their biosynthesis as a way to adapt to HL environments (Matus et al., 2009; Azuma et al., 2012). Carbonell-Bejerano et al. (2014) demonstrated that UV radiation upregulated a number of genes encoding transcription factors (e.g., MYBs and bHLH) that in turn activated flavonol biosynthetic genes [putative lyases, chalcone synthases, flavonol

TABLE 2 | An analysis of the photosynthetic pigments and volatile aroma compounds (2014/2015 season).

	Development	Exposure	UVB-attenuation	Exposure x Development	UVB-attenuation x Development	UVB-attenuation x Exposure	UVB-attenuation x Exposure x Development
Photosynthetic pigments							
Total carotenoids	6969.66	108.26	0.11	143.63	2.91	1.64	3.76
Neoxanthin	5290.28	5.56	3.44	34.75	0.60	4.81	5.45
β -Carotene + Lutein	4964.43	40.05	1.75	92.44	6.79	3.21	3.94
Chlorophyll β	4874.49	4.88	2.56	29.28	9.93	1.57	1.00
β -carotene	3946.08	39.94	2.88	56.21	4.89	3.64	3.90
Total xanthophylls	3532.44	207.91	24.29	143.68	1.79	0.79	0.07
Total chlorophylls	2844.18	7.81	1.03	24.82	3.92	0.65	0.35
Lutein	2407.50	18.29	0.00	110.95	4.99	0.86	0.40
Chlorophyll a	2203.64	8.62	0.63	22.16	2.49	0.41	0.21
Lutein epoxide	2019.62	163.13	29.35	131.01	4.88	24.76	40.76
Violaxanthin	1815.88	0.85	0.48	40.42	11.49	0.03	0.89
Carotene:Chlorophyll	1156.30	3.84	0.91	3.94	0.23	0.11	3.50
β -carotene + Lutein:Total Carotenoids	733.40	98.97	3.85	60.23	2.87	4.69	1.83
Lx:L (ratio)	584.61	86.36	47.86	138.58	3.61	0.30	30.05
DEPS (ratio)	281.07	592.13	13.11	64.35	8.32	1.94	0.03
V + A + Z	161.48	250.02	22.85	72.91	7.14	17.08	4.92
Antheraxanthin	125.00	261.87	3.13	140.63	2.35	13.86	4.57
Chlorophyll a:Chlorophyll b	114.44	54.70	2.90	11.46	0.11	12.99	7.32
Zeaxanthin	33.04	195.24	19.86	44.25	7.05	13.36	4.07
Volatile compounds							
β -Damascenone	1195.01	44.39	0.35	12.22	0.14	0.35	0.14
4-Terpineol	475.91	25.92	0.13	23.18	0.69	0.12	0.69
Mono-terpenes	438.47	37.45	0.05	7.69	1.37	0.03	1.28
α -terpinene	391.26	38.33	0.45	25.32	1.80	0.46	1.81
Geranylacetone	314.23	0.98	4.29	29.85	0.88	3.82	1.10
Cineol	299.63	0.03	0.39	0.03	0.39	0.39	0.39
Hotrienol	257.80	211.77	19.15	91.96	4.49	5.82	1.85
Norisoprenoids	238.93	1.49	6.26	33.02	3.97	2.79	1.03
Alcohols	234.48	207.44	15.19	89.72	4.21	3.43	2.79
Limonene	211.48	189.98	2.07	12.80	11.16	2.07	11.16
α -Terpinolene	205.19	66.92	0.08	23.89	1.22	0.05	1.23
Linalool	167.91	115.64	17.71	104.16	22.44	18.61	21.66
Sabinene	153.27	21.32	1.30	13.05	0.40	0.00	2.90
Gama-Terpinene	143.93	29.53	0.57	12.20	1.54	0.77	1.35
6-Methyl-6-heptan-2-one	84.04	0.00	10.61	71.19	14.54	0.29	14.25
α -Terpineol	62.55	104.88	6.36	23.13	3.13	6.36	3.13
1-Octen-3-one	60.04	36.70	25.00	2.26	14.63	28.84	35.30
Trans-2,4-Heptadienal	41.84	8.88	1.39	5.92	2.25	9.62	2.79
Geraniol	39.74	27.02	18.35	23.64	15.30	18.35	15.30
N-Hexanal	26.38	0.82	0.15	13.22	0.07	5.32	18.58
β -Cyclocitral	24.35	20.41	11.05	9.22	15.94	11.05	15.94
2-Octenal	23.74	90.77	20.74	15.30	8.02	11.14	26.33
Nonenal	22.77	2.68	2.73	2.99	0.46	0.74	6.33
2-Hexanal	16.86	1.07	6.97	1.71	3.05	0.65	2.22
Carbonyl compounds	14.49	0.00	1.69	0.83	1.03	0.04	4.66
Trans-2-Hexanal	12.63	0.03	2.17	0.74	0.98	0.36	3.63
Octanal	11.01	32.36	0.92	9.34	3.41	3.59	6.96
3-Hexanol	10.25	2.27	0.51	0.87	2.40	25.24	4.13
β -ionone	9.06	2.14	0.08	1.59	2.66	0.08	2.66
2-Heptanal	5.39	90.95	11.79	21.84	5.33	9.84	23.08

The repeated measures ANOVA results for the listed parameters and individual compounds are reported as F-values. Values are scaled from highest (i.e., most significant) to lowest by color. Green indicates low F-values, while red indicates high F-values values. All insignificant values ($F \leq 3$) are colored in gray. Maximum ■; 50% ▲; minimum ■; insignificant ■■■.

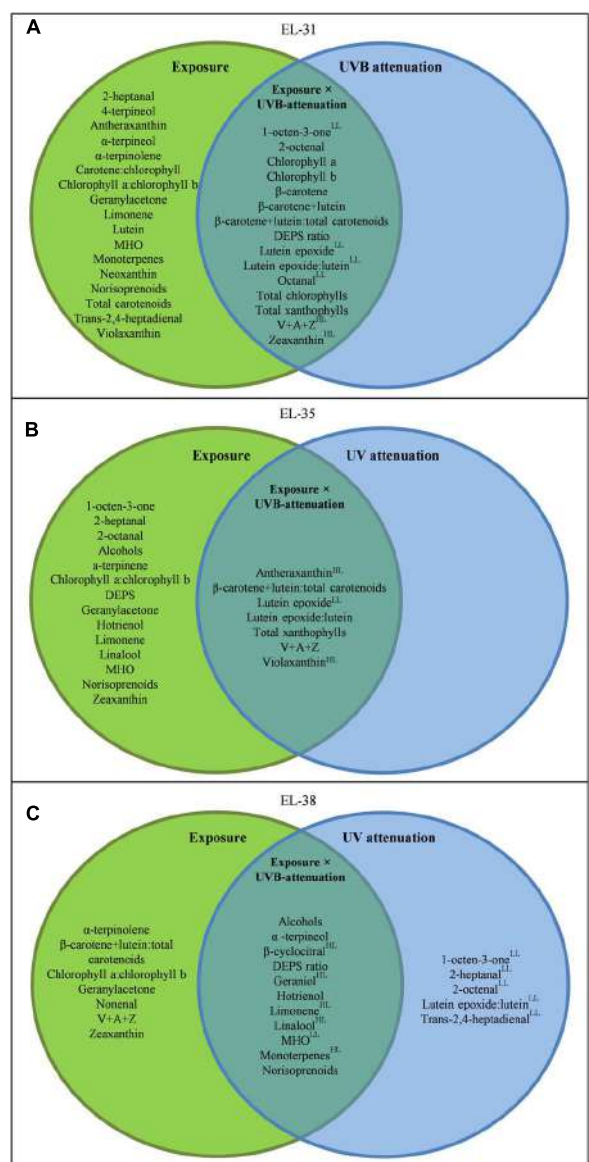


FIGURE 3 | A Venn diagram showing the compounds which responded to light exposure (green circle), UVB attenuation (blue circle) and both (intercept) in the early (A), véraison (B), and late (C) developmental stages. Compounds were selected based on significance in a repeated measures ANOVA and Fisher LSD Post Hoc tests (adjusted p -value, q -value ≤ 0.05). All metabolites presented have a q -value ≤ 0.05 . Metabolites with a \log_2 -fold-change of ≥ 0.5 are indicated by a “HL” for the high light- or “LL” for the low light microclimate.

synthases (FLS) and flavonol glycosyltransferases] in grape berries. FLS is a dedicated enzyme involved in flavonol biosynthesis (e.g., quercetin) and its transcriptional response to light has been demonstrated in Shiraz (Downey et al., 2004).

In this study the characterization of the microclimates confirmed exposure and UVB attenuation as the main treatment effect in both the HL and LL environments. Marked increases

in quercetin-glucoside contributed to a higher content of total polyphenolics in ripe berries in the HLcontrol (compared to HL-UVB), but not in the LL microclimate (Figure 6). The study illustrates that grapevine berries utilize polyphenolics as well as photosynthesis-related pigments in acclimation responses. These responses are differentially affected by UVB attenuation under HL and LL conditions in the different berry developmental stages. Since the carotenoid pigments are substrates for the formation of volatile aroma compounds (norisoprenoids) as ripening progresses, these volatile berry metabolites were also followed.

Grapevine Berries Displayed Metabolic Plasticity in their Response to Attenuated UVB and the Response Was Influenced by the Developmental Stage of the Berries

In the green berry stage (EL-31) the xanthophylls reacted to the variations in UVB. This modulation of xanthophylls in the photosynthetically active green berries indicated that within the field setting, acclimation to light stress occurred in the early developmental stages. The data showed that the violaxanthin- and the lutein epoxide cycles were functional in the photosynthetically active berries in the HL and LL microclimates. The amplitudes of the cycles were, however, responsive to solar radiation and UVB. Although these cycles appear to be functional in the photosynthetically active green berries, and are typically regarded as photo-protective measures, the major carotenoids and chlorophylls were not significantly affected (\log_2 -fold change ≤ 0.5) in either microclimate (HL or LL). This implies that the stress perceived by the photosynthetically active berries in the early developmental stages was mitigated by, for e.g., photoprotective mechanisms (e.g., non-photochemical quenching via the violaxanthin cycle) and photosynthesis was apparently unaffected (i.e., no evidence of photoinhibition and/or photodamage based on the core photosynthetic pigments). In the absence of UVB radiation, the berries required less zeaxanthin in HL microclimates, and conversely, less lutein epoxide in LL microclimates, to cope with the perceived stress and maintain active photosynthesis. The attenuation of UVB, however, potentially renders the plants more susceptible to damage as they are less acclimated than those plants exposed to UVB, especially in the LL microclimate. From numerous studies on photosynthetic organisms/tissues, it is known that the xanthophylls respond to light by way of the violaxanthin and/or lutein epoxide cycles (Demmig-Adams and Adams, 1996; García-Plazaola et al., 2007).

The photosynthetic efficiency of plants depends on their ability to adapt to natural daily variations in photon flux density. It is important that the photosynthetic plant tissues are able to absorb solar light and transfer the resulting energy to the relevant reaction centers under any light conditions. The light environment within a canopy is not fixed, but fluctuates in occurrence with the creation of gaps in the canopy or climatic changes (e.g., cloud cover). The alterations in the

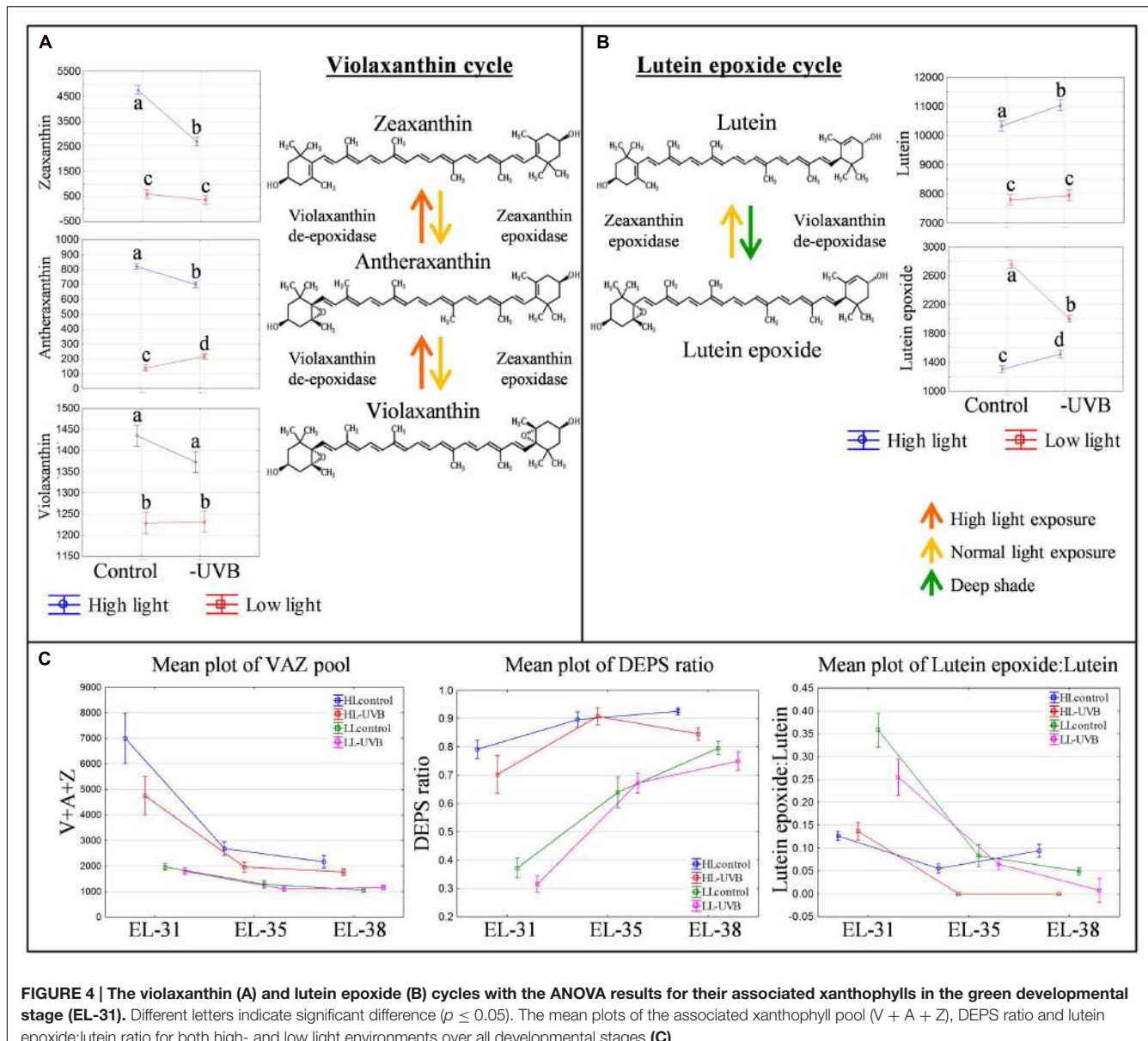


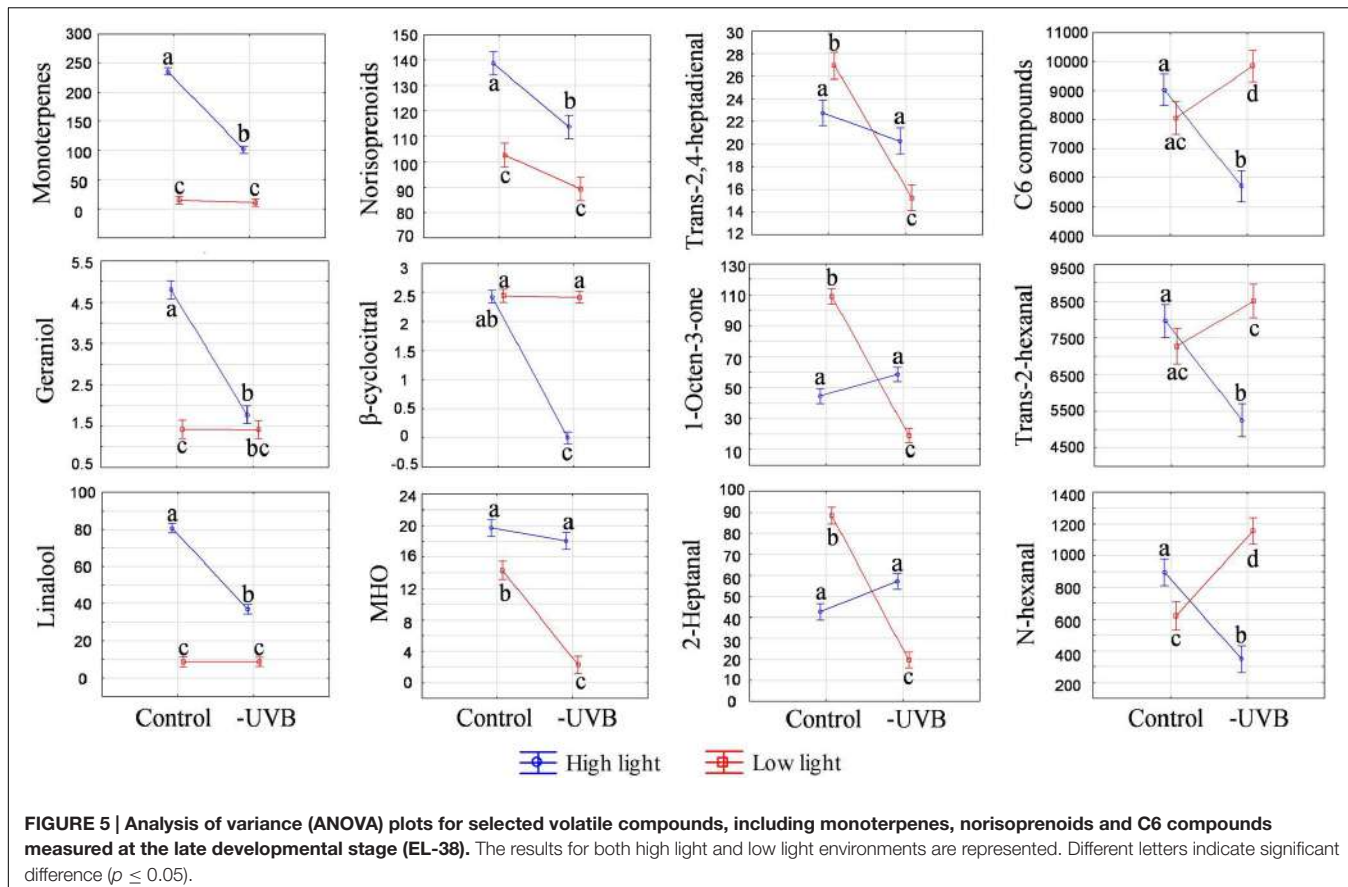
FIGURE 4 | The violaxanthin (A) and lutein epoxide (B) cycles with the ANOVA results for their associated xanthophylls in the green developmental stage (EL-31). Different letters indicate significant difference ($p \leq 0.05$). The mean plots of the associated xanthophyll pool (V + A + Z), DEPS ratio and lutein epoxide:lutein ratio for both high- and low light environments over all developmental stages (C).

light environment may be transitory (e.g., sunflecks), or more permanent (e.g., leaf removal). In response to the variations in light exposure, plants have developed several morphological, physiological and biochemical mechanisms to optimize the light harvesting process as well as to protect the photosystems and maintain optimal functioning (Walters and Horton, 1994; Demmig-Adams and Adams, 2006; Johnson et al., 2007; García-Plazaola et al., 2007; Vogelmann and Gorton, 2014). It is evident that berries have maintained this photoprotective ability and respond to stress in the same way as photosynthetically active leaves.

In the HL microclimate, UVB-exposure lead to increased production of berry volatiles (predominantly monoterpenes including geraniol, linalool and limonene with a \log_2 -fold change >1) in the later stages of berry development (from

véraison onward). Similar results were seen in Malbec berries in that increased UVB exposure resulted in an increase in monoterpane emissions at the pre-harvest developmental stage. These results were interpreted to suggest that monoterpenes were involved in protection from UVB radiation (Gil et al., 2013). The antioxidant potential of terpenes (isoprene, monoterpenes, sesquiterpenes and tetraterpenes such as carotenoids) is well documented (Loreto and Velikova, 2001; Loreto et al., 2004) and it is possible that this is one of their biological functions in older (sink) tissues (such as ripe berries and/or senescing tissues).

A similar result was seen in the norisoprenoids in the HL environment with the most responsive of them being β -cyclocitral. In a LL environment, MHO was seen to react in a similar way in that it was significantly reduced by

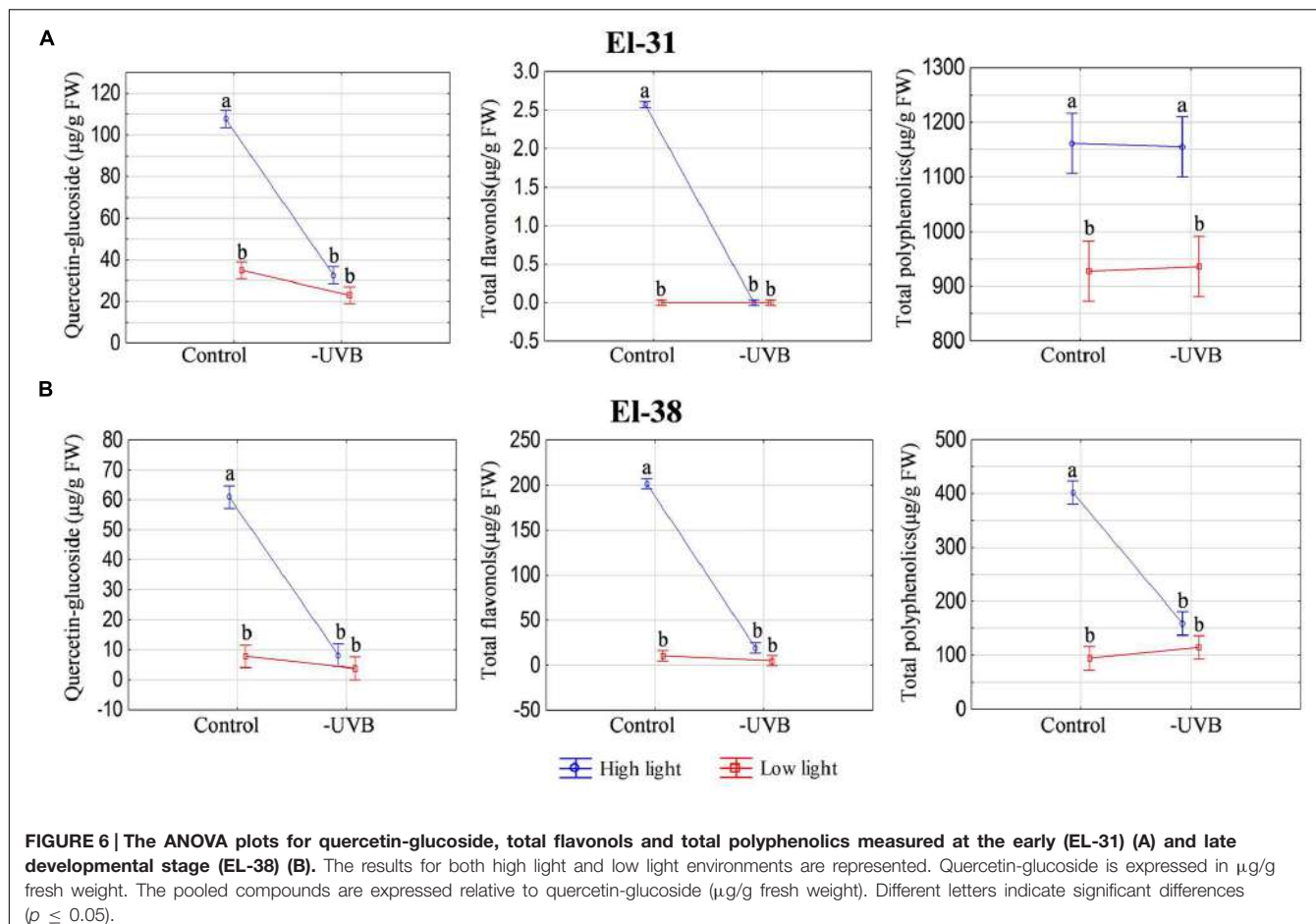


the attenuation of UVB. Norisoprenoids are formed via the degradation of carotenoids and the higher carotenoid content in HLcontrol berries may have directly resulted in the increased levels of norisoprenoids. Additionally, the derivatives of certain carotenoids are known to perform signaling functions in plants. Ramel et al. (2012) reported the rapid accumulation of β -cyclocitral upon exposure of *Arabidopsis* plants and the consequent reprogramming of gene expression to increase the capacity for photooxidative stress tolerance. The results of that study indicated that β -cyclocitral may serve as a signaling compound in plants which leads to the activation of oxidative stress defense mechanisms. Volatile carotenoid derivatives may therefore serve as sensing and signaling compounds when plants are subjected to stress as a way to mitigate potential damage. VOCs have been shown to increase in response to certain abiotic stresses (Possell and Loreto, 2013). It is speculated that volatile terpenes (e.g., monoterpenes) play important roles in the protection of plants from environmental stress (Loreto and Schnitzler, 2010; Carvalho et al., 2015). Although the exact mechanism is still unclear, the consistency of these links with stress warrants further investigation.

The higher C₆-compounds levels (e.g., *n*-hexanal, *trans*-2-hexanal) in the HLcontrol berries (versus the HL-UVB berries), indicates a role for UVB in the regulation and/or metabolism of these compounds. Leaf removal is typically used

in viticulture as a canopy management strategy to reduce the “green/vegetal” character of especially red cultivars (e.g., Cabernet Sauvignon). This green character is typically associated with pyrazines (predominantly methoxypyrazines), but can also be attributed to certain C₆-compounds (e.g., hexanal) and some monoterpenes (e.g., eucalyptol) (Allen et al., 1991; Fariña et al., 2005; Lund et al., 2009). C₆-compounds are produced via the lipoxygenase-hydroperoxide lyase (LOX-HPL) pathways and are developmentally regulated and known to be released during maceration or damage. Here we show that the UVB component of light contributes to the release of C₆ compounds implicating UV in the regulation the LOX-HPL pathway and consequently the metabolism of polyunsaturated fatty acids (PUFAs). Interestingly, in the LL environment in the later developmental stages, the LLcontrol berries had significantly lower levels of the C₆-compounds relative to the LL-UVB.

Attenuation of UVB in the LL environment decreased the levels of a number of straight chain aldehydes (e.g., 2-heptanal and *trans*-2,4-heptadienal) and a ketone (1-octen-3-one). These compounds therefore reacted similarly to the C₆ compounds in the HL environment, and again implicating UVB in the metabolism of PUFAs. It is clear that the level of light exposure will determine which substrates are metabolized and/or which compounds are formed in berries, displaying considerable plasticity in these responses.



Control Processes Over Non-photochemical Quenching, Photodamage and Photorepair Are Activated as Part of the Acclimation Responses and UVB Plays a Key Role

The increase in epoxidation state of the xanthophylls (as determined by the DEPS ratio) in the HL berries is due to higher zeaxanthin levels (versus violaxanthin) in the xanthophyll pool, and is indicative of a photosynthetic system that is utilizing non-photochemical quenching via zeaxanthin in the violaxanthin cycle. The response in the absence of UV (HL-UVB berries) is less than the HLcontrol, even though the incident PAR and bunch temperature are not significantly different. UVB exposure affects the amplitude of the violaxanthin cycle response (DEPS ratio due to different zeaxanthin levels). UVB radiation is known to affect the translation of psbA (D1 protein) in the photodamage/photorepair cycle, it is likely that in the absence of UVB (as in the HL-UVB), the photosystems recover quicker (via photorepair of photodamage) than in the presence of UVB radiation (as in the HLcontrol), and/or that the actual level of saturating conditions for photosynthesis are lower in the presence of UVB radiation and HL. These results provide a hypothesis for subsequent studies on UV effects on fruit physiology and

metabolism and are supported by literature from a number of fruits (Arakawa et al., 1985; Ubi et al., 2006; Calvenzani et al., 2010; Huyskens-Keil et al., 2012).

Additionally the lutein epoxide cycle is lower in the UVB attenuated LL treatments (LL-UVB). Lutein epoxide is formed in shade (deep/long term shade) and functions to protect the photosynthetic apparatus from sudden localized HL exposures (e.g., sunflecks). Although the PAR in the LLcontrol and the LL-UVB were similar (low but differing only in the incident UVB), the lutein epoxide cycle is less active in the absence of UVB (LL-UVB). It appears as if it is the UVB component of solar radiation that is required for the formation of lutein epoxide (and by extension the functioning of the lutein epoxide cycle in LL microclimate). It is evident that both cycles are required and simultaneously functional in photosynthetically active berries (albeit to varying degrees) to potentially cope with the continuously varying light conditions in the microclimate: zeaxanthin in HL and lutein epoxide in LL, with UVB affecting the absolute amounts present in photosynthetically active berries.

These responses to varying light conditions are well known and well described in photosynthetic research on photosynthetic organs (predominantly leaves); but the reports for the response of fruit to UVB exposure appears to be limited to the formation of metabolites with antioxidant or “sunscreen” activity

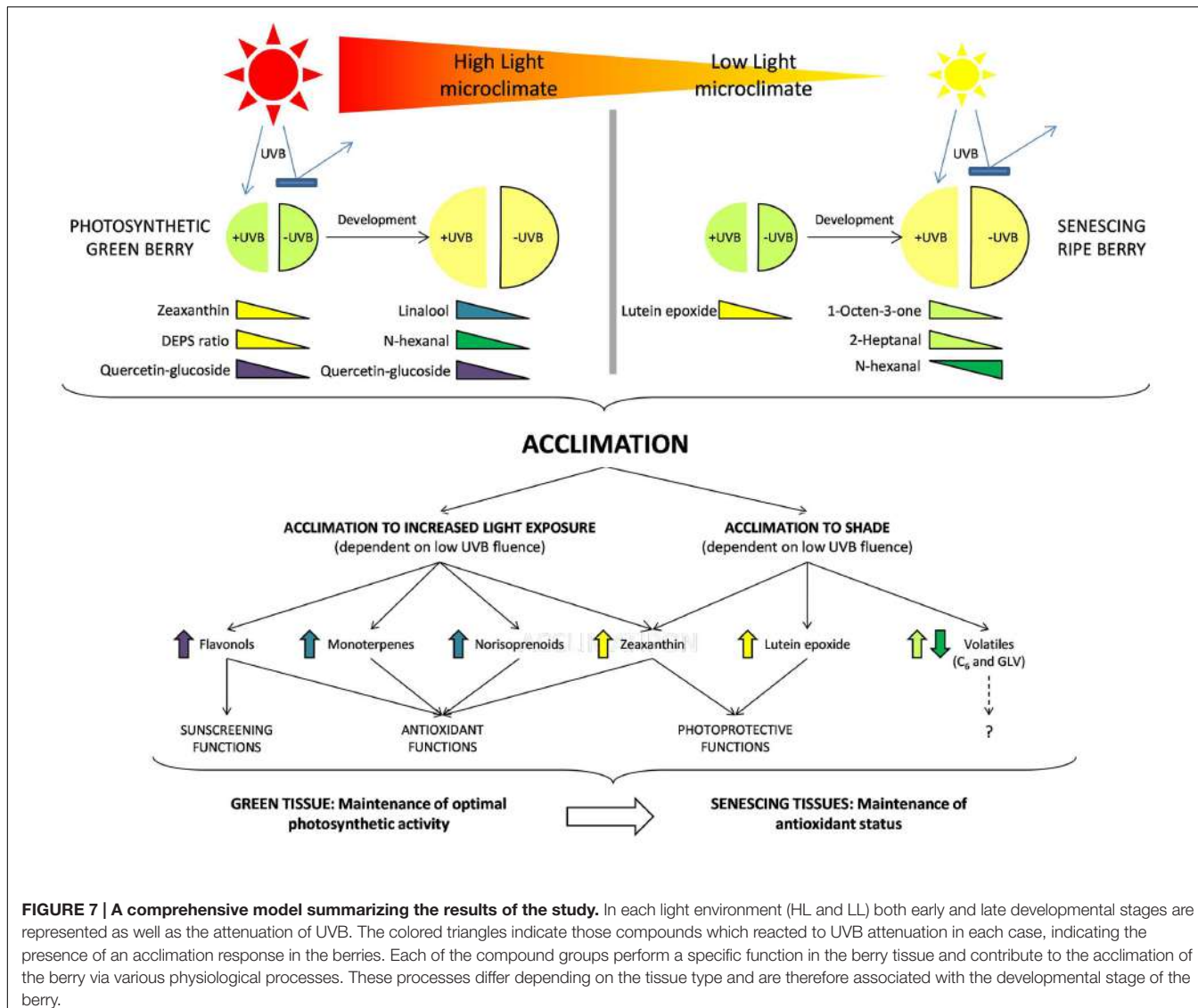


FIGURE 7 | A comprehensive model summarizing the results of the study. In each light environment (HL and LL) both early and late developmental stages are represented as well as the attenuation of UVB. The colored triangles indicate those compounds which reacted to UVB attenuation in each case, indicating the presence of an acclimation response in the berries. Each of the compound groups perform a specific function in the berry tissue and contribute to the acclimation of the berry via various physiological processes. These processes differ depending on the tissue type and are therefore associated with the developmental stage of the berry.

(polyphenolics, anthocyanins, flavonols, etc.). Increased exposure of the grape berries has been shown to result in the increase of polyphenolics and certain aromatic compounds in the berry tissues (Bureau et al., 2000; Tardaguila et al., 2010; Diago et al., 2012; Gil et al., 2013; Zhang et al., 2014; Song et al., 2015). It is tempting to speculate that the formation of these latter compounds represent molecular fingerprints of long term acclimation responses of early stage (i.e., photosynthetically active) fruits attempts at protecting photosynthesis distally (by reflecting incident radiation in predominantly the exposed skins and/or via general antioxidants to mitigate the damage of reactive oxygen species). The carotenoids (specifically the xanthophylls: zeaxanthin, antheraxanthin and lutein epoxide), however, are intrinsically linked to photosynthesis and are therefore probably the more direct/local response to saturating light conditions on the photosynthetic process (as on-site antioxidants or by direct non-photochemical quenching of reactive oxygen species). It could be that it is the failure of carotenoids and

other lipophilic antioxidants present in the photosynthetic membranes (of green berries), to mitigate stress that trigger the long(er) term responses involving acclimation and other photomorphogenic responses to deal with the consequence of continued photodamage (e.g., structural changes to the skin composition and the accumulation of polyphenolics in the skin).

The metabolic outcomes of these acclimation responses and the level of stress perceived in the different microclimates clearly impacts berry composition. It has been confirmed that in both leaves (Joshi et al., 2013; Juvany et al., 2013) and berries (Carbonell-Bejerano et al., 2014; Liu et al., 2015) young photosynthetically active tissues respond differently to increased exposure compared to older tissue (old, senescing leaves or ripe berries). **Figure 7** proposes an overview model of the respective responses and highlights the importance of the developmental stage (early or late) as well as the microclimate (HL or LL) on the metabolites that are differentially produced

and proposed to play a role in the acclimation responses. The data presented supports the hypothesis that plants in shade are less acclimated and consequently more susceptible (on e.g., a clear day) than the exposed (HL) more acclimated counterparts (typically displaying higher flavonols, higher photo-protective xanthophylls, and/or antioxidant volatiles, depending on the developmental stage). In the absence of UVB, less acclimation has potentially occurred in the LL-UVB and the plants will be more susceptible (to e.g., sunflecks) than the more acclimated HL-UVB counterparts. Here we show that these general plant responses are active in grapevine berries with developmental stages displaying distinctive responses.

AUTHOR CONTRIBUTIONS

MV conceived and planned the study. CJ implemented and maintained the viticultural treatments and monitored the vineyard. CJ and PY carried out berry sampling. CJ did the climatic data processing and analysis, processing and analysis of the berry samples together with HE-B which performed the UPLC, HPLC, and GC-MS analysis. CJ performed the data integration and processing for the above compounds. CJ, HE-B, and PY performed data analysis. CJ, PY, and MV drafted the initial manuscript, all authors contributed to the final manuscript.

ACKNOWLEDGMENTS

The authors would like to recognize the following people for their contributions toward this study: Ms Zelmari Coetzee for her assistance with the viticultural treatments, logger installation and sampling; Dr. Katja Suklje and Prof Alain Deloire for useful discussions during the planning stages of the study; Ms Varsha Premsagar for her assistance with sample processing; Mrs Anke Berry and Ms Louise Dautrey for their assistance with sampling processing and analysis; Mr Lucky Mokwena for his assistance with the implementation of the GC-MS method for volatile aroma compound analysis; Dr Albert Strever for his help with the statistical analysis. The study was financially supported with grants from Wine Industry Network for Expertise and Technology (Winetech), Department of Science and Technology (DST), the National Research Foundation (NRF) and the Technology and Human Resources for Industry Programme (THRIP).

SUPPLEMENTARY MATERIAL

The Supplementary Material for this article can be found online at: <http://journal.frontiersin.org/article/10.3389/fpls.2016.00786>

REFERENCES

- Alexanderson, E., Jacobson, D., Vivier, M. A., Weckwerth, W., and Andreasson, E. (2014). Field-omics—understanding large-scale molecular data from field crops. *Front. Plant Sci.* 5:286. doi: 10.3389/fpls.2014.00286

FIGURE S1 | The experimental layout of the treatments within the plot (A) and the four light environments created by leaf removal and UVB attenuation (B).

FIGURE S2 | The mean hourly seasonal (from berry set to harvest) solar radiation and UV radiation data (mean \pm 95% confidence interval) for each light environment measured in the 2014/2015 experimental season. The first hour is from 00h00 to 01h00.

FIGURE S3 | The seasonal (2014/2015) bunch and canopy minimum, maximum, and mean (\pm SD) temperatures for all light environments and the corresponding kinetics showing the mean hourly bunch and canopy temperatures (mean \pm 95% confidence interval) measured in the 2014/2015 experimental season. The first hour is from 00h00 to 01h00.

FIGURE S4 | (A) The total sugars and total organic acid contents measured over berry development and the ripening parameters determined at harvest (2011/2012 season). **(B)** The ripening parameters measured for the last experimental season (2014/2015 season).

FIGURE S5 | Orthogonal partial least squares – discriminant analysis (OPLS-DA) models generated for all metabolic data over both experimental seasons for developmental stage (A) and light exposure (B). Each OPLS-DA is accompanied by a co-efficient plot of compounds which contributed most to the respective models. These were chosen according to the individual variable importance plots (VIP's) and included the top compounds with a VIP \geq 0.5. Shapes of the sample icons denote the respective developmental stages: EL-31 (●), EL-35 (▲) and EL-38 (■).

FIGURE S6 | Orthogonal partial least squares – discriminant analysis models generated for all metabolic data over both experimental seasons for the early (A) and late (B) developmental stages separately. The attenuation of UVB was used as the y-factor in both models. Each OPLS-DA is accompanied by a co-efficient plot of compounds which contributed most to the respective models. These were chosen according to the individual variable importance plots (VIP's) and included the top compounds with a value above 0.5. Shapes of the sample icons denote the respective exposure: High Light (■) and Low Light (●).

TABLE S1 | Calibration curve of volatile organic compounds used in this study and analyzed by HS-SPME and GC single-quadrupole-MS.

TABLE S2 | Selected ions used for the integration of the peak area of the respective compounds of interest as well as their retention time on the Zebron column and quantifier molecules analyzed by HS-SPME and GC single-quadrupole-MS.

TABLE S3 | An analysis of the metabolic data from the first experimental season (2011/2012 season). The repeated measures ANOVA results for the listed parameters and individual compounds are reported as F-values. Values are scaled from highest (most significant) to lowest by color. Green indicates low F-values (significant), while red indicates high F-values values (more significant). All insignificant values are highlighted in gray. Maximum ■; 50% ▲; minimum ▼; insignificant □.

TABLE S4 | A table listing the measured contents of all the compounds \pm SD for both experimental seasons. The \log_2 -fold changes and corresponding p-values between the HL control/HL-UVB and LL control/LL-UVB contrasts are calculated and listed for each compound at each developmental stage. Blocks highlighted in red indicate significant difference ($p \leq 0.05$).

Allen, M. S., Lacey, M. J., Harris, R. L., and Brown, W. V. (1991). Contribution of methoxypyrazines to Sauvignon blanc wine aroma. *Am. J. Enol. Vitic.* 42, 109–112.

Arakawa, O., Hori, Y., and Ogata, R. (1985). Relative effectiveness and interaction of ultraviolet-B, red and blue light in anthocyanin synthesis of

- apple fruit. *Physiol. Plant.* 64, 323–327. doi: 10.1111/j.1399-3054.1985.tb0347.x
- Azuma, A., Yakushiji, H., Koshita, Y., and Kobayashi, S. (2012). Flavonoid biosynthesis-related genes in grape skin are differentially regulated by temperature and light conditions. *Planta* 236, 1067–1080. doi: 10.1007/s00425-012-1650-x
- Barros, E. P., Moreira, N., Pereira, G. E., Leite, S. G. F., Rezende, C. M., and de Pinho, P. G. (2012). Development and validation of automatic HS-SPME with a gas chromatography-ion trap/mass spectrometry method for analysis of volatiles in wines. *Talanta* 101, 177–186. doi: 10.1016/j.talanta.2012.08.028
- Blanke, M. M., and Lenz, F. (1989). Fruit photosynthesis. *Plant Cell Environ.* 12, 31–46. doi: 10.1111/j.1365-3040.1989.tb01914.x
- Bureau, S. M., Razungles, A. J., and Baumes, R. L. (2000). The aroma of muscat of Frontignan grapes: effect of the light environment of vine or bunch on volatiles and glycoconjugates. *J. Sci. Food Agric.* 80, 2012–2020. doi: 10.1002/1097-0010(200011)80:14<2012::AID-JSFA738>3.0.CO;2-X
- Calvenzani, V., Martinelli, M., Lazzari, V., Giuntini, D., Dall'Asta, C., Galaverna, G., et al. (2010). Response of wild-type and high pigment-1 tomato fruit to UV-B depletion: flavonoid profiling and gene expression. *Planta* 231, 755–765. doi: 10.1007/s00425-009-1082-4
- Carbonell-Bejerano, P., Diago, M.-P., Martínez-Abaigar, J., Martínez-Zapater, J. M., Tardáguila, J., and Núñez-Olivera, E. (2014). Solar ultraviolet radiation is necessary to enhance grapevine fruit ripening transcriptional and phenolic responses. *BMC Plant Biol.* 14:183. doi: 10.1186/1471-2229-14-183
- Carvalho, L. C., Coito, J. L., Colaco, S., Sangiogo, M., and Amancio, S. (2015). Heat stress in grapevine: the pros and cons of acclimation. *Plant Cell Environ.* 38, 777–789. doi: 10.1111/pce.12445
- Cramer, G. R., Urano, K., Delrot, S., Pezzotti, M., and Shinozaki, K. (2011). Effects of abiotic stress on plants: a systems biology perspective. *BMC Plant Biol.* 11:163. doi: 10.1186/1471-2229-11-163
- Dal Santo, S., Tornielli, G. B., Zenoni, S., Fasoli, M., Farina, L., Anesi, A., et al. (2013). The plasticity of the grapevine berry transcriptome. *Genome Biol.* 14:r54. doi: 10.1186/gb-2013-14-6-r54
- Demmig-Adams, B., and Adams, W. W. (1996). The role of xanthophyll cycle carotenoids in the protection of photosynthesis. *Trends Plant Sci.* 1, 21–26. doi: 10.1016/S1360-1385(96)80019-7
- Demmig-Adams, B., and Adams, W. W. (2006). Photoprotection in an ecological context: the remarkable complexity of thermal energy dissipation. *New Phytol.* 172, 11–21. doi: 10.1111/j.1469-8137.2006.01835.x
- Diago, M. P., Ayestarán, B., Guadalupe, Z., Poni, S., and Tardáguila, J. (2012). Impact of prebloom and fruit-Set basal leaf removal on the flavonol and anthocyanin composition of Tempranillo grapes. *Am. J. Enol. Vitic.* 63, 367–376. doi: 10.5344/ajev.2012.11116
- Downey, M. O., Harvey, J. S., and Robinson, S. P. (2004). The effect of bunch shading on berry development and flavonoid accumulation in Shiraz grapes. *Aust. J. Grape Wine Res.* 10, 55–73. doi: 10.1111/j.1755-0238.2004.tb0008.x
- Eichhorn, K. W., and Lorenz, D. H. (1977). Phanologische entwicklungsstadien der rebe. *Nachr. Dtsch. Pflanzenschutzd.* 29, 119–120.
- Eyéghé-Bickong, H. A., Alexandersson, E. O., Gouws, L. M., Young, P. R., and Vivier, M. A. (2012). Optimisation of an HPLC method for the simultaneous quantification of the major sugars and organic acids in grapevine berries. *J. Chromatogr. B Analyt. Technol. Biomed. Life Sci.* 885–886, 43–49. doi: 10.1016/j.jchromb.2011.12.011
- Fariña, L., Boido, E., Carratu, F., Versini, G., and Dellacassa, E. (2005). Terpene compounds as possible precursors of 1,8-cineole in red grapes and wines. *J. Agric. Food Chem.* 53, 1633–1636. doi: 10.1021/jf040332d
- Favery, J. J., Stec, A., Gruber, H., Rizzini, L., Oravecz, A., Funk, M., et al. (2009). Interaction of COP1 and UVR8 regulates UV-B-induced photomorphogenesis and stress acclimation in *Arabidopsis*. *EMBO J.* 28, 591–601. doi: 10.1038/emboj.2009.4
- García-Plazaola, J. I., Matsubara, S., and Osmond, C. B. (2007). The lutein epoxide cycle in higher plants: its relationships to other xanthophyll cycles and possible functions. *Funct. Plant Biol.* 34, 759–773. doi: 10.1071/FP07095
- Gil, M., Bottini, R., Berli, F., Pontin, M., Silva, M. F., and Piccoli, P. (2013). Volatile organic compounds characterized from grapevine (*Vitis vinifera* L. cv. Malbec) berries increase at pre-harvest and in response to UV-B radiation. *Phytochemistry* 96, 148–157. doi: 10.1016/j.phytochem.2013.08.011
- Gregan, S. M., Wargent, J. J., Liu, L., Shinkle, J., Hofmann, R., Winefield, C., et al. (2012). Effects of solar ultraviolet radiation and canopy manipulation on the biochemical composition of Sauvignon Blanc grapes. *Aust. J. Grape Wine Res.* 18, 227–238. doi: 10.1111/j.1755-0238.2012.00192.x
- Hideg, E., Jansen, M. A. K., and Strid, A. (2013). UV-B exposure, ROS, and stress: inseparable companions or loosely linked associates? *Trends Plant Sci.* 18, 107–115. doi: 10.1016/j.tplants.2012.09.003
- Huyskens-Keil, S., Eichholz, I., Kroh, L. W., and Rohn, S. (2012). UV-B induced changes of phenol composition and antioxidant activity in black currant fruit (*Ribes nigrum* L.). *J. Appl. Bot. Food Qual.* 81, 140–144.
- Johnson, M. P., Havaux, M., Triantaphylidès, C., Ksas, B., Pascal, A. A., Robert, B., et al. (2007). Elevated zeaxanthin bound to oligomeric LHCII enhances the resistance of *Arabidopsis* to photooxidative stress by a lipid-protective, antioxidant mechanism. *J. Biol. Chem.* 282, 22605–22618. doi: 10.1074/jbc.M702831200
- Joshi, P., Nayak, L., Misra, A. N., and Biswal, B. (2013). “Response of mature, developing and senescing chloroplasts to environmental stress,” in *Plastid Development in Leaves during Growth and Senescence*, eds B. Biswal, K. Krupinska, and U. C. Biswal (Amsterdam: Springer), 641–668.
- Juvany, M., Müller, M., and Munné-Bosch, S. (2013). Photo-oxidative stress in emerging and senescing leaves: a mirror image? *J. Exp. Bot.* 64, 3087–3098. doi: 10.1093/jxb/ert174
- Kolb, C. A., Kopecký, J., Riederer, M., and Pfundel, E. E. (2003). UV screening by phenolics in berries of grapevine (*Vitis vinifera*). *Funct. Plant Biol.* 30, 1177–1186. doi: 10.1071/FP03076
- Lashbrooke, J. G., Young, P. R., Strever, A. E., Stander, C., and Vivier, M. A. (2010). The development of a method for the extraction of carotenoids and chlorophylls from grapevine leaves and berries for HPLC profiling. *Aust. J. Grape Wine Res.* 16, 349–360. doi: 10.1111/j.1755-0238.2010.00097.x
- Li, J., Yang, L., Jin, D., Nezames, C. D., Terzaghi, W., and Deng, X. W. (2013). UV-B-induced photomorphogenesis in *Arabidopsis*. *Protein Cell* 4, 485–492. doi: 10.1007/s13238-013-3036-7
- Liu, L., Gregan, S., Winefield, C., and Jordan, B. (2015). From UVR8 to flavonol synthase: UV-B-induced gene expression in Sauvignon blanc grape berry. *Plant Cell Environ.* 38, 905–919. doi: 10.1111/pce.12349
- Loreto, F., and Schnitzler, J. P. (2010). Abiotic stresses and induced BVOCs. *Trends Plant Sci.* 15, 154–166. doi: 10.1016/j.tplants.2009.12.006
- Loreto, F., and Velikova, V. (2001). Isoprene produced by leaves protects the photosynthetic apparatus against ozone damage, quenches ozone products, and reduces lipid peroxidation of cellular membranes. *Plant Physiol.* 127, 1781–1787. doi: 10.1104/pp.010497
- Loreto, F., Pinelli, P., Manes, F., and Kollist, H. (2004). Impact of ozone on monoterpene emissions and evidence for an isoprene-like antioxidant action of monoterpenes emitted by *Quercus ilex* leaves. *Tree Physiol.* 24, 361–367. doi: 10.1093/treephys/24.4.361
- Lund, C. M., Thompson, M. K., Benkwitz, F., Wohler, M. W., Triggs, C. M., Gardner, R., et al. (2009). New Zealand Sauvignon blanc distinct flavor characteristics: sensory, chemical, and consumer aspects. *Am. J. Enol. Vitic.* 60, 1–12.
- Martínez-Lüscher, J., Morales, F., Delrot, S., Sánchez-Díaz, M., Gomés, E., Aguirreolea, J., et al. (2013). Short- and long-term physiological responses of grapevine leaves to UV-B radiation. *Plant Sci.* 213, 114–122. doi: 10.1016/j.plantsci.2013.08.010
- Matus, J. T., Loyola, R., Vega, A., Peña-Neira, A., Bordeu, E., Arce-Johnson, P., et al. (2009). Post-veraison sunlight exposure induces MYB-mediated transcriptional regulation of anthocyanin and flavonol synthesis in berry skins of *Vitis vinifera*. *J. Exp. Bot.* 60, 853–867. doi: 10.1093/jxb/ern336
- Pontin, M. A., Piccoli, P. N., Francisco, R., Bottini, R., Martínez-Zapater, J. M., and Lijavetzky, D. (2010). Transcriptome changes in grapevine (*Vitis vinifera* L.) cv. Malbec leaves induced by ultraviolet-B radiation. *BMC Plant Biol.* 10:224. doi: 10.1186/1471-2229-10-224
- Possell, M., and Loreto, F. (2013). “The role of volatile organic compounds in plant resistance to abiotic stresses: responses and mechanisms,” in *Biology Controls*

- and Models of Tree Volatile Organic Compound emissions*, eds Ü. Niinemets and R. K. Monson (Amsterdam: Springer), 209–235.
- Ramel, F., Birtic, S., Ginies, C., Soubigou-Taconnat, L., Trianaphylides, C., and Havaux, M. (2012). Carotenoid oxidation products are stress signals that mediate gene responses to singlet oxygen in plants. *Proc. Natl. Acad. Sci. U.S.A.* 109, 5535–55 doi: 10.1073/pnas.1115982109
- Schultz, H. R., Löhneritz, O., Bettner, W., Balo, B., Linsenmeier, A., Jähnisch, A., et al. (1998). Is grape composition affected by current levels of UV-B radiation? *VITIS-J. Grapevine Res.* 37, 191–192.
- Song, J., Smart, R., Wang, H., Dambergs, B., Sparrow, A., and Qian, M. C. (2015). Effect of grape bunch sunlight exposure and UV radiation on phenolics and volatile composition of *Vitis vinifera* L. cv. Pinot noir wine. *Food Chem.* 173, 424–431. doi: 10.1016/j.foodchem.2014.09.150
- Steel, C. C., and Keller, M. (2000). Influence of UV-B irradiation on the carotenoid content of *Vitis vinifera* tissues. *Biochem. Soc. Trans.* 28, 883–885. doi: 10.1042/bst0280883
- Tardaguila, J., de Toda, F. M., Poni, S., and Diago, M. P. (2010). Impact of early leaf removal on yield and fruit and wine composition of *Vitis vinifera* L. Graciano and Carignan. *Am. J. Enol. Vitic.* 61, 372–381.
- Thayer, S. S., and Björkman, O. (1990). Leaf xanthophyll content and composition in sun and shade determined by HPLC. *Photosyn. Res.* 23, 331–343. doi: 10.1007/BF00034864
- Tian, B., Harrison, R., Jaspers, M., and Morton, J. (2015). Influence of ultraviolet exclusion and of powdery mildew infection on Sauvignon Blanc grape composition and on extraction of pathogenesis-related proteins into juice. *Aust. J. Grape Wine Res.* 21, 417–424. doi: 10.1111/ajgw.12135
- Tilbrook, K., Arongaus, A. B., Binkert, M., Heijde, M., Yin, R., and Ulm, R. (2013). The UVR8 UV-B photoreceptor: perception, signaling and response. *Arabidopsis Book* 11:e0164. doi: 10.1199/tab.0164
- Ubi, B. E., Honda, C., Bessho, H., Kondo, S., Wada, M., Kobayashi, S., et al. (2006). Expression analysis of anthocyanin biosynthetic genes in apple skin: effect of UV-B and temperature. *Plant Sci.* 170, 571–578. doi: 10.1016/j.plantsci.2005.10.009
- Vogelmann, T. C., and Gorton, H. L. (2014). “Leaf: light capture in the photosynthetic organ,” in *The Structural Basis of Biological Energy Generation*, ed. M. F. Hohmann-Marriott (Amsterdam: Springer), 363–377.
- Walters, R. G., and Horton, P. (1994). Acclimation of *Arabidopsis thaliana* to the light environment: changes in composition of the photosynthetic apparatus. *Planta* 195, 248–256. doi: 10.1007/BF00199685
- Young, P., Eyeghe-Bickong, H. A., du Plessis, K., Alexandersson, E., Jacobson, D. A., Coetzee, Z. A., et al. (2016). Grapevine plasticity in response to an altered microclimate: sauvignon Blanc modulates specific metabolites in response to increased berry exposure. *Plant Physiol.* 170, 1235–1254.
- Zhang, H., Fan, P., Liu, C., Wu, B., Li, S., and Liang, Z. (2014). Sunlight exclusion from Muscat grape alters volatile profiles during berry development. *Food Chem.* 164, 242–250. doi: 10.1016/j.foodchem.2014.05.012

Conflict of Interest Statement: The authors declare that the research was conducted in the absence of any commercial or financial relationships that could be construed as a potential conflict of interest.

Copyright © 2016 Joubert, Young, Eyéghé-Bickong and Vivier. This is an open-access article distributed under the terms of the Creative Commons Attribution License (CC BY). The use, distribution or reproduction in other forums is permitted, provided the original author(s) or licensor are credited and that the original publication in this journal is cited, in accordance with accepted academic practice. No use, distribution or reproduction is permitted which does not comply with these terms.



OPEN ACCESS

Edited by:

Laurent Deluc,
Oregon State University, USA

Reviewed by:

Serge Delrot,
University of Bordeaux, France

Christopher Davies,

Commonwealth Scientific and
Industrial Research Organisation,

Australia

***Correspondence:**

Claudio Bonghi
claudio.bonghi@unipd.it

†Present Address:

Massimiliano Corso,
Laboratoire de Physiologie et de
Génétique Moléculaire des Plantes,
Campus de la Plaine - Université Libre
de Bruxelles, Brussels, Belgium

Specialty section:

This article was submitted to
Plant Physiology,
a section of the journal
Frontiers in Plant Science

Received: 24 September 2015

Accepted: 15 January 2016

Published: 09 February 2016

Citation:

Corso M, Vannozzi A, Ziliotto F, Zouine M, Maza E, Nicolato T, Vitulo N, Meggio F, Valle G, Bouzayen M, Müller M, Munné-Bosch S, Lucchin M and Bonghi C (2016) Grapevine Rootstocks Differentially Affect the Rate of Ripening and Modulate Auxin-Related Genes in Cabernet Sauvignon Berries. *Front. Plant Sci.* 7:69. doi: 10.3389/fpls.2016.00069

Grapevine Rootstocks Differentially Affect the Rate of Ripening and Modulate Auxin-Related Genes in Cabernet Sauvignon Berries

Massimiliano Corso^{1,2†}, **Alessandro Vannozzi**^{1,2}, **Fiorenza Ziliotto**¹, **Mohamed Zouine**³, **Elie Maza**³, **Tommaso Nicolato**¹, **Nicola Vitulo**⁴, **Franco Meggio**^{1,2}, **Giorgio Valle**⁴, **Mondher Bouzayen**³, **Maren Müller**⁵, **Sergi Munné-Bosch**⁵, **Margherita Lucchin**^{1,2} and **Claudio Bonghi**^{1,2*}

¹ Department of Agronomy, Food, Natural resources, Animals and Environment, University of Padova Agripolis, Legnaro, Italy

² Centro Interdipartimentale per la Ricerca in Viticoltura e Enologia, University of Padova, Conegliano, Italy, ³ Genomics and

Biotechnology of Fruit Laboratory, Institut National Polytechnique de Toulouse, Toulouse, France, ⁴ Centro di Ricerca

Interdipartimentale per le Biotecnologie Innovative, University of Padova, Padova, Italy, ⁵ Department of Vegetal Biology,

University of Barcelona, Barcelona, Spain

In modern viticulture, grafting commercial grapevine varieties on interspecific rootstocks is a common practice required for conferring resistance to many biotic and abiotic stresses. Nevertheless, the use of rootstocks to gain these essential traits is also known to impact grape berry development and quality, although the underlying mechanisms are still poorly understood. In grape berries, the onset of ripening (véraison) is regulated by a complex network of mobile signals including hormones such as auxins, ethylene, abscisic acid, and brassinosteroids. Recently, a new rootstock, designated M4, was selected based on its enhanced tolerance to water stress and medium vigor. This study investigates the effect of M4 on Cabernet Sauvignon (CS) berry development in comparison to the commercial 1103P rootstock. Physical and biochemical parameters showed that the ripening rate of CS berries is faster when grafted onto M4. A multifactorial analysis performed on mRNA-Seq data obtained from skin and pulp of berries grown in both graft combinations revealed that genes controlling auxin action (*ARF* and *Aux/IAA*) represent one of main categories affected by the rootstock genotype. Considering that the level of auxin tightly regulates the transcription of these genes, we investigated the behavior of the main gene families involved in auxin biosynthesis and conjugation. Molecular and biochemical analyses confirmed a link between the rate of berry development and the modulation of auxin metabolism. Moreover, the data indicate that this phenomenon appears to be particularly pronounced in skin tissue in comparison to the flesh.

Keywords: fruit development, polyphenols biosynthesis, auxin conjugation, transcriptional program, grapevine

INTRODUCTION

In Europe, *Vitis vinifera* varieties are grown as scion grafted onto a rootstock. At first, grafting was adopted with the aim of preventing devastation to European viticulture by Phylloxera. This gradually imposed the use of rootstocks as general practice and the development of new rootstock genotypes became an important issue in modern viticulture (Whiting, 2004). The use of rootstocks was proved to be beneficial in terms of adaptation to different soil types and to biotic (e.g., soil borne pests) and abiotic (e.g., salinity, water or oxygen deficit) factors (Marguerit et al., 2012; Tramontini et al., 2013; Corso et al., 2015). Rootstocks can also be used to confer other advantages affecting physiological processes at the scion level, such as biomass accumulation, quality yields, vine vigor, and grape berry quality (Walker et al., 2000; Gregory et al., 2013; Berdeja et al., 2015). The beneficial effects of rootstocks on stress resistance and vegetative growth represent an extremely important issue in viticulture, but their effect on grape development rates and on berry quality also warrants investigation. Although it is widely known that the rootstock influences grapevine reproductive performance and berry development (Kidman et al., 2013), studies specifically addressing the relationship between a given graft combination and the berry ripening evolution are still lacking.

Grape berry development exhibits a double-sigmoid pattern characterized by two phases of rapid growth separated by a lag phase during which little or no growth occurs (Coombe and McCarthy, 2000). Several hormones participate in the control of grape berry development and ripening, such as auxin (IAA), ethylene, abscisic acid (ABA), gibberellins (GAs), cytokinins (CKs), and brassinosteroids (BRs) (Davies and Böttcher, 2009). The early stages of berry development, from fertilization to fruit set, are mainly driven by IAA, CKs, and GAs to promote cell division and cell expansion. Although these hormones have a pivotal role in berry development, they are mostly produced by the seeds (Giribaldi et al., 2010). Thereafter, the changes occurring from pre-véraison to full ripening are associated with sequential increases in ethylene, brassinosteroids, and ABA content (Kuhn et al., 2013). Exogenous applications of hormones positively modulate many ripening-related processes such as anthocyanin accumulation and the uptake/storage of sugars in berries, via the re-programming of gene expression (Chervin et al., 2008; Giribaldi et al., 2010; Böttcher et al., 2011; Ziliotto et al., 2012). In particular, exogenous application of auxin and its analogs at pre-véraison stage causes a shift in ripening and a repression of several ripening-related genes (Davies et al., 1997; Böttcher et al., 2011; Ziliotto et al., 2012). Based on these observations it has been postulated that a decrease in IAA content is necessary to trigger the onset of ripening (Deluc et al., 2007; Ziliotto et al., 2012). This hypothesis has been confirmed by the observation that berries with a slow ripening progression have a high seed-to-berry weight ratio associated with high auxin and low ABA content (Gouthu and Deluc, 2015). Böttcher et al. (2010) speculated that in grapevine, the auxin decrease and maintenance of low IAA active forms may be due to their conjugation with amino acids, mediated by the auxin-responsive Gretchen Hagen 3 (GH3) proteins. However, to

further understanding into the role of auxin in fruit development and ripening it is necessary to consider not only the hormone concentration but also the downstream signaling events. Auxin signaling is initiated through binding of the hormone to the Transport Inhibitor Response1/Auxin Signaling F-Box protein (TIR1/AFB) and Auxin/Indole Acetic Acid (Aux/IAA) protein co-receptors, which results in the targeting of Aux/IAA proteins for degradation. The degradation of Aux/IAA proteins allows the release of Auxin Response Factors (ARF), the transcription factors that regulate the expression of auxin-responsive genes. The expression of Aux/IAAs and ARFs during fruit development and ripening has been extensively studied in many species (Pattison et al., 2014) and in particular in those bearing fleshy fruits (Audran-Delalande et al., 2012; Zouine et al., 2014), although to a lesser extent in grapevine (Çakir et al., 2013; Wan et al., 2014).

Recently, it was demonstrated that grafting the same scion on different rootstock induces extensive transcriptional re-programming in the shoot apex and in berries, particularly for genes involved in hormone signaling (Cookson and Ollat, 2013; Berdeja et al., 2015). This observation is in agreement with the hypothesis for a role of rootstock in the control of scion growth and reproductive activity by the modulation of hormone signaling pathways (Gregory et al., 2013). In order to clarify this aspect, we conducted a physical, biochemical, and transcriptional analysis on berries obtained from *V. vinifera* cv Cabernet Sauvignon (CS) plants grafted onto M4, a rootstock characterized by high tolerance to stress and medium vigor (Meggio et al., 2014), and 1103 Paulsen (1103P), a vigorous commercial rootstock. Data indicated that the ripening rate in berries of CS grafted onto M4 (CS/M4) was faster than those grown on CS/1103P combination. To investigate the relationship existing between the rootstock and the ripening rate in both the graft combinations, we analyzed the berry transcriptome during development and ripening by mean of mRNA-Seq analysis. Molecular analyses indicated that grafting the same variety (CS) on different rootstocks (1103P and M4) alters the expression of several genes, including those belonging to the main multigenic families involved in auxin biosynthesis, conjugation, and action and, consequently, the auxin levels in skin and flesh. A possible consequence of this alteration is a change in the berry ripening rate. This phenomenon was more pronounced in the berry skin in comparison to the flesh.

MATERIALS AND METHODS

Plant Material, Experimental Design and Meteorological Data

Sampling was performed in 2011 and 2012 on *V. vinifera* cv Cabernet Sauvignon plants grafted onto 1103P (*V. berlandieri* × *V. rupestris*) and M4 [(*V. vinifera* × *V. berlandieri*) × *V. berlandieri* × cv Ressegquier n.1] rootstocks located in Verona, Italy (Novaglie, 45°28'42.4"N, 11°02'40.4"E; Pasqua vigneti e cantine) and grown from 2003 in open field on a clay-calcareous soil. All vines were of the same age and were grafted in 2002. The two graft combinations were growth

in adjacent rows, with north–south orientation. Meteorological data, were registered from the meteorological station of Grezzana ($45^{\circ} 30' 35.22''$ N, $11^{\circ} 00' 48.54''$ E, 156 m a. s. l.) and collected by the Regional Agency for the Environmental Protection of Veneto (ARPAV), Italy. The dataset consisted of meteorological time series from January 1992 to December 2012, a series of 20 years that enabled climatological study to be performed. Meteorological data used for the purposes of the study consisted of precipitations (mm) and air temperature ($^{\circ}$ C) measured at 2 m.

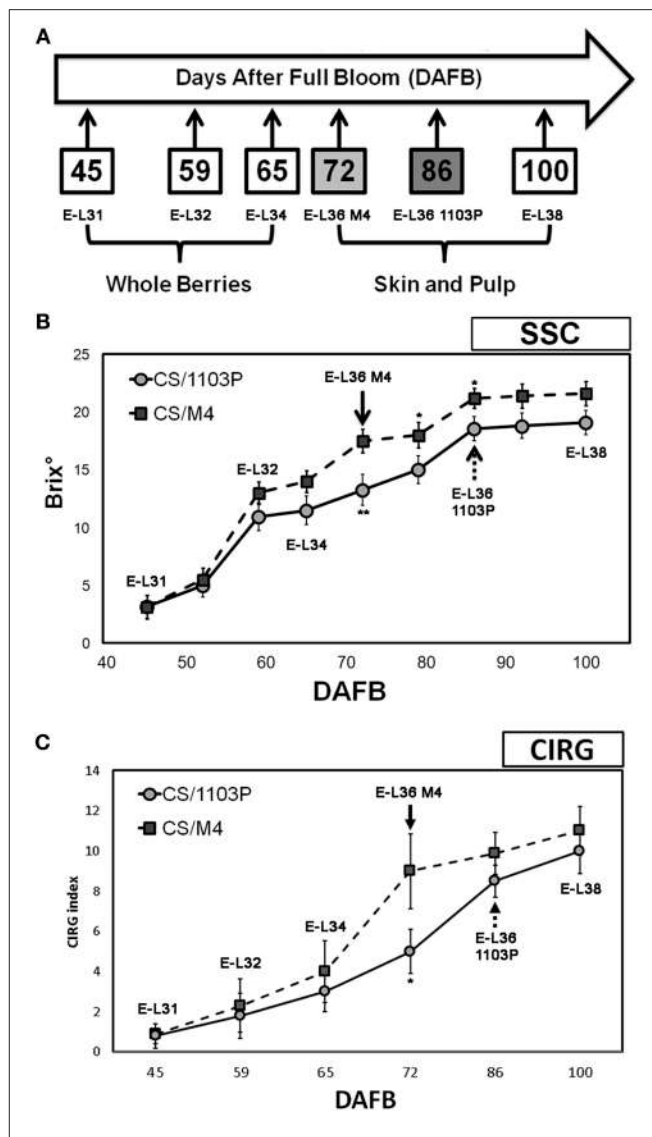
During both the growing seasons (2011 and 2012), berries grown on CS/1103P and CS/M4 graft combinations were sampled at five developmental stages following the modified Eichhorn and Lorenz (E-L) developmental scale proposed by Coombe (1995).

The evolution of berry development and ripening on both graft combinations was monitored by measuring the sugar content and the skin pigmentation. Total Soluble Solids and colorimetric analysis were determined in 100 berries collected from 10 different plants (one bunch per plant) for each time point and graft combination considered in the experiment. Color analyses were carried out with a CR-10 colorimeter (Konica-Minolta Holdings Inc., Tokyo, Japan) based on the $L^*a^*b^*$ space, the defining brightness (L^* , from white to black), and the chromatic coordinates (a^* , from red to green; b^* , from yellow to blue). Other parameters, such as hue angle (h), chroma (C), and Color Index for red Grapes (CIRG) were also calculated according to Carreño et al. (1995). At pre-véraison stages (E-L31, E-L32, and E-L34) the whole berries were considered, whereas at E-L36 and E-L38 stages, skin and pulp were sampled separately (Figure 1A).

Samplings at E-L36 stage were performed at 72 DAFB (Days After Full Bloom) for CS/M4 and 86 DAFB for CS/1103P when berries showed similar sugar content and skin color, whereas samplings at E-L31, E-L32, E-L34, and E-L38 corresponded to similar date in the two graft combinations and precisely to 45, 59, 65, and 100 DAFB (Figure 1A). In 2012 berries were collected at the same E-L stages considered in 2011. Two biological replicates, sampled in 2011, were used for mRNA-Seq, while three biological replicates, sampled in 2012, were considered for quantitative RT-PCR (qRT-PCR). Each replicate was composed of 100 berries sampled from 50 different bunches (two berries collected from the median position of each cluster) according to the CIRG.

RNA-Seq and Quantitative RT-PCR Analyses

Total RNA for transcriptome sequencing was extracted from samples collected at E-L31, E-L36, and E-L38 using the perchlorate method as reported by Ziliotto et al. (2012). Poly (A) mRNA was purified from total RNA using the Dynabeads “mRNA direct kit” (Invitrogen pn 610.12). Samples for Ligation Sequencing were prepared according to the SOLiD Whole transcriptome library preparation protocol (pn 4452437 Rev. B). Reads were aligned to the reference grape genome using PASS aligner (Campagna et al., 2009). The percentage identity was set to 90% with one gap allowed whereas the quality filtering parameters were set automatically by PASS. Moreover,



a minimum reads length cut-off of 50 and 30 nt was set for the forward sequences and reverse reads, respectively. The spliced reads were identified using the procedure described in PASS manual (<http://pass.cribi.unipd.it>). Forward and reverse reads were aligned independently on the reference genome. PASS-pair was used from the PASS package to perform the pairing between forward and reverse reads and to select only those sequences that are uniquely aligned. The version 1 (V1) of grape gene prediction (<http://genomes.cribi.unipd.it/grape>) was used as a reference genome, whereas htseq-counts program (<http://www-huber>.

embl.de/users/anders/HTSeq/doc/count.html) was adopted to quantify gene transcripts abundance. Gene expression data have been submitted to Gene Expression Omnibus (GEO) (accession no. SRA110619) at the NCBI (<https://www.ncbi.nlm.nih.gov/geo/>). Quantitative RT-PCRs (qPCR) were performed as described in Ziliotto et al. (2012). Gene specific primers are listed in **Supplementary Table S1**.

Statistical and Bioinformatics Analysis

DEseq R package (<http://www.r-project.org>) was used to perform the statistical analyses for discovering differentially expressed genes (DEGs). In order to evaluate the single effects of the rootstock (R: 1103P and M4), tissue (T: whole berries, skin and pulp), and phenological phase (PP: E-L31, pre-véraison; E-L36, mid/late véraison; E-L38, ripening) on gene expression, a multifactorial analysis was conducted using the multi-factor designs method of *DEseq* (Anders and Huber, 2010) (<http://bioconductor.org/packages/release/bioc/html/DESeq.html>). This method evaluates the weight of each factor considered in the analysis (R, T, and P) and its impact on DEGs, according to a false discovery rate (FDR) corrected *p*-value lower than 0.05. Enrichment analysis was performed for each set of DEGs (R, T, and P) by using BiNGO tool (Maere et al., 2005) with the built-in Fisher's exact test function and an FDR corrected *p*-value lower than 0.05. Hierarchical clustering analysis on mRNA-Seq data was carried out using Multi Experiment Viewer software (MeV; <http://www.tm4.org>; Saeed et al., 2006). Expression values used for the analysis were filtered based on the 5% of their median. Principal Component Analysis (PCA) and related graphs were carried out using “prcomp” and “scatterplot3d” R packages, respectively.

LC-ESI-MS/MS Analysis of IAA and IAA-Asp in CS/M4 and CS/1103P Berries

The samples processed for the mRNA-Seq analysis at E-L31, E-L36, and E-L38, together with those collected at E-L32 and E-L34, were also used for LC-MS/MS quantification. IAA and IAA-Asp were extracted and quantified from 100 mg of tissue as described by Müller and Munné-Bosch (2011) with some modifications. Sample tissue was spiked with [²H₅]IAA and [²H₅]IAA-Asp as internal standards and then extracted with 0.2 ml methanol, isopropanol, and glacial acetic acid (20:79:1, v/v/v) using ultra sonication (4–7°C). After centrifugation (14,000 × g for 15 min at 4°C), the supernatant was collected and the pellet re-extracted with 0.2 ml of extraction solvent. Then, the supernatants were combined, centrifuged (14,000 × g for 5 min at 4°C) and filtered through a 0.22 μm PTFE filter to be analyzed with an UPLC/ESI-MS/MS system. The LC system consisted of an Aquity UPLCTM System (Waters, Milford, MA USA) and samples (5 μl) were first separated on a C18 Kinetex column (50 × 2.1 mm, 1.7 μm; Phenomenex, Macclesfield, UK) using the following solvent conditions: 0–4 min linear gradient from 99% of solvent A to 1%, held for 0.2 min, from 1% of solvent A to 99% in 0.2 min and held for 0.6 min. Gradient solvents consisted of water and 0.05% glacial acetic acid (solvent A) and acetronitrile with 0.05% glacial acetic acid (solvent B). MS/MS experiments and detection were performed on an API 3000

triple quadruple mass spectrometer (PE Sciex, Concord, Ont., Canada) by multiple reactions monitoring (MRM) in negative ion mode. The optimized MS/MS conditions were determined in infusion experiments using purified IAA and IAA-Asp and their isotopically labeled internal standards. MRM transitions were 174/130 for IAA and 179/135 for [²H₅]IAA with the collision energy (CE) of –15 eV and collision cell exit potential (CXP) of –15 eV. MRM transition of IAA-Asp was 289/88 and 294/89 for [²H₅] IAA-Asp with CE of –36 eV and CXP of –15 eV. IAA and IAA-Asp quantification were performed by a ten-point calibration curve including [²H₅]IAA and [²H₅]IAA-Asp as internal standards using Analyst™ software (PE Sciex, Concord, Ont., Canada). The data were subjected to a Duncan's multiple-range test, performed using “agricolae” R package.

RESULTS

Biochemical and Colorimetric Analyses Showed Different Berry Ripening Evolution in CS/M4 and CS/1103P Graft Combinations

Berries grown on CS/1103P and CS/M4 graft combinations were sampled at five developmental stages following the modified Eichhorn and Lorenz developmental scale proposed by Coombe (1995). The criteria used for evaluating the evolution of grape development and ripening were the measurement of sugar content (SSC) and the CIRG values (**Figure 1**). Developmental stages considered in the study were defined as follows: (a) E-L 31: small hard green berries accumulating organic acids; (b) E-L 32: beginning of bunch closure, berries tight at touch; (c) E-L 34: stage immediately preceding véraison (onset of ripening) characterized by green berries; E-L 36: sugar (15–18°Brix) and anthocyanins accumulation and active growth due to cell enlargement (mid/late véraison) (Fortes et al., 2011) and E-L 38: harvest time. Biochemical and physical measurements performed on berries during 2011 growing season indicated different rate of berry development (**Figure 1**). The pre-véraison stages (E-L31-34) were reached almost simultaneously by berries grown in both graft combinations, as indicated by the similar evolution of SSC and CIRG (**Figures 1B,C**), while the ripening rate was different. In fact, the SSC (17.1°Brix ± 1.5) and CIRG (8.2 ± 2.1) values showed by CS/M4 berries at 72 DAFB (E-L36) were reached by CS/1103P berries at 86 DAFB. At harvest (E-L38) berries from both graft combinations had similar SSC values suggesting a recovery of the CS/1103P combination respect to CS/M4. Similar results were obtained by analysing the skin color evolution. Based on CIRG index values, the pigmentation of berry skin in CS/1103P displayed a 14-days delay compared to CS/M4, while at harvest (E-L38) berries from both graft combinations reached the same CIRG value, confirming a recovery from CS/1103P (**Figure 1C, Supplementary Figure S1**). The different evolution of berry development and ripening in CS/1103P and CS/M4 berries was observed also in 2012 (**Supplementary Figure S2**), although the two growing seasons were characterized by significant differences in temperature excursions as described in **Supplementary Data S1**.

Whole Transcriptome Analysis Revealed that M4 and 1103P Differently Modulate the Expression of Auxin-Related Genes in CS Berries

In order to confirm from a molecular point of view the delay observed in ripening rate between the two graft combinations, we performed a comparative mRNA-Seq transcriptome profiling on CS/M4 and CS/1103P berries collected at E-L31, E-L36, and E-L38. Approximately 2 billion paired-end reads (75 and 35 bp length for forward and reverse reads, respectively) were produced, with a total number of reads for each sample ranging from 36 to 65 million and a median of 52 million reads (**Supplementary Table S2**). On average, 91% of the reads passed the quality control test (filter based on read length after trimming the low quality bases) and were mapped to the PN40024 12X V1 grape reference genome (Jaillon et al., 2007; <http://genomes.cribi.unipd.it/grape>), producing approximately 20–42 million unique mapping reads depending on the sample considered. The rate of read mapping on known genes was on average 87% and the number of predicted genes covered at least by five independent reads was approximately 63% (**Supplementary Table S2**). A PCA performed on mRNA-Seq counts normalized and filtered ($n > 10$) confirmed that both in skin and flesh the transcriptome of CS/1103P and CS/M4 berries collected at E-L31 and E-L38 clustered together, as well as those of berries sampled at E-L36, although sampled at different DAFB (**Figure 2**).

A multifactorial statistical analysis on mRNA-Seq data was performed to identify those genes whose expression is influenced by the effects of three factors: the rootstock (R, M4, or 1103P); the tissue type (T, whole berry, skin, or pulp) and the phenological phase (PP, E-L31, E-L36, or E-L38), on the transcriptome responses. The singular (R, T, P) impact of each component on genes expression was calculated according to a FDR corrected *p*-value lower than 0.05. A complete list of DEGs whose expression is influenced by these factors is reported in **Supplementary Table S3**, while **Figure 3** provides a graphical representation of the total amount of DEGs influenced by each single component. Amongst these, 2358 genes were differentially expressed due to different rootstocks. Expanding the comparison to include different tissue types revealed 4297 genes showed differential expression. The majority of DEGs were influenced by the phenological phase, with 5743 transcripts showing altered expression. In order to identify specific metabolic pathways differentially regulated by M4 and 1103P rootstocks in CS berries, DEGs resulting from multifactorial analysis were associated to their respective GO terms, and a GO enrichment analysis was carried out for each dataset (**Figure 3** and **Supplementary Table S4**). Enriched GO terms associated with metabolic and physiological processes (i.e., photosynthesis, carbohydrate metabolism, aromatic compound metabolism, and phenylpropanoid metabolism) were identified amongst those DEGs affected by either single or combined factors, whereas GO terms related to regulatory mechanisms such as hormone metabolism and action were overrepresented only in those DEGs influenced by a single factor. Amongst these we considered of particular interest were the categories related to response to

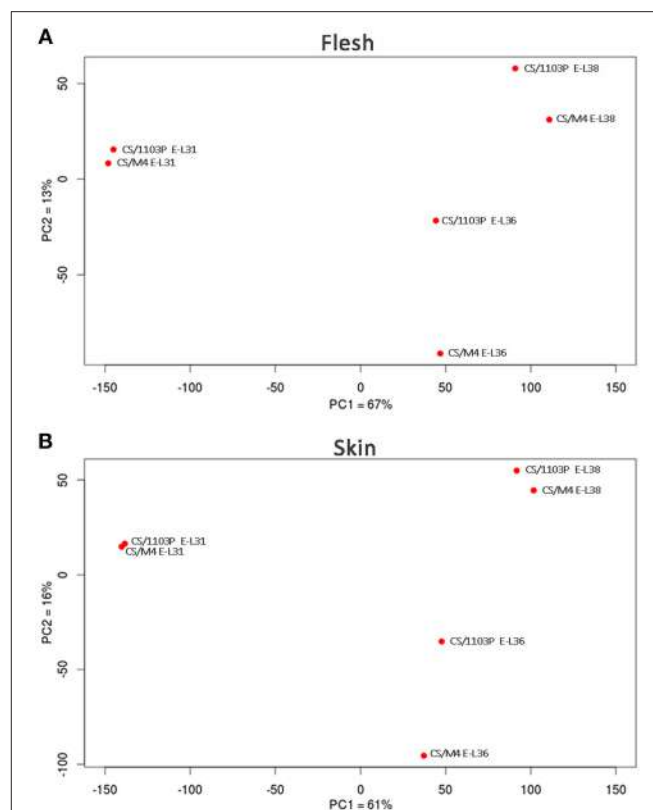


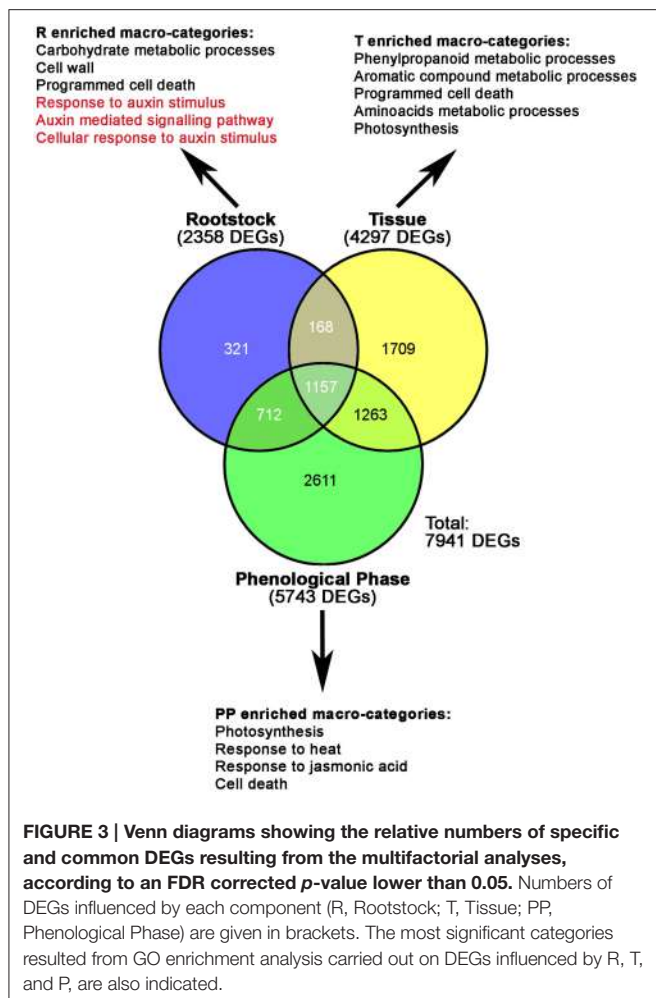
FIGURE 2 | Bidimensional PCA plot of row transcriptome data.

Cabernet Sauvignon (CS) grafted onto 1103P (CS/1103P) and M4 (CS/M4) samples distribution according to PC1 and PC2. Two separate PCAs were carried out for flesh (A) and skin (B) mRNA-seq data. Percent of variance is also reported for each component on the corresponding axes.

auxin stimulus (GO: 9733), auxin mediated signaling pathway (GO: 9734), and cellular response to auxin stimulus (GO: 71365), not only because of the role of this hormone in grape berry development, but also because the expression of genes belonging to these categories was affected exclusively by the rootstock (**Figure 3** and **Supplementary Table S4**).

A large number of genes belonging to these auxin-related GO categories were found to encode for Auxin/Indole-3-Acetic Acid (Aux/IAA) and the Auxin Response (ARF) transcription factors, representing two key families of auxin-response regulators (**Supplementary Tables S4, S5**). Recently, Çakir et al. (2013) and Wan et al. (2014) performed a genomic characterization of both the ARF and Aux/IAA gene families in grapevine. In the current study we proposed and used a new classification of both gene families (together with the GH3), based on the grapevine gene nomenclature system developed by Grimpel et al. (2014), as illustrated in **Supplementary Results S1**.

Based on the notion that Aux/IAA and ARF TFs interact with each other to finely regulate the auxin-signaling pathway, we considered genes belonging to these families together. **Figure 4A** shows the expression and hierarchical clustering of a subgroup of Aux/IAA and ARF members, excluding those genes scarcely represented by mRNA-Seq reads, in order to avoid



misinterpretation of results due to their contribution. Based on their expression profile, genes were divided into five clusters. The majority of the *Aux/IAA* and *ARF* genes were found in Cl.1 and 3. Most of the genes belonging to Cl.3 cluster, and specifically those found in the Cl3-II subgroup, were expressed exclusively at pre-véraison stage. This included both *Aux/IAAs* (*VviIAA15b*, -38, and -39) and *ARFs* (*VviARF6*, -6b, 16, 24, -25, -26, and 27) members. Although these genes showed a similar behavior in both genotypes, the induction observed in berries collected from CS/M4 was markedly higher than that observed in berries collected from CS/1103P. That was particularly true for *VviIAA15b*, *VviARF16b*, *VviARF25* and *VviARF27*. Only *VviIAA36* and *VviIAA40*, although belonging to Cl.3-I, were also expressed at E-L36, both in skin and pulp tissues. Similar to what was observed for members belonging to cluster Cl.3-II, the induction observed in CS/M4 berries was much higher compared to what observed in CS/1103P. The fact that *Aux/IAA* and *ARF* are known to physically interact to regulate the auxin signaling pathway and that *Aux/IAA* and *ARF* genes belonging to the Cl.3 cluster were strictly correlated in term of expression raises some questions about the possible interactions amongst them.

The opposite pattern was observed for members belonging to cluster Cl.1, mainly expressed in flesh and at those developmental stages following véraison. Genes belonging to cluster Cl.1-I were induced exclusively in the pulp of berries at ripening phase (apart from *VviIAA15a* and -44 which were induced only in the pulp of CS/M4 berries at E-L36), whereas genes belonging to cluster Cl.1-II were induced at E-L36 and E-L38.

Less clear was the behavior of genes belonging to clusters Cl.2, Cl.4, and Cl.5, although the latter appeared to be composed of genes preferentially expressed at pre-véraison and ripening stages in pulp. Biochemical and colorimetric data showed that the differences in the rate of berry development between the two graft combinations were limited to the onset of ripening. For this reason we focused our attention on those *Aux/IAA* and *ARF* genes belonging to cluster Cl.3-II, characterized by a higher expression at pre-véraison stages and whose differential behavior could be associated to the different ripening rate observed in the two graft combinations. In order to validate and expand results obtained from the mRNA-Seq data, we performed a quantitative RT-PCRs on *VviIAA15b* and *VviARF25*, representing those Cl.3-II members showing the highest difference in fold change between CS/1103P and CS/M4, at E-L31, 32, 34, 36, and 38. Both genes were showing the highest expression in CS/M4 at the pre-véraison stages (E-L31 and E-L32) (Supplementary Figure S3). In 2012, the expression profile of *VviARF25* and *VviIAA15b* was confirmed. This result reinforces the hypothesis for a role in the transition from the immature to mature fruit development stage.

CS/1103P and CS/M4 Berries Show a Shift in Auxin Homeostasis during Ripening

The positive relationship between auxin level and *Aux/IAA* transcription has been well documented (Zenser et al., 2001). Based on this observation, to investigate whether the differences observed in the expression of *ARF* and *Aux/IAA* genes in CS/M4 and CS/1103P berries were associated to differences in auxin homeostasis, we measured the level of free and conjugated IAA in berry samples collected in 2011. The level of free (IAA) and conjugated (IAA-Asp) auxin is shown in Figure 5. In berry flesh, no significant differences in IAA and IAA-Asp content were found between the two graft combinations. In comparison, at the skin level, their accumulation appeared to follow different kinetics. Indeed, M4 induced a significantly higher accumulation of free auxin at 65 (E-L34) and 72 (E-L36 M4) DABF, compared to that detected in CS/1103P berries. Later on, the two graft combinations showed similar level of IAA. As for IAA-Asp, CS/M4 showed a quantity two-fold higher than 1103P at E-L34 stage. During véraison CS/1103P berries appeared to accumulate more IAA-Asp than CS/M4 while at harvest no significant differences were observed.

The relative mRNA-Seq expression of genes involved in auxin biosynthesis and conjugation is graphically represented in Figures 6A,7A, regardless whether they were or not included amongst those DEGs obtained by the multifactorial analysis. Considering genes involved in auxin biosynthesis, the hierarchical clustering on mRNA-Seq data split auxin-biosynthetic genes into two sub-groups (Figure 6A). In this regard, considered genes can be divided into early-expressed

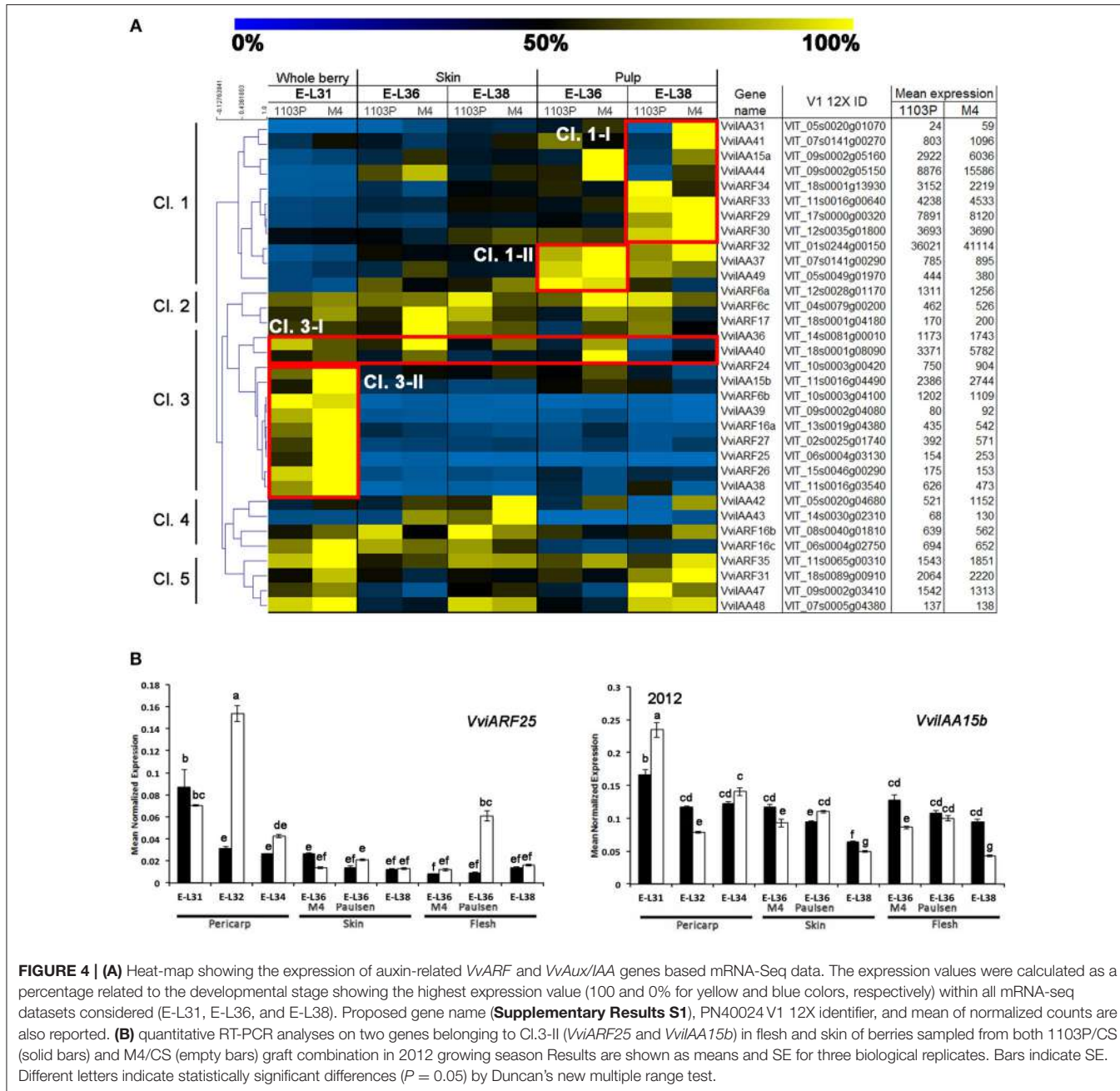


FIGURE 4 | (A) Heat-map showing the expression of auxin-related *VvARF* and *VvAux/IAA* genes based mRNA-Seq data. The expression values were calculated as a percentage related to the developmental stage showing the highest expression value (100% for yellow and 0% for blue colors, respectively) within all mRNA-seq datasets considered (E-L31, E-L36, and E-L38). Proposed gene name (**Supplementary Results S1**), PN40024 V1 12X identifier, and mean of normalized counts are also reported. **(B)** quantitative RT-PCR analyses on two genes belonging to Cl.3-II (*VviARF25* and *VviAA15b*) in flesh and skin of berries sampled from both 1103P/CS (solid bars) and M4/CS (empty bars) graft combination in 2012 growing season. Results are shown as means and SE for three biological replicates. Bars indicate SE. Different letters indicate statistically significant differences ($P = 0.05$) by Duncan's new multiple range test.

(E-L31, Cl.2) in whole berries and late-expressed (E-L36 and E-L38, Cl.1) in skin. Considering their high mRNA-Seq expression (**Figure 6A**), *VviYUC1* (Cl. 1) and *VviTAR4* (Cl. 2) were selected for qRT-PCRs (**Figure 6B**). Both in 2011 (**Supplementary Figure S3**) and 2012, (**Figure 6B**), the expression profile of *VviTAR-4* and *VviYUC1* genes was assessed. *VviTAR-4* was found to be more highly expressed at pre-véraison stages in CS/M4 than in CS/1103P, while *VviYUC1* transcripts were more highly accumulated at E-L36 in CS/M4 and at E-L38 in CS/1103P.

A closer relationship was observed between IAA-Asp and GH3 transcript levels (**Figures 5,7A,B**). Hierarchical

cluster analysis (**Figure 7A**) led to the identification of three main subgroups. Amongst them, Cl. 3 represented the most interesting one, being characterized by the presence of genes such as *VviGH3-9*, *VviGH3-24*, and *VviGH3-22*, which were strongly expressed at pre-véraison stage in CS/M4 but not in CS/1103P. The behavior of one of these genes (*VviGH3-22*) was also confirmed by qPCR in 2011 (**Supplementary Figure S3**) and 2012 (**Figure 7B**). Less obvious was the expression of genes belonging to other clusters. We also considered the expression pattern of *VviGH3-21*, which, based on mRNA-Seq data (**Figure 7A**) appeared to be highly expressed in skin tissue of CS/1103P at E-L38. Quantitative RT-PCR

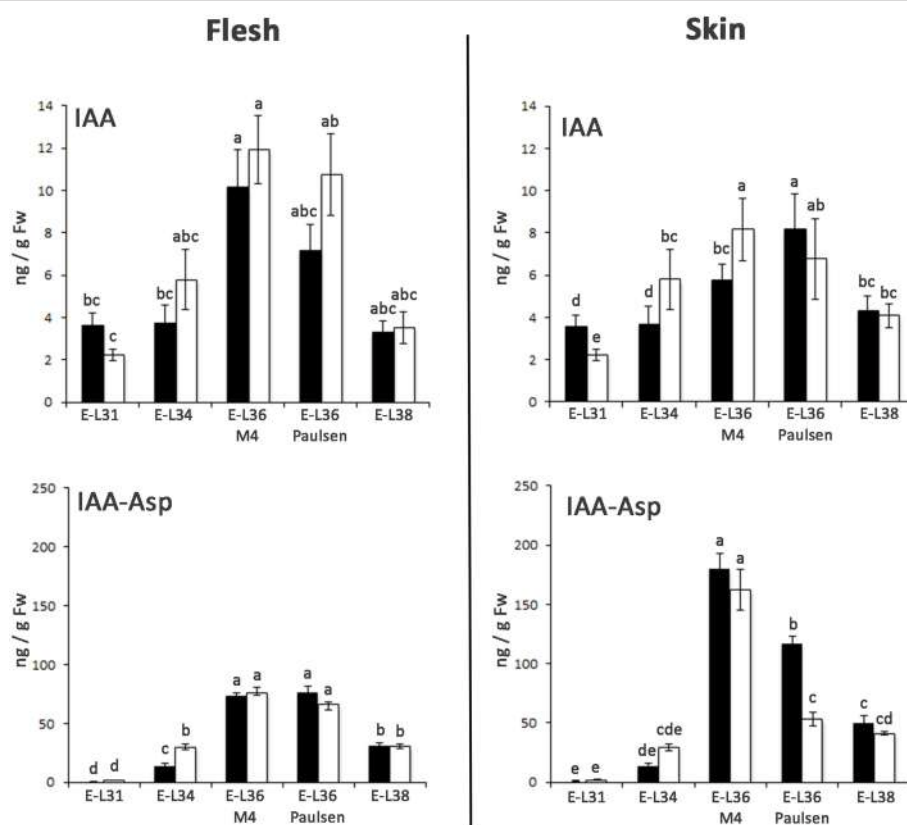


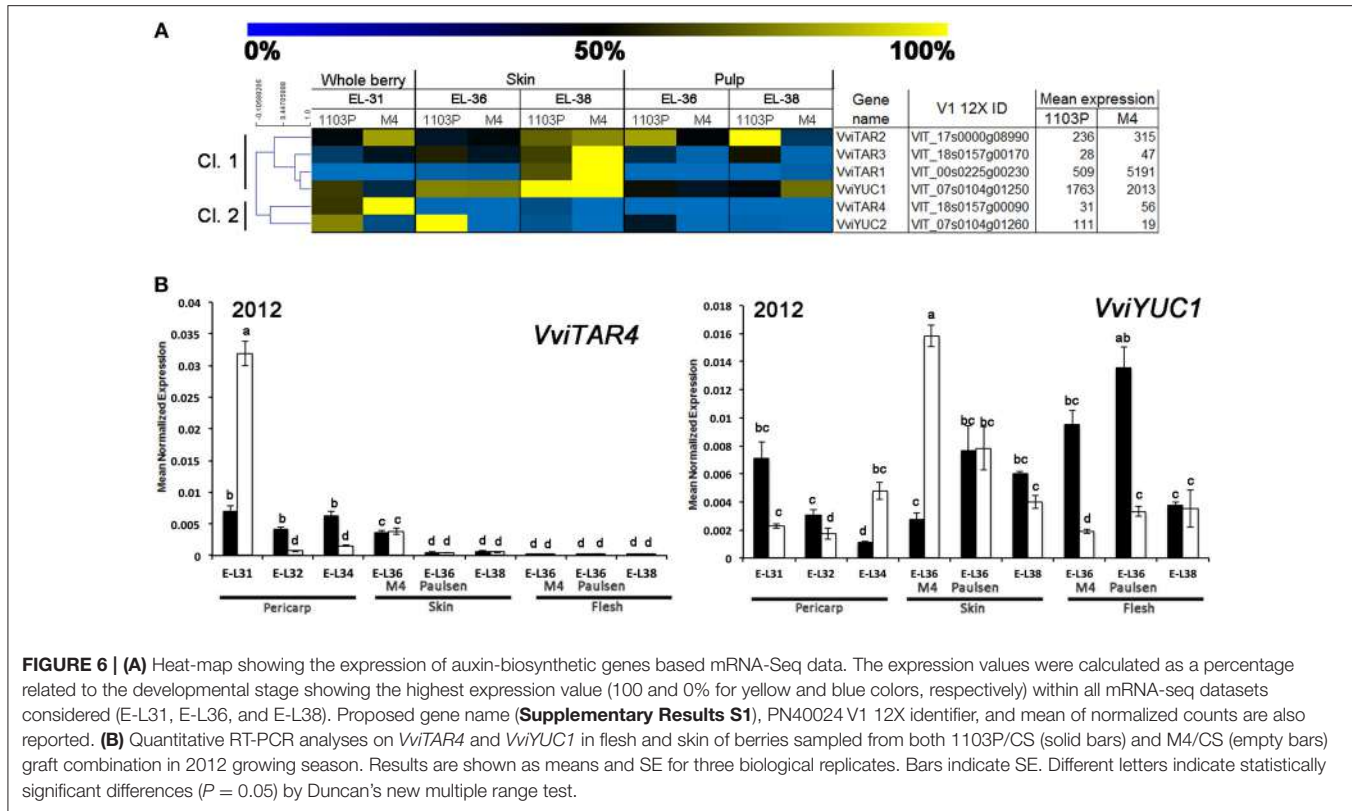
FIGURE 5 | Changes in levels of free IAA and IAA-Asp in flesh and skin of berries sampled from both 1103P/CS (solid bars) and M4/CS (empty bars) graft combination in 2011. IAA and the IAA-Asp were quantified by mean of LC-MS/MS at E-L31, E-L34, E-L36 M4, E-L36 Paulsen, and E-L38 developmental stages. Bars indicate SE of four replicates. Mean followed by the same letters are not statistically different at $P = 0.05$ (Duncan's multiple-range test).

validated this observation (Supplementary Figure S3 and Figure 7B).

The Expression Profile of Flavonoid-Related Genes Parallels the Levels of IAA-Asp in Grape Skin

CS/1103P and CS/M4 clearly display a differential regulation of auxin metabolism, as showed by free and conjugated IAA quantification (Figure 5) and molecular analyses (Figures 4, 6, 7). This different behavior could lead to a different rate in the berry development and ripening (Figure 1) particularly evident in the skin, as pointed out by colorimetric measurements (Figure 1C, Supplementary Figures S1, S2B). In fact, skin color evolution and CIRG index indicated a delay in CS/1103P skin pigmentation and accumulation of flavonoids in comparison to what was observed in CS/M4 berries. The change in skin pigmentation was paralleled by changes in the transcript accumulation of flavonoid biosynthesis (phenylalanine ammonia lyase, *VviPAL3-like*; chalcone synthase 3, *VviCHS3*; flavonol synthase 1, *VviFLS1*; leucoanthocyanidin reductase 1 and 2, *VviLAR1* and *VviLAR2*), flavone- and flavonol- (*VviUFGT*) related genes (Supplementary Figure S4). In particular, the expression of *VviPAL3-like*, *VviCHS3*, *VviLAR2*, and *VviUFGT*

occurred earlier (E-L36 M4) and was higher in CS/M4 berries than in CS/1103P ones. To associate changes in IAA-asp concentration, CIRG value and *GH3* and flavonol-related gene expression to the evolution of skin pigmentation in CS/M4 and CS/1103P berries during ripening, a PCA analysis was carried out on samples collected at pre-véraison (E-L31 and E-L34 corresponding to 45 DAFB and 65 DAFB), during véraison (E-L36, 72 DAFB for M4 and 86 DAFB for 1103P), and ripening (E-L38, 100 DAFB; Figure 8). The first two PCA components explained the 77% of the variance, contributing with similar weights (PC1 = 45% and PC2 = 32%). Examination of the scores and loadings plots for PC1 vs. PC2 showed that the distribution of samples was based on the fruit developmental stages. Samples collected at the pre-véraison stage were clearly separated from those collected during véraison and ripening phases. The PCA analysis also revealed that the early pre-véraison stage (45 DAFB) was strictly associated to the accumulation of *VviGH3-22* transcripts, whereas the induction of other genes, such as *VviLAR2*, *VviGH3-23*, and *VviGH3-17*, marked the late pre-véraison stage (68 DAFB) in both graft combinations. At 72 DAFB, by the time CS/M4 berries almost completed the change of skin color (accompanied by the induction of *VviCHS3* and *VviUFGT* transcription), CS/1103P was still in pre-véraison stage and reached mid/late véraison (marked by the accumulation of



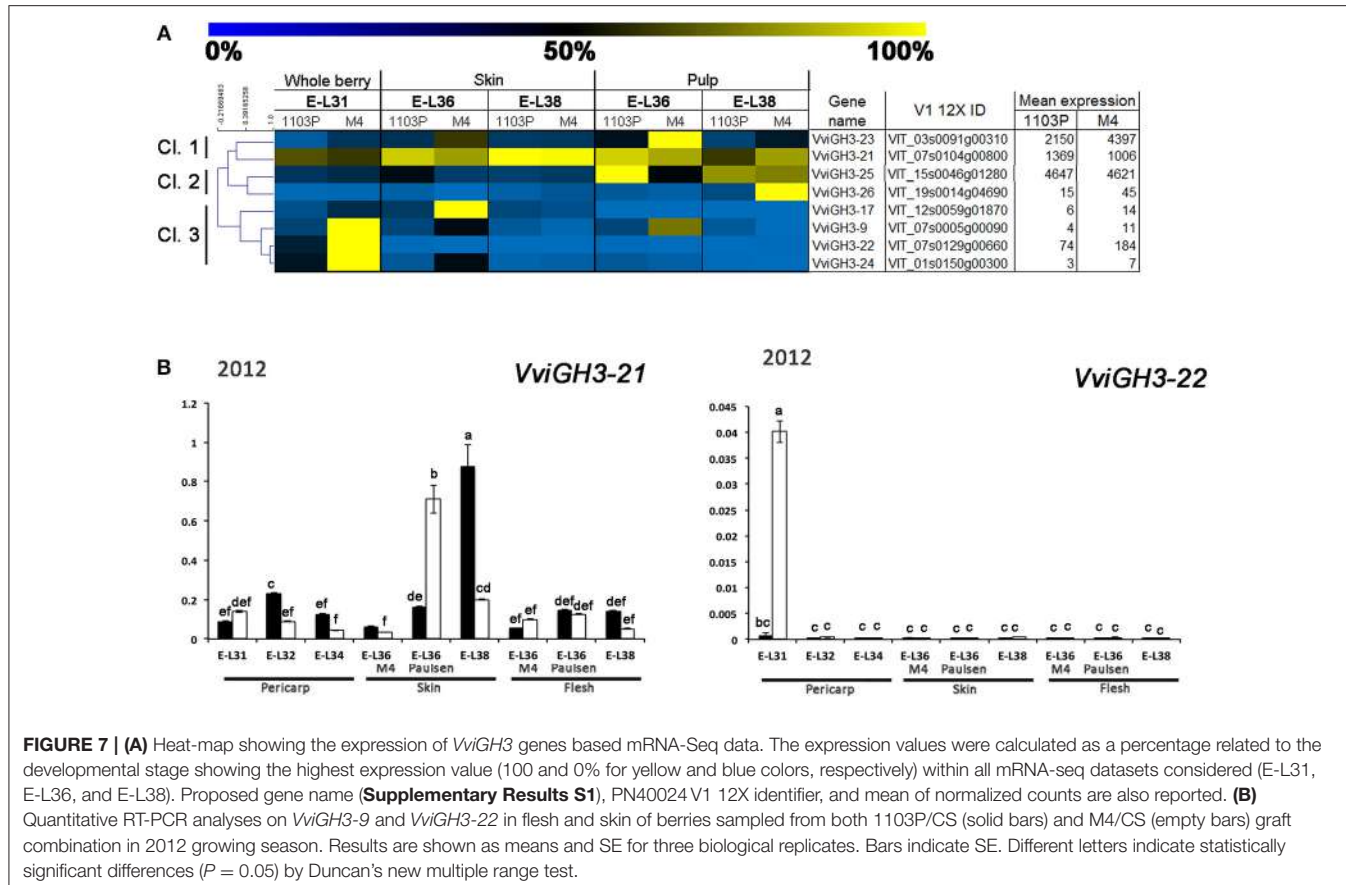
IAA-asp and flavonoids) at 86 DAFB. However, despite the delay displayed in ripening rate, CS/1103P berry collected at 100 DAFB clustered, on the basis of skin parameters, with those of CS/M4 suggesting their recovery of ripening progression. (Figure 7B).

DISCUSSION

The present study evaluated the effect of two grapevine rootstocks, the commonly used and vigorous 1103 P (*V. berlandieri* × *V. rupestris*) and the experimental genotype M4 [(*V. vinifera* × *V. berlandieri*) × *V. berlandieri* cv. Ressegueir n. 1], on *V. vinifera* cv. Cabernet Sauvignon berry development and ripening. The M4 genotype, developed by the DISAA department (University of Milan) was selected for its high tolerance to water deficit and salt exposure and was classified as a medium-vigorous rootstock (Meglio et al., 2014; Corso et al., 2015). The aim of the present study was to shed light on the impact of rootstocks on the scion berry development from a physiological and molecular point of view.

In our study we showed that the rate of berries ripening in CS plants grafted onto M4 is faster (in terms of sugar accumulation and change of skin color) than that observed in the CS/1103P combination (Figure 1). These results are in agreement and partially explained by previous studies showing that the use of the high vigor rootstock 1103P is associated to an extension of the vegetative cycle and a delay in ripening (Koundouras et al., 2008; Gambetta et al., 2012). Biochemical (Figure 1B) and colorimetric data (Figure 1C, Supplementary Figure S1) were also supported by molecular ones (Figure 2). Multifactorial

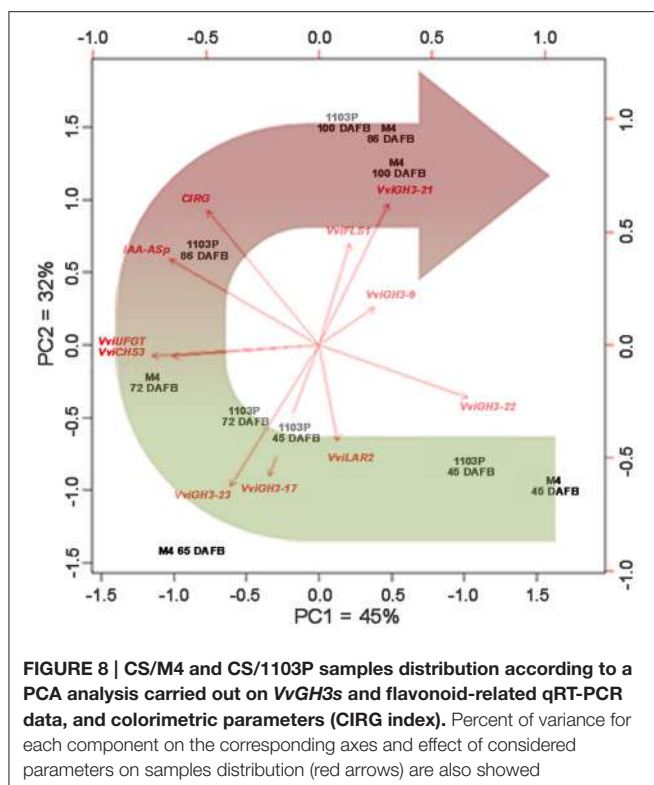
analyses conducted on mRNA-Seq data obtained from CS/1103P and CS/M4 berries at pre-véraison (E-L31), mid-late véraison (E-L36) and ripening (E-L38) indicated that the differential expression of 2358 genes (DEGs) is mainly affected by the rootstock (Figure 3; Supplementary Table S3). Enrichment analyses (Figure 3; Supplementary Table S4) evidenced that, amongst DEGs whose expression is influenced by the rootstock factor (R), many are associated to auxin-related functional categories. Amongst these categories the most prominent regarded genes involved in the auxin signal transduction. Auxin signal transduction is mediated by *Aux/IAA* and *ARF* genes (Pierre-Jerome et al., 2013), which appeared both differently modulated in the two graft combinations (Figure 4). In particular, those *Aux/IAA* and *ARF* genes more expressed at pre-véraison stage showed a higher accumulation of their transcripts in CS/M4 (Figure 5). Amongst these was *VviARF25*, very similar to the response repressor AtARF4 (Supplementary Results S1), which was recently demonstrated to interact with almost all *Aux/IAAs* and to show broad co-expression relationships with *Aux/IAA* genes (Piya et al., 2014). However, Kepinski (2007) suggested that specific pairs of *AUX/IAAs* and *ARFs* function depending on the tissue and developmental stage considered. In our study *VviARF25* was co-expressed with *VviIAA15b*, -38, and -39 (Figure 5). Thus, their products could interact forming putative pairs able to control the expression of auxin-inducible genes at the pre-véraison stage. This result suggests that the rootstock-dependent modulation of auxin action could be involved in the control of berry development rate, similarly to what already hypothesized by Cookson and Ollat (2013) for



what concerns the shoot development. At this regard, it was observed that many genes belonging to the functional categories IAA/auxin were both up- and down-regulated in shoot apical meristems of CS grafted on two different rootstocks, respectively Riparia Gloire de Montpellier and 1103P.

Together with genes involved in auxin action, CS berries grafted on 1103P and M4 rootstocks also showed different patterns of induction for genes involved in auxin biosynthesis and conjugation. Regarding auxin biosynthetic genes, *VviTARs* and *VviYUCCAs* were expressed at pre-véraison stages and during véraison, as previously observed by Böttcher et al. (2013). Although showing expression patterns only partially overlapping in the two growing season (**Figure 6**) considered, it's clear that the two rootstocks determined a different modulation of their transcript levels. Expression of auxin biosynthetic genes is partially overlapped with the differential IAA accumulation observed between CS/M4 and CS/1103P. This is particularly true for skin tissue, where M4 induces a significantly higher accumulation of auxin at 65 (E-L34) and 72 (E-L36 M4) DABF, compared to CS/110P (**Figure 5**). It is worth to note that difference in ripening rate between the two graft combinations parallels IAA-Asp accumulation in the skin and was coupled to an earlier and higher expression of genes involved in auxin biosynthesis (e.g., TAR4; **Figure 6B**) and action (i.e., *VviARF6a*, *VviARF6c*, *VivARF16a*, and *VviARF34*, **Figure 4A**) in CS/M4 berries. Together with auxin biosynthesis, the conjugation

process represented an important auxin homeostatic mechanism at pre-véraison stage. At this regard, of particular interest was the behavior of genes involved in auxin conjugation (*VvGH3s*), especially for those ones showing a peak of expression in pre-véraison phase (E-L31). Amongst these, *VviGH3-22* (VIT_07s0129g200660) was specifically expressed in pre-véraison stage in both graft combination (**Figure 7**) and at very low levels in all other developmental stages. This gene corresponds to *GH3-2* in the nomenclature proposed by Böttcher et al. (2011) (**Supplementary Results S2**), which described a similar behavior in CS and claimed it to be the most responsible gene for auxin homeostasis in pre-véraison. Both mRNA-Seq and qPCR analyses pointed out that *VviGH3-22* transcript is differentially accumulated between the two graft combinations, being much more expressed in CS/M4 than CS/1103P. This observation is in agreement with the higher ability of CS/M4 berries to conjugate IAA at pre-véraison stages (E-L34, **Figure 5**). Considering that the IAA-Asp conjugate might also represent a ripening signal in grapes (Böttcher et al., 2013), the early accumulation observed in CS/M4 at E-L34 (**Figure 5**) could be associated to the earlier onset of ripening in this graft combination. This shift in IAA-Asp accumulation was maintained along the whole ripening although was evident only at the skin level, where a higher accumulation of IAA-Asp was observed in CS/1103P. The different kinetic of IAA-Asp accumulation at these late stages could be associated to



the expression pattern of another *GH3* gene, namely *VviGH3-21*. This gene, corresponding to *GH3-8* described in Böttcher et al. (2011), encodes for a deduced protein representing an out layer respect to the other *GH3* members identified in grapevine and up to now its expression has not been investigated. In the present study *VviGH3-21* was found to be mainly expressed in the skin (**Figure 7B**) and at later stages compared to other *GH3* members. This observation could be associated to the later IAA conjugation observed in the skin and would be consistent with a delay in the ripening programme progression of skin respect to pulp as previously reported (Castellarin et al., 2011; Lijavetzky et al., 2012). The high expression of *VviGH3-21* in late ripening phases of CS/1103P berries compared to what observed in CS/M4 ones could be the result of the rootstock ability to modulate the transcriptome of grape berry. Recently, it was reported that the rootstock is able to modulate the expression of a number of genes in the scion (Cookson and Ollat, 2013; Berdeja et al., 2015; Kumari et al., 2015). In particular, Berdeja et al., (2015) reported that, in berries of Pinot noir plants undergoing water stress condition, the transcript level of genes involved in jasmonate metabolism changes based on the rootstock utilized (Kober 125 AA or Ritter 110). However, our results pointed out that skin colorimetric parameters of ripe berries (E-L 38) are similar between the two graft combinations suggesting an acceleration of ripening induced by 1103P rootstock at last stages of maturation. This result, although obtained in different graft combinations, could be associated to the observations reported by Gouthu et al. (2014) which showed that in a cluster, during the last phase of fruit developmental cycle, the ripening rate of under-ripe berries is higher than that measured in the ripest berries to reach a

synchronized development. This result indicated that, although starting with different timings, the ripening transcriptional programme has to be completed in a genetically defined temporal window independently by exogenous factors affecting the early phases of berry ripening initiation. Similarly, our results pointed out that rootstock is able to modulate the ripening rate but, later on, the genetic control of berry ripening is the main driving force leading to the achievement of full maturity. This result reinforces the assumption that the plasticity of ripening-related genes is mainly modulated by the developmental phase and almost unaffected by external stimuli (e.g., environmental conditions; Dal Santo et al., 2013). Nevertheless, the ripening initiation signal is not only linked to hormone dynamic but also to the status of sugar content, which in turn depends on the competition between the different sinks (Ho, 1988; Bobeica et al., 2015). In the sense using rootstocks characterized by different vigor could determine temporal variation in the duration of ripening programme influencing the relations between fruit and shoot sinks (favoring the shoot development in the case of vigorous rootstock) and, as consequence, the sugar uptake toward them.

CONCLUSIONS

Data presented here suggest that the regulation of auxin level is differently affected in the two scion /rootstock combinations and this is positively correlated with a different rate of grape berry development and ripening. The identification of links between signals controlling berry ripening and rootstock would be of great importance for a better understanding of the influence of rootstock on the scion performance. It has been postulated the ability of rootstock to induce high auxin levels in scion buds as the factor inducing the positive effect of vigorous peach rootstocks on scion branching (Sorce et al., 2006). Nowadays it is becoming evident that throughout the graft union occur a dynamic exchange of mobile signals [transcription factors, mRNAs, regulatory micro RNAs (miRNAs), small interfering RNAs (siRNAs), peptides, and proteins] between scion and rootstock (Haroldsen et al., 2012). Among mobile signals, small non-coding RNAs could play an important role in the regulation of complex processes as fruit development and ripening because of their ability to regulate gene expression in a much more tuneable manner (Vazquez et al., 2010). In this context, there are many evidences that the use of small RNAs, aside from pathogen resistance, down-regulation, and/or epigenetic modification of transcripts and genetic networks, could influence scion-specific characteristics, such as flowering time and fruit production or quality (Haroldsen et al., 2012). In addition to hormones (data presented here) investigations on the role of small RNAs, as well as, those of other signal molecules could help to better clarify the impact of rootstock on berry scion development and ripening.

AUTHOR CONTRIBUTIONS

MC, AV, ML, and CB developed the concept of the paper, wrote the paper, and together with MZ, EM, NV, MB, and GV performed the whole transcriptome and bioinformatic analyses; TN and FZ carried out qRT-PCR analyses, MM and SM

performed auxin quantification and FM collected and analyzed meteorological data. All authors discussed and commented on the manuscript.

FUNDING

This study was supported by the AGER “SERRES” project, grant n° 2010–2105. The cooperation among the international partners was supported by COST Action FA1106, Quality fruit.

ACKNOWLEDGMENTS

We are especially indebted to Pasqua vigneti e cantine (Novaglie, Verona, Italy) for the supply of plant materials.

SUPPLEMENTARY MATERIAL

The Supplementary Material for this article can be found online at: <http://journal.frontiersin.org/article/10.3389/fpls.2016.00069>

Supplementary Data S1 | Meteorological data originate from the Regional Agency for the Environmental Protection of Veneto (ARPAV), Italy.

Climatological data of decadal temperatures, rainfall, and temperature excursions for 2011–2012 compared to the period 1992–2012 are reported.

Supplementary Figure S1 | Colorimetric results of CS/1103P and CS/M4 berry.

Analyses were carried out at four time points corresponding to 45, 72, 86, and 100 DAFB.

Supplementary Figure S2 | Samplings of berries grown in both 1103P/CS and M4/CS graft combinations were performed at different stages of berry development and ripening.

Growing season: 2012. (A) Soluble solids content in CS/M4 (squares) and CS/1103P (circles) throughout fruit development. (B) CIRG values of CS/M4 (square) and CS/1103P (circle) graft combinations throughout fruit development. Bars represent the SD of 100 berries. CS/M4 and CS/1103P data from samples collected at the same DAFB were statistically treated using Student's *t*-test (**P* < 0.05; ***P* < 0.01).

Supplementary Figure S3 | Quantitative RT-PCR analyses on the following *VviYUC1*, *VviTAR4*, *Vvi ARF25*, *VviIAA15b*, *VviGH3-21*, and *VviGH3-22*

REFERENCES

- Anders, S., and Huber, W. (2010). Differential expression analysis for sequence count data. *Genome Biol.* 11:R106. doi: 10.1186/gb-2010-11-10-r106
- Audran-Delalande, C., Bassa, C., Mila, I., Regad, F., Zouine, M., and Bouzayen, M. (2012). Genome-wide identification, functional analysis and expression profiling of the Aux/IAA gene family in tomato. *Plant Cell Physiol.* 53, 659–672. doi: 10.1093/pcp/pcs022
- Berdeja, M., Nicolas, P., Kappel, C., Dai, Z. W., Hilbert, G., Peccoux, A., et al. (2015). Water limitation and rootstock genotype interact to alter grape berry metabolism through transcriptome reprogramming. *Hortic. Res.* 2:15012. doi: 10.1038/hortres.2015.12
- Bobeica, N., Poni, S., Hilbert, G., Renaud, C., Gomès, E., Delrot, S., et al. (2015). Differential responses of sugar, organic acids and anthocyanins to source-sink modulation in Cabernet Sauvignon and Sangiovese grapevines. *Front. Plant Sci.* 6:382. doi: 10.3389/fpls.2015.00382
- Böttcher, C., Burbidge, C. A., Boss, P. K., and Davies, C. (2013). Interactions between ethylene and auxin are crucial to the control of grape (*Vitis vinifera* L.) berry ripening. *BMC Plant Biol.* 13:222. doi: 10.1186/1471-2229-13-222
- Böttcher, C., Harvey, K., Forde, C. G., Boss, P. K., and Davies, C. (2011). Auxin treatment of pre-véraison grape (*Vitis vinifera* L.) berries both performed in flesh and skin of berries sampled from both 1103P/CS (solid bars) and M4/CS (empty bars) graft combination in 2011 growing season. Results are shown as means and SE for two biological replicates. Bars indicate SE. Different letters indicate statistically significant differences (*P* = 0.05) by Duncan's new multiple range test.
- Supplementary Figure S4 | Quantitative RT-PCR analyses on the following flavonoid-related genes: *VviPAL3-like* (VIT_13s0019g04460, A), *VviCHS3* (VIT_05s0136g00260, B), *VviLAR2* (VIT_17s0000g04150, C), *VviFLS1* (VIT_18s0001g03430, D), and *VviUGT* (VIT_16s0039g02230, E).** Transcript levels in CS/1103P (black) and CS/M4 (white) berries are shown as means of normalized expression ±SD.
- Supplementary Results S1 | Nomenclature of genes belonging to the grapevine ARF, Aux/IAA, and GH3 multigenic families.**
- Supplementary Table S1 | Primers used for qPCR analyses. V1 12X identifier (V1 12X ID), gene name, forward (FW sequence) and reverse (RV sequence) sequences are reported.**
- Supplementary Table S2 | (A)** Sequencing and alignment statistics. Sample name (Sample), replicate, paired-end Tag, total number of produced reads (Total), filtered reads after trimming (Filtered), good-quality reads (# Good), aligned and percentage of aligned reads (% Aligned), number of alignment (# alignment) are reported. **(B)** Summary of read number after pairing (F3 + F5). Sample name (Sample), library name (LibName), number of unique reads after pairing (Single), percentage of sequences that aligned on a gene (% ReadsOnGene), number of gene with at least five reads (# of genes) and percentage of genes with at least five reads (% of genes).
- Supplementary Table S3 | List of DEGs influenced by Rootstock (R), Tissue (T), and Phenological Phase (PP) components.** Numbers of DEG are given in brackets. PN40024 V1 12X annotation (V1 12X ID) and functional annotation (Funct. annot.) of DEGs are reported. Statistical analysis were carried out according to an FDR adjusted *p*-value lower than 0.05.
- Supplementary Table S4 | Over-enriched GO terms of genes differentially expressed influenced by rootstock (R), tissue (T), and phenological phase (P) factors.** For each term, the GO identifier (GO-ID), the complete Gene Ontology term (Description), the *p*-value and the FDR-corrected *P*-value (corr *p*-value) of the Fisher's exact test, the numbers of sequences in the test set (x) are provided.
- Supplementary Table S5 | Expression values (mean normalized mRNA-seq counts) of all 56 auxin-related genes.** Gene family, V1 12X annotation, gene name are reported. Graft combination (CS/1103P and CS/M4), considered tissue (whole berry, skin, and pulp) and phenological phase (E-L31, E-L36, and E-L38) are also indicated.
- delays ripening and increases the synchronicity of sugar accumulation. *Aust. J. Grape Wine R.* 17, 1–8. doi: 10.1111/j.1755-0238.2010.00110.x
- Böttcher, C., Keyzers, R. A., Boss, P. K., and Davies, C. (2010). Sequestration of auxin by the indole-3-acetic acid-amido synthetase GH3-1 in grape berry (*Vitis vinifera* L.) and the proposed role of auxin conjugation during ripening. *J. Exp. Bot.* 61, 3615–3625. doi: 10.1093/jxb/erq174
- Çakir, B., Kılıçkaya, O., and Olcay, A. (2013). Genome-wide analysis of Aux/IAA genes in *Vitis vinifera*: cloning and expression profiling of a grape Aux/IAA gene in response to phytohormone and abiotic stresses. *Acta Physiol. Plant.* 35, 365–377. doi: 10.1007/s11738-012-1079-7
- Campagna, D., Albiero, A., Bilardi, A., Cianiato, E., Forcato, C., Manavski, S., et al. (2009). PASS: a program to align short sequences. *Bioinformatics* 25, 967–968. doi: 10.1093/bioinformatics/btp087
- Carreño, J., Martínez, A., and Almela, L., and Fernández-López, J. A. (1995). Proposal of an index for the objective evaluation of the colour of red table grapes. *Food Res. Int.* 28, 373–377.
- Castellarin, S. D., Gambetta, G. A., Wada, H., Shackel, K. A., and Matthews, M. A. (2011). Fruit ripening in *Vitis vinifera*: spatiotemporal relationships among turgor, sugar accumulation, and anthocyanin biosynthesis. *J. Exp. Bot.* 62, 4345–4354. doi: 10.1093/jxb/err150

- Chervin, C., Tira-umphon, A., Terrier, N., Zouine, M., Severac, D., and Roustan, J. P. (2008). Stimulation of the grape berry expansion by ethylene and effects on related gene transcripts, over the ripening phase. *Physiol. Plant.* 134, 534–546. doi: 10.1111/j.1399-3054.2008.01158.x
- Cookson, S. J., and Ollat, N. (2013). Grafting with rootstocks induces extensive transcriptional re-programming in the shoot apical meristem of grapevine. *BMC Plant Biol.* 13:147. doi: 10.1186/1471-2229-13-147
- Coombe, B. G. (1995). Growth Stages of the Grapevine: adoption of a system for identifying grapevine growth stages. *Aust. J. Grape Wine R.* 1, 104–110. doi: 10.1111/j.1755-0238.1995.tb00086.x
- Coombe, B. G., and McCarthy, M. G. (2000). Dynamics of grape berry growth and physiology of ripening. *Aust. J. Grape Wine R.* 6, 131–135. doi: 10.1111/j.1755-0238.2000.tb00171.x
- Corso, M., Vannozzi, A., Maza, E., Vitulo, N., Meggio, F., Pitacco, A., et al. (2015). Comprehensive transcript profiling of two grapevine rootstock genotypes contrasting in drought susceptibility links the phenylpropanoid pathway to enhanced tolerance. *J. Exp. Bot.* 66, 5739–5752. doi: 10.1093/jxb/erv274
- Dal Santo, S., Tornielli, G. B., Zenoni, S., Fasoli, M., Farina, L., Anesi, A., et al. (2013). The plasticity of the grapevine berry transcriptome. *Genome Biol.* 4:r54. doi: 10.1186/gb-2013-14-6-r54
- Davies, C., Boss, P. K., and Robinson, S. P. (1997). Treatment of grape berries, a nonclimacteric fruit with a synthetic auxin, retards ripening and alters the expression of developmentally regulated genes. *Plant Physiol.* 115, 1155–1161.
- Davies, C., and Böttcher, C. (2009). “Hormonal control of grape berry ripening,” in *Grapevine Molecular Physiology & Biotechnology*, ed K. A. Roubelakis-Angelakis (Dordrecht: Springer Science+Business Media B.V.), 229–261.
- Deluc, L. G., Grimplet, J., Wheatley, M. D., Tillett, R. L., Quilici, D. R., Osborne, C., et al. (2007). Transcriptomic and metabolite analyses of Cabernet Sauvignon grape berry development. *BMC Genomics* 8:429. doi: 10.1186/1471-2164-8-429
- Fortes, A. M., Agudelo-Romero, P., Silva, M. S., Ali, K., Sousa, L., Maltese, F., et al. (2011). Transcript and metabolite analysis in Trincadeira cultivar reveals novel information regarding the dynamics of grape ripening. *BMC Plant Biol.* 11:149. doi: 10.1186/1471-2229-11-149
- Gambetta, G. A., Manuck, C. M., Drucker, S. T., Shaghahi, T., Fort, K., Matthews, M. A., et al. (2012). The relationship between root hydraulics and scion vigour across *Vitis* rootstocks: what role do root aquaporins play? *J. Exp. Bot.* 63, 6445–6455. doi: 10.1093/jxb/ers312
- Giribaldi, M., Géné, L., Delrot, S., and Schubert, A. (2010). Proteomic analysis of the effects of ABA treatments on ripening *Vitis vinifera* berries. *J. Exp. Bot.* 61, 2447–2458. doi: 10.1093/jxb/erq079
- Gouthu, S., and Deluc, L. G. (2015). Timing of ripening initiation in grape berries and its relationship to seed content and pericarp auxin levels. *BMC Plant Biol.* 15:46. doi: 10.1186/s12870-015-0440-6
- Gouthu, S., O’Neil, S. T., Di, Y., Ansarolia, M., Megraw, M., and Deluc, L. G. (2014). A comparative study of ripening among berries of the grape cluster reveals an altered transcriptional programme and enhanced ripening rate in delayed berries. *J. Exp. Bot.* 65, 5889–5902. doi: 10.1093/jxb/eru329
- Gregory, P. J., Atkinson, C. J., Bengough, A. G., Else, M. A., Fernández-Fernández, F., Harrison, R. J., et al. (2013). Contributions of roots and rootstocks to sustainable, intensified crop production. *J. Exp. Bot.* 64, 1209–1222. doi: 10.1093/jxb/ers385
- Grimplet, J., Adam-Blondon, A.-F., Bert, P.-F., Bitz, O., Cantu, D., Davies, C., et al. (2014). The grapevine gene nomenclature system. *BMC Genomics* 15:1077. doi: 10.1186/1471-2164-15-1077
- Haroldsen, V. M., Szczecba, M. W., Aktas, H., Lopez-Baltazar, J., Odias, M. J., Chi-Ham, C. L., et al. (2012). Mobility of Transgenic Nucleic Acids and Proteins within Grafted Rootstocks for Agricultural Improvement. *Front. Plant Sci.* 3:39. doi: 10.3389/fpls.2012.00039
- Ho, L. C. (1988). Metabolism and compartmentation of imported sugars in sink organs in relation to sink strength. *Annu. Rev. Plant. Physiol. Plant. Mol. Biol.* 39, 355–378. doi: 10.1146/annurev.pp.39.060188.002035
- Jaillon, O., Aury, J.-M., Noel, B., Pollicetti, A., Clepet, C., Casagrande, A., et al. (2007). The grapevine genome sequence suggests ancestral hexaploidization in major angiosperm phyla. *Nature* 449, 463–467. doi: 10.1038/nature06148
- Kepinski, S. (2007). The anatomy of auxin perception. *Bioessays* 29, 953–956. doi: 10.1002/bies.20657
- Kidman, C. M., Dry, P. R., McCarthy, M. G., and Collins, C. (2013). Reproductive performance of Cabernet Sauvignon and Merlot (*Vitis vinifera* L.) is affected when grafted to rootstocks. *Aust. J. Grape Wine R.* 19, 409–421. doi: 10.1111/ajgw.12032
- Koundouras, S., Tsialtas, I. T., Zioziou, E., and Nikolaou, N. (2008). Rootstock effects on the adaptive strategies of grapevine (*Vitis vinifera* L. cv. Cabernet Sauvignon) under contrasting water status: leaf physiological and structural responses. *Agr. Ecosyst. Environ.* 128, 86–96. doi: 10.1016/j.agee.2008.05.006
- Kuhn, N., Guan, L., Dai, Z. W., Wu, B. H., Lauvergeat, V., Gomès, E., et al. (2013). Berry ripening: recently heard through the grapevine. *J. Exp. Bot.* 65, 4543–4559. doi: 10.1093/jxb/ert395
- Kumari, A., Kumar, J., Kumar, A., Chaudhury, A., and Singh, S. P. (2015). Grafting triggers differential responses between scion and rootstock. *PLoS ONE* 10:e0124438. doi: 10.1371/journal.pone.0124438
- Lijavetzky, D., Carbonell-Bejerano, P., Grimplet, J., Bravo, G., Flores, P., Fenoll, J. M., et al. (2012). Berry flesh and skin ripening features in *Vitis vinifera* as assessed by transcriptional profiling. *PLoS ONE* 7:e39547. doi: 10.1371/annotation/fd93800a-3b3c-484d-97a9-190043309e4b
- Maere, S., Heymans, K., and Kuiper, M. (2005). BiNGO: a Cytoscape plugin to assess overrepresentation of Gene Ontology categories in Biological Networks. *Bioinformatics* 21, 3448–3449. doi: 10.1093/bioinformatics/bti551
- Marguerit, E., Brendel, O., Lebon, E., Van Leeuwen, C., and Ollat, N. (2012). Rootstock control of scion transpiration and its acclimation to water deficit are controlled by different genes. *New Phytol.* 194, 416–429. doi: 10.1111/j.1469-8137.2012.04059.x
- Meggio, F., Prinsi, B., Negri, A. S., Di Lorenzo, G. S., Lucchini, G., Pitacco, P., et al. (2014). Biochemical and physiological responses of two grapevine rootstock genotypes to drought and salt treatments. *Aust. J. Grape Wine R.* 20, 310–323. doi: 10.1111/ajgw.12071
- Müller, M., and Munné-Bosch, S. (2011). Rapid and sensitive hormonal profiling of complex plant samples by liquid chromatography coupled to electrospray ionization tandem mass spectrometry. *Plant Methods* 7, 37–47. doi: 10.1186/1746-4811-7-37
- Pattison, R. J., Csukasi, F., and Catalá, C. (2014). Mechanisms regulating auxin action during fruit development. *Physiol. Plantarum* 151, 62–72. doi: 10.1111/ppl.12142
- Pierre-Jerome, E., Moss, B. L., and Nemhauser, J. L. (2013). Tuning the auxin transcriptional response. *J. Exp. Bot.* 64, 2557–2563. doi: 10.1093/jxb/ert100
- Piya, S., Shrestha, S. K., Binder, B., Stewart, C. N., and Hewezi, T. (2014). Protein-protein interaction and gene co-expression maps of ARFs and Aux/IAAs in *Arabidopsis*. *Front. Plant Sci.* 5:744. doi: 10.3389/fpls.2014.00744
- Saeed, A., Bhagabati, N. K., Braisted, J. C., Liang, W., Sharov, V., Howe, E. A., et al. (2006). TM4 microarray software suite. *Methods Enzymol.* 411, 134–193. doi: 10.1016/S0076-6879(06)11009-5
- Sorce, M., Mariotti, L., Massai, R., and Lorenzi, R. (2006). The involvement of indoleacetic acid in paradormancy and sylleptic shoot development of grafted peach trees and hybrid rootstocks. *Eur. J. Horticult. Sci.* 71, 155–160.
- Tramontini, S., Vitali, M., Centoni, L., Schubert, A., and Lovisolo, C. (2013). Rootstock control of scion response to water stress in grapevine. *Environ. Exp. Bot.* 93, 20–26. doi: 10.1016/j.enexpbot.2013.04.001
- Vazquez, F., Legrand, S., and Windels, D. (2010). The biosynthetic pathways and biological scopes of plant small RNAs. *Trends Plant Sci.* 5, 337–345. doi: 10.1016/j.tplants.2010.04.001
- Walker, R. R., Read, P. E., and Blackmore, D. H. (2000). Rootstock and salinity effects on rates of berry maturation, ion accumulation and colour development in Shiraz grapes. *Aust. J. Grape Wine R.* 6, 227–239. doi: 10.1111/j.1755-0238.2000.tb00183.x
- Wan, S., Li, W., Zhu, Y., Liu, Z., Huang, W., and Zhan, J. (2014). Genome-wide identification, characterization and expression analysis of the auxin response factor gene family in *Vitis vinifera*. *Plant Cell Rep.* 33, 1365–1375. doi: 10.1007/s00299-014-1622-7
- Whiting, J. R. (2004). “Grapevine rootstocks,” in *Viticulture Volume 1: Resources*, eds P. R. Dry and B. G. Coombe (Adelaide, SA: Winetitles Media), 167–188.

- Zenser, N., Ellsmore, A., Leasure, C., and Callis, J. (2001). Auxin modulates the degradation rate of Aux/IAA proteins. *Proc. Natl. Acad. Sci. U.S.A.* 98, 11795–11800. doi: 10.1073/pnas.211312798
- Ziliotto, F., Corso, M., Rizzini, F. M., Rasori, A., Botton, A., and Bonghi, C. (2012). Grape berry ripening delay induced by a pre-véraison NAA treatment is paralleled by a shift in the expression pattern of auxin- and ethylene-related genes. *BMC Plant Biol.* 12:185. doi: 10.1186/1471-2229-12-185
- Zouine, M., Fu, Y., Chateigner-Boutin, A. L., Mila, I., Frasse, P., Wang, H., et al. (2014). Characterization of the tomato ARF gene family uncovers a multi-levels post-transcriptional regulation including alternative splicing. *PLoS ONE* 9:e84203. doi: 10.1371/journal.pone.0084203

Conflict of Interest Statement: The authors declare that the research was conducted in the absence of any commercial or financial relationships that could be construed as a potential conflict of interest.

Copyright © 2016 Corso, Vannozzi, Ziliotto, Zouine, Maza, Nicolato, Vitulo, Meggio, Valle, Bouzayen, Müller, Munné-Bosch, Lucchin and Bonghi. This is an open-access article distributed under the terms of the Creative Commons Attribution License (CC BY). The use, distribution or reproduction in other forums is permitted, provided the original author(s) or licensor are credited and that the original publication in this journal is cited, in accordance with accepted academic practice. No use, distribution or reproduction is permitted which does not comply with these terms.



Kaolin Foliar Application Has a Stimulatory Effect on Phenylpropanoid and Flavonoid Pathways in Grape Berries

Artur Conde^{1,2*}, Diana Pimentel^{1,2†}, Andreia Neves^{1,2}, Lia-Tânia Dinis¹, Sara Bernardo¹, Carlos M. Correia¹, Hernâni Gerós^{1,2,3} and José Moutinho-Pereira¹

¹ Centre for the Research and Technology of Agro-Environmental and Biological Sciences, University of Trás-os-Montes e Alto Douro, Vila Real, Portugal, ² Grupo de Investigação em Biologia Vegetal Aplicada e Inovação Agroalimentar (AgroBioPlant), Departamento de Biologia, Universidade do Minho, Braga, Portugal, ³ Department of Biology, Centre of Molecular and Environmental Biology, University of Minho, Braga, Portugal

OPEN ACCESS

Edited by:

Ana Margarida Fortes,
University of Lisbon, Portugal

Reviewed by:

Claudio Moser,

Fondazione Edmund Mach, Italy

Pablo Carbonell-Bejerano,

Instituto de las Ciencias de la Vid y del Vino, CSIC, Spain

*Correspondence:

Artur Conde

arturconde@bio.uminho.pt

[†]These authors have contributed equally to this work.

Specialty section:

This article was submitted to

Plant Physiology,

a section of the journal

Frontiers in Plant Science

Received: 12 February 2016

Accepted: 18 July 2016

Published: 08 August 2016

Citation:

Conde A, Pimentel D, Neves A, Dinis L-T, Bernardo S, Correia CM, Gerós H and Moutinho-Pereira J (2016) Kaolin Foliar Application Has a Stimulatory Effect on Phenylpropanoid and Flavonoid Pathways in Grape Berries. *Front. Plant Sci.* 7:1150.
doi: 10.3389/fpls.2016.01150

Drought, elevated air temperature, and high evaporative demand are increasingly frequent during summer in grape growing areas like the Mediterranean basin, limiting grapevine productivity and berry quality. The foliar exogenous application of kaolin, a radiation-reflecting inert mineral, has proven effective in mitigating the negative impacts of these abiotic stresses in grapevine and other fruit crops, however, little is known about its influence on the composition of the grape berry and on key molecular mechanisms and metabolic pathways notably important for grape berry quality parameters. Here, we performed a thorough molecular and biochemical analysis to assess how foliar application of kaolin influences major secondary metabolism pathways associated with berry quality-trait, leading to biosynthesis of phenolics and anthocyanins, with a focus on the phenylpropanoid, flavonoid (both flavonol- and anthocyanin-biosynthetic) and stilbenoid pathways. In grape berries from different ripening stages, targeted transcriptional analysis by qPCR revealed that several genes involved in these pathways—*VvPAL1*, *VvC4H1*, *VvSTSs*, *VvCHS1*, *VvFLS1*, *VvDFR*, and *VvUFGT*—were more expressed in response to the foliar kaolin treatment, particularly in the latter maturation phases. In agreement, enzymatic activities of phenylalanine ammonia lyase (PAL), flavonol synthase (FLS), and UDP-glucose:flavonoid 3-O-glucosyltransferase (UFGT) were about two-fold higher in mature or fully mature berries from kaolin-treated plants, suggesting regulation also at a transcriptional level. The expression of the glutathione S-transferase *VvGST4*, and of the tonoplast anthocyanin transporters *VvMATE1* and *VvABCC1* were also all significantly increased at véraison and in mature berries, thus, when anthocyanins start to accumulate in the vacuole, in agreement with previously observed higher total concentrations of phenolics and anthocyanins in berries from kaolin-treated plants, especially at full maturity stage. Metabolomic analysis by reverse phase LC-QTOF-MS confirmed several kaolin-induced modifications including a significant increase in the quantities of several secondary metabolites including flavonoids and anthocyanins in the latter ripening stages, probably resulting from the general stimulation of the phenylpropanoid and flavonoid pathways.

Keywords: grape berry, phenylpropanoids, flavonoids, secondary metabolites, metabolic changes, fruit quality, kaolin, stress mitigation

INTRODUCTION

Grapevine (*Vitis vinifera* L.) is a perennial woody plant with a great impact in the global economy, abundantly cultivated in areas with Mediterranean climates and spreading across temperate to semi-dry areas. Abiotic conditions, such as soil and atmospheric humidity, intense drought, and temperatures, have high impact on grape yield and wine quality (Chaves et al., 2010; Lovisolo et al., 2010). In Mediterranean areas, extended summer droughts and higher temperatures are increasingly expected (Fraga et al., 2012; Hannah et al., 2013) and climate change is undoubtedly having a negative impact in viticulture, including changes in grape-growing geographical area, therefore the development and application of stress mitigation strategies and of more sustainable agricultural practices is of utmost importance for grape production and winemaking industry.

In this context, the application of exogenous compounds that could maintain or even improve plant productivity or fruit quality under such environmental stresses are beginning to be experimented but, despite promising results yielded in some crops (Hose et al., 2000; Li et al., 2004; Seckin et al., 2009; Du et al., 2013; Zhou et al., 2014), in grapevine these strategies have so far been less explored. Kaolin, $\text{Al}_2\text{Si}_2\text{O}_5(\text{OH})_4$, is an inert clay mineral that reflects potentially damaging ultraviolet and infrared radiation and transmits photosynthetically active radiation, resulting in leaf temperature decrease and photosynthetic efficiency increase (Glenn and Puterka, 2005). Its exogenous application in leaves resulted in positive responses to abiotic stresses in apple, pomegranate and even olive tree (Glenn et al., 2001; Melgarejo et al., 2004; Khaleghi et al., 2015). In grapevines kaolin particle film induced cooler canopy temperatures, lower rates of stomatal conductance under non-limiting soil moisture conditions, protection of photosystem II structure and function in leaves exposed to heat and high solar radiation, and altered total soluble solids content and total anthocyanin amounts (Shellie and Glenn, 2008; Glenn et al., 2010; Ou et al., 2010; Song et al., 2012; Shellie, 2015; Dinis et al., 2016a,b). We recently observed that lower ROS quantities, increased hydroxyl radical scavenging and production of antioxidant compounds, including phenolics, apparently contributing to the protective effect of kaolin in grapevine (Dinis et al., 2016a), but little is known regarding the molecular mechanisms underlying these changes.

Secondary metabolites are indeed extremely important for fruit quality-trait and wine production, namely phenolics, since they contribute to color, flavor, aroma, texture, astringency, and stabilization of wine, and also exhibit antioxidant properties (reviewed by Teixeira et al., 2013). Phenolic compounds are divided in two major groups, nonflavonoid phenolics, and flavonoids (reviewed by Teixeira et al., 2013). Non-flavonoid phenolics comprise hydroxybenzoic acids, hydroxycinnamic acids, volatile phenolics and stilbenes, while flavonoids are C6-C3-C6 polyphenolic compounds and divided into flavonols, flavan-3-ols (catechins/epicatechins, proanthocyanidins, or condensed tannins) and anthocyanins (Kennedy et al., 2000; Verries et al., 2008). Grapevine anthocyanins are anthocyanidins glycosylated or acylglycosylated at the 3' position of the B ring, thus, flavonoid-3-O-monoglycosides, and are responsible for

the pigmentation of colored grape berries, from red through blue, hence for wine color (Castellarin et al., 2012). Two major secondary metabolic biochemical pathways underlie the synthesis of a wide range of important phenolic and flavonoid compounds, including anthocyanins: the phenylpropanoid pathway, with the enzyme phenylalanine ammonia lyase (PAL) playing a major role, and the flavonoid pathway, with several important enzymes involved in the formation of the different classes of flavonoids, discussed further ahead. Anthocyanins are stored in the vacuole after being transported across the tonoplast by primary or secondary transporters such as ATP-binding cassette (ABC) transporters (Francisco et al., 2013), as is the case of VvABCC1, dependent on the presence of reduced glutathione (GSH); or multidrug and toxic extrusion (MATE, or anthoMATE) transporters like MATE1 (or AM1) that use the H^+ gradient to transport mostly acylated anthocyanins (Gomez et al., 2009, 2011), respectively. Glutathione S-transferases (GSTs), with VvGST4 as a paradigmatic case, are very important in anthocyanin stabilization and transport to the vacuole via a non-covalent (ligandin) activity, and a correlation between anthocyanin accumulation and VvGST expression profile during berry ripening has already been established (Conn et al., 2008).

Environmental conditions have a strong influence on the secondary metabolism of grape berry cells (Teixeira et al., 2013), that is reflected in grape berry quality. High temperatures decreases anthocyanin biosynthesis and content (Spayd et al., 2002; Mori et al., 2007; Azuma et al., 2012; Carbonell-Bejerano et al., 2013). Genes encoding enzymes involved in flavonoid biosynthesis, as well as regulatory genes and UFGT enzymatic activity are differently affected by heat stress depending on the cultivar and whether these high temperatures are diurnal or nocturnal (Mori et al., 2005, 2007). Exposure to light, however, appears to promote a increase in phenolic, mostly flavonols, and, in many cases but not all, anthocyanin synthesis and content (Spayd et al., 2002; Fujita et al., 2006; Czembel et al., 2009; Matus et al., 2009; Azuma et al., 2012), but these responses have recently been proposed to be more complex (reviewed by Pillet et al., 2015). Mild water deficit can enhance anthocyanin and stilbenoid synthesis (Mattivi et al., 2006; Castellarin et al., 2007b; Deluc et al., 2011), however flavonol content is either unaltered or decreased (Deluc et al., 2009; Zarrouk et al., 2012). In fact, fruits from grapevines under severe water deficit stress can have lower synthesis and accumulation of phenolics, including anthocyanins, as often this stress is associated with superimposed very high temperatures in the vineyard edaphoclimate.

This work consisted of a thorough molecular and biochemical analysis with the objective of assessing the influence of a foliar application of kaolin on grape berry secondary metabolism. Transcriptional analyses by qPCR, as well as biochemical analyses including enzyme activity measurements, were performed on key metabolic pathways/molecular mechanisms involved in the biosynthesis of phenolics and anthocyanins, with a focus on phenylpropanoid, flavonoid (both flavonol- and anthocyanin-biosynthetic) and stilbenoid pathways. Metabolomic analysis by reverse phase LC-QTOF-MS was also performed to unveil kaolin-induced modifications on several important secondary metabolites in the latter ripening stages.

MATERIALS AND METHODS

Grapevine Field Conditions and Sampling

Whole grape berry samples were collected from field-grown “Touriga Nacional” cultivar grapevines (*Vitis vinifera* L.) grafted onto 110-R from the commercial vineyard “Quinta do Vallado,” in the Douro Demarcated Region (Denomination of Origin Douro/Porto), located at Peso da Régua, Portugal (41°09'44.5"N 07°45'58.2"W). The climate is typically Mediterranean-like, with a warm-temperate climate and dry and hot summers, with higher precipitation during winter but very low during the summer (Kottek et al., 2006). Vines were managed without irrigation and grown using standard cultural practices as applied by commercial farmers. Vineyard rows were located on a steep hill with an N-S orientation. Monthly maximum temperature (T_{\max}) and precipitation values (April to October) were reported in Dinis et al. (2016a).

Three vineyard rows, with 20 plants each, were sprayed in 17th July 2014, at the late green-phase and right before *véraison*, with 5% (w/v) Kaolin (Surround WP; Engelhard Corp., Iselin, NJ), according to previous work done by our team (Dinis et al., 2016a). A second application in the same day was done to ensure Kaolin adhesion uniformity. Other three vineyard lines, with 20 plants each, were maintained as control, i.e., without Kaolin application. All rows are located side-by-side (ensuring the same edaphoclimatic conditions) on a steep hill with an N-S orientation. The vines were 7 years-old, were trained to unilateral cordon and the spurs were pruned to two nodes each with 10–12 nodes per vine.

Grape berry samples treated with kaolin and without treatment, i.e., control, were randomly collected from different positions in the clusters of different plants from different rows in the vine at four ripening stages: on 23th July (late green phase), 21st August (*véraison*, ca. half of the berries per cluster colored), 3rd September (mature), and on 12th September (full mature); and immediately frozen in liquid nitrogen. In all ripening stages, sampling was performed in sunny and relatively hot days, so with relatively similar environmental conditions in all sampling dates. In the sampling procedure, 50–60 berries (about 5 per cluster) were collected always at the same time of the day, at 6.30 p.m. Phenological parameters of control vs. kaolin-treated fully-mature berries, respectively, were as follows: average berry weight—1.89 vs. 1.88 g, pH—3.98 vs. 3.94; total sugars—198.6 vs. 203.6 g/L. No apparent differences in skin to pulp ratio were noticed between control and kaolin-treated berries. The average water contents of control vs. kaolin-treated berries were as follows: 93.1 vs. 94.1% at green stage, 80.9 vs. 80.7% at veraison, 77.0 vs. 75.9% at mature stage, 74.5 vs. 74.4% at full maturation. For *véraison* sampling, a representative mix of colored and non-colored berries was obtained. This precaution procedure was adopted both in the cluster and for different clusters of the plant, with half of colored and half of non-colored berries collected from each condition and used for each experiment. The *véraison* rate was apparently similar between conditions with no apparent phonological displacement. No difference on *véraison* proportion between treatments was observable.

All berries selected for sampling were totally clean and without any trace or residue of kaolin. Berries were deseeded and ground to a fine powder under liquid nitrogen refrigeration and stored in -80°C. For RNA extraction, metabolite extraction and enzymatic activity assays, 6–8 randomly collected berries were used for grinding and sample homogenization.

Metabolomic Analysis by Reverse Phase LC-QTOF-MS

Reverse phase LC-QTOF-MS analysis was used to analyze how foliar kaolin application influenced grape berry secondary metabolome. Secondary metabolites were extracted from lyophilized powdered grape berry samples with 50% ethanol. After concentration in vacuum for ethanol removal, the extract was re-suspended with water. The aqueous solution was subsequently extracted with light petroleum and ethyl acetate, respectively. Samples were then evaporated under reduced pressure. Metabolite profiling analyses were performed with a liquid chromatography coupled to quadrupole time of flight-MS (LC-QTOF/MS) System (Agilent Technologies 1290 LC, 6540 MS, Agilent Technologies, Santa Clara, CA, USA) using reverse phase (RP) combined with positive ion ESI mode. A Zorbax Eclipse XDBC18 column (100 × 2.1 mm, 1.8 μm; Agilent Technologies) was used at 45°C and flow rate 0.6 mL/min with solvent A—water with 0.1% formic acid, and solvent B—acetonitrile with 0.1% formic acid. The gradient initiated from 25 to 95% B in 35 min, and returned to starting conditions in 1 min, with there-equilibration with 25% B for 9 min. For data acquisition, the TOF mass range was set from 50 to 1000 m/z. During the analysis two reference masses: 121.0509 m/z (C5H4N4) and 922.0098 m/z (C18H18O6N3P3F24) were continuously measured for constant mass correction and thus obtain the accurate mass. The capillary voltage was 3000 V with a scan rate of 1.0 scan per second. The nebulizer gas flow rate was 10.5 L/min.

Metabolite data were normalized using the dry (lyophilized) weight (DW) of the samples. For all experimental conditions, three independent and randomized runs were performed in all metabolomic analysis.

RNA Extraction

A total of 200 mg of grape berry tissue (without seeds) previously grounded in liquid nitrogen was used for total RNA extraction following the protocol by Reid et al. (2006) in combination with purification with RNeasy Plant Mini Kit (Qiagen). After treatment with DNase I (Qiagen), cDNA was synthesized from 1 μg of total RNA using Omniscript Reverse Transcription Kit of Qiagen.

Transcriptional Analysis by Real-Time qPCR

The expression of several target genes (Supplementary Table 1) in berries at different developmental stages from control and kaolin treated vines was analyzed by real-time qPCR. For that purpose, cDNA was synthesized from 1 μg of total RNA using Omniscript Reverse Transcription Kit (Qiagen). Real-time PCR analysis was

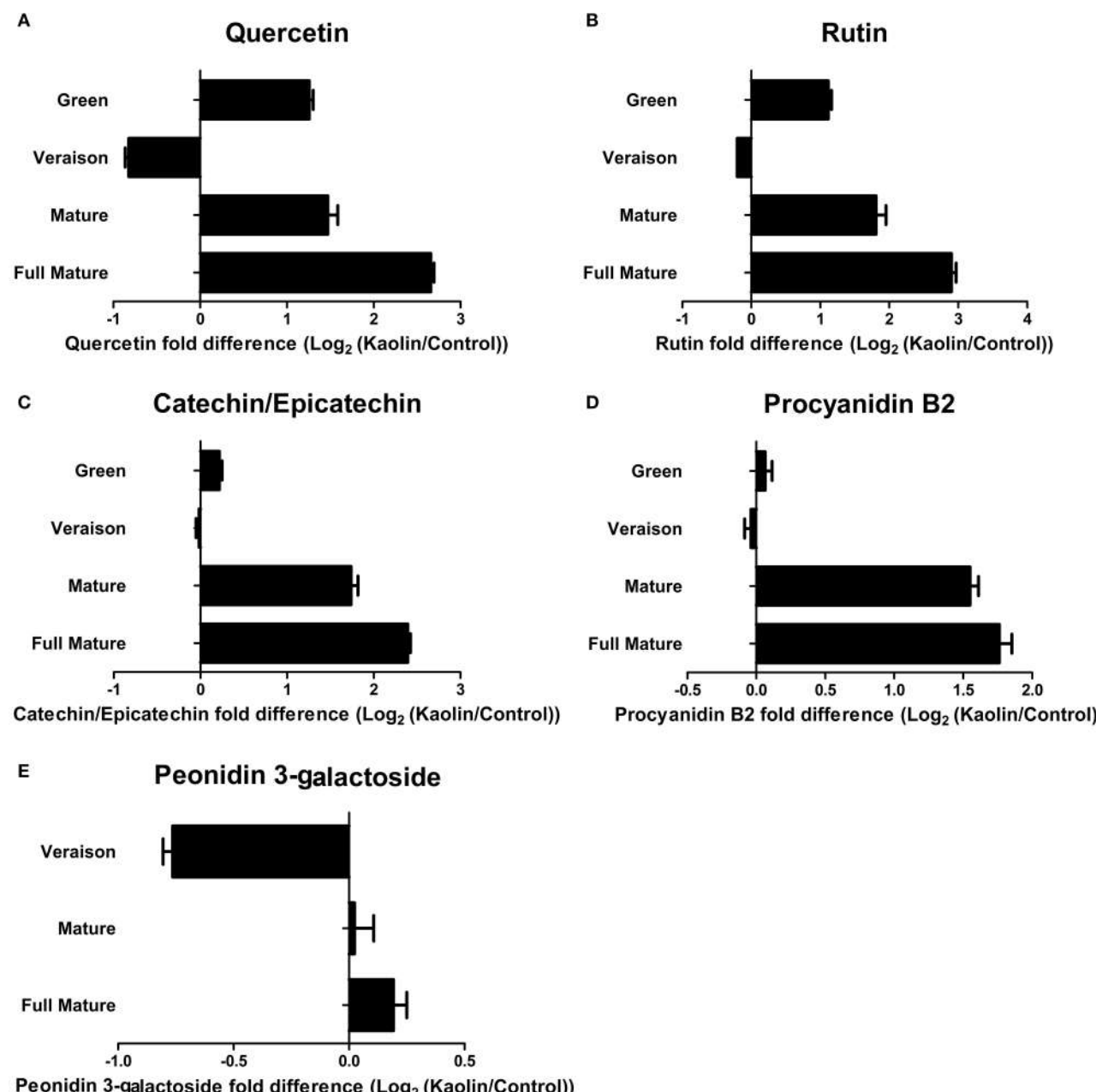


FIGURE 1 | Effect of kaolin application on the quantities of important secondary metabolites of grape berries. Relative amounts of (A) quercetin; (B) rutin; (C) catechin/epicatechin; (D) procyanodin B2, and (E) peonidin 3-galactoside (\log_2 transformation of kaolin/control fold variation), obtained by reverse phase LC-QTOF-MS, in grape berry tissues collected in four different maturation stages (green, véraison, mature, and full mature) from vines subjected to kaolin treatment and without application (control).

performed with QuantiTect SYBR Green PCR Kit (Qiagen) using 1 μL cDNA (diluted 1:10 in ultra-pure distilled water) in a final reaction volume of 10 μL per well. As reference genes, *VvACT1* (actin), and *VvGAPDH* (glyceraldehyde-3-phosphate dehydrogenase) were selected, as these genes were proven to be very stable and ideal for qPCR normalization purposes in grapevine (Reid et al., 2006). Gene specific primer pairs used for each target or reference gene are listed on Supplementary

Table 1 (Downey et al., 2003; Bogs et al., 2006; Conn et al., 2008; Gomez et al., 2009; Boubakri et al., 2013; Conde et al., 2015). Primers specifically designed for this work were obtained with the aid of QuantPrime (Arvidsson et al., 2008). Melting curve analysis was performed for specific gene amplification confirmation. The expression values were normalized by the average of the expression of the reference genes as described by Pfaffl (2001). For all experimental conditions tested, two

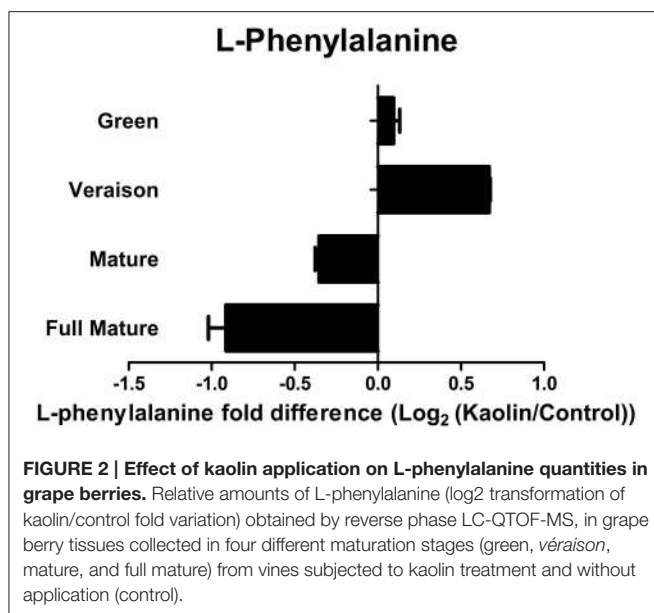


FIGURE 2 | Effect of kaolin application on L-phenylalanine quantities in grape berries. Relative amounts of L-phenylalanine (\log_2 transformation of kaolin/control fold variation) obtained by reverse phase LC-QTOF-MS, in grape berry tissues collected in four different maturation stages (green, véraison, mature, and full mature) from vines subjected to kaolin treatment and without application (control).

independent biological runs with mathematical triplicates were performed.

Protein Extraction

Total protein extraction from grape berry powder was performed as described by Stoop and Pharr (1993) with several modifications. Sample powder was thoroughly mixed with extraction buffer in an approximately 1:1 (v/v) powder:buffer ratio. Protein extraction buffer contained 50 mM Tris-HCl pH 8.9, 5 mM MgCl₂, 1 mM EDTA, 1 mM phenylmethylsulfonyl fluoride (PMSF), 5 mM dithiothreitol (DTT), and 0.1% (v/v) Triton X-100. The homogenates were thoroughly mixed and centrifuged at 18000xg for 20 min and the supernatants were maintained on ice and used for all enzymatic assays. Total protein concentrations of the extracts were determined by the method of Bradford (Bradford, 1976) using bovine serum albumin as a standard.

Phenylalanine Ammonia Lyase (PAL) Enzymatic Assay

PAL biochemical activity was determined in crude enzymatic extracts following the trans-cinnamic acid production at 41°C, in a total volume of 2 mL. The reaction mixture contained 0.2 mL of enzyme extract, 3.6 mM NaCl, and 25 mM L-phenylalanine (a saturating concentration that ensured that the reaction occurred at the V_{max}) as substrate in 50 mM Tris-HCl pH 8.9. The rate of conversion of L-phenylalanine to cinnamic acid was monitored continuously in the spectrophotometer at 290 nm. Reactions were initiated by the addition of L-phenylalanine.

Flavonol Synthase (FLS) Enzymatic Assay

FLS biochemical activity determination was performed as described by Li et al. (2012) with some modifications. Enzyme extraction was performed as described above, but for FLS

activity measurements the extracts were additionally purified with Amicon Ultra 4 Centrifugal Filters (Merck Millipore). FLS activity was determined following quercetin production at 37°C during 1 h in a total volume of 1 mL. The reactions were performed at pH 5.0 with 111 mM sodium acetate, 83 μ M 2-oxoglutaric acid, 42 μ M ferrous sulfate, 120 μ L of enzyme extract and started with 400 μ M dihydroquercetin, the substrate, at a saturating concentration that ensured V_{max} , and the production of quercetin was followed at 365 nm ($\epsilon = 13.2 \text{ mM}^{-1} \text{ cm}^{-1}$).

UDP-Glucose:Flavonoid 3-O-Glucosyltransferase (UGT) Enzymatic Assay

The biochemical activity of UGT was determined as described by Mori et al. (2005), with some adaptations. The assay mixture contained 100 mM sodium phosphate buffer pH 8.0, 1 mM UDP-glucose and 100 μ L enzyme extract, in a final volume of 500 μ L. The reaction was initiated with 1 mM quercetin as substrate (saturating concentration). The reaction mixture was incubated under gentle shaking for 30 min and the production of quercetin 3-glucoside was followed at 350 nm during 30 min ($\epsilon = 21877 \text{ M}^{-1} \text{ cm}^{-1}$).

Quantification of Total Phenolics and Anthocyanins

The concentration of total phenolics and anthocyanins was performed as described in our previous work (Dinis et al., 2016a). Briefly, the concentration of total phenolics was quantified by the Folin-Ciocalteu colorimetric method in berries from all experimental conditions. Total phenolics were extracted in 1.5 mL of pure methanol from 100 mg of berry grounded tissue. The homogenates were vigorously shaken for 15 min and subsequently centrifuged at 18000xg for 20 min. Twenty μ L of each supernatant were added to 1.58 mL of deionized water and 100 μ L of Folin reagent, vigorously shaken and incubated for 5 min in the dark before adding 300 μ L of 2M sodium carbonate. After 2 h of incubation in the dark, the absorbance of the samples was measured at 765 nm. Total phenolic concentrations were determined using a gallic acid calibration curve and represented as gallic acid equivalents (GAE). Anthocyanins were extracted from 150 mg of grape berry grounded tissue with 1 mL of 100% acetone. The suspension was vigorously shaken for 30 min. The homogenates were centrifuged for 20 min at 18000xg and the supernatants were collected. Anthocyanin extracts were diluted 1:10 in 25 mM potassium chloride solution pH 1.0 and absorbance was measured at 520 nm and 700 nm, using 25 mM potassium chloride solution pH 1.0 as blank. Total anthocyanin quantification was calculated in relation to cyanidin-3-glucoside equivalents, calculated by equation 1, per DW:

$$[\text{Total anthocyanins}] (\text{mg/L}) = \frac{(A_{520} - A_{700}) \times MW \times DF \times 1000}{\epsilon \times 1} \quad (1)$$

where MW is the molecular weight of cyanidin-3-glucoside (449.2 g mol⁻¹), DF is the dilution factor and ϵ is the molar extinction coefficient of cyanidin-3-glucoside (26900 M⁻¹ cm⁻¹).

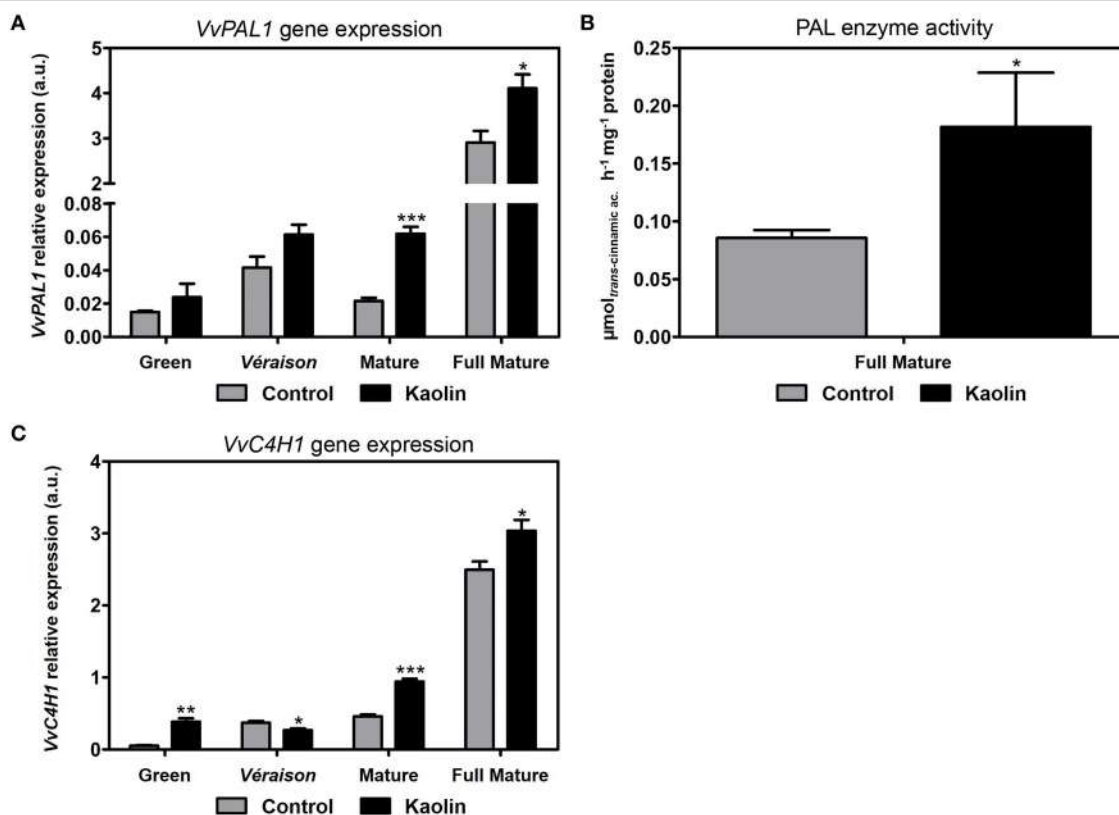


FIGURE 3 | Stimulatory effect of kaolin on the phenylpropanoid pathway. (A) Transcript levels of grapevine phenylalanine ammonia lyase 1 (*VvPAL1*) and cinnamate-4-hydroxylase 1 (*VvC4H1*) (**C**) in grape berries. **(B)** Phenylalanine ammonia lyase (PAL) total enzymatic activity, determined as V_{\max} in berries collected in the full mature stage (12th September) from vines treated with kaolin and without application (control). The assay was performed in triplicate. Values are the mean \pm SEM of three independent experiments. Asterisks indicate statistical significance (Student's *t*-test; $*P < 0.05$). Gene expression analyses were performed by real-time qPCR in grape berry tissues collected in four different maturation stages (green, véraison, mature, and full mature) from vines subjected to kaolin treatment and without application (control). *VvPAL1* and *VvC4H1* relative expression levels were obtained after normalization with the expression of the reference genes *VvACT1* and *VvGAPDH*. Two independent PCR runs with triplicates were performed for each tested mRNA. Values are the mean \pm SEM. Asterisks indicate statistical significance (Student's *t*-test; $*P < 0.05$; $**P < 0.01$; $***P < 0.001$).

Statistical Analysis

The results were statistically analyzed by Student's *t*-test using Prism vs. 5 (GraphPad Software, Inc.). For each condition, statistical differences between mean values are marked with asterisks (* $P < 0.05$; ** $P < 0.01$; *** $P < 0.001$).

RESULTS

Effect of Exogenous Kaolin Application on Grape Berry Secondary Metabolites

In a very recent study (Dinis et al., 2016a) we observed that a foliar treatment of cv. Touriga Nacional with kaolin significantly increased the total amount of phenolic compounds in mature and fully mature berries, and of anthocyanins in fully-mature berries only. Results obtained in the present work confirmed those observations, and demonstrated a significant increase of total phenolics in roughly 30% in the late-green phase, and unchanged concentrations in véraison (Supplementary Figure 1). In agreement, the quantities of quercetin (flavonol), rutin

(flavonol glucoside), catechin/epicatechin (monomeric flavan-3-ol), procyanidin B2 (proanthocyanidin), and peonidin 3-galactoside (anthocyanin), which were identified by reverse phase LC-QTOF-MS, were all substantially increased in berries from grapevines treated with kaolin (Figure 1).

Noticeably, LC-QTOF-MS analysis also showed that mature and fully mature berries from vines treated with kaolin had a significantly lower quantity of L-phenylalanine, the first metabolite to be converted (into *trans*-cinnamic acid) in the phenylpropanoid pathway, than berries from the control vines (Figure 2).

Transcriptional and Biochemical Activity Differences in the Phenylpropanoid Pathway

In our previous report (Dinis et al., 2016a) we showed that the transcript levels of a phenylalanine ammonia lyase gene (*VvPAL1*), that encodes an enzyme catalyzing the first step in the phenylpropanoid pathway in which *trans*-cinnamic acid

is produced, increased in the final maturation stages by 33% in berries from kaolin-treated plants. Here, we observed that *VvPAL1* transcripts also appeared to be slightly more abundant in berries from kaolin treated plants at the late-green and véraison stages (**Figure 3A**), in a trend that continued until the final maturation phase.

As the highest *VvPAL1* expression level occurred at the final ripening stage, here we determined the total PAL biochemical activity in crude extracts from fully mature berries. In agreement with the increase in *VvPAL1* transcript abundance, results showed a two-fold higher PAL specific activity in berries from vines subjected to kaolin treatment than in control berries (**Figure 3B**). As shown in **Figure 3C**, the steady-state transcript abundance of *VvC4H1*, which codes for a cinnamate-4-hydroxylase (C4H) that catalyzes the second reaction in the phenylpropanoid pathway, were also increased in berries from kaolin-treated plants, by 100% and approximately 20% at the mature and full mature stages, respectively.

Transcriptional Changes in Stilbene Biosynthetic Pathway

To evaluate how the stilbenoid pathway was influenced by foliar kaolin application, transcriptional analysis of *stilbene synthase 1* (*VvSTS1*), that encodes the first enzyme of this pathway, was performed. However, with the primer pair used for amplification, we actually amplified several STS family genes, which can provide a broader sense of the changes in this metabolic pathway. Stilbene synthase (STS) is responsible for the condensation of 4-coumaroyl-CoA with 3 molecules of malonyl-CoA producing resveratrol. The real-time qPCR analysis revealed that *VvSTS* transcript levels increase up to 1000-fold from mature to full mature stages, but kaolin application appeared to stimulate *VvSTS* transcription only in the mature stage (**Figure 4**).

Transcriptional and Biochemical Activity Changes in the Flavonoid Pathway—Biosynthesis of Flavonols, Flavanols, and Anthocyanins

Transcriptional changes in several important intermediates in the flavonoid pathway were also analyzed. This pathway is initiated by the action of chalcone synthase (CHS). As shown in **Figure 5A**, the expression of a paradigmatic chalcone synthase gene, *VvCHS1*, which is the better characterized chalcone synthase isoform in grapevine, was not constant during the season and was variably affected by kaolin. The highest steady-state transcript abundance quantity of *VvCHS1* was observed at the late-green stage, when the stimulatory effect of kaolin was more evident (five-fold increase over the control). However, kaolin application also stimulated *VvCHS1* transcription at the mature and full mature stage in a very subtle way, as we had reported before (Dinis et al., 2016a).

Flavonol Biosynthesis

Flavonol synthase (FLS) is the first enzyme of the flavonol biosynthetic branch of the flavonoid pathway. Gene expression analysis by qPCR revealed that *VvFLS1* was mostly expressed at

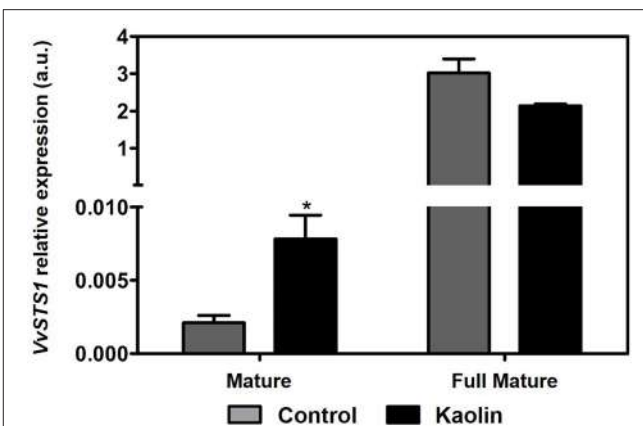


FIGURE 4 | Effect of kaolin application in the transcript levels of grapevine stilbene synthase 1 (*VvSTS1*) in mature and full mature grape berries. Gene expression analysis was performed by real-time qPCR in grape berry tissues collected from vines subjected to kaolin treatment and without application (control). *VvSTS1* relative expression levels were obtained after normalization with the expression of the reference genes *VvACT1* and *VvGAPDH*. Two independent PCR runs with triplicates were performed for each tested mRNA. Values are the mean \pm SEM. Asterisks indicate statistical significance (Student's *t*-test; **P* < 0.05).

the véraison and mature stages (**Figure 5B**), and then the steady-state transcript levels decreased abruptly at full mature stage. The stimulatory effect of kaolin application on *VvFLS1* expression was more evident in late green berries and at the mature stage, when a three-fold increase over the control was observed. Concordantly, in berries from kaolin-treated vines, the biochemical activity of FLS was also three-fold higher than in berries from untreated plants (**Figure 5C**)

Flavanol and Anthocyanin Biosynthesis

Dihydroflavonols are secondary metabolites that can enter in either anthocyanin or flavan-3-ol biosynthetic pathways. By catalyzing the reduction of dihydroflavonols to flavan-3,4-diols, the enzyme dihydroflavonol reductase (DFR) is responsible for the first committed step in the pathway leading to the synthesis of flavan-3-ols (or flavanol) compounds, a group that comprises catechin, epicatechin, epigallocatechin, other tannins and proanthocyanidins; and also in the pathway that culminates with the synthesis of anthocyanins. We observed that, in all developmental stages, *VvDFR1* expression was significantly higher in berries from vines treated with kaolin (**Figure 6A**), with increases by almost six-fold and two-fold, for instance, in the mature and full mature stages. The enzyme UDP-glucose:flavonol 3-O-glucosyl transferase (UFGT) catalyzes the final step of anthocyanin biosynthesis. The transcript levels of *VvUFGT* were noticeably higher in kaolin-treated than in control berries, particularly in the green (two-fold) and the mature (80%) stages, but also slightly, yet not statistically significant, in fully mature berries (**Figure 6B**). In agreement with the transcript abundance of the gene *VvUFGT1*, the UFGT specific activity was significantly enhanced by little more than two-fold, in mature berries from kaolin-treated

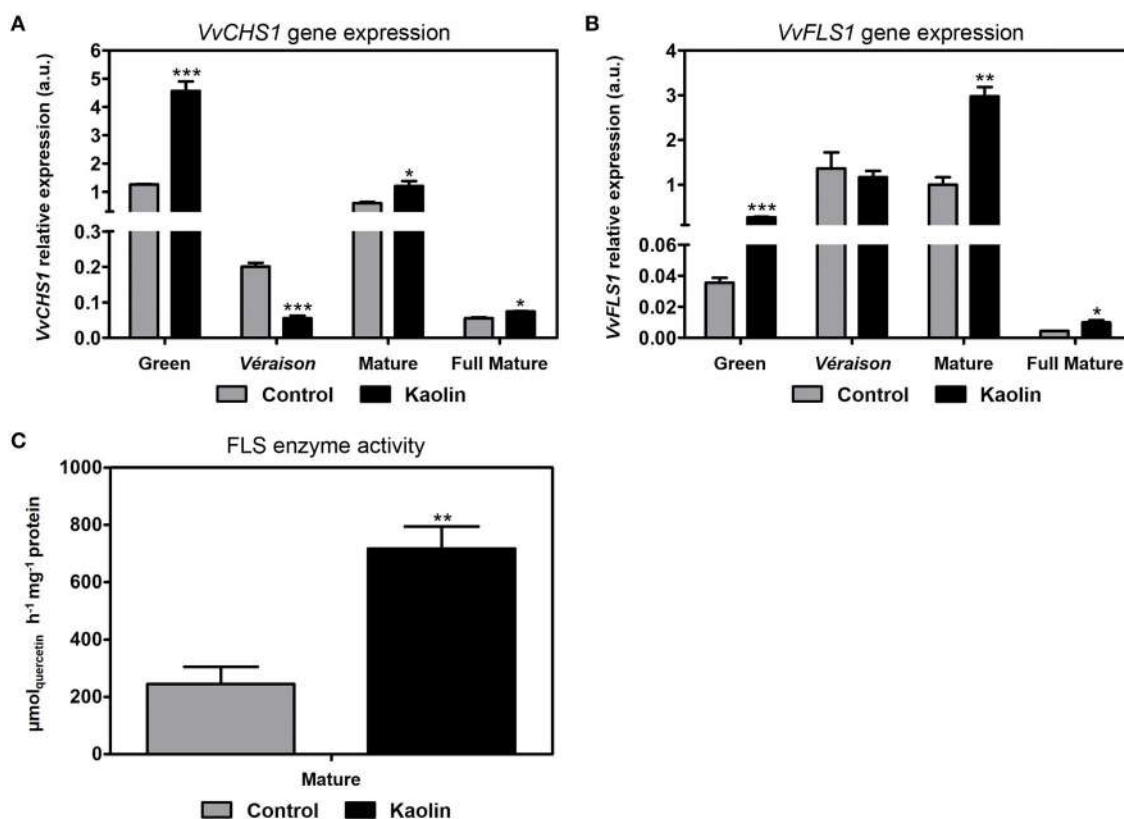


FIGURE 5 | Stimulatory effect of kaolin on chalcone synthase and flavonol synthase. **(A)** Transcript levels of chalcone synthase 1 (*VvCHS1*) and flavonol synthase 1 (*VvFLS1*) **(B)** in grape berries. Gene expression analyses were performed by real-time qPCR in grape berry tissues collected in four different maturation stages (green, véraison, mature, and full mature) from vines subjected to kaolin treatment and without application (control). *VvCHS1* and *VvFLS1* relative expression levels were obtained after normalization with the expression of the reference genes *VvACT1* and *VVGAPDH*. Two independent PCR runs with triplicates were performed for each tested mRNA. Values are the mean \pm SEM. Asterisks indicate statistical significance (Student's *t*-test; **P* < 0.05; ***P* < 0.001). **(C)** Flavonol synthase (FLS) total biochemical activity, determined as *V*_{max} in berries collected in the mature stage (3rd September) from vines treated with kaolin and without application (control). The assay was performed in triplicate. Values are the mean \pm SEM of three independent experiments. Asterisks indicate statistical significance (Student's *t*-test; ***P* < 0.01).

plants, while no differences were observed in full-mature berries (**Figure 6C**).

The gene *VvMYB5b* encodes a protein belonging to the R2R3-MYB family of transcription factors that has been unequivocally characterized as a regulator of the flavonoid pathway and as having a great role in anthocyanin- and proanthocyanidin-derived compounds accumulation (Deluc et al., 2008). Moreover, it is predominantly expressed during grape berry ripening, making it an ideal candidate to evaluate MYB-related regulation of anthocyanin biosynthetic pathway in the present work. As denoted in **Figure 7**, *VvMYB5b* appeared to be slightly up-regulated at the full mature stage, when kaolin application seemed to increase its expression, however the differences were not statistically significant between treatments.

Transcriptional Changes in Anthocyanin S-conjugation and Vacuolar Transport

Transcriptional changes in genes involved in anthocyanin S-conjugation and in vacuolar transport for intracellular storage

were also evaluated. The expression of the gene *VvGST4*, coding for glutathione S-transferase 4, was higher in berries under kaolin treatment in all development stages except in the full mature, with the three-fold increase in mature berries being most noticeable (**Figure 8A**). This enzyme is key in stabilizing anthocyanins by conjugating them with the reduced form of glutathione (GSH), a biochemical step that is required for the majority of anthocyanin vacuolar transport (Conn et al., 2008).

Gene expression of the tonoplast anthocyanin transporter *VvMATE1* was also strongly enhanced (by three-fold) in mature berries from kaolin-treated vines, and approximately two-fold higher than the control in the green stage (**Figure 8B**). On the other hand, the expression of another tonoplast anthocyanin transporter, *VvABCC1*, this one shown to strictly transport S-conjugated anthocyanins only, was very strongly upregulated in kaolin-treated berries at véraison by approximately 26-fold (**Figure 8C**). Interestingly, at the mature stage, the ripening phase when *VvMATE1* expression was very strongly upregulated in response to kaolin, *VvABCC1* transcript levels were higher in berries from untreated plants.

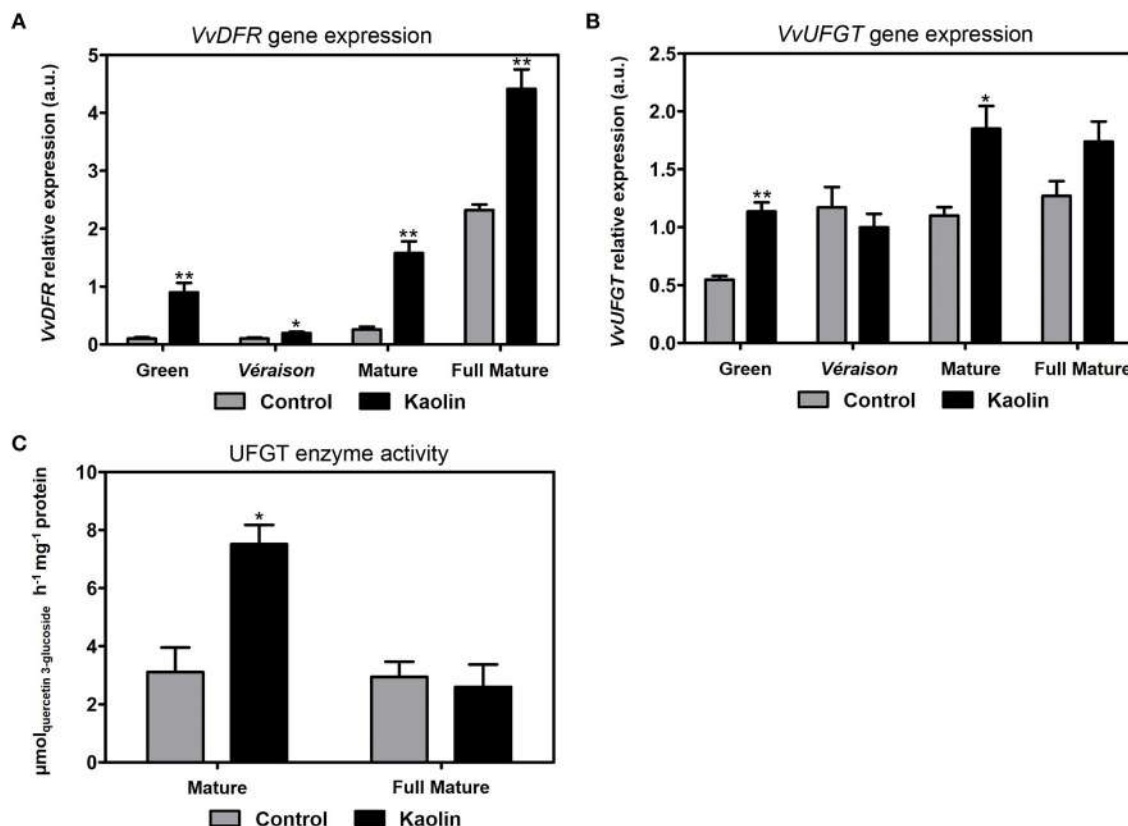


FIGURE 6 | Stimulatory effect of kaolin on key intervenients of anthocyanin biosynthesis. **(A)** Transcript levels of dihydroflavonol reductase (*VvDFR*) and UDP-glucose:flavonol 3-O-glucosyl transferase (*VvUGT*) **(B)** in grape berries. Gene expression analyses were performed by real-time qPCR in grape berry tissues collected in four different maturation stages (green, véraison, mature, and full mature) from vines subjected to kaolin treatment and without application (control). *VvDFR* and *VvUGT* relative expression levels were obtained after normalization with the expression of the reference genes *VvACT1* and *VvGAPDH*. Two independent PCR runs with triplicates were performed for each tested mRNA. Values are the mean \pm SEM. Asterisks indicate statistical significance (Student's *t*-test; **P* < 0.05; ***P* < 0.01). **(C)** UDP-glucose:flavonol 3-O-glucosyl transferase (UFGT) total biochemical activity, determined as *V_{max}* in berries collected in the mature (3rd September) and full mature (12th September) stages from vines treated with kaolin and without application (control). The assay was performed in triplicate. Values are the mean \pm SEM of three independent experiments. Asterisks indicate statistical significance (Student's *t*-test; **P* < 0.05).

DISCUSSION

This work, as well as a previous one (Dinis et al., 2016a) reinforce that the treatment of grapevine leaves with the inert clay mineral kaolin increases, in the mature grape berry, the quantities of phenolic compounds, including total phenolics and anthocyanins. This fact should have major implications in fruit and wine quality, while protecting plant against abiotic stress. Here, an analysis focused on secondary metabolism by reverse phase LC-QTOF-MS confirmed that the production in the grape berry of different classes of phenolic compounds—including flavonols, flavonol glucosides, flavan-3-ols, proanthocyanidins and anthocyanins, was indeed generally stimulated by foliar kaolin treatment of Touriga Nacional grapes. Furthermore, we showed here that the higher phenolic/anthocyanin content in response to kaolin is clearly due to a global stimulation of phenylpropanoid, flavonoid—flavonol and anthocyanin—pathways at the gene expression and/or protein activity (enzyme activity) levels. Indeed, a concerted and general increased in

the expression of many genes involved in these pathways, along with a significant increase in measured enzymatic activities were observed in the latter ripening stages.

Both *VvPAL1* and *VvC4H1* had higher expression in mature and fully mature berries from kaolin-treated vines, confirming that kaolin enhances this particular pathway that is fundamental for the following synthesis of stilbenes and flavonoids. The observed higher PAL enzymatic activity in fully mature berries from kaolin-treated vines also corroborates this assumption, and suggests that in this case the increased transcription levels of one PAL isoform (*VvPAL1*) do indeed provide strong evidence of a final increased biochemical activity. This increased biochemical activity of PAL, that is the result from the joint activity of all isoenzymes, may account for the observed lower levels of L-phenylalanine content in berries from kaolin-treated vines. Dai et al. (2014) demonstrated that increased L-phenylalanine amounts, the main precursor of phenolic biosynthesis, were not correlated with anthocyanin improvement. Here, we were able to observe the same, as lower L-phenylalanine contents were

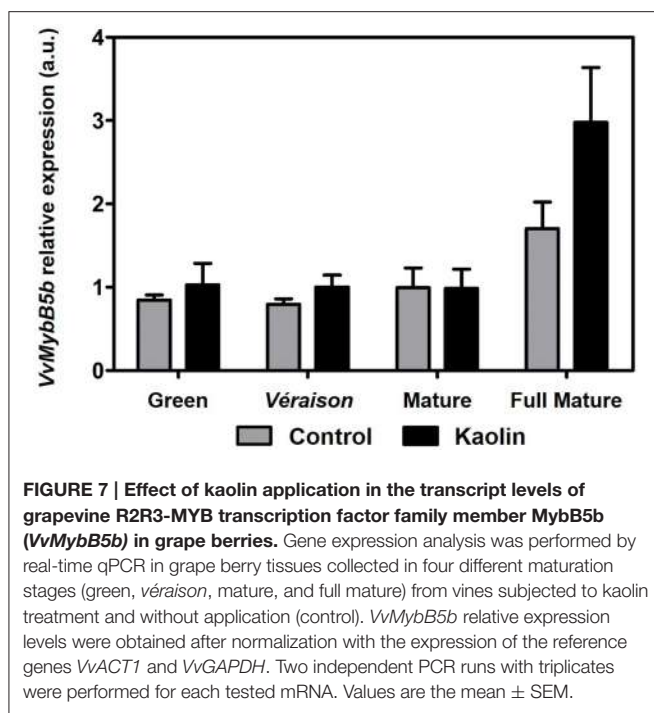


FIGURE 7 | Effect of kaolin application in the transcript levels of grapevine R2R3-MYB transcription factor family member MybB5b (*VvMybB5b*) in grape berries. Gene expression analysis was performed by real-time qPCR in grape berry tissues collected in four different maturation stages (green, véraison, mature, and full mature) from vines subjected to kaolin treatment and without application (control). *VvMybB5b* relative expression levels were obtained after normalization with the expression of the reference genes *VvACT1* and *VvGAPDH*. Two independent PCR runs with triplicates were performed for each tested mRNA. Values are the mean \pm SEM.

paralleled by an increase in total phenolics in kaolin-treated berries, and in PAL activity, thus, L-phenylalanine consumption.

The flavonols quercetin and rutin (a glycosylated quercetin-derivative) were successfully identified in the metabolomic analysis by LC-QTOF-MS and both were more abundant in berries from kaolin-treated vines especially at the latter ripening stages. This is in agreement with the enhanced flavonol biosynthetic pathway observed in berries from kaolin-treated vines, in particular at the mature stage. At that point, *VvFLS1* expression level was significantly higher in berries from kaolin-treated vines, which correlated very well with a significantly higher FLS activity, in the same proportion. Together with the correlation of PAL activity and *VvPAL1* transcripts, this shows that, in the secondary metabolic pathways we assessed, increased expression levels of a gene can be predictive/indicative of increased final enzymatic activity resulting from all possible isoforms, attesting our prospective qPCR analysis as a robust approach to assess the influence of kaolin on molecular mechanisms/biochemical pathways related with berry quality.

The four-fold increase in *VvCHS1* expression in green berries from kaolin-treated plants, the stage in which its expression was the highest, also suggests that an enhancement of this metabolic step that begins the flavonoids pathway could have played a role in the higher phenolics concentration observed in this phase.

Anthocyanins are responsible for berry color being, thus, an important quality trait of both fruit and red wine production. At the mature stage, berries are actively synthesizing anthocyanins in a process that stagnates in the very final ripening stage when the berries are ready for harvest. Fully mature berries from kaolin-treated vines had significantly more anthocyanins, in a process that appeared to be initiated in the mature phase. This difference could be explained by higher expression of

genes involved in anthocyanin biosynthesis and accumulation in the latter ripening stages of berries from kaolin-treated vines. *VvUFGT*, that glycosylates anthocyanidins/flavonols into anthocyanins using UDP-glucose as co-substrate, was indeed more expressed in mature berries from kaolin-treated vines, with a very good correlation with increased total UFGT higher enzymatic activity, just like the case of PAL and FLS, suggesting the increase in the transcription and activity of UFGT was key for increased anthocyanin concentrations. Like in the case of PAL, the enzymatic activity of UFGT is the clear-cut result from the joint action of all UFGT isoenzymes. Upstream, *VvDFR* expression was also enhanced in berries from kaolin-treated vines at the latter ripening stages, suggesting a whole stimulation of the anthocyanin synthesis pathway. Catechins/epicatechins, procyanidin B2, a proanthocyanidin, and the anthocyanin peonidin-3-galactoside were all also present in higher amounts in mature and fully mature berries from kaolin treated vines. This is in perfect agreement with the overall stimulation of phenylpropanoid and flavonoid pathways by foliar kaolin application. Moreover, anthocyanin stabilization and transport into the vacuole was also increased in berries during the major color change phases (véraison and mature) from kaolin-treated vines as demonstrated by increased *VvGST4*, *VvMATE1*, and *VvABCC1* transcripts.

Anthocyanin accumulation in the grape berry is known to be impaired by high temperatures (Spayd et al., 2002; Yamane et al., 2006; Mori et al., 2005, 2007), which suggests that the fact that foliar kaolin application leads to lower canopy temperatures might also contribute for the higher anthocyanin concentration in berries from kaolin-treated plants. Low anthocyanin accumulation at high temperatures has been reported to result from down-regulation of genes involved in anthocyanin biosynthesis (Mori et al., 2005, 2007; Carbonell-Berjano et al., 2013).

Mild water deficit has been observed to increase total anthocyanins and stilbenoids (Deluc et al., 2009, 2011; Castellarin et al., 2007a,b, 2012), and to up-regulate genes involved in the phenylpropanoid biosynthetic pathway (Deluc et al., 2009; Castellarin et al., 2007a,b, 2012). However, severe water deficit causes the opposite and results in lower anthocyanin synthesis and contents. Our results suggest that foliar kaolin application somehow had a stimulatory effect in phenolic and anthocyanin synthesis capacity, and a possible reduction of a severe water deficit stress to a milder form of stress induced by foliar kaolin application should not be ruled out. The recognized capacity of kaolin particle film in reducing part of the radiation that reaches plant tissues, thereby reducing canopy temperature and alleviating heat stress and sunburn, while stimulating photosynthesis (Dinis et al., 2016b), might also contribute for higher phenolic/anthocyanin concentrations in berries from kaolin-treated plants observed in this study, but a possible direct influence of silicon (Si) should not be ruled out, despite the reported inert nature of kaolin, and future studies to address this matter could provide valuable new insights, following previous reports showing that plants actively respond to Si supplementation, administrated in roots in forms other than kaolin, including the accumulation of

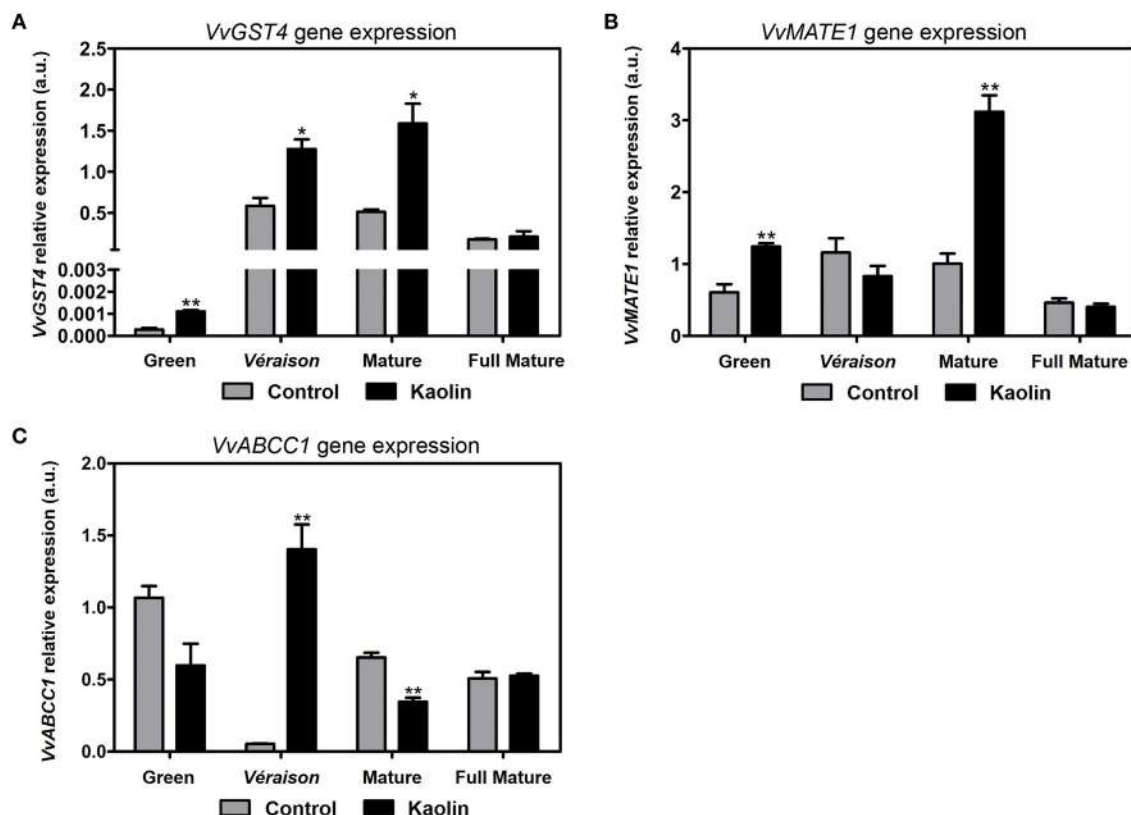


FIGURE 8 | Stimulatory effect of kaolin on the transcription of genes involved in anthocyanin S-conjugation and vacuolar transport capacity. (A) Transcript levels of glutathione S-transferase 4 (*VvGST4*) and of anthocyanin tonoplast transporters MATE1 (*VvMATE1*) (B) and ABCC1 (C) in grape berries. Gene expression analyses were performed by real-time qPCR in grape berry tissues collected in four different maturation stages (green, véraison, mature, and full mature) from vines subjected to kaolin treatment and without application (control). *VvGST4*, *VvMATE1*, and *VvABCC1* relative expression levels were obtained after normalization with the expression of the reference genes *VvACT1* and *VvGAPDH*. Two independent PCR runs with triplicates were performed for each tested mRNA. Values are the mean \pm SEM. Asterisks indicate statistical significance (Student's *t*-test; **P* < 0.05; ***P* < 0.01).

phenolics in rice (Zhang et al., 2013) and banana (Fortunato et al., 2014). It is also important to note that kaolin is known for increasing photosynthetic capacity in leaves, therefore increasing the synthesis of photoassimilates like sucrose. Interestingly, gene expression of several sugar transporters with a role in phloem unloading and/or post-phloem loading was increased in mature leaves and, most importantly, in mature and fully-mature berries (not shown) which might indicate an increased sugar transport capacity at the berry level as well as its accumulation or availability for feeding other metabolic pathways. In fact, several studies have shown a relationship between sugar and anthocyanin content (Pirie and Mullins, 1977; Hunter et al., 1991; Larronde et al., 1998; Dai et al., 2014), which suggests that sugar is important for the synthesis of secondary metabolites. Thus, it is plausible that kaolin-induced higher sugar transport and availability in the berry might also contribute to the stimulation of these secondary pathways. A somewhat interesting observation appears to be the very few changes generally observed at véraison. Abscisic acid concentration increases to reach its peak at this developmental phase of the berry and is responsible for the beginning of berry coloring and ripening

phase initiation (Castellarin et al., 2016), events that are markedly noticed by anthocyanin and other flavonoids accumulation. A possible explanation for the the fact that kaolin had no apparent effect at véraison might very well be the large concentrations of ABA comparing to the other phases, so that the regulation exerted by this hormone heavily controls the expression of the molecular mechanisms behind flavonoid and anthocyanin synthesis and superimposes any possible modification induced by the foliar kaolin treatment.

It is also important to note that, despite the absence of a factual skin:pulp ratio measurement in this study, no apparent changes in that regard were observed when collecting and processing the berry samples. So, despite not possible to completely rule out the influence of a slightly modified skin:pulp ratio by foliar application of kaolin, it appears not to be a contributor to the observed stimulated phenylpropanoid- and flavonoid-associated molecular mechanisms. In addition, no apparent changes were observed in berry softening, and alterations of brix, berry size and weight, and total acidity were negligible. However, a small contribution of possible indirect kaolin-induced skin thickening and/or phenology displacement, even though not

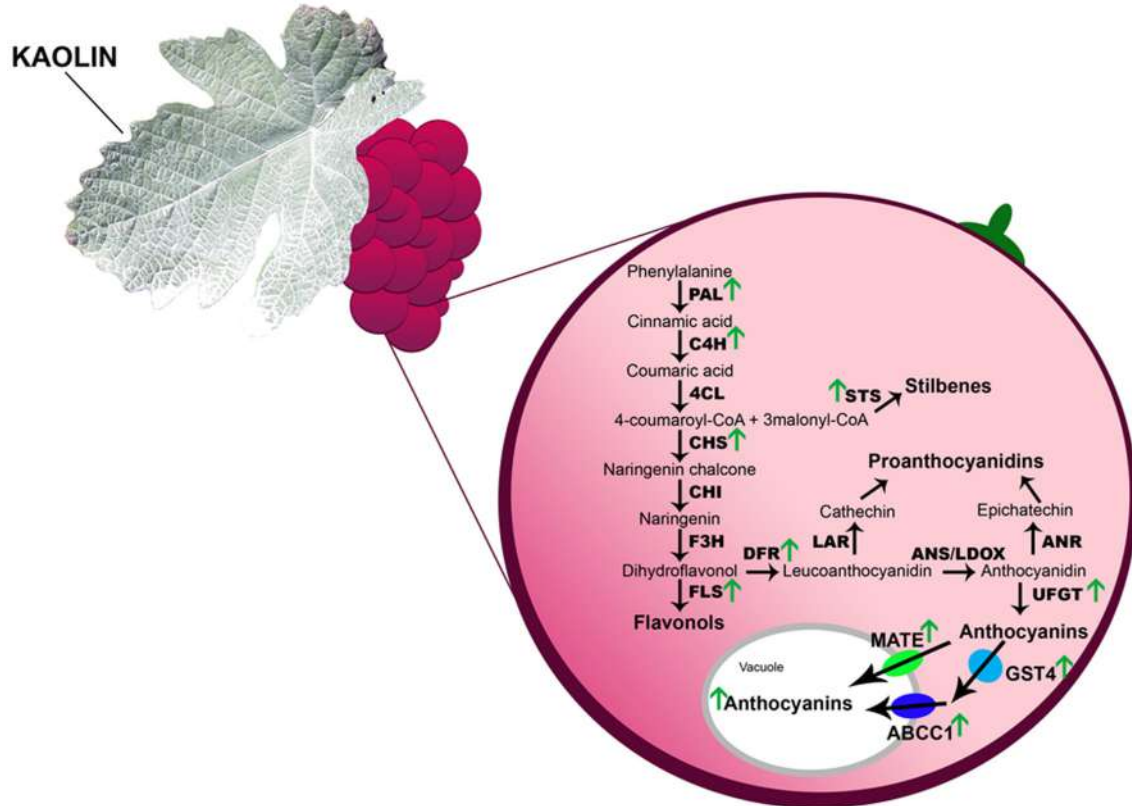


FIGURE 9 | Foliar kaolin application induced a general stimulation of phenylpropanoid and flavonoid pathways in grape berry cells. Molecular mechanisms studied in the present work are identified by the upper pointing green arrows that highlight increases of transcripts, biochemical activity or both we observed at any given point during berry ripening in response to kaolin application. CHS, chalcone synthase; CHI, chalcone isomerase; F3H, flavanone 3-hydroxylase; DFR, dihydroflavonol 4-reductase; ANS, anthocyanidin synthase; LDOX, leucoanthocyanin dioxygenase; LAR, leucoanthocyanidin reductase; ANR, anthocyanidin reductase; UFGT, UDPglucose:flavonoid 3-O-glucosyltransferase; FLS, flavonol synthase; GST4, glutathione S-transferase 4; MATE, anthocyanin multidrug and toxic extrusion transporters; ABCC1, ATP-binding cassette transporter; v, vacuole; cw, cell wall.

apparent in the current work, should not be completely ruled out, and should be carefully evaluated in future studies to confirm whether or not they are partially responsible for our observations on phenylpropanoid and flavonoid pathways. Additionally, thoroughly determined ripening indicators throughout berry development such as pH value or titratable acidity and total sugar content in a statistically significant manner is equally important to confirm that no phenology displacement occurs as consequence of foliar kaolin application.

In the present work, we showed that grape berries from kaolin-treated vines demonstrated generally enhanced phenolic-biosynthetic molecular mechanisms (Figure 9) that ultimately resulted in higher concentration of phenolics, including anthocyanins. These metabolic pathways are tightly associated with berry quality, and better grape berry quality translates into better wine quality, so, into added value to the winemaking industry, as these compounds are responsible for wine organoleptic properties, like color, flavor, astringency, and bitterness. The conjugation of kaolin application with other mitigation strategies based on viticultural practices or the application of other protective compounds with similar characteristics could also be potentially explored in the future.

In sum, exogenous kaolin application in grapevine leaves shows great potential as summer stress mitigation strategy because it positively impacts berry quality as a result of many molecular and biochemical changes in key secondary metabolic pathways such as phenylpropanoid and flavonoid pathways.

AUTHOR CONTRIBUTIONS

AC, HG, and JM designed the experiments. AC, DP, AN, LD, SB, and CC performed the experiments. AC and DP analyzed the data. AC, DP, and HG wrote the article. JM directed the study. All authors read and approved the manuscript.

FUNDING

The work was supported by European Union Funds (FEDER/COMPETE-Operational Competitiveness Programme—INNOVINE—ref. 311775, Enoexcel—Norte—07-0124-FEDER-000032 and INTERACT - NORTE-01-0145-FEDER-000017 - Linha VitalityWine - ON 0013), and by Portuguese national funds (FCT-Portuguese Foundation for Science

and Technology) under the project FCOMP-01-0124-FEDER-022692. AC was supported by Enoexcel—Norte—07-0124-FEDER-000032 and INTERACT - NORTE-01-0145-FEDER-000017.

ACKNOWLEDGMENTS

This work also benefited from the networking activities within the European funded COST ACTION FA1106 “QualityFruit.”

REFERENCES

- Arvidsson, S., Kwasniewski, M., Riaño-Pachón, D. M., and Mueller-Roeber, B. (2008). QuantPrime—a flexible tool for reliable high-throughput primer design for quantitative PCR. *BMC Bioinformatics* 9:465. doi: 10.1186/1471-2105-9-465
- Azuma, A., Yakushiji, H., Koshiba, Y., and Kobayashi, S. (2012). Flavonoid biosynthesis-related genes in grape skin are differentially regulated by temperature and light conditions. *Planta* 236, 1067–1080. doi: 10.1007/s00425-012-1650-x
- Bogs, J., Ebadi, A., McDavid, D., and Robinson, S. P. (2006). Identification of the flavonoid hydroxylases from grapevine and their regulation during fruit development. *Plant Physiol.* 140, 279–291. doi: 10.1104/pp.105.073262
- Boubakri, H., Poutaraud, A., Wahab, M. A., Clayeux, C., Baltenweck-Guyot, R., Steyer, D., et al. (2013). Thiamine modulates metabolism of the phenylpropanoid pathway leading to enhanced resistance to *Plasmopara viticola* in grapevine. *BMC Plant Biol.* 13:31. doi: 10.1186/1471-2229-13-31
- Bradford, M. M. (1976). A rapid and sensitive method for the quantitation of microgram quantities of protein utilizing the principle of protein-dye binding. *Anal. Biochem.* 72, 248–254. doi: 10.1016/0003-2697(76)90527-3
- Carbonell-Bejerano, P., Santa Maria, E., Torres-Perez, R., Royo, C., Lijavetzky, D., Bravo, G., et al. (2013). Thermotolerance responses in ripening berries of *Vitis vinifera* L. cv Muscat Hamburg. *Plant Cell Physiol.* 54, 1200–1216. doi: 10.1093/pcp/pct071
- Castellarin, S. D., Bavaresco, L., Falginella, L., Gonçalves, M., and Di Gaspero, G. (2012). “Phenolics in grape berry and key antioxidants,” in *The Biochemistry of the Grape Berry*, eds H. Gerós, M. Chaves, and S. Delrot (Sharjah: Bentham Science Publishers), 89–110.
- Castellarin, S. D., Gambetta, G. A., Wada, H., Krasnow, M. N., Cramer, G. R., Peterlunger, E., et al. (2016). Characterization of major ripening events during softening in grape: turgor, sugar accumulation, abscisic acid metabolism, colour development, and their relationship with growth. *J. Exp. Bot.* 67, 709–722. doi: 10.1093/jxb/erv483
- Castellarin, S. D., Matthews, M. A., Di Gaspero, G., and Gambetta, G. A. (2007a). Water deficits accelerate ripening and induce changes in gene expression regulating flavonoid biosynthesis in grape berries. *Planta* 227, 101–112. doi: 10.1007/s00425-007-0598-8
- Castellarin, S. D., Pfeiffer, A., Sivilotti, P., Degan, M., Peterlunger, E., and Gaspero, G. (2007b). Transcriptional regulation of anthocyanin biosynthesis in ripening fruits of grapevine under seasonal water deficit. *Plant. Cell Environ.* 30, 1381–1399. doi: 10.1111/j.1365-3040.2007.01716.x
- Chaves, M. M., Zarrouk, O., Francisco, R., Costa, J. M., Santos, T., Regalado, A. P., et al. (2010). Grapevine under deficit irrigation: hints from physiological and molecular data. *Ann. Bot.* 105, 661–676. doi: 10.1093/aob/mcq030
- Conde, A., Regalado, A., Rodrigues, D., Costa, J. M., Blumwald, E., Chaves, M. M., et al. (2015). Polyols in grape berry: transport and metabolic adjustments as a physiological strategy for water-deficit stress tolerance in grapevine. *J. Exp. Bot.* 66, 889–906. doi: 10.1093/jxb/eru446
- Conn, S., Curtin, C., Bezier, A., Franco, C., and Zhang, W. (2008). Purification, molecular cloning, and characterization of glutathione S-transferases (GSTs) from pigmented *Vitis vinifera* L. cell suspension cultures as putative anthocyanin transport proteins. *J. Exp. Bot.* 59, 3621–3634. doi: 10.1093/jxb/ern217
- Czemmel, S., Stracke, R., Weisshaar, B., Cordon, N., Harris, N. N., Walker, A. R., et al. (2009). The grapevine R2R3-MYB transcription factor VvMYBF1 regulates flavonol synthesis in developing grape berries. *Plant Physiol.* 151, 1513–1530. doi: 10.1104/pp.109.142059
- Dai, Z. W., Meddar, M., Renaud, C., Merlin, I., Hilbert, G., Delrot, S., et al. (2014). Long-term *in vitro* culture of grape berries and its application to assess the effects of sugar supply on anthocyanin accumulation. *J. Exp. Bot.* 65, 4665–4677. doi: 10.1093/jxb/ert489
- Deluc, L., Bogs, J., Walker, A. R., Ferrier, T., Decendit, A., Merillon, J.-M., et al. (2008). The transcription factor VvMYB5b contributes to the regulation of anthocyanin and proanthocyanidin biosynthesis in developing grape berries. *Plant Physiol.* 147, 2041–2053. doi: 10.1104/pp.108.118919
- Deluc, L. G., Decendit, A., Papastamoulis, Y., Mérial, J.-M., Cushman, J. C., and Cramer, G. R. (2011). Water deficit increases stilbene metabolism in Cabernet Sauvignon berries. *J. Agric. Food Chem.* 59, 289–297. doi: 10.1021/jf1024888
- Deluc, L. G., Quilici, D. R., Decendit, A., Grimpel, J., Wheatley, M. D., Schlau, K. A., et al. (2009). Water deficit alters differentially metabolic pathways affecting important flavor and quality traits in grape berries of Cabernet Sauvignon and Chardonnay. *BMC Genomics* 10:212. doi: 10.1186/1471-2164-10-212
- Dinis, L.-T., Bernardo, S., Conde, A., Pimentel, D., Ferreira, H., Félix, L., et al. (2016a). Kaolin exogenous application boosts antioxidant capacity and phenolic content in berries and leaves of grapevine under summer stress. *J. Plant Physiol.* 191, 45–53. doi: 10.1016/j.jplph.2015.12.005
- Dinis, L.-T., Ferreira, H., Pinto, G., Bernardo, S., Correia, C. M., and Moutinho-Pereira, J. (2016b). Kaolin-based, foliar reflective film protects photosystem II structure and function in grapevine leaves exposed to heat and high solar radiation. *Photosynthetica* 54, 47–55. doi: 10.1007/s11099-015-0156-8
- Downey, M., Harvey, J., and Robinson, S. (2003). Synthesis of flavonols and expression of flavonol synthase genes in the developing grape berries of Shiraz and Chardonnay (*Vitis vinifera* L.). *Aust. J. Grape Wine Res.* 9, 110–121. doi: 10.1111/j.1755-0238.2003.tb00261.x
- Du, Y.-L., Wang, Z.-Y., Fan, J.-W., Turner, N. C., He, J., Wang, T., et al. (2013). Exogenous abscisic acid reduces water loss and improves antioxidant defence, desiccation tolerance and transpiration efficiency in two spring wheat cultivars subjected to a soil water deficit. *Funct. Plant Biol.* 40, 494. doi: 10.1071/FP12250
- Fortunato, A. A., da Silva, W. L., and Rodrigues, F. Á. (2014). Phenylpropanoid pathway is potentiated by silicon in the roots of banana plants during the infection process of *Fusarium oxysporum* f. sp. *cubense*. *Phytopathology* 104, 597–603. doi: 10.1094/PHYTO-07-13-0203-R
- Fraga, H., Malheiro, A. C., Moutinho-Pereira, J., and Santos, J. A. (2012). An overview of climate change impacts on European viticulture. *Food Energy Secur.* 1, 94–110. doi: 10.1002/fes.314
- Francisco, R. M., Regalado, A., Ageorges, A., Burla, B. J., Bassin, B., Eisenach, C., et al. (2013). ABC1, an ATP binding cassette protein from grape berry, transports anthocyanidin 3-O-glucosides. *Plant Cell* 25, 1840–1854. doi: 10.1101/tpc.112.102152
- Fujita, A., Goto-Yamamoto, N., Aramaki, I., and Hashizume, K. (2006). Organ-specific transcription of putative flavonol synthase genes of grapevine and effects of plant hormones and shading on flavonol biosynthesis in grape berry skins. *Biosci. Biotechnol. Biochem.* 70, 632–638. doi: 10.1271/bbb.70.632
- Glenn, D. M., Cooley, N., Walker, R., Clingeleffer, P., and Shellie, K. (2010). Impact of kaolin particle film and water deficit on wine grape water use efficiency and plant water relations. *HortScience* 45, 1178–1187.
- Glenn, D. M., and Putterka, G. J. (2005). Particle films: a new technology for agriculture. *Hortic. Rev.* 31, 1–44. doi: 10.1002/9780470650882.ch1

We also thank Quinta do Vallado for gently displaying part of their vineyards to the field treatments employed in this work.

SUPPLEMENTARY MATERIAL

The Supplementary Material for this article can be found online at: <http://journal.frontiersin.org/article/10.3389/fpls.2016.01150>

- Glenn, D. M., Puterka, G. J., Drake, S. R., Unruh, T. R., Knight, A. L., Baherle, P., et al. (2001). Particle film application influences apple leaf physiology, fruit yield, and fruit quality. *J. Am. Soc. Hortic. Sci.* 126, 175–181.
- Gomez, C., Conejero, G., Torregrosa, L., Cheynier, V., Terrier, N., and Ageorges, A. (2011). *In vivo* grapevine anthocyanin transport involves vesicle-mediated trafficking and the contribution of anthoMATE transporters and GST. *Plant J.* 67, 960–970. doi: 10.1111/j.1365-313X.2011.04648.x
- Gomez, C., Terrier, N., Torregrosa, L., Vialet, S., Fournier-Level, A., Verries, C., et al. (2009). Grapevine MATE-Type proteins act as Vacuolar H⁺-dependent acylated anthocyanin transporters. *Plant Physiol.* 150, 402–415. doi: 10.1104/pp.109.135624
- Hannah, L., Roehrdanz, P. R., Ikegami, M., Shepard, A. V., Shaw, M. R., Tabor, G., et al. (2013). Climate change, wine, and conservation. *Proc. Natl. Acad. Sci. U.S.A.* 110, 6907–6912. doi: 10.1073/pnas.1210127110
- Hose, E., Steudle, E., and Hartung, W. (2000). Abscisic acid and hydraulic conductivity of maize roots: a study using cell- and root-pressure probes. *Planta* 211, 874–882. doi: 10.1007/s004250000412
- Hunter, J., De Villiers, O., and Watts, J. (1991). The effect of partial defoliation on quality characteristics of *Vitis vinifera* L. cv. Cabernet Sauvignon grapes. II. Skin color, skin sugar, and wine quality. *Am. J. Enol. Vitic.* 42, 13–18.
- Kennedy, J. A., Matthews, M. A., and Waterhouse, A. L. (2000). Changes in grape seed polyphenols during fruit ripening. *Phytochemistry* 55, 77–85. doi: 10.1016/S0031-9422(00)00196-5
- Khaleghi, E., Arzani, K., Moallemi, N., and Barzegar, M. (2015). The efficacy of kaolin particle film on oil quality indices of olive trees (*Olea europaea* L.) cv “Zard” grown under warm and semi-arid region of Iran. *Food Chem.* 166, 35–41. doi: 10.1016/j.foodchem.2014.06.006
- Kottek, M., Grieser, J., Beck, C., Rudolf, B., and Rubel, F. (2006). World map of the Köppen-Geiger climate classification updated. *Meteorol. Z.* 15, 259–263. doi: 10.1127/0941-2948/2006/0130
- Larronde, F., Kriza, S., Decendit, A., Cheze, C., Deffieux, G., and Mérillon, J. (1998). Regulation of polyphenol production in *Vitis vinifera* cell suspension cultures by sugars. *Plant Cell Rep.* 17, 946–950. doi: 10.1007/s002990050515
- Li, C., Bai, Y., Li, S., Chen, H., Han, X., Zhao, H., et al. (2012). Cloning, characterization, and activity analysis of a flavonol synthase Gene FtFLS1 and its association with flavonoid content in tartary buckwheat. *J. Agric. Food Chem.* 60, 5161–5168. doi: 10.1021/jf205192q
- Li, C., Yin, C., and Liu, S. (2004). Different responses of two contrasting *Populus davidiana* populations to exogenous abscisic acid application. *Environ. Exp. Bot.* 51, 237–246. doi: 10.1016/j.envexpbot.2003.11.001
- Lovisolo, C., Perrone, I., Carra, A., Ferrandino, A., Flexas, J., Medrano, H., et al. (2010). Drought-induced changes in development and function of grapevine (*Vitis* spp.) organs and in their hydraulic and non-hydraulic interactions at the whole-plant level: a physiological and molecular update. *Funct. Plant Biol.* 37, 98. doi: 10.1071/FP09191
- Mattivi, F., Guzzon, R., Vrhovsek, U., Stefanini, M., and Velasco, R. (2006). Metabolite profiling of grape: flavonols and anthocyanins. *J. Agric. Food Chem.* 54, 7692–7702. doi: 10.1021/jf061538c
- Matus, J. T., Loyola, R., Vega, A., Pena-Neira, A., Bordeu, E., Arce-Johnson, P., et al. (2009). Post-veraison sunlight exposure induces MYB-mediated transcriptional regulation of anthocyanin and flavonol synthesis in berry skins of *Vitis vinifera*. *J. Exp. Bot.* 60, 853–867. doi: 10.1093/jxb/ern336
- Melgarejo, P., Martínez, J. J., Hernández, F., Martínez-Font, R., Barrows, P., and Erez, A. (2004). Kaolin treatment to reduce pomegranate sunburn. *Sci. Hortic. (Amsterdam)* 100, 349–353. doi: 10.1016/j.scientia.2003.09.006
- Mori, K., Goto-Yamamoto, N., Kitayama, M., and Hashizume, K. (2007). Loss of anthocyanins in red-wine grape under high temperature. *J. Exp. Bot.* 58, 1935–1945. doi: 10.1093/jxb/erm055
- Mori, K., Sugaya, S., and Gemma, H. (2005). Decreased anthocyanin biosynthesis in grape berries grown under elevated night temperature condition. *Sci. Hortic. (Amsterdam)* 105, 319–330. doi: 10.1016/j.scientia.2005.01.032
- Ou, C., Du, X., Shellie, K., Ross, C., and Qian, M. C. (2010). Volatile compounds and sensory attributes of wine from Cv. Merlot (*Vitis vinifera* L.) grown under differential levels of water deficit with or without a kaolin-based, foliar reflectant particle film. *J. Agric. Food Chem.* 58, 12890–12898. doi: 10.1021/jf102587x
- Pfaffl, M. W. (2001). A new mathematical model for relative quantification in real-time RT-PCR. *Nucleic Acids Res.* 29, e45. doi: 10.1093/nar/29.9.e45
- Pillet, J., Berdeja, M., Guan, L., and Delrot, S. (2015). “Berry response to water, light and heat stresses,” in *Grapevine in a Changing Environment: A Molecular and Ecophysiological Perspective*, eds H. Geros, M. M. Chaves, H. M. Gil, and S. Delrot (Chichester, UK: John Wiley & Sons).
- Pirie, A., and Mullins, M. (1977). Interrelationships of sugars, anthocyanins, total phenols and dry weight in the skin of grape berries during ripening. *Am. J. Enol. Vitic.* 28, 204–209.
- Reid, K. E., Olsson, N., Schlosser, J., Peng, F., and Lund, S. T. (2006). An optimized grapevine RNA isolation procedure and statistical determination of reference genes for real-time RT-PCR during berry development. *BMC Plant Biol.* 6:27. doi: 10.1186/1471-2229-6-27
- Seckin, B., Sekmen, A. H., and Türkán, İ. (2009). An enhancing effect of exogenous mannitol on the antioxidant enzyme activities in roots of wheat under salt stress. *J. Plant Growth Regul.* 28, 12–20. doi: 10.1007/s00344-008-9068-1
- Shellie, K. (2015). Foliar reflective film and water deficit increase anthocyanin to soluble solids ratio during berry ripening in merlot. *Am. J. Enol. Vitic.* 66, 348–356. doi: 10.5344/ajev.2015.14121
- Shellie, K., and Glenn, D. M. (2008). Wine grape response to foliar particle film under differing levels of preveraison water stress. *HortScience* 43, 1392–1397.
- Song, J., Shellie, K. C., Wang, H., and Qian, M. C. (2012). Influence of deficit irrigation and kaolin particle film on grape composition and volatile compounds in Merlot grape (*Vitis vinifera* L.). *Food Chem.* 134, 841–850. doi: 10.1016/j.foodchem.2012.02.193
- Spayd, S. E., Tarara, J. M., Mee, D. L., and Ferguson, J. C. (2002). Separation of sunlight and temperature effects on the composition of *Vitis vinifera* cv. Merlot berries. *Am. J. Enol. Vitic.* 53, 171–182.
- Stoop, J. M. H., and Pharr, D. M. (1993). Effect of different carbon sources on relative growth rate, internal carbohydrates, and mannitol 1-oxidoreductase activity in celery suspension cultures. *Plant Physiol.* 103, 1001–1008.
- Teixeira, A., Eiras-Dias, J., Castellarin, S. D., and Gerós, H. (2013). Berry phenolics of grapevine under challenging environments. *Int. J. Mol. Sci.* 14, 18711–18739. doi: 10.3390/ijms140918711
- Verries, C., Guiraud, J.-L., Souquet, J.-M., Vialet, S., Terrier, N., and Ollé, D. (2008). Validation of an extraction method on whole pericarp of grape berry (*Vitis vinifera* L. cv. Shiraz) to study biochemical and molecular aspects of flavan-3-ol synthesis during berry development. *J. Agric. Food Chem.* 56, 5896–5904. doi: 10.1021/jf800028k
- Yamane, T., Jeong, S. T., Goto-Yamamoto, N., Koshita, Y., and Kobayashi, S. (2006). Effects of temperature on anthocyanin biosynthesis in grape berry skins. *Am. J. Enol. Vitic.* 57, 54–59.
- Zarrouk, O., Francisco, R., Pinto-Marijuan, M., Brossa, R., Santos, R. R., Pinheiro, C., et al. (2012). Impact of irrigation regime on berry development and flavonoids composition in Aragonez (Syn. Tempranillo) grapevine. *Agric. Water Manag.* 114, 18–29. doi: 10.1016/j.agwat.2012.06.018
- Zhang, G., Cui, Y., Ding, X., and Dai, Q. (2013). Stimulation of phenolic metabolism by silicon contributes to rice resistance to sheath blight. *J. Plant Nutr. Soil Sci.* 176, 118–124. doi: 10.1002/jpln.201200008
- Zhou, L., Xu, H., Mischke, S., Meinhardt, L. W., Zhang, D., Zhu, X., et al. (2014). Exogenous abscisic acid significantly affects proteome in tea plant (*Camellia sinensis*) exposed to drought stress. *Hortic. Res.* 1, 14029. doi: 10.1038/hortres.2014.29
- Conflict of Interest Statement:** The authors declare that the research was conducted in the absence of any commercial or financial relationships that could be construed as a potential conflict of interest.
- Copyright © 2016 Conde, Pimentel, Neves, Dinis, Bernardo, Correia, Gerós and Moutinho-Pereira. This is an open-access article distributed under the terms of the Creative Commons Attribution License (CC BY). The use, distribution or reproduction in other forums is permitted, provided the original author(s) or licensor are credited and that the original publication in this journal is cited, in accordance with accepted academic practice. No use, distribution or reproduction is permitted which does not comply with these terms.



Plasticity of the Berry Ripening Program in a White Grape Variety

Silvia Dal Santo^{1†}, Marianna Fasoli^{1,2†}, Stefano Negri^{1†}, Erica D'Incà¹, Nazareno Vicenzi³, Flavia Guzzo¹, Giovanni Battista Tornielli¹, Mario Pezzotti¹ and Sara Zenoni^{1*}

¹ Department of Biotechnology, University of Verona, Verona, Italy, ² E & J Gallo Winery, Modesto, CA, USA, ³ Unione Consorzi Vini Veneti DOC, Verona, Italy

Grapevine (*Vitis vinifera* L.) is considered one of the most environmentally sensitive crops and is characterized by broad phenotypic plasticity, offering important advantages such as the large range of different wines that can be produced from the same cultivar, and the adaptation of existing cultivars to diverse growing regions. The uniqueness of berry quality traits reflects complex interactions between the grapevine plant and the combination of natural factors and human cultural practices which leads to the expression of wine *typicity*. Despite the scientific and commercial importance of genotype interactions with growing conditions, few studies have characterized the genes and metabolites directly involved in this phenomenon. Here, we used two large-scale analytical approaches to explore the metabolomic and transcriptomic basis of the broad phenotypic plasticity of Garganega, a white berry variety grown at four sites characterized by different pedoclimatic conditions (altitudes, soil texture, and composition). These conditions determine berry ripening dynamics in terms of sugar accumulation and the abundance of phenolic compounds. Multivariate analysis unraveled a highly plastic metabolomic response to different environments, especially the accumulation of hydroxycinnamic and hydroxybenzoic acids and flavonols. Principal component analysis (PCA) revealed that the four sites strongly affected the berry transcriptome allowing the identification of environmentally-modulated genes and the plasticity of commonly-modulated transcripts at different sites. Many genes that control transcription, translation, transport, and carbohydrate metabolism showed different expression depending on the environmental conditions, indicating a key role in the observed transcriptomic plasticity of Garganega berries. Interestingly, genes representing the phenylpropanoid/flavonoid pathway showed plastic responses to the environment mirroring the accumulation of the corresponding metabolites. The comparison of Garganega and Corvina berries showed that the metabolism of phenolic compounds is more plastic in ripening Garganega berries under different pedoclimatic conditions.

OPEN ACCESS

Edited by:

Matthew Gillham,
University of Adelaide, Australia

Reviewed by:

Jin Chen,

Michigan State University, USA
Carlos Marcelino Rodriguez Lopez,
University of Adelaide, Australia

*Correspondence:

Sara Zenoni
sara.zenoni@univr.it

[†]These authors have contributed equally to this work.

Specialty section:

This article was submitted to
Plant Physiology,
a section of the journal
Frontiers in Plant Science

Received: 22 December 2015

Accepted: 20 June 2016

Published: 12 July 2016

Citation:

Dal Santo S, Fasoli M, Negri S, D'Incà E, Vicenzi N, Guzzo F, Tornielli GB, Pezzotti M and Zenoni S (2016) Plasticity of the Berry Ripening Program in a White Grape Variety. *Front. Plant Sci.* 7:970.
doi: 10.3389/fpls.2016.00970

INTRODUCTION

The quality traits of grapevine (*Vitis vinifera* L) berries for wine production reflect the outcome of complex interactions between the plant and its environment. In viticulture, the latter is defined as *terroir*, and it represents a combination of natural factors, such as climate, altitude, exposure, the geological characteristics of the soil, and the microbial community, together with human cultural

and production practices, which influence the expression of the berry traits and wine quality (White et al., 2009). The combination of a vine and a terroir is unique and is the basis of the term *typicity*, which describes the specific qualitative properties of wines (van Leeuwen et al., 2004). Typicity not only refers to geographically referenced wines but also includes collective taste memory, which has matured for a long time (Vaudour, 2002).

Grapevine is considered one of the most environmentally sensitive crops (Hannah et al., 2013) and it is characterized by broad phenotypic plasticity, i.e., the capacity of a single genotype to express different phenotypes under different environmental conditions (Bradshaw, 1965; Sultan, 2000). Phenotypic plasticity generates variability among berries, clusters, and vines within a vineyard (Dai et al., 2011) and it is often considered a disadvantage in viticulture because it can cause uneven maturity and large inter-seasonal variability (Clingeffer, 2010). However, genetic variability and plasticity also offer important benefits, such as the large range of different wines that can be produced from the same cultivar, and the adaptation of existing cultivars to specific growing regions (Dai et al., 2011). These phenotypic variations can be attributed to the effect of the environment on the expression of genes influencing plastic traits, mainly through transcriptomic and epigenomic reprogramming (Shaw et al., 2014).

Despite the scientific and commercial importance of genotype interactions with growing conditions, few studies have characterized the genes and metabolites directly involved in such phenotypic plasticity. Previously, we reported that $\geq 5\%$ of the transcriptome of the red berry cultivar Corvina was differentially modulated during berry ripening when comparing plants trained with different systems and rootstocks at sites with diverse pedoclimatic conditions representing a well-known viticultural area in the north of Italy (Dal Santo et al., 2013a). This suggests that the interaction between genotype (grapevine cultivar) and its growing conditions has a profound impact on berry gene expression, possibly affecting ripening and therefore wine quality traits. More recently, Anesi et al. (2015) identified different vine-growers on the basis of the unique metabolic profile of Corvina berries, and Young et al. (2015) described the plasticity of berry carotenoid metabolism in the white variety Sauvignon Blanc under different types of light exposure. These studies revealed few examples of a clear relationship between the plasticity of the berry metabolome and transcriptome, and highlighted the complexity of studying grapevine plasticity in open-field grown plants over multiple growing seasons. Under these conditions, the vines are simultaneously challenged by different external stimuli and are subjected to seasonal waves so that the assignment of a plastic change to a given viticultural practice and/or environmental factor can only be achieved using tailored statistical analysis.

Garganega is a white berry variety mainly cultivated in the Soave production area, which extends into the hills to the east of the Verona province, Italy (Calò et al., 2002). The soil of this production region has both volcanic and alluvial origins, and wines from Garganega berries cultivated in this area are characterized by complexity and longevity with a typical mineral tang. The typicity of Soave wines thus reflects the unique

interaction between the Garganega genotype and environmental factors such as the soil origin and composition, and the climatic conditions.

Here, we investigated metabolomic and transcriptomic plasticity during the ripening of Garganega berries representing a single clone cultivated at four sites characterized by different pedoclimatic conditions. To reduce the complexity as far as possible, we selected vineyards trained with similar agricultural practices, but different soil origins and altitudes. We found that the phenotype of the Garganega berries was highly plastic in different environments, indeed more plastic than ripening Corvina berries, particularly concerning the accumulation of phenolic compounds.

MATERIALS AND METHODS

Vineyard Features and Environmental Parameters

Vitis vinifera cv. Garganega, clone 4, provided by Vivai Coperativi di Rauscedo (VCR) samples were collected from four vineyards during the 2013 growing season at the same time of day (~ 10.30 a.m.). The parral training system rows were north-south oriented, and SO_4 was used as the rootstock. For all vineyards, the planting density was 3000–4000 vines/ha, with vines 10–15 years old. The vineyards were located in different areas of the Soave production region featuring diverse growing conditions, such as altitude and soil composition (Table 1). Meteorological data were kindly provided by the Cantina di Soave (Soave, Verona, Italy). Temperature and monthly precipitation (mm) measurements, and the number of rainy days, were obtained from recording stations using the Green Planet Platform (3a S.r.l., Torino, Italy) in the four vineyard sites studied in this project (Colognola ai Colli, Sarmazza di Monteforte d'Alpone, Soave and Ronca'; Supplementary Figure 1). Average daily temperatures were used to define the heat summation per month. Standard soil texture and chemical analysis was conducted by Enocentro Di Vassanelli C. & C. S.r.l. (Verona, Italy).

Sample Collection

Garganega berries were collected biweekly at four ripening stages, starting from veraison (the onset of ripening) and finishing at harvest (August 22nd, September 4th, September 17th, and September 30th 2013). For three vineyards (AP, VP, VH2), berries were harvested at the so-called “perfect ripening” stage, corresponding to a total soluble solids (TSS) content of 18.5° Brix and pH 3.3. This was never achieved by the VH1 berries. The $^{\circ}$ Brix of the berry juice was determined using a digital DBR35 refractometer (Giorgio Bormac S.r.l., Carpi, Italy). A single biological replicate was created by pooling about 30 berries collected from clusters of different vines, along one central vineyard row of an average of 70 vines. As the ripening variability within one single cluster is very large, we payed attention on collecting berries also from different position in the clusters. We repeated the same procedure for the other two biological replicates, but each time we collected berries from different clusters of different vines within the same row. This strategy allowed the collection of three biological replicates that represent

TABLE 1 | Description of collection sites.

Vineyard	Location in the soave area	Vineyard site	Altitude (m a.s.l.) ^a	Type of soil (% sand, clay, silt)	CaCO ₃ (% w/w) ^b	Vineyard training system	Rows facing direction	Vines/hectare	Vineyard Age (y) ^c	Rootstock ^d
AP	Colognola ai Colli	45°26'12.90"N, 11°10'30.10"E	84	32.5, 19.9, 47.6	total 22.8 active 16.8	Parral	North-south	3000	10–15	SO ₄
VP	Sarmazza (Monteforte d'Alpone)	45°26'5.27"N, 11°19'2.18"E	32	5.7, 7.5, 86.8	total 3.8 active 2.1	Parral	North-south	4000	10–15	SO ₄
VH1	Ronca'	45°30'9.99"N, 11°17'1.92"E	437	31.4, 10.0, 58.6	total 3.0 active 4.7	Parral	North-south	3000	10–15	SO ₄
VH2	Soave	45°25'28.86"N, 11°12'27.32"E	277	32.4, 4.6, 62.9	total 2.1 active 3.8	Parral	North-south	3500	10–15	SO ₄

^aMeters above sea level.^bDry matter.^cYears. ^dSO, Selection Oppenheim.

almost the entire variability of the vineyard. The same sampling collection procedure was applied at each sampling time point for each of the four vineyards, thus the experiment entailed the collection and analysis of 48 berry samples (four vineyards, four stages, three replicates). We removed the seeds from the berries of each biological replicates and the obtained pericarps were powdered with an automatic mill grinder (IKA®-Werke GmbH & Co. KG, Germany). The obtained frozen powder was used for both transcriptomic and metabolomic analyses.

RNA Extraction and Microarray Analysis

Total RNA was extracted from ~200 mg frozen berry powder using the Spectrum™ Plant Total RNA kit (Sigma-Aldrich, St. Louis, Missouri, USA) as previously described (Fasoli et al., 2012). A NimbleGen microarray 090818_Vitus_exp_HX12 chip (Roche, NimbleGen Inc., Madison, Wisconsin, USA) was hybridized with 5 µg total RNA per sample according to the manufacturer's instructions. The chip contained probes matching 29,549 predicted grapevine genes (<http://ddlab.sci.univr.it/FunctionalGenomics/>) representing ~98.6% of the genes predicted in the V1 annotation of the 12x grapevine genome (<http://srs.ebi.ac.uk/>), as well as 19,091 random probes used as negative controls. Arrays that meet the recommended quality metrics exhibit a background (averaged fluorescence intensity level of empty cells and random probes) of 450–500. Therefore, a fluorescence intensity value of 500 was used as the threshold to define gene expression, and averaged values across the entire dataset lower than 500 were considered to represent minimal/absent expression and were excluded from our analysis.

Reverse Transcription (RT) and Real Time qPCR

One microgram of extracted RNA was treated with 2 unit (U) of Turbo DNase (TURBO DNA-free kit—Ambion) according to the instructions provided with the commercial kit. DNase-treated RNA was then used for cDNA synthesis using the SuperScript III Reverse Transcriptase kit (Invitrogen) following the producer's indications. In order to assess if the cDNA had been properly produced, an amplification with primers designed on the 3' UTR of an Ubiquitin coding gene (VIT_16s0098g01190;

UbiFor 5'-TCTGAGGCTTCGTGGTGGTA-3' and UbiRev 5'-AGGCCTGCATAACATTTGCG-3') was performed.

Real Time qPCR was performed using GoTaq® Green Master Mix kit (Promega) to amplify a specific region of target genes (C4H, trans-cinnamate 4-monoxygenase, VvC4H-F: 5'-AA AGGGTGGGCAGTTCAGTT-3' and VvC4H-R: 5'-GGGG GGTGAAAGGAAGATAT-3'; MYB14, transcription factor MYB14, VvMYB14-F: 5'-TCTGAGGCCGGATATCAAAC-3' and VvMYB14-R: 5'-GGGACGCATCAAGAGAGTGT-3'; ANR, anthocyanidin reductase, VvANR-F: 5'-CAATACCAGTGTTC CTGAGC-3' and VvANR-R: 5'-AAACTGAACCCCTCTTCA C-3'; LAR1, leucoanthocyanidin reductase 1, VvLAR1-F: 5'-CA CATGCATGCGATTAGTCC-3' and VvLAR1-R: 5'-ACGAAT TTCACCCATGTTAC-3'). Reaction mix was composed of 1x GoTaq® Green Master Mix, 200 nM of each primer and 20 ng of cDNA in a final volume of 25 µl. The reaction was carried out on a StepOnePlus™ Real Time PCR System (Applied Biosystems) using the following cycling conditions: 95°C hold for 2 min followed by 40 cycles at 95°C for 15 s, 55°C for 30 s, 60° for 30 s, and 95°C for 15 s. Non-specific PCR products were identified by the dissociation curves. Amplification efficiency was calculated from raw data using LingRegPCR software (Ramakers et al., 2003). The mean normalized expression (MNE)-value was calculated for each sample referred to the ubiquitin expression according to the Simon equation (Simon, 2003). Standard error (SE)-values were calculated according to Pfaffl et al. (2002).

Statistical Analysis of the Transcriptome Dataset

Principal component analysis (PCA) was applied to the entire transcriptome dataset using SIMCA P+ v13 (Umetrics, San José, California, USA). Loadings of the first and second principal components were ordered, and genes within the first and last percentiles were extracted to investigate their expression profiles over time in the different vineyards. Multiclass significance analysis of microarrays (SAM) was carried out using TMeV v4.8 (<http://www.tm4.org/>) with a false discovery rate (FDR) of 0.01%, to extract genes that were significantly modulated during ripening in all four vineyards. The differentially expressed genes

were then filtered by applying a fold-change thresholds of ≥ 2 or ≤ -2 . To identify shared and specific transcriptomic ripening programs in the four vineyards, the selected differentially expressed genes (FDR 0.01%, $|FC| \geq 2$) were represented in a Venn diagram (Venny v2.0, <http://bioinfogp.cnb.csic.es/tools/venny/>). The differentially expressed genes were screened by calculating the coefficients of variation (CV) at the four developmental stages in each vineyard, and then the standard deviation (SD) among the four calculated CVs. This allowed to rank the shared genes by a quantitative measure of the intra-vineyard and inter-vineyard variability of expression during ripening. Transcripts scoring the highest standard deviations (the top 50 genes) were defined as the most plastic genes under our experimental conditions.

Functional Category Assignments and GO Enrichment Analysis

All grapevine transcripts were annotated against the V1 version of the 12x draft annotation of the grapevine genome. Gene Ontology annotations were assigned using the BiNGO v2.3 plug-in tool in Cytoscape v2.6 (<http://www.cytoscape.org/>) with PlantGOslim categories. Overrepresented PlantGOslim categories were identified using a hypergeometric test with a significance threshold of 0.05, after Benjamini and Hochberg correction with a FDR of 0.01 (Klipper-Aurbach et al., 1995).

Visualization of Grapevine Transcriptome Data

Information from the Nimblegen microarray platform was integrated using MapMan software (Thimm et al., 2004) as described for the Array Ready Oligo Set *Vitis vinifera* (grape), the AROS V1.0 Oligo Set (Operon, Qiagen, Hilden, Germany), and the Gene-Chip® *Vitis vinifera* Genome Array (Affymetrix Inc., Santa Clara, California, USA; Rotter et al., 2009). Mapping information and the annotation of the carotenoid biosynthesis and catabolic pathways were modified based on Young et al. (2012).

Extraction, Analysis, and Identification of Non-Volatile Metabolites

For each sample, 300 mg of frozen berry powder was extracted in three volumes of cold methanol acidified with 0.1% formic acid. After mixing, the samples were sonicated for 15 min at 4°C and then centrifuged at 16,000 $\times g$ for 10 min at 4°C. The supernatants were analyzed by reversed-phase high-performance liquid chromatography (RP-HPLC) coupled to electrospray ionization mass spectrometry (RP-HPLC-ESI-MS) or a diode array detector (RP-HPLC-DAD) after dilution (1:2 or 2:3, respectively) in LC-MS-grade water and passage through a 0.2- μm filter.

RP-HPLC analysis was carried out using a Beckman Coulter (Brea, California, USA) Gold 127 HPLC System equipped with a C18 guard column (7.5 \times 2.1 mm, 5 μm particle size) and an Alltech (Nicholasville, Kentucky, USA) RP C18 column (150 \times 2.1 mm, 3 μm particle size). Two solvents were used: 0.5% formic acid and 5% acetonitrile in water (solvent A) and

acetonitrile (solvent B). The gradient was set as follows: 0–10% B in 2 min, 10–20% B in 10 min, 20–25% B in 2 min, 25–70% B in 7 min, isocratic for 5 min, 70–90% B in 1 min, isocratic for 4 min, 90–0% B in 1 min, and 20 min equilibration. For each sample, 20 μL was injected at a flow rate of 0.2 mL min $^{-1}$. The HPLC instrument was coupled on-line with an Esquire 6000 ion trap mass spectrometer equipped with an ESI source (Bruker Daltonik GmbH, Bremen, Germany). MS data were collected using the Esquire Control v5.2 software, and processed using the Esquire Data Analysis v3.2 software (both provided by Bruker Daltonik GmbH). The instrument was set to induce positive and negative ionization in alternating mode. Mass spectra were recorded in the range 50–3000 m/z with a target mass of 400 m/z. MS/MS and MS³ mass spectra were recorded in positive and negative ionization modes in the range 50–3000 m/z with a fragmentation amplitude of 1 V. Nitrogen was used as the nebulizing gas (50 psi, 350°C) and drying gas (10 L min $^{-1}$). Helium was used as the collision gas. The vacuum pressure was 1.4 $\times 10^{-8}$ bar. Additional parameters: capillary source 4500 V; end plate offset –500 V; skimmer: 40 V; cap exit 121 V.

RP-HPLC-DAD analysis was carried out using a Beckman Coulter Gold 126 Solvent Module and Gold 168 Diode Array Detector. HPLC was carried out as above, with a larger injection volume of 100 μL . The wavelength range was 190–600 nm. Data were collected and analyzed using 32 Karat v7.0 (Beckman Coulter). Specific wavelengths were considered to represent the following classes of compounds: 280 nm (flavan-3-ols and their oligomers), 320 nm (hydroxycinnamic acid derivatives), and 350 nm (flavonols).

Metabolites were identified by comparing their retention times, m/z-values and MSⁿ fragmentation patterns with those of commercial standards in our in-house library. UV/vis spectra recorded by RP-HPLC-DAD were also used to support the LC-MS identification. Fragmentation patterns collected in online databases such as MassBank (<http://www.massbank.jp>) or reported in the literature were also considered, especially when no authentic standard compounds were available. Neutral losses of 132, 146, and 162 Da were considered diagnostic of the loss of pentose, deoxyhexose, and hexose sugar, respectively.

LC-MS Data Processing and Statistical Analysis

LC-MS chromatograms were converted to netCDF files for peak alignment and area extraction using MZmine (<http://mzmine.sourceforge.net/>). The resulting matrix was analyzed using SIMCA v.13.0 (Umetrix AB, Umeå, Sweden). Pareto scaling was applied to all analytical methods. Unsupervised PCA was used to identify the major clusters defined by the samples prior to supervised partial least squares discriminant analysis (PLS-DA) and orthogonal partial least squares discriminant analysis (OPLS-DA and O2PLS-DA) setting the classes according to the ripening stage for each vineyard location. PLS-DA models were validated using a permutation test (200 permutations) and the corresponding OPLS-DA/O2PLS-DA models were cross-validated by analysis of variance (ANOVA) with a threshold of $p < 0.01$.

Accession Numbers

Grape berry microarray expression data are available in the Gene Expression Omnibus under the series entry GSE75565 (<http://www.ncbi.nlm.nih.gov/geo/query/acc.cgi?acc=GSE75565>). The datasets supporting the Garganega metabolome analysis are included in this article and its supplementary files. The Corvina metabolomics data are available in the Metabolights database under the series entry MTBLS39.

RESULTS

Pedoclimatic Conditions Influence the Garganega Berry Ripening Process

Vitis vinifera cv. Garganega clone four berries were harvested from four different vineyards surrounding the Soave area, one of the most important wine production macro-areas in the province of Verona, Italy (Figure 1A). The vineyards were selected to maximize differences in environmental conditions (altitude and soil type) while minimizing differences in agricultural practices (training system, orientation of the rows, planting layout, vineyard age, and rootstock type; Table 1). The selected vineyards were characterized by a hill (VH1 and VH2) or plain (AP and VP) altitudinal position, and by an alluvial (AP) or volcanic (VP, VH1, and VH2) soil type (Table 1 and Figures 1A,B). The alluvial area (AP) featured almost twice the proportion of clay particles in the soil compared to the volcanic sites, among which the plain site (VP) was characterized by a silty soil with the lowest percentage of sand. VH1 and VH2 had similar soil textures, despite being located at different altitudes. The calcium carbonate component (total and active) was much lower in the VP, VH1, and VH2 vineyard sites than in the more calcareous alluvial AP site (Table 1). This is typical for “ando soils,” which developed on volcanic ash. Meteorological parameters were recorded, and the daily temperature data showed that more heat accumulated (heat summation per month) in the hillside areas in July, August, and September, but overall the heat summation was similar across all four vineyards (Supplementary Figure 1). Rainfall data showed greater variability among the areas albeit with no significant differences in terms of mm of rain per year, however VH2 was a more rainy area during the growing period (April 1st to October 31st in the Northern Hemisphere). Berry samples were harvested from all vineyards on the same day and three biological replicates were taken at each of the four developmental stages (Figure 1B). The TSS content was verified by measuring °Brix values (Figure 1C). Although the sampling date was aligned to the first developmental stage, the dynamics of TSS accumulation were unique to each vineyard. Interestingly, the two hillside vineyards showed the most divergent behavior: VH2 showed a steady increase in the TSS content whereas VH1 scored lowest for the accumulation of TSS.

Unraveling the Metabolome of Garganega Ripening Berry

Untargeted RP-HPLC-ESI-MS analysis was used to characterize the Garganega berry metabolome at each of the four vineyards (AP, VP, VH1, VH2) at four ripening stages, focusing on

moderately polar metabolites such as phenolic compounds. Data processing revealed 267 signals in negative ionization mode (Figure 2). The comparison of the fragmentation patterns with an in-house library of authentic standards and literature data led to the putative identification of 64 metabolites mainly representing the flavan-3-ols and their oligomers, phenolic acids, flavonol, and dihydroflavonol glycosides (Figure 2, Supplementary File 1). The major flavan-3-ol monomers were catechin (the most abundant) followed by epicatechin and two epigallocatechin isomers, whereas different types of oligomers were detected, including dimeric and trimeric procyanidins and prodelphinidins. Two galloylated derivatives were also identified as epicatechin gallate and procyanidin dimer gallate, and one compound was tentatively identified as a glycosilated procyanidin dimer (Maldini et al., 2009).

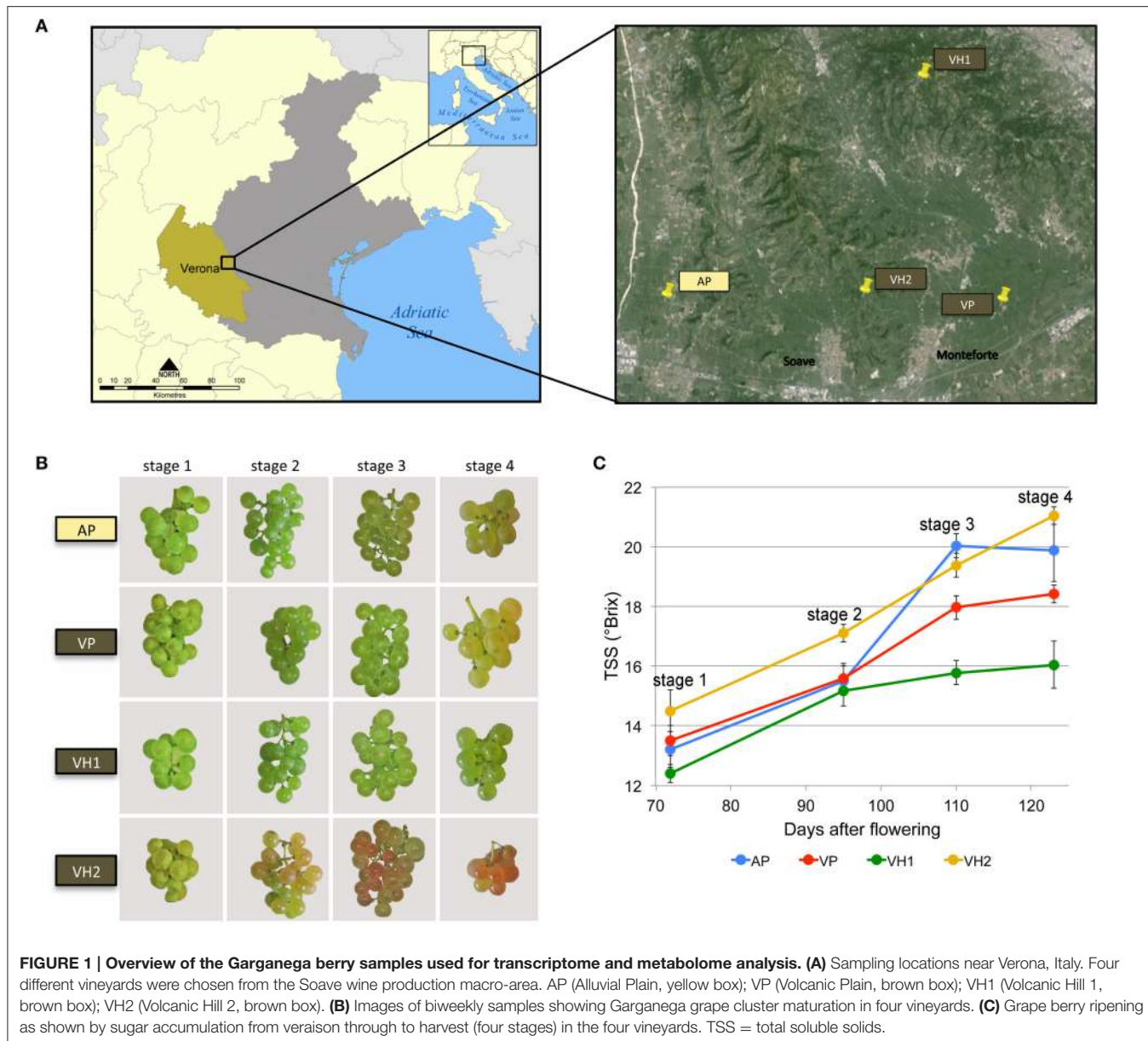
Another large group of metabolites corresponded to the hydroxycinnamic acids. Within this group, caffeoyltartaric acid was the most abundant, followed by coumaric and ferulic acid glycosides and tartaric acid esters (coutaric and fertaric acid). Minor signals were also assigned to the hexose esters of three benzoic acids (syringic, vanillic, and gallic acid).

Among the flavonols, the glycosides of quercetin, kaempferol, isorhamnetin, and myricetin were detected, as well as those of the dihydroflavonols, dihydroquercetin, and dihydrokaempferol. Other minor compounds were putatively identified, including two isomers of resveratrol glucoside, the phenylethanoid hydroxytyrosol glucoside, and an N-conjugated glycoside of tryptophan.

The Four Vineyards Show Different Trends in the Accumulation of Specific Metabolites during Ripening

The accumulation of metabolites among the four vineyards during ripening was initially compared by inspecting the entire data matrix by unsupervised multivariate PCA. Two partially overlapping clusters were observed for the VP and AP samples, whereas the VH1 and VH2 samples formed two independent clusters (Figure 3A). This clustering suggested that the two plain vineyards (AP, VP) shared similar metabolomes during the earlier stages of ripening, with differences emerging only during the last stage. In contrast, the two hillside vineyards (VH1, VH2) were characterized by distinct metabolomes from the earlier stages. These trends were confirmed by the comparison of phenolic compounds in the samples, revealing that the plain and hillside vineyards were characterized by different metabolomes throughout the ripening process (Figure 3B). These findings suggested that the Garganega berry metabolome is modulated during ripening according to the location of the vineyards.

In order to find metabolites that characterized the various groups of samples, we applied a supervised O2PLS-DA approach (Figure 4). The plain vineyards were analyzed together due to their similar behavior in the PCA, and this revealed an enrichment of metabolites (especially hydroxycinnamates) during ripening, with the dihydroflavonols and flavonols becoming particularly characteristic of the AP vineyard at stage 4 (Figures 4A,B). The hillside vineyard VH1 showed the



opposite trend, with many metabolites (particularly flavan-3-ols and their oligomers and phenolic acids) decreasing at the end of ripening. Dihydroflavonols and flavonols peaked during the third ripening stage and decreased toward the end of ripening, which is generally indicative of poor ripening and suggests that an unknown event inhibited the ripening process (**Figures 4C,D**). Flavan-3-ols and their oligomers characterized the first two ripening stages in the hillside vineyard VH2, but the dihydroflavonols and flavonols peaked during the third stage as described above (**Figures 4E,F**).

The Garganega Transcriptome Dataset Also Reveals Differences between Vineyards

Following microarray hybridization, the pericarp transcriptome dataset of the ripening Garganega berries was inspected by

PCA, confirming the consistency of the biological replicates (**Figure 5A**). PC1 explained 27.6% of the total variability and was attributed to differences in the ripening stage among the samples. Despite the small difference in PC1 at the first sampling point, the dynamics of ripening differed among the vineyards at the level of the transcriptome (**Figure 5A**). In particular, VH1 was characterized by a clear interruption of the ripening process, whereas VH2 reached a more advanced ripening stage. These differences corresponded to the increase in °Brix values in the VH1 and VH2 vineyards (**Figure 1C**) and strongly suggested that VH1 never reached the “full ripening” stage.

Differences among the vineyards were highlighted by visualizing the average trend of the first and last percentiles of the PC1 loadings (**Figure 5B**). As expected, the averaged trends of genes representing the first percentile increased during ripening, whereas those of genes representing the last percentile decreased.

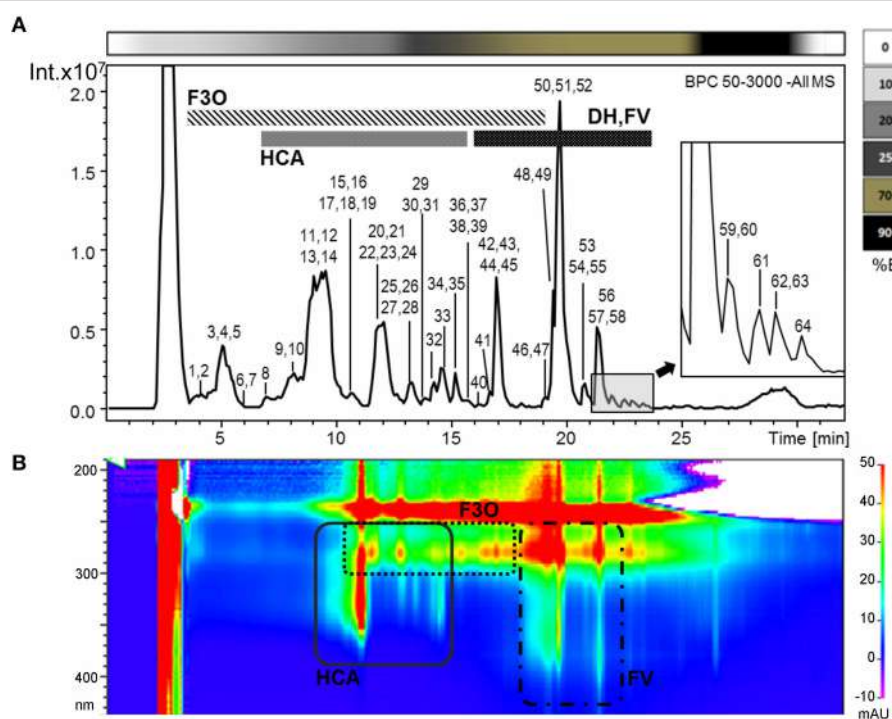


FIGURE 2 | (A) Base peak chromatogram of a Garganega methanolic extract recorded in negative ionization mode during RP-HPLC-ESI-MS analysis. The peaks numbers correspond to the metabolites identified in the Supplementary File 1 (column A) **(B)** Bidimensional RP-HPLC-DAD chromatogram recorded within the wavelength range 190–600 nm. F3O (flavan-3-ols and oligomers), HCA (hydroxycinnamic acid derivatives), DH (dihydroflavonol glycosides), FV (flavonol glycosides). The upper bar refers to the percentage of solvent B within the mobile phase.

In both cases, it was possible to rank the final ripening level reached in each vineyard on the basis of the averaged gene expression level at the final time point (VH2 > AP > VP > VH1). Interestingly, there was a larger difference in the expression level of the last percentile of the PC1 loadings compared to the first percentile of the PC1 loadings at the first time point (**Figure 5B**). This could explain the slight difference among samples at the first time point revealed by PC1 (**Figure 5A**), suggesting that the onset of ripening was predominantly defined by the downregulation rather than the upregulation of genes. We found that 55 genes among the positively-correlating PC1 loadings (26.96%) are already described as putative master regulators of ripening in five red berry varieties (Palumbo et al., 2014). In contrast, many photosynthesis-related genes were found among the negatively-correlating PC1 loadings, confirming that the suppression of photosynthesis is one of the main events driving the berry toward maturation (Fasoli et al., 2012; Supplementary File 2).

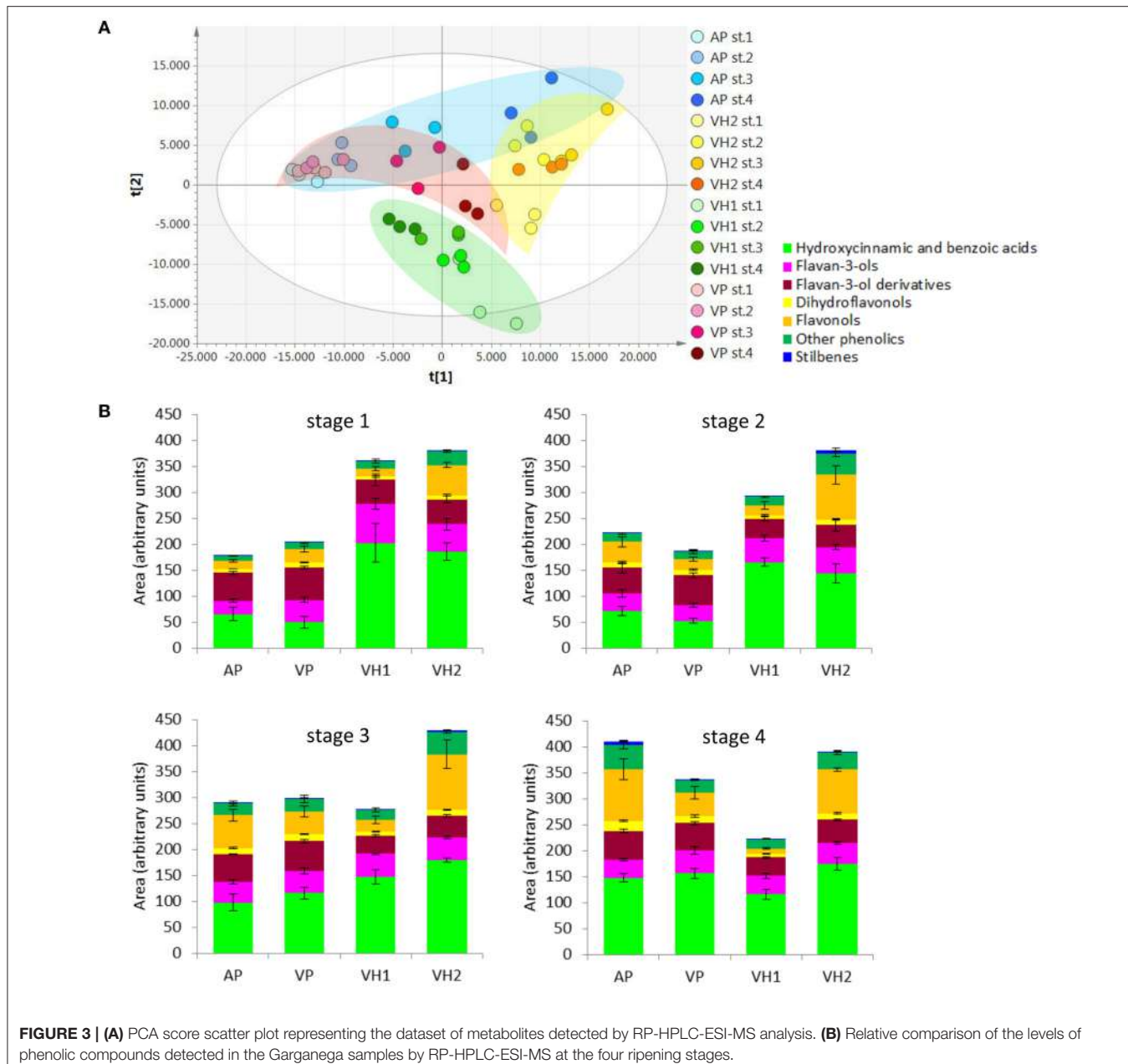
PC2 explained 16.5% of the total variability (**Figure 5A**) and mainly describes differences between vineyards. Such differences were already evident at the first time point, and showed that VH2 and VP were the two most distant conditions. Interestingly, these two vineyards followed opposite trends along PC2 during ripening, resulting in well-separated final stages. In contrast, only minor variations along PC2 were observed for the AP and VH1 vineyards during ripening (**Figure 5A**). These findings are well-supported by the averaged trends of the first and last percentiles of the PC2 loadings (**Figure 5C**). Major changes and

opposing trends in gene expression were observed for VP and VH2, whereas AP and VH1 showed different averaged levels of gene expression but little change during ripening. Interestingly, the PC2 first percentile loadings were expressed at a higher level overall than the last percentile loadings, suggesting the first percentile made the major contribution to the variability described by PC2.

The functional categories of the PC2 first percentile genes indicated that Carbohydrate metabolism, DNA, and RNA metabolic processes (transport, surveillance, and degradation) and Transport were key processes (Supplementary File 2). Only a few genes related to Secondary metabolism were found, including three encoding cinnamyl alcohol dehydrogenases (CADs). In contrast, the PC2 negative loadings were rich in Transcription factors, Pentatricopeptide repeat (PPR) proteins, and proteins related to Cellular homeostasis (Supplementary File 2).

Differences in Gene Expression Reflect Different Characteristics of the Four Vineyards

The plasticity of the ripening Garganega berry transcriptome in the four different vineyards was investigated by multiclass statistical analysis of microarrays (SAM) within each group of vineyard samples. A total of 12,931 transcripts were significantly modulated (Supplementary File 3) and, of these, 6272 scored



a fold change ($|FC| \geq 2$) in at least one condition. This revealed that vineyard VH2 featured the highest number of modulated genes (4782) and vineyard VH1 the lowest number (1224). In vineyards AP and VP, the number of differentially modulated genes with a $|FC| \geq 2$ was 1808 and 1441, respectively (Supplementary File 3 and **Figure 6A**). Interestingly, all four vineyards were characterized by a higher number of downregulated genes than upregulated genes (**Figure 6A**), confirming that berry ripening predominantly involves gene suppression rather than activation (Palumbo et al., 2014).

The significantly modulated genes were either specific or common among the four different vineyards (Supplementary

File 3 and **Figure 6B**). The VH2 vineyard featured the greatest number of specifically modulated genes, i.e., 56.48% of the VH2 modulated genes and 43.04% of all the modulated genes (**Figure 6B**). These genes were particularly enriched in functional categories related to stress, such as Death, Cell death, and Response to stress, as well as the categories Protein modification and Cell communication (Supplementary Figure 2). The 2701 genes specifically modulated in vineyard VH2 also included those encoding a large number of R proteins, other disease resistance proteins, and heat shock proteins, as well as 25 glutathione-S-transferases (GSTs), 16 CADs, and many terpene synthases (TPSs) involved in the production of distinct volatile compounds. Up to 90 genes

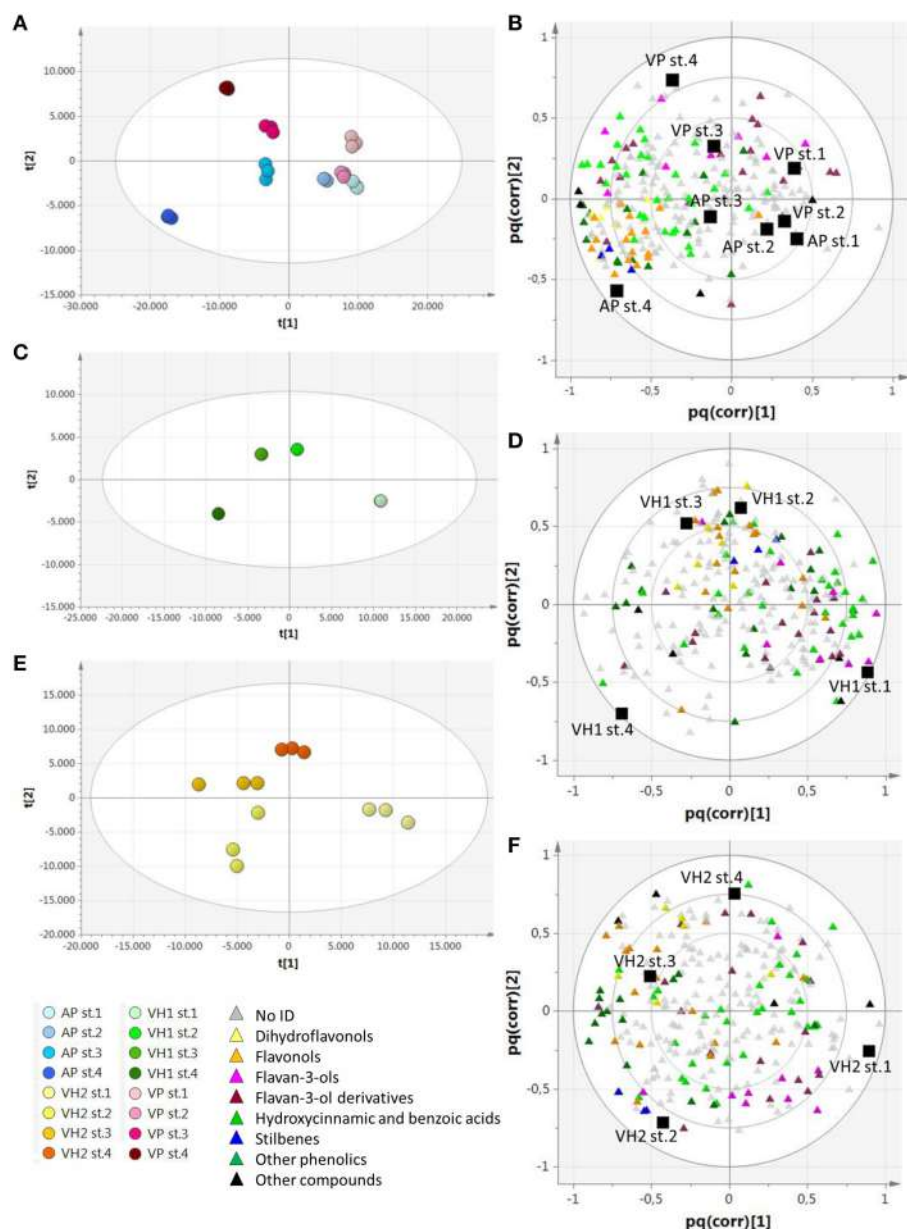


FIGURE 4 | O2PLS-DA score plots and correlation loading plots for the metabolites detected by RP-HPLC-ESI-MS analysis. (A,B): AP and VP samples; (C,D): VH1 samples; (E,F): VH2 samples. Sample clusters and groups of metabolites are depicted in different colors as shown in the legend.

encoding PRR-containing proteins were also found in this class (Supplementary File 3). PRR-containing proteins are thought to be involved in RNA metabolism (Barkan and Small, 2014) and show a high level of plasticity in Corvina berries (Dal Santo et al., 2013a). Many transporters, including 13 ABC transporters (Çakır and Kilickaya, 2013) and signal transduction-related transcripts, were found among the VH2-specific modulated genes. Interestingly, genes encoding nine histone proteins, a histone acetyltransferase (HAC1), and three histone-lysine N-methyltransferases were specifically modulated in the VH2 vineyard during berry ripening,

suggesting that histone modifications could play an important role in the plasticity of the Garganega berry transcriptome. Some of the VH2-specific transcripts also represented enzymes involved in carotenoid metabolism, i.e., *VvAAO3*, *VvLECY1*, *VvLBCY1*, *VvZEP2*, and *VvBCH1* (Young et al., 2012).

The transcriptional plasticity of carotenoid-related genes in ripening Garganega berries was investigated in more detail by screening the 12,931 modulated transcripts (Supplementary File 3) and visualizing the genes involved in carotenoid synthesis and catabolism (Young et al., 2012) using the MapMan heat

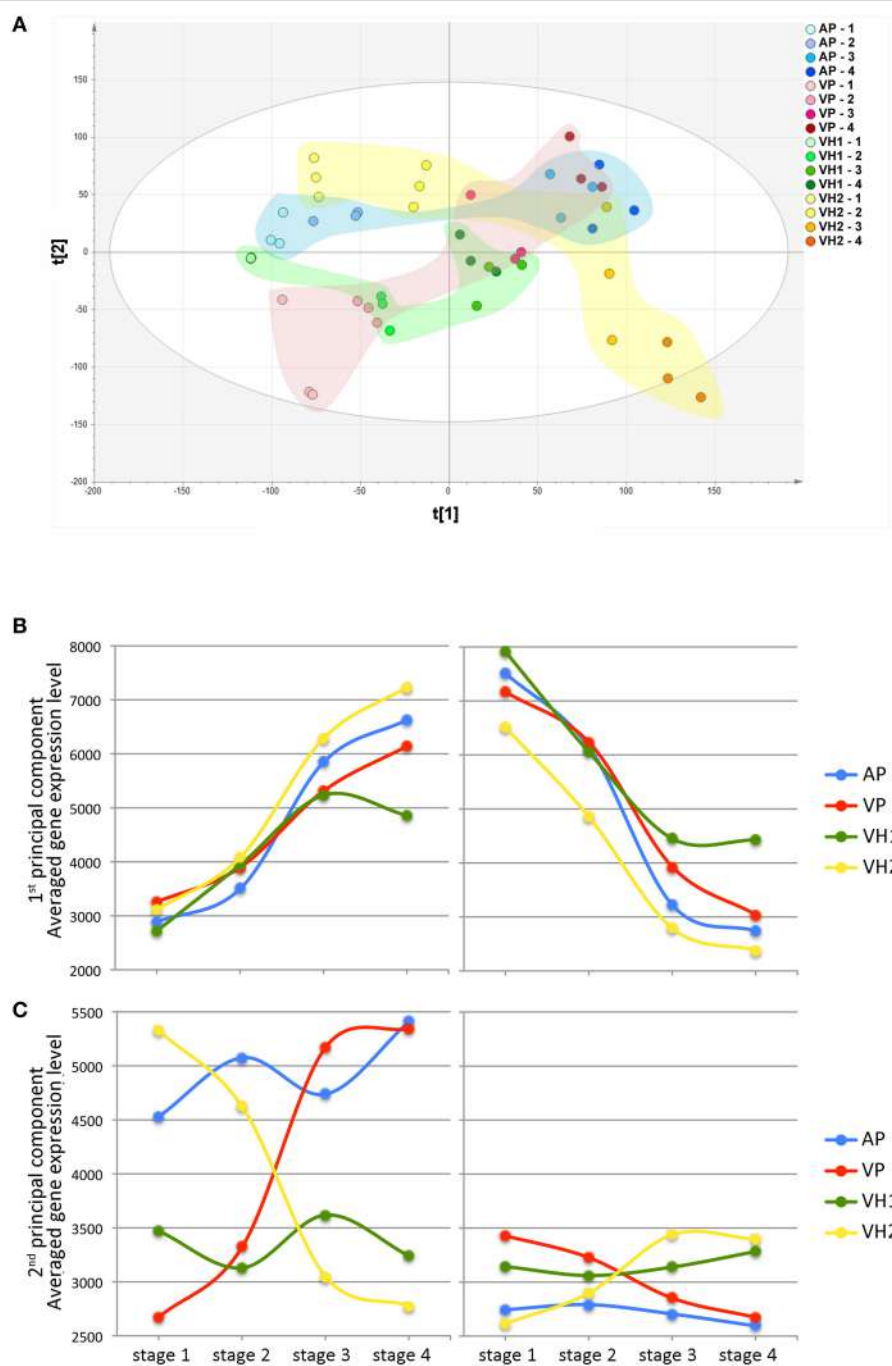
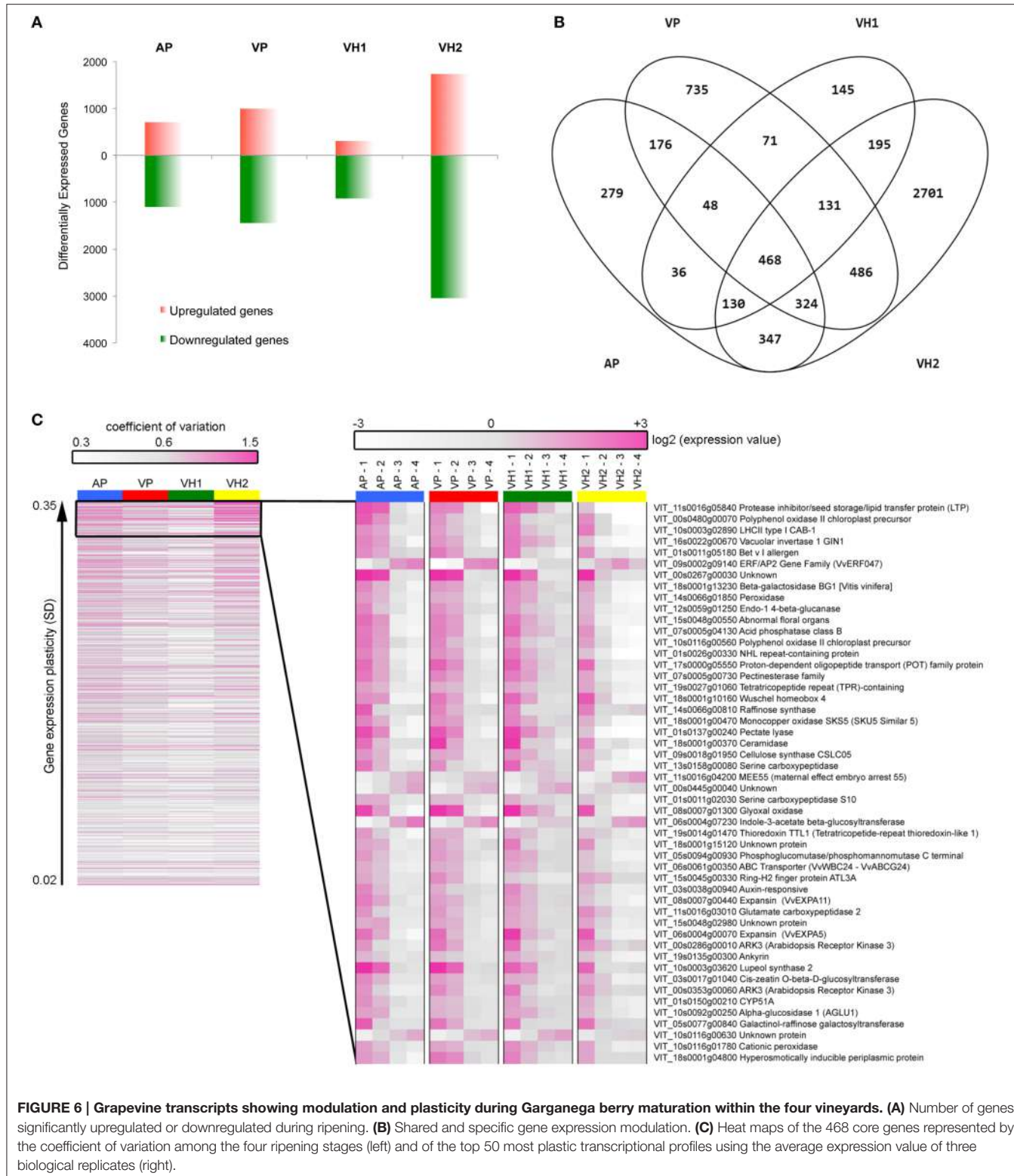


FIGURE 5 | Global gene expression trends in Garganega berries cultivated at four locations during ripening. (A) Variables and scores scatterplot of the PCA model ($R^2X = 0.748$, $Q^2cum = 0.582$) applied to the entire dataset. The expression profiles of genes positively (left) and negatively (right) correlated to the first (B) and second (C) principal components were selected within the first (positive) and the last (negative) percentile of each of the component loadings.

map representation (Supplementary Figure 3). Many genes in the carotenoid pathway were significantly modulated in one or more of the vineyards: VH2 featured 22 such genes, the highest number, VP and AP (both located on plains) featured eight and seven, respectively, and VH1 featured five. Genes representing all branches of the pathway were expressed in VH2, including the

common pathway to lycopene, the lutein branch, the β -carotene branch, abscisic acid (ABA) biosynthesis and degradation, and the cleavage of mature carotenoids to form apocarotenoids and strigolactone (Supplementary Figure 3). Only one carotenoid-related gene was significantly expressed in all four vineyards during berry ripening, i.e., *VvNCED3* representing the most



important enzyme in the ABA biosynthesis pathway (Sun et al., 2010).

VH1 featured the lowest number of specifically modulated genes, i.e., 11.85% of the VH1 modulated genes and 2.31%

of all the modulated genes (Figure 6B). Interestingly, GO analysis revealed the enrichment of the categories Secondary metabolic processes and Biosynthetic processes (Supplementary Figure 2). In particular, 15 stilbene synthases

(which synthesize resveratrol) and other genes representing the phenylpropanoid/flavonoid pathway were found among the VH1-specific genes (Supplementary File 3).

VP featured 735 specifically-modulated genes, i.e., 30.13% of the VP modulated genes and 11.72% of all the modulated genes (**Figure 6B**). GO analysis revealed the enrichment of the categories Death, Cell death, Lipid metabolic processes, and Cell communication (Supplementary Figure 2). Indeed, many genes involved in fatty acid biosynthesis, as well as those encoding R proteins, disease resistance proteins, and transporters, were found among the VP-specific modulated genes (Supplementary File 3).

Finally, AP featured 279 specifically-modulated genes, i.e., 15.43% of the AP modulated genes and 4.44% of all the modulated genes (**Figure 3B**). No significant GO category enrichment was revealed by BINGO analysis.

The Commonly Modulated Portion of the Transcriptome Contains Plastic Transcripts

A core of 468 genes (7.46% of all modulated genes as shown in **Figure 6B**) was found to represent the shared portion of the transcriptome, which was modulated in ripening Garganega berries regardless of the vineyard (Supplementary File 3). Interestingly, 65 core genes were also defined as switch genes, which are proposed to drive berries of five Italian red varieties from vegetative growth into the ripening phase (Palumbo et al., 2014). BINGO analysis revealed significant enrichment of the categories Photosynthesis, Generation of precursor metabolites and energy, and Carbohydrate metabolic processes (Supplementary Figure 2). Indeed, five genes representing the photosystem light harvesting complexes were found among the shared transcripts as well as many genes involved in specific carbohydrate metabolic processes, such as galactose, starch, and sucrose metabolism. The acidic vacuolar invertase *VvGIN1* and the sugar symporter *VvSUC2* were found among the common core genes (Supplementary File 3), and their expression increased simultaneously with post-veraison sugar accumulation (Davies and Robinson, 1996; Davies et al., 1999; Afoufa-Bastien et al., 2010).

After veraison, auxin levels decline sharply (Davies et al., 1997). Accordingly, many of the commonly modulated genes we identified are involved in auxin biosynthesis, transport, and signaling (Supplementary File 3), and others are related to cytokinins, ethylene, brassinosteroids, and salicylic acid. Furthermore, 39 of the genes were annotated as transcription factors, three of which have already been described as putative master regulators of berry ripening: LBD18, Myb TKI1, and *VvNAC11* (Palumbo et al., 2014). Finally, 52 transporters were significantly modulated in all four vineyards, indicating that intracellular transport plays a crucial role during the ripening of Garganega berries (Supplementary File 3).

We next analyzed the expression profiles of all 468 shared core genes to evaluate their transcriptional plasticity during berry development in the four vineyards. The heat map in **Figure 6C** (left panel) clearly shows that vineyard VH2 displayed the highest variability among the four developmental stages,

followed by vineyards AP and VP, whereas the dynamic range of gene expression in vineyard VH1 was more attenuated. We next focused on the top 50 genes scored by SD (**Figure 6C**, right panel). Most of these genes were downregulated, whereas only five were upregulated in ripening berries. The latter encoded ERF/AP2 transcription factor 47 (*VvERF047*), the maternal-effect embryo arrest protein 55, an indole-3-acetate β -glucosyltransferase, and two unknown proteins. The patterns of downregulation showed that the ripening process was delayed in vineyard VH1, was similar in the two vineyards located on plains (AP and VP) and was accelerated in VH2, confirming the °Brix trends (**Figure 1C**). For example, the expression of the photosystem light harvesting complex LHCII and the vacuolar invertase *VvGIN1* declined sharply after veraison in VH2 but declined gently from veraison to harvest in the other three vineyards. Many genes in the Cell wall metabolism category were found among the most plastic common genes expressed as described above, including a β -galactosidase, an endo-1,4- β -glucanase, a pectinesterase, a pectate lyase, the CSLC05 type cellulose synthase, and two expansins. Notably, the two expansin genes (*VvEXPAs* and *VvEXPAl*) have already been reported as markers of the veraison phenological phase (Dal Santo et al., 2013b) confirming that berry ripening was more advanced in VH2 than the other vineyards.

A Comparison between Garganega and Corvina Transcriptome Plasticity

In a previous study we evaluated the berry transcriptome plasticity of the red berry variety Corvina clone 48, through three consecutive growth years cultivated in 11 different vineyards in the Verona area (Dal Santo et al., 2013a). In order to compare the plasticity within red and white berry transcriptome during ripening, we chose four out of the 11 vineyards, basing our decision on the location (i.e., Soave and Valpolicella wine growing regions) and on the berry ripening stage (Supplementary File 4). This Corvina 36-sample reduced dataset (four vineyards, three developmental stages, three biological replicates) was then processed using the same statistical procedure described above for the Garganega berry transcriptome. We found that 2894 Corvina genes were significantly modulated (Supplementary Figure 4 and Supplementary File 5), representing 46.14% of all modulated genes in Garganega berries. This suggested that the white variety transcriptome could be modified to a greater extent by the ripening process and/or by the growing conditions compared to the red variety transcriptome.

We next compared the developmentally-regulated portion of each transcriptome focusing on the environmentally-sensitive genes, i.e., those genes expressed in one of the four selected vineyards. In the Corvina cultivar we identified 2021 genes representing 69.83% of all modulated Corvina genes whereas in the Garganega cultivar we identified 3860 genes representing 61.51% of all modulated Garganega genes (Supplementary Figure 4). Therefore, despite the significant difference in the total number of modulated genes during ripening, the vineyard-specific portion of the transcriptome was approximately the same size in the red and white berry

varieties. Specifically, the Garganega and Corvina varieties shared 409 genes (Supplementary File 6), which were particularly enriched in the GO categories Carbohydrate metabolic processes, Secondary metabolic processes, Lipid metabolic processes, and Photosynthesis (Supplementary Figure 5). These categories are therefore likely to be the most strongly influenced by the environment and may encompass the largest number of environmentally-sensitive genes.

The Phenylpropanoid Pathway is More Plastic in the White Berry Variety

The relative transcriptomic and metabolomic plasticity of Garganega and Corvina berries during ripening was determined by comparing gene expression and metabolite accumulation in the context of the phenylpropanoid/flavonoid pathway. The gene expression and phenolic profiles for each variety at veraison (stage 1), mid-maturity (stage 2), and in fully-ripe berries (stage 3; Supplementary File 4) are represented in **Figures 7A,B**, respectively.

Several differences between the varieties and locations were highlighted by this analysis. Some of the transcriptional trends changes were also confirmed by semi-quantitative Real Time RT-PCR analysis (Supplementary Figure 6). Garganega vineyard VH1 was characterized by a slight decline in the levels of hydroxycinnamic and hydroxybenzoic acids and the corresponding gene expression levels, whereas these compounds accumulated in the other three vineyards and the corresponding genes were induced. In particular, the caffeate 3-O-methyltransferase COMT2 (VIT_18s0072g00920) increased in vineyard AP, and the trans-cinnamate 4-monoxygenase VvC4H (VIT_06s0004g08150), which catalyzes the biosynthesis of p-coumarate from cinnamate, remained strongly expressed in vineyards VP and VH2 during ripening. The Garganega berries accumulated different amounts of these metabolites in different vineyards, mirroring the expression profiles of the corresponding genes. In contrast, a similar small decline in hydroxycinnamic and hydroxybenzoic acid levels was associated with Corvina berry ripening in all four vineyards, consistent with the overall downregulation of genes involved in the synthesis of these compounds. The hydroxycinnamic and hydroxybenzoic acid profiles differed substantially between the two varieties, and were more plastic in the white variety.

There was no substantial difference in resveratrol/stilbene accumulation in Garganega berries, even though stilbene synthases were upregulated in vineyard VH2, and the transcription factor VvMYB14 (VIT_07s0005g03340), which regulates the stilbene synthase gene family (Holl et al., 2013), was upregulated in vineyards VP and VH2. Stilbene accumulation correlated well with gene expression in Corvina berries, especially in the CC and PSP vineyards where the averaged expression level of stilbene synthase genes increased toward the final ripening stage.

The flavonol and dihydroflavonol content remained stable during the maturation of Garganega berries in vineyard VH1, whereas in the other vineyards a general increase in these compounds was observed. Flavonol synthase genes were

upregulated during berry ripening in the VH2 vineyard and, to a lesser extent, in vineyards AP and VP. In contrast, flavonols and dihydroflavonols accumulated in a similar manner in the four Corvina vineyards. This may reflect the slight but consistent increase in the averaged expression level of flavonol synthase and flavonoid glucosyltransferase genes during ripening.

The flavan-3-ols and their oligomers declined marginally in both cultivars and in the different vineyards, especially VH1 which featured the strongest reduction among the Garganega vineyards. This correlated with the pronounced decline in the expression of *VvANR* (anthocyanidin reductase, VIT_00s0361g00040) in Corvina berries, and *VvLAR2* (leucoanthocyanidin reductase 2, VIT_17s0000g04150) in Garganega berries, but did not correlate with the expression of *VvLAR1* (leucoanthocyanidin reductase 1, VIT_01s0011g02960), which remained high at the third ripening stage in the Corvina vineyard PM and the Garganega vineyards VP and VH1. Interestingly, the expression profiles of the two MYB transcription factors regulating this branch of the flavonoid pathway differed in the two varieties, i.e., *VvMYBPA1* was expressed more strongly in Garganega berries, whereas *VvMYBPA2* was expressed more strongly in Corvina berries.

DISCUSSION

We used two large-scale analytical approaches to explore metabolomic and transcriptomic changes during the ripening of Garganega berries, a *V. vinifera* white berry variety. In order to understand the molecular basis of the environmental impact on berry ripening, four vineyards were selected to maximize differences in environmental conditions and to minimize differences due to agricultural practices such as the training system, orientation of the rows, planting layout, vineyard age, and rootstock.

The four selected growing sites belong to the same production area and were chosen to ensure diverse environmental parameters such as soil origin, texture, and composition. The soils in three of the vineyards were characterized by a low percentage of sand and a low concentration of calcium carbonate, as expected given their volcanic origin, and the fourth was alluvial in origin with a high proportion of clay. Vineyards at different altitudes were chosen to maximize the environmental variability. However, despite the distance of 400 m between the lowest (32 m above sea level) and highest (437 m above sea level) vineyards, the meteorological parameters recorded at the four sites revealed little difference in heat unit accumulation and rainfall during the 2013 growing season. Even so, the number of rainy days during the pre-blooming period (i.e., pre-flowering period) was greater at the VH2 site and there was a higher temperature during July, August, and September. This may have contributed to the specific ripening behavior we observed. Indeed, the pedoclimatic conditions and other uncontrolled variables strongly influenced the ripening dynamics at each site in terms of sugar accumulation and the synthesis of phenolic compounds. The most divergent ripening dynamics were

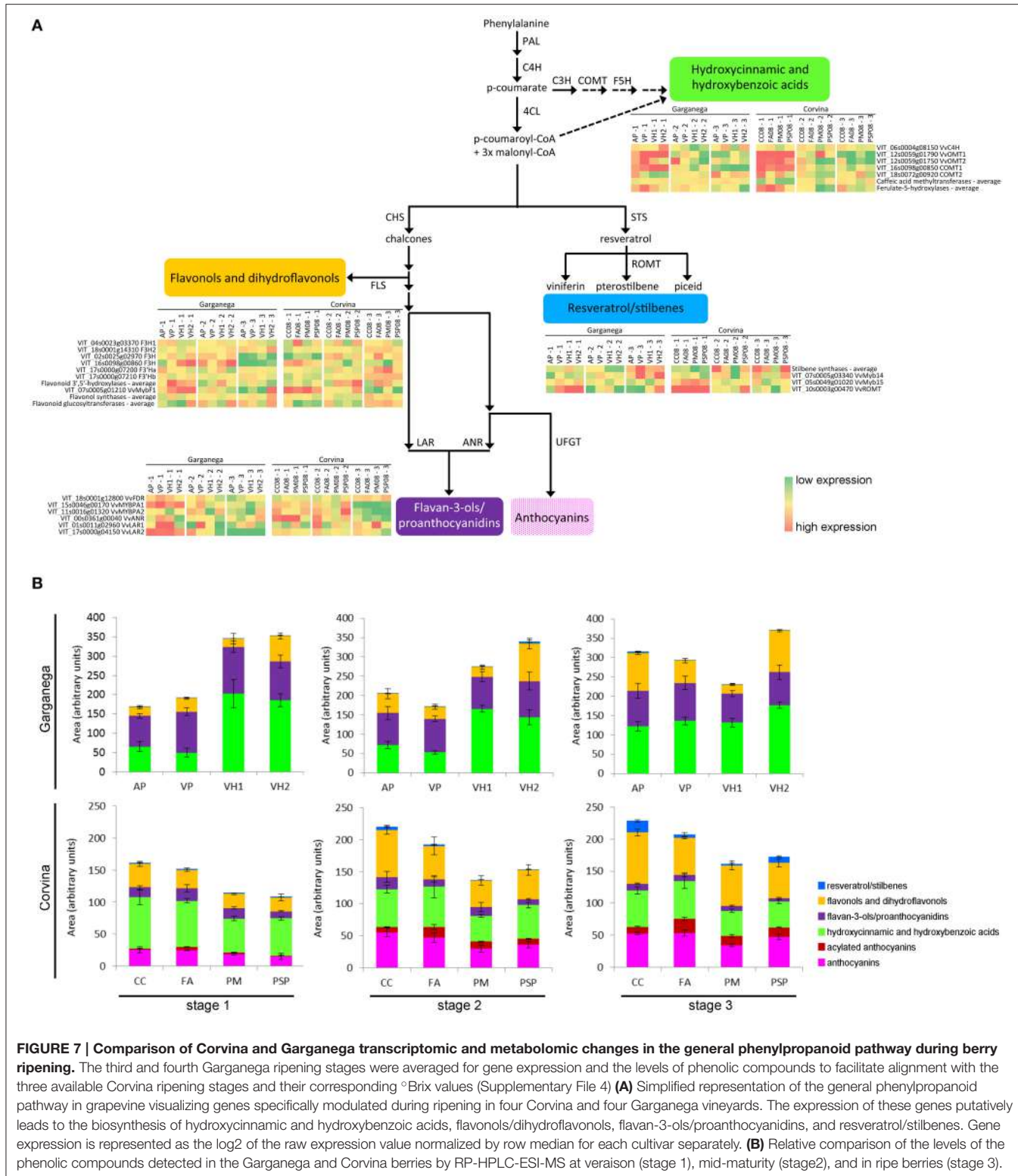


FIGURE 7 | Comparison of Corvina and Garganega transcriptomic and metabolomic changes in the general phenylpropanoid pathway during berry ripening. The third and fourth Garganega ripening stages were averaged for gene expression and the levels of phenolic compounds to facilitate alignment with the three available Corvina ripening stages and their corresponding °Brix values (Supplementary File 4) **(A)** Simplified representation of the general phenylpropanoid pathway in grapevine visualizing genes specifically modulated during ripening in four Corvina and four Garganega vineyards. The expression of these genes putatively leads to the biosynthesis of hydroxycinnamic and hydroxybenzoic acids, flavonols/dihydroflavonols, flavan-3-ols/proanthocyanidins, and resveratrol/stilbenes. Gene expression is represented as the log2 of the raw expression value normalized by row median for each cultivar separately. **(B)** Relative comparison of the levels of the phenolic compounds detected in the Garganega and Corvina berries by RP-HPLC-ESI-MS at veraison (stage 1), mid-maturity (stage 2), and in ripe berries (stage 3).

characterized by an early decline in sugar accumulation (VH1) and a consistent high sugar accumulation rate (VH2).

The phenolic fraction of the Garganega berry metabolome was investigated by HPLC-MS. The phenolic composition of

Garganega berries was found to be similar to that reported for another white berry cultivar, Albariño blanco (Di Lecce et al., 2014). One particularly relevant feature was the presence of a compound putatively identified as a myricetin derivative, a

flavonol that is normally absent from *V. vinifera* white grapes (Flamini, 2013). The quantitation of berry metabolites during ripening showed that the levels of the various classes of phenolic compounds, especially hydroxycinnamic acids and flavonols, were highly variable at veraison in the different vineyards, and that they changed in different and unpredictable ways during the subsequent stages. In the plain vineyards, the relative levels of hydroxycinnamic acid increased rapidly from stage 1 (veraison) to stage 4 (maturity), whereas the relative levels of flavonols increased in three of the four vineyards. Overall these results suggest that the phenolic fraction in Garganega berries is highly responsive to the pedoclimatic conditions encompassed by our study.

The investigation of transcriptomic data by PCA revealed that the four growing sites strongly affected the dynamics of the ripening berry transcriptome. The distribution of samples based on the first two components showed that PC1 describes the changes associated with berry development, as seen in previous transcriptome surveys (Lijavetzky et al., 2012; Pastore et al., 2013). This evidence is supported by the presence of many “switch” genes, representing putative master regulators of the shift from immature to mature growth (Palumbo et al., 2014), among the positive loadings of PC1, i.e., those upregulated during ripening. Furthermore, the presence of several photosynthesis genes among the negative loadings of PC1, i.e., those downregulated during ripening, reflected the progressive shutdown of photosynthesis associated with berry ripening, and further supports the directional distribution of samples on PC1 during the transcriptome changes underlying general berry development. This interpretation suggests that, despite the minor differences in PC1-values among samples collected at veraison, the ripening process was distinct in the four vineyards, with the greatest differences observed between high-altitude sites. Indeed, VH1 berries accumulated the lowest levels of TSS at harvest and yielded the lowest PC1-values, whereas VH2 berries, the richest in sugars, achieved the highest PC1-values at harvest. The distribution of samples along PC2 highlighted different and sometimes divergent behaviors accounting for the highly plastic responses of Garganega berries to the pedoclimatic conditions at the four growing sites. Interestingly, by focusing on the first and last percentiles of the PC2 loadings, we found that such plastic responses included the differential expression of genes mainly belonging to the same functional categories already assigned to plastic genes modulated in Corvina berries, e.g., DNA/RNA metabolic processes, Transport, Carbohydrate metabolism, Cellular processes, and Homeostasis (Dal Santo et al., 2013a). The large number of genes in the DNA/RNA metabolic process and transcriptional regulation categories in both cultivars strongly supports a key role for transcriptional and translational control in the transcriptomic plasticity of ripening berries (Dal Santo et al., 2013a). PC2 also contained several genes involved in carbohydrate metabolism, in particular genes encoding enzymes required for anaerobic metabolism (e.g., pyruvate decarboxylase, alcohol dehydrogenase, and aldehyde dehydrogenase), and those related to glycolysis and malic acid metabolism (e.g., pyruvate kinase,

phosphoenolpyruvate carboxylase, malate dehydrogenase, and malic enzyme).

Although we did not observe a clear relationship between the genes and enzymes responsible for malate metabolism, the direct influence of environmental conditions on malate metabolism was extensively characterized in early studies (Lakso and Kliewer, 1975, 1978) and also more recent studies (Sweetman et al., 2009, 2014) of berries ripening under diverse temperature regimes. The differential expression of genes involved in malate metabolism in Garganega berries grown at different sites may therefore reflect the distinct light and temperature conditions at each location.

Our investigation allowed to explore plasticity by identifying genes specifically modulated in each of the four vineyards. This revealed that VH2, characterized by accelerated ripening, featured the largest number of specifically modulated genes, especially several abiotic and biotic stress response genes whose expression was often associated with the berry maturation process (Tornielli et al., 2012) Secondary metabolism responded strongly to the environment particularly at the two high-altitude vineyards. Genes representing terpenoid, lignin, and carotenoid metabolism, as well as genes encoding GSTs, were all specifically modulated in vineyard VH2, whereas stilbene metabolism was most strongly affected in vineyard VH1.

The plasticity of phenylpropanoid metabolism is a well-known feature of grape berries and this confers many of the wine quality traits that represent specific terroirs (Teixeira et al., 2013). A strong correlation between phenylpropanoid accumulation and the expression of corresponding genes has recently been reported in Corvina berries (Dal Santo et al., 2013a; Anesi et al., 2015). The analysis of Sauvignon Blanc berries has likewise shown that carotenoid metabolism is highly responsive to the microclimate (Young et al., 2015). The analysis of carotenoid-related genes in Garganega berries revealed highly divergent expression profiles in the four vineyards, supporting the plastic behavior of this class of compounds which function to protect the photosynthetic membranes, promote the synthesis of ABA and strigolactone, and to generate volatile flavor/aroma compounds (Young et al., 2012).

The relative plasticity of Garganega berries at different sites was compared to the previously reported transcriptomic and metabolomic plasticity of Corvina berries (Dal Santo et al., 2013a; Anesi et al., 2015). We compared the number of differentially expressed genes detected when Corvina berries were ripened under four different environmental conditions and identified the environmentally sensitive portion of the developmentally regulated transcriptome. This revealed that the proportion of specifically modulated genes is similar in Corvina and Garganega berries, and many plastic genes are shared between the two varieties. We then focused on genes and metabolites involved in the phenylpropanoid/flavonoid pathway. The Garganega berries revealed vineyard-related trends in the accumulation or depletion of metabolites, whereas Corvina samples from all four sites showed highly similar metabolic trends during ripening, with a slight decline in the level of hydroxycinnamic acids and an increase in the levels of anthocyanins, flavonols, and stilbenes. The unique behavior of the Garganega cultivar, which increased (AP, VP), reduced (VH1), or maintained (VH2) the total level of phenolic compounds during ripening, together

with the greater metabolomic diversity at veraison compared to Corvina berries, strongly suggests that Garganega is much more plastic than Corvina in terms of the accumulation of phenolic compounds during ripening in different environments. Metabolic differences between the two varieties were also strongly supported by the consistency of the expression profiles of phenylpropanoid/flavonoid related genes during berry maturation.

In conclusion, this study provides an overview of the transcriptomic and metabolomic responses to different growing sites in Garganega, a white grapevine variety cultivated in the eastern hills of the Verona province. The typicity of Garganega wines depends on the unique effect of the growing area and climatic conditions on the grapevine genotype. This variety is therefore an excellent model to dissect the molecular mechanisms underlying *terroir*-dependent quality traits in wines and to improve the interpretation of phenotypic plasticity in grapevine. The sensitivity of phenylpropanoid/flavonoid metabolism to the Garganega growing site supports previous data based on the analysis of red cultivars highlighting the important role of phenolic plasticity in the investigation of plasticity in general. In this context, our results could help to define how different varieties interact with the environment to promote the accumulation of phenolic compounds, and thus help with the development of strategies to cope environmental changes or to enhance the phenolic composition of wines.

AUTHOR CONTRIBUTIONS

SDS and MF interpreted the bioinformatics data, coordinated the study, and wrote the manuscript. SN carried out the metabolomics analysis and helped to draft the manuscript. ED performed the microarray experiments and the qPCR analysis. MP contributed with supervision and coordination expertise. FG helped to interpret the metabolomics data and draft the

REFERENCES

- Afoufa-Bastien, D., Medici, A., Jeauffre, J., Coutos-Thevenot, P., Lemoine, R., Atanassova, R., et al. (2010). The *Vitis vinifera* sugar transporter gene family: phylogenetic overview and macroarray expression profiling. *BMC Plant Biol.* 10:245. doi: 10.1186/1471-2229-10-245
- Anesi, A., Stocchero, M., Dal Santo, S., Commisso, M., Zenoni, S., Ceoldo, S., et al. (2015). Towards a scientific interpretation of the terroir concept: plasticity of the grape berry metabolome. *BMC Plant Biol.* 15:191. doi: 10.1186/s12870-015-0584-4
- Barkan, A., and Small, I. (2014). Pentatricopeptide repeat proteins in plants. *Ann. Rev. Plant Biol.* 65, 415–442. doi: 10.1146/annurev-arplant-050213-040159
- Çakır, B., and Kilickaya, O. (2013). Whole-Genome survey of the putative ATP-binding cassette transporter family genes in *Vitis vinifera*. *PLoS ONE* 8:e78860. doi: 10.1371/journal.pone.0078860
- Bradshaw, A. D. (1965). “Evolutionary significance of phenotypic plasticity in plants,” in *Advances in Genetics*, ed M. Demerec (New York, NY: Academic Press), 115–155.
- Calò, A., Tomasi, D., Biscaro, S., Costacurta, A., Giorgessi, F., Lorenzoni, A., et al. (2002). *Le Vigne del Soave*. Verona: Consorzio Tutela Vini Soave e Recioto di Soave.
- Clingeffer, P. R. (2010). Plant management research: status and what it can offer to address challenges and limitations. *Aust. J. Grape Wine Res.* 16, 25–32. doi: 10.1111/j.1755-0238.2009.00075.x
- Dai, Z. W., Ollat, N., Gomes, E., Decroocq, S., Tandonnet, J. P., Bordenave, L., et al. (2011). Ecophysiological, genetic, and molecular causes of variation in grape berry weight and composition: a review. *Am. J. Enol. Vitic.* 62, 413–425. doi: 10.5344/ajev.2011.10116
- Dal Santo, S., Tornielli, G. B., Zenoni, S., Fasoli, M., Farina, L., Anesi, A., et al. (2013a). The plasticity of the grapevine berry transcriptome. *Genome Biol.* 14:r54. doi: 10.1186/gb-2013-14-6-r54
- Dal Santo, S., Vannonzi, A., Tornielli, G. B., Fasoli, M., Venturini, L., Pezzotti, M., et al. (2013b). Genome-wide analysis of the expansin gene superfamily reveals grapevine-specific structural and functional characteristics. *PLoS ONE* 8:e62206. doi: 10.1371/journal.pone.0062206
- Davies, C., Boss, P. K., and Robinson, S. P. (1997). Treatment of grape berries, a nonclimacteric fruit with a synthetic auxin, retards ripening and alters the expression of developmentally regulated genes. *Plant Physiol.* 115, 1155–1161.
- Davies, C., and Robinson, S. P. (1996). Sugar accumulation in grape berries – cloning of two putative vacuolar invertase cDNAs and their expression in grapevine tissues. *Plant Physiol.* 111, 275–283. doi: 10.1104/pp.111.1.275

manuscript. NV contributed to the design of the study. GBT participated in the design of the study, interpreted the microarray data and drafted the manuscript. SZ conceived, designed and supervised the study and wrote the manuscript.

FUNDING

This work was supported by Joint Project 2014, funded by the Regione Veneto, “Innovative molecular approaches to investigate the interaction between cultivar Garganega and Soave volcanic soil” between Consorzio Tutela Vini Soave e Recioto di Soave (Soave, Verona, Italy) and the Biotechnology Department of University of Verona. The INNOVINE European Project FP7-311775 “Combining innovation in vineyard management and genetic diversity for a sustainable European viticulture” also supported the present work which benefited from the networking activities coordinated under the EU-funded COST ACTION FA1106 “An integrated systems approach to determine the developmental mechanisms controlling fleshy fruit quality in tomato and grapevine.” SDS was financially supported by the Italian Ministry of University and Research FIRB RBFR13GHC5 project “The epigenomic plasticity of grapevine in genotype per environment interactions.”

ACKNOWLEDGMENTS

We thank the Consorzio Tutela Vini Soave e Recioto di Soave (Soave, Verona, Italy) and the associated vineyards for kindly providing the plant material. Ermanno Munari is acknowledged for valuable support during berry sampling.

SUPPLEMENTARY MATERIAL

The Supplementary Material for this article can be found online at: <http://journal.frontiersin.org/article/10.3389/fpls.2016.00970>

- Davies, C., Wolf, T., and Robinson, S. P. (1999). Three putative sucrose transporters are differentially expressed in grapevine tissues. *Plant Sci.* 147, 93–100. doi: 10.1016/S0168-9452(99)00059-X
- Di Lecce, G., Arranz, S., Jauregui, O., Tresserra-Rimbau, A., Quifer-Rada, P., and Lamuela-Raventos, R. M. (2014). Phenolic profiling of the skin, pulp and seeds of Albarino grapes using hybrid quadrupole time-of-flight and triple-quadrupole mass spectrometry. *Food Chem.* 145, 874–882. doi: 10.1016/j.foodchem.2013.08.115
- Fasoli, M., Dal Santo, S., Zenoni, S., Tornielli, G. B., Farina, L., Zamboni, A., et al. (2012). The Grapevine expression atlas reveals a deep transcriptome shift driving the entire plant into a maturation program. *Plant Cell* 24, 3489–3505. doi: 10.1105/tpc.112.100230
- Flamini, R. (2013). Recent applications of mass spectrometry in the study of grape and wine polyphenols. *ISRN Spectrosc.* 2013:813563. doi: 10.1155/2013/813563
- Hannah, L., Roehrdanz, P. R., Ikegami, M., Shepard, A. V., Shaw, M. R., Tabor, G., et al. (2013). Climate change, wine, and conservation. *Proc. Natl. Acad. Sci. U.S.A.* 110, 6907–6912. doi: 10.1073/pnas.1210127110
- Holl, J., Vannozzi, A., Czembel, S., D'Onofrio, C., Walker, A. R., Rausch, T., et al. (2013). The R2R3-MYB transcription factors MYB14 and MYB15 regulate stilbene biosynthesis in *Vitis vinifera*. *Plant Cell* 25, 4135–4149. doi: 10.1105/tpc.113.117127
- Klipper-Aurbach, Y., Wasserman, M., Braunschweig-Weintrob, N., Borstein, D., Peleg, S., Assa, S., et al. (1995). Mathematical formulae for the prediction of the residual beta cell function during the first two years of disease in children and adolescents with insulin-dependent diabetes mellitus. *Med. Hypotheses* 45, 486–490. doi: 10.1016/0306-9877(95)90228-7
- Lakso, A. N., and Kliewer, W. M. (1975). The influence of temperature on malic acid metabolism in grape berries: I. Enzyme responses. *Plant Physiol.* 56, 370–372. doi: 10.1104/pp.56.3.370
- Lakso, A. N., and Kliewer, W. M. (1978). The influence of temperature on malic acid metabolism in grape berries. II. temperature responses of net dark CO₂ fixation and malic acid pools. *Am. J. Enol. Vitic.* 29, 145–149.
- Lijavetzky, D., Carbonell-Bejerano, P., Grimplet, J., Bravo, G., Flores, P., Fenoll, J., et al. (2012). Berry flesh and skin ripening features in *Vitis vinifera* as assessed by transcriptional profiling. *PLoS ONE* 7:e39547. doi: 10.1371/journal.pone.0039547
- Maldini, M., Montoro, P., Piacente, S., and Pizza, C. (2009). ESI-MS, ESI-MS/MS fingerprint and LC-ESI-MS analysis of Proanthocyanidins from *Bursera simaruba* Sarg Bark. *Nat. Prod. Commun.* 4, 1671–1674.
- Palumbo, M. C., Zenoni, S., Fasoli, M., Massonnet, M., Farina, L., Castiglione, F., et al. (2014). Integrated network analysis identifies fight-club nodes as a class of hubs encompassing key putative switch genes that induce major transcriptome reprogramming during grapevine development. *Plant Cell* 26, 4617–4635. doi: 10.1105/tpc.114.133710
- Pastore, C., Zenoni, S., Fasoli, M., Pezzotti, M., Tornielli, G. B., and Filippetti, I. (2013). Selective defoliation affects plant growth, fruit transcriptional ripening program and flavonoid metabolism in grapevine. *BMC Plant Biol.* 13:30. doi: 10.1186/1471-2229-13-30
- Pfaffl, M. W., Horgan, G. W., and Dempfle, L. (2002). Relative expression software tool (REST (c)) for group-wise comparison and statistical analysis of relative expression results in real-time PCR. *Nucleic Acids Res.* 30:e36. doi: 10.1093/nar/30.9.e36
- Ramakers, C., Ruijter, J. M., Deprez, R. H. L., and Moorman, A. F. M. (2003). Assumption-free analysis of quantitative real-time polymerase chain reaction (PCR) data. *Neurosci. Lett.* 339, 62–66. doi: 10.1016/S0304-3940(02)01423-4
- Rotter, A., Camps, C., Lohse, M., Kappel, C., Pilati, S., Hren, M., et al. (2009). Gene expression profiling in susceptible interaction of grapevine with its fungal pathogen *Eutypa lata*: extending MapMan ontology for grapevine. *BMC Plant Biol.* 9:104. doi: 10.1186/1471-2229-9-104
- Shaw, J. R., Hampton, T. H., King, B. L., Whitehead, A., Galvez, F., Gross, R. H., et al. (2014). Natural selection canalizes expression variation of environmentally induced plasticity-enabling genes. *Mol. Biol. Evol.* 31, 3002–3015. doi: 10.1093/molbev/msu241
- Simon, P. (2003). Q-Gene: processing quantitative real-time RT-PCR data. *Bioinformatics* 19, 1439–1440. doi: 10.1093/bioinformatics/btg157
- Sultan, S. E. (2000). Phenotypic plasticity for plant development, function and life history. *Trends Plant Sci.* 5, 537–542. doi: 10.1016/S1360-1385(00)01797-0
- Sun, L. A., Zhang, M., Ren, J., Qi, J. X., Zhang, G. J., and Leng, P. (2010). Reciprocity between abscisic acid and ethylene at the onset of berry ripening and after harvest. *BMC Plant Biol.* 10:257. doi: 10.1186/1471-2229-10-257
- Sweetman, C., Deluc, L. G., Cramer, G. R., Ford, C. M., and Soole, K. L. (2009). Regulation of malate metabolism in grape berry and other developing fruits. *Phytochemistry* 70, 1329–1344. doi: 10.1016/j.phytochem.2009.08.006
- Sweetman, C., Sadras, V. O., Hancock, R. D., Soole, K. L., and Ford, C. M. (2014). Metabolic effects of elevated temperature on organic acid degradation in ripening *Vitis vinifera* fruit. *J. Exp. Bot.* 65, 5975–5988. doi: 10.1093/jxb/eru343
- Teixeira, A., Eiras-Dias, J., Castellarin, S. D., and Geros, H. (2013). Berry phenolics of grapevine under challenging environments. *Int. J. Mol. Sci.* 14, 18711–18739. doi: 10.3390/ijms140918711
- Thimm, O., Blasing, O., Gibon, Y., Nagel, A., Meyer, S., Kruger, P., et al. (2004). MAPMAN: a user-driven tool to display genomics data sets onto diagrams of metabolic pathways and other biological processes. *Plant J.* 37, 914–939. doi: 10.1111/j.1365-313X.2004.02016.x
- Tornielli, G. B., Zamboni, A., Zenoni, S., Delle Donne, M., and Pezzotti, M. (2012). “Transcriptomics and metabolomics for the analysis of grape berry development,” in *The Biochemistry of the Grape Berry*, eds H. Gerós, M. Chaves, and S. Delrot (Sharjah: Bentham Science Publishers), 218–240.
- van Leeuwen, C., Friant, P., Choné, X., Tregot, O., Koundouras, S., and Dubourdieu, D. (2004). Influence of climate, soil, and cultivar on terroir. *Am. J. Enol. Vitic.* 55, 207–217.
- Vaudour, E. (2002). The quality of grapes and wine in relation to geography: notions of terroir at various scales. *J. Wine Res.* 13, 117–141. doi: 10.1080/0957126022000017981
- White, M. A., Whalen, P., and Jones, G. V. (2009). Land and wine. *Nat. Geosci.* 2, 82–84. doi: 10.1038/ngeo429
- Young, P. R., Eyeghe-Bickong, H. A., du Plessis, K., Alexandersson, E., Jacobson, D. A., Coetze, Z. A., et al. (2015). Grapevine plasticity in response to an altered microclimate: sauvignon Blanc modulates specific metabolites in response to increased berry exposure. *Plant Physiol.* 170, 1235–1254. doi: 10.1104/pp.15.01775
- Young, P. R., Lashbrooke, J. G., Alexandersson, E., Jacobson, D., Moser, C., Velasco, R., et al. (2012). The genes and enzymes of the carotenoid metabolic pathway in *Vitis vinifera* L. *BMC Genomics* 13:243. doi: 10.1186/1471-2164-13-243
- Conflict of Interest Statement:** The authors declare that the research was conducted in the absence of any commercial or financial relationships that could be construed as a potential conflict of interest.
- The reviewer CR and handling Editor declared their shared affiliation, and the handling editor states that the process nevertheless met the standards of a fair and objective review.
- Copyright © 2016 Dal Santo, Fasoli, Negri, D'Inca, Vicenzi, Guzzo, Tornielli, Pezzotti and Zenoni. This is an open-access article distributed under the terms of the Creative Commons Attribution License (CC BY). The use, distribution or reproduction in other forums is permitted, provided the original author(s) or licensor are credited and that the original publication in this journal is cited, in accordance with accepted academic practice. No use, distribution or reproduction is permitted which does not comply with these terms.



Roostocks/Scion/Nitrogen Interactions Affect Secondary Metabolism in the Grape Berry

Aude Habran¹, Mauro Commissio², Pierre Helwi¹, Ghislaine Hilbert¹, Stefano Negri², Nathalie Ollat¹, Eric Gomès¹, Cornelis van Leeuwen¹, Flavia Guzzo^{2*} and Serge Delrot^{1*}

¹ UMR 1287, EGFV, Bordeaux Sciences Agro, Institut National de la Recherche Agronomique, Université de Bordeaux, Villenave d'Ornon, France, ² Biotechnology Department, University of Verona, Verona, Italy

OPEN ACCESS

Edited by:

Mario Pezzotti,
University of Verona, Italy

Reviewed by:

Essaid Alt Barka,
University of Reims
Champagne-Ardenne, France
Justine Vanden Heuvel,
Cornell University, USA

***Correspondence:**

Flavia Guzzo
flavia.guzzo@univr.it
Serge Delrot
serge.delrot@bordeaux.inra.fr

Specialty section:

This article was submitted to
Plant Physiology,
a section of the journal
Frontiers in Plant Science

Received: 12 February 2016

Accepted: 15 July 2016

Published: 09 August 2016

Citation:

Habran A, Commissio M, Helwi P, Hilbert G, Negri S, Ollat N, Gomès E, van Leeuwen C, Guzzo F and Delrot S (2016) Roostocks/Scion/Nitrogen Interactions Affect Secondary Metabolism in the Grape Berry. *Front. Plant Sci.* 7:1134. doi: 10.3389/fpls.2016.01134

The present work investigates the interactions between soil content, rootstock, and scion by focusing on the effects of roostocks and nitrogen supply on grape berry content. Scions of Cabernet Sauvignon (CS) and Pinot Noir (PN) varieties were grafted either on Riparia Gloire de Montpellier (RGM) or 110 Richter (110R) rootstock. The 4 roostock/scion combinations were fertilized with 3 different levels of nitrogen after fruit set. Both in 2013 and 2014, N supply increased N uptake by the plants, and N content both in vegetative and reproductive organs. Rootstock, variety and year affected berry weight at harvest, while nitrogen did not affect significantly this parameter. Grafting on RGM consistently increased berry weight compared to 110R. PN consistently produced bigger berries than CS. CS berries were heavier in 2014 than in 2013, but the year effect was less marked for PN berries. The berries were collected between veraison and maturity, separated in skin and pulp, and their content was analyzed by conventional analytical procedures and untargeted metabolomics. For anthocyanins, the relative quantitation was fairly comparable with both LC-MS determination and HPLC-DAD, which is a fully quantitative technique. The data show complex responses of the metabolite content (sugars, organic acids, amino acids, anthocyanins, flavonols, flavan-3-ols/procyanidins, stilbenes, hydroxycinnamic, and hydroxybenzoic acids) that depend on the rootstock, the scion, the vintage, the nitrogen level, the berry compartment. This opens a wide range of possibilities to adjust the content of these compounds through the choice of the roostock, variety and nitrogen fertilization.

Keywords: grapevine, berry, rootstock, nitrogen, metabolomics

Abbreviations: CS, Cabernet Sauvignon; DW, dry weight; ESI, electrospray ionization source; HPLC, High Pressure Liquid Chromatography; N, nitrogen; PN, Pinot Noir; LC-DAD, Liquid chromatography-diode array detector); LC-MS, Liquid chromatography-mass spectrometry; PCA, Principal Component Analysis; OPLS-DA, supervised Orthogonal Partial Least Square Discriminant Analysis; O2PLS-DA, Orthogonal Bidirectional Partial Least Square Discriminant Analysis; RGM, rootstock Riparia Gloire de Montpellier; 110 R, rootstock Richter.

INTRODUCTION

Since the early Twentieth-Century, most vineyards over the world (with the exceptions of Argentina, Australia, Chile, China) are grafted onto a rootstock of either a single American *Vitis* species or hybrids between *V. berlandieri*, *V. riparia*, *V. rupestris* (Whiting, 2004; Ollat et al., 2015). In addition to phylloxera, rootstocks contribute to the control of other soil-borne pests. They may also allow to withstand climate or adverse soil conditions such as drought, or high salt or lime content (Galet and Smith, 1998; Whiting et al., 2005), and to cope with problems of mineral nutrition (Keller et al., 2001; Lecourt et al., 2015). The rootstocks indirectly modify whole plant development by affecting the vigor of the scion (Tandonnet et al., 2010), biomass accumulation and distribution (Paranychianakis et al., 2004; Smart et al., 2006; Koundouras et al., 2008; Alsina et al., 2011), yield (Main et al., 2002; Jones et al., 2009), and phenology (Pongracz, 1983; Whiting et al., 2005). They are directly involved in water and ion uptake from the soil and their translocation to the upper part of the plant. It is therefore important to understand the interactions between soil content, rootstocks and scions.

Among the nutrients present in the soil solution, nitrogen is the most important for the control of vigor, yield, and berry quality. Increasing constraints are put on the use of nitrogen fertilization in order to avoid the pollution of ground water table. Even though grapevine requests smaller amounts of nitrogen than most other crops (30 kg/ha vs. 100–200 kg/ha), the ban of nitrogen fertilization on slopes steeper than 15% and its limitation in other conditions may be a problem in viticulture. This is particularly the case when intercropping is used, because the cover crop generally competes with the vines for nitrogen (Celette et al., 2009). Furthermore, the price of nitrogen fertilizers will increase due to the energy cost of their chemical synthesis.

In grapevine, assimilation of nitrogen may occur in the roots, trunk, stem, leaves and berries (Wermelinger et al., 1991). Therefore, various forms of nitrogen (nitrate, ammonium, amino acids, small peptides, proteins) may be found in these organs. Nitrogen is principally stored under the form of arginine (Nassar and Kliewer, 1966; Kliewer et al., 1967) and may be remobilized from the trunk and the roots toward the leaves, the stems and the fruits. This remobilization which occurs between bud burst and ripening depends on the reserves made during the previous year.

Premium wines are often obtained with grapevines that are grown on poor and superficial soils, and sometimes on slopes (Dela, 2000). Mild water deficit and moderate nitrogen availability direct berry metabolism toward the synthesis of phenolic and aromatic compounds. Excess nitrogen results in high vigor and increased *Botrytis cinerea* infection, which is detrimental to wine quality (Choné et al., 2001). Hence, the grape grower has to manage nitrogen supply in such a way that vegetative and reproductive growth is sufficient while nitrogen deficiency is avoided.

The present work investigates the interactions between soil content, rootstock and scion by focusing on the effects of rootstocks and nitrogen supply on berry content for two scion

varieties. Although some work has addressed the effects of nitrogen supply and rootstock effect on berry composition and wine quality, their combined action has only recently started to be investigated (Lecourt et al., 2015). In particular, non-targeted metabolite profiling has not yet been used to investigate these relationships in detail.

MATERIALS AND METHODS

Plant Material

Grapevines [*V. vinifera* cv. Cabernet-Sauvignon (CS) clone 169, and Pinot noir (PN) clone 777] grafted on either RGM clone 1 or 110R clone 152 rootstocks were used. The two varieties were chosen because of their contrasting profiles in secondary metabolites. RGM and 110R are rootstocks conferring, respectively, low and high vigor to the scion (Tandonnet et al., 2010). 128 plants corresponding to the four rootstock/scion combinations (110R/ CS; 110R/PN; RGM/CS; RGM/PN) were grafted in 2011. 32 plants/combination were planted in 10 L plastic pots containing loam, perlite and sand (4:3:3, v:v:v) and cultivated outside for the experiment. Vines were pruned with 2 spurs of 2 buds (4 buds per vine). Water and nutrients were supplied 3 times per day (1.2 L/day/plant) by drip irrigation with complete nutrient solutions. In 2013 and 2014, from budbreak to fruit set, all plants were supplied with a solution containing 1.4 mM nitrogen. After fruit set, 3 different concentrations of nitrogen were used for the fertirrigation: 0.8 mM N, 1.4 mM N, and 3.6 mM N (denominated N-, N0 and N+, respectively). Based on previous work (Hilbert et al., 2003; Lecourt et al., 2015), N-, N0 and N+ are considered as limited, mean and excessive nitrogen levels. Nitrogen was supplied as potassium nitrate, ammonium phosphate, calcium nitrate, ammonium sulfate and sequestrene. Except for nitrogen, all solution had the same non-limiting concentrations of other mineral elements. Leaf area was determined as described by Mabrouk et al. (1997). Ten plants per combination and per treatment were randomly distributed in the experiment.

Samples Collection

Three groups of three plants of each combination (rootstock/scion) were constituted to obtain three biological replicates. Berries were sampled during the 2013 and 2014 growing season at three time points, veraison (V), mid-maturity (MM, 30 days after mid-veraison), and maturity (M, 48 days after mid-veraison). Each biological replicate comprised twenty five berries randomly sampled at different anatomical and exposure positions of the clusters. All clusters were equally exposed to light. Berries were immediately frozen in liquid nitrogen and stored at -80°C . For the analysis, the skins were separated from the pulp and the seeds, frozen at -80°C and freeze-dried. The dried skins and pulp were powdered.

Plant Nitrogen (N) Status and Berry Nitrogen Content

The leaf blades and the petiole total nitrogen content were determined according to the Dumas method with an elemental auto-analyzer (Flash EA 1112 series, Thermo Fisher Scientific,

Courtalboeuf, France). In parallel, berry nitrogen content was assessed by Yeast Available Nitrogen (YAN) in grape juice at harvest. One hundred berries from each replicate were sampled and pressed. The juice was analyzed with a Fourier Transform Infra-Red spectrometer (FTIR, WineScan FOSS®, FRANCE, 92000 Nanterre).

Analysis of Primary Metabolites

Sugar and Organic Acid Analysis

An aliquot of 80 mg dry powder of samples (pulp and skin) was extracted, and sugar and organic acids were analyzed according to Bobeica et al. (2015).

Amino Acid Content

Amino acid concentration in berries was analyzed according to Pereira et al. (2006) with modifications. After derivatization with AccQ-Tag Ultra derivatization reagent (Waters, Milford, MA, USA), amino acids were analyzed using an UltiMate 3000 UHPLC system equipped with FLD-3000 Fluorescence Detector (Thermo Electron SAS, Waltham, MA USA). Separation was performed on a AccQ-Tag Ultra column, 2,1 × 100 mm, 1, 7 μm (Waters, Milford, MA, USA) at 37°C with elution at 0.5 ml min⁻¹ according to the following gradient (v/v): 0 min 93% A 4.2% B 2.8% C, 6.5 min 95% A 8.4% B 5.6% C, 9 min 78% A 13.2% B 8.8% C, 11 min 71% A 17.4% B 11.6% C linear for 2 min, 14 min 60% B 40% C linear for 1 min, 15 min 93% A 4.2% B 2.8% C (eluent A, sodium acetate buffer, 140 mM at pH 5.7; eluent B, acetonitrile; eluent C, water). Chromatograms corresponding to excitation at 250 nm and emission at 395 nm were recorded. The compounds were quantified by their peak area with Chromeleon software, version 7.1 (Thermo Electron SAS, Waltham, MA, USA) using external standards. Chemical standards were purchased from Sigma (St Louis, MO, USA). Twenty amino acids were identified and quantified as described by Pereira et al. (2006). The results were expressed in nmoles/g DW.

Untargeted Metabolomic Analyses

Powdered skins were extracted with forty volumes of ice cold methanol containing 10% of water and 0.1% formic acid; powdered pulps were extracted with ten volumes of ice cold methanol containing 10% of water. Extracts were sonicated at 40 kHz for 20 min in an ultrasonic bath (Falc Instruments, Bergamo, Italy) at room temperature, centrifuged for 15 min at 16,000 g at 4°C and finally stored at -20°C or immediately diluted for LC-MS (Liquid chromatography-mass spectrometry) and LC-DAD (Liquid chromatography-diode array detector) analyses. In detail, skin and pulp extracts were diluted 1:2 with water LC-MS grade for LC-MS, and respectively, 1:4 and 2:3 for LC-DAD. Finally, the solutions were filtered through 0.2 μm pore filters prior the injection.

The chromatographic analyses were carried out with two Beckman Coulter Gold 127 HPLC system (Beckman Coulter, Fullerton, CA) equipped with a C18 guard column (7.5 × 2.1 mm) and an analytical Alltima HP C18 column (150 × 2.1 mm, particule size 3 μm ; Alltech Associates Inc, Derfield, IL), linked with either a Bruker Esquire 6000 mass spectrometer or a System Gold 168 Diode Array Detector (Beckman Coulter). The HPLC

system was also on-line with a Beckman Coulter System Gold 508 autosampler in which samples were maintained at 4°C. Two solvents were used: 5% (v/v) acetonitrile, 0.5% (v/v) formic acid in water (solvent A) and 100% acetonitrile (solvent B). A solvent gradient was established from 0 to 10% B in 2 min, from 10 to 20% B in 10 min, from 20 to 25% B in 2 min, from 25 to 70% B in 7 min, isocratic flow for 5 min and from 70 to 90% in 1 min, and finally from 90 to 0% in 1 min. Then, the column was equilibrated for 20 min in 100% of solvent A. The injection volume was 20 μL for all samples.

The Bruker ion trap Esquire 6000 mass spectrometer was equipped with electrospray ionization source (ESI). The analyses were performed both in positive and negative modes, setting the scan among 50–3000 m/z and a target mass of 400 m/z. The ESI values were 50 psi and 350°C for the nitrogen nebulizing gas and 10 L/min for the drying gas. Mass spectra were recorded using an Averages of 5 spectra and Max Accu Time of 100 ms. The fragmentation was carried out in AutoMS, fragmenting molecules up to three times. Helium was injected to induce molecule fragmentation. MS data were collected with Bruker Daltonics Esquire 5.2 Control software and processed with Esquire 3.2 Data Analysis software (Bruker Daltonik GmbH, Bremen, Germany). MS data files were converted from .d extension to net.cdf and submitted to mzMine 2.10 (<http://mzmine.sourceforge.net>). The resulting data matrix, reporting the samples and the peak areas of the detected signals, was imported in Simca 13 (Umetrix, Sweden) software to perform the statistical analysis. Metabolite identification was performed by comparing the retention times, m/z and fragmentation patterns of a signal with those of authentic commercial standards included in our home-made library. When no match was observed, the m/z and the fragmentation pattern of the putative molecule were compared with those reported in literature or in on-line databases (massbank.jp; hmbd.ca).

The absorbances were recorded among 190–600 nm (UV-Vis) in LC-DAD analyses. Molecules identified as anthocyanins and hydroxycinnamic acid derivatives in LC-MS were confirmed by measuring their absorbance at 520 and 320 nm, respectively. For anthocyanin quantification, authentic commercial standard Kuromanin chloride (Sigma Aldrich) was earlier dissolved in methanol (Sigma Aldrich), diluted 1:2 with water and 20 μL were injected to the LC-DAD system. 0.01, 0.025, 0.05, 0.075, 0.1, 0.25, 0.5, 0.75, 1, 5, and 10 μg of standard were analyzed in triplicate and the peak areas at 520 nm were annotated. The final equation ($R^2:0.9994$) was used to assess the amount of the different grape anthocyanins as mg of Kuromanin's equivalents in 100 g of powder.

Statistical Analyses

The MS data matrix was imported into Simca 13 software (Umetrix, Sweden) and unsupervised Principal Component (PCA) and supervised Orthogonal Partial Least Square Discriminant (OPLS-DA) analyses were performed using centering and pareto scaling. The unsupervised PCA was carried out to observe homogeneous sample clusters that were used as Y classes in the supervised OPLS-DA. As final output,

molecules responsible for cluster separation in OPLS-DA were identified by plotting the pq(corr), i.e. the correlation between p (based on the X component, the metabolites) and q (based on the Y component, the classes), against p. The statistical analyses were validated by performing: (a) permutation test (200 permutations); (b) CV-ANOVA ($p < 0.05$); (c) t-test ($p < 0.05$) for a cluster characterizing molecule.

RESULTS

Plant Vigor

Plant Vigor was Estimated by Measurement of Pruning Weight, Leaf Surface Area, and Berry Yield

Pruning weights were higher in 2014 than in 2013 (Table 1). The pruning weight of CS plants depended on the rootstock genotype and tended to be higher when the scions were grafted on RGM than on 110R, while the rootstock did not affect the pruning weight for PN. In 2013, the pruning weight was increased by N supply, whatever the rootstock:scion combination, while this was not the case in 2014.

The rootstock genotype did not affect leaf area and nitrogen fertilization only increased the area of secondary leaves (Supplementary Table 1). Both the variety and the year significantly affected leaf area and interacted together.

While rootstock, variety and year affected berry weight at harvest, nitrogen did not have significant effect (Supplementary Table 2). Both in 2013 and 2014, grafting on RGM resulted in higher berry weight than grafting on 110R. PN consistently produced bigger berries than CS. CS berries were heavier in 2014 than in 2013, but the year effect was less marked for PN berries.

Nitrogen Uptake

Nitrogen uptake was assessed by measuring the N content of leaves (Table 2), petioles (Supplementary Table 3) and yeast assimilable nitrogen in the must (Supplementary Table 4). All these parameters concur to indicate that both in 2013 and 2014, N supply increased N uptake by the plants, and N content both in vegetative and reproductive organs. This is further supported by the amino acid analysis presented below (Table 3). The responses observed to N treatment did not significantly differ among the different rootstock/scion combinations tested.

Effects of Nitrogen Supply on Primary Metabolites in the Berries of Different Rootstock/Scion Combinations

Table 3 shows that for all samples, the sugar concentration was much higher in the pulp than in the skins, independently of the rootstock genotype and nitrogen supply. In CS, nitrogen supply did not affect the sugar content of the skin and of the pulp, while it decreased the sugar content of the pulp in PN berries.

ANOVA showed that the rootstock genotype significantly affected the skin content of organic acids, hexoses and amino acids in CS, while it only affected tartrate in CS pulp and malate in PN skin (Table 3A). For a given compartment (skin or pulp), and whatever the variety, the malate content was generally higher on 110R than on RGM, while the reverse was observed for tartrate (Table 3B).

Whatever the rootstock used, the malate content in CS was increased by higher nitrogen supply and this effect was also more

TABLE 1 | Pruning wood weight as affected by nitrogen supply.

Years	Scion/rootstock combination	Nitrate supply	Wood weight (g)	YAN (mg N/L)	Analysis of variance	Wood weight (g)	YAN (mg N/L)
2013	CS/RGM	N-	187.50 ± 34.18	120.00 ±	Years (Y)	***	—
		N+	242.50 ± 32.68	241.00 ±	Treatment (T)	*	***
	CS/110R	N-	164.50 ± 20.20	180.00 ±	Variety (V)	***	*
		N+	208.00 ± 14.94	252.00 ±	Rootstock (R)	**	NS
	PN/RGM	N-	155.00 ± 21.47	180.00 ±	Y/T	**	—
		N+	190.50 ± 10.92	215.00 ±	Y/V	***	—
	PN/110R	N-	158.00 ± 15.31	164.00 ±	V/R	*	NS
		N+	183.50 ± 11.07	223.00 ±	T/V	NS	NS
2014	CS/RGM	N-	298.00 ± 66.22	252.67 ± 45.79	Y/R	NS	—
		N+	255.50 ± 60.23	410.33 ± 11.68	T/R	NS	NS
	CS/110R	N-	266.00 ± 60.45	295.67 ± 30.83	Y/T/V	NS	—
		N+	266.11 ± 94.30	490.00 ± 26.00	Y/T/R	NS	—
	PN/RGM	N-	179.00 ± 28.07	268.00 ± 07.21	Y/V/R	NS	—
		N+	217.00 ± 26.10	518.00 ± 25.87	T/V/R	NS	NS
	PN/110R	N-	203.00 ± 44.11	260.33 ± 47.35	Y/T/V/R	NS	—
		N+	197.50 ± 50.84	568.00 ± 47.29			

Values are means of 3 independent replicates + SE. N-: 0.8 mM N; N+: 3.6 mM N. One factor (N treatment) Anova tests were made, as well as Tukey tests. For each rootstock/variety combination, a and b indicate significantly different values between N- and N+ treatment. ±Unique value. Statistical analyses were done using an analysis of variance with years (Y), rootstock (R), treatment (T), variety (V), and their interaction effects (ns, $P > 0.05$; * $P < 0.05$; ** $P < 0.01$; *** $P < 0.001$).

TABLE 2 | Leaf total N content as affected by nitrogen supply.

Years	Scion/rootstock combination	Nitrate supply	Leaf nitrogen content (%)	Petiole nitrogen content (%)	Analysis of variance	Leaf nitrogen content (%)	Petiole nitrogen content (%)
2013	CS/RGM	N-	1.00 ± 0.10a	0.23 ± 0.01	Years (Y)	**	NS
		N+	1.77 ± 0.41b	0.37 ± 0.12	Treatment (T)	***	*
	CS/110R	N-	1.14 ± 0.17a	0.25 ± 0.05	Variety (V)	**	NS
		N+	1.79 ± 0.30b	0.48 ± 0.18	Rootstock (R)	NS	NS
	PN/RGM	N-	1.10 [±]	0.28 [±]	Y/T	NS	NS
		N+	1.76 [±]	0.37 [±]	Y/V	NS	NS
	PN/110R	N-	1.12 [±]	0.21 [±]	V/R	NS	NS
		N+	1.87 [±]	0.37 [±]	T/V	NS	NS
	2014	CS/RGM	N-	1.10 ± 0.08a	0.38 ± 0.10	Y/R	NS
			N+	2.10 ± 0.09b	0.66 ± 0.10	T/R	NS
	CS/110R	N-	1.17 ± 0.20a	0.39 ± 0.04	Y/T/V	NS	NS
		N+	2.02 ± 0.07b	0.55 ± 0.12	Y/T/R	NS	NS
	PN/RGM	N-	1.43 ± 0.08a	0.33 ± 0.01	Y/V/R	NS	NS
		N+	2.22 ± 0.09b	0.63 ± 0.12	T/V/R	NS	NS
	PN/110R	N-	1.36 ± 0.04a	0.30 ± 0.02	Y/T/V/R	NS	NS
		N+	2.43 ± 0.02b	0.60 ± 0.08			

[±]Unique value. Values are means of 3 independent replicates + SE. N-: 0.8 mM N; N+: 3.6 mM N. One factor (N treatment) Anova tests were made, as well as Tukey tests. For each rootstock/variety combination, a and b indicate significantly different values between N- and N+ treatment. [‡]Unique value. Statistical analyses were done using an analysis of variance with years (Y), rootstock (R), treatment (T), variety (V), and their interaction effects (ns, P > 0.05; *P < 0.05; **P < 0.01; ***P < 0.001).

marked in the skin than in the pulp. This effect of nitrogen on malate content was absent for PN.

Nitrogen supply significantly increased the total amino acid content of the skin and pulp of the berries for almost all rootstock/scion combinations. However, the effect was less marked in PN skin, and even absent in PN pulp (**Table 3B**).

For the CS/RGM combination, increasing nitrogen supply strongly increased the amino acid concentration both in the skin and in the pulp in 2013 and 2014, although this effect was less marked in 2014 (**Table 3B**). Malate content was increased by higher nitrogen supply in the skin for both years, but only in 2013 for the pulp. The sugar concentration was much higher in the pulp than in the skin, but was not significantly affected by nitrogen.

For the CS/110R combination, higher nitrogen supply also strongly enhanced the total amino acid concentration in the skin, but less in the pulp. The treatment also increased the skin malate content for both years. There was no consistent effect of nitrogen status on the sugar content.

For the PN/RGM combination, there was no consistent effect of nitrogen supply on the organic acids, and a marginal decrease of sugars in 2013 (**Table 3B**). The amino acid content was increased by higher nitrogen supply, especially in the skin in 2013.

For the PN/110R combination, there was no marked effect of nitrogen supply on malate, tartrate and sugars. While the total amino acid concentration was increased by high nitrogen supply both in the skin and in the pulp, the glucose and fructose concentrations were diminished in the pulp.

The skin was generally more reactive than the pulp to the different parameters studied, and among these parameters,

the most sensitive were the malate and amino acid contents (**Table 3A**).

Effects of Nitrogen Supply on the Berries of Different Rootstock/Scion Combinations as Assessed by Untargeted Metabolomics

In order to investigate the impact of rootstock and different nitrogen status on the metabolome of grape berries, an untargeted LC-ESI-MS approach was developed with two different cultivars, Cabernet Sauvignon (CS), and Pinot Noir (PN). Two different rootstock (RGM and 110R) and three different nitrogen conditions (limited, 0.8 mM, N-; regular, 1.4 mM, N-0; excessive, 3.6 mM, N+) were used. Skin and pulp were analyzed separately.

The analysis in negative ionization mode allowed to detect secondary metabolites that mainly belong to the groups of anthocyanins, flavonols, flavan-3-ols/procyanidins, stilbenes, hydroxycinnamic, and hydroxybenzoic acids. The m/z values, retention time and putative identification of the detected molecules are reported in **Supplementary File 1**.

Since LC-MS based metabolomics is prone to effects such as matrix effect and ion suppression/enhancement that can impair the comparison between samples, we checked the performance of our analytical platform for relative quantitation. We compared the results of LC-MS determination with those obtained with HPLC-DAD, which is a fully quantitative technique. Nine samples randomly selected, with all their replicates, were analyzed by HPLC-DAD and compared with HPLC-MS. As shown in **Supplementary Figure 1**, the HPLC-DAD and HPLC-MS anthocyanin relative quantitation was fairly comparable.

The performance of our metabolomics platform on grape berry extracts has been extensively discussed in a previous paper (Toffali et al., 2011).

As a first approach, the two LC-MS datamatrix (pulp, skin) were preliminary explored by the unsupervised Principal Component Analysis (PCA). This analysis on skin datamatrix, showed, as expected, that the samples group primarily according to the cultivars (**Figure 1A**), then according to the ripening stage (**Figure 1A**), and finally according to the vintage (**Figure 1B**). Thus, separate Orthogonal Bidirectional Partial Least Square Discriminant Analysis (O2PLS-DA) models were built to highlight the main differences between the two cultivars, the three ripening stages and the two

vintages. PN and CS berries differed mainly for anthocyanin accumulation, more abundant in Cabernet Sauvignon, and for the different flavonoid distribution, with flavonols more abundant in CS and flavanones/flavanols more abundant in PN (**Supplementary Figure 2**). As minor difference, resveratrol is higher in mature Pinot noir grape berries. In terms of ripening, increases of resveratrol/stilbenes and significant changes in anthocyanins and flavonoid profiles were observed in both cultivars (**Supplementary Figures 2, 3**). The pulp datamatrix showed that CS contains much more tryptophan N-glucoside and less hydroxybenzoic acids than PN, and that both these metabolites increase during ripening (**Supplementary Figures 2E-G**).

TABLE 3 | Effect of nitrogen supply on the primary metabolites of berries for four rootstock/scion combinations.

(A)							
Year	Scion/rootstock combination	Nitrate supply	Malate (mmoles/g DW)	Tartrate (mmoles/g DW)	Glucose (mmoles/g DW)	Fructose (mmoles/g DW)	Total AA (nmol/mg DW)
2013	CS/RGM	Skin	N-	3.09 ± 0.31	6.45 ± 0.68	33.00 ± 2.97	19.27 ± 2.99
			N+	3.93 ± 0.29*	5.92 ± 0.68	31.08 ± 1.47	20.29 ± 1.18
		Pulp	N-	3.84 ± 0.36	5.25 ± 0.30	119.62 ± 31.21	98.56 ± 25.88
			N+	4.93 ± 0.92	5.88 ± 0.88	110.34 ± 18.52	94.90 ± 13.42
	CS/110R	Skin	N-	3.37 ± 0.21	5.81 ± 0.81	37.63 ± 0.26	24.10 ± 0.75
			N+	4.67 ± 0.50*	5.42 ± 0.23	32.24 ± 3.55	24.57 ± 5.48
		Pulp	N-	3.14 ± 0.39	3.56 ± 0.90	93.59 ± 27.37	84.53 ± 23.18
			N+	5.26 ± 0.77*	5.60 ± 0.82*	124.49 ± 49.31	107.17 ± 38.64
2014	PN/RGM	Skin	N-	3.19 ± 0.36	5.43 ± 0.26	33.35 ± 18.48	33.35 ± 15.02
			N+	3.41 ± 0.24	6.54 ± 0.28**	18.98 ± 1.87	22.52 ± 1.92
		Pulp	N-	2.13 ± 0.26	3.70 ± 0.08	77.87 ± 12.52	72.97 ± 12.74
			N+	2.50 ± 0.02	4.32 ± 0.13**	72.02 ± 18.98	67.59 ± 15.75
	PN/110R	Skin	N-	3.72 ± 0.17	6.05 ± 0.15	21.00 ± 4.02	24.36 ± 6.38
			N+	4.23 ± 0.28	5.90 ± 0.12	21.95 ± 1.92	26.81 ± 2.29
		Pulp	N-	2.74 ± 0.33	4.24 ± 0.18	92.48 ± 8.43	83.93 ± 4.04
			N+	3.18 ± 0.15	4.54 ± 0.19	67.19 ± 4.15*	64.16 ± 1.61**
2014	CS/RGM	Skin	N-	2.65 ± 0.19	6.10 ± 0.09	34.15 ± 3.16	22.00 ± 1.74
			N+	3.29 ± 0.66	6.39 ± 0.06*	27.95 ± 4.14	20.76 ± 2.77
		Pulp	N-	4.03 ± 1.56	6.05 ± 1.48	128.35 ± 34.35	115.51 ± 28.93
			N+	3.45 ± 0.11	4.43 ± 0.14	79.14 ± 9.24	70.94 ± 6.15
	CS/110R	Skin	N-	3.10 ± 0.49	5.60 ± 0.45	40.83 ± 1.91	26.78 ± 0.71
			N+	3.84 ± 0.69	5.78 ± 0.70	33.66 ± 0.52*	27.76 ± 1.29
		Pulp	N-	3.07 ± 0.49	4.75 ± 0.45	133.57 ± 38.13	113.69 ± 28.86
			N+	2.89 ± 0.17	3.63 ± 0.83	87.88 ± 23.69	82.02 ± 19.79
	PN/RGM	Skin	N-	3.06 ± 0.60	5.71 ± 0.51	26.57 ± 11.11	24.84 ± 10.32
			N+	5.27 ± 0.48**	6.22 ± 0.26	24.95 ± 2.12	26.56 ± 2.35
		Pulp	N-	3.24 ± 0.23	3.83 ± 0.41	79.32 ± 9.38	67.87 ± 7.00
			N+	4.85 ± 0.18***	4.50 ± 0.51	81.08 ± 17.71	66.88 ± 11.46
	PN/110R	Skin	N-	4.20 ± 0.71	5.72 ± 0.37	24.93 ± 2.93	25.94 ± 3.31
			N+	7.28 ± 0.72**	5.03 ± 1.00	22.14 ± 3.41	24.3 ± 2.75
		Pulp	N-	4.17 ± 2.03	4.78 ± 0.75	98.83 ± 24.72	81.29 ± 16.8
			N+	6.02 ± 0.11	4.23 ± 0.45	69.42 ± 0.50	61.8 ± 3.55

Raw values; asterisks indicate a significant statistical difference between N+ and N- treatments. Data shown are means ± standard deviation, n = 6. Statistical analyses have been done using a t-test, (*P < 0.05; **P < 0.01; ***P < 0.001).

		(B)					
		Analysis variance	Malate (mmoles/g DW)	Tartrate (mmoles/g DW)	Glucose (mmoles/g DW)	Fructose (mmoles/g DW)	Total AA (nmol/mg DW)
CS	Skin	Years (Y)	**	NS	*	NS	***
		Treatment (T)	***	NS	NS	***	***
		Rootstock (R)	*	*	***	***	*
		Y/T	NS	NS	NS	NS	NS
		Y/R	NS	NS	NS	NS	NS
		T/R	NS	NS	NS	NS	NS
		Y/T/R	NS	NS	NS	NS	NS
	Pulp	Years (Y)	**	NS	NS	NS	*
		Treatment (T)	NS	NS	NS	NS	**
		Rootstock (R)	NS	**	NS	NS	NS
PN	Skin	Years (Y)	***	NS	NS	NS	**
		Treatment (T)	***	NS	NS	NS	*
		Rootstock (R)	***	NS	NS	NS	NS
		Y/T	***	NS	NS	NS	NS
		Y/R	*	NS	NS	NS	NS
		T/R	NS	**	NS	NS	NS
		Y/T/R	NS	NS	NS	NS	NS
	Pulp	Years (Y)	***	NS	NS	NS	**
		Treatment (T)	**	NS	*	*	NS
		Rootstock (R)	*	*	NS	NS	NS
		Y/T	*	NS	NS	NS	NS
		Y/R	NS	NS	NS	NS	NS
		T/R	NS	*	*	NS	NS
		Y/T/R	NS	NS	NS	NS	NS

ANOVA analysis. Statistical analyses have been done using an analysis of variance with years (Y), rootstock (R), treatment (T), and their interaction effects (ns, $P > 0.05$; * $P < 0.05$; ** $P < 0.01$; *** $P < 0.001$). DW, dry weight.

The two cultivars were then analyzed separately in more details, using the above supervised approach, and considering only the more mature stages (mid-mature and mature) and the skin datamatrix. Both the cultivars showed rootstock-dependent differences (Figure 2): the CS-110R combination was more advantageous for secondary metabolites, especially anthocyanins, hydroxycinnamic acids, resveratrol/stilbenes and flavan-3-ols/procyanidins, compared with CS-RGM (Figures 2A,C,E). Also the combination PN-110R accumulated higher levels of anthocyanins, while the PN-RGM combination accumulated higher levels of hydroxycinnamic acids, flavan-3-ols/procyanidins, resveratrol/stilbenes (Figures 2B,D,F).

The four combinations (CS-110R, CS-RGM, PN-110R, and PN-RGM) were then analyzed under the different nitrogen nutrition conditions. The supervised O2PLS-DA multivariate analysis resulted in very weak models when the three different nitrogen supplementations were separately considered; the exclusion of the intermediate nitrogen supply resulted in stronger

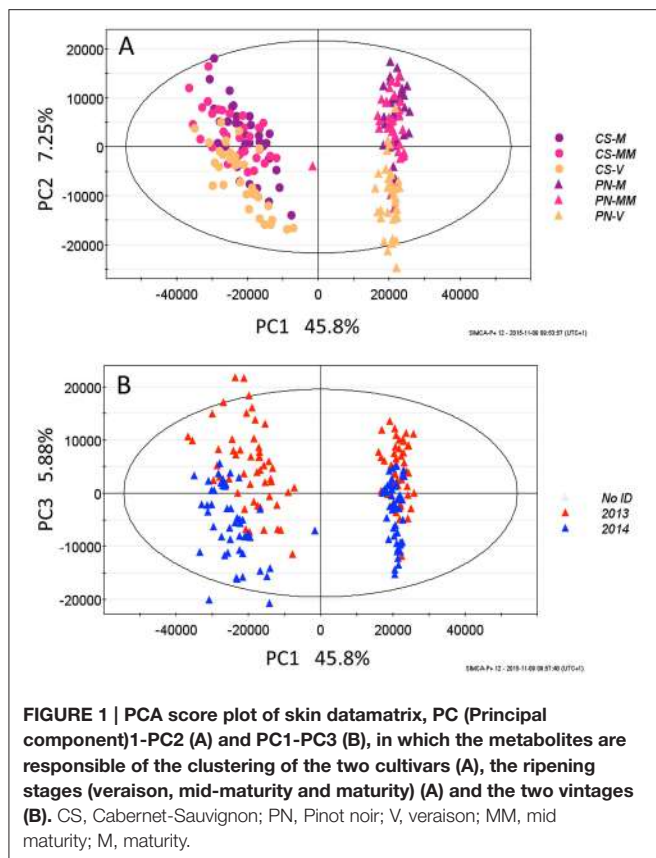
models. Thus, the effect of limited nitrogen supply was compared with higher nitrogen (Figure 3). In all four combinations between the two cultivars and the two rootstocks, excessive nitrogen supply decreased the accumulation of flavonoids and anthocyanins (Figure 3).

These effects were higher in PN than in Cabernet Sauvignon; in CS cultivar only cyanidin, delphinidin, and petunidin-based anthocyanins were affected by different levels of nitrogen nutrition, while in PN the peonidin-based anthocyanins were also affected.

The inhibition of accumulation of secondary metabolites caused by high nitrogen supplementation was higher when the scions were grafted on the 110R rootstock, compared with RGM (Supplementary Figure 4).

DISCUSSION

The berry content at harvest, which determines the quality of table grapes and is a major determinant for wines depend on



complex interactions between the rootstocks, the scion, and their respective environment (soil and atmosphere) that may be modified by a wide range of viticultural practices. To reach a precise control of berry content, and to face more easily current challenges like those raised by climate change, it is important to document and understand the different levers offered by the manipulation of rootstock/scion/environment interactions. The present study investigates the interactions between nitrogen level/rootstock genotype and scion genotype with targeted analytical procedures and an untargeted metabolomic approach.

A high vigor rootstock grafted by a scion Chardonnay (Ough et al., 1968) or Merlot (Stockert et al., 2013) tend to acquire more N, resulting in higher amounts of must amino-N than the intermediate and low growth promoting rootstocks. Our results (Table XX) partially confirm and precise this conclusion by comparing the skin and the pulp responses. The amino acid concentration was affected by the rootstock in the skin of CS, but not in the pulp, while the rootstock did not affect the amino acid content of PN berries.

Although nitrogen fertilization did not significantly affect berry size and impacted only marginally secondary leaf development, it significantly impacted the malate and amino acid content of berries for almost all rootstock/scion combinations. This effect of nitrogen on amino acids has already been described for other rootstock/scion combinations (Holzapfel and Treeby, 2007). The effects of nitrogen on malate are less expected. Our work also shows differential effects on a given treatment

on the skin and pulp compartment. The increase in malate induced by high nitrogen is more marked in CS skin and pulp. The rootstock genotype only affects tartrate in CS pulp and malate in PN skin. This underlines the complexity of the soil composition/rootstock/scion interactions, which may be selective for one variety, one rootstock, one compound and one berry compartment, and depend on year (climate). The analysis of primary metabolites suggest that the skin was the more reactive compartment, and this compartment was further analyzed by untargeted metabolomics.

This allowed to detect secondary metabolites belonging to the groups of anthocyanins, flavonols, flavan-3-ols/procyanidins, stilbenes, hydroxycinnamic, and hydroxybenzoic acids. A number of peaks are still unidentified. The samples separated according to varieties, ripening stage and vintage. In CS berries, the RGM rootstock favored a higher amount of anthocyanins, hydroxycinnamic acids, resveratrol/stilbenes and flavan-3-ols/procyanidins than the 110R rootstock.

Whatever the rootstock/scion combination, high nitrogen decreased the amounts of flavonoids and anthocyanins. This is in agreement with Soubeyrand et al. (2014) who found that low nitrogen supply significantly increased the anthocyanin level in Cabernet Sauvignon berries collected from field plants at two ripening stages (26 days post-véraison and maturity).

The present study show that these effects of nitrogen are variety-dependent, and do not concern all anthocyanins. They were stronger in PN than in CS. Only cyanidin, delphinidin, and petunidin-based anthocyanins were affected by nitrogen in CS berries, while the peonidin-based anthocyanins were also affected in PN berries.

Finally, the amounts of secondary metabolites caused by high nitrogen supply were more decreased in berries collected on scions grafted on 110R rootstock than on RGM (**Supplementary Figure 4**). As the present experiments were conducted in pots limiting rootstock development and as the vines were pruned similarly, the differences observed might be related more to a higher intrinsic capacity to retrieve and transport nitrogen for 110 R compared RGM than to vigor (vegetative development) *per-se*. Indeed, Lecourt et al. (2015) have shown that response to nitrate supply in grafted grapevines alter the root and shoot distribution of various ions in a genotype dependent way. Our former work (Berdeja et al., 2014) also showed that the rootstock genotype (110R, high vigor or 125 AA, low vigor) significantly impacted the total amount of anthocyanins of PN berries grown in field conditions. The proportion of 3', 4'-dihydroxy cyanidin and peonidin and 3', 4', 5'-trihydroxy delphinidin, malvidin, and petunidin slightly varied depending on the year, but was not clearly modified by rootstock or water supply.

The data described here show that untargeted metabolomics may be a powerful technique to detect the numerous and subtle changes depending on soil composition/rootstock/scion/climate interactions. The build up of adequate data bases and the combination of these data with RNAseq approaches would be very useful to decipher the overall response of berry metabolism, and the underlying gene expression changes to environmental cues and genetic background.

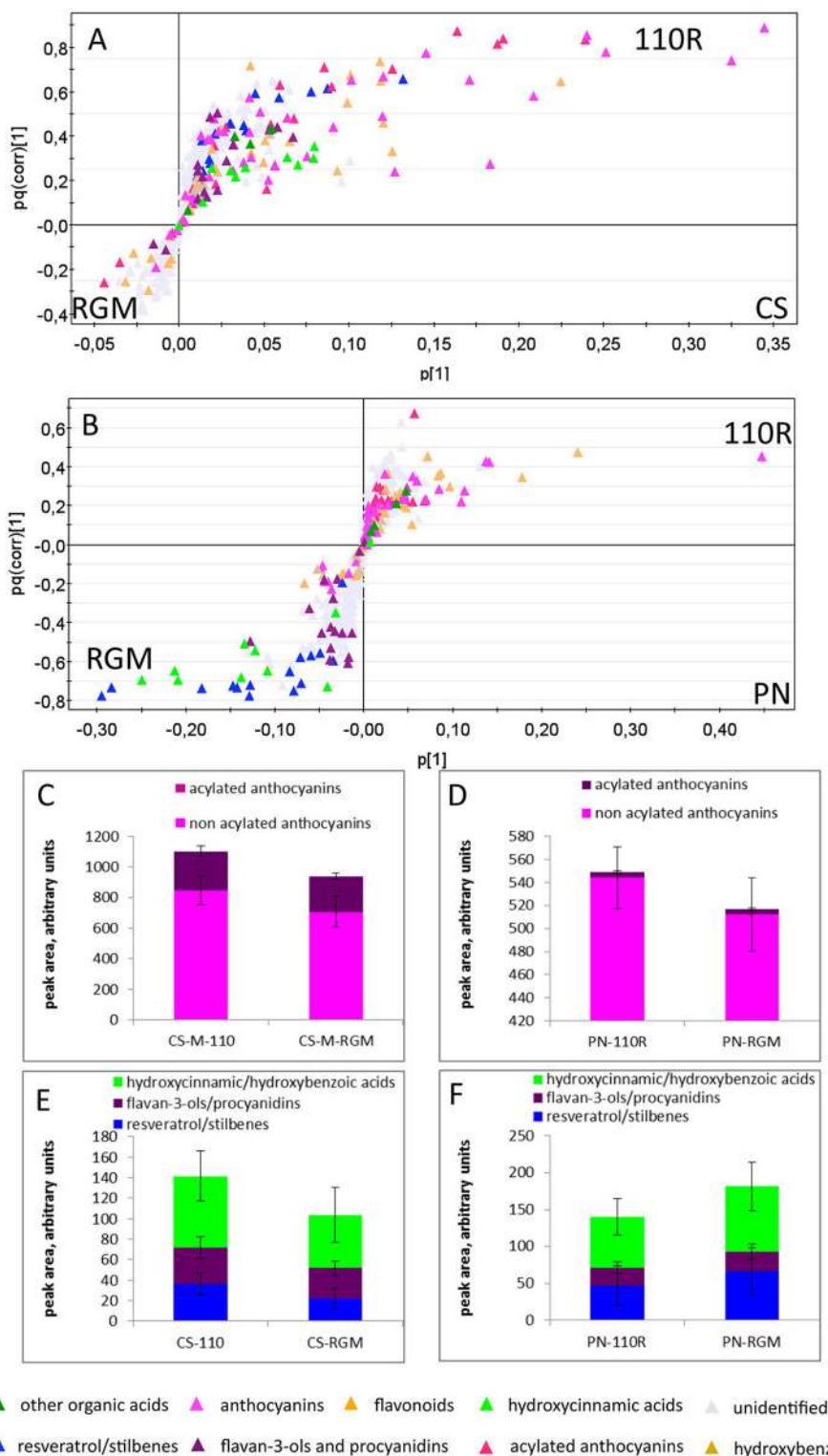


FIGURE 2 | O2PLS-DA loading plot (A,B) showing the CS-110R, PN-110R, CS-RGM, PN-RGM cultivar-rootstock consortia clustered according to the grape berries skin metabolites; in C-F the average relative levels of anthocyanins, hydroxycinnamic acids, flavan-3-ols/procyanidins and resveratrol/stilbenes of the four consortia are shown, \pm standard deviation. The high standard deviations of these data is expected and depend on their mixed nature, since for each consortia data of two ripening stages (M, MM), two vintages (2013 and 2014) and three nitrogen nutrition levels are clustered. CS, Cabernet-Sauvignon; PN, Pinot noir; 110R, 110R rootstock; RGM, RGM rootstock.

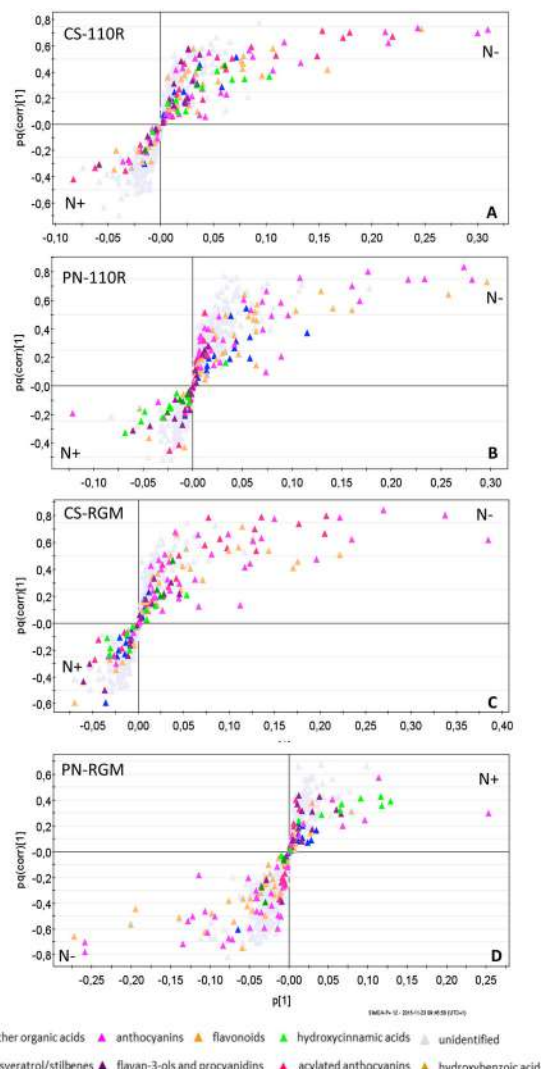


FIGURE 3 | O2PLS-DA loading plot showing the CS-110R, PN-110R, CS-RGM, PN-RGM samples in two nitrogen nutrition status ($N^- = 0.8 \text{ mM}$; $N^+ = 3.6 \text{ mM}$) clustered according to their skin grape berry metabolites. CS, Cabernet-Sauvignon; PN, Pinot noir; 110R, 110R rootstock; RGM, RGM rootstock.

AUTHOR CONTRIBUTIONS

CV and SD designed and oversaw the research. AH, GH, and PH performed the field experiments and berry sampling; AH, GH, SN, and MC did the metabolic and metabolomic analysis; AH and MC analyzed data. FG and SD drafted the ms. EG and NO critically revised the manuscript. All authors read and approved the final manuscript.

ACKNOWLEDGMENTS

The authors thank the Conseil InterProfessionnel du Vin de Bordeaux, and France Agrimer for supporting the Ph. D. work of AH, COST Action FA 1106 for providing a travel grant

and the Conseil Régional d'Aquitaine for general support. The authors also thank Bernard Douens and Christel Renaud for technical support, and ZhanWu Dai and Jean-Pascal Goutouly for scientific interactions.

SUPPLEMENTARY MATERIAL

The Supplementary Material for this article can be found online at: <http://journal.frontiersin.org/article/10.3389/fpls.2016.01134>.

Supplementary Figure 1 | Comparison between relative quantitation performances of HPLC-ESI-MS and HPLC-DAD: heat map representing the relative levels of each of the HPLC-DAD-detectable metabolites in a set of randomly selected samples, as detected by HPLC-DAD and HPLC-ESI-MS. Di, delphinidin; Cy, cyanidin; Pt, petunidin; Peo, peonidin; MV, malvidin; hx, hexose; ac, acetyl; cou, coumaroyl; 110R, 110R rootstock; RGM, RGM rootstock; V, veraison; MM, mid-maturity; M, maturity; N-: 0.8 mM nitrogen supply; N-0: 1.4 mM nitrogen supply; N+: 3.6 mM nitrogen supply.

Supplementary Figure 2 | Differences between Cabernet Sauvignon and Pinot noir cultivars grape berries explored by LC-MS-based untargeted metabolomics of skin (A–D) and pulp (E–G) grape berry: (A) and (E), O2PLS-DA loading plot. The high standard deviations of the average relative level of metabolite data is expected and depend on their mixed nature, since for each cultivar data of two ripening stages (M, MM), two vintages (2013 and 2014), two rootstock (110R and RGM) and three nitrogen nutrition levels are clustered. CS, Cabernet-Sauvignon; PN, Pinot noir; V, veraison; MM, mid mature; M, mature.

Supplementary Figure 3 | Evolution of grape berry ripening in Cabernet sauvignon (A,B) and Pinot noir (C,D) explored by LC-MS-based untargeted metabolomics of grape berry skin; (A,C): O2PLS-DA score plot; (B,D): O2PLS-DA loading plot. The high standard deviations of the average relative level of metabolite data is expected and depend on their mixed nature, since for each cultivar data for two rootstocks (110R and RGM) and three nitrogen nutrition levels are clustered. CS, Cabernet-Sauvignon; PN, Pinot noir; V, veraison; M, maturity.

Supplementary Figure 4 | Average relative level of metabolite in the grape berry skin of CS-110R, PN-110R, CS-RGM, PN-RGM cultivar-rootstock consortia in two conditions of nitrogen nutrition, +/- the standard deviation. The high standard deviations of the average relative level of metabolite data is expected and depend on their mixed nature, since for each cultivar data two ripening stages (mid maturity, maturity) and two vintages (2013, 2014) are clustered. CS, Cabernet-Sauvignon; PN, Pinot noir; 110R, 110R rootstock; RGM, RGM rootstock; N-: 0.8 mM nitrogen supply; N+: 3.6 mM nitrogen supply.

Supplementary File 1 | List of metabolites, isotopes, adducts, putatively identified by HPLC-ESI-MS in grape berries skin and pulp.

Supplementary Table 1 | Measurements of primary and secondary leaf area at harvest for the different rootstock/scion combinations fertilized by 0.8 mM (N-) or 3.6 mM (N+). Data shown are means \pm standard deviation, $n = 6$. Statistical analyses were done using an analysis of variance with years (Y), rootstock (R), treatment (T), variety (V), and their interaction effects (ns, $P > 0.05$; * $P < 0.05$; ** $P < 0.01$; *** $P < 0.001$).

Supplementary Table 2 | Measurements of berry weight at harvest for the different rootstock/scion combinations fertilized by 0.8 mM (N-) or 3.6 mM (N+). (A) The data are means \pm standard deviation, $n = 6$. (B) Statistical analyses have been done using an analysis of variance with years (Y), rootstock (R), treatment (T), variety (V), and their interaction effects (ns, $P > 0.05$; * $P < 0.05$; ** $P < 0.01$; *** $P < 0.001$).

Supplementary Table 3 | Petiole total N content as affected by nitrogen supply. Values are means of 3 independent replicates \pm SE. N- : 0.8 mM N ; N+ : 3.6 mM N. One factor (N treatment) Anova tests were made, as well as Tukey tests. For each rootstock/variety combination, a and b indicate significantly different values between N- and N+ treatment. . ‡ Unique value. Statistical analyses were done using an analysis of variance with years (Y), rootstock (R),

treatment (T), variety (V) and their interaction effects (ns, $P > 0.05$; * $P < 0.05$; ** $P < 0.01$; *** $P < 0.001$).

Supplementary Table 4 | Effect of nitrogen supply on yeast assimilable nitrogen (mg/L) in musts prepared from different rootstocks/scion

REFERENCES

- Alsina, M. M., Smart, D. R., Bauerle, T., De Herralde, F., Biel, C., Stockert, C., et al. (2011). Seasonal changes of whole root system conductance by a drought-tolerant grape root system. *J. Exp. Bot.* 62, 99–109. doi: 10.1093/jxb/erq247
- Berdeja, M., Hilbert, G., Dai, Z. W., Lafontaine, M., Stoll, M., Schultz, H. R., et al. (2014). Effect of water stress and rootstock genotype on Pinot Noir berry composition. *Aust. J. Grape Wine Res.* 20, 409–421. doi: 10.1111/ajgw.12091
- Boebeica, N., Poni, S., Hilbert, G., Renaud, C., Gomès, E., Delrot, S., et al. (2015). Differential responses of sugar, organic acids and anthocyanins to source-sink modulation in Cabernet Sauvignon and Sangiovese grapevines. *Front. Plant Sci.* 6:382. doi: 10.3389/fpls.2015.00382
- Celette, F., Findeling, A., and Gary, C. (2009). Competition for nitrogen in an unfertilized intercropping system: the case of an association of grapevine and grass cover in a Mediterranean climate. *Eur. J. Agron.* 30, 41–51. doi: 10.1016/j.eja.2008.07.003
- Choné, X., van Leeuwen, C., Chéry, P., and Ribéreau-Gayon, P. (2001). Terroir influence on water status and nitrogen status of non-irrigated Cabernet Sauvignon (*Vitis vinifera*). Vegetative development, must and wine composition. *Afr. J. Enol. Vitic.* 22, 8–15.
- Delas, J. (2000). *La Fertilisation de la Vigne*. France: Féret Bordeaux.
- Galet, P., and Smith, J. (1998). *Grape Varieties and Rootstock Varieties*. Chaintre: Oenoplurimédia.
- Hilbert, G., Soyer, J. P., Molot, C., Giraudon, J., Milin, S., and Gaudillere, J. P. (2003). Effects of nitrogen supply on must quality and anthocyanin accumulation in berries of cv. Merlot. *Vitis-Geilweilerhof* 42, 69–76.
- Holzapfel, B. P., and Treeby, M., T. (2007). Effects of timing and rate of N supply on leaf nitrogen status, grape yield and juice composition from Shiraz grapevines grafted to one of three different rootstocks. *Aust. J. Grape Wine Res.* 13, 14–22. doi: 10.1111/j.1755-0238.2007.tb00067.x
- Jones, T. H., Cullis, B. R., Clingleffer, P. R., and Rühl, E. H. (2009). Effects of novel hybrid and traditional rootstocks on vigour and yield components of Shiraz grapevines. *Aust. J. Grape Wine Res.* 15, 284–292. doi: 10.1111/j.1755-0238.2009.00061.x
- Keller, M., Kummer, M., and Vasconcelos, M. C. (2001). Reproductive growth of grapevines in response to nitrogen supply and rootstock. *Aust. J. Grape Wine Res.* 7, 12–18. doi: 10.1111/j.1755-0238.2001.tb00188.x
- Kliewer, W. M., Howarth, L., and Omori, M. (1967). Concentrations of tartaric acid and malic acid and their salts in *Vitis Vinifera* grapes. *Am. J. Enol. Vitic.* 18, 42–54.
- Koundouras, S., Tsialtas, I. T., Zioziou, E., and Nikolaou, N. (2008). Rootstock effects on the adaptive strategies of grapevine (*Vitis vinifera* L. cv. Cabernet-Sauvignon) under contrasting water status: leaf physiological and structural responses. *Agric. Ecosyst. Environ.* 128, 86–96. doi: 10.1016/j.agee.2008.05.006
- Lecourt, J., Lauvergeat, V., Ollat, N., Vivin, P., and Cookson, S. J. (2015). Shoot and root ionome responses to nitrate supply in grafted grapevines are rootstock genotype dependent. *Aust. J. Grape Wine Res.* 21, 311–318. doi: 10.1111/ajgw.12136
- Mabrouk, H., Carboneau, A., and Sinoquet, H. (1997). Canopy structure and radiation regime in grapevine. I. Spatial and angular distribution of leaf area in two canopy systems. *Vitis* 36, 119–124.
- Main, G., Morris, J., and Striegler, K. (2002). Rootstock effects on Chardonnay productivity, fruit, and wine composition. *Am. J. Enol. Vitic.* 53, 37–40.
- Nassar, A. R., and Kliewer, W. M. (1966). Free amino acids in various parts of *Vitis vinifera* at different stages of development. *Pro. Am. Soc. Horti. Sci.* 89, 281–284.
- Ollat, N., Peccoux, A., Papura, D., Esmeraud, D., Marguerit, E., Tandonnet, J. P., et al. (2015). “Rootstocks as a component of adaptation to environment,” in *Grapevine in a Changing Environment: A Molecular and Ecophysiological Perspective*, 68–75. Available online at: <http://eu.wiley.com/WileyCDA/WileyTitle/productCd-1118736052.html#>
- Ough, C. S., Cook, J. A., and Lider, L. A. (1968). Rootstock-scion interactions concerning wine making. II. Wine compositional and sensory changes attributed to rootstock and fertilizer level differences. *Am. J. Enol. Vitic.* 19, 254–265.
- Paranychianakis, N. V., Aggelides, S., and Angelakis, A. N. (2004). Influence of rootstock, irrigation level and recycled water on growth and yield of Soultanina grapevines. *Agric. Water Manag.* 69, 13–27. doi: 10.1016/j.agwat.2004.03.012
- Pereira, G. E., Gaudillere, J.-P., Pieri, P., Hilbert, G., Maucourt, M., Deborde, C., et al. (2006). Microclimate influence on mineral and metabolic profiles of grape berries. *J. Agric. Food Chem.* 54, 6765–6775. doi: 10.1021/jf061013k
- Pongracz, D. P. (1983). *Rootstocks for Grape Vines*. Cape: David Philip Pub.
- Smart, D. R., Breazeale, A., and Zufferey, V. (2006). Physiological changes in plant hydraulics induced by partial root removal of irrigated grapevine (*Vitis vinifera* cv. Syrah). *Am. J. Enol. Vitic.* 57, 201–209.
- Soubeyrand, E., Basteau, C., Hilbert, G., van Leeuwen, C., Delrot, S., and Gomès, E. (2014). Nitrogen supply affects anthocyanin biosynthetic and regulatory genes in grapevine cv. Cabernet-Sauvignon berries. *Phytochemistry* 103, 38–49. doi: 10.1016/j.phytochem.2014.03.024
- Stockert, C. M., Bisson, L. F., Adams, D. O., and Smart, D. R. (2013). Nitrogen status and fermentation dynamics for Merlot on two rootstocks. *Am. J. Enol. Vitic.* 64, 195–202. doi: 10.5344/ajev.2013.12065
- Tandonnet, J.-P., Cookson, S. J., Vivin, P., and Ollat, N. (2010). Scion genotype controls biomass allocation and root development in grafted grapevine. *Aust. J. Grape Wine Res.* 16, 290–300. doi: 10.1111/j.1755-0238.2009.00090.x
- Toffali, K., Zamboni, A., Anesi, A., Stoccero, M., Pezzotti, M., Levi, M., et al. (2011). Novel aspects of grape berry ripening and post-harvest withering revealed by untargeted LC-ESI-MS metabolomics analysis. *Metabolomics* 7, 424–436. doi: 10.1007/s11306-010-0259-y
- Wermelinger, B., Baumgärtner, J., and Gutierrez, A. P. (1991). A demographic model of assimilation and allocation of carbon and nitrogen in grapevines. *Ecol. Model.* 53, 1–26. doi: 10.1016/0304-3800(91)90138-Q
- Whiting, J. R. (2004). Grapevine rootstocks. *Viticulture* 1, 167–188.
- Whiting, M. D., Lang, G., and Ophardt, D. (2005). Rootstock and training system affect sweet cherry growth, yield, and fruit quality. *HortScience* 40, 582–586.
- Conflict of Interest Statement:** The authors declare that the research was conducted in the absence of any commercial or financial relationships that could be construed as a potential conflict of interest.
- The handling Editor declared a shared affiliation, though no other collaboration, with several of the authors MC, SN, FG and states that the process nevertheless met the standards of a fair and objective review.
- Copyright © 2016 Habran, Commissio, Helwi, Hilbert, Negri, Ollat, Gomès, van Leeuwen, Guzzo and Delrot. This is an open-access article distributed under the terms of the Creative Commons Attribution License (CC BY). The use, distribution or reproduction in other forums is permitted, provided the original author(s) or licensor are credited and that the original publication in this journal is cited, in accordance with accepted academic practice. No use, distribution or reproduction is permitted which does not comply with these terms.**



The Influence of Genotype and Environment on Small RNA Profiles in Grapevine Berry

Daniela Lopes Paim Pinto¹, Lucio Brancadoro², Silvia Dal Santo³, Gabriella De Lorenzis², Mario Pezzotti³, Blake C. Meyers^{4,5}, Mario E. Pè¹ and Erica Mica^{1,6*}

¹ Institute of Life Sciences, Sant'Anna School of Advanced Studies, Pisa, Italy, ² Department of Agricultural and Environmental Sciences-Production, Landscape, Agroenergy, University of Milan, Milan, Italy, ³ Laboratory of Plant Genetics, Department of Biotechnology, University of Verona, Verona, Italy, ⁴ Donald Danforth Plant Science Center, St. Louis, MO, USA, ⁵ Division of Plant Sciences, University of Missouri-Columbia, Columbia, MO, USA, ⁶ Genomics Research Centre, Agricultural Research Council, Fiorenzuola d'Arda, Italy

OPEN ACCESS

Edited by:

Mahmoud W. Yaish,
Sultan Qaboos University, Oman

Reviewed by:

Nataliya V. Melnikova,
Engelhardt Institute of Molecular
Biology (RAS), Russia
Douglas S. Domingues,
Sao Paulo State University, Brazil

*Correspondence:

Erica Mica
erica.mica@crea.gov.it

Specialty section:

This article was submitted to
Plant Physiology,
a section of the journal
Frontiers in Plant Science

Received: 19 February 2016

Accepted: 13 September 2016

Published: 05 October 2016

Citation:

Paim Pinto DL, Brancadoro L,
Dal Santo S, De Lorenzis G,
Pezzotti M, Meyers BC, Pè ME and
Mica E (2016) The Influence of
Genotype and Environment on Small
RNA Profiles in Grapevine Berry.
Front. Plant Sci. 7:1459.
doi: 10.3389/fpls.2016.01459

Understanding the molecular mechanisms involved in the interaction between the genetic composition and the environment is crucial for modern viticulture. We approached this issue by focusing on the small RNA transcriptome in grapevine berries of the two varieties Cabernet Sauvignon and Sangiovese, growing in adjacent vineyards in three different environments. Four different developmental stages were studied and a total of 48 libraries of small RNAs were produced and sequenced. Using a proximity-based pipeline, we determined the general landscape of small RNAs accumulation in grapevine berries. We also investigated the presence of known and novel miRNAs and analyzed their accumulation profile. The results showed that the distribution of small RNA-producing loci is variable between the two cultivars, and that the level of variation depends on the vineyard. Differently, the profile of miRNA accumulation mainly depends on the developmental stage. The vineyard in Riccione maximizes the differences between the varieties, promoting the production of more than 1000 specific small RNA loci and modulating their expression depending on the cultivar and the maturation stage. In total, 89 known vvi-miRNAs and 33 novel wvi-miRNA candidates were identified in our samples, many of them showing the accumulation profile modulated by at least one of the factors studied. The *in silico* prediction of miRNA targets suggests their involvement in berry development and in secondary metabolites accumulation such as anthocyanins and polyphenols.

Keywords: *Vitis vinifera*, Genotype x Environment (GxE), small RNAs, miRNAs, high throughput sequencing, berry

INTRODUCTION

The ability of a genotype to produce different phenotypes as a function of environmental cues is known as phenotypic plasticity (Bradshaw, 1965; Sultan, 2000; Pigliucci, 2001; Gratani, 2014). Phenotypic plasticity is considered one of the main processes by which plants, as sessile organisms, can face and adapt to the spatio-temporal variation of environmental factors (Nicotra et al., 2010; Palmer et al., 2012; Gratani, 2014).

Grapevine (*Vitis vinifera* L.) berries are characterized by high phenotypic plasticity (Dal Santo et al., 2013) and a genotype (cultivar or clone) can present variability within berries, among berries

in a cluster, and among vines (Gray, 2002; Keller, 2010). Berry phenotypic traits, such as the content of sugars, acids, phenolic, anthocyanins, and flavor compounds, are the result of cultivar (G) and environmental influences (E), and often strong G × E interactions (Sadras et al., 2007). Although grapevine plasticity in response to environmental conditions and viticulture practices may provide advantages related to the adaptation of a cultivar to specific growing conditions, it may also cause irregular ripening (Selvaraj et al., 1994) and large inter-seasonal fluctuations (Clingeleffer, 2010), which are undesirable characteristics for wine making (Keller, 2010).

Due to its complex nature, the study of phenotypic plasticity is challenging and the mechanisms by which the genes affecting plastic responses operate are poorly characterized (Holloway, 2002; DeWitt and Scheiner, 2003; Nicotra et al., 2010; Gianoli and Valladares, 2012; Gratani, 2014). In fact it is often difficult to assess the performance of different phenotypes in different environments (Schmitt, 1993; Schmitt et al., 1999; Callaway et al., 2003).

It has been suggested that genetic and epigenetic regulation of gene expression might be at the basis of phenotypic plasticity through the activation of alternative gene pathways (Schlichting and Pigliucci, 1993; Pigliucci, 1996) or multiple genes (Lind et al., 2015). Epigenetics has been proposed as crucial in shaping plant phenotypic plasticity, putatively explaining the rapid and reversible alterations in gene expression in response to environmental changes. This fine-tuning of gene expression can be achieved through DNA methylation, histone modifications and chromatin remodeling (Goldberg et al., 2007; Geng et al., 2013; Duncan et al., 2014).

Small non-coding RNAs (small ncRNAs) are ubiquitous and adjustable repressors of gene expression across a broad group of eukaryotic species and are directly involved in controlling, in a sequence specific manner, multiple epigenetic phenomena such as RNA-directed DNA methylation and chromatin remodeling (Bernstein and Allis, 2005; Fagegaltier et al., 2009; Ha et al., 2009; Swami, 2010; Burkhart et al., 2011; Castel and Martienssen, 2013; Duncan et al., 2014) and might play a role in genotype by environment (GxE) interactions. In plants, small ncRNAs are typically 20–24 nt long RNA molecules and participate in a wide series of biological processes controlling gene expression via transcriptional and post-transcriptional regulation (Finnegan and Matzke, 2003; Kim, 2005; Chen, 2009; Guleria et al., 2011; Lelandais-Briere et al., 2012; Matsui et al., 2013). Moreover, small RNAs have been recently shown to play an important role in plants environmental plasticity (Formey et al., 2014; Borges and Martienssen, 2016).

Fruit maturation, the process that starts with fruit-set and ends with fruit ripening (Coombe, 1976), has been largely investigated in fleshy fruits such as tomato and grapevine. These studies highlighted, among others, the vast transcriptomic reprogramming underlying the berry ripening process (Guillaumie et al., 2011; Matas et al., 2011; Lijavetzky et al., 2012), the extensive plasticity of berry maturation in the context of a changing environment (Dal Santo et al., 2013; Gapper et al., 2014), and the epigenetic regulatory network which contributes to adjust gene expression to internal and external

stimuli (Zhong et al., 2013; Liu et al., 2015). In particular, small RNAs, and especially microRNAs (miRNA), are involved, among others, in those biological processes governing fruit ripening (Karlova et al., 2013; Kullan et al., 2015).

In this work, we assessed the role of small ncRNAs in the plasticity of grapevine berries development, by employing next-generation sequencing. We focused on two cultivars of *Vitis vinifera*, Cabernet Sauvignon, and Sangiovese, collecting berries at four different developmental stages in three Italian vineyards, diversely located. First, we described the general landscape of small RNAs originated from hotspots present along the genome, examining their accumulation according to cultivars, environments and developmental stages. Subsequently, we analyzed miRNAs, identifying known and novel miRNA candidates and their distribution profiles in the various samples. Based on the *in silico* prediction of their targets, we suggest the potential involvement of this class of small RNAs in GxE interactions. The results obtained provide insights into the complex molecular machinery that connects the genotype and the environment.

MATERIALS AND METHODS

Plant Material

Two *V. vinifera* varieties Sangiovese (SG), a red Italian grape variety, and Cabernet Sauvignon (CS), an international variety, were grown side by side in three different Italian locations, representing traditional areas of Sangiovese cultivation in Italy with a long-standing winemaking tradition.

In order to reduce factors of variation, the age of the plants (between 10 and 12 years old), the clone type (Sangiovese clone R5 and Cabernet Sauvignon clone VCR23), the rootstock (*Vitis berlandieri* × *Vitis riparia*), the cultivation techniques (training system: low cordon; planting space: 2.40 × 0.8 m) and the health status were the same among all the locations.

The vineyards were located in Bolgheri (Bol), a coastal area of Tuscany, 50 m asl (above sea level) [GPS coordinates: SG 43.194090, 10.625186, CS 43.194622, 10.624392], in Montalcino (Mont) a mountain area of Tuscany, 195 m asl; [GPS coordinates: SG 42.980669, 11.433708, CS 42.985091, 11.435853] and in Riccione (Ric), a plain area of Emilia Romagna, 111 m asl; [GPS coordinates: SG 43.945261, 12.647235, CS 43.944372, 12.648995]. Further details on the environmental conditions of the vineyards are provided in Supplementary Figure 1.

Berries from four developmental stages were collected in two biological replicates, during the 2011 growing season, for a total of 48 samples (Table 1). The four sampled stages corresponded to pea size (ps), representing the first stage of berry development in this experimental plan, bunch closure (bc) also known as Lag Phase, 19–20 °Brix (19), which corresponds to 50% of sugar accumulation in berries, and harvest (hv), when the berries are fully ripened and the onset of sugar accumulation is over. About 200 berries per each developmental berry stage were sampled from upper, central and lower part of cluster, both from sun-exposed and shaded side and split in two biological replicates. Per each vineyard, the berries were collected from about 20 vines

selected in a single uniform row and immediately frozen in liquid nitrogen and stored at -80°C prior to analysis.

The libraries were named using the initials of the vineyard where the berries were collected, followed by the initial of the cultivar and the developmental stage. For example, the sample containing berries of Sangiovese, collected in Montalcino at pea size, was named Mont_SG_ps.

RNA Extraction and Small RNA Libraries Construction

RNA extraction was performed as described in Kullan et al. (2015). Briefly, total RNA was extracted from 200 mg of ground berries pericarp tissue (entire berries without seeds) using 1 ml of Plant RNA Isolation Reagent (Life Technologies) following manufacturer's recommendations.

The small RNA fraction was isolated from the total RNA using the mirPremier[®] microRNA Isolation kit (Sigma-Aldrich) and dissolved in DEPC water. All the steps suggested in the technical bulletin for small RNA isolation of plant tissues were followed except the "Filter Lysate" step, which was omitted. The quality and quantity of small RNAs were evaluated by a NanoDrop 1000 spectrometer (Thermo Fisher Scientific), and their integrity assessed by an Agilent 2100 Bioanalyzer using a small RNA chip (Agilent Technologies) according to the manufacturer's instructions.

Small RNA libraries were prepared using the TruSeq Small RNA Sample Preparation Kit (Illumina[®]), following all manufacturers' instructions. Forty-eight bar-coded small RNA libraries were constructed starting from 50 ng of small RNAs. The quality of each library was assessed using an Agilent DNA 1000 chip for the Agilent 2100 Bioanalyzer. Libraries were grouped in pools with six libraries each (6-plex).

The pools of libraries were sequenced on an Illumina Hiseq 2000 at IGA Technology Services (Udine, Italy).

The sequencing data were submitted to GEO-NCBI under the accession number GSE85611.

Bioinformatics Analysis of Sequencing Data

Adaptor sequences were trimmed and only reads ranging from 18 to 34 nt in length after adapter removal were kept. Retained reads were mapped to the reference *Vitis vinifera* L. genomic sequence V1 (PN40024, Jaillon et al., 2007) using Bowtie (Langmead et al., 2009) and reads perfectly aligned to the genome were retained. Reads matching rRNAs, tRNAs, snRNAs, and snoRNAs were excluded.

Read counts were normalized by the linear count scaling method TP4M (transcripts per 4 million), in order to reduce sequencing bias and to allow the comparison of small RNA accumulation from different libraries. The normalized abundance was calculated as:

$$\text{TPM abundance} = \left[\frac{\text{raw value}}{\left(\frac{\text{total genome matches} - \text{t/r/sn/snoRNA}}{\text{chloroplast mitochondria matches}} \right)} \right] \times n_{\text{base}}$$

TABLE 1 | List of berry samples of *Vitis vinifera* used for the construction of the small RNA libraries.

Vineyard	Variety	Developmental Stages	Replicate	Library Codes
Montalcino	Cabernet Sauvignon	Pea size	1	Mont_CS_ps_1
			2	Mont_CS_ps_2
		Bunch closure	1	Mont_CS_bc_1
			2	Mont_CS_bc_2
		19 °Brix	1	Mont_CS_19_1
			2	Mont_CS_19_2
		Harvest	1	Mont_CS_hv_1
			2	Mont_CS_hv_2
		Pea size	1	Mont_SG_ps_1
			2	Mont_SG_ps_2
Bolgheri	Sangiovese	Bunch closure	1	Mont_SG_bc_1
			2	Mont_SG_bc_2
		19 °Brix	1	Mont_SG_19_1
			2	Mont_SG_19_2
		Harvest	1	Mont_SG_hv_1
			2	Mont_SG_hv_2
		Pea size	1	Bol_CS_ps_1
			2	Bol_CS_ps_2
		Bunch closure	1	Bol_CS_bc_1
			2	Bol_CS_bc_2
Bolgheri	Cabernet Sauvignon	19 °Brix	1	Bol_CS_19_1
			2	Bol_CS_19_2
		Harvest	1	Bol_CS_hv_1
			2	Bol_CS_hv_2
		Pea size	1	Bol_SG_ps_1
			2	Bol_SG_ps_2
		Bunch closure	1	Bol_SG_bc_1
			2	Bol_SG_bc_2
		19 °Brix	1	Bol_SG_19_1
			2	Bol_SG_19_2
Riccione	Sangiovese	Harvest	1	Bol_SG_hv_1
			2	Bol_SG_hv_2
		Pea size	1	Ric_CS_ps_1
			2	Ric_CS_ps_2
		Bunch closure	1	Ric_CS_bc_1
			2	Ric_CS_bc_2
		19 °Brix	1	Ric_CS_19_1
			2	Ric_CS_19_2
		Harvest	1	Ric_CS_hv_1
			2	Ric_CS_hv_2
Riccione	Cabernet Sauvignon	Pea size	1	Ric_SG_ps_1
			2	Ric_SG_ps_2
		Bunch closure	1	Ric_SG_bc_1
			2	Ric_SG_bc_2
		19 °Brix	1	Ric_SG_19_1
			2	Ric_SG_19_2
		Harvest	1	Ric_SG_hv_1
			2	Ric_SG_hv_2

where n base is 4,000,000.

To perform the clustering analysis, the “hits-normalized-abundance” (HNA) values were calculated as:

$$HNA = \frac{TP4M}{Hits}$$

where $TP4M$ is the normalized abundance of each small RNA sequence mapping in a giving cluster and a *Hit* is defined as the number of loci at which a given sequence perfectly matches the genome.

One database was produced using the grapevine genome, and made available on the website (https://mpss.danforthcenter.org/dbs/index.php?SITE=grape_sRNA_GxE), in order to store and assist the visualization of all the sequenced libraries.

Static Clustering Analysis

The static clustering analysis was carried out as previously described by Lee et al. (2012), using a proximity-based pipeline built with custom Perl and database scripts (McCormick et al., 2011) and MySQL database queries, to group and quantify clusters of small RNAs. Briefly, the grapevine genome was divided into a series of windows of 500 bp, each window defined as a cluster. For every individual library, the small RNAs ranging from 21 to 24 nt and mapping in each cluster had their “hits-normalized-abundance” (HNA) summed up which determined the “cluster abundance.” The cluster abundance was averaged for the two replicates of each library. The clusters were annotated for gene and repeat information using the V1 annotation of the reference genome (Jaillon et al., 2007; Vitulo et al., 2014), allowing the characterization of specific small RNA-producing loci.

We set a selection criterion, by which a cluster was considered as expressed when the cluster abundance was equal or greater than 30 HNA. Additionally, when investigating the ratio between two cultivars in each environment (CS/SG ratio), only those clusters where the HNA of each library in the comparison was greater than or equal to 5 (library A \geq 5 HNA and library B \geq 5 HNA) and the sum of the cluster abundance of these same libraries was higher than 30 (library A + library B $>$ 30) were selected.

All the clustering analyses were performed using only two developmental stages for each cultivar: bunch closure was used to represent “green tissues” (g) and 19°Brix to represent “ripened tissues” (r).

Identification of Conserved miRNAs and Prediction of Novel Candidates

The identification of annotated (conserved or known) and novel (or species-specific) miRNAs was carried out applying a conservative and robust pipeline as described by Jeong et al. (2011) and Zhai et al. (2011), and successfully deployed in various published studies (Jeong et al., 2013; Xu et al., 2013; Ariket et al., 2014; Hu et al., 2015). Shortly, in order to recognize the conserved miRNAs, all small RNAs sequenced in the libraries were initially compared against all annotated vvi-miRNAs deposited in miRBase (version 20, Kozomara and Griffiths-Jones, 2014, <http://www.mirbase.org/>). Subsequently, the whole set of small RNAs passed through the five filters

designed according to the properties of validated plant miRNAs and their precursors (Meyers et al., 2008), keeping track of known miRNAs throughout the filtering. The filters included, but were not limited to, minimum abundance threshold (≥ 30 TP4M), size range (18–26 nt), maximum hits to the grapevine genome (1–20), strand bias (sense/total ≥ 0.9), and abundance bias [$(top1+top2)/total \geq 0.7$]. For each possible precursor found, the most abundant read was retained as the biologically active miRNA (also called “mature”) and in cases where both the 3'-end (3p) and the 5'-end (5p) reads were highly abundant (abundance greater than 200 TP4M), the two tags were kept.

All the known vvi-miRNAs identified by the pipeline were manually inspected, to ensure that the tags identified as known miRNAs were assigned correctly to their actual precursor, and to retrieve the most abundant isoform within the tags mapping in each precursor.

Regarding the novel miRNA candidates identified using this pipeline, only those for which the most abundant tag was 20, 21, or 22 nt were retained. They were compared with all the known mature plant miRNAs in miRBase (version 20) to identify homologs. Finally, novel candidates passed through a manual evaluation of precursor secondary structures, using the plant version of the UEA sRNA hairpin folding and annotation tool (Stocks et al., 2012) and the Mfold web server (Zuker, 2003), with default settings.

miRNA Accumulation and Statistical Analysis

A miRNA was considered as “expressed” only when the values of both biological replicates were greater than or equal to the threshold set at 10 TP4M. We defined a miRNA as “vineyard-, cultivar-, or stage-specific” when it was expressed only in a given vineyard, cultivar or one specific developmental stage.

Differentially expressed miRNAs were identified using the CLCbio Genomics Workbench (v.8, Qiagen, <http://www.qiagenbioinformatics.com/products/clc-genomics-workbench/>) using multiple comparison analysis. We loaded the total raw redundant reads from our 48 libraries in the CLCbio package and trimmed the adaptors, considering only reads between 18 and 34 nt. We annotated miRNAs against the user defined database, comprehending our set of 122 MIRNA loci and their corresponding mature sequences. For each library, the total counts of read perfectly mapping to the miRNA precursors was considered as the input of the expression analysis.

Given the main focus of our work, we aimed at identifying miRNAs differentially expressed between the two cultivars in the same environment and developmental stage (genotypic effect), or between the three vineyards in the same cultivar and in the same developmental stage (environmental effect). For this reason, we considered each developmental stage (12 libraries) and we performed the Empirical Analysis of digital gene expression (DGE), an implementation of the “Exact Test” present in the EdgeR Bioconductor package, as implemented in CLCbio software and estimating tagwise dispersion with pairwise comparisons and setting the significance threshold to FDR-adjusted $p \leq 0.05$.

Correlation Analysis

The normalized reads (TP4M) of all miRNAs identified in this study and also the cluster abundances obtained from the static clustering analysis were submitted to another *ad-hoc* normalization [$\log_{10}(1+TP4M)$ or $\log_{10}(1+HNA)$] for correlation analysis. This normalization was chosen because of the enormous range of abundance values that produced a log-unimodal distribution and may cause significant biases in the correlation analysis when performed using TP4M or HNA values. A unity was then added to the abundance value due to the presence of zero entries. After this addition, a value of zero still corresponds to zero of the $\log_{10}(1+TP4M)$ function, thus making consistent the comparisons among profiles.

The dendrogram was generated using the function `hclust` and the Pearson correlation was calculated using the function `cor` in R, based on the $\log_{10}(1+TP4M)$ or $\log_{10}(1+HNA)$ values for miRNAs and sRNA-generating loci respectively. Pearson's correlation coefficients were converted into distance coefficients to define the height of the dendrogram.

Heat maps were produced using MeV (MultiExperiment Viewer; Eisen et al., 1998) based on TP4M values of miRNAs abundance. The Venn diagrams were produced using the function `vennDiagram` in R, based on the miRNA list for each cultivar, environment and developmental stage.

Target Prediction

miRNA targets were predicted using miRferno, a built-in, plant-focused target prediction module of the software sPARTA (small RNA-PARE Target Analyzer; Kakrana et al., 2014). miRferno was run using the greedy prediction mode (`tarPred H`) and a seed-free system (`tarScore S`) for target scoring. The prediction was done in genic regions (`genomeFeature 0`) of the whole 12X version of the grapevine genome (Jaillon et al., 2007). The fasta file with spliced exons for each GFF transcript (V2.1.mRNA.fasta downloaded from <http://genomes.cribi.unipd.it/grape/>) of the V2.1 annotation (Vitulo et al., 2014) was used as "feature file." To reduce the number of false positives, only targets with a prediction score value smaller than 2.5 were retained (complete range of prediction score values: 0–10).

RESULTS

High-Throughput Sequencing Statistics

Small RNA libraries were constructed and sequenced for 48 samples of grapevine berries (Table 1). We obtained a total of 752,020,195 raw redundant reads (Supplementary Table 1). After adaptors trimming, 415,910,891 raw clean reads were recovered, ranging from 18 to 34 nt in length (Supplementary Table 1). Eliminating the reads mapping to rRNA, tRNA, snRNA, and snoRNA sequences, 199,952,950 reads represented by 20,318,708 distinct sequences, i.e., non-redundant sequences found in the 48 libraries (Supplementary Table 1), were perfectly mapped to the *V. vinifera* PN40024 reference genome (Jaillon et al., 2007).

The libraries were analyzed to assess the size distributions of mapped reads. Distinct peaks at 21- and 24-nt (Supplementary Figure 2) were observed in all the libraries. Consistent with previous reports in grapevine (Pantaleo et al., 2010) and other

plant species (Moxon et al., 2008; Ge et al., 2013), the 21-nt peak was the highest, comprising a higher proportion of redundant reads, whereas the 24-nt peak was less abundant. A few exceptions regarding the highest peak in the small RNA size profile were observed: Ric_SG_ps had the highest peak at 24-nt whereas Mont_CS_ps and Mont SG_bc did not show a clear difference between the 21- and the 24-nt peak.

Using the Pearson coefficients (Supplementary Table 2) we observed a strong association between the replicates as indicated by the high coefficients (ranging from 0.79 to 0.97).

To facilitate access and utilization of these data, we have incorporated the small RNAs into a website (https://mpss.danforthcenter.org/dbs/index.php?SITE=grape_sRNA_GxE). This website provides a summary of the library information, including samples metadata, mapped reads, and GEO accession numbers. It also includes pages for data analysis, such as quick summary of the abundances of annotated microRNAs from grapevine or other species. Small RNA-related tools are available, for example target prediction for user-specified small RNA sequences and matching criteria. Finally, and perhaps most importantly, a customized browser allows users to examine specific loci (genes or intergenic regions) for the position, abundance, length, and genomic context of matched small RNAs; with this information, coupled with the target prediction output, users can develop and assess hypotheses about whether there is evidence for small RNA-mediated regulation of grapevine loci of interest.

General Landscape of Small RNAs Distribution in Grapevine Berries in Different Environments

In order to investigate whether the overall distribution and accumulation of small RNA is affected by the interaction between different *V. vinifera* genotypes [Cabernet Sauvignon (CS) and Sangiovese (SG)] and environments [Bolgheri (Bol), Montalcino (Mont) and Riccione (Ric)], we investigated the regions in the grapevine genome from where a high number of small RNAs were being produced (sRNA-producing regions), by applying a proximity-based pipeline to group and quantify clusters of small RNAs as described by Lee et al. (2012).

The nuclear grapevine genome was divided in 972,413 adjacent, non-overlapping, fixed-size (500 bp) windows or clusters. To determine the small RNA cluster abundance, we summed the hits-normalized-abundance (HNA) values of all the small RNAs mapping to each of the 500 bp clusters, for each library (for details, see Materials and Methods). To reduce the number of false positives, we considered a cluster as expressed when the cluster abundance was greater than the threshold (HNA = 30) for a given library, eliminating regions where few small RNAs were generated, possibly by chance. Libraries from bunch closure, representing green berries, and 19 °Brix representing ripened berries, where used in this analysis. From the 972,413 clusters covering the whole grapevine genome, 4408 (0.45%) were identified as expressed (sRNA-producing regions) in at least one sample. As showed in Figure 1, CS-derived libraries have a higher number of expressed clusters when compared to SG-derived

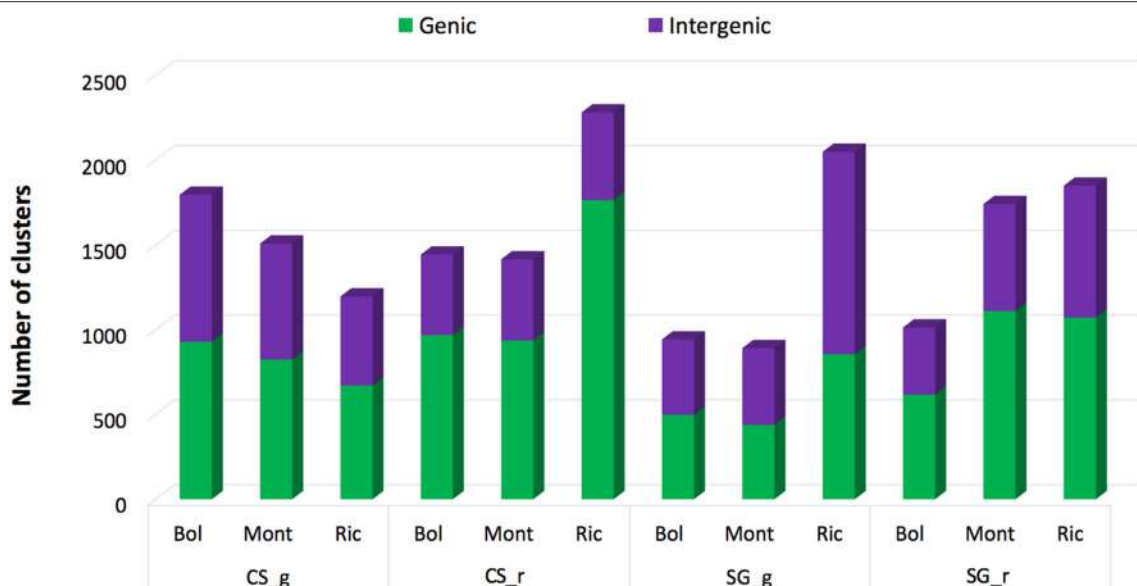


FIGURE 1 | Number of small RNA clusters expressed in ripened and green berries of grapevine collected from 2 different cultivars growing in 3 vineyards. The proportion of clusters located in Genic and Intergenic regions (based on the V1 grapevine genome annotation) is shown in green and blue respectively. CS, Cabernet Sauvignon; SG, Sangiovese; g, green; r, ripened; Bol, Bolgheri; Mont, Montalcino; Ric, Riccione. Green corresponds to bunch closure and ripened corresponds to 19 °Brix developmental stages.

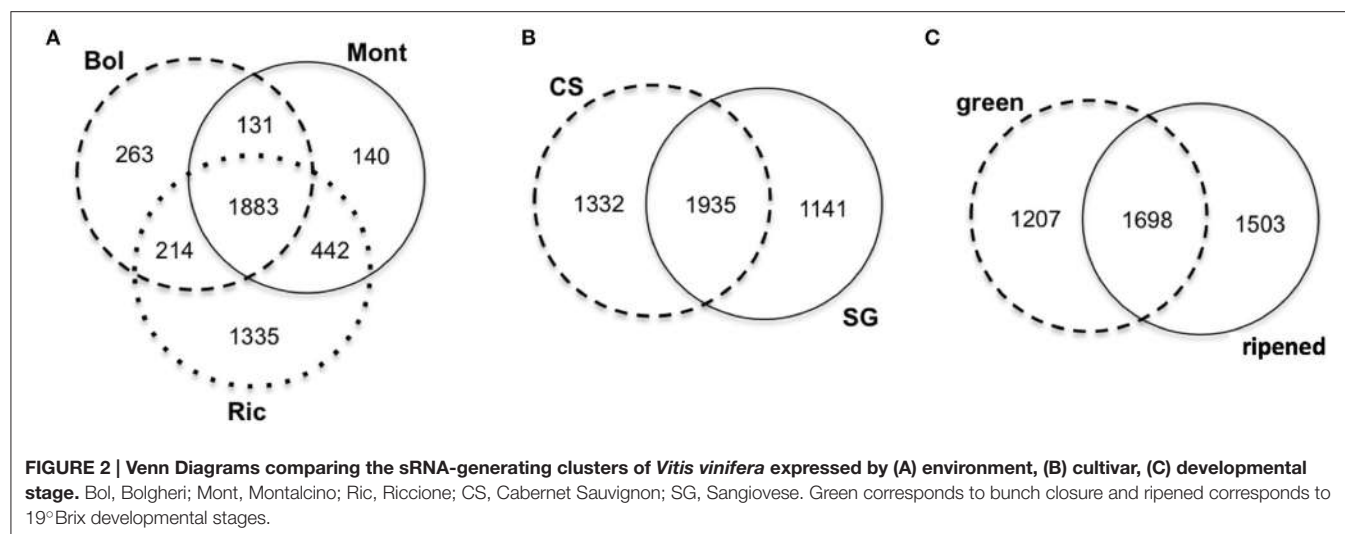
libraries of the same developmental stage and from the same vineyard. The exceptions were the Sangiovese green berries collected in Riccione and Sangiovese ripened berries collected in Montalcino, which have a higher number of expressed clusters than the respective CS ones. The two cultivars show a completely different small RNA profile across environments. When Cabernet berries were green, a higher number of sRNA-generating regions were found active in Bolgheri than in Montalcino and Riccione. Differently, ripened berries had the highest number of sRNA-producing regions expressed in Riccione, while Bolgheri and Montalcino show a similar level of expressed clusters (Figure 1). Sangiovese green berries instead show the highest number of active sRNA-generating regions in Riccione, and this number is twice the number found in Bolgheri and Montalcino that is similar. Ripened berries collected in Montalcino and Riccione show almost the same high level of sRNA-generating clusters, whereas those collected in Bolgheri present a lower number (Figure 1). We also noted that when cultivated in Bolgheri, neither Cabernet Sauvignon or Sangiovese change dramatically the number of expressed clusters during ripening, while in Riccione Cabernet Sauvignon shows a 2-fold increase of sRNA-producing clusters, which is not observed in Sangiovese.

Next, the small RNA-generating clusters were characterized on the basis of the genomic regions where they map, i.e., genic, intergenic and transposable elements. In general, when the berries were green, the numbers of sRNA-generating loci located in genic and intergenic regions were roughly equal in all environments and for both cultivars, except for Sangiovese berries collected in Riccione, which show a slight intergenic disposition of sRNA-producing regions (Figure 1). Differently, in ripened berries on average 65% of the sRNA-generating loci

were in genic regions, indicating a strong genic disposition of the sRNA-producing clusters (Figure 1). The shift of sRNA-producing clusters from intergenic to mostly genic is more pronounced in Cabernet Sauvignon berries collected in Riccione, with an increase of approximately 20% of expressed clusters in genic regions (Figure 1) when berries pass from the green to the ripened stage.

When comparing the clusters abundance among libraries, we found that 462 clusters were expressed in all libraries. The remaining 3946 expressed clusters were either shared among groups of libraries or specific to unique libraries. Interestingly, 1335 (30.3%) of the 4408 expressed clusters were specific to Riccione-derived libraries (Figure 2A). The other two environments showed a much lower percentage of specific clusters, 263 (6%) and 140 (3.2%) in Bolgheri and Montalcino respectively (Figure 2A). Comparing the expressed clusters between cultivars or developmental stages, we did not observe a similar discrepancy of specific clusters toward one cultivar or developmental stage; roughly the same proportion of specific clusters was found for each cultivar (Figure 2B) and for each developmental stage (Figure 2C). Among the 1335 specific clusters of Riccione, 605 were specific to Cabernet Sauvignon ripened berries and 499 to Sangiovese green berries. Other smaller groups of expressed clusters were identified as specific to one cultivar, one developmental stage or also one cultivar in a specific developmental stage.

When comparing the expressed clusters with the presence of transposable elements (TE) annotated in the grapevine genome (V1), we noticed that approximately 23% of the sRNA-generating regions were TE-associated. Sangiovese green berries from Riccione have the highest proportion (26%) of TE-associated



expressed clusters, while Cabernet Sauvignon ripened berries also from Riccione show the lowest proportion (13%) of TE-associated expressed clusters. Sangiovese berries (both green and ripened) have the highest percentage of expressed clusters located in TE when cultivated in Riccione, compared to the other two vineyards. Interestingly, Cabernet Sauvignon berries show the lowest proportion of TE-associated clusters when growing in Riccione (Figure 3A), independently from the berry stage.

In all the libraries, Long Terminal Repeat (LTR) retrotransposons were the most represented TE. More specifically, the gypsy family was the LTR class associated with the highest number of sRNA hotspots. The other classes of TE associated with the sRNA-generating regions can be visualized in Figure 3B.

The Distribution of sRNA-Producing Loci Is Variable between the Two Cultivars, and the Level of Variation Depends on the Vineyard

To determine the global relationship of small RNA-producing loci in the different environments, cultivars and developmental stages, we performed a hierarchical clustering analysis. As showed in Figure 4, the libraries clearly clustered according to the developmental stage and cultivar and not according to the environments. Ripened and green berries had their profile of sRNA-generating loci clearly distinguished from each other. Inside each branch of green and ripened samples, Cabernet Sauvignon and Sangiovese were also well separated, indicating that, the cultivar and the stage of development in which the berries were sampled modulate the outline of sRNA-producing loci more than the environment.

Notwithstanding the evidence that developmental stage and variety have the strongest effect in terms of distinguishing samples clustering, we were interested to verify the environmental influence on small RNA loci expression in the two cultivars. Thus, for each sRNA-generating cluster we

calculated the ratio between cluster abundance in Cabernet Sauvignon and Sangiovese (CS/SG) in each environment and developmental stage, thereby revealing the genomic regions with regulated clusters, considering a 2-fold change threshold, a minimum abundance of 5 HNA in each library and a minimum sum of abundance of 30 HNA (library A \geq 5 HNA and library B \geq 5 HNA; library A + library B $>$ 30 HNA; library A/library B \geq 2). Figure 5 shows how different environments affect the production of small RNAs. In Bolgheri, regardless the developmental stage there were many clusters with a very high abundance level in Cabernet Sauvignon (Figure 5A). In Montalcino (Figure 5B) and even more in Riccione (Figure 5C) we also observed differences between the expressions of clusters in the two cultivars, with ripened and green berries showing an almost opposite profile in terms of number of clusters more expressed in Cabernet Sauvignon or Sangiovese. When the berries were green, in Montalcino Cabernet Sauvignon shows the highest number of up-regulated clusters, while in Riccione, Sangiovese has the highest number of up-regulated clusters. The opposite behavior was noticed in ripened berries, with Sangiovese having the highest number of up-regulated clusters in Montalcino and Cabernet Sauvignon in Riccione (Figures 5B,C).

Notably, we observed a small percentage of regulated clusters (from 0.5 to 5%) exhibiting at least a 10-fold higher abundance of small RNA in Cabernet Sauvignon or Sangiovese when compared to each other (Figures 5A–C). An examination of those clusters showed that a substantial difference (50-fold or more) could exist between the cultivars, depending on the vineyard and the developmental stage. For example, in Riccione, a cluster matching a locus encoding a BURP domain-containing protein showed a fold change of 390 when comparing green berries of Sangiovese with Cabernet Sauvignon. The small RNAs mapping in this region were mainly 21-nt and produced from both strands (Figure 6). Similarly, the majority of the highly differentially expressed clusters (50-fold or more) showed a similar profile: strong bias toward 21-nt sRNAs and a low strand bias. These findings suggest that these small RNAs might be the product

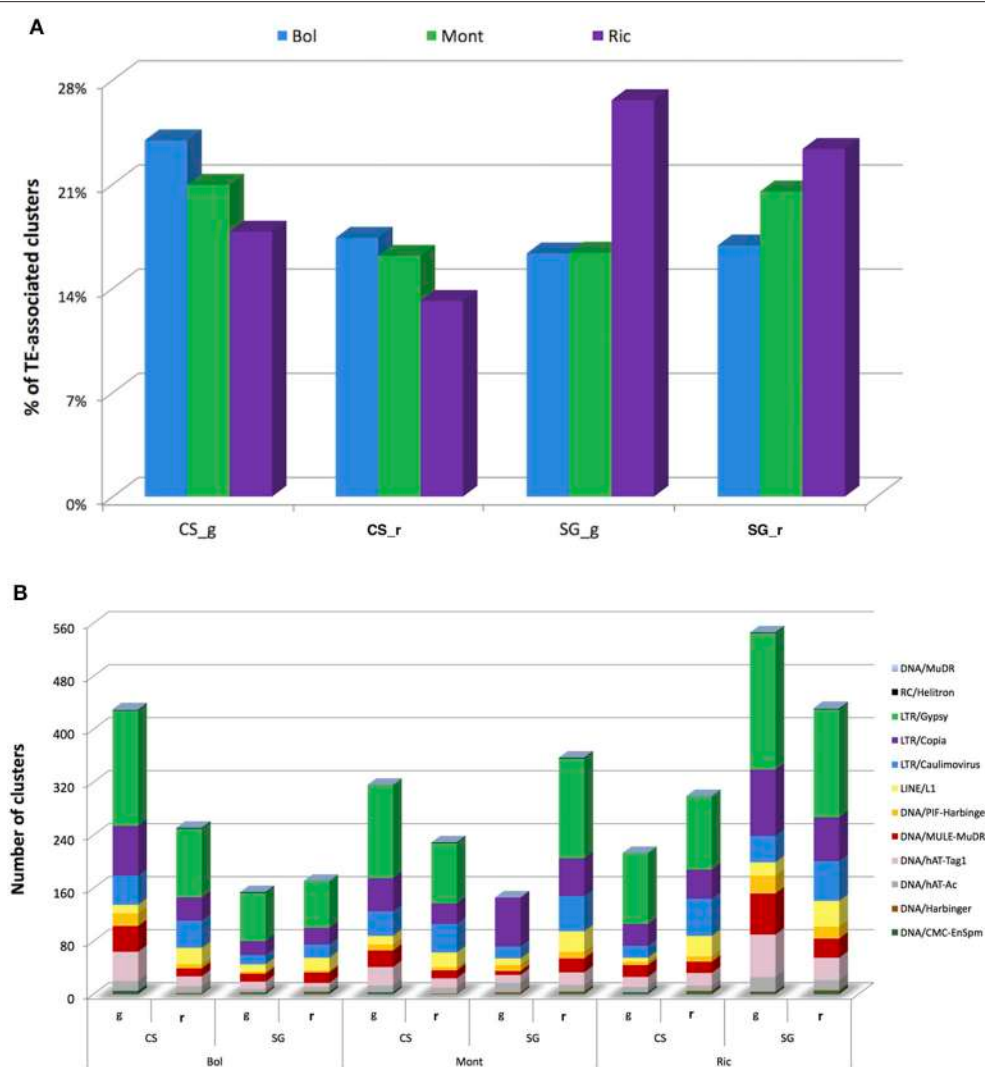


FIGURE 3 | Profile of small RNA-producing clusters expressed in ripened and green berries of grapevine collected from 2 different cultivars growing in 3 vineyards associated with Transposable Elements (TE). (A) Percentage of sRNA-producing clusters associated with TE in each sample. **(B)** Number of small RNA-generating clusters associated with different classes of TE in different samples. Bol, Bolgheri; Mont, Montalcino; Ric, Riccione; CS, Cabernet Sauvignon; SG, Sangiovese; g, green; r, ripened. Green corresponds to bunch closure and ripened corresponds to 19 °Brix developmental stages.

of RDR (RNA-dependent RNA) polymerase activity rather than degradation products of mRNAs.

miRNAs Identification and Target Prediction

We applied a pipeline adapted from Jeong et al. (2011) and Zhai et al. (2011) to identify annotated vvi-miRNAs, their variants, novel species-specific candidates and, when possible, the complementary 3p or 5p sequences. Starting from 25,437,525 distinct sequences from all the 48 libraries, the first filter of the pipeline removed sequences matching t/r/sn/snoRNAs as well as those that did not meet the threshold of 30 TP4M in at least one library or, conversely, that mapped in more than 20 loci of the

grapevine genome (considered overly repetitive to be a miRNA). Only sequences 18–26-nt in length were retained. Overall, 27,332 sequences, including 56 known vvi-miRNAs, passed through this first filter and were subsequently analyzed by a modified version of miREAP (<https://sourceforge.net/projects/mireap>) as described by Jeong et al. (2011). miREAP identified 1819 miRNA precursors producing 1108 unique miRNA candidates, including 47 known vvi-miRNA. Next, the sequences were submitted to the third filter to evaluate the single-strand and abundance bias retrieving only one or two most abundant miRNA sequence for each precursor previously identified. A total of 150 unique miRNA corresponding to 209 precursors were identified as candidate miRNAs. Among these 209 candidate precursors, 61 belonged to 31 known vvi-miRNA that passed all

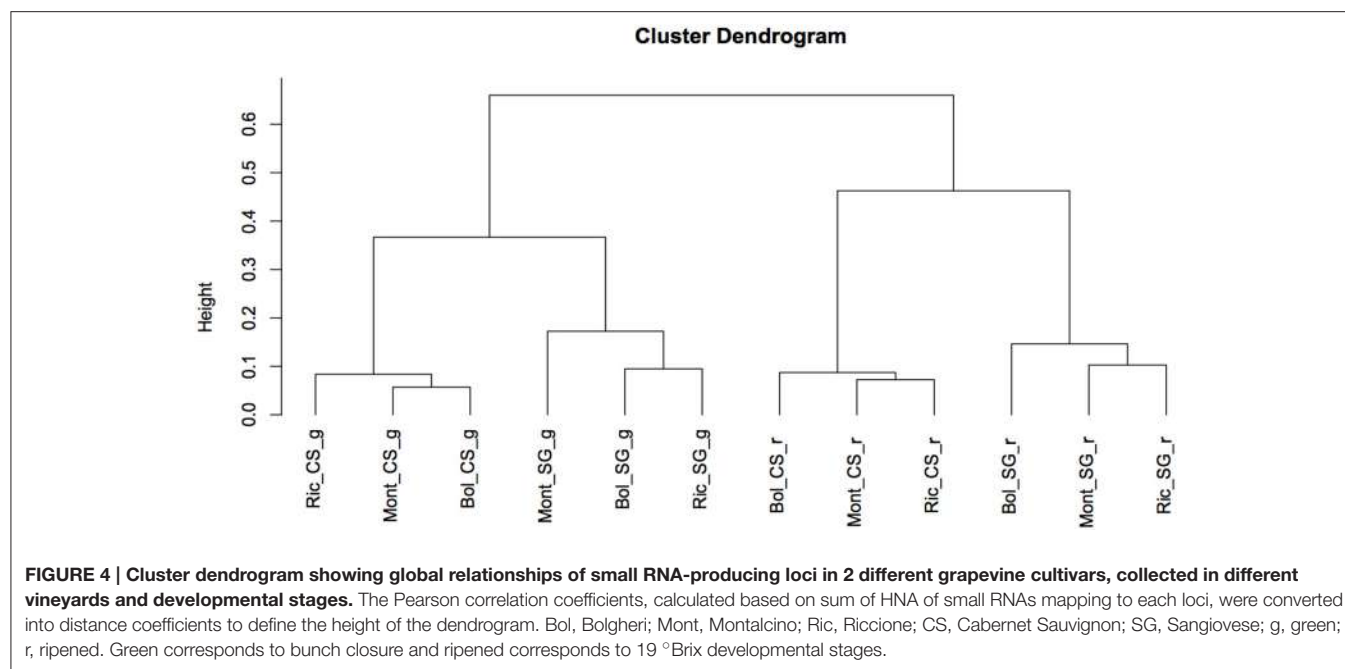


FIGURE 4 | Cluster dendrogram showing global relationships of small RNA-producing loci in 2 different grapevine cultivars, collected in different vineyards and developmental stages. The Pearson correlation coefficients, calculated based on sum of HNA of small RNAs mapping to each loci, were converted into distance coefficients to define the height of the dendrogram. Bol, Bolgheri; Mont, Montalcino; Ric, Riccione; CS, Cabernet Sauvignon; SG, Sangiovese; g, green; r, ripened. Green corresponds to bunch closure and ripened corresponds to 19 °Brix developmental stages.

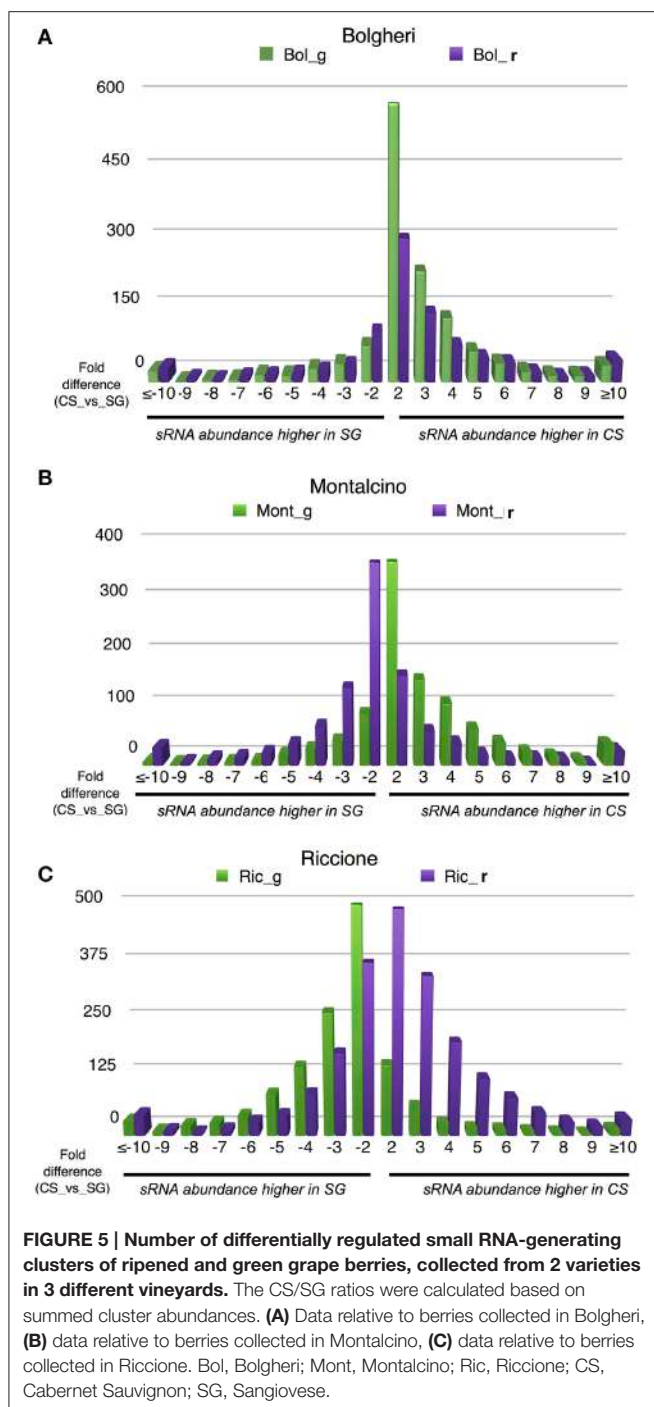
the filters and 148 were identified as putatively novel miRNA candidates. To certify that they were novel candidates rather than variants of known vvi-miRNAs we compared their sequences and coordinates with the miRNAs registered in miRBase (version 20, Kozomara and Griffiths-Jones, 2014). In order to reduce false positives and the selection of siRNA-like miRNAs, we considered only 20, 21, and 22 nt candidates whose stem-loop structures were manually evaluated (see Supplementary Figure 3). Eventually, 26 miRNAs homologous to other plant species were identified with high confidence. Twenty-two were new members of nine known *V. vinifera* families, whereas the other four belong to three families not yet described in grapevine (Table 2). For 16 homologs we were able to retrieve also the complementary sequence. Finally, excluding these 26 miRNAs and other si-RNA like miRNAs, we identified 7 completely novel *bona fide* miRNAs.

Apart from the 61 known vvi-miRNAs identified by the pipeline, we searched the dataset for others known vvi-miRNAs eliminated throughout the pipeline, looking for isomiRs that were actually more abundant than the annotated sequences. Their complementary 3p or 5p sequence was also retrieved when possible. Hence 89 known vvi-miRNAs were identified in at least one of our libraries (Table 3). Among the known vvi-miRNAs identified, 24 had an isomiR more abundant than the annotated sequence and 4 have the complementary sequence as the most abundant sequence mapping to their precursor. We found 16 vvi-miRNA isomiRs that were either longer or shorter than the annotated sequence, 7 vvi-miRNAs that mapped in the precursor in a position shifted with respect to the annotated ones and one miRNA that contains a nucleotide gap when compared to the annotated sequence (Table 3). An extreme case of shifted position was found in vvi-miRNA169c, where the annotated sequence had only 5 TP4M when summing its individual

abundance in the 48 libraries. Another sequence, shifted 16 bp as compared to its annotated position on the precursor had an abundance sum of 1921 TP4M, and was retained together with the annotated sequence, and named vvi-miRNA169c.1. For 36 of the 48 *V. vinifera* miRNA families deposited in miRBase we found at least one member.

An *in silico* prediction of miRNA targets was performed for the 191 mature miRNAs here identified. Using the miRferno tool (Kakrana et al., 2014), and considering only targets predicted with high stringency, 1192 targets were predicted for 143 miRNAs, including six completely novel vvi-miRNA candidates (Supplementary Table 3).

Two novel candidates (grape-m1191 and grape-m1355) seem to be involved in the regulation of important secondary metabolites biosynthesis. Among the six targets predicted for grape-m1191, the *TT12* gene (*transparent testa 12* - VIT_212s0028g01160) is known to be involved in the vacuolar accumulation of proanthocyanidins in grapevine (Marinova et al., 2007). For grape-m1355, 12 targets were predicted and all of them are involved in secondary metabolism pathways. Nine targets code a bifunctional dihydroflavonol 4-reductase (DFR) that is responsible for the production of anthocyanins (Davies et al., 2003), catalyzing the first step in the conversion of dihydroflavonols to anthocyanins (Boss and Davies, 2001). Another targeted gene codes a phenylacetaldehyde reductase (VIT_213s0064g00340) which, in tomato, was demonstrated to catalyze the last step in the synthesis of the aroma volatile 2-phenylethanol, important for the aroma and flavor (Tieman et al., 2007). Still this same miRNA candidate was predicted to target with high confidence (score = 0) a cinnamoyl reductase-like protein (VIT_203s0110g00350) that is part of polyphenol biosynthetic pathway (Martínez-Esteso et al., 2013). The grape-m1355 candidate maps on chromosome 3, exactly on the



first exon of its target (VIT_203s0110g00350.1), in a region where another two isoforms of the same gene are located (Supplementary Figure 4). The last target of this miRNA candidate, codes a cinnamyl alcohol dehydrogenase known to be involved in the lignin biosynthesis (Trabucco et al., 2013).

Other novel vvi-miRNA candidates seem to be involved in cell proliferation (grape-m0642 targets VIT_200s0291g00090, a cyclin-related protein with hydrolase activity) and in chloroplasts-related functions (grape-m1517 targets

VIT_203s0063g02020, a tic62 protein). Furthermore, for the new vvi-miRC482b candidate, besides the already known involvement of this miRNA family with disease resistance (Li et al., 2010) also predicted here, one predicted target encodes an anthocyanin 5-aromatic acyltransferase-like protein known to be involved in the biosynthesis of anthocyanin in different species (Provenzano, 2011).

As for the conserved known vvi-miRNAs, most of the well-established examples of miR-targets, such as miR156-SPB, miR166-HD-ZIP, miR171-GRAS, miR172-AP2, confirmed in several plant species and already predicted in grapevine, were also predicted here.

miRNA Accumulation among Vineyards and Genotypes

We studied miRNA profile of accumulation in the different samples. Using their normalized abundance (TP4M), i.e., their relative cloning frequency, we set an empirical cut off value equal to at least 10 TP4M in both biological replicates to consider a miRNA as expressed in a given library. Also, a miRNA was considered specific when it was expressed in one or more libraries of a unique cultivar, unique environment or unique developmental stage.

According to our established cut off, 175 miRNAs were classified as expressed in at least one of our libraries (Figure 7). The libraries constructed from Sangiovese berries at bunch closure collected in Bolgheri showed only 24 expressed miRNAs (Figure 7). For all the other libraries, expressed miRNAs ranged from 76 (Ric_SG_hv) to 148 (Ric_CS_hv) (Figure 7).

We found very few miRNAs specific to a given condition. The number of specific miRNAs for each cultivar, developmental stage and environment is reported in Figures 8A–C, respectively.

Thirty-nine vvi-miRNAs were highly expressed in almost all libraries [21 ubiquitous plus 18 expressed in all libraries except in Bol_SG_bc (Figure 9)], whereas other miRNAs had different accumulation patterns.

The normalized expression values of miRNAs were subjected to hierarchical clustering (HCL) and represented in a heat map (Figure 9). To examine the relatedness among cultivars, environments and developmental stages, we generated a correlation dendrogram (Figure 10). The dendrogram shows, as already suggested by the heatmaps, that a fundamental dichotomy emerges between ripened and green berries. The most evident pattern of expression is observed when comparing different developmental stages, and confirm previous observation of miRNA modulation during fruit ripening (Manning et al., 2006; Giovannoni, 2007; Carra et al., 2009; Sun et al., 2012; Cao et al., 2016). For example, some members of the vvi-miRNA156 family (f/i and the g-5p) were highly expressed in all ripened berries, but weakly or not expressed in green berries. Differently, vvi-miR396a-3p and vvi-miR396b-3p showed the opposite profile. Similarly, vvi-miR172d, vvi-miR166b-5p, vvi-miR166f-5p, and vvi-miR396d-5p were highly expressed in green berries but weakly expressed in ripened berries and the members of the vvi-miR319 family (b/f/g and c-3p) showed a gradient of decreasing abundance from pea size to harvest.

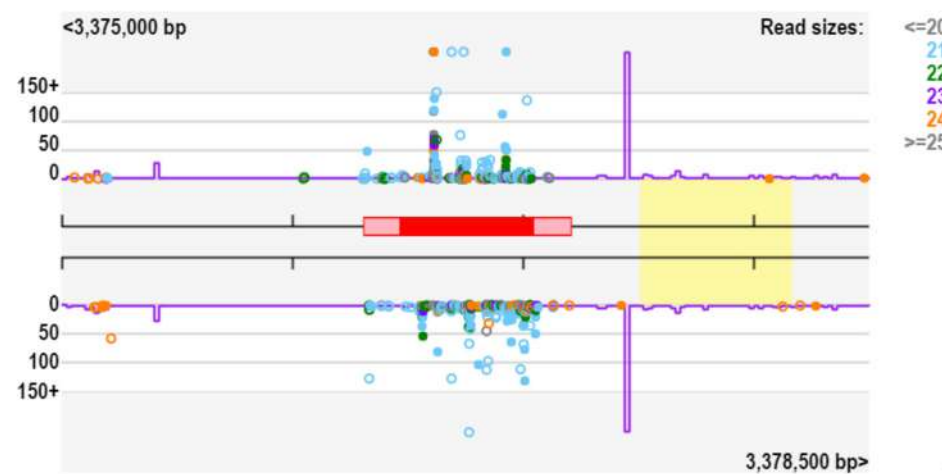
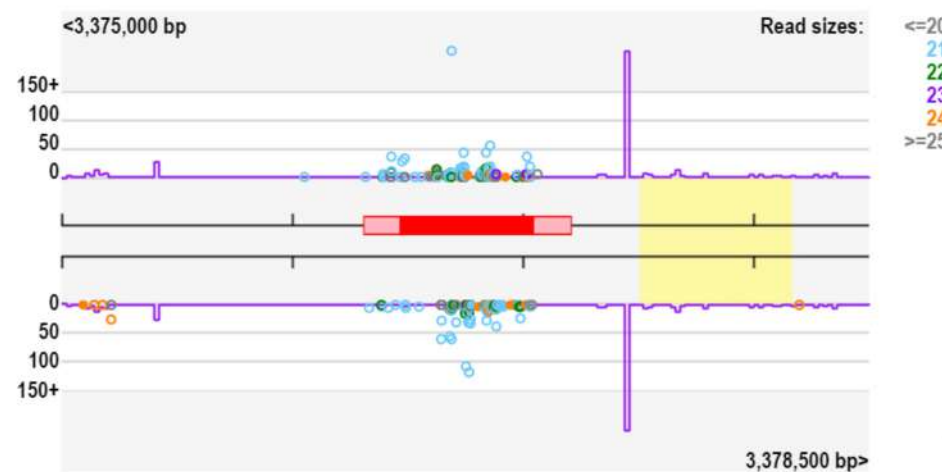
A Ric_SG_bc_2**B Ric_CS_bc_1**

FIGURE 6 | Small RNA-producing loci of *Vitis vinifera* berries with 390-fold change considering SG/CS. The gene in this locus (red box) codes for a protein annotated as “BURP domain-containing protein 3-like,” located on chromosome 4 (VIT_204s0008g04040). **(A)** Representation of small RNAs from Ric_SG_bc_2 mapping to this locus, **(B)** Representation of small RNAs from Ric_CS_bc_1 mapping to this locus. Violet line is the “k-mer” frequency and the yellow box indicate homology to a transposable element. Ric, Riccione; CS, Cabernet Sauvignon; SG, Sangiovese; bc, green, bunch closure developmental stages.

To gain statistical evidence of miRNA differential expression driven by the environment and/or genotype, we made pairwise comparisons, keeping constant the developmental stage, and evaluating the miRNA modulation among vineyards (Montalcino vs Bolgheri vs Riccione) or between cultivars (Cabernet Sauvignon vs Sangiovese). The analyses (with an FDR ≤ 0.05) reveal that some miRNAs are differentially expressed between the two genotypes grown in the same environment, but also that a number of miRNAs are modulated by the environment. In particular the number of differentially expressed miRNAs is higher in ripened berries (19 °Brix and at harvest), while no miRNAs are differentially expressed at bunch closure stage (Supplementary Table 4). In details, 14 reads are differentially expressed at pea size stage, in at least one comparison, corresponding to 6 distinct miRNA families;

27 reads are modulated at 19 °Brix stage, corresponding to 12 miRNA families and 35 reads are differentially expressed in berries at harvest, corresponding to 12 miRNA families. It is worth noting that 4 of the 6 families modulated in the berries at pea size, are still present among the miRNAs differentially expressed in the berries sampled at 19 °Brix and at harvest (miR166, miR3627, miR477, miR3636, and miR3640), even though not always in the same comparisons.

Some of the modulated miRNAs, both novel (grape-m1355, grape-m1191) and known (miR395, miR399, and miR396) are intriguingly connected to berry development and secondary metabolism, even though most of the modulated families are still uncharacterized, or with targets not clearly involved in berry ripening and development, and deserve further studies to fully understand their biological roles.

vi-miRC477c	19	12,889,963	12,890,080	+	TCCCTAAAGGCCTCCAATT	21	453	GTTGGAAAGCGGGGGGACCC	21	83,879
vi-miRC477i	20	16,672,963	16,673,080	-	TCCCTAAAGGCCTCCAATT	21	453	GTTGGAAAGCCTGGGGGACCC	21	83,879
vi-miRC477j	6	19,950,730	19,950,847	-	TCCCTAAAGGCCTCCAATT	21	453	GCTGGAAAGCGGATGGGGGACCC	21	62,642
vi-miRC477k	1	22,740,264	22,740,350	+	TCCCTAAAGGCCTCCAATT	21	453	GTTGGAAAGCGGGGGGACCC	21	83,879
vi-miRC477l	19	13,141,671	13,141,788	+	TCCCTAAAGGCCTCCAATT	21	453	GTTGGAAAGCCTGGGGGACCC	21	83,879
vi-miRC477m	19	13,510,093	13,510,210	+	TCCCTAAAGGCCTCCAATT	21	453	GTTGGAAAGCCTGGGGGACCC	21	83,879
vi-miRC477n	19	18,678,338	18,678,455	+	TCCCTAAAGGCCTCCAATT	21	453	GTTGGAAAGTGTGGGGGACCC	21	17,594
vi-miRC477o	19	18,872,706	18,872,824	-	TCCCTAAAGGCCTCCAATT	21	453	GTTGGAAAGTGGGGGGGACCC	21	30,683
vi-miRC477p	19	18,881,351	18,881,468	-	TCCCTAAAGGCCTCCAATT	21	453	GTTGGAAAGCCTGGGGGACCC	21	83,879
vi-miRC482a	14	19,755,466	19,755,588	-	GGATGGCTGAATTGGATA	20	189,848	TTCCCAATGCCGCCATTCAA	22	17,229
vi-miRC482b	1	3,865,560	3,865,686	+	CATGGGGGTTGGTAAGAGG	21	143,513	TCTTACCAACACCTCCCATTTC	22	37,745
vi-miRC530	6	17,896,112	17,896,288	+	TCTGCATTGCAACCTGCACT	21	19,330	AGGTGCAGGTGAAGGTGCAGA	21	207
vi-miRC530b	8	18,999,725	18,999,889	-	TCTGCATTGCAACCTGCACT	21	19,330	TAGATGATCATCAACAAACAA	21	12,436
vi-miRO827	5	24,742,113	24,742,240	-	TTTGTGCTGGTCATCTAGTC	22	6721	ACCGTCCTTCTGTATAAGC	21	1227
vi-miRC7122	5	6,820,719	6,820,833	-	TTACACAGAGAGATGACGGTGG	22	535	CCGAGAGGACTTAGTGGAC	21	1859
grape-m0642	17	3,771,923	3,772,046	+	GAGGTGATAGATCAGCAAGAG	21	31	TTGCTGAAOAAGAGAACCT	21	413
grape-m1188	29	1,474,782	1,474,863	+						
grape-m1191	29	469,980	470,068	-						
grape-m1355	3	13,241,508	13,241,588	-	GCGCGTTGGAGCAGGGAGCTT	21	740	AACACTGAATGATTGACCAG	21	90
grape-m1517	5	11,023,593	11,023,756	-				GGCACGACAGCTCTGGAGGCC	21	31
grape-m1577	6	6,902,214	6,902,359	-						
grape-m1738	8	21,905,716	21,905,814	-	TCGTAGTGGCTGCGAACAGCTCC	22	2406			

A temporary name has been given to each miRNA sequence either using a sequential numbering associated with the abbreviation *miRC* (miRNA Candidate) for those similar to other known plant miRNAs or using "grape-m" with a random numbering for those completely new candidates.

^aRefers to the genomic localization on the GRAPE_1CpV12Xv1 genome sequence.

^bNucleotide, sequence length of the microRNA.

^cSum of TPM values from 48 libraries.

TABLE 3 | List of reliable *Vitis vinifera* miRNAs from known miRNA precursors identified in Cabernet Sauvignon and Sangiovese derived small RNA libraries.

Family	miRNA	Chr ^a	Start ^a	End ^a	Strand ^a	5p Sequence	nt ^b	Abundance 5p ^c	3p Sequence	nt ^b	Abundance 3p ^c
wi-miR156	wi-miR156b	4	5,357,061	5,357,310	-	TGACAGAAGAGAGTGAGCAC	20	10,561	TGACAGAAGAGAGTGAGCAC	20	10,561
	wi-miR156c	4	848,207	848,307	-	TGACAGAAGAGAGTGAGCAC	20	10,561	TGCTCAOCTCTCTGTCAAC	23	1089
	wi-miR156d	11	7,623,202	7,623,334	-	TGACAGAAGAGAGTGAGCAC	20	234			
	wi-miR156e	11	1,504,195	1,504,301	-	TGACAGAGGGAGAGTGAGCAC	20	234			
	wi-miR156f	14	26,463,671	26,463,773	+	TTGACAGAAAGATAGAGGCAC	21	26,445	GCTCTCTAGACTCTGTCACTC	21	901
	wi-miR156g	17	3,046,310	3,046,441	-	TTGACAGAAAGATAGAGGCAC	21	26,445	TTGACAGAAAGATAGAGGCAC	21	26,445
	wi-miR156i	14	19,727,139	19,727,358	-	GAGCTCTTGAAGTCACAATAG	21	1644	TTGGATTGAAGGGAGCTATA	21	198,072
vv-miR159	wi-miR159c	17	2,609,190	2,609,409	-	GGATGOAGGGTTCATCGATC	21	365	TGATAAACCTCTGCATCCAG	21	130,041
vv-miR162	wi-miR162	17	4,716,504	4,716,636	+	TGGAGAACGGGCCACGTGCA	21	198	CATGTGCCCTCTCCCCATC	21	976
vv-miR164	wi-miR164a	7	3,287,412	3,287,590	-	TGGAGAACGGGCCACGTGCA	21	198			
	wi-miR164c	8	1,008,0445	10,080,636	+	AATGAGGTTTGATCCAAGATC	21	1886	TC TCGGACCAGGGCTTCATTC	21	1,172,737
	wi-miR164d	14	1,414,567	1,414,682	-	TGGAGAACGGGCCACGTGCA	21	198	GGAAATGTTGGCTGGCTCGAGG	21	120,762
vv-miR166	wi-miR166a	8	3,302,784	3,302,939	-	TGCGACAGGGCTTCATTC TC	21	10,941	TGCGACAGGGCTTCATTC TC	21	17,706,997
	wi-miR166b	12	17,937,384	17,937,510	+	GGAATGTTGCTGGCTCGAGG	21	54,367	TGCGACAGGGCTTCATTC CCC	21	17,706,997
	wi-miR166c	15	16,978,558	16,978,745	-	GATTGTTGCTGGCTCGAGG	21	2661	TGCGACAGGGCTTCATTC CCC	21	17,706,997
	wi-miR166d	16	21,405,202	21,405,388	-	GGAATGTTGCTGGCTCGAGG	21	54,367	TGCGACAGGGCTTCATTC CCC	21	17,706,997
	wi-miR166e	2	2,255,708	2,255,901	+	GGAATGTTGCTGGCTCGAGG	21	10,941	TGCGACAGGGCTTCATTC CCC	21	17,706,997
	wi-miR166f	7	19,450,000	19,450,127	+	GGAATGTTGCTGGCTCGAGG	21	262	TGCGACAGGGCTTCATTC CCC	21	17,706,997
	wi-miR166g	7	453,844	453,971	-	GGAATGTTGCTGGCTCGAGA	21	262	TGCGACAGGGCTTCATTC CCC	21	17,706,997
	wi-miR166h	5	6,741,189	6,741,288	-						
vv-miR167	wi-miR167b	14	7,137,373	7,137,501	+	TGAAAGTGGCCAGGATGATCT-	21	1143	AGATCATGTTGGAGTTTCAC	21	536
	wi-miR167d	20	7,490,493	7,490,606	+	TGAAAGCTGCCAGCATGATCT-	21	1143			
	wi-miR167e	5	5,845,370	5,845,489	+	TGAGCTGCCAGCATGATCT-	21	1143	AGATCATGTTGGAGTTTCAC	21	536
vv-miR168	wi-miR168	2	17,944,786	17,944,947	-	TGCGCTTGTGCAGGTGGGAA	21	43,188	CCGGCCCTGCATCAACTGAAT	21	3558
vv-miR169	wi-miR169c	4	2,265,913	2,266,028	-	CAGCCAGGATGACTTGGCGG	21	5			
	wi-miR169c.1	4	2,265,913	2,266,028	-	TGAGGAGTAGAATGAGAC	20	1921			
	wi-miR169e	14	25,082,574	25,082,756	-	TAGCCAGGATGACTTGC TCT	22	3136			
	wi-miR169g	8	21,104,448	21,104,568	+	CAGCCAGGATGACTTGC GA	21	13	*COGGCAAGTTGCTCTTGGCTAC	23	151
	wi-miR169r	11	16,415,128	16,415,239	+	TGAGTCAGGGATGACTTGC CC	21	11	*GGCAAGTTGACTTGACTCAGT	22	1181
	wi-miR169t	11	16,399,564	16,399,676	+	CGAGTCAGGGATGACTTGC GA	22	14	*GGCAAGTTGACTTGACTCAGT	22	1181
wi-miR171	wi-miR171b	12	5,542,396	5,542,529	-				- TTGAGCCGCCGTCAATAT TCC	24	1068
	wi-miR171i	17	893,536	893,632	+				TGATTGAGGCCGTGCCAAATAC	21	811
	wi-miR172d	8	12,667,173	12,667,279	+				TGAGAACTCTGATGATGCTGC -	23	6451
	wi-miR2111	8	15,368,664	15,368,748	-				GTCCCTCTGGTTGCAGATTACT	21	95
	wi-miR2950	7	14,340,406	14,340,517	+				TGGTGTGACGGGATGGAAATA	21	581
wi-miR319	wi-miR319b	1	4,189,556	4,189,753	+				TTGGACTGAAGGGAGCTCC-	21	9157
	wi-miR319c	2	855,548	855,756	-				TTGGACTGAAGGGAGCTCC-	21	9157

(Continued)

TABLE 3 | Continued

Family	miRNA	Chr ^a	Start ^a	End ^a	Strand ^a	5p Sequence	nt ^b	Abundance 5p ^c	3p Sequence	nt ^b	Abundance 3p ^c
	wi-miR319e	11	4,317,223	4,317,329	+				TTGGACTGAAAGGAGCTCCT	21	40,107
	wi-miR319f	6	9,137,252	9,137,445	+				TTGGACTGAAAGGAGCTCC-	21	9,157
	wi-miR319g	17	3,675,979	3,676,209	-	TCACAAAGTTCATCCAAAGCACCA	22	108,278	TTGGACTGAAAGGAGCTCC-	21	9,157
vi-miR3623	vi-miR3623	18	24,650,004	24,650,151	+	TTGTCGAGGAAGAAGCGGACT	22	2444	TTGGCTGCCTCTCTGTGACAAG	21	20,404
vi-miR3627	vi-miR3627	14	28,302,559	28,302,881	-	CGCATTTCAGCAGGCCAAG	21	1	TGGCTGCTGAGAAAATGTAGG-	22	12,342
vi-miR3629	vi-miR3629a	13	18,253,987	18,254,170	+	TGGCTGCTGAGAAAATGTAGG-	22	371		22	371
vi-miR3629c	vi-miR3629c	17	822,209	822,338	+	GGATTTGGGGCGATGGAAAGG	22	887	TTTCCCAGACCCCCAATAACCAA	22	1578
vi-miR3632	vi-miR3632	14	23,394,889	23,395,015	+	GGAATGGATGGTTAGGAGAG	20	45,786	TTCCTATACCAACCCATTCCCTA	22	1469
vi-miR3633	vi-miR3633a	17	5,521,913	5,522,060	+	GGAATGGTGGCTGGATCT	20	10,270	GTTCCTCATGCACATCCATTCTA	22	5610
vi-miR3633b	vi-miR3633b	17	5,521,557	5,521,691	+	GGCATAATGTGTGACGGAAAGA	21	1563	TTTCGGACTCTGGCACTCATGCCGT	23	753,254
vi-miR3634	vi-miR3634	17	5,681,202	5,681,314	-	GGCATATGTGTGACGGAAAGA	21	289	ATTATGTGOCACACATGCCCT	21	399
vi-miR3635	vi-miR3635	18	27,357,619	27,357,780	+	TGGGTTTGCTTCTGTAGATTTC	24	352	—	24	4495
vi-miR3636	vi-miR3636	16	5,414,817	5,414,967	-	TGTGGAGAACGAAAGTCGGAGAGT					
vi-miR3640	vi-miR3640	16	11,986,842	11,987,014	+	ACCTGATTGGTGTATGCTTTTGG	24	1321	—	24	1203
vi-miR390	vi-miR390	6	8,159,519	8,159,657	+	AAGCTOAGGAGGGATAGGGCC	21	5046	AAAGGCATCATCAATCAGGTAAATG		
vi-miR393	vi-miR393a	16	17,247,172	17,247,327	-	TGCAAAGGGATCGCATGTGATC	21	5152	ATCATGCTATCCCTTAGGAAAC	21	775
vi-miR393b	vi-miR393b	13	4,265,132	4,265,213	+	TGCCATTCTGTCCAACCTCC-	22	412			
vi-miR394	vi-miR394a	12	17,122,005	17,122,092	-	TTGGCATCTGTCCACCTCC	20	412			
vi-miR394b	vi-miR394b	18	1,413,038	141,3130	-						
vi-miR395	vi-miR395a	1	6,527,-921	6,528,019	+	CTGAAAGTTGGGGAAACTC	21	6899			
	vi-miR395c	1	6,499,899	6,500,020	-	CTGAAGTGTGTTGGGGAAACTC	21	6899			
	vi-miR395d	1	6,512,760	6,512,848	+	CTGAAGTGTGTTGGGGAAACTC	21	6899			
	vi-miR395e	1	6,505,233	6,505,354	+	CTGAAGTGTGTTGGGGAAACTC	21	6899			
	vi-miR395f	1	6,489,527	6,489,642	+	CTGAAGTGTGTTGGGGAAACTC	21	6899			
	vi-miR395h	1	6,566,637	6,566,758	+	CTGAAGTGTGTTGGGGAAACTC	21	6899			
	vi-miR395i	1	6,562,627	6,562,742	+	CTGAAGTGTGTTGGGGAAACTC	21	6899			
	vi-miR395j	1	6,553,011	6,553,126	+	CTGAAGTGTGTTGGGGAAACTC	21	6899			
	vi-miR395k	1	6,536,764	6,536,885	+	CTGAAGTGTGTTGGGGAAACTC	21	6899			
	vi-miR395l	1	6,559,083	6,559,199	+	CTGAAGTGTGTTGGGGAAACTC	21	6899			
vi-miR396	vi-miR396a	9	7,372,499	7,372,649	-	AAGAAAAGCTGTGGAGGACATGGC	24	2147			
	vi-miR396b	11	5,246,778	5,246,913	+	TTCCACAGCTTCTGTGAACTT	21	85,683	GTTCAGAAGAAAGCTGTGGGAAA	21	6917
	vi-miR396c	4	5,119,592	5,119,698	-	TTCCACAGCTTCTGTGAACTG	21	3900			
	vi-miR396d	11	5,253,095	5,253,244	-	TTCCACAGCTTCTGTGAACT-	21	7387	GTTCACAAATAAGCTGTGGGAAA	21	1899
vi-miR397	vi-miR397a	20	11,971,890	11,972,015	-	TCATTGAGTCAGCGGTGATG	21	432			
vi-miR398	vi-miR398b	6	16,503,544	16,503,633	-	TGTGTTCTCAGGTGCCCCCTG	21	16,121			
	vi-miR398c	6	15,575,579	15,575,668	+	TGTGTTCTCAGGTGCCCCCTG	21	16,121			

(Continued)

TABLE 3 | Continued

Family	miRNA	Chr ^a	Start ^a	End ^a	Strand ^a	5p Sequence	nt ^b	Abundance 5p ^c	3p Sequence	nt ^b	Abundance 3p ^c
vi-miR399	wi-miR399a	10	2,989,435	2,989,561	+	GTTGATTCTCCTTGGCAGA	21	503	TGCCAAAGGAGAATTGCCCTG	21	1289
	wi-miR399b	16	15,618,708	15,618,845	-				TGCCAAAGGAGAATTGCCCTG	21	2996
	wi-miR399c	15	15,232,197	15,232,281	+				TGCCAAAGGAGAATTGCCCTG	21	2996
	wi-miR399e	10	2,992,220	2,992,341	-				TGCCAAAGGAGAATTGCCGG	21	184
	wi-miR399h	10	2,983,543	2,983,634	+				TGCCAAAGGAGAATTGCCCTG	21	1289
	wi-miR399j	2	4,101,786	4,101,937	+	GGGCTTCTCCCTGGAGG	22	148	CGCCAAAGGAGAATTGCCCTG	21	113,055
vi-miR403	wi-miR403a	5	65,247	65,361	+				TAGATTACGCACAAAACTCG	21	82,567
	wi-miR403b	5	600,176	600,266	+				TAGATTACGCACAAAACTCG	21	82,567
	wi-miR403d	5	166,467	166,582	+	AGTTTGTGCGGAATCCAAQC	21	201	TAGATTACGCACAAAACTCG	21	82,567
	wi-miR403e	5	168,096	168,213	+				TAGATTACGCACAAAACTCG	21	82,567
	wi-miR403f	7	4,179,658	4,179,795	-	AGTTTGTGCGTGACTCTAAA	21	523	TAGATTACGCACAAAACTCG	21	82,567
vi-miR408	wi-miR408	7	5,011,920	5,012,056	+	CGGGGAGGAGGTAGTCATGG	21	3223	ATGCACTGCCCTCCCTGGC	21	6566
	wi-miR477	2	1,237,529	1,237,808	+	ACTCTCCTCAAGGGCTCT- G	22	513	CGAAGTCCTTGGGAGAGTGG	21	3289
vi-miR479	wi-miR479	16	21,573,744	21,573,866	+	TGTGGATTGGTTGGCTCATC	22	4449	CGAGGCCAACCAATATCACTC	21	46,073
	wi-miR482	17	5,523,009	5,523,155	+	*AATTGGAGAGTAGGAAAGCTT	22	139,166	TCITTCCTACTCCCTCCATTCC	22	42,801
vii-miR535	wi-miR535a	25	1,392,255	1,392,353	-	TGACAAACGAGAGAGCACGC	21	18,893			
	wi-miR535c	25	1,346,353	1,346,483	-	TGACAAACGAGAGAGCACGC	21	18,893	GTGCTCTCTGTCGCTGTCTATA	21	2191

^aRefers to the genomic localization on the GRAPE_IGGP12Xv1 genome sequence.^bNucleotide, sequence length of the microRNA.^cSum of TP4M values from 48 libraries.

-Missing nucleotide.

Nucleotides that differ from the annotated sequence are shown in red.

*Indicates that the most abundant sequence in our dataset does not correspond to the mature annotated miRNA, but to the star sequence.

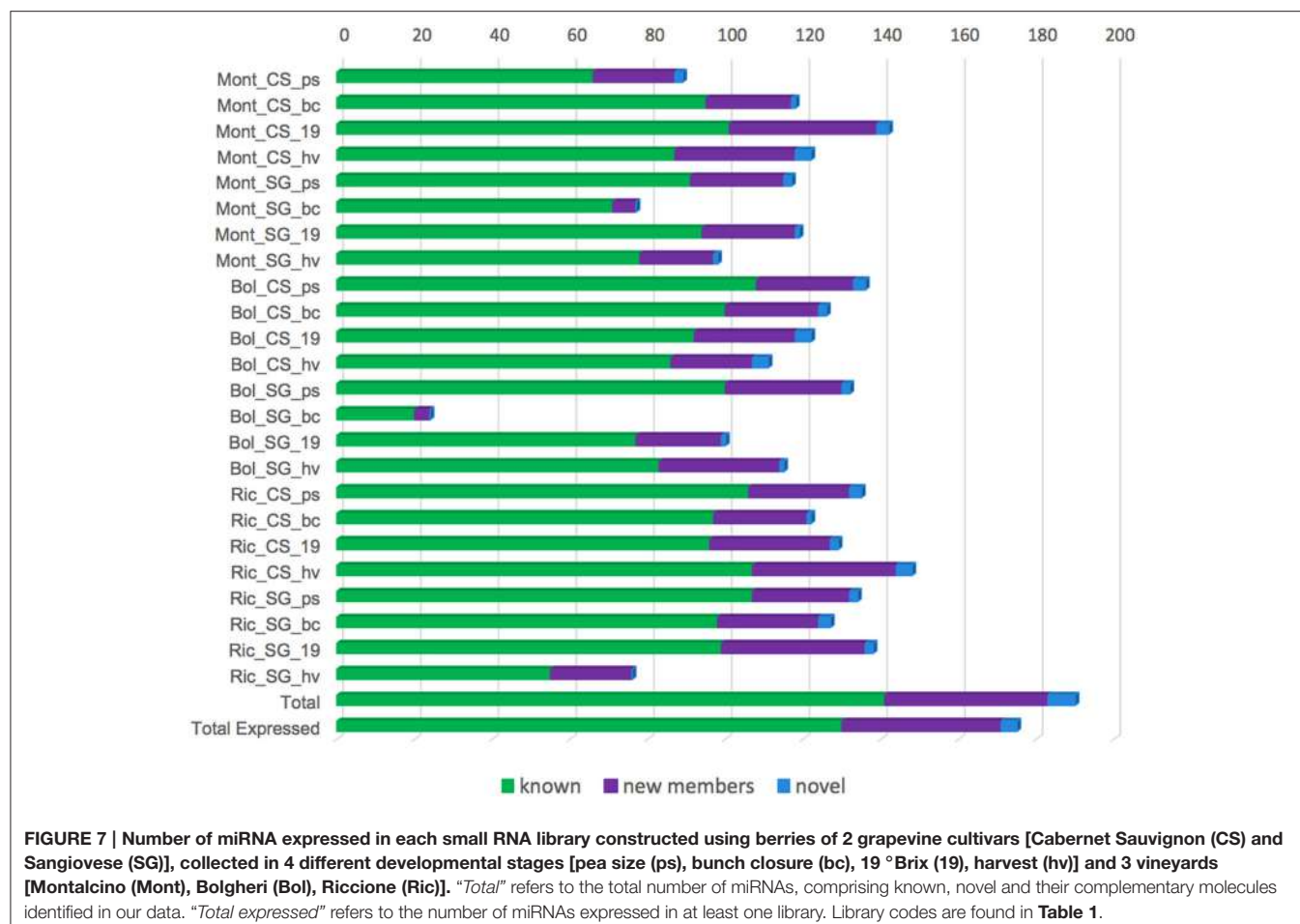


FIGURE 7 | Number of miRNA expressed in each small RNA library constructed using berries of 2 grapevine cultivars [Cabernet Sauvignon (CS) and Sangiovese (SG)], collected in 4 different developmental stages [pea size (ps), bunch closure (bc), 19 °Brix (19), harvest (hv)] and 3 vineyards [Montalcino (Mont), Bolgheri (Bol), Riccione (Ric)]. “Total” refers to the total number of miRNAs, comprising known, novel and their complementary molecules identified in our data. “Total expressed” refers to the number of miRNAs expressed in at least one library. Library codes are found in **Table 1**.

DISCUSSION

Using high throughput sequencing coupled with robust bioinformatics pipelines we analyzed small RNAs derived from the berries of Cabernet Sauvignon and Sangiovese, grown side-by-side in three vineyards, representative of different grapevine cultivation areas in Italy (Bolgheri, Montalcino, and Riccione). We obtained nearly 750 MB reads comprising a significant proportion of small (21–24 nt) RNAs. The size distribution profiles of our libraries were in general consistent with previous reports in berry grapevine, where the 21-nt class was more abundant than the 24-nt class (Pantaleo et al., 2010; Wang et al., 2012; Han et al., 2014; Kullan et al., 2015).

Our analysis revealed dynamic features of the regulatory network mediated by miRNAs and other small RNAs, at the basis of genotype-environment interactions.

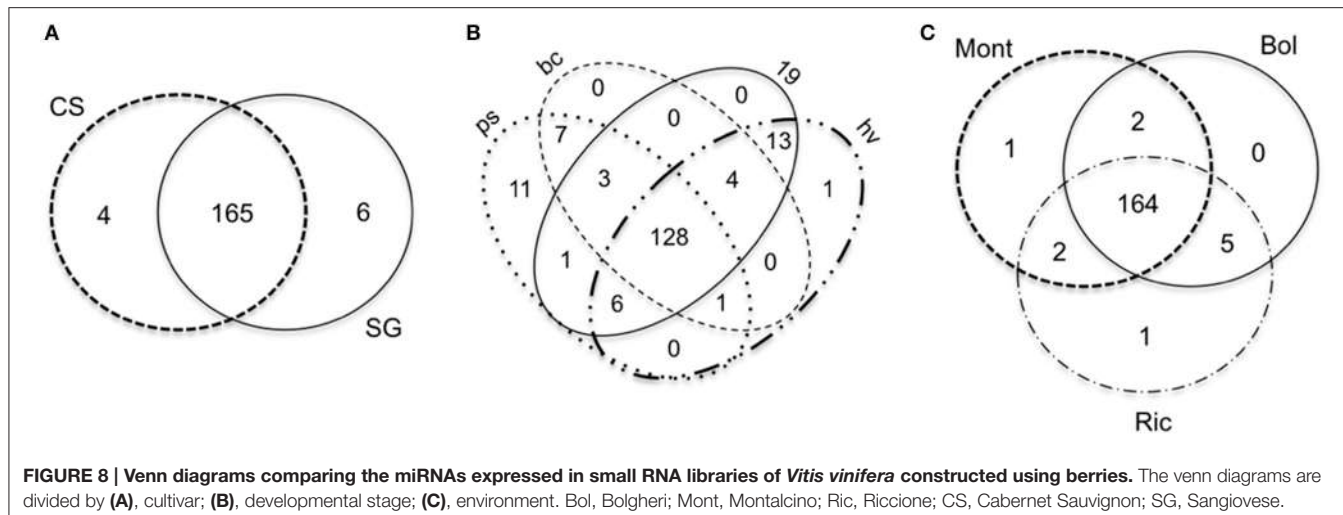
Genotype and Environment Effects on Small RNA Profiles

Plants evolved a series of pathways that generate small RNAs of different sizes with dedicated functions (Vazquez, 2006; Khraiwesh et al., 2012). Although the various small RNA classes have been intensively studied, we are still far from understanding

how many small RNA pathways exist, and how they are connected (Vazquez, 2006). Additionally, new classes of small non-coding RNAs continue to be discovered and many studies demonstrate a substantial redundancy and cross-talk between known small RNA pathways (Agarwal and Chen, 2009; Ghildiyal and Zamore, 2009; Bond and Baulcombe, 2014; Harding et al., 2014). Estimating the exact percentage of the plant genome covered by small RNA-generating loci still remains a challenge.

By applying static cluster analysis, we investigated small RNA abundances across the genome, identifying 4408 small RNAs producing hotspots. We analyzed their expression in different cultivars, environments and developmental stages, highlighting that the majority of the considered small RNA producing regions was modulated in different conditions. This suggests a strong influence of small RNAs in the response to environment in grapevine berries. Only 462 small RNA-generating loci, corresponding to about 10% of the total, were expressed in all the analyzed libraries, possibly involved in essential biological pathways.

Comparing the two cultivars, we observed, with few exceptions, that Cabernet Sauvignon berries have a higher number of expressed sRNA-generating loci than Sangiovese berries (**Figure 1**) when collected in the same conditions (i.e.,



vineyard and developmental stage). Considering the fact that small RNAs are implicated in the regulation of gene expression in several processes (Chen, 2009; Trindade et al., 2011), the higher number of small RNAs expressed in Cabernet Sauvignon compared to Sangiovese berries may reflect a buffering effect of small RNAs influencing grapevine response to diverse growing environments. We believe that these characteristics may have contributed to the wide diffusion of Cabernet Sauvignon, allowing its wide cultivation in almost all wine producing countries. This is not the case for Sangiovese whose cultivation is more restricted. It is worth noting that Sangiovese is considered a very unsettled grapevine cultivar (Poni, 2000), showing a wide range of variability in response to year, clone and bunch exposure (Rustioni et al., 2013). Differently, Cabernet Sauvignon is a cultivars showing less inter-annual differences in terms, for example, of concentration of secondary metabolites (Ortega-Regules et al., 2006).

To better evaluate varietal differences in response to the environment, we calculated the CS/SG ratio for the small RNA producing hotspots in the three vineyards. An interesting example is found in green berries sampled in Riccione. A region on chromosome 4 (3,376,501–3,377,000) showed a 390-fold change in the small RNA abundance, when comparing Cabernet vs. Sangiovese (**Figure 6**). Most of the reads produced in this region are 21 nt long and are also phased in intervals of 21 nt from both strands, typical of a *phased locus* (PHAS). The gene in this locus, also known as *VvRD22g*, encodes a BURP domain-containing protein, involved in an ABA-mediated abiotic stress response, which persists still after long periods of stress (Matus et al., 2014). The small RNAs profile suggests that the locus is regulated by *phased* siRNAs similarly to the mechanisms already described for PPR, NB-LRR, and MYB gene families (Howell et al., 2007; Zhai et al., 2011; Xia et al., 2013; Zhu et al., 2013). This is a clear example of GxE interactions since the BURP domain gene modulates *phased* siRNAs production in the two cultivars only when grown in Riccione.

When removing the threshold of minimum cluster abundance set to 5 HNA, in the CS/SG ratio, a high number of clusters

(ranging from 70 to 370 depending on the sample analyzed) with fold change greater than 50 was found, where one of the libraries has 0 HNA and the other any number greater than 30 HNA. This fact suggests a very strong modulation of the expression of small RNAs between the two cultivars, which is more or less pronounced depending on the vineyard where the berries were cultivated. A similar situation was observed comparing the expression level of small RNAs between reciprocal hybrids of *Solanum lycopersicum* and *S. pimpinellifolium* (Li et al., 2014).

The ripening process of grapevine berries is highly affected by the environment (van Leeuwen et al., 2004, 2007) and we observed the impact of the environment on the ripening process in the expression of small RNAs. The most relevant observation is that Riccione is very peculiar in relation to the activation of srRNA hotspots, as indicated by the high number of Riccione-specific clusters (**Figure 2A**) and by the extreme modification it induces in the CS/SG ratio (**Figure 5**): in Riccione in fact this ratio decreases in green berries and increases in ripened berries, and this is not observed in any other vineyard; in addition to this the already discussed example of BURP domain gene, is observed in Riccione, as well. Riccione is the most diverse environment when compared to Montalcino and Bolgheri. Riccione is located at the Adriatic coast and has a temperate sub-littoral climate, while Montalcino and Bolgheri are both located in Tuscany with typically Mediterranean climate.

Moreover, both cultivars show a peculiar profile of small RNA loci during berries ripening, in Riccione. The expression of small RNA loci in Cabernet Sauvignon berries drastically changed during development, especially when collected in Riccione (**Figure 1**), not only in the number of active loci but also in the different genic or intergenic disposition: ripened berries have a 2.6-fold increase in small RNA loci active in genic regions. Differently, when Sangiovese is grown in Riccione, there is a very high number of small RNA loci active in green berries, mainly associated to transposable elements that remains almost stable during development although the proportion of intergenic loci is reduced. Sangiovese berries collected in Montalcino show a 2.5-fold increase of small RNA producing loci during development.

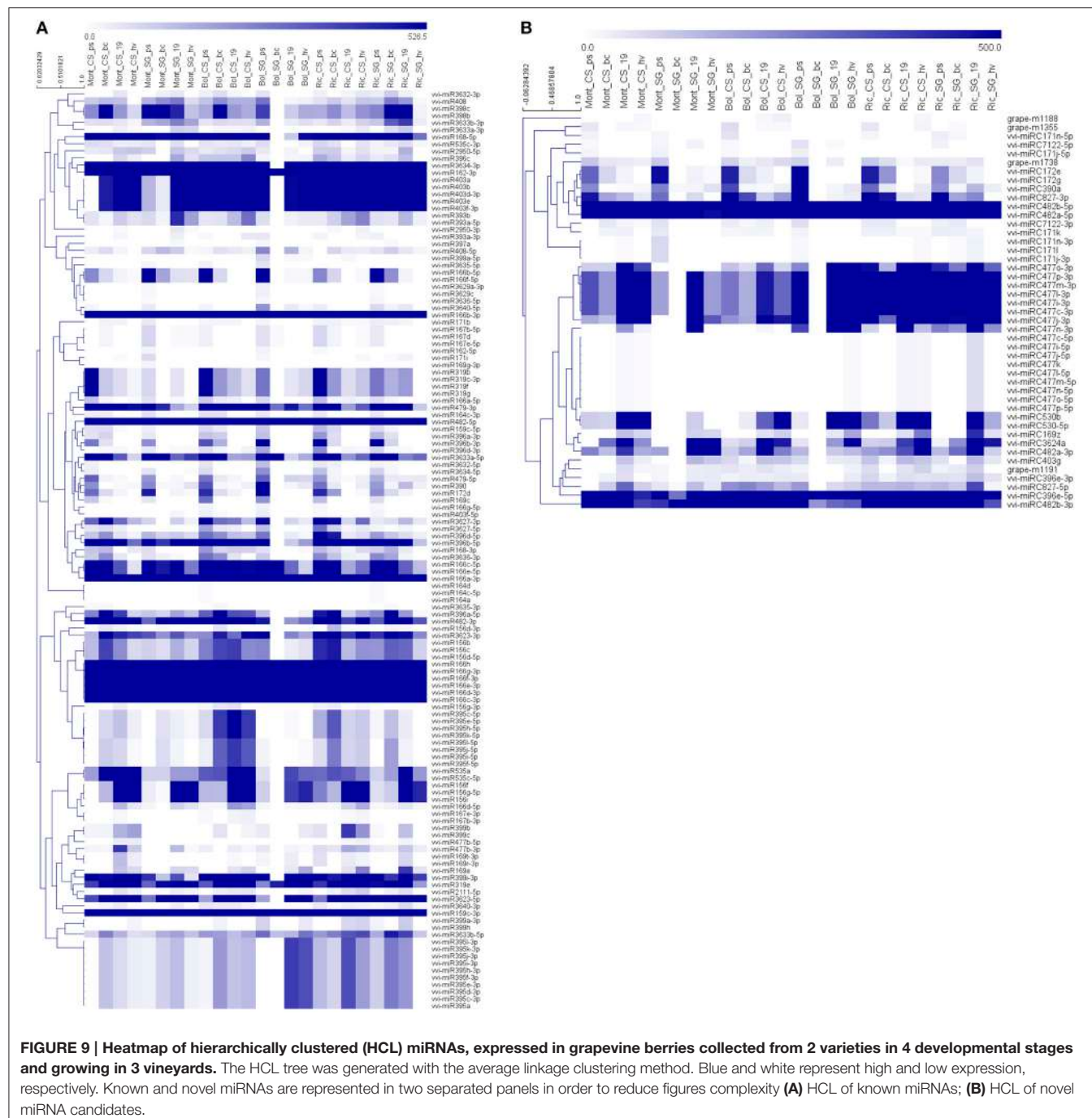


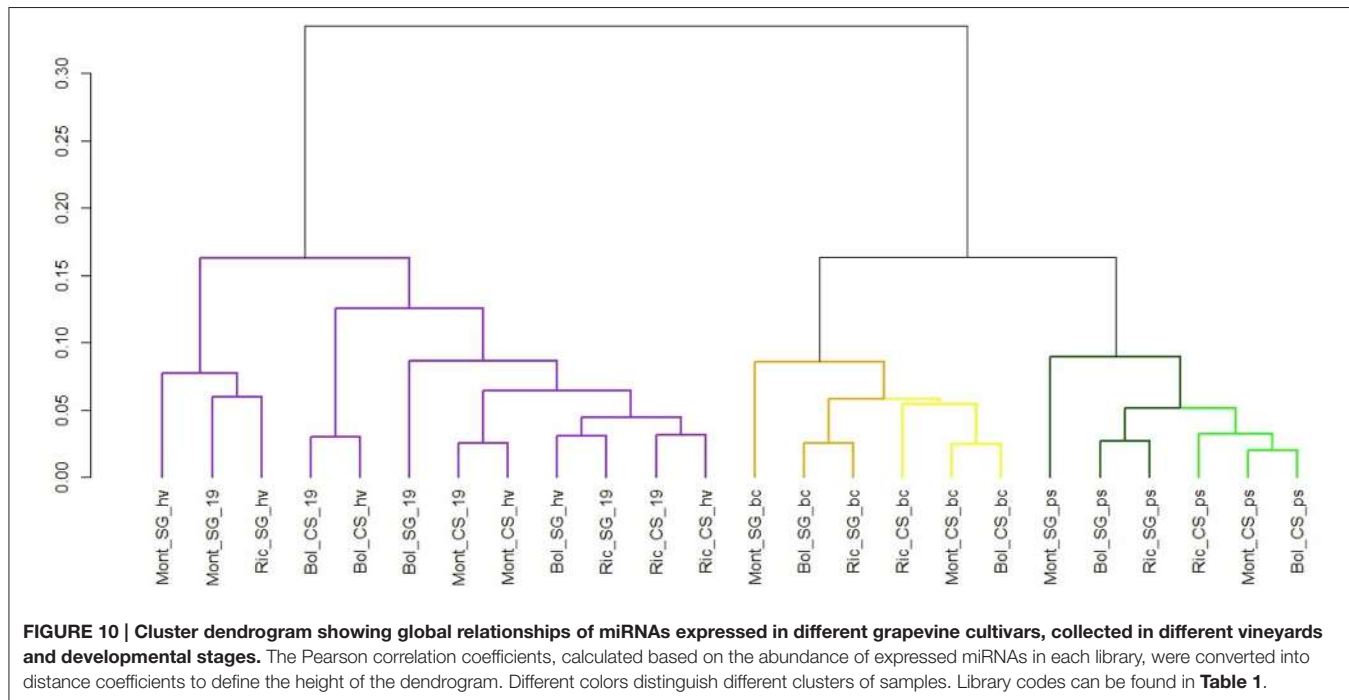
FIGURE 9 | Heatmap of hierarchically clustered (HCL) miRNAs, expressed in grapevine berries collected from 2 varieties in 4 developmental stages and growing in 3 vineyards. The HCL tree was generated with the average linkage clustering method. Blue and white represent high and low expression, respectively. Known and novel miRNAs are represented in two separated panels in order to reduce figures complexity **(A)** HCL of known miRNAs; **(B)** HCL of novel miRNA candidates.

Differences during berry development between the cultivars may explain their different behavior in different environments, and the characteristics of each vineyard may favor one or other variety according to their demands. For example, Sangiovese needs a long growing season (it is slow to ripen) with sufficient warmth to fully ripen (Poni, 2000). Consequently, cooler environments will require a reprogramming of Sangiovese gene expression in order to achieve ripening. Other factors such as composition of soil, level of humidity, photoperiod and density of cultivation may be exerting the same influence on the ripening

of the berries triggering the activation of different small RNA loci.

miRNAs Expression Is Mainly Dependent on the Developmental Stage but a Few miRNAs Are Directly Modulated by the Vineyard and the Cultivar

Applying a conservative pipeline to the analysis of our 48 small RNA libraries, we recognized 89 known and annotated grapevine



miRNAs. In addition, when compared to previous reports in grapevine (Alabi et al., 2012; Han et al., 2014; Wang et al., 2014) we identified 7 completely novel miRNAs plus 26 homologous to other plant species, but novel to grapevine. This is a remarkable number considering the stringency of our pipeline and that our study is based only on four developmental stages of berries.

The outline of miRNA accumulation across samples is different from that of sRNA-producing loci. While the expression of sRNA-generating regions allows distinguishing very well between ripened and green berries and also between cultivars (**Figure 4**), the accumulation of miRNAs shows a clear distinction only between ripened and green berries, and when the berries were green, we observe a further dichotomy separating the two cultivars and the two green developmental stages. The same pattern of miRNA accumulation among green and ripened berries of grapevine (cv. Corvina) was observed when we described the miRNA expression atlas of *Vitis vinifera* (Kullan et al., 2015).

Comparing the distribution of miRNAs expressed throughout our samples, we found a set of 39 miRNAs ubiquitous (21) or nearly ubiquitous (18) to all the libraries, and very few miRNAs specific of a cultivar, vineyard or developmental stage. All these 39 miRNAs belong to known vvi-miRNA families. With few exceptions, the same set of miRNAs was also found expressed in all the small RNA libraries constructed with different tissues of the grapevine cv. Corvina (Kullan et al., 2015), where the population of expressed miRNAs appears highly variable apart from a well-defined group of miRNAs, probably related to the basal metabolism. These findings are also consistent with previous report in grapevine where a small number of known tissue-specific miRNAs was described (Wang et al., 2014).

Considering the ripening process as shown in the heat maps (**Figure 9**), and the correlation dendrogram, it is clear that most miRNAs are modulated during the developmental process.

For some miRNA families, we observed the same peculiar patterns of miRNA accumulation, previously described in the grapevine miRNA atlas (Kullan et al., 2015), e.g., an increase of accumulation toward ripening for miR156 f/g/i, and a decrease for miR166c/e, miR172d, miR319, and miR396a/b, but this is not the main focus of our paper.

To establish genotype and environmental influence on miRNA modulation, we performed a statistical analysis that revealed a number of miRNAs differentially expressed. Being aware of the fact that we had only two biological replicates, we applied the exact test as implemented in the EdgeR package. This test has been recently judged a very robust tool that can be used in experiments similar to our, because of its low false positive rate and relative high true positive rate in the presence of a fold change higher than 4 (Schurch et al., 2016).

Considering berries at the same developmental stages, we compared Sangiovese vs. Cabernet Sauvignon in a given vineyard and Montalcino vs. Bolgheri, Montalcino vs. Riccione, and Bolgheri vs. Riccione keeping the cultivar fixed. In total we performed 9 pairwise comparisons for each developmental stage. In general, we observed that berries at 19 °Brix and at harvest show a higher number of differentially expressed miRNAs.

The most interesting examples are represented by two novel miRNAs, whose predicted targets are related to the biosynthesis and accumulation of secondary metabolites, which are of crucial importance in grapevine berries, since its quality depends mainly on its metabolites (Ali et al., 2010). The candidate grape-m1191 is differentially expressed in Sangiovese between Riccione and Bolgheri (Ric_SG_19 vs. Bol_SG_19) and was predicted to target the transparent-testa 12 gene (VIT_212s0028g01160) that encodes a multidrug secondary transporter-like protein (MATE) involved in the vacuolar accumulation of the flavonoid proanthocyanidin in different species including grapevine (Debeaujon et al., 2001; Bogs et al., 2007; Marinova et al.,

2007; Zhao et al., 2010). Also, in grapevine some studies provide evidences that the intracellular transport of acylated anthocyanins is catalyzed by a MATE transporter (Gomez et al., 2009; He et al., 2010).

The grape-m1355 seems to be involved in four different pathways, all related to secondary metabolites. It is differentially expressed in Montalcino between the two varieties (Mon_CS_hv vs. Mon_SG_hv) and was predicted to target a cinnamoyl reductase-like protein (CCR) (VIT_203s0110g00350), which is part of the polyphenol biosynthetic pathway (Leple et al., 2007); a cinnamyl alcohol dehydrogenase (VIT_206s0004g02380) involved in the lignin biosynthesis (Trabucco et al., 2013); a phenylacetaldehyde reductase (VIT_213s0064g00340), which catalyzes, in tomato, the last step in the synthesis of the volatile 2-phenylethanol, important for the aroma and flavor of many foods (Tieman et al., 2007); and different bifunctional dihydroflavonol 4-reductases (DFR) (see Supplementary Table 3). DFR catalyzes the first step in the conversion of dihydroflavonols to anthocyanins and are responsible for the production of colored anthocyanins (Boss and Davies, 2001; Davies et al., 2003). The same miRNA candidate was described in the grape miRNA atlas (Kullan et al., 2015) also predicted to target several genes of DFR-like and one CCR.

As for known miRNAs, several members of the miR395 family are differentially expressed at 19 °Brix and at harvest in Bolgheri and in both Bolgheri and Riccione, respectively, when comparing the two cultivars. Moreover, miR395f is differentially expressed also in CS at harvest between Montalcino and Bolgheri. This miRNA has been shown to target genes involved in Sulphate assimilation and metabolism (Liang and Yu, 2010; Kawashima et al., 2011; Matthewman et al., 2012), and hence it could be connected to flavonoid and stilbene pathways as suggested by Tavares et al. (2013).

miR399 family members are also differentially expressed in several comparisons: at 19 °Brix between Riccione and Bolgheri in CS and between Riccione and Montalcino in SG, plus in Montalcino between CS and SG. At harvest, miR399 are differentially expressed in SG in all the three comparisons among vineyards and in Riccione between CS and SG. miR399 is implicated in Phosphate homeostasis being rapidly up-regulated upon Pi starvation (Fujii et al., 2005). miR399 regulatory network has been shown to be important in flowering time (Kim et al., 2011) and was identified as a temperature-sensitive miRNA (Lee et al., 2010), however its characterization in fruit ripening is lacking, although intriguing.

miR396 family members are known to be regulated during organ development, targeting Growth Regulating Factors (Liu et al., 2009; Wang et al., 2011) and also in berry development (Kullan et al., 2015; Cao et al., 2016), and we observed their modulation during berry ripening in our data as well, but more interestingly, they are also differentially expressed between CS and SG in berries sampled in Bolgheri at 19 °Brix.

Finally, the investigation of the global relationships of different small RNA classes and miRNAs expressed in different grapevine cultivars, collected in different vineyards and developmental stages, suggests that although the vineyard may

influence their profile of abundance it probably does in less proportion than developmental stage and cultivar. Somehow, this behavior would be expected because although the epigenetic state is dynamic and responsive to both developmental and environmental signals, small RNAs in general and even more miRNAs are well known to play numerous crucial roles at each major stage of plants development (Jones-Rhoades et al., 2006; Chen, 2009, 2012). The results here described are in agreement with those reported in the grapevine miRNA atlas (Kullan et al., 2015), especially with respect to the clustering of berries according to their developmental stage, sustaining the idea that miRNAs influence organ identity and clearly separate green and ripened berries. Also, in the study of the grapevine transcriptome performed by Dal Santo et al. (2013), they observed that other factors such as year and developmental stage had more influence on the gene expression, rather than the environment.

AUTHOR CONTRIBUTIONS

DPP prepared small RNA libraries, performed the *in silico* analysis and wrote the paper. LB conceived the experimental plan and sampled biological material. SDS prepared plant material for RNA extraction, read critically the paper. GDL prepared plant material for RNA extraction, sampled the biological material, read critically the paper. MP conceived the work. MEP supported the lab work, contributed to data analysis and read critically the paper. BM gave a substantial contribution to *in silico* analysis. EM wrote the paper, prepared plant material for RNA extraction, supported small RNA libraries preparation and helped data analysis.

ACKNOWLEDGMENTS

This work was supported by the Doctoral School in Agrobiosciences of Scuola Superiore Sant'Anna and by the Valorizzazione dei Principali Vitigni Autoctoni Italiani e dei loro Terroir (Vigneto) project funded by the Italian Ministry of Agricultural and Forestry Policies. This work benefited from the networking activities within the European funded COST ACTION FA1106 “An integrated systems approach to determine the developmental mechanisms influencing fleshy fruit quality in tomato and grapevine.” SDS was financed by the Italian Ministry of University and Research FIRB RBFR13GHC5 project “The Epigenomic Plasticity of Grapevine in Genotype per Environment Interactions”. Research in the Meyers lab is supported by the US National Science Foundation Plant Genome Research Program (award #1339229). We wish to thank Jayakumar Belli Kullan for assistance with small RNA libraries preparation, Tzuu-fen Lee for useful discussion on clustering analyses and Mayumi Nakano for curating the database and GEO data submission.

SUPPLEMENTARY MATERIAL

The Supplementary Material for this article can be found online at: <http://journal.frontiersin.org/article/10.3389/fpls.2016.01459>

REFERENCES

- Agarwal, M. C. J., and Chen, X. (2009). "Endogenous small RNA pathways in *Arabidopsis*," in *Regulation of Gene Expression by Small RNAs*, Vol. xvii., eds R. K. Gaur and J. Rossi (Boca Raton, FL: CRC Press), 431.
- Alabi, O. J., Zheng, Y., Jagadeeswaran, G., Sunkar, R., and Naidu, R. A. (2012). High-throughput sequence analysis of small RNAs in grapevine (*Vitis vinifera* L.) affected by grapevine leafroll disease. *Mol. Plant Pathol.* 13, 1060–1076. doi: 10.1111/j.1364-3703.2012.00815.x
- Ali, K., Maltese, F., Choi, Y. H., and Verpoorte, R. (2010). Metabolic constituents of grapevine and grape-derived products. *Phytochem. Rev.* 9, 357–378. doi: 10.1007/s11101-009-9158-0
- Arikit, S., Xia, R., Kakrana, A., Huang, K., Zhai, J., Yan, Z., et al. (2014). An atlas of soybean small RNAs identifies phased siRNAs from hundreds of coding genes. *Plant Cell* 26, 4584–4601. doi: 10.1105/tpc.114.131847
- Bernstein, E., and Allis, C. D. (2005). RNA meets chromatin. *Genes Dev.* 19, 1635–1655. doi: 10.1101/gad.1324305
- Bogs, J., Jaffe, F. W., Takos, A. M., Walker, A. R., and Robinson, S. P. (2007). The grapevine transcription factor VvMYBPA1 regulates proanthocyanidin synthesis during fruit development. *Plant Physiol.* 143, 1347–1361. doi: 10.1104/pp.106.093203
- Bond, D. M., and Baulcombe, D. C. (2014). Small RNAs and heritable epigenetic variation in plants. *Trends Cell Biol.* 24, 100–107. doi: 10.1016/j.tcb.2013.08.001
- Borges, F., and Martienssen, R. A. (2016). The expanding world of small RNAs in plants. *Nat. Rev. Mol. Cell Biol.* 16, 727–741. doi: 10.1038/nrm4085
- Boss, P. K., and Davies, C. (2001). "Molecular biology of sugar and anthocyanin accumulation in grape berries," in *Molecular Biology and Biotechnology of the Grapevine*, ed K. Roubelakis-Angelakis (Dordrecht: Springer), 1–33.
- Bradshaw, A. D. (1965). "Evolutionary significance of phenotypic plasticity in plants," in *Advances in Genetics*, eds E. W. Caspari and J. M. Thoday (New York, NY: Academic Press), 115–155.
- Burkhart, K. B., Guang, S., Buckley, B. A., Wong, L., Bochner, A. F., and Kennedy, S. (2011). A pre-mRNA-associating factor links endogenous siRNAs to chromatin regulation. *PLoS Genet.* 7:e1002249. doi: 10.1371/journal.pgen.1002249
- Callaway, R. M., Pennings, S. C., and Richards, C. L. (2003). Phenotypic plasticity and interactions among plants. *Ecology* 84, 1115–1128. doi: 10.1890/0012-9658(2003)084[1115:PPAIAP]2.0.CO;2
- Cao, D., Wang, J., Ju, Z., Liu, Q., Li, S., Tian, H., et al. (2016). Regulations on growth and development in tomato cotyledon, flower and fruit via destruction of miR396 with short tandem target mimic. *Plant Sci.* 247, 1–12. doi: 10.1016/j.plantsci.2016.02.012
- Carra, A., Mica, E., Gambino, G., Pindo, M., Moser, C., Pé, M. E., et al. (2009). Cloning and characterization of small non-coding RNAs from grape. *Plant J.* 59, 750–763. doi: 10.1111/j.1365-313X.2009.03906.x
- Castel, S. E., and Martienssen, R. A. (2013). RNA interference in the nucleus: roles for small RNAs in transcription, epigenetics and beyond. *Nat. Rev. Genet.* 14, 100–112. doi: 10.1038/nrg3355
- Chen, X. (2009). Small RNAs and their roles in plant development. *Annu. Rev. Cell Dev. Biol.* 25, 21–44. doi: 10.1146/annurev.cellbio.042308.113417
- Chen, X. (2012). Small RNAs in development - insights from plants. *Curr. Opin. Genet. Dev.* 22, 361–367. doi: 10.1016/j.gde.2012.04.004
- Clingeleffer, P. R. (2010). Plant management research: status and what it can offer to address challenges and limitations. *Aust. J. Grape Wine Res.* 16, 25–32. doi: 10.1111/j.1755-0238.2009.00075.x
- Coombe, B. G. (1976). The Development of Fleshy Fruits. *Ann. Rev. Plant Phys.* 27, 207–228. doi: 10.1146/annurev.pp.27.060176.001231
- Dal Santo, S., Tornielli, G. B., Zenoni, S., Fasoli, M., Farina, L., Anesi, A., et al. (2013). The plasticity of the grapevine berry transcriptome. *Genome Biol.* 14:r54. doi: 10.1186/gb-2013-14-6-r54
- Davies, K., Schwinn, K., Deroles, S., Manson, D., Lewis, D., Bloor, S., et al. (2003). Enhancing anthocyanin production by altering competition for substrate between flavonol synthase and dihydroflavonol 4-reductase. *Euphytica* 131, 259–268. doi: 10.1023/A:1024018729349
- Debeaujon, I., Peeters, A. J., Leon-Kloosterziel, K. M., and Koornneef, M. (2001). The TRANSPARENT TESTA12 gene of *Arabidopsis* encodes a multidrug secondary transporter-like protein required for flavonoid sequestration in vacuoles of the seed coat endothelium. *Plant Cell* 13, 853–871. doi: 10.1105/tpc.13.4.853
- DeWitt, T. J., and Scheiner, S. M. (2003). *Phenotypic Plasticity: Functional and Conceptual Approaches*. New York, NY: Oxford University Press.
- Duncan, E. J., Gluckman, P. D., and Dearden, P. K. (2014). Epigenetics, plasticity, and evolution: how do we link epigenetic change to phenotype? *J. Exp. Zool. B Mol. Develop. Evol.* 322, 208–220. doi: 10.1002/jez.b.22571
- Eisen, M. B., Spellman, P. T., Brown, P. O., and Botstein, D. (1998). Cluster analysis and display of genome-wide expression patterns. *Proc. Natl. Acad. Sci. U.S.A.* 95, 14863–14868.
- Fagegaltier, D., Bougé, A.-L., Berry, B., Poisot, É., Sismeiro, O., Coppée, J.-Y., et al. (2009). The endogenous siRNA pathway is involved in heterochromatin formation in *Drosophila*. *Proc. Natl. Acad. Sci. U.S.A.* 106, 21258–21263. doi: 10.1073/pnas.0809280105
- Finnegan, E. J., and Matzke, M. A. (2003). The small RNA world. *J. Cell Sci.* 116, 4689–4693. doi: 10.1242/jcs.00838
- Formey, D., Sallet, E., Lelandais-Brière, C., Ben, C., Bustos-Sanmamed, P., Niebel, A., et al. (2014). The small RNA diversity from *Medicago truncatula* roots under biotic interactions evidences the environmental plasticity of the miRNAome. *Genome Biol.* 15:457. doi: 10.1186/s13059-014-0457-4
- Fujii, H., Chiou, T. J., Lin, S. I., Aung, K., and Zhu, J. K. (2005). A miRNA involved in phosphate-starvation response in *Arabidopsis*. *Curr. Biol.* 15, 2038–2043. doi: 10.1016/j.cub.2005.10.016
- Gapper, N. E., Giovannoni, J. J., and Watkins, C. B. (2014). Understanding development and ripening of fruit crops in an 'omics' era. *Hort. Res.* 1, 14034. doi: 10.1038/hortres.2014.34
- Ge, A., Shangguan, L., Zhang, X., Dong, Q., Han, J., Liu, H., et al. (2013). Deep sequencing discovery of novel and conserved microRNAs in strawberry (*Fragaria ananassa*). *Physiol. Plant.* 148, 387–396. doi: 10.1111/j.1399-3054.2012.01713.x
- Geng, Y., Gao, L., and Yang, J. (2013). "Epigenetic flexibility underlying phenotypic plasticity," in *Progress in Botany*, eds U. Lütge, W. Beyschlag, D. Francis, and J. Cushman (Berlin; Heidelberg: Springer), 153–163.
- Ghildiyal, M., and Zamore, P. D. (2009). Small silencing RNAs: an expanding universe. *Nat. Rev. Genet.* 10, 94–108. doi: 10.1038/nrg2504
- Gianoli, E., and Valladares, F. (2012). Studying phenotypic plasticity: the advantages of a broad approach. *Biol. J. Linn. Soc.* 105, 1–7. doi: 10.1111/j.1095-8312.2011.01793.x
- Giovannoni, J. J. (2007). Fruit ripening mutants yield insights into ripening control. *Curr. Opin. Plant Biol.* 10, 283–289. doi: 10.1016/j.pbi.2007.04.008
- Goldberg, A. D., Allis, C. D., and Bernstein, E. (2007). Epigenetics: a landscape takes shape. *Cell* 128, 635–638. doi: 10.1016/j.cell.2007.02.006
- Gomez, C., Terrier, N., Torregrosa, L., Vialet, S., Fournier-Level, A., Verriès, C., et al. (2009). Grapevine MATE-type proteins act as vacuolar H⁺-dependent acylated anthocyanin transporters. *Plant Physiol.* 150, 402–415. doi: 10.1104/pp.109.135624
- Gratani, L. (2014). Plant phenotypic plasticity in response to environmental factors. *Adv. Bot.* 2014:17. doi: 10.1155/2014/208747
- Gray, J. D. (2002). *The Basis of Variation in the Size and Composition of Grape Berries*. PhD, University of Adelaide.
- Guillaumie, S., Fouquet, R., Kappel, C., Camps, C., Terrier, N., Moncomble, D., et al. (2011). Transcriptional analysis of late ripening stages of grapevine berry. *BMC Plant Biol.* 11:165. doi: 10.1186/1471-2229-11-165
- Guleria, P., Mahajan, M., Bhardwaj, J., and Yadav, S. K. (2011). Plant small RNAs: biogenesis, mode of action and their roles in abiotic stresses. *Genom. Proteomics Bioinformatics* 9, 183–199. doi: 10.1016/S1672-0229(11)60022-3
- Ha, M., Lu, J., Tian, L., Ramachandran, V., Kasschau, K. D., Chapman, E. J., et al. (2009). Small RNAs serve as genetic buffer against genomic shock in *Arabidopsis* interspecific hybrids and allopolyploids. *Proc. Natl. Acad. Sci. U.S.A.* 106, 17835–17840. doi: 10.1073/pnas.0907003106
- Han, J., Fang, J., Wang, C., Yin, Y., Sun, X., Leng, X., et al. (2014). Grapevine microRNAs responsive to exogenous gibberellin. *BMC Genomics* 15:111. doi: 10.1186/1471-2164-15-111
- Harding, J. L., Horswell, S., Heliot, C., Armisen, J., Zimmerman, L. B., Luscombe, N. M., et al. (2014). Small RNA profiling of *Xenopus* embryos reveals novel miRNAs and a new class of small RNAs derived from intronic transposable elements. *Genome Res.* 24, 96–106. doi: 10.1101/gr.144469.112

- He, F., Mu, L., Yan, G. L., Liang, N. N., Pan, Q. H., Wang, J., et al. (2010). Biosynthesis of anthocyanins and their regulation in colored grapes. *Molecules* 15, 9057–9091. doi: 10.3390/molecules15129057
- Holloway, G. J. (2002). Phenotypic plasticity: beyond nature and nurture. *Heredity* 89, 410–410. doi: 10.1038/sj.hdy.6800153
- Howell, M. D., Fahlgren, N., Chapman, E. J., Cumbie, J. S., Sullivan, C. M., Givan, S. A., et al. (2007). Genome-wide analysis of the RNA-DEPENDENT RNA POLYMERASE6/DICER-LIKE4 pathway in *Arabidopsis* reveals dependency on miRNA- and tasiRNA-directed targeting. *Plant Cell* 19, 926–942. doi: 10.1105/tpc.107.050062
- Hu, H., Yu, D., and Liu, H. (2015). Bioinformatics analysis of small RNAs in pima (*Gossypium barbadense* L.). *PLoS ONE* 10:e0116826. doi: 10.1371/journal.pone.0116826
- Jaillon, O., Aury, J. M., Noel, B., Policriti, A., Clepet, C., Casagrande, A., et al. (2007). The grapevine genome sequence suggests ancestral hexaploidization in major angiosperm phyla. *Nature* 449, 463–467. doi: 10.1038/nature06148
- Jeong, D. H., Park, S., Zhai, J., Gurazada, S. G., De Paoli, E., Meyers, B. C., et al. (2011). Massive analysis of rice small RNAs: mechanistic implications of regulated microRNAs and variants for differential target RNA cleavage. *Plant Cell* 23, 4185–4207. doi: 10.1105/tpc.111.089045
- Jeong, D. H., Schmidt, S. A., Rymarquis, L. A., Park, S., Ganssmann, M., German, M. A., et al. (2013). Parallel analysis of RNA ends enhances global investigation of microRNAs and target RNAs of *Brachypodium distachyon*. *Genome Biol.* 14:R145. doi: 10.1186/gb-2013-14-12-r145
- Jones-Rhoades, M. W., Bartel, D. P., and Bartel, B. (2006). MicroRNAs and their regulatory roles in plants. *Annu. Rev. Plant Biol.* 57, 19–53. doi: 10.1146/annurev.arplant.57.032905.105218
- Kakrana, A., Hammond, R., Patel, P., Nakano, M., and Meyers, B. C. (2014). sPARTA: a parallelized pipeline for integrated analysis of plant miRNA and cleaved mRNA data sets, including new miRNA target-identification software. *Nucleic Acids Res.* 42:e139. doi: 10.1093/nar/gku693
- Karlova, R., van Haarst, J. C., Maliepaard, C., van de Geest, H., Bovy, A. G., Lammers, M., et al. (2013). Identification of microRNA targets in tomato fruit development using high-throughput sequencing and degradome analysis. *J. Exp. Bot.* 64, 1863–1878. doi: 10.1093/jxb/ert049
- Kawashima, C. G., Matthewman, C. A., Huang, S., Lee, B.-R., Yoshimoto, N., Koprivova, A., et al. (2011). Interplay of SLIM1 and miR395 in the regulation of sulfate assimilation in *Arabidopsis*. *Plant J.* 66, 863–876. doi: 10.1111/j.1365-313X.2011.04547.x
- Keller, M. (2010). Managing grapevines to optimise fruit development in a challenging environment: a climate change primer for viticulturists. *Aust. J. Grape Wine Res.* 16, 56–69. doi: 10.1111/j.1755-0238.2009.00077.x
- Khraiwesh, B., Zhu, J. K., and Zhu, J. (2012). Role of miRNAs and siRNAs in biotic and abiotic stress responses of plants. *Biochim. Biophys. Acta* 1819, 137–148. doi: 10.1016/j.bbagen.2011.05.001
- Kim, V. N. (2005). Small RNAs: classification, biogenesis, and function. *Mol. Cells* 19, 1–15.
- Kim, W., Ahn, H. J., Chiou, T.-J., and Ahn, J. H. (2011). The role of the miR399-PHO2 module in the regulation of flowering time in response to different ambient temperatures in *Arabidopsis thaliana*. *Mol. Cells* 32, 83–88. doi: 10.1007/s10059-011-1043-1
- Kozomara, A., and Griffiths-Jones, S. (2014). miRBase: annotating high confidence microRNAs using deep sequencing data. *Nucleic Acids Res.* 42, D68–D73. doi: 10.1093/nar/gkt1181
- Kullan, J. B., Paim Pinto, D. L., Bertolini, E., Fasoli, M., Zenoni, S., Tornielli, G. B., et al. (2015). miRVine: a microRNA expression atlas of grapevine based on small RNA sequencing. *BMC Genomics* 16:393. doi: 10.1186/s12864-015-1610-5
- Langmead, B., Trapnell, C., Pop, M., and Salzberg, S. L. (2009). Ultrafast and memory-efficient alignment of short DNA sequences to the human genome. *Genome Biol.* 10:R25. doi: 10.1186/gb-2009-10-3-r25
- Lee, H., Yoo, S. J., Lee, J. H., Kim, W., Yoo, S. K., Fitzgerald, H., et al. (2010). Genetic framework for flowering-time regulation by ambient temperature-responsive miRNAs in *Arabidopsis*. *Nucleic Acids Res.* 38, 3081–3093. doi: 10.1093/nar/gkp1240
- Lee, T.-F., Gurazada, S. G. R., Zhai, J., Li, S., Simon, S. A., Matzke, M. A., et al. (2012). RNA polymerase V-dependent small RNAs in *Arabidopsis* originate from small, intergenic loci including most SINE repeats. *Epigenetics* 7, 781–795. doi: 10.4161/epi.20290
- Lelandais-Briere, C., Sorin, C., Crespi, M., and Hartmann, C. (2012). Non-coding RNAs involved in plant responses to environmental constraints. *Biol. Aujourd’hui* 206, 313–322. doi: 10.1051/bio/2012032
- Leple, J. C., Dauwe, R., Morreel, K., Storme, V., Lapierre, C., Pollet, B., et al. (2007). Downregulation of cinnamoyl-coenzyme A reductase in poplar: multiple-level phenotyping reveals effects on cell wall polymer metabolism and structure. *Plant Cell* 19, 3669–3691. doi: 10.1105/tpc.107.054148
- Li, H., Deng, Y., Wu, T., Subramanian, S., and Yu, O. (2010). Misexpression of miR482, miR1512, and miR1515 increases soybean nodulation. *Plant Physiol.* 153, 1759–1770. doi: 10.1104/pp.110.156950
- Li, J., Sun, Q., Yu, N., Zhu, J., Zou, X., Qi, Z., et al. (2014). The role of small RNAs on phenotypes in reciprocal hybrids between *Solanum lycopersicum* and *S. pimpinellifolium*. *BMC Plant Biol.* 14:296. doi: 10.1186/s12870-014-0296-1
- Liang, G., and Yu, D. (2010). Reciprocal regulation among miR395, APS and SULTR2;1 in *Arabidopsis thaliana*. *Plant Signal. Behav.* 5, 1257–1259. doi: 10.4161/psb.5.10.12608
- Lijavetzky, D., Carbonell-Bejerano, P., Grimplet, J., Bravo, G., Flores, P., Fenoll, J., et al. (2012). Berry flesh and skin ripening features in *Vitis vinifera* as assessed by transcriptional profiling. *PLoS ONE* 7:e39547. doi: 10.1371/journal.pone.0039547
- Lind, M. I., Yarlett, K., Reger, J., Carter, M. J., and Beckerman, A. P. (2015). The alignment between phenotypic plasticity, the major axis of genetic variation and the response to selection. *Proc. Biol. Sci.* 282:20151651. doi: 10.1098/rspb.2015.1651
- Liu, D., Song, Y., Chen, Z., and Yu, D. (2009). Ectopic expression of miR396 suppresses GRF target gene expression and alters leaf growth in *Arabidopsis*. *Physiol. Plant.* 136, 223–236. doi: 10.1111/j.1399-3054.2009.01229.x
- Liu, R., How-Kit, A., Stammitti, L., Teyssier, E., Rolin, D., Mortain-Bertrand, A., et al. (2015). A DEMETER-like DNA demethylase governs tomato fruit ripening. *Proc. Natl. Acad. Sci. U.S.A.* 112, 10804–10809. doi: 10.1073/pnas.1503362112
- Manning, K., Tör, M., Poole, M., Hong, Y., Thompson, A. J., King, G. J., et al. (2006). A naturally occurring epigenetic mutation in a gene encoding an SBP-box transcription factor inhibits tomato fruit ripening. *Nat. Genet.* 38, 948–952. doi: 10.1038/ng1841
- Marinova, K., Pourcel, L., Weder, B., Schwarz, M., Barron, D., Routaboul, J.-M., et al. (2007). The *Arabidopsis* MATE transporter TT12 acts as a vacuolar flavonoid/H(+) -antiporter active in proanthocyanidin-accumulating cells of the seed coat. *Plant Cell* 19, 2023–2038. doi: 10.1105/tpc.106.046029
- Martínez-Esteso, M. J., Vilella-Antón, M. T., Pedreño, M. Á., Valero, M. L., and Bru-Martínez, R. (2013). iTRAQ-based protein profiling provides insights into the central metabolism changes driving grape berry development and ripening. *BMC Plant Biol.* 13:167. doi: 10.1186/1471-2229-13-167
- Matas, A. J., Yeats, T. H., Buda, G. J., Zheng, Y., Chatterjee, S., Tohge, T., et al. (2011). Tissue- and cell-type specific transcriptome profiling of expanding tomato fruit provides insights into metabolic and regulatory specialization and cuticle formation. *Plant Cell* 23, 3893–3910. doi: 10.1105/tpc.111.091173
- Matsui, A., Nguyen, A. H., Nakaminami, K., and Seki, M. (2013). *Arabidopsis* non-coding RNA regulation in abiotic stress responses. *Int. J. Mol. Sci.* 14, 22642–22654. doi: 10.3390/ijms141122642
- Matthewman, C. A., Kawashima, C. G., Húška, D., Csorba, T., Dalmary, T., and Kopriva, S. (2012). miR395 is a general component of the sulfate assimilation regulatory network in *Arabidopsis*. *FEBS Lett.* 586, 3242–3248. doi: 10.1016/j.febslet.2012.06.044
- Matus, J. T., Aquea, F., Espinoza, C., Vega, A., Cavallini, E., Dal Santo, S., et al. (2014). Inspection of the grapevine BURP superfamily highlights an expansion of RD22 genes with distinctive expression features in berry development and ABA-mediated stress responses. *PLoS ONE* 9:e110372. doi: 10.1371/journal.pone.0110372
- McCormick, K. P., Willmann, M. R., and Meyers, B. C. (2011). Experimental design, preprocessing, normalization and differential expression analysis of small RNA sequencing experiments. *Silence* 2:2. doi: 10.1186/1758-07X-2-2
- Meyers, B. C., Axtell, M. J., Bartel, B., Bartel, D. P., Baulcombe, D., Bowman, J. L., et al. (2008). Criteria for annotation of plant MicroRNAs. *Plant Cell* 20, 3186–3190. doi: 10.1105/tpc.108.064311
- Moxon, S., Jing, R., Szittya, G., Schwach, F., Rusholme Pilcher, R. L., Moulton, V., et al. (2008). Deep sequencing of tomato short RNAs identifies microRNAs

- targeting genes involved in fruit ripening. *Genome Res.* 18, 1602–1609. doi: 10.1101/gr.080127.108
- Nicotra, A. B., Atkin, O. K., Bonser, S. P., Davidson, A. M., Finnegan, E. J., Mathesius, U., et al. (2010). Plant phenotypic plasticity in a changing climate. *Trends Plant Sci.* 15, 684–692. doi: 10.1016/j.tplants.2010.09.008
- Ortega-Regules, A., Romero-Cascales, I., Lopez-Roca, J. M., Ros-Garcia, J. M., and Gomez-Plaza, E. (2006). Anthocyanin fingerprint of grapes: environmental and genetic variations. *J. Sci. Food Agric.* 86, 1460–1467. doi: 10.1002/jsfa.2511
- Palmer, C. M., Bush, S. M., and Maloof, J. N. (2012). “Phenotypic and developmental plasticity in plants,” in *Encyclopedia of Life Sciences* (Chichester: John Wiley & Sons, Ltd.), 1–9.
- Pantaleo, V., Szittyá, G., Moxon, S., Miozzi, L., Moulton, V., Dalmay, T., et al. (2010). Identification of grapevine microRNAs and their targets using high-throughput sequencing and degradome analysis. *Plant J.* 62, 960–976. doi: 10.1111/j.1365-313X.2010.04208.x
- Pigliucci, M. (2001). *Phenotypic Plasticity: Beyond Nature and Nurture*. Baltimore, MD: John Hopkins University Press.
- Pigliucci, M. (1996). How organisms respond to environmental changes: from phenotypes to molecules (and vice versa). *Trends Ecol. Evol.* 11, 168–173. doi: 10.1016/0169-5347(96)10008-2
- Poni, S. (2000). “Fisiologia di comportamento del Sangiovese. Aspetti di base e considerazioni applicative” in *Il Sangiovese: Atti del Simposio Internazionale*, ed ARSIA, (Firenze: ARSIA).
- Provenzano, S. (2011). *The Genetics of Anthocyanin Production, Accumulation and Display: A Comparative Study in Different species*. PhD, Vrije Universiteit.
- Rustioni, L., Rossoni, M., Failla, O., and Scienza, A. (2013). Anthocyanin esterification in Sangiovese grapes. *Ital. J. Food Sci.* 25, 131–141.
- Sadras, V. O., Stevens, R. M., Pech, J. M., Taylor, E. J., Nicholas, P. R., and McCarthy, M. G. (2007). Quantifying phenotypic plasticity of berry traits using an allometric-type approach: a case study on anthocyanins and sugars in berries of Cabernet Sauvignon. *Aust. J. Grape Wine Res.* 13, 72–80. doi: 10.1111/j.1755-0238.2007.tb00237.x
- Schluchting, C. D., and Pigliucci, M. (1993). Control of phenotypic plasticity via regulatory genes. *Am. Nat.* 142, 366–370. doi: 10.1086/285543
- Schmitt, J. (1993). Reaction norms of morphological and life-history traits to light availability in Impatiens capensis. *Evolution* 47, 1654–1668.
- Schmitt, J., Dudley, S., and Pigliucci, M. (1999). Manipulative approaches to testing adaptive plasticity: phytochrome-mediated shade-avoidance responses in plants. *Am. Nat.* 154, S43–S54. doi: 10.1086/303282
- Schurh, N. J., Schofield, P., Gierliński, M., Cole, C., Sherstnev, A., Singh, V., et al. (2016). How many biological replicates are needed in an RNA-seq experiment and which differential expression tool should you use? *RNA* 22, 839–851. doi: 10.1261/rna.053959.115
- Selvaraj, Y., Pal, D. K., Singh, R., and Roy, T. K. (1994). Biochemistry of uneven ripening in Gulabi grape. *J. Food Biochem.* 18, 325–340. doi: 10.1111/j.1745-4519.1994.tb00507.x
- Stocks, M. B., Moxon, S., Mapleson, D., Woolfenden, H. C., Mohorianu, I., Folkes, L., et al. (2012). The UEA sRNA workbench: a suite of tools for analysing and visualizing next generation sequencing microRNA and small RNA datasets. *Bioinformatics* 28, 2059–2061. doi: 10.1093/bioinformatics/bts311
- Sultan, S. E. (2000). Phenotypic plasticity for plant development, function and life history. *Trends Plant Sci.* 5, 537–542. doi: 10.1016/S1360-1385(00)01797-0
- Sun, X., Korir, N. K., Han, J., Shangguan, L. F., Kayesh, E., Leng, X. P., et al. (2012). Characterization of grapevine microR164 and its target genes. *Mol. Biol. Rep.* 39, 9463–9472. doi: 10.1007/s11033-012-1811-9
- Swami, M. (2010). An epigenetic silencing influence. *Nat. Rev. Genet.* 11:172. doi: 10.1038/nrg2755
- Tavares, S., Vesentini, D., Fernandes, J. C., Ferreira, R. B., Laureano, O., Ricardo-Da-Silva, J. M., et al. (2013). *Vitis vinifera* secondary metabolism as affected by sulfate depletion: diagnosis through phenylpropanoid pathway genes and metabolites. *Plant Physiol. Biochem.* 66, 118–126. doi: 10.1016/j.plaphy.2013.01.022
- Tieman, D. M., Lucas, H. M., Kim, J. Y., Clark, D. G., and Klee, H. J. (2007). Tomato phenylacetaldehyde reductases catalyze the last step in the synthesis of the aroma volatile 2-phenylethanol. *Phytochemistry* 68, 2660–2669. doi: 10.1016/j.phytochem.2007.06.005
- Trabucco, G. M., Matos, D. A., Lee, S. J., Saathoff, A. J., Priest, H. D., Mockler, T. C., et al. (2013). Functional characterization of cinnamyl alcohol dehydrogenase and caffeic acid O-methyltransferase in *Brachypodium distachyon*. *BMC Biotechnol.* 13:61. doi: 10.1186/1472-6750-13-61
- Trindade, I. S. D., Dalmay, T., and Fevereiro, P. (2011). “Facing the environment: small RNAs and the regulation of gene expression under abiotic stress in plants,” in *Abiotic Stress Response in Plants - Physiological, Biochemical and Genetic Perspectives*, ed A. V. Shanker (InTech), 113–136. Available online at: <http://www.intechopen.com/books/abiotic-stress-response-in-plants-physiological-biochemical-and-genetic-perspectives>
- van Leeuwen, C., Friant, P., Choné, X., Tregot, O., Koundouras, S., and Dubourdieu, D. (2004). Influence of climate, soil, and cultivar on Terroir. *Am. J. Enol. Vitic.* 55, 207–217.
- van Leeuwen, C. T. G. O., Choné, X., Gaudilleire, and J. P. Pernet, D. (2007). “Different environmental conditions, different results: the role of controlled environmental stress on grape quality and the way to monitor it,” in *Proceedings of the Thirteenth Australian Wine Industry Technical Conference*, ed. P. J. B. Williams and R. J. Pretorius (Adelaide: Australian Wine Industry Technical Conference Incorporated), 400.
- Vazquez, F. (2006). *Arabidopsis* endogenous small RNAs: highways and byways. *Trends Plant Sci.* 11, 460–468. doi: 10.1016/j.tplants.2006.07.006
- Vitulò, N., Forcato, C., Carpinelli, E. C., Telatin, A., Campagna, D., D'Angelo, M., et al. (2014). A deep survey of alternative splicing in grape reveals changes in the splicing machinery related to tissue, stress condition and genotype. *BMC Plant Biol.* 14:99. doi: 10.1186/1471-2229-14-99
- Wang, C., Han, J., Liu, C., Kibet, K. N., Kayesh, E., Shangguan, L., et al. (2012). Identification of microRNAs from Amur grape (*Vitis amurensis* Rupr.) by deep sequencing and analysis of microRNA variations with bioinformatics. *BMC Genomics* 13:122. doi: 10.1186/1471-2164-13-122
- Wang, C., Leng, X., Zhang, Y., Kayesh, E., Zhang, Y., Sun, X., et al. (2014). Transcriptome-wide analysis of dynamic variations in regulation modes of grapevine microRNAs on their target genes during grapevine development. *Plant Mol. Biol.* 84, 269–285. doi: 10.1007/s11103-013-0132-2
- Wang, L., Gu, X., Xu, D., Wang, W., Wang, H., Zeng, M., et al. (2011). miR396-targeted AtGRF transcription factors are required for coordination of cell division and differentiation during leaf development in *Arabidopsis*. *J. Exp. Bot.* 62, 761–773. doi: 10.1093/jxb/erq307
- Xia, S., Cheng, Y. T., Huang, S., Win, J., Soards, A., Jinn, T.-L., et al. (2013). Regulation of transcription of nucleotide-binding leucine-rich repeat-encoding genes SNC1 and RPP4 via H3K4 trimethylation. *Plant Physiol.* 162, 1694–1705. doi: 10.1104/pp.113.214551
- Xu, F., Liu, Q., Chen, L., Kuang, J., Walk, T., Wang, J., et al. (2013). Genome-wide identification of soybean microRNAs and their targets reveals their organ-specificity and responses to phosphate starvation. *BMC Genomics* 14, 66–66. doi: 10.1186/1471-2164-14-66
- Zhai, J., Jeong, D.-H., De Paoli, E., Park, S., Rosen, B. D., Li, Y., et al. (2011). MicroRNAs as master regulators of the plant NB-LRR defense gene family via the production of phased, trans-acting siRNAs. *Genes Dev.* 25, 2540–2553. doi: 10.1101/gad.177527.111
- Zhao, J., Pang, Y., and Dixon, R. A. (2010). The mysteries of proanthocyanidin transport and polymerization. *Plant Physiol.* 153, 437–443. doi: 10.1104/pp.110.155432
- Zhong, S., Fei, Z., Chen, Y. R., Zheng, Y., Huang, M., Vrebalov, J., et al. (2013). Single-base resolution methylomes of tomato fruit development reveal epigenome modifications associated with ripening. *Nat. Biotechnol.* 31, 154–159. doi: 10.1038/nbt.2462
- Zhu, Q.-H., Fan, L., Liu, Y., Xu, H., Llewellyn, D., and Wilson, I. (2013). miR482 Regulation of NBS-LRR Defense Genes during Fungal Pathogen Infection in Cotton. *PLoS ONE* 8:e84390. doi: 10.1371/journal.pone.0084390
- Zuker, M. (2003). Mfold web server for nucleic acid folding and hybridization prediction. *Nucleic Acids Res.* 31, 3406–3415. doi: 10.1093/nar/gkg595
- Conflict of Interest Statement:** The authors declare that the research was conducted in the absence of any commercial or financial relationships that could be construed as a potential conflict of interest.
- Copyright © 2016 Paim Pinto, Brancadoro, Dal Santo, De Lorenzis, Pezzotti, Meyers, Pé and Mica. This is an open-access article distributed under the terms of the Creative Commons Attribution License (CC BY). The use, distribution or reproduction in other forums is permitted, provided the original author(s) or licensor are credited and that the original publication in this journal is cited, in accordance with accepted academic practice. No use, distribution or reproduction is permitted which does not comply with these terms.



The Potential of the MAGIC TOM Parental Accessions to Explore the Genetic Variability in Tomato Acclimation to Repeated Cycles of Water Deficit and Recovery

Julie Ripoll^{1,2}, Laurent Urban² and Nadia Bertin^{1*}

¹ UR1115 Plantes et Systèmes de cultures Horticoles, INRA, Avignon, France, ² Laboratoire de Physiologie des Fruits et Légumes EA4279, Université d'Avignon et des Pays du Vaucluse, Avignon, France

OPEN ACCESS

Edited by:

Antonio Granell,
Consejo Superior de Investigaciones
Científicas, Spain

Reviewed by:

Jaime Prohens,
Universitat Politècnica de València,
Spain
Miquel A. Conesa,
Universitat de les Illes Balears, Spain

*Correspondence:

Nadia Bertin
nadia.bertin@avignon.inra.fr

Specialty section:

This article was submitted to
Plant Physiology,
a section of the journal
Frontiers in Plant Science

Received: 24 September 2015

Accepted: 07 December 2015

Published: 05 January 2016

Citation:

Ripoll J, Urban L and Bertin N (2016)
The Potential of the MAGIC TOM
Parental Accessions to Explore
the Genetic Variability in Tomato
Acclimation to Repeated Cycles
of Water Deficit and Recovery.
Front. Plant Sci. 6:1172.
doi: 10.3389/fpls.2015.01172

Episodes of water deficit (WD) during the crop cycle of tomato may negatively impact plant growth and fruit yield, but they may also improve fruit quality. Moreover, a moderate WD may induce a plant “memory effect” which is known to stimulate plant acclimation and defenses for upcoming stress episodes. The objective of this study was to analyze the positive and negative impacts of repeated episodes of WD at the plant and fruit levels. Three episodes of WD (−38, −45, and −55% of water supply) followed by three periods of recovery (“WD treatments”), were applied to the eight parents of the Multi-Parent Advanced Generation Inter-Cross population which offers the largest allelic variability observed in tomato. Predawn and midday water potentials, chlorophyll *a* fluorescence, growth and fruit quality traits [contents in sugars, acids, carotenoids, and ascorbic acid (AsA)] were measured throughout the experiment. Important genotypic variations were observed both at the plant and fruit levels and variations in fruit and leaf traits were found not to be correlated. Overall, the WD treatments were at the origin of important osmotic regulations, reduction of leaf growth, acclimation of photosynthetic functioning, notably through an increase in the chlorophyll content and in the quantum yield of the electron transport flux until PSI acceptors ($J_0^{\text{RE1}}/J^{\text{ABS}}$). The effects on fruit sugar, acid, carotenoid and AsA contents on a dry matter basis ranged from negative to positive to nil depending on genotypes and stress intensity. Three small fruit size accessions were richer in AsA on a fresh matter basis, due to concentration effects. So, fruit quality was improved under WD mainly through concentration effects. On the whole, two accessions, LA1420 and Criollo appeared as interesting genetic resources, cumulating adaptive traits both at the leaf and fruit levels. Our observations show that the complexity involved in plant responses, when considering a broad range of physiological traits and the variability of genotypic effects, represent a true challenge for upcoming studies aiming at taking advantage of, not just dealing with WD.

Keywords: fruit quality, MAGIC population, recovery period, *S. lycopersicum* L., water deficit

INTRODUCTION

Drought is a major threat for crop yield and improving agricultural productivity while reducing water use is a major issue. Indeed drought events are expected to increase in intensity, frequency, and geographic extent as a consequence of global change. Maintenance of plant productivity under limited water supply is a stress tolerance/acclimation trait, which shows inter- and intra-specific variation. In a recent review on fleshy fruits, Ripoll et al. (2014) championed the idea that drought can have positive effects on fruit quality while yield reduction could be minimized. However, developing plants adapted to drier conditions requires a better understanding of the physiological responses to WD. Many mechanisms may be involved in yield maintenance under WD conditions; in particular those involved in the reduction of water losses, in resource acquisition and allocation between source and sink organs, and in protection against oxidative stress (Ripoll et al., 2014). Exploring the existing genetic diversity in such traits opens new perspectives to address current challenges in the context of climate change. In tomato, current breeding methods have intensively selected yield or quality traits, while less attention has been paid to tolerance traits to abiotic stresses (Causse et al., 2001; Saliba-Colombani et al., 2001). MAGIC populations are an interesting source of genetic variability, since they display the largest allelic variability observed in different populations (Cavanagh et al., 2008). The eight parents of the MAGIC TOM S. *lycopersicum* L. have been selected for their higher rate of SNP differences among 360 others tomato accessions (Ranc, 2010), but to our knowledge these accessions were poorly characterized under stress conditions (Table 1). RIL populations have been developed from the MAGIC TOM population; they are used for genetic studies and breeding programs (Pascual et al., 2015). For instance a RIL population derived from an intraspecific cross between Cervil and Levovil, two of the eight MAGIC TOM parents (Saliba-Colombani et al., 2001), was used to identify QTLs of fruit quality (Chaïb et al., 2006). More recently, 119 recombinant inbred accessions derived from the same cross have been phenotyped and genotyped under two water regimes (control and moderate WD). This study revealed 11 interactive QTLs which determine genotypic expression as a function of watering regimes and which are associated to plant and fruit quality traits (Albert et al., 2015). This study concluded that large fruit tomatoes are more sensitive to drought than cherry tomatoes and that breeding for crop performance under conditions of deficit irrigation should aim at achieving trade-offs between fruit quality and yield.

Abbreviations: ANOVA, analysis of variance; AsA, ascorbic acid; AUC, area under the curve; DM, dry matter; MAGIC TOM, Multi-Parent Advanced Generation Inter-Cross population of Tomato; Plovdiv, genotype PlovdivXXIV (*S. lycopersicum* L.); PS, photosystems; RP, recovery period; RP1, recovery period 1; RP2, recovery period 2; RP3, recovery period 3; Stupicke, genotype Stupicke Polni Rane (*S. lycopersicum* L.); WD, water deficit; WD1, water deficit period 1; WD2, water deficit period 2; WD3, water deficit period 3. Parameters: $\Psi_{predawn}$, predawn water potential; Ψ_{midday} , midday water potential; Ψ_{soil} , soil water potential; F_V/F_M , maximum efficiency at which light absorbed by PSII is used for reduction of Q_A ; J_0^{RE1}/J^{ABS} , quantum yield of the electron transport flux until PSI acceptors; PI, Performance Index (Strasser et al., 2004).

Water deficit is known to impact the leaf physiological activity, usually resulting in a reduction of stomatal conductance, conduced to a reduction of photosynthetic activity, a decrease in growth and an increased risk of photo-oxidative stress (Tardieu et al., 2006). However, during RPs, mechanisms of plant defenses or acclimation are expected to be exacerbated by WD thanks to priming mechanisms (Bruce et al., 2007). Moreover, two successive stress periods may stimulate water uptake during the second stress period, resulting in a reduction of the negative impact of WD on plant growth (Al Gehani, 2005). During RP, growth may not completely recover depending on the duration and the intensity of WD. In tomato, when water supply is suppressed during the reproductive period (from 9 to 13 days), leaf water potential, stomatal conductance, and net photosynthesis rate can recover their initial values (Rahman et al., 1999). Cell wall extensibility which plays an important role in cell expansion, is less likely to recover after drought stress, arguably due to the rapid accumulation of abscisic acid (Mahdidi et al., 2011). However, in tomato, it has been observed that some Mediterranean drought adapted landraces tend to have thinner, more elastic cell walls, which allow them to maintain cell turgor by reducing cell volume, when cultivated under drought (Galmés et al., 2011). Under extreme WD, recovery may be partial due to damage on PSII. Indeed the synthesis of reactive oxygen species can increase under WD, and recovery depends on the quantity produced vs. the quantity scavenged (Xu et al., 2010). More generally, it has been demonstrated that “plant memory” of stress induces a faster activation of response mechanisms to other stressors (abiotic or biotic stress) through the common hormonal response pathways (Li and Zhang, 2012). The faster activation of defense response in primed plants is associated to an increased gene expression and to the accumulation of inactive signaling proteins and transcription factors (Bruce et al., 2007).

Regarding fruit quality (e.g., contents in soluble sugars, organic acids, carotenoids or C vitamin), the impact of WD may differ according to the stage of fruit development at the time of WD (reviewed in Ripoll et al., 2014). When WD occurs during the cell division stage, it may induce carbon starvation that negatively regulates cell division and consequently final fruit size. However, a positive effect on carbon supply to the remaining fruits has been suggested due to a negative regulation of fruit setting and fruit load. In peach (*Prunus persica* L.), WD has been shown to improve fruit sweetness, flavor and fruit size when applied during the stage of cell division and rapid endocarp hardening (Li et al., 1989; Vallverdu et al., 2012). In tomato, a moderate WD applied during the stage of cell division does not reduce fruit size, arguably due to important osmotic regulations (Ripoll et al., 2015). During the cell expansion stage, WD mainly impacts water flows between source and sink organs (Münch, 1930) through osmotic and turgor regulations. In peach, negative effects on yield have been observed associated with a decrease in fruit water content (Li et al., 1989; Girona et al., 2004). During ripening, which coincides with seed maturation, progressive softening, accumulation of pigments, sugars, and acids, and release of volatiles (Osorio et al., 2013), WD may interact with ethylene synthesis (Fray et al., 1994; Barry and Giovannoni, 2007). In

tomato, moderate WD during ripening reduces the accumulation of some carotenoids, whereas the effects on sugar accumulation seem to be genotype dependent (Ripoll et al., 2015). Different combinations of WD applied during flowering and fruit growth, or during flowering and ripening, showed that the improvement of fruit quality is counterbalanced by the decrease in yield when at least one development phase is exposed to intensive stress in oranges *Citrus sinensis* L. (García-Tejero et al., 2010). Thus, WD episodes followed by RP may impact fruit quality in a different way from single WD episode. For instance, fruit carotenoid content increases in tomato plants grown under WD and this increase is exacerbated after a second period of WD due to an increase in antioxidant enzyme activity during both the first WD period and the RP (Stoeva et al., 2010, 2012). So understanding the effect of WD on fruit quality is a complex issue due to the numerous factors involved, even though WD is generally expected to improve fruit quality (Ripoll et al., 2014). Similar observations have been made in response to moderate salt stress, involving similar mechanisms (e.g., Munns, 2002; De Pascale et al., 2007). Finally it appears that one could take advantage of the “memory effect” induced after a moderate WD, in order to promote fruit quality while minimizing yield reduction. Even though there is some evidence that WD can be used as a lever to increase quality of fruits, there is a lack of references about the effect of WD episodes of increasing intensity followed by periods of recovery.

In the present study, our objectives were: (i) to provide an overview of the beneficial and detrimental impacts of WD treatments at the plant and fruit levels, (ii) to assess the genetic variability of these responses, and (iii) to reveal interesting traits of plant acclimation to WD, which could be used in future breeding programs. The work was performed on the eight parents of the MAGIC TOM population. Plant and fruit responses were measured during three successive periods of WD of increasing intensity followed by RP (“WD treatments”), which is clearly an original feature of the present study. Moderate WD was achieved by reducing the supply of water by about 38% during the first WD period, 45% during the second WD period and 55% during the last WD period when compared to control plants. Predawn water potential, stem water potential at midday, chlorophyll content and chlorophyll *a* fluorescence as well as leaf composition (soluble sugars and organic acids) were assessed before and after each WD period. Fruit quality (soluble sugars, organic acids, carotenoids, and AsA contents) was measured on two batches of fruits which developed at different periods of the WD treatments.

MATERIALS AND METHODS

Plant Material and Experimental Conditions

The eight parents of the MAGIC TOM (**Table 1**) encompass four large-fruit accessions [Ferum, LA0147, Levovil, and Stupicke Polni Rane (here called Stupicke)], and four cherry accessions [Cervil, Criollo, LA1420, and PlovdivXXIVa (here called Plovdiv)]. All are indeterminate tomatoes. LA1420 seeds were provided by the Tomato Genetics Resource Centre, Davis, CA,

USA. Cervil and Levovil seeds were provided by Vilmorin Seed Company. The other accessions were supplied by the Tomato Genetic Resource Centre of INRA, Avignon, France (Causse et al., 2013).

The experiment was conducted during spring and summer 2012 in a glasshouse located near Avignon, France. Irrigation was calculated according to daily ETP (Penman, 1948), taking into account crop coefficients ($K_c = 40\%$ before treatments, 50–75% during the first WD, 75–100% from the first RP and 100% until the end of the experiment). The control irrigation met the evaporative demand. The WD treatments corresponded to three phases of WD of increasing intensity (-38, -45, and -55% of water supply when compared to control plants) followed by three RP (**Figure 1A**). Each WD and RP period lasted approximately 15 days. During recovery, WD was first reduced by half for 2 days and then brought back to the control level. Climate conditions (temperature, humidity, and light intensity) in the glasshouse were recorded every minute and data were averaged hourly throughout the experiment. Average day and night temperatures were stable until 12 June, i.e., until RP2 (around 25°C and 18°C, respectively). Temperatures increased during WD3 and RP3 (around 30°C and 22°C, respectively) due to seasonal effects. At the same time, the daily light integral increased in the glasshouse (from 5 to 11 MJ m⁻² day⁻¹), whereas average day and night humidity decreased (from 57 to 37% at daytime and from 80 to 60% at night) from WD1 to RP3. Plants were grown in 4 L pots filled with compost (substrate 460, Klasmann, Champety, France) distributed in two rows (control and stressed plants) of 80 plants each (10 plants per genotype) surrounded by border plants. The density was 1.3 plant m⁻².

The soil water potential (Ψ_{soil}) was measured daily with Watermark probes (Watermark 253, Campbell Scientific, Antony, France) placed at the opposite of the drippers (**Figure 1B**). One probe per treatment per genotype was used and connected to a data logging system (Data logger, Campbell Scientific, Antony, France). Results were converted into MPa using equation 8 given by Shock et al. (1998). In control conditions, Ψ_{soil} was rather stable until the WD3 period (-0.04 ± 0.01 MPa) and decreased during RP3 due to plant development (-0.05 ± 0.01 MPa). On the contrary, the soil water potential decreased to -0.09 ± 0.02, -0.29 ± 0.06, and -0.43 ± 0.04 MPa during WD1, WD2, and WD3, respectively. Nutrients were applied daily using a commercial solution (Liquoplant Rose, Plantin, Courthézon, France).

Flowers were pollinated three times a week using an electrical bee. Trusses were pruned according to final fruit weight (**Table 1**) in order to obtain comparable levels of competition among fruits for all genotypes (Cervil: 12 fruits per truss, Criollo: 10 fruits, LA1420: eight fruits, Plovdiv: eight fruits, Stupicke: six fruits, Ferum: five fruits, LA0147: five fruits, Levovil: four fruits). No chemical treatment was applied and *Macrolophus caliginosus* were released throughout the culture to protect plants from whiteflies.

Plant Measurements

Stem water potential was measured using a pressure chamber (SAM Précis 2000 Gradignan, France) at predawn and at solar

TABLE 1 | Some characteristics of the eight parents of the MAGIC TOM population selected for their high degree of allelic variability (Ranc, 2010).

Genotype	Cultivar	Fruit weight (g)	Duration of cell division (days)	Duration of cell expansion (days)	Duration of ripening (days)	Known resistance to stressor
Cervil	<i>S. lycopersicum</i> 'cerasiforme'	<5	14	25	10	Sensitive to saline stress (Manaa et al., 2011)
Criollo	<i>S. lycopersicum</i> 'cerasiforme'	<15	21	24	10	No reference
LA1420	<i>S. lycopersicum</i> 'cerasiforme'	<50	21	24	10	No reference
Plovdiv XXIVa	<i>S. lycopersicum</i> 'cerasiforme'	<50	20	25	10	No reference
Stupicke Polni Rane	<i>S. lycopersicum</i> 'esculentum'	<70	21	24	10	1. Stomatal closure after five days without irrigation (Hnilickova and Duffek, 2004) 2. Resistant to <i>Phytophthora infestans</i> (Petrikova et al., 2003) 3. Increased photosynthesis after 4 days at cold temperature (Hnilickova et al., 2002) 5. Strong emission of volatiles (Subrtova et al., 1985)
Ferum	<i>S. lycopersicum</i> 'esculentum'	<130	25	26	10	No reference
LA0147	<i>S. lycopersicum</i> 'esculentum'	<130	25	25	10	No reference
Levovil	<i>S. lycopersicum</i> 'esculentum'	<130	25	25	10	Tolerant to saline stress (Manaa et al., 2011)

All of them have an indeterminate growth pattern.

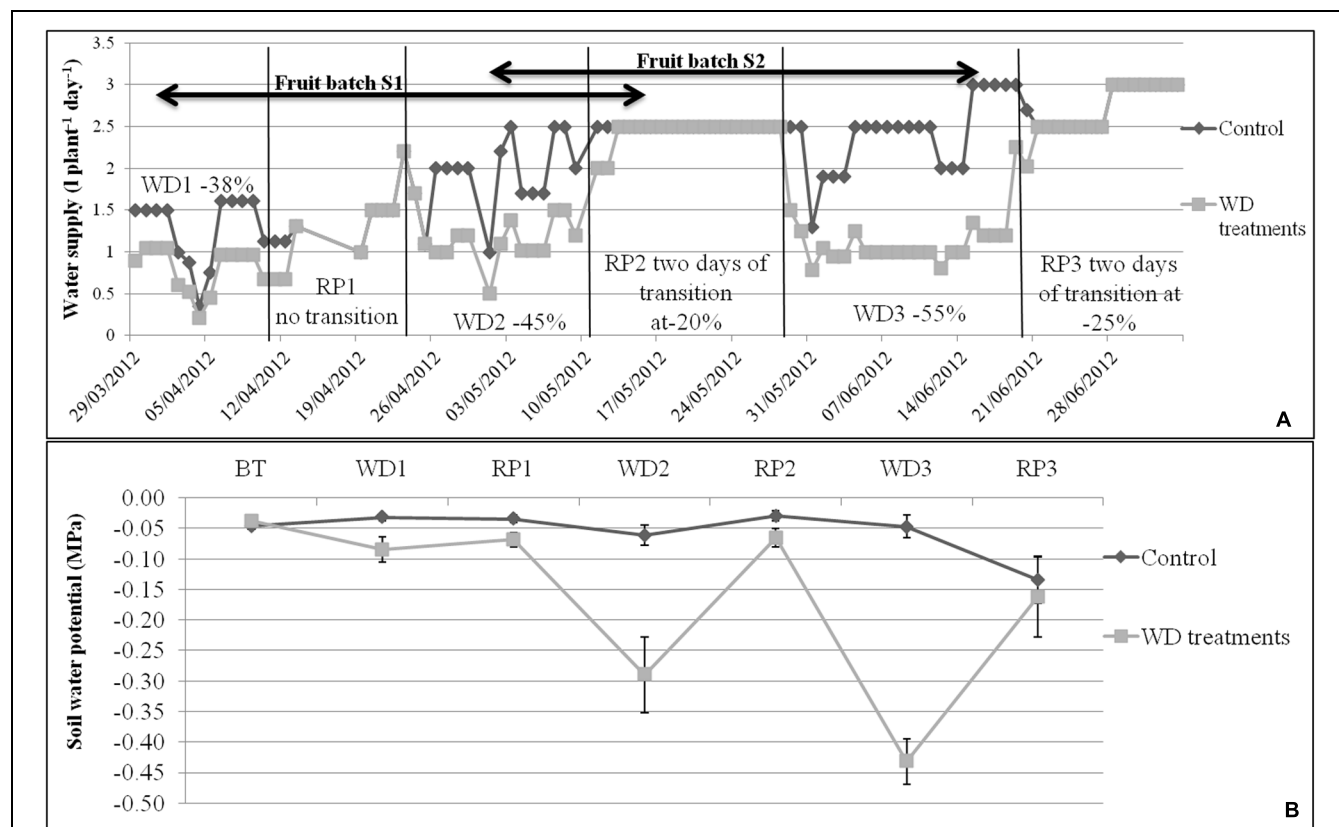


FIGURE 1 | (A) Water supply (water in $\text{l plant}^{-1} \text{ day}^{-1}$) for control and WD treatments, and **(B)** mean soil water potentials during each WD and RP period ($n = 8 \pm \text{SE}$), during the experiment period. Irrigation of control plants was monitored according to the measured potential evapotranspiration. The WD treatments consist in 3 cycles of WD of increasing intensity (-38, -45, and -55%) followed by RP periods. Transition periods of 2 days were applied after each WD period in order to reduce the risk of fruit blossom end rot. The fruit development periods of S1 and S2 lots are indicated by arrows.

noon (Ψ_{predawn} and Ψ_{midday}) at the end of each WD and RP period ($n \geq 4$ for a given genotype, 64 plants minimum). Leaves were bagged the day before, at nightfall.

Fluorescence of chlorophyll *a* was measured on dark adapted leaves (30 min.) using a fluorimeter (HANDY-PEA, Hansatech, King's Lynn, UK). Dark-adaptation allowed the PSII electron acceptor pool to be gradually re-oxidized to a point where all PSII reaction centers are capable of undertaking photochemistry. Measurements were carried out with an induction period of 1 s and leaves were illuminated to a light level of $3000 \mu\text{mol}$ photons $\text{m}^{-2} \text{s}^{-1}$. The measurements were carried out on non-senescing mature leaves, at around 11 a.m. during the last three days of each period ($n \geq 4$ for a given genotype, 64 plants minimum). The maximum photochemical efficiency of light harvesting of PSII (F_v/F_M), the PI of Strasser et al. (2004) and the quantum yield of the electron transport flux until PSI acceptors ($J_0^{\text{REI}}/J^{\text{ABS}}$; Stirbet and Govindjee, 2011) were calculated. The chlorophyll content was evaluated using a chlorophyll meter (SPAD 502, Konica-Minolta, Osaka, Japan) on adjacent leaves.

Plant leaf number and leaf length were measured at the end of each period ($n \geq 5$). The last day of the WD3 period, two non-senescing mature leaves, which were initiated during the WD treatments, were harvested on each plant and their specific leaf area ($n \geq 5$, 80 plants min.) was measured. Leaf area was measured with a Planimeter (Li-3100 C Area Meter, Li-Cor, Lincoln, NE, USA) and leaf dry weight was measured after seven days at 70°C in a ventilated oven.

Furthermore, at the end of each WD and RP period four leaflets of two mature leaves were harvested around 11 a.m. on five plants per genotype per treatment (80 plants in total), immediately frozen in liquid nitrogen and stored at -80°C , for biochemical analysis.

Fruit Measurements

The dates of anthesis of the successive trusses were recorded on all plants during the whole experiment. Thus, fruits could be pooled according to the developmental stage at the time of the WD treatments. The first pool of fruits (S1) was harvested during RP2, whereas WD1 occurred during the cell division period and WD2 during the cell expansion period. For the second pool of fruits (S2), WD2 occurred during the cell division period and WD3 during the cell expansion and ripening periods (Figure 1A). Fruit setting and abortion were recorded on the first eight trusses of each plant.

All measurements were performed on red mature fruits (breaker stage plus at least five days) harvested on five plants per genotype and per treatment (80 plants in total). Fruits were harvested at 11 a.m., avoiding the first proximal and the last distal fruits of each truss. Fruit diameter and fresh weight of all fruits were measured. Then fruits were frozen in liquid nitrogen and kept at -80°C prior to biochemical analysis of pericarp soluble sugars, organic acids, carotenoids, AsA, starch (only for Cervil), and DM contents. For biochemical analyses, fruits were pooled into five batches of three to five fruits for each treatment and genotype.

Biochemical Analyses

Soluble sugars and organic acids were extracted according to Gomez et al. (2002) and measured by HPLC method. Starch was measured on the supernatant after hydrolysis. The glucose released by starch hydrolysis was measured using the micro-method of Gomez et al. (2007) and starch content was calculated. DM content was measured after lyophilisation.

Assays of total, reduced and oxidized AsA content were carried out on ground powder conserved at -80°C using microplates and a plate reader, as previously described by Stevens et al. (2006). The absorbance was read at 550 nm. The specificity of the assay was checked by comparison with other known methods (Stevens et al., 2006). Carotenoids were extracted according to the method of Serino et al. (2009) and assayed by HPLC.

Statistical Analyses

All statistical analyses were performed using R3.1.0 (R Core Team, 2014). The evolution of physiological parameters over the experiment was compared between stressed and control plants using the AUCs. AUCs were calculated according to the Trapezoidal rule (Atkinson, 2008). Genotype and treatment effects on all parameters were analyzed by two-way ANOVA. The residue normality (ANOVA) was tested using the Shapiro-Wilk test (Royston, 1995). Levene's test was used to verify homoscedasticity of variances of the residues (Car package; Fox and Weisberg, 2011). When authorized, two-way ANOVA was performed and followed by multiple comparisons of means (Tukey test, lsmeans and multcompView packages; Graves et al., 2012 and Lenth, 2014, respectively). Alternatively, we used the non-parametric Kruskal-Wallis test (pgirmess package; Giraudoux, 2014). Heat-maps of the fruit traits were plotted according to control and WD treatments (gplots package; Warnes et al., 2014). Partial correlations network was built on plant and fruit data, based on the residues of the linear regressions (elimination of the genotype effect) and performed independently for the control and for the WD treatments (P threshold < 0.001 ; GGMselect, GeneNet, and igraph packages; Giraud et al., 2009; Schaefer et al., 2014, and Csardi and Nepusz, 2006, respectively). Finally, clustering analysis was performed on leaf and fruit data (FactoMineR package; Husson et al., 2014).

RESULTS

Mean Effects of the WD Treatments at the Plant and Leaf Levels

In order to evaluate the global plant response to the WD treatments, AUCs were calculated for Ψ_{predawn} , Ψ_{midday} , DM content, soluble sugars, organic acids, starch content, chlorophyll content, the maximum efficiency at which light absorbed by PSII is used for reduction of Q_A (F_v/F_M), the quantum yield of the electron transport flux until PSI acceptors ($J_0^{\text{REI}}/J^{\text{ABS}}$) and the PI index (Table 2). AUCs represent the cumulated response from the onset of the WD treatments until the end of WD3 (Figure 1).

TABLE 2 | Relative differences in plant and leaf traits between the WD treatments and the control.

	CERVIL	CRIOULLO	LA1420	PLOVDIV	STUPICKE	FERUM	LA0147	LEVOVIL
Predawn water potential	31.2	19.0	28.2	33.3	32.9	30.0	15.8	5.3
Midday stem water potential	12.7	28.4	7.0	14.3	13.6	54.9	20.8	-8.7
Length*number of leaves	7.0	-10.0	-3.0	-16.3	-5.2	-17.8	-8.6	-15.3
Fv/Fm	-1.7	-1.0	-2.3	-2.6	-3.0	-2.8	-2.7	-2.7
$J_0^{\text{RE1}}/J^{\text{ABS}}$	9.1	25.1	17.6	7.9	24.7	-0.6	23.1	11.1
PI	-12.6	-17.0	-19.8	-19.4	-11.1	-30.9	-9.2	-32.0
Chlorophyll content	1.7	6.8	10.9	2.7	16.1	4.5	1.8	17.0
Dry matter content	6.5	18.6	12.7	13.9	5.6	12.5	13.5	15.8
Citric acid	-18.1	-0.7	-6.9	3.7	-1.0	7.0	-7.4	-12.1
Malic acid	-7.3	9.4	38.1	23.9	30.6	25.5	5.2	41.6
Quinic acid	21.5	41.1	24.7	34.1	25.3	27.9	66.6	64.9
Total acids	-1.5	9.8	20.8	8.5	20.3	22.0	19.3	19.6
Glucose	14.1	16.4	35.5	36.6	143.1	9.9	59.1	129.9
Fructose	11.5	27.1	11.1	30.6	71.8	5.8	47.6	72.1
Sucrose	-5.0	12.4	4.4	9.6	8.6	5.7	17.3	10.5
Total sugars	8.3	20.8	6.6	41.9	14.6	65.1	29.1	62.3
Sugar/acid ratio	13.4	5.3	-160	29.3	-7.9	30.5	6.1	34.6
Starch	-4.9	79.2	12.8	242.0	101.5	195.5	101.3	212.4

Color scale:



Stem water potentials (in absolute values), leaf length \times leaf number, leaf metabolite contents (soluble sugars, organic acids, and starch on a DM basis) and parameters related to leaf photosynthetic activity were measured at the end of the WD for the eight parents of the MAGIC TOM (ranked in order of increasing fruit size). Relative differences were calculated based on total AUCs as: Parameter (%) = $\frac{\text{Mean WD} - \text{Mean Control}}{\text{Mean control}} \times 100$.

The percentages were scaled by color (green for high and red for low values). Significant differences are indicated by bold, italic, and underlined fonts for $P < 0.05$ (Two-way ANOVA test or Kruskal-Wallis test).

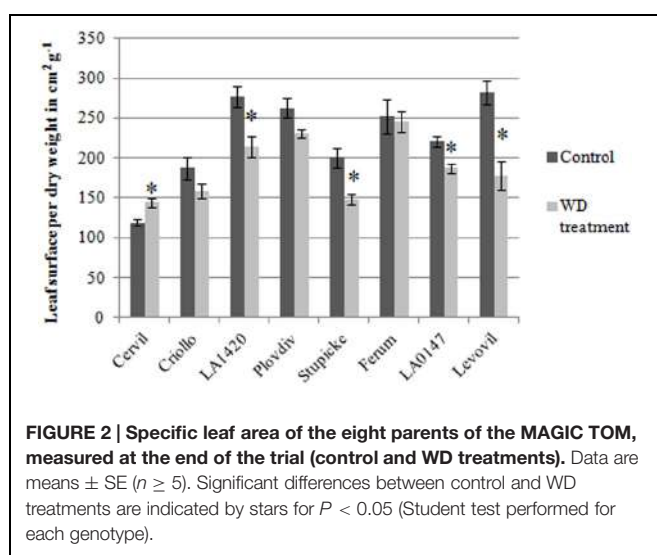


FIGURE 2 | Specific leaf area of the eight parents of the MAGIC TOM, measured at the end of the trial (control and WD treatments). Data are means \pm SE ($n \geq 5$). Significant differences between control and WD treatments are indicated by stars for $P < 0.05$ (Student test performed for each genotype).

RP3 was discarded because healthy non-senescent mature leaves were rare at this time.

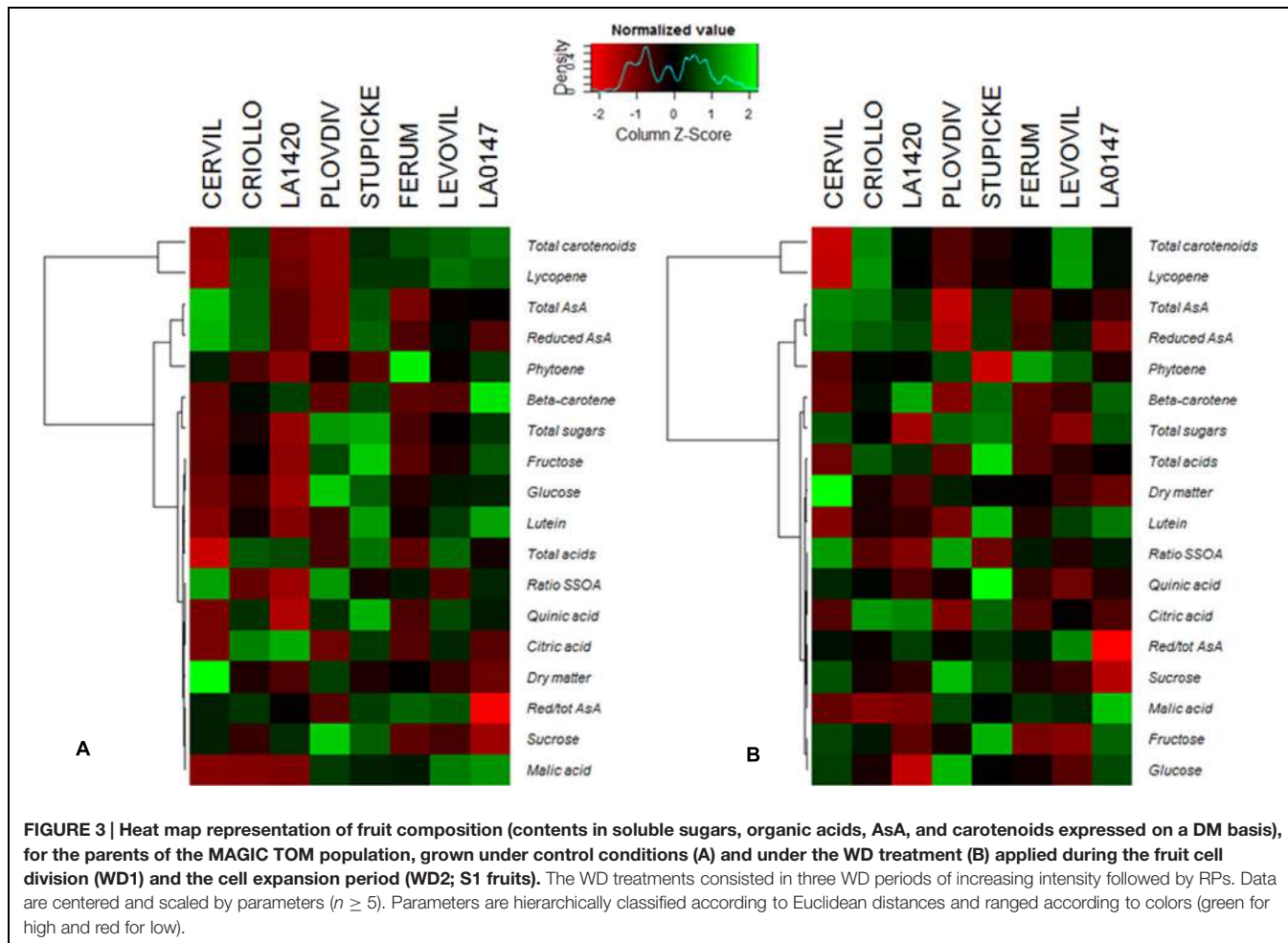
The F_v/F_m index decreased in response to the WD treatments in all genotypes except in Criollo. AUCs of PI index also significantly decreased for four genotypes (-19.4% in Plovdiv, -19.8% in LA1420, -30.9% in Ferum, and -32% in Levovil). On the contrary, $J_0^{\text{RE1}}/J^{\text{ABS}}$ increased in several genotypes (+25.1% in Criollo, +17.6% in LA1420, +24.7% in Stupicke, +23.1% in LA0147) as well as the relative chlorophyll content (+6.8% in

Criollo, +10.9% in LA1420, +2.7% in Plovdiv, and +16.1% in Stupicke). Then, leaf DM content (Table 2) increased due to the WD treatments (except in Cervil and Stupicke) as well as the contents in malic (except Cervil, Criollo and LA0147) and quinic acids, in glucose (except LA1420 and Ferum), in fructose (except Cervil, Criollo, and Ferum), and in starch (except Cervil and LA1420). The plant leaf area, assessed through leaf size and leaf number, significantly decreased in all genotypes except Cervil, LA1420, and Stupicke.

The specific leaf surface area measured at the end of the experiment on non-senescent mature leaves varied by a factor three among genotypes and it significantly decreased in response to the WD treatments in LA1420 (-26%), Stupicke (-26%), LA0147 (-15%) and Levovil (-36%) while it increased in Cervil (+21%), (Figure 2).

Effects of the WD Treatments on Fruit Size and Composition

A hierarchical clustering analysis, based on fruit composition variations (on a DM basis) among genotypes, is presented in Figure 3 for the first batch of fruits (S1). Clusters indicate fruit traits that co-varied under a given condition and highlight the differences in metabolite concentrations among genotypes. For both conditions, total soluble sugars, total organic acids, lutein, and β -carotene could be pooled together, as could be pooled together AsA and phytoene contents, on the one hand, and lycopene and total carotenoids contents, on the other hand. Figure 3 highlights contrasted composition among genotypes in



the control. For instance Cervil fruits which had the highest DM content, had the lowest content in total sugars, acids, carotenoids, and lycopene, but the highest content in total AsA on a DM basis. Similarly, LA1420 fruits were poor in all compounds except acids and β -carotene. On the contrary, Stupicke fruits were the richest in all compounds except phytoene. Similar results were observed in control fruits of the S2 fruits (data not shown).

Variations in fruit composition in response to the WD treatments are presented on a DM basis for S1 and S2 fruits (Tables 3 and 4, respectively). Though not significant, the decrease in fruit size and fresh mass was more pronounced in S2 fruits than in S1 fruits. For instance, on Levovil, the fruit fresh mass decreased by 42.8% in S2 fruits and by 13% in S1 fruits. Cervil S1 fruits were the less sensitive (Table 3). The number of set fruits measured on the eight first trusses was not significantly different between control and WD plants since inflorescences were pruned (data not shown).

On a DM basis, the variations in fruit composition were significant for five genotypes (Cervil, LA1420, Stupicke, LA0147, and Levovil; Table 3, S1 fruits). In the case of Cervil fruit, an increase in DM content (+8.9%), total soluble sugars (+20.3%), and starch content (+56.3%) was observed. Acid contents dropped in LA1420 fruits (-19.8% citric acid) and in LA0147

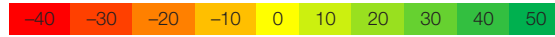
fruits (-30.6% malic acid). DM content was higher in Stupicke fruits (+12.7%), without any change in DM composition. In Levovil fruits, the β -carotene content was significantly reduced (-20.4%). Interestingly the contents in lycopene and carotenoids increased in four genotypes (Criollo, LA1420, Plovdiv, and LA0147), whereas total AsA content decreased in all genotypes except LA1420. However, these variations were not significant. Consistent results were observed in S2 fruits (Table 4) except for LA0147 whose contents in lycopene, carotenoids and total AsA were hardly affected. The fruit DM content increased in all genotypes (except Ferum) and to a larger extend in Cervil (+21%), LA1420 (+22.3%), and Levovil (+33.7%). Among soluble sugars, the sucrose content was more affected than glucose or fructose contents (+47.7% in Cervil and +61.8% in Stupicke).

On a fresh matter basis, sugars and quinic acid contents were significantly higher under WD in Cervil (respectively, +31.3 and +48.5% total sugar content in S1 and S2 fruits, and, respectively, +36.3 and +46.9% quinic acid content in S1 and S2 fruits) and in Levovil (+47% of total sugar and +44% of quinic acid for the S2 fruits; data not shown). In Stupicke only the quinic acid content was higher under WD (+35.6%, S1 fruits). For the S2 fruits, reduced and total AsA contents were higher in Cervil, LA1420,

TABLE 3 | Relative differences in fruit metabolite contents between the WD treatments and the control.

	CERVIL	CRIOLLO	LA1420	PLOVDIV	STUPICKE	FERUM	LA0147	LEVOVIL
Fruit size	2.3	-4.0	-6.8	4.2	-3.5	-3.7	-1.9	-5.6
Fresh weight	7.2	-5.7	-18.9	-3.3	-10.7	-11.0	-5.2	-12.7
Dry matter content	8.9	5.4	-0.3	-1.3	12.7	5.1	2.2	4.3
Glucose	19.6	7.9	7.1	-1.2	-2.9	6.8	-2.9	5.8
Fructose	20.5	6.1	12.9	-3.7	-1.8	5.0	-1.6	3.3
Sucrose	29.7	21.6	-19.6	11.9	9.3	36.9	8.7	-24.9
Total sugar	20.3	7.2	9.4	-2.1	-2.1	6.3	-2.1	4.3
Citric acid	9.4	-10.7	-19.8	-10.1	-4.7	-5.1	-20.0	-1.8
Malic acid	26.1	-6.6	-3.9	-5.9	-18.9	1.6	-30.6	1.1
Quinic acid	24.7	4.1	16.1	1.8	19.8	8.0	-10.4	1.2
Total acid	18.3	-4.9	-7.6	-3.8	3.5	1.7	-18.1	0.1
Sugar/acid ratio	0.6	12.2	18.0	2.0	-2.6	4.6	16.3	4.1
Lutein	-4.3	-6.6	45.5	-31.8	1.9	-15.2	-3.6	-14.2
Lycopene	-22.8	20.1	34.3	14.6	-11.6	-10.1	16.5	-12.3
Beta-carotene	-9.8	-0.2	24.5	-20.2	8.8	-6.9	1.9	-20.4
Phytoene	-19.7	30.6	48.6	27.3	-21.2	-6.2	29.4	-12.3
Total carotenoids	-21.4	19.9	35.3	14.4	-11.2	-9.4	17.2	-12.9
Reduced AsA	-9.0	-3.0	26.0	-16.0	-7.8	-7.0	-0.4	-17.2
Total AsA	-6.2	2.9	22.8	-17.3	-5.1	-1.3	-2.0	-12.1
Reduced/total AsA	-2.7	-6.0	2.3	1.5	-2.6	-5.8	1.7	-4.9
Starch	56.3							

Color scale:



Soluble sugars, organic acids, AsA, and carotenoids were measured on a dry mass basis for the eight MAGIC TOM parents. Relative differences were calculated as described in the legend of **Table 2**. The percentages were scaled by color (green for high and red for low values). S1 fruits were harvested at RP2 after a first WD period during cell division (WD1) and a second WD period during cell expansion (WD2). Significant differences are indicated by red bold, italic, and underlined fonts for $P < 0.05$ (Two-way ANOVA test or Kruskal-Wallis test).

and Plovdiv (respectively, +23.5, +31.2, and +30.3% reduced AsA, $P < 0.05$). So, metabolic and concentration effects added up for the compounds that increased both on a dry and fresh matter basis (mainly sugars and acids), whereas the negative effects of WD observed on a DM basis were mitigated by concentration effects, resulting in fruit quality homeostasis.

Partial Correlation Network and Clustering Among Leaf and Fruit Traits for Control and WD Treatments

A partial correlation network was built based on the AUCs calculated for the different leaf and fruit traits (**Figure 4**). Interestingly no leaf trait correlated to any fruit traits under both conditions. In control conditions, four independent leaf clusters emerged (**Figure 4A**). Positive correlations existed between leaf starch content and leaf DM content, between leaf malic acid content and Ψ_{predawn} , and between leaf fructose and glucose contents. Then PI correlated with $J_0^{\text{RE1}}/J^{\text{ABS}}$ and F_v/F_M . Concerning fruit traits, five independent clusters were found under control conditions. Fructose, glucose, and quinic acid contents were positively correlated one to each other, as well as lycopene and phytoene. Finally, fruit citric acid content, fruit malic acid content, and fruit lutein content were positively correlated one to each other while fruit fresh mass was negatively correlated with the fruit β -carotene content.

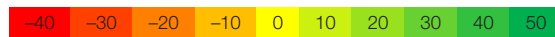
A different network was observed under the WD treatments when compared to the control (**Figure 4B**) suggesting that physiological acclimation processes were at play. At the leaf level, $J_0^{\text{RE1}}/J^{\text{ABS}}$ did not correlate any more with PI and F_v/F_M indexes. This observation suggests a regulation of the functioning of the photosynthetic machinery (**Table 2**). Leaf sugars (starch, fructose, and glucose) constituted an independent cluster. Leaf malic acid did not correlate anymore with Ψ_{predawn} but with leaf citric acid, due to the increase in organic acid contents (**Table 2**). Leaf DM content was positively correlated to leaf sucrose content instead of starch content. At the fruit level, the fruit DM content negatively correlated with the total ASA content, while the phytoene content was positively correlated with the lycopene content, as well as the lutein and β -carotene contents, the citric and quinic acid contents, and the glucose and fructose contents.

Clustering of the leaf and fruit traits measured in the experiment was realized for control (**Figure 5A**) and WD (**Figure 5B**) plants. Four clusters emerged for the control plants. LA1420 and Criollo were clustered according to their high fruit citric acid content and low leaf chlorophyll content. Levovil, Stupicke, and LA0147 stand out due to their similar malic acid and phytoene contents in fruits and by their low leaf glucose content. Ferum and Plovdiv were clustered due to their high PI index value and their low fruit AsA content. The cherry tomato Cervil constituted its own cluster due to its high starch, glucose,

TABLE 4 | Relative differences in fruit metabolite contents between the WD treatments and the control.

	CERVIL	CRIOLLO	LA1420	PLODIV	STUPICKE	FERUM	LA0147	LEVOVIL
Fruit size	-1.5	-9.7	-7.4	-9.1	-6.7	-1.0	-7.0	-14.7
Fresh weight	-0.2	-21.0	-20.2	-23.7	-16.1	-0.4	-18.6	-42.8
Dry matter content	<u>21.0</u>	14.0	<u>22.3</u>	9.0	8.7	-9.5	3.6	<u>33.7</u>
Glucose	23.9	-2.7	5.4	3.7	16.4	0.8	-1.8	10.3
Fructose	21.6	-1.5	0.9	3.5	12.3	5.9	-1.6	8.0
Sucrose	<u>47.7</u>	<u>102.2</u>	<u>42.3</u>	-4.7	<u>61.8</u>	-14.5	15.0	64.1
Total sugar	23.6	-0.7	3.7	3.3	15.2	3.0	-1.2	9.9
Citric acid	-4.0	1.4	<u>-27.0</u>	-4.6	-6.4	5.2	2.1	-21.5
Malic acid	-4.7	-4.3	14.6	4.0	-4.1	<u>-13.1</u>	0.3	<u>-33.4</u>
Quinic acid	<u>22.2</u>	-3.2	-6.7	5.0	-0.1	10.7	-0.3	7.6
Total acid	7.5	-0.8	-17.6	1.1	-3.5	5.7	1.0	-11.5
Sugar/acid ratio	15.0	-1.1	24.5	1.8	20.8	-2.3	-2.7	23.3
Lutein	-3.3	8.8	-20.9	28.8	10.8	29.4	32.9	-7.9
Lycopene	<u>-30.0</u>	<u>-11.8</u>	-4.1	1.2	<u>-11.8</u>	<u>41.3</u>	8.8	-9.9
Beta-carotene	-15.8	3.8	<u>-26.1</u>	-2.5	-7.7	<u>8.6</u>	6.4	<u>-24.6</u>
Phytoene	-18.3	-11.5	1.1	-9.2	-3.1	<u>44.2</u>	3.8	-0.3
Total carotenoids	<u>-27.5</u>	-11.2	-4.6	-0.4	<u>-10.7</u>	<u>40.9</u>	8.6	-9.8
Reduced AsA	7.7	-10.9	11.7	31.8	-7.2	11.8	5.8	-9.1
Total AsA	2.6	-7.4	10.4	19.8	-9.8	9.9	4.3	<u>-15.8</u>
Reduced/total AsA	4.8	-3.6	-0.1	11.0	3.3	1.4	0.9	8.0
Starch	<u>86.7</u>							

Color scale:



Soluble sugars, organic acids, AsA, and carotenoids were measured on a dry mass basis for the eight MAGIC TOM parents. Relative differences were calculated as described in the legend of **Table 2**. The percentages were scaled by color (green for high and red for low values). S2 fruits were harvested at WD3 (Cervil, Criollo, Plovdiv, and Stupicke) and RP3 (Levolv, LA1420, LA0147, and Ferum) after the first WD period during cell division (WD2) and a second WD period during cell expansion and ripening (WD3). Significant differences are indicated by red bold, italic, and underlined fonts for $P < 0.05$ (Two-way ANOVA test or Kruskal-Wallis test).

fructose, and malic acid contents in leaves and its high DM and low quinic acid contents in fruits. Similarly, four clusters emerged for the WD plants. Clustered genotypes did not necessarily respond to the WD treatments in the same way (**Table 2**). The first cluster includes Levovil, Stupicke, and Criollo, which have high fruit β -carotene content. LA1420, LA0147 and Ferum were clustered due to similar Euclidean distances without emergent traits. Plovdiv and Cervil constituted their own single cluster due to high glucose and low citric acid contents in leaves for Plovdiv, and to high DM content in fruits, high sucrose and fructose contents in leaves, and low Ψ_{predawn} and Ψ_{midday} values for Cervil.

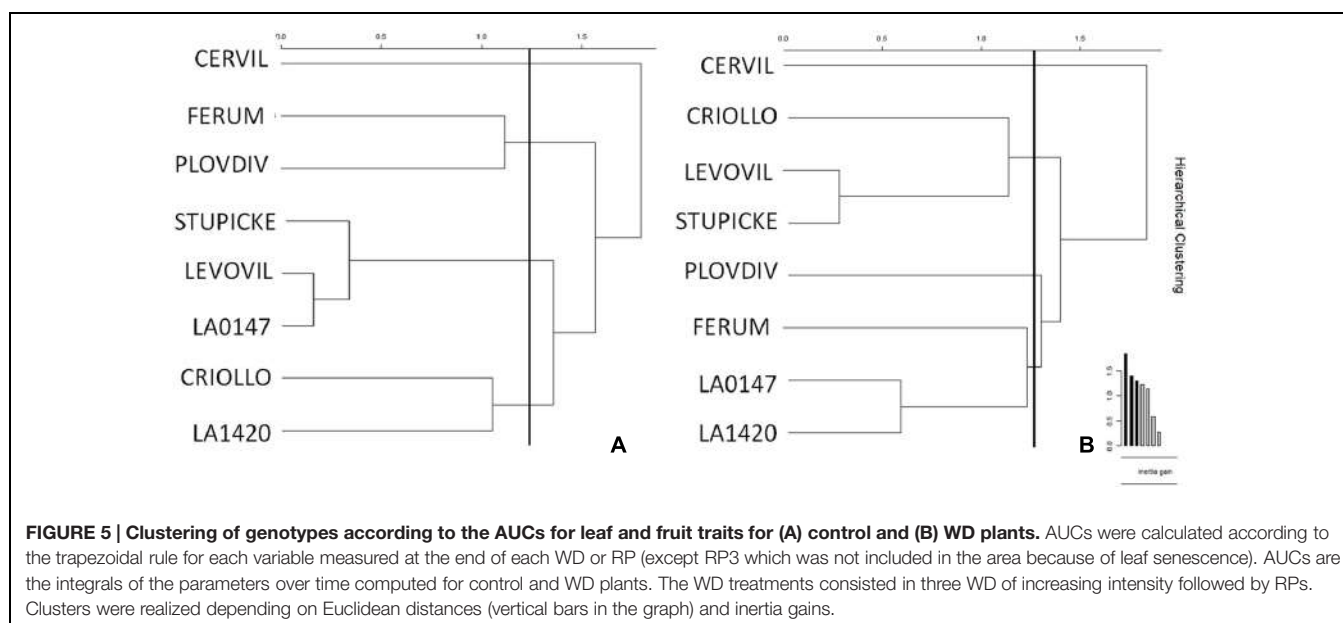
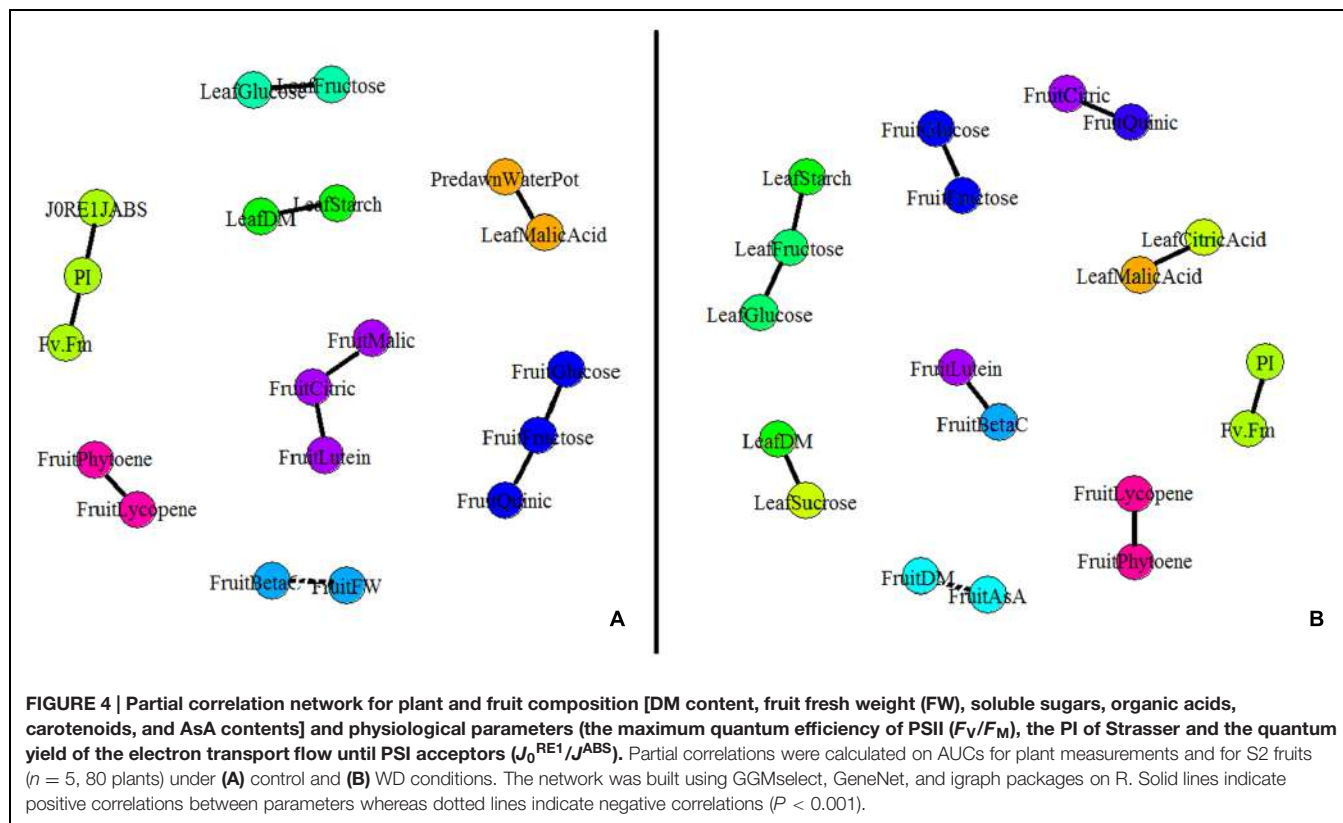
DISCUSSION

Leaf Responses to the WD Treatments Involved Osmotic and Photosynthetic Regulations

Current responses of plants submitted to WD encompass a decrease in plant water status and in water loss (as evidenced by a decrease in Ψ_{midday} , in stomatal conductance and in transpiration rate), a reduction of leaf growth, and osmotic regulations (Tardieu et al., 2006). In the present study, osmotic adjustment and photosynthetic adaptation seem to have prevailed in the response to the WD treatments, as evidenced by the

changes in leaf composition (increase in concentrations of soluble sugars and organic acids) and the relative stability of Ψ_{midday} except in Criollo and Ferum (**Table 2**). The absence of significant decrease in Ψ_{midday} may be explained by an increase in turgor. Indeed, when the elasticity modulus decreases, reflecting a decrease in cell wall rigidity, the decrease in turgor is mitigated during dehydration (Hsiao et al., 1976; Zimmermann, 1978), what probably happened in the present trial, although data are missing to substantiate this idea. Furthermore, the water status was not substantially affected, on the contrary to the carbon metabolism which was affected as reported in other studies (Chaves, 1991).

The parameters derived from analysis of the induction curve of maximum fluorescence of chlorophyll a are consistent with these ideas. A general decrease in F_v/F_m and to a larger extend in PI was observed in response to the WD treatments, as expected due to the sensitivity of PSII to WD conditions (Maxwell and Johnson, 2000). PI is a global index of performance (expressed in analogy to the Nernst potential) which is composed of three components: the force due to the concentration of active reaction centers, the force of the light reactions which is related to the quantum yield of primary photochemistry and the force related to the dark reactions (Živčák et al., 2008). PI has been defined as a “drought factor index” by Goltsev et al. (2012) during desiccation of beans *Phaseolus vulgaris* L., which is in accordance with the present observations on tomato. Moreover,



the increase in the quantum yield of the electron transport flux until PSI acceptors (J_0^{RE1}/J^{ABS}) could be explained by a return of electrons from PSI to PSII named the cyclic electron flow (Johnson, 2011), which is described as an orchestrator of the chloroplast energy budget, that increases in response to environmental stressors such as high light, WD simulated by low CO₂ supply, or extreme temperatures in higher plants

(Livingston et al., 2010; Johnson, 2011; Walker et al., 2014). The significant increase in quinic acid which was observed in all accessions in response to the WD treatments could be related to the increase in J_0^{RE1}/J^{ABS} . Indeed quinic acid has been described as a potential accelerator of the electron transport due to its capacity to act as a non-classical uncoupling factor on photophosphorylation (Barba-Behrens et al., 1993). Finally, the

increase in chlorophyll content in some genotypes, which is not compatible with photodamage in leaves, contributes to the idea that there was an efficient acclimation to maintain photosynthetic activity under WD.

In summary, the shifts in energy fluxes around PSII, the accumulation of starch in leaves and the decrease in the specific leaf surface area, which is a recognized if not specific consequence of WD, are all potent indicators that plants submitted to WD were indeed stressed (Chaves, 1991; Zgallai et al., 2005). They are also indicators of acclimation processes aiming at relieving the photosynthetic machinery from overheating, arguably as a consequence of decreased translocation to active growth areas. Finally, it appears that osmotic and photosynthetic regulations were highly involved in plant acclimation to successive episodes of WD. Such acclimation effects were observed in almost all accessions, but more clearly in Criollo, LA1420, and Stupicke. Overall, Cervil exhibited the weakest responses, suggesting that this genotype is poorly sensitive to WD as recently suggested by Albert et al. (2015).

The WD Treatments Reduced Fruit Growth Proportionally to the Increase in Stress Intensity and to Cumulative Effects of WD

Depending on its intensity, WD is expected to decrease fruit size and fruit water content, thus increasing the metabolite contents through a concentration effect. WD may also stimulate the accumulation of osmotic and antioxidant compounds (Ripoll et al., 2014). Despite the absence of a significant response, fruit size and weight were mainly reduced in S2 fruits by the WD treatments (except in the cherry tomato Cervil). These observations are not in accordance with others studies, where WD was reported to have positive effects on fruit growth, due to a negative regulation of fruit setting and to an increase of carbon supply to the remaining fruits (Li et al., 1989; Vallverdu et al., 2012). In the present study, the plant fruit load was regulated at similar level in control and WD plants, thus the maintenance of fruit growth arguably resulted from osmotic regulations and/or sugar compartmentation in the fruit (Ripoll et al., 2015). The reduction of fruit size and weight in S2 fruits is consistent with the idea that fruit yield decreases proportionally to the intensity of WD (Wang and Gartung, 2010). Competition for carbon was likely higher during the development of S2 fruits compared to S1 fruits, due to the cumulative effects of the three WD periods on the plant carbon budget. Moreover fruit growth of large fruit genotypes was more impacted by the WD treatments than fruits of small fruit genotypes, arguably due to higher carbon demand for large fruit growth. Indeed, in WD conditions, sink organ growth was suggested to be reduced mainly through carbon dependent mechanisms (Muller et al., 2011). However, water fluxes are indirectly linked to carbon metabolism through osmotic and turgor regulations, as discussed below. So, the genotypic differences observed in response to the WD treatments were arguably driven by the additive effects of differences in water flux on fruit expansion, of source-related differences

in carbon supply and of sink-related differences in carbon demand.

The WD Treatments Maintain Fruit Sugar and Acid Contents

As for fruit fresh weight, the increase in DM content was higher in S2 fruits than in S1 fruits, suggesting that S2 fruits were submitted to higher stress intensity than S1 fruits. An important increase in S2 fruits DM content was observed in response to the WD treatments in the large-fruit genotype Levovil as well as in the cherry tomato type Cervil. On the contrary, changes in DM composition were more pronounced in S1 fruits than in S2 fruits and responses were highly dependent on genotypes. Variations in fruit composition in response to WD may result either from dilution/concentration effects (Guichard et al., 2001; Etienne et al., 2013), from active solute accumulation (Lo Bianco et al., 2000; Hummel et al., 2010), or from starch breakdown, as observed in tomatoes under salinity-induced WD (Balibrea et al., 2003). Soluble sugars and organic acids (primarily malic and citric acids) are major osmotic compounds that accumulate in fleshy fruits and determine fruit taste. Previous studies on tomatoes showed an increase in fruit sugar content under WD depending on cultivars and timing of stress (Veit-Köhler et al., 1999; Bertin et al., 2000; Chen et al., 2014). In the present study, the total content in soluble sugars on a DM basis was not strongly affected by the WD treatments except in Cervil fruits which also accumulated large amounts of starch and acids. Thus, in cherry tomato the accumulation of starch, soluble sugars, and acids may be an adaptive strategy to maintain the phloem-to-fruit gradient of sugars and regulate cell turgor, sustaining fruit growth in WD conditions. Sucrose content on a DM basis was the most affected by the WD treatments among soluble sugars, but it represents only a minor part (<3%) of total soluble sugars in these genotypes. On a fresh weight basis, the increase in fruit sugar content in response to WD was observed only in Cervil and Levovil, which questions the idea that WD has a positive impact on fruit taste (Ripoll et al., 2014) and suggests that such effect strongly depends on genotype and WD intensity. The effects of WD on fruit acidity are more conflicting (Etienne et al., 2013). In many species (peach, clementine *Citrus clementina* Hort ex. Tan, mandarin *Citrus reticulata* B., pear *Pyrus* L., tomato), water supply has been shown to negatively correlate with organic acid content in ripe fruits, but in grapes *Vitis vinifera* L., nectarines *Prunus persica* var. *nucipersica* L. (Etienne et al., 2013) and tomatoes (Mitchell et al., 1991; Veit-Köhler et al., 1999; Bertin et al., 2000), this correlation has been shown to be positive.

Effects of the WD Treatments on Fruit Carotenoid and Ascorbic Acid Contents Ranged From Negative to Nil to Positive

Fruits supply a large range of health-promoting phytochemicals, of which secondary metabolites, primarily terpenoids (carotenoids, ABA, and others), and phenolic compounds, are the

largest group along with AsA. Of all of the environmental factors that play a stimulating role in the synthesis and accumulation of useful phytochemicals in fruits, moderate stress, and more specifically, controlled drought may influence the metabolism of these phytochemicals via at least two major mechanisms that are not mutually exclusive and that may even interact (Nora et al., 2012; Poiroux-Gonord et al., 2013; Fanciullino et al., 2014). Firstly, drought typically induces a decrease in net photosynthesis which reduces the supply of primary metabolites to the fruits that are the major source of precursors for the biosynthesis of phenolic compounds, carotenoids, and AsA. Secondly, drought may exacerbate oxidative stress and signaling which is known to directly and indirectly influence the biosynthetic pathways of these compounds in leaves (Fanciullino et al., 2014). In the present study, the effects of the WD treatments on fruit carotenoid content ranged on a DM basis from negative, to nil to positive depending on genotype and stress intensity (S1 and S2 fruits). This is in complete agreement with divergent responses reported in the litterature (reviewed by Ripoll et al., 2014). Similarly, total AsA was reduced in S1 fruits of all genotype but one (LA1420), whereas more variable effects were observed in S2 fruits. Many studies reported positive effects of WD on AsA (Zushi and Matsuzoe, 1998; Veit-Köhler et al., 1999; Favati et al., 2009; Murshed et al., 2013), but also indicated variable effects depending on genetic and seasonal factors or the intensity and duration of the treatment. In S1 fruits, carotenoid accumulation (on a DM basis) was increased in four genotypes and reduced in four other genotypes including cherry tomato and large-fruit genotypes. Taken together, our observations confirm previous observations (Poiroux-Gonord et al., 2013) that tend to refute the hypothesis that the supply of carbon to fruit determines carotenoid synthesis. In tomato fruits, the absence of correlation between sugars and reduced AsA content also suggests that fruit AsA content is not limited by leaf photosynthesis or sugar availability (Gautier et al., 2009). Variations in carotenoids and AsA content would therefore result from stress-induced cellular redox changes (Fanciullino et al., 2014). In tomato plants, AsA content has been suggested to correlate with resistance to WD (Zhang et al., 2011; Garchery et al., 2013). However in the present study, only one genotype (LA1420) exhibited an adaptive response at the fruit level through an increase in both carotenoid and AsA contents. On a fresh matter basis, the fruit content in phytonutrients was improved by the WD treatments only in the cherry tomato Cervil and in the small fruit size genotypes (LA1420 and Plovdiv) through an increase in reduced AsA. This increase resulted mainly from concentration effects than from metabolic stimulation, in agreement with recent findings (Ripoll et al., 2015).

CONCLUSION

In the present study, the WD treatments, which consisted in three successive cycles of moderate WD and recovery during the plant reproductive period, resulted in independent responses at the leaf and fruit levels. Considering parameters derived from

chlorophyll *a* fluorescence measurements and leaf composition, we may hypothesize that for some genotypes the cyclic electron flow (extrapolated from $J_0^{\text{REI}}/J^{\text{ABS}}$) and quinic acid content were involved in energy dissipation and regulation of oxidative stress during the WD treatments. Negative effects on fruit fresh weight were dependent on stress intensity, while beneficial effects on fruit taste (sugars and acids) and nutritional value were weak or even negative. Interestingly, high starch accumulation in fruit could be a potential asset to sustain fruit growth under WD. Considering a large range of plant and fruit traits, our observations clearly show that responses to drought are highly variable and that they strongly depend on genotypic effects and on the stage of development at the time WD is applied. On their whole, the present results demonstrate that drought could be exploited positively, and that repeated cycles of WD and recovery may be used to improve fruit taste and at the same time minimize fruit size reduction. A strategy for breeding would be to stack in one single genotype adaptive traits at the leaf and fruit levels. To this end, small-fruit genotypes, in particular LA1420 and Criollo, represent an interesting potential source of traits of interest, as far as acclimation is concerned. However, our capacity to take full advantage of drought events or controlled WD is clearly conditioned by a shift in our way of thinking. We need to explore the full variability of genotypic responses by taking into account a much broader range of crop performance criteria than the ones that are usually considered and by systematically including observations made at different stages of development. The complexity revealed by our observations clearly suggests that exploring the variability of genotypic responses represents a difficult task, but then it is our belief that this is how the issue of drought on crop performance should be addressed from now on, and that the reward will come up to the challenge.

AUTHOR CONTRIBUTIONS

This work is part of the Ph.D. thesis of JR, who significantly contributed to the experiment, the biochemical analyses, the statistical analyses, and the redaction of the article. Original idea of this project was developed by NB and LU, who contributed to the experimental protocol, the redaction of the article, and to the mentoring and training of JR

ACKNOWLEDGMENTS

The CTPS project TOMSEC and the ADAPTOM (ANR) project supported this work. J. Ripoll was supported by a Ph.D. fellowship of the *Federative Research Structure Tersys*. The authors thank the team of the UR1052 Genetics and Improvement of Fruit and Vegetables (INRA, Montfavet) for their strong implication in this study. The authors thank also the laboratory of biochemical analysis of the unit “Plantes et Systèmes de culture Horticoles” (INRA, Avignon) for their help in the analysis of all samples. We wish to thank Béatrice Brunel, Alain Goujon, and Jean-Claude l’Hôtel for technical assistance.

REFERENCES

- Albert, E., Gricourt, J., Bertin, N., Bonnefoi, J., Pateyron, S., Tamby, J. P., et al. (2015). Genotype by watering regime interactions in cultivated tomato: lessons from linkage mapping and gene expression. *Theor. Appl. Genet.* doi: 10.1007/s00122-015-2635-5 [Epub ahead of print].
- Al Gehani, I. (2005). *Effet des Stades D'Application et de L'Intensité de Stress Hydriques Répétés sur L'Etat Hydrique et la Croissance des Plantes et des Fruits de Tomate*. Ph.D. thèse, Aix-Marseille, Université d'Avignon et des pays du Vaucluse, Avignon.
- Atkinson, K. E. (2008). *An Introduction to Numerical Analysis*. New York, NY: John Wiley & Sons.
- Balibrea, M. E., Cuartero, J., Bolarin, M. C., and Perez-Alfocea, F. (2003). Sucrolytic activities during fruit development of *Lycopersicon* genotypes differing in tolerance to salinity. *Physiol. Plant.* 118, 38–46. doi: 10.1034/j.1399-3050.2003.00084.x
- Barba-Behrens, N., Carrasco-Fuentes, M. E., Castillo-Blum, S. E., Mendoza, J. L., Salazar, F., Tovar, A., et al. (1993). Coordination compounds quinic acid as decouplers on photosynthesis. *Biophys. Chem.* 47, 67–75. doi: 10.1016/0301-4622(93)80034-G
- Barry, C. S., and Giovannoni, J. J. (2007). Ethylene and fruit ripening. *J. Plant Growth Regul.* 26, 143–159. doi: 10.1007/s00344-007-9002-y
- Bertin, N., Guichard, S., Leonardi, C., Longuenesse, J. J., Langlois, D., and Navez, B. (2000). Seasonal evolution of the quality of fresh glasshouse tomatoes under Mediterranean conditions, as affected by air vapour pressure deficit and plant fruit load. *Ann. Bot. Lond.* 85, 741–750. doi: 10.1006/anbo.2000.1123
- Bruce, T. J. A., Matthes, M. C., Napier, J. A., and Pickett, J. A. (2007). Stressful “memories” of plants: evidence and possible mechanisms. *Plant Sci.* 173, 603–608. doi: 10.1016/j.plantsci.2007.09.002
- Causse, M., Desplat, N., Pascual, L., Le Paslier, M.-C., Sauvage, C., Bauchet, G., et al. (2013). Whole genome resequencing in tomato reveals variation associated with introgression and breeding events. *BMC Genomics* 14:791. doi: 10.1186/1471-2164-14-791
- Causse, M., Saliba-Colombani, V., Lesschaeve, I., and Buret, M. (2001). Genetic analysis of organoleptic quality in fresh market tomato. 2. Mapping QTLs for sensory attributes. *Theor. Appl. Genet.* 102, 273–283. doi: 10.1007/s001220051644
- Cavanagh, C., Morell, M., Mackay, I., Powell, W., Biotechnology, P., Leach, E. J., et al. (2008). From mutations to MAGIC: resources for gene discovery, validation and delivery in crop plants. *Curr. Opin. Plant Biol.* 11, 215–221. doi: 10.1016/j.pbi.2008.01.002
- Chaiß, J., Lecomte, L., Buret, M., and Causse, M. (2006). Stability over genetic backgrounds, generations and years of quantitative trait locus (QTLs) for organoleptic quality in tomato. *Theor. Appl. Genet.* 112, 934–944. doi: 10.1007/s00122-005-0197-7
- Chaves, M. M. (1991). Effects of water deficits on carbon assimilation. *J. Exp. Bot.* 42, 1–16. doi: 10.1093/jxb/42.1.1
- Chen, J., Kang, S., Du, T., Guo, P., Qiu, R., Chen, R., et al. (2014). Modeling relations of tomato yield and fruit quality with water deficit at different growth stages under greenhouse condition. *Agric. Water Manage.* 146, 131–148. doi: 10.1016/j.agwat.2014.07.026
- Csardi, G., and Nepusz, T. (2006). *The Igraph Software Package for Complex Network Research*. InterJournal Complex Systems 1695. Available at: <http://igraph.org>
- De Pascale, S., Martino, A., Raimondi, G., and Maggio, A. (2007). Comparative analysis of water and salt stress-induced modifications of quality parameters in cherry tomatoes. *J. Hortic. Sci. Biotechol.* 82, 283–289.
- Etienne, A., Genard, M., Lobit, P., Mbeguie-A-Mbeguie, D., and Bugaud, C. (2013). What controls fleshy fruit acidity? A review of malate and citrate accumulation in fruit cells. *J. Exp. Bot.* 64, 1451–1469.
- Fanciullino, A. L., Bidel, L. P. R., and Urban, L. (2014). Carotenoid responses to environmental stimuli: integrating redox and carbon controls into a fruit model. *Plant Cell Environ.* 37, 273–289. doi: 10.1111/pce.12153
- Favati, F., Lovelli, S., Galgano, F., Miccolis, V., Di Tommaso, T., and Candido, V. (2009). Processing tomato quality as affected by irrigation scheduling. *Sci. Hortic.* 122, 562–571. doi: 10.1016/j.scienta.2009.06.026
- Fox, J., and Weisberg, S. (2011). *An R Companion to Applied Regression*, 2nd Edn. Thousand Oaks CA: Sage.
- Fray, R. G., Wallace, A., Grierson, D., and Lycett, G. W. (1994). Nucleotide sequence and expression of a ripening and water stress-related cDNA from tomato with homology to the MIP class of membrane channel proteins. *Plant Mol. Biol.* 24, 539–543. doi: 10.1007/BF00024122
- Galmés, J., Conesa, M. A., Ochogavia, J. M., Perdomo, J. A., Francis, D. M., Ribas-Carbó, M., et al. (2011). Physiological and morphological adaptations in relation to water use efficiency in Mediterranean accessions of *Solanum lycopersicum*. *Plant Cell Environ.* 34, 245–260. doi: 10.1111/j.1365-3040.2010.02239.x
- Garchery, C., Gest, N., Do, P. T., Alhagdow, M., Baldet, P., Menard, G., et al. (2013). A diminution in ascorbate oxidase activity affects carbon allocation and improves yield in tomato under water deficit. *Plant Cell Environ.* 36, 159–175. doi: 10.1111/j.1365-3040.2012.02564.x
- García-Tejero, I., Romero-Vicente, R., Jimenez-Bocanegra, J. A., Martínez-García, G., Durán-Zuazo, V. H., and Muriel-Fernández, J. L. (2010). Response of citrus trees to deficit irrigation during different phenological periods in relation to yield, fruit quality, and water productivity. *Agric. Water Manage.* 97, 689–699. doi: 10.1016/j.agwat.2009.12.012
- Gautier, H., Massot, C., Stevens, R., Sérino, S., and Génard, M. (2009). Regulation of tomato fruit ascorbate content is more highly dependent on fruit irradiance than leaf irradiance. *Ann. Bot. Lond.* 103, 495–504. doi: 10.1093/aob/mcn233
- Giraud, C., Huett, S., and Verzelem, N. (2009). *Graph Selection with GGMselect*. Available at: <http://fr.arxiv.org/abs/0907.0619>
- Giroudoux, P. (2014). *Pgirmess: Data Analysis in Ecology*. R Package Version 1.5.9. Available at: Available at <http://CRAN.R-project.org/package=pgirmess>
- Girona, J., Marsal, J., Mata, M., Arbones, A., and DeJong, T. M. (2004). A comparison of the combined effect of water stress and crop load on fruit growth during different phenological stages in young peach trees. *J. Hortic. Sci. Biotechol.* 79, 308–315.
- Goltsev, V., Zaharieva, I., Chernev, P., Kouzmanova, M., Kalaji, H. M., Yordanov, I., et al. (2012). Drought-induced modifications of photosynthetic electron transport in intact leaves: analysis and use of neural networks as a tool for a rapid non-invasive estimation. *Biochim. Biophys. Acta* 1817, 1490–1498. doi: 10.1016/j.bbabi.2012.04.018
- Gomez, L., Bancil, D., Rubio, E., and Vercambre, G. (2007). The microplate reader: an efficient tool for the separate enzymatic analysis of sugars in plant tissues – validation of a micro-method. *J. Sci. Food Agric.* 87, 1893–1905. doi: 10.1002/jsfa.2924
- Gomez, L., Rubio, E., and Auge, M. (2002). A new procedure for extraction and measurement of soluble sugars in ligneous plants. *J. Sci. Food Agric.* 82, 360–369. doi: 10.1002/jsfa.1046
- Graves, S., Piepho, H.-P., Selzer, L., and Dorai-Raj, S. (2012). *mulcompView: Visualizations of Paired Comparisons*. R Package Version 0.1–5. Available at: <http://CRAN.R-project.org/package=multcompView>
- Guichard, S., Bertin, N., Leonardi, C., and Gary, C. (2001). Tomato fruit quality in relation to water and carbon fluxes. *Agronomie* 21, 385–392. doi: 10.1051/agro:2001131
- Hnilickova, H., and Duffek, J. (2004). The effect of water deficit and subsequent regeneration on selected physiological characteristics in tomatoes (*Lycopersicum esculentum* Mill.). *Sci. Agric. Bohem.* 35, 26–31.
- Hnilickova, H., Duffek, J., and Hnilicka, F. (2002). Effects of low temperatures on photosynthesis and growth in selected tomato varieties (*Lycopersicon esculentum* Mill.). *Sci. Agric. Bohemica* 33, 101–105.
- Hsiao, T. C., Acevedo, E., Fereres, E., and Henderson, D. W. (1976). Water stress growth, and osmotic adjustment. *Philos. Trans. R. Soc. Lond. B Biol. Sci.* 273, 479–500. doi: 10.1098/rstb.1976.0026
- Hummel, I., Pantin, F., Sulpice, R., Piñol, M., Rolland, G., Dauzat, M., et al. (2010). *Arabidopsis* plants acclimate to water deficit at low cost through changes of carbon usage: an integrated perspective using growth, metabolite, enzyme, and gene expression analysis. *Plant Physiol.* 154, 357–372. doi: 10.1104/pp.110.157008
- Husson, F., Josse, J., Le, S., and Mazet, J. (2014). *FactoMineR : Multivariate Exploratory Data Analysis and Data Mining with R*. R Package Version 1.26. Available at: <http://CRAN.R-project.org/package=FactoMineR>
- Johnson, G. N. (2011). Physiology of PSI cyclic electron transport in higher plants. *Biochim. Biophys. Acta* 1807, 384–389. doi: 10.1016/j.bbabi.2010.11.009
- Lenth, R. V. (2014). *Lsmeans: Least-Squares Means*. R Package Version 2.0.5.

- Li, S. H., Huguet, J. G., Schoch, P. G., and Orlando, P. (1989). Response of peach tree growth and cropping to soil water deficit at various phenological stages of fruit development. *J. Hortic. Sci.* 64, 541–552.
- Li, X., and Zhang, L. (2012). “SA and PEG-induced priming for water stress tolerance in rice seedling,” in *Information Technology and Agricultural Engineering*, Vol. 134, eds E. Zhu and S. Sambath (Heidelberg: Springer Berlin), 881–887.
- Livingston, A. K., Cruz, J. A., Kohzuma, K., Dhingra, A., and Kramer, D. M. (2010). An *Arabidopsis* mutant with high cyclic electron flow around photosystem I (hcef) involving the NADPH dehydrogenase complex. *Plant Cell* 22, 221–233. doi: 10.1105/tpc.109.071084
- Lo Bianco, R., Rieger, M., and Sung, S.-J. S. (2000). Effect of drought on sorbitol and sucrose metabolism in sinks and sources of peach. *Physiol. Plant.* 108, 71–78. doi: 10.1034/j.1399-3054.2000.108001071.x
- Mahdid, M., Kameli, A., Ehler, C., and Simonneau, T. (2011). Rapid changes in leaf elongation, ABA and water status during the recovery phase following application of water stress in two durum wheat varieties differing in drought tolerance. *Plant Physiol. Biochem.* 49, 1077–1083. doi: 10.1016/j.plaphy.2011.08.002
- Manaa, A., Ahmed, H. B., Valot, B., Bouchet, J. P., Aschi-Smiti, S., Causse, M., et al. (2011). Salt and genotype impact on plant physiology and root proteome variations in tomato. *J. Exp. Bot.* 62, 2797–2813. doi: 10.1093/jxb/erq460
- Maxwell, K., and Johnson, G. N. (2000). Chlorophyll fluorescence – a practical guide. *J. Exp. Bot.* 51, 659–668. doi: 10.1093/jexbot/51.345.659
- Mitchell, J. P., Shennan, C., Grattan, S. R., and May, D. M. (1991). Tomato fruit yields and quality under water deficit and salinity. *J. Am. Soc. Hortic. Sci.* 116, 215–221.
- Muller, B., Pantin, F., Génard, M., Turc, O., Freixes, S., Piques, M., et al. (2011). Water deficits uncouple growth from photosynthesis, increase C content, and modify the relationships between C and growth in sink organs. *J. Exp. Bot.* 62, 1715–1729. doi: 10.1093/jxb/erq438
- Münch, E. (1930). *Die Stoffbewegungen in der Pflanze*. Jena: Verlag von Gustav Fischer, 234.
- Munns, R. (2002). Comparative physiology of salt and water stress. *Plant Cell Environ.* 25, 239–250. doi: 10.1046/j.0016-8025.2001.00808.x
- Murshed, R., Lopez-Lauri, F., and Sallanon, H. (2013). Effect of water stress on antioxidant systems and oxidative parameters in fruits of tomato (*Solanum lycopersicum* L. cv. Micro-tom). *Physiol. Mol. Biol. Plants* 19, 363–378. doi: 10.1007/s12298-013-0173-7
- Nora, L., Dalmazo, G. O., Nora, F. R., and Rombaldi, C. V. (2012). “Controlled water stress to improve fruit and vegetable postharvest quality,” in *Water Stress*, eds Ismail Md. R. Mofizur and H. Hiroshi (Rijeka: InTech Open Science: Agricultural and Biological Sciences).
- Osorio, S., Scossa, F., and Fernie, A. R. (2013). Molecular regulation of fruit ripening. *Front. Plant Sci.* 4:198. doi: 10.3389/fpls.2013.00198
- Pascual, L., Desplat, N., Huang, B. E., Desgroux, A., Bruguier, L., Bouchet, J.-P., et al. (2015). Potential of a tomato MAGIC population to decipher the genetic control of quantitative traits and detect causal variants in the resequencing era. *Plant Biotechnol. J.* 13, 565–577. doi: 10.1111/pbi.12282
- Penman, H. L. (1948). Natural evaporation from open water, bare soil and grass. *Proc. R. Soc. Lond. A* 194, 120–145. doi: 10.1098/rspa.1948.0037
- Petrikova, K., Burg, P., and Pokluda, R. (2003). Evaluation of selected tomato varieties for the resistance against *Phytophthora infestans* (Mont.) de Bary and comparison of their earliness and yield. *Acta Hortic. Regiotecturae* 6, 40–43.
- Poiroux-Gonord, F., Fanciullino, A. L., Poggi, I., and Urban, L. (2013). Carbohydrate control over carotenoid build-up is conditional on fruit ontogeny in clementine fruits. *Physiol. Plant.* 147, 417–431. doi: 10.1111/j.1399-3054.2012.01672.x
- Rahman, S. M. L., Nawata, E., and Sakuratani, T. (1999). Effect of water stress on growth, yield and eco-physiological responses of four tomato (*Lycopersicon esculentum* Mill.) cultivars. *J. Jpn. Soc. Hortic. Sci.* 68, 499–504. doi: 10.2503/jjshs.68.499
- Ranc, N. (2010). *Analyse du Polymorphisme Moléculaire de Gènes de Composantes de la Qualité des Fruits dans les Ressources Génétiques Sauvages et Cultivées de Tomate; Recherche D'Associations Gènes/QTL*. Ph.D. thesis, Académie de Montpellier, Ecole Nationale Supérieure Agronomique de Montpellier, Montpellier.
- R Core Team (2014). *R: A Language and Environment for Statistical Computing*. Vienna: R foundation for Statistical Computing.
- Ripoll, J., Urban, L., Brunel, B., and Bertin, N. (2015). Water deficit effects on tomato quality depend on fruit developmental stage and genotype. *J. Plant Physiol.* 190, 26–35. doi: 10.1016/j.jplph.2015.10.006
- Ripoll, J., Urban, L., Staudt, M., Lopez-Lauri, F., Bidel, L. P. R., and Bertin, N. (2014). Water shortage and quality of fleshy fruits—making the most of the unavoidable. *J. Exp. Bot.* 65, 4097–4117. doi: 10.1093/jxb/eru197
- Royston, P. (1995). Remark as R94: a remark on algorithm AS 181: the W-test for normality. *Appl. Stat.* 44, 547–551.
- Saliba-Colombani, V., Causse, M., Langlois, D., Philouze, J., and Buret, M. (2001). Genetic analysis of organoleptic quality in fresh market tomato. 1. Mapping QTLs for physical and chemical traits. *Theor. Appl. Genet.* 102, 259–272. doi: 10.1007/s001220051643
- Schaefer, J., Opgen-Rhein, R., and Strimmer, K. (2014). *GeneNet: Modeling and Inferring Gene Networks*. R Package Version 1.2.11. Available at: <http://CRAN.R-project.org/package=GeneNet>
- Serino, S., Gomez, L., Costagliola, G., and Gautier, H. (2009). HPLC assay of tomato carotenoids: validation of a rapid microextraction technique. *J. Agric. Food Chem.* 57, 8753–8760. doi: 10.1021/jf902113n
- Shock, C. C. B., Michael, J., and Seddigh, M. (1998). “Calibration of watermark soil moisture sensors for irrigation management,” in *Proceedings of the International Irrigation Show*, (San Diego, CA: Irrigation Association), 139–146.
- Stevens, R., Buret, M., Garchery, C., Carretero, Y., and Causse, M. (2006). Technique for rapid, small-scale analysis of vitamin C levels in fruit and application to a tomato mutant collection. *J. Agric. Food Chem.* 54, 6159–6165. doi: 10.1021/jf061241e
- Stirbet, A., and Govindjee. (2011). On the relation between the Kautsky effect (chlorophyll a fluorescence induction) and Photosystem II: basics and applications of the OJIP fluorescence transient. *J. Photochem. Photobiol. B* 104, 236–257. doi: 10.1016/j.jphotobiol.2010.12.010
- Stoeva, N., Berova, M., Vassilev, A., Zlatev, Z., Kaymakanova, M., Ganeva, D., et al. (2012). Study on some enzyme activity in tomato plants during drought and recovery periods. *Agrarni Nauki* 4, 61–64.
- Stoeva, N., Berova, M., Zlatev, Z., Kaymakanova, M., Koleva, L., and Ganeva, D. (2010). Physiological test for evaluation of genotypes tolerance of tomato (*Solanum lycopersicum*) to water stress. *Agrarni Nauki* 2, 81–84.
- Strasser, R., Tsimali-Michael, M., and Srivastava, A. (2004). “Analysis of the chlorophyll a fluorescence transient,” in *Chlorophyll a Fluorescence*, Vol. 19, eds G. Papageorgiou and Govindjee (Dordrecht: Springer Netherlands), 321–362.
- Subrtova, D., Hubacek, J., Jankovsky, M., and Fialova, D. (1985). Volatile substances of tomatoes (*Lycopersicon esculentum*). *Rostlinna Vyroba* 31, 871–880.
- Tardieu, F., Cruziat, P., Durand, J.-L., Triboi, E., and Zivy, M. (2006). 1.1.2. Perception de la sécheresse par la plante. Conséquences sur la productivité et sur la qualité des produits récoltés. *ESCo Sécheresse Agric.* Chap. 1-1, 49–67.
- Vallverdu, X., Girona, J., Echeverria, G., Marsal, J., Behboudian, M. H., and Lopez, G. (2012). Sensory quality and consumer acceptance of ‘Tardibelle’ peach are improved by deficit irrigation applied during stage II of fruit development. *HortScience* 47, 656–659.
- Veit-Köhler, U., Krumbain, A., and Kosegarten, H. (1999). Effect of different water supply on plant growth and fruit quality of *Lycopersicon esculentum*. *J. Plant Nutr. Soil Sci.* 162, 583–588. doi: 10.1002/(SICI)1522-2624(199912)162:6<583::AID-JPLN583>3.0.CO;2-P
- Walker, B. J., Strand, D. D., Kramer, D. M., and Cousins, A. B. (2014). The response of cyclic electron flow around photosystem i to changes in photorespiration and nitrate assimilation. *Plant Physiol.* 165, 453–462. doi: 10.1104/pp.114.238238
- Wang, D., and Gartung, J. (2010). Infrared canopy temperature of early-ripening peach trees under postharvest deficit irrigation. *Agric. Water Manage.* 97, 1787–1794. doi: 10.1016/j.agwat.2010.06.014
- Warnes, G. R., Bolker, B., Bonebakker, L., Gentleman, R., Liaw, W. H. A., Lumley, T., et al. (2014). *gplots: Various R Programming Tools for Plotting Data*. R Package Version 2.14.2. Available at: <http://CRAN.R-project.org/package=gplots>
- Xu, Z., Zhou, G., and Shimizu, H. (2010). Plant responses to drought and rewetting. *Plant Signal. Behav.* 5, 649–654. doi: 10.4161/psb.5.6.11398

- Zgallaï, H., Steppe, K., and Lemeur, R. (2005). Photosynthetic, physiological and biochemical responses of tomato plants to polyethylene glycol-induced water deficit. *J. Int. Plant Biol.* 47, 1470–1478. doi: 10.1111/j.1744-7909.2005.00193.x
- Zhang, Y., Li, H., Shu, W., Zhang, C., Zhang, W., and Ye, Z. (2011). Suppressed expression of ascorbate oxidase gene promotes ascorbic acid accumulation in tomato fruit. *Plant Mol. Biol. Rep.* 29, 638–645. doi: 10.1007/s11105-010-0271-4
- Zimmermann, U. (1978). Physics of turgor- and osmoregulation. *Annu. Rev. Plant Physiol.* 29, 121–148. doi: 10.1146/annurev.pp.29.060178.001005
- Živčák, M., Brešić, M., Olšovská, K., and Slamka, P. (2008). Performance index as a sensitive indicator of water stress in *Triticum aestivum* L. *Plant Soil Environ.* 54, 133–139.
- Zushi, K., and Matsuzoe, N. (1998). Effect of soil water deficit on vitamin C, sugar, organic acid, amino acid and carotene contents of large-fruited tomatoes [*Lycopersicon esculentum*]. *J. Jpn. Soc. Hortic. Sci.* 67, 927–933. doi: 10.2503/jjshs.67.927

Conflict of Interest Statement: The authors declare that the research was conducted in the absence of any commercial or financial relationships that could be construed as a potential conflict of interest.

Copyright © 2016 Ripoll, Urban and Bertin. This is an open-access article distributed under the terms of the Creative Commons Attribution License (CC BY). The use, distribution or reproduction in other forums is permitted, provided the original author(s) or licensor are credited and that the original publication in this journal is cited, in accordance with accepted academic practice. No use, distribution or reproduction is permitted which does not comply with these terms.



Identification, Expression and IAA-Amide Synthetase Activity Analysis of Gretchen Hagen 3 in Papaya Fruit (*Carica papaya L.*) during Postharvest Process

Kaidong Liu^{1*}, Jinxiang Wang^{2,3}, Haili Li¹, Jundi Zhong¹, Shaoxian Feng¹, Yaoliang Pan¹ and Changchun Yuan^{1*}

¹ Life Science and Technology School, Lingnan Normal University, Zhanjiang, China, ² The State Key Laboratory for Conservation and Utilization of Subtropical Agro-Bioresources, South China Agriculture University, Guangzhou, China,

³ College of Agriculture and Root Biology Center, South China Agricultural University, Guangzhou, China

OPEN ACCESS

Edited by:

Antonio Granell,
CSIC, Spain

Reviewed by:

Alberto A. Iglesias,
National University of the Littoral,
Argentina
Clay Carter,
University of Minnesota, USA

*Correspondence:

Kaidong Liu
liukaidong2001@126.com
Changchun Yuan
yuanchangchun@163.com

Specialty section:

This article was submitted to
Plant Physiology,
a section of the journal
Frontiers in Plant Science

Received: 21 July 2016

Accepted: 03 October 2016

Published: 20 October 2016

Citation:

Liu K, Wang J, Li H, Zhong J, Feng S, Pan Y and Yuan C (2016)
*Identification, Expression and IAA-Amide Synthetase Activity Analysis of Gretchen Hagen 3 in Papaya Fruit (*Carica papaya L.*) during Postharvest Process.*
Front. Plant Sci. 7:1555.
doi: 10.3389/fpls.2016.01555

Auxin plays essential roles in plant development. Gretchen Hagen 3 (GH3) genes belong to a major auxin response gene family and GH3 proteins conjugate a range of acylsubstrates to alter the levels of hormones. Currently, the role of GH3 genes in postharvest physiological regulation of ripening and softening processes in papaya fruit is unclear. In this study, we identified seven CpGH3 genes in a papaya genome database. The CpGH3.1a, CpGH3.1b, CpGH3.5, CpGH3.6, and CpGH3.9 proteins were identified as indole-3-acetic acid (IAA)-specific amido synthetases. We analyzed the changes in IAA-amido synthetase activity using aspartate as a substrate for conjugation and found a large increase (over 5-fold) during the postharvest stages. Ascorbic acid (AsA) application can extend the shelf life of papaya fruit. Our data showed that AsA treatment regulates postharvest fruit maturation processes by promoting endogenous IAA levels. Our findings demonstrate the important role of GH3 genes in the regulation of auxin-associated postharvest physiology in papaya.

Keywords: auxin, GH3 gene family, papaya, postharvest, ripening, softening

INTRODUCTION

The ripening of fruit is a genetically controlled process that involves complex multi-hormonal crosstalk. Auxin (indole-3-acetic acid, IAA) is a ubiquitous signaling molecule that has a vital role in plant development and growth including cell elongation and division, organ differentiation, embryogenesis, lateral root elongation, shoot architecture, and fruit development (Quint and Gray, 2006; Teale et al., 2008). Along with the hormone ethylene, auxin plays vital roles in many aspects of fleshy fruit development including fruit set and fruit ripening (Jones et al., 2002; Ruan et al., 2012). In tomato, auxin functions to retard fruit ripening through interactions with other hormones, such as ethylene, abscisic acid (ABA), and jasmonic acid (JA) (Su et al., 2015). High concentrations of IAA are required for the biosynthesis of ethylene, which plays a significant role in fruit softening in “melting flesh” peaches at the late ripening stage (Pan et al., 2015).

Auxin coordinates plant development by regulating the expression of auxin response gene families such as *Aux/IAA* (auxin/indole acetic acid), *GH3* (Gretchen Hagen 3), *SAUR* (small auxin

up RNA), and *ARF* (auxin response factor) (Abel and Theologis, 1996). A recent transcriptome survey of strawberry fruit revealed dynamic changes in expression of auxin early response gene families during postharvest ripening (Chen et al., 2016). Such studies on the biological functions of auxin response genes help to elucidate the mechanisms underlying the regulation of auxin-mediated fruit ripening.

The protein structures and biological functions of *GH3* family members in model plant species have been studied in detail. The *GH3* family genes encode IAA-amido synthetases that are involved in endogenous auxin homeostasis through catalysis of auxin conjugation and by binding free IAA to amino acids (Staswick et al., 2005; Feng et al., 2015). The first *GH3* family member was isolated from soybean (*Glycine max*) and subsequently fully identified in the model plant *Arabidopsis thaliana* (Hagen et al., 1984; Takase et al., 2003, 2004). In plants, amino acid conjugation of diverse hormones, including JA, IAA, and salicylic acid (SA), control the concentrations of their bioactive forms to regulate developmental processes (Westfall et al., 2010, 2012). Recently, the crystal structures of the *GH3* family members benzoate-specific At $GH3.12/PBS3$ and JA-specific At $GH3.11/JAR1$ were reported. This analysis found a highly adaptable three-dimensional scaffold for the conjugation of amino acids to diverse acyl acid substrates; it also identified residues forming acyl acid binding sites in the *GH3* proteins and residues critical for amino acid recognition (Westfall et al., 2012). The auxin-conjugating enzyme *GH3.1* from grapevine (*V. vinifera*) has a similar structure to the *GH3* enzymes from *A. thaliana* (Peat et al., 2012). Based on structural details and acyl acid site comparisons, *GH3* proteins from different species can be assigned to eight subfamilies. *GH3* proteins belonging to subfamilies 1, 2, and 4 show a preference for JA, IAA, and benzoate substrates, respectively. *GH3* proteins belonging to subfamilies 3 and 5-8 have no well-defined substrates (Westfall et al., 2010, 2012).

In *A. thaliana*, the gene *WES1* encodes an auxin-conjugating enzyme that plays a role in hypocotyl growth by mediating phytochrome B-perceived light signals (Park et al., 2007). The mutant *ydk1-D*, a T-DNA insertion proximal to *AtGH3.2*, is dominant and displays a dwarf hypocotyl under both light and dark conditions (Takase et al., 2004). Two *GH3* gene homologs in *A. thaliana*, *DFL1*, and *DFL2*, regulate hypocotyl length and lateral root formation in response to light stimulation (Nakazawa et al., 2001; Takase et al., 2003). Several years ago, homeostasis of miR160 was reported to be involved in the regulation of adventitious root initiation in *A. thaliana* through targeting *AtARF17*, which encodes a negative regulator of *AtGH3.3*, *AtGH3.5*, and *AtGH3.6* expression (Sorin et al., 2005, 2006; Gutierrez et al., 2009). These results suggest that the *GH3* gene family is involved in adventitious root initiation (Gutierrez et al., 2012). In rice, some *GH3* genes were found to be related to stress responses and developmental regulation. Over-expression of *OsGH3.1* enhances resistance to fungal pathogens by inhibiting cell wall loosening and reducing auxin content (Domingo et al., 2009). In a similar manner to *OsGH3.1*, activation of *OsGH3.13* decreases endogenous auxin content and enhances rice drought tolerance (Zhang et al., 2009). *OsGH3.2* influences drought and

freezing tolerance through modulating ABA levels (Du et al., 2012). *OsGH3.5*, a downstream target gene of *OsARF19*, controls rice leaf angles by interacting with the brassinosteroid signaling pathway (Zhang et al., 2015).

In addition to model plant species, the *GH3* gene family has also been identified in fruit plants, including 11 members in citrus (*Citrus sinensis* L.), 15 in apple (*Malus × domestica*), 9 in grapevine (*Vitis vinifera* L.), and 2 in longan (*Dimocarpus longan* L.) (Böttcher et al., 2011; Kuang et al., 2011; Yuan et al., 2013; Xie et al., 2015). There is evidence that these *GH3* genes have a role in fruit setting, growth, and ripening (de Jong et al., 2009). In grape, expression of *VvGH3.1* increases at the onset of ripening. Activated IAA-amido synthetase conjugates IAA to amino acids and contributes to the establishment and maintenance of a low IAA concentration, which may accelerate the initiation of ripening (Böttcher et al., 2010). Expression of another grapevine *GH3* gene, *VvGH3.2*, can be induced by treatment with an auxinic compound in pre-ripening berries; this treatment increases the concentration of IAA-Asp and decreases the concentration of free IAA (Böttcher et al., 2011). These results indicate that *GH3* proteins have various roles in controlling fruit ripening in both auxin-dependent and JA-dependent manners.

As a climacteric fruit, papaya exhibits rapid softening and has a short-term shelf life, which significantly limits its market value (Jain et al., 2011). The elucidation of how endogenous hormones function in postharvest decay under different conditions is therefore of importance not only to plant biologists but also to agronomists (Gomez-Lobato et al., 2012; Chen et al., 2016). However, little is known of the roles of endogenous auxin in the postharvest maturation of papaya fruit. Our study provides comprehensive information on *GH3* gene expression patterns in different tissues and on the enzyme activities of IAA-amido synthetases under different postharvest conditions. These data will be important to the development of new postharvest strategies for papaya.

MATERIALS AND METHODS

Plant Materials and Treatments

We used the *Carica papaya* cultivar "Sunrise" in this study. Two-years-old trees planted in a 3 m × 3 m arrangement were provided with standard drip irrigation and fertilizer applications. The experimental field at Lingnan Normal University field experimental station in Zhanjiang City (Guangdong Province, China) has a tropical climate and experiences oceanic monsoons; it has an average daily temperature of 22.8°C, with a minimum of 15.7°C and a maximum of 28.8°C. The total yearly rainfall ranges between 1100 and 1800 mm. Five tissue samples were used for tissue-specific expression pattern analysis. In detail, the shoot, leaf, root samples were selected from 1-year-old papaya trees. The fruit samples were harvested from fruits at the color break stage (5% ≤ peel color ≤ 15% yellow) of 2-years-old trees. The flower samples were selected from mature flower with opened petals of 2-years-old trees. The selected were washed with deionized water, and then dipped in 75% (w/w) alcohol for 45 s to eliminate potential microbes.

Measurement of Fruit Firmness, Weight Loss, Total Soluble Solids, and Titratable Acidity

A hand-held fruit firmness tester (GY-J, Top Instrument Co, Ltd, Zhejiang, China) with an 8-mm probe attached to a digital force gauge was used to determine papaya firmness. The mean of five independent measurements was calculated for each papaya fruit and expressed in Newtons (N). Weight loss was estimated by measuring the weight of the whole papaya fruit from the beginning to the end of different storage periods. Weight loss was expressed as the percentage of initial weight. Fruits were packed in commercial boxes and stored at $20 \pm 1^\circ\text{C}$ and 85–90% relative humidity. The time points after harvest of 0, 5, 10, 15, 20, and 25 days were defined as postharvest stages 1–6, respectively.

Fruit pulp (5.0 g) from three replicates of five independent fruit for each treatment was prepared using a mortar and pestle in 50.0 mL distilled water. The homogenate was centrifuged at $15,000 \times g$ for 20 min at 4°C , and then the supernatant was used to measure total soluble solid content (%) with a hand-held refractometer (J1-3A, Guangdong Scientific Instruments, Guangzhou, China).

Respiration Rate Determination and Pericarp Color Characteristics Assay

The respiration rate was determined by conducting an infrared analysis. Five replicate groups of three papaya fruits from each treatment were weighed, and then sealed in a 2.4-L container at 25°C . An infrared gas analyzer (Li-6262 CO₂/H₂O analyzer, LI-COR, America) was used to monitor CO₂ concentration in the container. A colorimeter (Minolta, model CR-400, Tokyo, Japan) was used to determine the color characteristics of the papaya pericarp. Three independent points in the equatorial region of the papaya fruit skin were chosen to determine color characteristics. The method for assessing color characteristics has been described previously (Liu et al., 2014).

Identification of GH3 Genes in *Carica papaya*

A. thaliana GH3 protein sequences were used in a BLAST search of the *C. papaya* in Phytozome 10.1 database (<http://phytozome.jgi.doe.gov>). The sequences of the AtGH3 proteins are shown in Table S1. The maximum *e*-value acceptable in the BLAST search for identifying GH3 members was “ 10^{-3} .” The Hidden Markov Model (HMM) profiles of the GH3 gene family (Pfam: 03321, GH3 auxin-responsive promoter) were used to identify the candidate sequences (<http://pfam.xfam.org/>). All the obtained sequences were sorted as unique sequences for a further protein domain search using InterProScan Sequence Search (<http://www.ebi.ac.uk/Tools/pfa/iprscan/>). Motifs characteristic of CpGH3 proteins were investigated by Multiple Expectation Maximization for Motif Elicitation (MEME 4.10.2) web server (<http://meme.nbcr.net/meme/cgi-bin/meme.cgi>).

Phylogenetic Tree Construction and Intron-Exon Structure Analysis

ClustalW (<http://www.ebi.ac.uk/Tools/msa/clustalw2/>) was used to perform multiple sequence alignments on the identified CpGH3 protein sequences with the default parameters. Subsequently, GeneDoc (<http://www.ncbi.nlm.nih.gov/gfx/genedoc/>) was used to visualize the alignments. A phylogenetic tree was built using the MEGA5.1 software (<http://www.megasoftware.net/mega5/mega.html>) by neighbor-joining method for 19 *A. thaliana* and seven *C. papaya* GH3 protein sequences. Bootstrap values were calculated from 1000 iterations. Exon-intron organization of *CpGH3* genes were determined by comparing the coding sequences with their corresponding genomic sequences downloaded from the database Phytozome 10.1.

Cis-Element Analysis

The 1500-bp promoter regions of *CpGH3* genes were obtained and downloaded from Phytozome 10.1. An auxin response element (AuxRE: TGTCTC), an ABA responsive element (ABRE: YACGTGK), a SA responsive element (SARE: TGACG), a JA responsive element (JERE: AGACCGCC), and an ethylene responsive element (GCC: AGCCGCC) were used to scan the promoter regions of the *CpGH3*s. The results were confirmed using PLACE software (<http://www.dna.affrc.go.jp/PLACE/>).

RNA Isolation and Quantitative RT-PCR

Total RNAs from roots, shoots, leaves, flowers, and fruits from the different treatment groups were isolated with a plant RNeasy Mini kit (Qiagen, Hilden, Germany) according to the manufacturer's instructions. Genomic DNA contamination was removed using DNase I (TaKaRa, Dalian, China). The *CpActin* gene (evm.model.supercontig_18.238) was used as an internal standard to calculate relative fold differences based on comparative cycle threshold ($2^{-\Delta\Delta Ct}$) values. The qRT-PCR was performed as described previously (Yang et al., 2015). The primer sequences for the qRT-PCR were designed using Primer Premier 5 software and are listed in Table S2. The limit of detection and the amplification efficiency of the qRT-PCR was performed using 10-fold serial dilution of cDNA isolated from one sample (leaves), which was used to create the standard curve. The slopes and correlation coefficients of the standard curves were used to calculate the PCR efficiency primer pairs. In our experiment, the value of PCR efficiency (E) for each primer pair was calculated by formula: $E = \text{POWER}(10, 1/\text{slope}) - 1$. The value of PCR efficiency for each primer pair was between 0.9 and 1.1. The standard curves for absolute quantification RT-PCR of CpGH3 genes were showed in Figure S1. The fruits used in tissue-specific expression experiment are right before harvest, 150 days post-fertilization. To avoid the effects of environmental stress, the fruit samples were collected from a large number of independent papaya trees that were distributed throughout the test field. Five fruits from these samples were randomly assigned to each group for the qRT-PCR test.

Tissue Homogenization and Enzyme Activity Assay

One gram of pericarp and sarcocarp was excised from each papaya fruit and homogenized in 1 mL extraction buffer (50 mM Tris-HCl buffer containing 2 mM EDTA, protease inhibitor, and 5 mM 2-mercaptoethanol, pH 7.6) using a mortar and pestle. The homogenate was centrifuged at 12,000 × g for 30 min, and the supernatant was used for the enzyme activity assay. The assay was performed following the procedure described by Ostrowski and Jakubowska (2013). Briefly, enzyme activity was determined in a total volume of 15 μL buffer containing 50 mM Tris-HCl, pH 8.6, 2 mM IAA, 50 mCi mmol⁻¹, 10 mM aspartic acid, 5 mM ATP, 5 mM MGCl₂, and 2 mM DTT. Then, 6 μL of the supernatant fluid was used to start the reaction.

Protein Purification and Enzyme Assay

The coding regions of *CpGH3.1a*, *CpGH3.1b*, *CpGH3.5*, *CpGH3.6*, and *CpGH3.9* were amplified by PCR from a papaya cDNA template using gene-specific primers with additional restriction sites. The primer sequences are listed in Table S4. These PCR products were cloned into restriction sites of a pET-21(a)-His vector to generate GH3-His fusion protein. These five construct were expressed in *Escherichia coli* (DH5α) according to the manufacturer's protocol (Takara, Dalian, China). The expressed fusion proteins were purified with His GraviTrap columns (GE Healthcare, Little Chalfont, UK) and the protein concentration of each sample was determined using a Protein Quantification Kit-Rapid (SIGMA-ALDRICH, Shanghai, China). The assays about enzyme activity with IAA substrates were performed according to Ostrowski's description (Ostrowski and Jakubowska, 2013).

AsA Application, IAA Content and Ethylene Production Rate Measurements

For AsA application, fruits were randomly distributed two groups. One group was assigned to water (control treatment) and 250 mM AsA for 10 min. After treatment, the fruit were air-dried, packed into polyethylene bags (0.03 mm), and maintained at room temperature with 75% relative humidity. Three replicates were performed for each treatment.

For IAA content measurement, fruit samples were collected and washed three times in ddH₂O, and then blotted dry with a paper towel. A sample (50 mg) was obtained from each fruit. For IAA content measurement, 500 pg of ¹³C₆-IAA was added to each sample as an internal standard. ProElu C18 (<http://www.dikma.com.cn>) was used to purify the samples. Five independent biological replicates of each sample were used in our experiment, and IAA contents were determined using a FOCUS GC-DSQII (Thermo Fisher Scientific Inc., Austin, TX, USA). The experiment of IAA measurement was performed according to Liu's protocol (Liu et al., 2012).

For ethylene production measurement, two fruits in each of three replicates were placed in a 1000 mL flask for 1 h. Then, 1 mL space samples were collected and ethylene concentrations measured by flame ionization gas chromatography using a SP

6800 gas chromatograph fitted with a GDX-502 column held at 90°C.

Statistical Analysis

Differences between different groups of samples were calculated with Student's *t*-test at a significance level of 0.05 in software Excel. All the expression analysis was performed for five biological repeats and the values shown in figures represent the average values of five repeats, and the data are expressed as the mean and standard deviation (mean ± SD).

RESULTS

Identification and Phylogenetic Analysis of the GH3 Gene Family in *C. papaya*

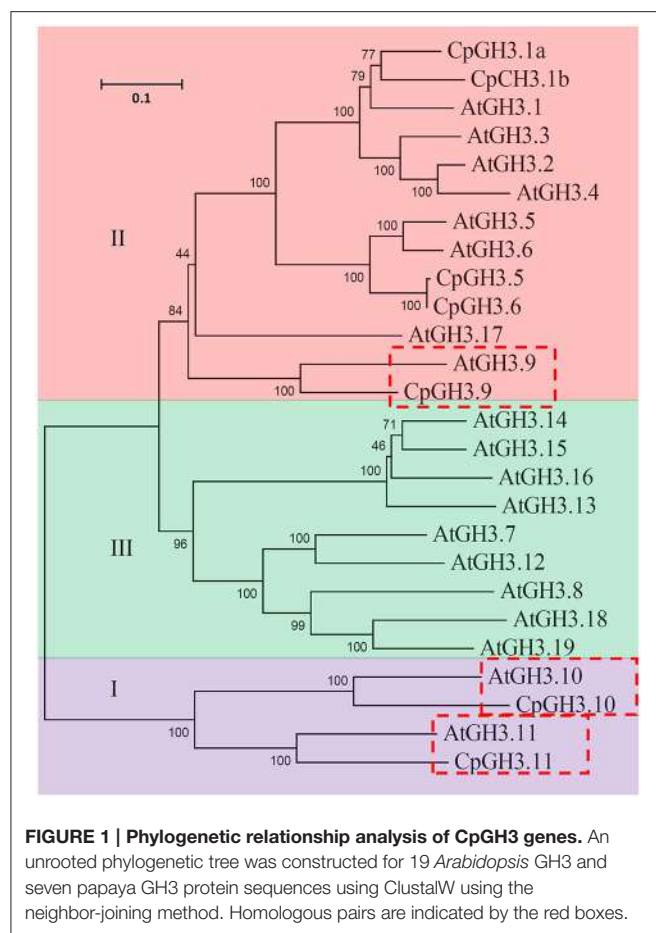
Seven GH3 genes were identified in *C. papaya*; these genes were all named according to the phylogenetic relationship between *C. papaya* and the model plant *A. thaliana*. The information on the *CpGH3* genes, including gene names, IDs, intron numbers, ORF lengths, and deduced polypeptide parameters, is summarized in Table S3. The sizes of the deduced *CpGH3* proteins varied from 421 amino acids (*CpGH3.9*) to 607 amino acids (*CpGH3.1a* and *CpGH3.1b*), molecular masses varied from 47.62 to 68.69 kDa, and predicted isoelectric points varied from 5.61 (*CpGH3.1b*) to 6.86 (*CpGH3.5*).

To investigate the relationship of the GH3 genes of *C. papaya* and *A. thaliana*, a phylogenetic tree was constructed for 19 *AtGH3* genes and the seven *CpGH3* genes. The results indicated that the GH3 gene family could be grouped into three major subfamilies, I, II, and III. Seven *CpGH3* genes were grouped into subfamilies I and III; no *CpGH3* gene belonged to subfamily III. Based on the phylogenetic relationship, three homologous pairs with high bootstrap values (>99) were identified between *CpGH3* and *AtGH3* families: *AtGH3.9/CpGH3.9*, *AtGH3.10/CpGH3.10*, and *AtGH3.11/CpGH3.11* (Figure 1). The exon-intron structures in the *CpGH3* gene family varied with one to three introns (Figure S2).

Multiple Sequence Alignments and Acyl Acid Substrate Prediction

Next, we performed a multiple sequence alignment of the 19 *AtGH3* protein sequences and seven *CpGH3* protein sequences. The alignment results showed that the *CpGH3* proteins all contained a highly conserved GH3 domain (Figure S3). Additionally, the MEME tool mapped three conserved motifs to all *CpGH3* proteins (Figure S4). The motif similarities with *AtGH3* proteins indicated that the functions of the *CpGH3* proteins could be predicted by this sequence comparison.

Based on the conserved amino acid residues, most *CpGH3* proteins could be assigned to the conjugate protein groups identified in *A. thaliana*. *CpGH3.11* was grouped into subfamily I that includes *AtGH3.11/JAR1* and which shows enzymatic activity with JA. *CpGH3.1a*, *CpGH3.1b*, *CpGH3.5*, *CpGH3.6*, and *CpGH3.9*, like *AtGH3.1-6*, *AtGH3.9*, and *AtGH3.17*, had IAA as the acyl acid substrate (Figure 2A). *CpGH3.10* in subfamily I has no currently identified substrates (Westfall et al., 2012). Furthermore, five putative IAA-synthetases, *CpGH3.1a*,



CpGH3.1b, *CpGH3.5*, *CpGH3.6*, and *CpGH3.9*, were chosen to analyze activity of the IAA amido synthetases. These GH3 proteins were purified from *E. coli* (Figure S5). Our data showed that these proteins are IAA-amido synthetases (Figure 2B).

Tissue-Specific Expression Patterns of *CpGH3* genes

Tissue-specific expression of the *CpGH3* genes was analyzed by absolute quantification RT-PCR. Transcripts of all *CpGH3* genes were detectable in different tissues and organs in papaya. *CpGH3.1a* and *CpGH3.9* were more highly expressed in the roots than in other organs; *CpGH3.10* and *CpGH3.11* were highly expressed in the leaves. Interestingly, the transcript level of *CpGH3.10* was very low in fruit, whereas *CpGH3.5* and *CpGH3.6* predominantly expressed in fruit (Figure 3).

Cis-Element Analysis and Hormone Responsive Expression of *CpGH3* Genes

Several phytohormone-related *cis*-elements, such as AuxRE, SARE, and JERE, have been identified in plants (Ulmakov et al., 1997; Paterson et al., 2004; Osakabe et al., 2014). Here, we scanned the 1500-bp upstream promoter regions of *CpGH3* genes for phytohormone-related *cis*-elements. Several such elements were identified, namely ABRE, AuxRE, and SARE; no JERE

sequences were found in these promoter regions. One AuxRE and one SARE element were present in the *CpGH3.1a* promoter; three SAREs were present in the *CpGH3.1b* promoter; two AuxREs were present in the *CpGH3.5* promoter; two ABREs were present in the *CpGH3.6* promoter; and two ABREs, two AuxREs, and two SAREs were present in the *CpGH3.11* promoter. The numbers of these hormone-related *cis*-elements in the upstream 1.5-kb regions of *CpGH3* genes are listed in Table S4.

CpGH3 Expression and IAA-Amido Synthetase Activity at Different Postharvest Stages

Genetic studies have revealed that fruit ripening and softening is mediated by auxin-responsive genes in an auxin homeostatic process (Pan et al., 2015). To elucidate the functions of *CpGH3* genes during the postharvest period, we analyzed the changes in expression levels at six different postharvest stages. Our analysis indicated that expression of most *CpGH3* genes changed significantly during fruit ripening and softening. *CpGH3.1a*, *CpGH3.6*, and *CpGH3.11* expression increased significantly, while *CpGH3.9* expression decreased significantly. Expression of two other *CpGH3* genes, *CpGH3.1b* and *CpGH3.5*, peaked at 15 days, and then declined slightly at 20 and 25 days (Figure 4A). Next, we examined changes in IAA-amido synthetase activity using aspartate as the substrate for conjugation. A large increase (over 5-fold) in enzyme activity was detected during the postharvest process. IAA-Asp synthetase activity was induced significantly at 10 days, and reached its peak at 15 days (Figure 4B).

Involvement of AsA in Maintenance of Shelf Life of Papaya Fruit

An enhanced AsA pool has been reported to be associated with good postharvest storage characteristics in various fruit species (Mellidou et al., 2012). However, the effects of AsA treatment on papaya fruit ripening are largely unknown. We found here that a 250 mM AsA treatment delayed the ripening process in papaya fruit (Figure 5A). The physiological data showed that the firmness of control fruit rapidly decreased and that 93.9% of their firmness was lost within 25 days after harvest. In contrast, the firmness of the AsA-treated fruit was slightly higher than the control fruit during postharvest storage (Figure 5B). The rate of CO₂ production showed the characteristic respiratory climacteric pattern during postharvest storage for 25 days. In control fruit, the respiration rate lightly increased within 10 days after harvest, and then decreased slowly. In the AsA-treated fruit, the respiration rate was lower than in control fruit within 10 days after harvest. CO₂ production peaked at 37.09 and 31.78 mg·kg⁻¹ FW h⁻¹ in the control and AsA-treated fruits, respectively, at 10 days (Figure 5C). Total soluble solids tended to increase during storage. However, the AsA treatment delayed the increase in total soluble solids compared to the controls (Figure 5D). Titratable acidities of the papaya fruit tended to decrease during postharvest storage. The AsA treatment delayed these decreases in titratable acidities compared with the control fruits, particularly between 10 and 20 days (Figure 5E).

A

Subfamily I	$\alpha 5$	$\beta 6$	217	239	$\beta 8-\beta 9$
AtGH3.11	F T D E L M E N T L Q L F R T A F F	ATTNV	V	I	HDYGSSEGW
CpGH3.11	F N D D L M D N T M Q I Y R T S F F	ATTNV	V	I	HDYGSSEGW
AtGH3.10	F T R H S A Q T T L Q I F R L S A A	ATTHY	A	I	ADYGSTESW
CpGH3.10	F T R H S S Q T T L Q V F K L A A A	ATTHY	A	I	ADYGSTESW
Subfamily II	$\alpha 5$	$\beta 6$	217	239	$\beta 8-\beta 9$
AtGH3.5	T I E E E L D R R S L L Y S L L M P V M	VLTSY	V	I	T M Y A S S E C Y
AtGH3.6	T I E E E L D R R S L L Y S L L M P V M	VLTSY	V	I	T M Y A S S E C Y
CpGH3.5	T I E E E L D R R S L L Y S L L M P V M	VLTSY	V	I	T M Y A S S E C Y
CpGH3.6	T I E E E L D R R S L L Y S L L M P V M	VLTSY	V	I	T M Y A S S E C Y
AtGH3.2	T I E E E L D R R Q Q L L Y S L L M P V M	VLTSY	V	I	T M Y A S S E C Y
AtGH3.4	T I E E E I N R R Q Q L L Y S L L M P V M	ALTSY	V	I	M I Y A S S E C Y
AtGH3.3	T I D E D M D R R Q Q L L Y S L L M P V M	VLTSY	V	I	T M Y A S S E C Y
CpGH3.1a	T I Q E E M D R R Q Q L L Y S L L M P V M	VLTSY	V	I	T M Y A S S E C Y
CpGH3.1b	T I H E E L D R R C L L Y S L L M P V M	VLTSY	V	I	T M Y A S S E C Y
AtGH3.1	T I K E E L D R R Q Q L L Y S L L M P V M	VLTSY	V	I	T M Y A S S E C Y
AtGH3.9	T I P E D L D R R Q Q L L Y N L L M P V M	VLTSY	V	I	T M Y A S S E C Y
CpGH3.9	- - - - -	VLTSY	V	I	T M Y A S S E C Y
AtGH3.17	S T A E E L E R K T F F Y S M L V P I M	VLTSY	V	I	T M Y A S S E C Y

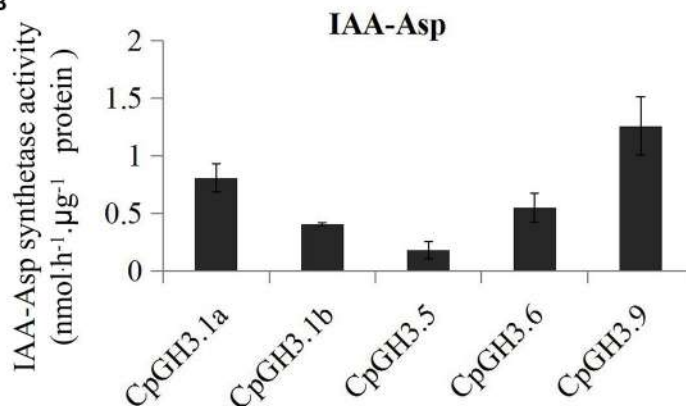
B

FIGURE 2 | Phylogenetic relationship analysis of GH3 family and sequence-based grouping of plant GH3 proteins based on acyl acid binding site residues. (A) CpGH3 and AtGH3 proteins are color coded according to their subgroup. Sequences corresponding to the residues of the $\alpha 5$ and $\alpha 6$ motifs, to residues 217 and 299 of AtGH3.12, and to the $\beta 8$ and $\beta 9$ motifs are indicated (Westfall et al., 2012). Conserved residues are highlighted by colored boxes. **(B)** Analysis of IAA-amido synthetases activities of CpGH3 proteins. All five GH3 proteins were purified from *E. coli*, and the *E. coli* with empty vector was used as negative control. The activities have been normalized to μg of protein.

IAA-Amido Synthetase Activities and the Expression of *CpGH3* Genes during Postharvest after AsA treatment

CpGH3 gene expression and IAA-amido synthetase activities were measured during the postharvest period in both control and AsA-treated fruits. The expression of *CpGH3.1a*, *CpGH3.1b*, and *CpGH3.5* was largely reduced by the AsA treatment during different postharvest stages. In contrast, *CpGH3.6* showed a small increase at postharvest 0 and 5 days, and was then reduced at postharvest 10–25 days. Expression of *CpGH3.9* slightly increased after AsA treatment. *CpGH3.6* showed over

10-fold reduction in expression level after postharvest 15 days (Figure 6A). At postharvest stages 0 and 5 days, IAA-amido synthetase activities were similar in control and AsA treated fruit. During 10–25 days, AsA treatment significantly reduced IAA-amido synthetase activity compared to controls (Figure 6B).

Endogenous IAA and Ethylene Production Rate Measurements

To examine the role of endogenous IAA during storage, IAA contents were measured in papaya fruit under different conditions. Endogenous IAA contents fell during the postharvest

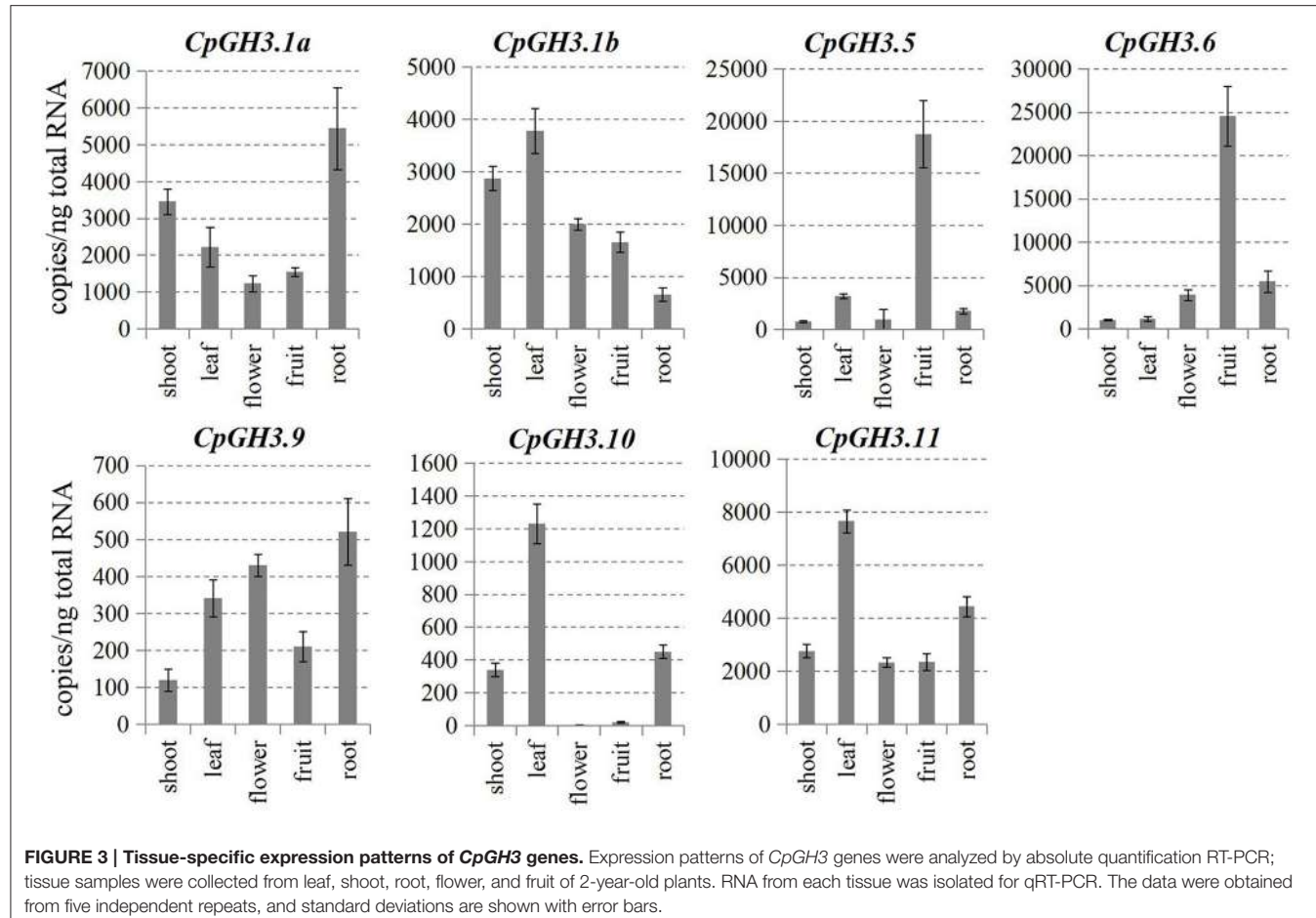


FIGURE 3 | Tissue-specific expression patterns of *CpGH3* genes. Expression patterns of *CpGH3* genes were analyzed by absolute quantification RT-PCR; tissue samples were collected from leaf, shoot, root, flower, and fruit of 2-year-old plants. RNA from each tissue was isolated for qRT-PCR. The data were obtained from five independent repeats, and standard deviations are shown with error bars.

period. Although IAA contents were consistent at 0 and 5 days, they then decreased significantly from 172 to 45 ng.g⁻¹ FW (fresh weight). In contrast to the controls, the IAA contents of the AsA-treated fruit only decreased to 71 ng.g⁻¹ FW (Figure 7). Thus, the AsA treatment may play a role in the retention of endogenous IAA during the postharvest period. Furthermore, previous studies have revealed that there is an ethylene-releasing peak during fruit ripening (Mo et al., 2008). In our study, production rate of ethylene climbed greatly with ripening and reached climacteric peak at the 10 days in the control, and then decreased gradually. In contrast to the control, the production rate of ethylene only increased 16.5 μL.kg⁻¹.h⁻¹, and reached its peak at the 15 days (Figure S6).

DISCUSSION

Papaya is a highly perishable fruit that undergoes a rapid softening process after harvest (Yao et al., 2014). Fruit ripening is associated with various hormone signals involved in the postharvest storage of fruits. GH3 proteins are among the most important downstream targets of auxin; GH3-mediated auxin homeostasis plays a vital part in the regulation of fruit ripening (Böttcher et al., 2010; Xie et al., 2015). Here, we

performed a systematic identification of *CpCH3* genes, and analyzed their expression patterns and synthetase activities at different postharvest stages. The data from these analyses provide insights into the underlying mechanisms linking auxin and fruit ripening in papaya.

Here, seven *GH3* genes were identified in the papaya genome. This number is considerably smaller than the 19 genes identified in *A. thaliana* (Staswick et al., 2005). The relatively small size of the papaya genome (372 Mbp) may be a possible explanation for the comparatively small number of *CpGH3* genes (Ming et al., 2008). The similarities in characteristic motifs and exon-intron structures of the *CpGH3* genes with those reported *AtGH3* genes supported our identification. The presence of conserved domains in the *CpGH3* proteins showed they were highly similar to *GH3* proteins of other model plant species (Staswick et al., 2005; Jain et al., 2006). This similarity suggests that *GH3* proteins might function in the same manner in different plant species. Furthermore, the phylogenetic analysis identified three orthologous gene pairs with high bootstrap values (100%), indicating a close relationship between the *A. thaliana* and papaya *GH3* gene families (Figure 1).

To identify potentially functional amino residues in the seven *CpGH3* proteins, we performed a multiple sequence alignment using the sequences of the 19 *AtGH3* proteins. We found that the

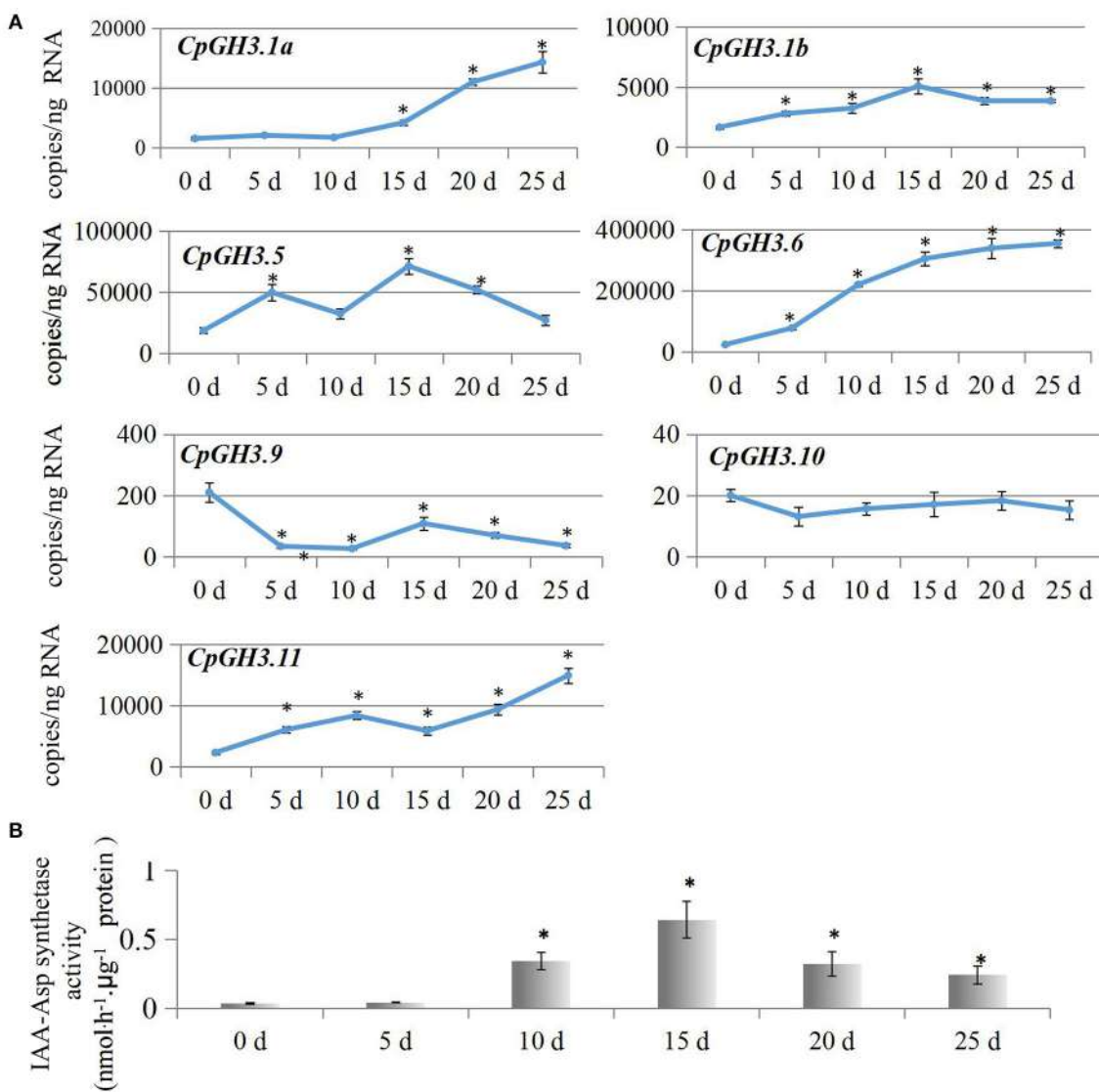


FIGURE 4 | Analysis of *CpGH3* gene expression patterns and IAA-amido synthetase activities during different postharvest stages. **(A)** Analysis of expression of *CpGH3* genes during different postharvest stages. **(B)** Enzymatic activities of IAA-amido synthetase. The data were obtained from five independent repeats, and standard deviations are shown with error bars. Significant differences ($P < 0.05$) between “stage 1” and the other postharvest stages are indicated by an asterisk.

CpGH3 proteins could be grouped into three subfamilies with different structures and different acyl acid substrate preferences (Wang et al., 2010). Recently, the crystal structures of two representative GH3 proteins, AtGH3.11 and AtGH3.12, were determined, and several specific secondary structures, such as the conserved motifs $\alpha 5$, $\alpha 6$, $\beta 8$, and $\beta 9$, were identified for acyl acid preferences (Westfall et al., 2012). Our data showed that five *CpGH3* proteins, *CpGH3.1a*, *CpGH3.1b*, *CpGH3.5*, *CpGH3.6*, and *CpGH3.9*, were grouped into subfamily II, and might function as IAA-specific amido synthetases. Interestingly, the $\alpha 5$ motif was absent from *CpGH3.9*, although the $\alpha 6$, $\beta 8$, and $\beta 9$ motifs were present and residues 217 and 239 showed high similarity to the other subfamily II GH3 proteins. The

acyl acid sites of IAA-using GH3 proteins have been reported to display consistent residues in the $\alpha 5$ motif (Westfall et al., 2012). Thus, the *CpGH3.9* protein was grouped into subfamily II as an IAA-specific amido synthetase. Previous studies have identified the activities of several known GH3s in different plant species. In grape berry, the activity of the indole-3-acetic acid-amido synthetase GH3-1 has been identified (Böttcher et al., 2010). Moreover, GH3-2 was also identified as an IAA-amido synthetase with similar amino acid preferences as GH3-1 by the same group (Böttcher et al., 2011). In pea, the IAA-amide synthetase activity of PsGH3-5 was determined with aspartate as a substrate (Ostrowski and Jakubowska, 2013). In our study, five of the seven *CpGH3* proteins showed IAA-specific

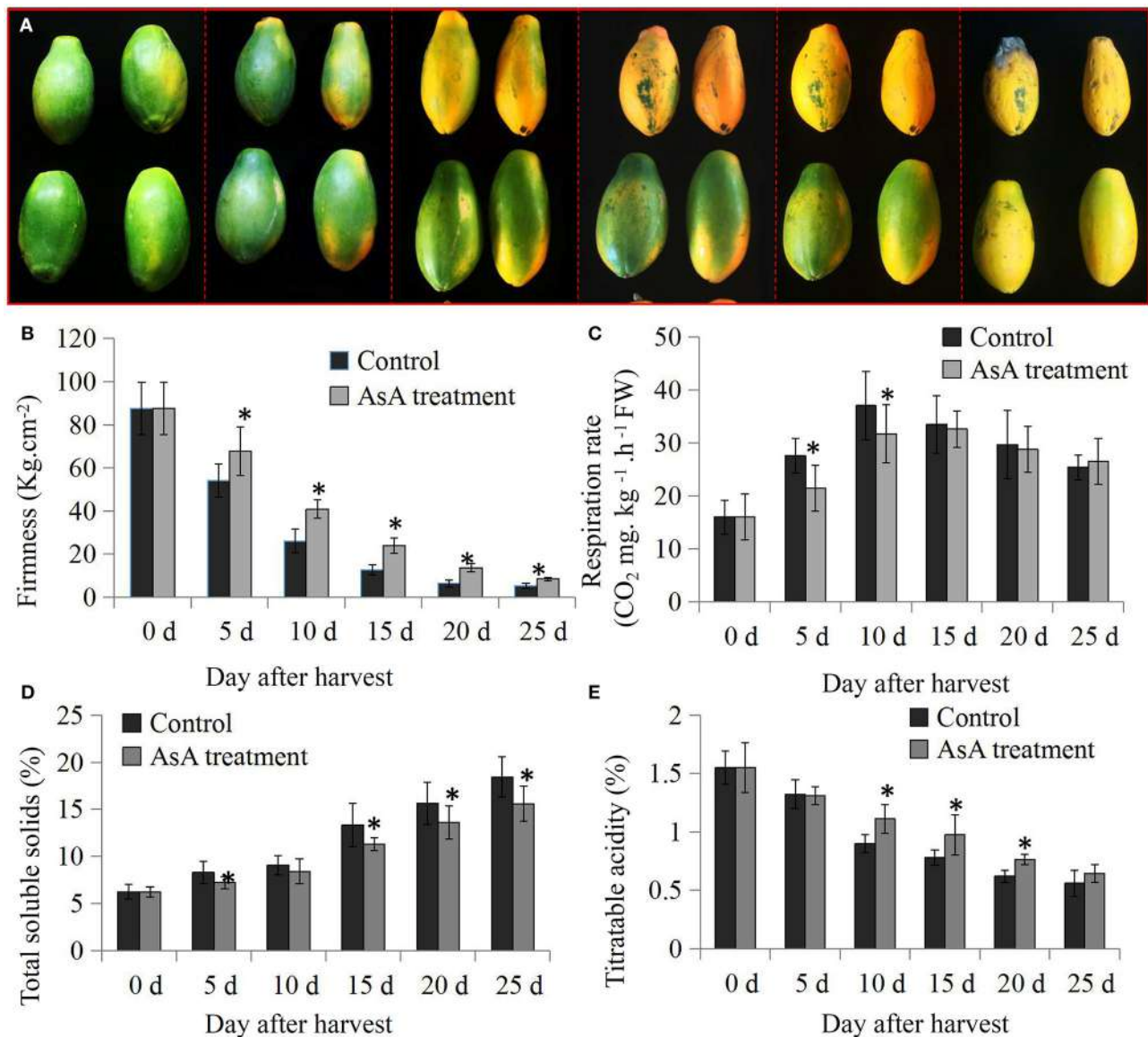


FIGURE 5 | Involvement of ascorbic acid (AsA) in maintenance of shelf life in papaya fruit. **(A)** Morphological differences between control and AsA-treated papaya fruit during the postharvest period. The changes in firmness **(B)**, respiration rate **(C)**, total soluble solids **(D)**, and titratable acidity **(E)** between the control and AsA-treated fruit after a 25 day postharvest storage period. Significant differences ($P < 0.05$) between the control and AsA-treated fruit at different postharvest stages are indicated by an asterisk.

amido synthetase activities, indicating their major roles in IAA-homeostasis.

Expression analyses suggest that *GH3* genes in different plant species have diverse roles in plant morphogenesis (Nakazawa et al., 2001; Takase et al., 2004; Khan and Stone, 2007; Kuang et al., 2011). Therefore, we analyzed the tissue-specific expression pattern of *CpGH3* genes to provide insights into their putative functions in papaya. *CpGH3.5* and *CpGH3.6* predominantly expressed in fruit, suggesting a possible role in auxin homeostasis during fruit development and ripening. Transcripts of *CpGH3.10* were virtually undetectable in fruit,

indicating that this gene had limited or no role during postharvest stages of fruit development. In tomato, several *SIGH3* genes show different patterns of expression in reproductive tissues or fruit development stages. In particular, *SIGH3.1* and *SIGH3.2* exhibit ripening-associated expression patterns (Kumar et al., 2012). In papaya, expression of *CpGH3.1a*, *CpGH3.6*, and *CpGH3.11* exhibited a fruit softening-associated up-regulation; the remaining *CpGH3* genes showed a constant level of expression during different postharvest stages (Figure 4A). The differential expression of *CpGH3* genes in a stage-specific manner during fruit ripening and softening is a common characteristic

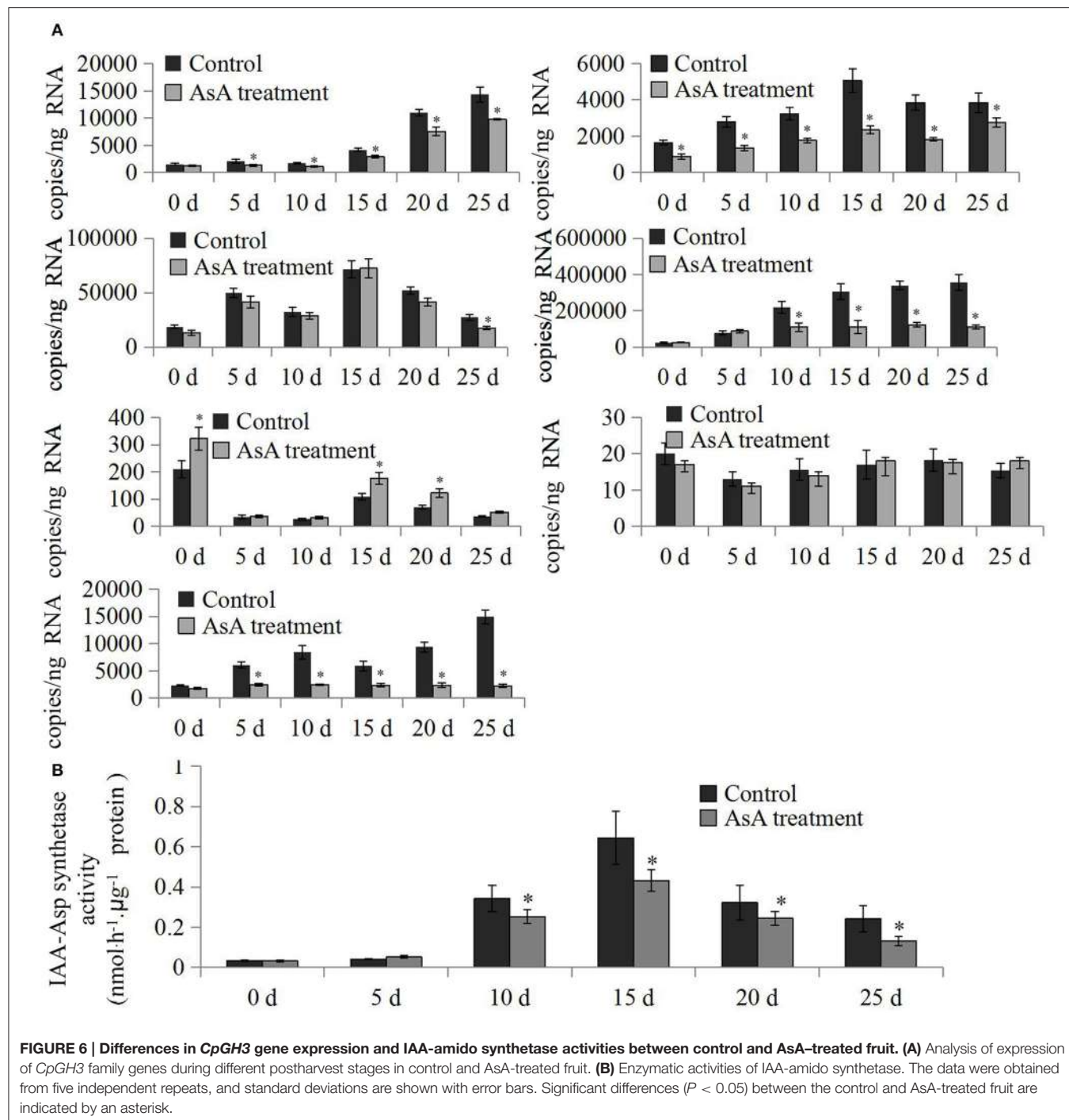


FIGURE 6 | Differences in *CpGH3* gene expression and IAA-amido synthetase activities between control and AsA-treated fruit. (A) Analysis of expression of *CpGH3* family genes during different postharvest stages in control and AsA-treated fruit. **(B)** Enzymatic activities of IAA-amido synthetase. The data were obtained from five independent repeats, and standard deviations are shown with error bars. Significant differences ($P < 0.05$) between the control and AsA-treated fruit are indicated by an asterisk.

of plant *GH3* genes (Böttcher et al., 2010; Kuang et al., 2011).

IAA is a well-studied inhibitor of ripening in both climacteric and non-climacteric fruits. A decrease in endogenous IAA levels is required for the initiation of ripening and has been reported to be a prerequisite for ripening to occur (Purgatto et al., 2002; Böttcher et al., 2010). It has been suggested that IAA-amido synthetase has an essential role in the ripening

process through inactivation of endogenous IAA in pungent pepper and grape vine (Liu et al., 2005; Böttcher et al., 2010). We examined IAA-amido synthetase activities in papaya using aspartate as a substrate for conjugation during postharvest stages. A significant increase in enzyme activity was observed after postharvest stage 3 (Figure 4B), although expression of only three *CpGH3* genes was up-regulated. The increased expression of *CpGH3.1a*, *CpGH3.6*, and *CpGH3.11* suggest they might

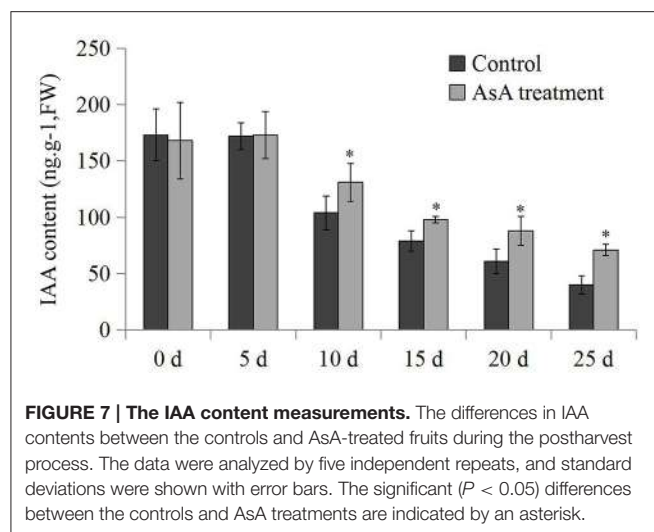


FIGURE 7 | The IAA content measurements. The differences in IAA contents between the controls and AsA-treated fruits during the postharvest process. The data were analyzed by five independent repeats, and standard deviations were shown with error bars. The significant ($P < 0.05$) differences between the controls and AsA treatments are indicated by an asterisk.

play a dominant role in the increase in enzyme activity during postharvest maturation. Interestingly, the mRNA levels of some *CpGH3* genes don't really correspond to enzymatic activity, suggesting the presence of diverse regulation manners in mRNA and protein levels. In fleshy fruit, the levels of endogenous IAA concentrations decline toward the onset of ripening (Buta and Spaulding, 1994). Many studies have reported that IAA levels are high at the early stages and then decrease to low levels at later ripening stages in non-climacteric fruit (Zhang et al., 2003; Symons et al., 2006). In *V. vinifera*, expression of *VvGH3.2* can be induced in pre-ripening berries by IAA treatment, and is associated with an increase in IAA-Asp levels and a decrease in free IAA levels (Böttcher et al., 2011). In common with these reports, IAA levels in papaya fruit were found to decline and to be relatively constant throughout the later stages of the postharvest period (Figure 7). Conjugation of IAA to amino acids is catalyzed by GH3 proteins, suggesting a negative feedback loop to regulate auxin homoeostasis (Staswick et al., 2005). The induced IAA-amido synthetase activities provide a possible explanation for the maintenance of low levels of endogenous IAA during the postharvest period in papaya fruit.

AsA is a well-known antioxidant that effectively regulates the enzymatic browning of fruits (Huang et al., 2014). The application of AsA is a useful approach to improve oxidative stress tolerance and to extend the shelf life of fruit (Zoldners et al., 2005; Liu et al., 2014). Several important postharvest physiological parameters, including fruit firmness, respiration rate, soluble solids content, and titratable acidity, were measured in the present study. Our analyses confirmed that AsA application delayed softening of papaya fruit (Figure 5). However, whether GH3 related IAA homoeostasis participated in this AsA-mediated effect is still largely unknown.

Analysis of *CpGH3* gene expression and enzymatic activities of CpGH3 proteins provided further insights into their possible

functions during postharvest fruit storage. The qRT-PCR data showed that the expression of most *CpGH3* genes was decreased by the AsA treatment compared with the control, although *CpGH3.9*, *CpGH3.6*, and *CpGH3.10* showed evidence of a slight induction effect. Clear differences were observed among the *CpGH3* genes in their responses to AsA treatment suggesting variations in the transcriptional regulation of these genes (Böttcher et al., 2015). On the basis of gene expression levels, IAA-amido synthetase activities were reduced by AsA treatments from 10 to 25 days compared to controls. Our data suggested that AsA treatment regulated postharvest fruit ripening and softening by promoting endogenous IAA levels. Moreover, fruits treated with AsA showed a relatively lower production rate of ethylene compared to the controls. It suggested that AsA delayed ripening by regulating auxin-ethylene balance. The higher IAA levels in AsA treated fruits would lead to lower ethylene levels.

In this study, we identified seven *CpGH3* genes in a papaya genome database. Our study provides comprehensive information on *GH3* gene expression patterns in different tissues and on the enzyme activities of IAA-amido synthetases under different postharvest conditions. These results further indicated an important role for *GH3* genes in the regulation of auxin-associated fruit postharvest changes. Our findings may provide a way to develop novel strategies for improving papaya fruit quality during postharvest storage.

AUTHOR CONTRIBUTIONS

KL, HL, and SF carried out the molecular studies. JZ and YP took care the plants. KL and JW drafted the manuscript. SF performed the statistical analysis. HL and SF conceived of the study, and participated in its design. CY acquired of funding and helped to draft the manuscript. All authors read and approved the final manuscript.

ACKNOWLEDGMENTS

This work was supported by the National Natural Science Foundation of China (grant no. 31201586); Science and Technology Program of Guangdong, China (grant no. 2014A020208138 and 2015A020208018); Natural Science Foundation of Guangdong Province, China (grant no. 2016A030307016); Natural Science Foundation of Lingnan Normal University (grant no. LZL1507); Collaborative Innovation Center Project of Lingnan Normal University (grant no. CIL1503). Editing of the manuscript was provided by International Science Editing company.

SUPPLEMENTARY MATERIAL

The Supplementary Material for this article can be found online at: <http://journal.frontiersin.org/article/10.3389/fpls.2016.01555>

REFERENCES

- Abel, S., and Theologis, A. (1996). Early genes and auxin action. *Plant Physiol.* 111, 9–17. doi: 10.1104/pp.111.1.9
- Böttcher, C., Boss, P. K., and Davies, C. (2011). Acyl substrate preferences of an IAA-amido synthetase account for variations in grape (*Vitis vinifera* L.) berry ripening caused by different auxinic compounds indicating the importance of auxin conjugation in plant development. *J. Exp. Bot.* 62, 4267–4280. doi: 10.1093/jxb/err134
- Böttcher, C., Burbidge, C. A., di Rienzo, V., Boss, P. K., and Davies, C. (2015). Jasmonic acid-isoleucine formation in grapevine (*Vitis vinifera* L.) by two enzymes with distinct transcription profiles. *J. Integr. Plant Biol.* 57, 618–627. doi: 10.1111/jipb.12321
- Böttcher, C., Keyzers, R. A., Boss, P. K., and Davies, C. (2010). Sequestration of auxin by the indole-3-acetic acid-amido synthetase GH3-1 in grape berry (*Vitis vinifera* L.) and the proposed role of auxin conjugation during ripening. *J. Exp. Bot.* 61, 3615–3625. doi: 10.1093/jxb/erq174
- Buta, J. G., and Spaulding, D. W. (1994). Changes in indole-3-acetic acid and abscisic acid levels during tomato (*Lycopersicon esculentum* Mill.) fruit development and ripening. *J. Plant Growth Regul.* 13, 163–166. doi: 10.1007/BF00196382
- Chen, J., Mao, L., Lu, W., Ying, T., and Luo, Z. (2016). Transcriptome profiling of postharvest strawberry fruit in response to exogenous auxin and abscisic acid. *Planta* 243, 183–197. doi: 10.1007/s00425-015-2402-5
- de Jong, M., Wolters-Arts, M., Feron, R., Mariani, C., and Vriezen, W. H. (2009). The *Solanum lycopersicum* auxin response factor 7 (SlARF7) regulates auxin signaling during tomato fruit set and development. *Plant J.* 57, 160–170. doi: 10.1111/j.1365-313X.2008.03671.x
- Domingo, C., Andrés, F., Tharreau, D., Iglesias, D. J., and Talón, M. (2009). Constitutive expression of OsGH3.1 reduces auxin content and enhances defense response and resistance to a fungal pathogen in rice. *Mol. Plant Microbe Interact.* 22, 201–210. doi: 10.1094/MPMI-22-2-0201
- Du, H., Wu, N., Fu, J., Wang, S., Li, X., Xiao, J., et al. (2012). A GH3 family member, OsGH3-2, modulates auxin and abscisic acid levels and differentially affects drought and cold tolerance in rice. *J. Exp. Bot.* 63, 6467–6480. doi: 10.1093/jxb/ers300
- Feng, S., Yue, R., Tao, S., Yang, Y., Zhang, L., Xu, M., et al. (2015). Genome-wide identification, expression analysis of auxin-responsive GH3 family genes in maize (*Zea mays* L.) under abiotic stresses. *J. Integr. Plant Biol.* 57, 783–795. doi: 10.1111/jipb.12327
- Gomez-Lobato, M. E., Civello, P. M., and Martínez, G. A. (2012). Effects of ethylene, cytokinin and physical treatments on BoPaO gene expression of harvested broccoli. *J. Sci. Food Agric.* 92, 151–158. doi: 10.1002/jsfa.4555
- Gutierrez, L., Bussell, J. D., Pacurar, D. I., Schwambach, J., Pacurar, M., and Bellini, C. (2009). Phenotypic plasticity of adventitious rooting in *Arabidopsis* is controlled by complex regulation of AUXIN RESPONSE FACTOR transcripts and microRNA abundance. *Plant Cell* 21, 3119–3132. doi: 10.1105/tpc.108.064758
- Gutierrez, L., Mongelard, G., Floková, K., Pacurar, D. I., Novák, O., Staswick, P., et al. (2012). Auxin controls *Arabidopsis* adventitious root initiation by regulating jasmonic acid homeostasis. *Plant Cell* 24, 2515–2527. doi: 10.1105/tpc.112.099119
- Hagen, G., Kleinschmidt, A., and Guilfoyle, T. (1984). Auxin-regulated gene expression in intact soybean hypocotyl and excised hypocotyl sections. *Planta* 162, 147–153. doi: 10.1007/BF00410211
- Huang, M., Xu, Q., and Deng, X. X. (2014). L-Ascorbic acid metabolism during fruit development in an ascorbate-rich fruit crop chestnut rose (*Rosa roxburghii* Tratt.). *J. Plant Physiol.* 171, 1205–1216. doi: 10.1016/j.jplph.2014.03.010
- Jain, M., Kaur, N., Tyagi, A. K., and Khurana, J. P. (2006). The auxin-responsive GH3 gene family in rice (*Oryza sativa*). *Funct. Integr. Genomics* 6, 36–46. doi: 10.1007/s10142-005-0142-5
- Jain, S. K., Verma, R. C., Murdia, L. K., Jain, H. K., and Sharma, G. P. (2011). Optimization of process parameters for osmotic dehydration of papaya cubes. *J. Food Sci. Technol.* 48, 211–217. doi: 10.1007/s13197-010-0161-7
- Jones, B., Frasse, P., Olmos, E., Zegzouti, H., Li, Z. G., Latché, A., et al. (2002). Down-regulation of DR12, an auxin-response-factor homolog, in the tomato results in a pleiotropic phenotype including dark green and blotchy ripening fruit. *Plant J.* 32, 603–613. doi: 10.1046/j.1365-313X.2002.01450.x
- Khan, S., and Stone, J. M. (2007). *Arabidopsis thaliana* GH3.9 influences primary root growth. *Planta* 226, 21–34. doi: 10.1007/s00425-006-0462-2
- Kuang, J. F., Zhang, Y., Chen, J. Y., Chen, Q. J., Jiang, Y. M., Lin, H. T., et al. (2011). Two GH3 genes from longan are differentially regulated during fruit growth and development. *Gene* 485, 1–6. doi: 10.1016/j.gene.2011.05.033
- Kumar, R., Agarwal, P., Tyagi, A. K., and Sharma, A. K. (2012). Genome-wide investigation and expression analysis suggest diverse roles of auxin-responsive GH3 genes during development and response to different stimuli in tomato (*Solanum lycopersicum*). *Mol. Genet. Genomics* 287, 221–235. doi: 10.1007/s00438-011-0672-6
- Liu, K., Kang, B. C., Jiang, H., Moore, S. L., Li, H., Watkins, C. B., et al. (2005). A GH3-like gene, CcGH3, isolated from *Capsicum chinense* L. fruit is regulated by auxin and ethylene. *Plant Mol. Biol.* 58, 447–464. doi: 10.1007/s11103-005-6505-4
- Liu, K., Yuan, C., Chen, Y., Li, H., and Liu, J. (2014). Combined effects of ascorbic acid and chitosan on the quality maintenance and shelf life of plums. *Sci. Hortic.* 176, 45–53. doi: 10.1016/j.scientia.2014.06.027
- Liu, X., Hegeman, A. D., Gardner, G., and Cohen, J. D. (2012). Protocol: high-throughput and quantitative assays of auxin and auxin precursors from minute tissue samples. *Plant Methods* 8:31. doi: 10.1186/1746-4811-8-31
- Mellidou, I., Keulemans, J., Kanellis, A. K., and Davey, M. W. (2012). Regulation of fruit ascorbic acid concentrations during ripening in high and low vitamin C tomato cultivars. *BMC Plant Biol.* 12:239. doi: 10.1186/1471-2229-12-239
- Ming, R., Hou, S., Feng, Y., Yu, Q., Dionne-Laporte, A., Saw, J. H., et al. (2008). The draft genome of the transgenic tropical fruit tree papaya (*Carica papaya* Linnaeus). *Nature* 452, 991–996. doi: 10.1038/nature06856
- Mo, Y., Gong, D., Liang, G., Han, R., Xie, J., and Li, W. (2008). Enhanced preservation effects of sugar apple fruits by salicylic acid treatment during post-harvest storage. *J. Sci. Food Agric.* 88, 2693–2699. doi: 10.1002/jsfa.3395
- Nakazawa, M., Yabe, N., Ichikawa, T., Yamamoto, Y. Y., Yoshizumi, T., Hasunuma, K., et al. (2001). DFL1, an auxin-responsive GH3 gene homologue, negatively regulates shoot cell elongation and lateral root formation, and positively regulates the light response of hypocotyl length. *Plant J.* 25, 213–221. doi: 10.1046/j.1365-313X.2001.00957.x
- Osakabe, Y., Yamaguchi-Shinozaki, K., Shinozaki, K., and Tran, L. S. (2014). ABA control of plant macroelement membrane transport systems in response to water deficit and high salinity. *New Phytol.* 202, 35–49. doi: 10.1111/nph.12613
- Ostrowski, M., and Jakubowska, A. (2013). GH3 expression and IAA-amide synthetase activity in pea (*Pisum sativum* L.) seedlings are regulated by light, plant hormones and auxinic herbicides. *J. Plant Physiol.* 170, 361–368. doi: 10.1016/j.jplph.2012.10.016
- Pan, L., Zeng, W., Niu, L., Lu, Z., Wang, X., Liu, H., et al. (2015). PpYUC11, a strong candidate gene for the stony hard phenotype in peach (*Prunus persica* L. Batsch), participates in IAA biosynthesis during fruit ripening. *J. Exp. Bot.* 66, 7031–7044. doi: 10.1093/jxb/erv400
- Park, J. E., Seo, P. J., Lee, A. K., Jung, J. H., Kim, Y. S., and Park, C. M. (2007). An *Arabidopsis* GH3 gene, encoding an auxin-conjugating enzyme, mediates phytochrome B-regulated light signals in hypocotyl growth. *Plant Cell Physiol.* 48, 1236–1241. doi: 10.1093/pcp/pcm086
- Paterson, A. H., Bowers, J. E., and Chapman, B. A. (2004). Ancient polyploidization predating divergence of the cereals, and its consequences for comparative genomics. *Proc. Natl. Acad. Sci. U.S.A.* 101, 9903–9908. doi: 10.1073/pnas.0307901101
- Peat, T. S., Böttcher, C., Newman, J., Lucent, D., Cowieson, N., and Davies, C. (2012). Crystal structure of an indole-3-acetic acid amido synthetase from grapevine involved in auxin homeostasis. *Plant Cell* 24, 4525–4538. doi: 10.1105/tpc.112.102921
- Purgatto, E., Oliveira do Nascimento, J. R., Lajolo, F. M., and Cordenunsi, B. R. (2002). The onset of starch degradation during banana ripening is concomitant to changes in the content of free and conjugated forms of indole-3-acetic acid. *J. Plant Physiol.* 159, 1105–1111. doi: 10.1078/0176-1617-00875
- Quint, M., and Gray, W. M. (2006). Auxin signaling. *Curr. Opin. Plant Biol.* 9, 448–453. doi: 10.1016/j.pbi.2006.07.006
- Ruan, Y. L., Patrick, J. W., Bouzayen, M., Osorio, S., and Fernie, A. R. (2012). Molecular regulation of seed and fruit set. *Trends Plant Sci.* 17, 656–665. doi: 10.1016/j.tplants.2012.06.005

- Sorin, C., Bussell, J. D., Camus, I., Ljung, K., Kowalczyk, M., Geiss, G., et al. (2005). Auxin and light control of adventitious rooting in *Arabidopsis* require ARGONAUTE1. *Plant Cell* 17, 1343–1359. doi: 10.1105/tpc.105.031625
- Sorin, C., Negroni, L., Balliau, T., Corti, H., Jacquemot, M. P., Davanture, M., et al. (2006). Proteomic analysis of different mutant genotypes of *Arabidopsis* led to the identification of 11 proteins correlating with adventitious root development. *Plant Physiol.* 140, 349–364. doi: 10.1104/pp.105.067868
- Staswick, P. E., Serban, B., Rowe, M., Tiriyaki, I., Maldonado, M. T., Maldonado, M. C., et al. (2005). Characterization of an *Arabidopsis* enzyme family that conjugates amino acids to indole-3-acetic acid. *Plant Cell* 17, 616–627. doi: 10.1105/tpc.104.026690
- Su, L., Diretto, G., Purgatto, E., Danoun, S., Zouine, M., Li, Z., et al. (2015). Carotenoid accumulation during tomato fruit ripening is modulated by the auxin-ethylene balance. *BMC Plant Biol.* 15:114. doi: 10.1186/s12870-015-0495-4
- Symons, G. M., Davies, C., Shavruk, Y., Dry, I. B., Reid, J. B., and Thomas, M. R. (2006). Grapes on steroids. Brassinosteroids are involved in grape berry ripening. *Plant Physiol.* 140, 150–158. doi: 10.1104/pp.105.070706
- Takase, T., Nakazawa, M., Ishikawa, A., Kawashima, M., Ichikawa, T., Takahashi, N., et al. (2004). ydk1-D, an auxin-responsive GH3 mutant that is involved in hypocotyl and root elongation. *Plant J.* 37, 471–483. doi: 10.1046/j.1365-313X.2003.01973.x
- Takase, T., Nakazawa, M., Ishikawa, A., Manabe, K., and Matsui, M. (2003). DFL2, a new member of the *Arabidopsis* GH3 gene family, is involved in red light-specific hypocotyl elongation. *Plant Cell Physiol.* 44, 1071–1080. doi: 10.1093/pcp/pcg130
- Teale, W. D., Ditengou, F. A., Dovzhenko, A. D., Li, X., Molendijk, A. M., Ruperti, B., et al. (2008). Auxin as a model for the integration of hormonal signal processing and transduction. *Mol. Plant* 1, 229–237. doi: 10.1093/mp/ssn006
- Ulmasov, T., Hagen, G., and Guilfoyle, T. J. (1997). ARF1, a transcription factor that binds to auxin response elements. *Science* 276, 1865–1868. doi: 10.1126/science.276.5320.1865
- Wang, S., Bai, Y., Shen, C., Wu, Y., Zhang, S., Jiang, D., et al. (2010). Auxin-related gene families in abiotic stress response in *Sorghum bicolor*. *Funct. Integr. Genomics* 10, 533–546. doi: 10.1007/s10142-010-0174-3
- Westfall, C. S., Herrmann, J., Chen, Q., Wang, S., and Jez, J. M. (2010). Modulating plant hormones by enzyme action: the GH3 family of acyl acid amido synthetases. *Plant Signal. Behav.* 5, 1607–1612. doi: 10.4161/psb.5.12.13941
- Westfall, C. S., Zubietta, C., Herrmann, J., Kapp, U., Nanao, M. H., and Jez, J. M. (2012). Structural basis for prereceptor modulation of plant hormones by GH3 proteins. *Science* 336, 1708–1711. doi: 10.1126/science.1221863
- Xie, R., Pang, S., Ma, Y., Deng, L., He, S., Yi, S., et al. (2015). The ARF, AUX/IAA and GH3 gene families in citrus: genome-wide identification and expression analysis during fruitlet drop from abscission zone A. *Mol. Genet. Genomics* 290, 2089–2105. doi: 10.1007/s00438-015-1063-1
- Yang, Y., Yue, R., Sun, T., Zhang, L., Chen, W., Zeng, H., et al. (2015). Genome-wide identification, expression analysis of GH3 family genes in *Medicago truncatula* under stress-related hormones and *Sinorhizobium meliloti* infection. *Appl. Microbiol. Biotechnol.* 99, 841–854. doi: 10.1007/s00253-014-6311-5
- Yao, B. N., Tano, K., Konan, H. K., Bédié, G. K., Oulé, M. K., Koffi-Nevry, R., et al. (2014). The role of hydrolases in the loss of firmness and of the changes in sugar content during the post-harvest maturation of *Carica papaya* L. var solo 8. *J. Food Sci. Technol.* 51, 3309–3316. doi: 10.1007/s13197-012-0858-x
- Yuan, H., Zhao, K., Lei, H., Shen, X., Liu, Y., Liao, X., et al. (2013). Genome-wide analysis of the GH3 family in apple (*Malus x domestica*). *BMC Genomics* 14:297. doi: 10.1186/1471-2164-14-297
- Zhang, S., Wang, S., Xu, Y., Yu, C., Shen, C., Qian, Q., et al. (2015). The auxin response factor, OsARF19, controls rice leaf angles through positively regulating OsGH3-5 and OsBRI1. *Plant Cell Environ.* 38, 638–654. doi: 10.1111/pce.12397
- Zhang, S. W., Li, C. H., Cao, J., Zhang, Y. C., Zhang, S. Q., Xia, Y. F., et al. (2009). Altered architecture and enhanced drought tolerance in rice via the down-regulation of indole-3-acetic acid by TLD1/OsGH3.13 activation. *Plant Physiol.* 151, 1889–1901. doi: 10.1104/pp.109.146803
- Zhang, X., Luo, G., Wang, R., Wang, J., and Himelrick, D. G. (2003). Growth and developmental responses of seeded and seedless grape berries to shoot girdling. *J. Am. Soc. Hortic. Sci.* 128, 316–323.
- Zoldner, J., Kiseleva, T., and Kaimish, I. (2005). Influence of ascorbic acid on the stability of chitosan solutions. *Carbohydr. Polym.* 60, 215–218. doi: 10.1016/j.carbpol.2005.01.013

Conflict of Interest Statement: The authors declare that the research was conducted in the absence of any commercial or financial relationships that could be construed as a potential conflict of interest.

Copyright © 2016 Liu, Wang, Li, Zhong, Feng, Pan and Yuan. This is an open-access article distributed under the terms of the Creative Commons Attribution License (CC BY). The use, distribution or reproduction in other forums is permitted, provided the original author(s) or licensor are credited and that the original publication in this journal is cited, in accordance with accepted academic practice. No use, distribution or reproduction is permitted which does not comply with these terms.

Advantages of publishing in Frontiers



OPEN ACCESS

Articles are free to read,
for greatest visibility



COLLABORATIVE PEER-REVIEW

Designed to be rigorous
– yet also collaborative,
fair and constructive



FAST PUBLICATION

Average 85 days from
submission to publication
(across all journals)



COPYRIGHT TO AUTHORS

No limit to article
distribution and re-use



TRANSPARENT

Editors and reviewers
acknowledged by name
on published articles



SUPPORT

By our Swiss-based
editorial team



IMPACT METRICS

Advanced metrics
track your article's impact



GLOBAL SPREAD

5'100'000+ monthly
article views
and downloads



LOOP RESEARCH NETWORK

Our network
increases readership
for your article

Frontiers

EPFL Innovation Park, Building I • 1015 Lausanne • Switzerland
Tel +41 21 510 17 00 • Fax +41 21 510 17 01 • info@frontiersin.org
www.frontiersin.org

Find us on

